British Journal of Pharmacology

November 1994

Volume 113 Number 3 pages 659–1078

Dr S J Coker
Department of Pharmacology
University of Liverpool
P.O. Box 147
LIVERPOOL L69 3BX

Br. J. Pharmacol. (1994), **113**, 659–661

SPECIAL REPORT

© Macmillan Press Ltd., 1994

Activation of BK_{Ca} channels in acutely dissociated neurones from the rat ventromedial hypothalamus by NS 1619

[1,3]Andrew J. Sellers & [2]Michael L.J. Ashford

Department of Pharmacology, Tennis Court Road, Cambridge, CB2 1QJ

NS 1619 activates the large-conductance Ca^{2+}-dependent K^+ channel (BK_{Ca}) in membrane patches isolated from rat ventromedial hypothalamic neurones. The activation is concentration dependent, with a maximal effect at less than 30 μM, reversible and can be inhibited by application of iberiotoxin to the extracellular membrane. NS 1619 does not activate ATP-K^+ channels present in the same neurones.

Keywords: BK_{Ca} channel, ATP-modulated K^+ channel, hypothalamus, NS 1619, potassium channel opener

Introduction ATP-sensitive K^+ (K_{ATP}) and large-conductance Ca^{2+}-dependent K^+ (BK_{Ca}) channels are present in glucose-receptive neurones of the rat ventromedial hypothalamus (VMHN; Ashford *et al.*, 1990; Treherne & Ashford, 1991). The K_{ATP} channel is not the classical (type 1) channel as found in pancreatic β-cells or heart, but a large-conductance non-rectifying version (type 2; Ashcroft & Ashcroft, 1990). The first-generation K^+ channel openers (levcromakalim, pinacidil, diazoxide and minoxidil sulphate), activators of type 1 K_{ATP} channels, do not activate either of these channel types in excised membrane patches (Sellers *et al.*, 1992). The benzimidazolone compound, NS 1619, activates BK_{Ca} channels in whole-cell and isolated patch recordings from bovine aortic smooth muscle cells (Olesen *et al.*, 1994), indicating that the site of action of this compound must be closely linked to, or part of, the BK_{Ca} channel complex. The aim of the present experiments was to evaluate the effects of NS 1619 on the BK_{Ca} and type 2 K_{ATP} channels that are recorded in patches isolated from VHMN neurones.

Methods Neurones were dissociated from the VMHN of rat brains using methods described previously (Ashford *et al.*, 1990). Briefly, VMHN nuclei were isolated from 350-μm-thick coronal brain slices and individual neurones were dissociated using enzyme treatment (collagenase and trypsin) and trituration. Neurones were plated into cell culture dishes and standard patch clamp techniques used (Hamill *et al.*, 1980). Channel activity was expressed as mean total current. All experiments were performed at 21–24°C.

Results The BK_{Ca} was identified by its conductance (245 pS) and voltage dependency (depolarization increasing channel activity). The channel was observed in 28 out of 43 membrane patches made from VMHN neurones. In every case, application of NS 1619 (5–20 μM) to inside-out patches containing BK_{Ca} channels induced a concentration-dependent and reversible increase in channel activity ($n = 8$; Figure 1a). Similarly, application of NS 1619 (5–20 μM) caused an increase in BK_{Ca} channel activity in outside-out membrane patches ($n = 13$; Figures 1b and 2a). In both membrane patch configurations no further increase in BK_{Ca} channel activity was observed with concentrations of NS 1619 greater than 30 μM (data not shown). Iberiotoxin (IbTx) blocks BK_{Ca} channels by directly occluding the external mouth of the pore region (Candia *et al.*, 1992). Figure 2a shows data recorded from an outside-out membrane patch bathed in quasiphysiological ion gradients. Application of 20 μM NS 1619 increased BK_{Ca} channel activity, an effect which was reversed by concomitant application of 35 nM IbTx. Type 2 K_{ATP} channels were identified by their conductance (135 pS), lack of voltage sensitivity and inhibition by ATP. NS 1619 (20 μM) caused no change in open-state probability of these neuronal K_{ATP} channels ($n = 5$; Figure 2b).

Discussion The first-generation potassium openers (e.g. levcromakalim, pinacidil and diazoxide), which induce relaxation of smooth muscle and cause hyperpolarization of many other tissues, are generally considered to activate K^+ channels identical or similar to type 1 K_{ATP} channels (Edwards & Weston, 1993). These agents have been observed to cause 'hyperpolarization-like' effects in many CNS preparations (Gandolfo *et al.*, 1989; Amoroso *et al.*, 1990; Schmid-Antomarchi *et al.*, 1990). However, no proof has been offered to suggest that these agents mediate these effects through *direct* activation of any specific K^+ channel type. Furthermore, type 2 K_{ATP} channels and BK_{Ca} channels in hypothalamic neurones have conclusively been shown to be insensitive to these agents (Sellers *et al.*, 1992). We propose that there is little or no evidence to suggest that lemakalim is directly activating (i.e. binding to the ion channel complex) any of the neuronal K^+ channels so far identified. Recently, Olesen *et al.* (1994) have described a novel benzimidazolone compound, NS 1619, which activates BK_{Ca} channels in aortic smooth muscle cells. We show here that NS 1619 activates hypothalamic BK_{Ca} channels in excised membrane patches. This activation is reversible, occurs at low concentrations of internal calcium and is inhibited by IbTx applied to the extracellular membrane of the channel. These data substantiate the observation that NS 1619 augments charybdotoxin sensitive whole-cell K^+ currents in cerebellar and cortical neurones (Olesen *et al.*, 1994). NS 1619 cannot activate K_{ATP} channels from neurones dissociated from the same brain region (these data) or K_{ATP} channels from pancreatic β-cells (Olesen *et al.*, 1994). In conclusion, these results clearly show that NS 1619 is selective for (at least) one neuronal K^+ channel type over another and also that NS 1619 is binding to a site which is closely associated with, or part of, the BK_{Ca} channel complex itself.

[1] Present address: Boyer Center of Molecular Medicine, Yale University Medical School, 295 Congress Avenue, New Haven, CT, USA.
[2]Present address: Vollum Institute for Advanced Biomedical Sciences, Oregon Health Services University, Portland, OR, USA.
[3]Author for correspondence.

We gratefully acknowledge the gift of NS 1619 from NeuroSearch, Denmark and the discussions provided by Dr Søren-Peter Olesen and Dr Ann Hayes of NeuroSearch and Glaxo respectively.

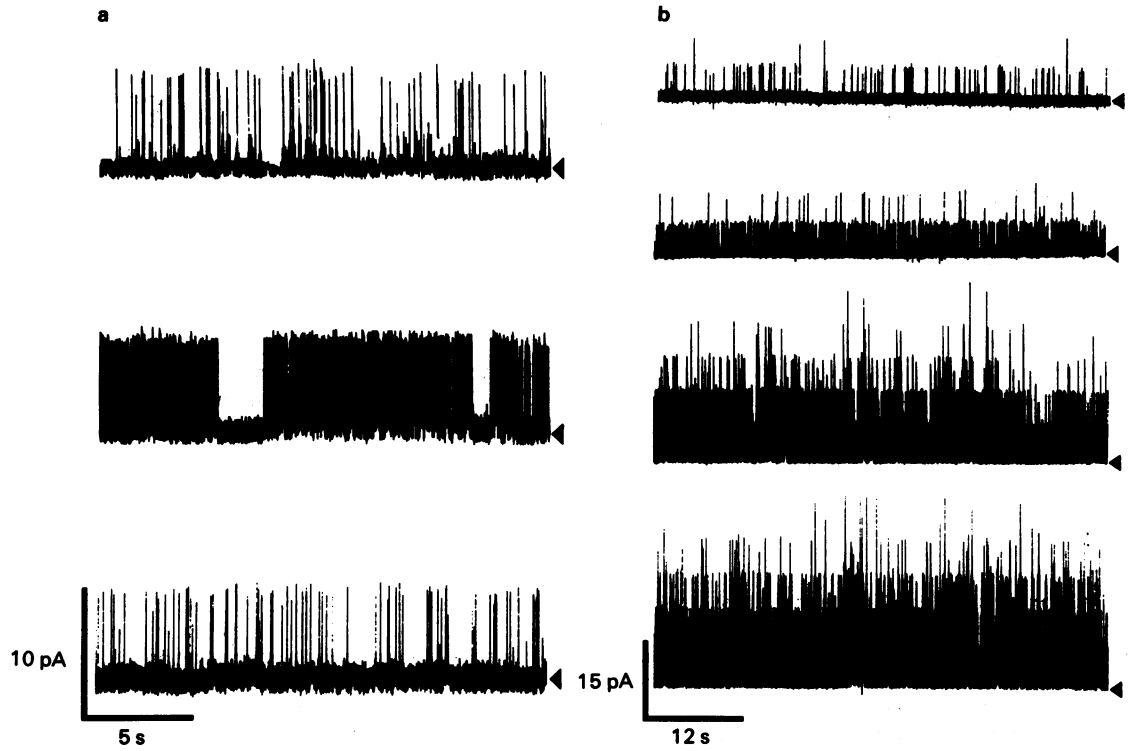


Figure 1 Effect of NS 1619 on VMHN BK_{Ca} channels. Data recorded from (a) an inside-out membrane patch and (b) an outside-out membrane patch. In both cases, patches were bathed in symmetrical K^+ solutions (< 10 nM free intracellular calcium) with E_M + 30 mV. Zero current levels are indicated by the arrows throughout. From top to bottom, traces show, with mean total current values in (a) control, 1.32 pA; 20 μM NS 1619, 5.37 pA; wash, 1.03 pA and (b) control, 0.81 pA; 5 μM NS 1619, 3.53 pA; 10 μM NS 1619, 8.68 pA; 20 μM NS 1619, 12.92 pA.

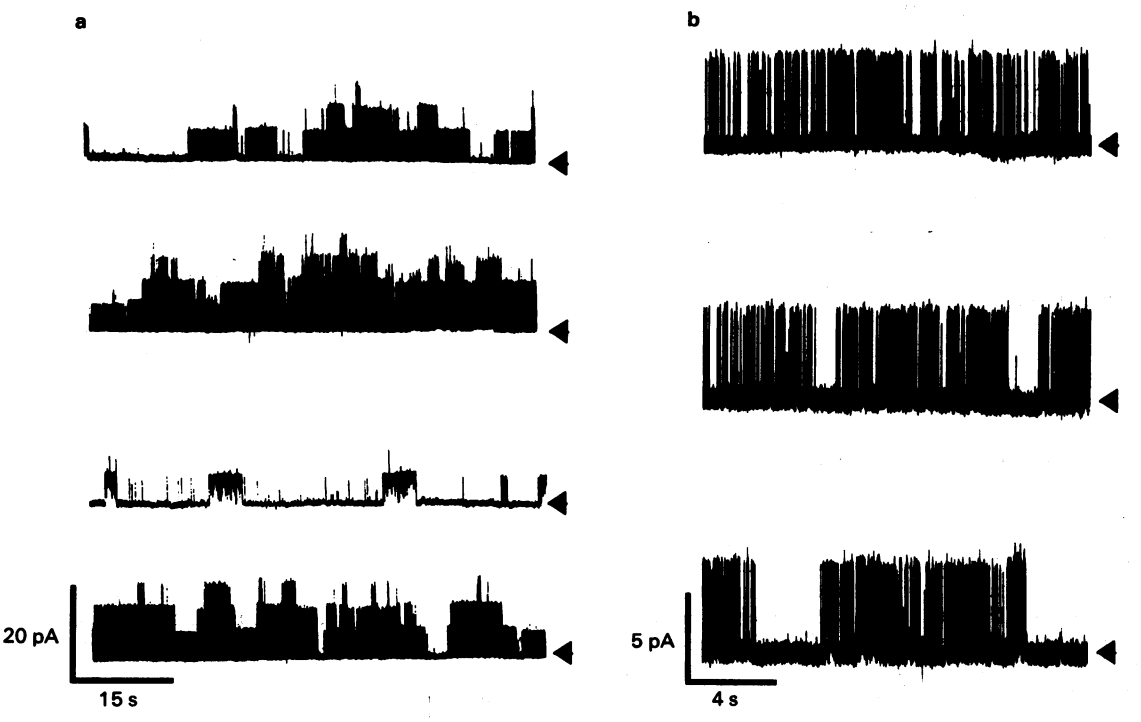


Figure 2 (a) The effects of NS 1619 are inhibited by IbTx. Data recorded from an outside-out membrane patch from a VMHN neurone bathed in quasiphysiological ion gradients (< 10 nM intracellular calcium). E_M + 20 mV. Traces show, with mean total current, from top to bottom; control, 8.70 pA; 20 μM NS 1619, 16.76 pA; 20 μM NS 1619 + 35 nM IbTx, 2.23 pA; and wash, 12.19 pA. (b) Lack of effect of NS 1619 on ATP-K^+ channels. Data recorded from an inside-out patch held at + 20 mV in symmetrical K^+ solutions. Traces show, from top to bottom, with mean total currents: control, 2.70 pA; 20 μM NS 1619, 2.61 pA; wash, 2.60 pA.

References

AMOROSO, S., SCHMID-ANTOMARCHI, H., FOSSET, M. & LAZDUNSKI, M. (1990). Glucose, sulfonylureas and neurotransmitter release: role of ATP-sensitive K^+ channels. *Science*, **247**, 852–854.

ASHCROFT, S.J.H. & ASHCROFT, F.M. (1990). Properties and functions of ATP-sensitive K-channels. *Cell. Signal.*, **2**, 197–214.

ASHFORD, M.L.J., BODEN, P.R. & TREHERNE, J.M. (1990). Glucose-induced excitation of hypothalamic neurones is mediated by ATP-sensitive K^+ channels. *Pflügers Arch.* **415**, 479–483.

CANDIA, S., GARCIA, M.L. & LATORRE, R. (1992). Mode of action of iberiotoxin, a potent blocked of the large-conductance Ca^{2+}-activated K^+ channel. *Biophys. J.*, **63**, 583–590.

EDWARDS, G. & WESTON, A.H. (1993). The pharmacology of ATP-sensitive potassium channels. *Annu. Rev. Pharmacol. Toxicol.*, **33**, 597–637.

GANDOLFO, G., GOTTESMAN, C., BIDARD, J.-N. & LAZDUNSKI, M. (1989). K^+ channel openers prevent epilepsy induced by the bee venom peptide MCD. *Eur. J. Pharmacol.*, **159**, 329–330.

HAMILL, O.P., MARTY, A., NEHER, E., SAKMANN, B. & SIGWORTH, F.J. (1981). Improved patch-clamp techniques for high-resolution current recording from cells and cell-free membrane patches. *Pflügers Arch.*, **391**, 85–100.

OLESEN, S.-P., MUNCH, E., MOLDT, P. & DREYER, J. (1994). Selective activation of Ca^{2+}-dependent K^+ channels by novel benzimidazolone. *Eur. J. Pharmacol.*, (in press).

SCHMID-ANTOMARCHI, H., AMOROSO, S., FOSSET, M. & LAZDUNSKI, M. (1990). K^+ channel openers activate brain sulfonylurea-sensitive K^+ channels and block neurosecretion. *Proc. Natl. Acad. Sci. USA*, **87**, 3489–3492.

SELLERS, A.J., BODEN, P.R. & ASHFORD, M.L.J. (1992). Lack of effect of potassium channel openers on ATP-modulated potassium channels recorded from rat ventromedial hypothalamic neurones. *Br. J. Pharmacol.*, **107**, 1068–1074.

TREHERNE, J.M. & ASHFORD, M.L.J. (1991). Calcium-activated potassium channels in rat dissociated ventromedial hypothalamic neurones. *J. Neuroendocrinol.*, **3**, 323–329.

(Received July 13, 1994
Accepted August 9, 1994)

Br. J. Pharmacol. (1994), **113**, 662–663

SPECIAL REPORT

© Macmillan Press Ltd., 1994

AT_1 receptor-mediated stimulation by angiotensin II of rat aortic fibronectin gene expression *in vivo*

[1]Shokei Kim, Kensuke Ohta, Akinori Hamaguchi, Takashi Omura, Kazunari Tominaga, Tokihito Yukimura, Katsuyuki Miura, Motoharu Tanaka & Hiroshi Iwao

Department of Pharmacology, Osaka City University Medical School, Osaka 545, Japan

Fibronectin plays an important role in various vascular diseases. A subpressor (200 ng kg^{-1} min^{-1}) or pressor (1000 ng kg^{-1} min^{-1}) dose of angiotensin II was continuously infused into rats by osmotic minipump for various times, to investigate the effects on aortic fibronectin gene expression. In rats infused with a subpressor dose of angiotensin II in which blood pressure was normal for 3 days, aortic fibronectin mRNA levels started to increase by 1.4 fold at 12 h and reached the maximal levels (increased by 3.1 fold) at 3 days. Treatment with TCV-116 (3 mg kg^{-1} day^{-1}), a non-peptide selective AT_1 receptor antagonist, completely inhibited the angiotensin II-induced increase in aortic fibronectin mRNA, while hydralazine (10 mg kg^{-1} day^{-1}) did not block this effect. Similar results were also obtained for a pressor dose of angiotensin II. Thus, angiotensin II directly stimulates aortic fibronectin gene expression *in vivo*, which is mediated by the AT_1 receptor but not by blood pressure.

Keywords: angiotensin II; fibronectin; AT_1 receptor; TCV-116; gene expression; blood pressure; transforming growth factor-β1; collagen

Introduction Recent studies suggest that angiotensin II (AII) may be involved not only in hypertension but also in various vascular diseases (Griendling *et al.*, 1993). However, the mechanism by which AII is responsible for vascular diseases *in vivo* remains to be elucidated. Fibronectin, the main extracellular matrix protein, influences cell adhesion and migration, and modulates vascular smooth muscle cells from a contractile to a synthetic phenotype, thus being implicated in vascular hypertrophy and neointimal formation (Ruoslahti, 1988; Glukhova *et al.*, 1989; Takasaki *et al.*, 1990). In this study, we have shown the importance of AII for aortic fibronectin gene expression *in vivo*.

Methods Eight-week-old male Wistar rats (Clea Japan, Japan), anaesthetized with ether, were implanted subcutaneously with an Alzet osmotic minipump (model 1003D or 2001, Alza Corp, USA) containing AII (Peptide Institute Inc., Japan) in saline or saline alone, and received a subpressor (200 ng kg^{-1} min^{-1}) or pressor (1000 ng kg^{-1} min^{-1}) infusion of AII for various times. For both doses, rats were separated into 4 groups: (1) saline-infused (control), (2) AII-infused, (3) AII-infused and TCV-116 (3 mg kg^{-1} day^{-1})-treated, and (4) AII-infused and hydralazine (10 mg kg^{-1} day^{-1})-treated groups. TCV-116 ((±)-1-(cyclohexyloxycarbonyloxy)-ethyl 2-ethoxy-1-[[2'-(1H-tetrazol-5-yl)biphenyl-4-yl] methyl]-1H-benzimidazole-7-carboxylate) (Takeda Chemical Industries, Ltd., Japan) (Shibouta *et al.*, 1993), a non-peptide selective AT_1 receptor antagonist, was given to rats by gastric gavage 24 h before implantation of the osmotic minipump to the end of AII infusion once a day. Hydralazine (Wako Pure Chemical Industries, Ltd., Japan), in the drinking water, was given to rats from 24 h before the start of AII infusion up to the end of AII infusion. At the indicated times, each group ($n = 4$) of rats was decapitated and the thoracic aortae were immediately excised, frozen in liquid nitrogen, pooled and stored at − 80°C until use.

RNA isolation and northern blot hybridization The detailed method was described in our previous paper (Kim *et al.*, 1994).

[1] Author for correspondence.

Results *Effect of AII infusion on blood pressure* For 200 ng kg^{-1} min^{-1} of AII, blood pressure (mean ± s.e.mean) of control, AII-infused, AII-infused and TCV-116-treated, and AII-infused and hydralazine-treated groups was 122 ± 1, 126 ± 2, 119 ± 2 and 120 ± 2 mmHg, respectively, at 2 days, and was 122 ± 2, 133 ± 2, 115 ± 5 and 118 ± 6 mmHg, respectively, at 3 days. As judged by ANOVA and Duncan's multiple range test, no statistically significant increase in blood pressure was produced by the infusion of 200 ng kg^{-1} min^{-1} of AII for 3 days, being consistent with the previous report by Simon & Altman (1992). In contrast, an infusion of 1,000 ng kg^{-1} min^{-1} increased blood pressure to 157 ± 8 mmHg ($P < 0.05$) on day 2, an effect which was completely inhibited by TCV-116 treatment.

Effects of AII infusion on aortic fibronectin mRNA levels As shown in Figures 1 and 2a, with a subpressor dose of AII, aortic fibronectin mRNA began to increase by 1.4 fold at 12 h after the infusion, gradually increased and reached a peak (3.1 fold) at 3 days. TCV-116 completely inhibited this increase in fibronectin mRNA at all time points examined, while hydralazine produced little inhibition, There was no significant increase in aortic TGF-β1, or type I or III collagen mRNA throughout AII infusion (Figure 1). The same experiments were repeated and similar results were obtained, thereby revealing that our observations were reproducible. A pressor dose of AII increased aortic fibronectin mRNA with a similar pattern to a subpressor dose (Figure 2), but failed to increase aortic TGF-β1 and types I and III collagen mRNAs throughout the infusion (data not shown).

Discussion We found that AII stimulated aortic fibronectin gene expression *in vivo* via the AT_1 receptor, but not via blood pressure. Fibronectin, the major extracellular matrix protein, modulates vascular smooth muscle cells from a contractile to a synthetic phenotype, causing cell proliferation (Ruoslahti, 1988). Fibronectin expression is increased in the hypertensive rat aorta (Takasaki *et al.*, 1990) and balloon-injured artery (Glukhova *et al.*, 1989), thereby supporting the contribution of fibronectin to vascular disease. Furthermore, Viswanathan *et al.* (1992) reported an increased AT_1 receptor expression in injured rat aorta. Therefore, our observations suggest that AII may participate in the development of vascular diseases by stimulating fibronectin expression.

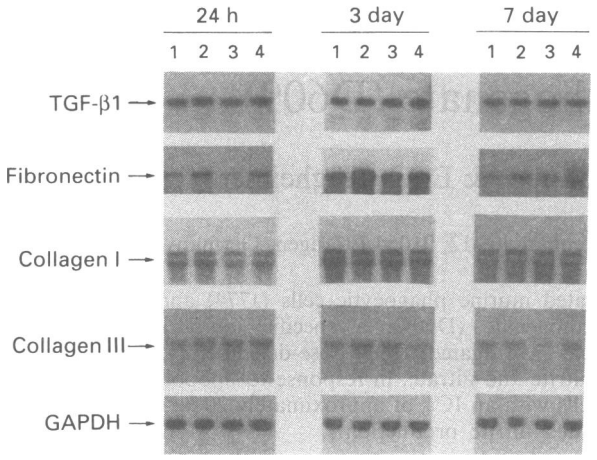


Figure 1 Representative autoradiograms of aortic mRNAs at 24 h, 3 days and 7 days after a subpressor (200 ng kg^{-1} min^{-1}) angiotensin II (AII) infusion. Lane 1, control rat; lane 2, AII-infused rat; lane 3, AII-infused and TCV-116-treated rat; lane 4, AII-infused and hydralazine-treated rat. In each group, aortic tissues were pooled from 4 rats. The size of mRNA was 2.5 kb for transforming growth factor-β1 (TGF-β1), 7.9 kb for fibronectin, 4.7 and 5.7 kb for α1(I) collagen (collagen I), 5.9 kb for α1(III) collagen (collagen III) and 1.4 kb for glyceraldehyde-3-phosphate dehydrogenase (GAPDH).

In this study, we also measured aortic TGF-β1 mRNA, because TGF-β1 stimulates fibronectin and collagen expressions (Border & Ruoslahti, 1992). Interestingly, in contrast to fibronectin, aortic TGF-β1 and types I and III collagen mRNAs were not stimulated by a subpressor or a pressor AII infusion. Thus, the AII-induced stimulation of aortic fibronectin expression *in vivo* seems to be a rather specific action and is not mediated by TGF-β1.

In conclusion, AII stimulates aortic fibronectin gene expression *in vivo*, via the AT_1 receptor but not via its pressor effect. Our present observations may partially explain the mechanism of the beneficial effects of inhibitors of the renin-angiotensin system on vascular diseases. However, further study is needed to elucidate the molecular mechanism of AII-induced vascular injury.

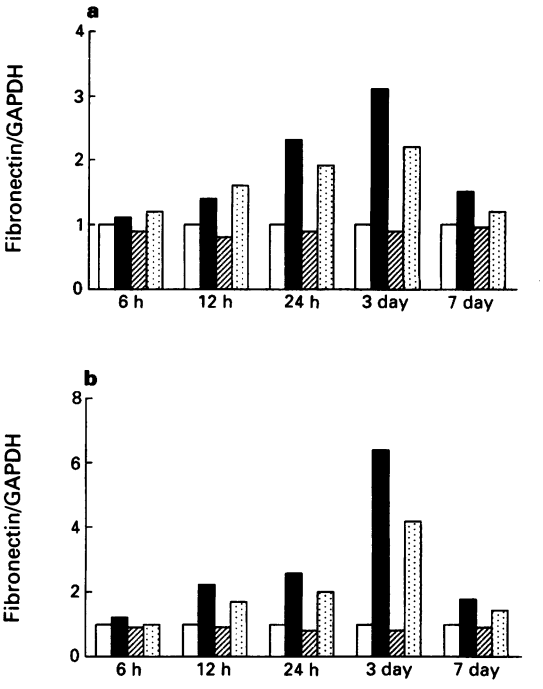


Figure 2 Aortic fibronectin mRNA levels at 6, 12, and 24 h, and 3 and 7 days after a subpressor (200 ng kg^{-1} min^{-1}) (a) and a pressor (1000 ng kg^{-1} min^{-1}) (b) angiotensin II (AII) infusion. The ordinate scale indicates aortic fibronectin mRNA levels, corrected for GAPDH mRNA levels. The value in the control group at each time point is represented as 1. Aortae were pooled from 4 rats in each group, and total RNA was extracted from the pooled aortae and subjected to northern blot analysis. Each column indicates control (open column), AII-infused (solid column), AII-infused and TCV-116-treated (hatched column) and AII-infused and hydralazine-treated groups (stippled column).

We are grateful to Drs R.O. Hynes, S.W. Qian, D. Rowe, Y.Yamada and Ph.Fort for the gift of cDNA for rat fibronectin, rat TGF-β1, rat α1 (I) collagen, mouse α1 (III) collagen, and rat GAPDH, respectively.

References

BORDER, W.A. & RUOSLAHTI, E. (1992). Transforming growth factor-β in disease: the dark side of tissue repair. *J. Clin. Invest.*, **90**, 1–7.

GLUKHOVA, M.A., FRID, M.G., SHEKHONIN, B.V., VASILEVSKAYA, T.D., GRUNWALD, J., SAGINATI, M. & KOTELIANSKY, V.E. (1989). Expression of extra domain A fibronectin sequence in vascular smooth muscle cells is phenotype dependent. *J. Cell. Biol.*, **109**, 357–366.

GRIENDLING, K.K., MURPHY, T.J. & ALEXANDER, R.W. (1993). Molecular biology of the renin-angiotensin system. *Circulation*, **87**, 1816–1828.

KIM, S., OHTA, K., HAMAGUCHI, A., OMURA, T., YUKIMURA, T., MIURA, K., INADA, Y., WADA, T., ISHIMURA, Y., CHATANI, F. & IWAO, H. Role of angiotensin II in renal injury of deoxycorticosterone acetate-salt hypertensive rats. *Hypertension*, (in press).

RUOSLAHTI, E. (1988). Fibronectin and its receptor. *Annu. Rev. Biochem.*, **57**, 375–413.

SHIBOUTA, Y., INADA, Y., OJIMA, M., WADA, T., NODA, M., SANADA, T., KUBO, K., KOHARA, Y., NAKA, T. & NISHIKAWA, K. (1993). Pharmacological profile of a highly potent and long-acting angiotensin II receptor antagonist, 2-ethoxy-1-((2'-(1H-tetrazol-5-yl)biphenyl-4-yl)methyl)-1H-benzimidazole-7-carboxylic acid (CV-11974), and its prodrug, (±)-1-(cyclohexyloxycarbonyloxy)-ethyl 2-ethoxy-1-((2'-(1H-tetrazol-5-yl)biphenyl-4-yl) methyl)-1H-benzimidazole-7-carboxylate (TCV-116). *J. Pharmacol. Exp. Ther.*, **266**, 114–120.

SIMON, G. & ALTMAN, S. (1992). Subpressor angiotensin II is a bifunctional growth factor of vascular muscle in rats. *J. Hypertens*, **10**, 1165–1171.

TAKASAKI, I., CHOBANIAN, A.V., SARZANI, R. & BRECHER, P. (1990). Effect of hypertension on fibronectin expression in the rat aorta. *J. Biol. Chem.*, **265**, 21935–21939.

VISWANATHAN, M., STROMBERG, C., SELTZER, A. & SAAVEDRA, J.M. (1992). Balloon angioplasty enhances the expression of angiotensin II AT1 receptors in neointima of rat aorta. *J. Clin. Invest.*, **90**, 1707–1712.

(Received June 7, 1994
Accepted July 13, 1994)

Br. J. Pharmacol. (1994), **113**, 664–668 © Macmillan Press Ltd, 1994

Induction of nitric oxide synthase activity in phagocytic cells inhibited by tricyclodecan-9-yl-xanthogenate (D609)

Klaus Tschaikowsky, [1]Michael Meisner, Frank Schönhuber & Erich Rügheimer

Institute of Anesthesiology, University of Erlangen-Nuremberg, Krankenhausstr. 12, 91054 Erlangen, Germany

1 The synthesis of nitric oxide (NO) by immune-stimulated murine phagocytic cells (J774) and the modulation of this synthesis by tricyclodecan-9-yl-xanthogenate (D609), a specific inhibitor of phosphatidylcholine-specific phospholipase C (PC-PLC), was investigated. D609 dose-dependently suppressed production of NO, as measured by the release of nitrite and nitrate, in response to lipopolysaccharide (LPS) and interferon-γ (IFN-γ) in intact cultured cells with an IC_{50} of approximately 20 μg ml^{-1}. D609 at 40 μg ml^{-1} completely abrogated immune-stimulated nitrite production.

2 The inhibitory effects of D609 on nitrite production were time-dependent and restricted to the first 18 h post-stimulation. D609 did not inhibit nitrite production in the cytosol of immune-stimulated phagocytes.

3 These findings indicate that the xanthogenate, D609, is a potent inhibitor of the induction of NO-synthase activity in immune-stimulated phagocytes. Furthermore, since D609 has been demonstrated to inhibit PC-PLC specifically, our findings suggest that the activation of this enzyme by LPS and IFN-γ is a proximal step in the signal transduction of inducible NO-synthase in phagocytic cells.

Keywords: Interferon-γ; lipopolysaccharide; nitrate; nitric oxide (NO); nitrite; murine macrophages, phospholipase C; protein kinase C; signal transduction; xanthogenates

Introduction

Nitric oxide (NO) has been recognized as an important mediator of various cellular activities. For example, NO regulates vascular tone and blood flow (Palmer *et al.*, 1987) and in sepsis, excess production of NO by macrophages and other cells activated by endotoxin and cytokines, is thought to induce massive vasodilatation and shock (Kilbourn *et al.*, 1990; Meyer *et al.*, 1992). Moreover, NO synthesized by macrophages contributes to their cytotoxic activity against bacteria (Granger *et al.*, 1990). NO reacts rapidly with water and oxygen to yield nitrite and nitrate, the accumulation of which provides a measure of NO production (Stuehr *et al.*, 1989).

As identified by molecular cloning, there are at least three distinct classes of nitric oxide synthases (NOS) producing NO. Two of them are dependent upon calcium/calmodulin and are constitutively expressed in rat brain (Bredt *et al.*, 1991) and in bovine and human endothelial cells (Lamas *et al.*, 1992; Marsden *et al.*, 1992), respectively. The other type of NOS (termed iNOS) is a Ca^{2+}-independent enzyme and is induced in macrophages, smooth muscle cells, hepatocytes, and fibroblasts several hours after exposure to some cytokines and endotoxin (LPS) (Moncada *et al.*, 1991).

To date, iNOS from murine macrophages has been cloned and characterized (Xie *et al.*, 1992), but little is known about the intracellular signal transduction mechanisms involved in the expression of iNOS. Glucocorticoids have been found to inhibit iNOS expression in activated endothelial cells (Radomski *et al.*, 1990). In addition, cytokines such as transforming growth factor-β, interleukin-4 (IL-4), macrophage deactivating factor, and IL-10 were shown to inhibit iNOS activity induced by interferon-γ (IFN-γ) but had no inhibitory effect on the NO release induced by IFN-γ plus lipopolysaccharide (LPS) (Ding *et al.*, 1990; Oswald *et al.*, 1992). Recently, inhibitors of nuclear transcription factor kappa B (NF-kB) and inhibitors of protein kinase C (PKC), a regulatory enzyme known to activate NF-kB (Gosh & Baltimore, 1990), have been shown to suppress the induction of iNOS activity in LPS- and IFN-γ-stimulated macrophages (Severn *et al.*, 1992; Mülsch *et al.*, 1993; Sherman *et al.*, 1993; Tschaikowsky *et al.*, 1994). These findings suggest that expression of iNOS is regulated by NF-kB.

We questioned, whether there is also a common signal proximal in the induction pathway of iNOS, mediating activation of NF-kB and subsequent synthesis of iNOS activity. Phosphatidylcholine-specific phospholipase C (PC-PLC) has recently been demonstrated to control the upregulaton of NF-kB in response to TNF (Schütze *et al.*, 1992). In these experiments, tricyclodecan-9-yl-xanthogenate (coded D609), previously described as an antiviral (Sauer *et al.*, 1984) and antitumoural (Amtmann & Sauer, 1990) compound, has been demonstrated to inhibit PC-PLC specifically (Schütze *et al.*, 1992). Additionally, D609 has been shown to suppress dose-dependently the TNF-induced release of diacylglycerol (DAG) (Schütze *et al.*, 1992).

In the present study, we investigated the role of D609 in the induction of iNOS activity in immune-stimulated murine macrophages, and discuss the role of PC-PLC and PKC in the signal transduction of iNOS.

Methods

Cell culture and treatment of cells

J774A.1 cells, a mouse macrophage-like cell line (American Type Culture Collection, Rockville, MD, U.S.A.) were grown continuously in 250 ml plastic bottles (Falcon). Supplemented modified Eagle's medium (SMEM) without Phenol red containing 10% heat-inactivated foetal bovine serum Heartline (endotoxin tested <50 pg ml^{-1}) 0.11 g l^{-1} sodium pyruvate, glucose 3.5 g l^{-1}, 100 u ml^{-1}penicillin, 100 μg ml^{-1} streptomycin and 2 mM L-glutamine was used as culture medium. Cells were harvested by centrifugation and then resuspended in culture medium. To induce NO-synthesis, cells were cultured at a concentration of 1×10^6 ml^{-1} in 24 well cluster plates (Costar). Two hours after incubation (37°C, 5% CO_2), medium was aspired to remove non-adherent cells and replaced by fresh, Phenol red-free culture medium adjusted to pH 7.0 (D609 is only active at pH ≤ 7.0), with various

[1] Author for correspondence.

concentrations of D609 that ranged from 0 (control) to 40 $\mu g\,ml^{-1}$, final concentration. After 1 h of incubation, iNOS activity was induced by adding 1 $\mu g\,ml^{-1}$ LPS (*E. coli* serotype 0111:B4) and 200 u ml^{-1} IFN-γ (final concentrations) either alone or in combination. If not stated otherwise, supernatants were collected at 18 h after stimulation. In subsequent time course experiments, D609 (30 $\mu g\,ml^{-1}$) was added to the cultures at 2, 6, 12 and 18 h after stimulation. In these experiments, cells were incubated (37°C, 5% CO_2) for 24 h, followed by recovery of the supernatant. Supernatants were subsequently analysed for nitrite and nitrate. Some wells were used to estimate the cytotoxic effect of D609 (10–40 $\mu g\,ml^{-1}$), LPS and IFN-γ. Cell viability at the end of the experiments, as assessed by Trypan blue exclusion, exceeded 90% at all concentrations of D609 and under all stimulatory conditions used.

Preparation of cytosol from stimulated macrophages

J774 cells grown in culture bottles were stimulated with LPS (1 $\mu g\,ml^{-1}$) and IFN-γ (200 u ml^{-1}). After 18 h of incubation (37°C, 5% CO_2), cells were harvested by mechanical agitation. After centrifugation (400 *g*, 10 min, 4°C), cells were washed in PBS and resuspended in deionized water containing protease inhibitors (0.1 mM phenylmethyl sulphonylfluoride, 5 $\mu g\,ml^{-1}$ aprotinin, 1 $\mu g\,ml^{-1}$ chymostatin, 5 $\mu g\,ml^{-1}$ pepstatin A; final concentrations). Cells were adjusted to a concentration of $10^7\,ml^{-1}$ and then lysed by three cycles of rapid freezing and thawing. Cell lysates were centrifuged (50,000 *g*, 1 h, 4°C), and aliquots of cytosol were stored at −70°C. Cytosol (70 µl) was incubated with 2 µl NADPH (30 mM), 4 µl L-arginine (30 mM), and 4 µl $MgCl_2$ (30 mM) for 2 h at 37°C. Under these conditions iNOS activity was optimal. For determination of the total amount of accumulated nitrate and nitrite, activated cytosol (80 µl) was further processed as described (nitrate assay). To assess the concentration of nitrite, residual NADPH, which interferes with the Griess reaction, was enzymatically oxidized to $NADP^+$ by addition of 10 µl of a quench solution (25 mM α-ketoglutarate, 0.15 M NH_4Cl, and 0.52 u L-glutamic dehydrogenase from *Proteus* species; final concentrations) (Marletta *et al.*, 1988). Complete oxidation of NADPH to NADP was achieved after 2 h of incubation at 37°C, as determined by the loss of absorbance at 340 nm (data not shown). Finally, 10 µl PBS was added and nitrite was determined as described below.

iNOS activity of the cytosol was defined as the amount of nitrite and nitrate produced per mg of protein and per minute of incubation. In some experiments N^G-monomethyl-L-arginine (0.5–5 mM) was added to the cytosol in order to determine whether the formation of nitrite and nitrate was due to iNOS activity.

Adherent cell protein determination

After complete recovery of the supernatant, remaining cell layers were washed with PBS and lysed in 1 ml PBS containing Triton X-100 (0.02%). Cell lysates were centrifuged (50,000 *g*, 1 h, 4°C) and stored at −20°C. The Pierce bicinchoninic acid method was used to determine protein concentrations, with human serum albumin as standard.

Determination of NO-production

Production of NO in the cell culture was determined by the accumulation of nitrite using a colorimetric assay based on the Griess reaction (Green *et al.*, 1982). Where indicated, nitrate in the sample was additionally measured.

Nitrite assay

Nitrite (NO_2-) concentration in samples of supernatant or activated cytosol was assessed as follows. Griess colour reagent was freshly prepared by combining (1:1) reagent A (0.1% N-(1-naphthyl)ethylenediamine) and reagent B (1%, w/v, sulphanilamide in 5% H_3PO_4). Samples (100 µl) were transferred to a 96 well plate (Costar). Colour reagent (100 µl) was added and after 30 min incubation at 21°C, absorbance was read at 560 nm using a MKII Titertek plate reader. Standard curves were constructed using sodium nitrite (0–120 µM) dissolved in Phenol red-free culture medium.

Nitrate assay

Samples of supernatant (70 µl) together with 2 µl NADPH (30 mM) and 8 µl distilled H_2 or activated cytosol (80 µl) were added per well of a 96 well plate (Costar). Complete reduction of nitrate (NO_3-) to nitrite was achieved by adding 10 µl *Aspergillus* nitrate reductase [EC 1.6.6.2.] and 60 min incubation at 37°C. Residual NADPH was quenched by addition of 10 µl freshly prepared quench solution. Nitrite concentration present before conversion of nitrate to nitrite was determined in parallel by using the same protocol, but adding PBS instead of nitrate reductase. Nitrate concentrations were calculated as difference between nitrite concentrations measured with and without nitrate reductase. Sodium nitrate standards were run in parallel to nitrite standards to verify complete conversion of nitrate to nitrite.

Reagents and media

Tricyclodecan-9-yl-xanthogenate (D609) was kindly provided by Dr G. Sauer, German Cancer Research Center, Heidelberg, Germany. D609 was freshly prepared as a 0.1% stock solution in distilled water and then further diluted in culture medium at pH 7.0. Recombinant mouse IFN-γ was obtained from Genzyme. The 'BCA Protein Assay' kit was purchased from Pierce Chemical Company. Culture medium and all other chemicals were purchased from Sigma.

Statistics

Results are presented as mean ± standard error of the mean (s.e.mean) and were compared by Student's *t* test for unpaired data. Only *P* values <0.05 were considered statistically significant. For multiple comparisons, analysis of variance (ANOVA) was performed. In case of significant *F* values, ANOVA was followed by *t* tests for unpaired data. The Bonferroni correction was used to correct the *t* statistic for the number of comparisons made between groups.

Results

LPS and IFN-γ, either alone or in combination, substantially induced expression of iNOS activity in J774 cells with a subsequent release of NO, as measured as NO_2^- after 18 h of incubation. Inhibition of PC-PLC by D609 added 1 h before stimulation, markedly diminished the production of NO_2^- in the supernatant of cells under all stimulatory conditions tested (Figure 1). However, when D609 was added directly to the activated cytosol of LPS- and IFN-γ-stimulated macrophages, no inhibitory effect on the enzyme activity of iNOS was found. Under the conditions chosen, production rate was 0.12 nmol $NO_2^-\,mg^{-1}$ protein min^{-1} which correlates well with the rate of nitrite production of 0.09 nmol mg^{-1} of protein min^{-1} reported for the cytosol of stimulated RAW 264.7 cells (Marletta *et al.*, 1988). Production rate for the total of NO_2^- and NO_3^-, that was reduced and measured as NO_2^-, was approximately 0.34 nmol $NO_2^-\,mg^{-1}$ protein min^{-1}. Nitrite production by the cytosol of stimulated macrophages was due to iNOS activity, since it could be completely abrogated by incubation with 5 mM NMMA (data not shown).

Therefore, activation of PC-PLC with the subsequent release of DAG seems to be a primary step in iNOS induc-

tion. At the end of each experiment, cell viability was above 90% in all groups. Moreover, adherent cell protein values from 10^6 J774 cells following 18 h of incubation were 149 ± 18 μg in the control group and did not differ significantly from the means of groups treated with D609 (data not shown). These findings indicate that the suppression of iNOS activity by D609 at the concentrations tested, can neither be explained by a cytotoxic nor by an inhibitory effect on cell proliferation. Additionally, the ratio of nitrite to nitrate in the supernatant was invariably about 55% to 45%, whereas in the stimulated cytosol, the ratio was about 35% to 65%, irrespective of the treatment. These ratios of nitrite to nitrate are in close agreement to results of previous studies (Iyengar *et al.*, 1987).

Inhibition of LPS- and IFN-γ-induced NO_2^-/NO_3^- production by D609 was dose-dependent (Figure 2). At 10 μg ml^{-1}, D609 induced significant suppression of NO_2^- production in J774 cells stimulated with LPS (1 μg ml^{-1}) and IFN-γ (200 u ml^{-1}). The IC_{50} value for inhibition of the nitrite release by D609 was approximately 20 μg ml^{-1}. At 40 μg ml^{-1}, added 1 h prior to stimulation, D609 suppressed the induction of iNOS activity by 90–100%.

We next carried out experiments to determine the time at which expression of iNOS activity was susceptible to inhibition by D609. As illustrated in Figure 3, D609 time-dependently inhibited the amount of NO_2^- accumulated after 24 h in the supernatant of stimulated cells. Up to 18 h after stimulation, we observed an almost linear relationship between the time D609 was present in the culture and the amount of inhibition. However, addition of D609 18 h after

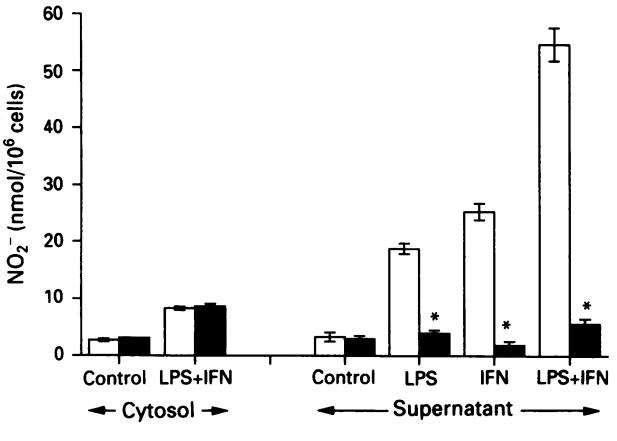


Figure 1 Effect of tricyclodecan-9-yl-xanthogenate (D609) on inducible nitric oxide synthase (iNOS) activity. Data represent the amount of nitrite (NO_2^-) in the supernatant and activated cytosol of stimulated murine J774 macrophages (means ± s.e.mean, $n = 8$) in the absence (open columns) or presence of D609 (30 μg ml^{-1}) (solid columns). Supernatants were collected at 18 h after stimulation. Cytosol prepared from stimulated cells (≈1.49 mg protein from 10^7 cells) was incubated (37°C, 5% CO_2) with L-arginine (1.5 mM), NADPH (0.75 mM) and $MgCl_2$ (1.5 mM) for 2 h. Subsequently, nitrate reductase was added. After 1 h of incubation (37°Ç, 5% CO_2), residual NADPH was enzymatically quenched, and the concentration of NO_2^- was determined. Pretreatment with D609 significantly inhibited NO_2^- production in the supernatant of cells stimulated by lipopolysaccharide (LPS; 1 μg ml^{-1}), interferon gamma (IFN; 200 u ml^{-1}), or both (LPS + IFN). D609 did not affect unstimulated cells (control) or iNOS activity in activated cytosol. *Indicates $P < 0.001$ versus stimulated cells without D609 (*t* test).

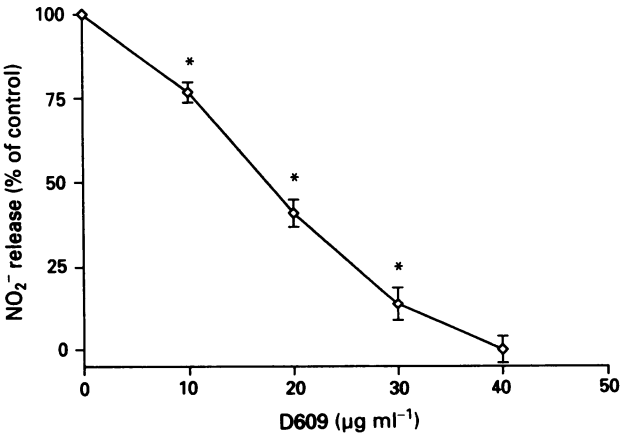


Figure 2 Dose-dependent inhibition of inducible nitric oxide synthase activity by D609. Macrophages were treated with D609 (0–40 μg ml^{-1}) 1 h prior to stimulation with lipopolysaccharide (1 μg ml^{-1}) plus interferon gamma (200 u ml^{-1}). After incubation for 18 h, supernatants were assayed for nitrite. Results are presented as means ± s.e.mean of duplicates from eight different experiments. *Indicates $P < 0.01$ versus mean of cells treated with the next lower concentration of D609 (ANOVA followed by *t* test).

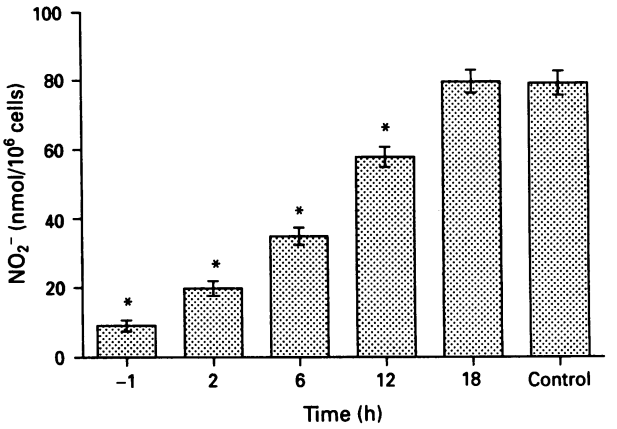


Figure 3 D609 inhibits the induction of nitrite (NO_2^-) synthesis, but not the activity of nitrite producing enzymes. Cells were incubated (37°C, 5% CO_2) with lipopolysaccharide (1 μg ml^{-1}) plus interferon gamma (200 u ml^{-1}) (zero time point) in the absence (control) or presence of D609 (30 μg ml^{-1}) added to the culture at the indicated times (−1 h to 18 h). The data represent the amount of NO_2^- accumulated in the supernatant at 24 h. D609 added at 18 h after stimulation did not reduce the concentration of NO_2^- as compared to control. Importantly, iNOS was still active between 18 h and 24 h, producing approximately 4.5 nmol NO_2^- (10^6 cells)$^{-1}$ h^{-1}). Results are given as means ± s.e.mean of duplicates from eight different experiments. *Indicates $P < 0.001$ versus control (*t* test).

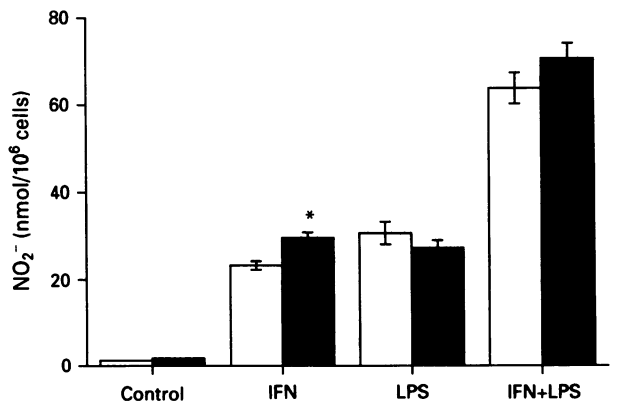


Figure 4 Effect of phorbol 12-myristate 13-acetate (PMA) on inducible nitric oxide synthase (iNOS) activity. Results represent the nitrite (NO_2^-) production (means ± s.e.mean, $n = 4$) in culture supernatant of unstimulated cells (control) and macrophages stimulated for 24 h by lipopolysaccharide (LPS; 1 μg ml^{-1}), interferon gamma (IFN; 200 u ml^{-1}), or both (LPS + IFN), in the absence (open columns) or presence of PMA (1 μg ml^{-1}) (solid columns). *Indicates $P < 0.05$ versus stimulated cells without PMA (*t* test).

the stimulation, did not reduce further accumulation of NO_2^- in the supernatant between 18 h and 24 h. Together with the finding that D609 did not inhibit enzyme activity of iNOS in the activated cytosol, this finding suggests that 18 h after co-stimulation with LPS and IFN-γ, macrophages stopped *de novo* synthesis of iNOS.

We also investigated whether activation of PKC could induce iNOS activity and eventually overcome the inhibitory effect by D609. In these experiments cells were incubated with PMA (1 $\mu g\,ml^{-1}$) that directly activates PKC, but not acidic sphingomyelinase (SM-ase) (Kolesnick, 1987). We found that PMA alone did not induce nitrite production. In combination with other stimuli, PMA enhanced only marginally the induction of iNOS activity by IFN-γ showing no significant effect on NO_2^- production induced by LPS and LPS + IFN-γ (Figure 4). Furthermore, addition of PMA to LPS and IFN-γ could not prevent the suppression of iNOS induction by D609 (data not shown).

Discussion

D609 dose-dependently reduced NO_2^- and NO_3^- production in response to LPS, IFN-γ and a combination of both. The ratio of nitrite to nitrate in the supernatant was unchanged by D609, excluding a shift within the oxidation products of NO. D609 did not inhibit NO production by iNOS present in lysates of stimulated J774 cells and was no longer inhibitory on NO production in cell cultures when added 18 h after stimulation. These findings indicate that D609 inhibits the induction of iNOS in response to LPS and IFN-γ. Induction of iNOS sensitive to D609 inhibition was found to be limited to the first 18 h post-stimulation, which is in close agreement with the kinetics of iNOS induction found by Ding *et al.* (1990).

The concentration of D609 needed for a 50% reduction in NO_2^- release was 20 $\mu g\,ml^{-1}$, which is nearly the same concentration as that needed to inhibit TNF-induced DAG release by 50% in the human monocytic cell line U937 (Schütze *et al.*, 1992). At 30–40 $\mu g\,ml^{-1}$, D609 completely abrogated NO production in response to LPS and IFN-γ. Again, this correlates well with finding of Müller-Decker (1989) showing that D609 at 30 $\mu g\,ml^{-1}$ almost completely blocked the phorbol ester-stimulated DAG release in hamster fibroblasts.

Together with the finding that D609 specifically inhibits PC-PLC, with no effects on phosphatidylinositol-specific PLC, phospholipase A_2 and phospholipase D (Schütze *et al.*, 1992), our results suggest that iNOS induction by LPS and IFN-γ depends on the activation of PC-PLC and the subsequent release of DAG. In a previous study, LPS has been demonstrated to induce hydrolysis of phosphatidyl-inositol-4,5-biphosphate in murine peritoneal macrophages (Pripic *et al.*, 1987).

Collectively, our results suggest that the activation of PC-PLC is a proximal signal in the induction of iNOS. In agreement with data from the literature, we propose the following signaling pathway as a model of iNOS expression: LPS and IFN-γ activate PC-PLC resulting in a release of DAG. DAG is a well-known activator of PKC, which has recently been implicated in iNOS induction in a study showing that iNOS induction can be blocked by inhibition of PKC (Severn *et al.*, 1992). Moreover, DAG released by PC-PLC has recently been shown to activate acidic SM-ase which subsequently produces ceramide (Schütze *et al.*, 1992). Both pathways, via PKC and via ceramide, lead to an activation of NF-kB (Gosh & Baltimore, 1990; Schütze *et al.*, 1992), that finally induces the expression of iNOS, as indicated by two recent studies (Mülsch *et al.*, 1993; Sherman *et al.*, 1993). It seems difficult, however, to determine which of the two pathways is more important for the induction of iNOS. Activation of PKC has been shown to induce activation of phosphatidylcholine-degrading phospholipase C with subsequent generation of DAG (Kolesnick & Paley, 1987; Müller-Decker, 1989). Thus, PKC may act as an endogenous amplifier for the acidic SM-ase-ceramide pathway. The finding that immune-stimulated iNOS activity is suppressed by inhibitors of PKC (Severn *et al.*, 1992; Tschaikowsky *et al.*, 1994), can therefore not provide clear-cut evidence on which is the prevailing pathway of iNOS induction. In our experiments, PMA, that activates PKC, but not acidic SM-ase (Kolesnick, 1987), enhanced only marginally induction of iNOS activity by IFN-γ, but could not induce iNOS activity *per se*, nor did it show a significant effect on iNOS induction by LPS and LPS + IFN-γ in the absence or presence of D609. These findings seem to favour the hypothesis that subsequent to activation of PC-PLC, both acidic SM-ase and PKC activation are necessary for iNOS induction, but neither pathway is sufficient to induce iNOS activity independently.

In conclusion, we have demonstrated that the xanthogenate D609 is a potent inhibitor of the induction of iNOS in immune-stimulated murine macrophages. Furthermore, our findings suggest that the activation of PC-PLC is a proximal step in the signal transduction of iNOS activity. However, clarification of the complete signal transduction pathway leading to iNOS expression awaits further investigations.

The authors wish to express their gratitude to Dr Sauer and Dr Amtmann (Deutsches Krebsforschungszentrum Heidelberg, Heidelberg, Germany) for the gift of D609.

References

AMTMANN, E. & SAUER, G. (1990). Tumor necrosis factor induces necrosis of human carcinoma xenografts in the presence of tricyclodecan-9-yl-xanthogenate and lauric acid. *Int. J. Cancer*, **45**, 1113–1118.

BREDT, D.S., HWANG, P.M., GLATT, C.E., LOWENSTEIN, C., REED, R.R. & SNYDER, S.H. (1991). Cloned and expressed nitric oxide synthase structurally resembles cytochrome P-450 reductase. *Nature*, **351**, 714–718.

DING, A., NATHAN, C.F., GRAYCAR, J., DERYNCK, R., STUEHR, D.J. & SRIMAL, S. (1990). Macrophage deactivating factor and transforming growth factors-β1, -β2, and -β3 inhibit induction of macrophage nitrogen oxide synthesis by IFN-γ. *J. Immunol.*, **145**, 940–944.

GOSH, S. & BALTIMORE, D. (1990). Activation in vitro of NF-kB by phosphorylation of its inhibitor IkB. *Nature*, **344**, 678–682.

GRANGER, D.L., HIBBS, J.B. Jr., PERFECT, J.R. & DURACK, D.T. (1990). Metabolic fate of L-arginine in relation to microbiostatic capability of murine macrophages. *J. Clin. Invest.*, **85**, 264–273.

GREEN, L.A., WAGNER, D.A., GLOGOWSKI, J., SKIPPER, P.L., WISHNOK, J.S. & TANNENBAUM, S.R. (1982). Analysis of nitrate, nitrite, and [^{15}N]nitrate in biological fluids. *Anal. Biochem.*, **1256**, 131–138.

IYENGAR, R., STUEHR, D.J. & MARLETTA, M. (1987). Macrophage synthesis of nitrite, nitrate, and N-nitrosamines: precursors and role of the respiratory burst. *Proc. Natl. Acad. Sci. U.S.A.*, **84**, 6369–6373.

KILBOURN, R.G., JUBRAN, A., GROSS, S.S., GRIFFITH, O.W., LEVI, R., ADAMS, J. & LODATO, R.F. (1990). Reversal of endotoxin-mediated shock by N^G-methyl-L-arginine, an inhibitor of nitric oxide synthesis. *Biochem. Biophys. Res. Commun.*, **172**, 1132–1138.

KOLESNICK, R.N. (1987). 1,2-Diacylglycerols but not phorbol ester stimulate sphingomyelin hydrolysis in GH3 pituitary cells. *J. Biol. Chem.*, **262**, 16759–16762.

KOLESNICK, R.N. & PALEY, A.E. (1987). 1,2-Diacylglycerols and phorbol ester stimulate phosphatidylcholine metabolism in GH3 pituitary cells. *J. Biol. Chem.*, **262**, 9204–9210.

LAMAS, S., MARSDEN, P.A., LI, G.K., TEMPST, P. & MICHEL, T. (1992). Endothelial nitric oxide synthase: molecular cloning and characterization of a distinct constitutive enzyme isoform. *Proc. Natl. Acad. Sci. U.S.A.*, **89**, 6348–6352.

MARLETTA, M.A., YOON, P.S., IYENGAR, R., LEAF, C.D. & WISHNOK, J.S. (1988). Macrophage oxidation of L-arginine to nitrite and nitrate: nitric oxide is an intermediate. *Biochemistry*, **27**, 8706–8711.

MARSDEN, P.A., SCHAPPERT, K.T., CHEN, H.S., FLOWERS, M., SUNDELL, C.L., WILCOX, J.N., LAMAS, S. & MICHEL, T. (1992). Molecular cloning and characterization of human endothelial nitric oxide synthase. *FEBS Lett.*, **307**, 287–293.

MEYER, J., TRABER, L.D., NELSON, S., LENTZ, C.W., NAKAZAWA, H., HERDON, D.N., NODA, H. & TRABER, D.L. (1992). Reversal of hyperdynamic response to continuous endotoxin administration by inhibition of NO synthesis. *J. Appl. Physiol.*, **73**, 324–328.

MONCADA, S.R., PALMER, M.J. & HIGGS, E.A. (1991). Nitric oxide: physiology, pathophysiology, and pharmacology. *Pharmacol. Rev.*, **43**, 109–142.

MÜLLER-DECKER, K. (1989). Interruption of TPA-induced signals by an antiviral and antitumoral xanthate compound: inhibition of a phospholipase c-type reaction. *Biochem. Biophys. Res. Commun.*, **162**, 198–205.

MÜLSCH, A., SCHRAY-UTZ, B., MORDVINTCEV, P.I., HAUSCHILDT, S. & BUSSE, R. (1993). Diethyldithiocarbamate inhibits induction of macrophage NO synthase. *FEBS Lett.*, **321**, 215–218.

OSWALD, I., GAZZINELLI, R.T., SHER, A. & JAMES, S.L. (1992). IL-10 synergizes with IL-4 and transforming growth factor-β to inhibit macrophage cytotoxic activity. *J. Immunol.*, **148**, 3578–3582.

PALMER, R.M.J., FERRIGE, A.G. & MONCADA, S. (1987). Nitric oxide release accounts for the biological activity of endothelium-derived relaxing factor. *Nature*, **327**, 524–526.

PRIPIC, V., WEIEL, J., SOMMERS, S., DIGUISEPPI, J., GONIAS, S.L., PIZZO, S., HAMILTON, T.A., HERMAN, B. & ADAMS, D.O. (1987). Effects of bacterial lipopolysaccharide on the hydrolysis of phosphatidyl-inositol-4,5-biphosphate in murine peritoneal macrophages. *J. Immunol.*, **139**, 526–533.

RADOMSKI, M.W., PALMER, R.M. & MONCADA, S. (1990). Glucocorticoids inhibit the expression of an inducible, but not the constitutive, nitric oxide synthase in vascular endothelial cells. *Proc. Natl. Acad. Sci. U.S.A.*, **87**, 10043–10047.

SAUER, G., AMTMANN, E., MELBER, K., KNAPP, A., MÜLLER, K., HUMMEL, K. & SCHERM, A. (1984). DNA and RNA virus species are inhibited by xanthates, a class of antiviral compounds with unique properties. *Proc. Natl. Acad. Sci. U.S.A.*, **81**, 3263–3267.

SCHÜTZE, S., POTTHOFF, K., MACHLEIDT, T., BERKOVIC, D., WIEGMANN, K. & KRÖNKE, M. (1992). TNF activates NF-kB by phosphatidylcholine-specific phospholipase C-induced 'acidic' sphingomyelin breakdown. *Cell*, **71**, 765–776.

SEVERN, A., WAKELAM, M.J.O. & LIEW, F.Y. (1992). The role of protein kinase C in the induction of nitric oxide synthesis by murine macrophages. *Biochem. Biophys. Res. Commun.*, **188**, 997–1002.

SHERMAN, M.P., AEBERHARD, E.E., WONG, V.Z., GRISCAVAGE, J.M. & IGNARRO, L.J. (1993). Pyrrolidine dithiocarbamate inhibits induction of nitric oxide sythase activity in rat alveolar macrophages. *Biochem. Biophys. Res. Commun.*, **191**, 1301–1308.

STUEHR, D.J., GROSS, S.S., SAKUMA, I., LEVI, R. & NATHAN, C.F. (1989). Activated murine macrophages secrete a metabolite of arginine with the bioactivity of endothelium-derived relaxing factor and the chemical reactivity of nitric oxide. *J. Exp. Med.*, **169**, 1011–1020.

TSCHAIKOWSKY, K., SCHÖNHUBER, F., MEISNER, M. & RÜGHEIMER, E. (1994). Involvement of phosphatidylcholine-specific phospholipase C and protein kinase C in induction of nitric oxide synthase in macrophages. *Int. Care Med.*, **20** Suppl. 1, S52.

XIE, Q.-W., CHO, H.J., CALAYCAY, J., MUMFORD, R.A., SWIDEREK, M., LEE, T.D, DING, A., TROSO, T. & NATHAN, C. (1992). Cloning and characterization of inducible nitric oxide synthase from mouse macrophages. *Science*, **256**, 225–228.

(Received March 15, 1994
Revised May 13, 1994
Accepted June 2, 1994)

Br. J. Pharmacol. (1994), **113**, 669–674 © Macmillan Press Ltd, 1994

Effects of cyclopiazonic acid on contractility and ecto-ATPase activity in guinea-pig urinary bladder and vas deferens

*†Airat U. Ziganshin, *Charles H.V. Hoyle, *†Lilia E. Ziganshina & [1]*Geoffrey Burnstock

*Department of Anatomy and Developmental Biology and Centre for Neuroscience, University College London, Gower Street, London WC1E 6BT and †Kazan Medical Institute, 49 Butlerov Street, Kazan, 420012, Russia

1 Cyclopiazonic acid (CPA), an inhibitor of sarcoplasmic ATPase, was tested on guinea-pig urinary bladder and vas deferens for its ability: (1) to modify contractile responses to electrical field stimulation (EFS), exogenous ATP, α,β-methylene ATP (α,β-meATP), carbachol, noradrenaline (NA), histamine, and KCl; (2) to affect ecto-ATPase activity; (3) to modify the release of ATP evoked by EFS.

2 In the urinary bladder, CPA (10 μM) potentiated contractile responses to EFS, exogenous ATP (100 μM), α,β-meATP (1 μM), carbachol (0.5 μM), histamine (30 μM) and KCl (30 mM). In the vas deferens, CPA (10 μM) potentiated responses to EFS, ATP, α,β-meATP, NA (100 μM) and KCl. CPA at a concentration of 1 μM had no effect on ATP-induced relaxation of carbachol-precontracted guinea-pig taenia coli, and at a concentration of 10 μM it markedly increased spontaneous contractile activity of taenia.

3 Ecto-ATPase was estimated to have V_{max} and K_m values of 0.98 nmol P_i 30 min^{-1} mg^{-1} wet tissue and 881 μM ATP in the urinary bladder, and 0.75 nmol P_i 30 min^{-1} mg^{-1} wet tissue and 914 μM ATP in the vas deferens, respectively. CPA at a concentration of 10 μM significantly inhibited ecto-ATPase activity by 18% in the urinary bladder and by 24% in the vas deferens.

4 In the guinea-pig vas deferens, CPA significantly potentiated ATP release evoked by EFS from 2.2 ± 0.8 (6) pmol ATP min^{-1} g^{-1} wet tissue to 35.2 ± 4.8 (6) pmol ATP min^{-1} g^{-1} wet tissue ($P<0.01$).

5 In conclusion, the potentiation of contractile responses of the guinea-pig urinary bladder and vas deferens by CPA has a non-specific character. CPA inhibited ecto-ATPase activity and increased ATP release, but these effects do not appear to contribute to the potentiation of P_{2x}-purinoceptor-mediated responses since the contractile actions of all the agonists studied were potentiated to the same extent.

Keywords: Cyclopiazonic acid; P_{2X}-purinoceptors; ecto-ATPase; guinea-pig smooth muscle

Introduction

It is now widely accepted that adenosine 5'-triphosphate (ATP) is a neurotransmitter that mediates responses via P_2-purinoceptors (Hoyle, 1992; Burnstock, 1993; Dubyak & El-Moatassim, 1993). However, it has been established that the amplitude of contractile responses of the guinea-pig urinary bladder and vas deferens evoked by exogenous ATP rarely approach those evoked by transmural electrical field stimulation (EFS) of purinergic nerves. On the other hand, in many systems, a stable analogue of ATP, α,β-methylene ATP (α,β-meATP), causes contractions about hundred times more effectively than ATP itself, and with a greater maximum amplitude. Thus, it seems likely that effects of endogenously released or exogenously applied ATP on P_2-purinoceptors may be limited by enzymatic degradation of ATP. Although the pharmacology and physiology of purinoceptors are being intensively investigated, the involvement of enzyme systems in purinergic neurotransmission is not completely understood. Ecto-ATPase (EC 3.6.1.3), the presence of which has been shown in a wide range of tissues, is one of the enzymes that could contribute to inactivation of external ATP at P_2-purinoceptors (see Ziganshin *et al.*, 1994). Inhibition of ecto-ATPase activity would be very useful for clarifying the distribution of and relationship between P_1(adenosine)- and P_2(ATP)-purinoceptors, as well as for potentiation of P_2-purinoceptor-mediated responses. Several compounds have been described as ecto-ATPase inhibitors (Smolen & Weissmann, 1978; Medzihradsky *et al.*, 1980; Zhao & Dhalla, 1989). However, only few of them have been examined for their ability to potentiate responses to ATP. Hourani & Chown (1989) tested some compounds on the guinea-pig urinary bladder and have shown that although suramin significantly inhibits ecto-nucleotidase activity, in their experiments it did not clearly change purinergic responses. Suramin has diverse biological activities (Voogd *et al.*, 1993) and is currently widely used as an antagonist of peripheral P_2-purinoceptors. It has been suggested that ATPases and P_2-purinoceptors have very similar ATP-binding domains at which suramin also binds, to cause inhibition of either ATP degradation or purinergic neurotransmission (Hoyle *et al.*, 1990), yet clear evidence for this is lacking.

Cyclopiazonic acid (CPA) has been described as a selective inhibitor of Ca^{2+}-ATPase in the sarcoplasmic reticulum of skeletal and smooth muscles (Kurebayashi & Ogawa, 1991; Imaizumi *et al.*, 1992). The compound is widely used as a pharmacological tool for investigating the role and turnover of intracellular Ca^{2+} (Schilling *et al.*, 1992; Uyama *et al.*, 1992; 1993). In the present study we investigated the effect of CPA on contractile responses of guinea-pig urinary bladder and vas deferens, and since we found potentiation of purinergic responses, we also examined the specificity of this potentiation and its ability to affect ecto-ATPase activity in these tissues.

Methods

Organ bath experiments

Male Dunkin Hartley guinea-pigs (250–400 g) were killed by a blow to the head and exsanguination. The urinary bladder and vasa deferentia were removed and longitudinal strips, approximately 2 mm by 10 mm, were prepared. The strips were suspended vertically in 10 ml organ baths for isometric recording of mechanical activity. An initial load of 1 g was applied to the strips which were then allowed to equilibrate

[1] Author for correspondence.

for at least 60 min. EFS was applied via two plantinum-wire rings 2.5 mm in diameter, 10 mm apart, through which the strip was threaded. The modified Krebs solution for these experiments had the following composition (mM): NaCl 133, KCl 4.7, $NaHCO_3$ 16.4, $MgSO_4$ 0.6, NaH_2PO_4 0.8, $CaCl_2$ 2.5 and glucose 7.7, and was gassed with 95% O_2/5% CO_2 (pH 7.3–7.4) and maintained at 36 ± 1°C. Contractions were recorded with a Grass FT0C3 force-displacement transducer and displayed on a Grass 79D ink-writing oscillograph. EFS was provided by a Grass S9 stimulator and applied at a given frequency (4–16 Hz) with a pulse width of 0.5 ms and supramaximal voltage, until a maximum contraction had been reached. ATP (100 μM), α,β-meATP (1 μM), carbachol (0.5 μM), histamine (30 μM), NA (100 μM) or KCl (30 mM) were added directly to the organ bath and washed out after a maximum contraction had been reached. Intervals of a least 30 min, with a wash every 10 min, were allowed after application of α,β-meATP in order to avoid desensitization, otherwise at least 10 min were allowed for washout. Responses to EFS and to agonists were examined in preparations before and after incubation with CPA at a concentration of 10 μM for at least 20 min. Since CPA was dissolved in dimethylsulphoxide (DMSO), control experiments were carried out to test the effect of the vehicle. In time-control preparations, which were carried out in parallel, but without incubation with CPA or vehicle, there were no significant difference between the first and second responses of tissues to EFS or to any agonists. All contractile responses were calculated as a percentage of the response evoked by EFS at a frequency of 16 Hz (at which the largest contraction was obtained) before incubation with any drug. Frequency-response relationships for EPS and the effects of two or three different agonists were obtained on each preparation.

Guinea-pig ventral taenia coli were dissected free and strips approximately 10 mm were prepared. Strips were suspended in 10 ml organ-baths containing Krebs solution. Tissues were allowed to equilibrate for at least 60 min after preloading initially with 1 g. A standard tone was induced with carbachol (0.05 μM) and when the contraction reached a plateau ATP (0.01–100 μM) was applied in a randomized manner at intervals of 10 min. The tissue was washed several times after the relaxation due to ATP had reached its maximum. After the first concentration-response relationship to ATP had been obtained, the tissue was incubated with CPA (1 or 10 μM) for at least 20 min and a second concentration-response relationship was constructed.

ATPase assay

The assay was carried out at 36 ± 1°C in buffer containing 10 mM 4-(2-hydroxyethyl)-1-piperazine-ethanesulphonic acid (HEPES), 135 mM NaCl, 5 mM KCl, 2 mM $CaCl_2$, 2 mM $MgCl_2$ and 10 mM glucose, pH 7.4. Smooth muscle preparations of the guinea-pig urinary bladder and vas deferens were prepared as for organ bath experiments. Single pieces of tissue (2–3 mg) were placed in 24-well cell culture dishes in 300 μl buffer and were pre-washed for 15–20 min. The pre-wash buffer was changed for 250 μl buffer containing 100 μM ATP and the tissues were incubated for 30 min and shaken continuously. Incubation was terminated by removing the buffer and adding it to 0.9 ml of a 2.5% (w/v) solution of sodium dodecyl sulphate (SDS) for inorganic phosphate assay. Tissues were again washed with buffer for 10–15 min and then incubated with 250 μl buffer containing 100 μM ATP and the compound tested (CPA, ouabain, oligomycin or sodium azide) for 30 min. When substrate specificity was tested, after the first incubation with ATP, the same tissue was incubated with 100 μM UTP, ADP, AMP, α,β-meATP or β,γ-methylene ATP. The buffer was again collected in SDS. For the inorganic phosphate assay, 1 ml of 1.25% (w/v) ammonium molybdate solution in 2 M HCl and 0.1 ml of 16% (w/v) Fiske and SubbaRow reducing agent (Sigma) were added to the samples. The solutions were transferred to cuvettes and left for 30 min at room temperature to develop colour. The inorganic phosphate was measured spectrophotometrically at 700 nm in a Bechman Du-65 Spectrophotometer. KH_2PO_4 was used as a phosphate standard. The amount of phosphate produced in the presence of CPA or other drugs (second incubation) was calculated as a percentage of that without any drugs (first incubation). All the results were expressed as mean ± s.e.mean of at least three experiments performed in quadruplicate. The kinetic constants (V_{max} and K_m) for enzymes were derived by Lineweaver-Burk plots at concentrations of ATP of 0.03–3 mM.

ATP release

Guinea-pig vasa deferentia were prepared as for organ bath experiments and suspended vertically between two platinum-wire rings 2.5 mm in diameter, 10 mm apart, through which the strips were threaded. The lower end was fixed to a rigid support and the upper end was attached to a Grass FT03C force-displacement transducer, and the tissue was given an initial load of 1 g. The tissues were continuously superfused at a rate of 1.5 ml min^{-1} with Krebs solution. The solution was gassed with 95% O_2 and 5% CO_2 and maintained at 36 ± 1°C. Tissues were allowed to equilibrate for at least 60 min before any procedure. The strips were stimulated for periods of 60 s with a pulse width of 0.5 ms at 8 Hz and 20 V and 30 min intervals. Superfusates were collected for 60 s before, during and for 60 s after stimulation and kept in liquid nitrogen for later ATP measurement. The second stimulation and collection of samples were made after 30 min of either perfusing the tissue with Krebs solution containing 10 μM CPA (experiment), 0.1% DMSO (vehicle control) or with just normal Krebs solution (control). The amount of ATP was measured in a Packard picolite detector by using luciferin-luciferase (Kirkpatrick & Burnstock, 1987). The results were expressed as pmol ATP released from 1 g wet blotted tissue for 1 min. We also calculated the S2/S1 ratio for each group, where S1 is the amount of ATP evoked by first stimulation of preparation, and S2 is the amount of ATP evoked by stimulation of the same preparation in the presence of CPA or vehicle.

Analysis of results

Means were compared by Student's paired and unpaired *t* tests. A probability of less than or equal to 0.05 was considered as significant. Data are presented as mean ± s.e.mean (*n*).

When concentration-response curves for ATP in taenia coli were constructed, the pD_2 values (negative logarithm of EC_{50}) in the absence and presence of CPA were calculated and were then used in Student's paired *t* tests.

Drugs

Cyclopiazonic acid, adenosine 5'-triphosphate disodium salt (ATP), uridine 5'-triphosphate sodium salt (UTP), adenosine 5'-diphosphate sodium salt (ADP), adenosine 5'-monophosphate sodium salt (AMP), α,β-meATP lithium salt, β,γ-methylene ATP sodium salt, ouabain, oligomycin, (-)-arterenol (noradrenaline), histamine dihydrochloride, carbamylcholine chloride (carbachol) and luciferin-luciferase were obtained from Sigma; sodium azide was supplied by Fisons (U.K.). Luciferin-luciferase was dissolved in sterile distilled water for a final concentration of 3 mg ml^{-1}. CPA was dissoved in DMSO for a stock solution of 10 mM. Oligomycin was dissolved in ethanol for a stock solution of 5 mg ml^{-1}. Ouabain was dissolved in buffer for a stock solution of 1 mM and used on the same day. Other compounds were dissolved in distilled water.

Results

Organ bath experiments

EFS (4–16 Hz) caused frequency-dependent contractions of urinary bladder detrusor muscle with the largest response at a frequency of 16 Hz (100%) and 37.6 ± 4.8% (5) and 72.4 ± 3.4% (5) at frequencies of 4 and 8 Hz respectively, relative to the response at 16 Hz. After 20 min incubation of tissue with CPA (10 μM) there was a significant potentiation of responses evoked by EFS at all frequencies. The responses increased to 81.4 ± 3.1% (5), 115.4 ± 2.4% (5) and 124.6 ± 2.7% (5), for 4,8 and 16 Hz respectively (in each case $P<0.01$, paired t test). CPA also significantly potentiated contractions evoked by ATP (100 μM), α,β-meATP (1 μM), carbachol (0.5 μM), histamine (30 μM) and KCl (30 mM) (Figures 1 and 2). CPA evoked spontaneous contractions or increased their amplitude in most preparations of urinary bladder. In the guinea-pig vas deferens, CPA at a concentration of 10 μM significantly potentiated contractions evoked either by EFS or exogenous ATP (100 μM), α,β-meATP (1 μM), NA (100 μM) and KCl (30 mM) (Figures 1 and 3). In both tissues, DMSO at a concentration of 0.1% (vehicle concentration) in the organ-bath had no effect on contractions evoked either by EFS or by any of the agonists.

In the guinea-pig taenia coli precontracted with carbachol (0.05 μM) ATP (0.01–100 μM) caused concentration-dependent relaxation with a pD_2 valve (negative log EC_{50}) of 6.11 ± 0.15 (4). CPA at a concentration of 10 μM greatly stimulated spontaneous activity of the taenea and also caused spontaneous relaxation of carbachol-precontracted tissue that did not permit proper concentration-response relationships to ATP to be constructed. At a concentration of 1 μM CPA had no effect on the ATP-induced relaxation of taenia coli, the pD_2 being 6.12 ± 0.18 (4).

ATPase assay

The rate of ATP (100 μM) hydrolysis as determined by the production of inorganic phosphate was linear for at least 60 min in both the guinea-pig urinary bladder and vas deferens. The amount of ATP cleft by the tissue during incubation (30 min) was about 2% of that added, thus indicating that there was no lack of the substrate for the reaction. The measured enzyme activity was estimated to have V_{max} and K_m values of 0.98 nmol P_i 30 min^{-1} mg^{-1} wet tissue and 881 μM ATP in the urinary bladder, and 0.75 nmol

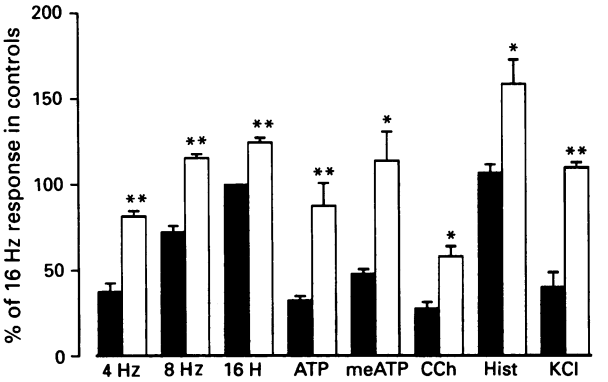


Figure 2 Contractions of guinea-pig isolated urinary bladder evoked by electrical field stimulation at different frequencies and exogenously applied ATP (0.1 mM), α,β-methylene ATP (meATP, 1 μM), carbachol (CCh, 0.05 μM), histamine (Hist, 30 μM) and KCl (30 mM) before (solid columns) and after incubation (for at least 20 min) with 10 μM cyclopiazonic acid (open columns). *$P<0.05$, **$P<0.01$, paired t test ($n = 4–6$).

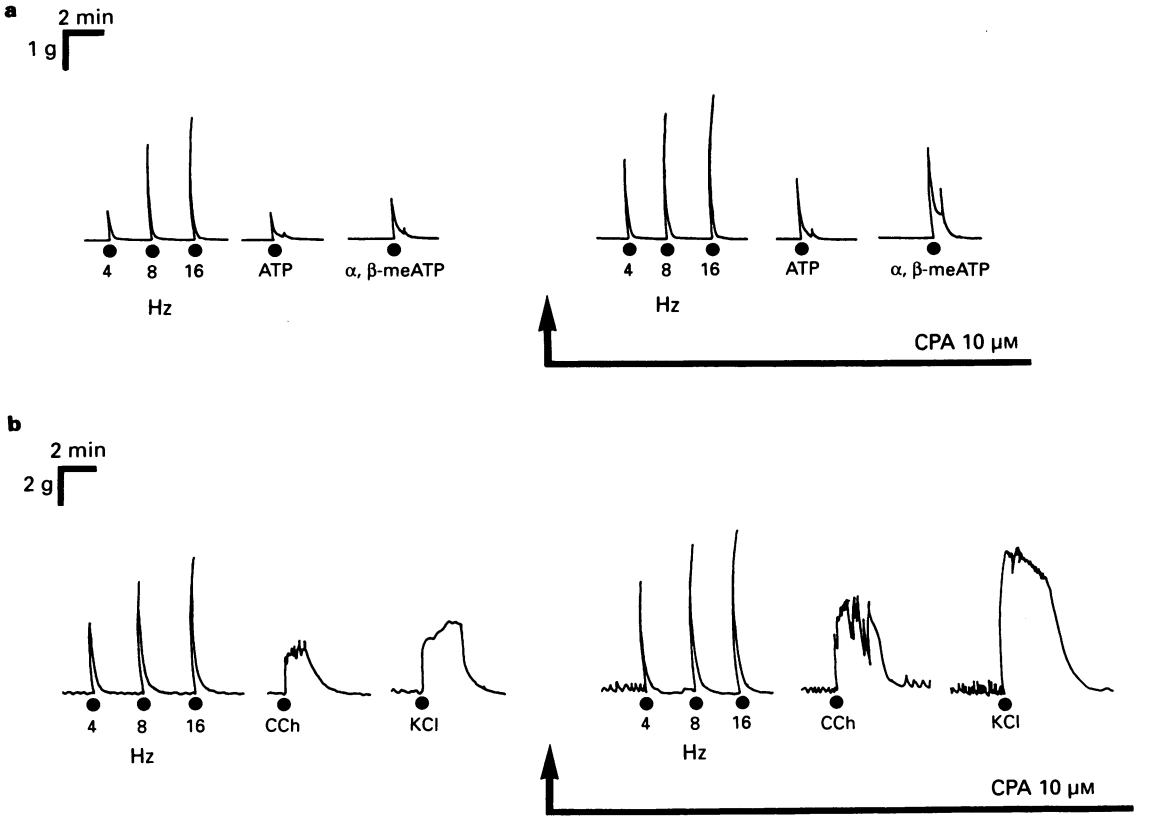


Figure 1 Original traces of contractions of guinea-pig isolated vas deferens (a) and urinary bladder (b) recorded before and after incubation (for at least 20 min) with 10 μM cyclopiazonic acid (CPA). Electrical field stimulation and administration of agonists are indicated by dots. Concentrations of agonist were: 0.1 mM ATP, 1 μM α,β-meATP, 0.05 μM carbachol (CCh) and 30 mM KCl. Note the potentiation of spontaneous activity in urinary bladder by CPA.

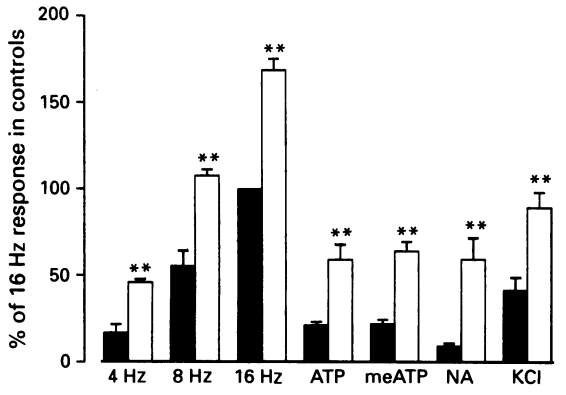


Figure 3 Contractions of guinea-pig isolated vas deferens evoked by electrical field stimulation at different frequencies and exogenously applied ATP (0.1 mM), α,β-methylene ATP (meATP, 1 μM), noradrenaline (NA, 0.1 mM) and KCl (30 mM) before (solid columns) and after incubation (for at least 20 min) with 10 μM cyclopiazonic acid (open columns). $^{**}P<0.01$, paired t test ($n=4-6$).

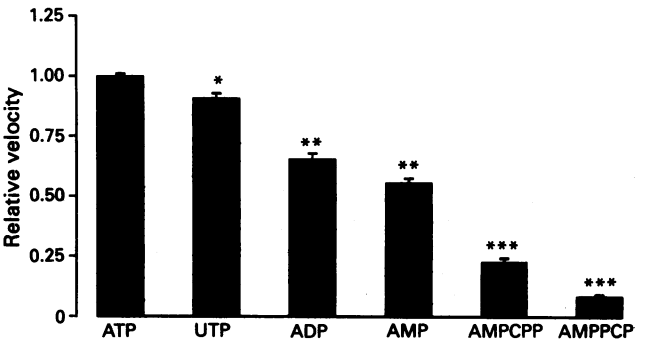


Figure 4 Comparison of relative velocities of guinea-pig urinary bladder ecto-ATPase when different substrates were used. ATP, UTP, ADP, AMP, α,β-methylene ATP (AMPCPP) and β,γ-methylene ATP (AMPPCP) were added at a final concentration of 100 μM, and P_i production was measured. $^{*}P<0.05$; $^{**}P<0.01$; $^{***}P<0.001$ against ATP group, paired t test ($n=12$).

P_i30 min^{-1} mg^{-1} wet tissue and 914 μM ATP in the vas deferens, respectively. In the guinea-pig urinary bladder, the rate of degradation of different nucleotides, used as substrates, at a concentration of 100 μM was ATP> UTP> ADP ≥ AMP> α,β-meATP ≥ β,γ-methylene ATP demonstrating that ATP was the preferential substrate (Figure 4). Similar results were obtained in the vas deferens (not shown).

At a concentration of 100 μM ATP, the actual rate of ATPase activity was 133.4 ± 12.2 (12) pmol P_i30 min^{-1} mg^{-1} wet tissue in the urinary bladder, and 164.7 ± 5.6 (18) pmol P_i30 min^{-1} mg^{-1} wet tissue in the vas deferens: these were taken as 100%. When ATP was replaced by β,γ-methylene ATP in the incubation medium the inorganic phosphate formation was 8.5 ± 0.8% (12) in urinary bladder and 0.8 ± 0.5% (12) in vas deferens of that when ATP was the substrate. When 100 μM α,β-meATP was added to the incubation medium as a substrate instead of ATP, the amount of inorganic phosphate produced was 23.0 ± 1.5% (12) in urinary bladder and 21.4 ± 3.4% (12) in vas deferens of that produced by the same concentration of ATP.

The activity measured was not due to secreted enzymes or release of intracellular enzymes, since the hydrolysis of ATP in buffer pre-incubated with tissue for 30 min and removed for ATPase assay was not more than 5% of the total basic activity. The spontaneous ATP breakdown when incubated in buffer without tissue for 30 min, as well as the amount of P_i released from the tissue during incubation time, was negligible.

Omission of Ca^{2+} alone from the incubation medium resulted in a 15% and 14% decrease of activity in the bladder and vas deferens, respectively. The absence of both Ca^{2+} and Mg^{2+} diminished ATP hydrolysis by 30% and 17% in urinary bladder and vas deferens respectively. When EDTA (1 mM) was added in Ca^{2+}- and Mg^{2+}-free buffer, the ATPase activity was 16.2 ± 1.3% (12) in the urinary bladder and 28.6 ± 1.4 (12) in the vas deferens, thus demonstrating that the activity being studied was due to a Ca^{2+}- and Mg^{2+}-dependent ATPase. Ouabain (1 mM), a specific inhibitor of transport Na^+, K^+-ATPase, and sodium azide (1 mM), an inhibitor of ATP-ADP diphosphohydrolase, and oligomycin (50 μg ml^{-1}), an inhibitor of mitochondrial ATPase, had no significant effect on ATP hydrolysis (not shown).

CPA (10 μM) caused significant inhibition of ATPase activity in both tissues. The enzyme activity was reduced to 82.2 ± 4.6% (12) in the urinary bladder and 76.1 ± 4.8% (12) in the vas deferens after incubation with CPA (in each case $P<0.05$, paired t test). DMSO (0.1%) had no significant effect on ATPase activity in either tissue.

ATP release

EFS stimulation of the guinea-pig vas deferens evoked ATP release about 1000 times greater than the spontaneous release of ATP (Table 1). In control experiments there was no statistically significant difference between the amount of ATP released during the first and second stimulation of the tissue. Superfusion of the tissue with Krebs solution containing 0.1% DMSO caused a significant decrease of ATP release evoked by EFS (Table 1). Addition of CPA (10 μM) to the perfusate did not affect the spontaneous release of ATP but caused a significant (based on absolute S2 values more than 15 fold) increase in EFS-evoked ATP release compared with the DMSO group (Table 1). The CPA-induced increase of ATP release was also detected when the samples were collected for 60 s after EFS.

Table 1 Effects of cyclopiazonic acid (CPA) on electrical field stimulation (EFS; 8 Hz, 0.5 ms, 20 V for 60 s) evoked release of ATP from guinea-pig vas deferens (pmol ATP min^{-1} g^{-1} wet tissue) in normal Krebs solution (control), after superfusion (30 min) with Krebs solution containing dimethylsulphoxide (DMSO, 0.1%; vehicle for CPA) and after superfusion (30 min) with Krebs solution containing CPA (10 μM)

	Before EFS	*During EFS*	*After EFS*
1st stimulation (S1)	0.0026 ± 0.0005 (27)	6.66 ± 1.39 (20)	0.0726 ± 0.0178 (23)
Control (S2)	0.0065 ± 0.0027 (8)	4.09 ± 1.34 (8)	0.0294 ± 0.0066 (7)
S2/S1		0.57 ± 0.16 (8)	
DMSO 0.1% (S2)	0.0015 ± 0.0007 (7)	2.16 ± 0.77 (6)*	0.0423 ± 0.0225 (7)
S2/S1		0.11 ± 0.05 (6)*	
CPA 10 μM (S2)	0.0040 ± 0.0020 (6)	35.19 ± 4.83 (6)**##	0.0225 ± 0.0197 (6)**#
S2/S1		18.11 ± 5.93 (6)*#	

$^{*}P<0.05$, $^{**}P<0.01$ against control; $\#P<0.05$, $\#\#P<0.01$ against DMSO group, paired t test.

Discussion

In the present study we have established that CPA potentiated contractions of guinea-pig urinary bladder and vas deferens evoked by all the stimuli employed, including EFS, different receptor agonists and the non-receptor stimulating agent, KCl. Thus, the inhibition of ecto-ATPase and the apparent increase of ATP release by CPA that we have also shown here, can hardly have contributed to the potentiation of P_{2X}-purinoceptor-mediated responses in these tissues. It is most likely that the CPA-induced potentiation of smooth muscle contractility is due to inhibition of the Ca^{2+}-dependent K^+-current (Suzuki *et al.*, 1992) and thus increased excitability of smooth muscle cells (Uyama *et al.*, 1993).

Although ecto-ATPase is widely expressed in different tissues and organs (Ziganshin *et al.*, 1994), there are as yet no clear indications of a physiological role for this enzyme, and the possibility exists that it is involved in purinergic neurotransmission as a transmitter-metabolizing enzyme (Pearson, 1985; Dubyak & El-Moatassim, 1993; Meghji, 1993). Welford *et al.*, (1986, 1987), testing this idea, have shown that the potency of many analogues of ATP is correlated with their resistance to hydrolysis in guinea-pig urinary bladder (P_{2X}-purinoceptors), but not in guinea-pig taenia coli (P_{2Y}-purinoceptors). Thus, at least in some tissues, inhibitors of ecto-ATPase should potentiate and/or prolong the effects of endogenously released or exogenously applied ATP.

In this study we have characterized ecto-ATPases in the guinea-pig urinary bladder and vas deferens, tissues that are known to possess P_{2X}-purinoceptors. Firstly, we have proved that the enzymes we dealt with were actually ecto-ATPases. The rank order of preferential substrates (where ATP appeared to be the favourite in both tissues), the dependence of the enzymes on Ca^{2+} and Mg^{2+}, the insensitivity of the enzymes to ouabain, oligomycin and sodium azide, inhibitors of intracellular ATPases, and the lack of enzyme activity in buffer preincubated with tissues, are all characteristics in agreement with known requirements for ecto-ATPases (Pearson, 1985), and indicate that the activity measured is that of ecto-ATPase.

In the presence of extracellular ATP, the reaction responsible for the increase of P_i in the medium by ecto-ATPase is $ATP \rightarrow ADP + P_i$. Although, as we have shown in this study, ADP (and AMP) can be cleaved by the enzyme, the amount of P_i coming from the degradation of these nucleotides in the presence of ATP cannot contribute significantly to the amount of P_i detected, since: (1) we have shown that ATP is a preferential substrate for the enzyme we tested; (2) 1–2 μM ADP produced from 100 μM ATP during the incubation time (less than 2% of added ATP was cleaved) cannot compete with the remaining amount (98–99 μM) of ATP for enzyme; (3) the theoretically possible degradation of AMP by 5′-nucleotidase (yielding P_i) would not have occurred in our system because of the known ability of ATP to inhibit this enzyme (Newby *et al.*, 1975; Stefanovic *et al.*, 1976; Pearson, 1985).

In the present study we found that CPA significantly inhibited the ecto-ATPase activity in both guinea-pig urinary bladder and vas deferens, and also potentiated contractions of these tissues mediated via P_{2X}-purinoceptors. However, it is unlikely that potentiation of purinergic responses by CPA is due to inhibition of ecto-ATPase activity, since CPA also potentiated contractions to carbachol, NA, histamine and KCl, as well as to EFS. Thus, the potentiation of contractility by CPA was non-specific. Similarly, it is unlikely that 24% of inhibition of enzyme activity was responsible for more than 15 fold increases of EFS-evoked release of ATP. It is more likely to be due to inhibition of the Ca^{2+}-dependent K^+-current (Suzuki *et al.*, 1992) causing prolongation of the action potential, leading to increased amount of neurotransmitter (ATP) being released. CPA at a concentration of 10 μM potentiated spontaneous contractions of urinary bladder and taenia coli. In the latter tissue it also caused spontaneous relaxation after precontraction by carbachol, which did not allow us to construct concentration-response relationships for ATP. CPA-evoked spontaneous contractions were not detected at a concentration of 1 μM. At this concentration CPA had no effect on ATP-induced relaxation of precontracted guinea-pig taenia coli, indicating that it did not affect P_{2Y}-mediated responses.

CPA mobilizes intracellular Ca^{2+} by inhibiting sarcoplasmic reticulum Ca^{2+}-ATPase (Kurebayashi & Ogawa, 1991; Imaizumi *et al.*, 1992). However, there are contradictions in the literature about the actual effect of CPA on contractility of smooth muscle cells. CPA reduces or abolishes contractions to caffeine in longitudinal smooth muscle strips from the guinea-pig ileum (Uyama *et al.*, 1992; 1993), in the rat aorta and in small mesenteric arteries (Shima & Blaustein, 1992). In Ca^{2+}-free solution, CPA concentration-dependently inhibits contractions to phenylephrine in the rabbit and rat aorta (Luo *et al.*, 1993; Low *et al.*, 1993), but in the presence of Ca^{2+}, CPA itself induces contraction of rat aorta (Low *et al.*, 1993), which is concentration-dependent, and less in endothelium-intact preparations than in endothelium-denuded aorta (Zheng *et al.*, 1993). Moreover, CPA potentiates contractions to KCl and 5-hydroxytryptamine (5-HT) in rat small mesenteric artery preparations, but in the rat aorta CPA has no consistent effect on contractions to 5-HT (Shima & Blaustein, 1992). Further, CPA causes endothelium-dependent relaxation of phenylephrine-precontracted rat aorta (Zheng *et al.*, 1993) probably via stimulation of synthesis of nitric oxide (Moritoki *et al.*, 1994), while in the rabbit aorta it inhibits relaxation by nitroglycerin and atrial natriuretic factor (Luo *et al.*, 1993). In the present study, the contractile agents, whose action were potentiated by CPA, included ATP, α,β-meATP, carbachol, NA, histamine and KCl. Contractions of the urinary bladder and vas deferens evoked by EFS of intramural nerves were also potentiated by CPA. Thus, in visceral smooth muscle preparations, CPA usually causes potentiation of contractions, which can be due to selectively suppressing Ca^{2+}-dependent K^+ current (Suzuki *et al.*, 1992) as well as increasing Ca^{2+}-influx through voltage-dependent Ca^{2+} channels (Uyama *et al.*, 1993). The CPA-induced increase of smooth muscle excitability appears to be similar to that of a K^+-blocker, 4-aminopyridine (Johns *et al.*, 1976; Hara *et al.*, 1980).

It is difficult to evaluate exactly the role of inhibition of ecto-ATPase by CPA in the potentiation of contractions mediated via P_{2X}-purinoceptors. It appears, however, that the main effect of CPA is at a level distal to receptor-occupancy since it potentiated the contractile actions of all the agents used, whether receptor-mediated or not.

The authors thank the Wellcome Trust (A.U.Z.) and the British Heart Foundation for financial support. The authors would also like to thank Dr P. Meghji for assistance with the biochemistry.

References

BURNSTOCK, G. (1993). Physiological and pathological roles of purines: An update. *Drug Dev. Res.*, **28**, 195–206.

DUBYAK, G.R. & EL-MOATASSIM, C. (1993). Signal transduction via P_2-purinoceptors for extracellular ATP and other nucleotides. *Am J. Pysiol.*, **265**, C577-C606.

HARA, Y., KITAMURA, K. & KURIYAMA, H. (1980). Actions of 4-aminopyridine on vascular smooth muscle tissues of the guinea-pig. *Br. J. Pharmacol.*, **68**, 99–106.

HOURANI, S.M.O. & CHOWN, J.A. (1989). The effects of some possible inhibitors of ectonucleotides on the breakdown and pharmacological effects of ATP in the guinea-pig urinary bladder. *Gen. Pharmacol.*, **20**, 413–416.

HOYLE, C.H.V. (1992). Transmission: Purines. In: *Autonomic Neuroeffector Mechanisms*. ed. Burnstock, G. & Hoyle, C.H.V. pp. 367–407. Chur: Harwood Academic Publishers.

HOYLE, C.H.V., KNIGHT, G.E. & BURNSTOCK, G. (1990). Suramin antagonizes responses to P_2-purinoceptor agonists and purinergic nerve stimulation in the urinary bladder and taenia coli. *Br. J. Pharmacol.*, **99**, 617–621.

IMAIZUMI, Y., SUZUKI, M., UYAMA, Y., MURAKI, K. & WATANABE, M. (1992). Effects of cyclopiazonic acid, a novel Ca^{2+}-ATPase inhibitor, on contractile response and an outward current in smooth muscle. *Jpn. J. Pharmacol.*, **58**, Suppl. 2, 401P.

JOHNS, A., GOLKO, D.S., LAUZON, P.A. & PATON, D.M. (1976). The potentiating effects of 4-aminopyridine on adrenergic transmission in the rabbit vas deferens. *Br. J. Pharmacol.*, **38**, 71–78.

KIRKPATRICK, K. & BURNSTOCK, G. (1987). Sympathetic nerve-mediated release of ATP from the guinea-pig vas deferens is unaffected by reserpine. *Eur. J. Pharmacol.*, **138**, 207–214.

KUREBAYASHI, N. & OGAWA, Y. (1991). Discrimination of Ca^{2+}-ATPase activity of the sarcoplasmic reticulum from actomyosin-type ATPase activity of myofibrils in skidded mammalian skeletal muscle fibres: distinct effects of cyclopiazonic acid on the two ATPase activities. *J. Muscle. Res. Cell Motil.*, **12**, 355–365.

LOW, A.M., KWAN, C.Y. & DANIEL, E.F. (1993). Functional alterations in the aorta of the spontaneously hypertensive rat: pharmacological assessment with cyclopiazonic acid. *Pharmacology*, **47**, 50–60.

LUO, D.-L., NAKAZAWA, M., ISHIBASHI, T., KATO, K. & IMAI, S. (1993). Putative, selective inhibitors of sarcoplasmic reticulum Ca^{++}-pump ATPase inhibit relaxation by nitroglycerin and atrial natriuretic factor of the rabbit aorta contracted by phenylephrine. *J. Pharmacol. Exp. Ther.*, **265**, 1187–1192.

MEDZIHRADSKY, F., CULLEN, E.I., LIN, H.L. & BOLE, G.G. (1980). Drug-sensitive ecto-ATPase in human leukocytes. *Biochem. Pharmacol.*, **29**, 2285–2290.

MEGHJI, P. (1993). Storage, release, uptake, and inactivation of purines. *Drug Dev. Res.*, **28**, 214–219.

MORITOKI, H., HISAYAMA, T., TAKEUCHI, S. KONDOH, W. & IMAGAWA, M. (1994). Relaxation of rat thoracic aorta induced by the Ca^{2+}-ATPase inhibitor, cyclopiazonic acid, possibly through nitric oxide formation. *Br. J. Pharmacol.*, **111**, 655–662.

NEWBY, A.C., LUZIO, J.P. & HALES, C.N. (1975). The properties and extracellular location of 5'-nucleotidase of the rat fat-cell plasma membrane. *Biochem. J.*, **146**, 625–633.

PEARSON, J.D. (1985). Ectonucleotidases: measurement of activities and use of inhibitors. In *Methods Used in Adenosine Research. Methods in Pharmacology*. ed. Paton, D.M. Vol. 6, pp. 83–107. New York: Plenum Press.

SCHILLING, W.P., CABELLO, O.A. & RAJAN, L. (1992). Depletion of the inositol 1,4,5-triphosphate-sensitive intracellular Ca^{2+} store in vascular endothelial cells activates the agonist-sensitive Ca^{2+}-influx pathway. *Biochem. J.*, **284 (Pt 2)**, 521–530.

SHIMA, H. & BLAUSTEIN, P. (1992). Modulation of evoked contractions in rat arteries by ryanodine, thapsigargin, and cyclopiazonic acid. *Circ. Res.*, **70**, 968–977.

SMOLEN, J.E. & WEISSMANN, G. (1978). Mg^{2+}-ATPase as a membrane ecto-enzyme of human granulocytes. Inhibitors, activators and response to phagocytosis. *Biochem. Biophys. Acta.*, **512**, 525–538.

STEFANOVIC, V., MANDEL, P. & ROSENBERG, A. (1976). Ecto-5'-nucleotidase of intact cultured C6 rat glioma cells. *J. Biol. Chem.*, **251**, 3900–3905.

SUZUKI, M., MURAKI, K., IMAIZUMI, Y. & WATANABE, M. (1992). Cyclopiazonic acid, an inhibitor of the sarcoplasmic reticulum Ca^{2+}-pump, reduces Ca^{2+}-dependent K^+ currents in guinea-pig smooth muscle cells. *Br. J. Pharmacol.*, **107**, 134–140.

UYAMA, Y., IMAIZUMI, Y. & WATANABE, M. (1992). Effects of cyclopiazonic acid, a novel Ca^{2+}-ATPase inhibitor, on contractile responses in skinned ileal smooth muscle. *Br. J. Pharmacol.*, **106**, 208–214.

UYAMA, Y., IMAIZUMI, Y. & WATANABE, M. (1993). Cyclopiazonic acid, an inhibitor of Ca^{2+}-ATPase in sarcoplasmic reticulum, increases excitability in ileal smooth muscle. *Br. J. Pharmacol.*, **110**, 565–572.

VOOGD, T.E., VANSTERKENBURG, E.L.M., WILTING, J. & JANSSEN, L.H.M. (1993). Recent research on the biological activity of suramin. *Pharmacol. Rev.*, **45**, 177–203.

WELFORD, L.A., CUSACK, N.J. & HOURANI, M.O. (1986). ATP analogues and the guinea-pig taenia coli: a comparison of the structure-activity relationships of ectonucleotidases with those of the P_2-purinoceptor. *Eur. J. Pharmacol.*, **129**, 217–224.

WELFORD, L.A., CUSACK, N.J. & HOURANI, M.O. (1987). The structure-activity relationships of ectonucleotidases and of excitatory P_2-purinoceptors: evidence that dephosphorylation of ATP analogues reduces pharmacological potency. *Eur. J. Pharmacol.*, **141**, 123–130.

ZHAO, D. & DHALLA, N.S. (1989). Influence of gramicidin S on cardiac membrane Ca^{2+}/Mg^{2+}ATPase activities and contractile force development. *Can. J. Physiol. Pharmacol.*, **67**, 546–552.

ZHENG, Z.F., GUAN, Y.Y. & KWAN, C.Y. (1993). Cyclopiazonic acid causes endothelium-dependent relaxation in rat aorta. *Chung. Kuo. Yao. Li. Hsueh. Poa.*, **14**, 21–26.

ZIGANSHIN, A.U., HOYLE, C.H.V. & BURNSTOCK, G. (1994). Ecto-enzymes and metabolism of extracellular ATP. *Drug Dev. Res.*, (in press).

(Received June 8, 1994
Revised July 8, 1994
Accepted July 14, 1994)

Br. J. Pharmacol. (1994), **113**, 675–680 © Macmillan Press Ltd, 1994

Modulation by endogenous prostanoids of the vasoconstrictor activity of endothelin-1 in the canine isolated, perfused spleen

[1]Dora M. Grassi-Kassisse, Edson Antunes, *Peter G. Withrington & Gilberto de Nucci

Department of Pharmacology, Faculty of Medical Sciences, UNICAMP, PO Box 6111, 13084-970, Campinas (SP), Brazil and *Faculty of Basic Medical Sciences, Queen Mary & Westfield College, Mile End Road, London E1 4NS

1 Endothelin-1 (ET-1, 0.4–200 pmol) was injected into the arterial circuit of the isolated perfused spleen of the dog in which splenic arterial perfusion pressure and spleen weight were recorded continuously.

2 Serial collection was made of splenic venous effluent before and after intra-arterial injection of ET-1 and assayed by direct radioimmunoassay for prostaglandin E_2 (PGE_2), 6-oxo-$PGF_{1\alpha}$ and thromboxane B_2 (TXB_2).

3 ET-1 caused graded arterial vasoconstriction of prolonged duration with small reductions in spleen weight at higher doses.

4 ET-1 cause a dose-related release of PGE_2, 6-oxo-$PGF_{1\alpha}$ and TXB_2 into the splenic venous effluent. The mean peak increase above the basal levels following 200 pmol of ET-1 was 800% for PGE_2, 233% for 6-oxo-$PGF_{1\alpha}$ and 205% for TXB_2.

5 Intra-arterial infusion of indomethacin significantly reduced the basal release of all three eicosanoids and significantly elevated the basal splenic vascular resistance. The release of all three eicosanoids in response to ET-1 and adrenaline (Ad) was significantly reduced by indomethacin and the accompanying increases in the splenic arterial vascular resistance were significantly potentiated at low doses of ET-1. The splenic arterial vascular responses to Ad were unchanged by indomethacin infusion.

6 These results indicate that the release of eicosanoids may modulate the splenic vascular responses to ET-1.

Keywords: Splenic vasoconstriction in dog; PGE_2; PGI_2; TXB_2; indomethacin; prostaglandins; eicosanoids; endothelin

Introduction

The 21 amino acid peptide, endothelin-1 (ET-1), was initially isolated from porcine cultured aortic endothelial cells and shown to possess potent vasoconstrictor potency of prolonged duration (Yanagisawa *et al.*, 1988). ET-1 was shown also to cause the release of the vasoactive prostanoids, prostaglandin E_2 (PGE_2), prostacyclin (PGI_2) and thromboxane A_2 (TXA_2) into the venous effluent of the rabbit isolated spleen (Rae *et al.*, 1989). It was proposed, therefore, that the two vasodilator prostanoids, PGE_2 and PGI_2, could act to limit the size and duration of vasoconstrictor responses to administered or released ET-1. The present experiments, in the canine isolated perfused spleen, were designed to address several questions related to this proposal. Firstly, to define quantitatively the relationship between the molar dose of ET-1 and both the absolute and relative amounts of prostanoids released into the splenic venous effluent. Secondly, to determine whether the cyclo-oxygenase inhibitor, indomethacin, significantly reduces the release of prostanoids from the spleen and thirdly, as a consequence of the foregoing, to establish whether basal splenic vascular smooth muscle tone and the splenic vascular responses to ET-1 were altered. Some of these results have been published in a preliminary form (Grassi-Kassisse *et al.*, 1993).

Methods

Spleen perfusion

The experiments were performed on ten dogs (mean weight 13.1 ± 1.4 kg) anaesthetized either with fentanyl (50–100 μg kg^{-1}, i.v.) and midazolam (0.3–1.0 mg kg^{-1}, i.m.) or pentobarbitone sodium (Sagatal, 30 mg kg^{-1}, i.v.) The surgical procedures involved in isolation of the spleen have been described in detail elsewhere (Corder *et al.*, 1987). Briefly, the spleen was isolated from all connections with the stomach, pancreas and omentum and, after ligation of the splenic artery and vein, removed from the donor. Heparin (5000 iu) was administered immediately prior to removal of the spleen. The splenic artery and vein were then cannulated and the spleen perfused via the arterial system with Krebs solution gassed with 95% O_2 and 5% CO_2 at 37°C. The arterial inflow was adjusted by means of a Watson Marlow pump to provide a perfusion pressure of about 40–60 mmHg and once this flow was established, it remained constant throughout the experiment. Splenic arterial perfusion pressure (SAPP) was measured with a strain gauge transducer (model PRC 21/3, Ugo Basile) incorporated into the splenic arterial line. Splenic arterial vascular resistance (SAVR) was calculated as the mean SAPP/mean splenic arterial flow. Changes in spleen volume were assessed indirectly by continuous weighing of the spleen on a digital balance with visual readings being taken at frequent set intervals (Green *et al.*, 1960; Boatman & Brody, 1964; Moerman *et al.*, 1969). At the end of each experiment the spleen was weighed.

Radioimmunoassay of eicosanoids

The splenic venous effluent was collected for timed samples during the control period before selected ET-1 administrations and for a set sequence following this. Subsequent analysis of eicosanoid release was performed by direct radioimmunoassay of 6-oxo-$PGF_{1\alpha}$ (breakdown product of PGI_2), TXB_2 (breakdown product of TXA_2) and PGE_2 without prior extraction. The radioimmunoassay procedure and the specificity of the antisera employed have been described previously (Salmon, 1978).

[1] Author for correspondence.

Drugs

(±)-Adrenaline, indomethacin, 6-oxo-$PGF_{1\alpha}$, TXB_2 and PGE_2 were obtained from Sigma (St. Louis, U.S.A.). Endothelin-1 was obtained from the Peptide Institute (Osaka, Japan). 5,6,8,9,11,12,14,15 (n)-[^{3}H]-TXB_2 (specific activity 140 Ci mmol^{-1}), 5,6,8,11,12,14,15 (n)-[^{3}H]-PGE_2 (specific activity 160 Ci mmol^{-1}) and 6-oxo-5,6,8,9,11,14,15 (n)-[^{3}H]-$PGF_{1\alpha}$ (specific activity 150 Ci mmol^{-1}) were purchased from Amersham International (Amersham, Bucks). Antisera for 6-oxo-$PGF_{1\alpha}$, PGE_2 and TXB_2 were a generous gift from J. Salmon (Wellcome Laboratories, Kent). Sagatal and heparin were obtained from May & Baker (Dagenham, Essex) and Roche (São Paulo, Brazil), respectively. Fentanyl and midazolam were obtained from Janssen (São Paulo, Brazil).

Adrenaline, endothelin-1 and indomethacin were dissolved in Krebs solution prior to intra-arterial injection. The composition of the Krebs solution was (mM): NaCl 118, $NaHCO_3$ 25, KCl 4.7, KH_2PO_4 1.2, $MgSO_4$ 1.17, $CaCl_2$ 2.5, and glucose 5.6. Bolus injections were of 1.0 ml and were immediately washed in with 0.5 ml of Krebs solution to provide a total constant injectate of 1.5 ml.

Calculations and statistics

Eicosanoid release is expressed in two forms. Firstly, as peak increase expressed either as a percentage of the basal release or in absolute amounts (pmol ml^{-1}). Secondly, the total amount of a given eicosanoid released by an injection of ET-1 was calculated by plotting individual sample activity (pmol/sample) against real time and estimating the total release by calculating the area under the curve (AUC). This value (pmol) was corrected by subtracting the total basal release over the same period of collection. Individual ED_{50} values for ET-1 and adrenaline were calculated as the molar intra-arterial dose required to cause a 50% increase (vasoconstriction) in the basal splenic arterial vascular resistance. Geometric means were then calculated with 95% confidence limits (CL). Unless stated otherwise, the results are presented as the arithmetic means ± standard error of the mean (s.e.mean). Significance of data was analysed by analysis of variance (ANOVA) and Student's paired t test for which $P<0.05$ was considered to indicate a significant difference.

Results

Control values

The mean spleen weight was 78.2 ± 15.3 g representing 0.57 ± 0.08% of the body weight. The mean splenic arterial inflow was 33.3 ± 4.1 ml min^{-1} giving an initial mean splenic arterial perfusion pressure of 40.7 ± 2.2 mmHg. The mean calculated splenic arterial vascular resistance was 2.0 ± 0.5 mmHg ml^{-1} min.

Effects of adrenaline and endothelin-1 on splenic vascular and capsular smooth muscle

Adrenaline Adrenaline (Ad) was injected close arterially over the dose range 0.05–540 nmol in seven experiments and the results were used as a basis for comparison of the molar potency and duration of action with the splenic vascular and capsular smooth muscle responses to ET-1. The splenic arterial response to doses of Ad above threshold consisted of a dose-dependent increase in splenic arterial perfusion pressure of relatively short duration (Figure 1). The ED_{50} for Ad was 15.3 nmol (CL: 4.5–51.7 nmol). Concomitant with this splenic vasoconstrictor response there was a reduction in spleen weight reflecting a reduction in spleen volume due to capsular smooth muscle contraction. The mean maximum reduction in spleen weight to Ad was 33 ± 6.3 g ($n = 7$).

Endothelin-1 ET-1 was administered as an intra-arterial bolus injection over the dose range 0.4–200 pmol. An increase in the splenic arterial perfusion pressure was recorded reflecting, under conditions of constant inflow, an increase in the splenic arterial vascular resistance. Both this splenic arterial vasoconstriction (Figure 1) and its prolonged duration (Table 1) were dose-dependent. A vasodilator phase in the splenic arterial response to ET-1 was not observed in these preparations. The mean ED_{50} for the splenic vasoconstrictor

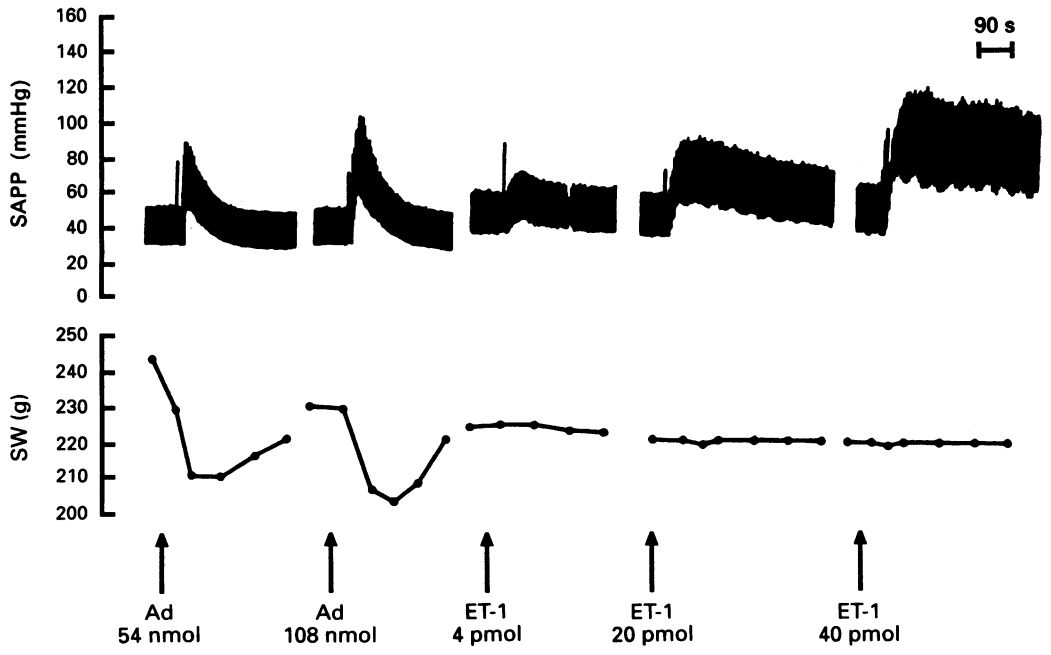


Figure 1 Canine isolated spleen (75 g) perfused with Krebs solution at constant flow (22 ml min^{-1}). Experimental records illustrating the graded increases in splenic arterial perfusion pressure (SAPP) and reductions in spleen volume (SW) in response to the close-arterial bolus injection of endothelin-1 (ET-1; 4.0, 20 and 40 pmol) and adrenaline (Ad; 54 and 108 nmol). The vascular responses to ET-1 are prolonged compared with those to Ad and the reductions in spleen weight, accompanying the vasoconstrictor responses to ET-1 are very small.

response to ET-1 was 9.5 pmol (CL: 4.5–20.4 pmol). Reductions in spleen weight which reflect reductions in the spleen volume and contractions of the splenic capsular smooth muscle were seen only at the highest dose of ET-1 (200 pmol); the mean maximum reduction in spleen volume caused by ET-1 was 6.2 ± 2.5 g ($n = 5$).

Table 1 Times to 50% recovery (min) of the splenic vasoconstriction induced by endothelin-1 (ET-1, 0.4–200 pmol)

ET-1 (pmol)	*50% recovery* (min)
0.4	1.1 ± 0.9
2	4.5 ± 0.6
4	9.2 ± 2.1
20	10.4 ± 0.8
40	18.6 ± 5.1
200	18.5 ± 2.5

Results are expressed as mean ± s.e.mean of seven experiments.

Release of prostanoids in response to splenic intra-arterial injections

Endothelin-1 In ten spleen perfusions, ET-1 was injected intra-arterially over the dose-range 0.4–200 pmol. The splenic smooth muscle responses were recorded and, in the majority of the perfusions, splenic venous samples were collected at three doses of ET-1 (4.0, 40 and 200 pmol) for up to 7.5 min after the injections. The samples were subsequently assayed for prostanoids by radioimmunoassay. Increased levels of prostanoids were detected in the venous effluent within 1.5 min of ET-1 administration. These levels returned to basal values before the end of sample collection and generally also before the return of the concomitant increases in smooth muscle activity (Figure 2). Within a given experi-

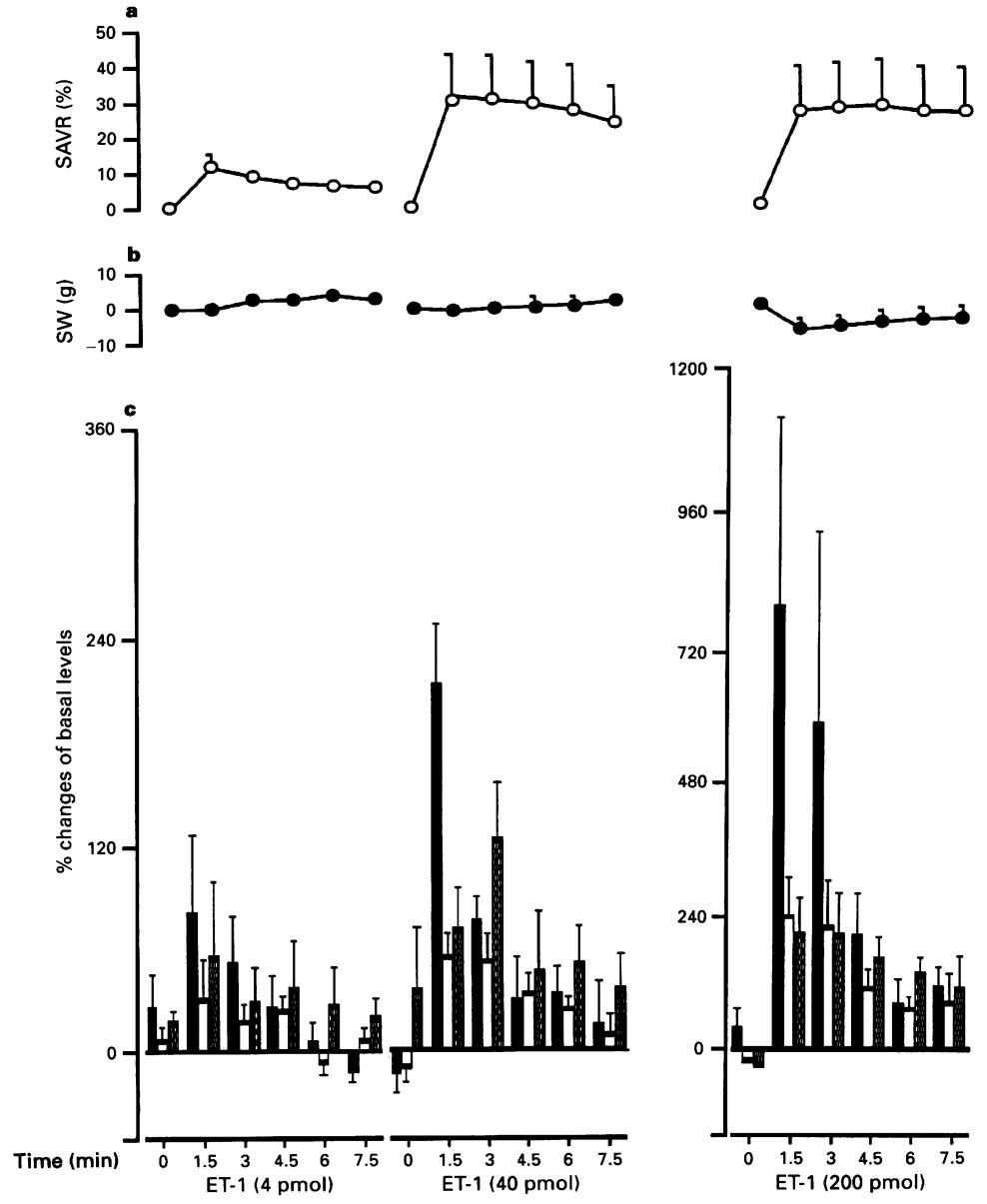


Figure 2 The temporal relationship between the release of vasoactive prostanoids into the splenic venous effluent and the concomitant changes in vascular and capsular smooth muscle activity in response to three intra-arterial doses of endothelin-1 (ET-1; 4.0, 40 and 200 pmol). Changes in (a) splenic arterial vascular tone (expressed as percentage increases above basal SAVR), (b) splenic capsular smooth muscle (expressed as changes in spleen weight) and (c) splenic effluent levels of PGE_2 (solid columns), 6-oxo-$PGF_{1\alpha}$ (open columns) and TXB_2 (hatched columns) given as percentage increases above basal levels. Note the change in scale in (c) for ET-1 (200 pmol).

ment and also when expressed as the group mean, the total amounts of individual prostanoids released and the peak concentrations of each achieved in the splenic venous effluent were related to the dose of ET-1 (Figure 2).

PGE_2 The mean basal release of PGE_2 into the splenic venous effluent samples prior to ET-1 and Ad injections was 290 ± 64 pmol min^{-1} ($n = 7$) or 7.9 ± 2.3 pmol ml^{-1}. The release of PGE_2 was related to the ET-1 dose (Figure 2) with the mean peak increase being $82.4 \pm 49.5\%$ ($n = 6$), $214 \pm 37\%$ ($n = 7$) and $784 \pm 343\%$ ($n = 4$) of the basal value at 4.0, 40 and 200 pmol of ET-1, respectively. These values were significantly different ($P < 0.05$) from each other. The total amount (AUC) of PGE_2 released by 200 pmol ET-1 was 2459 ± 880 pmol ($n = 4$).

6-oxo-$PGF_{1\alpha}$ The mean basal release of 6-oxo-$PGF_{1\alpha}$ into the splenic venous effluent was 217 ± 39 pmol min^{-1} ($n = 7$) or 6.3 ± 1.5 pmol ml^{-1}. There was a clear dose-related increase of 6-oxo-$PGF_{1\alpha}$ in the venous effluent following ET-1 administration (Figure 2). The mean peak increase of 6-oxo-$PGF_{1\alpha}$ release above basal levels was $30.5 \pm 26.5\%$ ($n = 6$), $56 \pm 15.5\%$ ($n = 7$) and $233 \pm 70\%$ ($n = 4$) for 4.0, 40 and 200 pmol ET-1 respectively (Figure 2). The mean peak release following 200 pmol of ET-1 was significantly different from those at 4.0 and 40 pmol of ET-1 ($P < 0.05$). The mean total amount of 6-oxo-$PGF_{1\alpha}$ (AUC) released by 200 pmol of ET-1 was 768 ± 94.4 pmol ($n = 4$). In addition, the total amounts of 6-oxo-$PGF_{1\alpha}$ were significantly less than the total amounts of PGE_2 released into the venous effluent by the same dose of ET-1 (200 pmol; $P < 0.05$).

TXB_2 The mean splenic venous basal release of TXB_2 was 459 ± 78 pmol min^{-1} ($n = 7$) or 13.3 ± 1.8 pmol ml^{-1}. As with PGE_2 and 6-oxo-$PGF_{1\alpha}$, there was a dose-related increase in TXB_2 in the splenic venous blood following ET-1 administration (Figure 2). The mean peak increases in splenic venous TXB_2 above basal values were $56 \pm 48\%$ ($n = 6$), $107 \pm 41\%$ ($n = 7$) and $205 \pm 81\%$ ($n = 4$) following the administration of 4.0, 40 and 200 pmol of ET-1. The total amount of TXB_2 (AUC) released by administration of 200 pmol ET-1 was 1507 ± 751 pmol ($n = 4$).

The ratios of eicosanoids (peak percentage increase) released at different doses of ET-1 were calculated using the amount of 6-oxo-$PGF_{1\alpha}$ released at any injection as the standard and equating this to 1.0. Under these conditions, the mean ratios of 6-oxo-$PGF_{1\alpha}$:TXB_2:PGE_2 released by 4.0, 40 and 200 pmol of ET-1 were 1.0:1.8:2.7, 1.0:2.2:3.8 and 1.0:0.9:3.4, respectively.

Adrenaline In all the perfusion experiments, samples of venous effluent were collected and assayed after a single dose of Ad (54 nmol) intended to be used in comparisons before and after indomethacin. The mean elevation of splenic arterial vascular resistance was $57.4 \pm 10.8\%$ of the basal tone and the mean reduction in the spleen weight was 15.3 ± 8.7 g ($n = 4$). The mean % increase in peak effluent concentrations of PGE_2, 6-oxo-$PGF_{1\alpha}$ and TXB_2 were 290.7 ± 98.5, 141.7 ± 29.8 and 86.7 ± 33.4, respectively ($n = 4$ each).

Effects of indomethacin infusion on splenic smooth muscle activity and the release of prostanoids

Indomethacin (5.6 μM) was infused into the splenic arterial line and its effects on basal and stimulated splenic prostanoid release, basal smooth muscle tone and subsequent responses to ET-1 and Ad established.

Basal levels of prostanoids in the splenic venous effluent Fifteen minutes after the start of the indomethacin infusion splenic venous samples were collected for assay prior to each administration of ET-1. Following indomethacin, the

Table 2 The effects of indomethacin on (a) the peak splenic venous effluent concentrations (pmol ml^{-1}) of prostaglandin E_2 (PGE_2), 6-oxo-$PGF_{1\alpha}$ and thromboxane A_2 (TXA_2) and (b) the maximum increase in spenic arterial vascular resistance (% SAVR) in response to three bolus doses of endothelin (ET-1)

	ET-1 (pmol)											
	4.0				40				200			
	PGE_2	*6-oxo-$PGF_{1\alpha}$*	*TXA_2*	*% SAVR*	*PGE_2*	*6-oxo-$PGF_{1\alpha}$*	*TXA_2*	*% SAVR*	*PGE_2*	*6-oxo $PGF_{1\alpha}$*	*TXA_2*	*% SAVR*
Krebs alone	9.2 ± 2.8	6.4 ± 1.7	27.1 ± 4.5	11.0 ± 3.0	16.9 ± 4.3	7.6 ± 1.3	27.0 ± 7.7	44.1 ± 16	63.6 ± 9.5	23.0 ± 6.7	41.4 ± 14	61.1 ± 7.5
	*	*	*	*	*	*	*		*	*	*	
Krebs + indomethacin (5.6 μM)	1.3 ± 0.1	3.2 ± 1.7	4.8 ± 2.6	21.6 ± 6.9	2.1 ± 0.6	0.8 ± 0.4	0.8 ± 0.2	25.2 ± 4.7	10.9 ± 3.3	14.0 ± 0.4	5.4 ± 3.5	84.5 ± 40

Values are mean ± s.e.mean.
*Significantly different ($P < 0.05$) from the results with Krebs alone.

Table 3 Indomethacin potentiates the increase in splenic arterial vascular resistance induced by low doses of endothelin-1 (ET-1)

ET-1 (pmol)	*Before Indo*	*During Indo*
0.4	0.7 ± 0.3	6.3 ± 1.8*
2	4.9 ± 2.0	9.3 ± 3.0*
4	11 ± 3.0	21.6 ± 6.9*
20	26.1 ± 6.4	50.3 ± 34.3
40	44.1 ± 15.7	25.2 ± 4.7
200	61.1 ± 7.5	84.5 ± 39.6

Results (mean ± s.e.mean of seven experiments) are expressed as the mean percentage (%) increases in splenic arterial vascular resistance in response to ET-1 before and during indomethacin infusion (Indo, 5.6 μM).
*$P<0.05$ when compared with values before Indo infusion.

mean basal levels of PGE_2, 6-oxo-$PGF_{1\alpha}$ and TXB_2 were 1.2 ± 0.3, 0.7 ± 0.2 and 2.1 ± 1.1 pmol ml^{-1}, respectively. These values were all significantly less than the basal splenic effluent levels prior to the infusion of indomethacin ($P<0.05$ in all cases; $n=3$).

Basal splenic smooth muscle tone Approximately 15 min after the start of each intra-arterial indomethacin infusion, there was a gradual and prolonged increase in perfusion pressure reflecting splenic arterial vasoconstriction. The mean increase in splenic arterial vascular resistance caused by indomethacin infusion was 18.3 ± 3.5% of the control ($n=6$). This value was significantly greater than the basal splenic arterial vascular resistance before indomethacin ($P<0.05$).

Release of prostanoids by ET-1 and Ad In four perfusions, splenic venous samples were collected at set intervals following three doses of ET-1 (4.0, 40 and 200 pmol) before and after indomethacin and were assayed for PGE_2, 6-oxo-$PGF_{1\alpha}$ and TXB_2. The peak concentrations of all three eicosanoids in the splenic effluent in response to ET-1 were significantly reduced during the indomethacin infusion (Table 2). The release of prostanoids by Ad was also significantly reduced ($P<0.05$) by indomethacin since the mean peak effluent concentrations of PGE_2, 6-oxo-$PGF_{1\alpha}$ and TXB_2 were 17.4 ± 8.2%, 10.5 ± 4.4% and 4.0 ± 2.1% of the basal values, respectively.

Splenic capsular and vascular responses to ET-1 and Ad In seven experiments, ET-1 (0.4–200 pmol) was administered before and during indomethacin infusion. Indomethacin significantly potentiated the increases in splenic arterial vascular resistance induced by low doses of ET-1 (0.4, 2.0 and 4.0 pmol; $P<0.05$; Table 3). In contrast, indomethacin did not significantly affect the changes in splenic arterial vascular tone evoked by Ad (66.5 ± 23.5%) or the changes in spleen weight in response to ET-1 (200 pmol; 8.3 ± 4.3 g; $P>0.7$) or Ad (54 nmol; 21.5 ± 15.9 g; $P>0.4$).

Discussion

The present experiments in the canine isolated, perfused spleen complement and substantially enlarge the initial observations on the rabbit isolated spleen (Rae *et al.*, 1989) for which it was reported that the intra-arterial administration of ET-1 caused the release of various eicosanoids into the splenic venous effluent. Rae *et al.* (1989) demonstrated that the predominant eicosanoid released by intra-arterial infusion of 10 nM ET-1 was PGE_2; although the venous effluent levels of 6-oxo-$PGF_{1\alpha}$ and TXB_2 were also increased, these increases were not significant. The experiments described here show that the amount of any individual eicosanoid released is determined by the bolus molar dose of ET-1 and that at the three doses studied in detail, the peak venous concentrations of PGE_2 were significantly elevated above control levels whilst only at the two higher doses of ET-1, were there significant increases in 6-oxo-$PGF_{1\alpha}$ and TXB_2.

In the canine spleen, the predominant eicosanoid released was PGE_2; the mean maximum release at 200 pmol ET-1 was nearly 800% above the basal level. The mean maximum increases for 6-oxo-$PGF_{1\alpha}$ and TXB_2 at the same dose of ET-1 were 233% and 205%, respectively. This profile of release differs both qualitatively and quantitatively from other tissues. In the rabbit kidney (Rae *et al.*, 1989), the main eicosanoid released was PGI_2; there was a significant elevation in PGE_2 with no detectable increase in the venous levels of TXA_2. In contrast, in guinea-pig isolated lungs (de Nucci *et al.*, 1988) there was a dose-dependent and sustained release of PGI_2 and TXA_2 although different patterns of release were observed in isolated rat (de Nucci *et al.*, 1988) and rabbit (Lidbury, 1990) lung. These different patterns of eicosanoid release most likely reflect the varying distribution of endothelin receptors and the enzyme (PGI_2 synthase, TXA_2 synthase) profiles of the cell populations within individual vascular beds.

PGE_2, the major cyclo-oxygenase product released by ET-1 in the spleen, is synthesized by endothelial cells (Ager *et al.*, 1982) and macrophages (Gordon *et al.*, 1976). Prostacyclin is released mainly by endothelial cells (Moncada *et al.*, 1976) whereas TXA_2 is released essentially by platelets (Hamberg *et al.*, 1975). The spleen contains a substantial population of both fixed and mobile macrophages together with lymphocytes within the splenic white pulp. Endothelial cells line the extensive sinusoidal network which forms the microvasculature of the spleen and platelets may be distributed both within the sinusoidal network and outside in the red and white pulp (Fujita *et al.*, 1985; Weiss *et al.*, 1985).

In the spleen, the time-course of the appearance of each eicosanoid was of relatively short duration, was similar for each at any particular dose of ET-1 and was clearly less than the concomitant changes in splenic vascular and capsular smooth muscle. This may indicate that different ET receptor mechanisms are involved in vascular smooth contraction and in stimulating eicosanoid release. Two ET receptor subtypes have been reported (Arai *et al.*, 1990; Sakurai *et al.*, 1990): a selective receptor ET_A expressed by smooth muscle cells (Lin *et al.*, 1991) and a non-selective receptor ET_B expressed by vascular endothelial cells (Sakamoto *et al.*, 1991). In the rabbit isolated kidney BQ-123, a selective ET_A antagonist, significantly reduced both the vasoconstrictor response to ET-1 and the concomitant release of prostacyclin, indicating that ET_A receptors are implicated in both processes (Télémaque *et al.*, 1993). Our results suggest that the splenic vascular response to ET-1 represents a balance between direct vasoconstriction on the one hand and vasodilatation due to eicosanoid release from endothelial cells, macrophages and other cell types present in the splenic microcirculation on the other. The receptors responsible for this eicosanoid release within the spleen have not yet been fully characterized. In the present experiments, one consequence of receptor activation was a substantial molar amplification in the release of individual eicosanoids. Thus, for example, 200 pmol ET-1 led to the subsequent release into the venous effluent of 770 pmol 6-oxo-$PGF_{1\alpha}$, 2460 pmol PGE_2 and 1510 pmol TXB_2.

The concomitant infusion of the cyclo-oxygenase inhibitor indomethacin led to a significant elevation in splenic arterial vascular resistance indicative of splenic arterial vasoconstriction. Similarly, in conscious rats with chronically implanted flow probes, intravenous indomethacin leads to vasoconstriction in renal, mesenteric and hindlimb vascular beds (Gardiner *et al.*, 1990). In addition, in the canine spleen there was a significant reduction in the basal splenic venous levels of all three eicosanoids (PGE_2, PGI_2 and TXA_2). We conclude therefore that in the spleen there is a basal release of

predominantly vasodilator eicosanoids, the action of which is to constantly reduce arterial inflow resistance and to ensure adequate and appropriate perfusion through the splenic microcirculation.

The ET-1-induced increases in all three eicosanoids in the splenic venous effluent were significantly reduced by the concomitant infusion of indomethacin. However, the proposal by Rae *et al.* (1989) that the ET-evoked release of vasodilator prostanoids limits the vasoconstrictor properties of ET-1 is only partially justified by the present experiments. Only at the lower doses of ET-1 was vasoconstrictor potency significantly enhanced by inhibition of eicosanoid synthesis indicating that at these lower doses of ET-1 the predominant eicosanoids released are the vasodilators, PGI_2 and PGE_2. At the higher doses of ET-1, the marked and prolonged vasoconstrictor responses were unattenuated by indomethacin suggesting that at these doses the vasodilator properties of PGE_2 and PGI_2 may be countered by the concomitant presence of vasoconstrictor agents including TXA_2. The potentiation by indomethacin of the vasoconstrictor responses to the lower doses of ET-1 may reflect the predominant balance *in vivo* since estimates of plasma levels of ET-1 are in the lower picomolar range (Knothe *et al.*, 1992; Ozdemir *et al.*, 1992).

D.M.G.K. is supported by Fundação de Amparo à Pesquisa do Estado de São Paulo (FAPESP). P.G.W. received travel grants from the Royal Society (London) and FAPESP (São Paulo).

References

AGER, A., GORDON, J.L., MONCADA, S., PEARSON, J.D., SALMON, J.A. & TREVETHICK, M.A. (1992). The effects of isolation and culture on prostaglandin synthesis by porcine aortic endothelial and smooth muscle cells. *J. Cell Physiol.*, **110**, 9–16.

ARAI, S., HORI, S., ARAMORI, I., OHKUBO, H. & NAKANISHI, S. (1990). Cloning and expression of a cDNA encoding an endothelin receptor. *Nature*, **348**, 730–732.

BOATMAN, D.L. & BRODY, M.J. (1964). Analysis of vascular responses in the spleen. *Am. J. Physiol.*, **207**, 155–161.

CORDER, R., LOWRY, P.J. & WITHRINGTON, P.G. (1987). Actions of the peptides, neuropeptide Y and peptide YY, on the vascular and capsular smooth muscle of the isolated, blood-perfused spleen of the dog. *Br. J. Pharmacol.*, **90**, 785–790.

DE NUCCI, G., THOMAS, R., D'ORLEANS-JUSTE, P., ANTUNES, E., WALDER, C., WARNER, T. & VANE, J.R. (1988). The pressor effects of circulating endothelin are limited by its removal in the pulmonary circulation and by the release of prostacyclin and EDRF. *Proc. Natl. Acad. Sci. U.S.A.*, **85**, 9797–9800.

FUJITA, T., KASHIMURA, M. & ADACHI, K. (1985). Scanning electron-microscopy and terminal circulation. *Experientia*, **41**, 167–179.

GARDINER, S.M., COMPTON, A.M. & BENNETT, T. (1990). Effects of indomethacin on the regional haemodynamic responses to low doses of endothelins and sarafatoxin. *Br. J. Pharmacol.*, **100**, 158–162.

GORDON, D., BRAY, M.A. & MORLEY, J. (1976). Control of lymphokine secretion by prostaglandins. *Nature*, **262**, 401.

GRASSI-KASSISSE, D.M., ANTUNES, E., WITHRINGTON, P.G. & DE NUCCI, G. (1993). Effects of indomethacin on endothelin-1 evoked vasoconstriction and release of eicosanoids from the isolated, perfused canine spleen. *J. Physiol.*, **467**, 128P.

GREEN, H.D., OTTIS, K. & KITCHEN, T. (1960). Autonomic stimulation and blockade on canine splenic inflow, outflow and weight. *Am. J. Physiol.*, **198**, 423–428.

HAMBERG, M., SVENSSON, J. & SAMUELSSON, B. (1975). Thromboxanes: a new family of biologically active compounds derived from prostaglandin endoperoxides. *Proc. Natl. Acad. Sci. U.S.A.*, **172**, 2994–2998.

KNOTHE, C., BOLDT, J., ZICKMANN, B., BALLESTEROS, M., DAPPER, F. & HEMPELMANN, G. (1992). Endothelin plasma levels in old and young patients during open heart surgery: correlations to cardiopulmonary and endocrinology parameters. *J. Cardiovasc. Pharmacol.*, **20**, 664–670.

LIDBURY, P.S. (1990). Endothelium-derived mediators and platelet function. *PhD Thesis, University of London.*

LIN, H.Y., KAGI, I.H., WINKEL, G.K., IVES, H.I. & LODISH, H.F. (1991). Cloning and functional expression of a vascular smooth muscle endothelin-1 receptor. *Proc. Natl. Acad. Sci. U.S.A.*, **88**, 3185–3189.

MOERMAN, E.J., SCAPAGNINI, U. & DE SCHAEPDRYVER, A.F. (1969). Adrenergic receptors in the isolated perfused dog spleen. *Eur. J. Pharmacol.*, **5**, 279–285.

MONCADA, S., GRYGLEWSKI, R., BUNTING, S. & VANE, J.R. (1976). An enyzme isolated from arteries transforms prostaglandin endoperoxides to an unstable substance that inhibits platelet aggregation. *Nature*, **263**, 663–665.

OZDEMIR, S., SAATCI, U,. BESBAS, N., BAKKALOGLU, A., OZEN, S. & KORAY, Z. (1992). Plasma atrial natriuretic peptide and endothelin levels in acute poststreptococcal glomerulonephritis. *Pediatr. Nephrol.*, **6**, 519–522.

RAE, G.A., TRYBULEC, M., DE NUCCI, G. & VANE, J.R. (1989). Endothelin-1 releases eicosanoids from the rabbit isolated perfused kidney and spleen. *J. Cardiovasc. Pharmacol.*, **13**, S89–S92.

SAKAMOTO, A., YANAGISAWA, M., SAKURAI, T., TAKUWA, Y., YANAGISAWA, H. & MASAKI, T. (1991). Cloning and functional expression of human cDNA for the ET_B endothelin receptor. *Biochem. Biophys. Res. Commun.*, **178**, 656–663.

SAKURAI, T,. YANAGISAWA, M., TAKUWAT, Y., MIYAZAKI, H., KIMURA, S., GOTO, K. & MASAKI, T. (1990). Cloning of a cDNA encoding a non-isopeptide-selective subtype of the endothelin receptor. *Nature*, **348**, 732–735.

SALMON, J.A. (1978). A radioimmunoassay for 6-keto-prostaglandin $F_{1\alpha}$. *Prostaglandins*, **15**, 383–397.

TÉLÉMAQUE, S., GRATTON, J.P., CLAING, A. & D'ORLEANS-JUSTE, P. (1993). Endothelin-1 induces vasoconstriction and prostacyclin release via the activation of endothelin ET_A receptors in the perfused rabbit kidney. *Eur. J. Pharmacol.*, **237**, 275–281.

WEISS, L., POWELL, R. & SCHIFFMAN, F.J. (1985). Terminating arterial vessels in red pulp of human spleen; a transmission electron microscopic study. *Experientia*, **41**, 233–242.

YANAGISAWA, M., KURIHARA, H., KIMURA, S., TOMOBE, Y., KOBAYASHI, M,. MITSUI, Y., YAZAKI, Y., GOTO, K. & MASAKI, T. (1988). A novel potent vasoconstrictor peptide produced by vascular endothelial cells. *Nature*, **332**, 411–415.

(Received August 13, 1993
Revised May 16, 1994
Accepted May 24, 1994)

Br. J. Pharmacol (1994), **113**, 681–686 © Macmillan Press Ltd, 1994

Contribution of ATP and nitric oxide to NANC inhibitory transmission in rat pyloric sphincter

Prajitno Soediono & [1]Geoffrey Burnstock

Department of Anatomy and Developmental Biology and Centre for Neuroscience, University College London, Gower Street, London WC1E 6BT

1 Changes in isometric tension were recorded from circular muscle strips of rat pyloric sphincter *in vitro*, in response to electrical field stimulation and exogenously applied muscle relaxants.

2 Concentration-response relationships were studied for relaxations to exogenously applied adenosine 5'-triphosphate (ATP) and two analogues, 2-methylthioATP (2-MeSATP) and α,β-methylene ATP (α,β-MeATP). These drugs evoked concentration-dependent relaxation of rat pyloric sphincter with an order of potency 2-MeSATP > ATP >> α,β-MeATP, indicating the presence of P_{2y}-purinoceptors. The IC_{50} value of each nucleotide was: 2-MeSATP, 5.0×10^{-8} M; ATP, 7.9×10^{-6} M; α,β-MeATP showed only slight activity at a concentration of 0.1 mM.

3 Frequency-response relationships for relaxations evoked by electrical field stimulation (EFS) were studied in the absence and presence of 10 μM N^G-nitro-L-arginine methyl ester (L-NAME, an inhibitor of nitric oxide (NO) synthesis) and 20 μM reactive blue 2 (a P_{2y}-purinoceptor antagonist). It was found that these substances significantly reduced the relaxant response of rat pyloric sphincter to EFS by 40% and 50% respectively. In the presence of both L-NAME and reactive blue 2 the responses were reduced by 75%.

4 Concentration-response relationships were studied for ATP and 2-MeSATP in the presence of L-NAME. It was found that L-NAME did not significantly inhibit the relaxant responses to these drugs.

5 Concentration-response relationships for ATP and noradrenaline were studied in the presence of reactive blue 2 (20 μM); the P_{2y}-antagonist significantly inhibited the relaxant response to ATP, but not that to noradrenaline.

6 The distribution of nitric oxide synthase in rat pyloric sphincter was investigated immunohistochemically, with immunoreactive nerve fibres found throughout the circular muscle layer and myenteric plexus of the sphincter.

7 While abundant vasoactive intestinal polypeptide (VIP)-containing nerve fibres were demonstrated immunohistochemically in the pyloric sphincter, relaxations to VIP (1 nM–0.3 μM) were not observed in this preparation.

8 It is concluded that ATP, acting through P_{2y}-purinoceptors, and NO contribute to NANC inhibitory neurotransmission in rat pyloric sphincter. NO appeared to contribute to the later component of NANC relaxation. The action of ATP was not mediated by NO, and VIP did not contribute to the NANC inhibitory responses in this preparation.

Keywords: Pyloric sphincter; nitric oxide; ATP; NANC; inhibition

Introduction

A major part of the autonomic innervation to the gastrointestinal tract is by non-adrenergic non-cholinergic (NANC) neurones, although the precise nature of transmitters involved remains controversial. In sphincteric regions of the gut, this NANC innervation is mainly inhibitory and is physiologically important in the relaxation of sphincters for the passage of ingested solids.

Vasoactive intestinal polypeptide (VIP) has been proposed as a candidate mediator for NANC innervation in stomach (Grider *et al.*, 1985), pyloric sphincter (Allescher *et al.*, 1989) and internal anal sphincter (Biancini *et al.*, 1985). However VIP does not mimic the electrophysiological actions of the final NANC transmitter *in vitro* (Daniel *et al.*, 1986, 1991). Functional (Allescher *et al.*, 1989) and biochemical (Torphy *et al.*, 1986) evidence has been presented suggesting that VIP is not the final NANC inhibitory transmitter in pyloric and lower oesophageal sphincters.

Adenosine 5'-triphosphate (ATP) and nitric oxide (NO) have also been put forward as inhibitory transmitters in the gut. The evidence for ATP as a transmitter in the gut is substantial (Burnstock *et al.*, 1970; Hoyle & Burnstock, 1989). NO was first identified as endothelium-derived relaxing factor (EDRF) but, subsequently, has been proposed as a putative NANC inhibitory transmitter in a number of tissues (for review see Rand, 1992). NO formation is catalysed by nitric oxide synthase (NOS). Investigations of brain NOS show that the primary substrate is arginine, forming citrulline and NO, and requiring Ca^{2+} and reduced nicotinamide adenine dinucleotide phosphate (NADPH). Because of its instability, NO cannot be localized in tissues. The purification of NOS has allowed antisera to be raised, and permitted immunohistochemical localization of this enzyme (Bredt & Snyder, 1990). Enzymatic blockade of NO production with arginine methyl esters reduces or blocks the inhibitory NANC responses in a variety of tissues, including the lower oesophageal sphincter (Tottrup *et al.*, 1991), ileocolonic junction (Boeckxstaens *et al.*, 1990) and the canine pyloric sphincter (Allescher *et al.*, 1992). In the canine ileocolonic junction, it was shown that the relaxant action of ATP is mediated by NO or an NO-releasing substance (Boeckxstaens *et al.*, 1991). A recent study of the NANC inhibitory responses in the rabbit portal vein has shown that both NO and ATP are involved in the NANC inhibitory

[1] Author for correspondence.

response (Brizzolara *et al.*, 1993), while studies in rat intestine have also proposed NO and ATP as cotransmitters (Belai & Burnstock, 1994).

In the present study the roles of ATP, VIP and NO in the NANC inhibitory innervation of rat pyloric sphincter were investigated. The receptor subtype mediating the effect of ATP in this tissue was also investigated and the possibility that the action of ATP is mediated through NO was examined. The distribution of the NO synthesizing enzyme NOS, and of VIP, was also studied immunohistochemically.

Methods

Male Sprague-Dawley rats (275–325 g) were killed by asphyxiation with CO_2. The gastric antrum and proximal duodenum were removed *en bloc*, opened along the greater curvature of the stomach and pinned flat. The junction between the gastric and duodenal mucosa was identified, the mucosa removed and a strip 2 mm wide was cut immediately proximal to this junction. This muscle strip was found to contain the thickened band of circular muscle, considered to be the anatomical representation of the pyloric sphincter and the only region to produce consistent relaxation to transmural electrical stimulation, as described by Anuras *et al.* (1974) in the opossum, cat and man. Silk ligatures were attached to each end of the muscle strip. One end was then tied to a rigid support and the other end to a force displacement transducer (Grass FT30C) to record isometric tension. The tissue was placed in a 5 ml organ bath containing modified Krebs-Ringer solution of the following composition (mM): NaCl 133, KCl 4.7, $NaHCO_3$ 16.4, $MgSO_4$ 0.6, $NaHPO_4$ 1.4, $CaCl_2$ 2.5 and glucose 7.7, aerated with 95% O_2-5% CO_2 at 37°C. Electrical field stimulation (EFS) was applied through 2 platinum wire rings 2.5 mm in diameter and 1 cm apart, through which the muscle preparation was threaded. Changes in tension were recorded on a Grass ink-writing oscillograph; 1 g of tension was applied. The tissue was allowed to equilibrate for at least 1 h. All strips were weighed and found to weigh within 2 standard deviations of the mean weight. Experiments with noradrenaline were performed at resting tension in the presence of atropine (2.3 μM). All other experiments were performed at resting tension and in the presence of atropine (2.3 μM), phentolamine (3.55 μM) and propranolol (3.8 μM).

Frequency-response relationships

The relationship between frequency of nerve stimulation (100 V, 0.25 ms, 0.5–32 Hz, 30 s stimulation every 5 min) and tissue response was studied in the absence, then presence of N^G-nitro-L-arginine methyl ester (L-NAME) (10 μM) or reactive blue 2 (20 μM). Frequency-response relationships constructed in the presence of L-NAME were repeated in the presence of L-arginine (1 mM). Finally, experiments were repeated in the presence of tetrodotoxin (3 μM).

Concentration-response relationships

The relationship between drug-concentration and tissue-response was investigated for noradrenaline, VIP, ATP and 2-methylthioATP (2-MeSATP) adding each agonist in a cumulative fashion. The concentration-response relationship for the purinoceptor agonist α,β-methylene ATP (α,β-MeATP) was studied under non-cumulative conditions, allowing at least 20 min between doses to prevent desensitization. Experiments with ATP were repeated in the presence of L-NAME (10 μM) and reactive blue 2 (20 μM); experiments with noradrenaline were repeated in the presence of reactive blue 2 (20 μM).

Drugs used

The following drugs were used: adenosine 5'-triphosphate (ATP); α,β-methylene ATP (α,β-MeATP); N^G-nitro-L-arginine methyl ester (L-NAME); L-arginine; noradrenaline bitartrate salt; vasoactive intestinal polypeptide (VIP); tetrodotoxin and reactive blue 2 (all obtained from Sigma Pharmaceuticals, U.K.); 2-methylthioATP (2-MeSATP) (Research Biochemicals Inc., U.K.); atropine sulphate (Phoenix Pharmaceuticals, U.K.); phentolamine mesylate (Ciba, U.K.) and propranolol hydrochloride (ICI, U.K.). All drugs were administered as aqueous solutions in microliter volumes and were prepared on the day of experimentation. Solutions of noradrenaline contained 300 μM ascorbic acid. The stock solution of tetrodotoxin (1 mM, in citrate buffer, pH 4.8) was stored at −20°C.

Preparation of results and statistical analysis

Results are shown as the % relaxation compared to the maximal relaxation of the tissue to EFS. Sodium nitroprusside (SNP) was initially used to determine maximal relaxa-

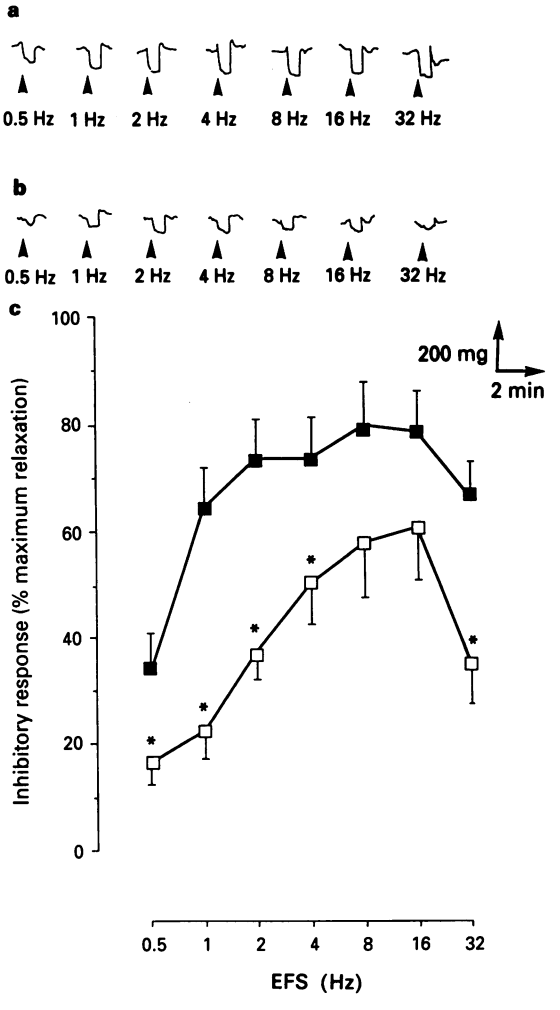


Figure 1 The effect of N^G-nitro-L-arginine methyl ester (L-NAME, 10 μM) on relaxations of rat pyloric sphincter to electrical field stimulation (EFS). (a) Before the application of L-NAME (10 μM) EFS caused relaxation of the sphincter. (b) A record taken 20 min after the application of L-NAME showing a reduction in relaxations to EFS. Arrowheads indicate the start of stimulation. (c) Frequency-response relationships representative of the effect of L-NAME on EFS. Responses in the absence (■, $n = 10$) and presence (□, $n = 10$) of L-NAME (10 μM) are shown. Data show mean response ± s.e. mean expressed as the % of the maximal relaxant response. *Indicates significance against the control group; $P \leq 0.05$.

tion. However EFS was found to produce a greater relaxant response than SNP in this preparation. Results are shown as mean ± standard error (s.e.) mean for the number of preparations indicated. For statistical analysis a paired Student's *t* test was used. *P* values of less than 0.05 were considered to be significant.

Immunohistochemistry

After dissection, the pyloric sphincter was fixed in 4% (w/v) paraformaldehyde in 0.1 M phosphate buffered saline (PBS) pH 7.3 for 4 h at 4°C. Tissues were then washed in 7% (w/v) sucrose in PBS containing 0.01% (w/v) sodium azide and stored at 4°C for at least 18 h in the same solution.

The tissues were mounted in embedding medium (Tissue-Tek OCT compound, Miles Inc., U.S.A.) and 10 μM longitudinal sections were cut on a cryostat (Reichart-Jung) at −25°C. The sections were thaw-mounted on gelatine coated slides and incubated in humid chambers at room temperature for 16 h with rabbit polyclonal antisera, diluted 1:3000, to NOS (Abbott, U.S.A.) or VIP (INC, U.K.). The preparations were washed three times in PBS and incubated with biotin-conjugated goat anti-rabbit immunoglobulin (Amersham, U.K.) at a dilution of 1:500 for 1 h, washed again with PBS, and then incubated with streptavidin-fluorescein isothiocyanate (FITC) conjugate (Amersham, U.K.) at a dilution of 1:250 for 1 h. Immunoreactivity was viewed with a Zeiss microscope and photographed with Kodak Tmax 3200 film.

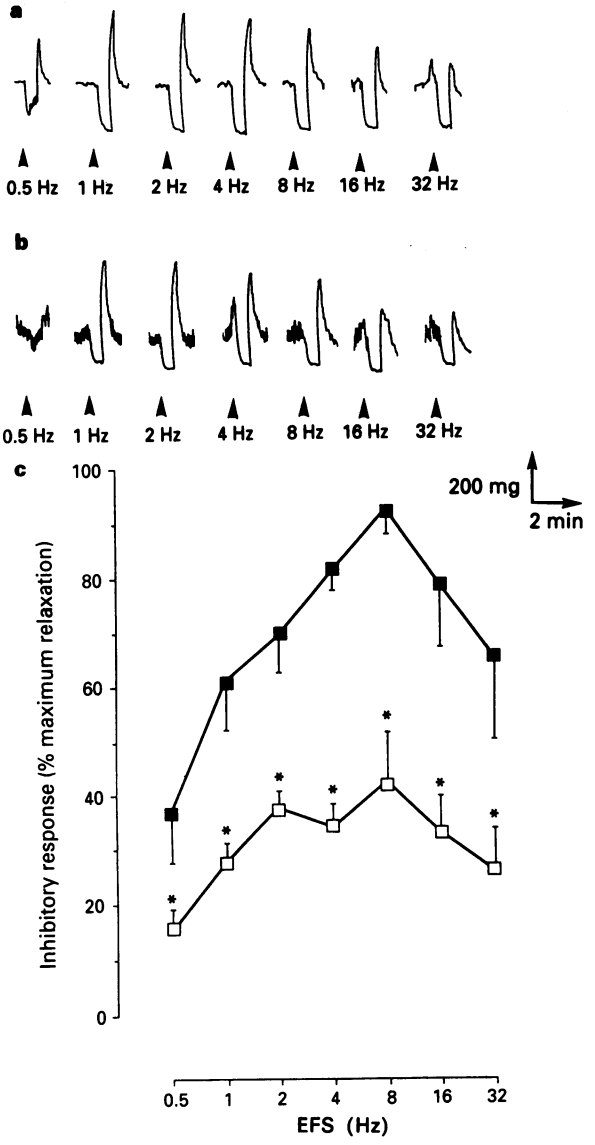


Figure 2 The effect of reactive blue 2 (20 μM) on relaxations of rat pyloric sphincter to EFS. (a) Before the application of reactive blue 2 (20 μM), EFS caused relaxation of the sphincter, followed by a rebound contraction. (b) 20 min after the application of reactive blue 2 there is a reduction in the relaxations to EFS. Arrowheads indicate the start of stimulation. (c) Frequency-response relationships showing the effect of EFS on rat pyloric sphincter. Responses in the absence (■, $n = 9$) and presence (□, $n = 9$) of reactive blue 2 (20 μM) are shown. Data show mean response ± s.e. mean expressed as the % of the maximal relaxation. *Indicate significance against the control group. $P \leq 0.05$.

Results

Effect of L-NAME, reactive blue 2 and tetrodotoxin on NANC relaxations induced by electrical field stimulation

EFS for 30 s (100 V, 0.25 ms, 0.5–32 Hz) induced relaxation in rat pyloric sphincter. These relaxations were fast in onset and were often followed by a rebound contraction. At high frequencies (≥ 16 Hz) the relaxation often extended beyond the period of stimulation. Tetrodotoxin (3 μM) abolished relaxations induced by EFS. L-NAME (10 μM; Figure 1) significantly reduced relaxations induced by EFS; the maximum reduction, 41.8% ± 6.0, occurred at 1 Hz. Relaxant responses were reduced by 22.0% ± 11.2 and 17.9% ± 14.9 at 8 and 16 Hz respectively, however these reductions were not significant. Reactive blue 2 (20 μM; Figure 2) significantly ($P \leq 0.05$) reduced relaxations induced by EFS at all frequencies, the relaxant response at 8 Hz was reduced by 50.1% ± 5.8. In the presence of both L-NAME and reactive blue 2 the relaxant response to EFS at 8 Hz was reduced by 75% ± 6.48 ($n = 6$).

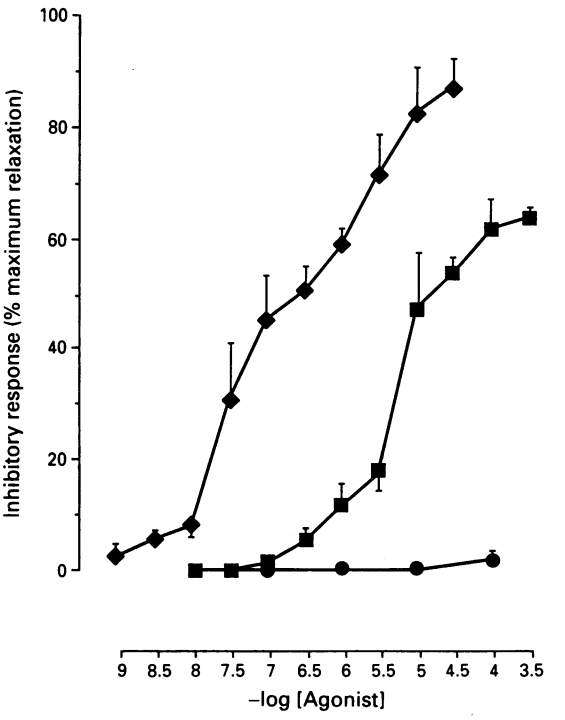


Figure 3 Concentration-response relationships showing the effect of ATP (■, $n = 8$), 2-MeSATP (◆, $n = 8$) and α,β-MeATP (●, $n = 8$) on isolated pyloric sphincter strips from rat. Data show mean response ± s.e mean expressed as the % of the maximal relaxation. *Indicates significance against the control group; $P \leq 0.05$. For abbreviations, see text.

Effect of L-arginine on the inhibitory effect of L-NAME

L-Arginine (1 mM) reversed the inhibitory effect of L-NAME by 54.2% ± 19.3 at 8 Hz, this reversal was not significant.

Effect of exogenous application of ATP, 2-MeSATP, α,β-MeATP and VIP

Exogenous application of ATP and 2-MeSATP relaxed the pyloric sphincter in a concentration-dependent fashion (Figure 3). 2-MeSATP was the most potent agonist but did not reach a maximum at the concentrations used (1 nM–30 μM); from these data an IC_{50} value of 5.0×10^{-8} M was calculated. Relaxations to ATP (IC_{50} 7.9×10^{-6} M) reached a maximum at 0.3 mM. α,β-MeATP was only slightly active at a concentration of 0.1 mM, showing a low affinity for the P_2-purinoceptors (P_{2y}-subtype) involved. Exogenous application of VIP (1 nM–0.3 μM) elicited no response in this preparation.

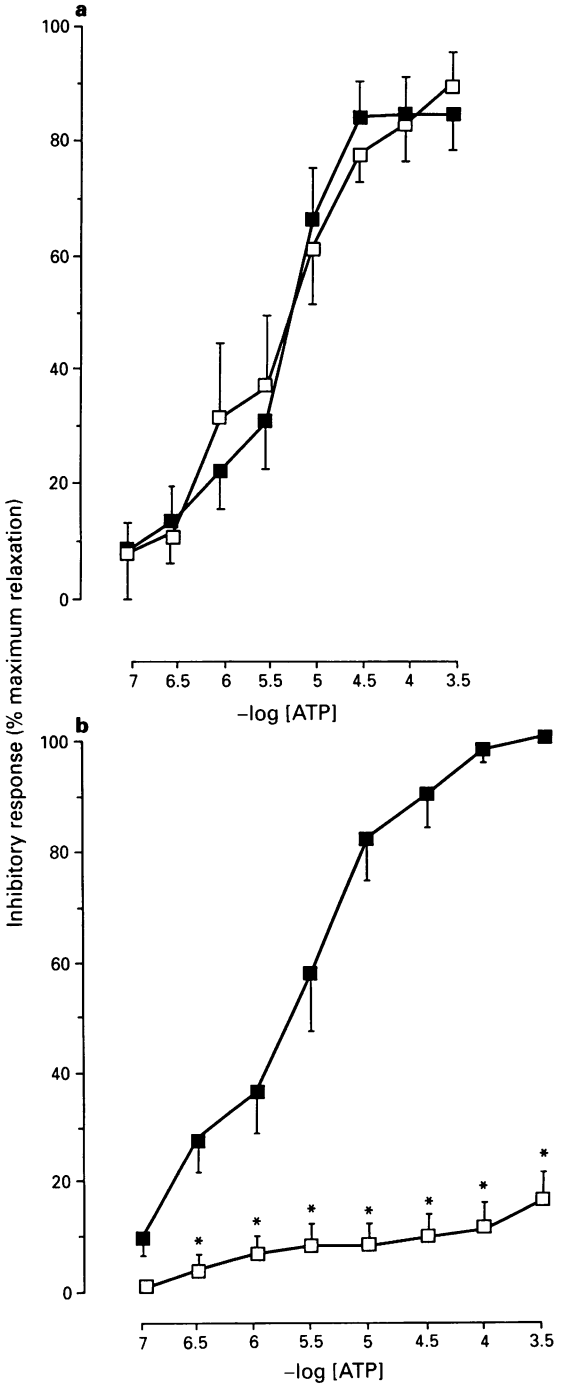


Figure 4 Concentration-response relationships showing the effect of ATP on isolated pyloric sphincter strips from rat. (a) The responses in the absence (■, $n = 10$) and presence (□, $n = 10$) of N^G-nitro-L-arginine methyl ester (L-NAME, 10 μM). (b) Responses in the absence (■, $n = 10$) and presence (□, $n = 10$) of reactive blue 2 (20 μM) are shown. Data show mean response ± s.e. mean expressed as the % of the maximal relaxation. *Indicates significance against the control group; $P \leqslant 0.05$.

Effect of L-NAME and reactive blue 2 on drug-induced relaxations

L-NAME did not significantly inhibit the relaxations evoked by exogenous application of ATP (Figure 4a), suggesting that ATP acts directly on smooth muscle and not indirectly through NO. Reactive blue 2 did significantly ($P \leqslant 0.05$) inhibit the relaxations evoked by exogenous application of ATP at concentrations above 0.3 μM. At the highest concentration (0.3 mM) the relaxant effect of ATP was inhibited by 84% ± 5 (Figure 4b). Reactive blue 2 had no inhibitory effect on the relaxations caused by exogenous application of noradrenaline (Figure 5), indicating its antagonistic actions were selective to ATP at this concentration.

Immunohistochemistry

The thickened circular muscle region of the pyloric region was found to have numerous NOS-like immunoreactive nerve fibres (Figure 6a). Immunoreactive fibres and nerve cell bodies were also seen in the myenteric plexus of the sphincter. The region also contained an abundant supply of VIP-like immunoreactive fibres within the circular muscle of the sphincter (Figure 6b). The myenteric plexus contained many VIP-like immunoreactive nerve fibres but no immunoreactive nerve cell bodies were seen.

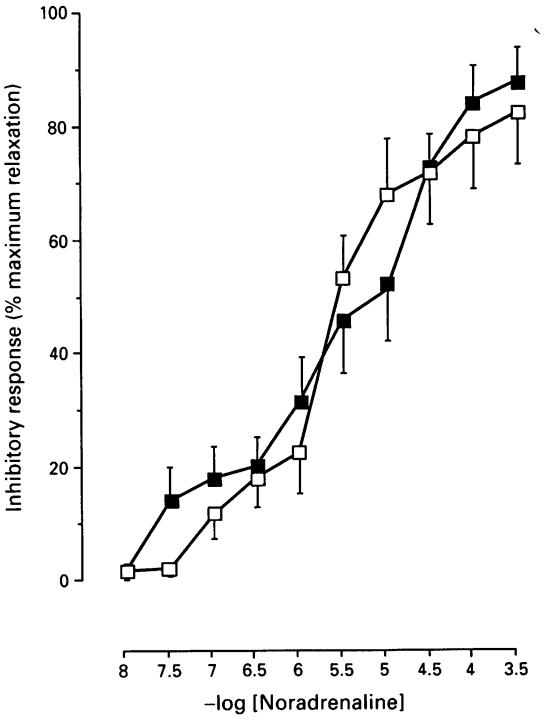


Figure 5 Concentration-response relationships showing the effect of noradrenaline on isolated pyloric sphincter strips from rat. Responses in the absence (■, $n = 10$) and presence (□, $n = 10$) of reactive blue 2 (20 μM) are shown. Data show mean response ± s.e. mean expressed as the % of the maximal relaxation. No significant difference between the points was found.

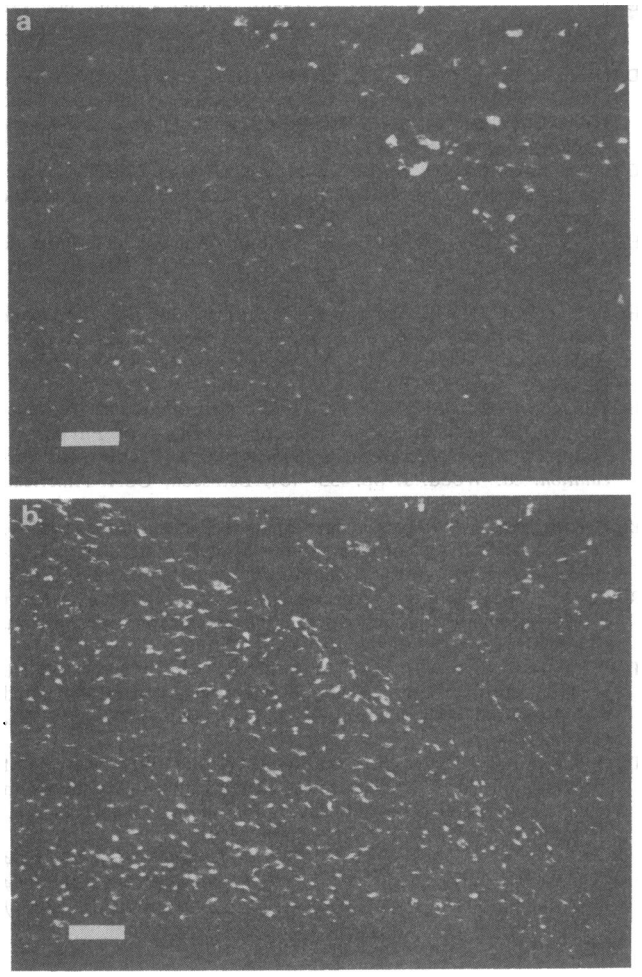


Figure 6 (a) Immunofluorescence micrograph of nitric oxide synthase (NOS)-like immunoreactivity in the pyloric sphincter region of rat. The circular muscle region of the sphincter shows fibres labelled with NOS-like immunofluorescence (calibration bar = 450 μm). (b) Immunofluorescence micrograph of vasoactive intestinal polypeptide (VIP)-like immunoreactivity in the pyloric sphincter region of rat. A dense distribution of VIP-like immunofluorescent fibres is seen within the circular muscle of the sphincter. (Calibration bar = 450 μm).

Discussion

Until recently, the most likely candidate for the inhibitory NANC response seen in the pyloric sphincter was considered to be VIP (Allescher *et al.*, 1989). However, the failure of VIP to produce consistent results *in vitro* (Daniel *et al.*, 1991) suggested that it was either not the final NANC transmitter or that some other NANC transmitter was present.

NO is synthesized from L-arginine by a cytosolic enzyme which appears to be related to NADPH-diaphorase in neuronal and endothelial cells. Recent studies in rat anococcygeus muscle (Li & Rand, 1989), opossum lower oesophageal sphincter (Tottrup *et al.*, 1991) and canine pyloric sphincter (Allescher *et al.*, 1992) suggested that NO or some related substance is involved in NANC responses *in vitro* and *in vivo*. This study shows that NO is a NANC neurotransmitter in rat pyloric sphincter, as has been previously demonstrated in canine pyloric sphincter *in vivo* and *in vitro* (Allescher *et al.*, 1992), on the basis of the reductions in relaxations to EFS induced by L-NAME and the reversal of this effect by L-arginine. However, this study showed that blockade of NO synthesis did not completely abolish relaxations of the sphincter to EFS.

ATP has been suggested as a NANC inhibitory transmitter in a wide variety of tissues (see Hoyle, 1992). Rat pyloric sphincter can be included in this list based on the reduction of relaxations to EFS in the presence of reactive blue 2 and the response to exogenous application of ATP and its analogues. The relative potency of ATP and its alkylthio derivative (2-MeSATP) is consistent with the classification for a purinoceptor of the P_{2y} subtype. The putative P_{2y} antagonist, reactive blue 2 (Burnstock & Warland, 1987), reduced relaxations of the sphincter to EFS and to exogenous application of ATP. Reactive blue 2 did not effect the relaxation caused by exogenous application of noradrenaline, implying that the action of reactive blue 2 is selective at the concentration used in this study and that there is a P_{2y}-purinoceptor mediated component to NANC relaxation in rat pyloric sphincter.

Studies of the canine ileocolonic junction have shown that NO is the final effector of NANC inhibitory neurotransmission in this tissue, mediating the action of EFS and exogenously applied ATP (Boeckxstaens *et al.*, 1991). The present study showed that relaxations evoked by ATP and EFS were not blocked fully by L-NAME, indicating that the action of ATP is not mediated by NO.

NOS-like immunoreactivity has been shown in several gut tissues in rat, including the ileum and colon (Belai *et al.*, 1992). The results of this study show that the pyloric sphincter of the rat also displays NOS-like immunoreactivity. The pyloric sphincter was also found to have a dense distribution of VIP-like immunoreactive nerve fibres as previously observed by Alumets *et al.* (1979), the absence of VIP-like immunoreactive nerve cell bodies may be due to a lack of colchicine pretreatment. Since exogenous application of VIP did not elicit a response the role of VIP in this preparation is unclear, but may involve neuromodulation of excitatory transmission as the basis for its reported inhibitory actions. Alternatively, it was found by Allescher *et al.* (1989) that injection of VIP into the canine gastroepiploic artery inhibited spontaneous and acetylcholine-induced pyloric contractions, but that *in vitro* muscle strips did not respond to exogenous application of VIP. It has also been shown that VIP is involved in slow inhibitory junction potentials in guinea-pig ileum but that this effect is masked by an excitatory potential mediated by a concomitant release of substance P (He & Goyal, 1993). Further investigation of rat pyloric sphincter may reveal an action of VIP *in vivo* or that inhibitory actions of VIP are masked by contraction mediated by release of substance P.

This study provides evidence that both ATP, acting directly on P_{2y}-purinoceptors, and NO contribute to the NANC inhibitory response of rat pyloric sphincter. Even though VIP-like immunoreactivity was present in the sphincteric region, exogenously applied VIP did not elicit a response in this preparation.

P.S. was funded by a departmental research scholarship.

References

ALLESCHER, H., DANIEL, E., DENT, J. & FOX, J. (1989). Inhibitory function of VIP/PHI and galanin in the canine pylorus. *Am. J. Physiol.*, **256**, G789–G797.

ALLESCHER, H., TOUGAS, G., VERGARA, P., LU, S. & DANIEL, E. (1992). Nitric oxide as a noncholinergic nonadrenergic inhibitory transmitter in the canine pylorus *in vivo*. *Am. J. Physiol.*, **262**, G695–G702.

ALUMETS, J., FAHRENKRUG, F., HÅKANSON, R., SCHAFFELITZKY DE MUCKADELL, O., SUNDLER, F. & UDDMAN, R. (1979). A rich VIP nerve supply is characteristic of sphincters. *Nature*, **280**, 155–156.

ANURAS, S., COOKE, A. & CHRISTENSSEN, J. (1974). An inhibitory innervation of the gastroduodenal junction. *J. Clin. Invest.*, **54**, 529–535.

BELAI, A. & BURNSTOCK, G. (1994). Evidence for coexistence of ATP and nitric oxide in non-adrenergic, non-cholinergic (NANC) inhibitory neurones in the rat ileum, colon and anococcygeus muscle. *Cell Tissue Res.*, (in press).

BELAI, A., SCHMIDT, H.H.W., HOYLE, C.H.V., HASSELL, C.J.S., SAFFREY, M.J., MOSS, J., FÖRSTERMANN, U., MURAD, F. & BURNSTOCK, G. (1992). Colocalisation of nitric oxide synthase and NADPH-diaphorase in the myenteric plexus of the rat gut. *Neurosci. Lett.*, **143**, 60–64.

BIANCINI, P., WALSH, J. & BEHAR, J. (1985). Vasoactive intestinal polypeptide: a neurotransmitter for relaxation of the rabbit internal anal sphincter. *Gastroenterology*, **89**, 867–874.

BOECKXSTAENS, G., PELCKMANS, P., BULT, H., DE MAN, J., HERMAN, A. & VAN MEARCKE, Y. (1990). Non-adrenergic non-cholinergic relaxation mediated by nitric oxide in the canine ileocolonic junction. *Eur. J. Pharmacol.*, **190**, 239–246.

BOECKXSTAENS, G., PELCKMANS, P., BULT, H., DE MAN, J., HERMAN, A. & VAN MEARCKE, Y. (1991). Evidence for nitric oxide as mediator of non-adrenergic non-cholinergic relaxation induced by ATP and GABA in the canine gut. *Br. J. Pharmacol.*, **102**, 434–438.

BREDT, D. & SNYDER, S. (1990). Isolation of nitric oxide synthase, a calmodulin requiring enzyme. *Proc. Natl. Acad. Sci. USA*, **87**, 682–685.

BRIZZOLARA, A., CROWE, R. & BURNSTOCK, G. (1993). Evidence for the involvement of both ATP and nitric oxide in the NANC inhibitory neurotransmission in the rabbit portal vein. *Br. J. Pharmacol.*, **109**, 606–608.

BURNSTOCK, G., CAMPBELL, G., SATCHELL, D. & SMYTHE, A. (1970). Evidence that adenosine triphosphate or a related nucleotide is the transmitter substance released by non-adrenergic inhibitory nerves in the gut. *Br. J. Pharmacol.*, **40**, 668–688.

BURNSTOCK, G. & WARLAND, J. (1987). P_2-Purinoceptors of two subtypes in the rabbit mesenteric artery: reactive blue 2 selectively inhibits responses mediated via the P_{2y}- but not the P_{2x}-purinoceptor. *Br. J. Pharmacol.*, **90**, 383–391.

DANIEL, E., JAGER, L. & JURY, J. (1986). Neither a purine nor VIP is the mediator of inhibitory nerves of opossum oesophageal circular smooth muscle. *J. Physiol.*, **382**, 489–508.

DANIEL, E., WOSKOWSKA, Z., CYPRIS, S. & FOX-THRELKELD, J. (1991). VIP release from canine intestine is inversely and indirectly related to motor activity of circular muscle (Abstract). *Gastroenterology*, **100**, A434.

GRIDER, J., CABLE, M., SAID, I. & MAKHLOUF, G. (1985). Vasoactive intestinal polypeptide (VIP) as neural mediator of gastric relaxation. *Am. J. Physiol.*, **248**, G73–G78.

HE, X. & GOYAL, R. (1993). Nitric oxide involvement in the peptide VIP-associated I.J.P. in guinea-pig ileum. *J. Physiol.*, **461**, 485–499.

HOYLE, C.H.V. (1992). Transmission: Purines. In *The Autonomic Nervous System*. Vol 1: *Autonomic Neuroeffector Mechanisms*. ed. Burnstock, G. & Hoyle, C.H.V. pp. 367–407. Chur, Switzerland: Harwood Academic Publishers.

HOYLE, C.H.V. & BURNSTOCK, G. (1989). Neuromuscular transmission in the gastrointestinal tract. In *Handbook of Physiology*, Section 6: *The Gastrointestinal System*, Vol. 1. *Motility and Circulation*. ed. Wood, J. pp. 435–464. Bethseda, USA: American Physiological Society.

LI, C. & RAND, M. (1989). Evidence for a role of nitric oxide in the neurotransmitter system mediating relaxation of the rat anococcygeus muscle. *Clin. Exp. Pharmacol. Physiol.*, **16**, 933–938.

RAND, M. (1992). Nitrergic transmission: Nitric oxide as a mediator of non-adrenergic non-cholinergic neuro-effector transmission. *Clin. Exp. Pharmacol. Physiol.*, **19**, 147–169.

TORPHY, T., FINE, C., BURMAN, M., BARNETTE, M. & ORMSBEE III, S. (1986). Lower oesophageal sphincter relaxation is associated with increased cyclic nucleotide content. *Am. J. Physiol.*, **251**, G786–G793.

TOTTRUP, A., KNUDSEN, M. & GREGERSEN, H. (1991). The role of the L-arginine-nitric oxide pathway in relaxation of the opossum lower oesophageal sphincter. *Br. J. Pharmacol.*, **104**, 113–116.

(Received April 20, 1994
Revised May 31, 1994
Accepted June 1, 1994)

Br. J. Pharmacol. (1994), **113**, 687–692 © Macmillan Press Ltd, 1994

The interaction between salmeterol and β_2-adrenoceptor agonists with higher efficacy on guinea-pig trachea and human bronchus *in vitro*

Britt-Louise Källström, Jacob Sjöberg & [1]Bertil Waldeck

Department of Pharmacology 2, Astra Draco AB, Box 34, S-221 00 Lund, Sweden

1 In guinea-pig tracheal preparations precontracted with 1 μmol l^{-1} carbachol, formoterol, procaterol, fenoterol, salmefamol, salbutamol and terbutaline (in that order of potency) caused a concentration-dependent and almost complete, relaxation. However, under these conditions, the maximum relaxation by salmeterol was approximately 30% of the maximum attainable relaxation.

2 We have therefore explored the ability of salmeterol to inhibit the relaxant response to β_2-adrenoceptor agonists of different chemical structure and relatively higher efficacy in smooth muscle preparations from guinea-pig trachea and human bronchus.

3 With 1 μmol l^{-1} salmeterol in the organ bath, the concentration-effect curves for the other agonists were shifted to the right in a variable way by 1.8–2.8 log units, fenoterol and salbutamol being the extremes.

4 When 20 μmol l^{-1} sulfonterol, another low efficacy β_2-adrenoceptor agonist, was substituted for salmeterol, the difference in the magnitude of the rightward shift between fenoterol and salbutamol was eliminated.

5 In the human bronchus, formoterol and terbutaline had a higher apparent efficacy than salmeterol. With 1 μmol l^{-1} salmeterol in the organ bath, the concentration-effect curve for formoterol was shifted 2.7 log units to the right.

6 Salmeterol inhibits, competitively, relaxant responses to β_2-adrenoceptor agonists with higher efficacy. The degree of inhibition seems to be dependent on the agonist used. This contrasts with results obtained with sulfonterol and suggests that salmeterol interacts with the β_2-adrenoceptor in a complex way.

Keywords: β-Adrenoceptor agonists; salmeterol; formoterol; guinea-pig trachea; human bronchus

Introduction

Much of the current interest in bronchodilator β-adrenoceptor agonists is now devoted to the long-acting compounds formoterol and salmeterol. While the clinical efficacy and duration of action of these compounds appear to be very similar when inhaled (Rabe *et al.*, 1993b), there are some interesting differences. Thus, the onset of action of salmeterol appears to be slower than that observed with shorter acting compounds (Beach *et al.*, 1992) while formoterol does not appear to differ in this respect (Wegener *et al.*, 1992). These clinical findings are consistent with observations made on isolated airway smooth muscle preparations (Jeppsson *et al.*, 1989; Johnson *et al.*, 1993). Moreover, salmeterol has a lower efficacy than salbutamol as assessed *in vitro* (Ball *et al.*, 1991; Lindén *et al.*, 1993) and inhibits competitively, agonists with higher efficacy, such as isoprenaline (Dougall *et al.*, 1991) and formoterol (Waldeck & Källström, 1991; Jeppsson *et al.*, 1992), in guinea-pig trachea. Due to its delayed onset and long duration of action, salmeterol is not recommended as rescue medication (Beach *et al.*, 1992), and other β-adrenoceptor agonists are recommended for this purpose.

Against this background, we felt it important to investigate the interaction between salmeterol and currently used β_2-adrenoceptor agonists with respect to relaxation of airway smooth muscle. Since salmeterol appears to interact with the β_2-adrenoceptor in a rather complex way (Jack, 1991; Nials *et al.*, 1993), we raised the question of whether agonists with different chemical structures may differ in their ability to overcome the inhibition by salmeterol. Thus, we have included in our study two resorcinol-derivatives of phenylethanolamine, namely terbutaline and fenoterol, two saligenin-deriviates, salbutamol and salmefamol, and two compounds with a nitrogen-function related to the 3-position on the phenyl ring, formoterol and procaterol (Figure 1). In some control experiments sulfonterol, another low efficacy β_2-adrenoceptor agonist (Kaiser *et al.*, 1975; Waldeck *et al.*, 1986) was substituted for salmeterol. Most of the experiments have been carried out on tracheal smooth muscle from guinea-pig, but some confirmatory studies were made on human bronchial strips.

Methods

Guinea-pig trachea

Male Dunkin-Hartley guinea pigs (Møllegaard, Denmark), weighing 200–350 g, were anaesthetized with pentobarbitone and exsanguinated by cutting the subclavian arteries. The trachea was removed and placed in a dissection bath filled with oxygenated Krebs solution (composition: see below) at room temperature. The trachea was freed from connective tissue and cut into sections comprising two cartilage rings. Surgical silk (4–0) was fastened to the cartilage on either side of the muscle bridge and the cartilage was then cut open ventrally.

Human bronchus

Macroscopally normal pulmonary tissue (kindly supplied by Dr Leif Johansson, Department of Pathology, University of Lund) was obtained from patients undergoing lung resection for carcinoma. A coarse separation of bronchii from vascular and parenchymal tissue was done less than 3 h after the

[1] Author for correspondence.

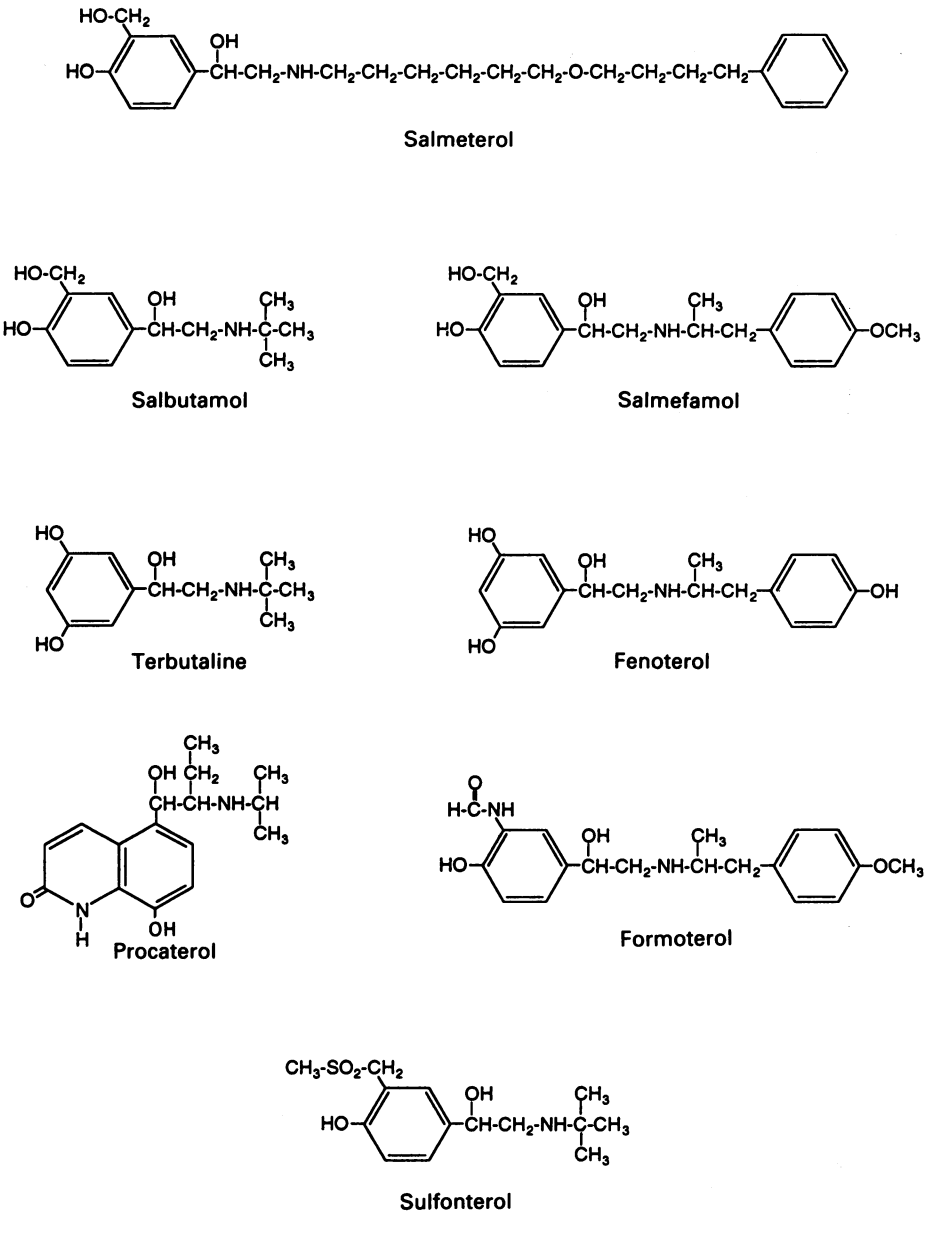


Figure 1 Chemical structures of the compounds investigated.

resection. The specimens were stored in oxygenated Krebs solution at 4–6°C overnight. The next morning, bronchial strips (from bronchii 2–5 mm i.d.) were dissected out and threads of surgical silk were fastened to each end of the strip.

General procedure

The preparations were mounted in waterjacketed organ baths (40 ml) containing Krebs solution (mM: NaCl 118, KCl 4.7, $CaCl_2$ 2.5, $MgSO_4$ 1.16, $NaHCO_3$ 25, KH_2PO_4 1.18, D-glucose 11.1) at 37°C. The solution was continuously oxygenated with 5% CO_2 in 95% O_2. A basal tension of 5 mN was applied and the tissues were allowed to stabilize. Isometric tension was continuously recorded with Grass force-displacement transducers (FTO3), connected to a Grass model 7D polygraph. The signals were transformed in an NB-MIO-16L-9 analogue digital converting board and registered in a Macintosh IIfx computer with a data acquisition and evaluation programme made with the LabVIEW 2 signal-processing software (National Instruments, Austin, Texas, U.S.A.).

During the stabilization period, which lasted 1 h for guinea-pig tracheal strips and 2 h for human bronchial preparations, the Krebs solution was changed every 15 min. The guinea-pig tracheal strips were tested by adding 0.1 μmol l^{-1} carbachol to the bath followed by 2.3 μmol l^{-1} terbutaline and a subsequent 60 min rinsing and recovery period. Due to the extended time for stabilization, this test procedure was not performed on human bronchi. Tone was induced by adding carbachol, 0.5 or 1 μmol l^{-1}, 15–20 min before addition of the relaxant compounds. Preparations which did not respond with contractile and relaxant effects were discarded. Each preparation was used for one experiment only.

In the interaction studies, a supramaximum concentration of salmeterol, sulfonterol or the vehicle was added to the organ baths 60 min before the cumulative addition of the test substances. The preparation was allowed to equilibrate, usually about 10 min, at each dose stage. Maximum relaxation was established by adding 10 μmol l^{-1} isoprenaline followed by 1 mmol l^{-1} theophylline at the end of the experiment. Relaxant effects were calculated as a percentage of the maximum relaxation induced by theophylline (1 mmol l^{-1}) added at the end of each cumulative concentration-effect curve. Isoprenaline was used to unmask a possible irreversible component of the inhibition by salmeterol.

Concentration-effect curves for the test compounds, obtained with and without salmeterol or sulfonterol, were constructed with the aid of a flexible ruler. In each curve with salmeterol, or sulfonterol, a point was taken from a position midway between the residual relaxing effect of the partial agonist and the maximum relaxation of the test compound. This value (in log units) was substracted from the mean log EC_{50} of the control curve. The difference was regarded as the log of the concentration-ratio (Dougall *et al.*, 1991). This mid-point estimate results in greater concentration-ratios than the iso-effective point estimate used by us in a previous study (Jeppsson *et al.*, 1992) but may be less sensitive to deviations in the slope parameter.

Drugs and solutions

The drugs used were carbamylcholine chloride and (−)-isoprenaline hydrochloride (Sigma Chemical Co., U.S.A.); (±)-salbutamol sulphate (Leiras Pharmaceuticals); (±)-salmefamol (Allen & Hanbury, Ltd, U.K.); (±)-fenoterol hydrobromide (Boehringer-Inghelheim KG, Germany); (±)-procaterol hydrochloride (Warner-Lambert Company, Ann Arbor, U.S.A.); (±)-sulfonterol (Smith Kline & French, Penn, U.S.A.); (±)-terbutaline sulphate, (±)-salmeterol base, (±)-formoterol fumarate and theophylline (Astra Draco AB, Sweden). The drugs were dissolved in saline, when necessary with the aid of acetic acid. In order to prevent oxidation, the stock solutions contained 0.5 mmol l^{-1} ascorbic acid.

The racemates of the β-adrenoceptor agonists were used throughout since the pure enantiomers were available only for a few of them. However, all pharmaceutical preparations for clinical use contain the racemates and, so far, there is no indication of an interaction at β-adrenoceptors between the enantiomers (Jeppsson *et al.*, 1984; Trofast *et al.*, 1991; Johnson *et al.*, 1993).

Statistical evaluation

Data are expressed as means ± s.e.mean with the number of experiments in parentheses. The concentration-ratios, in log units, were compared by Analysis of variance (Anova) and statistical significances were determined with Dunnett's test. The significance of differences observed in human bronchi was determined using Student's *t* test. $P<0.05$ was considered statistically significant.

Results

Guinea-pig trachea

All of the β-adrenoceptor agonists tested caused concentration-dependent relaxation of the guinea-pig tracheal smooth muscle contracted with 1 μmol l^{-1} carbachol (Figure 2). With the exception of salmeterol (and sulfonterol, see below), all of the agonists caused virtually complete (90–100%) relaxation, but that to 1 μmol l^{-1} salmeterol was only about 30%. In the presence of salmeterol at this concentration, the effect of the other β_2-adrenoceptor agonists was attenuated, and the concentration-response curves were shifted to the right. The magnitude of this shift ranged from 1.8 to 2.8 log units, fenoterol and salbutamol being the extremes (Table 1). For salbutamol, in the presence of salmeterol, maximum relaxation was not achieved with concentrations up to 100 μmol l^{-1} and the shift was calculated on the assumption that the curve would reach the control level. In general, the maximum relaxation to theophylline did not exceed that produced by 10 μmol l^{-1} isoprenaline.

The experiment with salbutamol was repeated with a ten fold lower concentration of salmeterol. The relaxant effect of salmeterol, 0.1 μmol l^{-1}, *per se* was comparable to the effect observed with 1 μmol l^{-1} (Figure 2). This result indicates that the concentration-response curve had reached a plateau and is compatible with previous observations made under similar experimental conditions (Jeppsson *et al.*, 1992; Lindén *et al.*, 1993). In the presence of 0.1 μmol l^{-1} salmeterol there was, at most, a two fold (0.3 log units) rightward shift of the concentration-response curve for salbutamol. The average time to reach effect equilibrium after each dose given in the cumulative concentration-effect curves was 9 min. This time was the same with and without salmeterol and independent of the agonist used. Salmeterol, however, was given 60 min to equilibrate.

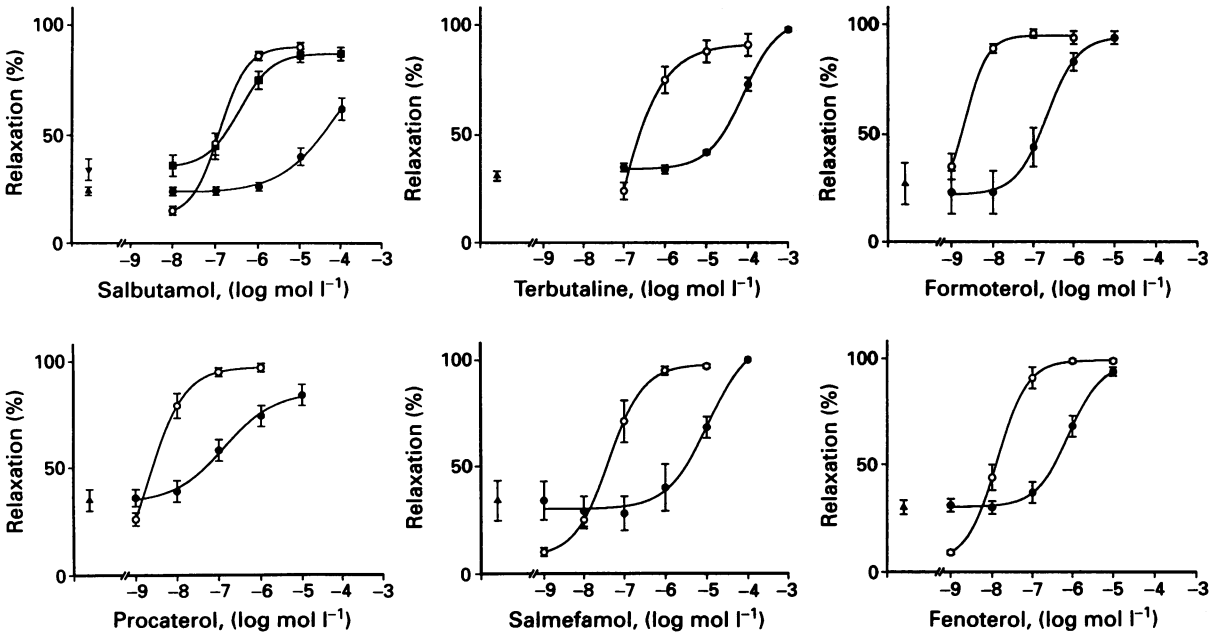


Figure 2 Inhibition of salmeterol of the relaxing effect of a series of β_2-adrenoceptor agonists in the guinea-pig trachea. Tone was induced by carbachol (1 μmol l^{-1}). Concentration-effect curves were obtained without (○) and with (●) 1 μmol l^{-1} salmeterol; in some experiments 0.1 μmol l^{-1} salmeterol (■). The effects of salmeterol *per se* (▲ 1 μmol l^{-1} and ▼ 0.1 μmol l^{-1}) are indicated to the left. The data are the means ± s.e. of 6–8 experiments.

Table 1 Inhibition, expressed as concentration-ratios, by salmeterol (1 μmol l^{-1}) of the relaxant effect of a series of β_2-adrenoceptor agonists on the guinea-pig trachea

Compound	*pD_2 without salmeterol*	*log concentration-ratio*	*Significantly different from salbutamol/terbutaline*	
Salbutamol	6.89 ± 0.10 (9)	2.83 ± 0.19 (6)	–	NS
Terbutaline	6.63 ± 0.10 (6)	2.55 ± 0.09 (6)	NS	–
Formoterol	8.76 ± 0.09 (6)	2.17 ± 0.07 (6)	$P<0.01$	NS
Salmefamol	7.28 ± 0.18 (6)	2.03 ± 0.09 (6)	$P<0.01$	$P<0.05$
Procaterol	8.37 ± 0.09 (6)	1.94 ± 0.11 (6)	$P<0.01$	$P<0.01$
Fenoterol	7.74 ± 0.12 (8)	1.81 ± 0.10 (6)	$P<0.01$	$P<0.01$

Data, means ± s.e., from experiments shown in Figure 2.

Table 2 Inhibition, expressed as concentration-ratios, by sulfonterol (20 μmol l^{-1}) of the relaxant effect of a series of β_2-adrenoceptor agonists on the guinea-pig trachea

Compound	*pD_2 without sulfonterol*	*log concentration-ratio*	*Significantly different from salbutamol*
Salbutamol	7.33 ± 0.12 (6)	2.81 ± 0.03 (6)	–
Formoterol	8.99 ± 0.14 (6)	2.59 ± 0.07 (6)	$P<0.05$
Fenoterol	8.04 ± 0.12 (6)	2.65 ± 0.03 (6)	NS

Data, means ± s.e. from experiments shown in Figure 3.

In separate control experiments sulfonterol was substituted for salmeterol. The relaxation induced by 20 μmol l^{-1} sulfonterol at the start of the cumulative addition of the agonist was about 11% (Figure 3). Like salmeterol, sulfonterol shifted the concentration-response curves for salbutamol, formoterol and fenoterol to the right. However, compared with the results obtained with salmeterol (Table 1), the difference in concentration-ratios between salbutamol and fenoterol disappeared and that between salbutamol and formoterol was largely eliminated when sulfonterol was used as antagonist (Table 2).

Human bronchus

Formoterol, terbutaline and salmeterol caused concentration-dependent relaxation of the human bronchial smooth muscle contracted with 0.5 μmol l^{-1} carbachol (Figure 4). The relaxation to formoterol and terbutaline was almost complete (~90%), whereas that to salmeterol achieved only about 40%. Formoterol was about 400 times more potent than terbutaline ($P<0.001$). The relaxant potency of salmeterol was intermediate between those of formoterol and terbutaline, but the effect was variable (two out of 10 preparations responded with an increase in tone).

In preparations contracted by 1 μmol l^{-1} carbachol (approximate EC_{50}) the relaxation to 1 μmol l^{-1} salmeterol was reduced to about 20% while the maximum relaxation to formoterol was 80–90% (Figure 5). In the presence of salmeterol (1 μmol l^{-1}) the concentration-effect curve of formoterol was shifted to the right by 2–3 log units ($P<0.01$).

Discussion

According to the basic principles for agonist/antagonist interaction, a competitive antagonist, or a partial agonist, causes a parallel shift to the right of the concentration-effect curve of an agonist with higher efficacy (Ruffolo, 1982). The magnitude of this shift is determined by the concentration of the antagonist and its affinity for the receptor. All agonists acting on the same receptor should be equally inhibited. Salmeterol caused an apparently parallel shift of the concentration-effect curves for all the agonists studied with the possible exception of salbutamol and procaterol. These two

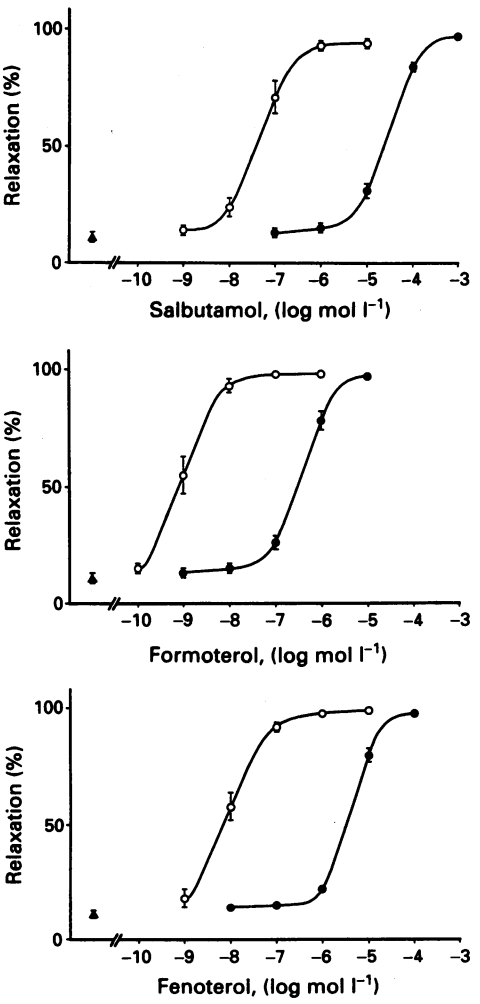


Figure 3 Inhibition of sulfonterol of the relaxant effect of a series of β_2-adrenoceptor agonists in the guinea-pig trachea. Tone was induced by carbachol (1 μmol l^{-1}). Concentration-effect curves were obtained without (○) and with (●) 20 μmol l^{-1} sulfonterol. The effect of sulfonterol *per se* (▲) is indicated to the left. The data are the means ± s.e. of 6 experiments.

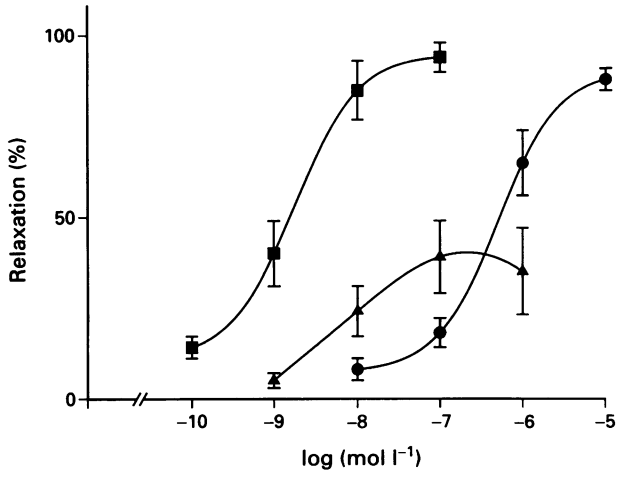


Figure 4 Relaxation by formoterol (■), terbutaline (●) and salmeterol (▲) of the human bronchus. Tone was induced by carbachol (0.5 μmol l^{-1}). The data are the means ± s.e. of 7–10 experiments.

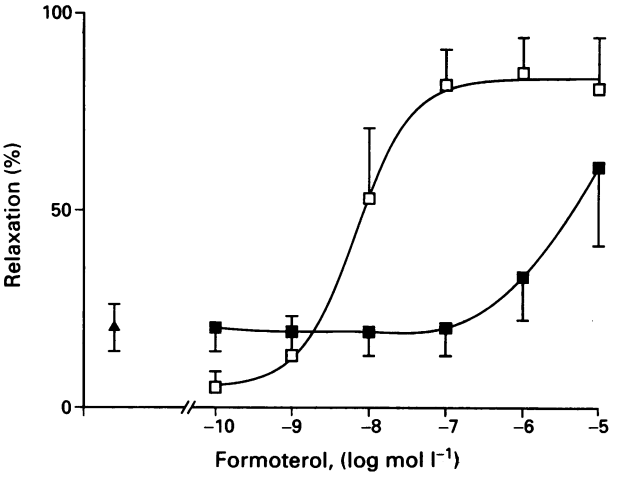


Figure 5 Inhibition by salmeterol of the relaxant effect of formoterol in human bronchus. Tone was induced by carbachol (1 μmol l^{-1}). Concentration-effect curves were obtained without (□) and with (■) 1 μmol l^{-1} salmeterol. The effect of salmeterol *per se* (▲) is indicated to the left. The data are the means ± s.e. of 3 preparations from two lungs.

β_2-agonists showed concentration-effect curves, which tended to be less steep in the presence of salmeterol. It should be recalled that Dougall *et al.* (1991), using adrenaline and isoprenaline as agonists, noted significantly less steep concentration-effect curves in the presence of salmeterol as compared to control curves. These authors interpreted this as non conformance with simple competition. However, the magnitude of the rightward shift in our study was different for the different agonists, both salbutamol and terbutaline were more inhibited than procaterol and fenoterol.

A number of factors may contribute to experimental results deviating from the general rules of agonist/antagonist interaction depicted above. Firstly, during non-equilibrium conditions, the results obtained may indicate differences in diffusion rate rather than differences in, for example, drug-receptor interaction. Thus the pA_2-value of 5.9 reported for salmeterol, with formoterol as agonist, on the oxidative respiratory burst in guinea-pig eosinophils was considered an under-estimation due to non-equilibrium conditions (Rabe *et al.*, 1993a). The pA_2 value for salmeterol estimated against formoterol in guinea-pig trachea was 7.4 (Jeppsson *et al.*, 1992), a value compatible with the present results and with the pK_i-value calculated from binding data on rat lung membranes (Brittain *et al.*, 1988; Coleman *et al.*, 1990). The time to reach effect equilibrium for the agonists in our experiments was in general 8–9 min per dose and did not appear to be different in the presence or absence of salmeterol. Thus, non-equilibrium conditions are less likely to have caused the differences observed.

Secondly, in the presence of a β_2-selective antagonist, a non-selective β-agonist may relax guinea-pig tracheal smooth muscle via β_1-adrenoceptors (O'Donnell & Wanstall, 1981; Johansson *et al.*, 1984). This may explain why the highly β_2-selective ligand, salmeterol inhibited the relaxant effect of isoprenaline only slightly (Jeppsson *et al.*, 1992). It could also explain the large difference in salmeterol-induced displacement observed between salbutamol and fenoterol, the latter being a less β_2-selective agonist, largely due to its higher efficacy at β_1-adrenoceptors (Brittain *et al.*, 1976). However, procaterol, which is much more β_2-selective than salbutamol (Yabuuchi, 1977), is more like fenoterol than salbutamol with respect to interaction with salmeterol, so other factors must also be considered.

A third possibility is related to the anomalous binding properties of salmeterol. In addition to binding to the β_2-adrenoceptor proper, salmeterol appears to interact more or less irreversibly, with an exosite (Bradshaw *et al.*, 1987; Nials *et al.*, 1993). The chemical structure of the competing agonist or antagonist, will then be critical for the interaction. Taking this into consideration, it is interesting to note than salbutamol and terbutaline, which have a relatively small substituent on the nitrogen atom, were inhibited to a larger extent than compounds with an extended substitution in this position, for example, formoterol and fenoterol. The anomalous binding of salmeterol is further highlighted by the experiments with sulfonterol. This low efficacy agonist inhibited salbutamol, formoterol and fenoterol to approximately the same extent. Moreover, on the spontaneously contracted guinea-pig trachea salbutamol and fenoterol (β_2-selective), but not isoprenaline (unselective), produced superimposable Schildt plots with the highly β_2-selective adrenoceptor antagonist, ICI 118.551 (O'Donnell & Wanstall, 1981).

A number of β-adrenoceptor antagonists with different chemical structures were tested for their ability to reverse the inhibitory effect of salmeterol on electrically stimulated guinea-pig trachea preparations (Nials *et al.*, 1993). These authors did not note any differences in inhibitory effects between the antagonists with regard to their interaction with salmeterol and isoprenaline, respectively. However, the agonist/antagonist interaction was not expressed in quantitative terms and a further analysis is warranted.

On the human bronchus the concentration-response curve to formoterol was shifted to the right in the presence of increasing concentrations of carbachol, consistent with functional antagonism (Buckner & Saini, 1975). Moreover, the maximum relaxation achieved by salmeterol decreased, which is expected from an agonist with a relatively low efficacy. These results confirm, and extend, previous observations on isolated preparations from human bronchi (Ball *et al.*, 1991; Coleman *et al.*, 1991; Naline *et al.*, 1994). Terbutaline and formoterol displayed an efficacy higher than that of salmeterol as judged from the maximum relaxation achieved. The relaxant effect of formoterol on the human bronchus appeared to be competitively inhibited by salmeterol in a way similar to that observed on the guinea-pig trachea. Naline *et al.* (1994) in their study on human bronchus found that salmeterol inhibited the relaxation by adrenaline in a way that they judged as noncompetitive, again indicating a complex interaction of salmeterol with other β-adrenoceptor agonists.

The clinical consequences of the low efficacy of salmeterol have not been fully evaluated. In mild asthmatics, salmeterol does not seem to attenuate the effect of salbutamol, the combined effects of the two drugs being largely additive (Smyth *et al.*, 1993). However, in a very recent case report

(Ulrik & Kok-Jensen, 1994) it appeared that a patient who was a poor responder to salmeterol improved significantly after formoterol. In our experiments on human bronchus, half maximum contraction was induced by carbachol. This condition is difficult to translate into clinical terms. But it cannot be excluded that in patients with severe bronchoconstriction, undue overuse of salmeterol may cause attenuation of the effect of a β_2-adrenoceptor agonist with higher efficacy.

We are indebted to Dr Anders Källén for expert statistical advice.

References

BALL, D.I., BRITTAIN, R.T., COLEMAN, R.A., DENYER, L.O.H., JACK, D., JOHNSON, M., LUNTS, L.H.C., NIALS, A.T., SHELDRICK, K.E. & SKIDMORE, I.F. (1991). Salmeterol, a novel, long-acting β_2-adrenoceptor agonist, characterization of pharmacological activity *in vitro* and *in vivo*. *Br. J. Pharmacol.*, **104**, 665–671.

BEACH, J.R., YOUNG, C.L., STENTON, S.C., AVERY, A.J, WALTERS, E.H. & HENDRICK, D.J. (1992). A comparison of the speeds of action of salmeterol and salbutamol in reversing metacholine-induced bronchoconstriction. *Pulm. Pharmacol.*, **5**, 133–135.

BRADSHAW, J.R., BRITTAIN, R.T., COLEMAN, R.A., JACK, D., KENNEDY, I., LUNTS, L.H.C. & SKIDMORE, I.F. (1987). The design of salmeterol, a long-acting selective β_2-adrenoceptor agonist. *Br. J. Pharmacol.*, **92**, 590P.

BRITTAIN, R.T., DEAN, C.M. & JACK, D. (1976). Sympathomimetic bronchodilator drugs. *Pharmacol. Ther. Bull.*, **2**, 423–462.

BRITTAIN, R.T., JACK, D. & SUMNER, M.J. (1988). Further studies on the long duration of action of salmeterol, a new selective β_2-stimulant bronchodilator. *J. Pharm. Pharmacol.*, **40**, 93P.

BUCKNER, C.K. & SAINI, R.K. (1975). On the use of functional antagonism to estimate dissociation constants for beta adrenergic receptor agonists in isolated guinea-pig trachea. *J. Pharmacol. Exp. Ther.*, **194**, 565–574.

COLEMAN, R.A., JOHNSON, M., NIALS, A.T. & SUMNER, M.J. (1990). Salmeterol, but not formoterol, persists at β_2-adrenoceptors *in vitro*. *Br. J. Pharmacol.*, **99**, 121P.

COLEMAN, R.A., NIALS, A.T., VARDEY, C.J., RABE, K.F. & MAGNUSSEN, H. (1991). Effects of salmeterol, albuterol and formoterol on human bronchial smooth muscle. *Am. Rev. Resp. Dis.*, **145**, A391.

DOUGALL, I.G., HARPER, D., JACKSON, D.M. & LEFF, P. (1991). Estimation of the efficacy and affinity of the β_2-adrenoceptor agonist salmeterol in guinea-pig trachea. *Br. J. Pharmacol.*, **104**, 1057–1061.

JACK, D. (1991). A way of looking at agonism and antagonism: Lessons from salbutamol, salmeterol and other β-adrenoceptor agonists. *Br. J. Clin. Pharmacol.*, **31**, 501–514.

JEPPSSON, A.-B., JOHANSSON, U. & WALDECK, B. (1984). Steric aspects of agonism and antagonism at β-adrenoceptors: experiments with the enantiomers of terbutaline and pindolol. *Acta. Pharmacol. Toxicol.*, **54**, 285–291.

JEPPSSON, A.-B., KÄLLSTRÖM, B.-L. & WALDECK, B. (1992). Studies on the interaction between formoterol and salmeterol in guinea-pig trachea in vitro. *Pharmacol. Toxicol.*, **71**, 272–277.

JEPPSSON, A.-B., LÖFDAHL, C.-G., WALDECK, B. & WIDMARK, E. (1989). On the predictive value of experiments in vitro in the evaluation of the effect duration of bronchodilator drugs for local administration. *Pulm. Pharmacol.*, **2**, 81–85.

JOHANSSON, L.-H., PERSSON, H. & ROSENGREN, E. (1984). Is there any evidence of β_1-adrenoceptors mediating relaxation of guinea-pig lung parenchyma? *Acta Pharmacol. Toxicol.*, **54**, 346–351.

JOHNSON, M., BUTCHERS, P.R., COLEMAN, R.A., NIALS, A.T., STRONG, P., SUMNER, M.J., VARDEY, C.J. & WHELAN, C.J. (1993). The pharmacology of salmeterol. *Life Sci.*, **52**, 2131–2143.

KAISER, C., SCHWARTZ, M.S., COLELLA, D.F. & WARDELL, Jr. J.R. (1975). Adrenergic agents. 3. Synthesis and adrenergic activity of some catecholamine analogs bearing a substituted sulfonyl or sulfonylalkyl group in the metaposition. *J. Med. Chem.*, **18**, 674–683.

LINDÈN, A., BERGENDAL, A., ULLMAN, A., SKOOGH, B.-E. & LÖFDAHL, C.-G. (1993). Salmeterol, formoterol, and salbutamol in the isolated guinea pig trachea: differences in maximum relaxant effect and potency but not in functional antagonism. *Thorax*, **48**, 547–553.

NALINE, E., ZHANG, Y., QIAN, Y., MAIRON, N., ANDERSON, G.P., GRANDORDY, B. & ADVENIER, C. (1994). Relaxant effects and durations of action of formoterol and salmeterol on the isolated human bronchus. *Eur. Respir. J.*, **7**, 914–920.

NIALS, A.T., SUMNER, M.J., JOHNSON, M. & COLEMAN, R.A. (1993). Investigations into factors determining the duration of action of the β2-adrenoceptor agonist, salmeterol. *Br. J. Pharmacol.*, **108**, 507–515.

O'DONNELL, S.R. & WANSTALL, J.C. (1981). Pharmacological approaches to the characterization of β-adrenoceptor populations in tissues. *J. Auton. Pharmacol.*, **1**, 305–312.

RABE, K.F., GIEMBYCZ, M.A., DENT, G., PERKINS, R.S., EVANS, P. & BARNES, P.J. (1993a). Salmeterol is a competitive antagonist at β-adrenoceptors mediating inhibition of respiratory burst in guinea-pig eosinophils. *Eur. J. Pharmacol.*, **231**, 305–308.

RABE, K.F,. JÖRRES, R., NOWAK, D., BEHR, N. & MAGNUSSEN, H. (1993b). Comparison of the effects of salmeterol and formoterol on airway tone and responsiveness over 24 hours in bronchial asthma. *Am. Rev. Respir. Dis.*, **147**, 1436–1441.

RUFFOLO, R.R. Jr. (1982). Important concepts of receptor theory. *J. Auton. Pharmacol.*, **2**, 277–295.

SMYTH, E.T., PAVORD, I.D., WONG, C.S., WISNIEWSKI, A.F.Z., WILLIAMS, J. & TATTERSFIELD, A.E. (1993). Interaction and dose equivalence of salbutamol and salmeterol in patients with asthma. *Br. Med. J.*, **306**, 543–545.

TROFAST, J., ÖSTERBERG, K., KÄLLSTRÖM, B.-L. & WALDECK, B. (1991). Steric aspects of agonism and antagonism at β-adrenoceptors: synthesis of and pharmacological experiments with the anantiomers of formoterol and their diastereomers. *Chirality*, **3**, 443–450.

ULRIK, C.S. & KOK-JENSEN, A. (1994). Different bronchodilating effect of salmeterol and formoterol in an adult asthmatic. *Eur. Respir. J.*, **7**, 1003–1005.

WALDECK, B., JEPPSSON, A.-B. & WIDMARK, E. (1986). Partial agonism and functional selectivity: a study on β-adrenoceptor mediated effects in tracheal, cardiac and skeletal muscle. *Acta Pharmacol. Toxicol.*, **58**, 209–218.

WALDECK, B. & KÄLLSTRÖM, B.-L. (1991). Salmeterol inhibits the relaxing effect of formoterol on guinea-pig tracheal smooth muscle: evidence for partial agonism at β_2-adrenoceptors. *Br. J. Pharmacol.*, **104**, 402P.

WEGENER, T., HEDENSTRÖM, H. & MELANDER, B. (1992). Rapid onset of action of inhaled formoterol in asthmatic patients. *Chest*, **102**, 535–538.

YABUCHI, Y. (1977). The β-adrenoceptor stimulant properties of OPC-2009 on guinea-pig isolated tracheal, right atrial and left atrial preparations. *Br. J. Pharmacol.*, **61**, 513–521.

(Received June 7, 1994
Accepted June 17, 1994)

Br. J. Pharmacol. (1994), **113**, 693–698 © Macmillan Press Ltd, 1994

Cyclo-oxygenase and nitric oxide synthase isoforms in rat carrageenin-induced pleurisy

[1]Annette Tomlinson, Ian Appleton, Adrian R. Moore, Derek W. Gilroy, Dean Willis, Jane A. Mitchell & Derek A. Willoughby

Department of Experimental Pathology, The William Harvey Research Institute, St. Bartholomew's Hospital Medical College, Charterhouse Square, London, EC1M 6BQ

1 The profiles of cyclo-oxygenase (COX) and nitric oxide synthase (NOS) isoforms were determined in the rat carrageenin-induced pleurisy model of acute inflammation.

2 The enzymes were assessed in peripheral blood leucocyte (PBL) cell pellets taken from untreated animals and at 2, 6 and 24 h after injection of the irritant in pleural exudate cell pellets and lung homogenates.

3 COX activity was assessed by the generation of prostacyclin (PGI_2, measured as the stable metabolite, 6-keto prostaglandin $F_{1\alpha}$) and prostaglandin E_2 (PGE_2). Western blot analysis and immunohistochemistry were also carried out.

4 NOS activity was based on the conversion of [^{3}H]-L-arginine to [^{3}H]-L-citrulline in the presence (total NOS activity) or absence of Ca^{2+} (inducible NOS; iNOS).

5 Peripheral blood leucocyte samples contained low levels of COX activity. In pleural exudate cell pellets, COX activity peaked at 2 to 6 h after injection of the carrageenin. At 24 h, COX activity was significantly reduced.

6 Western blot analysis demonstrated that the inducible isoform of COX (COX-2), was the predominant enzyme at all time points. Low levels of COX-2 were seen in PBLs. In pleural exudate cell pellets maximal COX-2 protein levels were seen at 2 h.

7 Immunohistochemistry confirmed the findings of Western blot studies. Approximately 10% of polymorphonuclear neutrophils (PMNs) in PBLs from untreated animals were immunopositive for COX-2. In cell pellet smears from carrageenin-induced pleurisy taken 2 h after injection of the irritant, PMNs were also the major source of COX-2 immunoreactivity. A small proportion of macrophages and mesothelial cells were also immunolabelled for COX-2.

8 Low levels of NOS activity were seen in PBLs. In pleural exudates NOS activity was maximum at 6 h and greatly reduced by 24 h. This activity was solely attributable to iNOS.

9 The present results illustrated a similar profile of COX and NOS activity in the carrageenin-induced pleurisy model of acute inflammation. It was demonstrated that COX-2 and iNOS were the predominant isoforms of their respective enzymes.

Keywords: Inducible cyclo-oxygenase; COX-2; nitric oxide synthase; inflammation; carrageenin pleurisy

Introduction

Arachidonic acid is an integral part of cell membrane phospholipids. The release of free arachidonic acid is via the rate limiting action of phospholipase A_2 on phosphatidylcholine or phospholipase C on phosphatidylinositol. Once generated, arachidonic acid is converted to prostaglandin G_2 (PGG_2) followed by PGH_2 and subsequently to prostaglandins and thromboxanes by the cyclo-oxygenase (COX) pathway (see Vane & Botting, 1987). Inhibition of COX is the mechanism of action of non-steroidal anti-inflammatory drugs (NSAIDs; Vane, 1971). Recently, two isoforms of COX have been identified, a constitutive COX (COX-1) and a mitogen-inducible COX (COX-2; see Xie *et al.*, 1992). We have shown *in vitro*, that NSAIDs have a differential inhibitory capacity on the two COX isoforms (Mitchell *et al.*, 1993a). This raises the possibility that selective inhibition of the predominant isoform of COX in inflammation, may prove more effective than conventional therapies.

Nitric oxide (NO) is a free radical involved in neurotransmission, cell mediated cytotoxicity and endothelium-dependent relaxation of vascular smooth muscle (for review see Moncada *et al.*, 1991). A number of cell types are capable of generating NO via nitric oxide synthase (NOS) from L-arginine (for review of NOS isoforms see Forstermann *et al.*, 1991). A constitutive, calcium-dependent isoform of NOS is present in endothelial cells, neurones and platelets (Radomski *et al.*, 1990). A second, calcium-independent isoform of NOS (iNOS) can be induced in endothelial cells, macrophages, vascular smooth muscle cells and fibroblasts.

Acute inflammation is characterized by vasodilatation, plasma extravasation and polymorphonuclear neutrophil (PMN) influx. Vasodilatation induced by a number of agents including bradykinin, histamine, substance P, 5-hydroxytryptamine and thrombin, is dependent on the release of a relaxing factor derived from the endothelium (endothelium-derived relaxing factor; EDRF) which has been shown to be identical to NO (Palmer *et al.*, 1987). In contrast, the vasodilatation induced by the COX metabolites PGE_2 and PGI_2 is independent of the endothelium, acting directly on smooth muscle cells (Chand & Altura, 1981; Cherry *et al.*, 1982). The observation that the vasodilator effects of numerous agents involved in the inflammatory process are mediated by NO signifies a role for this molecule in inflammation, although at present the precise role is obscure. However, modulation of the inflammatory response has been demonstrated in a number of models using inhibitors of NOS. For example, treatment with the NOS inhibitor N^G-monomethyl-L-arginine protects against immune complex-induced inflammation (Mulligan *et al.*, 1991) and use of

[1] Author for correspondence.

N^G-nitro-L-arginine methyl ester suppresses adjuvant-induced arthritis (Ialenti *et al.*, 1993).

Although the products of COX and NOS are implicated in inflammation, the relative contribution of the different isoforms of these enzymes has not been fully established. We have shown previously, that in a murine model of chronic granulomatous inflammation, inducible COX and NOS are the predominant isoforms of their respective enzymes (Vane *et al.*, 1994). Here we have extended these studies and characterized COX and NOS activity in the rat carrageenin-induced pleurisy model of acute inflammation.

Methods

Induction of pleurisy

Male Wistar rats (200 ± 20 g) were anaesthetized with ether and 150 µl of a 1% carrageenin solution in 0.9% NaCl injected into the pleural cavity (Velo *et al.*, 1973). Exudates were collected at 2, 6 and 24 h after injection of the irritant, by pleural lavage with 1 ml protease inhibitory buffer containing: trisodium citrate (3.15%), phenylmethylsulphonyl fluoride (1 mM), pepstatin A (1.5 mM) and leupeptin (0.2 mM) in 10 mM phosphate buffered saline (PBS) pH 7.3, Any exudates with blood contamination were rejected. Cells were counted in a Coulter counter, model Dn (Coulter Electronics Ltd., Luton). Each sample was centrifuged at 800 *g* for 10 min and the resultant cell pellet prepared as outlined below. At all time points lungs from experimental animals were dissected out and samples taken for subsequent procedures. Peripheral blood leucocytes (PBL) from untreated animals were used as control.

Preparation of peripheral blood leucocytes

Blood samples from untreated animals were taken by cardiac puncture and placed immediately in protease inhibitory buffer. Samples were centrifuged at 800 *g* for 10 min, the supernatant discarded and the red blood cells flash lysed by resuspending the cell pellet in 10 ml distilled water for 10 s, followed immediately by the addition of 10 ml, 2 × concentrated protease inhibitory buffer. Cellular debris was removed by two successive centrifugation (800 *g* for 10 min) and resuspension steps. Leucocyte integrity was assessed morphologically by smearing and staining with haematoxylin and eosin.

Assessment of COX activity

Cell pellets from pleural exudates and PBLs were sonicated and tissues from lungs were homogenized at 4°C in protease inhibitory buffer, in a ratio of 5:1 (v/w). The protein concentration in the homogenates was measured by the Bradford assay (Bradford *et al.*, 1976), with bovine serum albumin (BSA) used as standard. Homogenates were incubated at 37°C for 30 min in the presence of excess arachidonic acid (30 µM). The samples were boiled and centrifuged at 10,000 *g* for 30 min. The concentration of 6-keto $PGF_{1\alpha}$ or PGE_2 present in the supernatant was measured by radioimmunoassay. Results are expressed as ng eicosanoid per mg protein per 30 min (ng mg^{-1} 30 min^{-1}).

Western blot analysis

Cell pellets from pleural exudates and PBLs were lysed by the addition of protease inhibitory buffer containing 1% Triton X100 and boiled (10 min) with gel loading buffer (Tris, 50 mM; SDS, 10%; glycerol, 10%; 2-mercapthoethanol, 10%; bromophenol blue, 2 mg per ml) in a ratio of 1:1 and centrifuged at 10,000 *g*, for 10 min. The protein concentrations of supernatants were determined as above, and total protein-equivalents (17 µg) for each sample separated on 10% sodium dodecyl sulphate-polyacrylamide mini-gels (Hoefer; Staffordshire) using the Laemmli buffer system and transferred to polyvinylidene difluoride membranes (Millipore, Hertfordshire). Nonspecific IgGs were blocked with 5% dried milk protein and incubated with specific antibody to COX-1 or COX-2 (both 1:1,000). Bands were detected with an amplified alkaline phosphatase kit and developed with nitroblue tetrazolium (NBT)-5-bromo-4-chloro-3-indonyl phosphate (BCIP). Rainbow marker and pre-stained blue protein markers were used for molecular weight determinations. In experiments using COX-2 antibody, protein equivalents from rat seminal vesicles served as a positive control.

Immunohistochemistry

Peripheral blood and exudate cell samples were smeared onto poly-L-lysine coated slides and allowed to air dry. Prior to immunolabelling or histological staining, smears were fixed in 4% paraformaldehyde in 0.1 M phosphate buffer for 1 h or acetone for 10 min. Endogenous peroxidases were quenched with 0.3% H_2O_2 in methanol and sections washed with 0.1% Triton X100 in PBS. Non-specific binding of IgG's was blocked using normal goat serum (NGS) 1:50 in 0.1% essentially globulin free BSA in PBS. The sections were incubated overnight with polyclonal rabbit anti-COX-1 (1:300) or polyclonal rabbit anti-COX-2 (1:400) at 4°C, washed and incubated for a further 30 min with biotinylated goat anti-rabbit secondary antibody. Following a further 30 min incubation with Vectastain ABC horseradish-peroxidase, the substrate (0.05% diaminobenzidine tetrahydrochloride in 0.05 M Tris buffer pH 7.6) was added for the appropriate time period (5–10 min). This resulted in positive immunoreactivity labelling brown. Primary antiserum was replaced with NGS, as a negative control. Morphological observations were confirmed by use of the routine histological stain, haematoxylin and eosin.

Morphometric analysis

Differential cell counts and the number of immunopositive cells per unit area were determined using a 21 mm eye piece graticule (model NEII, Graticules Ltd.). Results are expressed as the percentage of total cells from an average of $n = 8$ smears, 1000 cells per smear, for peripheral blood and exudate samples at each time point.

Assessment of NOS activity

NOS activity was measured as the ability of exudate and peripheral blood samples to convert [^{3}H]-L-arginine to [^{3}H]-L-citrulline. Samples were prepared as for assessment of COX activity and incubated at room temperature for 30 min in the presence of NADPH (1 mM), calmodulin (30 nM), L-valine (50 mM), tetrahydrobiopterin (5 µM), calcium (2 mM) and a mixture of unlabelled and [^{3}H]-L-arginine (10 µM). In experiments to assess the contribution of the iNOS (calcium-independent) to the total NOS activity, calcium was replaced with EGTA (1 mM). In addition, L-citrulline formation was determined in the absence of NADPH as a measure of nonspecific conversion of L-arginine. Incubations were terminated by the addition of 1 ml HEPES (20 mM, pH 5.5) containing EGTA (1 mM) and EDTA (1 mM). The newly formed L-citrulline was separated from L-arginine by passing the reaction mixture over Dowex columns (1 ml) and the eluted labelled material was measured in a Beckman scintillation counter.

Materials

Radiolabelled prostanoids and Rainbow protein markers were obtained from Amersham International, Buckinghamshire. Polyclonal rabbit anti-COX-1 and polyclonal rabbit

anti-COX-2 were obtained from Cayman Chemicals, MI, U.S.A. Amplified alkaline phosphatase kit and NBT-BCIP colour development reagents were from Bio-Rad Laboratories Ltd., Hemel Hempstead. Biotinylated secondary antibody and ABC Elite kit were from Vector Laboratories, Peterborough. All other chemicals were from Sigma Chemical Co., Poole.

Statistics

Results are expressed as the mean ± s.e.mean for (n) experiments. Statistical analysis was determined by Student's unpaired t test, with a P value of <0.05 considered significant.

Results

Exudate volume and cell count

The COX activity in PBL cell pellets, and carrageenin-induced pleural exudate cell pellets and lung homogenates 6 h and reached a peak of 1.63 ± 0.23 ml at 24 h. The rise in exudate volume was paralleled by an increase in cell influx. At 2 h the total number of cells per ml exudate fluid was $8.9 \pm 2.4 \times 10^6$, this rose to $53.1 \pm 10.9 \times 10^6$ at 6 h and was maximal at 24 h ($111.5 \pm 16.9 \times 10^6$). This is illustrated in Figure 1.

COX activity (PGE_2)

The COX activity in PBL cell pellets, and carrageenin-induced pleural exudate cell pellets and lung homogenates was assessed by the generation of PGE_2 and 6-keto $PGF_{1\alpha}$. Peripheral blood leucocytes from untreated animals contained barely detectable levels of COX activity, as determined by PGE_2 generation. At 2 h after injection of carrageenin, 49.1 ± 10.7 ng PGE_2 per mg protein per 30 min (ng mg^{-1} protein 30 min^{-1}) were generated by the exudate cell pellet (Figure 2a). This fell at 6 h and was significantly reduced ($P<0.01$) by 24 h to 0.9 ± 0.1 ng PGE_2 mg^{-1} protein 30 min^{-1}. In lungs from affected animals low levels of PGE_2 were seen at 2 (5.8 ± 1 ng mg^{-1} protein 30 min^{-1}), 6 (4.1 ± 0.5 ng mg^{-1} protein 30 min^{-1}) and 24 h (4.06 ± 0.5 ng mg^{-1} protein 30 min^{-1}). However, no significant differences between time points was observed for PGE_2 levels in lung homogenates (see Figure 2a).

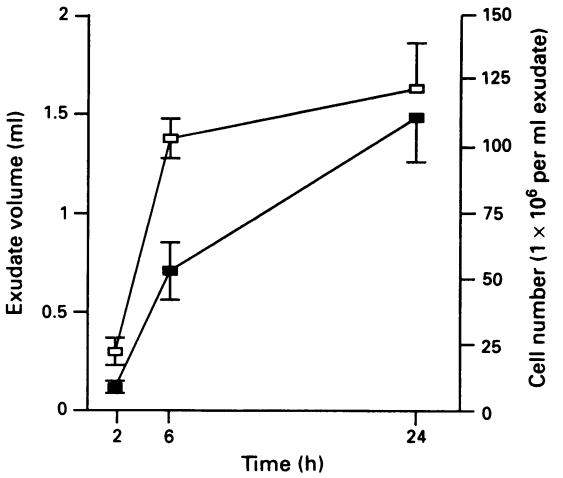


Figure 1 Time course of exudate volume (□) and inflammatory cell influx (■) in the rat carrageenin-induced pleurisy. Each point represents the mean ± s.e.mean from $n = 8$ experiments.

COX activity (6-keto $PGF_{1\alpha}$)

It was not possible to detect 6-keto $PGF_{1\alpha}$ liberation in PBL samples. The profile of 6-keto $PGF_{1\alpha}$ in cell pellets from pleural exudates and lung homogenates is illustrated in Figure 2b. In the case of carrageenin-induced pleural cell pellets the production of 6-keto $PGF_{1\alpha}$ was similar, but always proportionally greater than that of PGE_2. Maximal levels of 6-keto $PGF_{1\alpha}$ in exudate samples were seen at 6 h (128.1 ± 32.6 ng mg^{-1} protein 30 min^{-1}) and were significantly ($P<0.01$) reduced to 14.5 ± 2.5 ng mg^{-1} protein 30 min^{-1}, at 24 h. The production of 6-keto $PGF_{1\alpha}$ by lung homogenates was significantly lower than in exudate cell pellets at all time points, with levels of 38.4 ± 12.3, 26.4 ± 6.7 and 14.3 ± 2.9 ng mg^{-1} protein 30 min^{-1} at 2, 6 and 24 h respectively. No statistically significant difference was observed between time points.

Western blot analysis

At all time points, barely detectable levels of COX-1 protein were discerned (data not shown). The COX-2 protein levels in seminal vesicles, PBLs and carrageenin exudate cell pellets are shown in Figure 3. Low levels of COX-2 were seen in PBLs. The intensity of COX-2 labelling in exudate cell pellets varied, with maximal levels at 2 h in $n = 8$ experiments, whereas in 2 out of the total 10 experiments, the peak occurred at 6 h. A characteristic doublet at 72 and 74 kDa

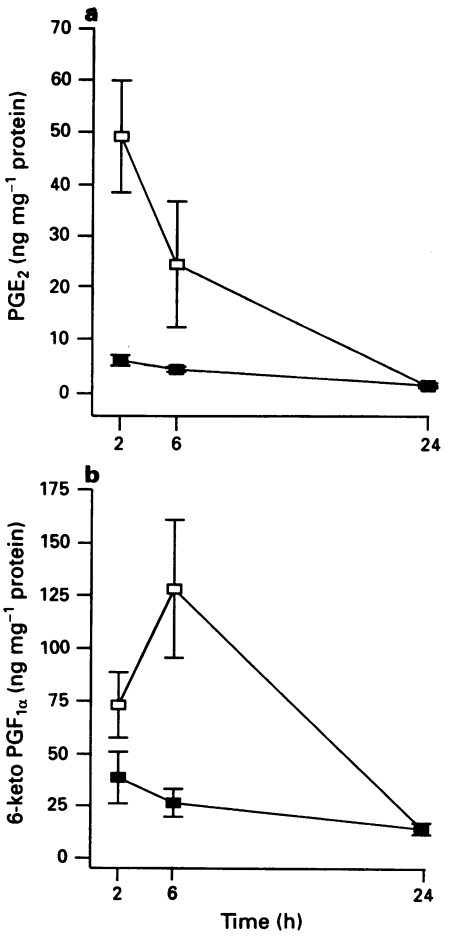


Figure 2 Production of prostaglandin E_2 (PGE_2) (a) and 6-keto $PGF_{1\alpha}$ (b) by homogenates of cell pellets from pleural exudates (□) and lungs (■) from the rat carrageenin-induced pleural model of acute inflammation. Prostaglandins were measured at 2, 6 and 24 h after injection of the irritant. Peripheral blood leucocyte pellets from untreated rats contained little or no COX activity. Each point represents the mean ± s.e.mean from $n = 8$ experiments.

was observed in samples taken at 2 h. In all experiments COX-2 protein was present at lower levels at 24 h. At 6 and 24 h a band at approximately 60 kDa was also seen, which was always less intense than the 72 kDa band. At all time points the levels of COX-2 protein from carrageenin-induced pleural cell pellets were lower than protein equivalents from seminal vesicles.

Immunohistochemistry

In peripheral blood smears, COX-2 immunoreactivity was specifically localized to a discrete population of PMNs and monocytes. Morphometric analysis revealed that of the PMN population, 9.3 ± 1.94% were observed to label positively for COX-2. In the case of the mononuclear cell population this figure was lower with only 0.25 ± 0.08% of monocytes labelling.

At 2 h after injection of the carrageenin, the profile of cells from the exudate smears was as follows: 58% PMNs, 8% macrophages, 17% lymphocytes and 17% mesothelial cells (cells lining the pleural cavity). Of the PMN population 84 ± 6.5% were observed to label for COX-2, 82.5 ± 5.1% of macrophages and 53 ± 9.9% of mesothelial cells. No lymphocytes were seen to label for COX-2.

The cell profile at 6 h changed and consisted of 88% PMNs, 10% macrophages, 1.5% lymphocytes and 0.5% mesothelial cells; 69.5 ± 6.5% of the PMNs labelled for COX-2, 13 ± 4% macrophages and 25 ± 2.5% mesothelial cells. No lymphocytes showed COX-2 immunoreactivity.

At 24 h after injection of the carrageenin the exudate cell profile was 63% PMNs, 36% macrophages, 0.6% lymphocytes and 0.4% mesothelial cells. Of the total number of PMNs present 87 ± 3% showed COX-2 immunoreactivity and 15 ± 5.8% of macrophages. The positive immunoreactivity associated with PMNs in a 24 h carrageenin-induced pleurisy is shown in Figure 4.

NOS activity

Cell pellets of PBLs contained barely detectable levels of NOS activity. In cell pellets from carrageenin-induced pleurisy, high levels of total NOS activity were measured at 2 h reaching a maximum at 6 h (550.6 ± 107.7 pmol L-citrulline 30 min^{-1}) (Figure 5). By 24 h, the level of activity was significantly ($P < 0.01$) reduced to 15.2 ± 5.6 pmol L-citrulline. The proportion of total NOS activity due to iNOS was determined by the exclusion of calcium. The profile of iNOS paralleled that of total NOS reaching a peak at 6 h

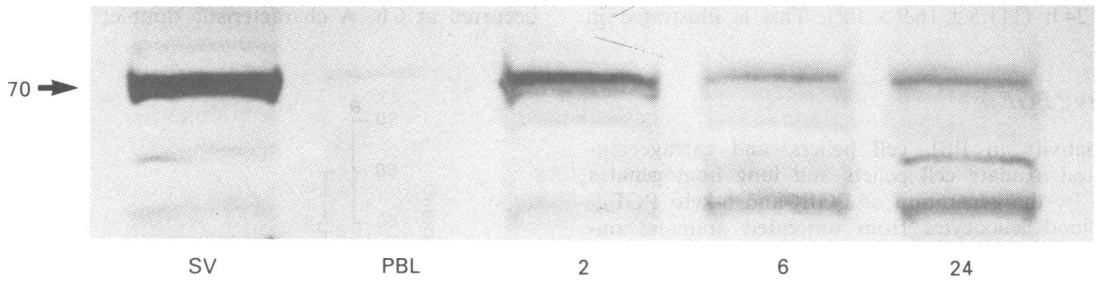


Figure 3 Western blot of the levels of COX-2 protein from extracts of seminal vesicles (SV), peripheral blood leucocytes (PBL) and exudate cell pellets from the rat carrageenin-induced pleural model of inflammation, taken at 2, 6 and 24 h after injection of the irritant. The specific antibody to COX-2 recognised a protein which migrated at 72 kDa molecular weight when compared to protein standards. The levels of COX-2 protein in cell pellets were always lower than in seminal vesicle controls. Note the characteristic doublet at 72 and 74 kDa in the 2 h time point. Note also the presence of a second band at approximately 60 kDa in the exudate samples. Western blots primed with a selective antibody to COX-1 showed low levels of protein, which remained constant throughout the depicted time course (data not shown).

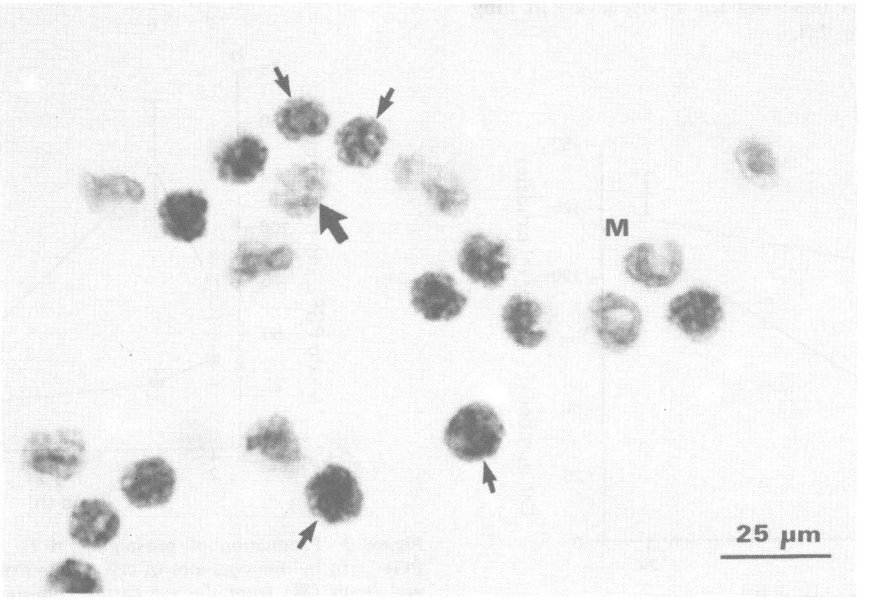


Figure 4 Immunolocalization of COX-2 in a cell smear derived from a rat carrageenin-induced pleurisy taken 24 h after injection of the irritant. The specific localization to PMNs is shown (arrows). Note however, the lack of labelling in a proportion of PMNs (large arrow) and some macrophages (M).

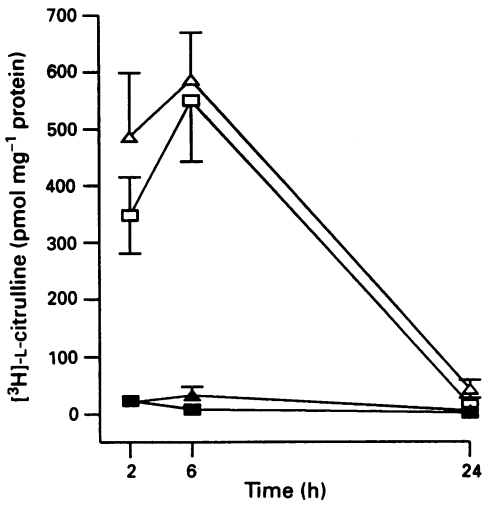


Figure 5 Total NOS activity in homogenates of cell pellets from pleural exudates (□) and lungs (■) from the rat carrageenin-induced pleural model of acute inflammation. NOS activity was measured at 2, 6 and 24 h after injection of the irritant. The calcium-independent activity (iNOS) of cell pellets (△) and lungs (▲) is also shown. Each point represents the mean ± s.e.mean from $n = 8$ experiments.

(587.3 ± 82.6 pmol L-citrulline) with a significant ($P < 0.01$) reduction in activity by 24 h (43.5 ± 15.8 pmol L-citrulline). Detectable levels of calcium-dependent NOS and iNOS activity were seen in lung homogenates, but no significant differences in activity were observed throughout the time course (see Figure 5). The generation of L-citrulline was significantly ($P < 0.001$) reduced in the absence of the essential co-factor NADPH in all samples measured (data not shown).

Discussion

The principal findings of this study are that, in the rat carrageenin-induced pleurisy the predominant isoforms of COX and NOS are COX-2 and iNOS. Furthermore, approximately 10% of circulating PMNs expressed the inducible isoform of COX, i.e. COX-2.

The activity of COX was assessed by the generation of the arachidonic metabolites PGE_2 and the stable metabolite of PGI_2, 6-keto $PGF_{1\alpha}$. In the case of PGE_2, the levels were maximal at 2 h after injection of the carrageenin, whereas 6-keto $PGF_{1\alpha}$ levels were greatest at 6 h. This may be due to differences in the kinetics of their respective isomerases. The peak of COX activity between 2–6 h is consistent with earlier studies measuring prostanoid levels in carrageenin-induced pleural exudates (Velo *et al.*, 1973). The results of the Western blot analysis confirm the findings of Otto *et al.* (1993) where, using murine COX-2 run on SDS-polyacrylamide gel electrophoresis, a 72 and 74 kDa doublet was observed due to N-glycosylation at Asn 580. Glycosylation of COX-2 is essential for enzymic activity, however, glycosylation at Asn 580 has no effect on activity. As the time course progressed a second protein band at approximately 60 kDa occurred, which was most intense at 24 h. This may represent COX-2 degradation products and could explain the decreased COX activity seen at 24 h. Western blot analysis demonstrated that PBLs contained COX-2 protein. The results also show correlation of the activity data for PGE_2, with levels of COX-2 protein, the peak occurring at 2 h after injection of the carrageenin (see Figure 3). In conjunction with the results of the immunohistochemistry, which revealed that a proportion of PMNs were labelled for COX-2, this may indicate that the rapid induction of COX activity seen at 2 h is primarily due to the influx of PMNs. Monocytes were also immunopositive for COX-2, although these formed a small proportion in relation to the number of PMNs labelled. Only a minority of peripheral blood PMNs were immunolabelled for COX-2. This may be due to the process of *ex vivo* extraction, which might result in their activation, or could be an indication that circulating PMNs have a basal level of expression of COX-2, which upon exposure to an inflammatory stimulus is rapidly utilised. Mesothelial cells of the pleural cavity and macrophages were also shown to label positively for COX-2 and could therefore in addition to PMNs contribute to the high levels of COX activity seen at 2 h.

At 24 h, COX activity and protein levels diminished. The percentage of PMNs in the exudate decreased, whereas macrophage numbers had increased. However, although the proportion of PMNs which labelled for COX-2 remained constant, the percentage of immunopositive macrophages decreased. This seems to indicate that as the inflammation progresses, the COX-2 present in macrophages is down regulated, but is unaffected in PMNs. Endothelial cells, once stimulated to produce PGI_2 become unresponsive to the effects of restimulation due to deactivation of COX (Kent *et al.*, 1983; Brotherton & Hoak, 1983). Unlike PMNs, macrophages have a longer life span. Hence, the decrease in COX-2 immunoreactivity seen in macrophages may be due to down regulation after exposure to the initial stimulus. *In vitro*, as promonocytes differentiate into monocytes/macrophages their ability to liberate prostaglandin is increased (Koehler *et al.*, 1990). The findings of the present study showed that a proportion of macrophages were immunolabelled for COX-2. Whether this represents a facet of maturity or is under the constraint of exogenous factors present in the inflammatory exudate requires further investigation. COX and NOS activity was detected in lungs from affected animals. However, the levels were always lower than in pleural exudate cell pellets, indicating that the induction of COX and NOS was localized to the site of injection i.e. the pleural cavity.

We have also shown that NOS activity was similar in profile to COX. In the pleural exudate cell pellet, maximal NOS activity occurred at 6 h after injection of the carrageenin and was significantly decreased after 24 h. Furthermore, it was found that this activity was solely attributed to iNOS, as depletion of calcium from the reaction mixture had no effect on subsequent levels of activity. Both constitutive and inducible forms of NOS are reported to be present in PMNs (Wright *et al.*, 1989; McCall *et al.*, 1989; 1991), whilst macrophages contain iNOS (Iyengar *et al.*, 1987; Marletta *et al.*, 1988). It is possible therefore, that at 6 h after injection of the irritant, the newly influxed monocytes/ macrophages, although representing only 10% of the total exudate cell population, may be responsible for this activity. In macrophages, high levels of NO feedback to switch off iNOS activity, due to NO binding to the haem moiety of the enzyme (Griscavage *et al.*, 1993). Interestingly, NO may also account for the decreased COX activity seen at 24 h as NO can inhibit PGI_2 release (Mitchell *et al.*, 1993b). Hence, the decrease in NOS and COX activity seen at 24 h could be due to a self modulatory, NO-mediated, negative feedback loop.

This study has demonstrated that, in the rat carrageenin-induced pleurisy model of acute inflammation, inducible COX and NOS are the predominant isoforms of their respective enzymes. As the inflammation progressed and the cell population changed from PMN to mononuclear dominated, there was an accompanying decrease in COX and NOS activity. It is possible that in acute inflammation the use of selective inhibitors of COX-2 and iNOS may be more beneficial than existing therapies.

This work was part supported by a grant from ONO Pharmaceutical Co., Ltd., Osaka, Japan. I.A. is a recipient of a Royal Society, Smith and Nephew Research fellowship. D.W. is supported by a grant from Laboratories OM, Geneva, Switzerland.

References

BRADFORD, M.M. (1976). A rapid and sensitive method for the quantitation of microgram quantities of protein utilizing the principle of protein-dye binding. *Anal. Biochem.*, **72**, 248–254.

BROTHERTON, A.F. & HOAK, J.C. (1983). Prostacyclin biosynthesis in cultured vascular endothelium is limited by deactivation of cyclooxygenase. *J. Clin. Invest.*, **72**, 1255–1261.

CHAND, N. & ALTURA, B.M. (1981). Acetylcholine and bradykinin relax intrapulmonary arteries by acting on endothelial cells: role in lung vascular diseases. *Science*, **213**, 1376–1380.

CHERRY, P.D., FURCHGOTT, R.F., ZAWADZKI, J.V. & JOTHIANANDAN, D. (1982). The role of endothelial cells in the relaxation of isolated arteries by bradykinin. *Proc. Natl. Acad. Sci. U.S.A.*, **79**, 2106–2111.

FORSTERMANN, U., SCHMIDT, H.H.H.W., POLLOCK, J.S., SHENG, H., MITCHELL, J.A., WARNER, T.D., NAKANE, M. & MURAD, F. (1991). Isoforms of Nitric Oxide Synthase, Characterization and purification from different cell types. *Biochem. Pharmacol.*, **42**, 1849–1857.

GRISCAVAGE, J.M., ROGERS, N.E., SHERMAN, M.P. & IGNARRO, L.G. (1993). Inducible nitric oxide synthase from a rat alveolar macrophage cell line is inhibited by nitric oxide. *J. Immunol.*, **151**, 6329–6337.

IALENTI, A., MONCADA, S. & DI ROSSA, M. (1993). Modulation of adjuvant arthritis by endogenous nitric oxide. *Br. J. Pharmacol.*, **110**, 701–706.

IYENGAR, R., STUEHR, D.J. & MARLETTA, M.A. (1987). Macrophage synthesis of nitrite, nitrate and N-nitrosamines: precursors and role in respiratory burst. *Proc. Natl. Acad. Sci. U.S.A.*, **84**, 6369–6374.

KENT, R.S., DIEDRICH, S.L. & WHORTON, A.R. (1983). Regulation of vascular prostaglandin synthesis by metabolites of arachidonic acid in perfused rabbit aorta. *J. Clin. Invest.*, **72**, 455–465.

KOEHLER, L., HASS, R., WESSEL, K., DEWITT, D.L., KAEVER, V., RESCH, K. & GOPPELT-STRUEBE, M. (1990). Altered arachidonic acid metabolism during differentiation of the human monoblastoid cell line U937. *Biochim. Biophys. Acta.*, **1042**, 395–403.

MCCALL, T.B., BOUGHTON-SMITH, N.K., PALMER, R.M.J., WHITTLE, B.J.R. & MONCADA, S. (1989). Synthesis of nitric oxide from L-arginine by neutrophils. *Biochem. J.*, **261**, 293–296.

MCCALL, T.B., PALMER, R.M.J. & MONCADA, S. (1991). Induction of nitric oxide synthase in rat peritoneal neutrophils and its inhibition by dexamethasone. *Eur. J. Immunol.*, **21**, 2523–2527.

MARLETTA, M.A., YOON, P.S., IYENGAR, R., LEAF, C.D. & WISHNOK, J.S. (1988). Macrophage oxidation of L-arginine to nitrite and nitrate: nitric oxide is an intermediate. *Biochemistry*, **27**, 8706–8718.

MITCHELL, J.A., AKARASEREENONT, P., THIEMERMANN, C., FLOWER, R.J. & VANE, J.R. (1993a). Selectivity of nonsteroidal antiinflammatory drugs as inhibitors of constitutive and inducible cyclooxygenase. *Proc. Natl. Acad. Sci. USA*, **90**, 11693–11697.

MITCHELL, J.A., SWIERKOSZ, T.A., WARNER, T.D., GROSS, S., THIEMERMANN, C. & VANE, J.R. (1993b). Regulation of prostacyclin synthesis by the release of endogenous nitric oxide in response to bacterial lipopolysaccharide. *Br. J. Pharmacol.*, **109**, 4P.

MONCADA, S., PALMER, R.M.J. & HIGGS, E.A. (1991). Nitric oxide: physiology, pathophysiology, and pharmacology. *Pharmacol. Rev.*, **43**, 109–142.

MULLIGAN, M.S., HEVEL, J.M., MARLETTA, M.A. & WARD, P.A. (1991). Tissue injury caused by deposition of immune complexes is L-arginine dependent. *Proc. Natl. Acad. Sci. U.S.A.*, **88**, 6338–6342.

OTTO, J.C., DEWITT, D.L. & SMITT, W.L. (1993). N-glycosylation of prostaglandin endoperoxide synthases 1 and 2 and their orientations in the endoplasmic reticulum. *J. Biol. Chem.*, **268**, 18234–18242.

PALMER, R.M.J., FERIGIE, A.G. & MONCADA, S. (1987). Nitric oxide release accounts for the biological activity of endothelium-derived relaxing factor. *Nature*, **327**, 524–527.

RADOMSKI, M.W., PALMER, R.M.J. & MONCADA, S. (1990). Characterization of the L-arginine: nitric oxide pathway in human platelets. *Br. J. Pharmacol.*, **101**, 325–332.

VANE, J.R. (1971). Inhibition of prostaglandin synthesis as a mechanism of action for aspirin-like drugs. *Nature*, **231**, 232–235.

VANE, J.R. & BOTTING, R. (1987). Inflammation and the mechanisms of action of anti-inflammatory drugs. *FASEB J.*, **1**, 89–96.

VANE, J.R., MITCHELL, J.A., APPLETON, I., TOMLINSON, A., BISHOP-BAILEY, D., CROXTALL, J. & WILLOUGHBY, D.A. (1994). Inducible isoforms of cyclooxygenase and nitric oxide synthase in inflammation. *Proc. Natl. Acad. Sci. U.S.A.*, **91**, 2046–2050.

VELO, G.P., DUNN, C.J., GIROUD, J.P., TIMSIT, J. & WILLOUGHBY, D.A. (1973). Distribution of prostaglandins in inflammatory exudate. *J. Pathol.*, **111**, 149–158.

WRIGHT, C.D., MULSCH, A., BUSSE, R. & OSSWALD, H. (1989). Generation of nitric oxide by human neutrophils. *Biochem. Biophys. Res. Commun.*, **160**, 813–819.

XIE, W., ROBERTSON, D.L. & SIMMONS, D.L. (1992). Mitogen-inducible prostaglandin G/H synthase: a new target for nonsteroidal antiinflammatory drugs. *Drug. Dev. Res.*, **25**, 249–265.

(Received January 27, 1994
Revised May 3, 1994
Accepted June 17, 1994)

Br. J. Pharmacol. (1994), **113**, 699–702 © Macmillan Press Ltd, 1994

Atypical β-adrenoceptors in the rat isolated common carotid artery

Mabayoje Ayotunde Oriowo

Department of Pharmacology & Toxicology, Faculty of Medicine, Kuwait University, P.O. Box 24923, Safat 13110, Kuwait

1 The possible existence of atypical β-adrenoceptors in vascular smooth muscle of the rat common carotid artery was examined in this study.

2 Isoprenaline produced concentration-dependent relaxation of noradrenaline (10^{-7} M) precontracted ring segments of the carotid artery. The relaxation was not affected by endothelial denudation.

3 Propranolol (10^{-8} M–3×10^{-7} M) shifted the isoprenaline curve to the right without suppressing the maximum response. However, the slope (0.74) of the Schild plot was significantly ($P<0.05$) less than 1.

4 Salbutamol (β_2), CGP 12177 and BRL 37344 (β_3) also concentration-dependently relaxed noradrenaline precontracted artery segments. These relaxations were not affected by propranolol (10^{-7} M). Pretreatment of the artery segments with BRL 37344 did not desensitize the tissue to the relaxant effect of isoprenaline, CGP 12177 and salbutamol.

5 It is concluded that atypical β-adrenoceptors exist in vascular smooth muscle of the common carotid artery.

Keywords: Rat common carotid artery; atypical β-adrenoceptors; (±)-CGP 12177; BRL 37344

Introduction

β-Adrenoceptors were classified into β_1- and β_2-adrenoceptors based on the differential affinities of some tissues to a series of sympathomimetic amines by Lands *et al.* (1967a). Since then, there have been reports of responses produced by β-adrenoceptor agonists which are relatively insensitive to propranolol and other β-adrenoceptor antagonists. Such responses include lipolysis in rat adipose tissue (Arch *et al.*, 1984; Wilson *et al.*, 1984), relaxation of rat proximal (Bianchetti & Manara, 1990) and distal colon (McLaughlin & MacDonald, 1990; Kirkham & Kelly, 1992), fundus (McLaughlin & MacDonald, 1991) and guinea-pig ileum (Bond & Clarke, 1988). These atypical β-adrenoceptors are designated β_3-adrenoceptors (Arch, 1989). The distribution of these receptors is not limited to the gastrointestinal tract. Clark & Bertholet (1983) demonstrated a vasorelaxant effect of pindolol, a non-specific β-adrenoceptor antagonist with significant intrinsic sympathomimetic activity in canine isolated perfused mesenteric vessels. A similar observation has also been made in the rat aorta precontracted with KCl (Doggerell, 1990). In both instances, the vasorelaxant effect of pindolol was not significantly inhibited by propranolol, thus suggesting the presence of an atypical β-adrenoceptor subtype different from the conventional β_1- and β_2-adrenoceptors. In a recent study, it was shown that propranolol antagonized the vasorelaxant effect of isoprenaline in the rat aorta (Gray & Marshall, 1992). However, the K_B value (3×10^{-8} M) was much less than values of $1-3 \times 10^{-9}$ M expected from an action on conventional β_1- and β_2-adrenoceptors. This observation would probably support the presence of atypical β-adrenoceptors in the rat aorta. The present studies were designed to determine the possible existence of β_3-adrenoceptors in vascular smooth muscles of the rat.

Methods

Sprague-Dawley rats of either sex weighing 150–200 g were used in this study. Each rat was anaesthetized with chloroform and bled through a cut in the abdominal aorta. The common carotid arteries were isolated and carefully cleaned of any connective tissue. Thereafter ring segments (3–4 mm) were set up for isometric tension recording, in a 30.0 ml organ bath containing Krebs solution of the following composition (mM): NaCl 119, $NaHCO_3$ 25, KCl 4.7, $MgSO_4$ 1.5, $CaCl_2$, 2.5, KH_2PO_4 1.2 and glucose 11.0. The solution was bubbled continuously with a 95% O_2 and 5% CO_2 gas mixture. The pH was approximately 7.4. To obtain relaxant responses, the arterial segments were contracted with noradrenaline (10^{-7} M). This concentration of noradrenaline usually produced about 85–90% of the maximum contraction in this tissue. Ascending concentrations of the agonists were added cumulatively to generate a concentration-response curve. Unless otherwise stated, the endothelium was maintained intact as shown by the ability of carbachol (10^{-6} M) to relax noradrenaline precontracted ring segments. When antagonists were used, each antagonist concentration was added to the bath and allowed to equilibrate with the tissue for 30 min before the agonist concentration-response curve was repeated. In all cases, only one agonist/antagonist pair was tested on any one preparation and only one antagonist concentration was tested on each preparation. Antagonist potency was expressed as the pA_2 value obtained according to Arunlakshana & Schild (1959). Antagonism was assumed to be competitive when the slope of the Schild regression line was not significantly different from 1. In preliminary experiments, the potency of isoprenaline was not affected by including cocaine (3×10^{-6} M) and deoxycorticosterone acetate (10^{-5} M) in the Krebs solution to block uptake$_1$ and uptake$_2$ respectively. These blockers were therefore not routinely used in this study.

Drug solutions

The following drugs were used in this study; carbachol hydrochloride, (−)-noradrenaline (arterenol) hydrochloride, (±)-propranolol hydrochloride (all from Sigma), (±)-CGP 12177 (4-[3-[1,1-dimethyl(ethyl)amino]-2-hydroxypropoxy]-1, 3-dihydro-2H-benzimidazol-2-one hydrochloride), salbutamol, (±)-isoprenaline (isoproterenol) hydrochloride (RBI) and BRL 37344, (**R*R***)-(±)-[4-[2-[2-(3-chlorophenyl)-2-

[1] Author for correspondence.

hydroxyethylamino]propyl]phenoxyacetic acid (courtesy of Smithkline Beecham, Epsom, Surrey). All the compounds were dissolved in distilled water or dilute hydrochloric acid.

Statistical analysis

Results are presented as mean ± s.e. of n number of experiments. Mean values were compared by Student's t test and differences between mean values were accepted as significant when $P<0.05$.

Results

Isoprenaline (10^{-8} M–10^{-5} M), produced concentration-dependent relaxation of noradrenaline (10^{-7} M) precontracted ring segments of the rat common carotid artery (Figure 1). The pD_2 value was 7.1 ± 0.1 ($n = 8$). In all cases, isoprenaline produced 100% relaxation (of the induced tone) and in some cases, even a little relaxation below the baseline. The relaxation was rapid in onset and the peak response was attained within 90 s. Propranolol (10^{-8} M–3×10^{-7} M) shifted the isoprenaline concentration-response curve to the right without reducing the maximum response (Figure 2). The Schild plot gave a straight line with a slope of 0.74 ± 0.07. As this value was significantly ($P<0.05$) less than 1, the X-intercept (8.85) was therefore strictly not a pA_2 value. Isoprenaline (10^{-8} M–10^{-5} M) relaxed the precontracted ring segments of the carotid artery with or without the endothelium.

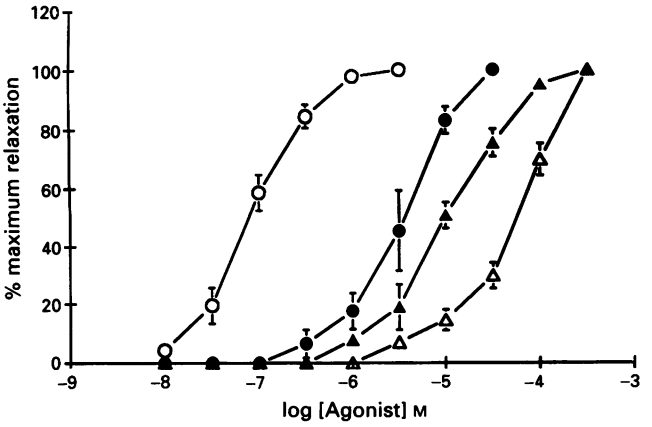


Figure 1 Inhibitory effect of isoprenaline (○), CGP 12177 (●), salbutamol (▲) and BRL 37344 (△) on ring segments of rat common carotid artery precontracted with noradrenaline (10^{-7} M). Each point represents the mean ± s.e. of 4–8 experiments.

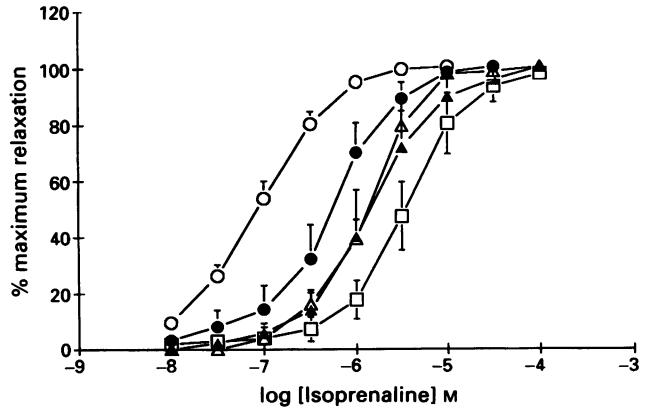


Figure 2 Concentration-response curves for isoprenaline in the absence (○) and in the presence of propranolol 10^{-8} M (●), 3×10^{-8} M (△), 10^{-7} M (▲) and 3×10^{-7} M (□). Each point represents the mean ± s.e. of 4 experiments.

Relaxant effects of selective β-adrenoceptor agonists on the precontracted carotid artery

CGP 12177 (10^{-6} M–3×10^{-5} M), BRL 37344 (10^{-5} M–3×10^{-4} M) and salbutamol (10^{-6} M–10^{-4} M) also concentration-dependently (Figure 1) relaxed ring segments of the carotid artery contracted with noradrenaline (10^{-7} M). The relaxant effects of CGP 12177 and salbutamol were rapid in onset and a peak response was usually attained within 120 s. On the other hand, the relaxant effect of BRL 37344 was slow in onset and the peak response was achieved in about 5–8 min. Removal of the endothelium did not modify the relaxant effect of CGP 12177, BRL 37344 and salbutamol. pD_2 values were 5.4 ± 0.1 ($n = 8$), 4.3 ± 0.1 ($n = 5$) and 5.1 ± 0.1 ($n = 4$) for CGP 12177, BRL 37344 and salbutamol respectively. CGP 12177, BRL 37344 and salbutamol were full agonists in this preparation producing the same maximum response as isoprenaline. Propranolol (10^{-7} M) did not significantly ($P>0.05$) affect the relaxant responses to CGP 12177, BRL 37344 and salbutamol. pD_2 values for these agonists in the absence and also in the presence of propranolol (10^{-7} M) are shown in Table 1. This concentration of propranolol (i.e. 10^{-7} M) produced a concentration-ratio of approximately 30 against isoprenaline.

Effect of pretreatment with BRL 37344 on the relaxant effect of isoprenaline, CGP 12177 and salbutamol

Since it has been consistently observed in non-vascular smooth muscles that pretreatment of the tissues with BRL 37344 induces cross-desensitization to other agonists acting on atypical β-adrenoceptors (e.g. McLaughlin & MacDonald, 1990), an attempt was made to determine whether such a phenomenon can occur in a vascular smooth muscle preparation. This was done by establishing concentration-response curves to isoprenaline, CGP 12177 and salbutamol (in the presence of propranolol, 10^{-7} M, to block β_1- and β_2-adrenoceptor subtypes) before and after BRL 37344 (10^{-4} M). The results show that in artery segments treated with BRL 37344 (10^{-4} M) for 30 min, there was no reduction in the potency of isoprenaline (Figure 3). There was also no change in the maximum response. The relaxant effects of CGP 12177 and salbutamol were also not modified by pretreating the tissues with BRL 37344. pD_2 values for the agonists before and after pretreatment with BRL 37344 (10^{-4} M) are shown in Table 2. As shown in Figure 3, a pre-exposure of the arterial segments to BRL 37344 did not affect the response to a subsequent addition of the same concentration of BRL 37344.

Discussion

β-Adrenoceptors in vascular smooth muscles were initially classified as β_2-adrenoceptors (Lands *et al.*, 1967b). Later studies using more selective agonists and antagonists have shown that vasodilatation could result from activation of β_1- or β_2-adrenoceptor subtypes. For example, while β_2-adrenoceptors predominate in the guinea-pig pulmonary artery (O'Donnell & Wanstall, 1985) and human saphenous vein (Ikezono *et al.*, 1987), β_1-adrenoceptors appear to predominate in the rabbit facial vein (McPherson & Bevan,

Table 1 Effect of propranolol on the relaxant effect of CGP 12177, BRL 37344 and salbutamol in ring segments of the rat common carotid artery precontracted with noradrenaline (10^{-7} M)

	pD_2 values	
Agonist	*Control*	*Propranolol (10^{-7} M)*
CGP 12177	5.4 ± 0.1 ($n = 8$)	5.4 ± 0.1 ($n = 8$)
BRL 37344	4.3 ± 0.1 ($n = 5$)	4.5 ± 0.07 ($n = 6$)
Salbutamol	5.5 ± 0.2 ($n = 4$)	5.4 ± 0.1 ($n = 4$)

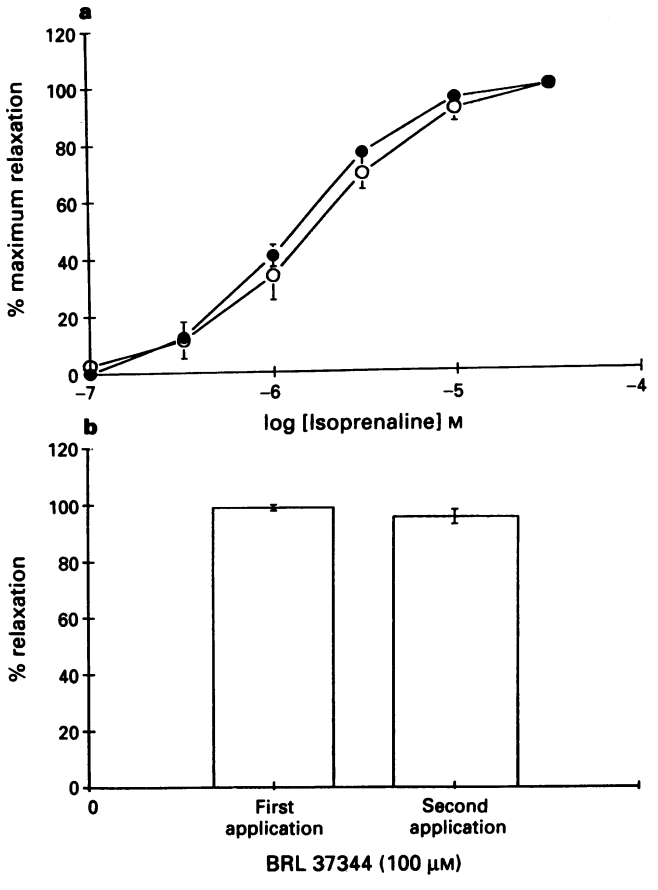


Figure 3 Concentration-response curves for isoprenaline before (○) and after (●) pretreatment with BRL 37344 (10^{-4} M) for 30 min (a) and the effect of pretreatment with BRL 37344 (10^{-4} M) on the relaxant response to a subsequent addition of BRL 37344 (b) on noradrenaline-precontracted rat common carotid artery segments.

Table 2 Effect of pretreatment with BRL 37344 (10^{-4} M, for 30 min) on the relaxant potency of Isoprenaline, CGP 12177 and salbutamol in ring segments of the common carotid artery precontracted with noradrenaline (10^{-7} M)

	pD_2 values	
Agonist	*Before BRL 37344*	*After BRL 37344*
Isoprenaline	5.8 ± 0.1 ($n = 4$)	5.9 ± 0.1 ($n = 4$)
CGP 12177	5.6 ± 0.1 ($n = 4$)	5.6 ± 0.1 ($n = 4$)
Salbutamol	5.4 ± 0.2 ($n = 4$)	5.4 ± 0.2 ($n = 4$)

1987), coronary and cerebral arteries (Edvinsson & Owman, 1974; Edvinsson *et al.*, 1976). In most other vessels, the isoprenaline-induced relaxation is mediated mainly via β_2-adrenoceptor activation with a little contribution from β_1-adrenoceptors (Taira *et al.*, 1977; Cohen & Wiley, 1978; O'Donnell & Wanstall, 1985). Isoprenaline and propranolol are non-selective β_1- and β_2-adrenoceptor agonist and antagonist respectively. It would therefore be expected that propranolol would antagonize isoprenaline competitively. However, results obtained in the present study show that even though propranolol produced a surmountable antagonism of isoprenaline-induced relaxation of precontracted ring segments of the rat common carotid artery, the antagonism did not satisfy the criteria for competitive antagonism. The Schild-plot was a straight line with a slope of 0.74 which was significantly different from 1. These results are therefore consistent with isoprenaline interacting with two sites having high and low affinities for propranolol probably corresponding to β_1- and β_2-adrenoceptor subtypes (high affinity) and atypical (β_3?) β-adrenoceptors (low affinity). It seems unlikely that β_2-adrenoceptors are involved in the relaxant response to isoprenaline in the carotid artery based on the very low potency of salbutamol in this preparation. Salbutamol is a potent and selective β_2-adrenoceptor agonist. pD_2 values reported in the literature vary from 7.0 in the guinea-pig lung strip (Schreurs *et al.*, 1980) to 8.3 in uterine smooth muscle (Granger *et al.*, 1985). The low pD_2 value (approximately 5.0) obtained in the present study is therefore not consistent with activation of β_2-adrenoceptors. This is supported by the fact that the potency ratio isoprenaline:salbutamol is greater than 100, a value that is about 10 fold greater than the usual potency ratio of about 10 observed in tissues containing conventional β_2-adrenoceptors (Arch *et al.*, 1984; Piercy, 1988). The high isoprenaline:salbutamol potency ratio observed in this study is similar to that obtained in brown adipose tissue of the rat (Arch *et al.*, 1984). Confirmation of salbutamol interacting with an atypical rather than conventional β_2-adrenoceptors was provided by the observation that propranolol (10^{-7} M) did not significantly affect salbutamol-induced relaxation of the carotid artery. This concentration of propranolol is at least 10 times its pA_2 value at conventional β_2-adrenoceptor sites. A similar conclusion was reached concerning the rabbit jejunum where propranolol antagonized salbutamol with a pA_2 value of 6.6 (Norman & Leathard, 1990).

CGP 12177 is a potent non-selective β_1- and β_2-adrenoceptor antagonist (Staehelin *et al.*, 1983; Bahouth & Malbon, 1988). It is also an agonist at atypical β-adrenoceptors, stimulating thermogenesis in brown adipose tissues (Mohell & Dickers, 1989) and lipolysis in white adipose tissues (Langin *et al.*, 1991) of the rat. In the present study, CGP 12177 behaved as a full agonist producing the same maximum relaxation of the precontracted carotid artery and was equipotent with isoprenaline (in the presence of propranolol, 10^{-7} M, to block β_1- and β_2-adrenoceptors). The relaxant effect of CGP 12177 was not antagonized by propranolol (10^{-7} M) thus confirming interaction of CGP 12177 with atypical β-adrenoceptors in the carotid artery. Another selective agonist used to demonstrate the presence of atypical β-adrenoceptors in the carotid artery is BRL 37344. This compound is a potent stimulant of lipolysis in both brown and white adipose tissues of the rat (Arch *et al.*, 1984; Wilson *et al.*, 1984). The lipolytic effect of BRL 37344 was not antagonized by propranolol at the usual β_1- and β_2-adrenoceptor blocking doses. BRL 37344 also potently relaxed smooth muscles of the gastrointestinal tract including the rat proximal colon (Bianchetti & Manara, 1990), distal colon (McLaughlin & McDonald, 1990; Kirkham & Kelly, 1992), gastric fundus (McLaughlin & Macdonald, 1991) and oesophagus (de Boer *et al.*, 1993), guinea-pig colon (Coleman *et al.*, 1987) and ileum (Bond & Clarke, 1988). These responses were resistant to antagonism by propranolol. Results obtained in the present study showed that BRL 37344 relaxed the precontracted ring segments of the carotid artery. The relaxation was slow in onset and took a longer time (compared with isoprenaline, CGP 12177 and salbutamol) to attain a peak response. This is similar to the slowly developing relaxation induced by BRL 37344 in smooth muscles of the gastrointestinal tract. However, the potency was very low (5.0) compared to values previously reported for other tissues such as the rat distal colon (McLaughlin & MacDonald, 1990; Kirkham & Kelly, 1992) and oesophagus (de Boer *et al.*, 1993). It is however close to the value obtained in the rat fundus (McLaughlin & MacDonald, 1991). The reason for this rather poor potency is not known.

Cross-desensitization to all agonists is a common occurrence in tissues pretreated with BRL 37344. In the rat distal colon for example, pretreatment of the tissue with BRL 37344 resulted in a rightward shift of the dose-response curve to isoprenaline and BRL 37344 (McLaughlin & MacDonald, 1990). This phenomenon has been interpreted as indicating a common site of action for the agonists. In the present study,

pretreatment of the tissues with BRL 37344 did not reduce either the potency of or the maximum response to isoprenaline, CGP 12177 and salbutamol. This could suggest that the atypical β-adrenoceptors in the carotid artery may differ from that in the gut tissues or that the coupling mechanism is not irreversibly affected by BRL 37344.

It was therefore concluded that there are atypical β-adrenoceptors mediating relaxation in the rat common carotid artery and that CGP 12177 might be a useful compound for identifying such receptors in vascular smooth muscles. The physiological significance of these atypical β-adrenoceptors in the vascular smooth muscle cannot be determined from this set of results. However, the receptor might be involved in the regulation of blood flow to some organs. For example, β_3-adrenoceptor mediated vasodilatation is mainly seen in vessels of the skin and fat in conscious dogs (Shen *et al.*, 1992).

The technical assistance of Mrs Elizabeth A. Kadavil is gratefully acknowledged. The author is also grateful to SmithKline Beecham pharmaceuticals for financial assistance.

References

ARCH, J.R.S. (1989). the brown adipocyte β-adrenoceptor. *Proc. Nutr. Soc.*, **48**, 215–233.

ARCH, J.R.S., AISWORTH, A.T., CAWTHORNE, M.A., PIERCY, V., SENNITT, M.V., THODY, V.E., WILSON, C. & WILSON, S. (1984). Atypical β-adrenoceptors on brown adipocytes as target for anti-obesity drugs. *Nature*, **309**, 363–365.

ARUNLAKSHANA, O. & SCHILD, H.O. (1959). Some quantitative uses of drug antagonists. *Br. J. Pharmacol. Chemother.*, **14**, 48–58.

BAHOUTH, S.W. & MALBON, C.C. (1988). Subclassification of beta adrenergic receptors of rat fat cells: a re-evaluation. *Mol. Pharmacol.*, **34**, 318–326.

BIANCHETTI, A. & MANARA, L. (1990). In vitro inhibition of intestinal motility by phenylethanolaminotetralines: evidence for atypical β-adrenoceptors in the rat colon. *Br. J. Pharmacol.*, **100**, 831–839.

DE BOER, R.E.P., BROUWER, F. & ZAAGSMA, J. (1993). The β-adrenoceptors mediating relaxation of rat oesophageal muscularis mucosae are predominantly of the β_3-, but also of the β_2-subtype. *Br. J. Pharmacol.*, **110**, 442–443.

BOND, R.A. & CLARKE, E.C. (1988). Agonist and antagonist characterisation of a putative adrenoceptor with distinct pharmacological properties from the α and β subtypes. *Br. J. Pharmacol.*, **95**, 723–734.

CLARK, B.J. & BERTHOLET, A. (1983). Effects of pindolol on vascular smooth muscle. *Gen. Pharmacol.*, **14**, 117–119.

COHEN, M.L. & WILEY, K.S. (1978). Rat jugular vein relaxes to norepinephrine, phenylephrine and histamine. *J. Pharmacol. Exp. Ther.*, **205**, 400–409.

COLEMAN, R.A., DENYER, L.H. & SHELDRICK, K.E. (1987). β-Adrenoceptors in guinea-pig gastric fundus – are they the same as the atypical β-adrenoceptors in rat adipocytes? *Br. J. Pharmacol.*, **90**, 40P.

DOGGRELL, S.A. (1990). Relaxant and β_2-adrenoceptor blocking activities of (±)-, (+)- and (−)-pindolol on the rat isolated aorta. *J. Pharm. Pharmacol.*, **42**, 444–446.

EDVINSSON, L. & OWMAN, C. (1974). Pharmacological characterization of adrenergic alpha and beta receptors mediating the vasomotor responses of cerebral arteries in vitro. *Circ. Res.*, **35**, 835–849.

EDVINSSON, L., OWMAN, C. & SJOBERG, N.O. (1976). Autonomic nerves, mast cells and amine receptors in human brain vessels: a histochemical and pharmacological study. *Brain Res.*, **115**, 377–393.

GRANGER, S.E., HOLLINGWORTH, M. & WESTON, A.H. (1985). A comparison of several calcium antagonists on uterine, vascular and cardiac muscles from the rat. *Br. J. Pharmacol.*, **85**, 255–262.

GRAY, D.W. & MARSHALL, I. (1992). Novel signal transduction pathway mediating endothelium-dependent relaxation in rat thoracic aorta. *Br. J. Pharmacol.*, **107**, 684–690.

IKEZONO, K., ZERKOWSKI, H.-R., BECKERINGH, J.J., MICHEL, M.C. & BRODDE, O.-E. (1987). Beta-2 adrenoceptor-mediated relaxation of the isolated human saphenous vein. *J. Pharmacol. Exp. Ther.*, **241**, 294–299.

KIRKHAM, D.M. & KELLY, J. (1992). Direct comparison of the rat atypical β-adrenoceptors mediating white adipocyte lipolysis and colonic relaxation. *Br. J. Pharmacol.*, **105**, 231P.

LANDS, A.M., ARNOLD, A., MCAULIFF, J.P., LUDUENA, F.P. & BROWN, T.G. (1967a). Differentiation of receptor systems activated by sympathomimetic amines. *Nature*, **214**, 597–598.

LANDS, A.M., LUDUENA, F.P. & BUZZO, H.J. (1967b). Differentiation of receptors responsive to isoproterenol. *Life Sci.*, **6**, 2241–2249.

LANGIN, D., PORTILLO, M.P., SAULINER-BLACHE, J.S. & LAFONTAN, M. (1991). Coexistence of three beta-adrenergic receptor subtypes in white fat cells of various mammalian species. *Eur. J. Pharmacol.*, **199**, 291–301.

MCLAUGHLIN, D.P. & MACDONALD, A. (1990). Evidence for the existence of atypical β-adrenoceptors (β_3-adrenoceptors) mediating relaxation in the rat distal colon. *Br. J. Pharmacol.*, **101**, 569–574.

MCLAUGHLIN, D.P. & MACDONALD, A. (1991). Characterization of catecholamine-mediated relaxations in rat isolated fundus: evidence for an atypical β-adrenoceptor. *Br. J. Pharmacol.*, **103**, 1351–1356.

MCPHERSON, G.A. & BEVAN, J.A. (1987). Specialization in beta-1 and beta-2 adrenoceptor distribution in veins of the rabbit face: relationship to myogenic tone and sympathetic nerve innervation. *J. Pharmacol. Exp. Ther.*, **240**, 99–105.

MOHELL, N. & DICKER, A. (1989). The beta adrenergic radioligand [3]CGP 12177, generally classified as an antagonist, is a thermogenic agonist in brown adipose tissue. *Biochem. J.*, **261**, 401–405.

NORMAN, B.J. & LEATHARD, H.L. (1990). Evidence that an atypical β-adrenoceptor mediates the inhibition of spontaneous rhythmical contractions of rabbit isolated jejunum induced by ritodrine and salbutamol. *Br. J. Pharmacol.*, **101**, 27–30.

O'DONNELL, S.R. & WANSTALL, J.C. (1985). Responses to the β_2-selective agonist procaterol of vascular and atrial preparations with different functional β-adrenoceptor populations. *Br. J. Pharmacol.*, **84**, 227–235.

PIERCY, V. (1988). Method for assessing the activity of drugs at β_1- and β_2-adrenoceptors in the same animal. *J. Pharmacol. Method*, **20**, 125–133.

SCHREURS, A.J.M., TERPSTRA, G.K., RAAIJMAKERS, J.A.M. & NIJKAMP, F.P. (1980). Effects of vaccination with Haemophilus influenza on adrenoceptor function of tracheal and parenchymal strips. *J. Pharmacol. Exp. Ther.*, **215**, 691–696.

SHEN, Y.-T., MANDERS, W.T., ZHANG, H. & VATNER, S.F. (1992). β3-Adrenergic receptor peripheral vascular regulation in conscious dogs. *Circulation*, **86**, Suppl. 1, I-297.

STAEHELIN, M., SIMONS, P., JAEGGI, K. & WIGGER, N. (1983). CGP 12177 A hydropholic beta-adrenergic receptor radioligand reveals high affinity binding of agonists to intact cells. *J. Biol. Chem.*, **258**, 3496–3502.

TAIRA, N., YABUUCHI, Y. & YAMASHITA, S. (1977). Profile of beta-adrenoceptors in femoral, superior mesenteric and renal vascular beds of dogs. *Br. J. Pharmacol.*, **59**, 577–583.

WILSON, C., WILSON, S., PIERCY, V., SENNITT, M.V. & ARCH, J.R.S. (1984). The rat lipolytic beta-adrenoceptor: studies using novel beta-adrenoceptor agonists. *Eur. J. Pharmacol.*, **100**, 309–319.

(Received February 1, 1994
Revised May 20, 1994
Accepted June 16, 1994)

Br. J. Pharmacol. (1994), **113**, 703–710 © Macmillan Press Ltd, 1994

Electrophysiological subtypes of inhibitory P_1 purinoceptors on myenteric neurones of guinea-pig small bowel

[1]F.L. Christofi & J.D. Wood

Department of Physiology, College of Medicine, The Ohio State University, Columbus, Ohio 43210, U.S.A.

1 Conventional intracellular microelectrode techniques were used to subclassify P_1 purinoceptors linked to reduction of cell input resistance, steady-state hyperpolarization of the membrane potential, or inhibition of fast e.p.s.ps, in neurones of microdissected myenteric plexus preparations from guinea-pig ileum. The potencies of P_1 purinoceptor agonists were estimated in neurones that were current clamped to a fixed membrane potential.

2 In AH/Type 2 neurones, the A_2 agonist, CGS 21680, the A_1 agonist, CCPA or the mixed A_1–A_2 agonist, NECA, suppressed excitability by reducing input resistance (40–50% max.) and causing hyperpolarization (20–25 mV max.). CGS 21680 (0.1–1 μM) enhanced the after-hyperpolarizing potential.

3 From cumulative dose-response data, the potency order for reducing input resistance was CCPA (IC_{50} = 5.1 ± 2.2 nM) >>> CGS 21680 (IC_{50} = 5.6 ± 2.5 μM). This effect was reversed by the A_1 antagonist, CPT (EC_{50} = 65 ± 11 nM).

4 In contrast, the potency order for membrane hyperpolarization was CCPA (IC_{50} = 61 ± 23 nM) = CGS 21680 (IC_{50} = 290 ± 90 nM) ⩾ NECA (IC_{50} = 450 ± 100 nM). Hyperpolarization elicited by CCPA was sensitive to the A_1–A_2 antagonist, DPSPX.

5 Agonists suppressed fast e.p.s.ps, but not DMPP responses, with an order of CCPA (IC_{50} = 8.1 ± 3.0 nM) >>> CGS 21680 (IC_{30} = 10 ± 2.9 μM).

6 In conclusion, the excitability of AH/Type 2 neurones is suppressed by activation of high affinity A_1 receptors that may be linked to a cyclic AMP-dependent pathway, leading to increase in calcium-dependent potassium conductance and enhancement of the after-hyperpolarizing potential. Activation of lower affinity non A_1 receptors linked to a cyclic AMP-independent pathway reduces excitability and leads mainly to a steady-state hyperpolarization. Adenosine also suppresses nicotinic cholinergic transmission by activating presynaptic high affinity A_1 receptors.

Keywords: P_1 purinoceptors; adenosine A_1 receptors; myenteric plexus; enteric nervous system; electrophysiology; potassium conductance; cyclic AMP; fast e.p.s.p.; acetylcholine release

Introduction

Burnstock (1978) classified purinoceptors into P_1 and P_2 subtypes; at P_2 sites, the preferred agonists are ATP and ADP and at P_1 sites, they are adenosine and AMP. P_1 purinoceptors were subclassified into A_1 and A_2 adenosine receptors according to the ability of adenosine and related analogues to cause respective inhibition or stimulation of adenylyl cyclase activity (Londos *et al.*, 1977; Van Calker *et al.*, 1979). A_2 receptors were further subdivided into high affinity A_{2a} and lower affinity A_{2b} (Bruns *et al.*, 1986; Jarvis *et al.*, 1989). The A_1–A_2 definition has come to rely mainly on the potency profile and sensitivity of P_1 purinoceptor agonists or antagonists, since evidence for receptor-cyclase coupling often does not exist and there is evidence for receptor coupling to cyclase-independent pathways (Trussel & Jackson, 1987; Yakel *et al.*, 1988; Broad & Cook, 1993).

Adenosine A_1 receptors which predominate on both cholinergic and tachykinergic terminals of myenteric neurones (Gustaffson *et al.*, 1985; Christofi & Cook, 1986; Broad *et al.*, 1992) are involved in inhibition of neuroeffector transmission in the small bowel (Gustaffson *et al.*, 1991; Christofi & Cook, 1987; Christofi *et al.*, 1990). Gustaffson *et al.* (1991) recently subclassified the peripheral receptor into a lower affinity A_{1b} receptor to distinguish it from central higher affinity A_{1a} receptors.

Several lines of evidence suggest that inhibitory adenosine receptors, distinct from A_1 receptors, may also exist on enteric neurones (Buckley & Burnstock, 1983; Gustaffson *et al.*, 1985; Christofi & Cook, 1987; Christofi *et al.*, 1990; Barajas-Lopez *et al.*, 1991). The neuronal non A_1 inhibitory receptor in myenteric ganglia is likely to be located on the somas of AH/Type 2 neurones which display postsynaptic responses to adenosine, because the other predominant neuronal type, the S/Type 1 neurone, apparently lacks postsynaptic inhibitory adenosine receptors (Zafirov *et al.*, 1985; Palmer *et al.*, 1987a), but displays excitatory responses to both adenosine and ATP (Katayama & Morita, 1989).

Adenosine reduces neuronal excitability in both central neurones (Green & Haas, 1991) and myenteric AH/Type 2 neurones (Palmer *et al.*, 1987a) by eliciting a steady-state hyperpolarization of the membrane potential and by enhancing postspike after-hyperpolarizing potentials. Both responses are accompanied by a reduction in cell input resistance.

In cortical neurones, two distinct adenosine receptors may mediate enhancement of after-hyperpolarizing potentials and steady-state hyperpolarization of the membrane potential, since there is a potency difference for adenosine between these two responses (Greene & Haas, 1985; 1991). Furthermore, adenosine affects two different potassium conductances in striatal (Trussel & Jackson, 1987) and hippocampal neurones (Gerber *et al.*, 1989), which further suggests the expression of two distinct receptors. The electrophysiology of adenosine in myenteric AH/Type 2 neurones is similar to that in central nervous neurones, raising the possibility that two distinct inhibitory receptors may also be expressed on AH/Type 2 neurones.

The after-hyperpolarizing potential is modulated by intracellular adenosine 3′:5′-cyclic monophosphate (cyclic AMP) levels and adenosine enhances the AHP in both central (Haas, 1984; Madison & Nicoll, 1986) and myenteric neur-

[1] Author for correspondence.

ones (Zafirov *et al.*, 1985; Palmer *et al.*, 1987a,b; Xia *et al.*, 1993; Christofi & Wood, 1993a). The available evidence fits the hypothesis that the enhancement of the afterhyperpolarizing potential and reduction in cell input resistance observed in AH/Type 2 neurones, may involve adenosine A_1-mediated reduction in neuronal cyclic AMP. However, the receptor subtype involved in these responses remains unknown.

The recent availability of more selective agonists for A_1 (Lohse *et al.*, 1988; Christalli *et al.*, 1988) and A_2 (Hutchinson *et al.*, 1989; Jarvis *et al.*, 1989) receptors is proving useful in further identification and subclassification of P_1 purinoceptors. Electrophysiological findings indicate that P_1 purinoceptor agonists suppress excitatory postsynaptic potentials (e.p.s.ps) in all categories of myenteric neurones, by acting at presynaptic receptors. Agonists also unmask prominent slow i.p.s.ps by suppressing slow e.p.s.ps in myenteric AH/Type 2 neurones (Christofi & Wood, 1993b). Limited structure-activity data with selective adenosine analogues suggest an interaction at presynaptic A_1 receptors. Selective A_1 and A_2 agonists also depress neuronal excitability in myenteric AH/Type 2 neurones (Christofi *et al.*, 1993). A more rigorous analysis of the potency profile of agonists at pre- and postsynaptic receptors has not been carried out.

The aim of this study was to use intracellular recording techniques to test the general hypothesis that adenosine suppresses neuronal excitability in myenteric neurones by activating two distinct P_1 purinoceptors. Receptors were classifed according to relative potencies (IC_{50} values) of selective A_1 and A_2 agonists in causing a reduction in cell input resistance, steady-state hyperpolarization or inhibition of fast e.p.s.ps. Adenosine antagonists were used to verify the P_1 purinoceptor nature of the interaction(s). Some of the results were previously presented in abstract form (Christofi & Wood, 1993c).

Methods

Intact myenteric plexus preparation

Adult male guinea-pigs, weighing 300–500 g, were killed by stunning and subsequent exsanguination. This method was approved by the Institutional Laboratory Animal Care and Use Committee of The Ohio State University. The segment of ileum was pinned flat with the mucosal side up to Sylgard 184 encapsulating resin (Dow Corning, Midland, MI, U.S.A.) in a dissection dish containing ice-cold Krebs solution. Fine forceps were used to remove the mucosa, submucosal plexus, and inner muscle layers and to expose the myenteric plexus on the underside of the longitudinal muscle layer. A 2.0 × 1.0 cm segment of the preparation was pinned to Sylgard in a 2.0-ml recording chamber. The tissue was superfused with Krebs solution warmed to 37°C and gassed with 95% O_2:5% CO_2 (pH 7.3–7.4), at a rate of 10–15 ml min^{-1}. The composition of the Krebs solution was (in mM): NaCl 120, $CaCl_2$ 2.5, $MgCl_2$ 1.2, NaH_2PO_4 1.35, $NaHCO_3$ 14.4 and glucose 11.5.

Intracellular recording technique

The myenteric ganglia were visualized with Hoffman Modulation Contrast optics and epi-illumination. Ganglia were immobilized with 100 μm L-shaped stainless steel wires placed on either side of the ganglion, perpendicular to the longitudinal muscle axis. Transmembrane electrical potentials were recorded with conventional intracellular microelectrodes filled with 3 M KCl and having resistances of 80–120 MΩ. The preamplifier (M767, World Precision Instruments) had bridge circuitry for intraneuronal injection of electrical current through the recording electrode. All data were recorded on magnetic tape for later analysis. The input resistance of the cells was estimated from the slopes of ohmic current-voltage plots as described previously (Grafe *et al.*, 1980). Current injection was controlled by a programmed pulse generator that delivered a sequence of six 200-ms rectangular hyperpolarizing pulses that increased with constant increments at 1 s intervals. Impaled neurones were classifed as S/Type 1, AH/Type 2 or Type 3 neurones according to reported criteria (Hirst *et al.*, 1974; Wood, 1989). AH/Type 2 neurones have a characteristic long-afterhyperpolarizing potential lasting from 4–20 s and 5–20 mV in amplitude that is absent in S/Type 1 neurones. Type 3 neurones do not display action potentials with intrasomal injection of depolarizing current of any magnitude, but have fast and slow e.p.s.ps. S/Type 1 neurones always have fast e.p.s.ps.

Experimental protocols

Impaled neurones were equilibrated and membrane potentials stabilized for 15 min before they were exposed to adenosine compounds. To determine the potency profiles of agonists in causing a reduction in input resistance and hyperpolarization in AH/Type 2 neurones, the membrane potential was initially current clamped to − 56 mV. Cells were exposed to increasing concentrations of P_1 purinoceptor agonists in a cumulative fashion at 7 min intervals. In cumulative drug-addition experiments, AH/Type 2 neurones whch displayed less than 12% spontaneous recovery (tachyphylaxis) from the maximum effect at each concentration were used in the analysis. In 60% of AH/Type 2 neurones, dose-response data was collected for both input resistance and hyperpolarization. The relative potency of agonists determined from cumulative-dose response data was compared with that determined from non-cumulative-dose response data for a restricted number of drug concentrations.

Fast e.p.s.ps were evoked in S/Type 1, AH/Type 2 and Type 3 neurones, by applying single electrical shocks (0.5–1.0 ms duration) to interganglionic connectives with electrodes made from Teflon-insulated Pt-wire (20 μm diam.) and an S-88 square-wave stimulator (Grass Instruments). To determine the inhibitory potency of agonists on fast e.p.s.ps, the membrane potentials of myenteric neurones was current-clamped to − 75 mV. For fast e.p.s.ps, data were pooled from all three cell types and no differences in adenosine receptors between cell types were assumed. Cumulative-dose response curves were constructed for each agonist, at 7 min intervals. Six fast e.p.s.ps were averaged in control and test conditions and data were normalized to % of control fast e.p.s.p. amplitude.

Abbreviations

The following abbreviations are used: ACh, acetylcholine; DMPP, (1,1-dimethyl-4-phenyl-piperazinium iodide); CCPA, (2-chloro-N^6-cyclopentyladenosine); CGS 21680, (2-[*p*-(carboxyethyl) phenylethylamino]-5′-N-ethylcarboxamidoadenosine); NECA, (5′N-ethyl-carboxamidoadenosine; CPT, (8-cyclopentyl-1,3-dimethylxanthine); DPSPX, (1,3-dipropyl-8-p-sulphophenylxanthine).

Drugs

The neurones were exposed to adenosine and its synthetic analogues CCPA, NECA and CGS 216180, the antagonists CPT and DPSPX, forskolin (H_2O soluble form) and hexamethonium, by adding the substances to the superfusion solution. Forskolin and DMPP were also applied by microejection from fine-tipped pipettes (tip diameter, 10–20 μm) with nitrogen pulses of controlled pressure and duration (Picospritzer, General Valve Corp., East Hanover, NJ, U.S.A). The pipettes contained fast green to visualize the distribution of the ejected substances in the perfusion chamber. The tips of the pipettes were positioned 20–50 μm from the impaled neurone. All drugs were dissolved in distilled water. Adenosine compounds and forskolin were pur-

chased from Research Biochem Inc. (Natick, MA, U.S.A.). CGS 21680 that was used in some studies was a kind gift from Dr R.A. Lovell at Ciba-Geigy Corporation (Summit, NJ, U.S.A.). Agents acting on cholinoceptors were purchased from Sigma (St. Louis, MO, U.S.A.).

Statistical analysis

Mean values ± s.e.mean are reported. For some experiments, the IC_{50} value (half-maximal inhibitory concentration) for each agonist was obtained from individual sigmoid cumulative dose-response curves (5 to 7 agonist concentrations), fitted by a non-linear curve fitting programme (DeLean *et al.*, 1978). Mann-Whitney nonparameteric unpaired two tail *t*-tests were used to assess differences between IC_{50} values. In addition, all cumulative dose-response data obtained in each neurone (2 to 8 agonist concentrations) were pooled for each agonist response and plotted using slidewrite software programme (4.1 version, Advanced Graphics Software, Inc., Carlsbad, CA, U.S.A.). For multiple comparisons between corresponding agonist concentrations on these dose-response curves, the significance of differences was evaluated by ANOVA followed by the modified *t* test according to Bonferroni. Statistical significance was inferred with corrected Bonferroni *P* values of <0.05. Illustrated curves represent the spline function through the data points.

Results

Results were analysed for 126 of 136 neurones from 59 guinea-pigs. These neurones represented 95 AH/Type 2, 16 Type 3 and 25 S/Type 1 neurones.

Postsynaptic effects of agonists acting on adenosine receptors in AH/Type 2 neurones

AH/Type 2 neurones used in the intracellular dose-response analysis had a mean resting membrane potential of -59 ± 1.4 mV ($n = 32$, 95% confidence limits between -56 and -62 mV). The mean input resistance of AH/Type 2 neurones that were current clamped at -56 mV was 92 ± 5.7 MΩ ($n = 31$, 95% confidence limits between 80 and 102 MΩ).

The agonists CGS 21680, CCPA or NECA (1 nM–10 μM) suppressed excitability in forskolin-responsive AH/Type 2 neurones (Figure 1). Agonists suppressed excitability by reducing cell input resistance, and causing hyperpolarization (Figure 1). CGS 21680 enhanced postspike after-hyperpolarizing potentials at concentrations ranging from 0.1–1 μM ($n = 10$, Figure 2).

P_1 purinoceptor agonists elicited hyperpolarization in 80 of 95 (84%) AH/Type 2 neurones. There was a linear 1:1 inverse relationship between hyperpolarization and the resting membrane potential of the neurones (Figure 3). The

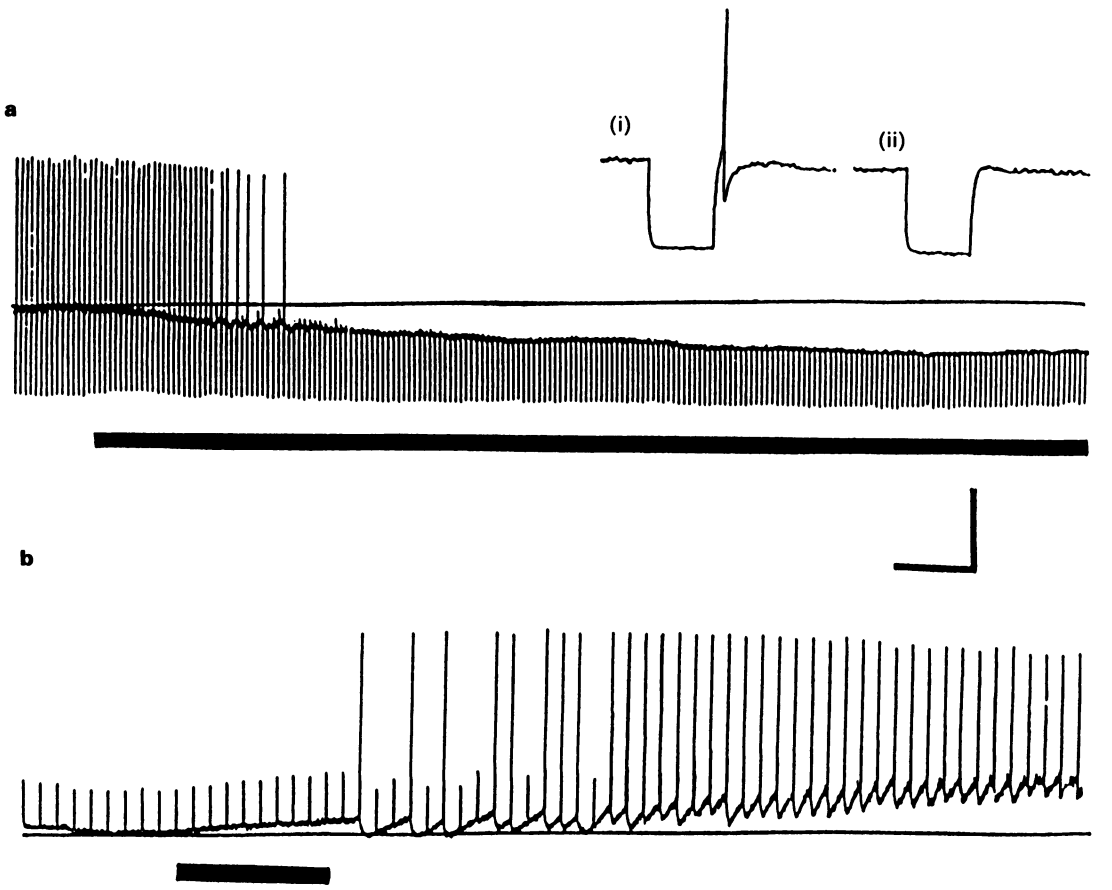


Figure 1 Inhibitory action of the A_2 agonist, CGS 21680, on the excitability characteristics of a myenteric AH/Type 2 neurone of the guinea-pig small bowel. (a) CGS 21680 (200 nM) suppressed excitability by causing a 24 mV hyperpolarization of the membrane potential which was associated with a reduction in cell input resistance. A decrease in the amplitude of the electrotonic potentials evoked by the hyperpolarizing current pulses indicates a reduction in input resistance. The anodal-break action potentials which occurred at the offset of the hyperpolarizing current pulses were suppressed by CGS 21680. (a(i)) Expanded time scale showing a single anodal-break response (current parameters: 100 ms duration; 0.5 nA) in the absence of CGS 21680. (a(ii)) Inhibited anodal-break response with CGS 21680. (b) Excitatory response to the adenylyl cyclase activator forskolin (5 μM) in the same neurone. The resting membrane potential (-60 mV) was current-clamped to -56 mV. The horizontal bars represent the length of time the drug was applied to the superfusion solution. Calibrations: vertical, 30 mV; horizontal, 15 s.

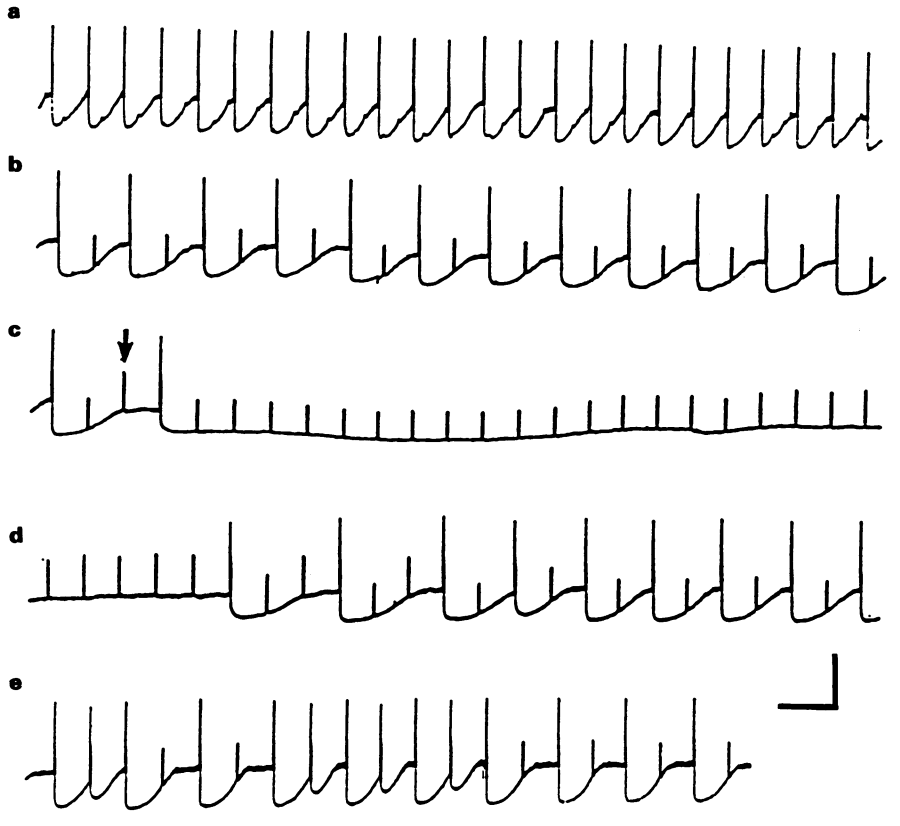


Figure 2 Action of CGS 21680 on the postspike after-hyperpolarizing potential of a myenteric AH/Type 2 neurone of the guinea-pig small bowel. Action potentials were evoked by intrasomal injection of depolarizing current pulses. (a) Control excitability; (b) a concentration of 0.2 μM CGS 21680 caused an increase in the duration of the afterhyperpolarizing potential (record begins after 1 min superfusion of CGS 21680). (c) A higher concentration of CGS 21680 (1 μM) applied at the arrow, quickly abolished the action potentials. At the offset of the final action potential, the afterhyperpolarizing potential did not recover and was observed as a sustained 23 mV hyperpolarization of the membrane potential. (d,e) Continuous records showing recovery beginning with a 3 min washout of CGS 21680 in Krebs solution. The resting membrane potential (− 64 mV) of the recorded neurone was current-clamped at − 56 mV. Calibrations: vertical, 20 mV; horizontal, 5 s.

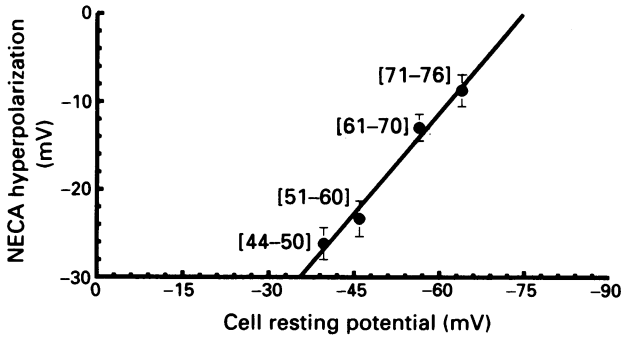


Figure 3 Linear 1:1 inverse relationship between the resting membrane potential and NECA-induced hyperpolarization of the membrane potential in myenteric AH/Type 2 neurones of the guinea-pig small bowel. The numbers in parentheses denote the range of resting membrane potentials pooled to calculate x-axis values. The data were fit by linear regression with a correlation coefficient of 0.999. Each point on the line represents the mean ± s.e.mean from 9 to 10 AH/Type 2 neurones.

maximum hyperpolarization for each agonist is shown in Table 1. At maximally-effective concentrations (1 μM), agonists caused a decrease in cell input resistance in 89 of 95 (93%) AH/Type 2 neurones. In nine of these responsive neurones (11.1%), there was no apparent hyperpolarization associated with the reduction in input resistance. Other AH/Type 2 neurones which responded with a depolarization and increase in excitability (Christofi *et al.*, 1993) with A_2 agonists were excluded from this drug analysis.

Potency profile of P_1 purinoceptor agonists

The membrane hyperpolarization and reduction in cell input resistance persisted in the continued presence of P_1 purinoceptor agonist in the Krebs superfusate. This permitted the relative potencies of agonists to be determined by cumulative drug addition. Figure 4a illustrates the cumulative-dose hyperpolarization curves for CGS 21680, CCPA and NECA. The IC_{50} value for each agonist in causing hyperpolarization is shown in Table 1. The potency profile of agonists was CGS 21680 = CPA ≥ NECA. In each of four additional AH/Type 2 neurones, in which stable recordings were made for 2 h, complete agonist-hyperpolarization dose-response relations were obtained for both CGS 21680 and CCPA. CGS 21680 was nearly equipotent with CCPA (Figure 4b).

Cumulative dose-response analysis for adenosine agonists in reducing cell input resistance (Figure 5a,b) revealed a potency order of CCPA >>> CGS 21680 (Figure 5c). The IC_{50} values for agonists are stated in Table 2 along with potency ratios. CCPA was also more potent in reducing input resistance than in causing hyperpolarization in the same AH/Type 2 neurones ($n = 3$, Figure 5d).

Non-cumulative dose-response analysis for P_1 purinoceptor agonists

In another series of experiments, each neurone was exposed to a single concentration of each agonist for 5 min. Other

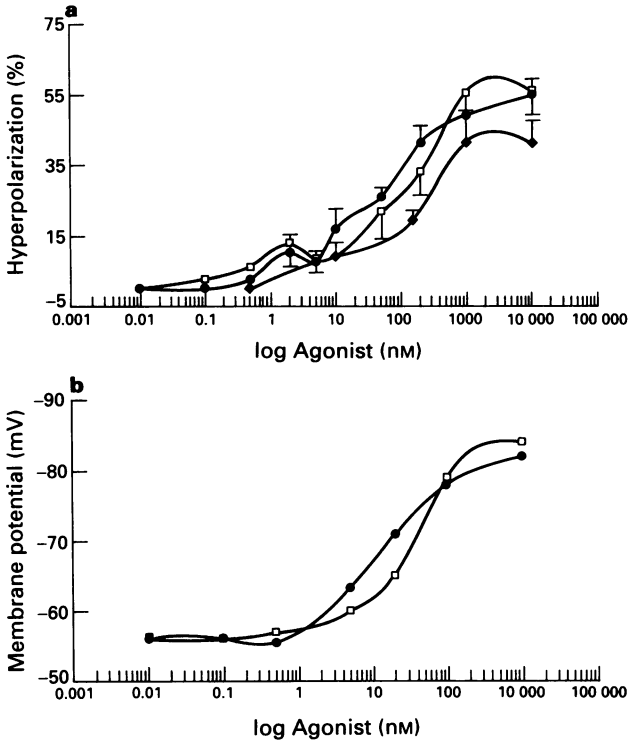


Figure 4 Cumulative dose-hypopolarization curves for P_1 purinoceptor agonists in myenteric AH/Type 2 neurones of the guinea-pig small bowel: (□) CGS 21680; (○) CCPA; (◆) NECA. The potency order of agonists is CGS 21680 = CCPA ⩾ NECA. The resting membrane potential of the neurones was current clamped at − 56 mV. Data from each preparation were normalized to the percentage of the control current-clamped membrane potential at − 56 mV. Two to six concentrations of agonist were exposed to each of 49 neurones in a cumulative fashion at 7 min intervals. Each data point represents the mean ± s.e.mean for six to eight neurones. (b) Dose-response relations for the A_1 agonist CCPA (●) and the A_2 agonist CGS 21680 (□) in eliciting hyperpolarization of the membrane potential in the same AH/Type 2 neurone. The IC_{50}s for CCPA and CGS 21680 were 100 nM and 250 nM, respectively; the potency order remained as CCPA = CGS 21680.

Table 1 Potency of P_1 purinoceptor agonists in causing hyperpolarization in AH/Type 2 neurones of the guinea-pig small intestinal myenteric plexus

Agonist	*Hyperpolarization* (% control) [a]IC_{50}	[b]*Maximum hyperpolarization* (mV)	n
CCPA	61 ± 23 nM	25 ± 3.5	10
CGS 21680	290 ± 90 nM	27 ± 3.0	10
NECA	450 ± 100 nM	20 ± 2.3	9
[c]CGS 21680:CCPA	4.8		
NECA:CCPA	7.4		
NECA:CGS 21680	1.6		

[a]The data represents the mean ± s.e.mean of the IC_{50} values estimated from the best fit (De Lean, 1978) of 5 to 6 individual dose-response curves constructed with cumulative addition of 5 to 7 concentrations of agonist.
[b]Neurones were exposed to a 10 μM concentration of agonist; *n*, number of neurones used to estimate maximum hyperpolarization; the membrane potential was current-clamped to − 56 mV.
The Mann-Whitney unpaired 2 tail *t* test was used to compare differences between IC_{50} values; CCPA vs CGS 21680, $P > 0.05$; CCPA vs NECA, $P < 0.05$; CGS 21680 vs NECA, $P > 0.05$.
[c]Ratio of IC_{50} values = potency ratio. For abbreviations, see text.

agonists were tested at 15 min intervals only in those cells that completely recovered from the effect of the previous agonist. Non-cumulative analysis gave the same results as cumulative analysis.

Data for membrane hyperpolarization were expressed as a percentage of the current-clamped membrane potential of − 56 mV. The hyperpolarizations produced by 5 nM CCPA (− 7.8 ± 3.1%, $n = 6$), 5 nM CGS 21680 (− 8.4 ± 3.0%, $n = 6$) and 5 nM NECA (− 9.3 ± 4.1, $n = 6$) were not significantly different from each other ($P > 0.05$). At a 200 nM concentration of each agonist, CCPA (− 41.6 ± 4.9, $n = 6$) caused the same hyperpolarization ($P > 0.05$) as CGS 21680 (− 35.4 ± 4.9, $n = 6$). NECA (− 19.3 ± 3.3, $n = 6$) caused a significantly smaller hyperpolarization than CCPA or CGS 21680 ($P < 0.05$). The apparent potency order for agonists on causing hyperpolarization ($n = 25$) remained as CGS 21680 = CCPA ⩾ NECA.

The reduction in cell input resistance by agonists was expressed as a percentage of the resting cell input resistance of each neurone that was current-clamped at − 56 mV. A concentration of 5 nM CCPA reduced the cell input resistance by − 22.0 ± 4.3% ($n = 6$), whereas 5 nM CGS 21680 did not affect the cell input resistance (− 0.0 ± 0.0%, $n = 6$); differences between agonist are significantly different ($P < 0.003$). At a 200 nM concentration, CCPA (− 45.8 ± 5.9%, $n = 6$) was significantly more effective ($P < 0.002$) than CGS 21680 (− 9.2 ± 7.2%, $n = 7$) in reducing input resistance. The apparent order of potencies of agonists for reducing the input resistance remained as CCPA >>> CGS 21680.

Competitive blockade with xanthine derivatives

The hyperpolarization induced by 0.2 μM CCPA (− 40.6 ± 5.0%, $n = 6$) was blocked in the presence of the mixed A_1–A_2 adenosine receptor antagonist DPSPX (− 7.3 ± 2.5%, 2 μM, $n = 6$). DPSPX also reversed the effect on cell input resistance (data not shown). The reduction in cell input resistance by CCPA was dose-dependently reversed by the A_1 selective antagonist, CPT ($P < 0.001$). The EC_{50} for CPT was 65 ± 11 nM ($n = 3$); a small membrane hyperpolarization (2 to 6 mV) or no hyperpolarization occurred in these cells, and therefore the effect of the antagonist was mostly to block the reduction in input resistance mediated by CCPA.

Presynaptic inhibition of fast e.p.s.ps

S/Type 1 neurones had relatively low resting membrane potentials (− 38 to − 53 mV) and higher input resistances (135 to 300 MΩ) than AH/Type 2 neurones. Type 3 neurones had membrane potentials ranging from − 64 to − 78 mV and input resistances ranging between 40 and 65 MΩ throughout recording periods (0.5–1.5 h). The nicotinic cholinergic nature of the fast e.p.s.ps was confirmed by hexamethonium (20 μM) blockade in all cell types. CGS 21680 or CCPA dose-dependently and reversibly suppressed or abolished fast e.p.s.ps in 17 of 21 S/Type 1, 4 of 4 AH/Type 2 and 8 out of 10 Type 3 neurones that received fast cholinergic inputs, without affecting the postsynaptic action of the nicotinic agonist DMPP ($n = 16$). The potency order of agonists was CCPA >>> CGS 21680 in suppressing fast e.p.s.ps (Figure 6, Table 2). In 2 S/Type 1 neurones, in which complete dose-inhibition curves on fast e.p.s.ps were obtained for both CCPA and CGS 21680, the potency order of CCPA >>> CGS 21680 was retained (data not shown). The receptor nature of the adenosine inhibition of fast e.p.s.ps has been established (Christofi & Wood, 1993b).

Discussion

P_1 purinoceptor subtypes on myenteric neurones

The present study revealed that a unitary P_1 purinoceptor mediates both presynaptic inhibition of fast e.p.s.ps in

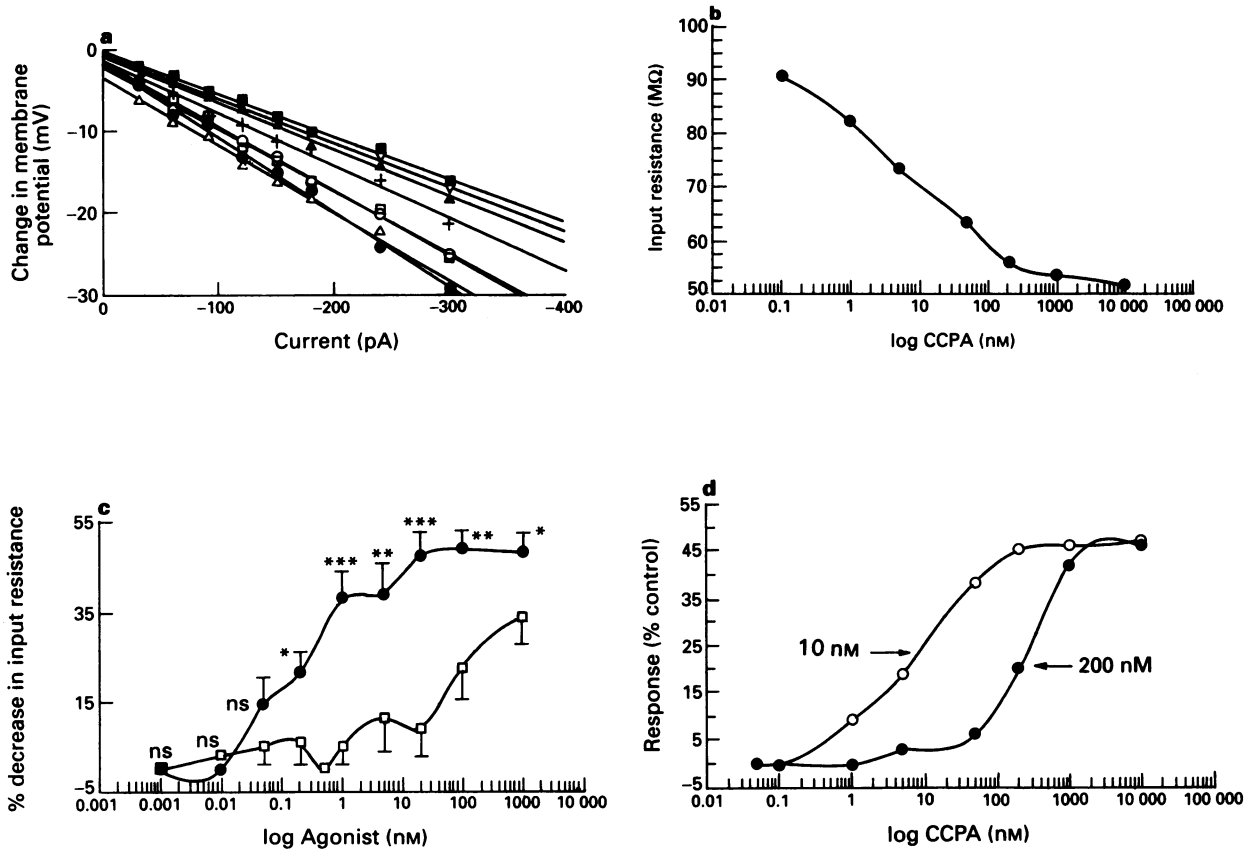


Figure 5 Effect of P_1 purinoceptor agonists on cell input resistance in myenteric AH/Type 2 neurones of guinea-pig small bowel. (a) Effect of CCPA on current-voltage ($I-V$) plots, that were obtained by intrasomal injection of incremental increases in hyperpolarizing current. $I-V$ relations were constructed in the presence of cumulative increases in CCPA concentration at 7 min intervals. The decrease in the slope of the $I-V$ plots was used to calculate the decrease in cell input resistance produced by CCPA. (●) Control; (△) 1 nM CCPA; (○) 5 nM CCA; (+) 50 nM CCPA; (▲) 200 nM CCPA; (▽) 1 μM CCPA; (■) 10 μM CCPA: (□) recovery after 20 min washout in Krebs solution. (b) Dose-response curve for CCPA extrapolated from the slopes of individual $I-V$ plots in (a). (c) Cumulative dose-response relations for adenosine agonists on reducing cell input resistance in AH/Type 2 neurones: (●) CCPA; (□) CGS 21680. Two to seven concentrations of each agonist were exposed to each of 30 neurones. Each data point represents the mean ± s.e.mean of six to nine neurones. ANOVA indicated a $P<0.0001$ between data points. Post-tests between pairs of values at each concentration of agonist on the curves yielded the following Bonferroni P values: ns, $P>0.05$; $*P<0.05$; $**P<0.01$; $***P<0.001$. (d) Potency of the A_1 agonist CCPA in reducing input resistance (○) and causing hyperpolarization (●) in the same AH/Type 2 neurone. CCPA was 20 fold more potent in reducing input resistance than in causing hyperpolarization. The resting potential of the AH/Type 2 neurones was current clamped to − 56 mV.

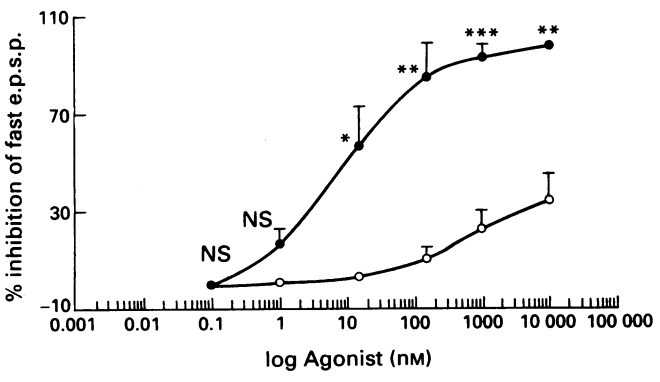


Figure 6 Dose-response relations for selective adenosine analogues as inhibitors of fast e.p.s.ps in neurones of the guinea-pig small intestinal myenteric plexus. Seventeen neurones were exposed to two to five concentrations of agonist in a cumulative fashion, at 7 min intervals. Each data point is the mean ± s.e.mean for 5–7 neurones. The resting potential was current clamped at − 75 mV. (●) CCPA; (○) CGS 21680. ANOVA indicated significant differences ($P<0.0001$) between data points at concentrations greater than 1 nM. Post-tests between pairs of values at each concentration of agonist on the curves yielded the following Bonferroni P values: NS, $P>0.05$; $*P<0.05$; $**P<0.01$; $***P<0.001$.

myenteric neurones, and postsynaptic inhibition of excitability in AH/Type 2 neurones. Our findings support the existence of high affinity adenosine A_1 receptors like those in the brain (Lohse *et al.*, 1988; Jarvis *et al.*, 1989; Lupica *et al.*, 1990; Gustaffson *et al.*, 1991). This conclusion is supported by data showing micromolar potency for the selective A_2 agonist CGS 21680, nanomolar potency of the highly selective A_1 agonist CCPA and a potency order of CCPA >>> CGS 21680 at both pre- and postsynaptic receptors. Furthermore, the potency of the selective A_1 antagonist, CPT (Daly *et al.*, 1987) at somal receptors on AH/Type 2 neurones is the same as its K_D at high affinity A_1 receptors on hippocampal neurones (Haas & Green, 1991).

This study provided novel electrophysiological evidence for heterogeneity of inhibitory P_1 purinoceptors on AH/Type 2 neurones. The pharmacology of adenosine analogues strongly suggests that hyperpolarization occurs mainly by activating a receptor that is distinct from A_1 receptors. The potency profile of CGS 21680 = CCPA ≥ NECA does not fit the profile of an A_1 or an A_2 inhibitory P_1 purinoceptor subtype, and is different from the profile obtained for high affinity A_1 sites. This different agonist profile could not be attributed to methodology, because differences in relative potencies of agonists were verified: (1) in cells with current clamped mem-

Table 2 Potency of adenosine analogues at pre- and postsynaptic P_1 purinoceptors on neurones of the guinea-pig small intestinal myenteric plexus

Agonist	*% reduction in input resistance* IC_{50}	[b]*% inhibition of fast e.p.s.ps* IC_{50}
CCPA	5.2 ± 2.2 nM	8.1 ± 3.1 nM
CGS 21680	5.6 ± 2.5 μM	[c]1.0 ± 2.9 μM
	Potency ratios A_2:A_1	
[d]CGS 21680: CCPA	1087	> 1260
[d]CCPA		

[a]Input resistance estimated from current-voltage plots according to Grafe *et al.* (1980). The membrane potential of AH/Type 2 neurones was current-clamped at − 56 mV.
[b]The membrane potential of S/Type 1 and Type 3 neurones was current-clamped at − 75 mV.
[a,b]Data represent the mean ± s.e.mean of IC_{50} values estimated from the best fit of six individual dose-effect curves constructed with cumulative additions of 5 to 7 concentrations of agonists; the difference between the IC_{50} values of CCPA and CGS 21680 is statistically significant; the Mann-Whitney unpaired 2 tail t test gave a $P = 0.033$.
[c]IC_{50} value is the maximum (30%) inhibition of fast e.p.s.ps observed with CGS 21680 at 10 μM concentration.
[d]Ratio of IC_{50} values = potency ratio.

brane potentials, (2) by both cumulative and non-cumulative drug addition, (3) in the same AH/Type 2 neurone, as well as, (4) in some cells which had a reduction in cell input resistance, without any apparent hyperpolarization.

The postspike after-hyperpolarizing potential of cortical neurones is enhanced at relatively low concentrations of adenosine, whereas at higher concentrations, the steady-state hyperpolarization predominates (Green & Haas, 1985; 1991), suggesting the existence of two distinct receptors. In our studies, the concentrations of CGS 21680 (0.1–1 μM) needed to enhance the after-hyperpolarizing potential are consistent with its activation of high affinity A_1 receptors. In fact, activation of high affinity A_1 receptors reduces input resistance and therefore must also enhance the after-hyperpolarization, since these responses represent the same ionic conductance (Wood, 1989). Higher concentrations of agonists than those needed to saturate A_1 sites mainly elicit a steady-state hyperpolarization via a lower affinity non A_1 receptor. Since hyperpolarization and reduction in input resistance are inextricably linked responses, we suggest that overlapping activation of the two predominant receptors by A_1 and A_2 agonists, especially at higher concentrations, is the reason for the lack of difference between agonist potencies on hyperpolarization. The non A_1 receptor may possibly represent an A_3 receptor subtype (Jacobson, 1994).

Signalling mechanisms coupled to P_1 purinoceptors

Enhancement of the postspike after-hyperpolarizing potential and reduction in input resistance in AH/Type 2 neurones may represent the physiological correlates of adenosine-mediated reduction in neuronal cyclic AMP (Haas, 1984; Madison & Nicoll, 1986; Zafirov *et al.*, 1985; Palmer *et al.*, 1987a). It was recently confirmed that nanomolar concentrations of the A_1 agonist, CCPA, were also sufficient to inhibit cyclic AMP formation, and CPT completely blocked this inhibition in isolated myenteric ganglia (Xia *et al.*, 1993).

In our study, the prolonged hyperpolarization occurs mainly via a non A_1 receptor and is therefore, by definition, also linked to a cyclic AMP-independent pathway, as is the case in central neurones (Trussell & Jackson, 1987; Green & Haas, 1991). As shown in other systems (Yakel *et al.*, 1988), including the enteric nervous system (Broad & Cook, 1993; Christofi *et al.*, 1993), multiple signalling mechanisms may contribute to the actions of adenosine in AH/Type 2 neurones. Furthermore, selectivity of action of adenosine at pre- and post-synaptic receptors may arise from the coupling of different signalling pathways to the respective A_1 receptors (Bruns *et al.*, 1987; Dunwiddie & Fredholm, 1989) on myenteric neurones.

The linear 1:1 inverse relationship shown to exist between P_1 purinoceptor-mediated hyperpolarization and the resting membrane potential of each AH/Type 2 neurone suggests that the ionic mechanism involves opening of potassium channels, as reported previously (Palmer *et al.*, 1985; 1987a). Adenosine hyperpolarization and reduction in cell input resistance involves a steady-state potassium current (Haas & Green, 1988). High affinity A_1 and lower affinity non A_1 receptors on AH/Type 2 neurones may be linked to two different potassium conductances (Trussell & Jackson, 1987; Gerber *et al.*, 1989). The A_1 receptor is likely to be linked to a $G_i$protein-adenylyl cyclase complex (Zgombick *et al.*, 1989). Activation of the receptor would lead to a reduction in intraneuronal cyclic AMP levels and eventual increase in potassium conductance to reduce excitability in AH/Type 2 neurones. We speculate that the non A_1 receptor (steady-state hyperpolarization) is linked directly to a potassium channel, or to other, as yet unidentified, intracellular signalling pathways.

Conclusions

Adenosine inhibits excitability in AH/Type 2 neurones, by acting at high affinity A_1 inhibitory receptors that are probably linked to a cyclic AMP-dependent pathway. A_1 activation leads to enhancement of the postspike after-hyperpolarization and increase in potassium conductance. Activation of lower affinity non A_1 receptors that are linked to a cyclic AMP-independent pathway leads mainly to a steady-state hyperpolarization produced by an increase in potassium conductance. Adenosine also inhibits ACh release and suppresses nicotinic cholinergic transmission to myenteric neurones by activating high affinity A_1 receptors. The findings establish adenosine as a critical inhibitory neuromodulator in myenteric ganglia, with an intricate neuropharmacology.

This research was supported by National Institutes of Health (NIH) Grants R29 DK-44179 to F.L.C. and RO1 DK37238 to J.D.W.

References

BARAJAS-LOPEZ, C., SUPRENANT, A. & NORTH, R.A. (1991). Adenosine A-1 and adenosine A-2 receptors mediate presynaptic inhibition and postsynaptic excitation in guinea-pig submucosal neurons. *J. Pharmacol. Exp. Ther.*, **258**, 490–495.

BROAD, R.M. & COOK, M.A. (1993). Multiple signaling mechanisms contribute to adenosine-mediated inhibition of substance P release from myenteric ganglia. *J. Gastroint. Mot.*, **5**, 183 (Abstr.).

BROAD, R.M., McDONALD, T.J., BRODIN, E. & COOK, M.A. (1992). Adenosine A_1 receptors mediate inhibition of tachykinin release from perifused enteric nerve endings. *Am. J. Physiol.*, **262**, G525–G531.

BRUNS, R.F., LU, G.H. & PUGSLEY, T.A. (1986). Characterization of the A_2 receptor labeled by [^{3}H]-NECA in rat striatal membranes. *Mol. Pharmacol.*, **29**, 331–346.

BRUNS, R.F., LU, G.H. & PUGSLEY, T.A. (1987). Adenosine receptor subtypes: binding studies. In *Topics and Perspectives in Adenosine Research*. ed. Gerlach, E. & Becker, B.F. pp. 59–73. Berlin: Springer.

BUCKLEY, N., BURNSTOCK, B. (1983). Autoradiographic demonstration of peripheral binding sites using [^{3}H]NECA. *Brain Res.*, **269**, 374–377.

BURNSTOCK, G. (1978). In *Cell Membrane Receptors for Drugs and Hormones: A Multidisciplinary Approach*, ed. Bolis, L. & Straub, R.W. pp. 107–118. New York: Raven Press.

CHRISTALLI, G., FRANCHETTI, P., GRIFANTINI, M. & VITTORIO, S. (1988). Adenosine receptor agonists: synthesis and biological evaluation of 1-deaza analogs of adenosine derivatives. **31**, 1179–1183.

CHRISTOFI, F.L., BAIDAN, L.V., FERTEL, R.H. & WOOD, J.D. (1993). Adenosine A_2 agonists excite a subset of AH/type 2 neurons and elevate cAMP levels in myenteric ganglia. *FASEB J.*, **7**, A1079 (Abstr.).

CHRISTOFI, F.L. & COOK, M.A. (1986). Affinity of various purine nucleosides for adenosine receptors on purified myenteric varicosities compared to their efficacy as presynaptic inhibitors of acetylcholine release. *J. Pharmacol. Exp. Ther.*, **237**, 305–311.

CHRISTOFI, F.L. & COOK, M.A. (1987). Possible heterogeneity of adenosine receptors present on myenteric nerve endings. *J. Pharmacol. Exp. Ther.*, **243**, 302–309.

CHRISTOFI, F.L., McDONALD, T.J. & COOK, M.A. (1990). Adenosine receptors are coupled negatively to release of tachykinin(s) from enteric nerve endings. *J. Pharmacol. Exp. Ther.*, **253**, 290–295.

CHRISTOFI, F.L. & WOOD, J.D. (1993a). Effects of pituitary adenylate cyclase activating peptide on morphologically identified myenteric neurons in guinea-pig small bowel. *Am. J. Physiol.*, **264** (*Gastroint. Liver Physiol.* **27**), G414–G421.

CHRISTOFI, F.L. & WOOD, J.D. (1993b). Presynaptic inhibibtion by adenosine A_1 receptors on guinea-pig small intestinal myenteric neurones. *Gastroenterology*, **104**, 1420–1429.

CHRISTOFI, F.L. & WOOD, J.D. (1993c). Adenosinergic A_1 and non-A_1 actions on myenteric neurones in guinea-pig small bowel. *Gastroenterology*, **104**, A346 (Abstr.).

DALY, J.W., UKENA, D. & JACOBSON, K.A. (1987). Analogues of adenosine, theophylline, and caffeine: selective interactions with A_1 and A_2 adenosine receptors. In *Topics and Perspectives in Adenosine Research*. ed. Gerlach, E. & Becker, B.F. pp. 23–36. Berlin: Springer.

DeLEAN, A., MUNSON, P.J. & ROBARDS, D. (1978). Simultaneous analysis of families of sigmoidal curves: application to bioassay, radioligand assay and physiological dose–response curves. *Am. J. Physiol.*, **235**, E97–E102.

DUNWIDDIE, T.V. & FREDHOLM, B. (1989). Adenosine A_1 receptors inhibit adenylate cyclase activity and neurotransmitter release and hyperpolarize pyramidal neurons in rat hippocampus. *J. Pharmacol. Exp. Ther.*, **249**, 31–37.

GERBER, U., GREENE, R.W., HAAS, H.L. & STEVENS, D.R. (1989). Characterization of inhibition mediated by adenosine in the hippocampus of the rat *in vitro*. *J. Physiol.*, **417**, 567–578.

GRAFE, P., MAYER, C. & WOOD, J.D. (1980). Synaptic modulation of calcium-dependent potassium conductance in myenteric neurons. *J. Physiol.*, **305**, 235–240.

GREENE, R.W. & HAAS, H.L. (1985). Adenosine actions on CA1 pyramidal neurones in rat hippocampal slices. *J. Physiol.*, **366**, 119–127.

GREENE, R.W. & HAAS, H.L. (1991). The electrophysiology of adenosine in the mammalian central nervous system. *J. Neurobiol.*, **36**, 329–341.

GUSTAFFSON, L.E., WILKUND, N.P., LUNDIN, J. & HEDQVIST, P. (1985). Characterization of pre- and post-junctional adenosine receptors in guinea-pig ileum. *Acta Physiol. Scand.*, **123**, 195–203.

GUSTAFFSON, L.E., WIKLUND, C.U., WIKLUND, N.P. & STELIUS, L. (1991). Subclassification of neuronal adenosine receptors. In *Purines in Cellular Signaling: Targets for new drugs*. ed. Jacobson, K.A., Daly, J.W. & Manganiello, V. pp. 200–205. New York: Springer-Verlag.

HAAS, H.L. (1984). Histamine potentiates neuronal excitation by blocking a calcium-dependent potassium conductance. *Agents Actions*, **16**, 3–4.

HAAS, H.L. & GREEN, R.W. (1988). Endogenous adenosine inibits hippocampal CA1 neurones: further evidence from extra- and intracellular recording. *Arch. Pharmacol.*, **337**, 561–565.

HIRST, G.D.S., HOLMAN, M.E. & SPENCE, I. (1974). Two types of neurons in the myenteric plexus of duodenum in the guinea-pig. *J. Physiol.*, **236**, 303–315.

HUTCHISON, A.J., WEBB, R.L., OEI, H.H., GHAI, G.R., ZIMMERMAN, M.R. & WILLIAMS, M. (1989). CGS 21680C, an A_2 selective adenosine receptor agonist with preferential hypotensive activity. *J. Pharmacol. Exp. Ther.*, **251**, 47–55.

JACOBSON, M.A. (1994). Cloning and expression of human adenosine receptor subtypes. *Drug Dev. Res.*, **31**, 281 (Abstr.).

JARVIS, M.F., SCHULZ, R., HUTCHISON, A.J., DO, U.H., SILLS, M.A. & WILLIAMS, M. (1989). [^{3}H] CGS 21680, a selective A_2 receptor agonist directly labels A_2 receptors in rat brain. *J. Pharmacol. Exp. Ther.* **251**, 888–893.

KATAYAMA, Y. & MORITA, K. (1989). Adenosine 5'-triphosphate modulates membrane potassium conductance in guinea-pig myenteric neurons. *J. Physiol.*, **408**, 373–390.

LOHSE, M., KLOTZ, K.-N., SCHWABE, U., CRISTALLI, G., VITTORI, S. & GRIFANTINI, M. (1988). 2-Chloro-N^6-cyclopentyladenosine: a highly selective agonist at A_1 adenosine receptors. *Naunyn Schmied. Arch. Pharmacol.*, **337**, 687–689.

LONDOS, C., COOPER, D.M.F. & WOLFF, J. (1977). Subtypes of external adenosine receptors. *Proc. Natl. Acad. Sci. U.S.A.*, **77**, 2551–2554.

LUPICA, C.R., CASS, W.A., ZAHNISER, N.R. & DUNWIDDIE, T.V. (1990). Effects of the selective A_2 receptor agonist CGS 21680 on in vitro electrophysiology, cAMP formation and dopamine release in rat Hippocampus and Striatum. *J. Pharmacol. Exp. Ther.*, **252**, 1134–1141.

MADISON, D.V. & NICOLL, R.A. (1986). Cyclic adenosine 3',5'-monophosphate mediates beta-receptor actions of noradrenaline in rat hippocampal pyramidal cells. *J. Physiol.*, **372**, 245–259,

PALMER, J.M., WOOD, J.D. & ZAFIROV, D.H. (1987a). Purinergic inhibition in the small intestine myenteric plexus of the guinea-pig. *J. Physiol.*, **387**, 357–369.

PALMER, J.M., WOOD, J.D. & ZAFIROV, D.H. (1987b). Transduction of aminergic and peptidergic signals in enteric neurones of the guinea-pig. *J. Physiol.*, **387**, 371–383.

TRUSSELL, L.O. & JACKSON, M.B. (1987). Dependence of an adenosine-activated potassium current on a GTP-binding protein in mammalian central neurones. *J. Neurosci.*, **7**, 3306–3316.

TRUSSELL, L.O. & JACKSON, M.B. (1989). Potassium currents coupled to an A_1 receptor by a G-protein in cultured central neurones. In *Adenosine Receptors in the Nervous System*. ed. Ribeiro, J.A. pp. 177–185. New York: Taylor & Francis.

VAN CALKER, D., MULLER, M. & HAMPRECHT, B. (1979). Adenosine regulates via two different types of receptors, the accumulation of cyclic AMP in cultured brain cells. *J. Neurochem.*, **33**, 999–1005.

WOOD, J.D. (1989). Electrical and synaptic behaviour for enteric neurones. In *Handbook of Physiology: The Gastrointestinal System, Motility and Circulation*. ed. Wood, J.D. Volume 1, Section 6. pp. 465–517. Bethesda, Maryland: American Physiological Society.

XIA, Y., FERTEL, R.H. & WOOD, J.D. (1993). Interactions of biogenic amines, brain-gut peptides and purine nucleotides with adenylate cyclase in signal transduction for slow synaptic excitation (slow EPSP) in enteric neurons (abstract). *J. Gastrointest. Mot.*, **5**, 225.

YAKEL, J.L., TRUSSELL, L.O. & JACKSON, M.B. (1988). Cytoplasmic modulation of transmitter gated K channels in cultured mammalian central neurons. In *Calcium and Ion Channel Modulation*. ed. Grinnell, A.D., Armstrong, D. & Jackson, M.B. pp. 291–302. New York: Plenum.

ZAFIROV, D.H., PALMER, J.M. & WOOD, J.D. (1985). Adenosine inhibits forskolin-induced excitation in myenteric neurons. *Eur. J. Pharmacol.*, **113**, 143–144.

ZGOMBICK, J.M., BECK, S.G., MAHLE, C.D., CRADDOCK-ROYAL, B. & MAAYANI, S. (1989). Pertussis toxin-sensitive guanine nucleotide-binding protein(s) couple adenosine A_1, and 5-hydroxytryptamine$_{1A}$ receptors to the same effector systems in the rat hippocampus: biochemical and electrophysiological studies. *Mol. Pharmacol.*, **35**, 484–494.

(Received December 3, 1993
Revised May 25, 1994
Accepted June 20, 1994)

Br. J. Pharmacol. (1994), **113**, 711–716 © Macmillan Press Ltd, 1994

Antagonistic properties of McNeil-A-343 at 5-HT_4 and 5-HT_3 receptors

[1]A. Sagrada, *G.B. Schiavi, †E. Cereda & *H. Ladinsky

Departments of Pharmacology, *Biochemistry and †Medicinal Chemistry, Boehringer Ingelheim Italy, Via Lorenzini 8, 20139 Milan, Italy

1 This study describes the *in vitro* interaction of the muscarinic ligand McNeil-A-343 with two 5-hydroxytryptamine (5-HT) receptor subtypes, the 5-HT_4 and 5-HT_3 receptors, using functional as well as radioligand binding studies.

2 In the rat oesophageal muscularis mucosae, precontracted with carbachol, McNeil-A-343 was a competitive antagonist (pA_2 6.2) of the 5-HT_4 receptor which mediates the relaxation induced by 5-HT. The compound *per se* relaxed the oesophagus at high concentration only ($\geq$ 10 μM), an effect unchanged by desensitization of the 5-HT_4 receptor with 10 μM 5-methoxytryptamine. In the same preparation in the absence of tone, McNeil-A-343 displaced the carbachol concentration-response curve to the right, yielding an apparent affinity (pA_2) of 4.9 for muscarinic receptors.

3 In the rat isolated superior cervical ganglion preparation, after blockade of muscarinic and nicotinic receptors, McNeil-A-343 caused a concentration-dependent depolarization that was unaffected by 100 nM ondansetron. The concentration-fast depolarization curve to 5-HT, mediated by the 5-HT_3 receptor, was displaced to the right by McNeil-A-343, which showed an apparent affinity (pA_2) of 4.8 for the 5-HT_3 subtype.

4 In binding studies, McNeil-A-343 recognized a single population of 5-HT_4 receptors in pig caudate nucleus, with a pK_I of 5.9. The binding affinity of McNeil-A-343 for 5-HT_3 receptors in NG 108-15 cells was approximately four times lower (pK_I 5.3). Binding affinities (pK_I) for muscarinic receptor subtypes in rat tissues were 5.3 (M_1, cortex), 5.2 (M_2, heart) and 4.9 (M_3, submandibular glands), respectively.

5 McNeil-A-343 is an antagonist at 5-HT_4 and 5-HT_3 receptors; the interaction of the compound with these receptor subtypes (notably the 5-HT_4) occurs in a range of concentrations which generally overlaps that relevant to the interaction with muscarinic receptors.

Keywords: McNeil-A-343; 5-hydroxytryptamine; 5-HT_4 receptors; 5-HT_3 receptors; muscarinic receptors; M_1 receptors

Introduction

McNeil-A-343 (4-[[N-(3-chlorophenyl)carbamoyl]oxy]-2-butynyltrimethylammonium chloride) was first described by Roszkowski (1961) as an unusual ganglionic stimulant, the *in vivo* action of which was unexpectedly blocked by atropine. A subsequent reappraisal of its properties (Goyal & Rattan, 1978; Hammer & Giachetti, 1982) resulted in the proposal that this compound might be a fundamental tool in the subclassification of muscarinic receptors. Although non-selective in terms of binding properties to muscarinic receptor subtypes (Eglen *et al.*, 1987), this compound has the peculiarity of displaying a functional selectivity for the putative M_1 subtype, where it exerts agonistic activity, compared to M_2 and M_3 muscarinic receptors, which are usually blocked, with few exceptions, by McNeil-A-343 (see Eglen & Whiting, 1986, for a review). Explanations of this profile, high efficacy at the M_1 receptor (Micheletti & Schiavone, 1990) and differences in receptor reserve between tissues (Eglen *et al.*, 1987) have been proposed.

Besides these actions at muscarinic receptors, McNeil-A-343 has been shown to have additional pharmacological properties. Some of them have been characterized, such as the inhibitory effect on noradrenaline reuptake (Allen *et al.*, 1972) and the stimulation (Roszkowski, 1961) or blockade of nicotinic receptors (Wakade *et al.*, 1986); the precise mechanism of other actions of McNeil-A-343, not attributable to the interaction with muscarinic receptors, has remained unresolved (e.g. Jaramillo & Volle, 1967). Within the framework of a more complete characterization of the profile of McNeil-A-343, we provide evidence in this study that this compound interacts with two 5-hydroxytryptamine (5-HT) receptor subtypes, 5-HT_3 and 5-HT_4, in a range of concentrations quite close to that significant for its activity at muscarinic receptors.

[1] Author for correspondence.

Methods

Functional studies on isolated tissues

5-HT_4 and muscarinic receptors The interaction of McNeil-A-343 with the 5-HT_4 receptor was evaluated in the rat oesophageal muscularis mucosae preparation, according to Baxter *et al.* (1991). The tunica muscularis mucosae of the intrathoracic oesophagus from male Sprague-Dawley rats (175–225 g; Charles River, Calco, Italy) was isolated and suspended in a 10 ml organ bath containing Tyrode solution of the following composition (mM): NaCl 136, KCl 2.7, $MgCl_2 \cdot 6H_2O$ 1.0, $NaH_2PO_4 \cdot H_2O$ 0.4, $NaHCO_3$ 11.9, $CaCl_2$ 1.8, glucose 5.6. Cocaine (30 μM), corticosterone (30 μM) and methysergide (1 μM) were added to the solution, that was kept at 37°C and aerated with 95% O_2:5% CO_2. Tissues were placed under 2.5 mN tension; responses were recorded isometrically (Basile 7005 transducer) on a chart recorder (Basile Gemini). After 30 min equilibration period, tissues were incubated with 100 μM pargyline for 30 min, and then washed repeatedly. The oesophagus was contracted with 3 μM carbachol (a concentration which produced 70% of the maximum response to the cholinoceptor agonist under these conditions); after stabilization of the contraction in response to carbachol, cumulative concentration-response curves to either McNeil-A-343 or 5-HT were constructed. In order to evaluate the agonistic activity of McNeil-A-343, the compound was cumulatively applied before and after equilibra-

tion with 5-methoxytryptamine (5-Me-OT, 10 μM, for 100 min). In the studies on the 5-HT_4 antagonistic properties of the muscarinic ligand, curves in response to 5-HT were constructed before and after addition of McNeil-A-343 (1–10 μM, 60 min equilibration period). Two concentration-response curves were obtained in each preparation.

In separate experiments, the interaction of McNeil-A-343 with muscarinic receptors was investigated in the same preparation uncontracted with carbachol. To this end, either cumulative concentration-response curves to McNeil-A-343 were constructed, or the antagonism of cumulative concentration-response curves to carbachol by McNeil-A-343 (100 μM, 60 min incubation period) was evaluated.

5-HT_3 receptor Superior cervical ganglia were isolated from male Sprague-Dawley rats (150–175 g; Charles River, Calco, Italy), desheathed under a microscope and submerged in a three-compartment bath; the central compartment, containing the ganglion body, was continuously perfused (2 ml min^{-1}) with modified Krebs-Henseleit solution at 25°C (composition mM: NaCl 125, KCl 5, KH_2PO_4 1.2, $CaCl_2$ 2.5, $MgSO_4$ 1.2, $NaHCO_3$ 25, glucose 10). The solution contained paroxetine (1 μM), scopolamine methylbromide (1 μM) and hexamethonium (100 μM), in order to block 5-HT uptake sites (Ireland *et al.*, 1987) muscarinic and nicotinic receptors, respectively. The d.c. potential between the ganglion body and the postganglionic trunk was recorded with a grease-gap technique (Newberry & Priestley, 1987). After a 60 min equilibration period, consecutive applications of 100 μM 5-HT were made (75 s perfusion time; 20 min interval between subsequent applications), until two equal-sized responses were obtained. Afterwards, two non-cumulative concentration-response curves were constructed, either to McNeil-A-343 or to 5-HT; the former compound was tested before and after perfusion with 100 nM ondansetron (90 min equilibration period), the latter before and after 30 μM McNeil-A-343 (60 min).

Radioligand binding studies

5-HT_4 receptor 5-HT_4 receptor binding was performed on membranes from pig caudate nucleus by the method described by Schiavi *et al.* (1994). Displacement experiments were performed by incubating 980 μl of the homogenate (final tissue dilution 1:70) at 30°C for 30 min in the presence of 0.1 nM [^{3}H]-GR 113808 (Grossman *et al.*, 1993) and different concentrations of McNeil-A-343 dissolved in the assay buffer (50 mM HEPES buffer, pH 7.4). Incubation volume was 1 ml. The reaction was terminated by rapid filtration and washing (3 × 2 ml of ice cold buffer with total duration of filtration being less than 10 s) using an IH-110 INOTECH cell harvester (type G7 glass filters, INOTECH). The filters were added to 4 ml of scintillation cocktail (Filter Count, Packard), and radioactivity was counted by liquid scintillation spectrometry. The specific binding of [^{3}H]-GR 113808 (defined as the binding displaceable by 10 μM BIMU 1) was about 80% of total binding.

5-HT_3 receptor 5-HT_3 receptor binding was performed on membranes from neuroblastoma × glioma NG 108-15 hybrid cells, according to the method of Hoyer & Neijt (1987). Displacement experiments were performed by incubating the homogenate, diluted to have about 150 μg protein ml^{-1} final concentration, at 30°C for 30 min in the presence of 0.3 nM [^{3}H]-itasetron ([^{3}H]-DAU 6215; Giraldo *et al.*, 1992) and different concentrations of McNeil-A-343 dissolved in the assay buffer. Incubation volume was 1 ml. Incubation was stopped by rapid filtration as described above. The specific binding of [^{3}H]-itasetron (defined as the binding displaceable by 3 μM MDL 72222) amounted to about 95% of total binding. Protein was determined by the method of Bradford (1976).

Muscarinic receptors Binding curves from displacement experiments were derived as previously described (Hammer *et al.*, 1986): 0.5 nM [^{3}H]-pirenzepine was used to label the M_1 receptor in cerebral cortex, and 0.3 nM [^{3}H]-N-methylscopolamine ([^{3}H]-NMS) was used to label all muscarinic receptors in the other tissues. Final tissue concentrations were (w/v): cerebral cortex, 1:200; heart, 1:300; submandibular glands, 1:150. 1 ml of homogenate was incubated at 30°C for 45 min in the presence of the marker ligand and different concentrations of McNeil-A-343. Free radioligand was separated from bound by filtration to terminate the experiment, as described above. Non-specific binding was estimated in the presence of 1 μM quinuclidinylbenzilate (QNB) and was less than 10% of total binding.

Analysis of results

All agonist concentration-effect curves were fitted to a general logistic function (Parker & Waud, 1971) using a non-linear iterative fitting programme (GraphPAD InPlot, GraphPAD Software Inc., Version 3.13). Equipotent concentration ratios (CR) were calculated at the EC_{50} level, in individual preparations, between the curve in the presence of antagonist and the control curve. Antagonist affinity of McNeil-A-343 at the 5-HT_4 receptor was estimated according to Arunlakshana & Schild (1959); apparent affinities at 5-HT_3 and muscarinic receptors were calculated according to the equation: $pA_2 = -\log([\text{Antagonist}]/\text{CR}-1)$ (Furchgott, 1972).

Binding parameters for drug competition studies were calculated by means of the Hewlett-Packard 3357 Laboratory Automation System. Corrected IC_{50} (K_I) values were calculated from the IC_{50}s after correction for the radioligand occupancy shift by the Cheng & Prusoff (1973) equation. K_D values for tritiated ligands, used in the calculations, were found in the respective displacement binding experiments with cold ligand to be the following: [^{3}H]-itasetron, 0.8 nM; [^{3}H]-GR 113808, 0.3 nM; [^{3}H]-NMS, 0.8 nM (heart), 0.5 nM (submandibular gland); [^{3}H]-pirenzepine, 12 nM.

Significance testings were carried out with Student's unpaired *t* test. Values were considered significantly different when $P<0.05$. Data are expressed as means ± s.e.mean.

Drugs

Drugs obtained from commercial sources were : 5-hydroxytryptamine hydrochloride (5-HT), 5-methoxytryptamine hydrochloride (5-Me-OT), carbachol chloride, cocaine hydrochloride, corticosterone, pargyline hydrochloride (Sigma Chemical Co., St. Louis, MO, U.S.A.); hexamethonium chloride (Fluka AG, Buchs, Switzerland).

Drugs synthesized in our laboratories were: BIMU 1 (3-ethyl-2,3-dihydro-N-[endo-8-methyl-8-azabicyclo(3.2.1)oct-3-yl]-2-oxo-1H-benzimidazole-1-carboxamide, hydrochloride), GR 113808 ([1-[2(methylsulphonylamino)ethyl]-4-piperidinyl] methyl-1-methyl-1H-indole-3-carboxylate, maleate), MDL 72222 (1αH,3α,5αH-tropan-3-yl-3,5-dichlorobenzoate, hydrochloride), McNeil-A-343.

The following drugs were kindly donated: methysergide hydrogenmaleate, from Sandoz (Basel, Switzerland); ondansetron hydrochloride dihydrate, from Glaxo Ltd. (Ware, UK); paroxetine hydrochloride hemihydrate, from Smith-Kline Beecham Pharmaceutical (Harlow, UK); quinuclidinylbenzilate (QNB), from Karl Thomae GmbH (Biberach, Germany); scopolamine methylbromide, from Boehringer Ingelheim KG (Ingelheim, Germany).

Radioligands were obtained as follows: [^{3}H]-GR 113808, specific activity of 82–85 Ci $mmol^{-1}$, was purchased from Amersham International (Bucks, UK); [^{3}H]-itasetron (2,3-dihydro-N-[endo-8-methyl-8-azabicyclo(3.2.1)oct-3-yl]-2-oxo-1H-benzimidazol-1-carboxamide, hydrochloride), specific activity of 88 Ci $mmol^{-1}$, was synthesized by Amersham International (Bucks, UK); [^{3}H]-NMS (79 Ci $mmol^{-1}$) and [^{3}H]-

pirenzepine (87 Ci mmol^{-1}) were purchased from New England Nuclear (Boston, MA, U.S.A.).

All other drugs and reagents, of the highest purity grade available, were purchased from commercial sources. Drugs were dissolved in distilled water, with the exception of corticosterone (dimethylsulphoxide). 5-HT and 5-Me-OT solutions were prepared daily.

Results

Functional studies

In the rat oesophageal muscularis mucosae, precontracted with carbachol, 5-HT (0.3 nM–10 μM) caused a concentration-dependent relaxation, with a pD_2 of 8.00 ± 0.18, and a maximum relaxation of 73 ± 5% of the carbachol-induced tone ($n = 12$); (Figure 1). This response was antagonized with high affinity (pA_2 8.97 ± 0.17; $n = 9$) by the 5-HT$_4$ receptor antagonist, GR 113808 (Gale *et al.*, 1994). McNeil-A-343 (0.1–300 μM), when administered *per se* in cumulative fashion upon the carbachol-induced tone, was virtually devoid of activity up to 3 μM; higher concentrations relaxed the oesophagus in concentration-dependent fashion, causing complete relaxation of carbachol tone (Figure 1). In order to investigate whether this effect was mediated by 5-HT$_4$ receptors, McNeil-A-343 was tested, during the same experiment, after 100 min incubation with 10 μM 5-Me-OT, which abolished the relaxant effect of 5-HT (not shown) by desensitizing the 5-HT$_4$ receptor (Baxter & Clarke, 1992). This treatment failed to alter the concentration-response curve to McNeil-A-343 (Figure 1). The possible antimuscarinic nature of this effect was then verified in the uncontracted rat oesophageal muscularis mucosae: in this case, cumulative application of McNeil-A-343 (0.1–300 μM) did not affect basal tonus, except for a negligible contraction at 300 μM (< 10% of carbachol maximum effect). However, McNeil-A-343 (100 μM) displaced to the right the concentration-response curve to carbachol, yielding a pA_2 value of 4.92 ± 0.04 at muscarinic receptors ($n = 4$) (Table 1).

The concentration-relaxation curve to 5-HT, in the precontracted oesophagus, was displaced rightward by McNeil-A-343 (1–10 μM) in concentration-dependent manner ($n = 3$–5 each); (Figure 2). A small increase in the magnitude of the 5-HT-induced relaxation was sometimes observed in the curves constructed after incubation with 3 or 10 μM McNeil-A-343, compared to the respective control curves. Schild analysis of the antagonistic effect provided an affinity estimate (pA_2) of 6.25 ± 0.09 for McNeil-A-343, with slope of the regression line not different from unity (1.02 ± 0.10; $P > 0.05$) (Figure 2, Table 1). In order to overcome the antimuscarinic effect afforded by the higher concentration of McNeil-A-343, the concentration of carbachol had to be doubled in 3 out of 5 experiments in the presence of 10 μM McNeil-A-343, so as to maintain the original tension of the preparation in the absence of the antagonist (Baxter & Clarke, 1992).

In the rat isolated superior cervical ganglion, the pD_2 of 5-HT (1–100 μM) with respect to the fast depolarization that is mediated by 5-HT$_3$ receptors (Newberry & Gilbert, 1989), was 5.41 ± 0.06 ($n = 4$). Ondansetron (100 nM) had an apparent affinity (pA_2) of 8.59 ± 0.19 for the 5-HT$_3$ receptor in this preparation ($n = 4$). During nicotinic and muscarinic receptor blockade, McNeil-A-343 (3–300 μM) depolarized the ganglion in a concentration-related fashion, with pD_2 of 4.55 ± 0.03 ($n = 4$); superfusion with 100 nM ondansetron did not modify either the potency of McNeil-A-343 (pD_2 4.61 ± 0.06, after ondansetron) or the maximum response to the compound ($P > 0.05$; $n = 4$). In order to assess the possible 5-HT$_3$ antagonistic properties of McNeil-A-343, the compuond was superfused at 30 μM concentration for 60 min, after constructing a concentration-depolarization curve to 5-HT. The rapid depolarization produced by McNeil-A-343 itself faded slightly during the equilibrium period; the following curve to 5-HT was shifted to the right and slightly, non-significantly depressed in its maximum response ($P > 0.05$; $n = 3$) (Figure 3). The apparent affinity of McNeil-A-343 for ganglionic 5-HT$_3$ receptor was 4.76 ± 0.02 (Table 1).

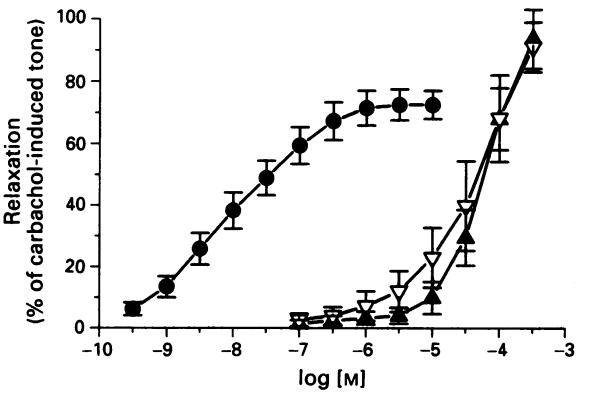


Figure 1 Rat oesophageal muscularis mucosae: cumulative concentration-response curves to 5-hydroxytryptamine (●) and to McNeil-A-343 before (▲) and after (△) desensitization of 5-HT$_4$ receptors with 10 μM 5-methoxytryptamine. Points are means with s.e.means (5-HT: $n = 12$; McNeil-A-343: $n = 4$).

Table 1 Affinity estimates for McNeil-A-343 at 5-hydroxytryptamine (5-HT) and muscarinic receptors, as determined in functional and binding studies

Functional assay	*Receptor*	*pA_2*	*Slope*
Rat oesophageal muscularis mucosae	5-HT$_4$	6.25 (0.09)	1.02 (0.10)
Rat oesophageal muscularis mucosae	Muscarinic	4.92 (0.04)†	–
Rat superior cervical ganglion	5-HT$_3$	4.76 (0.02)†	–
Binding assay	*Receptor*	*pK_I*	*nH*
Pig caudate nucleus	5-HT$_4$	5.92 (0.06)	0.81 (0.03)
NG 108-15 cells	5-HT$_3$	5.30 (0.01)	0.95 (0.02)
Rat cortex	M_1	5.26 (0.01)	0.88 (0.02)
Rat heart	M_2	5.25 (0.01)	0.76 (0.02)*
Rat submandibular gland	M_3	4.88 (0.01)	0.86 (0.02)

In functional studies, 3 to 5 replicates were obtained with each concentration of the antagonist. Agonists were 5-HT (5-HT$_4$ and 5-HT$_3$ receptors) and carbachol (muscarinic receptor).
†Calculated according to Furchgott (1972), see methods.
Estimates obtained from binding studies are means of 3 to 6 determinations performed in duplicate. Ligands were [^{3}H]-GR 113808 (5-HT$_4$ receptor), [^{3}H]-itasetron (5-HT$_3$ receptor), [^{3}H]-pirenzepine (M_1 receptor), [^{3}H]-NMS (M_2 and M_3 receptors).
Standard errors of the means are given in parentheses. *$P < 0.05$, Student's t test.

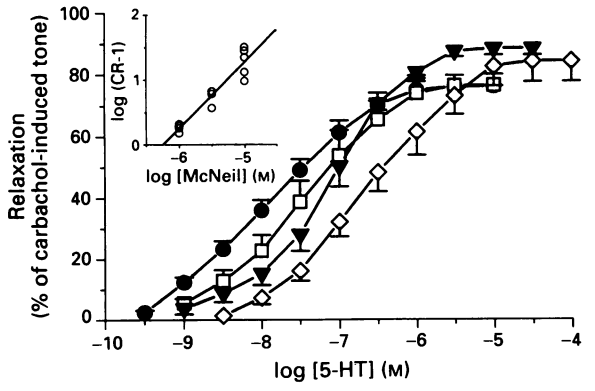


Figure 2 Concentration-response curves to 5-hydroxytryptamine (5-HT) in the rat oesophageal muscularis mucosae, in the absence (●) and presence of 1 μM (□), 3 μM (▼) and 10 μM (◇) McNeil-A-343. Points are means with s.e.means ($n = 3-5$). Inset: Schild plot for the antagonism of 5-hydroxytryptamine-induced relaxation by McNeil-A-343. Points are individual observations; the slope of the regression line (1.02 ± 0.10) is not significantly different from unity ($P > 0.05$).

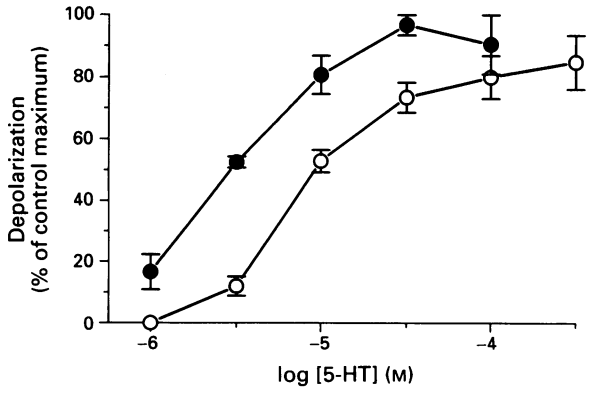


Figure 3 Non-cumulative concentration-depolarization curves to 5-hydroxytryptamine (5-HT) in the rat isolated superior cervical ganglion, before (●) and after (○) perfusion with 30 μM McNeil-A-343 for 60 min. Points are means ± s.e.mean ($n = 3$).

Binding studies

McNeil-A-343 bound to 5-HT_4 receptors in the pig caudate nucleus, with a pK_I of 5.92 ± 0.06; the affinity for the 5-HT_3 subtype in NG 108-15 cells was about 4 times lower (pK_I 5.30 ± 0.01) (Table 1). Binding affinity to muscarinic receptor subtypes in rat tissues is shown, for comparison, in Table 1: the affinity of McNeil-A-343 for M_1 and M_2 muscarinic receptors was comparable to that for the 5-HT_3 receptor, whereas the value obtained at the M_3 subtype was even slightly lower. Binding curves of McNeil-A-343 displayed Hill coefficients not significantly different from unity in all of the assays, and could be described adequately by a one-binding site model, except for that at the M_2 muscarinic subtype (n_H 0.76 ± 0.02; $P < 0.05$) (Table 1).

Discussion

The present study shows that the muscarinic ligand McNeil-A-343 recognizes the 5-HT_4 and 5-HT_3 receptor subtypes, with affinities comparable to those observed at muscarinic receptors, and exerts antagonistic activity at these 5-HT sites.

5-HT_4 receptors were first characterized in the brain (Dumuis *et al.*, 1988), and subsequently identified in peripheral organs from different species (for a review, see Bockaert *et al.*, 1992). We investigated the activity of McNeil-A-343 at the 5-HT_4 receptor located in the rat oesophageal muscularis mucosae, and found that in this preparation McNeil-A-343 behaved as a competitive antagonist of 5-HT, over the concentration range explored (1–10 μM). Indeed, high concentrations of the compound itself produced relaxation of the carbachol-contracted tissue. That the relaxation by McNeil-A-343 was unrelated to 5-HT_4 receptor stimulation, however, was clearly shown by the failure of 5-methoxytryptamine, which desensitizes the receptor site (Baxter *et al.*, 1991), to prevent the effect of McNeil-A-343. On the other hand, the antimuscarinic nature of this activity is strongly suggested by the fact that the compound, when tested on the uncontracted preparation, was not a muscarinic agonist; conversely, it displaced to the right the concentration-response curve to carbachol, yielding an affinity estimate for muscarinic receptors of the tunica muscularis mucosae compatible with its potency at causing relaxation of carbachol tone. An analogous relaxant effect, dependent on muscarinic blockade, has been previously shown after high concentrations of other 5-HT_4 ligands (Baxter *et al.*, 1991; Baxter & Clarke, 1992). The affinity of McNeil-A-343 for muscarinic receptors actually hampered the investigation of a broader range of concentrations of the compound for the antagonism at 5-HT_4 receptors: indeed, in some of the experiments in the presence of 10 μM McNeil-A-343, the concentration of carbachol had to be increased, to obtain a tissue tension comparable to that of the control curve (Baxter & Clarke, 1992). An additional observation was an increased maximum response to 5-HT in the presence of high concentrations of McNeil-A-343, compared to the control response: this is reminiscent of the phenomenon noticed in this preparation by Waikar *et al.* (1993), and attributed to blockade of the action of endogenous 5-hydroxytryptamine by 5-HT_4 receptor antagonists.

The recent characterization by our group of the 5-HT_4 binding site in the pig caudate nucleus (Schiavi *et al.*, 1994) led us to ascertain the properties of McNeil-A-343 in this tissue: consistent with the functional estimate of affinity for the 5-HT_4 receptor, a pK_I of 5.92 was obtained from the binding studies.

In the rat isolated superior cervical ganglion, we confirmed that McNeil-A-343 exerts a depolarizing effect resistant to muscarinic and nicotinic receptor blockade (Brown *et al.*, 1980). The attempt to demonstrate whether this activity is due to 5-HT_3 receptor stimulation, however, gave negative results: the effect was not antagonized by 100 nM ondansetron, which displays high affinity at rat ganglionic 5-HT_3 receptors (this study; Butler *et al.*, 1988), and it remains, therefore, an unexplained finding. Despite its own depolarizing effect, McNeil-A-343 was shown to be an antagonist at the 5-HT_3 receptor in this preparation: in fact, the concentration-response curve to 5-HT was displaced to the right by McNeil-A-343 without depression of the maximum response, even though it was constructed upon a partial depolarization by McNeil-A-343 itself. From this study, an estimate was obtained of the apparent affinity of McNeil-A-343 for the 5-HT_3 receptor (pA_2 4.76) that is approximately three times lower than that obtained from binding experiments in NG 108-15 cell membranes (pK_I 5.30).

By examining the affinities of McNeil-A-343 for 5-HT_4, 5-HT_3 and muscarinic receptors (Table 1), it emerges that all these drug-receptor interactions occur in a narrow concentration range. This conclusion applies also to the comparison between the functional estimate of the affinity at the 5-HT_4 receptor of the present study (pA_2 6.25), and the potency of McNeil-A-343 at putative M_1 muscarinic receptors, previously determined by means of *in vitro* functional studies (pD_2 in rabbit vas deferens: 6.08–6.25, Eltze, 1988; 5.81, Sagrada *et al.*, 1994; pD_2 in rat duodenum: 6.31, Micheletti & Schiavone, 1990). It is therefore tempting to speculate that the relatively high affinity of McNeil-A-343 for 5-HT_4 and 5-HT_3 receptors, compared to that for muscarinic sites, might have a bearing on some of the effects that have been

observed upon administration of this compound. For instance, 5-HT_4 antagonism by McNeil-A-343 might participate in the inhibitory effect of the compound on the phasic motility of the small intestine, an effect mainly, but not completely, mediated by M_1 receptor stimulation (Fox *et al.*, 1985). This is conceivable in the light of the role played by 5-HT_4 receptor activation in facilitating acetylcholine release from myenteric fibres and, consequently, smooth muscle contractility (see Bockaert *et al.*, 1992, for a review). In this connection, some, albeit few data are so far available concerning the effect of 5-HT_4 antagonists *per se* on gastrointestinal motility. On the one hand, SDZ 205557 and ICS 205930 do not interfere with *in vitro* basal peristaltic activity (Craig & Clarke, 1991; Costall *et al.*, 1993); on the other hand, an inhibitory effect of DAU 6285 has been observed on the gastric emptying of liquids in the dog (Rizzi *et al.*, 1994). Further studies with potent and selective antagonists are needed to clarify this matter. The 5-HT_3 antagonistic properties of the compound, conversely, might be implicated in the blockade of transmission produced by this compound in the cat superior cervical ganglion after preganglionic electrical stimulation (Jaramillo & Volle, 1967), given the presence of 5-HT_3 receptors on the superior cervical ganglia from different species (Azami *et al.*, 1985; Newberry *et al.*, 1991). In this regard, it is worth noting that the existence of species variants of the 5-HT_3 receptor has been postulated, based on the differences in affinities of 5-HT_3 receptor antagonists between tissues of different species (Butler *et al.*, 1990; Newberry *et al.*, 1991): it is therefore possible that the contribution to the McNeil-A-343 response, resulting from 5-HT_3 receptor blockade, might vary according to the species employed.

From a chemical point of view, classical 5-HT_3 and 5-HT_4 receptor ligands can be grouped into benzamido (or benzoate) benzimidazolone and indole derivatives, according to their aromatic moiety (Turconi *et al.*, 1991). Ondansetron and GR 113808, the reference compounds used in this study, bind with nanomolar and subnanomolar affinity, respectively, to 5-HT_3 and 5-HT_4 receptors (Kilpatrick *et al.*, 1987; Grossman *et al.*, 1993), and additionally discriminate between these two receptor subtypes by nearly one-thousand times (Gale *et al.*, 1994; Schiavi *et al.*, 1994). Despite its much lower potency and narrower selectivity profile, McNeil-A-343 represents a rather unusual structure within this field: in this molecule, a phenylcarbamoyloxy group serves as a bulky moiety, and it is linked to a quaternary cationic head through a butyne spacer. McNeil-A-343 cannot clearly be included in any of the three aforementioned classes, and can therefore be considered to represent a new chemical entity in the area of 5-HT_4 and 5-HT_3 receptors ligands. The development of potent and selective antagonists, structurally unrelated to the classical 5-HT_4 ligands, might help in settling some unresolved issues, as, for example, the significance of the so-called 'benzamide binding site' and its relationship to the 5-HT_4 receptor (see Bockaert *et al.*, 1992). It should also be mentioned that McNeil-A-343 appears to be endowed with a certain degree of selectivity within the 5-HT receptor family, since in binding experiments, 5-HT_{1A} and 5-HT_2 receptors show lower affinity for this compound ($K_I > 30\ \mu M$ at either site; E. Monferini, personal communications), with respect to the receptors reported here.

In conclusion, this study demonstrates additional pharmacological properties of the muscarinic ligand McNeil-A-343 at 5-HT_4 and 5-HT_3 receptors, which may account for some of the yet unexplained functional effects of this important pharmacological tool.

The authors thank M.S. Brunet, M.P. Duranti and M.L. Giudici for capable technical assistance; Dr N. Grippa for support in the analysis of results; Dr F. Borsini, Dr E. Giraldo and Dr A. Schiavone for helpful criticisms.

References

ALLEN, G.S., RAND, M.J. & STORY, D.F. (1972). Effects of McNeil-A-343 and DMPP on the uptake and release of [^{3}H]-noradrenaline by guinea-pig atria. *Br. J. Pharmacol.*, **45**, 480–489.

ARUNLAKSHANA, O. & SCHILD, H.O. (1959). Some quantitative uses of drug antagonism. *Br. J. Pharmacol. Chemother.*, **14**, 48–58.

AZAMI, J., FOZARD, J.R., ROUND, A.A. & WALLIS, D.I. (1985). The depolarising action of 5-hydroxytryptamine on rabbit vagal primary afferent and sympathetic neurones and its selective blockade by MDL 72222. *Naunyn-Schmied. Arch. Pharmacol.*, **328**, 423–429.

BAXTER, G.S. & CLARKE, D.E. (1992). Benzimidazolone derivatives act as 5-HT_4 receptor ligands in rat oesophagus. *Eur. J. Pharmacol.*, **212**, 225–229.

BAXTER, G.S., CRAIG, D.A. & CLARKE, D.E. (1991). 5-Hydroxytryptamine$_4$ receptors mediate relaxation of the rat oesophageal tunica muscularis mucosae. *Naunyn-Schmied. Arch. Pharmacol.*, **343**, 439–446.

BOCKAERT, J., FOZARD, J.R., DUMUIS, A. & CLARKE, D.E. (1992). The 5-HT_4 receptor: a place in the sun. *Trends Pharmacol. Sci.*, **13**, 141–145.

BRADFORD, M.M. (1976). A rapid and sensitive method for the quantitation of microgram quantities of protein utilising the principle of protein-dye binding. *Anal. Biochem.*, **72**, 248–254.

BROWN, D.A., FATHERAZI, S., GARTHWAITE, J. & WHITE, R.D. (1980). Muscarinic receptors in rat sympathetic ganglia. *Br. J. Pharmacol.*, **70**, 577–592.

BUTLER, A., ELSWOOD, C.J., BURRIDGE, J., IRELAND, S.J., BUNCE, K.T., KILPATRICK, G.J. & TYERS, M.B. (1990). The pharmacological characterization of 5-HT_3 receptors in three isolated preparations derived from guinea-pig tissues. *Br. J. Pharmacol.*, **101**, 591–598.

BUTLER, A., HILL, J.M., IRELAND, S.J., JORDAN, C.C. & TYERS, M.B. (1988). Pharmacological properties of GR38032F, a novel antagonist at 5-HT_3 receptors. *Br. J. Pharmacol.*, **94**, 397–412.

CHENG, Y.C. & PRUSOFF, W.H. (1973). Relationship between the inhibition constant (K_I) and the concentration of inhibitor which causes 50 percent inhibition (I_{50}) of an enzymatic reaction. *Biochem. Pharmacol.*, **22**, 3099–3108.

COSTALL, B., NAYLOR, R.J. & TULADHAR, B.R. (1993). 5-HT_4 receptor mediated facilitation of the emptying phase of the peristaltic reflex in the guinea pig isolated ileum. *Br. J. Pharmacol.*, **110**, 1572–1578.

CRAIG, D.A. & CLARKE, D.E. (1991). Peristaltis evoked by 5-HT and renzapride: evidence for putative 5-HT_4 receptor activation. *Br. J. Pharmacol.*, **102**, 563–564.

DUMUIS, A., BOUHELAL, R., SEBBEN, M., CORY, R. & BOCKAERT, J. (1988). A non-classical 5-hydroxytryptamine receptor positively coupled with adenylate cyclase in the central nervous system. *Mol. Pharmacol.*, **34**, 880–887.

EGLEN, R.M., KENNY, B.A., MICHEL, A.D. & WHITING, R.L. (1987). Muscarinic activity of McNeil-A-343 and its value in muscarinic receptor classification. *Br. J. Pharmacol.*, **90**, 693–700.

EGLEN, R.M. & WHITING, R.L. (1986). Muscarinic receptor subtypes: a critique of the current classification and a proposal for a working nomenclature. *J. Auton. Pharmacol.*, **5**, 323–346.

ELTZE, M. (1988). Muscarinic M_1- and M_2-receptors mediating opposite effects on neuromuscular transmission in rabbit vas deferens. *Eur. J. Pharmacol.*, **151**, 205–221.

FOX, J.E.T., DANIEL, E.E., JURY, J. & ROBOTHAM, H. (1985). Muscarinic inhibition of canine small intestinal motility in vivo. *Am. J. Physiol.*, **248**, G526–G531.

FURCHGOTT, R.F. (1972). The classification of adrenoceptors (adrenergic receptors). An evaluation from the standpoint of receptor theory. In *Handbook of Experimental Pharmacology*, ed. Blaschko, H. & Muscholl, E., Vol. 33, pp. 283–335. Berlin: Springer-Verlag.

GALE, J.D., GROSSMAN, C.J., WHITEHEAD, J.W.F., OXFORD, A.W., BUNCE, K.T. & HUMPHREY, P.P.A. (1994). GR113808: a novel, selective antagonist with high affinity at the 5-HT_4 receptor. *Br. J. Pharmacol.*, **111**, 332–338.

GIRALDO, E., SCHIAVI, G.B., LADINSKY, H. & MONFERINI, E. (1992). Binding characteristics of [^{3}H]DAU 6215, a new 5-HT_3 receptor antagonist, in NG 108-15 cells and rat entorhinal cortex. In *2nd International Symposium on Serotonin: From Cell Biology to Pharmacology and Therapeutics*. Abstract Book p. 42. Houston, Texas (U.S.A.), September 15–18, 1992.

GOYAL, R.K. & RATTAN, S. (1978). Neurohumoral, hormonal and drug receptors for the lower oesophageal sphincter. *Gastroenterol.*, **74**, 598–619.

GROSSMAN, C.J., KILPATRICK, G.J. & BUNCE, K.T. (1993). Development of a radioligand binding assay for 5-HT_4 receptors in guinea-pig and rat brain. *Br. J. Pharmacol.*, **109**, 618–624.

HAMMER, R. & GIACHETTI, A. (1982). Muscarinic receptor subtypes: M1 and M2. Biochemical and functional characterization. *Life Sci.*, **31**, 2991–2998.

HAMMER, R., GIRALDO, E., SCHIAVI, G.B., MONFERINI, E. & LADINSKY, H. (1986). Binding profile of a novel cardioselective muscarine receptor antagonist, AF-DX 116, to membranes of peripheral tissues and brain of the rat. *Life Sci.*, **38**, 1653–1662.

HOYER, D. & NEIJT, H.C. (1987). Identification of serotonin 5-HT_3 recognition sites by radioligand binding in NG108-15 neuroblastoma-glioma cells. *Eur. J. Pharmacol.*, **143**, 291–292.

IRELAND, S.J, STRAUGHAN, D.W. & TYERS, M.B. (1987). Influence of 5-hydroxytryptamine uptake on the apparent 5-hydroxytryptamine antagonist potency of metoclopramide in the rat isolated superior cervical ganglion. *Br. J. Pharmacol.*, **90**, 151–160.

JARAMILLO, J. & VOLLE, R.L. (1967). Nonmuscarinic stimulation and block of a sympathetic ganglion by 4-(m-chlorophenylcarbamoyloxy)-2-butynyltrimethylammonium chloride (McNeil-A-343). *J. Pharmacol. Exp. Ther.*, **157**, 337–345.

KILPATRICK, G.J., JONES, B.J. & TYERS, M.B. (1987). Identification and distribution of 5-HT_3 receptors in rat brain using radioligand binding. *Nature*, **330**, 746–748.

MICHELETTI, R. & SCHIAVONE, A. (1990). Functional determination of McNeil-A-343 affinity for M_1 muscarinic receptors. *J. Pharmacol. Exp. Ther.*, **253**, 310–314.

NEWBERRY, N.R., CHESHIRE, S.H. & GILBERT, M.J. (1991). Evidence that the 5-HT_3 receptors of the rat, mouse and guinea-pig superior cervical ganglion may be different. *Br. J. Pharmacol.*, **102**, 615–620.

NEWBERRY, N.R. & GILBERT, M.J. (1989). 5-Hydroxytryptamine evokes three distinct responses on the rat superior cervical ganglion in vitro. *Eur. J. Pharmacol.*, **162**, 197–205.

NEWBERRY, N.R. & PRIESTLEY, T. (1987). Pharmacological differences between two muscarinic responses of the rat superior cervical ganglion *in vitro*. *Br. J. Pharmacol.*, **92**, 817–826.

PARKER, R.B. & WAUD, D.R. (1971). Pharmacological estimation of drug receptor dissociation constants. Statistical evaluation: I. Agonists. *J. Pharmacol. Exp. Ther.*, **177**, 1–12.

RIZZI, C.A., SAGRADA, A., SCHIAVONE, A., SCHIANTARELLI, P., CESANA, R., SCHIAVI, G.B., LADINSKY, H. & DONETTI, A. (1994). Gastroprokinetic properties of the benzimidazolone derivative BIMU 1, an agonist at 5-hydroxytryptamine$_4$ and antagonist at 5-hydroxytryptamine$_3$ receptors. *Naunyn-Schmied. Arch. Pharmacol.*, **349**, 338–345.

ROSZKOWSKI, A.P. (1961). An unusual type of sympathetic ganglionic stimulant. *J. Pharmacol. Exp. Ther.*, **132**, 156–170.

SAGRADA, A., DURANTI, P., GIUDICI, L. & SCHIAVONE, A. (1994). Himbacine discriminates between putative muscarinic M_1 receptor-mediated responses. *Life Sci.*, **54**, PL305–PL310.

SCHIAVI, G.B., BRUNET, S., RIZZI, C.A. & LADINSKY, H. (1994). Identification of serotonin 5-HT_4 recognition sites in the porcine caudate nucleus by radioligand binding. *Neuropharmacol.*, **33**, 543–549.

TURCONI, M, SCHIANTARELLI, P., BORSINI, F., RIZZI, C.A., LADINSKY, H. & DONETTI, A. (1991). Azabicycloalkyl benzimidazolones: interaction with serotoninergic 5-HT_3 and 5-HT_4 receptors and potential therapeutic implications. *Drugs of the Future*, **16**, 1011– 1026.

WAIKAR, M.V., HEGDE, S.S., FORD, A.P.D.V. & CLARKE, D.E. (1993). Pharmacological analyses of endo-6-methoxy-8-methyl-8-azabicyclo [3.2.1] oct-3-yl-2,3-dihydro-2-oxo-1H-benzimidazole-1-carboxylate hydrochloride (DAU 6285) at the 5-hydroxytryptamine$_4$ receptor in the tunica muscularis mucosae of rat esophagus and ileum of guinea-pig: role of endogenous 5-hydroxytryptamine. *J. Pharmacol. Exp. Ther.*, **264**, 654–661.

WAKADE, A.R., KAHN, R., MALHOTRA, R.K., WAKADE, C.G. & WAKADE, T.D. (1986). McNeil-A-343, a specific agonist of M_1-muscarinic receptors, exerts antinicotinic and antimuscarinic effects in the rat adrenal medulla. *Life Sci.*, **39**, 2073–2080.

(Received March 21, 1994
Revised June 15, 1994
Accepted June 20, 1994)

Br. J. Pharmacol. (1994), **113**, 717–722 © Macmillan Press Ltd, 1994

Effects of bradykinin B_2 receptor antagonism on the hypotensive effects of ACE inhibition

Hervé Bouaziz, Yves Joulin, Michel Safar & [1]Athanase Benetos

Department of Internal Medicine, Broussais Hospital, and INSERM (U337), Paris, France

1 The aim of this study was to determine the participation of endogenous bradykinin (BK) in the antihypertensive effects of the angiotensin converting enzyme inhibitor (ACEI), perindoprilat, in the spontaneously hypertensive rat (SHR) on different salt diets.

2 Conscious SHRs receiving either a low or a high NaCl diet were used in order to evaluate the respective roles of angiotensin II suppression and bradykinin stimulation in the acute hypotensive effects of perindoprilat. Two different B_2 receptor antagonists (B 4146 and Hoe 140) were used after bolus administration of 7 mg kg^{-1} of the ACEI, perindoprilat. In separate animals, Hoe 140 was administered before the injection of perindoprilat. In other experiments, the effects of Hoe 140 on the hypotensive effects of the calcium antagonist, nicardipine, were tested.

3 The different NaCl diets had no effect on baseline blood pressure. Hoe 140 injection before ACE inhibition did not modify blood pressure. Perindoprilat caused more marked hypotension in the low salt-fed rats than in the high salt animals ($P<0.01$). Administration of Hoe 140 or B4146 after perindoprilat significantly reduced the antihypertensive effects of perindoprilat in the different groups, but this effect was more pronounced in high salt-fed rats. However, in SHRs receiving Hoe 140 before perindoprilat, the antihypertensive effect of perindoprilat was completely abolished in both high or low salt diet rats. In separate experiments we confirmed that Hoe 140 did not affect the hypotensive efficacy of the calcium antagonist, nicardipine.

4 Our study shows that inhibition of endogenous bradykinin degradation participates in the acute antihypertensive effects of perindoprilat in SHRs. The role of bradykinin is more pronounced following exposure to a high salt diet i.e., when the renin-angiotensin system is suppressed. Blockade of bradykinin B_2 receptors by Hoe 140 before administration of perindoprilat completely abolished the hypotensive effect of perindoprilat suggesting an increased role of bradykinin in the onset of hypotensive action of ACE inhibitors. However, the exact mechanism of this interaction remains unclear.

Keywords: Bradykinin receptor antagonist; ACE inhibition; NaCl diet; spontaneously hypertensive rats

Introduction

Since angiotensin converting enzyme (ACE), also known as kininase II, catabolizes bradykinin to inactive fragments, it has been suggested for a long time that a potentiation of the effects of endogenous bradykinin is implicated in the antihypertensive action of converting enzyme inhibitors (Erdös, 1975; Thurston *et al.*, 1978; Swartz *et al.*, 1979). However, due to the lack of specific bradykinin antagonists, conclusions from earlier studies were largely based on indirect evidence (Thurston *et al.*, 1978; Swartz *et al.*, 1979). The discovery of specific bradykinin B_2 receptor antagonists by Vavrek & Stewart (1985) offered new possibilities to demonstrate that potentiation of endogenous bradykinin contributed effectively to the antihypertensive actions of angiotensin converting enzyme inhibitors, in different experimental models (Benetos *et al.*, 1986; Carbonell *et al.*, 1988; Seino *et al.*, 1989). However this conclusion has been contested by some authors (Waeber *et al.*, 1986; Aubert *et al.*, 1987). These discrepancies may be related to differences among the experimental procedures, including the strain of rats, the type of bradykinin antagonist, and the study design. The recent development of a new highly potent, long lasting, bradykinin B_2 receptor antagonist (Lembeck *et al.*, 1991; Wirth *et al.*, 1991) may avoid some of the disadvantages of the older antagonists (Waeber *et al.*, 1986; Mulinari *et al.*, 1988) and permit a better study of the role of endogenous bradykinin in the cardiovascular effects of ACEI in the different experimental models (Bao *et al.*, 1988; Linz & Shölkens, 1992). Recently, the group of Linz and Shölkens (1992) reported that in aortic banded hypertensive rats, the bradykinin activation by ACEI seems to be more important than angiotensin II (AII) suppression for the prevention of cardiac hypertrophy, whereas for regression of hypertrophy the inverse was observed, i.e. a predominant role of AII and an insignificant participation of the bradykinin pathway (Shölkens & Lintz, 1993). These results indicate that the respective roles of these two systems in the cardiovascular effects of ACEI can be very different in various experimental conditions. Another major factor that can influence the activity of both the renin-angiotensin and the bradykinin systems is the amount of NaCl in the diet (Carretero & Scicli, 1991; Swales, 1990). To our knowledge, there are no data available concerning the respective roles of the renin-angiotensin and the bradykinin pathways in the hypotensive effects of ACE inhibitors, as a function of a NaCl diet.

Therefore, the aim of the present work was to study the role of endogenous bradykinin in the hypotensive effects of ACE inhibition in spontaneously hypertensive rats (SHRs) following a regular low (0.4%) or a high (7%) NaCl diet.

The role of bradykinin was evaluated by the use of specific antagonists of the B_2 receptors administered before or after the injection of the ACEI, perindoprilat.

Methods

Sixty-nine male SHRs were used in these experiments. The rats were obtained from IFFA CREDO France at 3 months of age. Half the animals received, for a period of 4 weeks, a regular 0.4% NaCl diet (LS), whereas the other half received a high 7% NaCl diet (HS). Both diets contained the same

[1] Author for correspondence at: Service de Médecine Interne, Hôpital Broussais, 96, rue Didot, 75014 Paris, France.

amount of potassium (0.205 mEq g^{-1}). The feed was provided by UAR France. Tap water was provided *ad libitum* throughout the study. During this period, all rats were housed in our animal room (U337, INSERM Paris France) at a constant temperature (23 ± 1°C) and humidity, with a 12 h light-dark cycle.

The day prior to experimentation, the rats were anaesthetized with intraperitoneal pentobarbitone (60 mg kg^{-1}). The right femoral and carotid arteries were cannulated for direct arterial pressure recording and drug administration, respectively. On the day of experimentation, the animals were conscious and unrestrained in individual plastic cages. Blood pressure and heart rate were recorded continuously with a Statham pressure transducer, Gould Brush pressure computer and Gould Brush 2400 recorder (Gould, Cleveland, Ohio). Two sets of experiments were performed.

First set of experiments (Groups I to VI, Table 1)

The rats were divided into 6 groups (Table 1). Groups I, II (LS), IV and V (HS) received a placebo injection (0.2 ml of 0.9% NaCl solution) followed 20 min later by the ACEI, perindoprilat, at a dose of 7.0 mg kg^{-1}. This dose is able to inhibit by almost 100% the plasma and tissue ACE, and shows a maximal hypotensive effect in SHR (Laubie *et al.*, 1984). In pilot experiments we tested 4 different doses of this drug, 0.7, 2, 7 and 12 mg kg^{-1}, in 4 low and 4 high salt fed rats. With the dose of 7 mg kg^{-1} we obtained a maximal hypotensive effect in both groups. The hypotensive effect reached a plateau 15 to 20 min after injection and lasted several hours. Thirty min later, the bradykinin B_2 antagonists (BKA) were administered. In groups I and IV, the B_2 receptor antagonist, Hoe 140, was given (Lembeck *et al.*, 1991; Wirth *et al.*, 1991) in bolus doses of 500 μg kg^{-1}, whereas in Groups II and V, the BKA B4146 (Vavrek & Stewart, 1985) was infused at a dose of 40 μg kg^{-1} min^{-1}. In groups III and VI, we first administered the same dose of Hoe 140 (500 μg kg^{-1}) and perindoprilat was injected 20 min later, followed by an injection of placebo. This procedure (BKA-ACEI-placebo) was not followed with the B4146 for practical reasons. This antagonist has a very short half life, and, therefore, very large amounts of this drug need to be infused during the entire experimental procedure (Vavrek & Stewart, 1985). In contrast, Hoe 140 has a long half life and a single injection of the compound is able to block the bradykinin receptors before and at least 30 min after the injection of the ACE inhibitor (Lembeck *et al.*, 1991; Wirth *et al.*, 1992). The dose of Hoe 140 we administered was the same as used in previous studies by Bao *et al.* (1992) and Lintz & Shölkens (1992). Higher doses of these two B_2 receptor antagonists were not used in order to avoid any non specific effect and especially an activation of the sympathetic system (Aubert *et al.*, 1987; Mulinari *et al.*, 1988).

Table 1 Experimental procedure in the different groups

		First set of experiments			
Groups (n)	*NaCl diet*	*MBP*	*First inj.*	*Second inj.*	*Third inj.*
I (8)	LS	165 ± 18	Placebo	Perind	Hoe 140
II (8)	LS	172 ± 16	Placebo	Perind	B 4146
III (7)	LS	163 ± 10	Hoe 140	Perind	Placebo
IV (8)	HS	183 ± 17	Placebo	Perind	Hoe 140
V (8)	HS	167 ± 13	Placebo	Perind	B 4146
VI (7)	HS	180 ± 7	Hoe 140	Perind	Placebo

		Second set of experiments			
Groups (n)	*NaCl diet*	*MBP*		*First day*	*Second day*
VII (6)	LS	177 ± 20	A	Pl-Nicard	Hoe 140-Nicard
			B	Hoe 140-Nicard	Pl-Nicard
VIII (6)	LS	174 ± 18	A	Pl-Perind	Hoe 140-Perind
			B	Hoe 140-Perind	Pl-Perind
IX (5)	HS	170 ± 12	A	Pl-Nicard	Hoe 140-Nicard
			B	Hoe 140-Nicard	Pl-Nicard
X (6)	HS	174 ± 14	A	Pl-Perind	Hoe 140-Perind
			B	Hoe 140-Perind	Pl-Perind

n = number of rats, Pl = placebo, Perind = perindoprilat, nicard = nicardipine, LS = 0.4% NaCl diet, HS = 7% NaCl diet.

Second set of experiments (Groups VII to X, Table 1)

These experiments were performed after the first set of experiments and aimed to determine if the bradykinin antagonist, Hoe 140, had any effect on hypotensive responses to nicardipine (i.e. in the absence of ACE inhibition).

Four groups of rats were used (Table 1). Experiments were performed over 2 days, in conscious rats. The first day rats received (after randomization) placebo or Hoe 140 (500 μg kg^{-1}). Groups VII_A (LS) and IX_A (HS) received an intra-arterial injection of the calcium antagonist, nicardipine (15 μg kg^{-1}). This dose was chosen after pilot experiments in order to obtain a similar effect to the perindoprilat hypotensive effect. With nicardipine the plateau effect is reached very early (3 to 5 min after injection) and its duration does not exceed 10 min.

Perindoprilat (7.0 mg kg^{-1}) was administered to Groups $VIII_A$ (LS) and X_A (HS). The following day the same procedure was followed after inversion of the placebo, Hoe 140 administration (Groups VII_B-X_B). The order of drug injections (placebo/Hoe 140) was not an influential factor in the blood pressure response, and therefore subgroups A and B were pooled for statistical analysis (Table 1).

Drugs

The bradykinin receptor antagonist B4146 (Hyp^3, Thi^{5,8}, D-Phe^7)-BK was obtained from Novachem, Clery en Vexin, France. Nicardipine was obtained from Sigma Chimie, Saint-Quentin-Fallavier, France. The bradykinin receptor antagonist, Hoe 140 (D-Arg, [Hyp^3, Thi^5, D-Thi^7, Oic^8]-BK was kindly provided by Hoechst AG, Frankfurt/Main, Germany. Perindoprilat was kindly provided by Servier, Courbevoie, France. All drugs were diluted in saline. The volume of the different bolus injections was 0.2 ml and of the B4146 infusion 0.1 ml min^{-1}.

Statistics

Blood pressure and heart rate values presented in the Results section were recorded 25 to 30 min after the injections of placebo, perindoprilat or Hoe 140, respectively (e.g. during the plateau effect). For B4146, values reported are those recorded between the 8th and the 10th min of the infusion, and for nicardipine 8 to 10 min after drug injection.

All results are expressed as mean ± s.d. In the first set of experiments, the effect of the drugs on mean blood pressure (MBP) and heart rate were tested by a repeated measure ANOVA. Differences between low and high salt fed rats were performed with Student's unpaired *t* test. In the second set of experiments a 1 way ANOVA was used to evaluate the effects of the Hoe 140 pretreatment on MBP changes following treatment with perindoprilat or nicardipine. When the *F* value was significant, a non parametric Keuls-Newman test was used. A $P<0.05$ was considered significant.

Results

Table 1 shows the values of baseline MBP in the different groups of rats. No statistical difference was observed between groups fed with a high or a low salt diet. Placebo saline

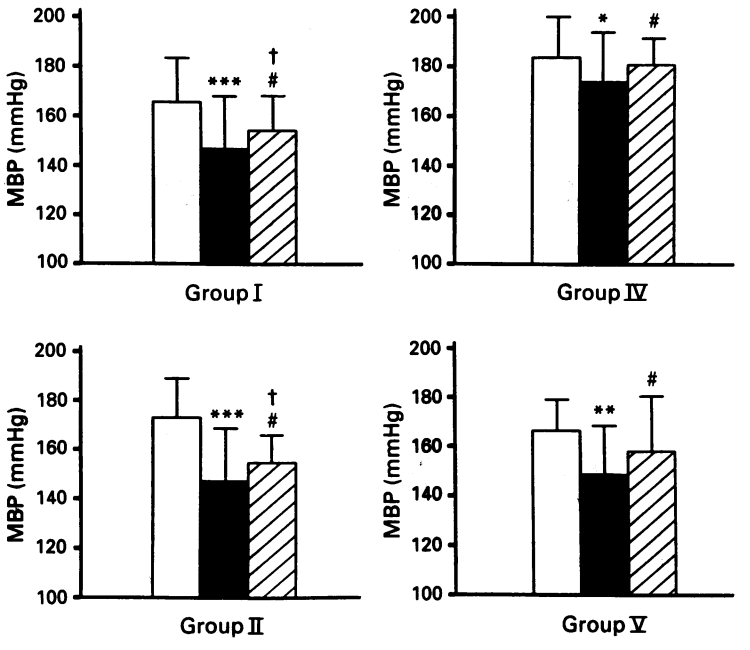


Figure 1 Mean blood pressure (MBP) values following administration of placebo, angiotensin converting enzyme inhibitor (ACEI), perindoprilat, and bradykinin B_2 receptor antagonists Hoe 140 (Groups I and IV) or B 4146 (Groups II and V). Groups I and II were given a 0.4% NaCl diet whereas groups IV and V had a 7% NaCl diet. Open columns, placebo; solid columns, perindoprilat; hatched columns, bradykinin antagonist. $*P<0.05$; $**P<0.01$, $***P<0.001$, perindopril vs placebo; $\#P<0.05$, bradykinin antagonist vs perindopril; $\dagger P<0.05$, bradykinin antagonist vs placebo.

injection had no effect on blood presure in any of the studied rats. Figure 1 shows the results obtained in groups I, II, IV and V when the bradykinin antagonists were administered after the injection of perindoprilat.

In the low salt fed rats, perindoprilat decreased MBP by a mean of 23 ± 4 mmHg (19 ± 5 and 26 ± 5 mmHg in gr I and II, respectively). The subsequent injection of Hoe 140, or infusion of B4146, increased MBP in a similar way by 8 ± 2 and 7 ± 2 mmHg, respectively ($P<0.05$ vs MBP before BKA). This increase in MBP started about 1 min after the beginning of the B4146, and persisted throughout the 10 min infusion. Thereafter, MBP returned to preinfusion levels, 2 to 3 min after the end of perfusion. In the Hoe 140 groups, the increase in MBP was present about 5 min after the injection but pressure did not return to the preinjection level, consistent with the long lasting duration of action of Hoe 140.

Our results show that the administration of the two BKA, attenuated the hypotensive effects of perindoprilat by 42% and 30% in Groups I (Hoe 140) and II (B4146), respectively.

In groups fed a high salt diet, the injection of perindoprilat significantly reduced MBP by a mean of 14 ± 4 mmHg (10 ± 2 and 18 ± 4 mmHg in groups IV and V, respectively). The comparison of the hypotensive effects of perindoprilat in high vs low NaCl diet showed that the ACEI was less effective in the former groups ($P<0.05$). The administration of the BK antagonists significantly increased blood pressure in both groups IV and V by 7 ± 2 and 10 ± 4 mmHg, respectively ($P<0.05$) (Figure 1), showing that B_2 receptor blockade attentuated the hypotensive effects of perindoprilat by 70 and 58% in these two groups respectively.

In groups III (LS) and VI (HS) (Figure 2), the administration of Hoe 140 before ACE inhibition had no significant effect on MBP. Heart rate was slightly reduced by 35 ± 20 beats min^{-1} but this difference was not statistically significant. The subsequent injection of perindoprilat did not induce any changes in blood pressure, showing that with prior B_2 receptor blockade, with Hoe 140, the hypotensive effects of the ACE inhibitor were completely abolished in both low and high salt fed rats (Figure 2).

In the second set of experiments the hypotensive effects of nicardipine were not modified by pretreatment with the Hoe 140 in any of the studied groups. In Group VII, MBP decreased after nicardipine by 48 ± 10 mmHg following placebo pretreatment and by 41 ± 7 mmHg after Hoe 140 pretreatment (Figure 3). In high salt fed rats (Group IX) the efficacy of nicardipine was similar to the low salt groups and

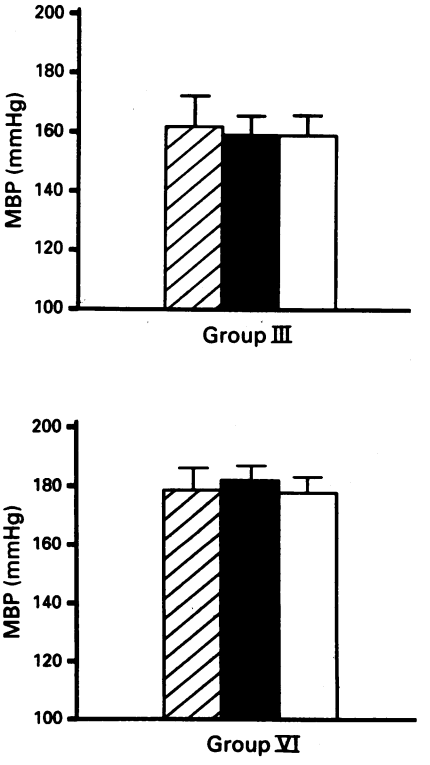


Figure 2 Mean blood pressure values following administration of bradykinin B_2 receptor antagonist, Hoe 140, ACEI perindoprilat and placebo, in 0.4% NaCl fed (Group III) and 7% NaCl fed (Group VI) rats. Hatched columns, bradykinin antagonist; solid columns perindoprilat; open columns, placebo.

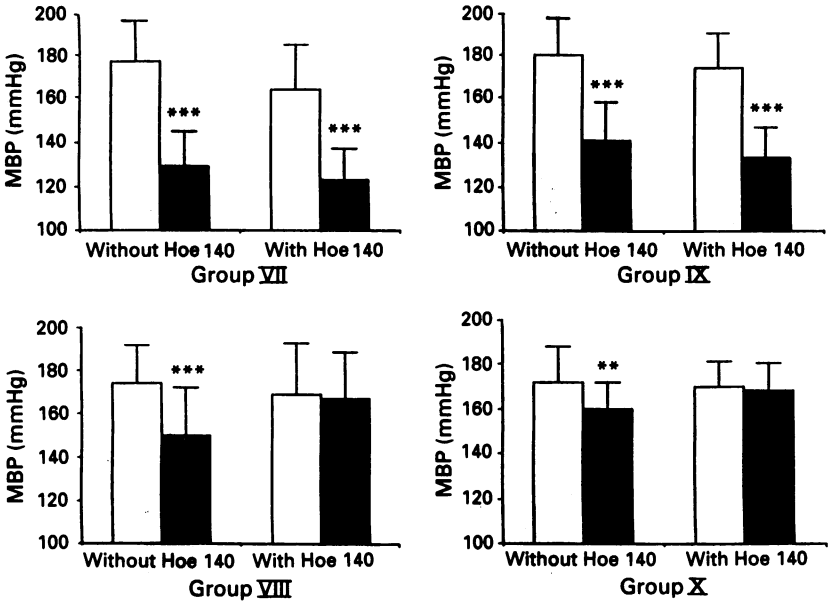


Figure 3 Mean blood pressure (MBP) values in the second set of experiments. The effects of nicardipine (upper panel) or perindoprilat (lower panel) are shown with or without pretreatment with the bradykinin B_2 receptor antagonist Hoe 140. Groups VII and VIII received a 0.4% NaCl diet whereas Groups IX and X received a 7% NaCl diet. Open columns, placebo; solid columns, after perindoprilat or nicardipine. $^{**}P<0.01$, $^{***}P<0.001$, nicardipine or perindoprilat vs placebo.

again there was no modification by pretreatment with Hoe 140 (39 ± 10 mmHg after placebo pretreatment and 41 ± 11 mmHg after Hoe pretreatment).

On the contrary, when perindoprilat was used, we obtained similar results to those observed in the first series of experiments, i.e. an abolition of the antihypertensive effects of the ACEI when rats were pretreated with the Hoe 140. In the low salt diet (Group VIII), MBP decreased after perindoprilat by 23 ± 8 mmHg after placebo pretreatment and by 2 ± 3 mmHg after Hoe 140 pretreatment. Finally in Group X (HS diet), perindoprilat decreased MBP by 12 ± 5 mmHg after placebo treatment and by 2 ± 1 mmHg following Hoe 140 pretreatment.

No changes of heart rate were recorded in any of the studied groups after the different treatments, except a very transient acceleration 2 to 3 min after nicardipine administration.

Discussion

The present study was designed to evaluate the participation of endogenous bradykinin in the acute hypotensive effects of the ACEI, perindoprilat, as a function of salt diet. We chose a dose of perindoprilat having a maximal hypotensive effect. Moreover, in order to understand the mechanisms of action of ACE inhibitors better we administered the bradykinin B_2 receptors antagonists before or after ACE inhibition.

The lack of increase in blood pressure following administration of Hoe 140 before perindoprilat shows that, in SHR, bradykinin does not seem to participate significantly in blood pressure regulation during basal conditions. In a previous study, we assessed the role of bradykinin in the blood pressure regulation of Dahl sensitive (DS) and resistant (DR) rats, fed a low or a high salt diet (Benetos *et al.*, 1993). In that study, we observed that in the salt sensitive strain, during a low salt diet, bradykinin played an important role in controlling blood pressure levels and that a high salt diet was able to inhibit endogenous bradykinin. On the other hand, in the salt-resistant animals (DR, SHR) no significant haemodynamic effects were observed after bradykinin blockade, showing that in these strains, bradykinin was not a major determinant of basal blood pressure regulation (Benetos *et al.*, 1992; 1993).

In all groups studied, bradykinin B_2-receptor blockade after perindoprilat injection significantly attenuated the hypotensive effects of ACE inhibition. This result shows that endogenous bradykinin activation by the ACEI has a vasodepressor action. An interesting finding of our study is that both BK antagonists induced the same increase in blood pressure, despite differences in their structure and pharmacokinetics. This result reduces the possibility of the existence of non-specific actions of these compounds on the blood pressure. In these groups, NaCl diet influences the respective roles of BK activation and AII diminution following administration of perindoprilat. Thus, while the absolute values of MBP elevation after BKA were similar in the various groups, the relative role of BK was much higher in the HS diet rats, since the MBP decrease after perindoprilat, was less pronounced in these latter groups. The latter observation can be explained by the fact that during a HS diet, a significant suppression of the renin angiotensin system occurs (Laubie *et al.*, 1984; Swales, 1990; Carretero & Scicli, 1991), and, therefore, the blockade of this system following ACEI has minor antihypertensive effects. Thus, in high salt fed rats, the major cause of ACEI-induced hypotension seems to be related to the activation of endogenous bradykinin.

Surprisingly, different results were obtained when perindoprilat was given after bradykinin receptor blockade with Hoe 140. In this latter case we observed a complete abolition of the hypotensive effects of perindoprilat in both low and high NaCl fed rats.

Similar results were observed by Linz & Schölkens (1992) in aortic-banding-induced hypertension. In that study, Hoe 140 completely abolished the hypotensive effects of ramiprilat (1 mg kg^{-1}) despite high renin-angiotensin activity in this experimental model. This effect was not observed by Cachofeiro *et al.* (1992), who reported that reduction in blood pressure induced by ramiprilat or captopril was curtailed in SHR pretreated with a B_2 receptor antagonist. In this last study, the schedule of the treatment was different since the B_2 receptor antagonist was given 15 min before administration of the ACE inhibitor and was followed up for 75 min. Moreover, the B_2 receptor antagonists were different, since Cachofeiro *et al.* (1992) used B3824 instead of Hoe 140. Both these compounds are selective and specific to B_2 receptors. However, Hoe 140 is much more potent than B3824 and has a very long lasting effect (Lembeck *et al.*, 1991)

which could be due to a non-competitive antagonist activity (Rhaleb *et al.*, 1992).

Several hypotheses could be suggested in order to explain the abolition of the hypotensive effects of perindoprilat in Hoe 140 pretreated rats: (1) It could be related to the blockade of the B_2 but not B_1 receptors by Hoe 140. In this condition and in the presence of perindoprilat which increases the plasma level of bradykinin, Hoe 140 could potentiate the effect of bradykinin and especially Des-Arg-bradykinin on the B_1 receptors. Actually, since kininase I (carboxypeptidase M) is not affected by ACE inhibition, an increase in Des-Arg-BK (B_1 receptor agonist) is expected (Ishida *et al.*, 1989). In fact Des-Arg-BK may increase blood pressure, since the weak direct hypotensive action of this peptide is overwhelmed by a pressor effect of released catecholamines through the B_1 receptor stimulation (Stewart, 1979). In a more recent study, Dominiak *et al.* (1992) showed that catecholamine and more especially adrenaline release occurred by both bradykinin and Des-Arg-BK, suggesting that both B_1 and B_2 receptors are involved. These effects were potentiated after administration of ACEI. This hypothesis could explain the paradoxical vasoconstriction that has been reported by Gardiner & Bennet (1992) in renal and mesenteric arteries after administration of bradykinin in the presence of captopril or perindopril. However, Bao *et al.* (1992) clearly demonstrated the absence of catecholamine stimulation in rats treated with ACEI, ramipril and Hoe 140.

Recently, Momose *et al.* (1993) reported that endothelin-1 (ET-1) secretion by human endothelial cells was inhibited by bradykinin via the B_2 receptor and stimulated by bradykinin via the B_1 receptor. In this condition, and in the presence of a non-competitive specific B_2 receptor antagonist, BK at a high plasma level could stimulate the ET-1 secretion via the B_1 receptor and induce some local vasoconstriction which could neutralise the renin-angiotensin-dependent hypotensive effect of perindoprilat.

(2) Hoe 140 could have some other, non-specific actions independent of BK receptor blockade. This hypothesis cannot be completely excluded. However, some previous data, as well as our results, make this suggestion improbable: (i) Hoe 140 has been described as a specific and selective B_2 receptor antagonist without any agonistic effect at the doses used in these experiments (Lembeck *et al.*, 1991; Wirth *et al.*, 1991); (ii) when administered before perindoprilat, no hypertensive effects were observed, and (iii) as we observed in the second set of experiments, the compound did not modify the hypotensive effects of nicardipine, showing that Hoe 140 has no influence on the peripheral vasorelaxation induced by other bradykinin-independent pathways.

In conclusion, our study shows that inhibition of endogenous bradykinin degradation participates in the acute antihypertensive effects of perindoprilat in SHRs. The role of bradykinin is more pronounced following an exposure to a high salt diet, i.e. when the renin-angiotensin system is suppressed. Blockade of bradykinin B_2 receptors by Hoe 140 before administration of perindoprilat completely abolished the hypotensive effect perindoprilat suggesting an increased role of bradykinin in the onset of the hypotensive action of ACE inhibitors. However other mechanisms, still unknown can be involved in this interaction.

References

AUBERT, J.F., WAEBER, B., NUSSBERGER, J., VAVREK, R., STEWART, J.M. & BRUNNER, H.R. (1987). Lack of a role of circulating bradykinin in the blood pressure response to acute angiotensin converting enzyme inhibition in rats. *Agents Actions*, **22**, 349–354.

BAO, G., GOHLKE, P., QADRI, F. & UNGER, T. (1992). Chronic kinin receptor blockade attenuates the antihypertensive effect of ramipril. *Hypertension*, **20**, 74–79.

BENETOS, A., BOUAZIZ, H. & SAFAR, M. (1992). Salt sensitivity and bradykinin activity in rats. *Agents Actions*, Suppl 38, III, 228–234.

BENETOS, A., BOUAZIZ, H. & SAFAR, M. (1993). Endogenous bradykinin activity in Dahl rats. *J. Cardiovasc. Pharmacol.*, **21**, 101–104.

BENETOS, A., GAVRAS, H., STEWART, J.M., VAVREK, R.J., HATINOGLOU, S. & GAVRAS, I. (1986). Vasodepressor role of endogenous bradykinin assessed by a bradykinin antagonist. *Hypertension*, **8**, 971–974.

CACHOFEIRO, V., SAKAKIBARA, T. & NASJLETTI, A. (1992). Kinins, nitric oxide and the hypotensive effect of captopril and ramiprilat in hypertension. *Hypertension*, **19**, 138–145.

CARBONELL, L.F., CARRETERO, O.A., STEWART, J.M. & SCICLI, A.G. (1988). Effects of a kinin antagonist on the acute antihypertensive activity of enalaprilat in severe hypertension. *Hypertension*, **11**, 239–243.

CARRETERO, O.A. & SCICLI, A.G. (1991). Local hormonal factors (intracrine, autocrine and paracrine) in hypertension. *Hypertension*, **18** (Suppl I), I-58–I-69.

DOMINIAK, P., SIMON, M., BLÖCHL, A. & BRENNER, P. (1992). Changes in peripheral sympathetic outflow of pithed SHRs after bradykinin and DesArg-Bradykinin infusions: influence of converting enzyme inhibition. *J. Cardiovasc. Pharmacol.*, **20** (Suppl 9), S35–S38.

ERDÖS, E.G. (1975). Angiotensin 1 converting enzyme. *Circ. Res.*, **36**, 247–255.

GARDINER, S.M. & BENNET, T. (1992). Involvement of nitric oxide in the regional haemodynamic effects of perindoprilat and captopril in hypovolaemic Brattleboro rats. *Br. J. Pharmacol.*, **107**, 1181–1191.

ISHIDA, H., SCICLI, A.G. & CARRETERO, O.A. (1989). Role of angiotensin converting enzyme and other peptidases in in vivo metabolism of kinins. *Hypertension*, **14**, 322–327.

LAUBIE, M., SCHIAVI, P., VINCENT, M. & SCHMITT, H. (1984). Inhibition of angiotensin-I-converting enzyme with S 9490: biochemical effects, interspecies differences and role of sodium diet in haemodynamic effects. *J. Cardiovasc. Pharmacol.*, **6**, 1076–1082.

LEMBECK, F., GRIESBACHER, T., ECKHARDT, M., HENKE, S., BREIPOHL, G. & KNOLLE, J. (1991). New, long-acting potent bradykinin antagonist. *Br. J. Pharmacol.*, **102**, 297–304.

LINZ, W. & SCHÖLKENS, B.A. (1992). A specific B_2-bradykinin receptor antagonist Hoe 140 abolishes the antihypertrophic effect of ramipril. *Br. J. Pharmacol.*, **105**, 771–772.

MOMOSE, N., FUKUO, K., MORIMOTO, S. & OGIHARA, T. (1993). Captopril inhibits endothelin-1 secretion from endothelial cells through bradykinin. *Hypertension*, **21**, 921–924.

MULINARI, R., BENETOS, A., GAVRAS, I. & GAVRAS, H. (1988). Vascular and sympathoadrenal response to bradykinin and a bradykinin analogue. *Hypertension*, **11**, 754–757.

RHALEB, N.E., ROUISSI, N., JUKIC, D., REGOLI, D., HENKE, S., BREIPOHL, G. & KNOLLE, J. (1992). Pharmacological characterisation of a new highly potent B2 receptor antagonist (HOE 140: D-Arg- [Hyp^3, Thi^5, D-Tic^7, Oic^8] bradykinin). *Eur. J. Pharmacol.*, **210**, 115–120.

SCHÖLKENS, B.A. & LINTZ, W. (1993). Cardioprotective actions of bradykinin in myocardial ischemia and left ventricular hypertrophy. Oral Communication In *Kinins*, 1993, Brazil.

SEINO, M., ABE, K., NUSHIRO, N., OMATA, K. & YOSHINAGA, J. (1989). Role of endogenous bradykinin in the acute depressor effect of angiotensin converting enzyme inhibitor captopril – assessed by a competitive antagonist of bradykinin. *Clin. Exp. Hypertens.*, (A), **11**, 35–43.

STEWART, J.M. (1979). Chemistry and biologic activity of peptides related to bradykinin. In *Bradykinin, Kallidin, and Kallikrein*, Vol. 25 Suppl *Handbook of Experimental Pharmacology* ed. Erdos, E.G. pp. 227–272. Berlin: Springer-Verlag.

SWALES, J.D. (1990). *Dietary Sodium Restriction in Hypertension: Pathophysiology, Diagnosis and Management*. ed. Laragh, J.H. & Brenner, B.M. Ch. 126, pp. 2011–2019. New York: Raven Press.

SWARTZ, S.L., WILLIAMS, G.H., HOLLENBERG, N.K., MOORE, T.J. & DLUHI, R. (1979). Converting enzyme inhibition in essential hypertension: the hypotensive response does not reflect only reduced angiotensin II formation. *Hypertension*, **1**, 106–111.

THURSTON, H. & SWALES, J.D. (1978). Converting enzyme inhibitor and saralasin infusion in rats: evidence for an additional vasodepressor property of converting enzyme inhibitor. *Circ. Res.*, **42**, 588–592.

VAVREK, R.J. & STEWART, J.M. (1985). Competitive antagonists of bradykinin. *Peptides*, **6**, 161–164.

WAEBER, B., AUBERT, J.G., VAVREK, R., STEWART, J.M., NUSSBERGER, J. & BRUNNER, H.R. (1986). Role of bradykinin in blood pressure regulation of conscious spontaneously hypertensive rats. *J. Hypertens.*, **4** (Suppl 6), S597–S598.

WIRTH, K., HOEK, F.J., ALBUS, U., LINZ, W., ANAGNOSTOPOULOS, H., HENKE, S.T., BREIPOHL, G., KÖNING, W., KNOLLE, J. & SCHÖLKENS, B.A. (1991). HOE 140 a new potent and long acting bradykinin-antagonist: *in vivo* studies. *Br. J. Pharmacol.*, **102**, 774–777.

(Received January 21, 1994
Revised June 8, 1994
Accepted June 22, 1994)

Br. J. Pharmacol. (1994), **113**, 723–728 © Macmillan Press Ltd, 1994

Pharmacological evidence of distinct α_1-adrenoceptor subtypes mediating the contraction of human prostatic urethra and peripheral artery

[1]Akihiko Hatano, Hitoshi Takahashi, Makoto Tamaki, Takeshi Komeyama, Takako Koizumi & Masayuki Takeda

Department of Urology, Niigata University School of Medicine, Asahimachi 1, Niigata 951, Japan

1 The α_1-adrenoceptor subtypes mediating contractions of the smooth muscle in human prostatic urethra and branches of internal iliac artery were characterized in isometric contraction experiments.

2 Phenylephrine produced concentration-dependent contractions in both the urethra and artery. These responses were competitively inhibited by prazosin, WB4101 and 5-methyl-urapidil, and the slopes of Schild plots for all these antagonists were close to unity.

3 The pA_2 values for prazosin were not significantly different between the urethra (9.42 ± 0.11; mean ± s.d.) and artery (9.50 ± 0.27), while the pA_2 values for WB4101 and 5-methyl-urapidil in the human prostatic urethra (8.94 ± 0.19 and 8.42 ± 0.14, respectively) were significantly greater than in the branches of human internal iliac artery (7.94 ± 0.21 and 7.43 ± 0.22, respectively; $P<0.01$).

4 Pretreatment with chlorethylclonidine (CEC) at concentrations ranging from 0.1 μM to 100 μM attenuated the maximum contraction to phenylephrine in a concentration-dependent manner in both the urethra and artery. However, the urethra was significantly less affected by CEC than the artery. The pD'_2 values (negative logarithm of the molar concentration of antagonist which reduced the maximum contraction to one half) in the urethra and artery were 4.35 ± 0.27 and 5.20 ± 0.37, respectively ($P<0.01$).

5 The present results indicate that there are distinct populations of α_1-adrenoceptor subtypes in the human prostatic urethra and branches of the internal iliac artery. The α_1-adrenoceptors responsible for the contraction of the human internal iliac artery branches are predominantly α_{1B}-subtype, whereas those in the human prostatic urethra are considered to be not α_{1B}, but α_{1C} or possibly α_{1A} or $\alpha_{1A/D}$-subtype.

Keywords: α_1-Adrenoceptor subtype; human urethra; human artery; phenylephrine-induced contraction; prazosin; WB4101; 5-methyl-urapidil; chlorethylclonidine

Introduction

α_1-Adrenoceptors have been subclassified according to their pharmacological properties into two receptor subtypes designated α_{1A} and α_{1B}. The α_{1A}-subtype shows high affinity for WB4101, benoxathian and 5-methyl-urapidil, and has little sensitivity to an irreversible alkylating agent, chlorethylclonidine (CEC), whereas the α_{1B}-subtype exhibits low affinity for the above-mentioned competitive antagonists and is potently inactivated by CEC (Morrow & Creese, 1986; Han *et al.*, 1987a,b; Minneman *et al.*, 1988; Gross *et al.*, 1988).

In recent years, molecular biological studies have revealed the existence of three genes encoding α_1-adrenoceptor subtypes, α_{1A} (rat: Lomasney *et al.*, 1991), α_{1B} (hamster: Cotecchia *et al.*, 1988) and α_{1C} (bovine: Schwinn *et al.*, 1990). In addition, another gene coding for a novel α_{1D}-subtype has been cloned (rat: Perez *et al.*, 1991). Identification of α_1-adrenoceptor subtypes in human various tissues is difficult. As regards the subtypes of α_1-adrenoceptors in human prostatic smooth muscles, several pharmacological and molecular biological studies have been reported (Chapple *et al.*, 1991; Lepor *et al.*, 1993a,b; Testa *et al.*, 1993; Price *et al.*, 1993). However, subclassification of α_1-adrenoceptors in human urethra and blood vessels has received little attention (Chapple *et al.*, 1991; Testa *et al.*, 1993).

The clinical effect of α_1-adrenoceptor antagonists for bladder outlet obstruction has already been established. Caine *et al.* (1975) first reported the pharmacological evidence that the human prostatic capsule and prostatic adenoma were rich in α-adrenoceptors. Subsequently, the efficacy of nonselective α-adrenoceptor antagonists, such as phenoxybenzamine and phentolamine, for the treatment of symptomatic bladder outlet obstruction was reported (Caine *et al.*, 1976; McGuire *et al.*, 1976; Awad *et al.*, 1976). In patients with benign prostatic hypertrophy, it was found that phentolamine reduced the intraurethral pressure in all portions of the urethra and inhibited noradrenaline-induced contraction of the isolated prostate, prostatic capsule and prostatic urethra (Furuya *et al.*, 1982). More recently, the α-adrenoceptors in these tissues were characterized as α_1- and α_2-adrenoceptors (Lepor & Shapiro, 1984; Kunisawa *et al.*, 1985; Gup *et al.*, 1990), and the selective α_1-adrenoceptor antagonists, such as prazosin or terazosin, have been reported as superior to nonselective α-blockers in safety and efficacy (Hedlund *et al.*, 1983; Kawabe *et al.*, 1990; Lepor *et al.*, 1990; Jardin *et al.*, 1991). The clinical effects of these antagonists are dose-dependent, but the development of systemic side effects restricts the maximum therapeutic dose. The most common adverse events associated with current selective α_1-antagonists are light-headedness, weakness and dizziness (Lepor *et al.*, 1990), which may be mediated by vascular and cerebral α_1-adrenoceptors. To avoid such adverse events, differentiation of α_1-adrenoceptor subtypes between human urethra and artery, as well as development of α_1-blockers selective for the human urethra, is essential. Consequently, this study was designed to identify α_1-adrenoceptor subtypes mediating contraction of the smooth muscle in human prostatic urethra and peripheral artery by isometric contraction technique.

[1] Author for correspondence at present address: Department of Urology, New York University Medical Center, 550 First Avenue, New York, NY 10016, U.S.A.

Methods

Human prostatic urethra in the region from the bladder neck to the proximal end of the colliculus seminalis and branches of the internal iliac artery, such as the superior vesical artery or obturator artery, were used. These tissues were obtained at the time of surgery from 19 males, aged 51 to 83 years (65.9 average), undergoing total cystectomy and pelvic lymph node dissection for urinary bladder tumour. Patients who had symptomatic bladder outlet obstruction, macroscopically obvious benign prostatic hyperplasia, urethral involvement of urinary bladder tumour, or prostatic cancer were excluded from this study. No patient had received irradiation, anticancer chemotherapy, or α_1-blocker administration prior to the surgery. Informed consent was obtained from each patient. These resected tissues were preserved at 4°C in oxygenated Krebs-Henseleit solution just after excision, and were used for the experiments within 24 h.

Preparation of tissue specimens

Urethral mucosa and prostate were removed from the smooth muscle layer of the normal prostatic urethra, and the artery was cleaned of adherent fatty and connective tissues. Then transverse smooth muscle strips measuring approximately 10 × 3 mm were prepared from the prostatic urethra, and ring media preparations, approximately 2 mm in diameter and 5 mm in length, were obtained from the branches of internal iliac artery. In order to avoid the possible involvement of endothelium-derived relaxing factor in the mechanical response (Furchgott, 1981), the endothelium of each segment of the artery was removed by rubbing them with a metal sound. Each preparation was suspended in an organ bath containing 10 ml modified Krebs-Henseleit buffer (mM): NaCl 111.0, KCl 5.9, $CaCl_2$ 2.5, $MgCl_2$ 1.2, NaH_2PO_4 1.2, $NaHCO_3$ 25.0 and glucose 11.5. The baths were maintained at 37°C, pH 7.4 and continuously aerated with a gas mixture consisting of 95% O_2 and 5% CO_2. A resting tension of 1 g was applied and the isometric contraction was recorded through a force-displacement transducer (T-7, Orientec, Japan) coupled to an amplifier unit (1829, Nihon Denki San-ei, Japan) and ink oscillographs (Servocorder, SR6211-2L, Graphtec, Japan). The preparations were equilibrated for at least 60 min before starting the experiments.

Phenylephrine concentration-response experiments

We used phenylephrine as an agonist in both tissues in order to eliminate the involvement of postjunctional α_2-adrenoceptors. Concentration-response curves for phenylephrine were obtained by direct administration of the drug into the bathing media in a cumulative fashion (10 nM–10 mM). Propranolol (1 μM) and atropine (1 μM) were added to the bathing solution 10 min before the phenylephrine concentration-response experiments in order to block β-adrenoceptors and muscarinic receptors, respectively.

In preliminary experiments, we confirmed the reproducibility of the concentration-response curves in each preparation. After determination of control concentration-response curves, the preparations were washed 3 times with a drug-free buffer and allowed to equilibrate for about 60 min prior to the next cumulative dose experiments. Competitive antagonists of α_1-adrenoceptors, prazosin (1–30 nM), WB-4101 (10–300 nM), and 5-methyl-urapidil (10–300 nM) were applied 30 min before the contractile response to phenylephrine in the presence of each antagonist. This procedure was repeated with 3 or 4 different but increasing concentrations of the antagonist in the same preparation. The competitive antagonistic activities were expressed as pA_2 values which were calculated according to the method of Arunlakshana & Schild (1959).

Chlorethylclonidine-pretreatment

Effects of chlorethylclonidine (CEC), an irreversible antagonist of α_1-adrenoceptors were also investigated. After determination of control concentration-response curves, the preparations were repetitively treated with CEC (at final concentrations ranging from 0.1 to 100 μM) for a total of 80 min; following the initial application, CEC was renewed 3 times every 20 min, because previous reports (Minneman *et al.*, 1988; Suzuki *et al.*, 1990) and our preliminary experiments showed that the incomplete access of the highly water-soluble CEC to α_1-adrenoceptor-binding sites could be overcome by repetitive treatments. After CEC pretreatment, the preparations were extensively washed with fresh Krebs-Henseleit solution for 30 min (7 repeats at 5 min intervals, 5 times each repeat), and then cumulative concentration-response curves for phenylephrine were obtained. The antagonistic activities of CEC were expressed as pD'_2 values (negative logarithm of the molar concentration of antagonist which reduce the maximum contraction to one half; Ariëns & van Rossum, 1957).

Drugs

Phenylephrine hydrochloride, prazosin hydrochloride, WB4101 hydrochloride (N-[2-(2,6-dimethoxy-phenoxy)ethyl]-2,3-dihydro-1,4-benzodioxin-2-methanamine hydrochloride), 5-methyl-urapidil, chlorethylclonidine and (±)-propranolol hydrochloride were purchased from Research Biochemicals Inc. (Natick, MA, U.S.A.). Atropine sulphate monohydrate was purchased from Wako Pure Chemical Industries Ltd. (Osaka, Japan).

Statistical analyses

Experimental values are given as a mean ± standard deviation (s.d.). Results were analysed by Student's *t* test for unpaired observation and a probability of less than 0.05 was considered significant.

Results

Effects of the competitive antagonists on phenylephrine-induced contraction

α_1-Adrenoceptor stimulation by phenylephrine produced concentration-dependent contractions in the human urethra and branches of the internal iliac artery. These contractile responses were antagonized by prazosin, WB4101 and 5-methyl-urapidil, resulting in rightward parallel shifts of the concentration-response curves (Figures 1, 2 and 3). The slopes of Schild plots for all antagonists tested were close to unity (Table 1), suggesting that these antagonists competitively inhibited the contractile responses elicited by phenylephrine in both tissues. Prazosin inhibited the phenylephrine responses at lower concentrations than WB4101 or 5-methyl-urapidil in both the urethra and the artery, thus resulting in higher pA_2 values. The pA_2 values for prazosin in the urethra and artery were 9.42 ± 0.11 and 9.50 ± 0.27, respectively (Table 1), and there was no significant difference in the pA_2 values between the two tissues. The pA_2 values for WB4101 in the urethra and artery were 8.94 ± 0.19 and 7.94 ± 0.21, respectively, and those for 5-methyl-urapidil were 8.42 ± 0.14 and 7.43 ± 0.22 (Table 1). Thus the pA_2 values for WB4101 and 5-methyl-urapidil in the urethra were significantly greater than those in the artery ($P<0.01$).

Effects of chlorethylclonidine on phenylephrine-induced contractions

Chlorethylclonidine (CEC) which is an irreversible alkylating agent of α_1-adrenoceptors (LeClerc *et al.*, 1980) attenuated

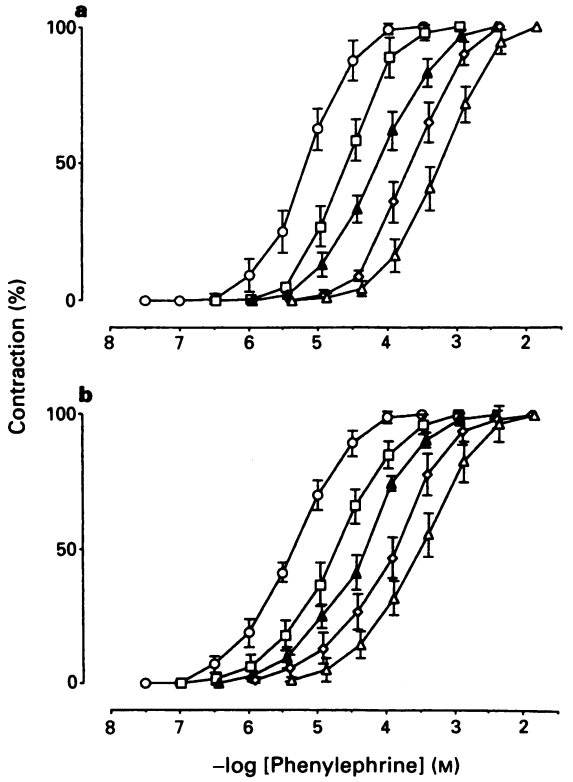


Figure 1 Effects of prazosin on the concentration-response curves for phenylephrine in the human prostatic urethra (a) and branches of the internal iliac artery (b). (○) Control; (□) 1 nM prazosin; (▲) 3 nM prazosin; (◇) 10 nM prazosin; (△) 30 nM prazosin. Each value is presented as the mean ± s.d. (bar) of 8 experiments.

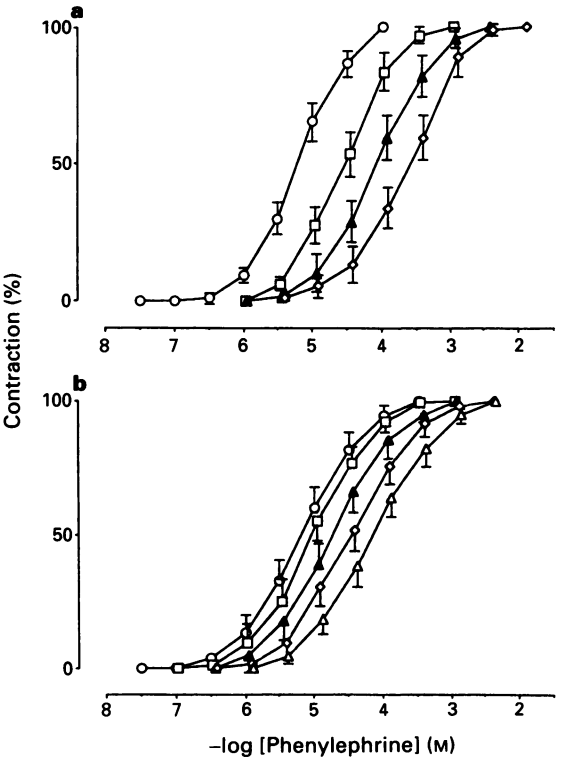


Figure 3 Effects of 5-methyl-urapidil (5-MeU) on the concentration-response curves for phenylephrine in the human prostatic urethra (a) and branches of the internal iliac artery (b). (○) Control; (□) 10 nM 5-MeU; (▲) 30 nM 5-MeU; (◇) 100 nM 5-MeU; (△) 300 nM 5-MeU. Each value is presented as the mean ± s.d. of 7 (a) and 9 (b) experiments.

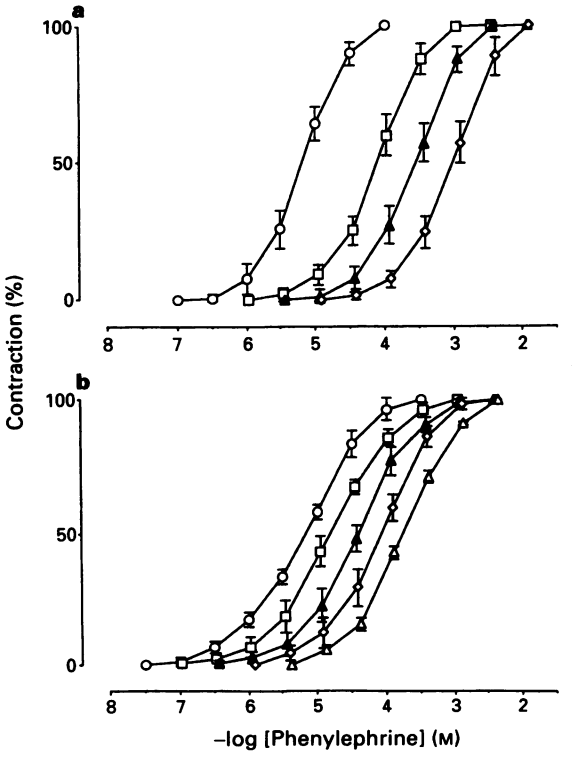


Figure 2 Effects of WB4101 on the concentration-response curves for phenylephrine in the human prostatic urethra (a) and branches of the internal iliac artery (b). (○) Control; (□) 10 nM WB4101; (▲) 30 nM WB4101; (◇) 100 nM WB4101; (△) 300 nM WB4101. Each value is presented as the mean ± s.d. of 11 (a) and 8 (b) experiments.

the maximum contractile responses induced by phenylephrine in both tissues in a concentration-dependent manner (Figure 4). However, the urethra was less affected by CEC than was the artery. Pretreatment with 10 μM and 100 μM CEC abolished about 55% and 90%, respectively, of the contractile response elicited by phenylephrine in the artery, while it abolished about 30% and 60% in the urethra. The pD'_2 value for CEC in the branches of the internal iliac artery (5.20 ± 0.37) was significantly greater than that in the prostatic urethra (4.35 ± 0.27) ($P<0.01$; Table 2).

Discussion

In this study, we have confirmed the distinction of α_1-adrenoceptor subtypes in the smooth muscle between the human prostatic urethra and branches of the internal iliac artery by the isometric contraction technique using WB4101, 5-methyl-urapidil and chlorethylclonidine as selective antagonists. This is the first report on the comparison of the α_1-adrenoceptor subtypes mediating the contraction of the smooth muscle in the human urethra and peripheral artery.

Originally, α_1-adrenoceptors which have high affinity for prazosin were subdivided into α_{1A}- and α_{1B}-adrenoceptor subtypes based on the affinities of WB4101, benoxathian (Morrow & Creese, 1986; Han *et al.*, 1987a) and 5-methyl-urapidil (Gross *et al.*, 1988) and sensitivities to the Ca^{2+} channel blocker, nifedipine (Han *et al.*, 1987a) in various tissues of rat, and also based on the ability of the alkylating agent CEC to inactivate the α_{1B} but not the α_{1A}-subtype (Han *et al.*, 1987b; Minneman *et al.*, 1988).

In the present study, the pA_2 values for WB4101 and 5-methyl-urapidil, which were thought to be α_{1A}-selective antagonists, were significantly higher in the urethra than in the artery, and the pD'_2 values for CEC were significantly

Table 1 pA_2 values of prazosin, WB4101 and 5-methyl-urapidil (5-MeU) in the human prostatic urethra and branches of the internal iliac artery

Antagonist	n	Urethra pA_2	Slope	n	Artery pA_2	Slope	Student's t test
Prazosin	8	9.42 ± 0.11	0.98	8	9.50 ± 0.27	0.90	NS
WB4101	11	8.94 ± 0.19	1.07	8	7.94 ± 0.21	0.97	$P<0.01$
5-MeU	7	8.42 ± 0.14	1.07	9	7.43 ± 0.22	1.06	$P<0.01$

Data shown are mean ± standard deviation, n = number of experiments. NS = not significant.

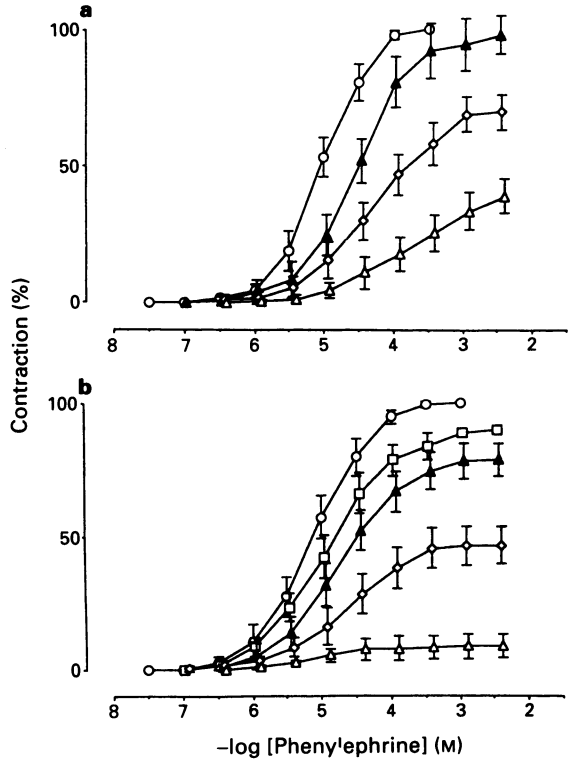


Figure 4 Effects of pretreatment with chlorethylclonidine (CEC) on phenylephrine-induced contraction of the human prostatic urethra (a) and branches of the internal iliac artery (b). (○) Control; (□) 0.1 μM CEC; (▲) 1 μM CEC; (◇) 10 μM CEC; (△) 100 μM CEC. Each value is expressed as % maximal response to phenylephrine is the mean ± s.d. (bar) of 6 (a) and 5 (b) experiments.

Table 2 pD'_2 values of chlorethylclonidine (CEC) in the human prostatic urethra and branches of the internal iliac artery

Antagonist	n	Urethra pD'_2	n	Artery pD'_2	Student's t test
CEC	6	4.35 ± 0.27	5	5.20 ± 0.37	$P<0.01$

Data shown are mean ± standard deviation, n = number of experiments. pD'_2: negative logarithms of the molar concentration of antagonist which reduce the maximum contraction to one half.

higher in the artery than in the urethra. Thus, the artery showed low affinities for WB4101 and 5-methyl-urapidil, and high susceptibility to inactivation by CEC. The α_1-adrenoceptor subtype responsible for the contraction of smooth muscles of human peripheral arteries therefore should be considered to belong to the α_{1B}-subtype. On the other hand, the human prostatic urethra showed higher affinities for WB4101 and 5-methyl-urapidil, which suggested that the α_1-subtype mediating the contraction of the human urethral smooth muscles might be the α_{1A}-subtype. However, the urethra displayed a considerable degree of sensitivity to inactivation by CEC, although it was significantly less than in the artery. This result does not agree with the fact that the pretreatment with CEC produced no effect on the contractile response of rat vas deferens (Han *et al.*, 1987b) which is considered to be mediated predominantly by α_{1A}-adrenoceptors (Aboud *et al.*, 1993). Thus, the α_1-adrenoceptors in the human prostatic urethra may be a mixture of α_{1A}- and α_{1B}-subtypes. In rat mesenteric artery and portal vein, α-adrenergic contractile responses are supposed to be mediated by a mixture of both α_{1A}- and α_{1B}-subtypes because both CEC and nifedipine partially attenuated noradrenaline-induced contractions, and WB4101 had moderate potencies in those tissues (Han *et al.*, 1990). Takayanagi *et al.* (1991) showed that, in rabbit common iliac artery, the concentration-response curve for phenylephrine was shifted by a lower concentration of WB4101, with no further shift being evident when a higher concentration of WB4101 was used, and demonstrated that, in rabbit aorta, two pA_2 values for WB4101 could be estimated according to computer-assisted analysis of the nonlinear Schild plot for an antagonism between phenylephrine and WB4101. Consequently, it was suggested that the rabbit aorta and the common iliac artery contained both α_{1A}- and α_{1B}-subtypes. In the present experiments, however, phenylephrine-induced concentration-responses curves in the urethra were shifted by WB4101 and 5-methyl-urapidil in a parallel manner and the Schild plots for both antagonists were linear with the slope close to unity. Thus, we could not obtain evidence of involvement of more than two adrenoceptor subtypes in the contraction of the human prostatic urethra by functional experiments.

Recent molecular biological studies revealed the existence of at least three distinct genes coding for α_1-adrenoceptors of mammals, namely α_{1A}- (Lomasney *et al.*, 1991), α_{1B}- (Cotecchia *et al.*, 1988) and α_{1C}-receptors (Schwinn *et al.*, 1990). Moreover, the clone of a novel α_{1D}-subtypes has been reported (Perez *et al.*, 1991). It is now widely accepted that CEC inactivates all of these cloned α_1-adrenoceptor subtypes, whereas the classical 'pharmacological' α_{1A}-subtype is considered resistant to this alkylating agent (Han *et al.*, 1987b; Minneman *et al.*, 1988) and it has not yet been identified by molecular cloning techniques. The cloned rat α_{1A}-adrenoceptor is now regarded as identical to rat α_{1D}-adrenoceptor (the DNA sequences of these two receptors were identical, except for two codons), and thus Schwinn & Lomasney (1992) have proposed designating it as the $\alpha_{1A/D}$-adrenoceptor. Pharmacological properties of the cloned α_1-adrenoceptor subtypes (α_{1B}, α_{1C} and $\alpha_{1A/D}$) have been studied by ligand binding experiments using membranes from COS-7 or HeLa cells transfected with the expression vector containing each cDNA (Schwinn *et al.*, 1990; Lomasney *et al.*, 1991; Perez *et al.*, 1991; Schwinn & Lomasney, 1992). Testa *et al.* (1993) evaluated the affinities of diverse α_1-antagonists for the α_1-adrenoceptor subtypes by a receptor binding technique using membranes of rat hippocampus pretreated with CEC (classical α_{1A}), rat liver (α_{1B}) and rabbit liver (α_{1C}). According to these reports, the pK_i values for prazosin were 9.03 in rat classical α_{1A} (Testa *et al.*, 1993), 9.25–9.60 in hamster and rat α_{1B} (Schwinn *et al.*, 1990; Lomasney *et al.*, 1991; Perez *et al.*,

1991; Testa *et al.*, 1993), 9.00–9.57 in bovine and rat α_{1C} (Schwinn *et al.*, 1990; Lomasney *et al.*, 1991; Testa *et al.*, 1993), and 9.48–9.49 in rat $\alpha_{1A/D}$ (Lomasney *et al.*, 1991; Perez *et al.*, 1991), all of which showed almost equivalent values. The pA_2 values for prazosin in our study were 9.42 in the urethra and 9.50 in the artery, being close to the above-mentioned pK_i values. The pK_i values for WB4101 derived from those binding studies were 8.89 in classical α_{1A} (Testa *et al.*, 1993), 7.54–8.23 in α_{1B} (Schwinn *et al.*, 1990; Lomasney *et al.*, 1991; Perez *et al.*, 1991; Testa *et al.*, 1993), 8.89–9.26 in α_{1C} (Schwinn *et al.*, 1990; Lomasney *et al.*, 1991; Testa *et al.*, 1993), and 8.67–8.72 in $\alpha_{1A/D}$ (Lomasney *et al.*, 1991; Perez *et al.*, 1991). The pK_i values for 5-methyl-urapidil were 8.33 in classical α_{1A} (Testa *et al.*, 1993), 6.47–7.39 in α_{1B} (Perez *et al.*, 1991; Schwinn & Lomasney, 1992; Testa *et al.*, 1993), 7.76–8.16 in α_{1C} (Schwinn & Lomasney, 1992; Testa *et al.*, 1993), and 6.48–7.82 in $\alpha_{1A/D}$ (Perez *et al.*, 1991; Schwinn & Lomasney, 1992). It is noteworthy that WB4101 has high affinity for α_{1C} and $\alpha_{1A/D}$ subtypes, and 5-methyl-urapidil has high affinity for the α_{1C}-subtype and low affinity for the $\alpha_{1A/D}$-subtype as well as the α_{1B}-subtype, although they have been regarded as α_{1A}-selective antagonists. The pA_2 values of the human artery for WB4101 and 5-methyl-urapidil found in this study were 7.94 and 7.43, which were comparable to the pK_i values of hamster and rat α_{1B}-receptors. On the other hand, the pA_2 value of the human urethra for WB4101 (8.94) and 5-methyl-urapidil (8.42) were close to the pK_i values of rat classical α_{1A}- and bovine and rat α_{1C}-receptors. These findings suggest that the human peripheral artery contains predominantly the α_{1B}-adrenoceptor subtype, and the human prostatic urethra primarily α_{1A} or α_{1C}; however it is unknown which receptor is the chief one in the urethra.

In the binding study of transfected COS-7 cells, pretreatment with 100 μM CEC for 10 min inactivated 98% of the cloned hamster α_{1B}-receptor, while 72% of the rat $\alpha_{1A/D}$-receptor was inactivated by the same pretreatment (Perez *et al.*, 1991). Exposure to 100 μM CEC for 20 min also inactivated 95% of the cloned hamster α_{1B}-receptor and 68% of the bovine α_{1C}-receptor (Schwinn *et al.*, 1990). In our study, preincubation of the artery with 10 μM and 100 μM CEC for 80 min caused 55% and 90% decrease in maximum contraction, respectively, and thus high susceptibility of the human artery to CEC was demonstrated. Accordingly, it is strongly suggested that the α_1-adrenoceptor subtype mediating the contraction of the branches of human internal iliac artery is mainly the α_{1B}-subtype. In the human urethra in our study, preincubation with 10 μM and 100 μM CEC for 80 min elicited 30% and 60% reduction in maximum contraction, respectively; thus a fairly high susceptibility of the urethra to blockade by CEC was demonstrated. In the light of these findings, we consider the α_1-adrenoceptor subtype responsible for the contraction of the human prostatic urethra may be primarily the α_{1C}- or $\alpha_{1A/D}$-subtype rather than the classical α_{1A}-subtype. In contrast to our results, Testa *et al.* (1993) reported that the number of specific [^{3}H]-prazosin binding sites in the human prostatic urethral membranes was not affected by pretreatment with CEC for 30 min, and they concluded that the α_{1A}-subtype is the main α_1-adrenoceptor present in the urethra. This discrepancy may be due to the difference in the method of CEC-pretreatment. Also in our preliminary experiments, a single pretreatment with CEC up to 10 μM for 10–30 min hardly affected the contractile responses in both the urethra and artery.

It is clear from this study that it is at present difficult to identify definitively functional α_1-adrenoceptors with the materials available. But we have confirmed that the α_1-adrenoceptors in the human prostatic urethra are apparently different from those in the human peripheral artery, and our findings have important clinical implications for the possibility that an α_1-adrenoceptor antagonist with low affinity for the α_{1B}-subtype may attain a therapeutic response to bladder outlet obstruction with fewer side effects. To determine the exact adrenoceptor subtypes in the human urethra and artery, application of molecular biological techniques to the human tissues are essential.

We thank the staff of the Department of Urology, Niigata University Hospital, and Dr Ryuji Takaki, Dr Tsutomu Nishiyama and Dr Sho Nakamura for offers of human tissues. This work was supported in part by the Grant-In-Aid for Scientific Research from the Ministry of Education, Science and Culture of Japan, Suzuki Memorial Urological Grant, and Yujin Memorial Grant.

References

ABOUD, R., SHAFII, M. & DOCHERTY, J.R. (1993). Investigation of the subtypes of α_1-adrenoceptor mediating contractions of rat aorta, vas deferens and spleen. *Br. J. Pharmacol.*, **109**, 80–87.

ARIENS, E.J. & VAN ROSSUM, J.M. (1957). pD_X, pA_X and pD'_X values in the analysis of pharmacodynamics. *Arch. Int. Pharmacodyn.*, **110**, 275–299.

ARUNLAKSHANA, O. & SCHILD, H.O. (1959). Some quantitative uses of drug antagonists. *Br. J. Pharmacol. Chemother.*, **14**, 48–58.

AWAD, S.A., DOWNIE, J.W., LYWOOD, D.W., YOUNG, R.A. & JARZYLO, S.V. (1976). Sympathetic activity in the proximal urethra in patients with urinary obstruction. *J. Urol.*, **115**, 545–547.

CAINE, M., RAZ, S. & ZEIGLER, M. (1975). Adrenergic and cholinergic receptors in the human prostate, prostatic capsule and bladder neck. *Br. J. Urol.*, **47**, 193–202.

CAINE, M., PFAU, A. & PERLBERG, S. (1976). The use of alpha-adrenergic blockers in benign prostatic obstruction. *Br. J. Urol.*, **48**, 255–263.

CHAPPLE, C.R., BURT, R.P. & MARSHALL, I. (1991). α_1-Adrenoceptor subtypes in the human prostate and inferior epigastric artery. *Neurourol. Urodyn.*, **10**, 306–308.

COTECCHIA, S., SCHWINN, D.A., RANDALL, R.R., LEFKOWITZ, R.J., CARON, M.G. & KOBILKA, B.K. (1988). Molecular cloning and expression of the cDNA for the hamster α_1-adrenergic receptor. *Proc. Natl. Acad. Sci. U.S.A.*, **85**, 7159–7163.

FURCHGOTT, R.F. (1981). The requirement for endothelial cells in the relaxation of arteries by acetylcholine and some vasodilators. *Trends Pharmacol. Sci.*, **2**, 173–176.

FURUYA, S., KUMAMOTO, Y., YOKOYAMA, E., TSUKAMOTO, T., IZUMI, T. & ABIKO, Y. (1982). Alpha-adrenergic activity and urethral pressure in prostatic zone in benign prostatic hypertrophy. *J. Urol.*, **128**, 836–839.

GROSS, G., HANFT, G. & RUGEVICS, C. (1988). 5-Methyl-urapidil discriminates between subtypes of the α_1-adrenoceptor. *Eur. J. Pharmacol.*, **151**, 333–335.

GUP, D.I., SHAPIRO, E., BAUMANN, M. & LEPOR, H. (1990). Autonomic receptors in human prostate adenomas. *J. Urol.*, **143**, 179–185.

HAN, C., ABEL, P.W. & MINNEMAN, K.P. (1987a). α_1-Adrenoceptor subtypes linked to different mechanisms for increasing intracellular Ca^{2+} in smooth muscle. *Nature*, **329**, 333–335.

HAN, C., ABEL, P.W. & MINNEMAN, K.P. (1987b). Heterogeneity of α_1-adrenergic receptors revealed by chlorethylclonidine. *Mol. Pharmacol.*, **32**, 505–510.

HAN, C., LI, J. & MINNEMAN, K.P. (1990). Subtypes of α_1-adrenoceptors in rat blood vessels. *Eur. J. Pharmacol.*, **190**, 97–104.

HEDLUND, H., ANDERSSON, K.-E. & EK, A. (1983). Effects of prazosin in patients with benign prostatic obstruction. *J. Urol.*, **130**, 275–278.

JARDIN, A., BENSADOUN, H., DELALUCHE-CAVALLOR, M.C. & ATTALI, P. (1991). Alfuzosin for the treatment of benign prostatic hypertrophy. *Lancet*, **337**, 1457–1461.

KAWABE, K., UENO, A., TAKIMOTO, Y., ASO, Y., KATO, H. & YM617 CLINICAL STUDY GROUP (1990). Use of an α_1-blocker, YM617, in the treatment of benign prostatic hypertrophy. *J. Urol.*, **144**, 908–912.

KUNISAWA, Y., KAWABE, K., NIIJIMA, T., HONDA, K. & TAKENAKA, T. (1985). A pharmacological study of alpha adrenergic receptor subtypes in smooth muscle of human urinary bladder base and prostatic urethra. *J. Urol.*, **134**, 396–398.

LECLERC, G., ROUOT, B., SCHWARTZ, J., VELLY, J. & WERMUTH, C.G. (1980). Studies on some para-substituted clonidine derivatives that exhibit an α-adrenoceptor stimulant activity. *Br. J. Pharmacol.*, **71**, 5–9.

LEPOR, H., KNAPP-MALONEY, G. & SUNSHINE, H. (1990). A dose titration study evaluating terazosin, a selective, once-a-day α_1-blocker for the treatment of symptomatic benign prostatic hyperplasia. *J. Urol.*, **144**, 1393–1398.

LEPOR, H. & SHAPIRO, E. (1984). Characterization of alpha$_1$ adrenergic receptors in human benign prostatic hyperplasia. *J. Urol.*, **132**, 1226–1229.

LEPOR, H., TANG, R., MERETYK, S. & SHAPIRO, E. (1993a). Alpha$_1$ adrenoceptor subtypes in the human prostate. *J. Urol.*, **149**, 640–642.

LEPOR, H., TANG, R. & SHAPIRO, E. (1993b). The alpha-adrenoceptor subtype mediating the tension of human prostatic smooth muscle. *Prostate*, **22**, 301–307.

LOMASNEY, J.W., COTECCHIA, S., LORENZ, W., LEUNG, W.-Y., SCHWINN, D.A., YANG-FENG, T.L., BROWNSTEIN, M., LEFKOWITZ, R.J. & CARON, M.G. (1991). Molecular cloning and expression of the cDNA for the α_{1A}-adrenergic receptor. *J. Biol. Chem.*, **266**, 6365–6369.

MCGUIRE, E.J., WAGNER, F.M. & WEISS, R.M. (1976). Treatment of autonomic dysreflexia with phenoxybenzamine. *J. Urol.*, **115**, 53–55.

MINNEMAN, K.P., HAN, C. & ABEL, P.W. (1988). Comparison of α_1-adrenergic receptor subtypes distinguished by chlorethylclonidine and WB 4101. *Mol. Pharmacol.*, **33**, 509–514.

MORROW, A.L. & CREESE, I. (1986). Characterization of α_1-adrenergic receptor subtypes in rat brain: a reevaluation of [^{3}H]WB4101 and [^{3}H]prazosin binding. *Mol. Pharmacol.*, **29**, 321–330.

PEREZ, D.M., PIASCIK, M.T. & GRAHAM, R.M. (1991). Solution-phase library screening for the identification of rare clones: isolation of an α_{1D}-adrenergic receptor cDNA. *Mol. Pharmacol.*, **40**, 876–883.

PRICE, D.T., SCHWINN, D.A., LOMASNEY, J.W., ALLEN, L.F., CARON, M.G. & LEFKOWITZ, R.J. (1993). Identification, quantification, and localization of mRNA for three distinct alpha$_1$ adrenergic receptor subtypes in human prostate. *J. Urol.*, **150**, 546–551.

SCHWINN, D.A., LOMASNEY, J.W., LORENZ, W., SZKLUT, P.J., FREMEAU, R.T. Jr., YANG-FENG, T.L., CARON, M.G., LEFKOWITZ, R.J. & COTECCHIA, S. (1990). Molecular cloning and expression of the cDNA for a novel α_1-adrenergic receptor subtype. *J. Biol. Chem.*, **265**, 8183–8189.

SCHWINN, D.A. & LOMASNEY, J.W. (1992). Pharmacologic characterization of cloned α_1-adrenoceptor subtypes: selective antagonists suggest the existence of a fourth subtype. *Eur. J. Pharmacol. Mol. Pharmacol.*, **227**, 433–436.

SUZUKI, E., TSUJIMOTO, G., TAMURA, K. & HASHIMOTO, K. (1990). Two pharmacologically distinct α_1-adrenoceptor subtypes in the contraction of rabbit aorta: each subtype couples with a different Ca^{2+} signalling mechanism and plays a different physiological role. *Mol. Pharmacol.*, **38**, 725–736.

TAKAYANAGI, I., HARADA, M., KOIKE, K. & SATOH, M. (1991). Differences in α_1-adrenoceptor mechanisms for phenylephrine and tizanidine in rabbit thoracic aorta and common iliac artery. *Can. J. Physiol. Pharmacol.*, **69**, 1819–1824.

TESTA, R., GUARNERI, L., IBBA, M., STRADA, G., POGGESI, E., TADDEI, C., SIMONAZZI, I. & LEONARDI, A. (1993). Characterization of α_1-adrenoceptor subtypes in prostate and prostatic urethra of rat, rabbit, dog and man. *Eur. J. Pharmacol.*, **249**, 307–315.

(Received December 12, 1993
Revised June 2, 1994
Accepted June 22, 1994)

Br. J. Pharmacol. (1994), **113**, 729–736 © Macmillan Press Ltd, 1994

The anticonvulsant and behavioural profile of L-687,414, a partial agonist acting at the glycine modulatory site on the N-methyl-D-aspartate (NMDA) receptor complex

M.D. Tricklebank, L.J. Bristow, P.H. Hutson, P.D. Leeson, M. Rowley, K. Saywell, L. Singh, F.D. Tattersall, L. Thorn & B.J. Williams

Merck Sharp and Dohme Research Laboratories, Neuroscience Research Centre, Terlings Park, Eastwick Road, Harlow, Essex CM20 2QR

1 The anticonvulsant and behavioural effects of the glycine/NMDA receptor partial agonist, L-687,414 (**R**(+)-*cis*-β-methyl-3-amino-1-hydroxypyrrolid-2-one) have been investigated in rodents.

2 L-687,414 dose-dependently antagonized seizures induced by N-methyl-D,L-aspartic acid (NMDLA, ED_{50} = 19.7 mg kg^{-1}), pentylenetetrazol (PTZ, ED_{50} = 13.0 mg kg^{-1}) and electroshock (ED_{50} = 26.1 mg kg^{-1}) when given intravenously 15 min before test, in male Swiss Webster mice but was most potent against audiogenic seizures induced by a 120 dB bell in DBA/2 mice (ED_{50} = 5.1 mg kg^{-1}, i.p., 30 min before test).

3 L-687,414 also induced impairments of performance in a rotarod test in both Swiss Webster and DBA/2 mice and the ratio [rotarod MED:anticonvulsant ED_{50}] varied between 0.9 and 5, depending on the convulsant used.

4 Similar behaviours to those seen after administration of the non-competitive NMDA receptor antagonist, MK-801 (head weaving, body rolling, hyperlocomotion) were seen in the mouse after giving L-687,414, although the peak effect occurred at a dose (100 mg kg^{-1}) which was 5–20 times the anticonvulsant ED_{50}s, depending on the convulsant used. Unlike MK-801, however, doses of L-687,414 that were behaviourally stimulant did not increase dopamine turnover in the nucleus accumbens.

5 Consistent with the interaction of L-687,414 with the glycine/NMDA receptor, the anticonvulsant, ataxic and motor stimulant effects of the compound were significantly attenuated by the glycine/NMDA receptor agonist, D-serine (10–100 μg per mouse, i.c.v.).

6 The results show that L-687,414 is a potent, orally active anticonvulsant with a more benign pharmacological profile than antagonists acting at the ion channel of the NMDA receptor complex. The compound is a useful tool with which to probe the functional role of the glycine co-agonist site *in vivo*.

Keywords: Glycine co-agonist site; N-methyl-D-aspartate (NMDA) receptor; L-687,414; anticonvulsant; behaviour; PCP-like effects; dopamine turnover

Introduction

The N-methyl-D-aspartate (NMDA) subtype of excitatory amino acid receptors is thought to consist of a multiple grouping of modulatory sites in addition to a recognition site for the neurotransmitter itself. This has given rise to at least four distinct classes of NMDA receptor antagonists: those acting (i) competitively at the neurotransmitter recognition site (e.g. CPP, (3-(2-carboxypiperazin-4-yl)-propyl-1-phosphonic acid, Davies *et al.*, 1986); (ii) by blocking the associated ion channel (e.g. phencyclidine, (PCP, Anis *et al.*, 1983) and dizocilpine (MK-801, Wong *et al.*, 1987)); (iii) at a site mimicked by combination of the NMDAR1 and NMDAR2B subunits of the NMDA receptor complex (e.g. ifenprodil, Williams, 1993) and (iv) by antagonizing the co-agonist actions of glycine (e.g. 7-chlorokynurenic acid (Kemp *et al.*, 1988) and **R**(+)-1-hydroxy-3-aminopyrrolid-2-one ((+)-HA-966, Singh *et al.*, 1990a).

Each of the four classes of NMDA antagonist has neuroprotective properties. However, in rodent, NMDA channel blockers are also characterized by their ability to induce 'PCP-like' behavioural effects that include the induction of a complex motor syndrome that progresses to ataxia with increasing dose, and cross-generalisation in drug discrimination studies (for review, see Willetts *et al.*, 1991). Competitive NMDA receptor antagonists share many of these behavioural properties, although they are generally less potent (relative to anticonvulsant doses) and less 'PCP-like' than the channel blockers (Tricklebank *et al.*, 1989; Willetts *et al.*, 1991).

Compounds that attenuate the actions of NMDA via the glycine and ifenprodil recognition sites are currently few in number and less well-characterized behaviourally. However, initial studies indicate that both ifenprodil and (+)-HA-966 are devoid of PCP-like properties, suggesting that antagonists acting at these modulatory sites may have distinct advantages over NMDA channel blockers. In this study, the anticonvulsant and behavioural effects of the low efficacy glycine/NMDA receptor partial agonist, L-687,414 (**R**(+)-*cis*-β-methyl-3-amino-1-hydroxypyrrolid-2-one), a more potent derivative of (+)-HA-966 (Leeson *et al.*, 1993), have been investigated. *In vitro*, L-687,414 inhibits strychnine-insensitive [^{3}H]-glycine binding to rat cerebral cortex synaptic membranes (pIC_{50} = 5.8) and glycine-potentiated NMDA responses with a pK_b of 6.2 in cultured cortical neurones and is thus about 10 fold more potent than (+)-HAA-966 (Leeson *et al.*, 1993). However, like (+)-HA-966, L-687,414 has some intrinsic activity at the glycine receptor having an efficacy level of approximately 7% of the maximum response to glycine in cortical neurones.

[1] Author for correspondence.

Methods

Animals

Experiments were performed on male Swiss Webster (20–30 g) or DBA/2 (8–10 g, 22–23 days of age) mice or Sprague Dawley rats (350–450 g) obtained from Bantin and Kingman, Hull, U.K. Animals were housed in groups of five under a 12 h light/dark cycle (lights on at 07 h 00 min) with food and water freely available. All procedures described below followed the laws governing animal experimentation in the United Kingdom. Animals subjected to techniques inducing convulsions were killed humanely within 2 min of experiencing a tonic seizure.

Intracerebroventricular injections

For the intraventricular (i.c.v.) injection of compounds, mice were anaesthetized with isoflurane and the skull exposed. Injections (5 μl) were made at lambda with a 3.5 mm long, 27 gauge needle attached to a 10 μl Hamilton microsyringe and the wound sealed with epoxy resin. Injections of dye by this procedure led to a uniform distribution of injectate throughout the ventricular system within 10 min.

Audiogenic seizures

Exposure of DBA/2 mice at 22–23 days of age to a 120 dB, 1.4 kHz bell induced wild running progressing to tonic extension of the limbs within 7–10 s of the onset of the sound. Groups of 8 mice were injected intraperitoneally with 4–5 doses of the test compound, 30 min before test. Animals not convulsing after exposure to the sound for 30 s were considered protected. The dose protecting 50% of the mice (ED_{50}) was calculated by probit analysis.

Seizures induced by N-methyl-D,L-aspartic acid or pentylenetetrazol

Groups of 8 Swiss Webster mice were injected subcutaneously with either N-methyl-D,L-aspartic acid (NMDLA, 500 mg kg^{-1}) or pentylenetetrazol (PTZ, 120 mg kg^{-1}) and the latency to the onset of tonic seizures noted over the following 30 min. Test compounds were given 15 min (intravenously) or 30 min (orally) before administration of the convulsant. Animals not convulsing within the 30 min observation period were considered protected. ED_{50} values were determined by probit analysis.

Anticonvulsant effects were also examined in the rat. For these studies, test compounds were injected i.v., 15 min before the i.v. injection of PTZ (80 mg kg^{-1}). In control animals, tonic seizures were induced within 1 min of injection of PTZ. Animals not convulsing were considered protected.

Seizures induced by electroshock

Tonic seizures were induced in Swiss Webster mice by application of electroshock (0.5 mA, 0.5 s) via corneal electrodes. Test compounds were given intravenously to groups of 8 mice, 30 min before application of shock. The number of mice protected from tonic limb extension was determined in each dose group.

Motor co-ordination

Animals were first trained to remain for 120 s on a rotarod apparatus revolving at 15 (mouse) or 8 (rat) r.p.m. Animals falling several times were discarded. The time animals were subsequently able to remain on the rod was determined 15 or 30 min after injection of the test compounds. The duration of each trial was 120 s.

The PCP-like behavioural syndrome

Quantification of lateral head movements (head weaves), side-to-side movements of the hind quarters (body rolls) and locomotion, behaviours characteristic of the syndrome induced in rodents by non-competitive NMDA receptor antagonists such as phencyclidine (PCP) and MK-801 (Tricklebank *et al.*, 1989), was carried out in Swiss Webster mice. Animals were first habituated to a perspex observation box (250 × 250 × 250 mm high) for 30 min. The test compound was then injected i.v. and the animal replaced in the cage. Fifteen min later, the above behaviours were scored (number of head weaves, body rolls and quadrants of the cage entered) for 5 min by an observer unaware of the drug treatment administered.

Locomotor activity

Swiss Webster mice were placed in individual perspex cages (230 × 200 × 210 mm high) lined with wire grids (pore size × 10 × 10 mm) to permit climbing. Each cage contained two parallel infrared photocells at the base of the cage to record cage crossing (number of consecutive beam breaks). Output from the photocells was linked to a BBC Master microcomputer and recorded at 10 min intervals. Following a 2 h habituation period, the animals were injected intravenously with either MK-801 (0.0625–1 mg kg^{-1}) or L-687,414 (75–200 mg kg^{-1}) and activity recorded for the following 2 h.

Determination of dopamine, HVA and DOPAC in mouse brain

Mice were injected with either MK-801 (0.05–1 mg kg^{-1}, i.v.), L-687,414 (5–106 mg kg^{-1}, i.v.) or 0.9% NaCl (10 ml kg^{-1}). Thirty min later, the animals were decapitated. Brains were removed and the striatum and nucleus accumbens dissected using a steel punch. Following storage at − 70°C, tissue was homogenised in 10 volumes of 0.4 M perchloric acid containing 0.1% sodium metabisulphite, 0.01% cysteine and 0.0035% EDTA and centrifuged at 3,000 *g* for 20 min. Monoamines in the supernatant were separated by high pressure liquid chromatography and the concentrations of dopamine, 3,4-dihydroxyphenylacetic acid (DOPAC) and homovanillic acid (HVA) determined electrochemically as described by Hutson *et al.* (1991).

Drugs

L-687,414 (R(+)-*cis*-β-methyl-3-amino-1-hydroxypyrrolid-2-one maleate) and dizocilpine (MK-801) were synthesized by Merck Sharp and Dohme Research Laboratories. Phencyclidine HCl was obtained from Ultrafine Chemicals Ltd (Salford, U.K.). Compounds were dissolved in 0.9% NaCl and injected in a volume of 10 ml kg^{-1} (mouse) or 1 ml kg^{-1} (rat) by routes specified in the text. Doses of L-687,414 refer to the free base. Corrections for salt forms were not made for MK-801 maleate or phencyclidine HCl.

Results

Anticonvulsant studies in the mouse

Given intravenously, L-687,414 dose-dependently inhibited seizures induced in the mouse by NMDLA (ED_{50} = 19.7 mg kg^{-1}, Figure 1), PTZ (ED_{50} = 13.0 mg kg^{-1}, Figure 2) and electroshock (ED_{50} = 26.1 mg kg^{-1}, Figure 2). The compound was also orally active against seizures induced by NMDLA (Figure 1) and by electroshock (ED_{50}s = 32.8 mg kg^{-1} and 44 mg kg^{-1} respectively, Figure 1 and Table 1). L-687,414 was most potent when administered by the i.p. route against seizures induced by sound in DBA/2 mice (ED_{50} = 5.1 mg kg^{-1}, Figure 3).

The involvement of the glycine/NMDA receptor in the anticonvulsant effect of L-687,414 in the mouse was determined by examining the ability of the i.c.v. administration of the glycine receptor agonist, D-serine (3–100 μg per mouse), to reverse the anticonvulsant effect of a 60 mg kg^{-1} (i.v.) dose of L-687,414 against seizures induced by NMDLA. When co-administered with L-687,414 15 min before injection of NMDLA, D-serine (100 μg per mouse, i.c.v.) attenuated the increase in seizure latency to a value not significantly different from that of animals given only drug vehicles (Figure 4).

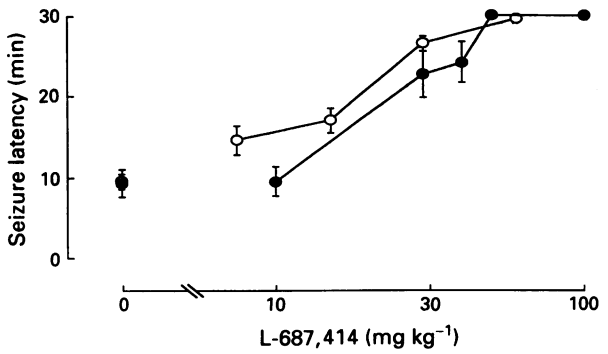


Figure 1 The effect of L-687,414 on seizures induced by N-methyl-D,L-aspartate (NMDLA) in the mouse. Male Swiss Webster mice were injected intravenously (○) or orally (●) with L-687,414 15 or 30 min respectively before the subcutaneous injection of NMDLA (500 mg kg^{-1}) and the latency to tonic seizure noted over the following 30 min. The results are shown as the mean (± s.e.mean) latency to convulse of 8 animals per dose group.

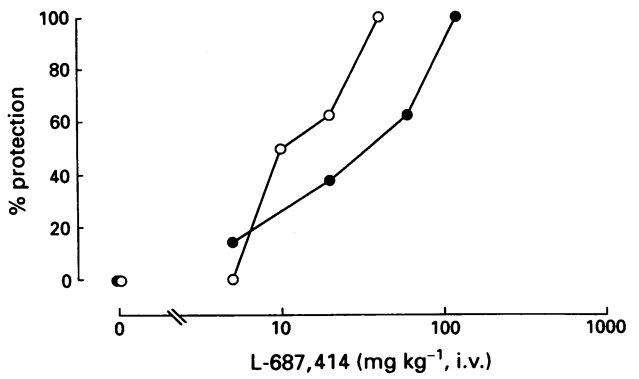


Figure 2 The effect of L-687,414 on seizures induced by pentylenetetrazol (PTZ) or electroshock in the mouse. Male Swiss Webster mice were injected intravenously with L-687,414 15 min before the subcutaneous injection of 120 mg kg^{-1} PTZ (○) or application of electroshock (0.5 mA, 0.5 s) via corneal electrodes (●). Protection was defined as the absence of tonic seizures within 30 min of injection of PTZ or immediately after exposure to electroshock. There were 8 animals in each dose group.

Anticonvulsant studies in the rat

In the rat, L-687,414 was somewhat weaker against seizures induced by an intravenous bolus injection of PTZ (ED_{50} = 61.3 mg kg^{-1}, i.v., Table 2) than against seizures induced by the subcutaneous injection of PTZ in the mouse (Table 1). In contrast, the non-competitive NMDA receptor antagonist, MK-801, potently antagonized PTZ-induced seizures in the rat with an ED_{50} (0.2 mg kg^{-1}, Table 2) similar to that seen in the subcutaneous PTZ model in the mouse.

The overall anticonvulsant profile of L-687,414 is summarized in Table 1.

Effects on motor co-ordination

L-687,414 dose-dependently induced impairments of performance on the rotarod in the mouse (Figures 3 and 5). However, in both DBA/2 and Swiss Webster mice, the ratio [rotarod MED: anticonvulsant ED_{50}] varied between 0.9 and 5, depending on the convulsant used (Table 1). In the rat, the lowest dose of L-687,414 to decrease the latency to fall from the rotarod significantly was 20 mg kg^{-1}, giving a ratio of 0.3 (Table 1).

In the Swiss Webster mouse, administration of D-serine (10–100 μg per mouse, i.c.v.) immediately before injection of L-687,414 (60 mg kg^{-1}, i.v.) prevented the impairment of rotarod performance determined 15 min later (Figure 6). D-Serine itself was without effect on rotarod performance (results not shown).

The PCP-like behavioural syndrome

MK-801 (0.063–1 mg kg^{-1}) induced head weaving, body rolling and hyperlocomotion in the mouse although, with the

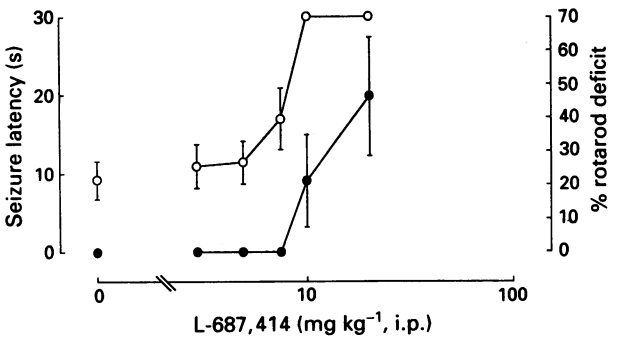


Figure 3 The effect of L-687,414 on seizures induced by sound and on rotarod performance in DBA/2 mice. Groups of 8 mice were trained to remain for 120 s on a rotarod revolving at 15 r.p.m. Thirty min after the i.p. injection of L-687,414 the animals were re-tested for their latency to fall from the rotarod (maximum 120 s) and immediately exposed to a 120 dB, 1.4 kHz bell and the latency to the onset of a tonic seizure noted (maximum 30 s). Results are shown as the mean (± s.e.mean) latency to convulse (○) or the mean (± s.e.mean) percentage deficit in rotarod performance (●) calculated as 100 × (120 − latency to fall (s)/120).

Table 1 Summary of the anticonvulsant and ataxic properties of L-687,414

	Test	*Strain*	*Route*	*Anticonvulsant* ED_{50} (mg kg^{-1})	*Rotarod MED* (mg kg^{-1})	*Rotarod MED* / *Anticonvulsant* ED_{50}
Mouse	Audiogenic	DBA/2	i.p.	5.1	27.3	5.3
	NMDLA	Swiss W.	i.v.	19.7	44.0	2.2
	NMDLA	Swiss W.	p.o.	32.8	40.0	1.2
	PTZ	Swiss W.	i.v.	13.0		3.4*
	Electroshock	Swiss W.	i.v.	26.1		1.5*
			p.o.	44.0		0.9*
Rat	PTZ	S. Dawley	i.v.	61.3	20.0	0.3

*Calculated assuming the minimum effective dose to be 40 mg kg^{-1}.
For experimental details, see Methods. For abbreviations, see text.

exception of body rolling, the dose-response relationship was biphasic (Figure 7 and Table 3), probably reflecting the progressive inability of the animals to move as ataxia increased in severity and the righting reflex was lost.

A similar, though less intense behavioural profile was seen with L-687,414 (Figure 7 and Table 3) although the dose required for the peak effect (100 mg kg^{-1}) was 5–20 times greater than the dose required to block audiogenic or NMDLA-induced seizures. The maximum head weaving score obtained in mice given L-687,414 was approximately 50% of that achieved with MK-801 but the maximum scores for locomotion and body rolling were similar. Each of these behaviours was attenuated by the i.c.v. administration of D-serine, given 15 min before injection of L-687,414 (100 mg kg^{-1}, i.v., Figure 8).

Locomotor activity

MK-801 increased locomotor activity over the dose range of 0.0625 mg kg^{-1} to 0.25 mg kg^{-1}. Higher doses of MK-801 induced much lower but longer lasting levels of hyperactivity, the effect of 1 mg kg^{-1} still being significant at the end of the 2 h observation period (Figure 9).

L-687,414 also increased locomotor activity, the peak effect being about 75% of the maximum score seen with MK-801

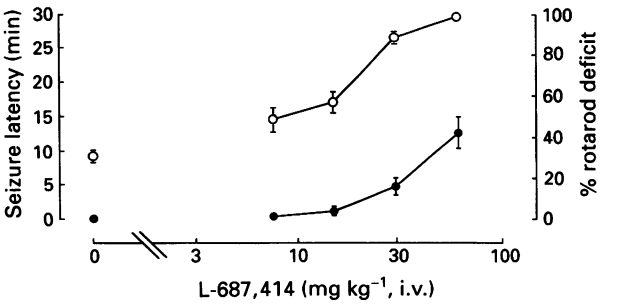


Figure 5 The effect of L-687,414 on seizures induced by N-methyl-D,L-aspartate (NMDLA) and on rotarod performance in Swiss Webster mice. Groups of 8 mice were trained to remain for 120 s on a rotarod revolving at 15 r.p.m. Fifteen min after the i.v. injection of L-687,414 the animals were re-tested for their latency to fall from the rotarod (maximum 120 s) and immediately injected with NMDLA (500 mg kg^{-1}, s.c.) and the latency to the onset of a tonic seizure noted (maximum 30 min). Results are shown as the mean (± s.e.mean) latency to convulse (○) or the mean (± s.e.mean) percentage deficit in rotarod performance (●) calculated as 100 × (120 − latency to fall (s)/120).

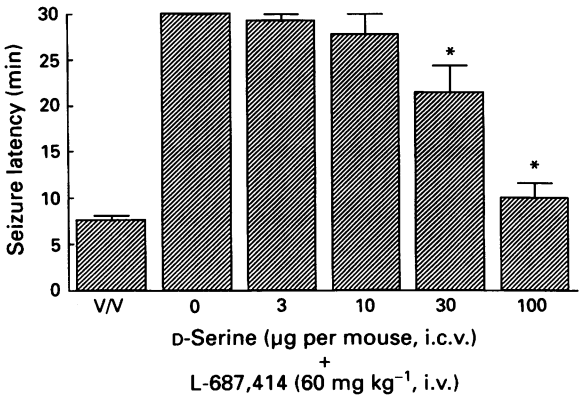


Figure 4 Effect of D-serine on the anticonvulsant action of L-687,414. D-Serine or saline was injected i.c.v. under isoflurane anaesthesia. The mice were then immediately given L-687,414 (60 mg kg^{-1}, i.v.). Fifteen min later, N-methyl-D,L-aspartate (NMDLA) was injected and the animals were observed for 30 min for the onset of a tonic seizure. The results are shown as the mean (± s.e.mean) latency to convulse. *Significantly different from animals given only L-687,414, $P<0.05$ (ANOVA followed by Dunnett's t test).

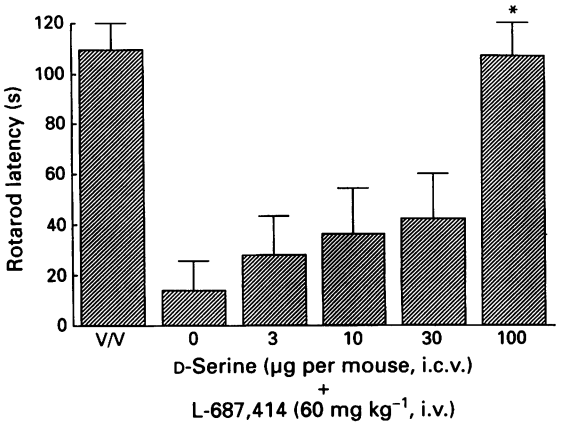


Figure 6 Effect of D-serine on the rotarod deficit induced by L-687,414. Swiss Webster mice were first trained to remain on a rotarod revolving at 15 r.p.m. D-Serine or saline was then injected i.c.v. under isoflurane anaesthesia. The mice were then immediately given L-687,414 (60 mg kg^{-1}, i.v.). Fifteen min later, the mice were re-tested on the rotarod and the latency to fall noted. The results are shown as the mean (± s.e.mean) latency to fall from the rotarod ($n = 8$ per group). *Significantly different from animals given only L-687,414, $P<0.05$ (ANOVA followed by Dunnett's t test).

Table 2 The anticonvulsant effects of MK-801 and L-687,414 against seizures induced by pentylenetetrazol in the rat

	Dose (mg kg^{-1}, i.v.)	*No. Protected* / *No. Tested*	
Saline		0/16	
MK-801	0.0625	2/16	
	0.125	10/16	
	0.25	17/24	
	0.5	13/16	
	1.0	14/15	
	2.0	16/16	$ED_{50} = 0.2$ mg kg^{-1}
Saline		0/8	
L-687,414	20	0/8	
	40	2/8	
	80	5/8	
	100	7/8	
	160	8/8	$ED_{50} = 61.3$ mg kg^{-1}

Male Sprague Dawley rats were given MK-801 or L-687,414. Fifteen minutes later they were injected intravenously with pentylenetetrazol (80 mg kg^{-1}). Animals not convulsing within 1 min of injection were considered protected.
ED_{50} values were calculated by probit anaysis.

and occurring within minutes of injection at a dose of 100 mg kg^{-1} (Figure 9). The hyperactivity response to L-687,414 was transient however, the scores of drug and vehicle-treated animals being indistinguishable by 40 min after injection. A dose of 200 mg kg^{-1} L-687,414 did not increase motor activity at any time after injection.

Effects on dopamine metabolism

The concentrations of DOPAC, HVA and the ratio ([DOPAC] + [HVA])/[DA], an index of dopamine (DA) turnover, significantly increased in the mouse nucleus accumbens following the intravenous injection of MK-801: alterations in the striatum were smaller in magnitude and not statistically significant (Table 4). With L-687,414 (5–106 mg kg^{-1}, i.v.), no significant effects on the concentrations of DOPAC or HVA or on the ratio ([DOPAC] + [HVA])/[DA] were seen in either the nucleus accumbens or the striatum (Table 4).

Discussion

Excitatory amino acid receptor antagonists acting at the ion channel of the NMDA receptor complex are anticonvulsant and neuroprotective agents. However, in rodents these compounds also activate mesocorticolimbic dopamine systems, induce hyperlocomotion, stereotypy and ataxia and cross-generalize with PCP-like drugs of abuse (e.g. ketamine and

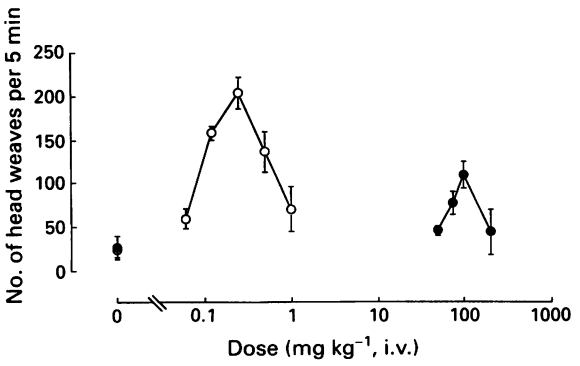


Figure 7 The induction of head weaving in the mouse by MK-801 and L-687,414. Male Swiss Webster mice were first habituated to a perspex observation cage for 30 min. MK-801 (○) or L-687,414 (●) were then injected intravenously and the animals returned to the cage. Fifteen min later, the number of lateral head movements (head weaves) was scored for 5 min by an observer unaware of the drug treatments. Results are shown as the mean (± s.e.mean) number of head weaves of 8 mice per group.

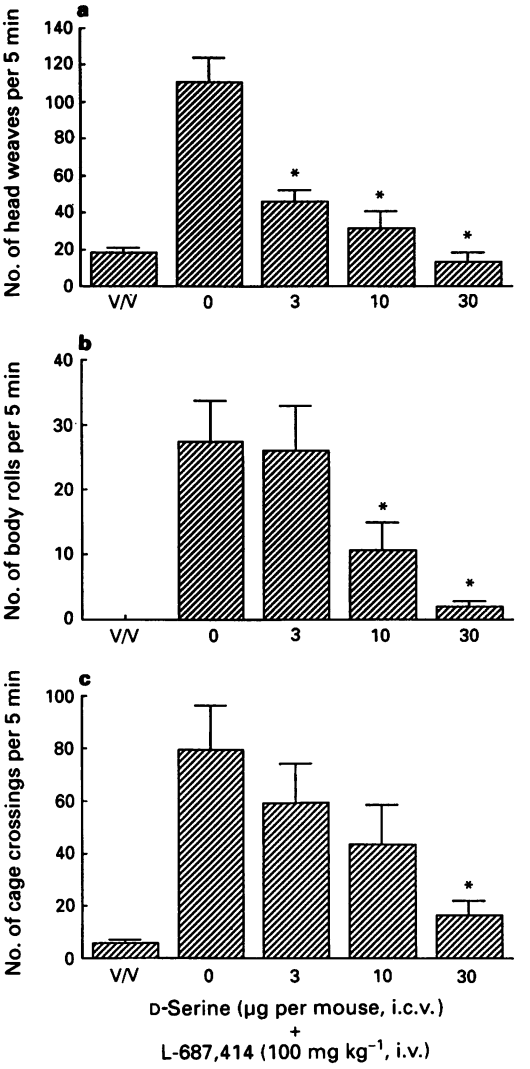


Figure 8 Effect of D-serine on the behaviours induced by L-687,414. Male Swiss Webster mice were first habituated to a perspex observation cage for 30 min. D-Serine or saline was then injected i.c.v. under isoflurane anaesthesia. Fifteen min later, a dose of 100 mg kg^{-1} L-687,414 was injected intravenously and the animals returned to the cage. After a further 15 min, the number of (a) lateral head movements (head weaves), (b) body rolls and (c) quadrants of the cage entered were scored for 5 min by an observer unaware of the drug treatments. Results are shown as the mean (± s.e.mean) number of each behaviour counted ($n = 8$ mice per group). *Significantly different from animals given only L-687,414, $P < 0.05$ (ANOVA followed by Dunnett's t test).

Table 3 Behaviours induced by MK-801 and L-687,414 in the mouse

	Dose (mg kg^{-1}, i.v.)	*No. of head weaves*	*No. of body rolls*	*No. of quadrants entered*
Saline		33 ± 7	0	13 ± 3
MK-801	0.063	60 ± 11	0	64 ± 23
	0.125	159 ± 7	0	120 ± 15*
	0.25	205 ± 18*	4 ± 2	76 ± 20*
	0.5	137 ± 23*	10 ± 5*	44 ± 13
	1.0	71 ± 26	6 ± 4	6 ± 4
Saline		28 ± 8	0	18 ± 7
L-687,414	50	46 ± 5	5 ± 2	46 ± 6
	75	78 ± 13	12 ± 3*	79 ± 17*
	100	110 ± 16*	14 ± 4*	126 ± 26*
	200	45 ± 26	11 ± 7	3 ± 2

Swiss Webster mice were injected intravenously with MK-801 or L-687,414 and 15 min later observed for 5 min during which time the number of head weaves, body rolls and quadrants of the observation cage entered were counted. Results are the means ± s.e.mean of 8 animals per group.
*$P < 0.05$ vs saline-treated animals (Dunnett's t test).

the benzomorphans) in drug discrimination paradigms (for review, see Willetts et al., 1991). Antagonism of the actions of NMDA can also be achieved by blocking the glycine co-agonist site on the NMDA receptor complex. Little is known of the behavioural pharmacology of glycine/NMDA receptor antagonists, however, since there are few compounds available that readily penetrate the CNS on systemic injection. Glycine-site antagonists that have been examined in some detail include 7-chlorokynurenic acid and the low efficacy partial agonist, (+)-HA-966 (Koek & Colpaert, 1990; Singh et al., 1990a,b,c; Hutson et al., 1991; Bristow et al., 1993), the general conclusion being that anticonvulsant effects can be maintained in the absence of PCP-like behavioural stimulation.

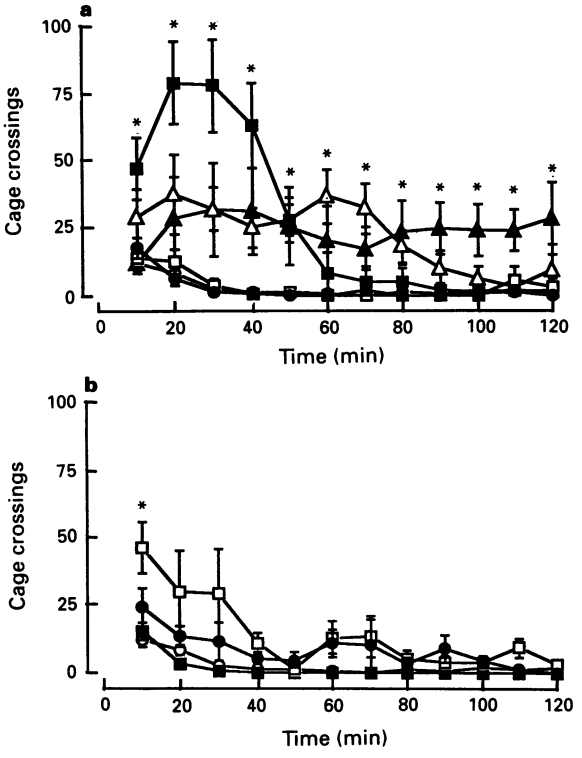


Figure 9 Effect of (a) MK-801 and (b) L-687,414 on locomotor activity. Male Swiss Webster mice were habituated for 2 h to automated photocell activity cages. Saline (○), MK-801 (● 0.0625 mg kg^{-1}, □ 0.125 mg kg^{-1}, ■ 0.25 mg kg^{-1}, △ 0.5 mg kg^{-1}, ▲ 1 mg kg^{-1}) or L-687,414 (● 75 mg kg^{-1}, □ 100 mg kg^{-1}, ■ 200 mg kg^{-1}) were then injected intravenously and the animals returned to the cages. The number of cage crossings (the number of consecutive beam breaks) were then monitored and recorded at 10 min intervals for a total of 2 h. Results are shown as the mean (± s.e.mean) number of cage crossings ($n = 8$ animals per group). *Significantly different from animals given saline, $P < 0.05$ (ANOVA with repeated measures followed by Dunnett's t test).

L-687,414 offers distinct advantages as a tool for investigating the functions of the glycine modulatory site over analogues of kynurenic acid and (+)-HA-966: the compound has higher affinity for the receptor and high bioavailability. These properties in the whole animal are demonstrated by the much lower ED_{50} compared to (+)-HA-966 to block seizures induced by NMDLA (19.7 mg kg^{-1} vs. 900 mg kg^{-1}, i.v., Singh et al., 1990a) and the relatively small differences in anticonvulsant potency seen when L-687,414 was given by the oral and intravenous routes.

The large difference in potency between (+)-HA-966 (Singh et al., 1990a) and L-687,414 in blocking NMDLA-induced seizures (45 fold) is, however, greater than would have been anticipated from the approximate 10 fold increase in affinity for the glycine site. In the audiogenic seizure model, the difference in potency between the two compounds does reflect their respective affinities *in vitro* and the discrepancy with NMDLA may be a function of (i) the more powerful convulsant stimulus offered by NMDLA, (ii) the higher degree of intrinsic activity of (+)-HA-966 at the glycine site or, (iii) a combination of these together with pharmacokinetic factors. That the anticonvulsant effects of both L-687,414 and (+)-HA-966 are mediated by the glycine modulatory site is indicated by the ability of similar doses of the glycine receptor agonist, D-serine, to reverse the protective action of both compounds against NMDLA (Figure 4 and Singh et al., 1990a).

L-687,414 was also active against seizures induced by pentylenetetrazol and electroshock, although in the former case, the compound was considerably weaker in the rat than in the mouse while MK-801 was equipotent in both species. The severity of the convulsant stimulus may again be a factor here since in the rat, PTZ was given as an intravenous bolus with seizures developing almost immediately whilst in the mouse the compound was given subcutaneously, taking about 10–12 min for a tonic seizure to occur.

As with the non-competitive NMDA receptor antagonist, MK-801, L-687,414 was found to impair the motor co-ordination necessary to maintain position on a revolving rotarod. The impairment in rotarod performance was reversed by administration of D-serine, consistent with the effect being mediated by the glycine modulatory site. However, unlike MK-801 (Tricklebank et al., 1989) the ataxia induced by L-687,414 occurred at doses that were often higher than those required for protection from seizures, giving a 'therapeutic window' of between 1 and 5 fold, depending on the seizure model employed for comparison. The largest window was seen with audiogenic seizures which again might be a

Table 4 Effect of MK-801 on dopamine metabolism in the striatum and nucleus accumbens of the mouse

		Nucleus accumbens			*Striatum*		
	Dose (mg kg^{-1})	*DOPAC* (ng g^{-1})	*HVA* (ng g^{-1})	$\frac{DOPAC + HVA}{DA}$	*DOPAC* (ng g^{-1})	*HVA* (ng g^{-1})	$\frac{DOPAC + HVA}{DA}$
Saline		674 ± 50	764 ± 61	0.29 ± 0.003	917 ± 65	1210 ± 68	0.25 ± 0.005
MK-801	0.05	693 ± 69	776 ± 37	0.30 ± 0.006	1013 ± 93	1427 ± 86	0.27 ± 0.01
	0.01	790 ± 75	964 ± 71	0.33 ± 0.18	1049 ± 144	1668 ± 119	0.29 ± 0.01
	0.5	1032 ± 65*	1133 ± 93*	0.40 ± 0.012*	1236 ± 142	1781 ± 142	0.31 ± 0.02
	1.0	1112 ± 30*	1170 ± 96*	0.41 ± 0.02*	1139 ± 79	1461 ± 111	0.28 ± 0.01
Saline	–	660 ± 45	788 ± 71	0.27 ± 0.02	808 ± 43	1023 ± 75	0.21 ± 0.02
L-687,414	5	727 ± 47	526 ± 47	0.20 ± 0.01	767 ± 52	1044 ± 69	0.21 ± 0.02
	16	652 ± 53	470 ± 23	0.21 ± 0.02	716 ± 92	1085 ± 79	0.20 ± 0.02
	53	723 ± 39	510 ± 44	0.23 ± 0.03	809 ± 101	1025 ± 47	0.20 ± 0.02
	106	960 ± 78	674 ± 109	0.28 ± 0.02	1327 ± 197	1683 ± 448	0.26 ± 0.07

Swiss Webster mice were injected intravenously with either MK-801 or L-687,414 and killed 30 min later. Values shown are the mean concentrations or concentration ratios ± s.e.mean of 4–5 animals per group.
*$P < 0.05$ vs saline-treated mice (Dunnett's t test).

reflection of a lower relative intensity of the convulsant stimulus to overcome.

With respect to the motor stimulation and stereotypy characteristic of non-competitive NMDA ion channel blockers and absent in animals given (+)-HA-966 or 7-chlorokynurenic acid (Tricklebank & Saywell, 1990; Koek & Colpaert, 1990; Bristow *et al.*, 1993), it is perhaps surprising that such behaviour was clearly seen after giving L-687,414. Head weaving, body rolling and hyperlocomotion were all present after intravenous injection of the compound with maximum intensities that were between 50% and 75% of those seen with MK-801 and occurring within the first 30 min of administration. The intensity of each behavioural component was attenuated by D-serine, again indicating the involvement of the glycine modulatory site in their genesis. However, a significant window between the anticonvulsant and peak stimulant doses was clearly apparent, ranging from 5 to 20 fold, depending on the convulsant used. With MK-801, no such window was found (Tricklebank *et al.*, 1989).

It is likely that the stimulation of motor activity induced by non-competitive NMDA receptor antagonists is mediated by increased release of dopamine, particularly in mesolimbic brain regions (French & Vantini, 1984; Tiedtke *et al.*, 1990; Rao *et al.*, 1990; Criswell *et al.*, 1993). Unlike MK-801, however, L-687,414 did not increase the concentration of HVA or DOPAC or alter dopamine turnover, as expressed by the ratio of ([DOPAC] + [HVA])/[DA], in the nucleus accumbens or striatum, even after administration of high doses. This suggests that changes in dopamine metabolism might be secondary to the increase in motor activity. However, since the behavioural response to L-687,414 was transient, it may be that changes in dopamine release were of insufficient duration and/or magnitude to be reflected in increased metabolite concentrations.

The interoceptive stimulus properties of PCP, as measured in drug discrimination paradigms, are thought to be mediated by blockade of the NMDA receptor (Tricklebank *et al.*, 1987; 1989; Willetts & Balster, 1989; Koek *et al.*, 1990; Singh *et al.*, 1990c). High doses of L-687,414 induced the majority of animals tested to choose the PCP lever, indicating that a degree of stimulus similarity exists between the compounds (Bourson & Tricklebank, 1991). However, the selection of the PCP lever induced by L-687,414 did not occur without a marked reduction in response rate, suggesting that the stimuli were not identical. Indeed, in animals trained to discriminate L-687,414 from saline, PCP did not generalize to the stimulus at doses above or below those reducing response rate whilst a structurally unrelated glycine/NMDA receptor antagonist, L-695,902 (7-chloro-4-hydroxy-3-methoxycarbonyl-2-quinolone, Rowley *et al.*, 1993) completely generalized without alteration of response rate (Bourson & Tricklebank, unpublished observations).

The relatively high degree of PCP-appropriate responding induced by L-687,414 contrasts with that seen with competitive NMDA receptor antagonists acting at the neurotransmitter recognition site. Similarly, the intensity of behavioural stimulation seen with L-687,414 appears to be greater than that seen with some (Tricklebank *et al.*, 1989), but perhaps not all (Koek & Colpaert, 1990; Svensson *et al.*, 1991) competitive NMDA receptor antagonists and is certainly greater than that seen with (+)-HA-966, 7-chlorokynurenic acid (Koek & Colpaert, 1990; Tricklebank & Saywell, 1990; Bristow *et al.*, 1993) and L-695,902 (Tricklebank *et al.*, 1993). It is difficult at the present time to reconcile these differences. Partial agonism does not seem to be a factor given the wholly antagonist actions of 7-chlorokynurenate and L-695,902. Some differences may be related to the relatively low affinity of the drugs for the glycine site and/or their slow brain penetration, although the probable existence of subtypes of the NMDA receptor (Moriyoshi *et al.*, 1991; Monyer *et al.*, 1992) raises the possibility that differential receptor subtype selectivity could account for some aspects of the varied profile of competitive, non-competitive and glycine/NMDA receptor antagonists. It is also possible that the intrinsic activities of compounds varies across subtypes so that, for example, an efficacy of 7% obtained with L-687,414 against cortical NMDA receptors (Leeson *et al.*, 1993) may be very different in an area predominantly expressing a non-cortical receptor subtype.

In conclusion, L-687,414 should prove to be a valuable tool for determining the behavioural relevance of the glycine modulatory site on the NMDA receptor complex. It is clearly premature, however, to define the functional properties of glycine site antagonists on the basis of a single compound and the availability of higher affinity ligands is keenly awaited. Nevertheless, in addition to the anticonvulsant properties described above, L-687,414 has also been shown to be neuroprotective in models of cerebral ischaemia (Gill *et al.*, 1991) and at neuroprotective doses did not increase cerebral glucose metabolism, distort cortical neuronal morphology or increase blood pressure, in contrast to MK-801 (Hargreaves *et al.*, 1993). It is also notable that in the photosensitive baboon photo-induced myoclonus was completely antagonized by L-687,414 at doses devoid of motor impairment (Smith & Meldrum, 1992), giving rise to the hope that some forms of epilepsy in man would be amenable to treatment with glycine/NMDA receptor antagonists at doses below those producing adverse behavioural effects.

The authors thank Dr R.G. Hill for advice and critical reading of the manuscript.

References

ANIS, N.A., BERRY, S.C., BURTON, N.R. & LODGE, D. (1983). The dissociative anaesthetics, ketamine and PCP, selectively reduce excitation of central mammalian neurones by N-methyl-aspartate. *Br. J. Pharmacol.*, **79**, 565–575.

BOURSON, A. & TRICKLEBANK, M.D. (1991). The discriminative stimulus properties of the glycine/NMDA receptor antagonist, L, 687,414. *Fund. Clin. Pharmacol.*, **5**, 443.

BRISTOW, L.J., HUTSON, P.H., THORN, L. & TRICKLEBANK, M.D. (1993). The glycine/NMDA receptor antagonist, **R**-(+)-HA-966, blocks activation of the mesolimbic dopaminergic system induced by PCP and dizocilpine (MK-801) in rodents. *Br. J. Pharmacol.*, **108**, 1156–1163.

CRISWELL, H.E., JOHNSON, K.B., MUELLER, R.A. & BREESE, G.R. (1993). Evidence for involvement of brain dopamine and other mechanisms in the behavioral action of the N-methyl-D-aspartic acid antagonist MK-801 in control and 6-hydroxydopamine-lesioned rats. *J. Pharmacol. Exp. Ther.*, **265**, 1001–1010.

DAVIES, J., EVANS, R.H., HERLING, P.L., JONES, A.W., OLVERMAN, H.J., POOK, P. & WATKINS, J.C. (1986). CPP, a new potent and selective NMDA antagonist. Depression of central neuron responses, affinity for [^{3}H]D-AP5 binding sites on brain membranes and anticonvulsant activity. *Brain Res.*, **382**, 169–173.

FRENCH, E.D. & VANTINI, G. (1984). Phencyclidine-induced locomotor activity in the rat is blocked by 6-hydroxydopamine lesions of the nucleus accumbens: comparisons to other psychomotor stimulants. *Psychopharmacol.*, **82**, 83–88.

GILL, R., HARGREAVES, R.J. & KEMP, J.A. (1991). Neuroprotective effects of the glycine site antagonist (+)cis-4-methyl-HA-966 (L-687,414) in rat focal ischaemia model. *J. Cereb. Blood Flow Metab.*, **11**, Suppl. 2, S304.

HARGREAVES, R.J., RIGBY, M., SMITH, D. & HILL, R.G. (1993). Lack of effect of L-687,414 ((+)-*cis*-4-methyl-HA-966), an NMDA receptor antagonist acting at the glycine site, on cerebral glucose metabolism and cortical neuronal morphology. *Br. J. Pharmacol.*, **110**, 36–42.

HUTSON, P.H., BRISTOW, L.J., THORN, L. & TRICKLEBANK, M.D. (1991). R-(+)-HA-966, a glycine/NMDA receptor antagonist, selectively blocks the activation of the mesolimbic dopamine system by amphetamine. *Br. J. Pharmacol.*, **103**, 2037–2044.

KEMP, J.A., FOSTER, A.C., LEESON, P.D., PRIESTLEY, T., TRIDGETT, R., IVERSEN, L.L. & WOODRUFF, G.N. (1988). 7-Chlorokynurenic acid is a selective antagonist at the glycine modulatory site of the N-methyl-D-aspartate receptor complex. *Proc. Natl. Acad. Sci. U.S.A.*, **85**, 6547–6550.

KOEK, W. & COLPAERT, F.C. (1990). Selective blockade of N-methyl-D-aspartate (NMDA)-induced convulsions by NMDA antagonists and putative glycine antagonists: relationship with phencyclidine-like behavioral effects. *J. Pharmacol. Exp. Ther.*, **252**, 349–357.

KOEK, W., WOODS, J.H. & COLPAERT, F.C. (1990). N-methyl-D-aspartate antagonism and phencyclidine-like activity: a drug discrimination analysis. *J. Pharmacol. Exp. Ther.*, **253**, 1017–1025.

LEESON, P.D., WILLIAMS, B.J., ROWLEY, M., MOORE, K.W., BAKER, R., KEMP, J.A., PRIESTLEY, T., FOSTER, A.C. & DONALD, A.E. (1993). Derivatives of 1-hydroxy-3-aminopyrrolidin-2-one (HA-966). Partial agonists at the glycine site of the NMDA receptor. *Biorg. Med. Chem. Lett.*, **3**, 71–76.

MONYER, H., SPRENGEL, R., SCHOEPFER, R., HERB, A., HIGUCHI, M., LOMELI, H., BURNASHEV, N., SAKMANN, B. & SEEBURG, P.H. (1992). Heteromeric NMDA receptors: molecular and functional distinction of subtypes. *Science*, **256**, 1217–1221.

MORIYOSHI, K., MASU, M., ISHII, T., SHIGEMOTO, R., MIZUNO, N. & NAKANISHI, S. (1991). Molecular cloning and characterization of the rat NMDA receptor. *Nature*, **354**, 31–37.

RAO, T.S., KIM, H.S., LEHMANN, J., MARTIN, L.L. & WOOD, P.L. (1990). Selective activation of dopaminergic pathways in the mesocortex by compounds that act at the phencyclidine (PCP) binding site: tentative evidence for PCP recognition sites not coupled to N-methyl-D-aspartate (NMDA) receptors. *Neuropharmacol.*, **29**, 225–230.

ROWLEY, M., LEESON, P.D., STEVENSON, G.I., MOSELEY, A.M., STANSFIELD, I., SANDERSON, I., ROBINSON, L., BAKER, R., KEMP, J.A., MARSHALL, G.R., FOSTER, A.C., GRIMWOOD, S., TRICKLEBANK, M.D. & SAYWELL, K. (1993). 3-Acyl-4-hydroxyquinolin-2(1H)-ones. Systemically active anticonvulsants acting by antagonism at the glycine site of the N-methyl-D-aspartate receptor complex. *J. Med. Chem.*, **36**, 3386–3396.

SINGH, L., DONALD, A.E., FOSTER, A.C., HUTSON, P.H., IVERSEN, L.L., IVERSEN, S.D., KEMP, J.A., LEESON, P.D., MARSHALL, G.R., OLES, R.J., PRIESTLEY, T., THORN, L., TRICKLEBANK, M.D., VASS, C.A. & WILLIAMS, B.J. (1990a). Enantiomers of HA-966 (3-amino-1-hydroxypyrrolid-2-one) exhibit distinct central nervous system effects: (+)-HA-966 is a selective glycine/N-methyl-D-aspartate receptor antagonist, but (−)-HA-966 is a potent γ-butryolactone-like sedative. *Proc. Natl. Acad. Sci. U.S.A.*, **87**, 347–351.

SINGH, L., MENZIES, R. & TRICKLEBANK, M.D. (1990b). The discriminative stimulus properties of (+)-HA-966, an antagonist of the glycine/N-methyl-D-aspartate receptor. *Eur. J. Pharmacol.*, **186**, 129–132.

SINGH, L., WONG, E.F.H., KESINGLAND, A.C. & TRICKLEBANK, M.D. (1990c). Evidence against involvement of the haloperidol-sensitive sigma recognition site in the discriminative stimulus properties of (+)-N-allylnormetazocine ((+)-SKF 10,047). *Br. J. Pharmacol.*, **99**, 145–151.

SMITH, S.E. & MELDRUM, B.S. (1992). The glycine-site NMDA receptor antagonist, R-(+)-cis-β-methyl-3-amino-1-hydroxypyrrolid-2-one, L-687,414 is anticonvulsant in baboons. *Eur. J. Pharmacol.*, **211**, 109–111.

SVENSSON, A., PILELBLAD, E. & CARLSSON, M. (1991). A comparison between the non-competitive NMDA antagonist dizocilpine (MK-801) and the competitive NMDA antagonist D-CPPene with regard to dopamine turnover and locomotor-stimulatory properties in mice. *J. Neurol. Transm.* [GenSect], **85**, 117–129.

TIEDTKE, P.I., BISCHOFF, C. & SCHMIDT, W.J. (1990). MK-801-induced stereotypy and its antagonism by neuroleptic drugs. *J. Neural Trans.*, **81**, 173–182.

TRICKLEBANK, M.D., KEMP, J.A., RIGBY, M., TATTERSALL, D., MARSHALL, G., SAYWELL, K., BOURSON, A., LEESON, P.D., KULAGOWSKI, J.J., ROWLEY, M., MAWER, I.M & HILL, R.G. (1993). The pharmacological profile of the glycine/NMDA receptor antagonist, L-695,902 and related 4-hydroxy-2-quinolones. Abstracts of the meeting *Focus on Epilepsy II. Antiepileptic Drugs in the 1990s: Current and Investigational Therapies.* Whistler, Canada, p. 24.

TRICKLEBANK, M.D. & SAYWELL, K. (1990). Behavioural properties of antagonists acting at the glycine modulatory site on the NMDA receptor/ion channel complex. *Neurosci. Abst.*, **16**, 462.

TRICKLEBANK, M.D., SINGH, L., OLES, R.J., PRESTON, C. & IVERSEN, S.D. (1989). The behavioural effects of MK-801: a comparison with antagonists acting non-competitively and competitively at the NMDA receptor. *Eur. J. Pharmacol.*, **167**, 127–135.

TRICKLEBANK, M.D., SINGH, L., OLES, R., WONG, E.H.F. & IVERSEN, S.D. (1987). A role for receptors of N-methyl-D-aspartic acid in the discriminative stimulus properties of phencyclidine. *Eur. J. Pharmacol.*, **141**, 497–501.

WILLETTS, J. & BALSTER, R.L. (1989). Effects of competitive and noncompetitive N-methyl-D-aspartate (NMDA) antagonists in rats trained to discriminate NMDA from saline. *J. Pharmacol. Exp. Ther.*, **251**, 627–633.

WILLETTS, J., BALSTER, R.L. & LEANDER, J.D. (1991). The behavioural pharmacology of NMDA receptor antagonists. *Trends Pharmacol. Res.*, **11**, 423–428.

WILLIAMS, K. (1993). Ifenprodil discriminates subtypes of the N-methyl-D-aspartate receptor: selectivity and mechanisms at recombinant heteromeric receptors. *Mol. Pharmacol.*, **44**, 851–859.

WONG, E.H.F., KEMP, J.A., PRIESTLEY, T., KNIGHT, A.R., WOODRUFF, G.N. & IVERSEN, L.L. (1986). The anticonvulsant MK-801 is a potent N-methyl-D-aspartate antagonist. *Proc. Natl. Acad. U.S.A.*, **83**, 7104–7108.

(Received March 30, 1994
Revised June 15, 1994
Accepted June 22, 1994)

Br. J. Pharmacol. (1994), **113**, 737–740 © Macmillan Press Ltd, 1994

Neuropeptide Y inhibits potassium-stimulated glutamate release through Y_2 receptors in rat hippocampal slices *in vitro*

[1]Susanne Greber, Christoph Schwarzer & [2]Günther Sperk

Department of Pharmacology, University of Innsbruck, 6020 Innsbruck, Austria

1 We investigated the effects of neuropeptide Y (NPY), peptide YY (PYY), NPY_{13-36}, NPY_{18-36}, [Leu[31]][Pro[34]]NPY and of pancreatic polypeptide Y (PPY) on calcium-dependent, potassium-stimulated glutamate release in superfused rat hippocampal slices.

2 NPY, PYY and the Y_2 receptor agonist NPY_{13-36} equipotently inhibited the release of glutamate. The half-maximal response was observed at about 10 nM in a dose-dependent manner (3 to 100 nM). Maximal inhibition of 50 to 60% was obtained at 100 nM. At higher concentrations of the peptides (300 nM and 1 μM) this inhibition was partially or entirely reversed. Porcine NPY_{13-36} and NPY_{18-36} inhibited glutamate release by about 44% at 100 nM.

3 The specific Y_1 receptor agonist, [Leu[31]][Pro[34]]NPY, caused an insignificant increase in glutamate release at 100 to 300 nM concentrations. PPY had no effect on potassium-evoked glutamate release in hippocampal slices at concentrations of 30 nM to 1 μM.

4 The experiments support previous electrophysiological data. They suggest a potent inhibitory action of NPY through NPY-Y_2 receptors on the release of the excitatory amino acid glutamate in rat hippocampus. Especially under conditions of increased NPY synthesis, such as in epilepsy, this mechanism may be of pathophysiological relevance.

Keywords: Glutamate; hippocampus; neuropeptide Y; NPY-Y_2 receptor; presynaptic inhibition; hippocampal slice; epilepsy; neurotransmitter release

Introduction

Neuropeptide Y (NPY), a 36-amino acid peptide is a member of a family of peptides that also includes peptide YY (PYY) and pancreatic polypeptide Y (PPY) (Tatemoto, 1982; Tatemoto *et al.*, 1982). NPY is abundant in the central and peripheral nervous system (Allen *et al.*, 1983; Chronwall *et al.*, 1985; DeQuidt & Emson, 1986; Morris, 1989). Two receptor subtypes (Y_1 and Y_2) equally recognizing NPY and PYY have been defined by receptor binding studies (Aicher *et al.*, 1991; Dumont *et al.*, 1993). A specific ligand of the Y_1 receptor is the NPY derivative [Leu[31]][Pro[34]]NPY (Fuhlendorff *et al.*, 1990). Selective agonists of the Y_2 receptor are amino-terminally truncated analogues of NPY such as NPY_{13-36} (Wahlestedt *et al.*, 1986). Both receptor subtypes are abundant in the central nervous system (Walker & Miller, 1988; Martel *et al.*, 1990; Gehlert *et al.*, 1992; Dumont *et al.*, 1993). The existence of a third receptor species (Y_3) with low affinity for PYY has been postulated recently (Grundemar *et al.*, 1991).

A variety of behavioural effects are observed after infusion of NPY into the central nervous system. Thus NPY stimulates food and water intake through Y_1 receptors (Stanley & Leibowitz, 1985; Danho *et al.*, 1988). It facilitates memory retention probably via Y_2 receptors (Flood & Morley, 1989). Activation of Y_1 or Y_2 receptors may affect locomotor behaviour in an inhibitory or stimulatory fashion, respectively (Heilig & Murison, 1987; Heilig *et al.*, 1988). Blockade of Y_1 receptor synthesis by infusion of an antisense oligonucleotide to Y_1 receptor mRNA into the amygdala has an anxiogenic effect (Wahlestedt *et al.*, 1993).

Induction of NPY expression has been observed in various animal models of epilepsy (Marksteiner & Sperk, 1988; Stenfors *et al.*, 1989; Marksteiner *et al.*, 1989, 1990a; Bellmann *et al.*, 1991). Mossy fibres, which represent an important excitatory pathway of the hippocampal formation, exhibit a marked and long lasting increase in NPY immunoreactivity (Marksteiner *et al.*, 1990b; Sperk *et al.*, 1992). It has been conjectured that NPY released during epileptic seizures may serve a protective role in inhibiting glutamate release from mossy fibre terminals (Marksteiner *et al.*, 1990b). Electrophysiological studies supported this proposal: NPY exerts a presynaptic inhibitory effect on the glutamatergic transmission at Schaffer collateral/CA1 synapses and at mossy fibre/CA3 synapses of the hippocampus (Colmers *et al.*, 1985; 1988; Haas *et al.*, 1987; Klapstein & Colmers, 1993). These effects seem to be mediated by presynaptic Y_2-receptors possibly by inhibiting Ca^{2+} influx through N-type Ca^{2+} channels (Colmers *et al.*, 1991; Toth *et al.*, 1993). Thus the aim of our present study was to investigate the effects of NPY and NPY receptor agonists on glutamate release in superfused slices of the rat hippocampus by means of biochemical methods.

Methods

Superfusion experiments

Adult male Sprague-Dawley rats (300–350 g; Versuchstierzuchtanstalt, Himberg, Austria) were decapitated and their brains were rapidly removed into ice-cold Krebs-Henseleit-Tris buffer (composition mM: NaCl 118, KCl 4.8, $MgSO_4$ 1.3, $CaCl_2$ 1.2, $NaHCO_3$ 15, KH_2PO_4 1.2, Tris 10, glucose 10, adjusted to pH 7.3 by gassing with 95% O_2/5% CO_2). Superfusion experiments were performed according to Burke & Nadler (1988). The hippocampi were removed and 300 μm thick transverse slices were obtained with a McIlwain tissue chopper. Two slices were transferred to a small circular nylon mesh net located in a superfusion chamber (Singer, 1988). They were covered by a second nylon mesh net and superfused at a flow rate of 1 ml min^{-1} with the above buffer. The medium was continuously gassed with 95% O_2/5% CO_2. The system was kept at 34°C. Transmitter release was induced by increasing the K^+ concentration (usually to 40 mM) for 90 s. The Na^+ concentration was correspondingly reduced. The

[1] Present address: Pediatric University Clinics, Vienna, Austria.
[2] Author for correspondence at: Dept. of Pharmacology, Peter-Mayr-Str. 1a, Innsbruck, Austria.

slices were stimulated twice (after about 50 and 100 min respectively).

The respective peptide was added to the superfusion medium 8 min before the second pulse of elevated K^+. The system was changed to a previously well gassed buffer (50 ml contained in a siliconized glass flask). The respective NPY analogue (in 500 µl 1.1% bovine serum albumin) was admixed immediately before use. In order to avoid extensive foaming and adsorption of the peptide to the glass flask, gassing was stopped. (This interruption of gassing for 9.5 min did not affect the basal or the K^+ stimulated glutamate release). The peptide was included in the same way in the medium containing elevated K^+. After the stimulation period the perfusion system was changed back to the original continuously gassed superfusion medium. Four perfusion chambers were used in parallel. In the control experiments slices were superfused in the same way, including bovine serum albumin without peptide, prior to and during the second K^+-stimulus. Fractions of 1 ml were collected and lyophilized. At the end of the experiment the brain slices were transferred to 1 ml 0.1 M $HClO_4$ and sonicated. The homogenate was centrifuged (15,000 *g*, 10 min). The supernatants were diluted 1:80 with 0.4 M $NaBO_4$ buffer, pH 10.0 for determination of tissue glutamate. Pellets were solubilized in 0.5 M NaOH for protein determination (Lowry *et al.*, 1951). Recovery of NPY, NPY_{13-36}, NPY_{18-36} and PYY as monitored by radioimmunoassay (Bellmann *et al.*, 1991). The NPY analogues cross-reacted about 10 to 30% with our NPY antibody. The recovery of the peptides was generally more than 95%; values were therefore not corrected. The antibody did not significantly crossreact with [Leu^{31}][Pro^{34}] NPY or PPY.

Determination of glutamate by h.p.l.c.

Amino acids were determined by high performance liquid chromatrography (h.p.l.c.) and fluorimetric detection after pre-column derivatization with *o*-phthaldialdehyde. The lyophilized samples were solubilized in 200 µl 0.4 M $NaBO_4$ buffer, pH 10.0, containing 400 nM L-cysteic acid (Sigma) as internal standard. Aliquots (120 µl) of the samples were placed into an automatic h.p.l.c. injection system (Hitachi-Merck) refrigerated at 6°C. Each sample was reacted with 20 µl *o*-phthaldialdehyde reagent immediately prior to injection. (The *o*-phthaldialdehyde reagent was prepared daily by solubilizing 5 mg *o*-phthaldialdehyde in 93 µl methanol and adding of 833 µl 0.4 M $NaBO_4$ buffer, pH 9.5 and 4 µl β-mercaptoethanol. The mixture was incubated at room temperature overnight before use). The reaction was stopped after 90 s by addition of 80 µl 1 M phosphate buffer pH 1.5 and mixing. An aliquot of 180 µl was then injected into the h.p.l.c.

Separation of amino acids was performed with a C18 reversed phase column (Merck, LiChrospher 100, 5 µm, 4 × 125 mm). The mobile phase consisted of a mixture of a 0.1 M NaH_2PO_4 buffer, pH 6.2 containing 20% methanol (eluent A) and a 0.01 M NaH_2PO_4 buffer, pH 5.8, 80% methanol (eluent B). The column was eluted isocratically for 7 min with 95% eluent A and 5% eluent B followed by a gradient increasing the concentration of eluent B to 50% during 3 min at a flow rate of 1 ml min^{-1}. After washing the column with eluent B for 5 min and equilibrating it with 95% eluent A/5% eluent B (5 min) the next sample was applied. The amino acids were monitored with a fluorescence detector (Shimadzu, RF 530) at 340 nm excitation and 455 emission. The glutamic acid derivative eluted after 8 min and was quantified with external standards (1 to 50 pmol) included after every sixth sample. The recovery was determined by the internal standard L-cysteic acid.

The amount of potassium-stimulated glutamate release was calculated from those two fractions obtained during stimulation with high K^+. Basal release rates were estimated from the fractions prior to stimulation and were subtracted. The ratio of glutamate released during the second and the first stimuli (S_2/S_1) was calculated. It was 1.02 ± 0.08 ($n = 32$) in control experiments.

Human NPY_{13-36} was custom synthesized by Neosystems (Strasbourg, France) and purified by h.p.l.c. All other neuropeptides were obtained from Peninsula (Great Britain).

Results

After a recovery period of about 30 min a basal release rate of glutamate of 4 to 7 pmol mg^{-1} protein min^{-1} was observed. Elevated K^+ concentrations caused a dose-dependent increase in glutamate release. At 40 mM KCl (90 s) 416 ± 32 (17) pmol glutamate mg^{-1} protein was released during a period of 2 min representing about 0.6% of total glutamate in the slices. This release was Ca^{2+}-dependent. Substituting Ca^{2+} in the superfusion medium by 2 mM EGTA reduced the K^+-stimulated release by 90% (Figure 1b). Rates of basal and K^+-stimulated release of aspartate were 34 ± 3.3 (12) and 107 ± 3.4 (7) pmol mg^{-1} protein min^{-1}, respectively. Markedly elevated aspartate release (accompanied by elevated glutamate release) was observed only occasionally and was taken as indicator for Ca^{2+}-independent release. These experiments were not included.

NPY at concentrations of 30 to 100 nM inhibited potassium-stimulated glutamate release by 45 to 55% (Figure 2). PYY and the Y_2 receptor agonist NPY_{13-36} were about as potent as NPY (Figure 2, Table 1). In Figure 2 dose-response

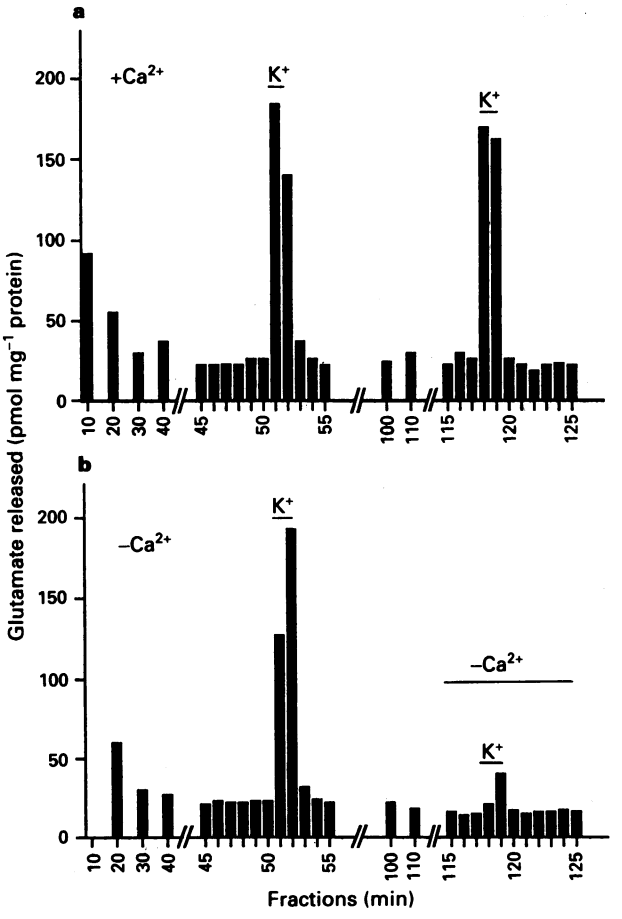


Figure 1 K^+-stimulated glutamate release from hippocampal slices and its Ca^{2+} dependency. (a) Two hippocampal slices (300 µm) were superfused. For stimulation K^+ concentration was increased to 50 mM for 90 s. Glutamate was determined in 1 ml (1 min) fractions by h.p.l.c. (b) Eight min prior to the second stimulus Ca^{2+} was substituted by 2 mM EGTA.

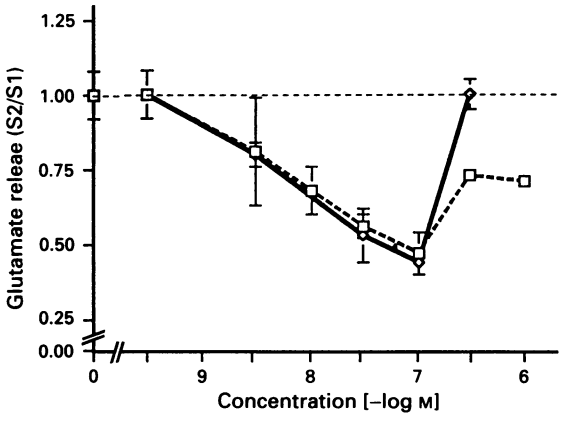


Figure 2 Dose-response curve for inhibition of K^+-stimulated glutamate release by rat NPY (—◇—) and rat NPY_{13-36} (- -□- -). S_2/S_1 values were calculated from K^+-stimulated release in the presence and absence of the respective peptides.

relationships for NPY and NPY_{13-36} are shown. Maximal inhibition (56%) was observed at a concentration of 100 nM. Half maximal inhibition was obtained at about 10 nM. At concentrations of 300 nM to 1 μM, inhibition of K^+-evoked glutamate release by NPY_{13-36} was less prominent (about 30%) or entirely reversed (NPY, PYY, Figure 2, Table 1).

In Table 1 the efficacies of NPY and of the NPY analogues in inhibiting glutamate release are compared. At concentrations of 100 nM, porcine NPY_{13-36} and NPY_{18-36} were slightly less effective (about 44% inhibition) than rat NPY, rat NPY_{13-36} and PYY (56% inhibition). PYY had no significant inhibitory action upon glutamate release. There was a slight increase in release of the amino acid in the presence of 100 nM [Leu^{31}][Pro^{34}]NPY.

Discussion

Our experiments show equipotent inhibitory actions of NPY, PYY and the Y_2 receptor agonist NPY_{13-36} on K^+-stimulated glutamate release in hippocampal slices. The specific Y_1 receptor agonist [Leu^{31}][Pro^{34}] NPY lacked this inhibitory action on glutamate release. The experiments are in good agreement with electrophysiological data by Colmers and coworkers (Colmers *et al.*, 1985; 1988; 1991; Klapstein & Colmers, 1993). The authors demonstrated an inhibitory action of NPY upon excitatory postsynaptic potentials and population spikes in CA1 and CA3 pyramidal neurones after orthodromic stimulation. This action of the peptide is mediated by presynaptic Y_2 receptors (Colmers *et al.*, 1988; 1991).

The present experiments demonstrate this effect of NPY and the Y_2 receptor agonist NPY_{13-36} at low concentrations (half maximal inhibition at about 10 nM) in superfused slices of the rat hippocampus. Maximal inhibition of glutamate release occurred at 100 nM NPY and was about 55%. This suggests that not all glutamate terminals may be under inhibitory control of the peptide. This is in agreement with Colmer's results and the observation that NPY for example was inactive at perforant path–granule cell synapses (Klapstein & Colmers, 1993).

It is also interesting that maximal inhibition of glutamate release observed at 100 nM was attenuated at higher concentrations of NPY, PYY and NPY_{13-36} (300 nM and 1 μM). The latter effect could be mediated through a different type of NPY receptor. Monet *et al.* (1992) reported an agonist action of NPY with glutamate at the N-methyl-D-aspartate receptor at high nM concentrations. Stimulation of these receptors would result in enhanced release of glutamate. It also may be possible that NPY_{13-36} exerts a partially antagonistic action at the higher concentrations. Such an antagonistic action has been reported for NPY_{18-36} on the inhibitory action of NPY upon isoprenaline-stimulated adenylyl cyclase in cardiac ventricular membranes (Balasubramaniam & Sheriff, 1990). The low concentrations of NPY required for inhibition of glutamate release are in favour of a physiological role for this mechanism.

The sites for this action of NPY on glutamate release within the hippocampal formation may be at CA1 pyramidal neurones innervated by Schaffer's collaterals or at mossy fibre-CA3, commisural-CA3 and CA3-CA3 synapses (Klapstein & Colmers, 1993). The cellular origin of NPY exerting this action is not entirely clear. NPY is contained at high concentrations in interneurones throughout the hippocampus (Köhler *et al.*, 1986). A recent electron microscopy study indicates the presence of NPY immunoreactive varicosities in immediate apposition to glutamatergic presynaptic terminals (Milner & Veznedaroglu, 1992). NPY originating from these neurones may control glutamate release under physiological conditions.

Another compartment that may release NPY is the glutamatergic nerve terminal itself. No NPY, however, has been found in granule cells or in pyramidal neurones of untreated rats (Köhler *et al.*, 1986; Morris, 1989). In epileptic rats, however, a markedly augmented and long lasting expression of NPY has been observed in granule cells of the dentate gyrus and, transiently, also in CA1 and CA3 pyramidal neurones (Marksteiner *et al.*, 1990b; Sperk *et al.*, 1992). Pre-existing Y_2 receptors may serve as targets for NPY released together with glutamate from these neurones. The peptide is released at a high rate during epileptic seizures. It then may exert its action by supressing the release of the excitatory neurotransmitter and inhibiting seizure propagation.

We thank E. Rupp and Dr S. Lang for determination of NPY analogues. We are indebted to Dr E.A. Singer, Department of Pharmacology, Vienna for providing the perfusion chambers. Some of the peptides were donated by Dr P.A. Czernilofsky, Bender Austria. The work was supported by the Austrian Science Foundation and the Dr Legerlotz-Foundation.

Table 1 The effects of neuropeptide Y (NPY) and NPY analogues on K^+-stimulated glutamate release

	% inhibition at		
	30 nM	100 nM	300 nM
NPY_{1-36} (rat)	47 ± 8.7 (3)*	56 ± 2.0 (3)*	− 0.2 ± 5.3 (7)
PYY (rat)	ND	52 ± 9.8 (4)*	− 17 (2)
NPY_{13-36} (rat)	44 ± 3.6 (5)**	56 ± 5.1 (6)***a	27 ± 1.5 (3)
NPY_{13-36} (porcine)	ND	44 ± 2.1 (3)*	ND
NPY_{18-36} (porcine)	ND	44 (2)	ND
[Leu^{31}][Pro^{34}]NPY (porcine)	11 ± 0.4 (3)	− 18 ± 1.4 (5)	− 0.1 ± 15.3 (5)
PPY	ND	7.3 ± 7.0 (3)	ND

*$P<0.005$, **$P<0.001$ significantly different vs controls; [a]$P<0.05$ significantly different vs 30 nM (Student's t test); ND, not determined. Data represent mean reduction in S_2/S_1 values expressed as % of control values ± s.e.mean. (n) = number of experiments.

References

AICHER, S.A., SPRINGSTON, M., BERGER, S.B., REIS, D.J. & WAHLESTEDT, C. (1991). Receptor-selective analogs demonstrate NPY/PYY receptor heterogeneity in rat brain. *Neurosci. Lett.*, **130**, 32–36.

ALLEN, Y.S., ADRIAN, T.E., ALLEN, J.M., TATEMOTO, K., CROW, T.J., BLOOM, S.R. & POLAK, J.M. (1983). Neuropeptide Y distribution in the rat brain. *Science*, **221**, 877–879.

BALASUBRAMANIAM, A. & SHERIFF, S. (1990). Neuropeptide Y (18–36) is a competitive antagonist of neuropeptide Y in rat cardiac ventricular membranes. *J. Biol. Chem.*, **266**, 14724–14727.

BELLMANN, R., WIDMANN, R., OLENIK, C., MEYER, D.K., MAAS, D., MARKSTEINER, J. & SPERK, G. (1991). Enhanced rate of expression and biosynthesis of neuropeptide Y after kainic acid induced seizures. *J. Neurochem.*, **56**, 525–530.

BURKE, S.P. & NADLER, J.V. (1988). Regulation of gutamate and aspartate release from slices of the hippocampal CA1 area: effects of adenosine and baclofen. *J. Neurochem.*, **51**, 1541–1551.

CHRONWALL, B.M., DIMAGGIO, D.A., MASSARI, V.J., PICKEL, V.M., RUGGIERO, D.A. & O'DONOHUE, T.L. (1985). The anatomy of neuropeptide-Y containing neurones in rat brain. *Neuroscience*, **15**, 1159–1181.

COLMERS, W.F., KLAPSTEIN, G.J., FOURNIER, A., ST-PIERRE, S. & TREHERNE, K.A. (1991). Presynaptic inhibition by neuropeptide Y in rat hippocampal slice *in vitro* is mediated by a Y_2 receptor. *Br. J. Pharmacol.*, **102**, 41–44.

COLMERS, W.F., LUKOWIAK, K. & PITTMAN, Q.J. (1985). Neuropeptide Y reduces orthodromically evoked population spike in rat hippocampal CA1 by a possibly presynaptic mechanism. *Brain Res.*, **346**, 404–408.

COLMERS, W.F., LUKOWIAK, K. & PITTMANN, Q.J. (1988). Neuropeptide Y action in the hippocampal slice: site and mechanism of presynaptic inhibition. *J. Neurosci.*, **8**, 3827–3837.

DANHO, W., TRISCARI, J., VINCENT, G., NAKAJIMA, T., TAYLOR, J. & KAISER, E.T. (1988). Synthesis and biological evaluation of pNPY fragments. *Int. J. Pept. Prot. Res.*, **32**, 496–505.

DEQUIDT, M.E. & EMSON, P.C. (1986). Distribution of neuropeptide Y-like immunoreactivity in the rat central nervous system II. Immunohistochemical analysis. *Neuroscience*, **18**, 545–618.

DUMONT, Y., FOURNIER, A., ST.-PIERRE, S. & QUIRION, R.K (1993). Comparative characterization and autoradiographic distribution of neuropeptide Y receptor subtypes in the rat brain. *J. Neurosci.*, **13**, 73–86.

FLOOD, J. & MORLEY, J. (1989). Dissociation of the effects of neuropeptide Y on feeding and memory: evidence for pre- and post-synaptic mediation. *Pept.*, **10**, 963–966.

FUHLENDORFF, J., GETHER, U. AAKERLUND, L., LANGELAND-JOHANSEN, N., THOGERSEN, H., MELBERG, S.G., OLSEN, U.B., THASTRUP, O. & SCHWARTZ, T.W. (1990). [Leu^{31},Pro^{34}] neuropeptide Y: a specific Y_1 receptor agonist. *Proc. Natl. Acad. Sci. U.S.A.*, **87**, 182–186.

GEHLERT, D.R., GACKENHEIMER, S.L. & SCHOBE, D.A. (1992). [Leu^{31}-Pro^{34}]neuropeptide Y identifies a subtype of ^{125}I-labelled peptide YY binding sites in the rat brain. *Neurochem. Int.*, **21**, 45–67.

GRUNDEMAR, L., WAHLESTEDT, C. & REIS, D.J. (1991). Neuropeptide Y acts at an atypical receptor to evoke cardiovascular depression and to inhibit glutamate responsiveness in the brainstem. *J. Pharmacol. Exp. Ther.*, **258**, 633–638.

HAAS, H.L., HERMAN, A., GREENE, R.W. & CHAN-PALAY, V. (1987). Action and location of neuropeptide tyrosine (Y) on hippocampal neurons of the rat in slice preparations. *J. Comp. Neurol.*, **257**, 208–215.

HEILIG, M. & MURISON, R. (1987). Intracerebroventricular neuropeptide Y (NPY) suppresses home cage and open field activity in the rat. *Regul. Pept.*, **19**, 221–231.

HEILIG, M, WAHLESTEDT, C. & WIDERLÖV, E. (1988). Neuropeptide Y (NPY)-induced suppression of activity in the rat: evidence of NPY receptor heterogeneity and for interaction with α-adrenoceptors. *Eur. J. Pharmacol.*, **157**, 205–213.

KLAPSTEIN, G.J. & COLMERS, W.F. (1993). On the sites of presynaptic inhibition by neuropeptide Y in rat hippocampus in vivo. *Hippocampus*, **3**, 103–112.

KÖHLER, C., ERIKSSON, L.G., DAVIES, S. & CHAN-PALAY, V. (1986). Neuropeptide Y innervation of the hippocampal region in the rat and monkey brain. *J. Comp. Neurol.*, **244**, 384–400.

LOWRY, O.H., ROSEBOUGH, N.J., FARR, A.L. & RANDALL, R.J. (1951). Protein measurement with the Folin phenol reagent. *J. Biol. Chem.*, **193**, 265–275.

MARKSTEINER, J., LASSMANN, H., SARIA, A., HUMPEL, C., OLENIK, C., MEYER, D.K. & SPERK, G. (1990a). Neuropeptide levels after pentylenetetrazol kindling in the rat. *Eur. J. Neurosci.*, **2**, 98–103.

MARKSTEINER, J., ORTLER, M., BELLMANN, R. & SPERK, G. (1990b). Neuropeptide, Y biosynthesis is markedly induced in mossy fibers during temporal lobe epilepsy of the rat. *Neurosci. Lett.*, **112**, 143–148.

MARKSTEINER, J. & SPERK, G. (1988). Concomitant increase of somatostatin, neuropeptide Y and glutamate decarboxylase in the frontal cortex of rats with decreased seizure threshold. *Neuroscience*, **26**, 379–385.

MARKSTEINER, J., SPERK, G. & MAAS, D. (1989). Differential increases in brain levels of neuropeptide Y and vasoactive intestinal polypeptide after kainic acid-induced seizures in the rat. *Naunyn-Schmied. Arch. Pharmacol.*, **339**, 173–177.

MARTEL, J.C., FOURNIER, A., ST. PIERRE, S. & QUIRION, R. (1990). Quantitative autoradiographic distribution of [^{125}I]Bolton-Hunter neuropeptide Y receptor binding sites in rat brain. Comparison with [^{125}I]peptide YY receptor sites. *Neuroscience*, **36**, 255–283.

MILNER, T.A. & VEZNEDAROGLU, E. (1992). Ultrastructural localization of neuropeptide Y-like immunoreactivity in the rat hippocampal formation. *Hippocampus*, **2**, 107–126.

MONNET, F.P., DEBONNEL, G., FOURNIER, A. & DEMONTIGNY, C. (1992). Neuropeptide Y potentiates the N-Methyl-d-Aspartate response in the CA_3 dorsal hippocampus. Involvement of a subtype of Sigma receptor. *J. Pharmacol. Exp. Ther.*, **263**, 1219–1225.

MORRIS, B.J. (1989). Neuronal localisation of neuropeptide Y gene expression in rat brain. *J. Comp. Neurol.*, **290**, 358–368.

SINGER, E.A. (1988). Transmitter release from brain slices elicited by single pulses: a powerful method to study presynaptic mechanisms. *Trends Pharmacol. Sci.*, **9**, 274–276.

SPERK, G., MARKSTEINER, J., GRUBER, B., BELLMANN, R., MAHATA, M. & ORTLER, M. (1992). Functional changes in neuropeptide Y and somatostatin containing neurones induced by limbic seizures in the rat. *Neuroscience*, **50**, 831–846.

STANLEY, B.G. & LEIBOWITZ, S.F. (1985). Neuropeptide Y injected in the paraventricular hypothalamus: a power stimulant of feeding behaviour. *Proc. Natl. Acad. Sci. U.S.A.*, **82**, 3940–3943.

STENFORS, C., THEODORSSON, E. & MATHE, A.A. (1989). Effect of repeated electroconvulsive treatment on regional concentrations of tachykinins, neurotensin, vasoactive intestinal polypeptide, neuropeptide Y, and galanin in rat brain. *J. Neurosci. Res.*, **24**, 445–450.

TATEMOTO, K. (1982). Neuropeptide Y: Complete amino acid sequence of the brain peptide. *Proc. Natl. Acad. Sci. U.S.A.*, **79**, 5485–5489.

TATEMOTO, K., CARLQUIST, M. & MUTT, V. (1982). Neuropeptide Y: a novel brain peptide with structural similarities to peptide YY and pancreatic polypeptide. *Nature*, **296**, 659–660.

TOTH, P., VYTAUTAS, P., BINDOKAS, P., BLEAKMAN, D., COLMERS, W. & MILLER, R. (1993). Mechanism of presynaptic inhibition by neuropeptide Y at sympathetic nerve terminals. *Nature*, **364**, 635–639.

WAHLESTEDT C., PICH, E.M., KOOB, G.F., YEE, F. & HEILIG, M. (1993). Modulation of anxiety and neuropeptide Y-Y1 receptors by antisense oligodeoxynucleotides. *Science*, **259**, 528–531.

WAHLESTEDT, C., YANAIHARA, N. & HAKANSON, R. (1986). Evidence for different pre- and post-junctional receptors for neuropeptide Y and related peptides. *Regul. Pept.* **13**, 307–318.

WALKER, M.W. & MILLER, R.J. (1988). ^{125}I-neuropeptide Y and ^{125}I-peptide YY bind to multiple receptor sites in rat brain. *Mol. Pharmacol.*, **34**, 779–792.

(Received April 5, 1994
Revised June 16, 1994
Accepted June 27, 1994)

Br. J. Pharmacol. (1994), **113**, 741–748 © Macmillan Press Ltd, 1994

Failure of CGS15943A to block the hypotensive action of agonists acting at the adenosine A_3 receptor

[1]M. Patel, M.J. Sheehan & P. Strong

Cellular Sciences, Glaxo Research and Development Ltd., Park Road, Ware, Herts, SG12 0DP

1 Adenosine receptor agonists were evaluated for their activity at the putative adenosine A_3 receptor which mediates a 'xanthine-resistant' hypotensive response in the anaesthetized rat. The compounds tested were: the A_1/A_3 receptor agonist, N-[2-(4-aminophenyl)ethyl]adenosine (APNEA), the non-selective adenosine receptor agonist, 5'-N-ethylcarboxamidoadenosine (NECA), the adenosine A_1 receptor-selective agonists, N-[(1S,*trans*)-2-hydroxycyclopentyl]adenosine (GR79236) and N^6-cyclopentyl adenosine (CPA), the A_{2a} receptor-selective agonists, 2-[[2-[4-(2-carboxyethyl) phenyl] ethyl] amino]-N-ethylcarboxamidoadenosine (CGS21680) and 2-phenylaminoadenosine (CV1808), and the moderately A_{2b} selective agonist, N-[(2-methylphenyl)methyl]adenosine (metrifudil).

2 In confirmation of literature findings, APNEA (1–1000 nmol kg^{-1}) induced hypotension and bradycardia; the hypotension was not blocked by pretreatment with the xanthine antagonist, 8-*P*-sulphophenyltheophylline (8-sPT; 40 mg kg^{-1}, i.v.), whereas the bradycardia was attenuated. The non-xanthine antagonist, 9-fluoro-2-(2-furyl)-5,6-dihydro [1,2,4]triazolo{1,5-c}-quinazin-5-imine (CGS15943A; 3 mg kg^{-1} i.v.), also attenuated the bradycardia without affecting the hypotension.

3 The adenosine A_1 receptor-selective agonists, GR79236 and CPA, both produced dose-dependent falls in blood pressure and heart rate which were antagonized by 8-sPT (40 mg kg^{-1}) and CGS15943A (3 mg kg^{-1}).

4 The adenosine A_{2a} receptor-selective agonists, CGS21680 and CV1808, produced only a hypotensive response which was antagonized by 8-sPT (40 mg kg^{-1}) and to a much greater extent by CGS15943A (3 mg kg^{-1}), consistent with the response being mediated solely by A_{2a} receptors.

5 The modestly A_{2b} receptor-selective agonist, metrifudil, produced a dose-dependent fall in blood pressure and at higher doses a fall in heart rate. The hypotension induced by metrifudil was not antagonized by either 8-sPT (40 mg kg^{-1}) or CGS15943A (3 mg kg^{-1}) even though the bradycardia was abolished, suggesting that this agonist activates the putative A_3 receptor.

6 The non-selective adenosine receptor agonist, NECA, produced a hypotension and bradycardia that was attenuated by 8-sPT (40 mg kg^{-1}), confirming previous work. The non-xanthine antagonist, CGS15943A (3 mg kg^{-1}), also attenuated the hypotension and bradycardia. The bradycardia was blocked to a much greater extent, suggesting that NECA may therefore induce hypotension partly by activating the putative A_3 receptor.

7 In conclusion, we have confirmed that the putative A_3 receptor mediating hypotension in the anaesthetized rat is not blocked by 8-sPT, and further shown that it is not blocked by CGS15943A. The A_{2a} agonists CGS21680 and CV1808 showed no discernible activity at the A_3 receptor, whereas APNEA, NECA, CPA and metrifudil appear to activate this receptor. The adenosine A_1 receptor agonist, GR79236, shows considerable selectivity for the A_1 receptor but may activate the A_3 receptor at high doses.

Keywords: Adenosine A_3 receptor, GR79236; CGS21680; CV1808; APNEA; hypotension; anaesthetized rat

Introduction

In addition to the A_1, A_{2a} and A_{2b} sub-types of adenosine receptors, the characteristics of which we have recently evaluated in functional studies (Gurden *et al.*, 1993), adenosine A_3 receptors have recently been cloned from rat (Zhou *et al.*, 1992), sheep (Linden *et al.*, 1993) and human (Salvatore *et al.*, 1993) sources.

There is at present very little work described in the literature that addresses the nature of the physiological processes which adenosine A_3 receptors may control. However, in recent publications it has been suggested that activation of these receptors induces a hypotensive effect in both pithed and anaesthetized rats (Fozard & Carruthers 1993a; Fozard & Hannon, 1994). The features of the response which suggest that it is mediated by A_3 receptors are (i) its occurrence in response to administration of N-[2-(4-aminophenyl)ethyl] adenosine (APNEA; Fozard & Carruthers, 1993a), (ii) its resistance to blockade by 8-(*P*-sulphophenyl]theophylline (8-sPT) and 1,3-dipropyl-8-cyclopentylxanthine (DPCPX; Fozard & Carruthers, 1993a; Carruthers & Fozard, 1994), (iii) its inhibition by pertussis toxin (Carruthers & Fozard, 1993) and (iv) its inhibition by (albeit high doses of) the antagonist BW-A522 (3-(3-iodo-4-aminobenzyl)-8-(4-oxyacetate)-1-propylxanthine; Fozard & Hannon, 1994). An interesting feature of these studies has been the observation that other adenosine derivatives routinely used in the study of adenosine receptors, including 5'-N-ethylcarboxamidoadenosine (NECA) and R-phenylisopropyladenosine (R-PIA), also have affinity for A_3 receptors and induce an 8-sPT-resistant hypotension in rats (Fozard & Carruthers, 1993a).

In our recent work (Gurden *et al.*, 1993) we identified the A_1-receptor selective agonists, GR79236 (N-[(1S,*trans*)-2-hydroxycyclopentyl] adenosine) and CPA (N^6-cyclopentyl adenosine), the modestly A_{2b} receptor-selective agonist, metrifudil (N-[(2-methylphenyl)methyl] adenosine) and the A_{2a}-receptor selective agonists CGS21680 (2-[[2-[4-(2-carboxyethyl) phenyl] ethyl] amino]-N-ethylcarboxamidoadenosine) and CV1808 (2-phenylaminoadenosine) as being particularly useful in the receptor classification of adenosine receptor-mediated responses. Accordingly, the aims of this study were

[1] Author for correspondence.

to investigate the extent to which GR79236, metrifudil and CV1808 are able to elicit an 8-sPT-resistant hypotensive response in the anaesthetized rat, and to confirm the findings of Fozard & Carruthers (1993b) for CPA and CGS21680. In addition, we have also investigated the effects of pretreatment with CGS15943A (9-fluoro-2-(2-furyl)-5,6-dihydro [1,2,4] triazolo{1,5-c}-quinazin-5-imine), a potent non-xanthine adenosine receptor blocking drug which shows a 6 fold selectivity for A_1 receptors over A_2 receptors (Williams *et al.*, 1987), on cardiovascular responses to APNEA, NECA, CPA, GR79236, metrifudil, CGS21680 and CV1808. A preliminary account of this work has been published in abstract form (Patel *et al.*, 1994).

Methods

Female AH/A Wistar rats weighing 190–250 g were anaesthetized with sodium pentobarbitone (60 mg kg^{-1}), and a cannula inserted via a tracheostomy to facilitate spontaneous respiration. The right external jugular vein was cannulated for the continuous infusion of a maintenance dose of sodium pentobarbitone (100 μg kg^{-1} min^{-1}) and the left external jugular vein was cannulated for the administration of drugs (agonists and antagonists). The right carotid artery was cannulated with a heparinized catheter (50 unit ml^{-1} heparin in 0.9% w/v NaCl solution; i.d. = 0.50 mm) for measurement of blood pressure. The heart rate was derived from the blood pressure record. Body temperature was maintained at 37°C by means of a heated mat and a lamp, and all parameters were displayed on a Devices M19 chart recorder.

After a 10–15 min stabilization period, two priming doses of adenosine (300 nmol kg^{-1}) were administered as bolus doses in 0.1 ml volume with a time interval of 3 min. After a further 10 min stabilization period, dose-response curves to agonists were constructed by cumulative bolus injection, the intervals between doses being sufficient to allow a plateau response to develop. In the experiments with the adenosine receptor antagonists, either 8sPT (40 mg kg^{-1}) or CGS15943A (1–10 mg kg^{-1}), drug or vehicle was injected intravenously 5 min before establishing dose-response curves to the agonists. All drugs were given in a 0.1 ml dose volume. Only one agonist dose-response curve was generated per animal.

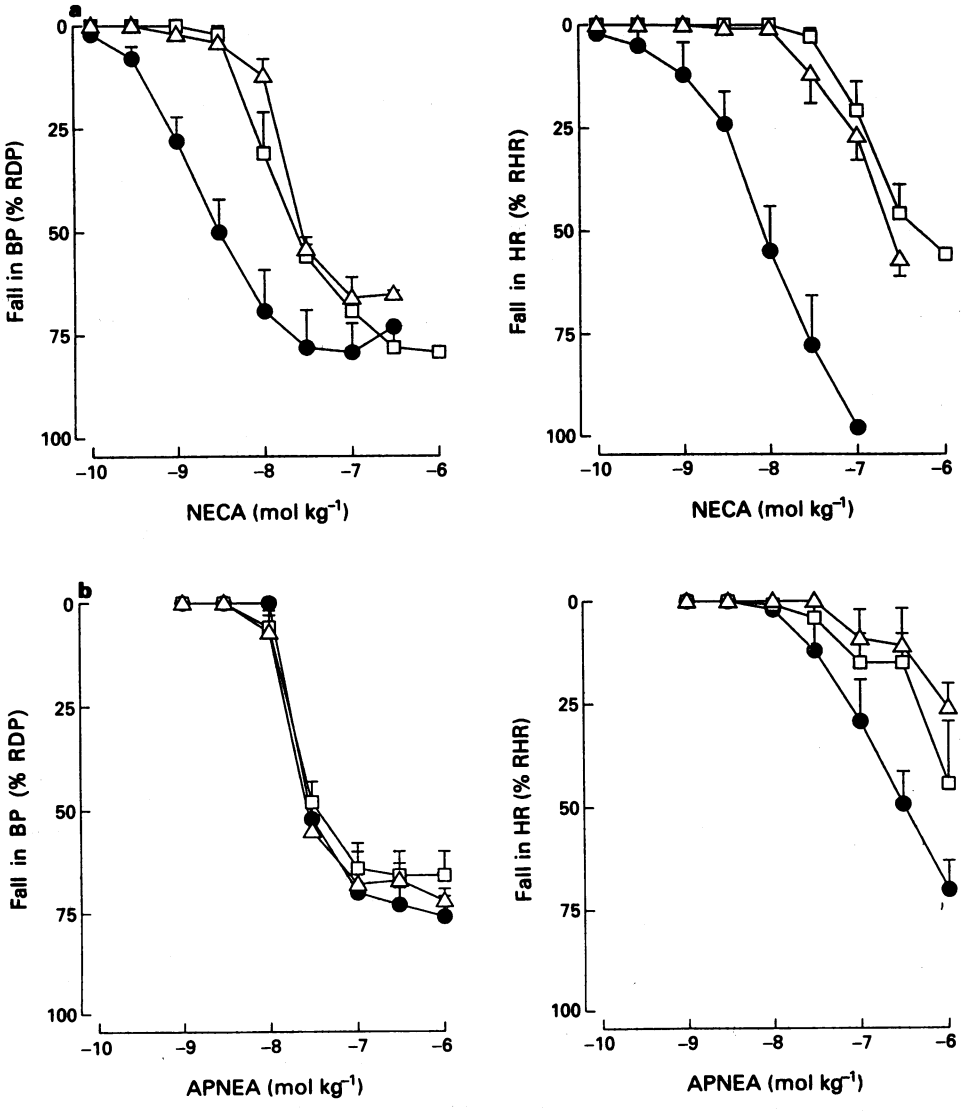


Figure 1 Effects of pretreatment with 8-sPT or CGS15943A on the cardiovascular responses to NECA (a) and APNEA (b) in the anaesthetised rat; (●) untreated controls; (□) animals pretreated with 8-sPT (40 mg kg^{-1}); (△) animals pretreated with CGS15943A (3 mg kg^{-1}) given 5 min prior to the agonist dose-response curve (DRC). The resting diastolic blood pressure (BP) and resting heart rate (HR) values just prior to starting the agonist DRC were as follows. NECA (control); 140 ± 6 mmHg, 473 ± 14 beats min^{-1} (n = 4); NECA (8-sPT): 102 ± 14 mmHg, 452 ± 22 beats min^{-1} (n = 5); NECA (CGS15943A): 119 ± 6 mmHg, 448 ± 13 beats min^{-1} (n = 4); APNEA (control): 109 ± 10 mmHg, 440 ± 34 beats min^{-1} (n = 4); APNEA (8-sPT): 130 ± 12 mmHg, 420 ± 22 beats min^{-1} (n = 5); APNEA (CGS15943A): 131 ± 4 mmHg, 457 ± 18 beats min^{-1} (n = 4). For abbreviations, see text.

Drugs

The following compounds were used: adenosine (Sigma Chemical Co.); CV1808 (2-(phenylamino)adenosine) and CGS21680 (2-[[2-(4-[2-carboxyethyl)phenyl]ethyl] amino] -*N*-ethylcarboxamindoadenosine) and 8-*p*-sulphophenyltheophylline (batches from both Research Biochemicals Inc and Chemistry Division, Glaxo Research and Development); NECA (5'-N-ethylcarboxamidoadenosine), CPA (N^6-cyclopentyladenosine), metrifudil (N-[(2-methylphenyl)methyl] adenosine), CGS15943A (9-fluoro-2-(2-furyl)-5,6-dihydro [1,2,4]triazolo{1,5-c}-quinazin-5-imine), APNEA (N-[2-(4-aminophenyl)ethyl] adenosine) and GR79236 (N-[(1S, *trans*)-2-hydroxycyclopentyl] adenosine) were synthesized in the Chemistry Division (Glaxo Research and Development).

GR79236, CPA, NECA, APNEA, metrifudil and CGS21680 were dissolved in 50 µl 1 M HCl and made up to volume in 0.9% (w/v) NaCl solution (saline). CV1808 was dissolved in 200 µl 1 M HCl + 200 µl 1 M NaOH and made up to volume in saline. A stock concentration of 100 µmol ml^{-1} was used for the agonists. The antagonists, 8sPT and CGS15943A, were prepared in dimethylsulphoxide (DMSO); administration of either 8sPT or CGS15943A did not alter resting blood pressure or heart rate. Administration of 0.1 ml DMSO vehicle produced a transient fall in blood pressure and heart rate which returned to pre-dose levels within 2 min.

Analysis of data

Hypotension was measured as the fall in diastolic pressure in mmHg, and expressed as a percentage of the resting diastolic pressure. Bradycardia was measured as the fall in heart rate in beats min^{-1}, and expressed as a percentage of the resting heart rate. The effective dose required to produce a fall in blood pressure of 40% or a fall in heart rate of 40% (ED_{40} BP and ED_{40} HR respectively) were expressed in nmol kg^{-1} and were determined by graphical interpolation. Dose-ratios (DR) were determined by dividing the ED_{40} value obtained from the antagonist pretreated groups by the ED_{40} value obtained from the control groups. Data are presented as the arithmetic mean ± s.e.mean, or geometric mean with 95% confidence interval as appropriate, from 3 or more animals per dose group. Significant differences between treatment groups in ED_{40} values were determined with Student's *t* test for unpaired data. Resting diastolic blood pressure and heart

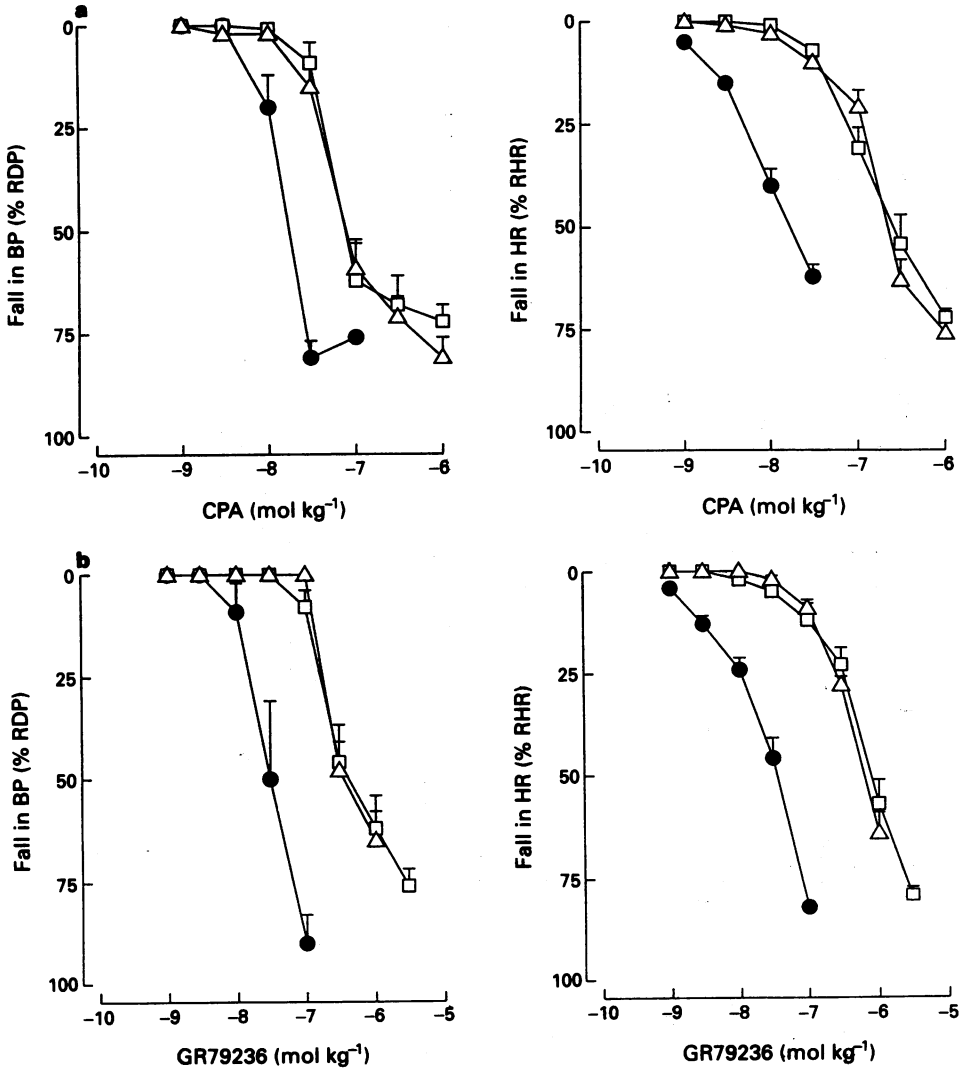


Figure 2 Effects of pretreatment with 8-sPT or CGS15943A on the cardiovascular response to CPA (a) and GR79236 (b) in the anaesthetized rat; (●) untreated controls; (□) animals pretreated with 8-sPT (40 mg kg^{-1}); (Δ) animals pretreated with CGS15943A (3 mg kg^{-1}) given 5 min prior to the agonist dose-response curve (DRC). The resting diastolic blood pressure (BP) and resting heart rate (HR) values just prior to starting the agonist DRC were as follows: CPA (control); 135 ± 10 mmHg, 455 ± 19 beats min^{-1} ($n = 4$); CPA (8-sPT): 136 ± 23 mmHg, 433 ± 25 beats min^{-1} ($n = 4$); CPA (CGS15943A): 119 ± 15 mmHg, 385 ± 24 beats min^{-1} ($n = 4$); GR79236 (control): 114 ± 23 mmHg, 460 ± 27 beats min^{-1} ($n = 4$); GR79236 (8-sPT): 125 ± 4 mmHg, 404 ± 20 beats min^{-1} ($n = 5$); GR79236 (CGS15943A): 123 ± 3 mmHg, 460 ± 9 beats min^{-1} ($n = 4$). For abbreviations, see text.

Table 1 Cardiovascular effects of adenosine agonists and their blockade by 8-sPT and CGS15943A

	Control		*8-sPT-treated*[c]					*CGS15943A-treated*[d]				
	BP ED_{40}[a] (nmol kg^{-1})	*HR* ED_{40}[a]	*BP* ED_{40}[a] (nmol kg^{-1})	*HR* ED_{40}[a]	*Dose-ratio* *BP*[b]	*HR*[b]	n	*BP* ED_{40}[a] (nmol/kg^{-1})	*HR* ED_{40}[a]	*Dose-ratio* *BP*[b]	*HR*[b]	n
NECA	2 (0.5–10)	11 (3–41)	12 (6–23)	323* (82–1272)	6	29	5	21 (16–27)	149* (92–243)	3	14	4
APNEA	25 (14–43)	164 (44–615)	27 (19–38)	774* (497–1205)	1	5	5	27 (6–120)	>880*	1	>7	4
CPA	14 (8–21)	19 (4–100)	72 (28–180)	156* (61–401)	5	8	4	62 (39–98)	178* (118–268)	5	10	4
GR79236	25 (9–72)	23 (14–37)	307* (104–896)	496* (328–750)	12	21	5	302* (131–697)	466* (315–689)	12	20	4
CGS21680	7 (4–12)	>1000	90* (27–298)	>1000	13	–	5	947* (498–1799)	>3000	135	–	4
CV1808	21 (8–51)	>1000	941* (497–1779)	>10000	45	–	5	3009* (1214–7459)	>10000	143	–	5
Metrifudil	18 (16–21)	649 (432–976)	61 (30–128)	10000	4	–	7	37 (22–62)	10000	2	–	5

Values are mean + 95% confidence interval.
[a]dose to lower BP and HR by 40%; [b]BP or HR ED_{40} (control)/BP or HR after antagonist; [c]40 mg kg^{-1} or [d]3 mg kg^{-1} given 5 min prior to agonist DRC
*denotes the means are significantly different from controls, $P<0.05$.

Table 2 Cardiovascular effects of APNEA and GR79236 and their blockade by CGS15943A

	Control		*CGS15943A-treated*[c]					*CGS15943A-treated*[d]				
	BP ED_{40}[a] (nmol kg^{-1})	*HR* ED_{40}[a]	*BP* ED_{40}[a] (nmol kg^{-1})	*HR* ED_{40}[a]	*Dose-ratio* *BP*[b]	*HR*[b]	n	*BP* ED_{40}[a] (nmol/kg^{-1})	*HR* ED_{40}[a]	*Dose-ratio* *BP*[b]	*HR*[b]	n
APNEA	25 (14–43)	164 (44–615)	35 (10–122)	658 (187–2315)	1	4	3	44 (29–68)	5811* (2422–13940)	2	35	4
GR79236	25 (9–72)	23 (14–37)	145* (66–340)	124* (83–184)	6	5	4	544* (226–1310)	1115* (771–1612)	24	48	4

Values are mean + 95% confidence interval.
[a]dose to lower BP and HR by 40%; [b]BP or HR ED_{40} (control)/BP or HR after antagonist; [c]1 mg kg^{-1} or [d]10 mg kg^{-1} given 5 min prior to agonist DRC
*denotes the means are significantly different from controls, $P<0.05$.

rate values for each group of experiments are given in the figure legends.

Results

The resting diastolic blood pressure of a representative group of anaesthetized rats was 126 ± 3 mmHg, with a resting heart rate of 417 ± 14 beats min^{-1} ($n = 15$). Two priming doses of adenosine (300 nmol kg^{-1}) administered as single intravenous bolus doses produced a fall in blood pressure of 43 ± 4 mmHg, associated with a fall in heart rate of 65 ± 5 beats min^{-1}, and 46 ± 4 mmHg, with a fall in heart rate of 71 ± 7 beats min^{-1}, for the first and second priming dose respectively.

NECA and APNEA

The non-selective adenosine receptor agonist NECA (0.1–300 nmol kg^{-1}), and the A_1/A_3 agonist APNEA (1–1000 nmol kg^{-1}), produced dose-dependent falls in blood pressure and heart rate (Figure 1a,b). The antagonist 8-sPT (40 mg kg^{-1}) and CGS15943A (3 mg kg^{-1}) produced a smaller rightward displacement of the dose-response curve (DRC) to the hypotensive effect of NECA than to the bradycardic effect of NECA (Figure 1a; Table 1). Even more notably, the antagonists 8-sPT (40 mg kg^{-1}) and CGS15943A (3 mg kg^{-1}) were without effect on the hypotension observed with APNEA. However, both antagonists were able to produce a rightward displacement of the DRC to the bradycardia obtained with APNEA (Figure 1b; Table 1).

A_1 receptor-selective agonists, CPA and GR79236

The A_1-selective agonists, CPA and GR79236 (0.1–300 nmol kg^{-1}), also produced a dose-dependent fall in blood pressure and heart rate. Both agonists produced hypotension and bradycardia at approximately equieffective doses (Table 1). The antagonists 8-sPT (40 mg kg^{-1}) and CGS15943A (3 mg kg^{-1}) produced slightly smaller rightward displacements of the DRC to the hypotensive effects of GR79236 and CPA than to their bradycardic effects, although this difference was only significant for CPA ($P < 0.05$) (Figure 2a,b, Table 1).

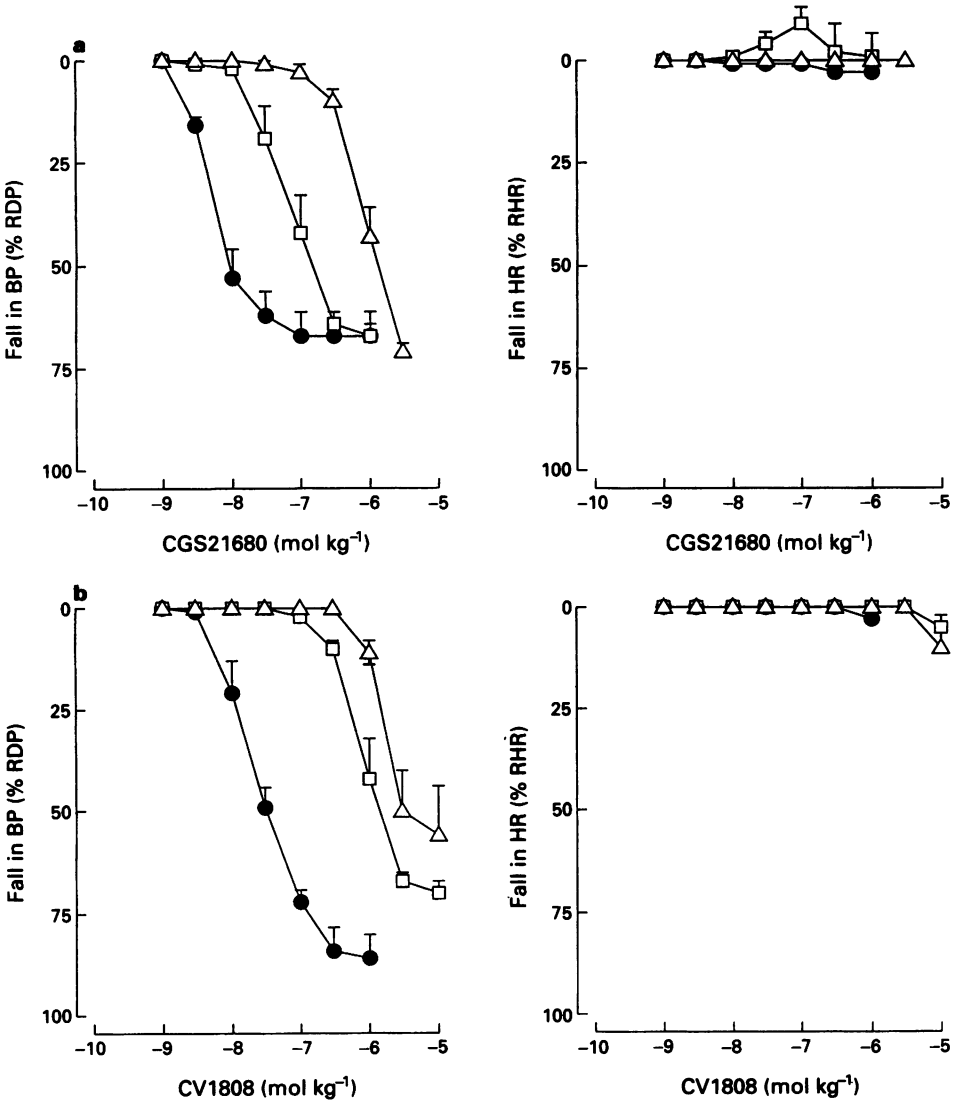


Figure 3 Effects of pretreatment with 8-sPT or CGS15943A on the cardiovascular responses to CGS21680 (a) and CV1808 (b) in the anaesthetized rat; (●) untreated controls; (□) animals pretreated with 8-sPT (40 mg kg^{-1}); (△) animals pretreated with CGS15943A (3 mg kg^{-1}) given 5 min prior to the agonist dose-response curve (DRC). The resting diastolic blood pressure (BP) and resting heart rate (HR) values just prior to starting the agonist DRC were as follows: CGS21680 (control); 112 ± 10 mmHg, 435 ± 20 beats min^{-1} ($n = 4$); CGS21680 (8-sPT): 132 ± 8 mmHg, 382 ± 17 beats min^{-1} ($n = 5$); CGS21680 (CGS15943A): 141 ± 7 mmHg, 427 ± 10 beats min^{-1} ($n = 4$).CV1808 (control): 106 ± 14 mmHg, 380 ± 25 beats min^{-1} ($n = 4$); CV1808 (8-sPT): 143 ± 7 mmHg, 428 ± 19 beats min^{-1} ($n = 5$); CV1808 (CGS15943A): 117 ± 4 mmHg, 372 ± 14 beats min^{-1} ($n = 5$). For abbreviations, see text.

A_{2a} receptor-selective agonists, CGS21680 and CV1808

The adenosine A_{2a} receptor selective agonists, CGS21680 (0.1–100 nmol kg^{-1}) and CV1808 (1–1000 nmol kg^{-1}), both produced a dose-dependent fall in blood pressure, with no significant effect on heart rate. Following administration of either 8-sPT (40 mg kg^{-1}) or CGS15943A (3 mg kg^{-1}), a rightward displacement of the DRC to the hypotensive effect of CGS21680 was observed, with CGS15943A (3 mg kg^{-1}) producing a much greater antagonism of this effect. A modest tachycardia was observed following 8-sPT treatment (Figure 3a; Table 1). Similarly, both 8-sPT (40 mg kg^{-1}) and CGS15943A (3 mg kg^{-1}) produced an antagonism of the hypotensive effect of CV1808, with CGS15943A being the more potent of the two antagonists (Figure 3b, Table 1).

A_{2b} receptor-selective agonist, metrifudil

The adenosine A_{2b} receptor-selective agonist, metrifudil (0.01–10 μmol kg^{-1}), also produced a dose-dependent hypotension and bradycardia. The metrifudil-induced hypotension occurred at lower doses than those causing bradycardia (Table 1). The hypotension induced by metrifudil was not significantly antagonized by either 8-sPT (40 mg kg^{-1}) or CGS15943A (3 mg kg^{-1}) (Figure 4a, Table 1); however, the bradycardia produced by metrifudil was attenuated by both antagonists (Figure 4b; Table 1).

Antagonism of the effects of APNEA and GR79236 by CGS15943A (1–10 mg kg^{-1})

The hypotension induced by APNEA has already been demonstrated to be resistant to blockade by both 8-sPT (40 mg kg^{-1}) and CGS15943A (3 mg kg^{-1}) (Figure 1a). This effect of APNEA was also resistant to blockade by a higher dose of CGS15943A (10 mg kg^{-1}) (Figure 5a; Table 2). However, CGS15943A (1–10 mg kg^{-1}) produced a dose-dependent rightward displacement of the APNEA-induced bradycardia (Figure 5a; Table 2). In contrast, CGS15943A (1–10 mg kg^{-1}) produced dose-dependent rightward displacements of the DRC to both the hypotension and bradycardia induced by GR79236 (Figure 5b; Table 2).

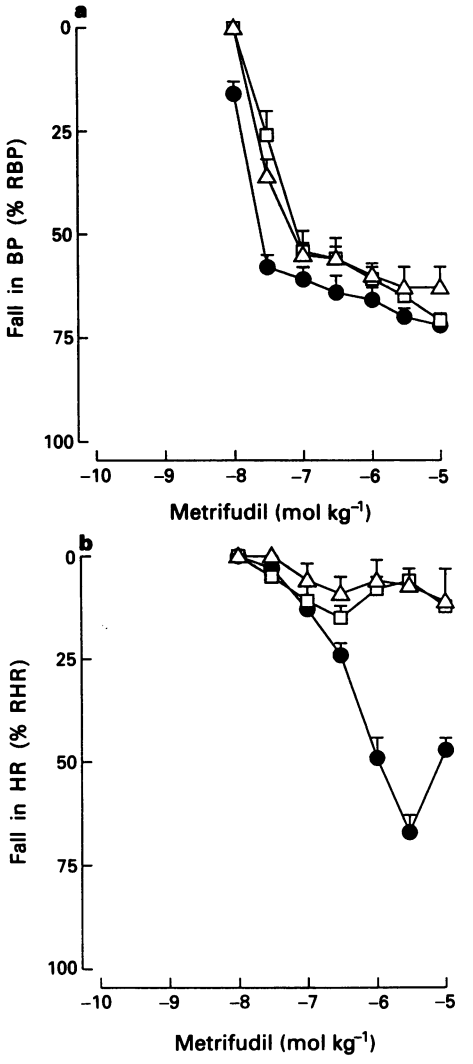


Figure 4 Effects of pretreatment with 8-sPT or CGS15943A on the cardiovascular responses to metrifudil in the anaesthetized rat; (●) untreated controls; (□) animals pretreated with 8-sPT (40 mg kg^{-1}); (△) animals pretreated with CGS15943A (3 mg kg^{-1}) given 5 min prior to the agonist dose-response curve (DRC). The resting diastolic blood pressure (BP) (a) and resting heart rate (HR) (b) values just prior to starting the agonist DRC were as follows. Metrifudil (control); 111 ± 9 mmHg, 370 ± 21 beats min^{-1} ($n = 4$); metrifudil (8-sPT): 147 ± 5 mmHg, 427 ± 12 beats min^{-1} ($n = 7$); metrifudil (CGS15943A) 134 ± 7 mmHg, 406 ± 22 beats min^{-1} ($n = 5$). For abbreviations, see text.

Discussion

The hypotension observed in the presence of blockade of A_1 and A_2 receptors in pithed or anaesthetized rats has been postulated to be an *in vivo* functional correlate for the adenosine A_3 receptor (Fozard & Carruthers, 1993a; Fozard & Hannon, 1994). In the present study we have attempted to characterize further the putative A_3 receptor mediating a hypotensive response in the anaesthetized rat to a range of adenosine agonists in the presence of A_1/A_2 receptor blockade with the xanthine antagonist 8sPT, or the non-xanthine antagonist CGS15943A (Ghai *et al.*, 1987). The initial characterization of CGS15943A suggested that this antagonist had a much greater affinity for adenosine receptors of the A_2 than the A_1 receptor subtype (Ghai *et al.*, 1987). However, recent studies in CHO cells transfected with human A_1, A_{2a} or A_{2b} receptors suggest that its selectivity is modest. For example, A_{2a} to A_1 selectivity may be as little as 5 fold and A_{2a} to A_{2b} selectivity only 20 fold (Rollins *et al.*, 1994) and so it may be more accurate to consider CGS15943A as an adenosine receptor antagonist with limited selectivity. Indeed, CGS15943A has previously been described as a non-selective adenosine receptor antagonist (Merkel *et al.*, 1993).

In the presence of a high dose of 8sPT, the agonists CPA, APNEA and NECA produced a fall in blood pressure at doses lower than those required for an effect on heart rate. In this respect, our results confirm the findings of Fozard and co-workers (1993a,b, 1994) suggesting that these agonists may cause hypotension by activating the A_3 adenosine receptor. Furthermore, the hypotensive response to APNEA remained unaffected after A_2/A_1 receptor blockade by high doses of CGS15943A (3 and 10 mg kg^{-1}) which clearly attenuated the effects of APNEA on heart rate. Thus the A_3 receptor appears to have little affinity for CGS15943A.

In the presence of CGS15943A (3 mg kg^{-1}), the selective A_1 receptor agonist CPA was found to mediate a hypotensive response at doses lower than those required to produce bradycardia. This is similar to the results obtained for CPA in the presence of a high dose of 8-sPT (Figure 2a, Table 1) and confirms the findings of Fozard & Carruthers (1993b). In contrast, under the same conditions GR79236 produced hypotension only at doses that also produced bradycardia. However, in the presence of a higher dose of CGS15943A (10 mg kg^{-1}), GR79236 may produce hypotension in the absence of significant bradycardia, although the dose-ratios for the falls in blood pressure and heart rate were not significantly different. It is unlikely that GR79236 produces a hypotensive response by activation of vascular A_2 receptors.

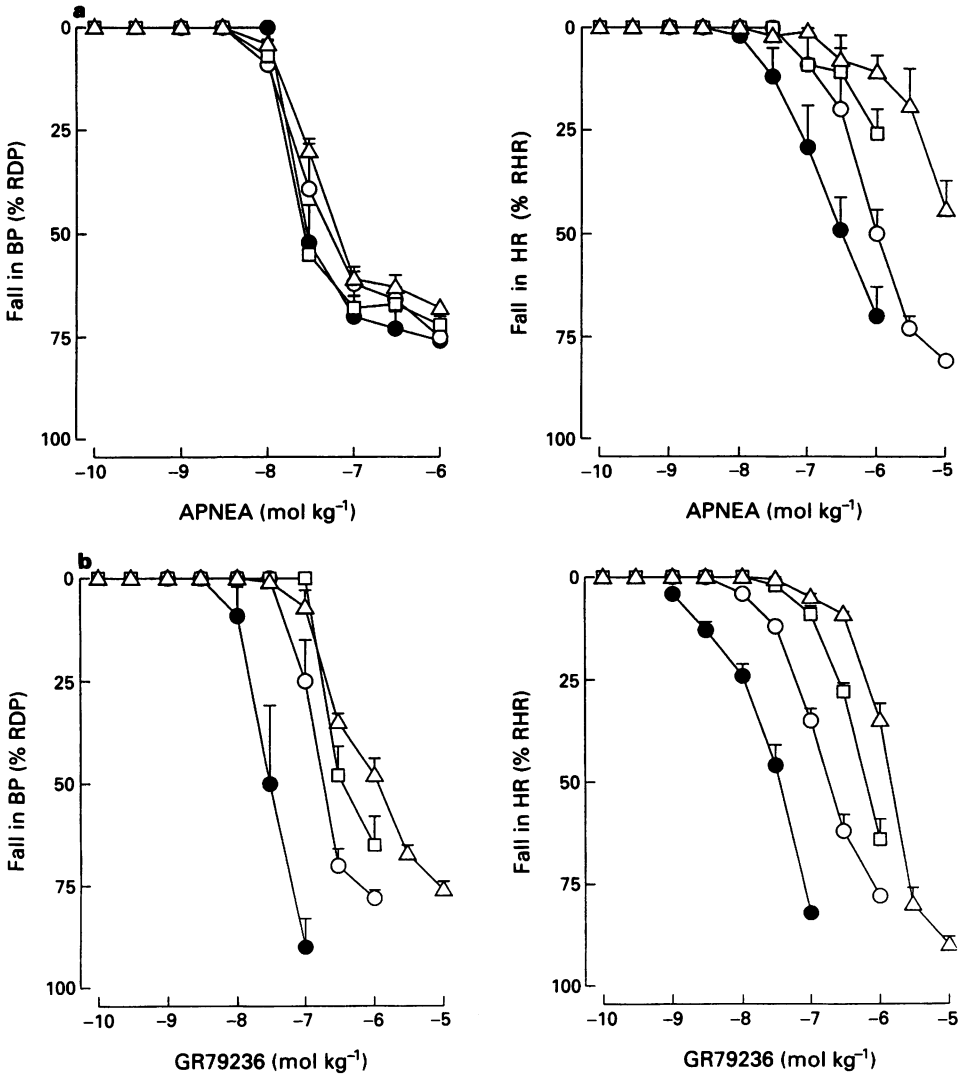


Figure 5 Effects of pretreatment with CGS15943A on the cardiovascular responses to APNEA (a) and GR79236 (b) in the anaesthetized rat; (●) untreated controls; (□) animals pretreated with CGS15943A (1 mg kg^{-1}); (□) CGS15943A (3 mg kg^{-1}),(△) CGS15943A (10 mg kg^{-1}) given 5 min prior to the agonist dose-response curve (DRC). The resting diastolic blood pressure (BP) and resting heart rate (HR) values just prior to starting the agonist DRC were as follows. (a) APNEA (control); 109 ± 10 mmHg, 440 ± 34 beats min^{-1} ($n = 4$); CGS15943A (1 mg kg^{-1}): 145 ± 9 mmHg, 370 ± 15 beats min^{-1} ($n = 3$); CGS15943A (3 mg kg^{-1}): 131 ± 5 mmHg, 457 ± 18 beats min^{-1} ($n = 4$); CGS15943A (10 mg kg^{-1}): 139 ± 19 mmHg, 402 ± 14 beats min^{-1} ($n = 4$). (b) GR79236 (control): 114 ± 22 mmHg, 460 ± 27 beats min^{-1} ($n = 4$); CGS15943A (1 mg kg^{-1}): 140 ± 6 mmHg, 412 ± 5 beats min^{-1} ($n = 4$); CGS15943A (3 mg kg^{-1}): 123 ± 3 mmHg, 460 ± 9 beats min^{-1} ($n = 4$): CGS15943A (10 mg kg^{-1}): 120 ± 10 mmHg, 385 ± 9 beats min^{-1} ($n = 4$).

Recent studies have shown that GR79236 has 300 fold selectivity for A_1 over A_2 receptors (Gurden *et al.*, 1993), and furthermore, both 8-sPT and CGS15943A were effective antagonists of the A_{2a}-mediated hypotensive response to CGS21680 and CV1808. Therefore it is possible that GR79236 may activate the A_3 receptor at high doses.

The modestly selective A_{2b} receptor agonist, metrifudil, also produced a profound hypotension with smaller effects on heart rate. The fall in blood pressure induced by metrifudil was not antagonized by either 8sPT or CGS15943A at doses that blocked A_{2a}-mediated responses, and since CGS15943A has approximately equal affinity for A_{2a} and A_{2b} receptors (Rollins *et al.*, 1994), the hypotensive response cannot be explained by an action at A_{2b} receptors. These data suggest that metrifudil may produce a hypotensive effect by the activation of the putative A_3 receptor and so is probably of limited value in studying A_{2b} receptors *in vivo*. Although the hypotension induced by metrifudil was resistant to blockade by 8sPT and CGS15943A, in a similar manner to that described for APNEA, the response was qualitatively different from that observed with APNEA. The response was slower in onset and had a longer duration to attainment of a maximum response. This qualitative difference between metrifudil and APNEA is not fully understood and merits further investigation.

In conclusion, our results not only support the findings of Fozard and co-workers but extend the characterization of agonists that have efficacy at this putative A_3 receptor to include metrifudil. Since the hypotensive response mediated by the A_3 receptor was also resistant to the non-xanthine antagonist CGS15943A, it is clear that the A_3 receptor can no longer be described as a xanthine-insensitive receptor. Indeed, the xanthine antagonist, BW-A522, has been shown to antagonize the response to APNEA in a surmountable manner, albeit with somewhat lower potency than would be expected from its affinity for the human and sheep A_3 receptor (Fozard & Hannon, 1994). The results also suggest that CGS15943A is a more potent antagonist than 8sPT at blocking both A_2 and A_1 receptors and would therefore be a more appropriate antagonist with which to study A_3-receptor-

mediated events in preparations where mixed populations of adenosine receptors exist. Finally, our study suggests that the selective A_1 receptor agonist, GR79236, and the A_{2a} receptor agonists, CGS21680 and CV1808, are without significant effect at the putative A_3 receptor and would therefore be suitable tools with which to investigate this novel receptor.

References

CARRUTHERS, A.M. & FOZARD, J.R. (1993). Effect of pertussis toxin treatment on the putative adenosine receptor-mediated hypotensive response in the rat. *Eur. J. Pharmacol.*, **250**, 185–188.

CARRUTHERS, A.M. & FOZARD, J.R. (1994). Hypotensive responses to the putative adenosine, A_3 agonist N^6-2-(4-aminophenyl) ethyladenosine in the rat. *Drug Dev. Res.*, **30**, 147–152.

FOZARD, J.R. & CARRUTHERS, A.M. (1993a). Adenosine A_3 receptors mediate hypotension in the angiotensin II-supported circulation of the pithed rat. *Br. J. Pharmacol.*, **109**, 3–5.

FOZARD, J.R. & CARRUTHERS, A.M. (1993b). The cardiovascular effects of A_1 and A_2 receptor agonists in the pithed rat: no role for glibenclamide-sensitive potassium channels. *Naunyn-Schmeid. Arch. Pharmacol.*, **347**, 192–196.

FOZARD, J.R. & HANNON, J.P. (1994). BW-A522 blocks adenosine A_3 receptor-mediated hypotensive responses in the rat. *Eur. J. Pharmacol.*, **252**, R5–R6.

GHAI, G., FRANCIS, J.E., DOTSON, R.A., HOPKINS, M.F., COTE, D.T., GOODMAN, F.R. & ZIMMERMAN, M.B. (1987). Pharmacological characterisation of CGS15943A: a novel non-xanthine adenosine antagonist. *J. Pharmacol. Exp. Ther.*, **242**, 784–790.

GURDEN, M.F., COATES, J., ELLIS, F., FOSTER, M., HORNBY, E., KENNEDY, I., MARTIN, D.P., STRONG, P., VARDEY, C.J. & WHEELDON, A. (1993). Functional characterisation of three adenosine receptor types. *Br. J. Pharmacol.*, **109**, 693–698.

LINDEN, J., TAYLOR, H.E., ROBEVA, A.S., TUCKER, A.L., STEHLE, J.H., RIVKEES, S.A., FINK, J.S. & REPPERT, S.M. (1993). Molecular cloning and functional expression of a sheep A_3 adenosine receptor with widespread tissue distribution. *Mol. Pharmacol.*, **44**, 524–532.

MERKEL, L.A., RIVERA, L.M., COLUSSI, D.J., PERRONE, M.H., SMITS, G.J. & COX, B.F. (1993). *In vitro* and *in vivo* characterisation of an A1-selective adenosine agonist, RG14202. *J. Pharmacol. Exp. Ther.*, **265**, 699–706.

PATEL, M., SHEEHAN, M.J. & STRONG, P. (1994). Cardiovascular effects of GR79236, APNEA and CGS21680 in the anaesthetised rat. *Br. J. Pharmacol.*, **112**, 505P.

ROLLINS, P.J., TURNER, S.J., AKPOGUMA, C.I.O. & RAY, K.P. (1994). Characterisation of human adenosine type 1, 2_a and 2_b receptors expressed in CHO cells. *Biochem. Soc. Trans.*, **22**, 195.

SALVATORE, C.A., JACOBSON, M.A., TAYLOR, H.E., LINDEN, J. & JOHNSON, R.G. (1993). Molecular cloning and characterisation of the human A_3 adenosine receptor. *Proc. Natl. Acad. Sci. U.S.A.*, **90**, 10365–10369.

WILLIAMS, M., FRANCIS, J., GHAI, G., BRAUNWALDER, A., PSYCHOYOS, S., STONE, G.A. & CASH, W.D. (1987). Biochemical characterisation of the triazoloquinazoline, CGS 15943, a novel non-xanthine antagonist. *J. Pharmacol. Exp. Ther.*, **241**, 415–420.

ZHOU, Q.-Y., LI, C., OLAH, M.E., JOHNSON, R.A., STILES, G.L. & CIVELLI, O. (1992). Molecular cloning and characterisation of an adenosine receptor: the A_3 adenosine receptor. *Proc. Natl. Acad. Sci. U.S.A.*, **89**, 7432–7436.

(Received April 22, 1994
Revised June 21, 1994
Accepted June 27, 1994)

Br. J. Pharmacol. (1994), **113**, 749–756 © Macmillan Press Ltd, 1994

Role of interleukin-5 in enhanced migration of eosinophils from airways of immunized guinea-pigs

[1]Eliane Coëffier, Danielle Joseph & B. Boris Vargaftig

Unité de Pharmacologie Cellulaire, Unité Associée Institut Pasteur-INSERM no. 285, 25, Rue du Dr. Roux, 75015, Paris, France

1 Platelet activating factor (PAF), leukotriene B_4 (LTB_4) and interleukin-5 (IL-5) are potent chemoattractants for guinea-pig eosinophils, which may be involved in eosinophil recruitment and up-regulation in allergic diseases. Eosinophils from the bronchoalveolar lavage fluid (BALF) of ovalbumin-sensitized guinea-pigs were collected 24 h after antigen provocation and migration induced by PAF, LTB_4 and rhIL-5 was studied.

2 Total BALF content and distribution of eosinophils were greater in immunized, ovalbumin-challenged guinea-pigs ($5.0 \pm 0.8 \times 10^6$/guinea-pig; $12 \pm 1\%$) than in immunized, saline-challenged animals ($3.0 \pm 0.7 \times 10^6$/guinea-pig; $7 \pm 1\%$).

3 The chemoattraction of eosinophils isolated on a metrizamide gradient was studied in micro-Boyden chambers, results being expressed as the number of migrating cells (mean ± s.e.mean). PAF and LTB_4-induced migration of eosinophils from immunized and OA-challenged guinea-pigs were significantly enhanced, as compared to immunized and saline-challenged animals (170 ± 36 vs 35 ± 9 migrating eosinophils for 10 nM PAF; 271 ± 60 vs 110 ± 19 for 1 nM LTB_4).

4 The IL-5 antibody TRFK-5, *in vivo*, reduced eosinophil recruitment in BALF of antigen-challenged immunized animals as well as the enhanced responsiveness of eosinophils from the challenged animals, suggesting a role for IL-5 in the priming of eosinophils *in vivo*.

5 In contrast to TRFK-5, nedocromil sodium reduced to a similar extent eosinophil, macrophage and lymphocyte recruitment into the BALF of antigen-challenged, but failed to down-regulate the enhanced responsiveness of eosinophils from the challenged animals.

6 The increased eosinophil content in lungs from antigen-challenged guinea-pigs is thus selectively reduced by the anti-IL-5 antibody, which also attenuates the concomitant enhancement of the eosinophil responsiveness, supporting the concept that IL-5 is essential for recruitment and priming of eosinophils *in vivo*. In contrast, nedocromil sodium reduced non-selectively the total cell recruitment to the airways, but failed to attenuate the enhanced responsiveness of those eosinophils which migrated, indicating that its effects involve a different target.

Keywords: Bronchopulmonary allergy; eosinophils; anti-IL-5 antibody; interleukin-5

Introduction

Increased numbers of eosinophils in blood and bronchoalveolar lavage fluid (BALF) are frequently observed in patients with bronchial asthma (De Monchy *et al.*, 1985), as initially recognized by Hüber & Koessler (1922), but neither the mechanisms of eosinophil recruitment into tissues undergoing allergic reactions nor their pathophysiological role have been elucidated (Frigas & Gleich, 1986; Venge, 1990). PAF and leukotriene (LT) B_4 are two recognized inflammatory mediators which share the ability to induce eosinophil chemoattraction *in vitro* (Czarnetzki & Mertensmeier, 1985; Wardlaw *et al.*, 1986; Coëffier *et al.*, 1991a) and *in vivo* (Silbaugh *et al.*, 1987; Lellouch-Tubiana *et al.*, 1988; Arnoux *et al.*, 1988; Sanjar *et al.*, 1990). T-cells also play an important role in the induction of eosinophilia, particularly via three well characterized factors, interleukin-3 (IL3) (Lopez *et al.*, 1987), granulocyte-macrophage colony-stimulating factor (GM-CSF) (Thorne *et al.*, 1986) and interleukin-5 (IL-5) (Sanderson *et al.*, 1985; Campbell *et al.*, 1987; Yokota *et al.*, 1987) known to stimulate eosinophilopoiesis. IL-5 specifically facilitates the terminal differentiation and proliferation of eosinophils (Yamaguchi *et al.*, 1988b), as well as their survival, viability, and antibody-dependent cytotoxicity (Yamaguchi *et al.*, 1988a; Lopez *et al.*, 1988; Secor *et al.*, 1990) and is the first haemopoietic factor whose elaboration *in vivo* may explain the selective eosinophilia and eosinophil activation in disease (Coffman *et al.*, 1990; Sher *et al.*, 1990; Sedgwick *et al.*, 1991).

IL-5 can induce migration of guinea-pig (Coëffier *et al.*, 1991b), mice (Yamaguchi *et al.*, 1988a) and human (Wang *et al.*, 1989) eosinophils. In addition, human recombinant (hr) IL-5 primes very intensively guinea-pigs eosinophils for an enhanced migration by PAF and LTB_4 (Coëffier *et al.*, 1991b) as well as human eosinophils to other chemoattractants (Warringa *et al.*, 1992). This priming may be important for bronchopulmonary hyperresponsiveness and indeed lungs from immunized and antigen-boosted guinea-pigs become hyperresponsive, undergoing a more intense bronchoconstriction and releasing more mediators than controls when stimulated with PAF (Pretolani *et al.*, 1988). Lungs from boosted animals contain more eosinophils than paired controls as well as a target with the hrIL-5 interacts, allowing for a very intense priming upon the subsequent stimulation with PAF (Pretolani *et al.*, 1992). Since this target may be the eosinophil, we hypothesized that eosinophils from sensitized and antigen-challenged animals might also be hyperresponsive *in vitro*.

In order to understand better the role and mechanisms of this *in vivo* priming, experiments were performed comparing TRFK-5, a specific monoclonal antibody against IL-5 (Gulbenkian *et al.*, 1992) with the anti-allergic compound nedocromil sodium, which down-regulates the enhanced responsiveness of sensitized lungs to PAF (Pretolani *et al.*, 1990).

[1] Author for correspondence.

Methods

Sensitization procedure

Male Hartley guinea-pigs (weighing 500 g) from the Saint-Antoine breeding (Pleudaniel, France), were sensitized s.c. with a mixture containing ovalbumin (10 μg) and $Al(OH)_3$ (1 mg) dispersed in 0.5 ml of 0.15 M NaCl (saline). Non-sensitized animals received a mixture containing $Al(OH)_3$ (1 mg) dispersed in 0.5 ml of 0.15 M NaCl. Fourteen days later, guinea-pigs were challenged by the intra-nasal instillation of ovalbumin (3 mg ml^{-1} in 0.15 M sterile saline, 1 mg per animal) or saline alone, under protection of mepyramine (1 mg kg^{-1}, i.p.), to prevent acute anaphylaxis. TRFK-5 was administered i.p. at 30 μg kg^{-1} 2 h before the intra-nasal challenge. This dose was shown to be effective in suppressing eosinophil infiltration by antigen in guinea-pig BALF (Gulbenkian *et al.*, 1992). Nedocromil sodium was administered twice s.c. at 30 mg kg^{-1}, 10 min before and 9 h after the intra-nasal challenge with ovalbumin. Control animals were treated with saline.

Harvest of bronchoalveolar cells

Airway eosinophils were obtained by bronchoalveolar lavage 24 h after the intra-nasal challenge. Guinea-pigs were anaesthetized with sodium pentobarbitone (34 mg kg^{-1}, i.p.) Bronchoalveolar cells were collected in 10 successive lavages using 5 ml aliquots of sterile saline at room temperature through a polyethylene tracheal cannula. The 10 successive lavages from one animal were pooled and each individual bronchoalveolar lavage sample (50 ml) was supplemented with 20 iu ml^{-1} heparin just after lavage (Laboratories Choay, Paris, France) and centrifuged separately (475 *g*, 10 min, 20°C). Heparin prevents cell aggregation through metrizamide gradient and, as shown previously, has no effect on guinea-pig eosinophils (Coëffier *et al.*, 1991a). The cells recovered in the bronchoalveolar pellets providing from two to three animals were then pooled in 3 ml of metrizamide 18%. The cells were counted with a Malassez haemacytometer and the cell purity was analysed after cytocentrifugation by a modified May-Grünwald-Giemsa staining (Diff-Quik, American Scientific Products, Mc Gaw Park, IL, U.S.A.) and the viability was estimated with the Trypan Blue exclusion test.

Purification of guinea-pig eosinophils from BALF

Eosinophils were isolated on a metrizamide gradient according to a modification (Coëffier *et al.*, 1991a) of the method of Vadas *et al.* (1979). Gradients were prepared by placing the bronchoalveolar cell pellet in 3 ml metrizamide at 18% in a 15 ml plastic Falcon tube and underlaying this solution with a series of 3 ml volumes of discontinuous metrizamide gradient (20, 22, 24% metrizamide). After two centrifugations (180 *g*, 11 min, 20°C and 2200 *g*, 11 min, 20°C) the cells were collected from each density interface and washed once in HBSS. After counting with a Malassez haemocytometer, eosinophil numbers were adjusted to 4×10^6 ml^{-1} in RPMI 1640 containing L-glutamine (2 mM), 0.4% BSA and 27 mM HEPES. The cell purity was controlled after cytocentrifugation and a modified May-Grünwald-Giemsa staining (Diff-Quick, American Scientific Products, McGaw Park, IL, U.S.A.) and the viability was estimated with the Trypan Blue exclusion test.

Migration studies

Eosinophil migration was performed according to a modification of the Boyden chamber technique as described by Coëffier *et al.* (1991b), using micropore filters with a 3 μm pore size. Stock solutions of PAF, FMLP, rhIL-5, C5a and lyophilized LTB_4 were diluted in RPMI 1640 containing 2 nM L-glutamine, 0.05% BSA and 27 mM HEPES. Approximately 25 μl of the buffer or of the attractant solution were dispended into the lower wells, such that a slight excess was added and a meniscus formed. The prewet filter (RPMI 1640 containing 2 mM L-glutamine and 27 mM HEPES) was carefully placed over the entire set of wells. The silicone gasket and upper chamber were added and secured firmly in place and 50 μl of the cell suspension were added to the upper wells. A clean microscope slide was placed over the upper wells to reduce evaporation during incubation and to avoid leakage into the interwell spaces. The chamber was incubated at 37°C with CO_2 for 2 h. During this time, the cells settled to the filter surface by gravity. The filters were removed, fixed briefly (2–4 s) in absolute methanol and stained with Gill's haematoxylin. The rectangular filters were cut and mounted on microscope slides. Buffer controls were tested in four to six samples and each agonist concentration was tested in triplicate. The results were quantified by counting the number of cells in fields which have migrated to 40 μm using an optical grid at 400 × magnification.

Materials and buffers

Lipid-free bovine serum albumin (BSA), gamma globulin fraction II, calcium ionophore A23187, formyl-L-methionyl-L-leucyl-L-phenylalanine (FMLP), human recombinant C5a, calcium ionophore A23187, N-2-hydroxyethylpiperazine-N'-2-ethanesulphonic acid (HEPES) and metrizamide were from Sigma Chemical Co. (St. Louis, MO. U.S.A.) LTB_4 was from Cascade (Berkshire, UK). $Al(OH)_3$ was from Merck (Darmstadt, Germany). Synthetic PAF (1-0-hexadecyl-2-acetyl-*sn*-glycero-3-phosphorylcholine) was from Bachem (Budendorf, Switzerland). Recombinant human interleukin 5 (rhIL-5) was from Immugenex (Los Angeles, CA, U.S.A.). Chicken ovalbumin (OA) was from Miles (Naperville, IL, U.S.A.). Sodium pentobarbitone was from Clin-Midy (Montpellier, France). Mepyramine maleate was from Rhône-Poulenc-Rorer (Vitry sur Seine, France). Nedocromil sodium, a generous gift of Dr A. Norris (Fisons, UK) was dissolved in saline at the concentration of 100 mg ml^{-1} and further diluted in saline. In preliminary phases of this study, TRFK-5-derived rat antimouse IL-5 antibody was a generous gift from Dr R.W. Egan of Schering-Plough Research (Bloomfield, NJ, U.S.A.). Later, TRFK-5 was purchased from Immugenex (Los Angeles, CA, U.S.A.).

Buffers were: L-glutamine-free RPMI 1640, containing 2 g/l sodium bicarbonate from Eurobio, Paris, France and Ca^{2+} and Mg^{2+}-free Hank's balanced salt buffer (HBSS) from Gibco (Paisley, UK).

The 48-wells microtaxis chambers and the cellulose nitrate filters (3 μm pore size) were purchased from Neuro Probe, Inc. (Cabin John, MD, USA).

Expression of results

Results are expressed as the number of eosinophils migrating at 40 μm (mean ± s.e.mean) through the cellulose nitrate filter in the presence of the agonist and of the solvent alone. The variability of the results was evaluated by the coefficient of variation among individual observations per test and among triplicate values. The statistical significance of differences between means of various groups were tested using analysis of variance with the ANOVA test and $P < 0.05$ was considered significant.

Results

Interference of immunization and provocation with cell numbers and distribution

Immunization alone more than doubled the total number of cells recovered from the BALF 24 h after the intra-nasal instillation of antigen when compared with non-immunized

animals (Table 1). However, the main differences in the cell composition of BALF from actively sensitized guinea-pigs compared to non immunized animals were the number and proportion of eosinophils. Indeed, the eosinophil counts were further increased by antigen challenge ($5.0 \pm 0.8 \times 10^6$ eosinophils for immunized and challenged animals vs $0.6 \pm 0.4 \times 10^6$ for non immunized guinea-pigs). Finally, the proportion of eosinophils did not change in the unchallenged animals, being 5–8%, but reached 12% after provocation. The number of macrophages was also increased after sensitization and challenge; no difference in the number of the other cell types, i.e., polymorphonuclear neutrophils and lymphocytes, was detected (Table 1).

Eosinophil purification

Two populations of eosinophils were separated from the BALF of control and immunized animals upon the discontinuous metrizamide gradient, one of low density (at 20 and 22% of metrizamide, 20 ± 3 and 27 ± 4% of eosinophils for sensitized, saline-challenged and sensitized, ovalbumin-challenged guinea-pigs, respectively, $n = 12$) and another of high density (at 22 24% of metrizamide), of purity ranging between 67 and 96% (78 ± 3 and 82 ± 2% of eosinophils for sensitized, saline-challenged and ovalbumin-challenged guinea-pigs respectively, $n = 12$) (Figure 1). The intra-nasal provocation increased the number of low density eosinophils ($1.6 \pm 0.3 \times 10^6$ vs $0.9 \pm 0.2 \times 10^6$ eosinophils for sensitized saline-challenged and ovalbumin-challenged guinea-pigs, respectively, $n = 12-14$) (Figure 1). High density eosinophils were used for further experiments.

Increased migration of eosinophil from the guinea-pig BALF after challenge with ovalbumin

As shown in Figure 2, eosinophils collected from ovalbumin-challenged animals migrated to a larger extent than controls in response to PAF and LTB_4. PAF and LTB_4-induced migration of eosinophils from immunized and ovalbumin-challenged, was significantly increased, as compared to those of sensitized and saline-challenged, animals (170 ± 36 vs 35 ± 9 migrating eosinophils for 10 nM PAF; 271 ± 60 vs 110 ± 19 for 1 nM LTB_4). rhIL-5-induced migration was also significantly increased after the challenge (Table 2), whereas responses to C5a and to FMLP were non-significantly increased (373 ± 89 vs 224 ± 73 for 100 nM C5a and 64 ± 27 vs 35 ± 13 for 1 μM FMLP), the increased response corresponding to the enhancement of spontaneous migration. Furthermore, it appears that C5a elicited a dose-dependent migration of both saline- and antigen-challenged eosinophils when compared to controls in both groups. Ovalbumin itself, applied to the eosinophils, had no significant effect (Table 2).

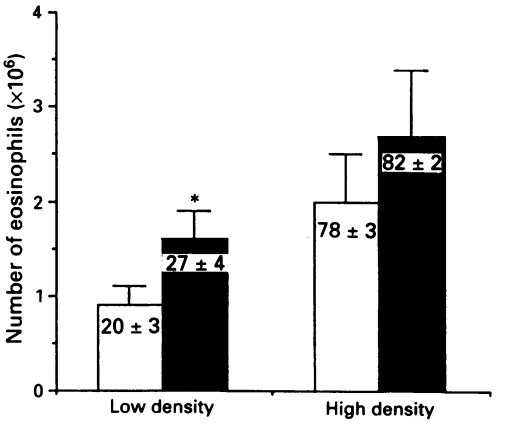


Figure 1 The intra-nasal provocation with antigen increased the number of low density eosinophils in the guinea-pig BALF. Eosinophils were separated from the BALF of saline (open columns) and ovalbumin-challenged (solid columns) sensitized guinea-pigs upon a discontinuous metrizamide gradient. Two populations of eosinophils were separated, one of low density (between 20 and 22% of metrizamide), and another of high density (between 22 and 24% of metrizamide). The results are expressed as the number of total eosinophils collected after the gradient (mean ± s.e.mean, $n = 12$). The numbers in the columns indicate the % of purity of each eosinophil population evaluated after cytocentrifugation and staining. *$P < 0.05$, comparison between sensitized, saline-challenged and sensitized, ovalbumin-challenged guinea-pigs.

Effect of TRFK-5, a specific monoclonal antibody against IL-5, on accumulation of eosinophils

In vitro, IL-5 primes guinea-pigs eosinophils for an enhanced migration by PAF and LTB_4 (Coëffier *et al.*, 1991b) and, accordingly, we hypothesized that eosinophils from antigen-challenged animals might be primed *in vivo* by IL-5 generated upon antigen challenge. Experiments were thus performed with TRFK-5-derived rat anti-mouse IL-5 antibody which cross-reacts with guinea-pigs. Injected i.p. 2 h before antigen challenge at 30 μg kg^{-1}, TRFK-5 inhibited eosinophil accumulation in BALF after ovalbumin provocation (Figure 3). TRFK-5 failed to modify the recruitment of macrophages, lymphocytes and neutrophils.

Effect of anti IL-5 on ex vivo *hyperresponsiveness of airway eosinophils*

Injected as above, TRFK-5 inhibited the enhancement of PAF and LTB_4-induced eosinophil migration observed with eosinophils from immunized and ovalbumin-challenged, as compared to immunized and saline-challenged, animals (Figure 4).

Table 1 Cell counts in bronchoalveolar lavage fluid from control and sensitized guinea-pigs

	Leukocytes	*Eosinophils*		*Macrophages*		*Neutrophils*		*Lymphocytes*	
Treatment	× 10^6/BAL	(%)	(× 10^6)	(%)	(× 10^6)	(%)	(× 10^6)	(%)	(× 10^6)
Unsensitized									
Saline-challenged	21.2 ± 5.7	8 ± 3	2.3 ± 1.1	67 ± 11	12.9 ± 4.0	18 ± 11	5.2 ± 3.5	7 ± 4	0.8 ± 0.5
Ovalbumin-challenged	10.9 ± 2.2	5 ± 2	0.6 ± 0.4	66 ± 7	6.9 ± 1.1	29 ± 8	3.5 ± 1.5	3 ± 1	0.3 ± 0.1
Sensitized									
Saline-challenged	41.7 ± 3.5	7 ± 1	3.0 ± 0.7	80 ± 2	33.4 ± 3.0	7 ± 1	2.7 ± 0.5	5 ± 1	1.9 ± 0.3
Ovalbumin-challenged	44.5 ± 5.0	12 ± 2*	5.0 ± 0.8*	75 ± 3	32.8 ± 3.4	9 ± 2	5.0 ± 1.6	5 ± 1	1.6 ± 0.4

Guinea-pigs were sensitized s.c. with 0.5 ml of saline containing 10 μg of ovalbumin dispersed in 1 mg $Al(OH)_3$.
Non-sensitized animals received 0.5 ml of saline containing 1 mg $Al(OH)_3$ alone. Guinea-pigs were challenged 14 days later by the intra-nasal instillation of ovalbumin (3 mg ml^{-1} in saline, 1 mg per animal) or saline alone, under protection of mepyramine (1 mg kg^{-1}, i.p.) Airway eosinophils were obtained by bronchoalveolar lavage 24 h after the intra-nasal challenge. Cells were counted and the cell purity was analysed after cytocentrifugation (mean ± s.e.mean, $n = 12-15$).
*Represents statistical significance ($P < 0.05$) from both the unsensitized and sensitized, ovalbumin-challenged groups as tested by ANOVA test.

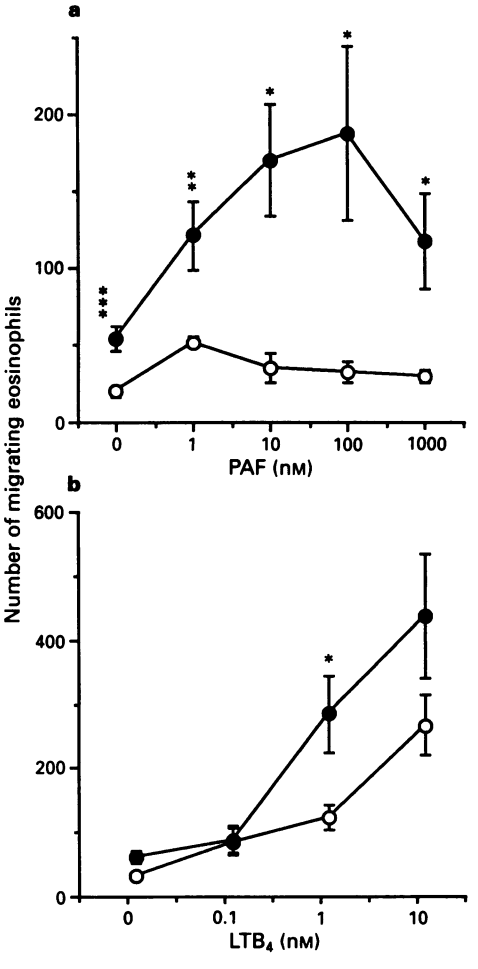


Figure 2 Increased migration of eosinophils from BALF of guinea-pig after challenge with ovalbumin: airway eosinophils were obtained by bronchoalveolar lavage performed 24 h after the challenge of sensitized guinea-pigs with 1 mg of ovalbumin by the intra-nasal route, control animals being treated with saline. The eosinophils were isolated on a metrizamide gradient and migration was studied as described under 'Methods'. Spontaneous, PAF (a) and LTB_4-induced (b) migration of eosinophils from sensitized and ovalbumin-challenged animals (●) was evaluated, as compared to that of sensitized and saline-challenged (○) animals. The results are expressed as the number of eosinophils migrating through the nitrocellulose filter (3 μm pore size) to 40 μm using a optical grid at 400 × magnification (mean ± s.e.mean of four to 16 experiments). $*P<0.05$; $**P<0.01$; $***P<0.001$, comparison between sensitized, saline-challenged and sensitized, ovalbumin-challenged guinea-pigs.

Modulation by nedocromil sodium of the enhanced responses of eosinophils from immunized and challenged guinea-pigs

To investigate its potential ability to interfere with eosinophils, nedocromil sodium was injected s.c. at 30 mg kg^{-1} 10 min before the intra-nasal provocation with ovalbumin and again after 9 h, i.e. 15 h before BALF collection.

As seen in Figure 5, nedocromil sodium markedly reduced the total number of cells recruited into the BALF of the challenged guinea-pigs, as well as that of macrophages, eosinophils and lymphocytes. In contrast to its effect on the total number of cells, nedocromil sodium failed to modify the pattern of cell recruitment in the BALF of guinea-pigs challenged with intra-nasal ovalbumin. Finally, as seen in Figure 4, eosinophils from the BALF of nedocromil sodium-treated and ovalbumin-challenged guinea-pigs, migrated as much with PAF or with LTB_4 as those from saline-challenged, animals, in contrast to the protective effect of TRFK-5.

Table 2 Chemotactic response of normodense eosinophils from bronchoalveolar lavage fluid of sensitized guinea-pigs towards C5a, FMLP, rhIL-5 and ovalbumn

Agonist	*Saline-challenged*	*Ovalbumin-challenged*
Control	17 ± 4	56 ± 11
C5a (nM)		
0.1	32 ± 3	48 ± 7
1	116 ± 35	67 ± 10
10	127 ± 51	116 ± 47
100	224 ± 73	373 ± 90
1000	224 ± 52	336 ± 113
FMLP 1 μM	36 ± 13	64 ± 25
rhIL-5 (ng ml^{-1})		
100	32 ± 4	61 ± 16
500	38 ± 4	115 ± 32*
Ovalbumin (μg ml^{-1})		
30	15 ± 4	69 ± 33
100	23 ± 5	51 ± 18

Airway eosinophils were obtained by bronchoalveolar lavage performed 24 h after the intra-nasal challenge. The eosinophils were isolated on a metrizamide gradient and migration was studied as described under Methods. Spontaneous (control), C5a, FMLP, rhIL-5 and ovalbumin-induced migration of eosinophils from sensitized and ovalbumin challenged animals (2nd column) was evaluated, as compared to that of sensitized and saline-challenged animals (first column). The results are expressed as the number of migrating eosinophils (mean ± s.e.mean of four to six experiments).
*Represents statistical difference ($P<0.05$, ANOVA test) from sensitized, saline-challenged and sensitized, ovalbumin-challenged guinea-pigs.

Discussion

The concept that inflammatory cells, particularly eosinophils, are involved with the development and/or expression of bronchopulmonary hyperresponsiveness is becoming increasingly popular. Airway and blood eosinophilia is associated with the allergen-induced late-phase bronchoconstriction in asthmatic patients (DeMonchy *et al.*, 1985) and in animal models of allergic asthma (Dunn *et al.*, 1988; Lellouch-Tubiana *et al.*, 1988), but little is known of the processes that control the infiltration of eosinophils *in vivo*.

In our study, the leukocyte numbers and the proportion of eosinophils in the BALF of ovalbumin-challenged guinea-pigs increased markedly. In agreement with Frick *et al.* (1989) and Rimmer *et al.* (1992), and in analogy with human blood eosinophils from allergic patients (Fukuda & Gleich, 1989), those eosinophils showed two densities and underwent a marked shift from high to low density cells. This deviation probably reflects the underlying eosinophil activation and loss of granular materials upon or after recruitment into the airways.

Eosinophils collected 24 h after provocation migrated more intensively in response to PAF and LTB_4 than those of paired immunized unchallenged animals. Furthermore, since the number of eosinophils recovered doubled during the 24 h interval between provocation and BALF collection, it is likely that at least part of the eosinophils exposed to PAF or to LTB_4 were additional to those already present in the BALF before the provocation. We do not know whether the additional cells were demarginated and then migrated to the BALF, underwent differentiation *in situ* or become available in increasing numbers by other mechanisms.

Enhancement of eosinophil function, in response to antigen challenge, has been previously reported by Cerasoli *et al.* (1991) who demonstrated that eosinophils from the airways of immunised guinea-pigs release more superoxide anion in response to antigen challenge and by Moser *et al.* (1992) who showed that eosinophils from allergic patients

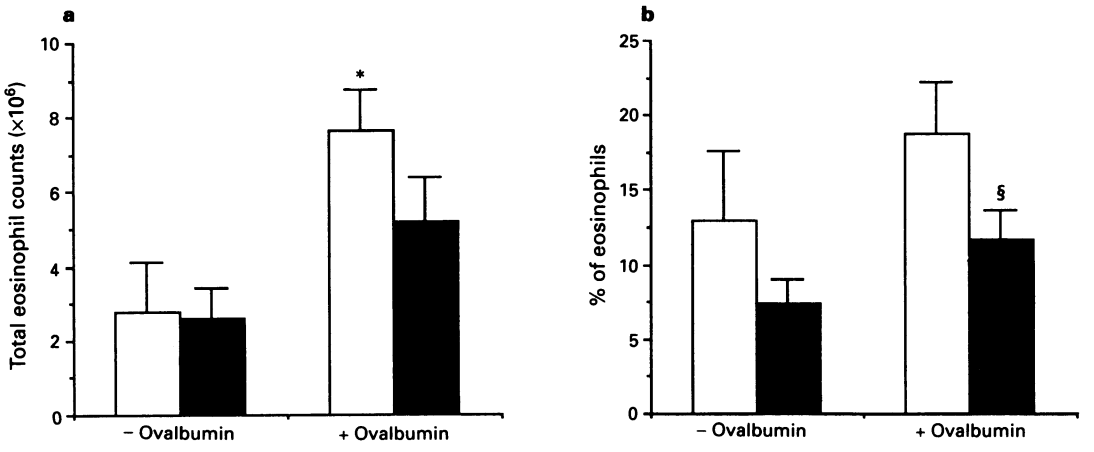


Figure 3 Interference of TRFK-5 with eosinophil recruitment into the BALF of guinea-pigs challenged with intra-nasal ovalbumin: TRFK-5 was administered i.p. at 30 $\mu g\,kg^{-1}$ 2 h before the intra-nasal challenge (solid columns). Control animals were treated with saline (open columns). Airway eosinophils were obtained by bronchoalveolar lavage performed 24 h after challenge. Cells were counted with a Malassez hemocytometer and the cell purity was analysed after cytocentrifugation and staining. The results are expressed as the total number of cells in the BALF (mean ± s.e. mean of four to 10 experiments). $*P<0.05$, comparison between sensitized, saline-challenged and sensitized, ovalbumin-challenged guinea-pigs, $\S P<0.05$, comparison between sensitized, solvent-treated and ovalbumin-challenged animals and sensitized, TRFK-5 treated and ovalbumin-challenged guinea-pigs.

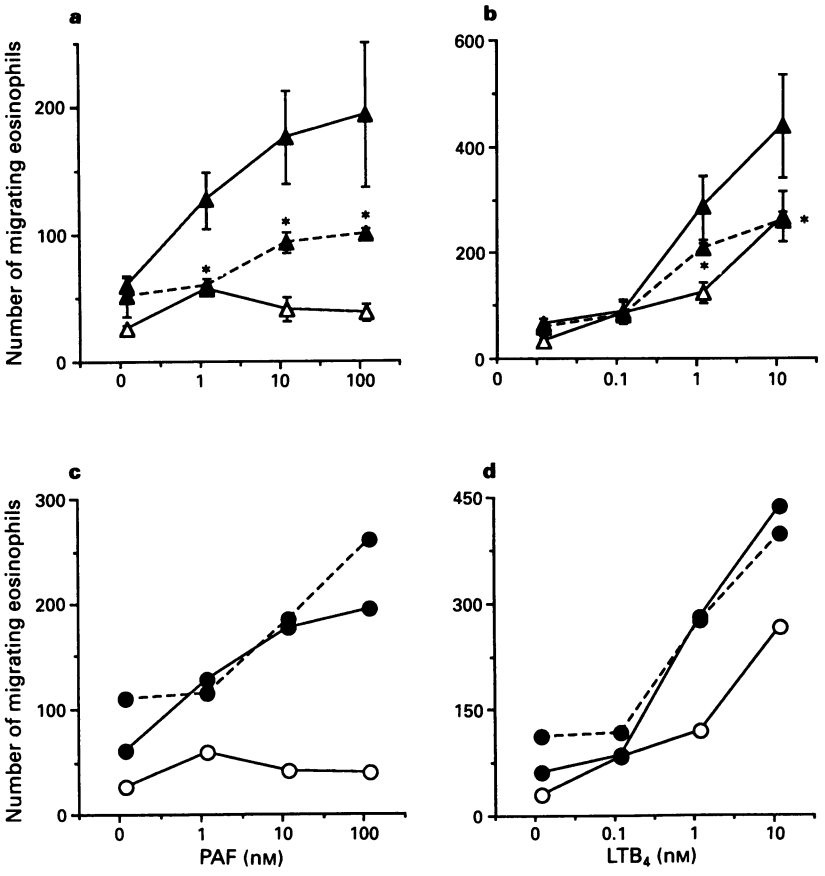


Figure 4 Modulation of the enhanced IL-5 responsiveness of airway eosinophils by anti-IL-5 antibody and nedocromil sodium: TRFK-5 (a,b) was administered i.p. at 30 $\mu g\,kg^{-1}$ 2 h before the intra-nasal challenge, control animals being treated with saline. Nedocromil sodium (c,d) or saline were injected s.c. at 30 $mg\,kg^{-1}$ 10 min before the intra-nasal provocation with ovalbumin or saline and again after 9 h, i.e., 15 h before BALF collection. Airway eosinophils were obtained by bronchoalveolar lavage performed 24 h after challenge. The eosinophils were isolated on a metrizamide gradient and migration was studied as described under Methods. Spontaneous, PAF and LTB_4-induced migration of eosinophils from TRFK-5 treated and ovalbumin-challenged (—▲—) guinea-pigs was evaluated, as compared to those of solvent-treated and ovalbumin-challenged (—▲—) and solvent-treated and saline-challenged sensitized animals (—△—). Spontaneous, PAF and LTB_4-induced migration of eosinophils from nedocromil sodium-treated and ovalbumin-challenged (—●—) was evaluated, as compared to those of solvent-treated and ovalbumin-challenged (—●—) and solvent-treated and saline-challenged (—○—), sensitized animals. The results are expressed as the number of migrating eosinophils (mean ± s.e.mean of four to 16 experiments). $*P<0.05$, comparison between sensitized, solvent-treated and ovalbumin-challenged animals and sensitized, TRFK-5-treated and ovalbumin-challenged guinea-pigs.

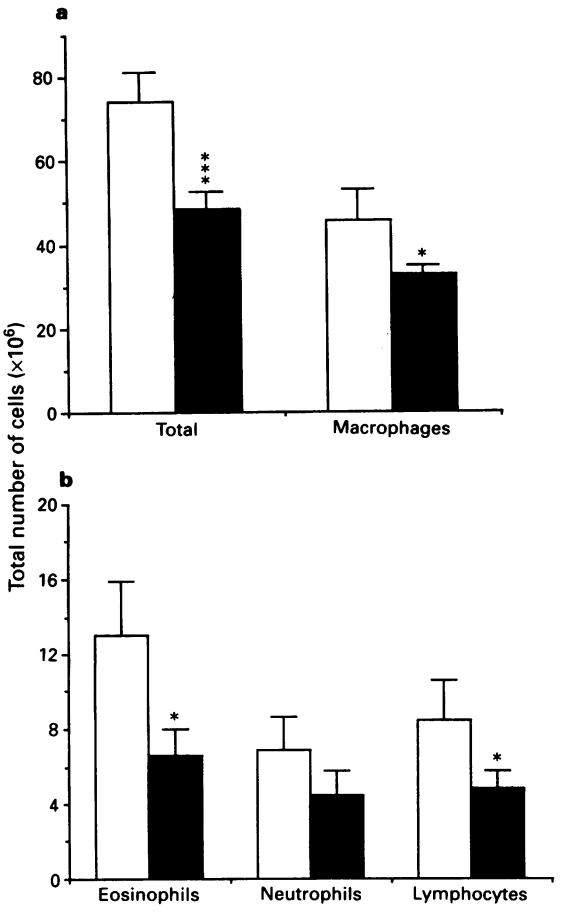


Figure 5 Interference of nedocromil sodium with cell recruitment into the BALF of guinea-pigs challenge with intra-nasal ovalbumin: nedocromil sodium (solid columns) or saline (open columns) were injected s.c. at 30 mg kg^{-1} 10 min before the intra-nasal provocation with ovalbumin and again after 9 h, i.e., 15 h before BALF collection. Airway eosinophils were obtained by bronchoalveolar lavage performed 24 h after challenge. Cells were counted with a Malassez haemocytometer and the cell purity was analysed after cytocentrifugation and staining. The results are expressed as the total number of cells in the BALF (mean ± s.e.mean of five to 12 experiments). *$P<0.05$, ***$P<0.001$, comparison between sensitized, solvent-treated and ovalbumin-challenged animals and sensitized, nedocromil-treated and ovalbumin-challenged guinea-pigs.

display an increased adherence and transmigration capacity. On the other hand, Sedgwick *et al.* (1992) compared the function of airway and blood eosinophil after *in vivo* antigen challenge and demonstrated that, after challenge, eosinophils from the BALF have an enhanced influx of intracellular calcium, generate more anion superoxide and express larger amounts of the integrin adherence receptor CR3 (CD 11b/CD 18).

Cytokines can modulate eosinophil responses (Silberstein *et al.*, 1986; Silberstein & David, 1986; Lopez *et al.*, 1988; Rothenberg *et al.*, 1988; Coëffier *et al.*, 1991b). There is now good evidence that IL-5 is the major, and possibly the only cytokine involved in the production of specific eosinophilia (reviewed in Sanderson, 1992). The likelihood that formation of IL-5 accounts for the selective recruitment of eosinophils is supported by the fact that it is a selective eosinophil chemoattractant (Wang *et al.*, 1989) which enhances the adhesion of eosinophils to endothelial cells, selectively as well (Walsh *et al.*, 1990).

Eosinophils from immunized and challenged animals became hyperresponsive to PAF and LTB_4. *In vitro*, IL-5 primes very intensively guinea-pig eosinophils for an enhanced migration in response to PAF and LTB_4 (Coëffier *et al.*, 1991b) and, accordingly, we hypothesized that eosinophils from immunized and antigen-challenged animals might be primed *in vivo* by IL-5 generated upon antigen challenge. Asthma is associated with an inflammatory reaction involving the infiltration of eosinophils, and *in situ* hybridization in mucosal bronchial biopsies in mild allergic asthmatics demonstrated mRNA encoding for IL-5, further supporting the concept that Th2 cells in the lung of allergic asthmatic individuals produce IL-5 which accounts for eosinophil recruitment and involvement (Hamid *et al.*, 1991). This led us to study whether IL-5 accounts for the *in vivo* eosinophil recruitment to the lungs and for hyperresponsiveness of guinea-pig eosinophils using TRFK-5, a specific monoclonal antibody against IL-5, TRFK-5 indeed inhibited *in vitro* eosinophil migration by rhIL-5. Administered *in vivo*, it reduced eosinophil recruitment to the BALF of antigen-challenged animals, and decreased the enhanced responsiveness of eosinophils collected from the challenged animals. The fact that TRFK-5 prevents lung and BALF eosinophilia has been already described for guinea-pigs (Gulbenkian *et al.*, 1992) and mice (Okudaira *et al.*, 1991). Our findings suggest that IL-5 produced at the site of an antigen invasion may participate in the mechanism of the local accumulation of eosinophils.

Recently, the cytokines GM-CSF, IL-3 and IL-5 have been demonstrated in the circulation of allergic asthmatic subjects (Walker *et al.*, 1991) and a significant increase in IL-5 concentrations was observed in BALF 48 h after segmental antigen bronchoprovocation (Sedgwick *et al.*, 1991). Lymphocytes from these patients secreted these cytokines spontaneously and after activation (Corrigan *et al.*, 1988; Walker *et al.*, 1991). These cytokines can convert normal eosinophils into a preactivated or primed state and herewith affect several eosinophil functions (reviewed in Weller, 1992). Interestingly, mRNA for IL-3, IL-4 and IL-5 and GM-CSF are detected in the skin during an allergen-induced late phase cutaneous reaction, supporting that T-cells of the Th2 phenotype infiltrate (or differentiate) at the site of inflammation (Kay *et al.*, 1991). Silva *et al.* (1993) showed that antigen-induced eosinophil infiltration into the guinea-pig airways is followed by a marked increase of the number of $CD4^+$ lymphocytes, a potential source of IL-5. Accordingly, the participants of the IL-5-induced up-regulation of lung function are indeed present in the allergen-stimulated guinea-pig, supporting its usefulness as a model for the human disease.

The effects of nedocromil sodium were compared to those of TRFK-5, since it down-regulates the bronchopulmonary hyperresponsiveness in the guinea-pig, induced by antigen (Pretolani *et al.*, 1990) or revealed by IL-5 (Pretolani *et al.*, 1992) and inhibits PAF- and LTB_4-induced chemoattraction of eosinophils of normal individuals (Bruijnzeel *et al.*, 1990). It seemed important to determine whether nedocromil sodium would show a similar profile as the *in vivo* neutralization of IL-5 with the antibody. In the present study, nedocromil sodium reduced antigen-induced migration to the BALF not only of eosinophils, but also of lymphocytes and macrophages, thus differing from TRFK-5. In addition, when eosinophil numbers were adjusted to perform the migration tests and the protective effect on migration was thus compensated for, no protection against the enhanced responses to PAF or to LTB_4 was noted, contrary to what has been reported for human eosinophils *in vitro* (Bruijnzeel *et al.*, 1990). Nedocromil sodium thus prevents nonspecifically the antigen-driven migration of inflammatory cells into guinea-pig lungs, but does not modify the ability of guinea-pig eosinophils to respond *ex vivo* to PAF or LTB_4. Thus TRFK-5 affected at least two different targets, i.e., migration and eosinophil priming, whereas nedocromil sodium interfered with migration of the inflammatory cells, and not only of eosinophils, but failed to affect the antigen-induced up-regulation of eosinophil migration.

In summary, PAF and LTB_4-induced migration of eosinophils from immunized and ovalbumin-challenged guinea-pigs were significantly enhanced, as compared to immunized and saline-challenged, animals. The IL-5 antibody TRFK-5 inhibited the *in vitro* migration of eosinophils induced by rhIL-5. *In vivo*, IL-5 antibody reduced eosinophil recruitment in BALF of antigen-challenged immunized animals as well as the enhanced responsiveness of eosinophils from the challenged animals, suggesting a role for IL-5 in the priming of eosinophils *in vivo*. Nedocromil sodium reduced to a similar extent eosinophil, macrophage and lymphocyte recruitment in the BALF of antigen-challenged and of saline-challenged immunized animals, but failed to down-regulate the enhanced responsiveness of eosinophils from the challenged animals. Our results supports the concept that IL-5 is important for recruitment and priming of eosinophils from the guinea-pig BALF.

References

ARNOUX, B., DENJEAN, A., PAGE, C.P, NOLIBE, D., MORLEY, J. & BENVENISTE, J. (1988). Accumulation of platelets and eosinophils in baboon lung after PAF-acether challenge. Inhibition by ketotifen. *Am. Rev. Respir. Dis.*, **137**, 855–860.

BRUIJNZEEL, P.L.B., WARRINGA, R.A.J., KOK, P.T.M. & KREUKNIET, J. (1990). Inhibition of neutrophil and eosinophil induced chemotaxis by nedocromil sodium and sodium cromoglycate. *Br. J. Pharmacol.*, **99**, 798–802.

CAMPBELL H.D., TUCKER, W.Q.J., HORT, Y., MARTINSON, M.E., MAYO, G., CLUTTERBUCK, E.J., SANDERSON, C.J. & YOUNG, I.G. (1987). Molecular cloning, nucleotide sequence, and expression of the gene encoding human eosinophil differentiation factor (Interleukin 5). *Proc. Natl. Acad. Sci. U.S.A.*, **84**, 6629–6633.

CERASOLI, F., TOCKER, J. & SELIG, W.M. (1991). Airway eosinophils from actively sensitized guinea-pigs exhibit enhanced superoxide anion release in response to antigen challenge. *Am. J. Respir. Cell Mol. Biol.*, **4**, 355–363.

COËFFIER, E., JOSEPH, D. & VARGAFTIG, B.B. (1991a). LTB_4, a potent chemotactic factor for purified guinea-pig eosinophils: interference of PAF-acether antagonists. *Int. J. Immunopharmacol.*, **13**, 273–280.

COËFFIER, E., JOSEPH, D. & VARGAFTIG, B.B. (1991b). Activation of guinea-pig eosinophils by human recombinant IL-5. Selective priming to Platelet-Activating Factor and interference with its antagonists. *J. Immunol.*, **147**, 2595–2602.

COFFMAN, R.L., SEYMOUR, B.W.P., HUDAK, S., JACKSON, J. & RENNICK, D. (1990). Antibody to interleukin-5 inhibits helminth-induced eosinophilia in mice. *Science*, **245**, 308–310.

CORRIGAN, C.J., HARTNELL, A. & KAY, A.B. (1988). T-lymphocyte activation in acute severe asthma. *Lancet*, **i**, 1129–1132.

CZARNETZKI, B.M. & MERTENSMEIER, R. (1985). *In vitro* and *in vivo* chemotaxis of guinea-pig leukocytes toward leukotriene B_4 and its ω-oxidation products. *Prostaglandins*, **30**, 5–10.

DE MONCHY, J.G.R., KAUFFMAN, H.K., VENGE, P., KOETER, G.H., JANSEN, H.M., SLUITER, H.J. & DE VRIES, K. (1985). Bronchoalveolar eosinophilia during allergen-induced later asthmatic reactions. *Am. J. Respir. Dis.*, **131**, 373–376.

DUNN, C.J., ELLIOTT, G.A., OOSTVEEN, J.A. & RICHARDS, I.M. (1988). Development of a prolonged eosinophil-rich inflammatory leukocyte infiltration in the guinea-pig asthmatic response to ovalbumin inhalation. *Am. Rev. Respir. Dis.*, **137**, 541–547.

FRICK, W.E., SEDGWICK, J.B. & BUSSE, W.W. (1989). The appearance of hypodense eosinophils in antigen-dependent late phase asthma. *Am. Rev. Respir. Dis.*, **139**, 1401–1406.

FRIGAS, E. & GLEICH, G.J. (1986). The eosinophil and the pathophysiology of asthma. *J. Allergy Clin. Immunol.*, **77**, 527–537.

FUKUDA, T. & GLEICH, G.J. (1989). Heterogeneity of human eosinophils. *J. Allergy Clin. Immunol.*, **83**, 369–373.

GULBENKIAN, A.R., EGAN, R.W., FERNANDEZ, X., JONES, H., KREUTNER, W., KUNG, T., PAYVANDI, F., SULLIVAN, L., ZURCHER, J.A. & WATNICK, A.S. (1992). Interleukin-5 modulates eosinophil accumulation in allergic guinea pig lung. *Am. Rev. Respir. Dis.*, **146**, 263–266.

HAMID, Q., AZZAWI, M., YING, S., MOQBEL, R., WARDLAW, A.J., CORRIGAN, C.J., BRADLEY, B., DURHAM, S.R., COLLINS, J.V., JEFFERY, P.K., QUINT, J. & KAY, A.B. (1991). Expression of mRNA for interleukin-5 in mucosal bronchial biopsies from asthma. *J. Clin. Invest.*, **87**, 1541–1546.

HUBER, H.L. & KOESSLER, K.K. (1992). The pathology of bronchial asthma. *Arch. Intern. Med.*, **30**, 689–760.

KAY, A.B., YIN, S., VARNEY, V., GAGA, M., DURHAM, S.R., MOQBEL, R., WARDLAW, A.J. & HAMID, Q. (1991). Messenger RNA expression of the cytokine gene cluster, interleukin 3 (IL-3), IL-4, IL-5, and Granulocyge/Macrophage Colony-stimulating Factor, in allergen-induced late-phase cutaneous reactions in atopic subjects. *J. Exp. Med.*, **173**, 775–778.

LELLOUCH-TUBIANA, A., LEFORT, J., SIMON, M.T., PFISTER, A. & VARGAFTIG, B.B. (1988). Eosinophil recruitment into guinea-pig lungs after PAF-acether and allergen administration. *Am. Rev. Respir. Dis.*, **137**, 948–954.

LOPEZ, A.F., TO, L.B., YANG, Y.-C., GAMBLE, J.R., SHANNON, M.F., BURNS, G.F., DYSON, P.G., JUTTNER, C.A., CLARK, S. & VADAS, M.A. (1987). Stimulation of proliferation, differentiation, and function of human cells by primate interleukin 3. *Proc. Natl. Acad. Sci. U.S.A.*, **84**, 2761–2765.

LOPEZ, A.F., SANDERSON, C.J., GAMBLE, J.R., CAMPBELL, H.D., YOUNG, I.G. & VADAS, M.A. (1988). Recombinant human interleukin 5 is a selective activator of human eosinophil function. *J. Exp. Med.*, **167**, 219–224.

MOSER, R., FEHR, J., OLIGIATI, L. & BRUIJNZEEL, P.L.B. (1992). Migration of primed human eosinophils across cytokine-activated endothelial cell monolayers. *Blood*, **79**, 2937–2945.

OKUDAIRA, H., NOGAMI, M., MATSUZAKI, G., DOHI, M., SUKO, M., KASUYA, S. & TAKATSU, K. (1991). T-cell-dependent accumulation of eosinophils in the lung and its inhibition by monoclonal anti-interleukin-5. *Intern. Arch. Allergy Appl. Immunol.*, **94**, 171–173.

PRETOLANI, M., LEFORT, J., LEDUC, D. & VARGAFTIG, B.B. (1992). Effect of human recombinant interleukin-5 on *in vitro* lung responsiveness to PAF in actively sensitized guinea-pigs. *Br. J. Pharmacol.*, **106**, 677–684.

PRETOLANI, M., LEFORT, J., SILVA, P.M.R., MALANCHÈRE, E., DUMAREY, C., BACHELET, M. & VARGAFTIG, B.B. (1990). Protection by nedocromil sodium of active immunization-induced bronchopulmonary alterations in the guinea-pig. *Am. Rev. Respir. Dis.*, **141**, 1259–1265.

PRETOLANI, M., LEFORT, J. & VARGAFTIG, B.B. (1988). Active immunization induces lung hyperresponsiveness in the guinea-pig. *Am. Rev. Respir. Dis.*, **138**, 1572–1578.

RIMMER, S.J., AKERMAN, C.L., HUNT, T.C., CHURCH, M.K., HOLGATE, S.T. & SHUTE, J.K. (1992). Density profile of bronchoalveolar lavage eosinophils in the guinea pig model of allergen-induced late-phase allergic responses. *Am. J. Respir. Cell Mol. Biol.*, **6**, 340–348.

ROTHENBERG, M.E., OWEN, W.F., SILBERSTEIN, D.S., WOODS, J., SOBERMAN, R.J., AUSTEN, K.F. & STEVENS, R.L. (1988). Human eosinophils have prolonged survival, enhanced functional properties, and become hypodense when exposed to human interleukin 3. *J. Clin. Invest.*, **81**, 1986–1992.

SANDERSON, C.J. (1992). Interleukin-5, eosinophils, and disease. *J. Am. Soc. Hematol.*, **79**, 3101–3109.

SANDERSON, C.J., WARREN, D.J. & STRATH, M. (1985). Identification of a lymphokine that stimulates eosinophil differentiation in vitro. Its relationship to interleukin 3, and functional properties of eosinophils produced in cultures. *J. Exp. Med.*, **162**, 60–74.

SANJAR, S., AOKI, S., BOUBEKEUR, K., CHAPMAN, I.D., SMITH, D., KINGS, M.A. & MORLEY, J. (1990). Eosinophil accumulation in pulmonary airways of guinea-pigs induced by exposure to an aerosol of platelet-activating factor: effect of anti-asthma drugs. *Br. J. Pharmacol.*, **99**, 267–272.

SECOR, W.E., STEWARD, S.J. & COLLEY, D.G. (1990). Eosinophils and immune mechanisms. VI. The synergistic combination of granulocyte-macrophage colony-stimulating factor and IL-5 accounts for eosinophil-stimulation promoter activity in *Schistosoma mansoni*-infected mice. *J. Immunol.*, **144**, 1484–1489.

SEDGWICK, J.B., CALHOUN, W.J., GLEICH, G.J., KITA, H., ABRAMS, J.S., SCHWARTZ, L.B., VOLOVITZ, B., BEN-YAAKOV, M. & BUSSE, W.W. (1991). Immediate and late airway response of allergic rhinitis patients to segmental antigen challenge. *Am. Rev. Respir. Dis.*, **144**, 1274–1281.

SEDGWICK, J.B., CALHOUN, W.J., VRTIS, R.F., BATES, M.E., MCALLISTER, P.K. & BUSSE, W.W. (1992). Comparison of airway and blood eosinophil function after in vivo antigen challenge. *J. Immunol.*, **149**, 3710–3718.

SHER, A., COFFMAN, R.L., HIENY, S., SCOTT, P. & CHEEVER, A.W. (1990). Interleukin 5 is required for the blood and tissue eosinophilia but not granuloma formation induced by infection with *Schistosoma mansoni*. *Proc. Natl. Acad. Sci. U.S.A.*, **87**, 61–65.

SILBAUGH, S.A., STENGEL, P.W., WILLIAMS, G.D., HERRON, D.K., GALLAGHER, P. & BAKER, S.R. (1987). Airway sensitization and lung granulocytes infiltration in the guinea-pig. *Am. J. Respir. Dis.*, **136**, 930–934.

SILBERSTEIN, D.S. & DAVID, J.R. (1986). Tumor necrosis factor enhances eosinophil toxicity to *Schistosoma mansoni* larvae. *Proc. Natl. Acad. Sci. U.S.A.*, **83**, 1055–1059.

SILBERSTEIN, D.S., OWEN, W.F., GASSON, J.C., DIPERSIO, J.F., GOLDE, D.W., BINA, J.C., SOBERMAN, R., AUSTEN, K.F. & DAVID, J.R. (1986). Enhancement of human eosinophil cytotoxicity and leukotriene synthesis by biosynthetic (recombinant) granulocyte-macrophage colony-stimulating factor. *J. Immunol.*, **137**, 3290–3294.

SILVA, J.R.L.E., BACHELET, C.-M., PRETOLANI, M., BAKER, D. & SCHEPER, R.J. (1993). Immunopathological alterations in the bronchi of immunised guinea-pigs. *Am. J. Respir. Cell Mol. Biol.*, **9**, 44–53.

THORNE, K.J.I., RICHARDSON, B.A., TAVERNE, J., WILLIAMSON, D.J., VADAS, M.A. & BUTTERWORTH, A.E. (1986). A comparison of eosinophil-activating factor (EAF) with other monokines and lymphokines. *Eur. J. Immunol.*, **16**, 1143–1149.

VADAS, M.A., DAVID, J.R., BUTTERWORTH, A., PISANI, N.T. & SIONGOK, T.A. (1979). A new method for the purification of human eosinophils and neutrophils, and a comparison of the ability of these cells to damage schistosomula of *Schistosoma mansoni*. *J. Immunol.*, **122**, 1228–1238.

VENGE, P. (1990). The human eosinophil in inflammation. *Agents Actions*, **29**, 122–126.

WALKER, C., VIRCHOW, J.C., BRUIJNZEEL, P.L.B. & BLASER, K. (1991). T cell subsets and their soluble products regulate eosinophilia in allergic and nonallergic asthma. *J. Immunol.*, **146**, 1829–1835.

WALSH, G.M., HARTNELL, A., WARDLAW, A.J., KURIHARA, K., SANDERSON, C.J. & KAY, A.B. (1990). IL-5 enhances the in vitro adhesion of human eosinophils, but not neutrophils, in a leucocyte integrin (CD11/18)-dependent manner. *Immunology*, **71**, 258–265.

WANG, J.M., RAMBALDI, A., BIONDI, A., CHEN, Z.G., SANDERSON, C.J. & MANTOVANI, A. (1989). Recombinant human interleukin 5 is a selective eosinophil chemoattractant. *Eur. J. Immunol.*, **19**, 701–705.

WARDLAW, A.J., MOQBEL, R., CROMWELL, O. & KAY, A.B. (1986). Platelet-activating Factor. A potent chemotactic and chemokinetic factor for human eosinophils. *J. Clin. Invest.*, **78**, 1701–1706.

WARRINGA, R.A.J., SCHWEIZER, T., MAILOE, T., KUIPER, P.H.M., BRUIJNZEEL, P.L.B. & KOENDERMAN, L. (1992). Modulation of eosinophil chemotaxis by interleukin-5. *Am. J. Respir. Cell Mol. Biol.*, **7**, 631–636.

WELLER, P.F. (1992). Cytokine regulation of eosinophil function. *Clin. Immunol. Immunopathol.*, **62**, S55–S59.

YAMAGUCHI, Y., HAYASHI, Y., SUGAMA, Y., MIURA, Y., KASAHARA, T., KITAMURA, S., TORISU, M., MITA, S., TOMINAGA, A., TAKATSU, K. & SUDA, T. (1988a). Highly purified murine interleukin 5 (IL-5) stimulates eosinophil function and prolongs in vitro survival. IL-5 is an eosinophil chemotactic factor. *J. Exp. Med.*, **167**, 1737–1742.

YAMAGUCHI, Y., SUDA, T., SUDA, J., EGUCHI, M., MIURA, Y., HARADA, N., TOMINAGA, A. & TAKATSU, K. (1988b). Purified interleukin 5 supports the terminal differentiation and proliferation of murine eosinophilic precursors. *J. Exp. Med.*, **167**, 43–56.

YOKOTA, T., COFFMAN, R.L., HAGIWARA, H., RENNICK, D.M., TAKEBE, Y., YOKOTA, K., GEMMELL, L., SHRADER, B., YANG, G., MEYERSON, P., LUH, J., HOY, P., PÈNE, J., BRIÈRE, F., SPITS, H., BANCHEREAU, J., DE VRIES, J., LEE, F.D., ARAI, N. & ARAI, K.-I. (1987). Isolation and characterization of lymphokine cDNA clones encoding mouse and human IgA-enhancing factor and eosinophil colony-stimulating factor activities: relationship to interleukin 5. *Proc. Natl. Acad. Sci. U.S.A.*, **84**, 7388–7392.

(Received January 24, 1994
Revised June 8, 1994
Accepted June 27, 1994)

Br. J. Pharmacol. (1994), **113**, 757–766 © Macmillan Press Ltd, 1994

The mechanism of the inhibitory effect of polyamines on the induction of nitric oxide synthase: role of aldehyde metabolites

Csaba Szabó, Garry J. Southan, [1]Christoph Thiemermann & John R. Vane

The William Harvey Research Institute, St. Bartholomew's Hospital Medical College, Charterhouse Square, London EC1M 6BQ

1 We have recently found that in the presence, but not in the absence, of foetal calf serum, spermine inhibits the production of nitric oxide (NO) in cultured J774.2 macrophages stimulated with bacterial endotoxin (lipopolysaccharide; LPS) or with γ-interferon (IFN), showing that polyamines may act as suppressants of NO-mediated immune functions. Here, we have studied the mechanisms and the specificity of this inhibitory action.

2 Other polyamines, as well as spermine, inhibit the formation of NO in cultured J774.2 macrophages, with the order of potency being spermine > spermidine >> putrescine = cadaverine. This inhibition of NO formation is not due to any cytotoxic effect of these agents for they neither reduced mitochondrial respiration nor increased the release of lactate dehydrogenase into the supernatant.

3 Spermine is not a direct inhibitor of the activity of iNOS in induced J774.2 cells as measured by its lack of effect on the conversion of L-arginine to L-citrulline in homogenates. Neither spermine, nor its metabolites, interfere with the production of nitrite from NO or act as scavengers of NO. Thus, spermine is an inhibitor of the induction of iNOS.

4 Spermine inhibits nitrite formation in the presence of foetal, newborn or adult bovine serum, but not rat or human serum.

5 The effect of sper mine on nitrite production can be prevented by isoniazid, hydrazine or hydroxylamine, inhibitors of spermine oxidase, as well as by phenylhydrazine, an aldehyde inhibitor. We have, therefore, tested the effects of spermine dialdehyde or malon dialdehyde on the induction of iNOS. Spermine dialdehyde (SDA, 10^{-5} M) inhibits nitrite formation by IFN-activated J774.2 cells in the absence of serum when given as a pretreatment but not when given 6 h after stimulation. In contrast, malon dialdehyde was ineffective. Thus, aldehyde metabolites of spermine, such as SDA, account for the inhibitory effect of polyamines on the induction of NOS *in vitro*.

6 The inhibitory effect of polyamines on iNOS induction appears to be fairly specific to iNOS, for spermine does not inhibit LPS-induced production of prostaglandin $F_{2\alpha}$ or tumour necrosis factor.

Keywords: Nitric oxide; lipopolysaccharide; interferon; spermine; spermidine; putrescine; cadaverine; spermine dialdehyde; immunosuppression; cyclo-oxygenase; tumour necrosis factor; pregnancy, cancer

Introduction

Endotoxin (bacterial lipopolysaccharide, LPS) interleukin-1, tumour-necrosis factor and γ-interferon (IFN) induce nitric oxide (NO) synthase (iNOS) in a variety of cells including macrophages. L-Arginine-derived NO serves as a cytotoxic molecule that plays a key role in the antimicrobial activity of activated macrophages, and may play a role in the process of allograft rejection (Stuehr & Nathan, 1989; Nathan & Hibbs, 1991; Nathan, 1992; Stuehr & Griffith, 1992; Green & Nacy, 1993; Langrehr *et al.*, 1993). The formation of NO can be inhibited by competitive inhibitors of NOS such as the L-arginine analogue, N^G-monomethyl-L-arginine (L-NMMA). The induction of iNOS in various cells *in vitro* can be inhibited by glucocorticoids, dihydropyridine calcium channel modulators and by certain cytokines, e.g. interleukin-4 (IL-4), IL-8, IL-10, transforming growth factor β (TGFβ) and platelet-derived growth factor (Stuehr & Nathan, 1989; Radomski *et al.*, 1990; Nathan & Hibbs, 1991; Nathan, 1992; Cunha *et al.*, 1993; Green & Nacy, 1993; Langrehr *et al.*, 1993; Szabó *et al.*, 1993a).

Polyamines are endogenous regulators of cell proliferation, differentation, functional activation and macromolecular biosynthesis although their mechanism of action is not clear (Gaugas, 1980; Selmeci *et al.*, 1985; Morgan, 1987). Certain polyamines inhibit the production of nitrite in immunostimulated macrophages (Szabó *et al.*, 1994; Pollack *et al.*, 1994). We have recently shown that spermine inhibits the production of NO in cultured J774.2 macrophages stimulated with bacterial endotoxin (lipopolysaccharide; LPS) or with γ-interferon (IFN) in the presence, but not in the absence, of foetal calf serum (FCS) (Szabó *et al.*, 1994). This study was designed to characterize this inhibitory action of spermine, by investigating in immuno-stimulated J774.2 macrophages in culture (i) whether polyamines other than spermine also inhibit nitrite accumulation, (ii) whether spermine has any direct effect on the activity of the iNOS, (iii) whether polyamines scavenge NO (and thereby e.g. form NO:spermine adducts) or alter the formation of nitrite and/or nitrate from NO, (iv) whether metabolism of polyamines plays a role in their inhibitory action, (v) the specificity of the serum needed for the inhibition and (vi) whether spermine also inhibits the induction of the cytokine-inducible isoform of cyclo-oxygenase (COX-2) or the production of tumour necrosis factor α (TNFα).

Methods

Cells and culture conditions

The mouse macrophage cell line J774.2 was cultured in Dulbecco's modified Eagle's medium (DMEM) with 4×10^{-3} M L-glutamine and 10% foetal calf serum (FCS) as described (Szabó *et al.*, 1993b). Cells were cultured in 96-well plates with 200 μl culture medium until they reached confluence.

[1] Author for correspondence.

Experimental protocols

To induce iNOS, fresh culture medium containing *E. coli* LPS (1 μg ml^{-1}) or IFN (50 U ml^{-1}) was added. Nitrite accumulation in the cell culture medium was measured after 24 h. To assess the effects of the polyamines spermine, spermidine, putrescine, cadaverine and N^1-acetylspermine (all at 10^{-6}–10^{-4} M) or L-NMMA (3×10^{-3} M) on nitrite production, the above agents were added to the medium either simultaneously with or 6 h after stimulation of iNOS induction with LPS or IFN. To investigate whether spermine affects the activity or the induction of iNOS, spermine was also added 0.5 h before as well as 2, 4 or 6 h after LPS; nitrite production was measured 24 h after LPS treatment. The effect of spermine or N^1-acetylspermine (10^{-6}–10^{-4} M) on LPS- or IFN-induced nitrite production was also tested in DMEM without FCS. Moreover, the effect of spermine (10^{-4} M) on the production of nitrite by LPS (1 μg ml^{-1}) was also investigated at various concentrations of FCS (0.01, 0.1, 0.3, 1 and 3%). The effect of spermine (10^{-5} M) on nitrite production was also studied in DMEM in the presence of various concentrations (1 and 10%) of bovine (foetal calf, newborn calf or adult) sera as well as in the presence of human or rat serum. In addition, the effect of LPS-binding protein (LBP, 0.01–10 μg ml^{-1}) was tested on the induction of NOS both in the presence and absence of FCS.

Isonicotinic acid hydrazine (INH) and hydroxylamine (1 μM–1 mM), were used as inhibitors of spermine oxidase, an enzyme present in FCS (Morgan, 1987; Seiler, 1990). Phenylhydrazine (10^{-5} and 10^{-4} M), an aldehyde inhibitor, and genistein, a tyrosine kinase inhibitor (Levitzki, 1992), were also tested on the inhibition of the nitrite accumulation by spermine (10^{-4} M) in macrophages stimulated by LPS.

To assess whether spermine or spermine dialdehyde (see below) reacts directly with nitrite or nitric oxide, spermine (10^{-4} M) was added to either sodium nitrite (3×10^{-6}–10^{-4} M) or to the NO donor, 3-morpholinosydnonimine-*N*-ethylcarbamide (SIN-1, 10^{-5}–10^{-3} M) (Feelisch *et al.*, 1989) and nitrite was determined 3 h thereafter.

The effect of spermine dialdehyde (SDA) and malon dialdehyde (MDA, both at 10^{-7}–10^{-4} M) on nitrite production by IFN was studied in DMEM with or without FCS. As SDA has a short half-life in culture medium (see Discussion), it was added three times to the medium (together with LPS as well as 2 and 4 h thereafter).

Nitrite measurement

Nitrite production, an indicator of NO synthesis, was measured in the supernatant of J774.2 macrophages as previously described (Szabó *et al.*, 1993a,b). Nitrite was measured by adding 100 μl of Griess reagent (1% sulphanilamide and 0.1% naphthylethylenediamide in 5% phosphoric acid) to 100 μl samples of cell culture medium. The optical density at 550 nm (OD_{550}) was measured by using an Anthos 1.2.1. microplate reader (Anthos Labtechnik, Salzburg, Austria). Nitrite concentrations were calculated by comparison with OD_{550} of standard solutions of sodium nitrite prepared in culture medium.

Cell viability and respiration

Cell viability was measured in 96-well plates using a colorimetric assay based on the standard kit obtained from Sigma (LDH Kit [LD]). Cells treated with 1% Triton X-100 for 24 h served as positive control.

Mitochondrial respiration, an indicator of cell viability, was assessed by the mitochondrial-dependent reduction of MTT [3-(4, 5-dimethylthiazol-2-yl)-2, 5-diphenyltetrazolium bromide] to formazan (Szabó *et al.*, 1993a). Cells in 96-well plates were incubated (37°C) with MTT (0.2 mg ml^{-1} for 60 min). Culture medium was removed by aspiration and the cells solubilized in dimethylsulphoxide (DMSO, 100 μl). The extent of reduction of MTT to formazan within cells was quantitated by meausurement of OD_{550} using the Anthos microplate reader. The calibration curve for MTT-formazan was prepared in DMSO. MTT-formazan production by cells was calculated as μg MTT-formazan per well per min and expressed as a percentage of the values obtained from untreated cells.

Nitric oxide synthase assay

J774.2 cells were grown to confluence in 75 cm^2 culture flasks containing 40 ml DMEM. To induce iNOS, fresh culture medium containing *E. coli* LPS (1 μg ml^{-1}) was added. After 8 h, cells were rinsed twice with ice-cold phosphate-buffered saline (PBS) and harvested with a Teflon cell-scraper into 5 ml volume of homogenization buffer composed of: 50 mM Tris HCl, 0.1 mM EDTA, 0.1 mM EGTA, 12 mM 2-mercaptoethanol and 1 mM phenylmethylsulphonyl fluoride (pH 7.4). Cell suspensions were centrifuged at 800 *g* for 10 min and the pelleted cells were homogenized in buffer (composition as above) on ice using an Ultra-Turrax T 25 homogenizer (Janke & Kunkel, IKA Labortechnik, Staufen i. Br., Germany). Conversion of [^{3}H]-L-arginine to [^{3}H]-L-citrulline was measured in the homogenates as described (Szabó *et al.*, 1993b). Briefly, cell homogenate (100 μl) was incubated in the presence of [^{3}H]-L-arginine (10 μM, 5 kBq/tube), NADPH (1 mM), calmodulin (30 nM) and EGTA (5 mM) for 35 min at 37°C in HEPES buffer (pH 7.5). The reaction was stopped by dilution with 1 ml of ice cold HEPES buffer (pH 5.5) containing EGTA (2 mM) and EDTA (2 mM). Reaction mixtures were applied to Dowex 50W (Na^+ form) columns and the eluted [^{3}H]-L-citrulline activity was measured by scintillation counting (Beckman, LS3801; Fullerton, CA, U.S.A.). Experiments performed in the absence of NADPH or in the presence of L-NMMA (3 mM) determined the extent of [^{3}H]-L-citrulline formation independent of a specific iNOS activity. By co-incubating the homogenates together with spermine (10^{-7}–10^{-4} M) in the presence of the above-mentioned cofactors for 35 min, we have investigated the direct effect of spermine on iNOS activity.

NO measurements using chemiluminescence

Appropriate volumes (150–300 μl) of samples of standard sodium nitrite and sodium nitrate solutions were injected through a septum into a reaction flask containing the reagent solution (see below), which was continuously flushed with nitrogen. The nitrogen and any NO produced was drawn through moisture and acid traps into a Dasibi 2107 chemiluminescence analyser (Dasibi Co, Japan), where NO was quantitated by its reaction with ozone (Cox & Frank, 1982; Walters *et al.*, 1987).

The reagent solutions used were: (a) 10 ml glacial acetic acid and 0.25 mg sodium iodide in 60 ml water at 85°C for conversion of nitrite and any potential spermine:NO adducts to NO; (b) 50 ml water containing 15.5 mg ferrous ammonium sulphate and 8 mg ammoniummolybdate for the conversion of both nitrate and nitrite to NO (Walters *et al.*, 1987). Moreover, NO was released from the authentic spermine: NO adduct (SperNO; a kind gift from Dr Larry Keefer at the National Cancer Institute, Frederick, U.S.A.) in the molar ratio of ~1.7 M NO/1 M adduct (i.e. ~85% of bound NO is released, $n = 3$). Under these conditions, N-nitroso compounds would also give a substantial response, and C-nitroso compounds a slight response.

All comparisons of NO detector responses were made using the same preparation of reagent solution, and dilution of the reagent solution did not exceed 10%. Under these conditions the coefficient of variation is <7%.

Addition of spermine to a solution of NO in water made no difference in the chemiluminescence response when it was injected into the reaction flask containing water at room

temperature. Repeated injections of NO, nitrite, nitrate or spermine:NO adducts over 30 min gave constant responses.

Measurements of tumour necrosis factor α

Murine TNFα was measured in 100 μl samples of cell culture supernatant using an ELISA kit (Genzyme, Kings Hill, Kent, UK) according to the manufacturer's instructions. Briefly, the kit is based on a solid-phase enzyme immunoassay employing the multiple antibody sandwich principle. A hamster monoclonal antibody specific for murine TNFα was coated on microtitre wells in a 96-well plate. TNFα present in standard, samples and tissue culture supernatants was captured by the solid-phase monoclonal antibody. Then a goat polyclonal anti-murine antibody, which binds to multiple epitopes on the TNFα contained on solid phase, was added. A third antibody, horseradish peroxidase-conjugated rabbit anti-goat IgG, was then added to bind anti-murine TNFα: murine TNFα immune complexes. The peroxidase enzyme was then reacted with peroxide substrate and OPD (chromagen) to produce colour which was proportional in intensity to the amount of TNFα present. Colour intenstiy was quantitated by measuring absorbance of 492 nm using the Anthos microplate reader. The presence of spermine (10^{-4} M) did not affect this assay ($n = 4$).

Measurement of prostaglandin $F_{2\alpha}$

Prostaglandin $F_{2\alpha}$ was measured in 100 μl samples of cell culture supernatant using a specific radioimmunoassay (Salmon, 1978). The presence of spermine (10^{-4} M) did not affect this assay ($n = 4$).

Materials

N^1-acetylspermine trihydrochloride, acrolein, bacterial lipopolysaccharide (*E. coli*, serotype No. 0127:B8), cadaverine hydrochloride, calmodulin, dexamethasone phosphate, DMEM, L-glutamine, hydroxylamine, isonicotinic acid, MTT, MTT-formazan, NADPH, phenylhydrazine hydrochloride, prostaglandin $F_{2\alpha}$ and anti-prostaglandin $F_{2\alpha}$ antibody, putrescine hydrochloride, sodium nitrite, spermidine hydrochloride, spermine hydrochloride and Dowex 50W anion exchange resin was obtained from Sigma Chemical Co. (Poole, Dorset, UK). N^G-methyl-L-arginine monoacetate (L-NMMA) and genistein were obtained from Calbiochem (Nottingham, UK). L-[2,3,4,5-^{3}H]-arginine hydrochloride was obtained from Amersham (Buckinghamshire, U.K.). Foetal and newborn calf serum and bovine serum were obtained from Advanced Protein Products (West Midlands, UK). Human serum and rat serum were prepared in our laboratory. Murine γ-interferon was obtained from Genzyme (West Malling, Kent, UK). Malon dialdehyde was purchased from Fluka (Gillinham, Dorset, UK). SIN-1 was a kind gift from Dr Rainer Henning at the Cassella AG (Frankfurt, Germany). Spermine dialdehyde was a kind gift from Drs Cathy Lau and Elizabeth Wang at the Marion Merrel Dow Laboratories (Don Mills, Ontario, Canada). Rabbit LPS-binding protein (LBP) was a kind gift of Dr Richard Ulevich at the Scripps Research Institute (La Jolla, CA, U.S.A.).

Statistical evaluation

All values in the figures and text are expressed as mean ± standard error of the mean of n observations. One-way

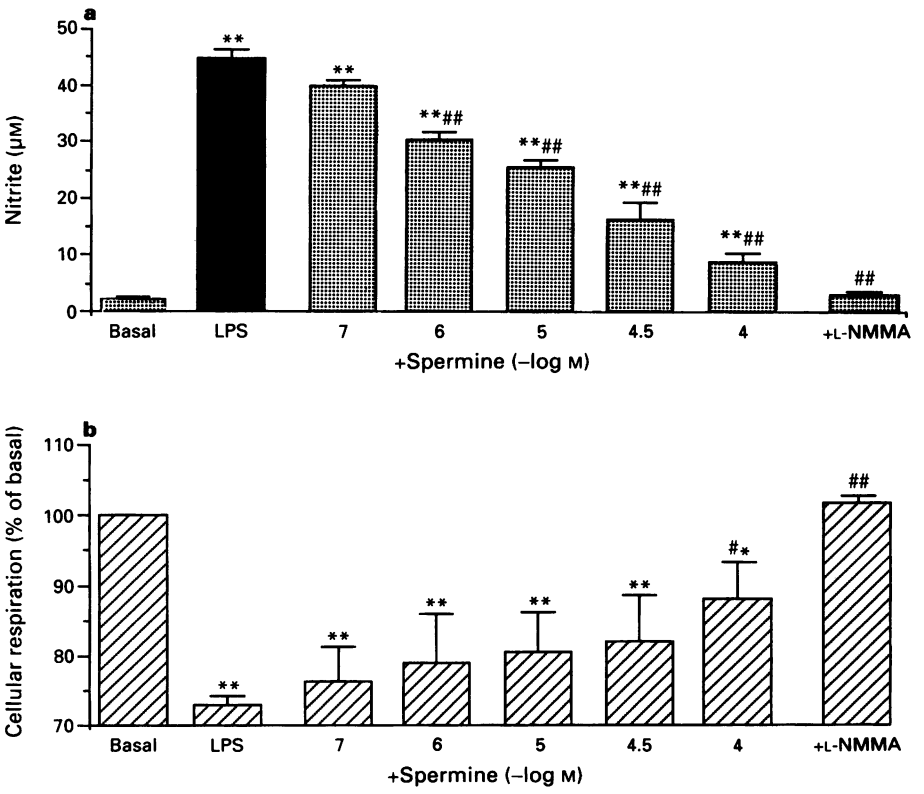


Figure 1 Spermine dose-dependently inhibits the formation of nitrite in J774.2 macrophages stimulated by LPS, without depressing cellular respiration. Depicted are the effects of spermine (10^{-7}–10^{-4} M) or L-NMMA (3×10^{-3} M) on nitrite accumulation (a), and on mitochondrial respiration (b) in J774.2 macrophages stimulated by LPS (1 μg ml^{-1}) for 24 h. Data are expressed as means ± s.e.mean of $n = 9$ wells from 3 experimental days. Formazan production in cells not treated with LPS amounted to 0.32 ± 0.07 μg formazan produced per well per min and was taken as 100%. $*P<0.05$ and $**P<0.01$ represent significant differences when compared to basal values. $\#P<0.05$ and $\#\#P<0.001$ represent significant differences when compared to the values seen with LPS. For abbreviations used in this and subsequent legends, see text.

analysis of variance was performed followed by an adjusted t test with P values corrected by the Bonferroni method. A P value less than 0.05 was considered to be statistically significant.

Results

Spermine inhibits the formation of NO

Nitrite concentration in the medium of J774.2 macrophages stimulated with LPS was 45 ± 2 μM after 24 h. Co-administration of spermine with LPS dose-dependently reduced the accumulation of nitrite in the medium (Figure 1a). The production of nitrite by these cells is due to NO, for the NOS inhibitor L-NMMA also inhibited nitrite accumulation.

The induction of iNOS in these cells was associated with an inhibition of mitochondrial respiration, which was also partially prevented by spermine (Figure 1b). Higher concentrations of spermine (at 10^{-3} M and above) caused a direct inhibition of mitochondrial respiration in J774.2 macrophages (data not shown). LPS caused a slight ($5 \pm 1\%$) increase in the LDH activity measured the culture medium of activated macrophages, which was unaffected by spermine or L-NMMA (not shown).

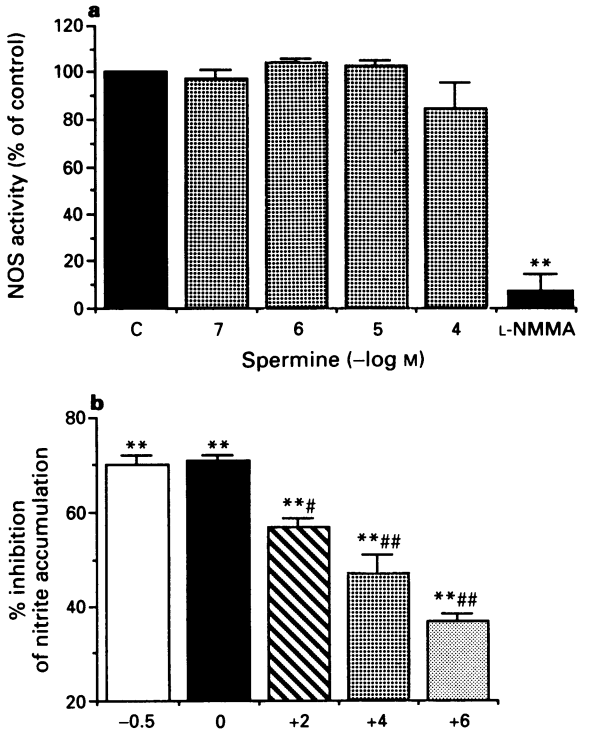


Figure 2 Spermine inhibits the induction of iNOS in response to LPS but it is not a direct inhibitor of iNOS activity. (a) The effect of spermine (10^{-6}–10^{-4} M) or L-NMMA (3×10^{-3} M) on the activity of iNOS in the homogenate of J774.2 macrophages. Data are expressed as means ± s.e.mean of triplicate determinations. iNOS activity in the homogenates was 2.07 ± 0.11 pmol mg^{-1} protein min^{-1} and was taken as 100%. $^{**}P<0.01$ represents significant inhibition. (b) The effect of spermine (3×10^{-5} M), when applied 0.5 h before LPS (– 0.5), together with LPS (0) or 2, 4 or 6 h after LPS (+ 2, + 4 and + 6, respectively) on nitrite accumulation in the medium of J774.2 macrophages stimulated by LPS (1 μg ml^{-1}) for 24 h. Data are expressed as means ± s.e.mean of $n = 9$ wells from 3 experimental days. $^{*}P<0.05$ and $^{**}P<0.01$ represent significant inhibition, when compared to control; $\#P<0.05$ and $\#\#P<0.01$ represent significant decrease in the extent of inhibition, when spermine is applied 2, 4 or 6 h after LPS.

Spermine inhibits the induction, but not activity of iNOS

Spermine did not affect citrulline formation in the homogenates of J774.2 cells that had been pretreated for 8 h with LPS (Figure 2a). The inhibitory effect of spermine on nitrite accumulation in the culture medium of J774.2 macrophages was reduced in time-dependent fashion when spermine was given 2, 4 or 6 h after LPS to the tissue culture medium (Figure 2b). When given 6 h after LPS, the inhibitory effect of spermine (3×10^{-5} M) was reduced from $71 \pm 1\%$ to $37 \pm 2\%$ ($n = 6$, $P<0.01$).

Changes in the formation of nitrite, nitrate or NO: spermine adducts are not involved in the inhibitory action of spermine

Spermine does not interfere with the Griess reaction, for spermine given to sodium nitrite did not alter the levels of nitrite measured (Figure 3a), nor did it alter the accumulation of nitrite caused by the NO donor SIN-1 (Figure 3b).

Nitrite was also measured by chemiluminescence and the respective values obtained were similar to the NO production measured with the Griess reaction either under conditions that would convert only nitrite to NO (Figure 4a), or under conditions that would convert nitrite, nitrate as well as potential spermine:NO adducts or N-nitroso-compounds to NO (not shown).

The inhibitory effect of spermine on iNOS induction is dependent on bovine serum

Spermine did not cause an inhibition of nitrite accumulation when FCS was omitted from the medium (Figure 5a). Under

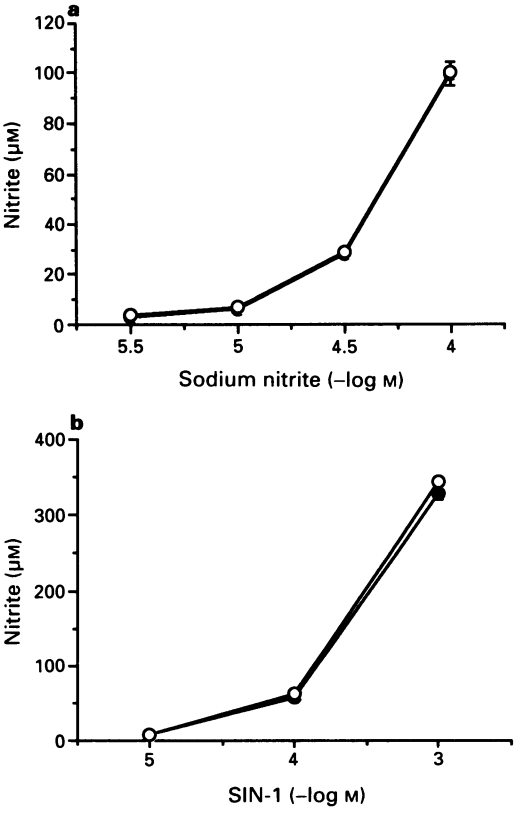


Figure 3 Spermine does not interfere with the Griess reaction and does not scavenge NO. Effect of spermine (10^{-4} M) on the levels of nitrite when sodium nitrite (3×10^{-6} M–10^{-4} M) is added to the culture medium (a) or on nitrite accumulation in the medium in response to the NO donor compound SIN-1 (10^{-5}–10^{-3} M). Data are expressed as means ± s.e.mean of quadriplicate wells: (●) nitrite levels in the absence of spermine; (○) nitrite levels in the presence of spermine.

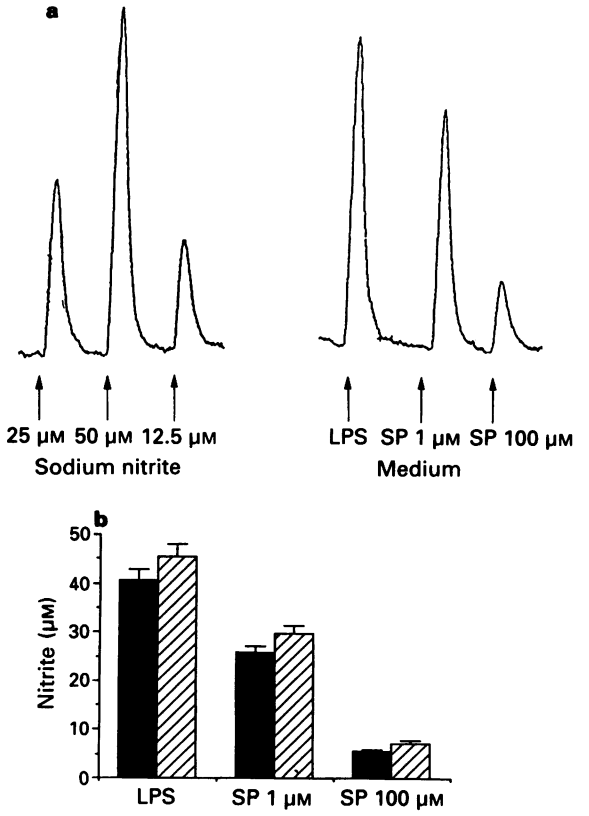


Figure 4 Spermine does not affect the conversion of NO to nitrite. (a) Chemiluminescence NO signals with various doses of sodium nitrite (left panel) or with tissue culture medium of J774.2 macrophages stimulated by LPS (1 μg ml^{-1}) for 24 h without (LPS) or with spermine (SP 1 μM and SP 100 μM). (b) Nitrite levels in the medium of J774.2 macrophages stimulated by LPS (1 μg ml^{-1}) for 24 h without (LPS) or with spermine (SP 1 μM and SP 100 μM), as determined by Griess reaction (hatched columns) or chemiluminescence (solid columns). Data are expressed as means ± s.e.mean of triplicate determinations.

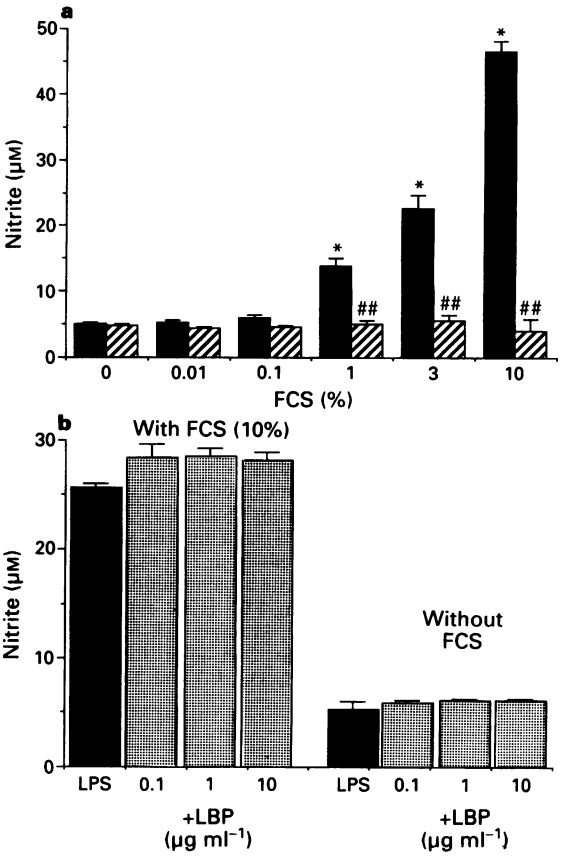


Figure 5 A serum factor, which is not LBP, is required for the induction of iNOS by LPS. Depicted are nitrite levels in the medium of J774.2 macrophages stimulated by LPS (1 μg ml^{-1}) for 24 h. (a) Nitrite production at various concentrations (0–10%) of FCS in the absence (solid columns) and in the presence of spermine (10^{-4} M, hatched columns). (b) Effect of LBP (0.1–10 μg ml^{-1}) on nitrite production in the presence of 10% FCS (left panel) and without FCS (right panel). Data are expressed as means ± s.e.mean of $n = 9$ wells from three experimental days. Nitrite concentrations in wells not treated with LPS were <2.6 μM at all concentrations of FCS and were not affected by LBP. $^{**}P<0.01$ represent significant differences when compared to basal values. $\#\#P<0.01$ represent significant differences with spermine when compared to the values seen with LPS alone.

these conditions, the formation of nitrite by LPS was largely attenuated. Re-addition of FCS restored the ability of LPS to induce nitrite, and hence, iNOS (Figure 5a). When iNOS was induced by γ-interferon (50 U ml^{-1}), spermine caused a concentration-dependent inhibition of nitrite accumulation only in the presence of FCS. In contrast to LPS, the induction of iNOS by γ-interferon was enhanced when FCS was omitted from the culture medium (Figure 6).

We have tested the possibility that the lack of LPS-binding protein, normally present in all animal sera including FCS, is responsible for the lack of iNOS induction in the absence of FCS. Surprisingly, addition of LBP (1–30 μg ml^{-1}) did not enhance iNOS induction by LPS (Figure 5b) or by IFN (not shown) either in the presence or absence of FCS.

The inhibitory effect of spermine on iNOS induction by LPS or γ-interferon was also seen when FCS was replaced with bovine newborn serum (NS) or adult bovine serum (BS) (10% or 1%) in the culture medium. In fact, in the presence of NS or BS, the inhibition of nitrite accumulation by spermine (10^{-5} M) was slightly enhanced (Figure 7).

Role of oxidized metabolites of spermine in the inhibitory action

In the presence of FCS (10%), the inhibitory effect of spermine on nitrite production elicited by LPS was partially prevented by INH or hydroxylamine (0.1–1 mM, inhibitors of spermine oxidase) (Figure 8). These agents themselves did not significantly affect the production of nitrite by LPS in the

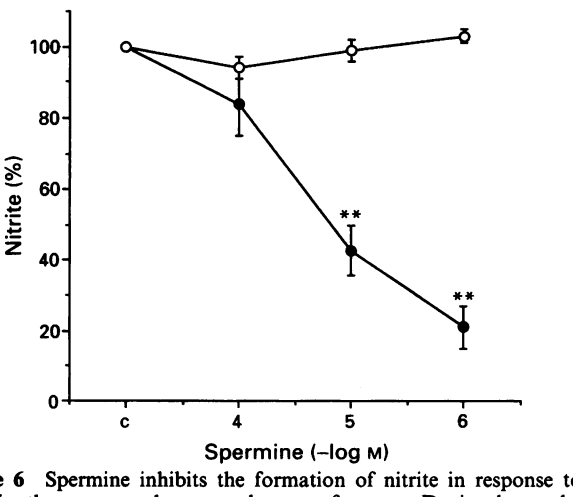


Figure 6 Spermine inhibits the formation of nitrite in response to IFN in the presence but not absence of serum. Depicted are the effect of spermine (10^{-7}–10^{-4} M) on nitrite accumulation in J774.2 macrophages stimulated by IFN (50 u ml^{-1}) for 24 h in the presence (●) or absence (○) of FCS (10%). Data are expressed as means ± s.e.mean of $n = 9$ wells from 3 experimental days. Nitrite in the medium at 24 h after IFN was 10 ± 1 μM in the absence and 28 ± 4 μM in the presence of serum; these values were considered as 100%. $^{*}P<0.05$ and $^{**}P<0.01$ represent significant inhibition of nitrite accumulation by spermine.

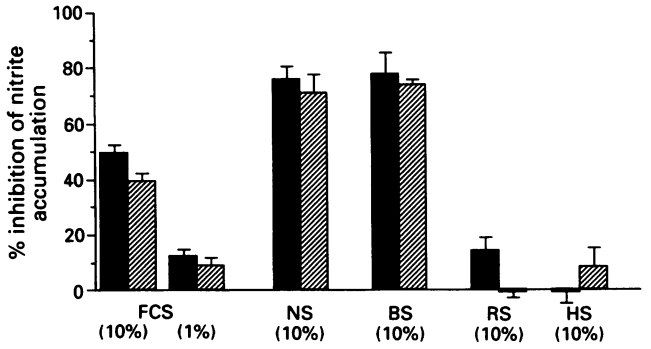


Figure 7 The inhibition of nitrite formation by spermine is only seen in the presence of bovine sera but not rat or human serum. Depicted are the effect of spermine (10^{-5} M) on nitrite accumulation in J774.2 macrophages stimulated by IFN (50 U ml^{-1}, solid columns) or LPS (1 μg ml^{-1}, hatched columns) for 24 h in the presence of FCS (FCS, 10 and 1%), newborn serum (NS, 10%), adult bovine serum (BS, 10%), rat serum (RS, 10%) and human serum (10%). Data (means ± s.e.mean of $n = 6-9$ wells from 2–3 experimental days) are expressed as % inhibition of nitrite accumulation. Nitrite production in the culture medium containing FCS (10% and 1%), NS, BS, RS and HS amounted to 71.6 ± 2.2; 31.6 ± 0.9; 35.5 ± 2.9; 39.1 ± 2 μM; 37.2 ± 1.0 and 37.6 ± 1.7 μM at 24 h after LPS and 48.1 ± 0.7; 66.1 ± 3.7; 42.7 ± 0.5, 45.5 ± 0.7; 33.5 ± 3 and 27.0 ± 1.4 μM at 24 h after IFN, respectively.

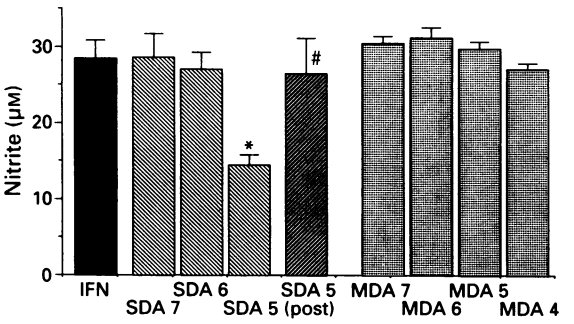


Figure 9 Spermine dialdehyde but not malon dialdehyde inhibits the induction of iNOS by IFN in serum-free medium. Depicted are the effects of spermine dialdehyde (SDA, $10^{-7}-10^{-5}$ M) and malon dialdehyde (MDA, $10^{-7}-10^{-5}$ M) applied together with IFN, or the effect of SDA applied 6 h after IFN (10^{-5}, post) on the nitrite accumulation in the medium of J774.2 macrophages stimulated by IFN (50 U ml^{-1}) for 24 h. Data are expressed as means ± s.e.mean of $n = 6-9$ wells from 2–3 experimental days. $^{*}P < 0.05$ represents significant inhibition of the effect on nitrite accumulation. $\#P < 0.05$ represents significant difference between the effect of SDA (10^{-5}) when applied together with LPS vs when given 6 h after LPS.

absence of spermine, nor did they affect mitochondrial respiration (data not shown). The aldehyde inhibitor, phenylhydrazine (10 or 100 μM), also attenuated the inhibitory effect of spermine (100 μM) on LPS-induced nitrite accumulation from 70 ± 9% (control) to 30 ± 2% and 8 ± 13%, respectively, ($n = 6$) (Figure 8).

Spermine can be metabolized by spermine oxidase to, *inter alia*, spermine dialdehyde (SDA) and malon dialdehyde (MDA). We found that SDA (10^{-5} M) inhibited the accumulation of nitrite in the culture medium of J774.2 cells stimulated with INF in the absence of serum (without being cytotoxic, not shown), but this effect was completely absent when it was added 6 h after IFN (Figure 9). In contrast, MDA (up to 10^{-4} M) did not inhibit nitrite formation (Figure 9). Like spermine (Figure 3), SDA did not directly affect the detection of nitrite by the Griess reaction, nor did it act as a scavenger of NO ($n = 6$, not shown).

The acetylated spermine metabolite N^1-acetylspermine caused an inhibition of nitrite accumulation that was similar to the one seen with spermine itself (Figure 10). Spermidine was less potent than spermine or its N^1-acetylated derivative,

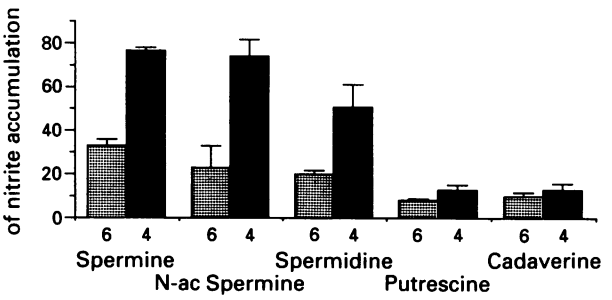


Figure 10 Polyamines inhibit LPS-induced nitrite production with variable potencies. Effect of spermine, N^1-acetyl-spermine (N-ac Spermine), spermidine, putrescine and cadaverine (10^{-6}, stippled columns and 10^{-4} M, solid columns) on nitrite accumulation in the medium of J774.2 macrophages stimulated by LPS (1 μg ml^{-1}) for 24 h. Nitrite concentration at 24 h after LPS was 60.7 ± 1.4 μM. Data are expressed as means ± s.e.mean of $n = 9$ wells from 3 experimental days.

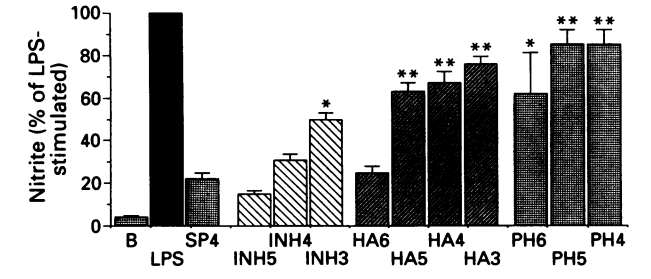


Figure 8 The inhibitory effect of spermine on nitrite accumulation is prevented by inhibitors of polyamine oxidase or by an aldehyde inhibitor. Depicted are the effects of isonicotinic acid (INH, $10^{-5}-10^{-3}$ M), hydroxylamine (HA, $10^{-6}-10^{-3}$ M) and phenhydrazine (PH $10^{-6}-10^{-4}$ M), applied together with spermine, on the inhibitory effect of spermine (SP, 10^{-4} M), on nitrite accumulation in the medium (with 10% FCS) of J774.2 macrophages stimulated by LPS (1 μg ml^{-1}) for 24 h. Data are expressed as means ± s.e.mean of $n = 6-9$ wells from 2–3 experimental days. $^{*}P < 0.05$ and $^{**}P < 0.01$ represent significant inhibition of the effect of spermine by INH, HA or PH.

whereas putrescine and cadaverine were virtually ineffective (Figure 10). The presence of foetal calf serum was also required for the inhibitory effect of spermidine or N^1-acetylspermine on LPS-induced nitrite accumulation (not shown).

Acrolein may be a metabolite of spermine under certain conditions. It is however, unlikely that acrolein significantly contributes to the effects of spermine or SDA on NO formation for acrolein (up to 10^{-5} M), unlike spermine, did not inhibit nitrite formation in response to LPS, while it became cytotoxic at higher concentrations ($n = 3$).

Spermine does not inhibit LPS-induced production of TNFα or prostaglandin $F_{2\alpha}$

In addition to causing the expression of iNOS and, hence, NO formation, LPS also induces the expression of a novel isoform of cyclo-oxygenase (COX-2) resulting in the accumulation of large amounts of cyclo-oxygenase products such as prostaglandin $F_{2\alpha}$ ($PGF_{2\alpha}$). Moreover, LPS causes the formation of murine TNFα in LPS-activated J774.2 cells (see: Discussion). Interestingly, this LPS-induced production of $PGF_{2\alpha}$ and murine TNFα was unaffected by spermine ($10^{-6}-10^{-4}$ M, Figure 11a and b).

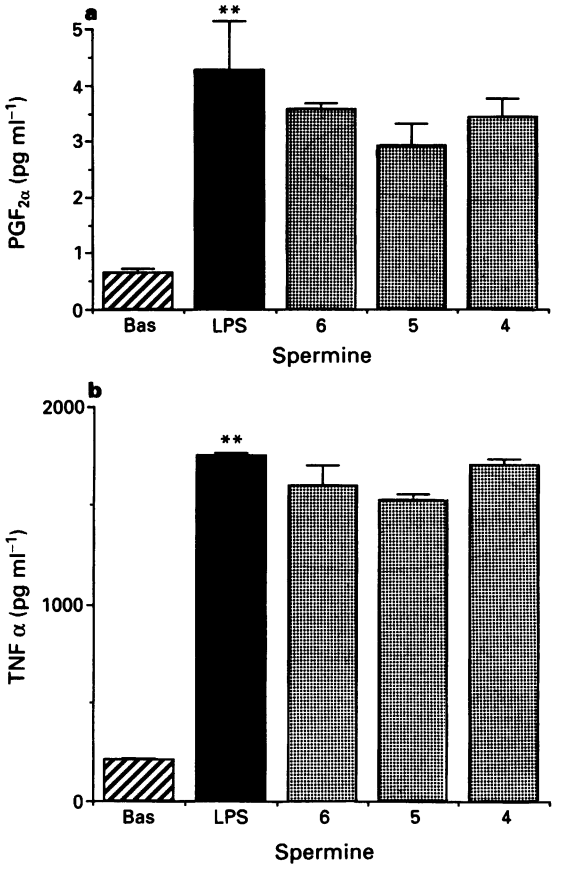


Figure 11 Spermine does not inhibit the LPS-induced induction of cyclo-oxygenase or the LPS-induced production of TNFα. Depicted are the effects of spermine (10^{-6}–10^{-4} M) on LPS-induced production of $PGF_{2\alpha}$ and (a) and TNFα (b) in the medium of J774.2 macrophages stimulated by LPS (1 μg ml^{-1}) for 24 h. Data are expressed as means ± s.e.mean of $n = 6$–9 wells from 2–3 experimental days. $^{**}P < 0.01$ represents significant increase in the production of $PGF_{2\alpha}$ or TNFα in response to LPS.

Discussion

The present study demonstrates that spermine, N^1 acetylspermine and spermidine, but not putrescine or cadaverine, inhibit the accumulation of nitrite in the medium of LPS-stimulated J774.2 macrophages. This inhibitory effect is dependent on the presence of bovine serum in the cell culture medium.

The hypothesis that spermine interferes with either induction or activity of iNOS, but not with NO directly (or with its detection), is supported by the findings that (i) neither spermine nor its metabolites scavenge NO or affect its conversion to nitrite or nitrate, (ii) spermine or its metabolites do not scavenge NO released by SIN-1 or bind to nitrite and (iii) similar levels of NO were determined by measuring nitrite with either the Griess reaction or chemiluminescence. Adducts of NO with spermine have recently been synthesized (Maragos *et al.*, 1991; Morley *et al.*, 1993). Formation of such adducts in the medium is not the mechanism by which spermine reduces the accumulation of nitrite in the medium, for any adducts of spermine with NO would also be converted to NO under the conditions used in our chemiluminescence experiments.

Spermine had no effect on the formation of citrulline by homogenates of J774.2 cells in which iNOS had previously been induced by LPS. Taken with the finding that spermine had a reduced potency when given to cells several hours after LPS, this strongly suggests that polyamines inhibit the induction of iNOS, rather than directly inhibiting iNOS activity.

The inhibitory effect of spermine was entirely dependent on the presence of serum. Moreover, the inhibition was observed either in the presence of foetal, newborn or adult bovine serum. Bovine serum contains polyamine oxidase (also known as spermine oxidase) (Tabor *et al.*, 1954; Yamada & Yasonobu, 1962) whereas spermine oxidase is not present in normal human or rodent sera (see Morgan, 1985; 1987). Our experiments with the spermine oxidase inhibitors, hydroxylamine and isonicotinic acid (Morgan, 1987; Seiler, 1990) demonstrate that the presence of this enzyme in the culture medium is a prerequisite to demonstrate an inhibitory effect of spermine on nitrite formation by LPS-activated J774.2 macrophages. Thus, we suggest that spermine oxidase converts spermine into active inhibitor(s) of iNOS induction by LPS or IFN. It is noteworthy that the levels of spermine oxidase in bovine serum increase after birth (Gahl & Pitot, 1982), which may explain our finding here (see Figure 7) that the degree of inhibition of iNOS induction afforded by spermine tended to increase when newborn or adult serum was used instead of FCS.

Spermine can be oxidized to N^1-acetylspermine by the enzymes polyamine oxidase and N-acetyltransferase (Gaugas, 1980; Selmeci *et al.*, 1985; Morgan, 1987). N^1-acetylspermine can then be further metabolized to e.g. carboxyethylputrescine, putrescine and/or aminopropionaldehyde (Gaugas, 1980; Selmeci *et al.*, 1985; Morgan, 1987) (see Figure 12). The finding that N^1-acetylspermine inhibits LPS-induced nitrite accumulation only in the presence, but not in the absence of serum, strongly suggests that the formation of N^1-acetylspermine and its subsequent further conversion may be involved in the inhibitory effect of spermine. Lower polyamine metabolites (such as putrescine), however, are much less potent inhibitors than spermine in J774.2 cells activated by LPS or IFN and, hence, are unlikely to play a major role in this inhibitory effect.

The inhibition of iNOS induction afforded by spermine in LPS-activated macrophages was prevented by phenylhydrazine, a compound that directly inactivates aldehydes. Thus, we suggest that aldehyde metabolites of spermine are involved in the observed inhibition. Such aldehyde metabolites could in principle directly inhibit the expression of iNOS or, alternatively, may be further metabolized to yield the active inhibitor. Potential aldehyde metabolites of spermine which may contribute to the inhibition of iNOS induction seen with spermine include spermine dialdehyde (SDA) or malon dialdehyde (MDA) which are generated from spermine by polyamine oxidases (Labib & Tomasi, 1981; Quash *et al.*, 1987; Lau *et al.*, 1990). MDA was ineffective in inhibiting nitrite production in LPS-activated macrophages, even when FCS was present, whereas SDA caused a significant inhibition of nitrite accumulation even in the absence of serum (Figure 9). However, the potency of SDA is less than the apparent potency of spermine. Thus, the formation of SDA by serum polyamine oxidases cannot fully account for the prevention of iNOS induction caused by spermine in J774.2 macrophages activated by LPS or IFN, especially for it is known that SDA has only a short half-life in the culture medium (Lau *et al.*, 1990). However, the formation of SDA may contribute to the inhibition of iNOS induction caused by spermine, and SDA may well synergize with other aldehyde metabolites. Thus, other, yet unidentified aldehyde metabolites of spermine must also contribute to the inhibition of iNOS induction seen with polyamines. Other aldehyde metabolites of spermine include small molecules such as propionaldehyde. Propionaldehyde has recently been proposed as an active aldehyde metabolite responsible for the inhibition of mast cell secretion by polyamines (Vliagoftis *et al.*, 1992).

The mechanism by which spermine or spermine-derived aldehydes inhibit the expression of iNOS warrants further investigation. Pharmacological agents that inhibit the induction of iNOS include glucocorticoids, growth factors, thrombin and dihydropyridine-type calcium channel modulators

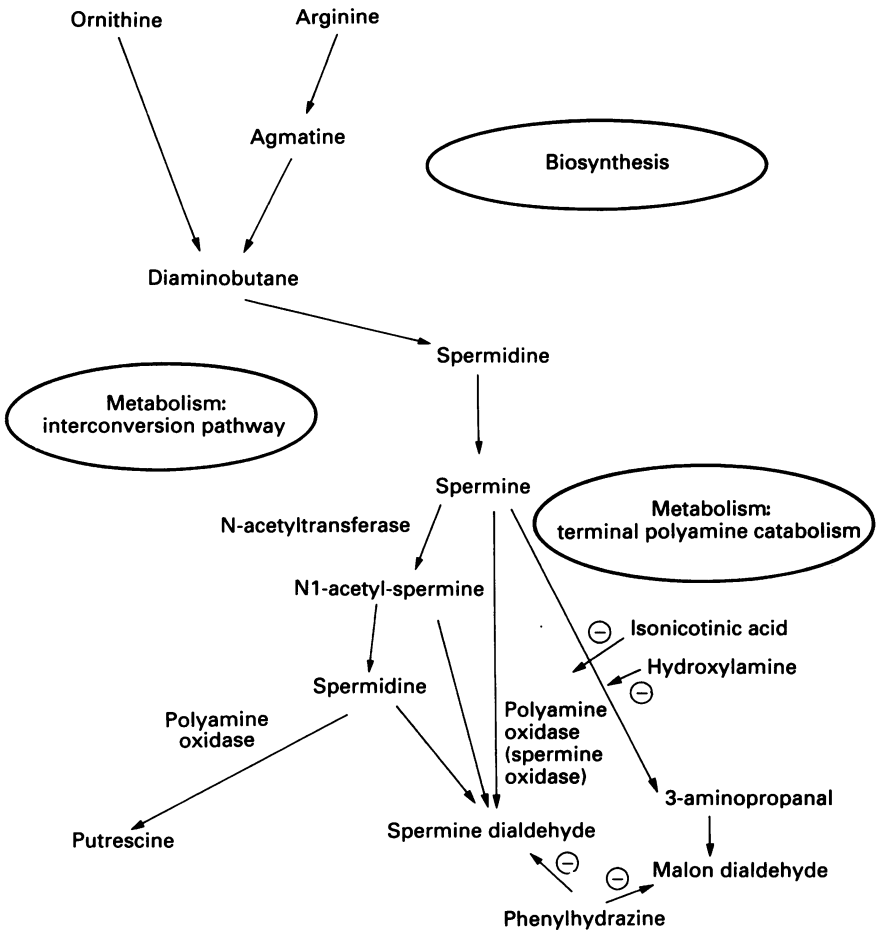


Figure 12 Metabolic pathways of polyamines in the presence of bovine serum.

(see Introduction), but their exact mode of action is not known. The induction of iNOS by LPS is, at least in part, dependent on the release of secondary cytokines such as TNFα and INF (*in vitro*) or TNFα, INF and interleukin-1 (*in vivo*) (Liew *et al.*, 1990; Evans *et al.*, 1992; Fortier *et al.*, 1992; Green *et al.*, 1993; Thiemermann *et al.*, 1992; Szabo *et al.*, 1993c). It is unlikely, however, that spermine or its metabolites inhibit the release of secondary cytokines for (i) spermine did not inhibit the release of TNFα in response to LPS; and (ii) spermine also inhibited nitrite production when iNOS was induced by IFN. Inhibition of tyrosine kinase has recently been shown to inhibit the induction of iNOS by LPS and IL-1 in cultured vascular smooth muscle cells (Marczin *et al.*, 1993) and in mouse peritoneal macrophages (Dong *et al.*, 1993). This mechanism is also involved in the induction of iNOS in J774.2 cells, for genistein, a tyrosine kinase inhibitor prevents nitrite production when given together with LPS, but its action is significantly reduced when given 6 h after the stimulus of induction (Szabo & Southan, unpublished data). There is also evidence for the involvement of the gene promoter region nuclear factor $NF_{\kappa}B$ (Sherman *et al.*, 1993) in the induction of iNOS. It is tempting to speculate that metabolites of spermine inhibit iNOS induction by interfering with the activity of tyrosine kinase and/or the activation of $NF\text{-}_{\kappa}B$. Although the mechanisms of the inhibitory effects of polyamines on iNOS induction reported here are unclear, it is likely that aldehyde metabolites of spermine interfere at a relatively early stage with the signal transduction pathway leading to the induction, i.e. prior to, or at the level of transcription.

Interestingly, in the absence of serum, the induction of iNOS by LPS, but not by IFN, was largely reduced, and the induction could be restored with re-addition of serum. Thus, the presence of a serum factor is necessary for the initiation of the induction process itself, but only with LPS and not IFN. A likely candidate might have been LPS-binding protein (LBP), a plasma protein that is required for many immunological actions of LPS. LBP is known to bind to LPS in order to activate the CD14 receptor located on the cell membrane (Raetz *et al.*, 1993; Hewerr & Roth, 1993). Here we show, however, that the lack of iNOS induction in the absence of serum is not simply due to the absence of LBP in the culture medium, and it must, therefore, be related to other factor(s) present in the serum (e.g. soluble CD14, growth factors, cytokines, hormones) or to other properties of serum (e.g. adherence properties). It is, however, noteworthy that the LBP-CD14 system is usually more functional at lower concentrations of LPS, rather than the relatively high ones used in the present study (Raetz *et al.*, 1991; Hewerr & Roth, 1993).

Polyamines are present in high concentrations in foetal and neoplastic tissues and in seminal fluid (Morgan & Illei, 1980). These tissues represent antigenic sites/challenges that often do not elicit appropriate immune response (Normann, 1985; Bulmer, 1992). In the presence of FCS, spermine and spermidine, but to a much lesser extent putrescine or cadaverine, inhibit the immune response in LPS-stimulated primary cell cultures of the spleen (Byrd *et al.*, 1977). Lau and co-workers (1984; 1990) described an immunosuppressant factor, originally termed suppression inhibitory factor, obtained from the supernatant of cultured mutant human lymphocytes, which they later identified as SDA (also known as dioxidized spermine). SDA may be useful in preventing graft-versus-host reactions in bone marrow transplantation (Lau *et al.*, 1992; Wang *et al.*, 1990).

The present study tentatively links these observations to

the induction of iNOS, a major cytotoxic macrophage effector molecule. Thus our data not only identify a novel inhibitor of iNOS induction (SDA) but also describe a possible mechanism for immunosuppression seen in tissues or biological fluids that contain high levels of polyamines. Our findings may have implications for the mechanism of host immunosuppression seen in pregnancy or in tumour-bearing organisms. For instance, it is well documented that pregnancy is associated with high levels of polyamines and polyamine oxidases in the plasma and in the amniotic fluid (Gaugas, 1980; Morgan & Illei, 1980; Gahl *et al.*, 1982). Moreover, many tumour cells also contain and secrete large amounts of polyamines. As polyamines are also produced by bacteria (Tait, 1985), they may serve as suppressants of the host immune response by inhibiting the induction of iNOS.

It is now evident that many of the actions of polyamines are dependent on their conversion by spermine oxidase. These effects of polyamines include the inhibition of lymphocyte proliferation and other immunosuppressive actions (Labib & Tomasi, 1981; Quan *et al.*, 1990; Lea *et al.*, 1991): inhibition of histamine release (Vligoftis *et al.*, 1992), and inhibition of neutrophil activation (Ferrante *et al.*, 1986). We, therefore, investigated the effect of spermine on other LPS-induced processes including the induction of COX-2 and the induction of the production of TNFα. LPS and several pro-inflammatory cytokines induce a distinct isoform of cyclooxygenase (COX-2) *in vitro* and *in vivo* that plays a key role e.g. in chronic inflammation (Masferrer *et al.*, 1992a,b; Vane, 1993). Our data show that spermine does not inhibit the induction of either COX-2 or the production of TNFα. Thus, we conclude that aldehyde metabolites of spermine are relatively selective inhibitors of the signal transduction pathway leading to the expression of iNOS in cultured macrophages.

This work was supported by a grant from Glaxo Group Research Ltd. C.S. is supported by the Lloyd's of London Tercentenary Foundation. C.T. is supported by a grant from the Commission of the European Communities (Biomed I, BMHI, CT 92/1893). The authors thank Dr Bruno Battistini for the assistance with the radioimmunoassay measurements and Ms Elizabeth Wood for expert assistance with the cell cultures.

References

BULMER, J. (1992). Immune aspects of pathology of the placental bed contributing to pregnancy pathology. *Balliere's Clin. Obstet. Gynecol.*, **6**, 461–488.

BYRD, W.J., JACOBS, D.M. & AMOS, M.S. (1977). Synthetic polyamines added to cultures containing bovine sera reversibly inhibit in vitro parameters of immunity. *Nature*, **267**, 621–623.

COX, R.D. & FRANK, C.W. (1982). Detection of nitrate and nitrite in blood and urine by chemiluminescence. *J. Anal. Toxicol.*, **5**, 148–152.

CUNHA, F.Q., MONCADA, S. & LIEW, F.Y. (1992). IL-10 inhibits the induction of nitric oxide synthase by INFγ in murine macrophages. *Biochem. Biophys. Res. Commun.*, **182**, 1155–1159.

DONG, Z., QI, X., XIE, K. & FIDLER, I.J. (1993). Protein tyrosine kinase inhibitors decrease induction of nitric oxide synthase activity in lipopolysaccharide-responsive and lipopolysaccharide-nonresponsive murine macrophages. *J. Immunol.*, **151**, 2717–2724.

EVANS, T., CARPENTER, A., SILVA, A. & COHEN, J. (1992). Differential effects of monoclonal antibodies to tumor necrosis factor alpha and gamma interferon on induction of hepatic nitric oxide synthase in experimental gram-negative sepsis. *Infect. Immun.*, **60**, 4133–4139.

FEELISCH, M., OSTROWSKI, J. & NOACK, E. (1989). On the mechanism of NO release from sydnonimines. *J. Cardiovasc. Pharmacol.*, **14** (suppl. 11), S13–S22.

FERRANTE, A., MAXWELL, G.M., RENCIS, V.O., ALLISON, A.C. & MORGAN, D.M.L. (1986). Inhibition of the respiratory burst of human neutrophils by the polyamine oxidase – polyamine system. *Int. J. Immunopharmacol.*, **8**, 411–417.

FORTIER, A.H., POSLINELLI, T., GREEN, S.J. & NACY, C.A. (1992). Activation of macrophages for destruction of Francisella tularensis: identification of cytokines, effector cells, and effector molecules. *Infect. Immun.*, **60**, 817–825.

GAHL, W.A. & PITOT, H.C. (1982). Polyamine degradation in foetal and adult bovine serum. *Biochem. J.*, **202**, 603–611.

GAUGUS, J.M. (1980). *Polyamines in Biomedical Research*. Chichester: John Wiley & Sons.

GREEN, S.J. & NACY, C.A. (1993). Antimicrobial and immunopathologic effects of cytokine-induced nitric oxide synthesis. *Current Op. Infect. Dis.*, **6**, 384–396.

GREEN, S.J., NACY, C.A., SCHREIBER, R.D., GRANGER, D.L., CRAWFORD, R.M., MELTZER, M.S. & FOSTER, A.H. (1993). Neutralization of gamma interferon and tumor necrosis factor alpha blocks in vivo synthesis of nitrogen oxides from L-arginine and protection against *Francisella tularensis* infection in *Mycobacterium bovis* BCG-treated mice. *Infect. Immun.*, **61**, 689–698.

HEWERR, J.A. & ROTH, R.A. (1993). Hepatic and extrahepatic pathobiology of bacterial lipopolysaccharides. *Pharmacol. Rev.*, **45**, 381–411.

LABIB, R.S. & TOMASI, T.B. (1981). Enzymatic oxidation of polyamines. Relationship to immunosuppressive properties. *Eur. J. Immunol.*, **11**, 266–269.

LANGREHR, J.M., HOFFMAN, R.A., LANCASTER, J.R. & SIMMONS, R.L. (1993). Nitric oxide – a new endogenous immunomodulator. *Transplantation*, **55**, 1205–1212.

LAU, C., BUDZ-TYMKIEWITZ, T.A., WANG, E.Y. & ISHAQUE, A. (1984). A mutant human T-cell line producing immunosuppressive factor(s). *Cellular Immunol.*, **87**, 35–52.

LAU, C., STANOJEV, D., VISCONTI, V., PANG, H., KREPINSKI, G., GREY, A., WANG, E. & ISHAQUE, A. (1990). Purification, characterization and structural elucidation of the active moiety of the previously called 'suppressor activating factor (SAF)'. *Cellular Immunol.*, **125**, 92–106.

LAU, C., WANG, E., ISHAQUE, A., JONES, K., WONG, B., KIMSTO, L. & CONANT, J. (1992). Spermine dialdehyde, a novel ex vivo purging agent for both allogeneic and autologous bone marrow transplantations. *Int. J. Immunopharmacol.*, **14**, 1081–1091.

LEA, R.G., PORAT, O., DAYA, S., FUJIWARA, K. & CLARK, D.A. (1991). The detection of spermine and spermidine in human in vitro fertilization supernatants and their relation to early embryo-associated suppressor activity. *Fertil. Steril.*, **56**, 771–775.

LEVITZKI, A. (1992). Tyrpostins: tyrosine kinase blockers as novel antiproliferative agents and dissectors of signal transduction. *FASEB J.*, **6**, 3275–3282.

LIEW, F.Y., LI, Y. & MILLOTT, S. (1990). Tumor necrosis factor synergizes with IFN in mediating killing of Leishmania major through the induction of nitric oxide. *J. Immunol.*, **145**, 4290–4297.

MARAGOS, C., MORLEY, D., WINK, D.A., DUNAMS, T.M., SAAVEDRA, J.E., HOFFMAN, A., BOVE, A.A., ISAAC, L., HRABIE, J.A. & KEEFER, L.K. (1991). Complexes of NO with nucleophiles as agents for the controlled biological release of nitric oxide. Vasorelaxant effects. *J. Med. Chem.*, **34**, 3242–3247.

MARCZIN, N., PAPAPETROPOULOS, A. & CATRAVAS, J.D. (1993). Tyrosine kinase inhibitors suppress endotoxin- and IL-1β-induced NO synthesis in aortic smooth muscle cells. *Am. J. Physiol.*, **265**, H1014–H1018.

MASFERRER, J.L., SEIBERT, K., ZWEIFEL, B.S. & NEEDLEMAN, P. (1992a). Endogenous glucocorticoids regulate an inducible cyclooxygenase enzyme. *Proc. Natl. Acad. Sci. U.S.A.*, **89**, 3917–3921.

MASFERRER, J.L., ZWEIFEL, B.S., SEIBERT, K. & NEEDLEMAN, P. (1992b). Selective regulation of cellular cyclooxygenase by dexamethasone and endotoxin in mice. *J. Clin. Invest.*, **86**, 1375–1379.

MORGAN D.M.L. (1985). Polyamine oxidases. *Biochem. Soc. Trans.*, **13**, 322–326.

MORGAN, D.M. (1987). Polyamines. *Essays Biochem.*, **23**, 82–115.

MORGAN, M.L. & ILLEI, G. (1980). Polyamine – polyamine oxidase interactin: part of maternal protective mechanism against foetal rejection. *Br. Med. J.*, **280**, 1295–1297.

MORLEY, D., MARAGOS, C.M., ZHANG, X.Y., BOIGNON, M., WINK, D.A. & KEEFER, L.K. (1993). Mechanism of vascular relaxation induced by the nitric oxide/nucleophile complexes, a new class of NO-based vasodilators. *J. Cardiovasc. Pharmacol.*, **21**, 670–676.

NATHAN, C.F. (1992). Nitric oxide as a secretory product of mammalian cells. *FASEB J.*, **6**, 3051–3064.

NATHAN, C.F. & HIBBS, J.B. (1991). Role of nitric oxide synthesis in macrophage antimicrobial activity. *Curr. Opin. Immunol.*, **3**, 65–70.

NORMANN, S.J. (1985). Macrophage infiltration and tumor progression. *Cancer Metastas. Rev.*, **4**, 277–291.

POLLACK, P., AEBERHARD, E. & SHERMAN, M. (1994). Effect of polyamines on inducible nitric oxide (NO) production. *FASEB J.*, **8**, A361 (abstr.).

QUAN, C.P., ROUX, C., PILL, J. & BOUVET, J.P. (1990). Delineation between T and B suppressive molecules from human seminal plasma: II. Spermine is the major suppressor of T-lymphocytes in vitro. *Am. J. Reprod. Immunol.*, **22**, 64–69.

QUASH, G., RIPOLL, H., GASSOLO, L., DOUTHEAU, A., SABA, A. & GORE, J. (1987). Malondialdehyde production from spermine by homogenates of normal and transformed cells. *Biochimie*, **96**, 101–108.

RADOMSKI, M.W., PALMER, R.M.J. & MONCADA, S. (1990). Glucocorticoids inhibit the expression of an inducible, but not the constitutive nitric oxide synthase in vascular endothelial cells. *Proc. Natl. Acad. Sci. U.S.A.*, **87**, 10043–10047.

RAETZ, C.R., ULEVICH, R.J., WRIGHT, S.D., SIBLEY, C.H., DING, A. & NATHAN, C.F. (1991). Gram-negative endotoxin: an extraordinary lipid with profound effects on eukaryotic signal transduction. *FASEB J.*, **5**, 2652–2660.

SALMON, J.A. (1978). A radioimmunoassay for 6-keto-$PGF_{1\alpha}$. *Prostaglandins*, **15**, 383–397.

SEILER, N. (1990). Polyamine metabolism. *Digestion*, **64** (suppl. 2), 319–330.

SELMECI, L., BROSNAN, M.E. & SEILER, N. (1985). *Recent Progress in Polyamine Research*. Budapest: Akademiai Kiado.

SHERMAN, M.P., AEBERHARD, E.E., WONG, V.Z., GRISCAVAGE, J.M., IGNARRO, L.J. (1993). Pyrrolidine thiocarbamate inhibits induction of nitric oxide synthase activity in rat alveolar macrophages. *Biochem. Biophys. Res. Commun.*, **191**, 1301–1308.

STUEHR, D.J. & GRIFFITH, O.W. (1992). Mammalian nitric oxide synthases. *Adv. Enzymol. Mol. Biol.*, **65**, 287–346.

STUEHR, D.J. & NATHAN, C.F. (1989). Nitric oxide: a macrophage product responsible for cytostasis and respiratory inhibition in tumor target cells. *J. Exp. Med.*, **169**, 1543–1555.

SZABO, C., SOUTHAN, G.J., WOOD, E., THIEMERMANN, C. & VANE, J.R. (1994). Inhibition by spermine of the induction of nitric oxide synthase in J774.2 macrophages: requirement of a serum factor. *Br. J. Pharmacol.*, **110**, 355–356.

SZABO, C., THIEMERMANN, C. & VANE, J.R. (1993a). Dihydropyridine modulators of calcium channels inhibit the induction of nitric oxide synthase by endotoxin in cultured J774.2 cells. *Biochem. Biophys. Res. Commun.*, **196**, 825–830.

SZABO, C., WU, C.C., MITCHELL, J.A., GROSS, S.S., THIEMERMANN, C. & VANE, J.R. (1993b). Platelet-activating factor contributes to the induction of nitric oxide synthase by bacterial lipopolysaccharide. *Circ. Res.*, **73**, 991–999.

SZABO, C., WU, C.C., GROSS, S.S., THIEMERMANN, C. & VANE, J.R. (1993c). Interleukin-1 contributes to the induction of nitric oxide synthase by endotoxin in vivo. *Eur. J. Pharmacol.*, **250**, 157–160.

TABOR, C., TABOR, H. & ROSENTHAL, S.M. (1954). Purification of amine oxidase from beef plasma. *J. Biol. Chem.*, **208**, 645–661.

TAIT, G.H. (1985). Bacterial polyamines, structures and biosynthesis. *Biochem. Soc. Trans.*, **13**, 316–318.

THIEMERMANN, C., WU, C.C., SZABO, C., PERRETTI, M. & VANE, J.R. (1993). Tumour necrosis factor is an endogenous mediator of the induction of nitric oxide synthase in endotoxin shock in the rat. *Br. J. Pharmacol.*, **110**, 177–182.

VANE, J.R. (1993). Towards a better aspirin. *Nature*, **215**, 215–216.

VLIAGOFTIS, H., BOUCHER, W.S., MAK, L.L. & THEODARIDES, T.C. (1992). Inhibition of mast cell secretion by oxidation products of natural polyamines. *Biochem. Pharmacol.*, **43**, 2237–2245.

WALTER, C.L., GILLIAT, P.N., PALMER, R.C. & SMITH, P.L. (1987). A rapid method for detection of nitrate and nitrite by chemiluminescence. *Food Addit. Contam.*, **4**, 133–140.

WANG, E., MASON CONANT, J., LI, D., VISCONTI, V., CHOURMOUZIS, E. & LAU, O. (1990). Ex vivo spermine dialdehyde treatment prevents lethal GVHD in a murine bone marrow transplantation model. *Bone Marrow Transplant*, **6**, 235–242.

YAMADA, H. & YASONOBU, K.T. (1962). Monoamine oxidase I, purification, crystallization and properties of plasma monoamine oxidase. *J. Biol. Chem.*, **237**, 1511–1516.

(Received May 6, 1994
Revised June 20, 1994
Accepted June 28, 1994)

Br. J. Pharmacol. (1994), **113**, 767–774 © Macmillan Press Ltd, 1994

Dual effects of tetrandrine on cytosolic calcium in human leukaemic HL-60 cells: intracellular calcium release and calcium entry blockade

Yuk-Man Leung, Chiu-Yin Kwan & [1]Tatt-Tuck Loh

Department of Physiology, Faculty of Medicine, University of Hong Kong, 5 Sassoon Road, Hong Kong

1 Tetrandrine (TET, a Ca^{2+} antagonist of Chinese herbal origin) and thapsigargin (TSG, an endoplasmic reticulum Ca^{2+} pump inhibitor) concentration-dependently mobilized Ca^{2+} from intracellular stores of HL-60 cells, with EC_{50} values of 20 μM and 0.8 nM, respectively. After intracellular Ca^{2+} release by 30 nM TSG, there was no more discharge of Ca^{2+} by TET (100 μM), and *vice versa*.

2 Pretreatments with 100 nM rauwolscine (α_2-adrenoceptor antagonist), 100 nM prazosin (α_1-adrenoceptor antagonist), 10 nM phorbol myristate acetate (PMA, a protein kinase C activator) or 100 nM staurosporine (a protein kinase C inhibitor) had no effect on 100 μM TET-induced intracellular Ca^{2+} release.

3 After intracellular Ca^{2+} release by 30 nM TSG in Ca^{2+}-free medium, readmission of Ca^{2+} caused a substantial and sustained extracellular Ca^{2+} entry. The latter was almost completely inhibited by 100 μM TET (IC_{50} of 20 μM) added just before Ca^{2+} readmission. In Ca^{2+}-containing medium, 30 nM TSG caused a sustained phase of cytosolic Ca^{2+} elevation, which could be abolished by 100 μM TET. TET was also demonstrated to retard basal entry of extracellular Mn^{2+} and completely inhibit TSG-stimulated extracellular Mn^{2+} entry.

4 TSG-induced extracellular Ca^{2+} entry was insensitive to the L-type Ca^{2+} channel blocker, nifedipine (1 μM), but was completely inhibited by the non-selective Ca^{2+} channel blocker La^{3+} (300 μM). Depolarization with 100 mM KCl did not raise the cytosolic Ca^{2+} level.

5 These data suggest that (a) TET and TSG mobilized the same Ca^{2+} pool and TET-induced intracellular Ca^{2+} release was independent of protein kinase C activity and α-adrenoceptor activation, and (b) TET blocked the voltage-insensitive Ca^{2+} entry pathway activated by TSG. These dual effects on HL-60 cells were also observed with hernandezine (HER), a TET-like compound and in another cell type, murine B lymphoma M12.4 cells.

Keywords: Tetrandrine; thapsigargin; hernandezine; calcium antagonist; cytosolic calcium; calcium release; human leukaemia; HL-60 cells

Introduction

Tetrandrine (TET), a *bis*-benzylisoquinoline alkaloid isolated from the Chinese medicinal herb *Stephania tetrandra*, has various pharmacological actions. It has been demonstrated clinically (Gao *et al.*, 1965) and in experimental animals (Qian *et al.*, 1983) to have a hypotensive effect, which in part could be due to its Ca^{2+} antagonistic properties (Jia *et al.*, 1985; Fang & Jiang, 1986). It has also been shown to cause suppression of fibroblast proliferation (Reist *et al.*, 1993) and collagen synthesis (Liu *et al.*, 1983), which might account for its anti-silicotic effect (Li *et al.*, 1981; Yu *et al.*, 1983). The anti-inflammatory effect of TET is most likely attributable to its inhibitory effects on immune cells such as B cells, mast cells, monocytes and neutrophils (Seow *et al.*, 1986; 1988; Teh *et al.*, 1988; Ferrante *et al.*, 1990). Not surprisingly, its various pharmacological actions are paralleled by its multiple modulatory effects at the molecular or signal transduction level. For instance, its Ca^{2+} antagonistic properties have been related to its inhibition of L-type and T-type Ca^{2+} channels (King *et al.*, 1988; Liu *et al.*, 1991; 1992; Rossier *et al.*, 1993), and receptor-mediated Ca^{2+} entry (Kwan *et al.*, 1992). In human lymphocytes, TET caused not only attenuation of extracellar Ca^{2+} entry, but also reduction of inositol trisphosphate production (Ioannoni *et al.*, 1989). There has been evidence that TET might bypass the plasma membrane receptor-effector coupling and act directly on intracellular messengers. For example, in human lymphocytes, protein kinase C (PK-C) activity stimulated with phorbol myristate acetate (PMA), a direct activator of PK-C, was inhibited by TET, suggesting that TET could possibly exert a direct inhibition on this intracellular signalling molecule (Ioannoni *et al.*, 1989).

Recently, Kwan & Wang (1993) observed that TET relaxed KCl-induced contraction in canine saphenous and mesenteric veins, but after washout, a transient contraction unexpectedly followed. This contraction upon washout of KCl was not observed with nifedipine or sodium nitroprusside as the relaxants. In rat alveolar type II cells, TET and chemically related compounds were shown to raise cytolosic free calcium concentration ($[Ca^{2+}]_i$) slightly (Miles *et al.*, 1993). Both contraction and $[Ca^{2+}]_i$ elevation induced by TET were observed in Ca^{2+}-containing medium, and therefore, whether the contraction and $[Ca^{2+}]_i$ elevation were due to interacellular Ca^{2+} release or extracellular Ca^{2+} entry is unknown. Nevertheless, these two novel phenomena cast serious doubt on TET being a selective and effective Ca^{2+} antagonist. In this work we investigated the effects of TET on $[Ca^{2+}]_i$ homeostasis of human leukaemic HL-60 cells. We describe here two novel effects of TET, namely, blockade of extracellular Ca^{2+} entry induced by thapsigargin (TSG, a selective endoplasmic reticulum Ca^{2+} pump inhibitor (Thastrup *et al.*, 1990; Lytton *et al.*, 1991)) and stimulation of Ca^{2+} release from intracellular stores. Entry of extracellular Ca^{2+} and release of Ca^{2+} from intracellular stores into the cytosol will hereafter be, for the sake of simplicity, referred to as Ca^{2+} entry and Ca^{2+} release, respectively. We have characterized the pharmacological properties of the Ca^{2+} entry

[1] Author for correspondence.

pathway that TET blocked and partially delineated the mechanism of TET-induced Ca^{2+} release. We have also shown that hernandezine (HER), a chemically related compound of TET, behaved very similarly to TET in HL-60 cells.

Methods

Cell culture

HL-60 cells and M12.4 cells obtained from American Type Culture Collection, Maryland, U.S.A., were maintained in RPMI 1640 medium (Sigma), supplemented with 10% foetal calf serum, 5 μg gentamycin ml^{-1} and penicillin/streptomycin (100 u ml^{-1}, 100 μg ml^{-1}) in a humidified atmosphere with 5% CO_2 at 37°C. The cells were split in a 1:5 ratio every two or three days.

$[Ca^{2+}]_i$ measurement

The method of measuring $[Ca^{2+}]_i$ was modified from the protocol described by Lambert & Nahorski (1990). Hank's buffered saline solution (HBSS), composed of (mM): NaCl 138, KCl 5.3, $MgSO_4$ 0.88, $CaCl_2$ 1.2, KH_2PO_4 0.44, Na_2HPO_4 0.34, glucose 5 and HEPES (N-[2-hydroxyethyl]-piperazine-N'-2-ethane sulphonic acid) 25 buffered at pH 7.4, was used for cell washing. HL-60 cells or M12.4 cells grown to a density of around 1.5×10^6 ml^{-1} were harvested, washed once in Ca^{2+}-containing HBSS and resuspended in serum-free RPMI 1640 medium at a cell density of about 2×10^7 ml^{-1}. Fura 2-acetoxymethyl (AM) ester was added to this cell suspension at a final concentration of 5 μM. The cell suspension was then incubated at 37°C for 45 min. Thereafter, the fura 2-loaded cells were washed two times in Ca^{2+}-containing HBSS and resuspended in the same buffer solution at a cell density of 2.8×10^6 ml^{-1}. Before experimentation on each sample, 1 ml of this cell suspension was centrifuged and the cell pellet was resuspended in 2 ml Ca^{2+}-free or Ca^{2+}-containing HBSS. Ca^{2+}-free HBSS was used when Ca^{2+} release from intracellular stores was to be detected. Ca^{2+}-containing HBSS was used when thapsigargin was to induce a sustained Ca^{2+} entry. This 2-ml cell suspension was then transferred to a quartz cuvette which contained a mini stirrer, and warmed at 37°C for about 3 min before addition of agonists or drugs. Fura 2 fluorescence was detected with a Hitachi F-4000 fluorescence spectrophotometer. Excitation and emission wavelengths were set at 340 mm and 500 nm respectively. For calibration, F_{max} was obtained by lysing the cells with 0.1% Triton X-100 and F_{min} by chelating Ca^{2+} with 20 mM EGTA. $[Ca^{2+}]_i$ was calculated according to Grynkiewicz *et al.* (1985). The basal $[Ca^{2+}]_i$ ranged from 70–110 nM.

In experiments under Ca^{2+}-free conditions, about 30 s before agonist or drug stimulation, a small amount of EGTA was added to the cell suspension to chelate contaminating Ca^{2+} to maintain a stable baseline which was important to help interpreting whether the Ca^{2+} release was transient or exhibiting a plateau phase. The amount of EGTA (22.5–100 μM) added to each sample in a given experiment was the same, but might vary in separate experiments, depending on the level of contaminating Ca^{2+}.

In experiments when La^{3+} was used to block Ca^{2+} entry, phosphate salts were omitted from the HBSS and the concentration of HEPES was reduced to 8 mM in order to avoid precipitation upon La^{3+} addition. Also, 1% foetal calf serum was included in the reaction medium to avoid La^{3+}-induced cell aggregation.

Mn^{2+} entry experiments

At 360 nm excitation wavelength, fura 2 fluorescence is insensitive to Ca^{2+} but quenchable by Mn^{2+}. Therefore, at this wavelength, a decrease in fura 2 fluorescence upon addition of Mn^{2+} indicated Mn^{2+} entry from the extracellular space into the cytosol (herafter simply referred to as Mn^{2+} entry), and this protocol has been used as a means to detect divalent cation entry, which is suggestive of Ca^{2+} channel opening (Merritt *et al.*, 1989). In this work, cell suspension in Ca^{2+}-free medium (without EGTA supplementation) was prepared as described above, and after a 3-min warming at 37°C, 0.5 mM Mn^{2+} was added for 1–1.5 min before the cells were exposed to pharmacological agents. Excitation and emission wavelengths were set at 360 nm and 500 nm respectively.

Materials

ATP, nifedipine, prazosin, rauwolscine, thapsigargin, phorbol myristate acetate, and fura 2-AM were obtained from Sigma Chemical Co., St. Louis, MO, U.S.A. CPA and staurosporine were purchased from Calbiochem, Richmond, CA, U.S.A. Foetal calf serum was purchased from Gibco BRL (Gaitherburg, MD, U.S.A.). TET (purity > 98%) from Jing-Hua Pharmaceutical Company (Zhejiang, China) and Aldrich (Milwaukee, WI, U.S.A.) were tested in preliminary experiments and both exhibited the dual effects of intracellular Ca^{2+} release and blockade of Ca^{2+} entry. Subsequently in all the experiments shown in this work, TET from the Jing-Hua Pharmaceutical Company was employed. Hernandezine (HER) was a generous gift from Professor G.Z. Liu of the China-Japan Friendship Hospital (Beijing, China). Both TET and HER were dissolved in 0.1 N HCl to yield a stock solution of 30 mM. The amount of vehicle added to the reaction medium did not affect the medium pH or the fluorescence reading.

Statistical analysis

Results are expressed as mean ± s.e. Student's paired *t* test was employed and differences were considered significant when $P < 0.05$.

Results

Relationship between the TET- and TSG-releasable Ca^{2+} pool

Both TET and TSG concentration-dependently released intracellular Ca^{2+} of HL-60 cells (Figure 1a,b). It is noteworthy that there was a plateau phase of the TET-induced Ca^{2+} release, which was distinct from the transient TSG-induced Ca^{2+} release (see the Discussion section). The concentration-response curves are shown in Figure 1c. TSG was more efficacious than TET ($[Ca^{2+}]_i$ elevation of 110 nM vs 49 nM). Furthermore, TSG was much more potent than TET (EC_{50} value of 0.8 nM vs 20 μM).

We then investigated the relationship between the TET- and TSG-sensitive intracellular Ca^{2+} pool(s). It can be demonstrated that during the time course of the TET-induced Ca^{2+} release, the Ca^{2+} release by 30 nM TSG was progressively inhibited so that after around 20 min, TSG did not cause further Ca^{2+} release (Figure 2a–d). Similarly, TET could release no more Ca^{2+} after the cells had been challenged with 30 nM TSG (Figure 2e). A prolonged treatment with a suboptimal concentration (0.6 nM) of TSG also substantially inhibited TET-induced Ca^{2+} release (Figure 2f). The Ca^{2+} pool dischargeable by cyclopiazonic acid (CPA), another microsomal Ca^{2+} pump inhibitor chemically unrelated to TSG (Mason *et al.*, 1991; Kwan & Deng, 1991), exactly overlapped with the TSG-sensitive pool (Leung *et al.*, 1994). TET could release only a very small amount of Ca^{2+} after prolonged treatment with a suboptimal concentration (3 μM) of CPA (Figure 2g). Taken together, the results suggest the the TET-sensitive Ca^{2+} pool exactly overlapped with the TSG/CPA-dischargeable Ca^{2+} pool.

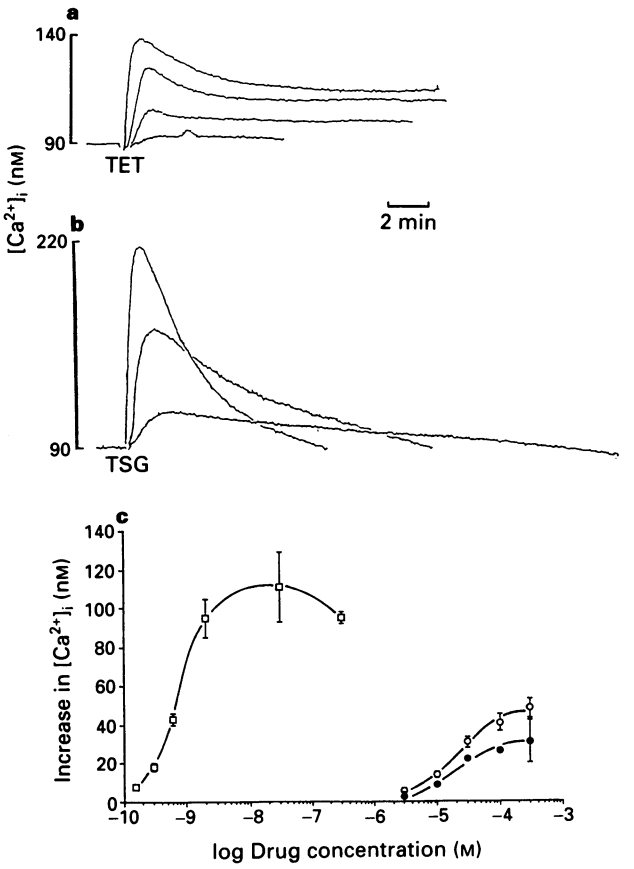


Figure 1 Ca^{2+} release elicited by TET and TSG. HL-60 cells in EGTA-supplemented Ca^{2+}-free HBSS were challenged with (a) various concentrations of TET (3, 10, 30 and 100 μM; from bottom trace to top), or (b) various concentrations of TSG (0.23, 0.6 and 30 nM; from bottom trace to top). Similar traces were obtained in at least 2 other separate experiments. Concentration-response curves of TSG (□) and TET (○, peak; ●, plateau phase) are shown in (c). Each point is the mean ± s.e. of 3–4 separate experiments. For abbreviations in this and subsequent legends, see text.

Roles of PK-C and α-adrenoceptors in TET-induced Ca^{2+} release?

There have been reports that suggest TET might affect PK-C activity (Ioannoni *et al.*, 1989; Kwan & Wang, 1993). We therefore tested whether TET released intracellular Ca^{2+} by activating or inhibiting PK-C. A brief treatment (3 min) with a PK-C activator, phorbol myristate acetate (PMA) (3 nM) caused a substantial (85 ± 6.7%; $n = 4$; $P < 0.05$) inhibition of ATP-induced Ca^{2+} release (Figure 3a,b). This inhibition could be readily reversed by a 5-min exposure to a PK-C inhibitor staurosporine (100 nM) before PMA treatment (Figure 3c). This indicates that staurosporine could significantly inhibit PK-C activity. Staurosporine did not qualitatively or quantitatively affect TET-induced Ca^{2+} release (Figure 3d,e). PMA (10 nM) caused almost complete (97.7 ± 0.3%; $n = 3$; $P < 0.05$) inhibition of ATP-induced Ca^{2+} release, but did not significantly suppress TET-induced Ca^{2+} release (87.5 ± 7.6% of the control value; $n = 3$; $P > 0.05$). These results suggest that TET-induced Ca^{2+} release was independent of PK-C activity. There has been evidence that TET could activate α_2-adrenoceptors in canine saphenous and mesenteric vein smooth muscles (Kwan & Wang, 1993). However, we can rule out the possible involvement of α_2-adrenoceptors in TET-induced Ca^{2+} release, since rauwolscine, an α_2-adrenoceptor antagonist, did not affect TET-induced Ca^{2+} release (95.9 ± 10.9% of the control value; $n = 3$; $P > 0.05$). Prazosin, an α_1-adrenoceptor antagonist also failed to affect TET-induced Ca^{2+} release (102.1 ± 7.1% of the control value; $n = 3$; $P > 0.05$).

TSG-induced Ca^{2+} entry could be blocked by TET, La^{3+} but not nifedipine

In a number of cells, depletion of intracellular Ca^{2+} stores stimulates Ca^{2+} entry into the cytosol (for reviews see Putney 1986; 1990). This 'capacitative Ca^{2+} entry' (CCE) also operates in HL-60 cells (Demaurex *et al.*, 1992; Alonso-Torre *et al.*, 1993). Emptying of intracellular Ca^{2+} stores by suboptimal concentrations of TSG or CPA induced a sustained Ca^{2+} entry upon Ca^{2+} readmission (Figure 4a,b). However, as shown in Figure 4c, TET did not induce any CCE (upper

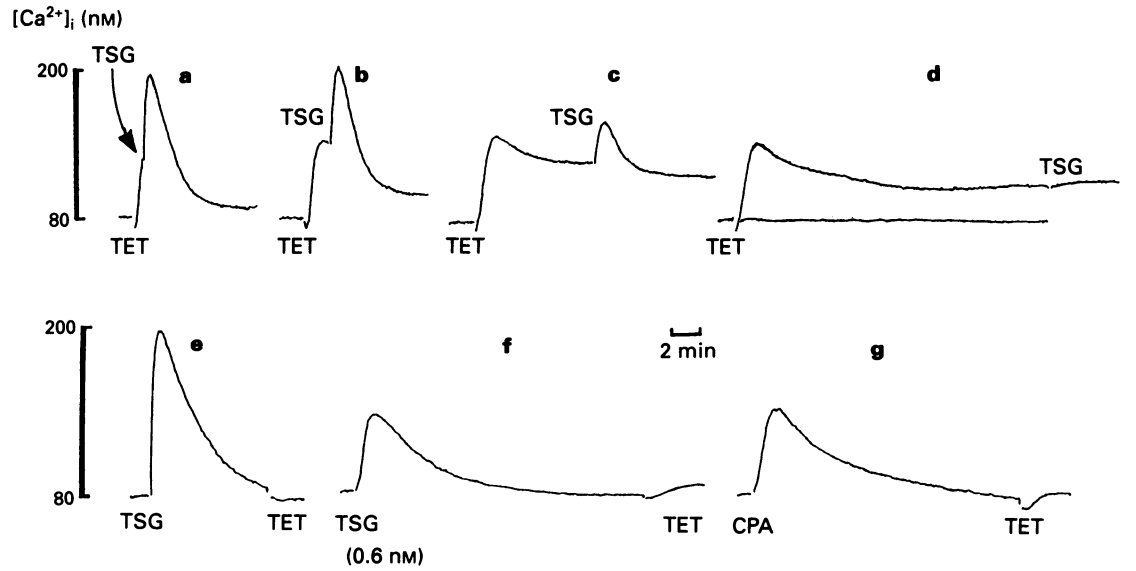


Figure 2 Relations of the TET-, TSG- and CPA-releasable pools. HL-60 cells in EGTA-supplemented Ca^{2+}-free HBSS were challenged with 100 μM TET and at different time points during the TET-induced Ca^{2+} release, 30 nM TSG was added (a–d). The lower trace in (d) was the baseline of the control (without any treatment with pharmacological agents). After Ca^{2+} release by 30 nM TSG (e), 0.6 nM TSG (f) or 3 μM CPA (g), 100 μM TET was added. Similar traces were obtained in 2 other separate experiments.

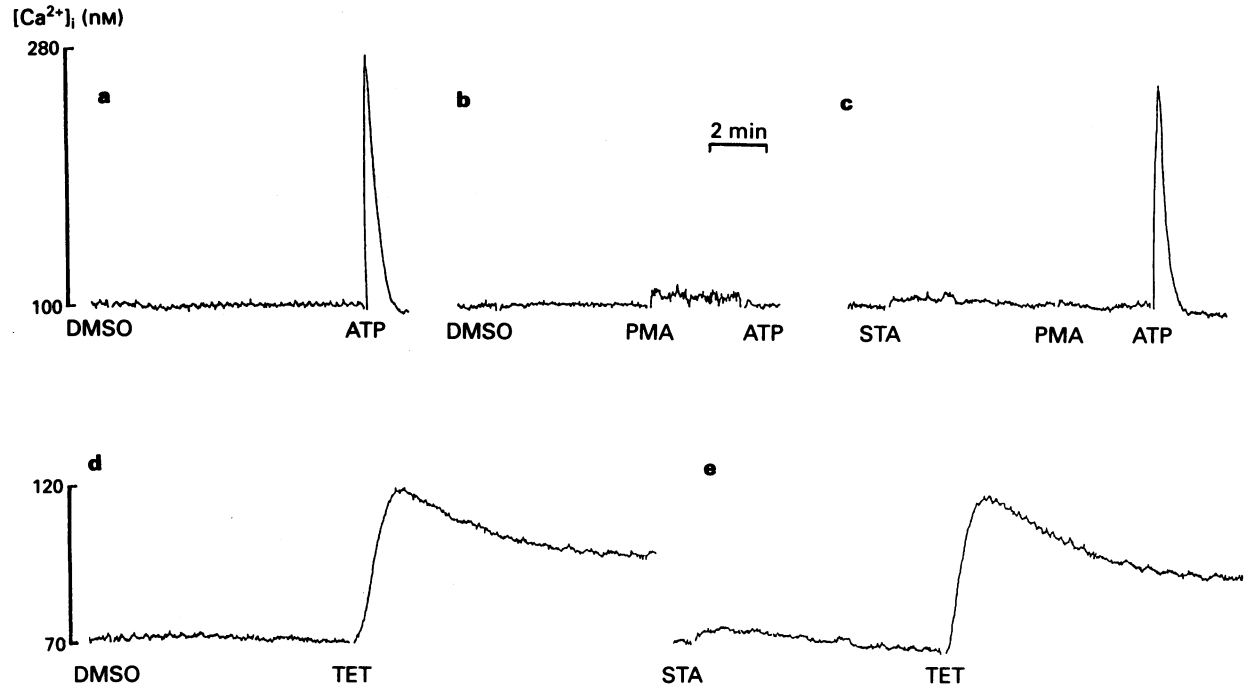


Figure 3 Effects of PMA and staurosporine (STA) on ATP- and TET-induced Ca^{2+} release. HL-60 cells in EGTA-supplemented Ca^{2+}-free HBSS were stimulated with 10 μM ATP (a); in (b), 10 μM ATP stimulation was preceded by 3 nM PMA treatment; and in (c), the inhibitory effect of PMA on ATP stimulation was reversed by 100 nM STA. 100 nM STA pretreatment did not affect TET-induced Ca^{2+} release (d and e). Similar traces were obtained in 2 other separate experiments.

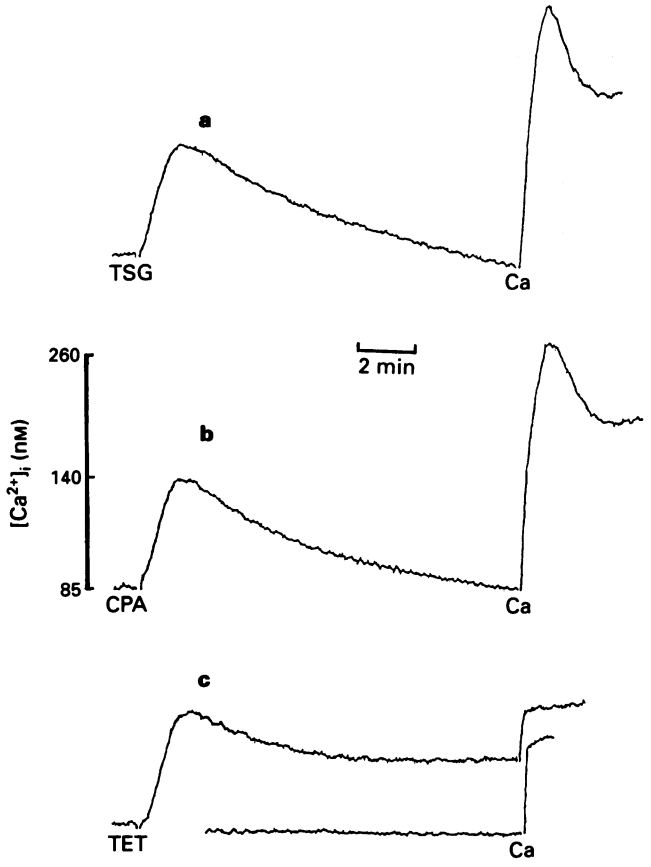


Figure 4 TET did not induce capacitative Ca^{2+} entry. HL-60 cells in EGTA-supplemented Ca^{2+}-free HBSS were treated with 0.6 nM TSG (a), 3 μM CPA (b), or 100 μM TET (c, upper trace) for approximately 12 min before readmission of 1.2 mM Ca^{2+}. In (c, lower trace), when 1.2 mM Ca^{2+} was readmitted to the control sample which had not been treated with any pharmacological agent, there was an increase in fluorescence. Similar traces were obtained in 2 other separate experiments.

trace): after TET-induced Ca^{2+} release, the increase in fluorescence upon Ca^{2+} readmission was unlikely to be Ca^{2+} entry, and was most possibly due to the saturation of leaked fura-2 with extracellular Ca^{2+} because such increase in fluorescence upon Ca^{2+} readmission was also observed even when there had not been any pretreatment (lower trace). The absence of CCE after TET-induced Ca^{2+} release suggests that TET might have blocked the CCE itself induced.

Results in Figure 5 show that TET blocked CCE induced by TSG. After Ca^{2+} release by TSG, addition of Ca^{2+} caused substantial and sustained Ca^{2+} entry, which could be abolished by TET pretreatment before Ca^{2+} readmission (Figure 5a,b). The fluorescence increase upon Ca^{2+} readmission in Figure 5a, as just explained, was most likely due to saturation of leaked fura-2 with Ca^{2+} (see Figure 5c). Using the protocol shown in Figure 5a, we obtained the concentration-inhibition curve for TET and estimated the IC_{50} of TET to be around 20 μM (Figure 6). That TET was able to inhibit CCE induced by TSG could also be observed if TET was added together with TSG (Figure 5d). In Ca^{2+}-containing medium, TSG caused a tonic elevation of $[Ca^{2+}]_i$ (Figure 5e). This tonic phase, presumably due to sustained Ca^{2+} entry, was abolished by TET. The biphasic $[Ca^{2+}]_i$ elevation induced by TSG in Ca^{2+}-containing medium was converted into a monophasic one if TET was added together with TSG (Figure 5f). The ability of TET to block TSG-induced CCE could also be demonstrated using the Mn^{2+} entry protocol (Figure 7). Addition of Mn^{2+} caused a gradual quench of fluorescence, which reflected basal Mn^{2+} entry. Treatment with TSG accelerated Mn^{2+} entry. TET substantially reduced basal Mn^{2+} entry and inhibited subsequent TSG-accerlerated Mn^{2+} entry. Basal Mn^{2+} entry was also substantially reduced if TET was added before Mn^{2+} (not shown).

The Ca^{2+} entry pathway activated by TSG-induced Ca^{2+} pool emptying, which have just been shown to be TET-sensitive, were pharmacologically characterized. The tonic phase of $[Ca^{2+}]_i$ elevation induced by TSG in Ca^{2+}-containing medium was not affected by the selective L-type Ca^{2+} channel antagonist nifedipine (NIF), but was abolished

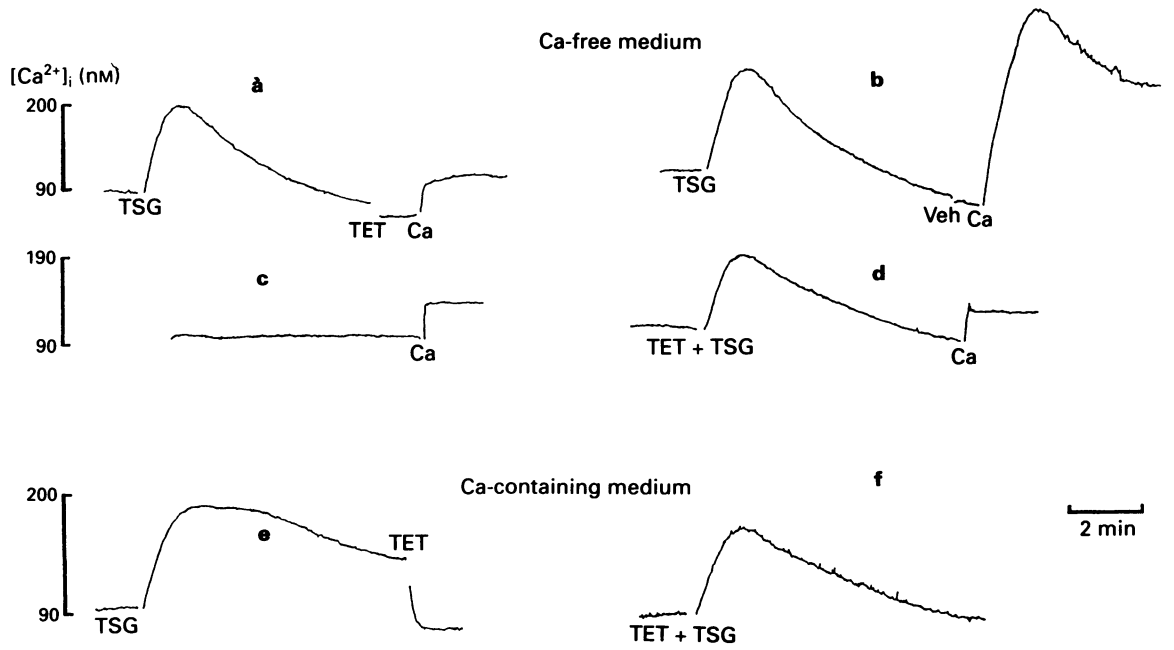


Figure 5 Blockade of TSG-induced Ca^{2+} entry by TET. Concentrations of TSG, TET, and Ca^{2+} used were 30 nM, 100 μM and 1.2 mM respectively. HL-60 cells in EGTA-supplemented Ca^{2+}-free HBSS were challenged with (a) TSG and then TET, (b) TSG and then vehicle (Veh; 6.7 μl 0.1 N HCl), or (d) TET and TSG simultaneously, before Ca^{2+} readmission. In (c), when Ca^{2+} was readmitted to the control sample which had not been treated with any pharmacological agent, there was an increase in fluorescence. Cells in Ca^{2+}-containing HBSS were exposed to TSG (e) or a combination of TSG and TET (f). In the former case, TET was added during the TSG-induced sustained $[Ca^{2+}]_i$ elevation. Similar traces were obtained in 2 other separate experiments.

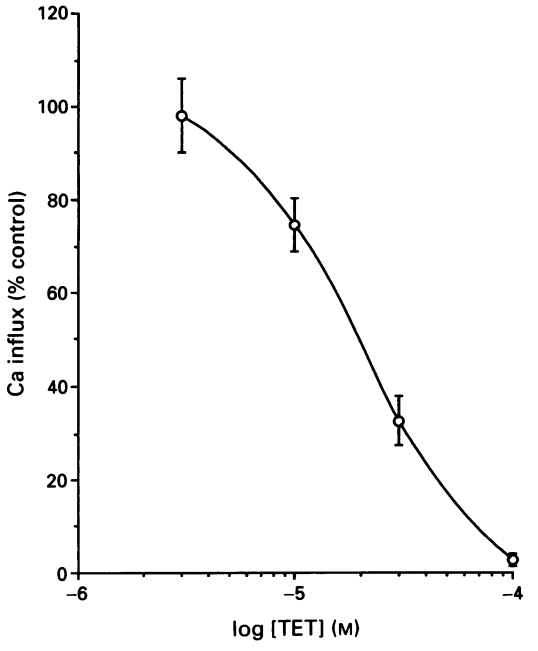


Figure 6 Concentration-dependent inhibitory effect of TET on TSG-induced Ca^{2+} entry. Using the protocol shown in Figure 5(a), various concentrations of TET were added after 30 nM TSG-induced Ca^{2+} release and before 1.2 mM Ca^{2+} readmission. The Ca^{2+} entry after TET treatment is expressed as a percentage of that of the control, in which only the vehicle (6.7 μl 0.1 N HCl) was added. Each point is the mean ± s.e. of 3 separate experiments.

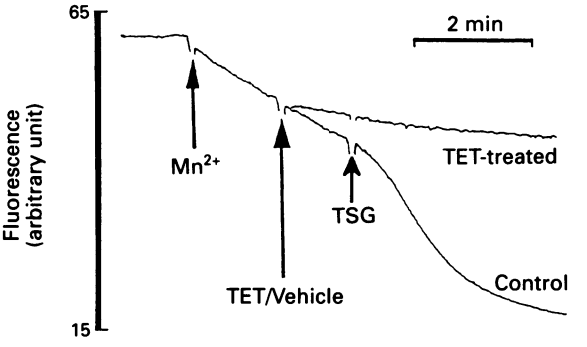


Figure 7 TET inhibited basal and TSG-stimulated Mn^{2+} entry. Addition of 0.5 mM Mn^{2+} to HL-60 cells in Ca^{2+}-free HBSS (without EGTA supplementation) caused a gradual quenching of fura-2 fluorescence at 360 nm excitation wavelength. Subsequently, cells were treated with vehicle (6.7 μl 0.1 N HCl) and then 30 nM TSG (lower trace), or 100 μM TET and then 30 nM TSG (upper trace). Similar traces were obtained in 2 other separate experiments.

by the non-selective Ca^{2+} channel blocker La^{3+} (Figure 8a). After TSG-induced Ca^{2+} release in Ca^{2+}-free medium, Ca^{2+} entry upon readmission of Ca^{2+} was not affected by prior treatment with NIF, but was abolished by La^{3+} (Figure 8b). Note that addition of La^{3+} after TSG-induced Ca^{2+} release in Ca^{2+}-free medium caused a fluorescence increase. This was most likely due to saturation of leaked fura-2 with La^{3+}, which has a fluorescence excitation spectrum qualitatively and quantitatively very similar to that of Ca^{2+} (Kwan & Putney, 1990).

Effects of TET and HER in HL-60 cells and M12.4 cells

The effects of hernandezine (HER), a compound chemically closely related to TET, on $[Ca^{2+}]_i$ homeostasis of HL-60 cells were examined. This compound, like TET, also induced a tonic phase of Ca^{2+} release and abolished the sustained TSG-induced $[Ca^{2+}]_i$ elevation in Ca^{2+}-containing medium (Figure 9a,b). Both TET and HER were able to exercise the dual effects of Ca^{2+} release and blockade of Ca^{2+} entry in another cell system (murine B lymphoma M12.4 cells) (Figure 9c–f). However, it is noteworthy that Ca^{2+} release induced by both compounds was less sustained and the

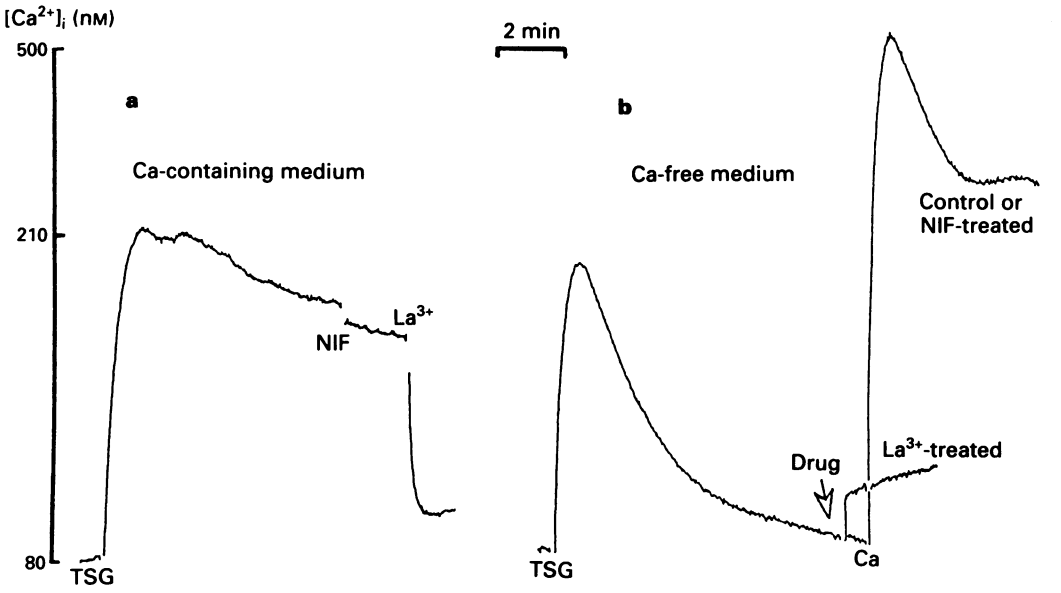


Figure 8 The TSG-induced Ca^{2+} entry pathway in HL-60 cells was inhibited by La^{3+} but insensitive to nifedipine (NIF). In (a), the TSG-induced sustained $[Ca^{2+}]_i$ elevation in Ca^{2+}-containing HBSS was insensitive to 1 μM NIF but abolished by 300 μM La^{3+}. In (b), cells in EGTA-supplemented Ca^{2+}-free HBSS were stimulated with 30 nM TSG. Subsequently, either 1 μM NIF or 300 μM La^{3+} was added before 1.2 mM Ca^{2+} readmission. The pattern and magnitude of Ca^{2+} entry in the control (no drug treatment) or after nifedipine treatment were nearly identical. Similar traces were obtained in at least 2 other separate experiments.

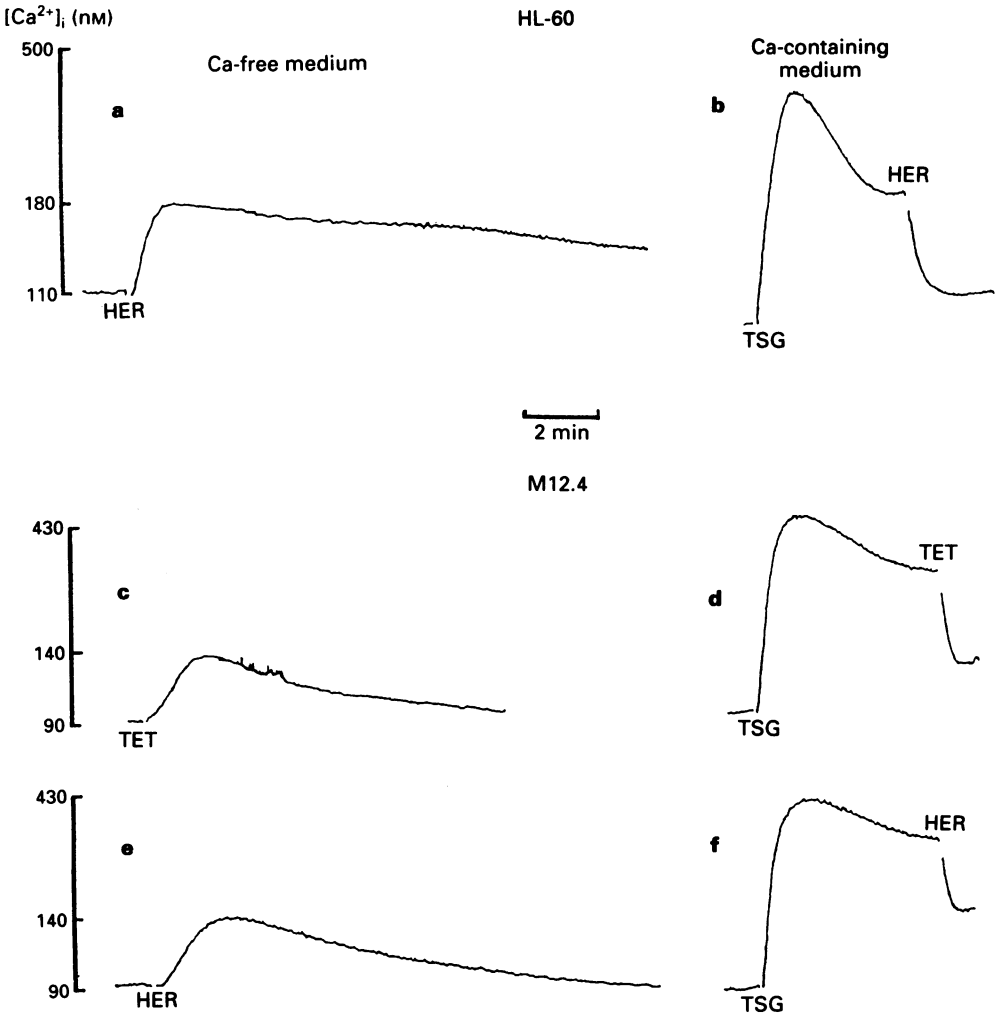


Figure 9 The dual effects of HER in HL-60 cells and those of HER and TET in M12.4 cells. In (a), HL-60 cells in EGTA-supplemented Ca^{2+}-free HBSS were challenged with 100 μM HER. In (c) and (e), M12.4 cells in EGTA-supplemented Ca^{2+}-free HBSS were challenged with 100 μM TET and 100 μM HER, respectively. In (b), where HL-60 cells were suspended in Ca^{2+}-containing HBSS, 100 μM HER was added during the 30 nM TSG-induced sustained $[Ca^{2+}]_i$ elevation. In (d) and (f), where M12.4 cells were suspended in Ca^{2+}-containing HBSS, 100 μM TET and 100 μM HER, respectively, were added during the 3 nM TSG-induced sustained $[Ca^{2+}]_i$ elevation. Similar traces were obtained in 2 other separate experiments.

blockade of Ca^{2+} entry by both compounds was only partial in M12.4 cells compared to those in HL-60 cells.

Discussion

Our work describes two novel pharmacological actions of TET, namely, mobilization of intracellular Ca^{2+} and blockade of capacitative Ca^{2+} entry induced by TSG. It is unlikely that TET released intracellular Ca^{2+} by opening the ryanodine-sensitive channel (Ca^{2+}-induced Ca^{2+} release channel) since ryanodine (0.1–10 μM) and caffeine (10 mM) did not cause any Ca^{2+} release in HL-60 cells (results not shown). It also does not seem that TET induced Ca^{2+} release by activating the IP_3 receptor-channel because of the following reasons: (1) IP_3-induced Ca^{2+} release (see, for example, the ATP-induced Ca^{2+} release shown in Figure 3) is characteristically very fast (peaking within seconds) and transient ($[Ca^{2+}]_i$ returning to basal level within 1–2 min). But the TET-induced Ca^{2+} release was relatively slow and long-lasting. (2) The IP_3-releasable pool was only a very minor fraction of the TSG-sensitive pool (Leung *et al.*, 1994). It is demonstrated here that the TSG-sensitive pool could be discharged fully by TET. The latter phenomenon, together with the almost identical initial kinetics of Ca^{2+} release by TET, TSG (0.6 nM), and CPA (3 μM), suggest that TET might cause Ca^{2+} release by inhibiting the microsomal Ca^{2+} pump. If it is the case, the lower efficacy of TET than TSG suggests that TET could not fully inhibit the microsomal Ca^{2+} pump.

It is obvious that the TET- and TSG-dischargeable Ca^{2+} pool exactly overlapped. However, it is difficult to explain why there was a sustained phase of TET-induced Ca^{2+} release in HL-60 cells (but not in M12.4 cells), a phenomenon in contrast to the transient TSG-induced Ca^{2+} release, irregardless of the concentration of TSG used. Given sufficient time, a suboptimal concentration (0.6 nM) of TSG could almost completely empty the TSG-sensitive pool: addition of TET afterwards did not release much Ca^{2+}. This indicates that most of the Ca^{2+} released was not recycled back into the pool, but was rather removed into the extracellular space (Ca^{2+} efflux). Given enough time, TET was also able to empty totally the TSG-sensitive pool, again implying that released Ca^{2+} was not recycled back into the pool. But in this case, $[Ca^{2+}]_i$ remained well above basal level, hinting that, to a certain extent, Ca^{2+} efflux was prevented. Therefore, TET might also inhibit Ca^{2+} efflux mechanism(s). If it is true that TET also inhibited Ca^{2+} efflux in HL-60 cells, it is puzzling why adding TET together with TSG (30 nM) did not produce a sustained phase of Ca^{2+} release. Also, it is interesting to note that after exposure to TET, the earlier TSG was added, the closer the $[Ca^{2+}]_i$ returned to basal level. We have not studied these phenomena further, and the only explanation we could offer is that perhaps TET does have a moderate inhibitory effect on Ca^{2+} efflux in HL-60 cells, but the high $[Ca^{2+}]_i$ raised by 30 nM TSG strongly activated Ca^{2+} efflux and dominated the inhibitory effect of TET.

Recently, it was shown that TET relaxed KCl-induced contraction in canine saphenous and mesenteric veins, and surprisingly, a transient contraction developed upon washout of KCl (Kwan & Wang, 1993). Such TET-induced contraction is believed to be mediated via α_2-adrenoceptor activation since rauwolscine (an α_2-antagonist), but not prazosin (an α_1-antagonist), abolished such contraction. However, our data do not suggest any involvement of α_2-adrenoceptor in TET-induced Ca^{2+} release. Data from Kwan & Wang (1993) also suggest that TET-induced contraction may result from the activation of the Na^+/H^+ exchanger, which could be a substrate of PK-C. It has been shown that TET could inhibit the activity of PK-C in human lymphocytes (Ioannoni *et al.*, 1989). Since we observed that the PK-C activator PMA and the PK-C inhibitor, staurosporine, did not have any significant effect on TET-induced Ca^{2+} release, we conclude that the latter is independent of PK-C activity.

That TET caused Ca^{2+} release, but did not induce any capacitative Ca^{2+} entry due to the emptying of the Ca^{2+} store, is not unexpected because TET exerts non-selective Ca^{2+} antagonistic actions: it blocks not only voltage-operated Ca^{2+} channels (King *et al.*, 1988; Liu *et al.*, 1991; 1992; Rossier *et al.*, 1993), but also voltage-insensitive Ca^{2+} entry (Kwan *et al.*, 1992). We show here in HL-60 cells that TET blocked the TSG-induced Ca^{2+} entry, which was via a La^{3+}-sensitive but nifedipine-insensitive Ca^{2+}-permeable pathway. We have also observed that there was no $[Ca^{2+}]_i$ elevation in response to high KCl-induced depolarization in Ca^{2+}-containing medium (not shown), indicating the lack of functional voltage-operated Ca^{2+} channels in HL-60 cells. Taken together, these data further confirm that TET is a non-selective Ca^{2+} antagonist.

Hernandezine (HER), a compound chemically very close to TET, and reportedly eliciting Ca^{2+} antagonistic effect in platelets (Ma *et al.*, 1991), also behaved similarly to TET in HL-60 cells. Furthermore, both compounds also blocked Ca^{2+} entry and caused Ca^{2+} release in M12.4 cells. Thus, the dual effects of TET and HER do not seem to exhibit cell-specificity. We are unable to tell whether TET-induced contraction in canine saphenous and mesenteric veins (Kwan & Wang, 1993) and slight $[Ca^{2+}]_i$ elevation in rat alveolar type II cells (Miles *et al.*, 1993) were due to internal Ca^{2+} release or not. It is because these phenomena were observed in Ca^{2+}-containing medium, therefore, the source of $[Ca^{2+}]_i$ elevation could be extracellular. But certainly TET does not cause Ca^{2+} release in all kinds of cells, for example, it did not release Ca^{2+} from intracellular stores of rat neutrophils (Hong *et al.*, 1989) and bovine adrenal glomerulosa cells (Rossier *et al.*, 1993).

Although TET, as a hypotensive agent, is inferior to the more selective and potent drugs like nifedipine and verapamil, it has been shown to be a clinically effective drug in the treatment of silicosis (Li *et al.*, 1981), a disease that hitherto has not been successfully under control by any conventional immunosupressive drugs. Undoubtedly, the molecular mechanism(s) by which TET acts on fibroblasts, the key cells in the formation of silicosis, warrants future investigation. With respect to the basic pharmacological research, it has already been demonstrated that TET could block not only L- and T-type Ca^{2+} channels (King *et al.*, 1988; Liu *et al.*, 1991; 1992; Rossier *et al.*, 1993), but also receptor-mediated Ca^{2+} entry (Kwan *et al.*, 1992). Here we show that TET also (1) released intracellular Ca^{2+}, probably by inhibiting microsomal Ca^{2+} pumps, and (2) blocked voltage-insensitive Ca^{2+} entry activated by TSG. Therefore, although TET itself may have limitations as a pharmacological tool for investigation of $[Ca^{2+}]_i$ homeostatic mechanisms, it could well be a promising lead compound for the synthesis of analogues that may serve as selective pharmacological probes for voltage-insensitive receptor-mediated Ca^{2+} entry or microsomal Ca^{2+} pumps.

The authors are grateful to Mr W.B. Wong for technical assistance. The work was supported by a UPGC grant No. 338-034-0003 and a CRCG grant No. 335/034/0058.

References

ALONSO-TORRE, S.R., ALVAREZ, J., MONTERO, M., SANCHEZ, A. & GARCIA-SANCHO, J. (1993). Control of Ca^{2+} entry into HL-60 and U937 human leukaemia cells by the filling state of the intracellular Ca^{2+} stores. *Biochem. J.*, **289**, 761–766.

DEMAUREX, N., LEW, D.P. & KRAUSE, K.-H. (1992). Cyclopiazonic acid depletes intracellular Ca^{2+} stores and activates an influx pathway for divalent cations in HL-60 cells. *J. Biol. Chem.*, **267**, 2318–2324.

FANG, D.C. & JIANG, M.X. (1986). A new calcium antagonist of Chinese medicinal origin: tetrandrine. *J. Hypertension*, **4** (suppl 6), S150–S152.

FERRANTE, S., SEOW, W.K., ROWAN-KELLY, B. & THONG, Y.H. (1990). Tetrandrine, a plant alkaloid, inhibits the production of tumour necrosis factor-alpha (cachectin) by human monocytes. *Clin. Exp. Immunol*, **80**, 232–235.

GAO, Y., CHANG, M.Y., MAO, H.Y., CHAO, H.Y. & CHEN, D.H. (1965). The clinical observation of tetrandrine in the treatment of 270 cases by hypertensive patients and hypertensive crisis. *J. Clin. Intern. Med.*, **13**, 504–507.

GRYNKIEWICZ, G., POENIE, M. & TSIEN, R.Y. (1985). A new generation of Ca^{2+} indicators with greatly improved fluorescence properties. *J. Biol. Chem.*, **260**, 3440–3450.

HONG, J.L., ZHOU, H.L. & BIAN, R.L. (1989). Effects of tetrandrine on cytoplasmic free calcium in rat neutrophils. *Acta Pharmacol. Sin.*, **10**, 533–537.

IOANNONI, B., CHALMERS, A.H., SEOW, W.K., MCCORMACK, J.G. & THONG, Y.H. (1989). Tetrandrine and transmembrane signal transduction: effect on phosphoinositide metabolism, calcium flux and protein kinase C translocation in human lymphocytes. *Int. Arch. Allergy Appl. Immunol.*, **89**, 349–354.

JIA, J.F., GAO, N.N., XIA, G.J., LUO, Q.F., FANG, D.C. & JIANG, M.X. (1985). Studies on the calcium antagonistic action of tetrandrine: IX. Effects of tetrandrine on contractility of isolated swine coronary artery strips. *Acta Acad. Med. Wuhan.*, **5**, 15–19.

KING, V.F., GARCIA, M.L., HIMMEL, D., REUBEN, J.P., LAM, Y.K.T., PAN, J.X., HAN, G.Q. & KACZOROWSKI, G.J. (1988). Interaction of tetrandrine with slowly inactivating calcium channels. Characterization of calcium channel modulation by an alkaloid of Chinese medicinal herb origin. *J. Biol. Chem.*, **263**, 2238–2244.

KWAN, C.Y. & DENG, H.W. (1991). Cyclopiazonic acid is a sarcoplasmic reticulum Ca^{2+} pump inhibitor of rat aortic muscle. *Acta Pharmacol. Sin.*, **12**, 53–58.

KWAN, C.Y., DENG, H.W. & GUAN, Y.Y. (1992). Tetrandrine is not a selective calcium channel blocker in vascular smooth muscle. *Acta Pharmacol. Sin.*, **13**, 385–390.

KWAN, C.Y. & PUTNEY, J.W. Jr. (1990). Uptake and intracellular sequestration of divalent cations in resting and methacholine-stimulated mouse lacrimal acinar cells. *J. Biol. Chem.*, **265**, 678–684.

KWAN, C.Y. & WANG, Z.L. (1993). Tetrandrine: a vasodilator of medicinal herb origin with a novel contractile effect on dog saphenous vein. *Eur. J. Pharmacol.*, **238**, 431–434.

LAMBERT, D.G. & NAHORSKI, S.R. (1990). Muscarinic-receptor-mediated changes in intracellular Ca^{2+} and inositol 1,4,5-trisphosphate mass in a human neuroblastoma cell line, SH-SY5Y. *Biochem. J.*, **265**, 555–562.

LEUNG, Y.M., KWAN, C.Y. & LOH, T.T. (1994). Cytosolic calcium pre-elevation amplifies agonist-induced calcium release in human leukemic HL-60 cells. *Biochem. J.* (in press).

LI, Q.L., XU, Y.H., ZHON, Z.H., CHEN, X.W., HUANG, X.G., CHEN, S.L. & ZHAN, C.X. (1981). The therapeutic effect of tetrandrine on silicosis. *Chin. J. Tuberc. Resp. Dis.*, **4**, 321–328.

LIU, B.C., ZOU, C.G. & LI, Y.R. (1983). Studies of the contents of glycosaminoglycans from lungs of silicotic rats and tetrandrine-treated silicotic rats. *Ecotoxicol. Environ. Safety*, **7**, 323–329.

LIU, Q.Y., KARPINSKI, E. & PANG, P.K.T. (1992). Tetrandrine inhibits both T and L calcium channel currents in ventricular cells. *J. Cardiovasc. Pharmacol.*, **20**, 513–519.

LIU, Q.Y., KARPINSKI, E., RAO, M.R. & PANG, P.K.T. (1991). Tetrandrine: a novel calcium channel antagonist inhibits type I calcium channels in neuroblastoma cells. *Neuropharmacology*, **30**, 1325–1331.

LYTTON, J., WESTLIN, M. & HANLEY, M.R. (1991). Thapsigargin inhibits the sarcoplasmic or endoplasmic reticulum Ca-ATPase family of calcium pumps. *J. Biol. Chem.*, **266**, 17067–17071.

MA, L.J., YIN, Z.Z. & LIU, G.Z. (1991). Effect of hernandezine on platelet aggregation and its mechanism of action. *Chin. J. Pharmacol. Toxicol.*, **5**, 41–43.

MASON, M.J., GARCIA-RODRIGUEZ, C. & GRINSTEIN, S. (1991). Coupling between intracellular Ca stores and the Ca permeability of the plasma membrane. Comparison of the effects of thapsigargin, 2,5-di-(tert-butyl)-1,4-hydroquinone, and cyclopiazonic acid in rat thymic lymphocytes. *J. Biol. Chem.*, **266**, 20856–20862.

MERRITT, J.E., JACOB, R. & HALLAM, T.J. (1989). Use of manganese to discriminate between calcium influx and mobilization from internal stores in stimulated human neutrophils. *J. Biol. Chem.*, **264**, 1522–1527.

MILES, P.R., BOWMAN, L., MA, J.K.H. & MA, J.Y.C. (1993). Alterations in alveolar type II cell metabolism induced by tetrandrine and other alkaloids. *Toxicol. Appl. Pharmacol.*, **119**, 142–149.

PUTNEY, J.W. Jr. (1986). A model for receptor-regulated calcium entry. *Cell Calcium.*, **7**, 1–12.

PUTNEY, J.W. Jr. (1990). Capacitative calcium entry revisited. *Cell Calcium*, **11**, 611–624.

QIAN, J.Q., THOOLEN, M.J.M.C., VAN MEEL, J.C.A., TIMMERMANS, P.B.M.W.M. & VAN ZWIETEN, P.A. (1983). Hypotensive activity of tetrandrine in rats. Investigation into its mode of action. *Pharmacology*, **26**, 187–197.

REIST, R.H., DEY, R.D., DURHAM, J.P., ROJANASAKUL, Y. & CASTRANOVA, V. (1993). Inhibition of proliferative activity of pulmonary fibroblasts by tetrandrine. *Toxicol. Appl. Pharmacol.*, **122**, 70–76.

ROSSIER, M.F., PYTHON, C.P., CAPPONI, A.M., SCHLEGEL, W., KWAN, C.Y. & VALLOTTON, M.B. (1993). Blocking T-type calcium channels with tetrandrine inhibits steroidogenesis in bovine adrenal glomerulosa cells. *Endocrinology*, **132**, 1035–1043.

SEOW, W.K., FERRANTE, A., GOH, D.B.H., CHALMERS, A.H., LI, S.Y. & THONG, Y.H. (1988). In vitro immunosuppressive properties of the plant alkaloid tetrandrine. *Int. Arch. Allergy Appl. Immunol.*, **85**, 410–415.

SEOW, W.K., LI, S.Y. & THONG, Y.H. (1986). Inhibitory effects of tetrandrine on human neutrophil and monocyte adherence. *Immunol. Lett.*, **13**, 83–88.

TEH, B.S., SEOW, W.K., CHALMERS, A.H., PLAYFORD, S., IOANNONI, B. & THONG, Y.H. (1988). Inhibition of histamine release from rat mast cells by the plant alkaloid tetrandrine. *Int. Arch. Allergy Appl. Immunol.*, **86**, 220–224.

THASTRUP, O., CULLEN, P.J., DROBAK, B.K., HANLEY, M.R. & DAWSON, A.P. (1990). Thaspsigargin, a tumor promoter, discharges intracellular Ca^{2+} stores by specific inhibition of the endoplasmic reticulum Ca^{2+}-ATPase. *Proc. Natl. Acad. Sci. U.S.A.*, **87**, 2466–2470.

YU, X.F., ZOU, C.G. & LIH, M.B. (1983). Observations of the effect of tetrandrine on experimental silicosis of rats. *Ecotoxicol. Environ. Safety*, **7**, 306–312.

(Received April 25, 1994
Revised June 13, 1994
Accepted June 29, 1994)

Br. J. Pharmacol. (1994), **113**, 775–780 © Macmillan Press Ltd, 1994

Antagonism by (R)- and (S)-trihexyphenidyl of muscarinic stimulation of adenylyl cyclase in rat olfactory bulb and inhibition in striatum and heart

[1]Pierluigi Onali, *Arne J. Aasen & Maria C. Olianas

Section on Biochemical Pharmacology, Department of Neurosciences, University of Cagliari, 09124 Cagliari, Italy and *Department of Pharmacy, University of Oslo, 0316 Oslo 3, Norway

1 Activation of muscarinic receptors in rat olfactory bulb stimulates adenylyl cyclase activity. This response was competitively antagonized by the (R)- and (S)-enantiomers of trihexyphenidyl with pA_2 values of 8.84 and 6.09, respectively.

2 Similarly, in rat striatal homogenates, muscarinic inhibition of adenylyl cyclase activity was antagonized by the (R)- and (S)-enantiomers with pA_2 values of 8.75 and 6.12, respectively.

3 In contrast, in rat myocardium the muscarinic inhibition of the adenosine 3':5'-cyclic monophosphate (cyclic AMP) formation was more weakly antagonized by trihexyphenidyl, with a particularly marked loss (15 fold) in activity of the (R)-enantiomer. The (R)- and (S)-enantiomers had pA_2 values of 7.64 and 5.72, respectively.

4 Each muscarinic response was completely antagonized by increasing concentrations of (R)-trihexyphenidyl with a Hill coefficient not significantly different from unity.

5 The present study shows that the muscarinic receptors coupled to stimulation of adenylyl cyclase in the olfactory bulb display high stereoselectivity for the enantiomers of trihexyphenidyl. The affinities of these receptors for the antagonists are similar to those shown by the striatal receptors. This finding supports the hypothesis that both the muscarinic stimulation of adenylyl cyclase in the olfactory bulb and the muscarinic inhibition of the enzyme in striatum are mediated by activation of a receptor subtype pharmacologically equivalent to the m4 gene product. On the other hand, the weaker affinities and the lower stereoselectivity for the trihexyphenidyl enantiomers exhibited by the muscarinic inhibition of adenylyl cyclase in the heart are consistent with the involvement of M_2 receptors in this response.

Keywords: Trihexyphenidyl enantiomers; muscarinic receptor subtypes; cyclic AMP; adenylyl cyclase; rat heart, rat striatum; rat olfactory bulb

Introduction

Activation of muscarinic cholinoceptor has been reported to inhibit adenylyl cyclase activity in different rat brain areas, such as corpus striatum (Olianas *et al.*, 1983), cerebral cortex (McKinney *et al.*, 1991) and hippocampus (Vickroy & Cadman, 1989). However, in rat olfactory bulb, muscarinic receptor agonists cause stimulation, rather than inhibition, of basal adenylyl cyclase activity (Onali & Olianas, 1990). The muscarinic stimulation does not require Ca^{2+} (Olianas & Onali, 1990), is prevented by *in vivo* treatment with pertussis toxin (Olianas & Onali, 1992) and is enhanced by concurrent activation of the enzyme by G_s-coupled neurotransmitter receptors (Olianas & Onali, 1993a). Unlike the muscarinic stimulation of adenosine 3':5'-cyclic monophosphate (cyclic AMP) accumulation described in cells either transfected with the muscarinic m1 receptor gene (Felder *et al.*, 1989) or naturally expressing the M_3 receptor subtype (Baumgold *et al.*, 1992), the muscarinic stimulation of adenylyl cyclase in rat olfactory bulb occurs independently of activation of phosphoinositide hydrolysis (Olianas & Onali, 1993b) and may result from a direct coupling of the receptors to the catalyst through guanosine-5'-triphosphate (GTP) binding regulatory proteins of the G_o/G_i family (Olianas & Onali, 1993a).

The pharmacological properties of the muscarinic receptors involved in this unique response appear different from those typically displayed by the M_1, M_2 and M_3 receptor subtypes. In fact, the muscarinic stimulation of adenylyl cyclase activity of rat olfactory bulb is highly sensitive to either classical M_2 antagonists, such as methoctramine and AF-DX 116, or M_3 antagonists, such as hexahydrosiladiphenidol and *p*-fluorohexahydrosiladiphenidol, and is moderately sensitive to the M_1 antagonists, pirenzepine (Olianas & Onali, 1991). The data so far accumulated have led to the hypothesis that the predominant receptor involved may be pharmacologically equivalent to the m4 gene product (M_4) (Olianas & Onali, 1991). However, because selective M_4 antagonists are not currently available, the characterization of the receptor subtype(s) involved requires the comparison amongst the increasing number of drugs which can discriminate between subtypes and with other responses with well characterized pharmacological profiles. Muscarinic receptor subtypes can be differentiated on the basis of their stereoselective interaction with chiral antagonists (Waelbroeck *et al.*, 1989). For the antimuscarinic drug, trihexyphenidyl, the ratio between the potencies of the (R)- and (S)-enantiomer, the eudismic ratio (Lehmann, 1986), has been found to differ markedly when the compounds were tested as antagonists of functional responses mediated by M_1, M_2 and M_3 receptors (Lambrecht *et al.*, 1988). Moreover, in radioligand binding studies employing the five cloned muscarinic receptors subtypes, (R)-trihexyphenidyl has been found to display high affinity for the m1 and m4 and low affinity for the m2 and m5 subtypes (Dorje *et al.*, 1991). In the present study we have investigated the sensitivity of the muscarinic stimulation of adenylyl cyclase in rat olfactory bulb to the antagonistic activity of the trihexyphenidyl enantiomers. For comparison, the compounds were also tested on the muscarinic inhibition of adenylyl cyclase in rat striatum and myocardium.

[1] Author for correspondence.

Methods

Tissue homogenization

Hearts, olfactory bulbs and striata were obtained from male Sprague-Dawley rats (200–350 g) killed by decapitation. Crude membrane preparations were obtained from each tissue according to the following procedures.

Hearts were perfused *in situ* with ice-cold saline solution, excised and minced with a razor blade. The tissue was homogenized in 10 volumes (v/w) of an ice-cold hypotonic homogenization buffer containing 10 mM 4-(2-hydroxyethyl)-1-piperazine-ethanesulphonic acid (HEPES)/NaOH, 1 mM ethylene glycol *bis* (β-aminoethyl ether)-*N,N'*-tetraacetic acid (EGTA), 1 mM $MgCl_2$ and 1 mM dithiothreitol (DTT) (pH 7.4) in a Polytron. The homogenate was filtered through two layers of gauze and centrifuged at 1,000 *g* for 10 min at 4°C. The supernatant was discarded and the pellet resuspended in 10 volumes of homogenization buffer. The tissue suspension was centrifuged at 28,000 *g* for 10 min at 4°C and the final pellet was resuspended in the same buffer at a protein concentration of 5.0 to 6.5 mg ml^{-1}.

Olfactory bulbs were rapidly dissected from the brain, stripped of meninges and homogenized by hand in 10 volumes of ice-cold hypotonic homogenization buffer. The homogenate was diluted six fold and centrifuged at 27,000 *g* for 20 min at 4°C. The pellet was resuspended in the same buffer and centrifuged as above. The final pellet was resuspended to a protein concentration of 1.0 to 1.5 mg ml^{-1}, incubated for 5 to 10 min in an ice-bath and then used for adenylyl cyclase assay. Striata were homogenized in 10 volumes of an ice-cold isotonic buffer containing 0.32 M sucrose, 10 mM HEPES/NaOH, 1 mM EGTA and 1 mM DTT (pH 7.4). The homogenate was diluted twofold and centrifuged at 1,000 *g* for 10 min at 4°C. The supernatant was aspirated and centrifuged at 11,000 *g* for 20 min at 4°C. The pellet was resuspended in 40 volumes of ice-cold hypotonic buffer containing all the constituents of the homogenization buffer except sucrose. The tissues was then centrifuged at 27,000 *g* for 20 min at 4°C and the final pellet was resuspended in hypotonic buffer to a protein concentration of 1.2 to 1.6 mg ml^{-1}. For each tissue, at lest three separate membrane preparations were tested.

Adenylyl cyclase activity

The enzyme activity was assayed in a 100 μl reaction mixture containing 50 mM HEPES/NaOH buffer (pH 7.4), 2.3 mM $MgCl_2$, 1.3 mM DTT, 0.3 mM EGTA 0.2 mM [α-^{32}P]adenosine-5'-triphosphate (ATP) (45–60 c.p.m. $pmol^{-1}$), 1 mM [^{3}H]-cyclic AMP (80 c.p.m. $nmol^{-1}$), 1 mM 3-isobutyl-1-methylxanthine, 5 mM phosphocreatine, 50 u ml^{-1} of creatine kinase, 100 μM GTP, 50 μg of bovine serum albumin, 10 μg of bacitracin, 10 kallikrein inhibitor units of aprotinin and 10 μM physostigmine. When the enzyme activity was assayed in the myocardium and striatum, the concentration of [α-^{32}P]ATP was 0.05 mM and 10 μM forskolin, a direct stimulator of adenylyl cyclase, was added to the reaction mixture to amplify the muscarinic inhibition. The incubation was started by adding the tissue preparation (40–70 μg of protein) and was carried out at 30°C for 10 min. [^{32}P]-cyclic AMP was isolated as described by Salomon *et al.* (1974).

Protein content was determined by the method of Bradford (1976), with bovine serum albumin used as a standard.

Statistical analysis

Results are reported as mean ± standard error of the mean (s.e.mean). Agonist concentration-response curves were analysed by a least squares curve fitting computer programme (Graph-Pad, ISI, Philadelphia, PA, U.S.A.). The antagonist effects were examined according to Schild analysis (Schild, 1947) and the potency of each antagonist was determined from the ratios between the EC_{50} values of the agonist estimated in the absence and in the presence of multiple concentrations of the antagonist. The pA_2 values were determined from the x intercepts and calculated by least squares regression analysis of the Schild plots, where the log of the dose ratios (DR) − 1 is plotted as a function of the antagonist concentration. The (**R**)-enantiomer was also tested for its ability to reverse completely the agonist response. In these experiments the effects of multiple concentrations of the antagonist on the response elicited by a fixed concentration of the agonist were determined. The data were analysed as competition curves by nonlinear regression analysis for models of one or two noninteracting sites. The antagonist inhibitory constant (K_i) was calculated according to the equation:

$$K_i = IC_{50}/1 + (A/EC_{50}) \quad (1)$$

where IC_{50} is the concentration of the antagonist producing half-maximal inhibition; A is the concentration of the agonist and EC_{50} is the agonist concentration producing half-maximal effect. The goodness of fit of the data to a one- versus a two site-model was evaluated by the *F* test of the sum of squares of residuals from both fittings considering a level of significance of $P<0.05$. For the easier comparison with the pA_2 values, K_i values were converted to the logarithmic form (pK_i). Statistical significance of the difference between means was determined by Student's *t* test.

Drugs

[α^{32}P]-ATP (30–40 Ci $mmol^{-1}$) and [2,8-^{3}H]-cyclic AMP (25 Ci $mmol^{-1}$) were purchased from Du Pont de Nemours (Bad Homburg, Germany). Forskolin was from Calbiochem (La Jolla, CA, U.S.A.). The enantiomers of trihexyphenidyl were synthesized in the laboratory of A.J.A. The absolute configurations of the (−)- and (+)-enantiomers are (**R**) and (**S**), respectively (Schjelderup *et al.*, 1987). Based on optical activity measurements, the enantiomeric excesses were estimated to be: (**R**)-(−)-trihexyphenidyl 99%, (**S**)-(+)-trihexyphenidyl 98%. Both enantiomers were in the hydrochloride form and were dissolved in distilled water. Physostigmine sulphate, acetylcholine hydrochloride (ACh) and the other compounds used for the adenylyl cyclase assay were purchased from Sigma Chemical Co. (St. Louis, MO, U.S.A.).

Results

Schild analysis

In rat olfactory bulb, ACh caused a concentration-dependent stimulation of adenylyl cyclase activity with an EC_{50} value of 0.370 ± 0.07 μM and a maximal effect corresponding to a 50.3 ± 6.1% increase of basal enzyme activity ($n = 12$, $P<0.001$). The slope value of the curve was 0.921 ± 0.06 and did not differ significantly from unity. In the presence of increasing concentrations of (**R**)-trihexyphenidyl the ACh response curve was progressively shifted to the right (Figure 1a). A Schild plot of (**R**)-trihexyphenidyl antagonism yielded a pA_2 value of 8.84 and a slope value of 0.908 (Table 1). (**S**)-Trihexyphenidyl shifted the ACh concentration-response curves only at concentrations or equal to higher than 1 μM (Figure 1b). The corresponding Schild plot yielded a straight line and a pA_2 value of 6.09.

In rat striatal membranes ACh maximally inhibited adenylyl cyclase activity by 23.5 ± 1.5% (*P* 0.001) with an EC_{50} value of 1.49 ± 0.12 μM ($n = 9$). (**R**)-trihexyphenidyl antagonized the ACh-induced inhibition of adenylyl cyclase in a concentration-dependent manner with a pA_2 value of 8.75 (Figure 2a; Table 1). Also for this muscarinic response, the (**S**)-enantiomer (Figure 2b) behaved as a weaker antagonist, displaying a pA_2 value of 6.12.

In the heart, ACh produced a concentration-dependent

inhibition of adenylyl cyclase with an EC_{50} value of $0.80 \pm 0.04\,\mu M$ and a maximal effect corresponding to a $45.6 \pm 5.5\%$ reduction of control enzyme activity ($n = 10$, $P < 0.001$). The (R)- and (S)-enantiomers counteracted the response to ACh with pA_2 values of 7.64 and 5.72, respectively (Figure 3).

The eudismic ratios for the antagonism of the muscarinic responses in olfactory bulb, striatum and heart were 562, 426 and 83, respectively.

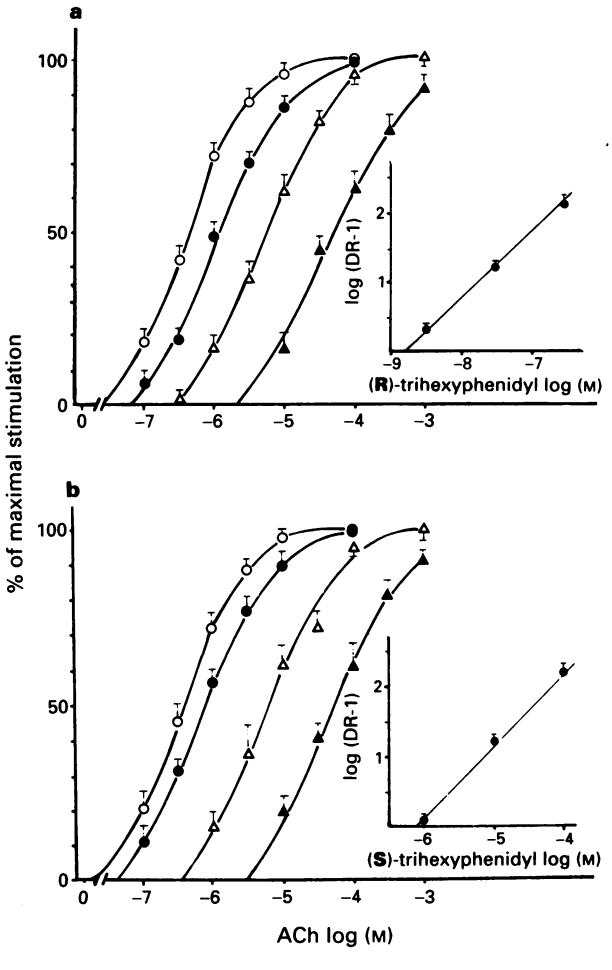


Figure 1 Antagonism of acetylcholine (ACh) stimulation of adenylyl cyclase activity of olfactory bulb by (R)- and (S)-trihexyphenidyl. (a) The enzyme activity was assayed at the indicated concentrations of ACh in the absence (○) and in the presence of 3 nM (●), 30 nM (△) and 300 nM (▲) (R)-trihexyphenidyl. Inset: Schild plot of the antagonism. (b) The enzyme activity was assayed in the absence (○) and in the presence of 1 μM (●), 10 μM (△) and 100 μM (▲) (S)-trihexyphenidyl. Inset: Schild plot of the antagonism. Data are the mean ± s.e.mean of three experiments for each antagonist. Enzyme activities (expressed as pmol cyclic AMP min^{-1} mg^{-1} protein ± s.e.mean) were: (a) basal 115.3 ± 2.7, ACh (100 μM) 169.2 ± 3.4 ($P < 0.01$); (b) basal 110.3 ± 1.8, ACh (100 μM) 161.9 ± 2.8 ($P < 0.01$).

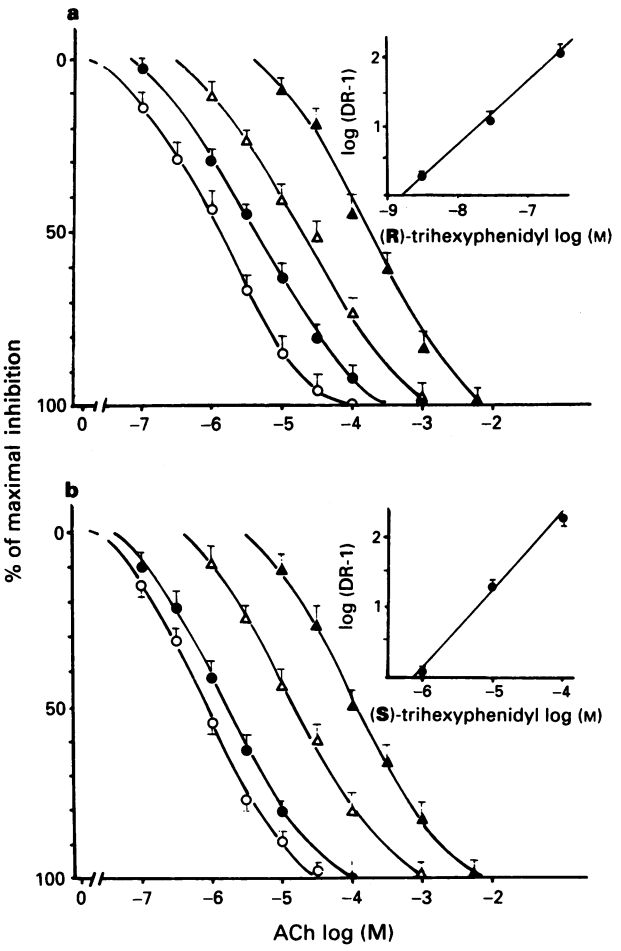


Figure 2 Antagonism of acetylcholine (ACh) inhibition of adenylyl cyclase activity of rat striatum by (R)- and (S)-trihexyphenidyl. (a) The enzyme activity was assayed at the indicated concentrations of ACh in the absence (○) and in the presence of 3 nM (●), 30 nM (△) and 300 nM (▲) (R)-trihexyphenidyl. Inset: Schild plot of the antagonism. (b) The enzyme activity was assayed in the absence (○) and in the presence of 1 μM (●), 10 μM (△) and 100 μM (▲) (S)-trihexyphenidyl. Inset: Schild plot of the antagonism. Data are the mean ± s.e.mean of three experiments for each enantiomer. Enzyme activities (expressed as nmol cyclic AMP min^{-1} mg^{-1} protein ± s.e.mean) were: (a) control, 2.96 ± 0.03, ACh (100 μM) 2.28 ± 0.04 ($P < 0.01$); (b) control 2.89 ± 0.02, ACh (100 μM) 2.21 ± 0.03 ($P < 0.01$).

Inhibition curves

Increasing concentrations of (R)-trihexyphenidyl completely antagonized both the stimulatory and inhibitory effects of ACh (Figure 4). The competition curves were monophasic with Hill coefficients not significantly different from unity (Table 2). Moreover, in each tissue no significant difference ($P > 0.05$) was found by fitting the data to either a two-sites or a one-site competition model. The apparent pK_i values of

Table 1 Affinity constants and eudismic ratios (R/S) of the enantiomers of trihexyphenidyl at muscarinic receptors coupled to stimulation of adenylyl cyclase activity in rat olfactory bulb and to inhibition of the enzyme in striatum and heart

	(R)-trihexyphenidyl		*(S)-trihexyphenidyl*		
Tissue	pA_2	slope	pA_2	slope	(R/S)
Olfactory bulb	8.84 ± 0.02	0.908 ± 0.07	6.09 ± 0.03	1.072 ± 0.04	562
Striatum	8.75 ± 0.05	0.910 ± 0.08	6.12 ± 0.07	1.068 ± 0.06	426
Heart	7.64 ± 0.03	1.050 ± 0.09	5.72 ± 0.05	1.098 ± 0.10	83

Data were obtained from the experiments shown in Figures 1–3. Each value is the mean ± s.e.mean of three experiments. Slope values of Schild plot regression lines were not significantly different from unity ($P > 0.05$). The eudismic ratios were calculated from the antilog of the difference between the pA_2 values of the (R)- and (S)-enantiomers.

(R)-trihexyphenidyl obtained from the competition curves (Table 2) were in good agreement with the corresponding pA_2 values.

Discussion

The present study shows that the stereoisomers of trihexyphenidyl are effective antagonists at muscarinic receptors coupled to either stimulation or inhibition of adenylyl cyclase. For each response examined, the antagonism appears to be competitive, since it is completely surmountable over a wide range of concentrations and is associated with Schild slopes not significantly different from unity. In agreement with previous observations (Barlow, 1971; Lambrecht *et al.*, 1988) the (R)-enantiomer is considerably (80–560 fold) more potent than the (S)-enantiomer. The affinity of the (R)-enantiomer for the muscarinic receptors of the olfactory bulb coupled to stimulation of adenylyl cyclase is similar to that estimated for the striatal receptors linked to inhibition of the enzyme. In terms of absolute values, the potencies of (R)-trihexyphenidyl in antagonizing the ACh effects in the olfactory bulb and striatum correlate well with the reported affinities of the compound for the cloned human m4 and m1 receptor subtypes and for the striatal M_4 sites (Dorje *et al.*, 1991; Waelbroeck *et al.*, 1992). The potency of the (R)-

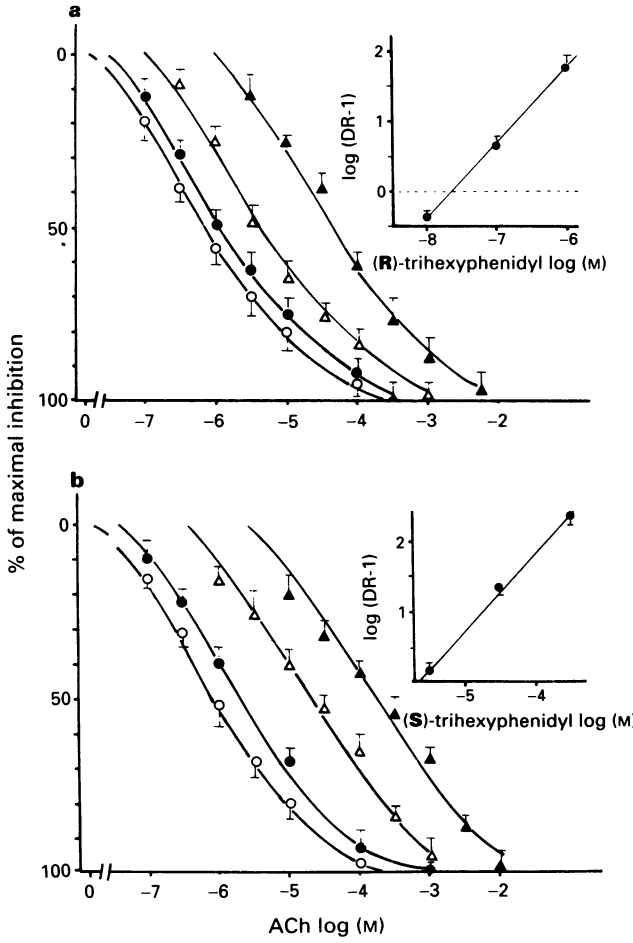


Figure 3 Antagonism of acetylcholine (ACh) inhibition of adenylyl cyclase activity of rat heart by (R)- and (S)-trihexyphenidyl. (a) The enzyme activity was assayed at the indicated concentrations of ACh in the absence (○) and in the presence of 10 nM (●), 100 nM (△) and 1000 nM (▲) (R)-trihexyphenidyl. Inset: Schild plot of the antagonism. (b) The enzyme activity was assayed in the absence (○) and in the presence of 3 μM (●), 30 μM (△) and 300 μM (▲) (S)-trihexyphenidyl. Inset: Schild plot of the antagonism. Data are the mean ± s.e.mean of three experiments for each antagonist. Enzyme activities (expressed as pmol cyclic AMP min^{-1} mg^{-1} protein ± s.e.mean) were: (a) control 70.2 ± 3.5, ACh (300 μM) 38.9 ± 2.3 ($P<0.001$); (b) control 65.9 ± 1.9, ACh (300 μM) 35.2 ± 1.5 ($P<0.001$).

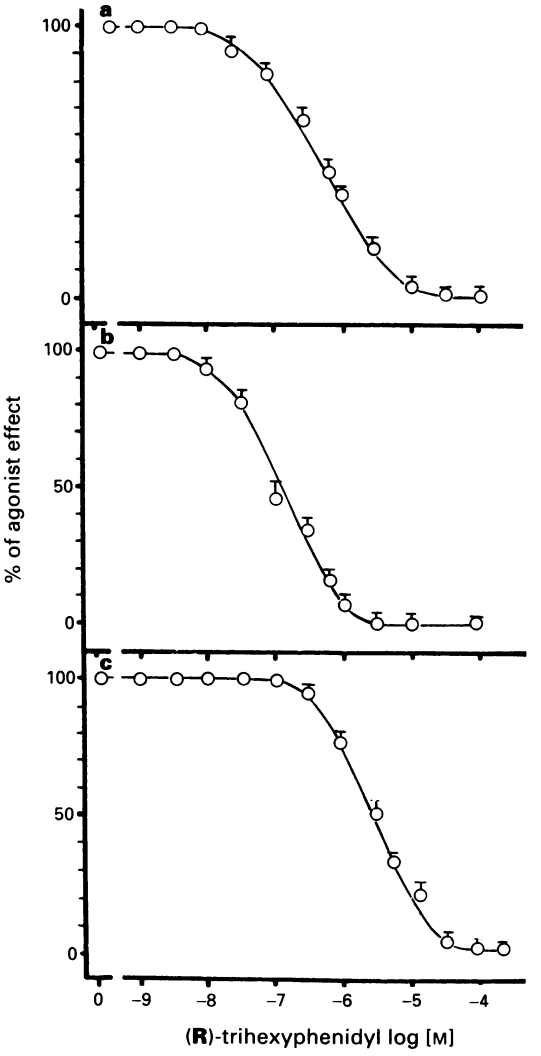


Figure 4 Concentration-dependent inhibition by (R)-trihexyphenidyl of the acetylcholine (ACh)-induced stimulation of adenylyl cyclase of rat olfactory bulb (a) and of the ACh-induced inhibition of the enzyme in rat striatum (b) and heart (c). In each tissue the enzyme activity was assayed as described under Methods at the indicated concentrations of the antagonist in the absence and in the presence of 100 μM ACh. Data are expressed as percentage of the maximal effect elicited by ACh and represent the mean ± s.e.mean of three experiments for each tissue. At the concentrations tested, (R)-trihexyphenidyl failed to affect the enzyme activity *per se*.

Table 2 Inhibition by (R)-trihexyphenidyl of acetylcholine effects on adenylyl cyclase in olfactory bulb, striatum and heart of rat

Tissue	pK_i	*Hill coefficient*
Olfactory bulb	8.77 ± 0.03	0.990 ± 0.03
Striatum	8.76 ± 0.04	1.040 ± 0.02
Heart	7.58 ± 0.02	1.100 ± 0.05

Data were obtained from the experiments shown in Figure 4. Each value is the mean ± s.e.mean of three experiments. pK_i values were calculated according to equation 1 described under Methods. Hill coefficients were not significantly different from unity ($P>0.05$).

enantiomer in antagonizing the ACh inhibition of adenylyl cylcase of rat myocardium is between 10 and 20 fold lower than that observed in the olfactory bulb and striatum and is quite close to its affinity for the cardiac M_2 sites (Waelbroeck *et al.*, 1992). Moreover, the 13–15 fold difference between the potencies in striatum and olfactory bulb and that in myocardium agrees with the selectivity of (R)-trihexyphenidyl for the M_1–M_4 sites versus the M_2 site observed previously (Waelbroeck *et al.*, 1992).

Unlike the (R)-enantiomer, (S)-trihexyphenidyl discriminates poorly between the muscarinic receptors coupled to adenylyl cyclase in the different tissues. Thus, the pA_2 values are only two fold higher in olfactory bulb and striatum than in myocardium. This finding is generally in agreement with the data obtained in functional and radioligand binding studies, in which (S)-trihexyphenidyl was found to possess almost equal affinities for the different muscarinic receptor subtypes (Lambrecht *et al.*, 1988; Dorje *et al.*, 1991; Waelbroeck *et al.*, 1992).

The eudismic ratios are high at the olfactory bulb and the striatal receptors and low at the myocardial receptors. This parameter represents an important discriminatory property of trihexyphenidyl enantiomers. The eudismic ratio of 83 found for the antagonism of ACh inhibition of adenylyl cyclase in myocardium is close to the value of 68 previously obtained for the antagonism of M_2-mediated negative inotropic effects in guinea-pig atrium (Lambrecht *et al.*, 1988) and with the values of 69 and 40 reported in radioligand binding assays of the M_2 receptor (Dorje *et al.*, 1991; Waelbroeck *et al.*, 1992). Thus, the sensitivity of the ACh inhibition of myocardial adenylyl cylcase to the trihexyphenidyl enantiomers is consistent with the involvement of the M_2 receptor subtype. On the other hand, eudismic ratios as high as those found in the present study for the antagonism of ACh effects in the olfactory bulb and striatum have been previously observed at the ileal and glandular M_3 receptors and at the striatal M_4 receptor (Lambrecht *et al.*, 1989; Waelbroeck *et al.*, 1992). Collectively, the antagonistic activity of trihexyphenidyl enantiomers clearly discriminates the olfactory bulb stimulatory receptor and the striatal inhibitory receptor from the putative cardiac M_2 inhibitory receptor.

On the basis of pharmacological data and in light of the distribution of the different molecular forms of muscarinic receptor in the brain, it has been proposed that the striatal muscarinic receptor coupled to inhibition of adenylyl cyclase is pharmacologically equivalent to the m4 gene product (M_4) (McKinney *et al.*, 1989; Elhert *et al.*, 1989). Previous studies have shown that the muscarinic stimulation of adenylyl cyclase in the olfactory bulb and the muscarinic inhibition of the enzyme in the striatum show similar sensitivities to a number of antagonists and have led to the hypothesis that a similar receptor subtype mediates the two responses (Olianas & Onali, 1991). The present finding that both the olfactory bulb and striatal receptors are blocked by (R)- and (S)-trihexyphenidyl with a similar potency provides support for the same classification being given to these receptors, i.e. M_4.

In conclusion, the present study shows that the muscarinic stimulation of adenylyl cyclase in rat olfactory bulb and the muscarinic inhibitions of the enzyme in striatum and heart are stereospecifically antagonized by the enantiomers of trihexyphenidyl and that the differential sensitivity to these drugs can be useful for identifying the receptor subtypes mediating these functional responses.

References

BARLOW, R.B. (1971). Differences in the stereospecificity of closely related compounds; a reinvestigation of the enantiomers of procyclidine, benzhexol and their metho- and etho-salts. *J. Pharm. Pharmacol.*, **23**, 90–97.

BAUMGOLD, J., PAEK, R. & YASUMOTO, T. (1992). Agents that stimulate phosphoinositide turnover also elevate cAMP in SK-N-SH human neuroblastoma cells. *Life Sci.*, **50**, 1755–1759.

BRADFORD, M.M. (1976). A rapid and sensitive method for the quantitation of microgram quantities of protein utilizing the principle of protein-dye binding. *Anal. Biochem.*, **72**, 248–254.

DORJE, F., WESS, J., LAMBRECHT, G., TACKE, R., MUTSCHLER, E. & BRANN, M.R. (1991). Antagonist binding profiles of five cloned human muscarinic receptor subtypes. *J. Pharmacol. Exp. Ther.*, **256**, 727–733.

EHLERT, F.J., DELEN, F.M., YUN, S.H., FRIEDMAN, D. & SELF, D.W. (1989). Coupling of subtypes of the muscarinic receptor to adenylate cyclase in the corpus striatum and heart. *J. Pharmacol. Exp. Ther.*, **251**, 660–671.

FELDER, C.C., KANTERMANN, R.Y., MA, A.L. & AXELROD, J. (1989). A transfected m1 muscarinic acetylcholine receptor stimulates adenylate cyclase via phosphatidylinositol hydrolysis. *J. Biol. Chem.*, **264**, 20356–20362.

LAMBRECHT, G., FEIFEL, R., MOSER, U., AASEN, A.J., WAELBROECK, M., CHRISTOPHE, J. & MUTSCHLER, E. (1988). Stereoselectivity of the enantiomers of trihexyphenidyl and its methiodide at muscarinic receptor subtypes. *Eur. J. Pharmacol.*, **155**, 167–170.

LEHMAN, F.P.A. (1986). Stereoisomerism and drug action. *Trends Pharmacol. Sci.*, **7**, 281–285.

MCKINNEY, M., ANDERSON, D.J., FORRAY, F. & EL-FAKAHANY, E. (1989). Characterization of the striatal M2 muscarinic receptor mediating inhibition of cyclic AMP using selective antagonists: a comparison with the brainstem M2 receptor. *J. Pharmacol. Exp. Ther.*, **250**, 565–572.

MCKINNEY, M., ANDERSON, D.J., VELLA-ROUNTREE, L., CONNOLLY, T. & MILLER, J.H. (1991). Pharmacological profiles for rat cortical M1 and M2 muscarinic receptors using selective antagonists: comparison with N1E-115 muscarinic receptors. *J. Pharmacol. Exp. Ther.*, **257**, 1121–1129.

OLIANAS, M.C. & ONALI, P. (1990). Ca2 +-independent stimulation of adenylate cyclase activity by muscarinic receptors in rat olfactory bulb. *J. Neurochem.*, **55**, 1083–1086.

OLIANAS, M.C. & ONALI, P. (1991). Muscarinic stimulation of adenylate cyclase activity of rat olfactory bulb. II. Characterization of the agonist sensitivity and comparison with muscarinic inhibition of the enzyme in striatum and heart. *J. Pharmacol. Exp. Ther.*, **259**, 680–686.

OLIANAS, M.C. & ONALI, P. (1992). Properties of muscarinic-stimulated adenylate cyclase activity in rat olfactory bulb. *J. Neurochem.*, **58**, 1723–1729.

OLIANAS, M.C. & ONALI, P. (1993a). Synergistic interaction of muscarinic and opioid receptors with Gs-linked neurotransmitter receptors to stimulate adenylyl cyclase activity of rat olfactory bulb. *J. Neurochem.*, **61**, 2183–2190.

OLIANAS, M.C. & ONALI, P. (1993b). Stimulation of phosphoinositide hydrolysis by muscarinic receptor activation in the rat olfactory bulb. *Biochem. Pharmacol.*, **45**, 281–287.

OLIANAS, M.C., ONALI, P., NEFF, N.H. & COSTA, E. (1983). Adenylate cyclase activity of synaptic membranes from rat striatum. Inhibition by muscarinic receptor agonists. *Mol. Pharmacol.*, **23**, 393–398.

ONALI, P. & OLIANAS, M.C. (1990). Positive coupling of cholinergic muscarinic receptors to adenylate cyclase activity in membranes of rat olfactory bulb. *Naunyn-Schmied. Arch. Pharmacol.*, **343**, 107–109.

SALOMON, Y., LONDOS, D. & RODBELL, M. (1974). A highly sensitive adenylate cyclase assay. *Anal. Biochem.*, **58**, 541–548.

SCHILD, H.O. (1947). pA, a new scale for measurement of drug antagonism. *Br. J. Pharmacol.*, **2**, 189–206.

SCHJELDERUP, L., HARBITZ, O., GROTH, P. & AASEN, A.J. (1987). Syntheses of (S)-(+)-trihexyphenidyl hydrochloride and (S)-(+)-procyclidine hydrochloride, two anticholinergics, using (S)-(−)-3-cyclohexyl-3-hydroxy-3-phenylpropanoic acid as chiral synthon. *Acta Chem. Scand.*, Ser. **B41**, 356–361.

VICKROY, T.W. & CADMAN, E.D. (1989). Dissociation between muscarinic receptor-mediated inhibition of adenylate cyclase and autoreceptor inhibition of [^{3}H] acetylcholine release in rat hippocampus. *J. Pharmacol. Exp. Ther.*, **251**, 1039–1044.

WAELBROECK, M., TASTENOY, M., CAMUS, J., FEIFEL, R., MUTSCHLER, E., STROHMANN, C., TACKE, R., LAMBRECHT, G. & CHRISTOPHE, J. (1989). Stereoselectivity of the interaction of muscarinic antagonists with their receptors. *Trends Pharmacol. Sci.*, **10** suppl. IV, 65–69.

WAELBROECK, M., CAMUS, J., TASTENOY, M., MUTSCHLER, E., STROHMANN, C., TACKE, R., SCHJELDERUP, L., AASEN, A., LAMBRECHT, G. & CHRISTOPHE, J. (1992). Stereoselective interaction of procyclidine, hexahydro-difenidol, hexbutinol and oxyphencyclimine, and of related antagonists, with four muscarinic receptors. *Eur. J. Pharmacol.-Mol. Pharmacol. Sect.*, **227**, 33–42.

(Received March 25, 1994
Revised June 15, 1994
Accepted July 4, 1994)

Br. J. Pharmacol. (1994), **113**, 781–788 © Macmillan Press Ltd, 1994

Facilitation by procaterol, a β-adrenoceptor agonist, of noradrenaline release in the pithed rat independently of angiotensin II formation

[1]P. Kotsonis & H. Majewski

Prince Henry's Institute of Medical Research, P.O. Box 5152, Clayton 3168, Victoria, Australia

1 The effects of the β_2-adrenoceptor agonist, procaterol, on sympathetic neuroeffector transmission were studied in the pithed adrenal demedullated rat to determine if generation of angiotensin II was involved in its effect. Pressor responses were elicited by either electrical stimulation (20 V, 2 Hz) of the entire spinal sympathetic outflow or methoxamine (0.1 mg kg^{-1}, i.v.).

2 Sodium nitroprusside (3 and 5 μg kg^{-1} min^{-1}, i.v.) produced hypotension and the pressor responses to both sympathetic nerve stimulation and methoxamine were reduced. This indicates that decreasing blood pressure in pithed rats reduces pressor responses. Procaterol (10 and 30 ng kg^{-1} min^{-1}, i.v.) also produced hypotension but did not alter pressor responses to sympathetic nerve stimulation. Nevertheless, procaterol (10 and 30 ng kg^{-1} min^{-1}, i.v.) did reduce pressor responses to methoxamine. Together these results suggest that procaterol may have enhanced sympathetic neurotransmitter release. This was confirmed in another series of experiments where procaterol (30 ng kg^{-1} min^{-1}, i.v.) increased plasma noradrenaline levels during sympathetic nerve stimulation.

3 Captopril (5 mg kg^{-1}, i.v.) produced hypotension and as expected reduced pressor responses to sympathetic nerve stimulation. When the hypotensive effect of captopril was abolished by concomitant vasopressin infusion (1.5–4.5 i mu kg^{-1} min^{-1}, i.v.), pressor responses to sympathetic nerve stimulation were restored to pre-captopril levels. In this situation procaterol (10 and 30 ng kg^{-1} min^{-1}, i.v.) reduced basal blood pressure and did not alter pressor responses to sympathetic nerve stimulation whereas the pressor responses were reduced by an equihypotensive infusion of sodium nitroprusside (3 and 5 μg kg^{-1} min^{-1}, i.v.). The lack of reduction of pressor responses after procaterol in the presence of captopril is indirect evidence that procaterol may have enhanced noradrenaline release independently of angiotensin II.

4 In another series of experiments, plasma noradrenaline levels elicited by sympathetic nerve stimulation were not altered by captopril (5 mg kg^{-1}, i.v.). In the presence of captopril (5 mg kg^{-1}, i.v.), procaterol (30 ng kg^{-1} min^{-1}, i.v.) no longer enhanced plasma noradrenaline levels during sympathetic nerve stimulation. However, since the dose of captopril is well above that required to block angiotensin converting enzyme (ACE) the effect may be non-specific. Therefore, the selective AT_1 receptor antagonist, losartan (10 mg kg^{-1}, i.v.), was also used. Losartan (10 mg kg^{-1}, i.v.) did not alter plasma noradrenaline levels during sympathetic nerve stimulation, and in the presence of losartan procaterol (30 ng kg^{-1} min^{-1}, i.v.) enhanced plasma noradrenaline levels during sympathetic nerve stimulation. This result further suggests that β-adrenoceptor facilitation of noradrenaline release from sympathetic nerves in the pithed rat occurs by a mechanism independent of angiotensin II generation.

Keywords: β-Adrenoceptors; angiotensin II; renin-angiotensin system; noradrenaline release; losartan; captopril; sympathetic nerves

Introduction

Sympathetic nerves possess prejunctional β_2-adrenoceptors, activation of which results in enhanced action potential-evoked transmitter release (for reviews see Majewski, 1983; Borkowski, 1988). The endogenous activator appears to be adrenaline which enhances action potential-evoked noradrenaline release both *in vitro* (Stjärne & Brundin, 1975; Majewski *et al.*, 1981) and *in vivo* (Majewski *et al.*, 1985). In general the level of facilitation of noradrenaline release is small (10–50%, Stjärne & Brundin, 1975; Majewski *et al.*, 1981) but recent experiments in conscious rats suggests that larger effects are possible (100–200%, Coppes *et al.*, 1993). This action of adrenaline has been implicated in the development of hypertension and adrenaline has been found not only to induce hypertension through a β-adrenoceptor-mediated mechanism (see Majewski & Rand, 1986; Floras, 1992) but also like other β_2-adrenoceptor agonists, increases vasoconstrictor responses to sympathetic nerve stimulation in isolated blood vessels (Kawasaki *et al.*, 1984) and in whole animals (Borkowski & Quinn, 1984; Schlicker *et al.*, 1988).

Up until the mid 1980's it was assumed that the β-adrenoceptors responsible for enhancing transmitter release were located on the nerve varicosities. Indeed, functional studies demonstrated their presence on sympathetic nerves of axonal sprouts (Weinstock *et al.*, 1978). However, Kawasaki *et al.* (1984) showed that a large proportion of the enhanced transmitter release after β-adrenoceptor activation was blocked by the angiotensin converting enzyme inhibitor, captopril, in the rat perfused mesentery. It was suggested that activation of β-adrenoceptor could induce the formation of angiotensin II locally and that angiotensin II enhanced noradrenaline release by activating a prejunctional angiotensin II receptor mechanism which is well described (for review see Zimmerman, 1981). Subsequently, β-adrenoceptor agonists were shown to evoke an overflow of angiotensin II-like immunoreactivity from rat perfused mesentery and this was antagonized by the angiotensin converting enzyme inhibitor, captopril (Nakamaru *et al.*, 1986). Further studies have shown that the facilitatory effects of β-adrenoceptor agonists on noradrenaline release can be inhibited by converting enzyme inhibitors and angiotensin II receptor blocking drugs (rat perfused mesenteric bed: Kawasaki *et al.*, 1984;

[1] Author for correspondence.

Nakamaru *et al.*, 1986; Draper *et al.*, 1989; and rat vena cava: Göthert & Kollecker, 1986; Ziogas & Story, 1991). However, no interaction between β-adrenoceptor-mediated facilitation of noradrenaline release and angiotensin II was seen in rat kidney (Rump & Majewski, 1987), rat anococcygeus muscle (Li *et al.*, 1988), rat atria (Mian *et al.*, 1989), rat tail artery and mouse atria (Rajanayagam *et al.*, 1989).

In vivo evidence for angiotensin II being involved in the release-enhancing effect of β-adrenoceptor agonists has come from experiments in pithed rats. Brokowski & Quinn (1984) using spontaneously hypertensive rats have shown that β-adrenoceptor agonists enhance vasoconstrictor responses to sympathetic nerve stimulation. Subsequently, Schlicker *et al.* (1988) proposed that this effect was in fact due to the generation of angiotensin II since the effect was reduced by both the angiotensin converting enzyme inhibitor, captopril, and the angiotensin receptor antagonist, saralasin. However, interpretation of pressor response data in the pithed rat is complicated since a number of studies have found that in the pithed rat, sympathetically induced vasopressor responses are critically affected by basal arterial pressure (Oldham & Scotcher, 1986) and anti-angiotensin drugs such as captopril depress sympathetic vasoconstrictor response largely due to the hypotension (e.g. Hatton & Clough, 1982).

The aim of the present study was to investigate further β-adrenoceptor/angiotensin II modulation of sympathetic neurotransmission in the pithed rat. This was done firstly, by negating the hypotensive effects of captopril by use of infusions of vasopressin so that the effects of captopril on pressor responses could be clearly assessed independently of blood pressure changes and secondly, by measuring plasma noradrenaline levels to provide an independent biochemical index of noradrenaline release.

Methods

Adrenal demedullation

Male Sprague-Dawley rats (240–350 g) were anaesthetized with an intraperitoneal (i.p.) injection of sodium methohexitone (25 mg kg^{-1}) and sodium amylobarbitone (63 mg kg^{-1}) and the adrenal demedullation was performed via bilateral flank incisions. Animals were then allowed to recover and were given normal food and water rations.

Pithed rats

Three to ten days after adrenal demedullation the rats were anaesthesized with an intraperitoneal (i.p.) injection of sodium methohexitone (25 mg kg^{-1}) and sodium amylobarbitone (63 mg kg^{-1}). The left carotid artery was cannulated with polyethylene tubing for the recording of arterial blood pressure and heart rate. The tubing was inserted as far as the aortic arch. The trachea was then cannulated. The right jugular vein was also cannulated with polyethylene tubing which was inserted as far as the right atrium. The rats were pithed through the orbit of the eye with a stainless steel rod (1.5 mm in diameter) which was passed down the spinal cord. A stainless steel needle, which acted as an indifferent electrode, was placed subcutaneously in the lower back and positioned parallel to the spinal cord.

After pithing, the rats were artifically respired with air (60 breaths min^{-1} and a volume of 2 ml 100 g^{-1} body weight). Tubocurarine (1 mg, i.v.) and atropine (1 mg kg^{-1}, i.v.) were given after pithing to prevent skeletal muscle contraction and muscarinic receptor activation during electrical stimulation of the entire spinal outflow, respectively. The rats were then allowed a 10–15 min equilibration period during which time blood pressure stabilised. Body temperature was maintained at 36°C.

After the equilibration period, the spinal cord was stimulated electrically through the pithing rod at a frequency of 2 Hz with 0.5 ms square wave pulses at a voltage of 20 V across the electrodes for 20 s. A 5 min period was allowed between stimulations to enable the diastolic pressure to return to pre-stimulation values. Seven consecutive equilibration stimulations were performed by which time the pressor responses were stable and reproducible. Then seven test stimulations (S1–S7) were performed with the first test stimulation (S1) taken as the pre-saline or drug control value. Drug or saline (0.9% NaCl, control) was infused after the first stimulation (S1) until the end of the experiment (S2–S7).

In another series of experiments, pressor responses were elicited with a bolus injection (i.v., left jugular vein) of methoxamine (0.1 mg kg^{-1}, in a volume of 0.1 ml, flushed with 0.1 ml saline). A 10 min period was allowed between each bolus injection of methoxamine to enable diastolic pressure to return to pre-stimulation values. Six consecutive equilibration methoxamine administrations were given by which time the pressor responses were stable and reproducible. Then seven test administrations were performed with the first administration (M1) taken as the pre-saline or drug control value. Drug or saline (0.9% NaCl, control) was infused after the first administration (M1) until the end of the experiment (M2–M7).

Plasma noradrenaline levels during sympathetic nerve stimulation

Animals were prepared as described and the spinal cord was stimulated electrically through the pithing rod at a frequency of 2 Hz with 0.5 ms square wave pulses at a voltage of 20 V across the electrodes for 90 s. Fifteen minutes was allowed between stimulations to ensure that diastolic blood pressure had returned to pre-stimulation values. There were two test stimulations (S1 and S2). Arterial blood (1.0 ml) was taken from the carotid artery over a 1 min period (starting 60 s after the onset of electrical stimulation) and immediately replaced with an equal volume blood taken from an anaesthetized donor rat. This ensured haemodynamic stability. The drug under investigation was administered either 5 or 10 min before the start of the second period of electrical stimulation. Upon completion of the experiment additional blood was taken for the determination of recoveries and pH adjustment for alumina chromatography.

Plasma noradrenaline analysis

The blood sample was immediately transferred into an ice-cold centrifuge tube containing 0.3 ml of 0.9% NaCl (with 50 iu ml^{-1} of heparin); 50 μl Na_2EDTA (100 mg ml^{-1}) and 50 μl Na_2SO_3 (125 mg ml^{-1}). The samples were then centrifuged (at 14,000 *g* for 20 min at 4°C) and an aliquot (0.85 ml) was transferred to a tube containing 0.1 ml 2 M $HCLO_4$; 50 μl Na_2EDTA (100 mg ml^{-1}) and 50 μl Na_2SO_3 (125 mg ml^{-1}); these tubes were frozen (−40°C) for up to a week. After thawing, the samples were centrifuged again (at 14,000 *g* for 20 min at 4°C) and an aliquot (0.9 ml) of the final supernatant was adjusted to pH 8.3–8.5 with 2 M Tris acetate buffer (≈170 μl). The samples were poured onto alumina (200 mg) in a glass column stoppered with a glass fibre filter. The columns were then washed two times with 1 ml H_2O. Then 500 μl of 0.1 M $HCLO_4$ was added to the column and the eluate was recirculated once.

The amount of noradrenaline in 100 μl $HClO_4$ eluate was determined by high-performance liquid chromatography (h.p.l.c.) coupled with electrochemical detection. A reverse phase column was used (EXCIL C18 5 μM–Alt 230, Activon, Australia). The solvent consisted of Na_2HPO_4 buffer 0.06 M, pH 3.10 containing 450–650 mg l^{-1} heptane sulphonic acid, 200 mg l^{-1} Na_2EDTA and 10–15 ml methanol. The electrochemical detection was an ESA Coulochem 5100 with an ESA 5011 analytical cell (ESA, Bedford, MA, U.S.A.). The first electrode potential was 0.06 V and the detecting electrode was 0.30 V. Recoveries were performed by adding

500 pg noradrenaline to a blood sample at the end of the experiment. The mean recovery of noradrenaline was 89.2% ± 2.7% ($n = 12$). Corrections were made for incomplete recovery.

Drugs and materials

Sodium methohexitone and sodium amylobarbitone (Lilly, Sydney, Australia); tubocurarine (Wellcome, Sydney, Australia); atropine sulphate (Astra, Ryde, Australia); sodium nitroprusside (Sigma, St Louis, U.S.A.); vasopressin (Parke-Davis, Caringbah, Australia). The following drugs were generously donated: captopril (Squibb, Melbourne, Australia); procaterol-HCl (Parke-Davis, Ann Arbor, Michigan, U.S.A.); methoxamine-HCl (Wellcome, Sydney, Australia); losartan (DuPont Merck Pharmaceutical Co., Wilmington, U.S.A.).

Captopril, sodium nitroprusside, vasopressin, losartan and methoxamine-HCl were freshly dissolved and diluted in 0.9% NaCl prior to use. In the case of methoxamine-HCl, saline solution also contained ascorbic acid (0.5 mg ml^{-1}). Procaterol-HCl was initially made up as a stock solution (1 mg ml^{-1}) in 0.01 M HCl (pH ≈ 2) and diluted with 0.9% NaCl on the day of use. This did not alter the pH of 0.9% NaCl.

Statistical analysis of results

All data are expressed as the mean ± standard error of the mean (s.e.mean). All groups of data were analysed with two-way analysis of variance (ANOVA). Probability levels of less than 0.05 ($P < 0.05$) were taken to indicate a significant difference.

Results

Base parameters

The base cardiovascular parameters are shown in Table 1. In the series of experiments where plasma noradrenaline levels in pithed adrenal demedullated rats were measured during sympathetic nerve stimulation the mean plasma noradrenaline levels were 424.3 ± 23.5 pg ml^{-1} ($n = 37$). In pithed adrenal demedullated rats, plasma adrenaline levels under basal conditions and during sympathetic nerve stimulation (2 Hz, 0.5 ms, 20 V, for 90 s) were below detectable levels (< 10 pg ml^{-1}). In the absence of nerve stimulation, plasma noradrenaline levels were also undetectable.

Pressor responses to sympathetic nerve stimulation

The β_2-adrenoceptor agonist, procaterol (10 and 30 ng kg^{-1} min^{-1}, i.v), did not affect pressor responses to sympathetic nerve stimulation (Figure 1b) but did reduce basal diastolic pressure (Figure 1a). To act as a control for the hypotensive effects of procaterol, the vasodilator sodium nitroprusside (SNP) was also used. In contrast to procaterol, SNP (3 and 5 μg kg^{-1} min^{-1}, i.v.) significantly reduced pressor responses to sympathetic nerve stimulation (Figure 1d) whilst the reduction in basal diastolic pressure was not significantly different from that produced by procaterol (compare Figure 1a and c). Heart rate was not altered by either procaterol or SNP (not shown).

Pressor responses to methoxamine

Procaterol (10 and 30 ng kg^{-1} min^{-1}, i.v.) significantly reduced blood pressure and pressor responses elicited by the α_1-adrenoceptor agonist, methoxamine (Figure 2a and b). Equihypotensive infusions of SNP (3 and 5 μg kg^{-1} min^{-1}, i.v.) also reduced pressor responses to methoxamine (Figure 2c and d). The reduction in basal diastolic blood pressure and pressor responses to methoxamine by SNP was not significantly different from that produced by procaterol (compare Figure 2a and c as well as b and d).

Effects of captopril on pressor responses to sympathetic nerve stimulation

The effects of procaterol were examined in the presence of captopril (5 mg kg^{-1}, i.v.) which reduced basal diastolic pres-

Table 1 Absolute values for cardiovascular parameters at first electrical stimulation (S1) or methoxamine administration (M1)

	Initial basal diastolic pressure (mmHg)	*Initial pressor response* (Δ mmHg)	*Initial heart rate* (beats min^{-1})
A Pithed rats: electrical stimulation (Figure 1)			
Control ($n = 4$)	34 ± 1	43 ± 3	393 ± 18
Procaterol ($n = 4$)	32 ± 1	46 ± 6	395 ± 13
SNP ($n = 5$)	32 ± 2	42 ± 7	377 ± 20
B Pithed rats: methoxamine (Figure 2)			
Control ($n = 4$)	37 ± 6	48 ± 11	362 ± 21
Procaterol ($n = 3$)	38 ± 3	54 ± 7	371 ± 16
SNP ($n = 5$)	39 ± 4	55 ± 3	366 ± 10
C Pithed rats: electrical stimulation captopril (Figure 3)			
Control ($n = 5$)	33 ± 3	26 ± 3	340 ± 19
Procaterol ($n = 5$)	32 ± 2	27 ± 2	327 ± 10
D Pithed rats: electrical stimulation captopril and vasopressin (Figure 4)			
Control ($n = 5$)	37 ± 2	27 ± 2	346 ± 9
Procaterol ($n = 7$)	34 ± 2	30 ± 4	336 ± 7
SNP ($n = 5$)	34 ± 2	32 ± 2	372 ± 15
E Pithed rats: electrical stimulation (Figure 5)			
Control ($n = 7$)	39 ± 2	42 ± 6	319 ± 22
Procaterol ($n = 7$)	36 ± 1	38 ± 4	289 ± 6
Captorpil ($n = 5$)	37 ± 3	33 ± 4	289 ± 6
Captopril + procaterol ($n = 6$)	34 ± 2	35 ± 4	277 ± 14
Losartan ($n = 6$)	39 ± 2	39 ± 7	322 ± 6
Losartan + procaterol ($n = 6$)	39 ± 3	39 ± 2	300 ± 3

In the experiments represented in Figure 1–5 consecutive measurements are made (S1–S7, M1–M7) and all results are expressed as a percentage of the initial value. The absolute values at S1 or M1 are shown above.

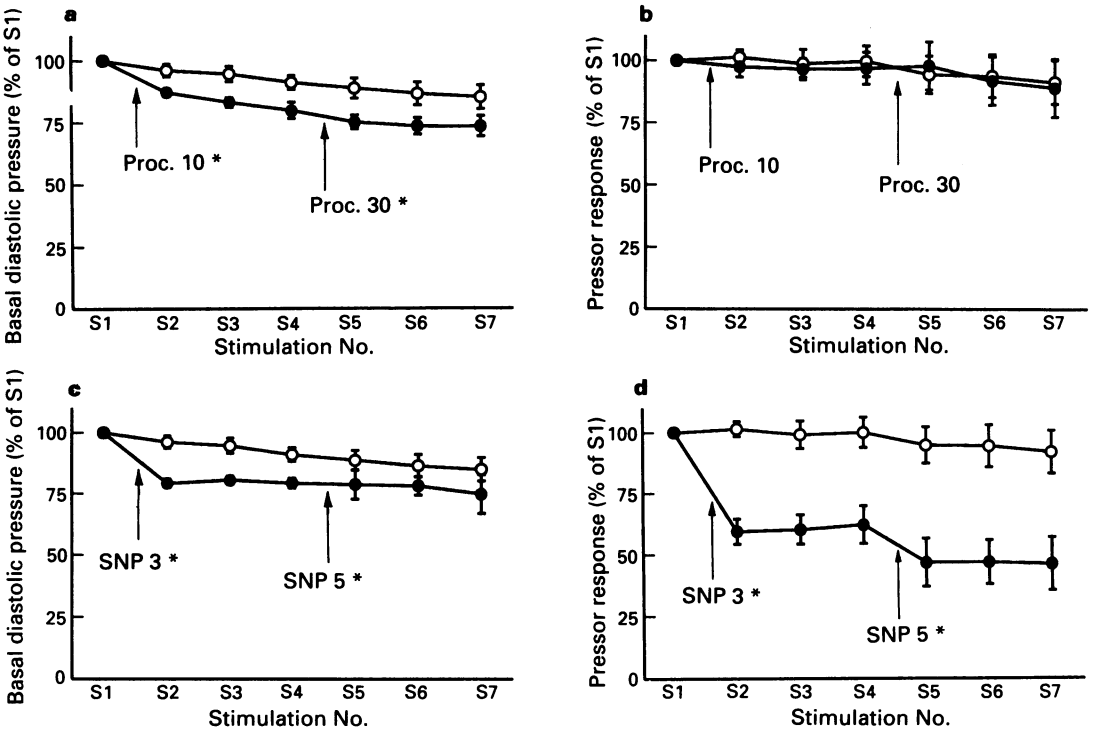


Figure 1 The effect of procaterol and sodium nitroprusside on basal diastolic pressure (a and c, respectively) and pressor responses (changes in diastolic pressure; b and d, respectively) to sympathetic nerve stimulation. There were 7 consecutive stimulations (S1–S7; 2 Hz, 0.5 ms, 20 V, for 20 s at 5 min intervals). Saline (0.9% NaCl, vehicle) or drug infusion began after the first stimulation (S1). All results are expressed as a percentage of S1: (○) indicate experiments where no drug was administered ($n = 4$) and (●) indicate either procaterol (a and b, Proc 10 and 30 ng kg^{-1} min^{-1}, $n = 4$) or sodium nitroprusside (c and d, SNP 3 and 5 μg kg^{-1} min^{-1}, $n = 5$) which were infused immediately after S1 and S4. Each symbol represents the mean with s.e.mean. A significant effect ($P < 0.05$, ANOVA) of procaterol or SNP at each dose is indicated by *. The hypotensive effects of SNP and procaterol were not significantly different ($P > 0.05$, ANOVA).

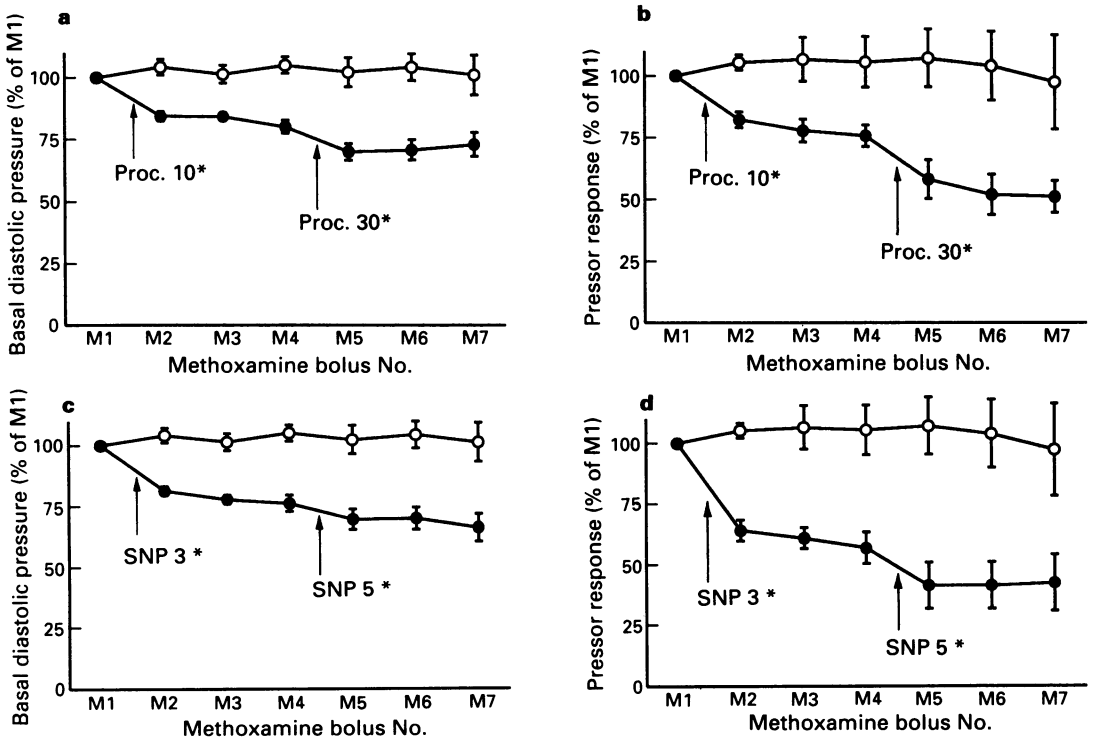


Figure 2 The effect of procaterol and sodium nitroprusside on basal diastolic pressure (a and c, respectively) and pressor responses (change in diastolic pressure; b and d, respectively) to methoxamine (0.1 mg kg^{-1}, i.v.). There were 7 consecutive methoxamine administrations (M1–M7; at 10 min intervals). Saline (0.9% NaCl, vehicle) or drug infusion began after the first methoxamine bolus (M1). All results are expressed as a percentage of M1: (○) indicate experiments where no drug was administered ($n = 4$) and (●) indicate either procaterol (a and b, Proc 10 and 30 ng kg^{-1} min^{-1}, $n = 3$) or sodium nitroprusside (c and d, SNP 3 and 5 μg kg^{-1} min^{-1}, $n = 5$) which were infused immediately after M1 and M4. Each symbol represents the mean with s.e.mean. A significant effect ($P < 0.05$, ANOVA) of procaterol or SNP at each dose is indicated by *. The hypotensive effects of SNP and procaterol were not significantly different ($P > 0.05$, ANOVA).

sure and pressor responses to sympathetic nerve stimulation (Figure 3a and b). In the presence of captopril, procaterol (10 and 30 ng kg^{-1} min^{-1}, i.v.) had no effect on the already reduced basal diastolic pressure or pressor responses to sympathetic nerve stimulation (Figure 3a and b). Heart rate was not altered by captopril (not shown).

In another series of experiments vasopressin (1.5–4.5 i mu kg^{-1} min^{-1}, i.v.) was given to negate the hypotensive effects of captopril. The infusion rate of vasopressin was adjusted to each experiment immediately after captopril administration (Figure 4a). In this case the pressor responses to sympathetic nerve stimulation were maintained at pre-captopril levels (Figure 4b) which contrasts the depressant action of captopril alone (Figure 3b). Procaterol (10 and 30 ng kg^{-1} min^{-1}, i.v.) did not reduce pressor responses to sympathetic nerve stimulation after the combination of captopril and vasopressin (Figure 4b). In contrast, in the same situation, SNP (3 and 5 μg kg^{-1} min^{-1}, i.v.) reduced basal diastolic pressure (Figure 4c) and pressor responses to sympathetic nerve stimulation (Figure 4d).

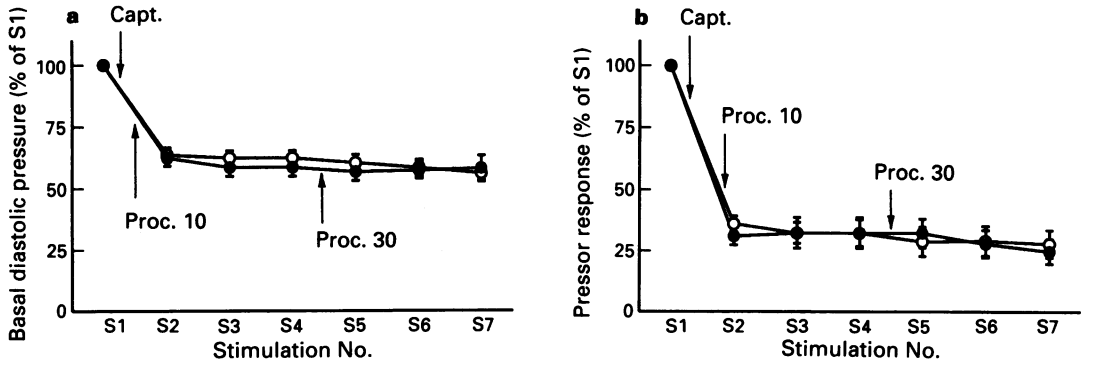


Figure 3 The effect of procaterol on basal diastolic pressure (a) and pressor responses (change in diastolic pressure; b) to sympathetic nerve stimulation in animals given captopril (Capt, 5 mg kg^{-1}, i.v., immediately after S1). There were 7 consecutive stimulations (S1–S7; 2 Hz, 0.5 ms, 20 V, for 20 s at 5 min intervals). Saline (0.9% NaCl, vehicle) or drug infusion began after the first stimulation (S1). All results are expressed as a percentage of S1: (○) indicate experiments ($n = 5$) where captopril but not procaterol was administered; (●) indicate experiments where animals were given captopril (between S1 and S2) in addition to procaterol 10 ng kg^{-1} min^{-1} (after S1, Proc 10, $n = 5$) and procaterol 30 ng kg^{-1} min^{-1} (after S4, Proc 30, $n = 5$). Each symbol represents the mean with s.e.mean. There was no significant effect of procaterol ($P > 0.05$, ANOVA).

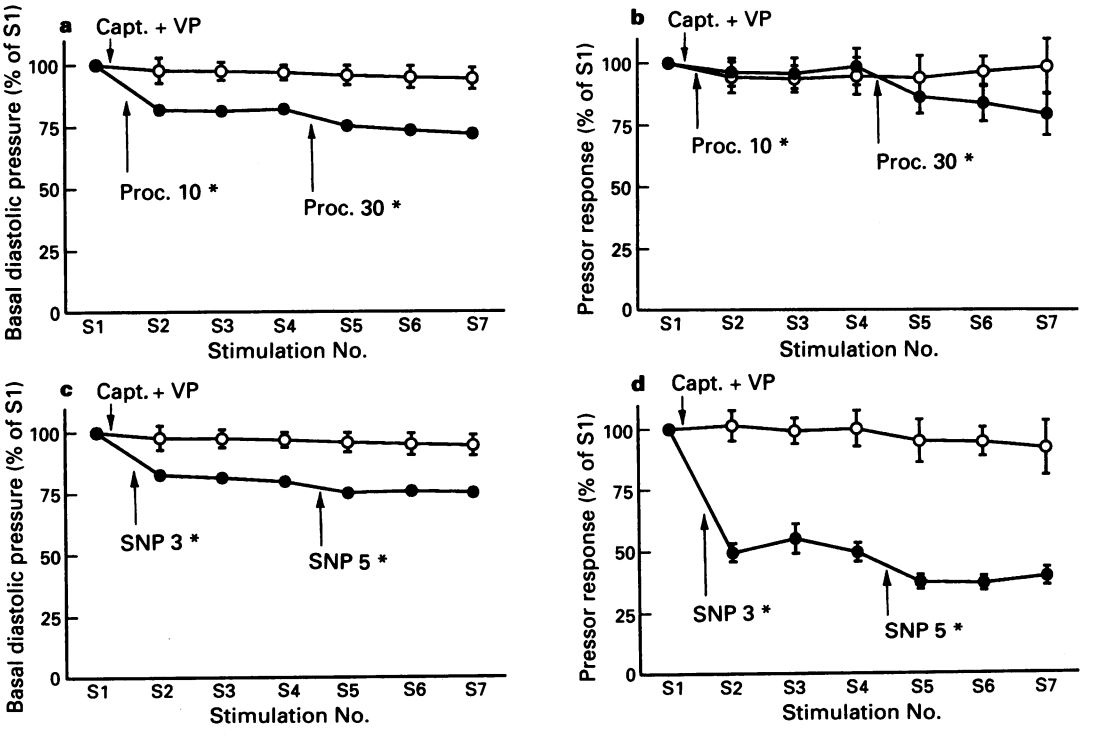


Figure 4 The effect of procaterol and sodium nitroprusside on basal diastolic pressure (a and c, respectively) and pressor responses (change in diastolic pressure; b and d, respectively) to sympathetic nerve stimulation in animals given captopril (Capt, 5 mg kg^{-1}, i.v., immediately after S1) and vasopressin (VP, 1.5–4.5 i mu kg^{-1} min^{-1}, i.v., immediately after S1 until the end of the experiment). There were 7 consecutive stimulations (S1–S7; 2 Hz, 0.5 ms, 20 V, for 20 s at 5 min intervals). All results are expressed as a percentage of S1. Saline (0.9% NaCl, vehicle) or drug infusion began after the first stimulation (S1): (○) indicate experiments ($n = 5$) where captopril and vasopressin were administered between S1 and S2; (●) indicate experiments where in addition to captopril and vasopressin, either procaterol (a and b, Proc 10 and 30 ng kg^{-1} min^{-1}, $n = 7$) or sodium nitroprusside (c and d, SNP 3 and 5 μg kg^{-1} min^{-1}, $n = 5$) were infused immediately after S1 and S4. Each symbol represents the mean with s.e.mean. A significant effect ($P < 0.05$, ANOVA) of procaterol or SNP at each dose is indicated by *. The hypotensive effects of SNP and procaterol were not significantly different ($P > 0.05$, ANOVA).

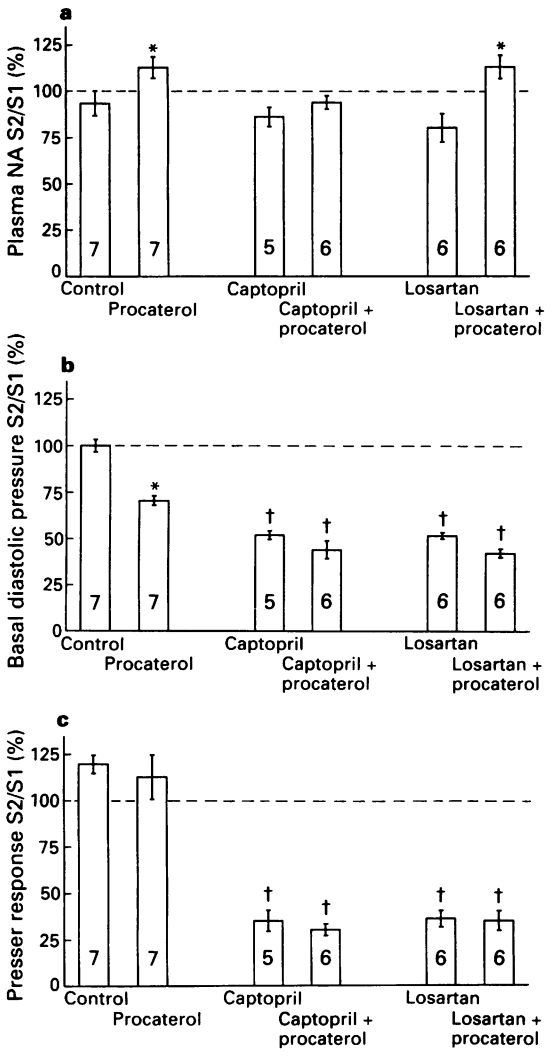


Figure 5 The effect procaterol infusion on plasma noradrenaline (NA) levels during sympathetic nerve stimulation (a). Also shown are the corresponding values of basal diastolic pressure (b) and pressor responses (change in diastolic pressure; c). There were 2 consecutive stimulations (S1 and S2; 2 Hz, 0.5 ms, 20 V, for 90 s at 15 min intervals). Saline (0.9% NaCl, vehicle) or drug infusion began after the first stimulation (S1). Drugs used were procaterol (30 ng kg^{-1} min^{-1}, i.v.), captopril (5 mg kg^{-1}, i.v.) and losartan (10 mg kg^{-1}, i.v.). All results are expressed as a percentage of the first stimulation (S1). The mean with s.e.mean is shown. A significant effect of procaterol ($P<0.05$, Student's t test) versus vehicle ($n=7$) or appropriate drug is indicated by *. A significant effect of drug ($P<0.05$, Dunnett's test) versus vehicle ($n=7$) is indicated by †.

Effects of procaterol on plasma noradrenaline levels during sympathetic nerve stimulation

In this series of experiments plasma noradrenaline levels in arterial blood during sympathetic nerve stimulation (2 Hz, 0.5 ms, 20 V, for 90 s) were measured. Procaterol (30 ng kg^{-1} min^{-1}, i.v.) significantly enhanced plasma noradrenaline levels compared to control but pressor responses to sympathetic nerve stimulation were not altered (Figure 5a and c).

Plasma noradrenaline levels during sympathetic nerve stimulation were not significantly altered by captopril (5 mg kg^{-1}, i.v., Figure 5a). However, in the presence of captopril, procaterol (30 ng kg^{-1} min^{-1}, i.v.) no longer significantly enhanced plasma noradrenaline levels during sympathetic nerve stimulation (Figure 5a). The AT_1 angiotensin receptor antagonist, losartan (10 mg kg^{-1}, i.v.), did not alter plasma noradrenaline during sympathetic nerve stimulation (Figure 5a) and the enhancement of plasma noradrenaline levels during sympathetic nerve stimulation produced by procaterol was not reduced by losartan (Figure 5a). All of the drugs which produced hypotension (captopril and losartan) reduced the pressor responses to sympathetic nerve stimulation (Figure 5b and c).

Discussion

There has been considerable debate about adrenaline activation of presynaptic β_2-adrenoceptors and the development of hypertension through facilitation of noradrenaline release from sympathetic nerves (see Majewski & Rand, 1986; Floras, 1992). An intriguing possibility has arisen that β_2-adrenoceptor facilitation of transmitter release is in fact mediated indirectly by local generation of angiotensin II (see Introduction). This hypothesis was the basis for the present study where we investigated the effect of the selective β_2-adrenoceptor agonist, procaterol, on pressor responses to thoracolumbar preganglionic sympathetic nerve stimulation in the pithed rat which was adrenal demedullated several days prior to experimentation to remove endogenous sources of circulating and tissue adrenaline (Majewski & Murphy, 1989).

It has been shown previously that infusions of procaterol, which did not affect resting blood pressure, enhanced pressor responses to sympathetic nerve stimulation in pithed spontaneously hypertensive rats (SHR) (procaterol, 10–13 ng kg^{-1} min^{-1}, Borkowski & Quinn, 1984) and pithed Wistar rats (procaterol, 13–21 ng kg^{-1} min^{-1}, Schlicker *et al.*, 1988). These effects are attributed to activation of β_2-adrenoceptors and enhanced sympathetic transmitter release since procaterol had no effect on pressor responses to exogenous noradrenaline (Borkowski & Quinn, 1984; Schlicker *et al.*, 1988). The studies of Borkowski & Quinn (1984) and Schlicker *et al.* (1988) imply that β_2-adrenoceptors responsible for enhancing transmitter release are more sensitive to agonists than β_2-adrenoceptors responsible for mediating vasodilatation. However, in our study we were unable to obtain an infusion of procaterol which altered pressor responses without affecting resting blood pressure. Low infusion rates of procaterol (1 and 3 ng kg^{-1} min^{-1}) did not affect resting blood pressure and did not affect responses to sympathetic nerve stimulation (not shown). Higher infusion rates (10 and 30 ng kg^{-1} min^{-1}), comparable to the previous studies of Borkowski & Quinn (1984) and Schlicker *et al.* (1988), reduced resting blood pressure but still had no effect on responses to sympathetic nerve stimulation.

Effects on resting blood pressure may be very important in pithed rats. Many studies have shown that reducing blood pressure with drugs in the pithed rat reduces the vasoconstrictor effects of drugs (e.g. Oldham & Scotcher, 1986; Hatton & Clough, 1982). In the present study the vasodilator sodium nitroprusside (SNP), which is a guanosine 3′:5′-cyclic monophosphate (cyclic GMP)-dependent vasodilator, reduced pressor responses to sympathetic nerve stimulation. SNP does not inhibit noradrenaline release (Waldman & Murad, 1987) and the effect is probably due to a reduction in postjunctional vasoconstrictor sensitivity since pressor responses to methoxamine were also reduced by SNP. This contrasts with the case of procaterol which reduced pressor responses to methoxamine but not sympathetic nerve stimulation and suggests that there may have been an underlying facilitation of sympathetic transmitter release by procaterol to compensate for the reduced postjunctional effectiveness. Indeed, when Borkowski & Quinn (1984) used an infusion of procaterol which lowered blood pressure (100 ng kg^{-1} min^{-1}) there was no effect on pressor responses to sympathetic nerve stimulation but there was a reduction in vasoconstrictor responses to noradrenaline, which is similar to the findings of the present study.

Procaterol (30 ng kg^{-1} min^{-1}) enhanced the plasma nora-

drenaline levels elicited by sympathetic nerve stimulation by 89 pg ml^{-1} (21%), which indicates facilitation of noradrenaline release. This enhancement is unlikely to be due to a reduction in noradrenaline plasma clearance since in most studies, β-adrenoceptor agonists either have no effect (Majewski *et al.*, 1982) or enhance noradrenaline plasma clearance (Cryer *et al.*, 1980). In other *in vivo* models including the anaesthetized and pithed rabbit (Schmidt *et al.*, 1984) and in man (Musgrave *et al.*, 1984) β-adrenoceptor agonists also enhance noradrenaline release.

To investigate a possible role of locally generated angiotensin II in the effect of procaterol, captopril (5 mg kg^{-1}) was used in the present study to block angiotensin II formation from angiotensin I. In this case captopril reduced pressor responses to sympathetic nerve stimulation as has been previously reported (e.g. Oldham & Scotcher, 1986). This effect was presumably due to the hypotension induced by captopril since subsequent vasopressin infusion, which prevented the hypotension, restored pressor responses. This observation further highlights the importance of resting blood pressure on pressor response in this model. It should be noted that vasopressin acts directly on vascular smooth muscle (Share, 1988) and is thought to have no effects on sympathetic transmitter release (Johnson *et al.*, 1974). In the presence of captopril and vasopressin, SNP reduced pressor responses to sympathetic nerve stimulation yet procaterol, which produced a similar degree of hypotension, had no effect on pressor responses suggesting that neurogenic vasoconstriction was still being facilitated. This result contrasts with that of Schlicker *et al.* (1988) who found that the facilitatory effect of procaterol on neurogenic responses was inhibited by captopril and the angiotensin receptor antagonist, saralasin. The discrepancy may be because in the latter case the pressor responses were themselves reduced by the anti-angiotensin drugs and this was not corrected for as in the present study.

When plasma noradrenaline levels were measured in the presence of captopril, it was found that procaterol no longer significantly enhanced plasma noradrenaline levels during sympathetic nerve stimulation, although there was a tendency for this to happen. In contrast, in the presence of the selective angiotensin II receptor (AT_1) blocking drug, losartan (10 mg kg^{-1}), procaterol still produced increases in noradrenaline release during sympathetic nerve stimulation. This dose was sufficient to block completely the pressor effects of infused angiotensin II in the pithed rat (Rechtman & Majewski, 1993). The discrepancy between the effects of captopril and losartan may be because the dose of captopril (5 mg kg^{-1}) (this dose blocked the facilitatory effects of procaterol on neurogenic responses in the study by Schlicker *et al.*, 1988) was high and and in excess of that required to block angiotensin converting enzyme activity and angiotensin II production (see Boura *et al.*, 1982; Clough *et al.*, 1982; where 0.01 and 0.1 mg kg^{-1} was sufficient, respectively). Indeed, in a previous study in the rat isolated kidney (Rump & Majewski, 1987) low concentrations of captopril (0.1 μM), which blocked angiotensin II formation from angiotensin I, had no effect on β-adrenoceptor facilitation of noradrenaline release whilst high concentrations of captopril (5 μM) did block β-adrenoceptor facilitation of noradrenaline release. In the same study (Rump & Majewski, 1987) the angiotensin receptor blocking agent, saralasin, did not affect β-adrenoceptor facilitation of noradrenaline release. Thus, high concentrations of captopril may affect noradrenaline release by angiotensin II-independent mechanisms. Whether this involves other substances affected by converting enzyme such as kinins, opioids and tachykinins, or other processes is unclear.

In conclusion, this study has demonstrated that pressor responses to sympathetic nerve stimulation are critically dependent on basal blood pressure in the pithed rat. It should be noted that the large reductions in pressor responses to sympathetic nerve stimulation by captopril and losartan were not accompanied by any change in plasma noradrenaline levels (compare Figure 5a and c) and thus are most likely to be due to the hypotension produced by these agents. If it is assumed that this can be taken into account by examining the changes in pressor responses to exogenous agonists or maintaining blood pressure with vasopressin infusion, then it appears that the β_2-adrenoceptor agonist, procaterol, facilitates neurogenic vasoconstriction by a mechanism independent of angiotensin II since this was not affected by captopril. Biochemical measurements of increments in plasma noradrenaline during nerve stimulation also support the proposal that procaterol enhances stimulation-induced noradrenaline release. This effect is not blocked by losartan and thus does not involve angiotensin receptors. However, the effects of captopril are equivocal with an indication that it may block the facilitatory effect of procaterol on plasma noradrenaline. However, this may be unrelated to blockade of angiotensin II since the dose of captopril was high.

This work was supported by a grant from the National Health and Medical Research Council of Australia. P.K. is a National Heart Foundation of Australia Postgraduate Research Scholar.

References

BOURA, A.L.A., HUI, S.-C.G., RECHTMAN, M.P. & WALTERS, W.A.W. (1982). Captopril inhibits pressor responses to peripheral sympathetic nerve activation in cats and rats. *Clin. Exp. Pharmacol. Physiol.*, **7**, 123–128.

BORKOWSKI, K.R. (1988). Pre- and postjunctional β-adrenoceptors and hypertension. *J. Autonom. Pharmacol.*, **8**, 153–171.

BORKOWSKI, K.R. & QUINN, P. (1984). Facilitation by β-adrenoceptors of stimulation-induced vasoconstriction in pithed spontaneously hypertensive rats. *J. Autonom. Pharmacol.*, **4**, 127–131.

CLOUGH, D.P., COLLIS, M.C., CONWAY, J., HATTON, R. & KEDDIE, J.R. (1982). Interaction of angiotensin-converting enyzme inhibitors with the function of the sympathetic nervous system. *Am. J. Cardiol.*, **49**, 1410–1414.

COPPES, R.P., SMIT, J., KHALI, N.N., BROUWER, F. & ZAAGSMA, J. (1993). Strong activation of vascular prejunctional β_2-adrenoceptors in freely moving rats by adrenaline released as a co-transmitter. *Eur. J. Pharmacol.*, **243**, 272–279.

CRYER, P.E., RIZZA, R.A., HAYMOND, M.W. & GERICH, J.E. (1980). Epinephrine and norepinephrine are cleared through beta-adrenergic but not alpha-adrenergic mechanisms in man. *J. Clin. Invest.*, **29** (suppl. 1), 1114–1118.

DRAPER, A.J., MEGHJI, S. & REDFERN, P.H. (1989). Enhanced presynaptic facilitation of vascular adrenergic neurotransmission in spontaneously hypertensive rats. *J. Autonom. Pharmacol.*, **9**, 103–111.

FLORAS, J.S. (1992). Epinephrine and the genesis of hypertension. *Hypertens*, **19**, 1–18.

GÖTHERT, M. & KOLLECKER, P. (1986). Subendothelial β_2-adrenoceptors in the rat vena cava: Facilitation of noradrenaline release via local stimulation of angiotensin II synthesis. *Naunyn-Schmied. Arch. Pharmacol.*, **334**, 156–165.

HATTON, R. & CLOUGH, D.P. (1982). Captopril interferes with neurogenic vasoconstriction in the pithed rat by angiotensin-dependent mechanisms. *J. Cardiovasc. Pharmacol.*, **4**, 116–123.

JOHNSON, E.M., MARSHALL, G.R. & NEEDLEMAN, P. (1974). Modification of the pressor responses to sympathetic nerve stimulation by the renin-angiotensin system in rats. *Br. J. Pharmacol.*, **51**, 541–546.

KAWASAKI, H., CLINE, W.H. & SU, C. (1984). Involvement of the vascular renin-angiotensin system in beta adrenergic receptor-mediated facilitation of vascular neurotransmission in spontaneously hypertensive rats. *J. Pharmacol. Exp. Ther.*, **231**, 23–32.

LI, C., MAJEWSKI, H. & RAND, M.J. (1988). Facilitation of noradrenaline release from sympathetic nerves in rat anococcygeus muscle by activation of prejunctional β-adrenoceptors and angiotensin receptors. *Br. J. Pharmacol.*, **95**, 385–392.

MAJEWSKI, H. (1983). Modulation of noradrenaline release through activation of presynaptic β-adrenoceptors. *J. Autonom. Pharmacol.*, **3**, 47–60.

MAJEWSKI, H., HEDLER, L., SCHURR, C. & STARKE, K. (1985). Dual effect of adrenaline on noradrenaline release in the pithed rabbit. *J. Cardiovasc. Pharmacol.*, **7**, 251–257

MAJEWSKI, H., HEDLER, L. & STARKE, K. (1982). The noradrenaline release rate in the anaesthetized rabbit: facilitation by adrenaline. *Naunyn-Schmied. Arch. Pharmacol.*, **321**, 20–27.

MAJEWSKI, H. & MURPHY, T.V. (1989). Beta-adrenoceptor blockade and sympathetic neurotransmission in the pithed rat. *J. Hypertens*, **7**, 991–996.

MAJEWSKI, H. & RAND, M.J. (1986). A possible role of epinephrine in the development of hypertension. *Med. Res. Rev.*, **6**, 467–486.

MAJEWSKI, H., RAND, M.J. & TUNG, L.H. (1981). Activation of prejunctional β-adrenoceptors in rat atria by adrenaline applied exogenously or released as a co-transmitter. *Br. J. Pharmacol.*, **73**, 669–679.

MIAN, M.A., MAJEWSKI, H. & RAND, M.J. (1989). Facilitation of noradrenaline release by isoprenaline in rat isolated atria does not involve angiotensin II formation. *Clin. Exp. Pharmacol. Physiol.*, **16**, 905–911.

MUSGRAVE, I.F., BACHMAN, A.W. & GORDON, R.D. (1984). Increased plasma noradrenaline during adrenaline infusion in man. *J. Hypertens*, **2** (suppl 3), 135–137.

NAKAMURA, M., JACKSON, E.K. & INAGAMI, T. (1986). β-Adrenoceptor mediated release of angiotensin II from mesenteric arteries. *Am. J. Physiol.*, **250**, H144–H148.

OLDHAM, A.A. & SCOTCHER, K.P. (1986). Interactions between angiotensin II, the sympathetic nervous system and blood pressure of the pithed rat. *Br. J. Pharmacol.*, **86**, 749P.

RAJANAYAGAM, M.A.S., MUSGRAVE, I.F., RAND, M.J. & MAJEWSKI, H. (1989). Facilitation of noradrenaline release by isoprenaline is not mediated by angiotensin II in mouse atria and rat tail artery. *Arch. Int. Pharmacodyn. Ther.*, **299**, 185–199.

RECHTMAN, M.P. & MAJEWSKI, H. (1993). A facilitatory effect of anti-angiotensin drugs on vagal bradycardia in the pithed rat and guinea-pig. *Br. J. Pharmacol.*, **110**, 289–296.

RUMP, L.C. & MAJEWSKI, H. (1987). Beta-adrenoceptor facilitation of norepinephrine release is not dependent on local angiotensin II formation in the rat isolated kidney. *J. Pharmacol. Exp. Ther.*, **243**, 1107–1112.

SCHLICKER, E., ERKENS, K. & GÖTHERT, M. (1988). Probable involvement of angiotensin II formation in the β_2-adrenoceptor-mediated facilitation of the neurogenic vasopressor response in the pithed rat. *Naunyn-Schmied. Arch. Pharmacol.*, **338**, 536–542.

SCHMIDT, H., SCHURR, C., HEDLER, L. & MAJEWSKI, H. (1984). Local modulation of noradrenaline release in vivo: presynaptic β_2-adrenoceptors and endogenous adrenaline. *J. Cardiovasc. Pharmacol.*, **6**, 641–649.

SHARE, L.A. (1988). Role of vasopressin in cardiovascular regulation. *Physiol. Rev.*, **68**, 1248–1284.

STJÄRNE, L. & BRUNDIN, J. (1975). Dual adrenoceptor-mediated control of noradrenaline secretion from human vasoconstrictor nerves: facilitation by β-receptors and inhibition by α-receptors. *Acta Physiol. Scand.*, **94**, 139–141.

WALDMAN, S.A. & MURAD, F. (1987). Cyclic GMP synthesis and function. *Pharmacol. Rev.*, **39**, 163–196.

WEINSTOCK, M., THOA, N.B. & KOPIN, I.J. (1978). β-Adrenoceptors modulate noradrenaline release from axonal sprouts in cultured rat superior cervical ganglia. *Eur. J. Pharmacol.*, **47**, 297–302.

ZIMMERMAN, B.G. (1981). Adrenergic facilitation by angiotensin: Does it serve a physiological function? *Clin. Sci.*, **60**, 343–348.

ZIOGAS, J. & STORY, D.F. (1991). Angiotensin II generation in the rat vena cava: Stimulation of local synthesis by β-adrenoceptor activation. *Naunyn-Schmied. Arch. Pharmacol.*, **343**, 31–36.

(Received May 11, 1994
Revised July 1, 1994
Accepted July 4, 1994)

Br. J. Pharmacol. (1994), **113**, 789–794 © Macmillan Press Ltd, 1994

Enhancement of retinal acetylcholine release by DAMGO: possibly a direct opioid receptor-mediated excitatory effect

M.J. Neal, S.J. Paterson & J.R. Cunningham

Department of Pharmacology, UMDS, St Thomas' Hospital, London SE1 7EH

1 An eye-cup preparation in anaesthetized rabbits was used to examine opioid modulation of acetylcholine (ACh) release from cholinergic neurones in the retina.

2 The μ-opioid receptor agonist, [D-Ala^2, MePhe^4, Gly-ol^5]-enkephalin (DAMGO), when applied locally to the retina at concentrations between 1–30 μM significantly increased the light-evoked release of ACh. The effect of DAMGO was completely blocked by the selective μ-receptor antagonist CTOP but the κ-receptor antagonist nor-binaltorphimine (norBNI) did not affect the action of DAMGO on ACh release indicating that the opioid produced its effect by activation of μ-receptors (the rabbit retina has negligible δ-receptors).

3 Blockade with bicuculline and strychnine of GABAergic and glycinergic inputs to the cholinergic neurones did not affect the action of DAMGO on ACh release. Also DAMGO did not reduce the potassium-evoked release of either GABA or glycine from rat isolated retinas.

4 Exposure of the rabbit retina to a combination of an A_1-adenosine receptor antagonist, 8-cyclopentyl-1,3 dipropylxanthine (DPCPX), and adenosine deaminase did not affect the enhancing action of DAMGO on the light-evoked release of ACh.

5 When the retina in the rabbit eye-cup was exposed to kainate, the release of ACh was increased by approximately three times the resting release. In the presence of DAMGO the kainate-evoked release of ACh was enhanced by 44%.

6 These experiments show that activation of μ-opioid receptors by DAMGO increases the release of ACh elicited by physiological stimulation (flickering light). Since we could find no evidence that DAMGO reduces inhibitory inputs to the cholinergic neurones, it seems that the enhancing action of DAMGO on the light-evoked release of ACh involves a direct excitatory effect rather than disinhibition. This conclusion is supported by the enhancing action of DAMGO on the kainate-evoked release of ACh because kainate is thought to act directly on the cholinergic neurones.

Keywords: Opioid receptors; ACh release; cholinergic neurones; retina; amacrine cell; opioids

Introduction

The retina is a part of the central nervous system that possesses cholinergic neurones (Neal, 1983). In the rabbit retina, Masland & Mills (1979) showed that these neurones were amacrine cells. About half of these cells are located in the inner nuclear layer and ramify narrowly in sublamina *a* of the inner plexiform layer. The other half of the cholinergic amacrine cells are displaced into the ganglion cell layer and these ramify narrowly in sublamina *b* of the inner plexiform layer. The cholinergic neurones in the retina are transiently responding cells and release acetylcholine (ACh) when the retina is stimulated with flickering light but not by changes in constant illumination (Massey & Neal, 1979).

The cholinergic neurones receive excitatory input from cone bipolar cells (Famiglietti, 1983; 1991) and ACh release studies using a rabbit eye-cup preparation have shown that the bipolar cell transmitter is an excitatory amino acid acting on kainate receptors (Cunningham & Neal, 1985; Linn *et al.*, 1991). The only known inhibitory inputs to the cholinergic neurones arise from glycinergic and GABAergic amacrine cells (Massey & Redburn, 1982; Cunningham & Neal, 1983). It has been claimed recently that adenosine has a tonic inhibitory action on cholinergic amacrine cells (Blazynski *et al.*, 1992) but the physiological significance of this is unknown.

Immunocytochemical studies have shown that many retinas possess enkephalinergic amacrine cells but the number of such neurones varies widely between different species (for review Brecha *et al.*, 1984). Enkephalinergic amacrine cells are particularly well developed in avian retinas, where over half of the enkephalinergic neurones stain also for glycine. This colocalization seems to be species specific and in a variety of non-mammalian retinas enkephalin has been shown to colocalize with GABA. In mammalian retinas, enkephalinergic amacrine cells are less well developed although they have been described in the guinea-pig retina (Altschuler *et al.*, 1982). In the rabbit retina, it has proved difficult to characterize enkephalinergic neurones but immunocytochemical studies have revealed a subpopulation of amacrine cells that stain for endo-oligopeptidase A, a putative enkephalin generating enzyme (Ferro *et al.*, 1991). Recently, we have used selective opioid ligands to characterize opioid binding sites in mammalian retinas (Cunningham *et al.*, 1992) and found that the rabbit retina possesses a significant number of opioid receptors which are predominantly of the μ-receptor subtype (85%). The remaining 15% of binding sites are of the κ-receptor subtype.

In a preliminary experiment in collaboration with Dr A. Corbett we have found that the rabbit retina possesses [Met^5]enkephalin and [Leu^5]enkephalin in a ratio of 3 to 1 (i.e. the same as brain) although the actual concentrations were only about 2–3% of those occurring in brain.

Opioids are thought to have a modulatory role in the central nervous system and they have consistently been shown to inhibit ACh release from the brain, (for example, Ruzicka & Jhamandas, 1991; Mulder *et al.*, 1991; Arenas *et al.*, 1991; Heijna *et al.*, 1992). The present study was undertaken to explore the possibility that μ-opioid receptor activation in the rabbit retina might modulate the release of ACh. We found that the μ-receptor agonist DAMGO enhanced the

[1] Author for correspondence.

light-evoked release of ACh apparently by a receptor-mediated excitatory action rather than by disinhibition.

Methods

Eye-cup preparation

The methods have been described in detail previously (Neal & Cunningham, 1982). Briefly, adult albino rabbits were anaesthetized with urethane (1.5 g kg^{-1}, i.p.) and a stainless-steel ring was sutured to the episclera to prevent collapse of the eye-cup. The cornea and iris were removed and this was followed by an intracapsular lens extraction and vitrectomy. The resulting eye-cup was filled for 30 min with Krebs Ringer bicarbonate containing [^{3}H]-ACh (0.5 μM) and then the retina was continuously irrigated for 60 min with fresh medium containing physostigmine (30 μM). A syringe mounted on a micromanipulator was used to place 0.5 ml of medium in the eye-cup and this was replaced at 5 min intervals. The total radioactivity in the resulting samples was measured by liquid scintillation counting. In previous experiments it was found that [^{3}H]-ACh represented 95–100% of the increase in total radioactivity evoked by light flashes. Therefore, in the present experiments, the increase in total radioactivity produced by stimulation with light was assumed to be due to an increase in the release of [^{3}H]-ACh.

The light source was a quartz halide bulb (100 W) and the initially dark-adapted retina was stimulated for 5 min periods by flickering light at 3 Hz (25% duty cycle; retinal illuminance, 650 lux).

The viability of the eye-cup preparation and the effects of drugs on the gross physiological response of the retina were assessed by electroretinography (ERG). None of the drugs used in the present study significantly affected the b-wave of the ERG, indicating that they had no major effects on the distal part of the retina (i.e. at the synapses between the photoreceptors and the bipolar cells).

Expression of results

The effects of light stimulation on the release of total radioactivity from the retina are expressed as the ratio of the peak-evoked release of radioactivity to the average release of radioactivity in the two samples immediately preceding stimulation. The resulting ratio is hereafter referred to as the 'light-evoked release of ACh'.

Analysis of results

In each rabbit experiment, the mean values of the light-evoked release of [^{3}H]-ACh in the presence or absence (controls) of the drug were calculated. Each drug was tested in three to six separate rabbit experiments and the light-evoked release of [^{3}H]-ACh was expressed as a percentage (mean ± s.e.mean) of that obtained in the absence of drug.

Isolated rat retinas

Male hooded Lister rats (150–200 g) were killed by cervical dislocation. The eyes were enucleated and the retinas dissected in Krebs bicarbonate medium at room temperature. In experiments on GABA release, retinas were taken from animals that had been treated with the irreversible GABA-T inhibitor, γ-vinyl-GABA (GVG) (250 mg kg^{-1} i.p.) 18 h before death (Neal & Shah, 1989).

In order to measure the release of GABA and glycine from the tissue, two entire rat retinas (approx 20 mg) were placed in a small perspex chamber (volume 0.5 ml) containing Krebs-bicarbonate medium (300 μl) at room temperature and were gently agitated by a stream of 5% CO_2 in oxygen. At 10 min intervals, the medium was drained off and replaced with fresh solution. The GABA and glycine in each of the resulting 10 min samples were measured by high performance liquid chromatography (h.p.l.c.). Potassium evoked release of GABA and glycine was achieved by exposing the tissues for one 10 min period to KCl (50 mM). The effect of drugs on the K-evoked release was examined by exposing the tissue to the drug in the collection period immediately preceding the addition of KCl and during exposure to KCl. GABA and glycine were analysed by reverse phase chromatography on a Varian 5000 h.p.l.c. using precolumn derivatisation with *o*-phthalaldehyde (Turnell & Cooper, 1981).

Statistical analysis

Values for the mean and standard error of the mean (s.e.mean) were calculated and compared using Student's *t* test for paired and unpaired analyses. Significant differences were assumed at a level of $P<0.05$.

Medium and chemicals

Krebs bicarbonate Ringer of the following composition was used (mM): NaCl 118.4, KCl 4.84, CaCl 2.4, $MgSO_4$ 1.8, KH_2PO_4 1.2, $NaHCO_3$ 25, glucose 9.5, gassed with a mixture of 5% CO_2 in oxygen. [Methyl-^{3}H]-choline chloride (Sp.Act. 85 Ci $mmol^{-1}$) was obtained from Amersham International. Vigabatrin (γ-vinyl-GABA) was a gift from Merrell Dow, Strasbourg, France; 8-cyclopentyl-1,3 dipropylxanthine (DP-CPX) and nor-binaltorphimine HCl (norBNI) were obtained from Research Biochemicals Inc; naloxone from Endo Laboratories; CTOP (Cys^2, Tyr^3, Orn^5, Pen^7 Amide) from Peninsula Laboratories, Inc; other chemicals (Analar grade) were obtained from BDH or Sigma.

Results

DAMGO enhances light-evoked release of ACh

When the rabbit retina was exposed to DAMGO (1–30 μM) in the eye-cup the resting release of ACh was not affected but the light-evoked release was significantly enhanced. This effect is illustrated in Figure 1 which shows a typical experiment where DAMGO increased the light-evoked release of ACh by 40%. The effect of different concentrations of DAMGO on the light-evoked release of ACh is summarized in Figure 2. The opioid significantly enhanced the light-evoked release of ACh at 1 μM and its maximum effect was produced at 30 μM.

The effect of a submaximal concentration of DAMGO (10 μM) on the light-evoked release of ACh was antagonized by naloxone (1 μM) (Figure 1) indicating that the action of DAMGO was mediated by opioid receptors. Since we had previously found that about 15% of the opioid binding sites in the rabbit retina are of the κ-type (Cunningham *et al.*, 1992), the effect of selective μ and κ-opioid receptor antagonists on the action of DAMGO was examined (there are negligible δ-binding sites). The results are summarized in Figure 2 and clearly show that the κ-receptor antagonist norBNI did not antagonize the enhancing effect of DAMGO on the light-evoked release, whilst the μ-receptor antagonist CTOP abolished the effect of DAMGO. It seems therefore that the enhancing effect of DAMGO on the light-evoked release of ACh from the retina is mediated predominantly by activation of μ-receptors. Naloxone and CTOP alone did not affect ACh release indicating that the cholinergic amacrine cells are not under enkephalinergic tone.

Effect of DAMGO unaffected by strychnine

The cholinergic amacrine cells receive inhibitory inputs from glycinergic and GABAergic amacrine cells. In order to test whether DAMGO enhanced the light-evoked release of ACh by reducing glycinergic inhibition, the effects of DAMGO

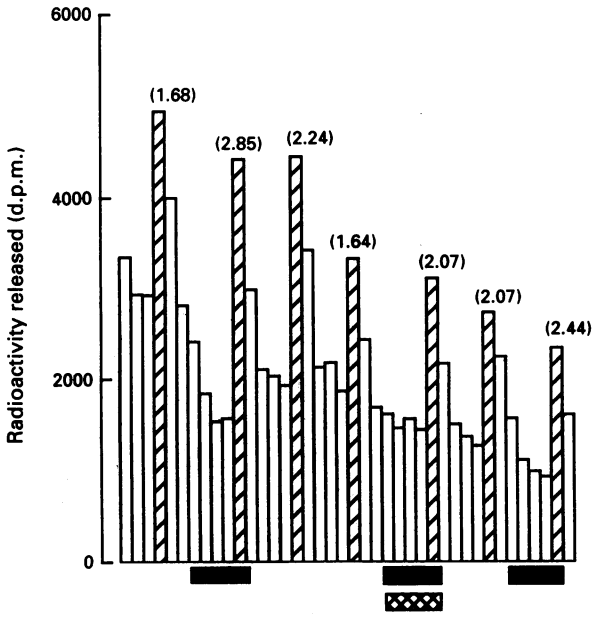


Figure 1 Effect of DAMGO (10 μM) (solid horizontal bar) and naloxone (1 μM) (cross-hatched horizontal bar) on the light-evoked release of ACh from the rabbit retina. Each column is a 5 min collection period. Hatched columns indicate stimulation with a flickering light (3 Hz, 25% duty cycle, 650 lux). Figures in parentheses indicate stimulated release/resting release and is taken as a measure of the 'light-evoked release of ACh. In this typical experiment, the mean control light-evoked release was 1.91 and this was increased to 2.65 in the presence of DAMGO. This experiment was repeated six times with similar results. For abbreviations in this and subsequent legends, see text.

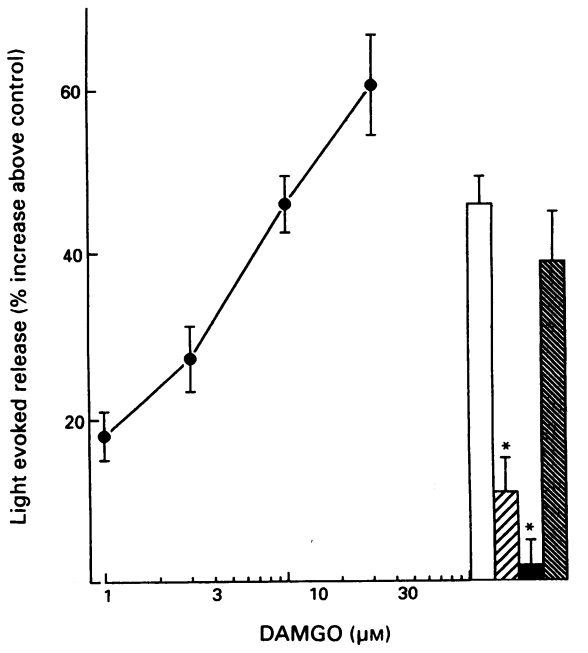


Figure 2 Effect of different concentrations of DAMGO on the light-evoked release of ACh from the rabbit retina (●). The columns show the effect of opioid receptor antagonists on the increase of light-evoked release of ACh caused by a submaximal (10 μM) concentration of DAMGO. Open column: light-evoked release of ACh in the presence of DAMGO (percentage of light-evoked release in absence of drug) widely hatched column: DAMGOC + naloxone (1 μM); solid column: DAMGOC + CTOP (0.1 μM); narrowly hatched column: DAMGOC + norBNI (0.1 μM). Each result is the mean of 3–4 separate rabbit experiments. S.e.mean are indicated and * indicates DAMGOC + antagonist is significantly different from DAMGO alone ($P < 0.001$).

(10 μM) were examined in the presence of strychnine (20 μM). This concentration of strychnine was used because we have previously shown that it prevents the inhibitory action of glycine (but not GABA) on ACh release (Cunningham & Neal, 1983). Strychnine had no significant effect on the action of DAMGO (Table 1).

Effect of DAMGO unaffected by bicuculline

When the retina was exposed to bicuculline (10 μM) the resting release of ACh was increased approximately 2 fold, an effect that has been reported previously (Cunningham & Neal, 1983). Bicuculline at this concentration has been shown to block the effects of exogenous $GABA_A$ receptor agonists on ACh release (Cunningham & Neal, 1983) but as shown in Table 1, it did not affect the action of DAMGO on the light-evoked release of ACh.

DAMGO did not inhibit GABA or glycine release from isolated retinas

As a further test to see whether DAMGO might enhance the evoked release of ACh by inhibiting GABA or glycine release, its effect on their release was examined in rat isolated retinas. When control isolated retinas were exposed to KCl (50 mM) the release of GABA and glycine was increased by 9.1 and 3.3 fold respectively (Figure 3). The KCl-evoked release of GABA and glycine in the presence of DAMGO was 9.8 and 3.5 respectively. Thus, the release of these transmitters was unaffected by DAMGO (Figure 3) supporting the conclusion that the opioid did not enhance ACh release by reducing GABA- or glycine-mediated inhibition.

Effect of DAMGO unaffected by adenosine antagonism

It has been suggested that adenosine may modulate transmitter release in the retina (for review Blazynski & Perez, 1991) and using the rabbit eye-cup preparation, Blazynski *et al.* (1992) found that the adenosine A_1-antagonist, DPCPX and adenosine deaminase increased the light-evoked release of ACh, suggesting that there is a tonic release of (inhibitory) adenosine. The possibility that DAMGO might enhance the light-evoked release of ACh by inhibiting the release of adenosine was tested by exposing the retina to DAMGO in the presence of both DPCPX (0.1 μM) and adenosine deaminase (1 u ml^{-1}). Although this combination of drugs would be expected to inhibit the action of endogenously released adenosine, it had no effect on the enhancement of the light-evoked release of ACh by DAMGO (Table 1). Thus, the

Table 1 Effect of antagonists on the enhancement of light-evoked acetylcholine (ACh) release caused by [D-Ala^2,MePhe^4,Gly-ol^5] enkephalin (DMAGO) (10 μM)

Antagonist	*Light-evoked release of ACh (% of release in presence of DAMGO alone)*	*Number of experiments*
Strychnine (20 μM)	100.6 ± 9.80	3
Bicuculline (10 μM)	97.7 ± 4.55	3
DPCPX (0.1 μM) and adenosine deaminase (1 u ml^{-1})	103.6 ± 6.15	3

The light-evoked release of ACh from the rabbit retina was measured in the presence of antagonist with and without DAMGO. The results are expressed as the mean of the percentage of release in the presence of DAMGO alone ± s.e.mean. None of the antagonists significantly affected the enhancing action of DAMGO on the light-evoked release of ACh. DPCPX: 8-cyclopentyl-1,3 dipropylxanthine.

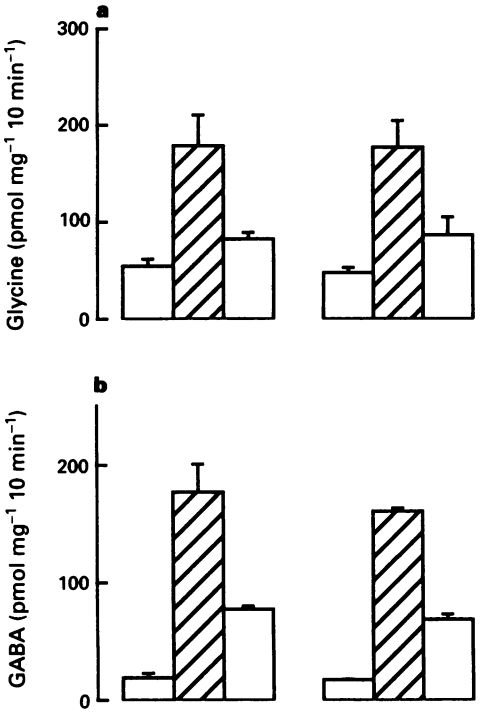


Figure 3 Effect of DAMGO (10 μM) on the potassium-evoked release of (a) glycine and (b) GABA from the rat isolated retina. Each column is a 10 min collection period. Stimulation of control retinas (left) with 50 mM KCl (hatched columns) significantly increased the release of both glycine ($n = 7$) and GABA ($n = 3$) ($P < 0.01$ and $P < 0.05$ respectively). When retinas were exposed to DAMGO (10 μM) (right) the K-evoked release of glycine and GABA was not significantly different from that occurring in the absence of the opioid. S.e.mean are indicated.

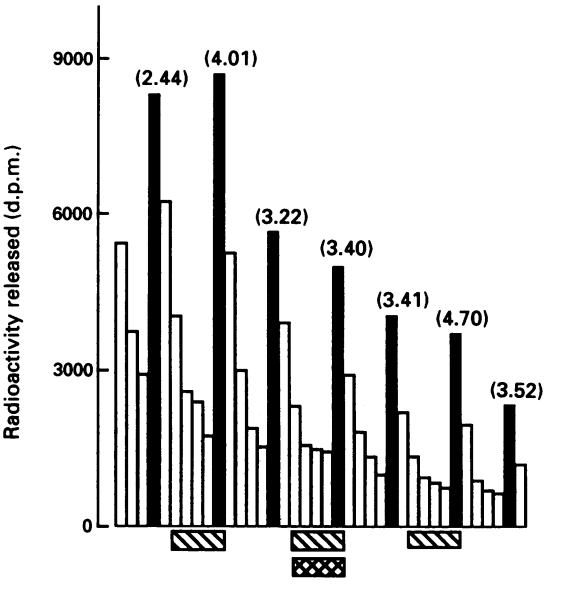


Figure 4 Typical rabbit eye-cup experiment showing that exposure of the retina to kainate (10 μM) (solid columns) for 5 min caused an approximately 3 fold increase in ACh release. In the presence of DAMGO (10 μM) (hatched horizontal bar) the kainate-evoked release of ACh was strikingly increased, an effect that was blocked by naloxone (1 μM) (cross-hatched horizontal bar).

increase in ACh release caused by DAMGO is unlikely to be due to an opioid mediated inhibition of adenosine release.

DAMGO enhances kainate-evoked ACh release

When the retina in the rabbit eye-cup was exposed to kainate (10 μM) (Figure 4) the release of ACh was increased approximately 3 fold. The kainate-evoked release of ACh was strikingly increased by DAMGO (10 μM) an effect that was blocked by naloxone (1 μM) (Figure 4). In five separate rabbit experiments DAMGO increased the kainate-evoked release of ACh by 43.6% ± 5.2 ($n = 5$). Since kainate has been reported to stimulate ACh release by a direct effect on cholinergic amacrine cells (Linn & Massey, 1992), the enhancement of its action by DAMGO is consistent with the idea that DAMGO might be acting directly on the cholinergic neurones.

Discussion

Opioids have been shown to modulate the release of many transmitters in both the central and peripheral nervous systems. The predominant effect of opioid receptor activation is to inhibit transmitter release and apparent excitatory effects have usually involved presynaptic inhibition of non-opioid inhibitory neurones (for review Leslie, 1987). Paton (1957) showed that morphine and 'related substances' inhibited the release of ACh from the coaxially stimulated guinea-pig ileum and many subsequent studies have shown that opioids inhibit ACh release from many areas of the brain (Leslie, 1987). The opioid receptors involved in the inhibition of ACh release differ not only in different brain areas but also in different species (Lapchak *et al.*, 1989). In some brain areas, activation of the different opioid receptors with selective agonists produces apparently opposite effects on ACh release. For example, Wichmann & Starke (1990) found that the electrically-evoked release of [^{3}H]-ACh from striatal slices was inhibited by μ and δ-receptor agonists but stimulated by the κ-receptor agonist, ethylketazocine. However, the effects of the latter drug were blocked by sulperide, and it was concluded that ethylketazocine disinhibited the cholinergic neurones. Nevertheless, it seems that opioid receptor activation can sometimes increase ACh release directly because κ- and δ-receptor agonists (but not μ-receptor agonists) enhance the potassium-evoked release of ACh from synaptosomes prepared from the electric organ of *Torpedo* (Oron *et al.*, 1991). In the present experiments, we found that the μ-receptor agonist, DAMGO, clearly enhanced the light-evoked release of ACh and we failed to find any evidence that this effect was due to disinhibition.

In the retina, the cholinergic neurones receive two known inhibitory inputs, one from glycinergic amacrine cells and one from GABAergic amacrine cells. In goldfish (Djamgoz *et al.*, 1981) and chicken isolated retinas (Watt *et al.*, 1984), opioids ([Met^5]-enkephalin, DADLE, morphine) have been found to decrease the potassium-evoked release of [^{3}H]-GABA from presumed GABAergic amacrine cells. At first sight it may seem that a similar action of opioids in the rabbit retina would account for the action of DAMGO on ACh release. However, in the rabbit retina cholinergic amacrine cells are under considerable GABA tone and blockade of $GABA_A$ receptors with bicuculline causes a striking increase in the resting release of ACh (Cunningham & Neal, 1983). If DAMGO had an inhibitory effect on GABA release in the rabbit retina, then one would expect the opioid to produce an increase in the resting release of ACh. Such an effect was never observed and furthermore the enhancing action of DAMGO on ACh release was not affected by bicuculline at a concentration that is known to block the effects of endogenously released GABA. The conclusion that DAMGO does not increase ACh release by inhibiting GABA release is also supported by our experiment using isolated rat retinas where

we found that DAMGO had no effect on the potassium-evoked release of endogenous GABA.

The only other major inhibitory transmitter in the retina is glycine, the release of which from the rabbit retina following stimulation with flashing light was demonstrated by Ehinger & Lindberg (1974). About 40–60% of amacrine cells accumulate [^{3}H]-glycine and immunohistochemical studies have confirmed that these cells are glycinergic (Marc 1988, for review). The glycinergic amacrine cells seem to be closely involved with the cholinergic amacrine cells and we have recently suggested that the cholinergic neurones in the rabbit retina provide an excitatory input to the glycinergic neurones which form an inhibitory loop back to the cholinergic amacrines (Neal & Cunningham, 1994). This inhibitory feedback is analogous to the Renshaw cell in the spinal cord but the cholinergic synapse is muscarinic. Recently, double immunostaining studies in the frog retina have indicated that all glycinergic amacrine cells possess cholinergic muscarinic receptors (Jardon *et al.*, 1992). Any drug which interrupts the inhibitory glycinergic feedback loop would be expected to enhance the light-evoked release of ACh from the retina. Thus, atropine and strychnine both enhance the light-evoked release of ACh (Cunningham *et al.*, 1983; Neal & Cunningham, 1994). Baclofen also increases the light-evoked release of ACh from the rabbit retina and we have shown that this is because the $GABA_B$ receptor agonist reduces the release of glycine from the glycinergic amacrine cells (Neal & Cunningham, 1994). In the present experiments we could find no evidence that DAMGO enhanced the light-evoked release of ACh by affecting glycinergic transmission. The action of the opioid on the rabbit retina was not affected by strychnine which occludes the action of baclofen (Neal & Cunningham, 1994). Furthermore, DAMGO did not affect the potassium-evoked release of glycine from rat isolated retinas, again in contrast to baclofen which clearly inhibits glycine release (Neal & Cunningham, 1994). Thus, we have found no evidence that the action of DAMGO on retinal ACh release involves a reduction in glycinergic inhibition.

Although glycinergic and GABAergic neurones provide the great majority of amacrine cells in the rabbit retina there are small populations that utilise other transmitters, e.g. dopamine, substance P, somatostatin, but these do not affect ACh release (Cunningham & Neal, 1983).

Recently, it has been suggested that adenosine may modulate transmitter release in the retina (for review Blazynski & Perez, 1991). Immunocytochemical studies have revealed subpopulations of neurones that contain adenosine (Braas *et al.*, 1987; Blazynski, 1989) and also the presence of adenosine deaminase (Senba *et al.*, 1986). In the rabbit retina, adenosine occurs in some amacrine cells, and in displaced amacrine cells, where it is colocalized with ACh. Since other studies have clearly established that ACh and GABA are colocated in these neurones (Brecha *et al.*, 1988) it seems that the displaced amacrine cells in the rabbit retina contain ACh, GABA and adenosine.

The physiological significance of adenosine in the retina is unknown but Perez *et al.* (1986) have reported that purines are continuously released from the rabbit retina. Furthermore, depolarization of the retina with high-potassium or glutamate increased the release of adenosine and other purines (Perez & Ehinger, 1989). Adenosine agonists decreased the potassium-evoked release of [^{3}H]-ACh from the rabbit retina suggesting that endogenously released adenosine might modulate ACh release. Evidence in support of this view was recently presented by Blazynski *et al.* (1992) who used the rabbit eye-cup preparation to show that the light-evoked release of ACh was increased when the retina was exposed to a selective A_1-receptor antagonist or adenosine deaminase (which presumably reduces the extracellular concentration of adenosine). These experiments support the view that in the retina there is a release of adenosine which apparently has a tonic inhibitory action on the cholinergic amacrine cells. The exact cellular location of the A_1-receptors involved in this inhibitory action of adenosine is not known.

In the present experiments, we found that a combination of DPCPX with adenosine deaminase did not affect the enhancing action of DAMGO on the light-evoked release of ACh. A slight problem was that DPCPX alone, or in combination with adenosine deaminase, did not increase the light-evoked release of ACH as described by Blazynski *et al.* (1992). Thus, we found no evidence in our preparation for a tonic inhibitory action of adenosine on ACh release and it seems unlikely that DAMGO enhances the light-evoked release of ACh by inhibiting the release of (inhibitory) adenosine. Furthermore, much of the adenosine in the rabbit retina is colocalized with ACh and it is difficult to believe that DAMGO could increase the release of ACh but decrease the release of adenosine from the same neurone.

Since we could find no evidence that DAMGO enhanced the release of ACh from the retina by reducing any known inhibitory input to the cholinergic amacrine cells, it seems that the effect of DAMGO on retinal ACh release might involve a direct excitatory effect on the cholinergic neurones. The normal excitatory input to the cholinergic amacrine cells is from cone bipolar cells which release an excitatory amino acid transmitter (glutamate?) which acts on kainate receptors (Cunningham & Neal, 1983). When the rabbit retina is exposed to kainate there is a large increase in ACh release and pharmacological studies suggest that kainate acts directly on the cholinergic amacrine cells (Linn & Massey, 1992). In the present experiments, we found that DAMGO not only increased the light-evoked release of ACh, but also enhanced the kainate-evoked release of ACh, a result that is consistent with the suggestion that DAMGO might be acting directly on the cholinergic neurones.

Our experiments provide no information on the conductance changes that underlie the action of DAMGO on ACh release. Presumably activation of μ-receptors on the cholinergic neurones either increases Ca-conductance or decreases K-conductance. Such changes have been described in sensory neurones where opioids have been found to evoke direct receptor-mediated excitatory effects (Crain & Shen, 1990). In summary, we have found that μ-receptor activation in the retina enhances the light-evoked release of ACh, and since we have not been able to find any evidence of a disinhibitory mechanism, we conclude that DAMGO has a direct excitatory action on cholinergic neurones. However, we cannot rule out the possibility that DAMGO acts by reducing the release of an as yet unknown inhibitory transmitter, although this seems rather unlikely.

References

ALTSCHULER, R.A., MOSINGER, J.L., HOFFMAN, D.W. & PARAKKAL, M.H. (1982). Immunocytochemical localization of enkephalin-like immunoreactivity in the retina of the guinea pig. *Proc. Natl. Acad. Sci. U.S.A.*, **79**, 2398–2400.

ARENAS, E., ALBERCH, J., PEREZ-NAVARRO, E., SOLSONA, C. & MARSAL, J. (1991). Neostriatal dopaminergic terminals prevent the GABAergic involvement in the mu- and delta-opioid inhibition of KCl-evoked endogenous acetylcholine release. *Brain Res.*, **556**, 349–352.

BLAZYNSKI, C. (1989). Displaced cholinergic GABAergic amacrine cells in the rabbit retina also contain adenosine. *Vis. Neurosci.*, **3**, 425–431.

BLAZYNSKI, C. & PEREZ, M.T.R. (1991). Adenosine in vertebrate retina: localization, receptor characterization and function. *Cell. Mol. Neurobiol.*, **11**, 463–484.

BLAZYNSKI, C., WOODS, C. & MATHEWS, G.C. (1992). Evidence for the action of endogenous adenosine in the rabbit retina: modulation of the light-evoked release of acetylcholine. *J. Neurochem.*, **58**, 761–767.

BRAAS, K.M., ZARBIN, M.A. & SNYDER, S.H. (1987). Endogenous adenosine and adenosine receptors localized to ganglion cells of the retina. *Proc. Natl. Acad. Sci. U.S.A.*, **84**, 3906–3910.

BRECHA, N.C., ELDRED, W., KULJIS, R.O. & KARTEN, H.J. (1984). Identification and localization of biologically active peptides in the vertebrate retina. *Prog. Retinal. Res.*, **3**, 185–226.

BRECHA, N.C., JOHNSON, D., PEICHL, L. & WÄSSLE, H. (1988). Cholinergic amacrine cells of the rabbit retina contain glutamate decarboxylase and γ-aminobutyric immunoreactivity. *Proc. Natl. Acad. Sci. U.S.A.*, **85**, 6187–6191.

CRAIN, S.M. & SHEN, K.F. (1990). Opioids can evoke direct receptor-mediated excitatory effects on sensory neurons. *Trends Pharmacol. Sci.*, **11**, 77–81.

CUNNINGHAM, J.R., DAWSON, C. & NEAL, M.J. (1983). Evidence for a cholinergic inhibitory feed-back mechanism in the rabbit retina. *J. Physiol.*, **340**, 455–468.

CUNNINGHAM, J.R. & NEAL, M.J. (1983). Effect of γ-aminobutyric acid agonists, glycine, taurine and neuropeptides on acetylcholine release from the rabbit retina. *J. Physiol.*, **336**, 563–577.

CUNNINGHAM, J.R. & NEAL, M.J. (1985). Effect of excitatory amino acids and analogues on [^{3}H]-acetylcholine release from amacrine cells of the rabbit retina. *J. Physiol.*, **366**, 47–62.

CUNNINGHAM, J.R., PATERSON, S.J. & NEAL, M.J. (1992). Comparison of opioid binding sites in mammalian retinas. *Exp. Eye Res.*, **55**, P51.

DJAMGOZ, M.B.A., STELL, W.K., CHIN, C.-A. & LAM, D.M.K. (1981). An opiate system in the goldfish retina. *Nature*, **292**, 620–623.

EHINGER, B. & LINDBERG, B. (1974). Light-evoked release of glycine from the retina. *Nature*, **251**, 727–728.

FAMIGLIETTI, E.V. (1983). ON and OFF pathways through amacrine cells in the mammalian retina: The synaptic connections of 'starburst' amacrine cells. *Vis. Res.*, **23**, 1265–1279.

FAMIGLIETTI, E.V. (1991). Synaptic organisation of 'starburst' amacrine cells in rabbit retina: Analysis of serial thin sections by electron microscopy and graphic reconstruction. *J. Comp. Neurol.*, **309**, 40–70.

FERRO, E.S., HAMASSAKI, D.E., CAMARGO, A.C.M. & BRITTO, L.R.G. (1991). Endo-oligopeptidase A, a putative enkephalin-generating enzyme, in the vertebrate retina. *J. Neurochem.*, **57**, 1643–1649.

HEIJNA, M.H., HOGENBOOM, F., MULDER, A.H. & SCHOFFELMEER, A.N. (1992). Opioid receptor-mediated inhibition of ^{3}H-dopamine and ^{14}C-acetylcholine release from rat nucleus accumbens slices. A study on the possible involvement of K^+ channels and adenylate cyclase. *Naunyn-Schmied. Arch. Pharmacol.*, **345**, 627–632.

JARDON, B., BONAVENTURE, N. & SCHERRER, E. (1992). Possible involvement of cholinergic and glycinergic amacrine cells in the inhibition exerted by the ON retinal channel on the OFF retinal channel. *Eur. J. Pharmacol.*, **210**, 201–207.

LAPCHAK, P.A., ARAUJO, D.M. & COLLIER, B. (1989). Regulation of endogenous acetylcholine release from mammalian brain slices by opiate receptors: hippocampus, striatum and cerebral cortex of guinea-pig and rat. *Neurosci.*, **31**, 313–325.

LESLIE, F.M. (1987). Methods used for the study of opioid receptors. *Pharmacol. Rev.*, **39**, 197–249.

LINN, D.M., BLAZYNSKI, C., REDBURN, D.A. & MASSEY, S.C. (1991). Acetylcholine release from the rabbit retina mediated by kainate receptors. *J. Neurosci.*, **11**, 111–122.

LINN, D.M. & MASSEY, S.C. (1992). GABA inhibits ACh release from the rabbit retina: A direct effect or feedback to bipolar cells? *Vis. Neurosci.*, **8**, 97–106.

MARC, R.E. (1988). The role of glycine in the mammalian retina. *Prog. Retinal Res.*, **8**, 67–107.

MASLAND, R.H. & MILLS, J.W. (1979). Autoradiographic identification of acetylcholine in the rabbit retina. *J. Cell. Biol.*, **83**, 159–178.

MASSEY, S.C. & NEAL, M.J. (1979). The light-evoked release of acetylcholine from the rabbit retina *in vivo* and its inhibition by GABA. *J. Neurochem.*, **32**, 1327–1329.

MASSEY, S.C. & REDBURN, D.A. (1982). A tonic γ-aminobutyric acid-mediated inhibition of cholinergic amacrine cells in rabbit retina. *J. Neurosci.*, **2**, 1633–1643.

MULDER, A.H., BURGER, D.M., WARDEH, G., HOGENBOOM, F. & FRANKHUYZEN, A.L. (1991). Pharmacological profile of various kappa-agonists at κ-, μ- and δ-opioid receptors mediating presynaptic inhibition of neurotransmitter release in the rat brain. *Br. J. Pharmacol.*, **102**, 518–522.

NEAL, M.J. (1983). Cholinergic mechanisms in the vertebrate retina. *Prog. Retinal Res.*, **2**, 191–212.

NEAL, M.J. & CUNNINGHAM, J.R. (1982). Vertebrate retina *in vivo*: a preparation for studying acetylcholine release from central cholinergic neurons. In *Progress in Cholinergic Biology: Model Cholinergic Synapses*. ed. Hanin, I. & Goldberg, A.M. pp. 249–269. New York: Raven Press.

NEAL, M.J. & CUNNINGHAM, J.R. (1994). Baclofen enhances amacrine cell acetylcholine release by reducing glycinergic feedback inhibition. *Invest. Ophthalmol. & Visual Sci.*, **35**, 1365.

NEAL, M.J. & SHAH, M.A. (1989). Baclofen and phaclofen modulate GABA release from slices of rat cerebral cortex and spinal cord but not from retina. *Br. J. Pharmacol.*, **98**, 105–112.

ORON, L., SARNE, Y. & MICHAELSON, D.M. (1991). Effect of opioid peptides on electrically evoked acetylcholine release from Torpedo electromotor neurones. *Neurosci Lett.*, **125**, 231–234.

PATON, W.D.M. (1957). The action of morphine and related substances on contraction and on acetylcholine output of coaxially stimulated guinea-pig ilium. *Br. J. Pharmacol.*, **12**, 119–127.

PEREZ, M.T.R., EHINGER, B., LINSTROM, K. & FREDHOLM, B.B. (1986). Release of endogenous and radioactive purines from the rabbit retina. *Brain Res.*, **398**, 106–112.

PEREZ, M.T.R. & EHINGER, B. (1989). Adenosine inhibits evoked acetylcholine release from the rabbit retina. *J. Neurochem.*, **52**, S157.

RUZICKA, B.B. & JHAMANDAS, K. (1991). The K(+)-evoked release of [^{3}H]acetylcholine from slices of rat globus pallidus: modulation by delta-opioid receptors. *Can. J. Physiol. Pharmacol.*, **69**, 414–418.

SENBA, E., DADDONA, P.E. & NAGY, J.I. (1986). Immunohistochemical localization of adenosine deaminase in the retina of the rat. *Brain Res. Bull.*, **17**, 209–217.

TURNELL, D.C. & COOPER, J.D.H. (1981). Rapid assay for amino acids in serum or urine by precolumn derivatization and reversed phase liquid chromatography. *Clin. Chem.*, **28**, 101–118.

WATT, C.B., SU, Y.-Y.T. & LAM, D.M.-K. (1984). Interactions between enkephalin and GABA in avian retina. *Nature*, **311**, 761–764.

WICHMANN, T. & STARKE, K. (1990). Modulation by muscarine and opioid receptors of acetylcholine release in slices from striato-striatal grafts in the rat. *Brain Res.*, **510**, 296–302.

(Received March 16, 1994
Revised June 6, 1994
Accepted July 6, 1994)

Br. J. Pharmacol. (1994), 113, 795–800 © Macmillan Press Ltd, 1994

Contribution of intra- and extracellular Ca^{2+} to noradrenaline exocytosis induced by ouabain and monensin from guinea-pig vas deferens

[1]Takeshi Katsuragi, Shusuke Ogawa & Tatsuo Furukawa

Department of Pharmacology, School of Medicine, Fukuoka University, Fukuoka 814-80, Japan

1 Contributions of intra- and extracellular Ca^{2+} to noradrenaline (NA) release evoked by increasing intracellular Na^+ concentrations (ouabain plus monensin) from adrenergic nerves of guinea-pig vas deferens were evaluated under conditions eliminating carrier-mediated NA release (with 100 μM cocaine).

2 Ouabain (100 μM) plus monensin (10 μM), unlike 100 mM KCl, produced a marked NA release which was unchanged by Ca^{2+}-removal.

3 In normal solution but not in Ca^{2+}-free solution, the release of NA evoked by ouabain plus monensin was reduced by adenosine, clonidine and neuropeptide Y, and by Ca^{2+}-channel blockers such as ω-conotoxin GVIA and nifedipine. The release of NA was also decreased by cromakalim in a glibenclamide-sensitive fashion.

4 In contrast, in the absence but not in the presence of Ca^{2+}, the drug-evoked NA release was inhibited by mitochondrial inhibitors (carbonylcyanide-*m*-chlorophenylhydrazone and oligomycin) and further by immobilizers of intracellular Ca^{2+} (TMB-8 and BAPTA-AM) and calmodulin antagonists (W-7 and trifluoperazine).

5 These findings suggest that the release of NA evoked by elevation of $[Na^+]_i$ from adrenergic nerves in the presence and absence of Ca^{2+} involves, in part, exocytotic processes which are triggered by depolarization-induced Ca^{2+} influx and by utilization of Ca^{2+} from intracellular Ca^{2+} store sites such as mitochondria, respectively.

Keywords: Noradrenaline release; extra- and intracellular Ca^{2+}; ouabain plus monensin; neuromodulators; Ca^{2+}-antagonists; guinea-pig vas deferens

Introduction

Ouabain, a cardiac glycoside, is generally used to inhibit Na^+-K^+ ATPase and subsequently, to block the Na^+ pump on the cell membrane (Akera, 1977; Török, 1989). There is accumulated evidence for a role of ouabain as a trigger in adrenergic (Paton, 1973; Nakazato *et al.*, 1978) or cholinergic (Paton *et al.*, 1971; Vizi, 1972; 1978) neurotransmission.

According to Nakazato and co-workers (1978), the increase in the noradrenaline (NA) output after exposure to ouabain was antagonized by Ca^{2+} removal from the medium. Recent studies, however, revealed that NA release evoked by ouabain but not by electrical stimulation or KCl, from adrenergic nerves of guinea-pig vas deferens (Katsuragi *et al.*, 1988) and heart (Kranzhöfer *et al.*, 1991), from rat tail artery (Palaty, 1981) and neocortical slices (Schoffelmeer *et al.*, 1988) was virtually unaffected or even enhanced in Ca^{2+}-free medium. Therefore, the mechanism underlying release of transmitters evoked by increasing $[Na^+]_i$ is still unknown. It has been hypothesized that the positive inotropic action (Orrego, 1984) and catecholamine release from bovine chromaffin cells (Török & Powis, 1990) evoked by cardiac glycosides may be caused by a Na^+-Ca^{2+} exchange mechanism across the cell membrane (Orrego, 1984). However, the contribution of mitochondrial Ca^{2+}, which might be released by reversal of Na^+-Ca^{2+} exchange between cytosol and mitochondria on raising $[Na^+]_i$, to the release of neurotransmitters remains to be clarified.

In recent studies (Katsuragi *et al.*, 1988), it has been shown that the application of monensin, a Na^+ ionophore (Pressman & Fahim, 1982), in combination with ouabain, produced a quick and marked increase in intracellular Na^+ concentration ($[Na^+]_i$) which results in massive release of NA from adrenergic nerves.

Accordingly, in the present study, the contribution of intra- and extracellular Ca^{2+} to NA release evoked from guinea-pig vas deferens by elevating $[Na^+]_i$ with ouabain plus monensin, was extensively evaluated in the presence and absence of Ca^{2+} by using presynaptic neuromodulators, such as clonidine and ω-conotoxin GVIA, intracellular Ca^{2+}-chelators, mitochondrial inhibitors and calmodulin antagonists.

Methods

Measurement of NA release

Male guinea-pigs (250–400 g) were stunned and bled. Both vasa deferentia were removed and dissected free of fascia and vascular tissue. Preparations were trimmed to 15 mm in length. These segments were suspended with an initial load of 0.7 g in an organ bath filled with 1 ml of Krebs solution (37°C) of the following composition (mM): NaCl 122, KCl 5.2, $CaCl_2$ 2.4, $MgSO_4 \cdot 7H_2O$ 1.2, $NaHCO_3$ 25.6, D-glucose 11, EDTA 0.03 and ascorbic acid 0.1. The bathing medium was constantly bubbled with 95% O_2 + 5% CO_2. Then, pargyline (10 μM; a monoamine oxidase inhibitor), U-0521 (50 μM; a catechol-*O*-methyltransferase inhibitor) and cocaine (100 μM: an amine uptake inhibitor) were added to the bath and kept there throughout the experiment to measure NA as the metabolically unchanged form. The addition of 100 μM cocaine also inhibits carrier-mediated Na^+-NA co-transport (Schömig *et al.*, 1988; Adam-Vizi, 1992). Thirty minutes after suspending the tissue, secretagogues such as ouabain and monensin, were introduced into the bath for the test period

[1] Author for correspondence.

of 40 min. Use of organic solvents such as ethanol was limited to 0.05% of the bathing medium without any solvent effect. The Ca^{2+}-free solution was made by removal of Ca^{2+} from Krebs solution and by the addition of 0.5 mM EGTA.

Medium (100 μl) was collected from the bath prior to, 0 (control), 10, 20, 30 and 40 min after administration of drugs such as ouabain. Following each sampling, fresh Krebs solution (100 μl) of the same composition as the experimental medium was added to the bath. Endogenous NA in the sample medium (100 μl) was adsorbed onto 50 mg of alumina (N-Super 1, ICN Biochemicals, Cleveland, OH, U.S.A.) in a centrifuge tube with a filter (0.22 μm) and centrifuged for 1 min with a microcentrifuge (6,400 r.p.m.). NA adsorbed on alumina was eluted with 0.2 N HCl (100 μl) through centrifugation as described above. At the end of the experiment, tissue wet weight was measured after blotting with filter paper. Amounts of NA in the aliquots (10 μl) were determined with a high performance liquid chromatography electrochemical detector system (h.p.l.c.-e.c.d., Yanagimoto MFG Co., Kyoto, Japan) equipped with a reversed phase column (Yanapak, ODS-T) as described previously (Katsuragi *et al.*, 1988; 1991). Briefly, the mobile phase consisted of 2.5 mM sodium-l-octane sulphonate, 10 μM EDTA:2Na and 163 ml of ethanol in 1000 ml of 0.1 M KH_2PO_4. The phosphate buffer was adjusted to pH 3.3 with phosphoric acid. Flow rate was 1.0 ml min^{-1} (25°C). Finally, because an amine-free medium (100 μl) was added to the bathing medium (900 μl) after sampling, experimental values of NA were compensated for this and expressed as μg g^{-1} wet weight of tissue or % of control.

Test inhibitors were applied in effective concentrations without affecting the basal release of NA.

Drugs

The drugs used were ouabain (E. Merk, Darmstadt, Germany); monensin (gift from Eli Lilly, Indianapolis, IN, U.S.A.); U-0521 (3,4-dihydroxy-2-methyl propiophenon; gift from Upjohn, Kalamazoo, MI, U.S.A.); cocaine hydrochloride (Takeda, Osaka, Japan); pargyline hydrochloride (Nacalai, Kyoto, Japan); adenosine hemisulphate, clonidine hydrochloride, nifedipine, CCCP (carbonyl cyanide-*m*-chlorophenylhydrazone), oligomycin, TMB-8 (3,4,5-trimethoxy benzoate 8-(*N*,*N*-diethyl amino) octyl ester), W-7 (N-(6-amino hexyl)-1-naphthalene sulphonamide), trifluoperazine (TFP; Sigma, St. Louis, MO, U.S.A.); neuropeptide Y, ω-conotoxin GVIA (Peptide Institute, Minoh, Japan); BAPTA-AM (1,2-*bis*(O-aminophenoxy) ethane-*N*,*N*,*N'*,*N'*-tetraacetic acid aminoethosy) (Dojin, Kumamoto, Japan); cromakalim (gift from Beecham, Harlow, U.K.) and glibenclamide (gift from Yamanouchi, Tokyo, Japan).

Statistical analysis

Differences between two means and between multiple means were tested for statistical significance by Student's *t* test and by one way analysis of variance (ANOVA) followed by Dunnett's test, respectively. A value of $P<0.05$ was considered to be significant.

Results

Effects of external Ca^{2+} on NA releases evoked by ouabain, monensin and KCl

Efflux of NA from adrenergic nerves of guinea-pig vas deferens was measured by sampling every 10 min for up to 40 min after administration of test drugs in the presence and absence of Ca^{2+} in the external medium. Ouabain (100 μM) and monensin (10 μM) in the presence of Ca^{2+} increased the total release of NA during 40 min by approximately 10 and 6 fold, respectively, from a basal efflux of 0.67 ± 0.05 μg g^{-1} wet weight ($n = 8$). The release of NA evoked by ouabain was further enhanced by concurrent administration of monensin. The NA release induced by ouabain plus monensin was unchanged by Ca^{2+} removal from the medium except for the first 10 min period after adding the secretagogues. Similarly, the basal release of NA was virtually unaffected by Ca^{2+}-free medium (Figure 1a). On the other hand, 100 mM KCl induced a much lower NA release of about 20% compared to that by ouabain plus monensin. The KCl-evoked NA release was largely inhibited by removal of Ca^{2+} (Figure 1b).

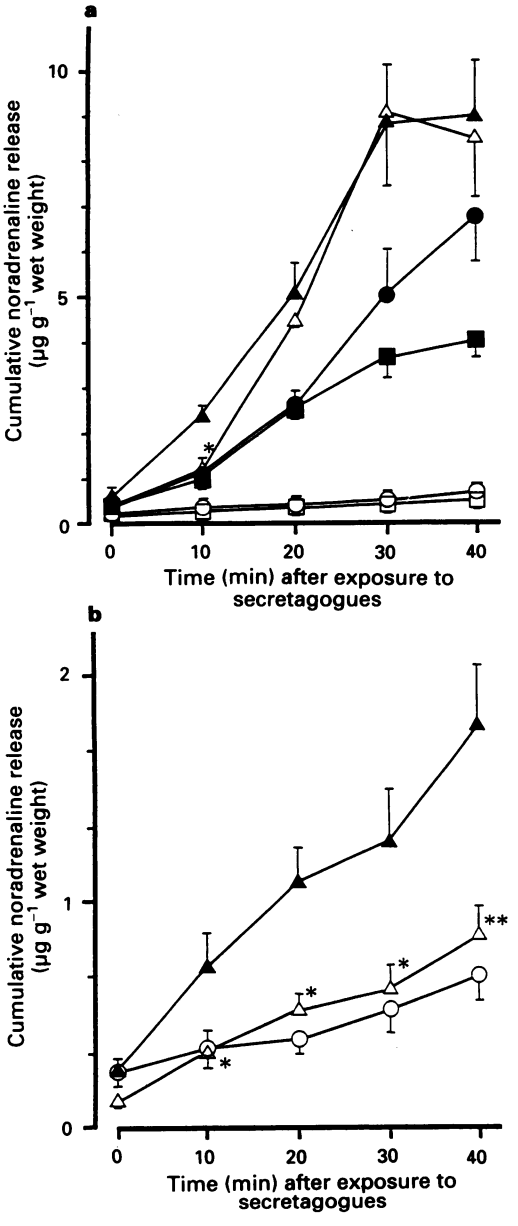


Figure 1 Effects of ouabain and/or monensin (a) and high KCl (b) on noradrenaline release from guinea-pig vas deferens in the presence and absence of Ca^{2+}. (a) (○) Basal release ($n = 8$); (□) basal release without Ca^{2+} ($n = 6$); (●), 100 μM ouabain ($n = 9$); (■) 10 μM monensin ($n = 5$); (▲) ouabain plus monensin ($n = 5$); (△) ouabain plus monensin without Ca^{2+} ($n = 5$). (b) (○) Basal release ($n = 8$); (▲) 100 mM KCl ($n = 5$); (△) 100 mM KCl without Ca^{2+} ($n = 4$). These experiments were carried out in the presence of Ca^{2+}, except for the experiment shown with (△). Sampling at 0 min was actually carried out 5 min before adding secretagogues. Values from each media sample which were collected cumulatively every 10 min up to 40 min are expressed as μg of noradrenaline per gram wet weight of tissue (mean ± s.e.mean). $*P<0.05$; $**P<0.01$ from control with Ca^{2+}.

$[Ca^{2+}]_o$-dependent effects of drugs on NA release evoked by ouabain plus monensin

The total NA released in the 40 min after administration of ouabain and monensin in normal medium was significantly inhibited by approximately 27%, 26% and 31% by addition of adenosine (30 μM), clonidine (30 μM) and neuropeptide Y (3 μM), respectively (Figure 2a).

In Ca^{2+}-free medium, inhibition of the evoked NA release by these drugs was no longer detectable (Figure 2b). ω-Conotoxin GVIA and nifedipine at a concentration of 0.3 μM also reduced the evoked NA release to 66% and 69%, respectively, in the presence of Ca^{2+}, although nifedipine, unlike ω-conotoxin GVIA, tended to decrease the release even in Ca^{2+}-free conditions. Furthermore, cromakalim (1 μM) reduced the evoked NA release in normal medium. This reduction by cromakalim did not occur in the presence of glibenclamide (1 μM), a K^+-channel blocker, or in the absence of Ca^{2+} (Figure 3). These findings, thus, show that the reduction by these test drugs of the NA release evoked by ouabain plus monensin in the presence, but not absence, of Ca^{2+} can be attributed to inhibition of Ca^{2+}-influx from the external medium.

None of the test drugs used here affected the basal NA release (data not shown).

Effects of drugs on NA release evoked by ouabain plus monensin in Ca^{2+}-free medium

Following exposure to 10 μM CCCP or 30 μM oligomycin (mitochondrial inhibitors), the NA release evoked by ouabain plus monensin from the adrenergic nerves was reduced by approximately 30% in Ca^{2+}-free medium, but was virtually unaffected in the presence of Ca^{2+} (Figure 4). The NA release caused by increasing $[Na^+]_i$ with ouabain plus monensin under Ca^{2+}-free conditions was inhibited by about 38%

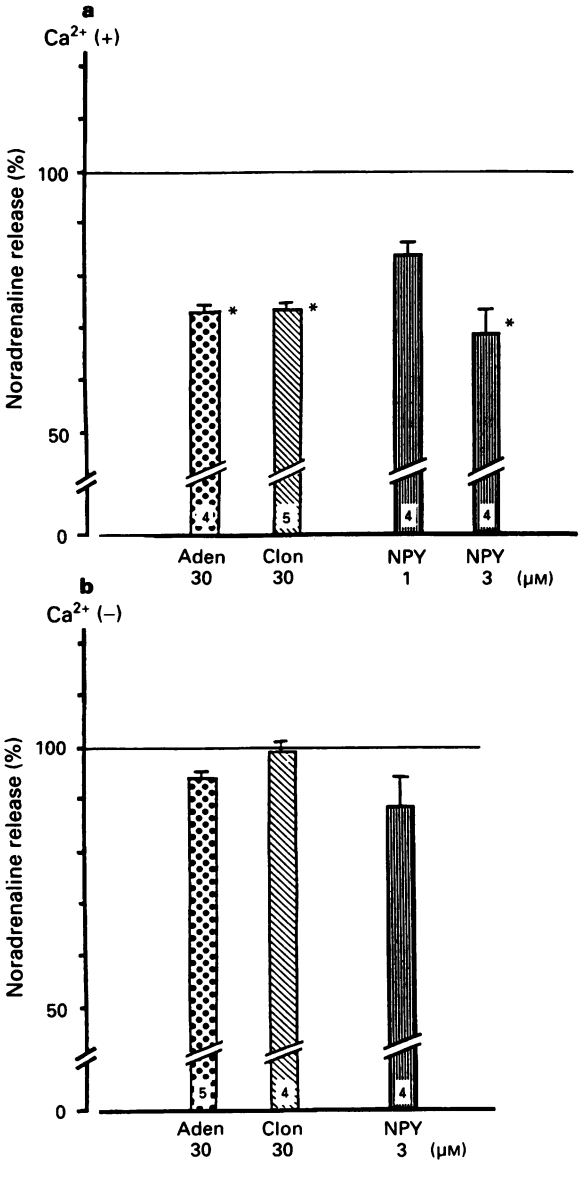


Figure 2 Effects of adenosine (Aden), clonidine (Clon) and neuropeptide Y (NPY) on noradrenaline release evoked by ouabain plus monensin in the presence (a) and absence (b) of Ca^{2+}. Cumulative release of noradrenaline over 40 min after concurrent administration of ouabain (100 μM) and monensin (10 μM) is expressed as % (mean ± s.e.mean) of the corresponding control; (a) 9.01 ± 1.27 μg g^{-1} wet weight 40 min^{-1}, $n = 5$; (b) 8.49 ± 1.32 μg g^{-1} wet weight, 40 min^{-1}, $n = 5$. A test drug was added to the bath 10 min before introduction of ouabain and monensin and remained during the experiment. Number of experiments is shown in each column. $^*P < 0.05$ from control.

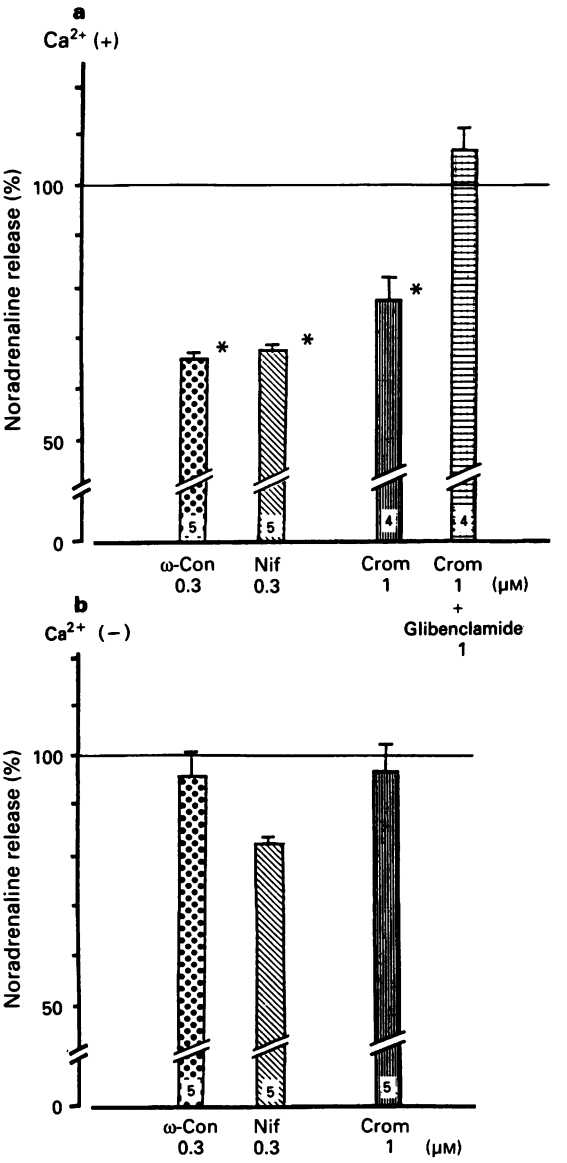


Figure 3 Effects of ω-conotoxin GVIA (ω-Con), nifedipine (Nif) and cromakalim (Crom) on noradrenaline release evoked by ouabain plus monensin in the presence (a) and absence (b) of Ca^{2+}. For details, see Figure 2. Glibenclamide was added 5 min before cromakalim. $^*P < 0.05$ from control.

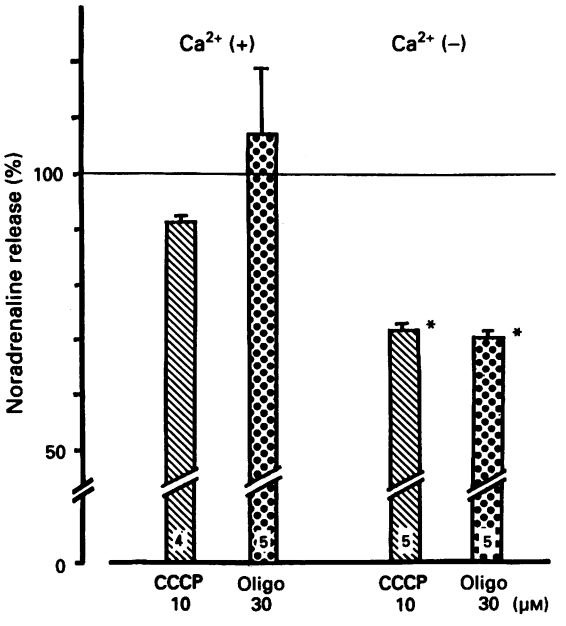


Figure 4 Effects of carbonyl cyanide-*m*-chlorophenylhydrazone (CCCP) and oligomycin (Oligo) on the noradrenaline release evoked by ouabain plus monensin in the presence and absence of Ca^{2+}. For details, see Figure 2. Test antagonists were added to the bath 20 min before administration of ouabain plus monensin. $*P<0.05$ from control.

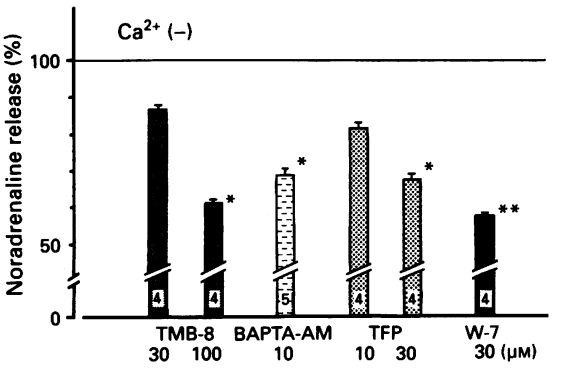


Figure 5 Effects of TMB-8, BAPTA/AM, TFP and W-7 on noradrenaline release evoked by ouabain plus monensin in the absence of Ca^{2+}. For details, see Figure 4. Protocol of sampling was identical with that in Figure 2b. $*P<0.05$; $**P<0.01$ from control. For abbreviations, see text.

Table 1 Effects of antagonists on basal noradrenaline release

Treatments	(μM)	(n)	*Released noradrenaline* (μg g^{-1} wet wt. 15 min^{-1}) mean ± s.e.mean	P
No treatment		(8)	0.38 ± 0.03	
Oligomycin	30	(5)	0.44 ± 0.08	NS
TFP	30	(8)	0.38 ± 0.04	NS
TMB-8	100	(6)	0.42 ± 0.06	NS
BAPTA/AM	10	(5)	0.40 ± 0.05	NS

Antagonists were added to the bath 15 min before sampling of basal noradrenaline release. NS, not significantly different from control. For abbreviations, see text.

and 31%, respectively, by 100 μM TMB-8, a blocker of intracellular Ca^{2+} mobilization, and 10 μM BAPTA-AM, an intracellular Ca^{2+}-chelator, suggesting that the NA release evoked by ouabain plus monensin, even in Ca^{2+}-free medium, may be elicited, in part, by using intracellular free Ca^{2+} (Figure 5). Finally, the effect of calmodulin antagonists on the evoked release of NA was assessed in the Ca^{2+}-free medium. This NA release was reduced by approximately 33% and 43%, respectively, following exposure to W-7 and TFP at 30 μM (Figure 5).

These antagonists did not significantly alter the basal release of NA from the tissue as illustrated in Table 1.

Discussion

We have found that ouabain plus monensin produced a marked and long-lasting release of NA from adrenergic nerves of the guinea-pig vas deferens, even in Ca^{2+}-free medium. The results described in this paper provide evidence that the mechanisms involved in this release of NA differ in Ca^{2+}-containing and Ca^{2+}-free medium.

The combination of inhibition of the Na^+-pump by ouabain and increase in Na^+ permeability by monensin (a Na^+ ionophore) will result in an accumulation of Na^+ and loss of K^+ in the axons. The reduction in the K^+ gradient will result in depolarization, which, in the presence of extracellular Ca^{2+} could trigger Ca^{2+} entry through voltage-sensitive Ca^{2+} channels and release of NA. However, the release of NA evoked by 100 mM KCl, which was Ca^{2+}-dependent, was small in comparison, suggesting that the increase in intracellular Na is likely to play an additional role in stimulating release. The release of NA evoked by ouabain plus monensin (with or without Ca^{2+}) increased with time during the first 30 min, and then stopped. This could be due to depletion of releasable NA from the nerve endings, since the NA content of the vas deferens is approximately 10 μg g^{-1} wet weight (unpublished data).

In the presence of Ca^{2+}, but not in its absence, the release of NA evoked by ouabain plus monensin was reduced by the addition of adenosine, clonidine and neuropeptide Y. The fact that these agents did not have an effect in the absence of Ca^{2+} supports the suggestion that they could be blocking NA release by reducing Ca^{2+} entry (adenosine: Hedqvist & Fredholm, 1976; Su, 1983; clonidine: Starke, 1977; neuropeptide Y: Lundberg & Stjärne, 1984). This view can be further supported by the finding that the evoked NA release was reduced by voltage-gated Ca^{2+} channel blockers such as ω-conotoxin GVIA and nifedipine, but again only in the presence of Ca^{2+}. It has been accepted that activation of N-type Ca^{2+} channels, which are sensitive to ω-conotoxin GVIA, plays an important role in the depolarization-dependent NA release from sympathetic neurones (Hirning *et al.*, 1988). Moreover, studies in the gastrointestinal tract provide evidence that the electrically-evoked ACh release from both the guinea-pig isolated colon (Lecchini *et al.*, 1991) and ileum (Katsuragi *et al.*, 1990) was inhibited by nifedipine but was enhanced by Bay K 8644. According to Artalejo & Garciá (1986), catecholamine release from cat adrenal glands evoked by ouabain, but not by A-23187 (a Ca^{2+}-ionophore), was strongly enhanced by Bay K 8644, indicating that catecholamine release induced by ouabain results from, in part, L-type Ca^{2+} channel activation via cell depolarization (Vizi, 1978). These findings, therefore, are highly consistent with our results.

In the present work with normal Krebs solution, cromakalim, an ATP-sensitive-K^+ channel opener, produced a decrease of evoked NA release, which was reversed by glibenclamide, an ATP sensitive-K^+ channel blocker (Nielsen-Kudsk *et al.*, 1990; Satoh *et al.*, 1991). This suggests that, under these conditions, the K^+-channel opener cromakalim can still hyperpolarize the nerve terminal membrane, thus reducing Ca^{2+} entry through voltage sensitive Ca^{2+} channels.

In contrast to the inhibitory action of these neuromod-

ulators, a mitochondrial inhibitor, oligomycin, inhibited the evoked NA release in the absence, but not in the presence, of Ca^{2+} in the medium. Similarly, CCCP, an uncoupler of mitochondria, was able to reduce the evoked NA release only in Ca^{2+}-free conditions. BAPTA/AM is a permeant derivative of BAPTA for binding cytosolic free Ca^{2+}. Thus, this chelator can inhibit intracellular Ca^{2+}-requiring processes such as synaptic transmission (Niesen *et al.*, 1991) and secretion from salivary glands (Mills *et al.*, 1991). TMB-8 is known as an inhibitor of Ca^{2+} release from intracellular stores, i.e. a Ca^{2+} immobilizer, and prevents Ca^{2+}-influx across the cell membrane (Kojima *et al.*, 1985). In our study, BAPTA/AM and TMB-8 also diminished NA release evoked by ouabain plus monensin in Ca^{2+}-free medium. In further studies, W-7 and TFP, Ca^{2+}/calmodulin antagonists, diminished the release of NA evoked by ouabain plus monensin in the Ca^{2+}-free medium. Therefore, a calmodulin-dependent process may be involved in NA release triggered by an increase of $[Na^+]_i$ in Ca^{2+}-free conditions.

These results suggest that increase of $[Na^+]_i$ may elicit reversed Na^+-Ca^{2+} exchange between cytosolic Na^+ and mitochondrial Ca^{2+} (Sandoval, 1981; Crompton, 1985). This mechanism must be of great importance in the Ca^{2+}-free solutions where Ca^{2+} entry cannot occur, but does not seem to occur in Ca^{2+}-containing solutions. This clearly suggests that the two conditions are rather different. It is possible that a greater accumulation of Na^+ and loss of K^+ may occur when the Na pump is blocked in Ca^{2+}-free solutions, than when Ca^{2+} is present, as has been seen in smooth muscle (Aickin *et al.*, 1987). The fact that cromakalim can reduce NA secretion evoked by ouabain and monensin in Ca^{2+}-containing solutions strongly suggests that the K^+ equilibrium potential is still positive to the resting potential, and the axon terminals must contain significant amounts of K^+. In Ca^{2+}-containing solutions although part of the release is triggered by Ca entry, and can be reduced by the test drugs, it is noticeable that even at high concentrations the test drugs only reduced the release by 30–35%, and never abolished it. This suggests that another, unknown mechanism of release is involved. It is possible that Ca^{2+}-loss from mitochondria via Na^+-Ca^{2+} exchange reduces oxidative ATP synthesis in this organelle (Cox & Matlib, 1993) and the consequent reduction of ATP at catecholamine store sites might trigger release of bound NA from the nerve terminals (Trifaro & Cubeddu, 1979).

In conclusion the release of NA caused by ouabain plus monensin seems to be complicated. In normal Ca^{2+} medium, NA release evoked by accumulation of $[Na^+]_i$ seems to involve an exocytotic release process, which is partly due to the depolarization-induced Ca^{2+} influx from the outer medium. However, in Ca^{2+}-free medium when intracellular Na^+ is probably higher, the NA release could be triggered by an exocytotic process by using intracellular Ca^{2+} derived from Ca^{2+} store sites such as mitochondria, e.g. via the Na^+-Ca^{2+} exchange transport mechanisms. In addition to these Ca^{2+}-requiring processes, there may be further unknown mechanisms involved in the massive release of NA following accumulation of $[Na^+]_i$.

This work was supported by a Grant-in-Aid for Scientific Research 02670102 from the Ministry of Education, Sciences and Culture of Japan (T.K.). The authors are grateful to Upjohn (U.S.A.), Eli Lilly (U.S.A.) and Yamanouchi (Japan) for kindly supplying U-0521, monensin and glibenclamide, respectively.

References

ADAM-VIZI, V. (1992). External Ca^{2+}-independent release of neurotransmitters. *J. Neurochem.*, **58**, 395–405.

AICKIN, C.C., BRADING, A.F. & WALMSLEY, D. (1987). An investigation of sodium-calcium exchange in the smooth muscle of guinea-pig ureter. *J. Physiol.*, **391**, 325–346.

AKERA, T. (1977). Membrane adenosine-triphosphatase: a digitalis receptor? *Science*, **198**, 569–574.

ARTALEJO, C.R. & GARCIA, A.G. (1986). Effects of Bay K 8644 on cat adrenal catecholamine secretory responses to A-231878 or ouabain. *Br. J. Pharmacol.*, **88**, 757–765.

COX, D.A. & MATLIB, M.A. (1993). Modulation of intramitochondrial free Ca^{2+} concentration by antagonists of Na^+-Ca^{2+} change. *Trends Pharmacol. Sci.*, **14**, 408–413.

CROMPTON, M. (1985). The regulation of mitochondrial calcium transport in heart. In *Current Topics in Membranes and Transport*. Vol. 25. ed. Shmoo, A.E. pp. 231–276. New York: Academic Press.

HEDQVIST, P. & FREDHOLM, B.B. (1976). Effects of adenosine on adrenergic transmission: prejunctional inhibition and postjunctional enhancement. *Naunyn-Schmied. Arch. Pharmacol.*, **293**, 217–223.

HIRNING, L.D., FOX, A.P., MCCLESKI, E.W., OLIVERA, B.A., THAYER, S.A., MILLER, R.J. & TSIEN, R.W. (1988). Dominant role of N-type Ca^{2+} channels in evoked release of norepinephrine from sympathetic neurons. *Science*, **239**, 57–61.

KATSURAGI, T., TOKUNAGA, T., MIYAMOTO, K., KURATOMI, L. & FURUKAWA, T. (1988). Norepinephrine and adenosine triphosphate release in different ratio from guinea pig vas deferens by high potassium chloride, ouabain and monensin. *J. Pharmacol. Exp. Ther.*, **247**, 302–308.

KATSURAGI, T., SHIRAKABE, K., OGAWA, S., SOEJIMA, O. & FURUKAWA, T. (1990). Involvement of dihydropyridine-sensitive Ca^{2+} channels in adenosine-evoked inhibition of acetylcholine release from guinea-pig ileal preparation. *J. Neurochem.*, **55**, 363–369.

KATSURAGI, T., TOKUNAGA, T., OGAWA, S., SOEJIMA, O., SATO, C. & FURUKAWA, T. (1991) Existence of ATP-evoked ATP release system in smooth muscles. *J. Pharmacol. Exp. Ther.*, **259**, 513–518.

KOJIMA, I., KOJIMA, K. & RASMUSSEN, H. (1985). Mechanism of inhibitory action of TMB-8 [8-(N,N-diethylamino)octyl-3,4,5-trimethoxy-benzoate] on aldosterone secretion in adrenal glomerulosa cells. *Biochem. J.*, **232**, 87–92.

KRANZHÖFER, R., HAASS, M., KURZ, T., RICHARDT, G. & SCHÖMIG, A. (1991). Effect of digitalis glycosides on norepinephrine release in the heart, dual mechanisms of action. *Cir. Res.*, **68**, 1628–1637.

LECCHINI, S., MARCOLI, M., DE PONTI, F.F., CASTELLETTI, C.A. & FRIGO, G.M. (1991). Selectivity of Ca^{2+} channel blockers in inhibiting muscular and nerve activities in isolated colon. *Br. J. Pharmacol.*, **102**, 735–741.

LUNDBERG, J.M & STJÄRNE, L. (1984). Neuropeptide Y (NPY) depresses the secretion of ^{3}H-noradrenaline and the contractile response evoked by field stimulation in the rat vas deferens. *Acta Physiol. Scand.*, **120**, 477–479.

MILLS, C.L., DORMER, R.L. & MCPHERSON, M.A. (1991). Introduction of BAPTA into intact rat submandibular acini inhibits mucin secretion in response to cholinergic and β-adrenergic agonists. *FEBS Lett.*, **289**, 141–144.

NAKAZATO, Y., OHGA, A. & ONODA, Y. (1978). The effect of ouabain on noradrenaline output from peripheral adrenergic neurones of isolated guinea-pig vas deferens. *J. Physiol.*, **278**, 45–54.

NIELSEN-KUDSK, J.E., BANG, L. & BRØNSGAAD, A.M. (1990). Glibenclamide blocks the relaxant of pinacidil and cromakalim in airway smooth muscle. *Eur. J. Pharmacol.*, **180**, 291–296.

NIESEN, C., CHARLTON, M.P. & CARLEN, P.L. (1991). Postsynaptic and presynaptic effects of the calcium chelator BAPTA on synaptic transmission in rat hippocampal dentate granule neurons. *Brain Res.*, **555**, 319–325.

ORREGO, F. (1984). Calcium and the mechanism of action of digitalis. *Gen. Pharmacol.*, **15**, 273–280.

PALATY, V. (1981). Release of noradrenaline from the rat tail artery induced by inhibition of the sodium pump in calcium free solution. *Can. J. Physiol. Pharmacol.*, **59**, 347–350.

PATON, D.M. (1973). Mechanism of efflux of noradrenaline from adrenergic nerves in rabbit atria. *Br. J. Pharmacol.*, **49**, 614–627.

PATON, W.D.M., VIZI, E.S. & ZAR, M.A. (1971). The mechanism of acetylcholine release from parasympathetic nerves. *J. Physiol.*, **215**, 819–849.

PRESSMAN, B.C. & FAHIM, M. (1982). Pharmacology and toxicology of the monovalent carboxylic ionophores. *Annu. Rev. Pharmacol. Toxicol.*, **22**, 465–490.

SANDOVAL, M.E. (1981). On the role of mitochondria in neurotransmitter release. In *Regulatory Mechanism of Synaptic Transmission*. ed. Tapia, R. & Cotman, C. pp. 187–203. New York: Plenum Press.

SATOH, K., YAMADA, H. & TAIRA, N. (1991). Differential antagonism by glibenclamide of the relaxant effects of cromakalim, pinacidil and nicorandil on canine large coronary arteries. *Naunyn-Schmied. Arch. Pharmacol.*, **343**, 76–82.

SCHOFFELMEER, A.N.M., HOGENBOOM, F. & MUDLER, A.H. (1988). Sodium dependent ^{3}H-noradrenaline release from rat neocortical slices in the absence of extracellular calcium: presynaptic modulation by μ-opioid receptor and adenylate cyclase activation. *Naunyn-Schmied. Arch. Pharmacol.*, **338**, 548–552.

SCHÖMIG, A., KURZ, T., RICHARDT, G. & SCHÖMIG, E. (1988). Neuronal sodium homeostasis and axoplasmic amine concentration determine calcium-independent noradrenaline release in normoxic and ischemic rat heart. *Circ. Res.*, **63**, 214–226.

STARKE, K. (1977). Regulation of noradrenaline release by presynaptic receptor systems. *Rev. Physiol. Biochem. Pharmacol.*, **77**, 1–124.

SU, C. (1983). Purinergic neurotransmission and neuromodulation. *Annu. Rev. Pharmacol. Toxicol.*, **23**, 397–411.

TÖRÖK, T.L. (1989). Neurochemical transmission and the sodium-pump. *Prog. Neurobiol.*, **32**, 11–76.

TÖRÖK, T.L. & POWIS, D.A. (1990). Catecholamine release from bovine cromaffin cells: the role of sodium-calcium exchange in ouabain-evoked release. *Exp. Physiol.*, **75**, 573–586.

TRIFARO, J.M. & CUBEDDU, X.L. (1979). Exosytosis as a mechanism of noradrenergic transmitter release. In *Trends in Autonomic Pharmacology*, Vol. 1. ed. Kalsner, S. pp. 195–249. Baltimore, Urban & Schwarzenberg.

VIZI, E.S. (1972). Stimulation by inhibition of (Na^+-K^+-Mg^{2+})-activated ATPase of acetylcholine release in cortical slices from rat brain. *J. Physiol.*, **226**, 95–117.

VIZI, E.S. (1978). Na^+-K^+-activated adenosinetriphosphatase as a trigger in transmitter release. *Neuroscience*, **3**, 367–384.

(Received March 31, 1994
Revised July 4, 1994
Accepted July 6, 1994)

Br. J. Pharmacol. (1994), **113**, 801–808 © Macmillan Press Ltd, 1994

The effect of hyperglycaemia on function of rat isolated mesenteric resistance artery

[1]Paul D. Taylor & Lucilla Poston

Division of Physiology, United Medical and Dental Schools Smooth Muscle Group, St. Thomas' Campus, London, SE1 7EH

1 Noradrenaline sensitivity and acetylcholine-induced relaxation were investigated in mesenteric resistance arteries from female Wistar rats (220–250 g) following exposure to isotonic supraphysiological glucose solutions (20 and 45 mM, in physiological buffer, 2 h incubation).

2 Arteries incubated in 20 mM glucose demonstrated enhanced noradrenaline sensitivity compared with those in physiological buffer.

3 Profoundly impaired endothelium-dependent relaxation to acetylcholine was observed in arteries incubated in 20 and 45 mM glucose.

4 Indomethacin (10 μM) normalized noradrenaline sensitivity in 20 mM glucose, but unmasked an enhanced maximum response in 20 and 45 mM glucose relative to controls.

5 Addition of L-arginine (0.1 mM) prevented the abnormality of acetylcholine-induced relaxation in the 20 mM glucose medium and significantly improved relaxation in 45 mM glucose.

6 The aldose reductase inhibitor, ponalrestat (10^{-5} M, ZENECA Pharmaceuticals), prevented impaired acetylcholine-mediated relaxation in 20 mM glucose and significantly improved relaxation in 45 mM glucose.

7 Indomethacin (10 μM) improved maximum relaxation but did not alter impaired sensitivity to acetylcholine in the high glucose media (20 and 45 mM).

8 Superoxide dismutase (SOD, 150 u ml^{-1}) also prevented impaired acetylcholine-induced relaxation in 20 mM glucose but not in 45 mM glucose.

9 Endothelium-independent relaxation to sodium nitroprusside (SNP, 10^{-9}–10^{-5} mM) was normal in 20 mM glucose but was slightly, although significantly impaired by 45 mM glucose.

10 Enhanced responsiveness of rat isolated mesenteric resistance arteries to noradrenaline caused by elevated glucose would appear to be mediated through abnormal cyclo-oxygenase activity and the reduced tonic release of nitric oxide.

11 Hyperglycaemia may lead to abnormal endothelium-dependent relaxation in these arteries through several mechanisms which include a role for increased free radical production, polyol pathway activation and altered L-arginine metabolism.

Keywords: Mesenteric resistance arteries; vascular endothelium; vascular smooth muscle; hyperglycaemia; nitric oxide; aldose reductase inhibitors; free radicals

Introduction

Abnormalities of the vascular endothelium may contribute to diabetic vascular dysfunction (Cohen & Tesamariam, 1992) including abnormal permeability and release of endothelium-derived vasoactive substances. Several studies in diabetic patients (de Tejada *et al.*, 1989; McVeigh *et al.*, 1992; McNally *et al.*, 1992; Elliot *et al.*, 1993) and the majority of studies of diabetic vascular function in chemically-induced animal models of diabetes, including some from our own laboratory (Taylor *et al.*, 1992; 1994a,c) have reported impaired endothelium-dependent relaxation (Oyama *et al.*, 1986; Pieper & Gross, 1988; Durante *et al.*, 1988; Kamata *et al.*, 1989; Tanz *et al.*, 1989; Mayhan, 1989; Abiru *et al.*, 1990; Tesfamariam *et al.*, 1990; Mayhan *et al.*, 1991; Cameron & Cotter, 1992). Although long suspected, it has only recently been proven that strict glycaemic control is associated with a lower incidence of vascular complications in diabetes (DDCT, 1993). Of the many metabolic disturbances of diabetes, hyperglycaemia is, therefore, the most likely cause of endothelial dysfunction. Indeed, Tesfamariam and coworkers have reported the impairment of endothelium-dependent relaxation in normal rabbit aorta following exposure to abnormally raised concentrations of glucose (Tesfamariam *et al.*, 1990; 1991; 1992; Tesfamariam & Cohen, 1992).

Several mechanisms have been proposed whereby hyperglycaemia might mediate endothelial dysfunction. These include a role for the glucose-stimulated increase in polyol pathway activity and the redox changes associated with increased sorbitol flux (Williamson *et al.*, 1990; Cameron & Cotter, 1992). Sorbitol accumulation may lead to cellular *myo*-inositol depletion and abnormal cell signalling (Greene *et al.*, 1987) and to subsequent inhibition of Na^+/K^+ ATPase (Gupta *et al.*, 1992). The activation of protein kinase C by glucose-induced *de novo* synthesis of diacylglycerol has also been implicated (Lee *et al.*, 1989; Tesfamariam *et al.*, 1991), together with increased production of constrictor prostanoids (Tesfamariam *et al.*, 1989) and the generation of oxygen-derived free radicals (Tesfamariam & Cohen, 1992). None of the functional studies investigating the mechanism of hyperglycaemia-induced endothelial dysfunction have been carried out in small arteries; all have been in conduit vessels which are minimally involved in diabetic vascular dysfunction.

In the present study we have examined the effects of acute hyperglycaemia on resistance artery function and have attempted to elucidate the various mechanisms involved. Since streptozotocin (STZ) diabetic rats have increased plasma glucose levels and osmolality (Hebden *et al.*, 1986) both of which may cause impaired vasodilatation (Korthuis *et al.*, 1987; Friedman, 1989), we have attempted to delineate the effect of glucose *per se* by using isotonic elevated glucose

[1] Author for correspondence.

media. Some of this work has been published as a preliminary report (Taylor *et al.*, 1994b).

Methods

Female Wistar rats (220–250 g) were killed by cervical dislocation and the mesentery was removed and placed in physiological saline solution (PSS). The control solution consisted of (mM): NaCl 119, $NaHCO_3$ 25, D-glucose 5.5, KH_2PO_4 1.18, $MgSO_47H_2O$ 1.17, KCl 4.7, $CaCl_2$ 2.5, ethylenediamine-tetra-acetic acid disodium salt (EDTA) 0.026. Third branch mesenteric arteries (approx internal diameter 275 μm) were dissected free of connective tissue under a light microscope and mounted as ring preparations on a small vessel myograph (Mulvany & Halpern, 1977) capable of measuring isometric tension. Arteries were bathed in PSS at 37°C and bubbled with 5% CO_2/95% O_2 and their passive tension and internal circumference were determined. The arteries were then set to an internal circumference equivalent to 90% of that which they would experience when relaxed *in situ* under a transmural pressure of 100 mmHg (the maximum active tension for the minimum resting tension is developed at approximately this circumference; Mulvany & Halpern, 1977). All arteries were subjected to a routine run-up procedure in which they were contracted for 2 min every 10 min on four occasions using the following protocol. The first and fourth contractions were produced with 5 μM noradrenaline in 125 mM potassium solution (KPSS, equimolar substitution of KCl for NaCl in PSS). The second was with 5 μM noradrenaline in PSS and the third with KPSS. Arteries failing to produce a maximum active tension equivalent to a pressure of 100 mmHg on the final contraction were rejected.

Arteries were then incubated for 2 h in either PSS or PSS containing raised concentrations of glucose. High glucose PSS (45 or 20 mM glucose) was prepared by the equimolar substitution of glucose for NaCl. As a control for the consequent lowering of sodium, arteries were incubated in PSS in which equimolar substitutions of N-methyl-D-glucamine were made for NaCl (equivalent to 45 mM glucose PSS), and these arteries did not differ significantly in their responses to agonists. The incubating medium was changed every 20 min. Arteries were then contracted for 2 min with 5 μM noradrenaline in KPSS prior to the continuation of the protocol. Dose-response curves were then constructed to noradrenaline (10^{-7}–10^{-5} M), with concentration increments at 3 min intervals. The organ bath was then washed out three times with PSS and a 10 min wash out period allowed before arteries were submaximally contracted with noradrenaline to achieve approximately 80% maximum response. After 3 min, relaxation of preconstricted arteries to acetylcholine was assessed by the addition of half log molar increments at 2 min intervals (10^{-9}–10^{-5} M). A similar protocol was observed for assessing relaxation to sodium nitroprusside (10^{-9}–10^{-5} M). A number of pharmacological inhibitors were employed which, unless otherwise stated, were present throughout the 2 h incubation period.

Some experiments were also carried out using arteries obtained from rats with experimentally-induced diabetes. Diabetes was induced in female Wistar rats by tail vein injection of STZ (45 mg kg^{-1}) in citrate buffer. Animals were killed at 7–10 weeks duration of diabetes (serum glucose concentrations, mmol l^{-1}, 45.3 ± 3.6, $n = 9$, *versus* controls 6.31 ± 0.4, $n = 14$, $P < 0.001$, (glucose oxidase methods; YSI Model 23 AM Glucose Analyzer)).

Drugs

Chemicals used in this investigation were noradrenaline (Winthrop Laboratories): acetylcholine, indomethacin, sodium nitroprusside, N^G-nitro-L-arginine methylester (L-NAME), L-arginine, superoxide dismutase (all from Sigma); streptozotocin (gift from Dr MacLeod, Upjohn Co. Kalamazoo, U.S.A.); ponalrestat (Statil, gift from ZENECA Pharmaceuticals, Macclesfield). Chemicals were prepared as stock solutions dissolved in PSS except for L-arginine which was solubilised in distilled water, pH balanced to 7.8; ponalrestat which was dissolved in dimethylsulphoxide (DMSO) and indomethacin which was prepared as a 1 mM stock solution in phosphate buffer consisting of (mM): KH_2PO_4 20, $NaH_2PO_42H_2O$ 120, pH balanced to 7.8. All concentrations are expressed as the final molar concentrations in the organ bath.

Statistical analysis

All values are given as the mean ± s.e.mean. Tension is given as active wall tension (mN mm^{-1} artery length) ± s.e.mean and the relaxation responses to acetylcholine and sodium nitroprusside as a percentage of the initial precontraction to noradrenaline. The negative log of the concentration of a drug required to produce 50% of the maximum response (pEC_{50}) was calculated as the mean ± s.e.mean of the individual pEC_{50}s using non linear regression, and the sigmoid equation of the curve fitting programme 'GraphPad' (GraphPad Software Inc., San Diego, CA, U.S.A.). Some data were not suitable for curve fitting, in which case maximum responses only were compared. Statistical comparisons of the pEC_{50} values and maximum responses between the experimental and control groups were achieved using Student's independent *t* test. Paired two-tailed *t* tests were employed in the comparisons of sequential concentration-effect curves in the presence and absence of inhibitors. Significance was assumed if $P < 0.05$.

Results

Noradrenaline responses

Arteries exposed to elevated glucose media for 2 h and control arteries contracted in a dose-dependent manner in response to increasing concentrations of noradrenaline (10^{-7}–10^{-5} M). Enhanced sensitivity to noradrenaline, compared to controls, was observed in arteries incubated in 20 mM but not 45 mM glucose PSS (pEC_{50}: arteries in 20 mM glucose 5.91 ± 0.06, $n = 12$, *versus* control PSS 5.72 ± 0.04, $n = 12$, $P < 0.05$, Figure 1a).

The addition of indomethacin (10 μM) to control arteries did not affect the sensitivity to noradrenaline but reduced the maximum response, however in 20 mM glucose, indomethacin reduced noradrenaline sensitivity such that the difference between control and glucose treated vessels was abolished (pEC_{50} 20 mM glucose + indomethacin 5.63 ± 0.07, $n = 8$, *versus* control PSS + indomethacin 5.57 ± 0.07, $n = 12$, NS). In addition the arteries in high glucose (20 and 45 mM) then exhibited an enhanced maximum response compared to arteries in control PSS (maximum response to noradrenaline [mNmm^{-1}]: 20 mM glucose + indomethacin 3.29 ± 0.27, $n = 8$, *versus* control PSS + indomethacin 2.48 ± 0.20, $n = 12$, $P < 0.05$; 45 mM glucose PSS with indomethacin 3.59 ± 0.31, $n = 12$, *versus* control PSS + indomethacin 2.48 ± 0.20, $n = 12$, $P < 0.01$) (Figure 1b).

Addition of N^G-nitro-L-arginine methyl ester (L-NAME, 0.1 mM, 10 min pre-incubation) to the media, (in the continued presence of 10 μM indomethacin), increased the maximum response of normal arteries to noradrenaline in control, but not in 20 mM or 45 mM glucose, significantly reducing the difference in maximum response observed between arteries in 45 mM glucose PSS + indomethacin and those in control PSS + indomethacin (maximum response to noradrenaline [mNmm^{-1}]: control PSS + indomethacin 2.48 ± 0.20, $n = 12$, *versus* 3.45 ± 0.22, $n = 11$, with L-NAME, $P < 0.005$; 45 mM glucose + indomethacin + L-NAME 4.00 ± 0.28, $n = 11$ *versus* control PSS + indomethacin + L-NAME

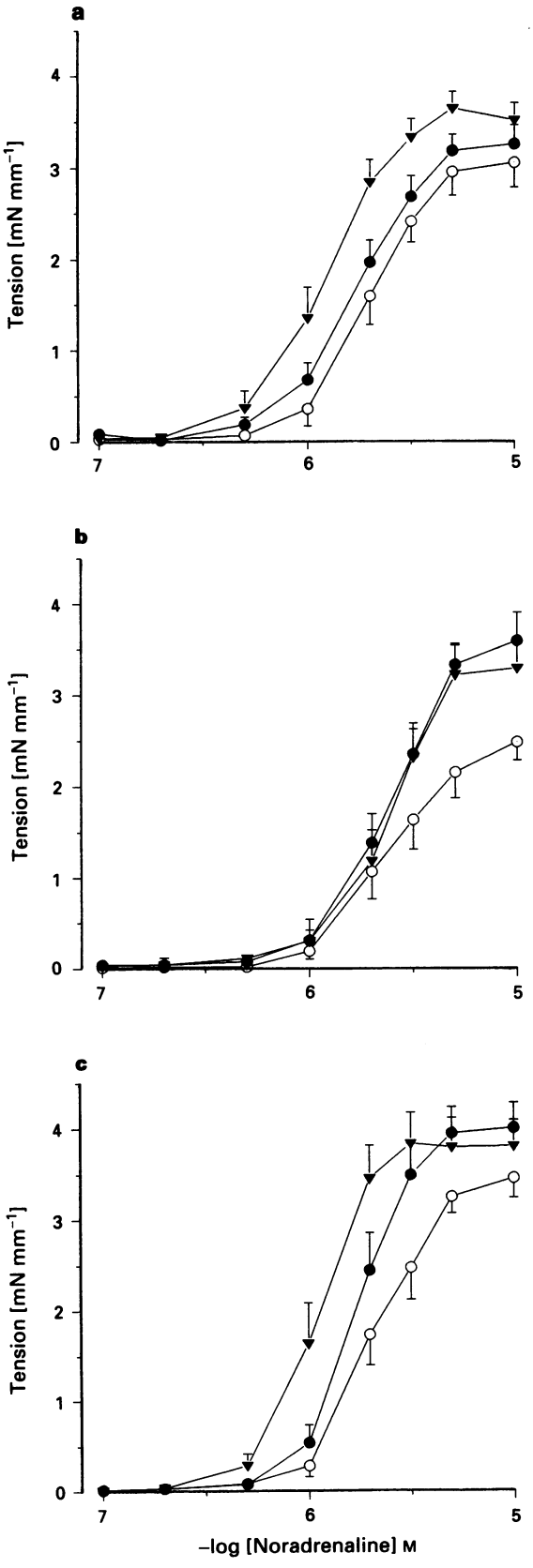


Figure 1 (a) Noradrenaline concentration-effect curves for normal mesenteric resistance arteries incubated for 2 h in 20 mM glucose (▼, $n = 12$), 45 mM glucose (●, $n = 13$), and control PSS (○, $n = 12$); (b) with the inclusion of indomethacin (10 μM), during 2 h incubation in 20 mM glucose (▼, $n = 8$), 45 mM (●, $n = 11$), and control PSS (○, $n = 12$); and (c) following the addition of the nitric oxide synthase inhibitor N^G-nitro-L-arginine methyl ester (L-NAME, 0.1 mM), in the continued presence of indomethacin (10 μM) following 2 h incubation in 20 mM glucose (▼, $n = 8$), 45 mM (●, $n = 11$), and control PSS (○, $n = 11$).

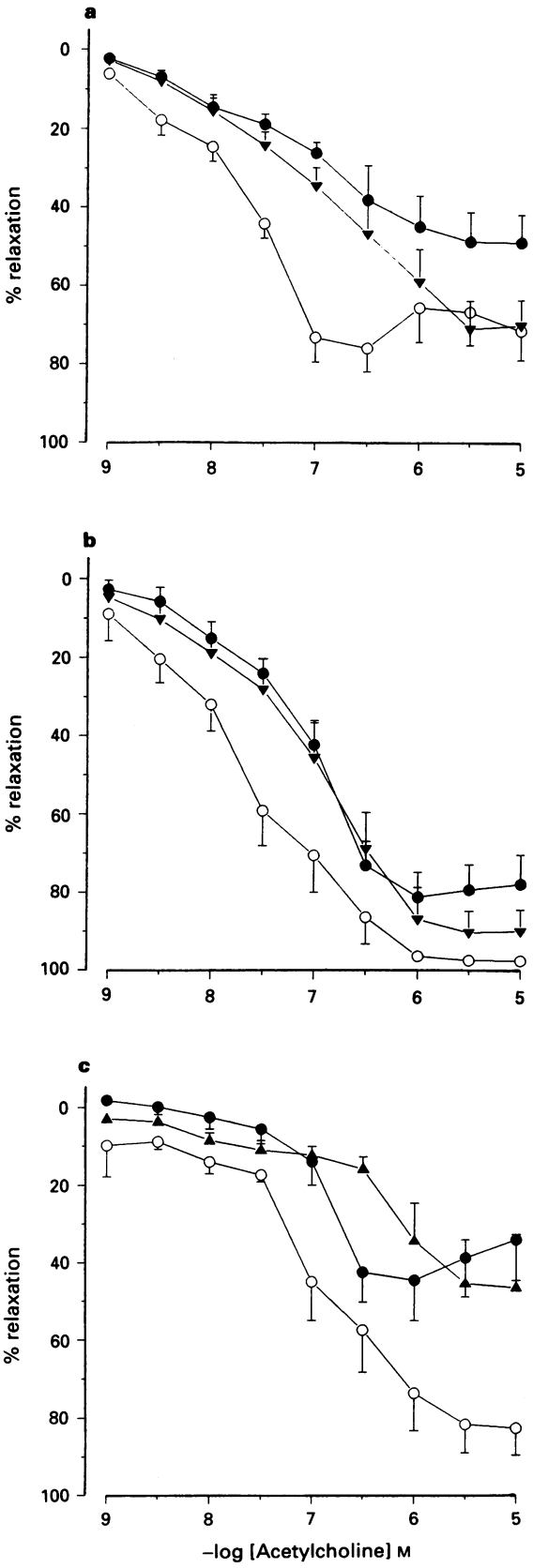


Figure 2 (a) Acetylcholine-induced relaxation in normal mesenteric resistance arteries precontracted with noradrenaline after 2 h incubation in 20 mM glucose (▼, $n = 12$), 45 mM glucose (●, $n = 11$), and control PSS (○, $n = 12$); (b) with the inclusion of indomethacin (10 μM), during 2 h incubation in 20 mM glucose (▼, $n = 8$), 45 mM glucose (●, $n = 12$), and control PSS (○, $n = 12$); and (c) following the addition of the nitric oxide synthase inhibitor N^G-nitro-L-arginine methyl ester (L-NAME, 0.1 mM), in the continued presence of indomethacin (10 μM) following 2 h incubation in 20 mM glucose (▼, $n = 8$), 45 m M glucose (●, $n = 11$), and control PSS (○, $n = 11$).

3.45 ± 0.22, $n = 11$, NS). The addition of neither the aldose reductase inhibitor, ponalrestat (10^{-5} M) nor L-arginine (10^{-4} M) corrected the enhanced noradrenaline sensitivity observed in normal arteries incubated in 20 mM glucose.

Endothelium-dependent relaxations

Incubation of arteries for 2 h in NaCl-substituted isosmotic 20 mM and 45 mM glucose PSS caused profound impairment of acetylcholine-induced relaxation compared to control (5.5 mM glucose) PSS: 20 mM glucose pEC_{50} 6.88 ± 0.12, $n = 12$ *versus* control PSS 7.54 ± 0.09, $n = 12$, $P < 0.001$, 45 mM glucose (curve fitting inappropriate) maximum relaxation to acetylcholine [% noradrenaline precontraction]: 48.8 ± 7.1, $n = 11$, *versus* control PSS 75.8 ± 5.9, $n = 12$, $P < 0.01$, the higher glucose concentration (45 mM) producing greater inhibition than the lower (20 mM) (maximum relaxation to acetylcholine in 45 mM glucose: 48.8 ± 7.1%, $n = 11$, *versus* 20 mM glucose 70.9 ± 7.2%, $n = 12$, $P < 0.05$) (Figure 2a).

The addition of indomethacin (10 μM) to the media significantly improved maximum relaxation in all groups (maximum relaxation [% noradrenaline precontraction]: 45 mM glucose 48.8 ± 7.1, $n = 11$, *versus* 45 mM glucose + indomethacin 81.9 ± 6.3, $n = 11$, $P < 0.005$; 20 mM glucose 70.9 ± 7.2, $n = 12$, *versus* 20 mM glucose + indomethacin 91.2 ± 5.0, $n = 8$, $P = 0.05$; control PSS 75.8 ± 5.9, $n = 12$, *versus* control PSS + indomethacin 98.5 ± 0.5, $n = 12$, $P < 0.001$). Indomethacin did not alter sensitivity to acetylcholine in any of the experimental groups, which was abnormal in arteries in both 20 mM and 45 mM glucose (pEC_{50}: 20 mM glucose + indomethacin 6.87 ± 0.20, $n = 8$, *versus* control PSS + indomethacin 7.68 ± 0.13, $n = 12$, $P < 0.05$; 45 mM glucose + indomethacin 7.06 ± 0.08, $n = 12$, *versus* control PSS + indomethacin, $P < 0.05$, Figure 2b).

The addition of 0.1 mM L-NAME to the media, in the continued presence of 10 μM indomethacin caused a significant attenuation of relaxation of normal arteries to acetylcholine in both 20 and 45 mM glucose and in control PSS (maximum relaxation [% noradrenaline precontraction]: 20 mM glucose + indomethacin 91.2 ± 5.0, $n = 8$ *versus* 20 mM glucose + indomethacin + L-NAME 46.3 ± 13.7, $n = 8$, $P < 0.01$; 45 mM glucose + indomethacin 81.2 ± 6.3, $n = 11$, *versus* 45 mM glucose + indomethacin + L-NAME 44.4 ± 10.5, $n = 11$, $P < 0.05$; control PSS + indomethacin 97.5 ± 0.5, $n = 11$ *versus* control PSS + indomethacin + L-NAME 82.5 ± 6.8, $n = 11$, $P < 0.05$). L-NAME affected greater inhibition of acetylcholine-induced relaxation in 20 and 45 mM glucose PSS than in control PSS ($P < 0.05$, Figure 2c).

L-Arginine (10^{-4} M) prevented the impaired relaxation of normal arteries to acetylcholine in 20 mM glucose (pEC_{50}, 7.34 ± 0.06, $n = 7$, *versus* control PSS + L-arginine 7.41 ± 0.20, $n = 12$, NS. However, with 45 mM glucose maximum relaxation to acetylcholine was not improved (maximum relaxation [% noradrenaline precontraction] 67.9 ± 8.4, $n = 14$, *versus* control PSS + L-arginine 95.2 ± 1.2, $n = 12$, $P < 0.01$, Figure 3).

The aldose reductase inhibitor, ponalrestat (10^{-5} M) was also effective in preventing the endothelial dysfunction in 20 mM glucose (pEC_{50}: 20 mM glucose + ponalrestat 7.49 ± 0.17, $n = 6$, *versus* control PSS + ponalrestat 7.75 ± 0.13, $n = 8$, NS) and significantly improved relaxation to acetylcholine in arteries incubated in 45 mM glucose PSS (maximum relaxation [% noradrenaline precontraction]: 45 mM

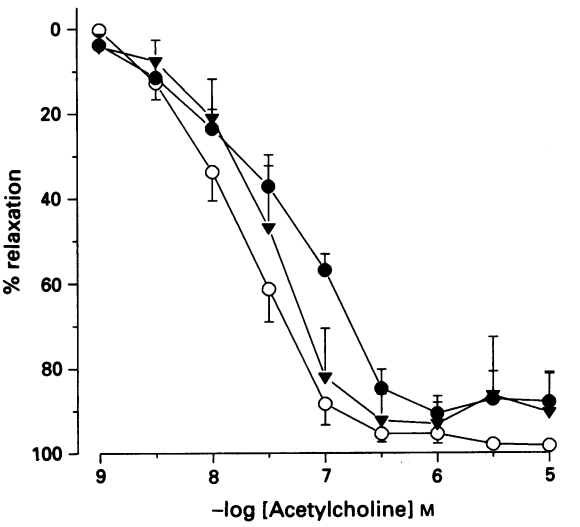


Figure 4 Acetylcholine-induced relaxation in normal mesenteric resistance arteries precontracted with noradrenaline, after 2 h incubation in 20 mM glucose (▼, $n = 6$), 45 mM glucose (●, $n = 7$) and control PSS (○, $n = 8$) in the presence of 10^{-5} M ponalrestat.

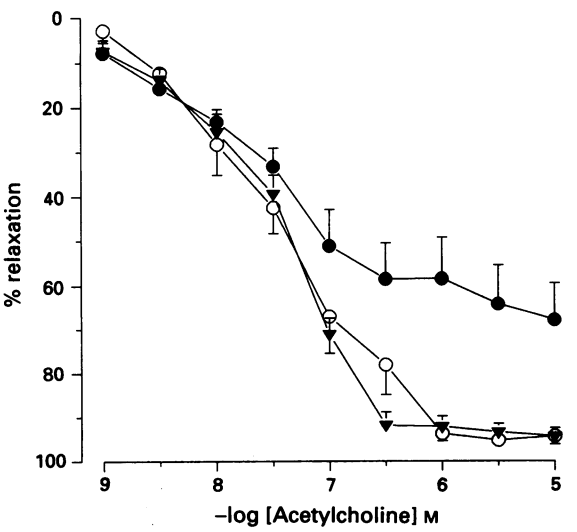


Figure 3 Acetylcholine-induced relaxation in normal mesenteric resistance arteries precontracted with noradrenaline, after 2 h incubation in 20 mM glucose (▼, $n = 7$), 45 mM glucose (●, $n = 14$) and control PSS (○, $n = 12$) in the presence of 10^{-4} M L-arginine.

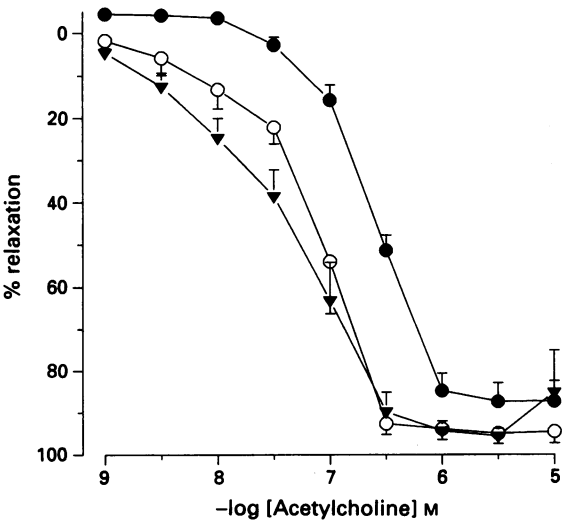


Figure 5 Acetylcholine-induced relaxation in normal mesenteric resistance arteries precontracted with noradrenaline, after 2 h incubation in 20 mM glucose (▼, $n = 8$), 45 mM glucose (●, $n = 6$) and control PSS (○, $n = 5$) in the presence of superoxide dismutase (SOD, 150 u ml^{-1}).

glucose 48.8 ± 7.1, $n = 11$, *versus* 45 mM glucose + ponalrestat 91.6 ± 2.6, $n = 7$, $P < 0.001$). However, the sensitivity of arteries to acetylcholine was significantly impaired in 45 mM glucose compared with control (pEC_{50}: 45 mM glucose + ponalrestat 7.18 ± 0.05, $n = 7$, *versus* control PSS + ponalrestat 7.75 ± 0.13, $n = 8$, $P < 0.01$, Figure 4).

Superoxide dismutase (SOD, 150 u ml^{-1}) also prevented impaired relaxation to acetylcholine in 20 mM glucose (pEC_{50}: 20 mM glucose + SOD 7.34 ± 0.12, $n = 8$, *versus* control PSS + SOD 7.08 ± 0.10, $n = 5$, NS). Maximum relaxation to acetylcholine in arteries incubated in 45 mM glucose was significantly improved by the addition of superoxide dismutase to the medium, but the sensitivity to acetylcholine was still impaired relative to control (maximum relaxation [% noradrenaline precontraction]: 45 mM glucose 48.8 ± 7.1, $n = 11$, *versus* 45 mM glucose + SOD 87.3 ± 4.4, $n = 6$, $P < 0.005$; pEC_{50}: 45 mM glucose + SOD 6.62 ± 0.04, $n = 6$, *versus* control + SOD 7.08 ± 0.10, $n = 5$, $P < 0.005$, Figure 5).

Endothelium-independent relaxation

Relaxation to the nitrovasodilator, sodium nitroprusside (SNP, 10^{-9}–10^{-5} M) in the presence of indomethacin (10 μM) and L-NAME (0.1 mM) was normal in arteries incubated in 20 mM glucose (pEC_{50}: 20 mM glucose 7.63 ± 0.10, $n = 8$, *versus* control PSS, NS), but was significantly impaired in arteries incubated for 2 h in 45 mM glucose (pEC_{50}: 45 mM glucose PSS 7.48 ± 0.07, $n = 12$, *versus* control PSS 7.78 ± 0.10, $n = 11$, $P < 0.05$).

Responses in diabetic arteries

Similar responses to noradrenaline were observed in the arteries of the diabetic rats as were found in the normal arteries in response to elevated glucose. Thus arteries from STZ-induced diabetic rats (7–10 weeks duration of STZ-diabetes) in PSS (5.5 mM glucose) + indomethacin, demonstrated normal sensitivity but an enhanced maximum contractile response to noradrenaline, when compared to arteries from non-diabetic animals (maximum response [$mNmm^{-1}$]: diabetic arteries + indomethacin 3.98 ± 0.21, $n = 13$, *versus* non-diabetic controls + indomethacin 2.53 ± 0.13, $n = 13$, $P < 0.0001$). Incubation of arteries from STZ-induced diabetic rats in 45 mM glucose PSS (similar to the serum glucose concentration of these animals) did not significantly alter the maximum response to noradrenaline which was equivalent to that of arteries from non-diabetic animals in the same medium. The addition of L-NAME did not significantly alter the maximum noradrenaline response of arteries from the diabetic animals incubated in normal PSS + indomethacin.

Diabetic rat arteries incubated in control PSS with indomethacin also demonstrated impaired relaxation to acetylcholine compared to normal arteries (pEC_{50}: diabetic arteries in control PSS 7.08 ± 0.17, $n = 7$, *versus* normal arteries 7.68 ± 0.13, $n = 12$, $P < 0.05$). The incubation of diabetic arteries in 45 mM glucose PSS with indomethacin did not further impair endothelium-dependent relaxation to acetylcholine (pEC_{50}: diabetic arteries in control PSS 7.08 ± 0.17, $n = 7$, *versus* diabetic arteries in 45 mM glucose PSS 6.93 ± 0.12, $n = 9$, NS).

Diabetic arteries incubated in normal PSS demonstrated normal relaxation to SNP in the presence of indomethacin (10 μM) and L-NAME (0.1 mM). However, diabetic arteries showed impaired relaxation in 45 mM glucose compared to normal PSS (diabetic arteries pEC_{50}: control PSS 7.77 ± 0.15, $n = 8$, *versus* 45 mM glucose 7.30 ± 0.06, $n = 9$, $P < 0.01$).

Discussion

These results demonstrate that enhanced sensitivity to noradrenaline can be induced in normal isolated mesenteric resistance arteries of the rat by incubation in abnormally high glucose. The maximum effect occurred at the lower of the two glucose concentrations and these data were almost identical to those we recently reported in mesenteric resistance arteries from STZ-induced diabetic rats (Taylor *et al.*, 1992; 1994a) which substantiated previous reports of enhanced pressor reactivity in conduit arteries (MacLeod & McNeill, 1985; Pieper & Gross, 1988; White & Carrier, 1988; Harris & Macleod, 1988; Cohen *et al.*, 1990). The more modest response to the higher glucose concentration implies an additional mechanism, perhaps a direct deleterious effect on the smooth muscle. The similarity of the data in the normal arteries in 20 mM glucose medium and those from the diabetic rats strongly suggests a central role for hyperglycaemia.

An abnormality of endothelium-derived relaxing or constricting factors may underly enhanced noradrenaline responses, since endothelial damage augments contractions of normal rat arteries to α-adrenoceptor agonists (Carrier & White, 1985; Durante *et al.*, 1988). Inhibition of cyclooxygenase using indomethacin caused a rightward shift of the noradrenaline response in the control and glucose-treated arteries, which would suggest inhibition of either basal or noradrenaline stimulated release of a constrictor prostanoid. However, this could also have been the result of the previous use of potassium in the run up period as Holden *et al.* (1992) have shown that potassium produces a long lasting increase in thromboxane A_2 synthesis. Nonetheless the difference in sensitivity between control and glucose treated arteries to noradrenaline was no longer evident in the presence of indomethacin. Agrawal & McNeill (1987) have similarly reported an indomethacin-sensitive increase in α-adrenoceptor responses in mesenteric arteries from diabetic rats. These data suggest that there is enhanced production of a constrictor prostanoid by hyperglycaemia and in diabetes, but indomethacin in addition to the inhibition of cyclooxygenase, also has some calcium channel inhibitory activity (Triggle, 1981). Since increased calcium channel activation has been reported in experimental diabetes (Chang *et al.*, 1993) indomethacin could be normalizing the response in elevated glucose through inhibition of calcium influx. Endothelium-derived relaxing factors also modify responses to vasoconstrictors in this vascular bed (Graves & Poston, 1993) and in this study, as in others, the inhibition of nitric oxide synthase by L-NAME (in the presence of indomethacin) augmented the maximum contractile response to noradrenaline in control arteries. L-NAME, however, had only a modest effect on maximal contraction in arteries in the hyperglycaemic medium, significantly reducing the difference in maximum response between arteries in glucose and in control PSS. This would imply that hyperglycaemia had reduced the spontaneous or tonic release of nitric oxide as we have reported in the arteries of the diabetic rat (Taylor *et al.*, 1992). There would, therefore, appear to be at least two pathways through which hyperglycaemia may enhance constrictor responses. An alternative explanation has been proposed (Simmons & Winegrad, 1992), which suggests that glucose may inhibit an adenosine stimulated component of Na^+/K^+ ATPase activity, so depolarizing the vascular smooth muscle and perhaps reducing a Na^+/K^+ ATPase stimulated hyperpolarizing factor (Vanhoutte, 1988). The stimulation of Na^+/K^+ ATPase is thought to occur through glucose-induced stimulation of aldose reductase (Simmons & Winegrad, 1992). However, inhibition of aldose reductase by ponalrestat did not prevent enhanced noradrenaline sensitivity in this study and therefore, does not support a role for this pathway.

Endothelium-dependent relaxation to acetylcholine in mesenteric resistance arteries from normal rats was profoundly impaired by incubation in elevated glucose medium (20 mM and 45 mM). This agrees with the observations of Tesfamariam and coworkers in rabbit aorta (Tesfamariam *et al.*, 1990, 1991; 1992; Tesfamarian & Cohen, 1992). There is,

however, a fundamental difference between the contributory pathways in the rat mesenteric arteries and the rabbit aorta. In the rabbit aorta, impaired relaxation was completely prevented by cyclo-oxygenase blockade and attributed to increased generation of vasoconstrictor prostanoids and associated free radicals (Tesfamariam *et al.*, 1990; Tesfamarian & Cohen, 1992). In contrast, indomethacin improved maximum relaxation in all groups in this study and the sensitivity to acetylcholine remained impaired in the high glucose media. This response to indomethacin is similar to that reported in the arteries of the diabetic rats in this and our previous report (Taylor *et al.*, 1992) and do not accord with the findings in diabetic rabbit aorta. Indomethacin has also been found not to alter impaired endothelium-dependent responses in diabetic rat aorta (Oyama *et al.*, 1986). There appear, therefore, to be important differences in the mechanism of endothelial dysfunction in these two models of diabetes.

Some previous studies, including our own, have been criticised for investigating diabetic artery function *in vitro* in euglycaemic medium. We report here that relaxation to acetylcholine is not significantly different between diabetic arteries incubated in 45 mM glucose and control PSS. This suggests that either the acute effects of hyperglycaemia are prolonged and irreversible, or that other mechanisms may be important in the long term. Inhibition of nitric oxide synthase by L-NAME caused greater inhibition of acetylcholine relaxation in high glucose than in normal glucose medium. This could be interpreted as there being a greater nitric oxide mediated component of relaxation in the high glucose experiment. Indeed, a recent study by Craier *et al.* (1993) in porcine aortic endothelial cells suggested that exposure to elevated glucose concentration results in enhanced nitric oxide formation through amplification of agonist-stimulated Ca^{2+} mobilization. Alternatively, it could be hypothesized that L-NAME is less effective when nitric oxide synthase activity is higher, and that greater inhibition in high glucose reflects reduced nitric oxide synthase activity. We have previously presented evidence that this occurs in arteries from diabetic rats (Taylor *et al.*, 1992) and this is supported by the experiments of Martin *et al.* (1992) which have shown L-NAME to be more effective in blocking acetylcholine-induced relaxation in rat aorta when phenoxybenzamine was used to inactivate a fraction of the muscarinic receptors. Nonetheless, L-NAME did not achieve complete blockade of relaxation in any of the experimental conditions which could indicate incomplete inhibition of nitric oxide synthase or implicate a separate component to acetylcholine-induced relaxation, possibly the endothelium-derived hyperpolarizing factor (EDHF), which has been clearly demonstrated in the same arteries by Garland & McPherson (1992). The results could also be interpreted, therefore, to suggest that glucose inhibits EDHF.

The nitric oxide precursor, L-arginine (10^{-4} M), prevented impaired relaxation to acetylcholine in 20 mM glucose, but did not affect relaxation in control PSS. This suggests that substrate availability for nitric oxide synthase is rate limiting under hyperglycaemic conditions, which could either occur as a result of impaired cellular arginine uptake or increased utilization, or alternatively reduced affinity of the nitric oxide synthase enzyme for L-arginine. In the rabbit aorta, Gupta *et al.* (1992) have found L-arginine supplementation prevents endothelium-dependent inhibition of Na^+/K^+ ATPase induced by hyperglycaemia suggesting reduced nitric oxide release may be responsible for the lowered enzyme activity. It is of interest that L-arginine, the intracellular concentration of which is generally considered not to be a rate limiting factor for nitric oxide synthase, also normalizes impaired endothelium-dependent relaxation in atherosclerosis, both in animals (Rossitch *et al.*, 1991; Girerd *et al.*, 1990) and in man (Drexler *et al.*, 1991). Thus, it is possible that hypercholesterolaemia and hyperglycaemia could affect nitric oxide synthase activity through a common metabolic pathway.

Most investigations suggest that nitric oxide synthase activity is reduced in diabetes, but one interpretation of the beneficial effect of L-arginine could be that nitric oxide synthase activity is sufficiently *raised* by hyperglycaemia so that the cell becomes L-arginine depleted. As mentioned previously, Craier *et al.* (1993) have suggested that glucose may stimulate nitric oxide release in porcine endothelial cells and one investigation in the diabetic rat aorta has suggested that nitric oxide synthase activity is increased. Langenstroer & Pieper (1992) have reported that reduced relaxation to acetylcholine is the result of massive inactivation by oxygen-derived free radicals, of an underlying increased nitric oxide synthesis (unmasked with superoxide dismutase). It is unfortunate, therefore, that the *in vitro* studies of arteries from diabetic animals, including our own, have never included L-arginine in the organ bath, which could have masked an underlying increase in nitric oxide synthesis. However, this criticism cannot be directed towards *in vivo* studies in diabetic animals and man which have demonstrated impaired endothelium-dependent relaxation in the presence of physiological concentrations of L-arginine.

It has been proposed that hyperglycaemia may impair nitric oxide production in vascular endothelium through the stimulation of the polyol pathway (Cameron & Cotter, 1992). In one of the proposed effector pathways, redox changes associated with increased sorbitol flux can lead to increased utilisation, and may reduce availability, of cellular NADPH, an essential cofactor of nitric oxide synthase (Cameron & Cotter, 1992). In the present study the aldose reductase inhibitor, ponalrestat, prevented impaired relaxation to acetylcholine in 20 mM glucose, and significantly improved but did not completely prevent impaired relaxation in 45 mM glucose PSS. This is in accord with the study of Tesfamariam *et al.* (1992) in which an aldose reductase inhibitor prevented glucose-induced (44 mM) endothelial dysfunction in normal rabbit aorta, and with two studies which have found treatment *in vivo* with aldose reductase inhibitors reverses endothelium dysfunction in diabetic animals (Cameron & Cotter, 1992; Tesfamariam *et al.*, 1993). However, in a recent study in this laboratory, diabetic rats treated with ponalrestat (100 mg kg^{-1} day^{-1}) over a 10 week period still demonstrated impaired endothelium-dependent relaxation in the isolated perfused mesenteric circulation (Taylor *et al.*, 1994c) suggesting that, in the long term, mechanisms other than the stimulation of aldose reductase may contribute to endothelial dysfunction in this circulation.

The protective effect of superoxide dismutase (SOD, 150 u ml^{-1}) on glucose-induced impairment of acetylcholine relaxation, suggests a role for oxygen-derived free radicals in the blunted response. SOD has also been shown to improve endothelium-dependent relaxation in diabetic rat aorta (Hattori *et al.*, 1991), and glucose-induced impairment of acetylcholine relaxation in rabbit aorta (Tesfamariam & Cohen, 1992) which occurs as a result of increased cyclooxygenase activity. An alternative source of oxygen-derived free radicals might also be the autoxidation of glucose (Wolff & Dean, 1987). Increased free radical generation might also explain the impaired response of the arteries to sodium nitroprusside in elevated glucose as free radicals would reduce the efficacy of this nitric oxide donor (Ignarro *et al.*, 1980). Similar experiments carried out in the presence of superoxide dismutase would help to validate this assumption. The alternative explanation, that 45 mM glucose has a non-specific deleterious effect upon vascular smooth muscle relaxation could be investigated by determining the effect of glucose on the response to other non-cyclic GMP-dependent vasodilators. Responses to sodium nitroprusside were not impaired in the diabetic arteries incubated in normal glucose but were abnormal in 45 mM glucose, indicating an additional and acute effect of hyperglycaemia.

In conclusion, this study suggests a central role for glucose in the development of vascular functional changes associated with experimental diabetes. Using several pharmacological

agents we have identified a number of contributory pathways. Since the sum total of the individual contributions is obviously greater than the net effect of hyperglycaemia a degree of overlap undoubtedly occurs. For example, stimulation of aldose reductase can theoretically lead to both an increase in free radicals, through a reduction in free radical scavenging (Dvornik, 1987), and a reduction in nitric oxide synthase activity (Cameron & Cotter, 1992). Moreover, a link has been hypothesized between the production of constrictor prostanoids and the generation of free radicals (Tesfamariam & Cohen, 1992). Further studies with combinations of agents would determine the degree of overlap. It should be noted that some important differences exist between the mechanisms involved in hyperglycaemia-induced endothelial dysfunction and those we have identified in the small mesenteric arteries of rats with streptozotocin-induced diabetes (Taylor *et al.*, 1992; 1994a,c). Since these were investigated in a euglycaemic medium, it would appear that diabetes is associated with long term modification of endothelial function. Whether these are secondary to the initial and acute effects of hyperglycaemia remains to be determined. However, the arteries from the diabetic rats demonstrated no further endothelial dysfunction in a hyperglaemic compared to a euglycaemic medium, suggesting that chronic modification of the endothelium may occur in response to hyperglycaemia.

This work was funded through a collaborative PhD studentship between the Medical Research Council and ZENECA Pharmaceuticals.

References

ABIRU, T., KAMATA, K., MIYATA, N. & KASUYA, Y. (1990). Differences in vascular responses to vasoactive agents of basilar artery and aorta from rabbits with alloxan-induced diabetes. *Can. J. Physiol. Pharmacol.*, **68**, 882–888.

AGRAWAL, D.K. & MCNEILL, J.H. (1987). The effect of diabetes on vascular smooth muscle function in normotensive and spontaneously hypertensive rat mesenteric artery. *Can. J. Physiol. Pharmacol.*, **65**, 2274–2280.

CAMERON, N.E. & COTTER, M.A. (1992). Impaired contraction and relaxation in aorta from streptozotocin-diabetic rats: role of polyol pathway. *Diabetologia*, **35**, 1011–1019.

CARRIER, G.O. & WHITE, R.E. (1985). Enhancement of alpha-1 and alpha-2 adrenergic agonist-induced vasoconstriction by removal of endothelium in rat aorta. *J. Pharmacol. Exp. Ther.*, **232**, 682–687.

CHANG, K.C., CHUNG, S.Y., CHONG, W.S., SUH, J.S. *et al.* (1993). Possible superoxide radical-induced alteration of vascular reactivity in aortas from streptozotocin-treated rats. *J. Pharmacol. Exp. Ther.*, **266**, 992–1000.

COHEN, R.A. & TESFAMARIAM, B. (1992). Diabetes mellitus and the vascular endothelium. In: *Hyperglycaemia, Diabetes and Vascular Disease*. ed. Rudderman, N., Brownlee, M. & Williamson, J.R. pp. 223–249. New York: Oxford University Press.

COHEN, R.A., TESFAMARIAM, B., WEISBROD, R.M. & ZITNAY, K.M. (1990). Adrenergic denervation in rabbits with diabetes mellitus. *Am. J. Physiol.*, **259**, H55–H61.

CRAIER, W.F., WASCHER, T.C., LACKENER, L., TOPLAK, H., KREJS, G.J. & KUKOVETZ, W.R. (1993). Exposure to elevated D-glucose concentrations modulates vascular endothelial cell vasodilatory responses. *Diabetes*, **42**, 1497–1505.

DIABETES CONTROL AND COMPLICATIONS TRIAL RESEARCH GROUP. (1993). The effect of intensive treatment of diabetes on the development and progression of long-term complications in insulin-dependent diabetes mellitus. *N. Engl. J. Med.*, **329**, 977–986.

DREXLER, H., ZEIHER, A.M., MEINZER, K. & JUST, H. (1991). Correction of endothelial dysfunction in coronary microcirculation of hypercholesterolaemic patients by L-arginine. *Lancet*, **338**, 1546–1550.

DURANTE, W., SEN, A.K. & SUNAHARA, F.A. (1988). Impairment of endothelium-dependent relaxation in aortae from spontaneously diabetic rats. *Br. J. Pharmacol.*, **94**, 463–468.

DVORNIK, D. (1987). Hyperglycaemia in the pathogenesis of diabetic complications. In *Aldose Reductase Inhibition. An Approach for the Prevention of Diabetic Complications*. ed. Porte, D. pp. 69–151. New York: Biomedical Information Corporation.

ELLIOT, T.G., COCKROFT, J.R., GROOP, P.H, VIBERTI, G.C. & RITTER, J.M. (1993). Inhibition of nitric oxide synthesis in forearm vasculature of insulin-dependent diabetic patients: blunted vasoconstriction in patients with microalbuminuria. *Clin. Sci.*, **85**, 687–693.

FRIEDMAN, J.J. (1989). Vascular sensitivity to and reactivity to norepinephrine in diabetes mellitus. *Am. J. Physiol.*, **256**, H1134–H1138.

GARLAND, C.J. & MCPHERSON, G.A. (1992). Evidence that nitric oxide does not mediate the hyperpolarisation and relaxation to acetylcholine in the rat small mesenteric artery. *Br. J. Pharmacol.*, **105**, 429–435.

GIRERD, X.J., HIRSCH, A.T., COOKE, J.P., DZAU, V.J. & CREAGER, M.A. (1990). L-arginine augments endothelium-dependent vasodilation in cholesterol-fed rabbits. *Circ. Res.*, **67**, 1301–1308.

GRAVES, J. & POSTON, L. (1993). Beta adrenergic mediated relaxation of rat isolated mesenteric resistance arteries: a role for the endothelium and nitric oxide. *Br. J. Pharmacol.*, **108**, 631–637.

GREENE, D.A., LATTIMER, S.A. & SIMA, A.A.F. (1987). Sorbitol, phosphoinositides, and sodium potassium-ATPase in the pathogenesis of diabetic complications. *N. Engl. J. Med.*, **316**, 599.

GUPTA, S., SUSSMAN, I., MCARTUR, C.S., TORNHEIM, K., COHEN, R.A. & RUDERMAN, N.B. (1992). Endothelium dependent inhibition of Na^+/K^+ ATPase activity in rabbit aorta by hyperglycaemia. Possible role of endothelium derived nitric oxide. *J. Clin. Invest.*, **90**, 727–732.

HARRIS, K.H. & MACLEOD, M. (1988). Influence of the endothelium on contractile responses of arteries from diabetic rats. *Eur. J. Pharmacol.*, **153**, 55–64.

HATTORI, Y., KAWASAKI, H., ABE, K. & KANNO, M. (1991). Superoxide dismutase recovers altered endothelium-dependent relaxation in diabetic rat aorta. *Am. J. Physiol.*, **261**, H1086–H1094.

HEBDEN, R.A., GARDINER, S.M., BENNETT, T. & MACDONALD, I.A. (1986). The influence of streptozotocin-induced diabetes mellitus on fluid and electrolyte handling in rats. *Clin Sci.*, **70**, 111–117.

HOLDEN, K., SNEDDON, J.M. & MUNBY, J. (1992). KCl-induced augmentation of α_1-adrenoceptor pressor responsiveness in the rat mesenteric vascular bed (MVB) is thromboxane-dependent. *Br. J. Pharmacol.*, **106**, 16P.

IGNARRO, L.J., EDWARDS, J.C., GRUETTER, B.K., OHLSTEIN, E.H. & GRUETTER, C.A. (1980). Possible involvement of S-nitrosothiols in the activation of guanylate cyclase by nitroso compounds. *FEBS Lett.*, **110**, 275–278.

KAMATA, K., MIYATA, N. & KASUYA, Y. (1989). Impairment of endothelium-dependent relaxation and changes in levels of cyclic GMP in aorta from streptozotocin-induced diabetic rats. *Br. J. Pharmacol.*, **97**, 614–618.

KORTHUIS, R.J., BENOIT, J.N., KVIETYS, P.R., LAUGHLIN, M.H., TAYLOR, A.E. & GRANGER, D.N. (1987). Intestinal hypermia in experimental diabetes mellitus. *Am. J. Physiol.*, **253**, G26–G32.

LANGENSTROER, P. & PIEPER, G.M. (1992). Regulation of spontaneous EDRF release in diabetic rat aorta by oxygen free radicals. *Am. J. Physiol.*, **263**, H257–H265.

LEE, T.-S., SALTSMAN, K.A., OHASHI, H. & KING, G.L. (1989). Activation of protein kinase C by elevation of glucose concentration: proposal for a mechanism in the development of diabetic vascular complications. *Proc. Natl. Acad. Sci. U.S.A.*, **86**, 5141–5145.

MACLEOD, K.M. & MCNEILL, J.H. (1985). Influence of chronic experimental diabetes on contractile response of rat isolated blood vessels. *Can. J. Physiol. Pharmacol.*, **63**, 52–57.

MARTIN, G.R., BOLOFO, M.L. & GILES, H. (1992). Inhibition of endothelium-dependent vasorelaxation by arginine analogues: a pharmacological analysis of agonist and tissue dependence. *Br. J. Pharmacol.*, **105**, 643–652.

MAYHAN, W.G. (1989). Impairment of endothelium-dependent dilatation of cerebral arterioles during diabetes mellitus. *Am. J. Physiol.*, **256**, H621–H625.

MAYHAN, W.G., SIMMONS, L.K. & SHARPE, G.M. (1991). Mechanism of impaired responses of cerebal arterioles during diabetes mellitus. *Am. J. Physiol.*, **260**, H319–H326.

MCNALLY, P.G., WATT, P.A.C., BURDEN, A.C., HEARNSHAW, J.R. & THURSTON, H. (1992). Impaired vascular contraction and endothelium-dependent relaxation in normotensive Type 1 diabetes. *Diab. Med.*, **9**, 32A.

MCVEIGH, G.E., BRENNAN, G.M., JOHNSTON, G.D., MCDERMOTT, B.J., MCGRATH, L.T., HENRY, W.R., ANDREWS, J.W. & HAYES, J.R. (1992). Impaired endothelium-dependent and independent vasodilation in patients with Type 2 (non-insulin-independent) diabetes mellitus. *Diabetologia*, **35**, 771–776.

MULVANY, M.J. & HALPERN, W. (1977). Contractile properties of small arterial resistance arteries in spontaneously hypertensive and normotensive rats. *Circ. Res.*, **41**, 19–26.

OYAMA, Y., KAWASAKI, H., HATTORI, Y. & KANNO. M. (1986). Attenuation of endothelium-dependent relaxation in aorta from diabetic rats. *Eur. J. Pharmacol.*, **131**, 75–78.

PIEPER, G.M. & GROSS, G.J. (1988). Oxygen free radicals abolish endothelium dependent relaxation in diabetic rat aorta. *Am. J. Physiol.*, **255**, H825–833.

ROSSITCH Jr. E., ALEXANDER III, E., MCBLACK, P. & COOKE, J.P. (1991). L-arginine normalizes endothelial function in cerebral vessels from hypercholesterolemic rabbits. *J. Clin. Invest.*, **87**, 1295–1299.

SIMMONS, D.A. & WINEGRAD, A.I. (1992). Mechanisms in rabbit aorta for hyperglycaemia-induced alterations in angiotensin II and norepinephrine effects. *Diabetologia*, **35**, 725–729.

TANZ, R.D., CHANG, K.S.K. & WELLER, T.S. (1989). Histamine relaxation of aortic rings from diabetic rats. *Agents Actions*, **28**, 2–8.

TAYLOR, P.D., MCCARTHY, A.L., THOMAS, C.R. & POSTON, L. (1992). Endothelium-dependent relaxation and noradrenaline sensitivity in mesenteric resistance arteries of streptozotocin-induced diabetic rats. *Br. J. Pharmacol.*, **107**, 393–399.

TAYLOR, P.D., OON, B., THOMAS, C.R. & POSTON, L. (1994a). Prevention by insulin treatment of endothelial dysfunction but not enhanced noradrenaline-induced contractility in mesenteric resistance arteries from streptozotocin-induced diabetic rats. *Br. J. Pharmacol.*, **111**, 35–41.

TAYLOR, P.D., THOMAS, C.R. & POSTON, L. (1994b). The effect of acute hyperglycaemia on endothelial function in isolated rat mesenteric resistance arteries. *Diab. Med.*, **10**, S32.

TAYLOR, P.D., WICKENDEN, A.D., MIRLEES, D. & POSTON, L. (1994c). Endothelial function in the isolated perfused mesentery and aortae of rats with streptozotocin-induced diabetes: effects of treatment with the aldose reductase inhibitor, ponalrestat. *Br. J. Pharmacol.*, **111**, 42–48.

DE TEJADA, I.S., GOLDSTEIN, I., AZADZOI, K., KRANE, R.J. & COHEN, R.A. (1989). Impaired neurogenic and endothelium-mediated relaxation of penile smooth muscle from diabetic men with impotence. *New Engl. J. Med.*, **320**, 1025–1030.

TESFAMARIAM, B., BROWN, M.L. & COHEN, R.A. (1991). Elevated glucose impairs endothelium-dependent relaxation by activating protein kinase C. *J. Clin. Invest.*, **87**, 1643–1648.

TESFAMARIAM, B., BROWN, M.L. & COHEN, R.A. (1992). Aldose reductase and myo-inositol in endothelial cell dysfunction caused by elevated glucose. *J. Pharmacol. Exp. Ther.*, **263**, 153–157.

TESFAMARIAM, B., BROWN, M.L., DEYKIN, D. & COHEN, R.A. (1900). Elevated glucose promotes generation of endothelium-derived vasoconstrictor prostanoids in rabbit aorta. *J. Clin. Invest.*, **85**, 929–932.

TESFAMARIAM, B. & COHEN, R.A. (1992). Free radicals mediate endothelial cell dysfunction caused by elevated glucose. *Am. J. Physiol. (Heart Circ. Physiol.)*, **263**, H321–H326.

TESFAMARIAM, B., JAKUBOWSKI, J.A. & COHEN, R.A. (1989). Contraction of diabetic rabbit aorta caused by endothelium-derived PGH_2-TxA_2. *Am. J. Physiol.*, **257**, H1327–H1333.

TESFAMARIAM, B., PALACINO, J.J., WEISBROD, R.M. & COHEN, R.A. (1993). Aldose reductase inhibition restores endothelial cell function in diabetic rabbit aorta. *J. Card. Pharmacol.*, **21**, 205–211.

TRIGGLE, D.J. (1981). Calcium antagonists. Basic chemical and pharmacological aspects. In *New Perspectives on Calcium Antagonists*. ed. Weiss, G.B. pp. 1–18. Bethesda, MD: American Physiological Society.

VANHOUTTE, P.M. (1988). The endothelium-modulator of vascular smooth muscle tone. *N. Engl. J. Med.*, **319**, 512–513.

WHITE, R.E. & CARRIER, G.O. (1988). Enhanced vascular α-adrenergic neuroeffector system in diabetes: importance of calcium. *Am. J. Physiol.*, **255**, H1036–H1042.

WILLIAMSON, J.R., OSTROW, E., EABES, D., CHANG, K., ALISON, W., KILO, C. & SHERMAN, W.R. (1990). Glucose induced microsvascular functional changes in nondiabetic rats are stereospecific and are prevented by an aldose reductase inhibitor. *J. Clin. Invest.*, **80**, 1167–1172.

WOLFF, S.P. & DEAN, R.T. (1987). Glucose autooxidation and protein modification: the potential role of autooxidative glycosylation in diabetes. *Biochem. J.*, **245**, 246–250.

(Received December 13, 1993
Revised June 20, 1994
Accepted July 5, 1994)

Br. J. Pharmacol. (1994), **113**, 809–814 © Macmillan Press Ltd, 1994

The effect of non-steroidal anti-inflammatory drugs on the accumulation and release of interleukin-1-like activity by peritoneal macrophages from the mouse

A.K. Bahl, M.M. Dale & [1]J.C. Foreman

Department of Pharmacology, University College London, Gower Street, London WC1E 6BT

1 The non-steroidal anti-inflammatory drugs (NSAIDs) indomethacin, 10 and 100 μM, piroxicam, 100 μM, and sodium meclofenamate, 1 and 100 μM, potentiated the lipopolysaccharide (LPS)-stimulated release of interleukin-1 (IL-1)-like activity from mouse peritoneal macrophages. Aspirin up to 100 μM was without effect. The drugs did not themselves stimulate the release of IL-1-like activity at the concentrations used.

2 LPS, 1 μg ml^{-1}, stimulated prostaglandin E_2 production by mouse peritoneal macrophages and this was totally inhibited by aspirin, 100 μM, indomethacin, 1 μM, piroxicam, 10 μM and sodium meclofenamate, 0.1 μM.

3 The potentiation of LPS-stimulated release of IL-1-like activity produced by indomethacin, 100 μM, piroxicam, 100 μM, or sodium meclofenamate, 10 μM, was inhibited by prostaglandin E_2, (PGE_2) 10 ng ml^{-1}.

4 Aspirin, 100 μM, indomethacin, 100 nM to 10 μM, piroxicam, 1 to 100 μM, and sodium meclofenamate, 10 nM, all potentiated cell-associated IL-1-like activity in LPS- stimulated macrophages. The drugs had no effect on cell-associated IL-1-like activity by themselves.

5 Exogenous PGE_2, 2 to 30 ng ml^{-1}, inhibited the cell-accumulation of IL-1-like activity stimulated by LPS in the presence of indomethacin, 1 μM, or sodium meclofenamate, 0.1 μM.

6 The 5-lipoxygenase inhibitors BWA4C, 0.01 to 10 μM, and L-651,392, 0.01 to 10 μM, had no effect on LPS-stimulated released or cell-associated IL-1-like activity. Over the same concentration-ranges, neither of the 5-lipoxygenase inhibitors affected released or cell-associated IL-1-like activity in LPS-stimulated mouse macrophages in the presence of indomethacin, 1 μM.

7 The synthetic diacylglycerol, DiC_8, 10 to 200 μM, did not itself increase released or cell-associated IL-1-like activity but in the presence of the diacylglycerol kinase inhibitor, R59022, 10 μM, DiC_8 increased released and cell-associated IL-1-like activity. The activity of DiC_8 on released and cell-associated IL-1-like activity was not increased by indomethacin, 100 μM.

8 NSAIDs increase LPS-induced cell-associated IL-1-like activity in mouse macrophages by inhibiting the formation of cyclo-oxygenase products such as PGE_2 but at higher concentrations the NSAIDs potentiate LPS-induced release of IL-1-like activity by a mechanism independent of cyclo-oxygenase inhibition. The potentiation of the release of IL-1-like activity appears not to be related to an effect of NSAIDs on either 5-lipoxygenase or diacylglycerol metabolism.

Keywords: Non-steroidal anti-inflammatory drugs; mouse macrophages; interleukin-1; cyclo-oxygenase; prostaglandin E_2; 5-lipoxygenase; diacylglycerol

Introduction

Although non-steroidal anti-inflammatory drugs (NSAIDs) are widely used in the treatment of inflammatory joint disease, there is some evidence that they may promote joint destruction in osteoarthritis in man (Newman & Ling, 1985; Rashad *et al.*, 1989) and in animal models (Kalbhen, 1982; Maier & Wilhelmi, 1983). Indomethacin has been shown to potentiate T-lymphocyte proliferation *in vitro* (Lewis & Barret, 1986) and plasma extravasation (Raud *et al.*, 1987). Both indomethacin and sodium meclofenamate potentiate superoxide production by human neutrophils (Dale & Penfield, 1987; Twomey *et al.*, 1989). Interleukin-1 release by macrophages has also been shown to be potentiated by NSAIDs (Oppenheim *et al.*, 1980; Brandwein, 1986; Knudsen *et al.*, 1986; Kunkel *et al.*, 1986; Sandborg *et al.*, 1986). In contrast, some studies have failed to demonstrate any effect of NSAIDs on IL-1 release (Phadke *et al.*, 1986; Eden & Turino, 1986; Otterness *et al.*, 1988).

Interleukin-1 (IL-1) has a number of biological actions which are consistent with a role as an inflammatory mediator (Dinarello, 1989). There are two forms of IL-1: IL-1α and IL-1β which are translated from two separate mRNA's (Dinarello, 1989). The pro-peptides resulting from the translation of the mRNA's have different residence times within the cytoplasm and different biological activities. The IL-1α pro-peptide resides in the cytoplasm for 10 to 15 h compared with 3 to 4 h for the IL-1β pro-peptide (Hazuda *et al.*, 1988). The difference in cytoplasmic residence times appears to reflect different rates of secretion. Maximal IL-1β secretion occurs 2 h after lipopolysaccharide (LPS) stimulation of macrophages whereas the maximal rate of IL-1α secretion occurs 13 h after stimulation (Hazuda *et al.*, 1988). Processing of the IL-1 pro-peptides is not necessary for secretion from the cell and the kinetics of the release of IL-1β pro-peptide and mature form are identical (Hazuda *et al.*, 1988). The IL-1α pro-peptide and the mature form are similar in biological activity (Mosley *et al.*, 1987) whereas the IL-1β pro-peptide is biologically inactive and may be converted to a biologically active form extracellularly by a variety of proteases present in inflammatory exudates (Beuscher *et al.*, 1990; Hazuda *et al.*, 1990). Recently, a unique cytoplasmic cysteine protease has been identified which cleaves the IL-1β pro-peptide to its

[1] Author for correspondence.

mature form, Thornberry et al. (1992) have termed this enzyme, IL-1β-converting enzyme. A number of studies have also provided evidence that some IL-1 remains in association with the cell membrane (Kurt-Jones et al., 19885a,b; 1986; Conlon et al., 1987; Beuscher & Cotton, 1988).

Although there is evidence that PGE_2 inhibits IL-1 release from macrophages (Kunkel et al., 1986) and that this may explain the potentiation by NSAIDs of IL-1 release, the potentiating action of NSAIDs on superoxide generation by human neutrophils appears to be unrelated to the inhibition of PGE_2 synthesis by these drugs (Dale & Penfield, 1987; Twomey & Dale, 1992). There also remains the controversy in the literature regarding the ability of NSAIDs to potentiate IL-1 production from macrophages. This controversy may, in part, reflect the non-selective and insensitive bioassays that have been used to quantitate IL-1 production.

Hence, the aim of this study was to investigate the action of several NSAIDs on IL-1 production by macrophages in response to stimulation by lipopolysaccharide (LPS), using an improved assay, and to relate the effects of the NSAIDs to the inhibition of prostaglandin synthesis. Since IL-1 can remain associated with or within the cells, this study considers the differential effects of NSAIDs on released and cell-associated IL-1. In addition, the possibility that NSAIDs regulate IL-1 production by inhibiting the metabolism of diacylglycerol is investigated since this has previously been postulated as a proinflammatory activity of NSAIDs with respect to superoxide generation by neutrophils. (Dale & Penfield, 1987; Twomey & Dale, 1992).

Methods

Preparation of macrophages

The animals used were 8 to 12 week old male BKW mice (Bantin & Kingman, Hull). The mice were killed by asphyxiation in CO_2 and then doused with 70% industrial methylated spirit. Five ml of phosphate-buffered saline (nominally free of Ca^{2+} and Mg^{2+}) and chilled to 4°C was introduced into the peritoneal cavity and agitated. The peritoneal washings were removed and those from 5 mice were pooled. The cells were washed three times with phosphate-buffered saline by alternate centrifugation at 300 *g* for 8 min and then resuspension. The cells were finally resuspended in RPMI-1640 medium to which 5% (v/v) heat-inactivated foetal calf serum, 2 mM glutamine and gentamycin 50 $\mu g\,ml^{-1}$ had been added (supplemented RPMI). At this stage the cell viability as judged by trypan blue exclusion was greater than 95% and the cell population comprised 50 to 60% macrophages when stained for non-specific esterase.

The cells, at a density of $10^6\,ml^{-1}$ were placed in a 24 well tissue culture plate so that each well contained 10^6 cells. After incubation for 2 h at 37°C in an atmosphere of 95% air and 5% CO_2, the non-adherent cells were removed from the wells by gentle rinsing with supplemented RPMI-1640. The cell monolayer remaining in the wells comprised about 90% macrophages and these adherent cells were used for the experiments.

Experimental protocols

The experiments were performed by adding 1 ml of serum-free RPMI containing the reagents appropriate to the protocol, to the cells in the wells. Unless otherwise indicated, the cells were then incubated for 20 h at 37°C in 95% air and 5% CO_2. At the end of the incubation, the cell-free supernatants were removed from the wells and retained for appropriate assays. RPMI (300 μl) containing 10% (v/v) heat-inactivated foetal calf serum was added to the cells in each well. The tissue culture plates were then frozen to − 75°C and thawed to room temperature to fracture the cells. Cell disruption was completed by sonication for 15 min, the volume of each well was made up to 1 ml and the disrupted cell suspensions were used for appropriate assays.

Assay of interleukin-1

The assay used is based on that described by Gearing et al. (1987). The assay relies on the ability of IL-1 to stimulate the production of IL-2 from a sub-class of murine T cell thymoma cells: EL4 NOB1. The IL-2 released from the EL4 NOB1 cells is directly proportional to the concentration of IL-1 in contact with the cells, and the IL-2 produced is quantitated by its ability to support the viability and proliferation of the cytotoxic T cell line: CTLL. Supernatants from cells or disrupted cell suspensions were serially diluted in RPMI containing 5% (v/v) heat-inactivated foetal calf serum; 100 μl of appropriate sample dilution (1 in 100 for supernatants and 1 in 1000 for disrupted cell suspension) was placed in a well of a tissue culture plate together with 100 μl of a suspension of EL4 NOB1 cells ($2 \times 10^6\,ml^{-1}$). These dilutions provide amounts of IL-1-like activity which fall on the linear part of the concentration-response curve for IL-1 and EL4 NOB1 cells. Incubation was carried out at 37°C for 24 h in 95% air and 5% CO_2. After incubation, 50 μl of the supernatant from the EL4 NOB1 cells was removed and frozen to − 75°C to kill any cells that might be present. After thawing the samples, 50 μl of a suspension of CTLL cells ($8 \times 10^5\,ml^{-1}$) were added to give a final volume of 100 μl. Incubation was carried out at 37°C for 24 h in 95% air and 5% CO_2.

After the incubation, the viability of CTLLs was assessed by the method of Tada et al. (1986). A volume of 20 μl of 3-(4,5-dimethyl-thiazol-2-yl)-2,5-di-phenyltetrazolium bromide (MTT), 5 $mg\,ml^{-1}$ in phosphate buffered saline was added to each well of the culture plate and a further incubation was carried out at 37°C for 4.5 h in 95% air and 5% CO_2. Next, 100 μl of a solution of sodium dodecyl sulphate, 100 $mg\,ml^{-1}$ in HCl, 0.01 M, was added to each well and the plates were returned to the incubator for a further 12 h.

The absorbance of each well was measured at 570 nm with a reference wavelength of 630 nm in a MAXline Vmax microplate reader. The absorbance of each sample was proportional to the amount of IL-2 released from the EL4 NOB1 cells, and this, in turn, was proportional to the amount of IL-1-like activity released from the macrophages and incubated with the EL4 NOB1 cells (Gearing et al., 1987). The assay, which does not discriminate between IL-1α and IL-1β, was sufficiently sensitive to detect human recombinant IL-1α at levels of 0.3 $pg\,ml^{-1}$.

The bioassay at the stage of EL4 NOB1 culture has been shown to be selective for IL-1 and we have shown that the supernatants generated from macrophages in these experiments did not maintain the viability of CTLL. Hence, the activity assayed is very likely to be IL-1 but since this has not been confirmed with a monoclonal antibody, the activity is referred to as IL-1-like.

In all protocols, drugs and stimuli were tested directly and independently on CTLL cells and EL4 NOB1 cells to ensure that they did not interfere with the assay. PGE_2 above 1 $ng\,ml^{-1}$ inhibited the response of EL4 NOB1 cells to recombinant IL-1 and hence, in experiments involving the addition of exogenous PGE_2, supernatant from the macrophages were diluted to ensure no interference from PGE_2 in the IL-1 assay. PGE_2 had no effect on CTLL cells at concentrations up to 30 $ng\,ml^{-1}$. In all supernatants that were assayed for IL-1 biological activity, the concentration of PGE_2 was below that required to produce inhibition of EL4 NOB1 or CTLL cells.

Assay of prostaglandin E_2

PGE_2 was assayed with a commercial radioimmunoassay kit (NEN Research Products).

Data analysis

The data presented in Figures 1, 2 and 4 have been subjected to repeated measures ANOVA. Post-analysis was conducted by Tukey-Kramer multiple comparison tests. The data in Figures 3 and 6 have been subjected to the Student's paired *t* test.

Materials

Materials used in the experiments were obtained from the following sources: Sigma Chemical Co., Poole, Dorset: aspirin, DiC_8, indomethacin, lipopolysaccharide, MTT, piroxicam, prostaglandin E_2, sodium dodecyl sulphate. Gibco Ltd, Paisley: foetal calf serum, gentamycin, glutamine, phosphate buffered saline (nominally free of Ca^{2+} and Mg^{2+}), RPMI-1640, trypan blue. Parke Davis & Co., Pontypool: sodium meclofenamate. Recombinant IL-1α was a gift from Dr A. Sedgwick, Roche, Welwyn, BWA4C (*N*-(3-phenoxycinnamyl)-acetohydroxamic acid) and L-651,392 (4-bromo-2,7-dimethoxy-3H-phenothiazin-3-one) were gifts from Wellcome Research Laboratories, Beckenham and Merk, Sharp & Dohme, Hoddesdon respectively. RHC 80267 was a gift from Dr C.A. Sutherland, Revlon Health Care, N.Y., U.S.A. R59022 was a gift from Janssen Pharmaceutica, Belgium. All other general reagents were of Analar or equivalent quality.

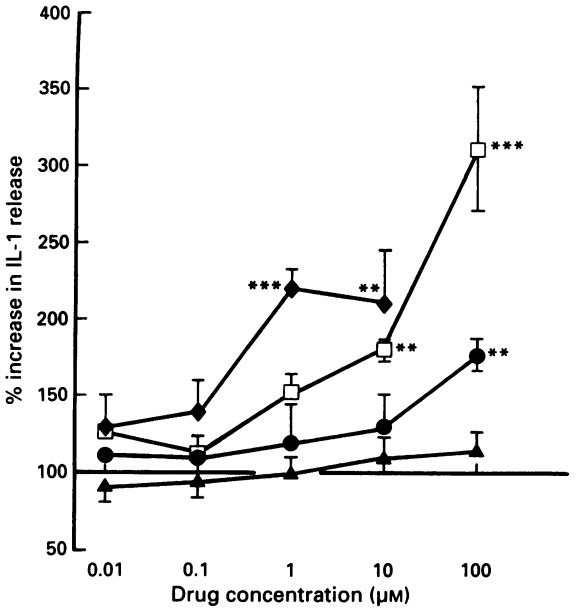


Figure 1 The effect of non-steroidal anti-inflammatory drugs on the release of interleukin-1 (IL-1)-like activity from mouse peritoneal macrophages: (□) indomethacin; (●) piroxicam; (◆) sodium meclofenamate; (▲) aspirin. The data are the means ± s.e.mean from 4 separate experiments where the release of IL-1 is expressed as a percentage of the value obtained when macrophages were stimulated with LPS, 1 μg ml^{-1} alone (control) which was equivalent to 20 ± 5 absorbance units. Significant differences from control are denoted: $^{**}P < 0.01$; $^{***}P < 0.001$.

Results

Initial experiments showed that LPS, 1 μg ml^{-1} stimulated the release of IL-1-like activity from mouse macrophages. The amount of IL-1-like activity (with 95% confidence intervals) released into the supernatant rose from a basal level of 10 pg ml^{-1} (1–35), ($n = 6$) to 300 pg ml^{-1} (95–600) following LPS stimulation ($n = 6$). The basal release of IL-1-like activity probably results from trace amounts of LPS present in the culture media and adherence of the cells to the tissue culture plate. For all subsequent experiments, the levels of IL-1-like activity generated were not expressed in pg ml^{-1} but are shown as an activity relative to that generated by cells treated with LPS, 1 μg ml^{-1} alone. Figure 1 shows concentration-response curves for the potentiation by four NSAIDs of LPS-induced release of IL-1-like activity from resident peritoneal macrophages of the mouse. Piroxicam, 100 μM, indomethacin, 10 and 100 μM and sodium meclofenamate, 1 and 10 μM all potentiated the release of LPS-induced IL-1-like activity. Aspirin up to 100 μM was without effect. The order of potency of the drugs for the potentiation of LPS-induced release of IL-1-like activity was: sodium meclofenamate > indomethacin > piroxicam, but the greatest effect was seen with indomethacin 100 μM. None of the NSAIDs used released detectable IL-1-like activity in the absence of LPS (data not shown). The concentrations of NSAIDs used did not have cytotoxic effects on macrophages, as judged by the ability of the cells to exclude trypan blue, by the ability of the cells to convert MTT (a marker of intact mitochrondrial metabolic activity) and by morphological examination.

Figure 2 shows the inhibition by four NSAIDs of LPS-induced PGE_2 generation by mouse peritoneal macrophages. All four NSAIDs inhibited PGE_2 generation induced by LPS. Total inhibition of PGE_2 generation was achieved with aspirin 100 μM, indomethacin, 1 μM, piroxicam, 10 μM and sodium meclofenamate, 0.1 μM.

Figure 3 shows the effect of adding exogenous PGE_2, 10 ng ml^{-1} on LPS-induced release of IL-1-like activity from mouse peritoneal macrophages in the presence of potentiating concentrations of three NSAIDs. The potentiation of LPS-induced release of IL-1-like activity by indomethacin, 100 μM, piroxicam, 100 μM and sodium meclofenamate,

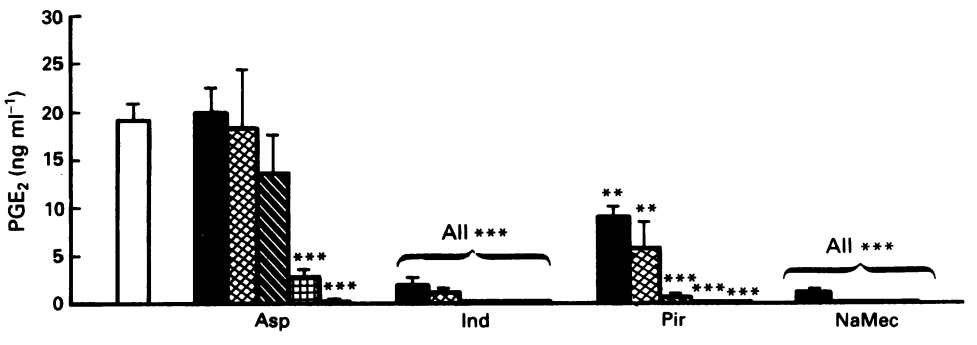


Figure 2 The effect of non-steroidal anti-inflammatory drugs on prostaglandin E_2 (PGE_2) synthesis by mouse peritoneal macrophages stimulated with LPS, 1 μg ml^{-1}. LPS, 1 μg ml^{-1} alone □; LPS 1 μg ml^{-1} with NSAID (aspirin, Asp; indomethacin, Ind; piroxicam, Pir; sodium meclofenamate, Na Mec) at a concentration of 10 nM (■), 100 nM (▩), 1 μM (▧), 10 μM (▦), 100 μM (▨). The data are the means ± s.e. mean from 4 separate experiments. Significant inhibition is shown as: $^{**}P < 0.01$, $^{***}P < 0.001$.

10 μM was reversed, in each case, by the addition of exogenous PGE_2.

Initial experiments showed that LPS, 1 μg ml^{-1} stimulated the accumulation of cell-associated IL-1-like activity in mouse macrophages. The amount of IL-1-like activity (with 95% confidence intervals) associated with the disrupted cell suspension rose from a basal level of 55 pg ml^{-1} (20–65), (n = 6) to 950 pg ml^{-1} (480–1500) following LPS stimulation (n = 6). Figure 4 shows the concentration-response relationships for four NSAIDs on cell-associated IL-1-like activity induced by LPS, 1 μg ml^{-1}. Sodium meclofenamate, 0.01 to 10 μM, piroxicam, 1 to 100 μM, indomethacin, 0.1 to 100 μM and aspirin, 100 μM, all potentiated LPS-induced cell-associated IL-1-like activity in mouse peritoneal macrophages. The order of potency for this effect of the NSAIDs on LPS-induced cell-associated IL-1-like activity was: sodium meclofenamate > indomethacin > piroxicam > aspirin. None of the NSAIDs used had any effect on cell-associated IL-1-like activity in the absence of the LPS stimulus (data not shown). For indomethacin, piroxicam and sodium meclofenamate, there was a reversal of the potentiation of cell-associated IL-1-like activity at the highest concentration used of each drug (Figure 4).

Figure 5 shows that the addition of exogenous PGE_2 2 to 30 ng ml^{-1} caused a concentration-dependent inhibition of the potentiation by indomethacin (1 μM) and sodium meclofenamate (0.1 μM) of LPS-induced cell-associated IL-1 in mouse macrophages.

The effect of two selective 5-lipoxygenase inhibitors, BWA4C (Tateson et al., 1988) and L-651,392 (Guindon et al., 1987) was examined on the released and cell-associated IL-1-like activity stimulated by LPS, 1 μg ml^{-1} in the presence of indomethacin, 1 μM. Neither of the 5-lipoxygenase inhibitors, 0.01 to 10 μM had any effect on released or cell-associated IL-1-like activity under these conditions. In addition the two 5-lipoxygenase inhibitors, at the same concentrations, did not cause any change in LPS-stimulated release of IL-1-like activity or the level of cell-associated IL-1-like activity in the absence of NSAIDs (data not shown).

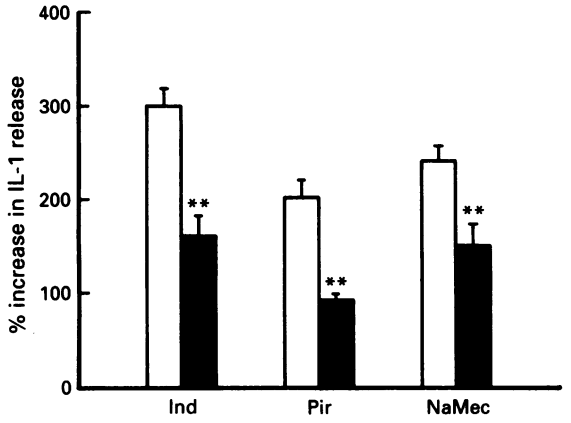


Figure 3 The effect of exogenous prostaglandin E_2 (PGE_2) on the potentiation by non-steroidal anti-inflammatory drugs of LPS-induced IL-1 release from mouse peritoneal macrophages. The data are the means ± s.e.mean from 3 separate experiments. Open columns, NSAID alone; solid columns NSAID + PGE_2, 10 ng ml^{-1}. The responses are expressed as a percentage of the IL-1 released by LPS, 1 μg ml^{-1} alone which was equivalent to 23 + 11 absorance units. Significant effect of PGE_2 is denoted. **P < 0.01, Ind, indomethacin; Pir, piroxicam; Na Mec, sodium meclofenamate.

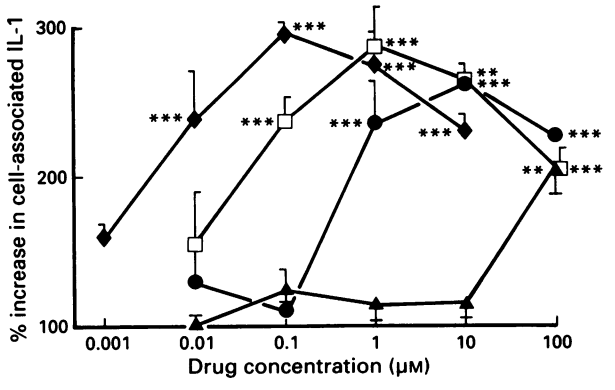


Figure 4 The effect of non-steroidal anti-inflammatory drugs: indomethacin; piroxicam; sodium meclofenamate; aspirin, on cell-associated interleukin-1 (IL-1) in mouse peritoneal macrophages stimulated with LPS, 1 μg ml^{-1}: (◆) sodium meclofenamate; (□) indomethacin; (●) piroxicam; (▲) aspirin. The data are the means ± s.e.mean from 4 separate experiments where the IL-1 associated with the cell has been expressed as a percentage of the amount of IL-1 associated with cells treated with LPS 1 μg ml^{-1} alone (control) which was equivalent to 19 ± 7 absorbance units. Significant differences from control are denoted: **P < 0.01, ***P < 0.001.

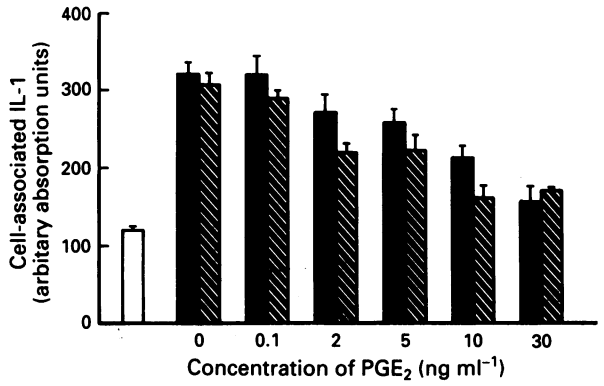


Figure 5 The effect of adding exogenous prostaglandin E_2 (PGE_2) on the cell-associated IL-1 in mouse macrophages stimulated with LPS 1 μg ml^{-1} in the presence indomethacin, 1 μM or sodium meclofenamate, 0.1 μM. Open columns LPS, 1 μg ml^{-1} alone; solid columns indomethacin, 1 μM + LPS, 1 μg ml^{-1} hatched columns sodium meclofenamate, 0.1 μM + LPS, 1 μg ml^{-1}. The data are the means ± s.e.mean from 4 separate experiments.

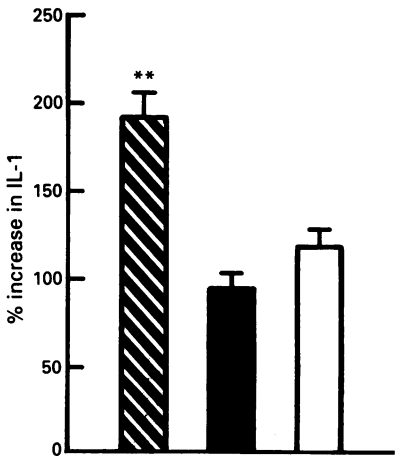


Figure 6 The effect of inhibitors of diacylglycerol kinase (R 59022, 10 μM), diacylglycerol lipase (RHC 80267, 10 μM) and indomethacin (100 μM) on IL-1 release from mouse macrophages stimulated with the synthetic diacylglycerol, DiC_8, 100 μM. Hatched column R59022, 10 μM + DiC_8 100 μM; solid column, RHC 80276, 10 μM + DiC_8, 100 μM; open column, indomethacin, 100 μM + DiC_8, 100 μM. The data are the means ± s.e.mean from 3 separate experiments. The responses have been expressed as a percentage of the IL-1 produced by DiC_8, 100 μM alone (control) which was equivalent to 27 + 9 absorbance units. Significant difference from control is denoted: **P < 0.01.

The synthetic diacylglycerol, DiC_8, 10 to 200 μM did not stimulate release of IL-1-like activity from mouse macrophages. However, in the presence of the diacylglycerol kinase inhibitor, R59022 (6-[2-[4-[(4-fluorophenyl)phenylmethylene]-1-piperidinyl]ethyl]-7-methyl-5H-thiazolo[3,2-α]pyrimidin-5-one) (De Chaffoy de Courcelles *et al.*, 1985), 10 μM, DiC_8 stimulated the release of IL-1-like activity. The diacylglycerol lipase inibitor, RHC 80267 (1,6-di (*o*-(carbamoyl)cyclohexanone oxime)hexane) (Sutherland & Amin, 1982), 10 μM was without effect. Indomethacin, 100 μM failed to enhance the action of DiC_8 on the release of IL-1-like activity from mouse macrophages (Figure 6).

Discussion

Although the bioassay used does not distinguish between the activity of IL-1α and IL-1β, the data presented in this paper demonstrate that NSAIDs produce a concentration-dependent potentiation of both released and cell-associated IL-1-like activity in resident peritoneal macrophages of the mouse stimulated by LPS. There are, however, important differences between the effects of the four NSAIDs on cell-associated and released IL-1-like activity from these cells. The potentiation of LPS-induced cell-associated IL-1-like activity was found to be a property of all four NSAIDs, including aspirin and it occurred at the same concentrations of the drugs which also inhibited PGE_2 generation by the macrophages. In contrast, the potentiation of LPS-induced release of IL-1-like activity was observed for only indomethacin, piroxicam and sodium meclofenamate: aspirin was without effect at the highest concentration tested (100 μM). Moreover, the potentiation of the release of IL-1-like activity occurred only at concentrations of the NSAIDs which were clearly in excess of the minimum concentration required to inhibit totally PGE_2 generation by the cells.

The potentiation of cell-associated IL-1-like activity induced by LPS stimulation appears to be related to the ability of the NSAIDs to inhibit PGE_2 synthesis in the cells. We draw this conclusion because the addition of exogenous PGE_2 causes a concentration-dependent inhibition of cell-associated IL-1-like activity in the presence of LPS and NSAIDs. Furthermore, the concentrations of NSAIDs which cause potentiation of LPS-induced IL-1-like activity are the same as those which inhibit PGE_2 synthesis in these macrophages, with the maximum potentiation of cell-associated IL-1-like activity occurring at the NSAID concentrations which are those minimally required to abolish PGE_2 synthesis. This conclusion is also consistent with data which show that PGE_2 can inhibit the translation of mRNA for IL-1 (Knudsen *et al.*, 1986).

In contrast to the action of the NSAIDs on LPS-induced cell-associated IL-1-like activity, the LPS-induced release of IL-1-like activity from the macrophages is potentiated by concentrations of NSAIDs which are in excess of those which just abolish PGE_2 synthesis. It is also worth pointing out that at these higher concentrations, the potentiation of LPS-induced cell-associated IL-1-like activity is reversed. Nevertheless, the potentiation of LPS-induced release of IL-1-like activity caused by higher concentrations of NSAIDs, whilst it may be independent of PGE_2 synthesis, is reversed by the addition of exogenous PGE_2.

We propose, therefore, that NSAIDs have two different actions on mouse peritoneal macrophages. First, inhibition of cyclo-oxygenase by the NSAIDs reduces the synthesis of PGE_2 and this removes a negative feedback signal on the translation of the mRNA for IL-1 and hence there is potentiation of cell-associated IL-1. Second, an effect of NSAIDs independent of the inhibition of cyclo-oxygenase appears to be responsible for the potentiation of LPS-induced release of IL-1 from the cell. It has been shown that concentrations of indomethacin higher than those required to inhibit prostaglandin production potentiate the release of superoxide from stimulated human neutrophils (Dale & Penfield, 1987). There is evidence that the potentiation of superoxide production by indomethacin is related to the ability of the drug to inhibit diacylglycerol metabolism, leading to a potentiation of protein kinase C activation (Dale & Penfield, 1987; Twomey & Dale, 1992). Using DiC_8, a synthetic diacylglycerol which stimulates protein kinase C, we have shown that provided the metabolism of DiC_8 is inhibited by blocking diacylglycerol kinase with R59022 (DeChaffoy de Courcelles *et al.*, 1985), then the release of IL-1-like activity is increased. However, we could find no evidence that indomethacin might be acting as an inhibitor of diacylglycerol metabolism in its effect on LPS-stimulated release of IL-1-like activity from mouse macrophages.

In this paper, we considered the possibility that the higher concentrations of NSAIDs might cause substrate diversion to 5-lipoxygenase and that the potentiation of IL-1 release might be caused by a product of 5-lipoxygenase activity. Alternatively, a 5-lipoxygenase product might normally down-regulate IL-1 release and the high concentrations of NSAIDs might remove this down-regulation by inhibiting 5-lipoxygenase. Two selective 5-lipoxygenase inhibitors, BWA4C and L-651,392 did not change indomethacin-induced potentiation of LPS-stimulated cell-associated or released IL-1-like activity. Moreover, these two 5-lipoxygenase inhibitors did not change the cell-associated or released IL-1-like activity from LPS-stimulated cells in the absence of indomethacin. It seems unlikely that 5-lipoxygenase products are involved in the NSAID-induced potentiation of IL-1 release from LPS-stimulated mouse peritoneal macrophages. Indeed, Parkar *et al.* (1990) have shown that leukotrienes are not involved in regulating IL-1 secretion from activated macrophages, but that study did not examine the role of leukotrienes on cell-associated IL-1.

The biological role of IL-1 that accumulates within cells is still uncertain; some authors have suggested that it may be involved in antigen presentation and activation of T-cells (Unanue *et al.*, 1987). NSAIDs by inhibiting the production of prostaglandins which serve to down-regulate IL-1 mRNA translation could potentiate the production of cell-associated IL-1 at inflammatory sites. Although the cyclo-oxygenase-independent action of the NSAIDs on mouse macrophages occurs over higher concentration-ranges, these concentrations may well have some significance *in vivo*. In one study of arthritic patients, a single dose of 50 mg of indomethacin produced a free plasma concentration of the drug of 1 to 8 μM (Emori *et al.*, 1973). In another study, a dose of 25 mg of indomethacin gave plasma concentrations of 1.5 to 8.5 μM (Hvidberg *et al.*, 1972). In practice, many patients with arthritis have to be given single doses of indomethacin up to 300 mg. From our data, it is clear that concentrations which can be achieved therapeutically can potentiate LPS-stimulated release of IL-1-like activity in the mouse peritoneal macrophage.

We are grateful to the Emily Le Rossignol Fund, University College London for financial support A.K.B. was in receipt of an M.R.C. Award for Training in Research Methods.

References

BEUSCHER, H.U. & COTTON, H.R. (1988). Structure and function of membrane IL-1. *Mol. Immunol.*, **25**, 1189–1199.

BEUSCHER, H.U., GUNTHER, C. & ROLLINGHOFF, M. (1990). IL-1β is secreted by activated murine macrophages as biologically inactive precursor. *J. Immunol.*, **144**, 2179–2183.

BRANDWEIN, S.R. (1986). Regulation of interleukin-1 production by mouse peritoneal macrophages. *J. Biol. Chem.*, **261**, 8624–8632.

CONLON, P.J., GRABSTEIN, K.H., ALPERT, A., PRICKETT, K.S., ITOP, T.P. & GILLIS, S. (1987). Localisation of mononuclear cell interleukin-1. *J. Immunol.*, **139**, 98–102.

DALE, M.M. & PENFIELD, A. (1987). Comparison of the effects of indomethacin, RHC80267 and RO59022 on superoxide production by 1-oleoyl,2-acetyl glycerol and A23187 in human neutrophils. *Br. J. Pharmacol.*, **92**, 63–68.

DE CHAFFOY DE COURCELLES, D., ROEVENS, P. & VAN DELL, H. (1985). R 59022 a diacylglycerol kinase inhibitor. *J. Biol. Chem.*, **260**, 15762–15770.

DINARELLO, C.A. (1989). Interleukin-1 and its biologically related cytokines. *Adv. Immunol.*, **48**, 153–205.

EDEN, E. & TURINO, G.M. (1986). Secretion of interleukin-1/leucocytic pyrogen from endotoxin-stimulated human alveolar macrophages is unaffected by indomethacin. *Immunopharmacol.*, **12**, 81–88.

EMORI, H.W., CHAMPION, G.D., BLUESTONE, R. & PAULUS, H.E. (1973). Simultaneous pharmacokinetics of indomethacin in serum and synovial fluid. *Ann. Rheum. Dis.*, **32**, 433–435.

GEARING, A.J., BIRD, C.R., BRISTOW, A., POOLE, S. & THORPE, R. (1987). A simple sensitive assay for interleukin-1 which is responsive to 10(3) U/ml of interleukin-2. *J. Immunol. Methods*, **99**, 7–11.

GUINDON, Y., GIRARD, Y., MAYCOCK, A., FORD-HUTCHINSON, A.W., ATKINSON, J.G., BELANGER, P.C., DALLOB, A., DOUGHERTTY, H. & EGAN, R. (1987). L-651,392: a novel potent and selective 5-lipoxygenase inhibitor. *Adv. Prostaglandin Thrombox. Leukotriene Res.*, **17A**, 554–557.

HAZUDA, D.J., LEE, J.C. & YOUNG, P.R. (1988). The kinetics of interleukin-1 secretion from activated monocytes. *J. Biol. Chem.*, **263**, 8473–8479.

HAZUDA, D.J., STRICKLER, J., KUEPPERS, F., SIMON, P.L. & YOUNG, P.R. (1990). Processing of precursor interleukin-1β and inflammatory disease. *J. Biol. Chem.*, **265**, 6318–6322.

HVIDBERG, E., LAUSEN, H.H. & JANSEN, J.A. (1972). Indomethacin: plasma concentrations and protein binding in man. *Eur. J. Clin. Pharmacol.*, **4**, 119–124.

KALBHEN, D.A. (1982). The inhibitory effects of steroidal and non-steroidal antirheumatic drugs on articular cartilage in osteoarthritis and its counteraction by a biological GAGA-peptide complex. *Z. Rheumatol.*, **41**, 202–211.

KNUDSEN, P.J., DINARELLO, C.A. & STROM, T.B. (1986). Prostaglandins posttranscriptionally inhibit monocyte expression of interleukin-1 activity by increasing intracellular cyclic adenosine monophosphate. *J. Immunol.*, **137**, 3189–3194.

KUNKEL, S.L., CHENSUE, S.W. & PHAN, S.H. (1986). Prostaglandins as endogenous mediators of interleukin-1 production. *J. Immunol.*, **136**, 186–192.

KURT-JONES, E.A., BELLER, D.I., MIZEL, S.B. & UNANUE, E.R. (1985a). Identification of a membrane associated IL-1 in macrophages. *Proc. Natl. Acad. Sci. U.S.A.*, **82**, 1204–1208.

KURT-JONES, E.A., KIELY, J. & UNANUE, E.R. (1985b). Conditions required for expression of membrane IL-1 on B cells. *J. Immunol.*, **135**, 1548–1550.

KURT-JONES, E.A., VIRGIN, H.W., UNANUE, I.V. & UNANUE, E.R. (1986). In vivo and in vitro expression of macrophage membrane IL-1 in response to soluble and particulate stimuli. *J. Immunol.*, **137**, 10–14.

LEWIS, G.P. & BARRETT, M.L. (1986). Immunosuppressive actions of prostaglandins and the possible increase in chronic inflammation after cyclo-oxygenase inhibitors. *Agents Actions*, **19**, 59–65.

MAIER, R. & WILHELMI, G. (1983). Evaluierung der wirkung von Analgetika/Antiphlogistika auf die Progredienz der spontenat der C57-black-Maus. *Z. Rheumatol.*, **42**, 232–234.

MOSLEY, B., DOWER, S.K., GILLIS, S. & COSMAN, D. (1987). Determination of the minimum polypeptide lengths of the functionally active sites of human interleukins 1 alpha and 1 beta. *Proc. Natl. Acad. Sci. U.S.A.*, **84**, 4572–4576.

NEWMAN, N.M. & LING, R.S.M. (1985). Acetabular bone destruction related to non-steroidal anti-inflammatory drugs. *Lancet*, **ii**, 11–13.

OPPENHEIM, J.J., KOOPMAN, W.J., WAHL, L.M. & DOUGHERTY, S.F. (1980). Prostaglandin E_2 rather than lymphocyte activating factor produced by activated human mononuclear cells stimulates increases in murine thymocyte cAMP. *Cell. Immunol.*, **49**, 64–73.

OTTERNESS, I.G., BLIVEN, M.L., ESKRA, J.D., REINKE, M. & HANSON, D.C. (1988). The pharmacologic regulation of interleukin-1 production: the role of prostaglandins. *Cell. Immunol.*, **114**, 385–397.

PARKAR, B.A., MCCORMICK, M.E. & FOSTER, S.J. (1990). Leukotrienes do not regulate interleukin-1 production by activated macrophages. *Biochem. Biophys. Res. Commun.*, **169**, 422–429.

PHADKE, K., CARLSON, D.G., GITER, B.D. & BUTLER, L.D. (1986). Role of interleukin 1 and interleukin 2 in rat and mouse arthritis models. *J. Immunol.*, **136**, 4085–4091.

RASHAD, S., REVELL, P., HEMINGWAY, A., LOW, F., RAINSFORD, K. & WALKER, F. (1989). Effect of non-steroidal anti-inflammatory drugs on the course of osteoarthritis. *Lancet*, **ii**, 519–521.

RAUD, J., DALHEN, S. & HEDQUIST, O. (1987). Prostaglandin E_2 reverses indomethacin-induced enhancement of acute allergic inflammation in the hamster cheek pouch. *Adv. Prostaglandin Thrombox. Leukotriene Res.*, **17**, 908–912.

SANDBORG, C.I., BERMAN, M.A., ANDREWS, B.S. & FRIOU, G.J. (1986). Increased production of an interleukin-1 (IL-1) inhibitor with fibroblast stimulating activity by mononuclear cells from patients with scleroderma. *Clin. Exp. Immunol.*, **66**, 312–319.

SUTHERLAND, C.A. & AMIN, D. (1982). Relative activities of rat and dog platelet phospholipase A_2 and diglyceride lipase. *J. Biol. Chem.*, **257**, 14006–14010.

TADA, H., SHIHO, O., KUROSHIMA, K., KOYAMA, M. & TSUKAMOTO, K. (1986). An improved colorimetric assay for interleukin-2. *J. Immunol. Methods*, **93**, 157–165.

TATESON, J.E., RANDALL, R.W., REYNOLDS, C.H., JACKSON, W.P., BHATTACCHERJEE, P., SALMON, J.A. & GARLAND, L.G. (1988). Selective inhibition of arachidonate 5-lipoxygenase by novel acetohydroxamic acids: biochemical assessment *in vitro* and *ex vivo*. *Br. J. Pharmacol.*, **94**, 528–539.

THORNBERRY, N.A., BULL, H.G., CALAYCAY, J.R., CHAPMAN, K.T., HOWARD, A.D., KOSTURA, M.J., MILLER, D.K., MOLINEAUX, S.M., WEIDNER, J.R., AUNINS, J., ELLISTON, K.O., AYALA, J.M., CASANO, F.J., CHIN, J., DING, G.J.-F., EGGER, L.A., GAFFNEY, E.P., LIMJUCO, G., PALYHA, O.C., RAJU, S.M., ROLANDO, A.M., SALLEY, J.P., YAMIN, T.-T., LEE, T.D., SHIVELY, J.E., MACCROSS, M., MUMFORD, R.A., SCHMIDT, J.A. & TOCCI, M.J. (1992). A novel hetrodimeric cysteine protease is required for interleukin-1β processing in monocytes. *Nature*, **356**, 768–774.

TWOMEY, B.M. & DALE, M.M. (1992). Cyclooxygenase-independent effects of non-steroidal anti-inflammatory drugs on the neutrophil respiratory burst. *Biochem. Pharmacol.*, **43**, 413–418.

TWOMEY, B.M., MUID, R.E. & DALE, M.M. (1989). The potentiation of human neutrophil superoxide generation by sodium meclofenamate. *Br. J. Pharmacol.*, **98**, 671P.

UNANUE, E.R., WEAVER, C.T., FULBRIGGE, R.C., KIELY, J.M. & CHAPLIN, D.D. (1987). Membrane IL-1: a key protein in antigen presentation. *Ann. Inst. Pasteur Immunol.*, **138**, 489–492.

(Received February 23, 1994
Revised July 7, 1994
Accepted July 11, 1994)

Br. J. Pharmacol. (1994), **113**, 815–822 © Macmillan Press Ltd, 1994

Evidence for P_2-purinoceptor-mediated inhibition of noradrenaline release in rat brain cortex

[1]Ivar von Kügelgen, Leni Späth & Klaus Starke

Pharmakologisches Institut, Hermann-Herder-Strasse 5, D-79104 Freiburg i. Br., Germany

1 Some postganglionic sympathetic axons possess P_{2Y}-like P_2-purinoceptors which, when activated, decrease the release of noradrenaline. We examined the question of whether such receptors also occur at the noradrenergic axons in the rat brain cortex. Slices of the brain cortex were preincubated with [^{3}H]-noradrenaline, then superfused with medium containing desipramine (1 μM) and stimulated electrically, in most experiments by trains of 4 pulses/100 Hz.

2 The selective adenosine A_1-receptor agonist, N^6-cyclopentyl-adenosine (CPA; 0.03–3 μM) as well as the non-subtype-selective agonist 5'-N-ethylcarboxamido-adenosine (NECA; 0.3–3 μM) reduced the evoked overflow of tritium, whereas the adenosine A_{2a}-receptor agonist, 2-*p*-(2-carbonylethyl)-phenethylamino-5'-N-ethylcarboxamido-adenosine (CGS-21680; 0.003–30 μM) and the adenosine A_3-receptor agonist N^6-2-(4-aminophenyl)ethyl-adenosine (APNEA; 0.03–3 μM) caused no change. Of the nucleotides tested, ATP (30–300 μM), adenosine-5'-O-(3-thiotriphosphate) (ATPγS; 30–300 μM), adenosine-5'-O-(2-thiodiphosphate) (ADPβS; 30–300 μM), P_1,P_4-di(adenosine-5')-tetraphosphate (Ap_4A; 30–300 μM) and the preferential P_{2Y}-purinoceptor agonist, 2-methylthio-ATP (300 μM) decreased the evoked overflow of tritium. The P_{2X}-purinoceptor agonist, α,β-methylene-ATP (3–300 μM) caused no change.

3 The A_1-selective antagonist, 8-cyclopentyl-1,3-dipropylxanthine (DPCPX; 10 nM) attenuated the effects of the nucleosides CPA (apparent pK_B value 9.8) and NECA as well as of the nucleotides ATP (apparent pK_B 9.3), ATPγS (apparent pK_B 9.2) and ADPβS (apparent pK_B 8.7). CGS-21680 and APNEA were ineffective also in the presence of DPCPX. The A_2-selective antagonist 1,3-dipropyl-8-(3,4-dimethoxystyryl)-7-methylxanthine (KF-17837) reduced the effects of CPA, NECA and ATPγS only when given at a concentration of 300 nM but not at 10 nM.

4 The P_2-purinoceptor antagonists, suramin (300 μM), reactive blue 2 (30 μM) and cibacron blue 3GA (30 μM) did not change the effect of CPA. Suramin and cibacron blue 3GA shifted the concentration-response curve of ATPγS to the right (apparent pK_B values 3.7 and 5.0, respectively). Reactive blue 2 also attenuated the effect of ATPγS, and cibacron blue 3GA attenuated the effect of ATP, but in these cases the agonist concentration-response curves were not shifted to the right. There was no antagonistic effect of suramin against ATP and ADPβS.

5 The results indicate that rat cerebrocortical noradrenergic axons possess, in addition to the known adenosine A_1-receptor, a separate purinoceptor for nucleotides (P_2) which, in contrast to the A_1-receptor, is blocked by suramin, reactive blue 2 and cibacron blue 3GA. Nucleotides such as ATP and ATPγS activate both receptors. Inconsistencies in antagonist effects against nucleotides are probably due to this activation of two receptors. The presynaptic P_2-purinoceptor is P_{2Y}-like, as it is in the peripheral sympathetic nervous system.

Keywords: Rat brain cortex; P_1-purinoceptor; P_2-purinoceptor; presynaptic purinoceptors; noradrenaline release; adenine nucleotides; adenosine 5'-O-(3-thiotriphosphate) (ATPγS); suramin; reactive blue 2; cibacron blue 3GA

Introduction

ATP inhibits the release of noradrenaline in dog subcutaneous adipose tissue (Fredholm, 1974), and adenosine inhibits the release of noradrenaline in rabbit kidney, guinea-pig vas deferens and, again, dog subcutaneous adipose tissue (Hedqvist & Fredholm, 1976). Since these initial observations, our knowledge of the presynaptic modulation of noradrenaline release by nucleosides and nucleotides has become complex, for two main reasons. First, nucleotides can act both as such and after dephosphorylation. Second, there are several presynaptic sites of action: (i) Presynaptic inhibition through adenosine receptors (P_1-purinoceptors) of the A_1 subtype is widespread (see Stone, 1981; Fredholm & Dunwiddie, 1988). Nucleotides also may produce inhibition through these receptors, both directly (Lukacsko & Blumberg, 1982; von Kügelgen *et al.*, 1989; 1992a; Fuder & Muth, 1993; Kurz *et al.*, 1993) and after breakdown to adenosine (e.g., De Mey *et al.*, 1979). (ii) Some noradrenergic terminal axons possess release-enhancing adenosine A_2- in addition to release-inhibiting A_1-receptors (Fuder *et al.*, 1992; Gonçalves & Queiroz, 1993; Rensing *et al.*, 1993). (iii) Presynaptic P_2-purinoceptors, sensitive to nucleotides but not nucleosides, are a third group, found at postganglionic sympathetic axons and mediating mainly inhibition (von Kügelgen *et al.*, 1989; 1993; 1994a; Fuder & Muth, 1993; Kurz *et al.*, 1993; Allgaier *et al.*, 1994; see also Stjärne & Åstrand, 1985), although facilitation of noradrenaline release has also been described (Miyahara & Suzuki, 1987; Sperlagh & Vizi, 1991; Allgaier *et al.*, 1994). (iv) As an alternative it has been suggested that adenosine as well as adenine nucleotides inhibit the release of noradrenaline at a common, novel, presynapatic purinoceptor that the authors call P_3 (Shinozuka *et al.*, 1988; Forsyth *et al.*, 1991; Todorov *et al.*, 1994).

To our knowledge, presynaptic P_2-purinoceptors have never been identified at central noradrenergic (or non-noradrenergic) neurones, despite studies with P_2-selective agonists (Stone & Cusack, 1989; von Kügelgen *et al.*, 1992a; for review see Hoyle & Burnstock, 1991). In a previous investigation we observed that the release of noradrenaline in brain cortex slices from rabbits was reduced through A_1- but

[1] Author for correspondence.

not changed through P_2-purinoceptors (von Kügelgen et al., 1992a). We have now carried out an analogous search in rats. Previous results suggest that rat cerebrocortical noradrenergic axons possess A_1-receptors (Harms et al., 1978; Craig & White, 1992). Reasons for the choice of the rat were the operation of P_2-purinoceptors at peripheral noradrenergic axons of this species (Fuder & Muth, 1993; Kurz et al., 1993; von Kügelgen et al., 1994a) as well as the cell bodies of the cerebrocortical noradrenergic neurones in the locus coeruleus (Tschöpl et al., 1992; Shen & North, 1993). Slices of rat brain cortex were preincubated with [^{3}H]-noradrenaline, and transmitter release was elicited by electric stimulation. Some of these results have been published in abstract form (von Kügelgen et al., 1994b).

Methods

Male Wistar rats weighing 250–300 g (Savo, Kisslegg, Germany) were killed by cervical dislocation and exsanguination. The brain was quickly removed and chilled. Two slabs were cut from the occipito-parietal cortex, parallel to the surface. The superficial slab, 0.2 mm thick, was discarded and round slices of 3.5 m diameter were punched from the second slab, 0.3 mm thick. Six to eight slices were preincubated at 37°C for 30 min in 2 ml medium containing (−)-[^{3}H]-noradrenaline, 0.1 μM. One slice was then transferred to each of six 0.16-ml superfusion chambers where it was held by a polypropylene mesh between platinum wire electrodes, 6 mm apart. The slices were superfused with [^{3}H]-noradrenaline-free medium for 107 min at a rate of 0.6 ml min^{-1} at 37°C. A Stimulator I (Hugo Sachs Elektronik, March-Hugstetten, Germany) operating in the constant voltage mode was used for electrical field stimulation. Three periods of stimulation were applied (rectangular pulses of 2 ms width and 12.5 V cm^{-1}, yielding a current strength of 18 mA). The first stimulation period was delivered after 20 min of superfusion and consisted of 18 pulses at 1 Hz. It was not used for determination of tritium overflow. The following two periods were delivered after 59 (S_1) and 89 (S_2) min of superfusion and consisted of a train of either 4 pulses/100 Hz or 60 pulses/1 Hz (identical parameters at S_1 and S_2 in each single experiment); unless stated otherwise, the parameters were 4 pulses/100 Hz. The collection of successive 3-min superfusate samples began 9 min before S_1. Some drugs (or solvents) were present in the medium throughout superfusion. Other drugs (or solvents) were added before S_2 (6 min before S_2 unless stated otherwise) and kept for the remainder of the experiment; the delay from addition to medium to arrival at tissue was about 60 s. After superfusion, each slice was solubilized in 0.5 ml Soluene-350 (Canberra Packard, Frankfurt am Main, Germany). Tritium was measured in superfusate samples and solubilized slices by liquid scintillation counting.

The medium used for incubation and superfusion contained (mM): NaCl 118, KCl 4.8, $CaCl_2$ 1.3, $MgSO_4$ 1.2, $NaHCO_3$ 25, KH_2PO_4 1.2, glucose 11, ascorbic acid 0.57, disodium EDTA 0.03. It was saturated with 5% CO_2 in O_2. The pH was adjusted to 7.4 with NaOH 1 M. The medium used for superfusion (but not that used for preincubation) contained desipramine 1 μM in order to block uptake$_1$.

The outflow of tritium was expressed as a fractional rate (min^{-1}) and the evoked overflow, obtained by subtraction of the estimated basal outflow, as a percentage of the tritium content of the slice (von Kügelgen et al., 1992a). For further evaluation of basal tritium efflux, ratios were calculated of the fractional rate of outflow in the 3-min interval before S_2 and in the 3-min interval before S_1 (b_2/b_1). For further evaluation of the electrically evoked overflow, ratios were calculated of the overflow elicited by S_2 and the overflow elicited by S_1 (S_2/S_1). S_2/S_1 ratios obtained in individual experiments with a test compound A added before S_2 were calculated as a percentage of the mean S_2/S_1 ratio in the appropriate control group (solvent instead of A). When the interaction of A, added before S_2, and a drug B, added throughout superfusion, was studied, the 'appropriate control' was a group in which B alone was used.

The following drugs were used: suramin hexasodium salt (Bayer, Wuppertal, Germany); (−)-[ring-2,5,6-^{3}H]-noradrenaline, specific activity 1.50 to 2.11 TBq mmol^{-1} (Du Pont, Dreieich, Germany); N^6-2-(4-aminophenyl)ethyl-adenosine (APNEA) (Prof. R.A. Olsson, Dept. of Internal Medicine, University of South Florida, Tampa, Florida, U.S.A.); 2-*p*-(2-carbonylethyl)-phenethylamino-5′-N-ethylcarboxamido-adenosine HCl (CGS-21680), N^6-cyclopentyl-adenosine (CPA), 8-cyclopentyl-1,3-dipropylxanthine (DPCPX), 2-methylthio-adenosine-5′-triphosphate tetrasodium salt (2-methylthio-ATP), reactive blue 2 (R-115 in RBI catalogue 1992-93; Colour Index No. 61211 in Society of Dyers and Colourists, 1971) (Research Biochemicals, Biotrend, Köln, Germany); yohimbine HCl (Roth, Karlsruhe, Germany); adenosine-5′-O-(2-thiodiphosphate) lithium salt (ADPβS), adenosine-5′-O-(3-thiotriphosphate) lithium salt (ATPγS), ATP disodium salt, cibacron blue 3GA (C-9534 in Sigma catalogue 1993; isomer of reactive blue 2 in which the sulphonic acid residue at the terminal benzene ring is in the *o*-position; see footnote on page 130 of von Kügelgen et al., 1994a), desipramine HCl, P_1,P_4-di(adenosine-5′)-tetraphosphate ammonium salt (Ap_4A), 5′-N-ethylcarboxamido-adenosine (NECA), indomethacin, α,β-methylene-adenosine-5′-diphosphate (α,β-methylene-ADP, APCP), α,β-methylene-adenosine-5′-triphosphate lithium salt (α,β-methylene-ATP, APCPP), N^G-nitro-L-arginine, tetrodotoxin (Sigma, Deisenhofen, Germany); 1,3-dipropyl-8-(3,4-dimethoxystyryl)-7-methylxanthine (KF-17837) (Dr F. Suzuki, Kyowa Hakko Kogyo, Pharmaceutical Research Laboratories, Sunto-Gun, Shizuoka-Ken, Japan). Solutions of drugs were prepared with distilled water, or (indomethacin) the KH_2PO_4- and $NaHCO_3$- containing stock solution of the medium, or (APNEA, CGS-21680, DPCPX, KF-17837) dimethyl sulphoxide (final concentration about 0.4 mM), or (CPA) ethanol (final concentration about 3 mM), or (tetrodotoxin) sodium acetate buffer (0.1 M, pH 4.8), or (NECA) tartaric acid (final concentration about 0.1 mM). Solutions of KF-17837 were protected from direct sunlight. Appropriate amounts of the solvents given before S_2 did not change basal tritium efflux or the evoked overflow. Dimethyl sulphoxide was added in all experiments throughout superfusion to make them directly comparable.

Means ± s.e.mean are given throughout. Differences between means were tested for significance by the Mann-Whitney test. $P<0.05$ or lower was taken as the criterion of statistical significance. For multiple comparisons with the same control, P levels were adjusted according to Bonferroni. n is the number of brain slices.

Results

Electrical stimulation by 4 pulses/100 Hz or 60 pulses/1 Hz sharply increased the outflow of tritium from rat brain cortex slices preincubated with [^{3}H]-noradrenaline (as in Figure 1 of Trendelenburg et al., 1993). In the presence of desipramine (1 μM) alone, which was always present throughout superfusion, the overflow elicited by 4 pulses/100 Hz at S_1 averaged 1.641 ± 0.025% of the tritium content of the tissue (corresponding to 96.8 ± 1.6 Bq; b_1, i.e. basal tritium efflux before S_1 was 0.00364 ± 0.00004 min^{-1}; $n = 323$), and the overflow elicited by 60 pulses/1 Hz at S_1 averaged 2.843 ± 0.081% of tissue tritium (b_1 0.00353 ± 0.00013 min^{-1}; $n = 30$). When no additional drug was administered between S_1 and S_2, b_2, i.e. the basal overflow of tritium before S_2, was slightly lower than b_1, and the outflow elicited by S_2 was similar to the overflow at S_1. For example, the control b_2/b_1 ratio for experiments with 4 pulses/100 Hz was 0.91 ± 0.05, and the control S_2/S_1 ratio was 1.02 ± 0.01 (desipramine alone present throughout superfusion; $n = 66$). Trains of 4

pulses/100 Hz were used except in experiments described at the end of the Results section.

Effects of adenine nucleosides and nucleotides

When added 6 min before S_2, the adenine nucleosides and nucleotides tested did not change the basal efflux of tritium (b_2/b_1) except for a slight decrease by CPA 300 nM and ATP 300 μM and a slight increase by Ap_4A 300 μM. As shown in Figure 1a, the selective adenosine A_1-receptor agonist CPA as well as the non-subtype-selective agonist NECA (Williams *et al.*, 1986) reduced the evoked overflow of tritium by about 30% maximally (no true maximum reached in the case of NECA). The selective adenosine A_{2a}-receptor agonist CGS-21680 (Jarvis *et al.*, 1989) and the preferential adenosine A_3-receptor agonist APNEA (Zhou *et al.*, 1992) caused no change (Figure 1a). Of the nucleotides examined, ATP, ATPγS, ADPβS, Ap_4A and the preferential P_{2Y}-purinoceptor agonist 2-methylthio-ATP (Kennedy, 1990; Hoyle & Burnstock, 1991) reduced the evoked overflow (Figure 1b). ATP and its metabolically more stable analogue ATPγS (Welford *et al.*, 1986) were equipotent and at the highest concentration tested, 300 μM, produced greater inhibition (by about 45%) than any other compound of Figure 1. The preferential

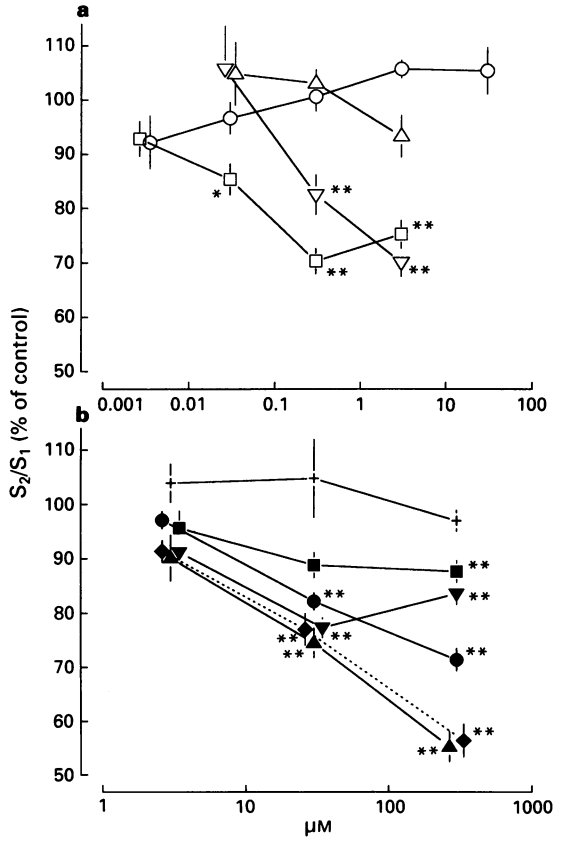


Figure 1 Effects of adenosine analogues (a) and adenine nucleotides (b) on electrically evoked tritium overflow from rat brain cortex slices preincubated with [^{3}H]-noradrenaline. Slices were stimulated twice by 4 pulses/100 Hz (S_1, S_2). N^6-2-(4-aminophenyl)ethyl-adenosine (APNEA, Δ), 2-*p*-(2-carbonylethyl)-phenethylamino-5'-N-ethylcarboxamido-adenosine (CGS-21680, ○), N^6-cyclopentyl-adenosine (CPA, □), 5'-N-ethylcarboxamido-adenosine (NECA, ▽), adenosine 5'-O-(2-thiodiphosphate) (ADPβS, ●), adenosine 5'-O-(3-thiotriphosphate) (ATPγS, ◆), ATP (▲), P_1, P_4-di(adenosine-5')-tetraphosphate (Ap_4A, ▼), α,β-methylene-ATP (+) or 2-methylthio-ATP (■) was added 6 min before S_2 for the remainder of the experiment. Ordinates, evoked tritium overflow: S_2/S_1 ratio obtained in individual tissue slices were calculated as a percentage of the average control (solvent) S_2/S_1 ratio. Means ± s.e.mean of 4–12 experiments. Significant differences from control: $^*P<0.05$ and $^{**}P<0.01$.

P_{2X}-purinoceptor agonist α,β-methylene-ATP (Kennedy, 1990; Hoyle & Burnstock, 1991) caused no change.

ATPγS 30 μM produced a similar decrease, irrespective of whether it was added 6 min (Figure 1b) or 12 min before S_2 (not shown; $n = 4$ for the 12-min experiment).

Interactions

Drugs tested for their interaction with nucleosides and nucleotides were added throughout superfusion (in addition to desipramine). They caused only minimal changes of the basal efflux of tritium (b_1), and only cibacron blue 3GA 30 μM caused a significant change (an increase by 21%) of the overflow evoked by S_1 (not shown). Nucleosides, nucleotides or their solvents were added before S_2. When solvent was administered before S_2, the b_2/b_1 ratio again was slightly below, and the S_2/S_1 ratio close to, unity (not shown).

We first tested the interaction with P_1-purinoceptor antagonists. DPCPX selectively blocks adenosine A_1-receptors (Bruns *et al.*, 1987; Lohse *et al.*, 1987). DPCPX 10 nM shifted the concentration-response curves of CPA, ADPβS, ATP and ATPγS to the right by similar degrees (Figure 2). From the shifts at the level of 15% inhibition, apaprent pK_B values of DPCPX against CPA, ADPβS, ATP and ATPγS of 9.8, 8.7, 9.3 and 9.2, respectively, were calculated (equation No. 4 of Furchgott, 1972). DPCPX 10 nM abolished the inhibition by NECA 0.3 and 3 μM but did not reverse it to an increase in evoked tritium overflow ($n = 6$ and 4, respectively; not shown). CGS-21680 0.3 and 30 μM and APNEA 3 μM were ineffective in the presence of DPCPX ($n = 4$ or 5; not shown) as they had been in the absence of the A_1 antagonist (Figure 1a).

KF-17837 is a P_1-purinoceptor antagonist which preferentially blocks the adenosine A_2-receptor (Shimada *et al.*, 1992; Jackson *et al.*, 1993). At a concentration of 10 nM, it failed to antagonize CPA 0.3 μM, NECA 0.3 μM and ATPγS 30 μM ($n = 4–7$; not shown). KF-17837 300 nM, however, significantly attenuated the effects of CPA 0.3 μM (S_2/S_1 ratio 85.4 ± 6.8% of control; $n = 6$) and ATPγS 30 μM (S_2/S_1 90.5 ± 4.5% of control; $n = 6$) and abolished the effect of NECA 0.3 μM on the evoked overflow of tritium ($n = 5$; not shown).

Antagonists at P_2-purinoceptors were the second group of drugs studied for their interaction with nucleosides and nucleotides. The non-subtype-selective P_2 antagonist, suramin (Dunn & Blakeley, 1988), when added throughout superfusion at a concentration of 300 μM, did not change the inhibitory effects of CPA, ADPβS and ATP but caused a small shift to the right of the concentration-response curve of ATPγS (Figure 3). The shift at the level of 25% inhibition corresponded to an apparent pK_B value of suramin against ATPγS of 3.7.

Reactive blue 2 is a preferential antagonist at P_{2Y}-purinoceptors (Burnstock & Warland, 1987; Houston *et al.*, 1987). Reactive blue 30 μM did not change the inhibition by CPA but attenuated the inhibition by ATPγS, 300 μM (Figure 4).

Selective antagonism against nucleotides was also observed with cibacron blue 3GA, an isomer of reactive blue 2 and also P_{2Y}-selective (e.g., Shirahase *et al.*, 1991; Boland *et al.*, 1992; for the nomenclature of reactive blue 2 and cibacron blue 3GA see footnote on p. 130 of von Kügelgen *et al.*, 1994a). Cibacron blue 3GA 30 μM left the effect of CPA unchanged, tended to reduce the effect of ADPβS, reduced significantly the effect of ATP 300 μM, and shifted the concentration-response curve of ATPγS to the right (Figure 5). The shift at the level of 25% inhibition corresponded to an apparent pK_B value of cibacron blue 3GA against ATPγS of 5.0.

The combination of cibacron blue 3GA (30 μM) with DPCPX (10 nM) was also tested. The mixture shifted the concentration-response curve of ATPγS beyond the antagonism caused by DPCPX alone (Figure 2d) and cibacron blue 3GA alone (Figure 5d). The shift beyond that produced

by DPCPX alone (Figure 2d), when read at the level of 10% inhibition, yielded an apparent pK_B for cibacron blue 3GA of 5.1, similar to the 5.0 value obtained in the absence of DPCPX (preceding paragraph).

In search for possible mediators of the inhibition by adenine nucleotides, ATPγS was administered in the combined presence of indomethacin and N^G-nitro-L-arginine which were added throughout superfusion at concentrations (10 μM each) known to block the synthesis of prostaglandins (Starke *et al.*, 1977) and nitric oxide (Knowles *et al.*, 1990), respectively. The inhibition by ATPγS 30 μM remained unchanged ($n = 5$; not shown).

The inhibitor of 5'-nucleotidase α,β-methylene-ADP, given throughout superfusion at a concentration (100 μM) blocking the breakdown of AMP to adenosine (Bruns, 1980; see also Cunha *et al.*, 1994), did not change the effect of ATPγS 30 and 300 μM ($n = 6$ and 7; not shown). When both α,β-methylene-ADP and cibacron blue 3GA 30 μM were present throughout superfusion, the concentration-response curve of ATPγS was shifted to the right to the same extent (see Figure 5d) as by cibacron blue 3GA alone ($n = 5$ per ATPγS concentration; not shown).

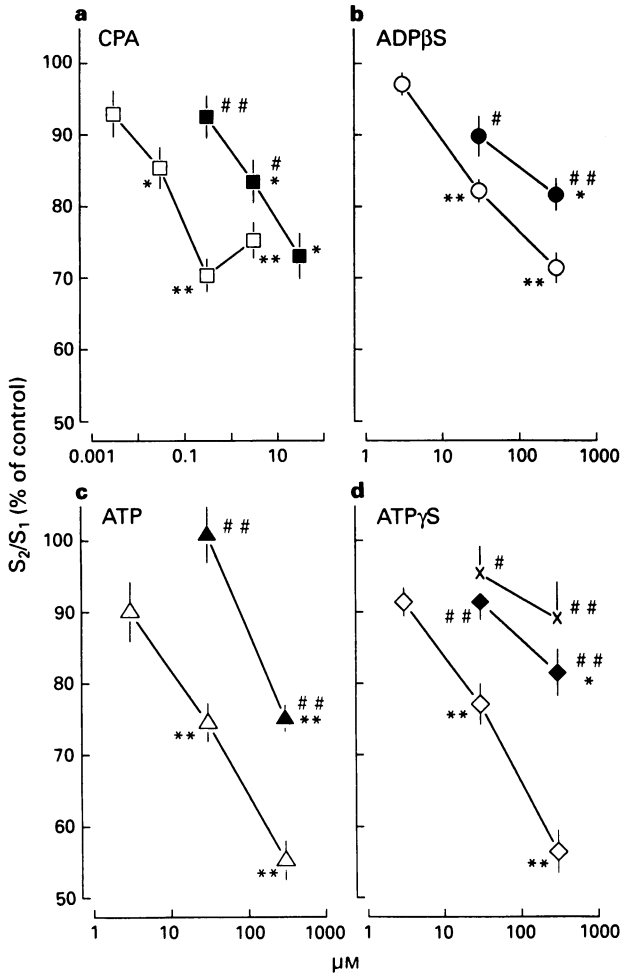


Figure 2 Interaction of purinoceptor agonists with 8-cyclopentyl-1,3-dipropylxanthine (DPCPX) or cibacron blue 3GA combined with DPCPX. Slices were stimulated twice by 4 pulses/100 Hz (S_1, S_2).N^6-cyclopentyl-adenosine (CPA, a), adenosine 5'-O-(2-thiodiphosphate) (ADPβS, b), ATP (c) or adenosine 5'-O-(3-thiotriphosphate)(ATPγS, d) was added 6 min before S_2 for the remainder of the experiment. Open symbols represent experiments in which CPA, ADPβS, ATP orATPγS was given alone (taken from Figure 1). Solid symbols represent experiments in which the medium contained DPCPX 10 nM throughout superfusion; (x) represents experiments in which the medium contained both cibacron blue 3GA 30 μM and DPCPX 10 nM throughout superfusion (d). Ordinates, evoked tritium overflow: S_2/S_1 ratios obtained in individual tissue slices were calculated as a percentage of the average S_2/S_1 ratio in the appropriate control group (solvent instead of agonists). Means ± s.e.mean of 4–12 experiments. Significant differences from corresponding control: $*P<0.05$ and $**P<0.01$. Significant differences from experiments in which CPA, ADPβS, ATP or ATPγS was given alone: $\#P<0.05$ and $\#\#P<0.01$.

Effects of purinoceptor antagonists, tetrodotoxin and yohimbine

When present throughout superfusion, the purinoceptor antagonists did not change the overflow of tritium evoked by 4 pulses/100 Hz (S_1) except for a small increase by cibacron blue 3GA 30 μM (see above). Drug effects on the electrically evoked overflow of tritium in this kind of experiment are assessed more accurately when the drugs are given before S_2 so that S_1 is a reference value for each brain slice. However, DPCPX 10 nM, suramin 300 μM and reactive blue 2 30 μM, also caused no change in evoked tritium overflow when applied before S_2, and the same was true for cibacron blue 3GA 30 μM. Two drugs unrelated to purines were administered: tetrodotoxin 0.3 μM abolished the overflow response to 4 pulses/100 Hz; yohimbine 1 μM was ineffective (Table 1).

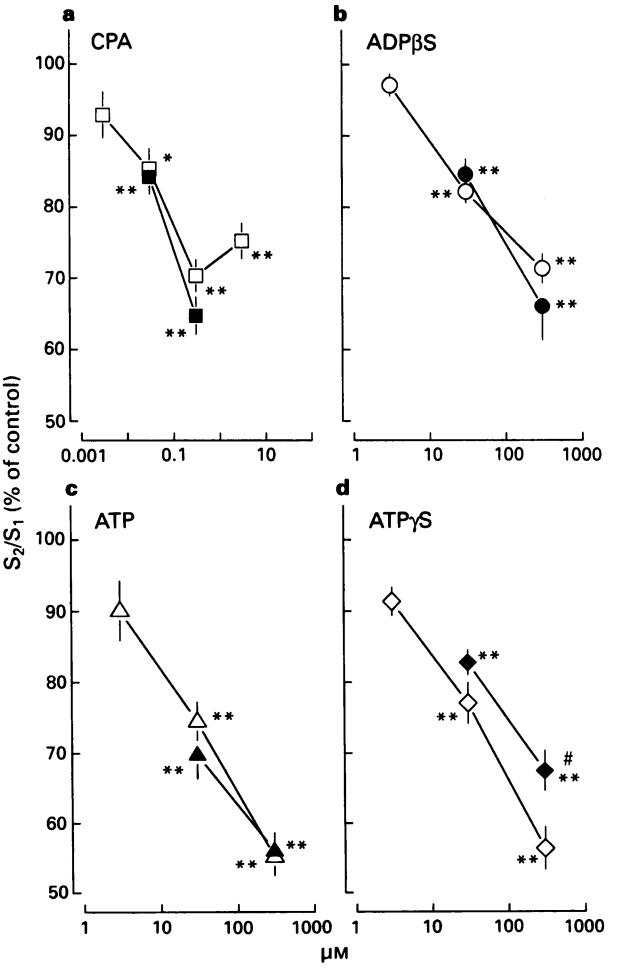


Figure 3 Interaction of purinoceptor agonists with suramin. Slices were stimulated twice by 4 pulses/100 Hz (S_1, S_2). N^6-cyclopentyl-adenosine (CPA, a), adenosine 5'-O-(2-thiodiphosphate) (ADPβS, b), ATP (c) or adenosine 5'-O-(3-thiotriphosphate) (ATPγS, d) was added 6 min before S_2 for the remainder of the experiment. Open symbols represent experiments in which CPA, ADPβS, ATP or ATPγS was given alone. Solid symbols represent experiments in which the medium contained suramin 300 μM throughout superfusion. Means ± s.e.mean of 5–14 experiments. Other details as in Figure 2.

Slices were stimulated by 60 pulses/1 Hz instead of 4 pulses/100 Hz in a final series of experiments. The purinoceptor antagonists again caused no change, whereas yohimbine now increased the evoked overflow of tritium 2.4 fold (Table 1).

Discussion

Under the conditions of the present experiments, the overflow of tritium, elicited by electrical stimulation in the presence of desipramine, reflects a quasi-physiological release of [^{3}H]-noradrenaline (see Taube *et al.*, 1977). The release evoked by 4 pulses/100 Hz was free from presynaptic α_2-autoinhibition as shown by the lack of effect of yohimbine (cf. Zier *et al.*, 1988). Hence, any potential interaction between presynaptic α_2-adrenoceptor and purinoceptor mechanisms was avoided.

Presynaptic adenosine A_1-receptors

Our experiments confirm the operation of release-inhibiting A_1-receptors at the noradreneregic terminal axons in rat brain cortex (Harms *et al.*, 1978; Craig & White, 1992) and indicate the absence of additional P_1-purinoceptor subtypes. In accord with this view, only the A_1-receptor agonist CPA and the non-subtype-selective agonist NECA, but neither the A_{2a}-receptor agonist CGS-21680 nor the A_3-receptor agonist APNEA altered the evoked overflow of tritium. CPA was about 8 times more potent than NECA in causing inhibition (Figure 1a), as it is at A_1 radioligand binding sites in rat brain membranes (Williams *et al.*, 1986). The adenosine A_1-receptor antagonist DPCPX shifted the concentration-response curve of CPA to the right with an apparent pK_B value (9.8) close to values found at presynaptic A_1-receptors in other rat tissues (9.3–9.7; Sebastião *et al.*, 1990; Fuder *et al.*, 1992; Kurz *et al.*, 1993). DPCPX also blocked the effect of NECA. On the other hand, the preferential adenosine A_2-receptor antagonist KF-17837 attenuated the effects of

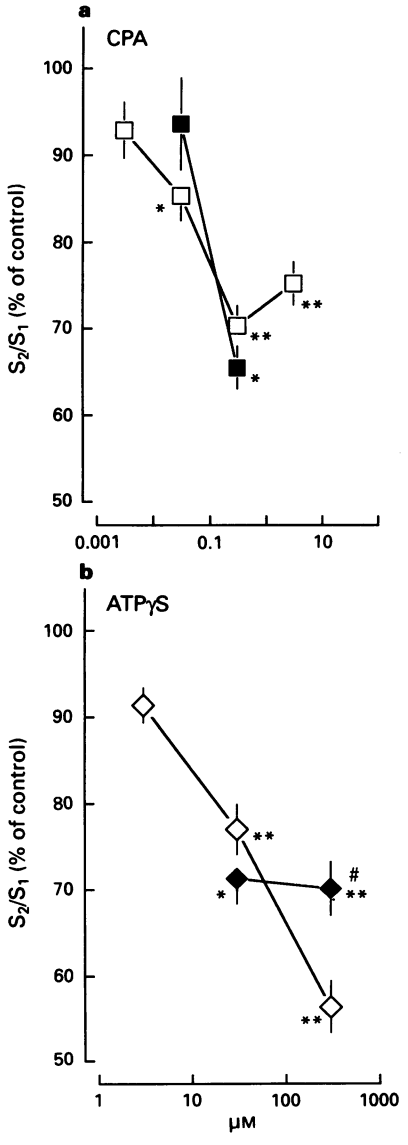


Figure 4 Interaction of purinoceptor agonists with reactive blue 2. Slices were stimulated twice by 4 pulses/100 Hz (S_1, S_2). N^6-cyclopentyl-adenosine (CPA, a) or adenosine 5′-O-(3-thiotriphosphate) (ATPγS, b) was added 6 min before S_2 for the remainder of the experiment. Open symbols represent experiments in which CPA or ATPγS was given alone. Solid symbols represent experiments in which the medium contained reactive blue 2 30 μM throughout the superfusion. Means ± s.e.mean of 5–12 experiments. Other details as in Figure 2.

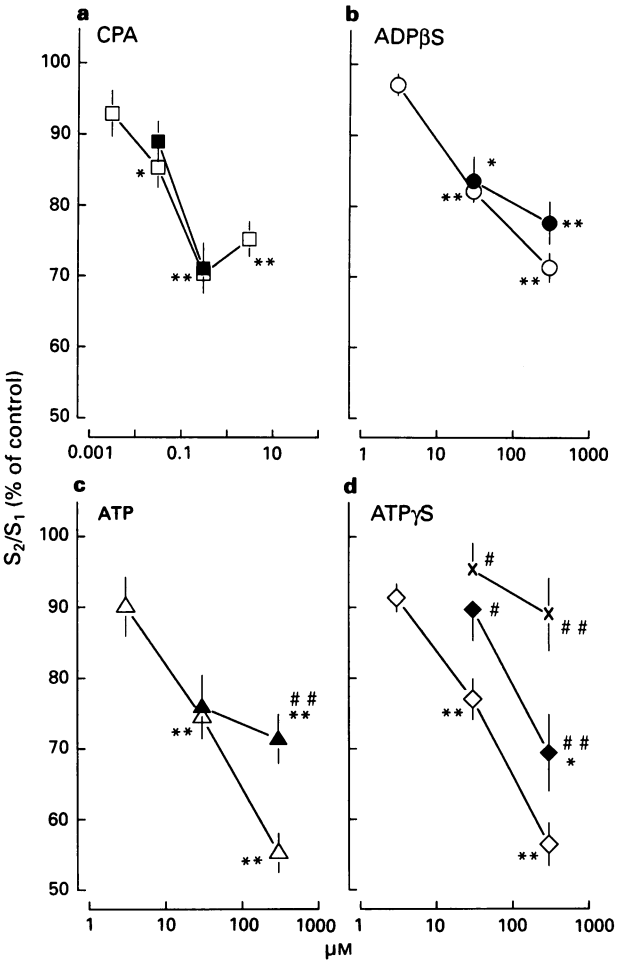


Figure 5 Interaction of purinoceptor agonists with cibacron blue 3GA or cibacron blue 3GA combined with 8-cyclopentyl-1,3-dipropylxanthine (DPCPX). Slices were stimulated twice by 4 pulses/100 Hz (S_1, S_2). N^6-cyclopentyl-adenosine (CPA, a) adenosine 5′-O-(2-thiodiphosphate) (ADPβS, b), ATP (c) or adenosine 5′-O-(3-thiotriphosphate) (ATPγS, d) was added 6 min before S_2 for the remainder of the experiment. Open symbols represent experiments in which CPA, ADPβS, ATP or ATPγS was given alone. Solid symbols represent experiments in which the medium contained cibacron blue 3GA 30 μM throughout superfusion; (x) represents experiments in which the medium contained both cibacron blue 3GA 30 μM and DPCPX 10 nM throughout superfusion (d; identical with (x) in Figure 2d). Means ± s.e.mean of 4–12 experiments. Other details as in Figure 2.

Table 1 Effects of purinoceptor antagonists, yohimbine and tetrodotoxin on electrically evoked tritium overflow

Drugs added 6 min before S_2	*S_2/S_1 (% of control) 4 pulses/100 Hz*	*n*	*60 pulses/1 Hz*	*n*
–	100.0 ± 1.2	10	100.0 ± 1.5	6
DPCPX (10 nM)	103.5 ± 1.9	6	109.4 ± 3.1	5
Suramin (300 μM)	101.1 ± 1.8	4	103.2 ± 2.0	5
Reactive blue 2 (30 μM)	95.0 ± 1.7	6	110.8 ± 7.6	5
Cibacron blue 3GA (30 μM)	107.1 ± 3.0	7	111.9 ± 5.6	5
Tetrodotoxin (0.3 μM)	3.1 ± 1.3**	6	–	
Yohimbine (1 μM)	97.8 ± 8.2	6	240.9 ± 14.4*	4

Slices were stimulated twice (S_1, S_2; pulse number and frequency indicated). Drugs or solvent were added 6 min before S_2 for the remainder of the experiment. S_2/S_1 ratios obtained in individual tissue slices were calculated as a percentage of the average control (solvent) S_2/S_1 ratio. DPCPX, 8-cyclopentyl-1,3-dipropylxanthine. Means ± s.e. mean of *n* experiments.
Significant differences from corresponding control: $^*P<0.05$ and $^{**}P<0.01$.

CPA and NECA only at the high concentration of 300 nM, close to its K_i for inhibition of radioligand binding to A_1-receptors in guinea-pig brain membranes (Shimada *et al.*, 1992). Finally, none of the agonists increased the evoked overflow of tritium, not even in the presence of DPCPX when a release-enhancing non-A_1 effect might have been unmasked (Brown *et al.*, 1990; Rensing *et al.*, 1993). The absence of release-enhancing A_2-purinoceptors contrasts with some other noradrenergic neurone systems (see Introduction).

The cerebrocortical presynaptic A_1-purinoceptors were sites of action not only of the nucleosides CPA and NECA. DPCPX shifted the concentration-inhibition curves of ADPβS, ATP and ATPγS to the right with apparent pK_B values (8.7 to 9.3) similar to the pK_B against CPA (9.8) and similar to values at presynaptic A_1-receptors in other rat tissues (9.3–9.7; see above). Blockade of 5'-nucleotidase by α,β-methylene-ADP did not attenuate the effect of ATPγS, indicating that breakdown of nucleotides to adenosine was not necessary for the inhibition. It has been suggested that adenosine and adenine nucleotides activate a common presynaptic receptor in some sympathetically innervated peripheral tissues and that this receptor is a novel subtype, P_3 (Shinozuka *et al.*, 1988; Forsyth *et al.*, 1991; Todorov *et al.*, 1994). While our results support the notion of a common presynaptic nucleoside and nucleotide receptor, the potent antagonist effect of DPCPX identifies the receptor in rat brain cortex as A_1. In this, the rat brain cortex noradrenergic axons would agree with the noradrenergic axons of rabbit brain cortex, rat vas deferens and mouse vas deferens (von Kügelgen *et al.*, 1992a; 1994a; Fuder & Muth, 1993; Kurz *et al.*, 1993; compare the studies on non-noradrenergic neurones by Moody *et al.*, 1984; Wiklund *et al.*, 1985; Rubino *et al.*, 1992; Cunha *et al.*, 1994). Adenine nucleotides also activate A_1-receptors in non-neural cells (Bailey *et al.*, 1992). One major component of the presynaptic inhibition by adenine nucleotides was, hence, A_1-mediated.

Presynaptic P_{2Y}-like purinoceptors

The nucleotides depressed the release of noradrenaline through a second site, a P_2-purinoceptor. One piece of evidence is the inhibition produced by 2-methylthio-ATP, a nucleotide selective for the P_{2Y}-subtype P_2-purinoceptor (Kennedy, 1990; Hoyle & Burnstock, 1991) and inactive at A_1-receptors (Tschöpl *et al.*, 1992; von Kügelgen *et al.*, 1992a). A more important piece of evidence is the observation that three P_2-purinoceptor antagonists, suramin, reactive blue 2 and cibacron blue 3GA, while not changing the effect of CPA, tended to attenuate or attenuated significantly the effect of the nucleotides, most consistently that of ATPγS (Figures 3–5).

Cibacron blue 3GA shifted the concentration-response curve of ATPγS to the right with an apparent pK_B value (5.0) similar to that found at the P_2-purinoceptors of the sympathetic axons of rat iris (4.7; Fuder & Muth, 1993). Virtually the same apparent pK_B (5.1) was obtained when the concentration-response curve of ATPγS in the presence of cibacron blue 3GA plus DPCPX was compared with the curve determined in the presence of DPCPX alone (Figure 2d); if DPCPX and cibacron blue 3GA had blocked the same receptor, the combination should have caused a much smaller shift beyond that caused by DPCPX alone (cf. Kurz *et al.*, 1993). The failure of indomethacin and N^G-nitro-L-arginine to attenuate the inhibition by ATPγS, excludes prostaglandins or nitric oxide as mediators of the effect of the nucleotide. Although alternatives are hard to exclude (see Starke, 1981), it seems most likely that the P_2-purinoceptors are located on the noradrenergic terminal axons themselves. Release-inhibiting P_2-purinoceptors have previously been demonstrated at the postganglionic sympathetic axons of mouse and rat vas deferens (von Kügelgen *et al.*, 1989; 1993; 1994a; Kurz *et al.*, 1993) and rat iris (Fuder & Muth, 1993) and at cultured chick postganglionic sympathetic neurones (Allgaier *et al.*, 1994). This is the first report of P_2-purinoceptors modulating transmitter release in the CNS.

One may ask why cibacron blue 3GA antagonized the effect of ATPγS more consistently than effects of ADPβS and ATP (Figure 5); why suramin antagonized only ATPγS but not ADPβS and ATP (Figure 3); why the antagonism of cibacron blue 3GA against ATP (Figure 5c) and of reactive blue 2 against ATPγS (Figure 4b) differed so markedly from a rightward shift; and why the apparent pK_B value of suramin against ATPγS (3.7) was lower than at other P_2-purinoceptors (for example 4.7 and 5.0 at P_{2X}- and P_{2Y}-purinoceptors in guinea-pig urinary bladder and taenia coli, respectively; Hoyle *et al.*, 1990). The likely common reason is the action of all nucleotides at two receptors, A_1 and P_2, a fact that leads to deviations from the rules valid for one-receptor systems (see p. 298 of Furchgott, 1972). ATPγS may have relied on the P_2 component to a greater extent than ADPβS and ATP and, hence, may have been more susceptible to P_2 antagonists, as it was at the presynaptic P_2-purinoceptors in mouse van deferens (von Kügelgen *et al.*, 1989). It should be noted that the apparent pK_B values of DPCPX against the nucleotides (8.7–9.3) also were slightly lower than the pK_B against CPA (9.8), possibly for the same reason, as suggested previously by Fuder & Muth (1993). Generally speaking, the 'apparent pK_B values' of the present study must be considered as rough affinity estimates, because of the two-receptor situation, because curve shifts often were small, and because only one antagonist concentration and few agonist concentrations were used.

The involvement of two receptors in the effect of nucleotides impedes the subclassification of the presynaptic P_2-purinoceptor. Nevertheless, the P_2-purinoceptor at postganglionic sympathetic neurones has been described as P_{2Y}-like (von Kügelgen *et al.*, 1989; 1994a; Fuder & Muth, 1993; Kurz *et al.*, 1993). The effect of 2-methylthio-ATP, combined with lack of effect of α,β-methylene-ATP, makes the presynaptic P_2-purinoceptor in rat brain cortex P_{2Y}-like as well. The antagonism by reactive blue 2 and cibacron blue 3GA is in accord with this view: both are P_{2Y}-selective and have previously been shown to block the presynaptic P_{2Y}-like purinoceptors in mouse vas deferens (von Kügelgen *et al.*, 1994a) and rat iris (Fuder & Muth, 1993). The rat cerebrocortical presynaptic P_2-purinoceptor differs, however, from classical P_{2Y}-purinoceptors at which 2-methylthio-ATP is known to act at nanomolar concentrations (see Fischer *et al.*, 1993). It also differs from the P_2-purinoceptor at the cell bodies of the noradrenergic neurones in the rat locus coeruleus, which mediates an increase in firing rate and

which has equally been classified as P_{2Y}-like (Illes & Nörenberg, 1993; Shen & North, 1993): in the locus coeruleus, 2-methylthio-ATP and α,β-methylene-ATP were about equipotent and more potent than ATP. The existence of several kinds of P_{2Y}-purinoceptor has recently been confirmed by molecular cloning (see Barnard *et al.*, 1994).

An endogenous input?

Presynaptic A_1-receptors are potential sites of action of endogenous adenosine (as well as adenine nucleotides; see above), and presynaptic P_{2Y}-like receptors are potential sites of action of endogenous ATP. Under the conditions of the present experiments, however, the receptors did not play this 'physiological' role: DPCPX and the P_2 antagonists caused no consistent increase in the release of [^{3}H]-noradrenaline, neither when the pulse trains were very brief (4 pulses/100 Hz) nor when they were longer (60 pulses/1 Hz) (cf. Harms *et al.*, 1978). Presynaptic α_2-autoinhibition, in contrast, depressed transmitter release during the 60 pulses/1 Hz trains, as shown by the effect of yohimbine (Table 1) and as expected (see Starke *et al.*, 1989). The results, of course, do not exclude an endogenous input to the presynaptic purinoceptors under other conditions. The release of noradrenaline is depressed by endogenous A_1-agonists in several tissues such as rat (Jonzon & Fredholm, 1984) and rabbit hippocampus (Jackisch *et al.*, 1985) and rabbit brain cortex (von Kügelgen *et al.*, 1992a,b). An endogenous agonist input to presynaptic P_2-purinoceptors has recently been demonstrated for the postganglionic sympathetic nerves of the mouse, rat and rabbit vas deferens (von Kügelgen *et al.*, 1993, 1994; Grimm *et al.*, 1994).

Conclusion

The noradrenergic axons of the rat brain cortex possess two release-inhibiting purinoceptor systems, A_1 and P_2. The A_1-receptors are activated by nucleosides such as CPA and also by (certain) nucleotides such as ATPγS and are blocked by DPCPX but not by suramin, reactive blue 2 and cibacron blue 3GA. The P_2-receptors are activated by nucleotides but not by nucleosides and are blocked by suramin, reactive blue 2 and cibacron blue 3GA but not by DPCPX; they are P_{2Y}-like. Neither purinoceptor was activated by an endogenous ligand under the present experimental conditions.

This study was supported by the Deutsche Forschungsgemeinschaft (SFB 325). We thank Professor Dr R.A. Olsson (University of South Florida, Dept. of Internal Medicine, Tampa, Florida, USA), Professor Dr H.J. Ruoff (Bayer, Fachbereich Klinische Forschung, Wuppertal, Germany) and Dr F. Suzuki (Kyowa Hakko Kogyo, Pharmaceutical Research Laboratories, Sunto-Gun, Shizuoka-Ken, Japan) for drugs.

References

ALLGAIER, C., PULLMANN, F., SCHOBERT, A., VON KÜGELGEN, I. & HERTTING, G. (1994). P_2 purinoceptors modulating noradrenaline release from sympathetic neurons in culture. *Eur. J. Pharmacol.*, **252**, R7–R8.

BAILEY, S.J., HICKMAN, D. & HOURANI, S.M.O. (1992). Characterization of P_1-purinoceptors mediating contraction of the rat colon muscularis mucosae. *Br. J. Pharmacol.*, **105**, 400–404.

BARNARD, E.A., BURNSTOCK, G. & WEBB, T.E. (1994). G protein-coupled receptors for ATP and other nucleotides: a new receptor family. *Trend Pharmacol. Sci.*, **15**, 67–70.

BOLAND, B., HIMPENS, B., VINCENT, M.F., GILLIS, J.M. & CASTEELS, R. (1992). ATP activates P_{2X}-contracting and P_{2Y}-relaxing purinoceptors in the smooth muscle of mouse vas deferens. *Br. J. Pharmacol.*, **107**, 1152–1158.

BROWN, S.J., JAMES, S., REDDINGTON, M. & RICHARDSON, P.J. (1990). Both A_1 and A_{2a} purine receptors regulate striatal acetylcholine release. *J. Neurochem.*, **55**, 31–38.

BRUNS, R.F. (1980). Adenosine receptor activation by adenine nucleotides requires conversion of the nucleotides to adenosine. *Naunyn-Schmied. Arch. Pharmacol.*, **315**, 5–13.

BRUNS, R.F., FERGUS, J.H., BADGER, E.W., BRISTOL, J.A., SANTAY, L.A., HARTMAN, J.D., HAYS, S.J. & HUANG, C.C. (1987). Binding of the A_1-selective adenosine antagonist 8-cyclopentyl-1,3-dipropylxanthine to rat brain membranes. *Naunyn-Schmied. Arch. Pharmacol.*, **335**, 59–63.

BURNSTOCK, G. & WARLAND, J.J.I. (1987). P_2-purinoceptors of two subtypes in the rabbit mesenteric artery: reactive blue 2 selectively inhibits responses mediated via the P_{2Y}- but not the P_{2X}-purinoceptor. *Br. J. Pharmacol.*, **90**, 383–391.

CRAIG, C.G. & WHITE, T.D. (1992). Low-level N-methyl-D-aspartate receptor activation provides a purinergic inhibitory threshold against further N-methyl-D-aspartate-mediated neurotransmission in the cortex. *J. Pharmacol. Exp. Ther.*, **260**, 1278–1284.

CUNHA, R.A., RIBEIRO, J.A. & SEBASTIÃO, A.M. (1994). Purinergic modulation of the evoked release of [^{3}H]acetylcholine from the hippocampus and cerebral cortex of the rat: role of ectonucleotidases. *Eur. J.Neurosci.*, **6**, 33–42.

DE MEY, J., BURNSTOCK, G. & VANHOUTTE, P.M. (1979). Modulation of the evoked release of noradrenaline in canine saphenous vein via presynaptic receptors for adenosine but not ATP. *Eur. J. Pharmacol.*, **55**, 401–405.

DUNN, P.M. & BLAKELEY, A.G.H. (1988). Suramin: a reversible P_2-purinoceptor antagonist in the mouse vas deferens. *Br. J. Pharmacol.*, **93**, 243–245.

FISCHER, B., BOYER, J.L., HOYLE, C.H.V., ZIGANSHIN, A.U., BRIZZOLARA, A.L., KNIGHT, G.E., ZIMMET, J., BURNSTOCK, G., HARDEN, T.K. & JACOBSON, K.A. (1993). Identification of potent, selective P_{2Y}-purinoceptor agonists: structure-activity relationships for 2-thioether derivatives of adenosine 5'-triphosphate. *J. Med. Chem.*, **36**, 3937–3946.

FORSYTH, K.M., BJUR, R.A. & WESTFALL, D.P. (1991). Nucleotide modulation of norepinephrine release from sympathetic nerves in the rat vas deferens. *J. Pharmacol. Exp. Ther.*, **256**, 821–826.

FREDHOLM, B.B. (1974). Vascular and metabolic effects of theophylline, dibuturyl cyclic AMP and dibuturyl cyclic GMP in canine subcutaneous adipose tissue in situ. *Acta Physiol. Scand.*, **90**, 226–236.

FREDHOLM, B.B. & DUNWIDDIE, T.V. (1988). How does adenosine inhibit transmitter release? *Trends Pharmacol. Sci.*, **9**, 130–134.

FUDER, H., BRINK, A., MEINCKE, M. & TAUBER, U. (1992). Purinoceptor-mediated modulation by endogenous and exogenous agonists of stimulation-evoked [^{3}H]noradrenaline release on rat iris. *Naunyn-Schmied. Arch. Pharmacol.*, **345**, 417–423.

FUDER, H. & MUTH, U. (1993). ATP and endogenous agonists inhibit evoked [^{3}H]-noradrenaline release in rat iris via A_1- and P_{2Y}-like purinoceptors. *Naunyn-Schmied. Arch. Pharmacol.*, **348**, 352–357.

FURCHGOTT, R.F. (1972). The classification of adrenoceptors (adrenergic receptors). An evaluation from the standpoint of receptor theory. In *Catecholamines. Handbook of Experimental Pharmacology*. ed. Blaschko, H. & Muscholl, E. Vol. 33, pp. 283–335. Berlin, Heidelberg, New York: Springer.

GONÇALVES, J. & QUEIROZ, G. (1993). Facilitatory and inhibitory modulation by endogenous adenosine of noradrenaline release in the epididymal portion of rat vas deferens. *Naunyn-Schmied. Arch. Pharmacol.*, **348**, 367–371.

GRIMM, U., FUDER, H., MOSER, U., BÄUMERT, H.G. MUTSCHLER, E. & LAMBRECHT, G. (1994). Characterization of the prejunctional muscarinic receptors mediating inhibition of evoked release of endogenous noradrenaline in rabbit isolated vas deferens. *Naunyn-Schmied. Arch. Pharmacol.*, **349**, 1–10.

HARMS, H.H., WARDEH, G. & MULDER, A.H. (1978). Adenosine modulates depolarization-induced release of ^{3}H-noradrenaline from slices of rat brain neocortex. *Eur. J. Pharmacol.*, **49**, 305–308.

HEDQVIST, P. & FREDHOLM, B.B. (1976). Effects of adenosine on adrenergic neurotransmission; prejunctional inhibition and postjunctional enhancement. *Naunyn-Schmied. Arch. Pharmacol.*, **293**, 217–223.

HOUSTON, D.A., BURNSTOCK, G. & VANHOUTTE, P.M. (1987). Different P_2-purinergic receptor subtypes of endothelium and smooth muscle in canine blood vessels. *J. Pharmacol. Exp. Ther.*, **241**, 501–506.

HOYLE, C.H.V. & BURNSTOCK, G. (1991). ATP receptors and their physiological roles. In *Adenosine in the Nervous System*. ed. Stone, T.W. pp. 43–76. London: Academic Press.

HOYLE, C.H.V., KNIGHT, G.E. & BURNSTOCK, G. (1990). Suramin antagonizes responses to P_2-purinoceptor agonists and purinergic nerve stimulation in the guinea-pig urinary bladder and taenia coli. *Br. J. Pharmacol.*, **99**, 617–621.

ILLES, P. & NÖRENBERG, W. (1993). Neuronal ATP receptors and their mechanism of action. *Trends Pharmacol. Sci.*, **14**, 50–54.

JACKISCH, R., FEHR, R. & HERTTING, G. (1985). Adenosine: an endogenous modulator of hippocampal noradrenaline release. *Neuropharmacology*, **24**, 499–507.

JACKSON, E.K., HERZER, W.A. & SUZUKI, F. (1993). KF17837 is an A_2 adenosine receptor antagonist in vivo. *J. Pharmacol. Exp. Ther.*, **267**, 1304–1310.

JARVIS, M.F., SCHULZ, R., HUTCHISON, A.J., DO, U.H., SILLS, M.A. & WILLIAMS, M. (1989). [^{3}H]CGS 21680, a selective A_2 adenosine receptor agonist directly labels A_2 receptors in rat brain. *J. Pharmacol. Exp. Ther.*, **251**, 888–893.

JONZON, B. & FREDHOLM, B.B. (1984). Adenosine receptor mediated inhibition of noradrenaline release from slices of the rat hippocampus. *Life Sci.*, **35**, 1971–1979.

KENNEDY, C. (1990). P_1- and P_2-purinoceptor subtypes – an update. *Arch. Int. Pharmacodyn. Ther.*, **303**, 30–50.

KNOWLES, R.G., PALACIOS, M., PALMER, R.M.J. & MONCADA, S. (1990). Kinetic characteristics of nitric oxide synthase from rat brain. *Biochem. J.*, **269**, 207–210.

KURZ, K., VON KÜGELGEN, I. & STARKE, K. (1993). Prejunctional modulation of noradrenaline release in mouse and rat vas deferens: contribution of P_1 and P_2-purinoceptors. *Br. J. Pharmacol.*, **110**, 1465–1472.

LOHSE, M.J., KLOTZ, K.N., LINDENBORN-FOTINOS, J., REDDINGTON, M., SCHWABE, U. & OLSSON, R.A. (1987). 8-Cyclopentyl-1,3-dipropylxanthine (DPCPX) – a selective high affinity antagonist radioligand for A_1 adenosine receptors. *Naunyn-Schmied. Arch. Pharmacol.*, **336**, 204–210.

LUKACSKO, P. & BLUMBERG, A. (1982). Modulation of the vasoconstrictor response to adrenergic stimulation by nucleosides and nucleotides. *J. Pharmacol. Exp. Ther.*, **222**, 344–349.

MIYAHARA, H. & SUZUKI, H. (1987). Pre- and post-junctional effects of adenosine triphosphate on noradrenergic transmission in the rabbit ear artery. *J. Physiol.*, **389**, 423–440.

MOODY, C.J., MEGHJI, P. & BURNSTOCK, G. (1984). Stimulation of P_1-purinoceptors by ATP depends partly on its conversion to AMP and adenosine and partly on direct action. *Eur. J. Pharmacol.*, **97**, 47–54.

RENSING, C., RENSING, H., HERTTING, G. & JACKISCH, R. (1993). Evidence for facilitatory adenosine A_2 receptors modulating noradrenaline release in the rabbit hippocampus. *Naunyn-Schmied. Arch. Pharmacol.*, **347**, R68.

RUBINO, A., AMERINI, S., LEDDA, F. & MANTELLI, L. (1992). ATP modulates the efferent function of capsaicin-sensitive neurones in guinea-pig isolated atria. *Br. J. Pharmacol.*, **105**, 516–520.

SEBASTIÃO, A.M., STONE, T.W. & RIBEIRO, J.A. (1990). The inhibitory adenosine receptor at the neuromuscular junction and hippocampus of the rat: antagonism by 1,3,8-substituted xanthines. *Br. J. Pharmacol.*, **101**, 453–459.

SHEN, K.Z. & NORTH, R.A. (1993). Excitation of rat locus coeruleus neurons by adenosine 5'-triphosphate: ionic mechanism and receptor characterization. *J. Neurosci.*, **13**, 894–899.

SHIMADA, J., SUZUKI, F., NONAKA, H., ISHII, A. & ICHIKAWA, S. (1992). (E)-1,3-Dialkyl-7-methyl-8-(3,4,5-trimethoxystyryl)xanthines: potent and selective adenosine A_2 antagonists. *J. Med. Chem.*, **35**, 2342–2345.

SHINOZUKA, K., BJUR, R.A. & WESTFALL, D.P. (1988). Characterization of prejunctional purinoceptors on adrenergic nerves of the rat caudal artery. *Naunyn-Schmied. Arch. Pharmacol.*, **338**, 221–227.

SHIRAHASE, H., USUI, H., SHIMAJI, H., KURAHASHI, K. & FUJIWARA, M. (1991). Endothelium-independent and endothelium-dependent contractions mediated by P_{2X}- and P_{2Y}-purinoceptors in canine basilar arteries. *J. Pharmacol. Exp. Ther.*, **256**, 683–688.

SOCIETY OF DYERS AND COLOURISTS (1971). *Colour Index* (3rd edition), Vol. 4. Bradford: Lund Humphries.

SPERLAGH, B. & VIZI, E.S. (1991). Effect of presynaptic P_2 receptor stimulation on transmitter release. *J. Neurochem.*, **56**, 1466–1470.

STARKE, K. (1981). Presynaptic receptors. *Annu. Rev. Pharmacol. Toxicol.*, **21**, 7–30.

STARKE, K., GÖTHERT, M. & KILBINGER, H. (1989). Modulation of neurotransmitter release by presynaptic autoreceptors. *Physiol. Rev.*, **69**, 864–989.

STARKE, K., PESKAR, B.A., SCHUMACHER, K.A. & TAUBE, H.D. (1977). Bradykinin and postganglionic sympathetic transmission. *Naunyn-Schmied. Arch. Pharmacol.*, **299**, 23–32.

STJÄRNE, L. & ÅSTRAND, P. (1985). Relative pre- and postjunctional roles of noradrenaline and adenosine 5'-triphosphate as neurotransmitters of the sympathetic nerves of guinea-pig and mouse vas deferens. *Neuroscience*, **14**, 929–946.

STONE, T.W. (1981). Physiological roles for adenosine and adenosine 5'-triphosphate in the nervous system. *Neuroscience*, **6**, 523–555.

STONE, T.W. & CUSACK, N.J. (1989). Absence of P_2-purinoceptors in hippocampal pathways. *Br. J. Pharmacol.*, **97**, 631–635.

TAUBE, H.D., STARKE, K. & BOROWSKI, E. (1977). Presynaptic receptor systems on the noradrenergic neurones of rat brain. *Naunyn-Schmied. Arch. Pharmacol.*, **299**, 123–141.

TODOROV, L.D., BJUR, R.A. & WESTFALL, D.P. (1994). Inhibitory and facilitatory effects of purines on transmitter release from sympathetic nerves. *J. Pharmacol. Exp. Ther.*, **268**, 985–989.

TRENDELENBURG, A.U., LIMBERGER, N. & STARKE, K. (1993). Presynaptic α_2-autoreceptors in brain cortex: α_{2D} in the rat and α_{2A} in the rabbit. *Naunyn-Schmied. Arch. Pharmacol.*, **348**, 35–45.

TSCHÖPL, M., HARMS, L., NÖRENBERG, W. & ILLES, P. (1992). Excitatory effects of adenosine 5'-triphosphate on rat locus coeruleus neurones. *Eur. J. Pharmacol.*, **213**, 71–77.

VON KÜGELGEN, I., KURZ, K. & STARKE, K. (1993). Axon terminal P_2-purinoceptors in feedback control of sympathetic transmitter release. *Neuroscience*, **56**, 263–267.

VON KÜGELGEN, I., KURZ, K. & STARKE, K. (1994a). P_2-purinoceptor-mediated autoinhibition of sympathetic transmitter release in mouse and rat vas deferens. *Naunyn-Schmied. Arch. Pharmacol.*, **349**, 125–132.

VON KÜGELGEN, I., SCHÖFFEL, E. & STARKE, K. (1989). Inhibition by nucleotides acting at presynaptic P_2-receptors of sympathetic neuro-effector transmission in the mouse isolated vas deferens. *Naunyn-Schmied. Arch. Pharmacol.*, **340**, 522–532.

VON KÜGELGEN, I., SPÄTH, L. & STARKE, K. (1992a). Stable adenine nucleotides inhibit [^{3}H]-noradrenaline release in rabbit brain cortex slices by direct action at presynaptic adenosine A_1-receptors. *Naunyn-Schmied. Arch. Pharmacol.*, **346**, 187–196.

VON KÜGELGEN, I., SPÄTH, L. & STARKE, K. (1992b). Adenosine but not an adenine nucleotide mediates tonic purinergic inhibition, as well as inhibition by glutamate, of noradrenaline release in rabbit brain cortex slices. *Naunyn-Schmied. Arch. Pharmacol.*, **346**, 677–684.

VON KÜGELGEN, I., SPÄTH, L. & STARKE, K. (1994b). Presynaptic P_2-purinoceptors inhibiting the release of [^{3}H]-noradrenaline in rat brain cortex slices. *Naunyn-Schmied. Arch. Pharmacol.*, **349**, R80.

WELFORD, L.A., CUSACK, N.J. & HOURANI, S.M.O. (1986). ATP analogues and the guinea-pig taenia coli: a comparison of the structure-activity relationships of ectonucleotidases with those of the P_2-purinoceptor. *Eur. J. Pharmacol.*, **129**, 217–224.

WIKLUND, N.P., GUSTAFSSON, L.E. & LUNDIN, J. (1985). Pre- and postjunctional modulation of cholinergic neuroeffector transmission by adenine nucleotides. Experiments with agonist and antagonist. *Acta Physiol. Scand.*, **125**, 681–691.

WILLIAMS, M., BRAUNWALDER, A. & ERICKSON, T.J. (1986). Evaluation of the binding of the A-1 selective adenosine radioligand, cyclopentyladenosine (CPA), to rat brain tissue. *Naunyn-Schmied. Arch. Pharmacol.*, **332**, 179–183.

ZHOU, Q.Y., LI, C., OLAH, M.E., JOHNSON, R.A., STILES, G.L. & CIVELLI, O. (1992). Molecular cloning and characterization of an adenosine receptor: the A_3 adenosine receptor. *Proc. Natl. Acad. Sci. U.S.A.*, **89**, 7432–7436.

ZIER, G., DROBNY, H., VALENTA, B. & SINGER, E.A. (1988). Evidence against a functional link between noradrenaline uptake mechanisms and presynaptic alpha-2 adrenoceptors. *Naunyn-Schmied. Arch. Pharmacol.*, **337**, 118–121.

(Received April 22, 1994
Revised June 30, 1994
Accepted July 11, 1994)

Br. J. Pharmacol. (1994), **113**, 823–830 © Macmillan Press Ltd, 1994

Agonist-induced desensitization of histamine H_1 receptor-mediated inositol phospholipid hydrolysis in human umbilical vein endothelial cells

G. McCreath, I.P. Hall & [1]*S.J. Hill

Department of Medicine and *Department of Physiology and Pharmacology, Medical School, Queen's Medical Centre, Nottingham NG7 2UH

1 The regulation of histamine-induced [^{3}H]-inositol phosphate formation was studied in human cultured umbilical vein endothelial cells (HUVEC).

2 Histamine (EC_{50} 4.8 μM) produced a 12.7 fold increase in [^{3}H]-inositol phosphate formation over basal levels. Prior exposure to 0.1 mM histamine (2 h) produced a 78% reduction in the response to subsequent histamine (0.1 mM) challenge. The IC_{50} for this histamine-induced desensitization was 0.9 μM.

3 The inositol phosphate response to histamine (0.1 mM) was inhibited by phorbol dibutyrate (IC_{50} 40 nM; maximal reduction 64%). This effect was antagonized by both staurosporine (100 nM) and Ro 31-8220 (10 μM). However, the histamine-induced desensitization of the H_1-receptor-mediated inositol phosphate response was insensitive to the protein kinase inhibitors, staurosporine, Ro 31-8220, K252a and KN62.

4 Prior exposure to sodium nitroprusside (100 μM), forskolin (10 μM) or dibutyryl cyclic AMP (1 mM) had no effect upon histamine-induced [^{3}H]-inositol phosphate formation.

5 NaF (20 mM) and thrombin (EC_{50} 0.4 u ml^{-1}) also induced inositol phosphate formation in HUVEC. Histamine pretreatment (0.1 mM, 10–120 min) failed to modify the inositol phosphate response to a subsequent NaF or thrombin challenge.

6 We conclude that the desensitization of histamine H_1-receptor-mediated [^{3}H]-inositol phosphate formation occurs at the level of the receptor and involves a mechanism independent of activation of protein kinase A, G, or C, or calcium calmodulin-dependent protein kinase II.

Keywords: Histamine H_1-receptor; desensitization; inositol phosphate hydrolysis; endothelial cells

Introduction

Prolonged exposure of many G protein coupled receptors to an agonist results in a reduced physiological response which may be due to receptor desensitization, sequestration or down regulation (Wojcikiewicz *et al.*, 1993). The mechanism underlying these effects have been extensively studied using the β_2-adrenoceptor as a model. For this receptor, short term (< 1 h) exposure to agonist results in receptor desensitization which is mediated through two different mechanisms, involving adenosine 3′:5′-cyclic monophosphate (cyclic AMP)-dependent phosphorylation of specific sites in the third intracellular loop of the receptor (Lohse *et al.*, 1990; Hausdorff *et al.*, 1989; 1990), and cyclic AMP-independent phosphorylation of residues in the cytoplasmic tail of the receptor by a specific family of receptor kinases named β-adrenoceptor kinases (βARK: Benovic *et al.*, 1986; 1987; Kolbilka, 1992; Ostrowski *et al.*, 1992; Lefkowitz, 1993; Inglese *et al.*, 1993). In the case of β-ARK, the phosphorylation of the β_2-adrenoceptor is rapidly followed by the binding of a protein (β-arrestin 1 or 2) which interferes with the coupling of the receptor with its G-protein (Lefkowitz, 1993; Lohse *et al.*, 1992).

Sequestration (which is manifest by a loss of cell surface receptors to an intracellular compartment) quickly follows the more rapid uncoupling of β_2-receptors from G_s-proteins (Yu *et al.*, 1993; Barak *et al.*, 1994). Following agonist removal, sequestered receptors can be recycled to the cell surface (Yu *et al.*, 1993). It has been suggested that receptor sequestration may represent a mechanism by which receptors can be dephosphorylated and recycled to re-establish normal responsiveness (Barak *et al.*, 1994). Longer term exposure of the β_2-adrenoceptor to agonists leads to an overall loss of cellular receptors (downregulation) as a result of receptor degradation via the lysosomes and altered receptor expression (Hadcock *et al.*, 1989; Kolbilka, 1992).

Less is known of the mechanisms underlying desensitization of phospholipase C (PLC)-coupled recpetors. Stimulation of PLC-coupled receptors results in the formation of the two intracellular second messengers, inositol 1,4,5 trisphosphate (Ins 1,4,5 P_3) and diacylglycerol. Binding of Ins(1,4,5)P_3 to its receptor on the endoplasmic reticulum results in the release of calcium from intracellular stores whilst diacylgylcerol is able to activate protein kinase C (Berridge, 1987). Studies with transfected muscarinic m3 receptors in CHO cells have shown that desensitization occurs following exposure to agonist, and that this effect is temporally associated with receptor phosphorylation (Tobin & Nahorski, 1993; Tobin *et al.*, 1993). Similarly, both α_1-adrenoceptors (in smooth muscle cells) and cholecystokinin receptors (in pancreatic acinar cells) are phosphorylated and desensitize following short term agonist exposure (Leeb-Lundberg *et al.*, 1987; Klueppelberg *et al.*, 1991). However, these effects all occur rapidly following agonist exposure and less is known about the mechanisms underlying the longer term effects of agonist on the regulation of PLC-coupled receptors.

A number of histamine H_1 receptor-mediated responses in isolated tissues and immortalised cell lines have been shown to desensitize following prolonged agonist exposure (Taylor & Richelson, 1979; Donaldson & Hill, 1985; Lurie *et al.*, 1985; Brown *et al.*, 1986; Leurs *et.al.*, 1990; Bristow & Zamani, 1993; Bristow *et al.*, 1993; Daykin *et al.*, 1993). The mechanisms underlying this process are poorly defined and in particular controversy exists over the potential role of protein

[1] Author for correspondence.

kinase C. In order to investigate some of the mechanisms underlying desensitization of the human histamine H_1 receptor in a non-transformed cell line, we have studied the regulation of histamine-induced inositol phospholipid hydrolysis in human umbilical vein endothelial cell (HUVEC).

Methods

Cell culture

Human umbilical vein endothelial cells (HUVEC) were isolated from human umbilical cord veins as previously described (Jaffe *et al.*, 1973). Briefly, under sterile conditions the vessel lumen was incubated with collagenase (0.5 mg m^{-1} in M-199; type II) at 37°C for 10 min and dissociated endothelial cells flushed out with a 10 ml syringe. The cells obtained were pelleted by centrifugation (1200 r.p.m., 10 min) and resuspended in M-199 supplemented with 10% foetal calf serum, 10% newborn calf serum, penicillin (100 u ml^{-1}), streptomycin (100 $\mu g\ ml^{-1}$), heparin (90 $\mu g\ ml^{-1}$) and endothelial cell growth factor (20 $\mu g\ ml^{-1}$). These cells were then plated in 1% gelatin-coated 25 cm^2 tissue-culture flasks and incubated at 37°C in humidified air/CO_2 (95:5). When confluent (usually 4–5 days), monolayer primary cultures were passaged using trypsin/EDTA solution (0.05/0.02%) into 75 cm^2 flasks or 24-well cluster dishes for experimental purposes. Cells were used between passage 3 and 7. Cells were indentified as endothelial in origin by immunocytochemistry using standard methods. The antibodies used were Rabbit Anti-human Factor VIII (1:80) and FITC Anti-rabbit IgG (1:20) (Sigma, England).

Inositol phospholipid hydrolysis

Monolayer cell cultures in 24-well cluster dishes were prelabelled with [^{3}H]-*myo*-inositol (1 μCi/well) for 24 h in inositol-free M199 containing dialysed 10% FCS, dialysed 10% NCS and 2 mM glutamine. Prelabelled cells were then washed twice with 1 ml Hanks/HEPES buffer pH (7.4) (HBSS with 20 mM HEPES) and incubated at 37°C for 20 min in the presence of 10 mM LiCl. Where appropriate, antagonists were added at the beginning of this incubation period. For desensitization experiments, histamine or phorbol dibutyrate (PdBu) were added for the final 2 h of the prelabelling period and, where appropriate, staurosporine or Ro 31-8220 were added for the final 3 h of this period. Agonists were finally added in 10 μl Hanks/HEPES buffer and the incubation continued for 45 min unless otherwise stated in the text. Incubations were terminated by the addition of 1 ml of precooled(−20°C) methanol/0.12M HCl (1:1 v/v). Cells were left for at least 2 h at −20°C. Total [^{3}H]-inositol phosphates in the supernatant of the disrupted cell monolayers were finally quantified by anion-exchange chromatography as previously described (Daykin *et al.*, 1993).

Inositol phospolipid labelling

Inositol phospholipid labelling was studied as previously described (Daykin *et al.*, 1993). In brief, cells were treated, and incubations terminated, as described in the previous section. Following overnight storage at −20°C, the supernatant was removed and 600 μl of chloroform/methanol/HCl (100:200:1) was added to each well. The remainder of the disrupted cell monolayer was scraped into solution and the contents of each well was removed and transferred to microcentrifuge tubes. 200 μl of chloroform and 200 μl of H_2O were added to each tube, samples were vortexed and then centrifuged at 1500 g for 10 min. 150 μl aliquots of the chloroform phase containing the labelled phospholipids were then removed from each sample, dried overnight, and counted for tritium.

Data analysis

All figures except Figure 1 show mean data from n separate individual experiments. EC_{50} values were determined in individual experiments by the logistic regression package Graphpad. Values in the text are mean ± s.e.mean of values obtained in individual experiments. EC_{50} represents the concentration of agonist required to produce 50% of the maximal response; IC_{50} represents the concentration of drug required to reduce the maximal response by 50%. In experiments examining the effect of protein kinase C activators and/or inhibitors upon histamine-induced inositol phosphate formation, results were always expressed as a % of the control response to 0.1 mM histamine. Data were analyzed by paired or unpaired t test as appropriate.

Materials and chemicals

Medium-199 (M-199), foetal calf serum (FCS) and trypsin/EDTA solution were purchased from Northumbria Biological Ltd. (Northumberland, England). Newborn calf serum (NCS), penicillin/streptomycin and Hanks balanced salt solution (HBSS) were obtained from GIBCO (Paisley, Scotland). L-Glutamine was purchased from Flow Laboratories (High Wycombe, England) and endothelial cell growth factor (ECGF) from Advanced Protein Products (West Midlands, England). Ro 31-8220 (3-{1-[3-(2-isothioureido)propyl]indol-3-yl}-4-(1-methylindol-3-yl)-3-pyrrolin-2,5-dione) was a kind gift from Roche. [^{3}H]-*myo*-inositol (specific activity 16.5 μCi ml^{-1}) was obtained from NEN DuPont. (Herts., England). KN 62 {1-[*N*,*O*-bis(1,5-isoquinolinesulphonyl)-*N*-methyl-L-tyrosyl]-4-phenylpiperazine} and K252a [(8**R**,9**S**,11**S**)-(−)-9-hydroxy-9-methoxycarbonyl-8-methyl-2,3,9,10-tetrahydro-8,11-epoxy-1H,8H,11H-2,7b,11a-triazodibenzo(a,g)cycloocta(cde)trinden-1-one] were obtained from Calbiochem-Novabiochem (Nottingham, England). Tissue culture flasks/plates were obtained from Costar (High Wycombe, England). All other reagents were obtained from Sigma Chemical Co. (Dorset, England).

Results

Effect of histamine on inositol phosphate formation in HUVEC

In the presence of LiCl, histamine produced concentration-related [^{3}H]-inositol phosphate formation in HUVEC (Figure 1). The mean response to 0.1 mM histamine was a 12.7 ± 0.3 (n = 65) fold increase in total [^{3}H]-inositol phosphate accumulation over basal (unstimulated) levels. In the absence of LiCl, a marked reduction in the magnitude of the inositol phosphate response to histamine was observed (maximum response 2.5 fold over basal, n = 3). Hence all further experiments were performed in the presence of LiCl. The EC_{50} value for histamine-induced inositol phosphate formation was 4.8 ± 0.2 μM (n = 47). The time course for the accumulation of inositol phosphates in response to stimulation by 0.1 mM histamine was linear for periods up to 40 min (n = 5) (Figure 2). Histamine-induced [^{3}H]-inositol phosphate formation was antagonized by the H_1-selective antagonist, mepyramine (K_d = 6.0 ± 0.7nM, n = 8) (Figure 1). In contrast, the H_2-selective antagonist, tiotidine (10 μM) and H_3-selective antagonist, thioperamide (10 μM) were without significant effect upon the inositol phosphate response to histamine (data not shown, n = 4 for each antagonist).

Histamine-induced desensitization of H_1-mediated inositol phosphate accumulation

Prior exposure of HUVEC to increasing concentrations of histamine (0.1 μM–0.1 mM) for 2 h resulted in concentration-dependent desensitization of the inositol phosphate response

observed following rechallenge with histamine (0.1 mM) (Figure 3a). The IC_{50} for desensitization with histamine was 0.9 ± 0.2 μM ($n = 10$) and the maximum reduction observed following pre-exposure to 0.1 mM histamine was $78 \pm 3.0\%$ ($n = 10$, $P < 0.05$ compared to non-desensitized cells) (Figure 3a). Figure 3b shows the effect of pre-exposure to histamine (0.1 mM) for 2 h upon the inositol phosphate response seen with a subsequent 45 min challenge with increasing concentrations of histamine. Similar experiments performed in the presence (during the 2 h desensitization period) of either thioperamide (10 μM, $n = 3$) or tiotidine (10 μM, $n = 3$) provided no evidence for the involvement of either histamine H_2- or H_3-receptors in the desensitization process. The onset of desensitization was rapid in these experiments and was clearly evident at the first time point measured (10 min) (Figure 4). Furthermore, the time course of the response to histamine (0.1 mM) was markedly different in desensitized cells (compared to control cells) and began to plateau between 15 and 30 min (Figure 2). The amount of [^{3}H]-inositol present in the membrane phospholipid compartment was not significantly altered by prior incubation with histamine (0.1 mM) ($n = 4$).

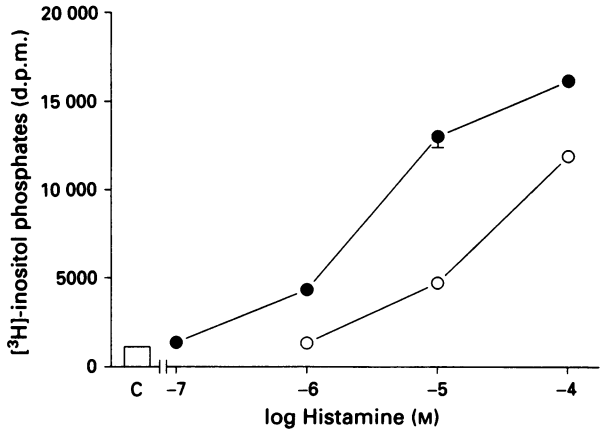


Figure 1 Accumulation of [^{3}H]-inositol phosphates in response to histamine (45 min) in the presence (○) and absence (●) of the H_1-receptor selective antagonist, mepyramine (50 nM) in HUVEC. Each point represents the mean ± s.e.mean of data obtained from a single experiment. Similar results were obtained in seven further experiments.

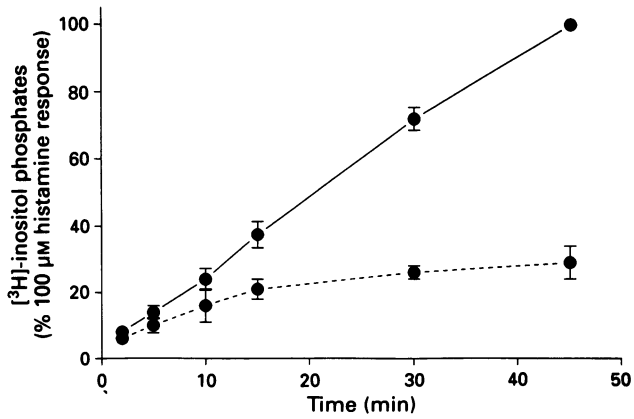


Figure 2 Time course of histamine (0.1 mM) H_1-receptor-mediated [^{3}H]-inositol phosphate accumulation in HUVEC in non-desensitized cells (solid line) and cells previously exposed to histamine (0.1 mM) for 2 h (dashed line). Each point represents the mean ± s.e.mean of data obtained in three separate experiments. Data are expressed as a % of the histamine (0.1 mM) response in naive cells.

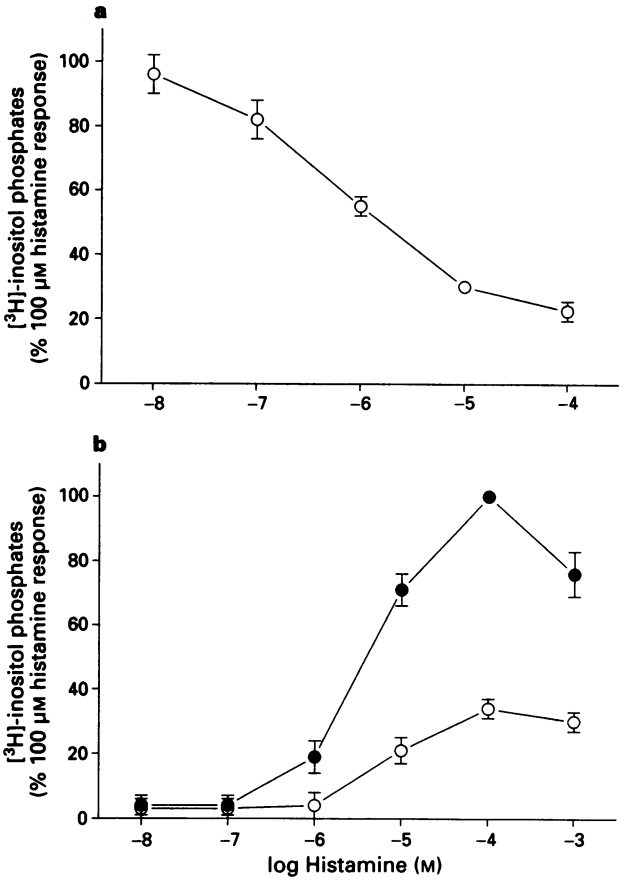


Figure 3 The formation of [^{3}H]-inositol phosphates in response to histamine (0.1 mM, 45 min) in HUVEC following 2 h pre-exposure to a range of concentrations of histamine (a); (b) shows the [^{3}H]-inositol phosphate response to 45 min exposure to a range of concentrations of histamine in control cells (●) and in cells following 2 h pre-exposure to histamine (0.1 mM) (○). Each point represents the mean ± s.e.mean of data obtained from seven (a) and five (b) individual experiments. Data are expressed as a % of the histamine (0.1 mM) response in naive cells.

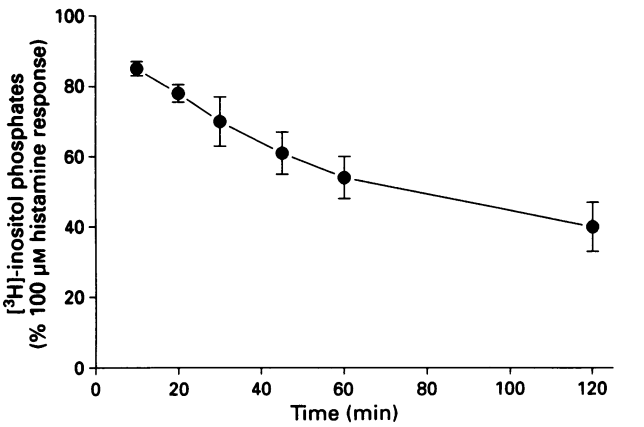


Figure 4 The time course of desensitization of histamine-induced [^{3}H]-inositol phosphate formation in HUVEC. Cells were exposed to 0.1 mM histamine for 10–120 min before replacement of the buffer with Hanks/HEPES containing LiCl. Cells were then rechallenged with 0.1 mM histamine 20 min later and incubations terminated after a further 45 min. Data are mean values (± s.e.mean) from six separate experiments and are expressed as a % of the histamine response in naive cells. Pretreatment with histamine did not significantly alter the basal rate of [^{3}H]-inositol phosphate formation when compared with naive cells (not shown). Data are expressed as % of the histamine (0.1 mM) response in naive cells.

Effect of phorbol dibutyrate upon histamine-induced inositol phosphate formation

The effect of pre-exposure of HUVEC to increasing concentrations of the protein kinase C activator, phorbol dibutyrate (PdBu) for 2 h upon the inositol phosphate response to 0.1 mM histamine is shown in Figure 5a. PdBu pretreatment produced a concentration-dependent reduction ($IC_{50} = 40 \pm 0.2$ nM, max. reduction $= 64 \pm 1.8\%$; $n = 6$, $P < 0.05$) of the inositol phosphate response seen with histamine (0.1 mM). Exposure of HUVEC to the protein kinase C inhibitor, staurosporine (100 nM) prior to, and during, PdBu treatment inhibited the PdBu-induced inhibition of H_1-mediated inositol phosphate formation (Figure 5a). Similar results were obtained when the protein kinase C selective inhibitor, Ro 31-8220 (10 μM) Davis *et al.*, 1989) was used to reverse PdBu-mediated inhibition of histamine-induced inositol phosphate formation in HUVEC (Figure 5b).

Effect of staurosporine and Ro 31-8220 upon desensitization of histamine-induced inositol phosphate formation in HUVEC

Exposure to staurosporine (100 nM) for 1 h prior to, and during histamine pretreatment did not significantly inhibit histamine-induced desensitization of the histamine-induced inositol phosphate response at any concentration examined ($P > 0.05$) (Figure 6a). The non-selective protein kinase inhibitor K252a (1 μM) was also without significant effect on the desensitization of the histamine-induced inositol phosphate response (2 experiments). Pre exposure of HUVEC to Ro 31-8220 (10 μM) for 1 h before and during, histamine pretreatment produced a small but significant inhibition ($15 \pm 2\%$, $P < 0.05$) of histamine-induced desensitization of inositol phosphate formation ($n = 5$) (Figure 6b). The calcium calmodulin kinase II inhibitor KN62 (20 μM: applied 1 h prior to histamine) had no significant effect upon histamine-induced desensitization of the H_1 receptor-mediated inositol phosphate response (Figure 6c).

Effect of histamine pretreatment on the NaF response

Stimulation of HUVEC for 45 min with the G protein activator, NaF (20 mM), induced an inositol phosphate res-

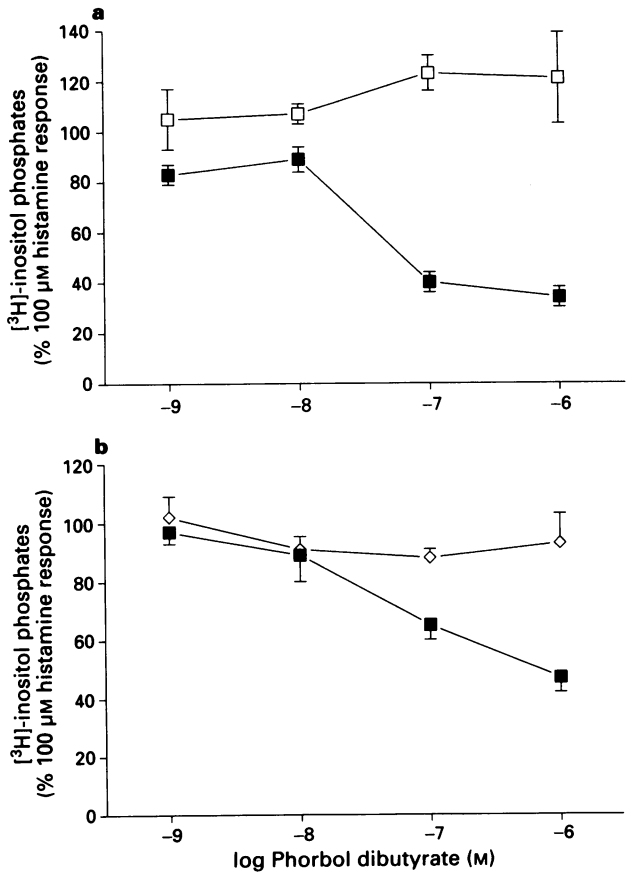


Figure 5 Accumulation of [^{3}H]-inositol phosphates in response to 0.1 mM histamine (45 min) following 2 h pre-incubation with a range of concentrations of phorbol dibutyrate (PdBu) (■), staurosporine (100 nM) plus PdBu (□, a) and Ro 31-8220 (10 μM) plus PdBu (◇, b). Staurosporine or Ro 31-8220 were added 1 h prior to PdBu. Each point represents the mean ± s.e.mean of data obtained from six (a) and three (b) separate experiments. Data are expressed as a % of the histamine (0.1 mM) response in naive cells.

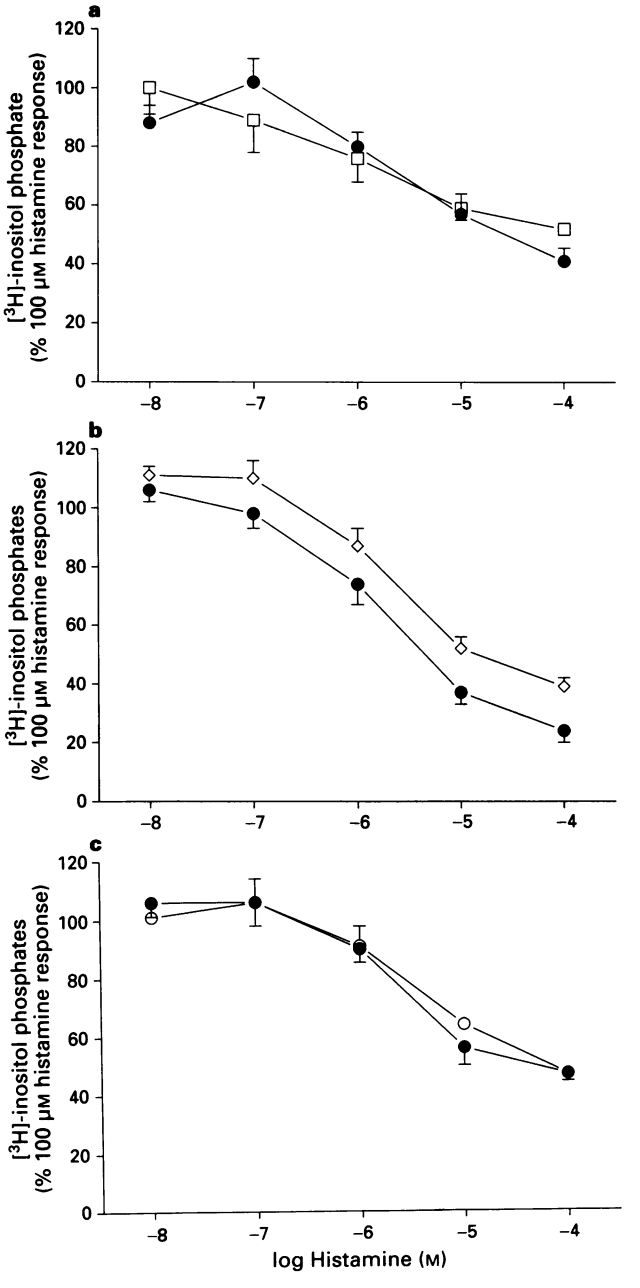


Figure 6 Accumulation of [^{3}H]-inositol phosphates in response to 0.1 mM histamine (45 min) following 2 h pre-incubation with a range of concentrations of histamine (●), staurosporine (100 nM) plus histamine (□, a), Ro 31-8220 (10 μM) plus histamine (◇, b) and KN-62 (20 μM) plus histamine (○, c). Staurosporine, Ro 31-8220 and KN-62 were added 1 h prior to histamine. Each point represents the mean ± s.e.mean of data obtained from four (a), five (b) and three (c) separate experiments. Data are expressed as a % of the histamine (0.1 mM) response in naive cells.

ponse which amounted to 68 ± 5% of the response to histamine (0.1 mM) ($n = 3$). Following pretreatment of cells with histamine (0.1 mM) for 10–120 min, HUVEC were rechallenged for 45 min with either NaF (20 mM) or histamine (0.1 mM). In this series of experiments, prior exposure to 0.1 mM histamine (120 min) produced a 72 ± 1% reduction (compared to control cells) of the response to a subsequent challenge with 0.1 mM histamine, the magnitude of this effect therefore being similar to that seen in previous experiments (see Figure 3a). In contrast, histamine pretreatment (10–120 min) failed to alter significantly the response to subsequent challenge with NaF (Figure 7).

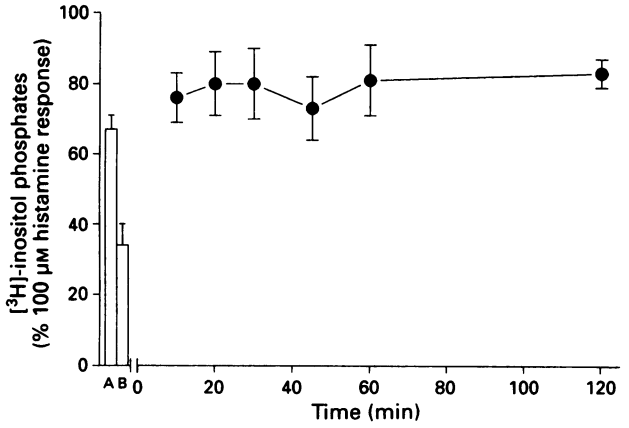


Figure 7 Inositol phosphate formation in response to stimulation with 20 mM NaF (45 min) in non-desensitized HUVEC (column A) as compared with the response to 20 mM NaF in HUVEC which have been pre-exposed at various time points (1–120 min) to histamine (0.1 mM) (●). The column marked B represents histamine-induced [3H]-inositol phosphate formation (45 min, 0.1 mM) following 2 h pre-exposure to 0.1 mM histamine. Each point represents the mean ± s.e.mean of three separate experiments. Data are expressed as a % of the histamine (0.1 mM) response in naive cells.

Lack of effect of forskolin or nitroprusside preincubation on histamine-induced desensitization

Prior incubation of HUVEC with nitroprusside (10 μM) had no significant effect upon the response to a subsequent challenge with histamine (Figure 8a). Prior exposure to forskolin (10 μM) failed to modulate the histamine inositol phosphate response in HUVEC (Figure 8b). In addition, prior exposure to the stable, membrane permeant analogue of cyclic AMP, 8-bromo cyclic AMP (1 mM) failed to inhibit the response to a subsequent histamine challenge ($n = 4$, $P > 0.05$, data not shown) implying that cyclic AMP does not play a major role in desensitization of histamine H_1 receptor-induced inositol phosphate formation in HUVEC.

Effect of prior exposure to thrombin upon histamine-induced inositol phosphate formation

Prior exposure of HUVEC to thrombin (1 u ml^{-1}) for 2 h produced a small (20 ± 3.3%) reduction in the subsequent response to 0.1 mM histamine ($n = 7$, $P < 0.05$). However,

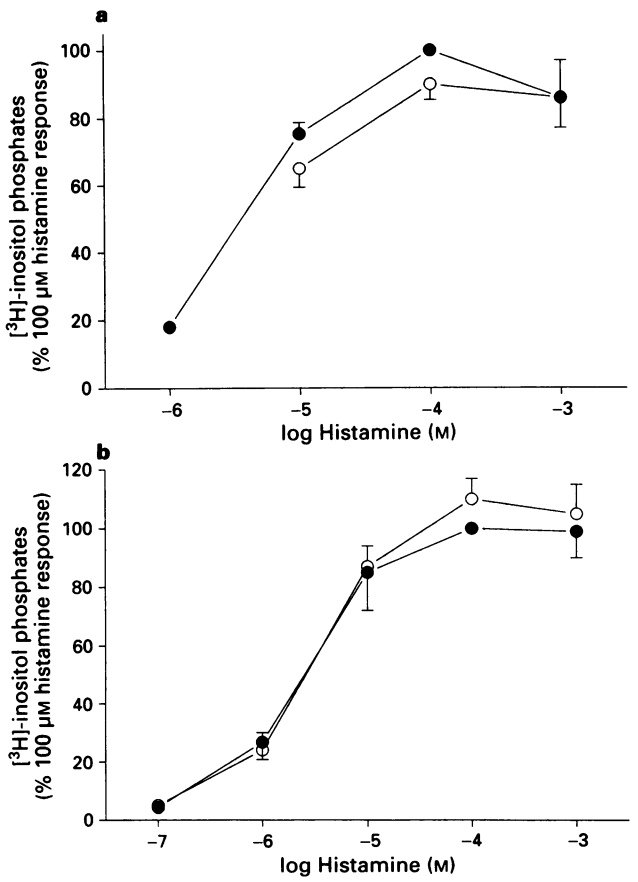


Figure 8 Accumulation of [3H]-inositol phosphates in response to histamine (●) following pre-incubation with nitroprusside (10 μM, 20 min, ○, a) or forskolin (10 μM, 2 h, ○, b). Each point represents the mean ± s.e.mean of data obtained from three separate experiments. Data are expressed as a % of the histamine (0.1 mM) response in naive cells.

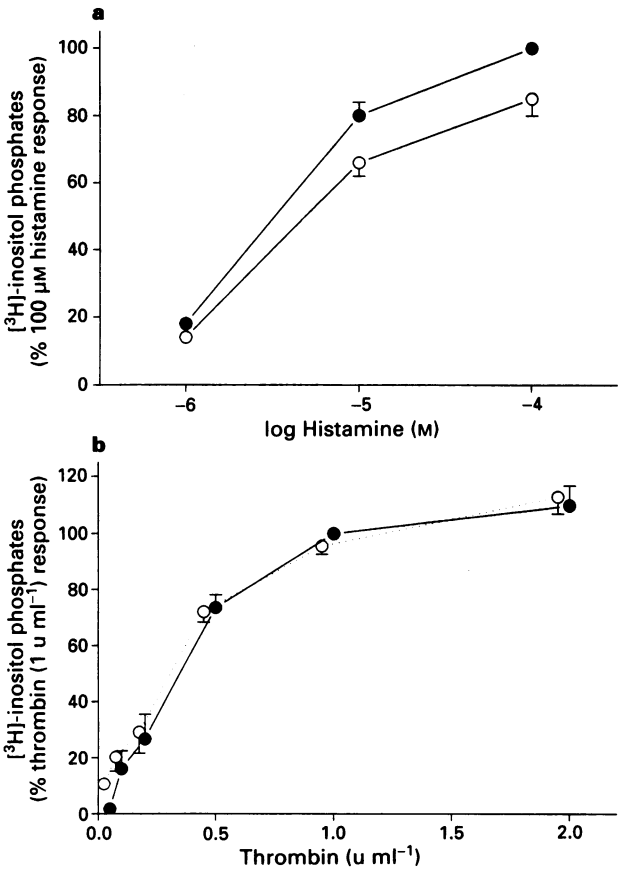


Figure 9 Accumulation of [3H]-inositol phosphates in response to histamine (●) following 2 h pre-incubation with thrombin (○) (1 u ml^{-1}, a); (b) shows the effect of prior incubation of HUVEC with histamine (0.1 mM, ○) upon the accumulation of [3H]-inositol phosphates in response to thrombin (1 u ml^{-1}) (●). Each point represents the mean ± s.e.mean of data obtained from seven (a) or four (b) separate experiments. Data are expressed as a % of the histamine (0.1 mM) response (a) or thrombin (1 u ml^{-1}) response (b) in naive cells.

exposure of cells to histamine (0.1 mM) during prelabelling had no significant effect upon the thrombin response (Figure 9b) indicating that histamine-induced desensitization of the H_1-receptor is homologous in HUVEC.

Discussion

In this study we have examined some of the mechanisms underlying the regulation of histamine-induced inositol phosphate responses in HUVEC following moderate to long term exposure to agonist. Histamine is a potentially important local mediator in HUVEC which causes a number of physiologically relevant effects including increased vascular permeability (Rotrosen & Gallin, 1986) and stimulation of the release of prostacyclin (Hallam *et al.*, 1988b), von Willebrand factor (Hamilton & Sims, 1987) and endothelium-derived relaxing factor (Chaudhuri *et al.*, 1991). As has been previously described, histamine was a potent inducer of inositol phosphate formation in these cells (Lo & Fan, 1987; Resink *et al.*, 1987; Pollock *et al.*, 1988). This effect appeared to be mediated through the H_1 receptor subtype because the H_1-selective antagonist, mepyramine, inhibited histamine-induced inositol phosphate formation with a K_d of 6 nM whereas appropriate concentrations of the H_2 and H_3 selective antagonists tiotidine (10 μM) and thioperamide (10 μM) did not produce significant effects upon this response. The K_d value for mepyramine is similar to that previously reported for other responses mediated through the H_1 receptor subtype (Hill, 1990).

Prior treatment of HUVEC with a maximally effective concentration of histamine (0.1 mM) for 10–120 min produced a marked and significant attenuation of the inositol phosphate response to a subsequent stimulation by histamine. This effect was relatively rapid in onset (an apparent desensitization could be observed at the earliest time measured i.e. 10 min) and could also be produced by low concentrations of agonist (IC_{50} 0.9 μM). Interestingly, the IC_{50} for this effect (0.9 μM) was lower than the EC_{50} for histamine-induced inositol phosphate formation itself (4.8 μM). This suggests that there may be a significant spare receptor reserve for the desensitization response in HUVEC. The desensitization produced by histamine pretreatment was not affected by antagonism of histamine H_2- and H_3-receptors by tiotidine (10 μM) and thiopermide (10 μM) respectively. Thus, the differences in IC_{50} and EC_{50} values could not be due to the involvement of H_2- or H_3-receptors in the desensitization process.

There are a number of possible mechanisms which could underlie this desensitization process. We have considered four possibilities: (a) that the diacylglycerol, which is produced as a consequence of phospholipase C activation, is able to feedback and inhibit H_1-receptor-mediated inositol phospholipid hydrolysis via the activation of protein kinase C; (b) that a cyclic AMP-dependent protein kinase A mechanism is involved as a consequence of the histamine-induced release and subsequent action of prostacyclin on adenylyl cyclase (Carter *et al.*, 1988); (c) that calcium/calmodulin dependent kinase mediates desensitization following the rise in $[Ca^+]_i$ which accompanies H_1-receptor activation in these cells (Rotrosen & Gallin, 1986; Hallam *et al.*, 1988a,b; Hamilton & Sims, 1987; Pollock *et al.*, 1988; Carter *et al.*, 1988; or (d) that protein kinase G has a role following the histamine-induced synthesis and action of nitric oxide (endothelium-derived relaxant factor) (Chaudhuri *et al.*, 1991).

Prior exposure of HUVEC to the adenylyl cyclase activator forskolin or to the membrane permeant analogue of cyclic AMP, dibutyryl cyclic AMP, failed to modulate significantly histamine-induced inositol phosphate formation suggesting that H_1-receptor-mediated desensitization may not be mediated by cyclic AMP. Similarly, the nitric oxide donor, and cyclic GMP elevator, sodium nitroprusside was not able to modify H_1-receptor-mediated phospholipase C activity. In contrast, prior exposure of HUVEC to the phorbol ester, phorbol dibutyrate (PdBu), produced a marked inhibition of histamine-induced inositol phosphate formation. The effect of PdBu was itself reversed by the protein kinase C inhibitors, staurosporine and Ro 31-8220. However, staurosporine (0.1 μM) did not modulate histamine-induced desensitization of H_1 receptor mediated inositol phosphate formation, and, although the more selective protein kinase C inhibitor Ro 31-8220 (10 μM) (Davis *et al.*, 1989) appeared to produce a small reversal (15%) of desensitization, this effect was markedly smaller than the effect of Ro 31-8220 upon PdBu-induced inhibition of the histamine response. These results suggest that protein kinase C plays only a minor role if any in the histamine-induced desensitization process.

Staurosporine is acknowledged to be a potent but rather non-selective inhibitor of protein kinase C (Ruegg & Burgess, 1989) and is in addition a relatively potent inhibitor of protein kinases A and G (Tamaoki *et al.*, 1986; Schachtele *et al.*, 1988; Tischler *et al.*, 1990). Consequently, the lack of effect of both staurosporine and the similarly non-selective kinase inhibitor K-252a (1 μM) (Kase *et al.*, 1987; Ruegg & Burgess, 1989; Tischler *et al.*, 1990) on histamine-induced desensitization supports the data obtained with forskolin and sodium nitroprusside, and appears to rule out a role for either cyclic AMP or cyclic GMP dependent kinases in this process. Interestingly, the selective Ca^+/calmodulin dependent kinase II inhibitor, KN-62 (20 μM) (Tokumitsu *et al.*, 1990) was also without effect on histamine-induced desensitization.

Desensitization appears to occur at the level of the receptor itself, rather than through a post-receptor mechanism (e.g. desensitization of phospholipase C), because prior exposure to histamine failed to modulate the inositol phosphate response to the G protein activator NaF. Prior exposure of HUVEC to thrombin (1 u ml^{-1}) produced only a small (20%) reduction in the subsequent response to 0.1 mM histamine. This finding suggests that thrombin may produce some degree of heterologous desensitization of the H_1 receptor via the production and action of diacylglycerol and protein kinase C. The lack of effect of histamine pretreatment on the subsequent responses to thrombin and NaF also confirms that there has been no marked change in the specific activity or availability of [^{3}H]-inositol phospholipids during the desensitization process; a finding which was confirmed by measurements of [^{3}H]-inositol incorporation into the membrane phospholipids. Also, because the inositol phosphate responses to thrombin, histamine and NaF are of similar magnitude, it seems unlikely that NaF and thrombin are acting predominantly on cells that are not affected by histamine. Furthermore, Pollock *et al.* (1988) have shown that thrombin and histamine act on the same population of HUVEC and Jacob *et al.* (1988) have reported that the majority of HUVEC respond to histamine. Taken together these data suggest that desensitization of histamine-induced inositol phosphate formation in HUVEC occurs through an H_1-receptor specific mechanism, and that this effect is not due to alteration in the specific activity of the membrane phospholipid pool following stimulation in the presence of LiCl. One possible explanation is that the H_1-receptor can be desensitized by a kinase analogous to one of the βARK family responsible in part for mediating β-adrenoceptor desensitization (Benovic *et al.*, 1986; Lohse *et al.*,1990).

Desensitization of histamine H_1-receptor-mediated intracellular events has been reported in many other cell and tissue types including neuroblastoma cell lines (Taylor & Richelson, 1979), HeLa cells (Bristow & Zamani, 1993a), guinea-pig cortex (Bristow *et al.*, 1993) and smooth muscle (Donaldson & Hill, 1985; Lurie *et al.*, 1985; Brown *et al.*, 1986; Leurs *et al.*, 1990; Daykin *et al.*, 1993). Qualitatively, the regulation of H_1 receptor mediated inositol phosphate formation in HUVEC appears to have similar characteristics to those observed in some other cell types. For example, the regulation of histamine-induced inositol phosphate formation in

HUVEC by phorbol esters, and the reversal of this effect by inhibitors of protein kinase C such as staurosporine, displays very similar characteristics to the responses seen in cultured airway smooth muscle cells, HeLa cells and DDT_1MF-2 cells (Bristow & Zamani, 1993; Daykin *et al.*, 1993; Hamilton & Sims, 1987; Dickenson & Hill, 1993). In most of these cell systems, however, the histamine-induced H_1-receptor desensitization appears to be independent of protein kinase C. However the role of other protein kinases has not been investigated in these other cell types.

Long term exposure of G-protein coupled receptors to agonist can result in reduced responses because of down regulation, involving loss of receptors from the cell. This can potentially be due to internalisation of receptor and increase receptor breakdown or to a reduction in the rate of receptor synthesis. We cannot exclude the possibility that down regulation could account for some of the reduced responsiveness seen following prior agonist exposure in HUVEC. However, down regulation usually occurs following exposure to agonist for periods longer than 2 h (Huganir & Greengard, 1990), and hence it seems likely that the majority of the reduction in responsiveness observed following prior histamine exposure in HUVEC is due to desensitization. From Figure 3, it is clear that desensitization reduced the maximum response to histamine. This could be due to phosphorylation of the receptor and uncoupling from the G-protein necessary for functional responses; however, it is also possible that receptor sequestration could have reduced the number of receptors available at the cell surface. Unfortunately, binding studies with [^{3}H]-mepyramine would be unlikely to help resolve this issue due to the physicochemical properties of this ligand which has access to both internalised and cell surface receptors (Bristow *et al.*, 1993; Hill, 1990).

In conclusion, therefore, we have shown that histamine H_1-receptor-mediated inositol phopholipid hydrolysis in cultured HUVEC can be attenuated by prior exposure of HUVEC to histamine. This effect occurs at the level of the receptor itself, is homologous, and does not appear to be mediated by activation of Ca^{2+}/calmodulin dependent kinase II or protein kinases A, G or C.

I.P.H. is supported by a National Asthma Campaign Senior Research Fellowship.

References

BARAK, L.S., TIBERI, M., FRREDMAN, N.J., KWATRA, M.M., LEFKOWITZ, R.J. & CARON, M.G. (1994). A highly conserved tyrosine residue in G-protein-coupled receptors is required for agonist-mediated β_2-adrenergic receptor sequestration. *J. Biol. Chem.*, **269**, 2790–2795.

BENOVIC, J.L., KUHN, H., WEYARD, I., CODINA, J., CARON, M.G. & LEFKOWITZ, R.J. (1987). Functional desensitization of the isolated beta-adrenergic receptor by the beta-adrenergic receptor kinase: potential role of an analog of the retinal protein arrestin (48kDa protein). *Proc. Natl. Acad. Sci. U.S.A.*, **84**, 8879–82.

BENOVIC, J.L., STRASSER, R.H., CARON, M.G. & LEFKOWITZ, R.J. (1986). Beta adrenergic receptor kinase: indentification of a novel protein kinase that phosphorylates the agonist-occupied form of the receptor. *Proc. Natl. Acad. Sci. U.S.A.*, **83**, 2797–801.

BERRIDGE, M.J. (1987). Inositol trisphosphate and diacylglycerol: two interacting second messengers. *Annu. Rev. Biochem.*, **56**, 159–193.

BRISTOW, D.R., BANFORD, P.C., BAJUSZ, I., VEDAT, A. & YOUNG, J.M. (1993). Desenitization of histamine H_1-receptor-mediated inositol phosphate accumulation in guinea pig cerebral cortex slices. *Br. J. Pharmacol.*, **110**, 269–274.

BRISTOW, D.R., & ZAMANI, M.R. (1993). Desensitization of histamine H_1-receptor-mediated inositol phosphate production in HeLa cells. *Br. J. Pharmacol.*, **109**, 353–359.

BROWN, D.R., PRENDIVILLE, P. & CAIN, C. (1986). α_1-adrenergic and H_1-histamine receptor control of intracellular Ca^{2+} in a muscle cell line: the influence of prior agonist exposure on receptor on receptor responsiveness. *Mol. Pharmacol.*, **29**, 531–539.

CARTER, T.D., HALLAM, T.J., CUSACK, N.J. & PEARSON, J.D. (1988). Regulation of P2-purinoceptor-mediated prostacyclin release from human endothelial cells by cytoplasmic calcium concentration. *Br. J. Pharmocol.*, **95**, 1181–1190.

CHAUDHURI, G, BUGA, G.M., GOLD, M.E., WOOD, K.S. & IGNARRO, L.J. (1991). Characterisation and actions of human umbilical endothelium derived relaxing factor. *Br. J. Pharmacol.*, **102**, 331–336.

DAVIS, P.D., HILL, C.H., KEECH, E., LAWTON, G., NIXON, J.S., SEDGWICK, A.D., WADSWORTH, J., WESTMACOTT, D. & WILKINSON, S.E. (1989). Potent selective inhibitors of protein kinase C. *FEBS Lett.*, **259**, 61–63.

DAYKIN, K., WIDDOP, S. & HALL, I.P. (1993). Control of histamine-induced inositol phospholipid hydrolysis in cultured human tracheal smooth muscle cells. *Eur. J. Pharmacol. (Mol. Pharmacol.)*, **246**, 135–140.

DICKENSON, J.M. & HILL, S.J. (1993). Homologous and heterologous desensitization of histamine H_1- and ATP-receptors in the smooth muscle cell line, DDT1MF-2: the role of protein kinase C. *Br. J. Pharmacol.*, **110**, 1449–1456.

DONALDSON, J. & HILL, S.J. (1985). Histamine-induced inositol phospholipid breakdown in the longitudinal smooth muscle of guinea-pig ileum. *Br. J. Pharmacol.*, **85**, 499–512.

HADCOCK, J.R., WANG, H. & MALBON, C.C. (1989). Agonist-induced destabilisation of beta-adrenergic receptor mRNA *J. Biol. Chem.*, **264**, 19928–33.

HALLAM, T.J., JACOB, R. & MERRITT, J.E. (1988a). Evidence that agonists stimulate bivalent-cation influx into human endothelial cells. *Biochem. J.*, **255**, 179–184.

HALLAM, T.J., JACOB, R. & NEEDHAM, L.A. (1988b). Thrombin-stimulated elevation of human endothelial-cell cytoplasmic free calcium concentration causes prostacyclin production *Biochem. J.*, **251**, 243–249.

HAMILTON, K.K. & SIMS, P.J. (1987). Changes in cytosolic Ca^{2-} associated with von Willebrand Factor release in human endothelial cells exposed to histamine: study of microcarrier cell monolayers using the fluorescent probe indo-1 *J. Clin. Invest.*, **79**, 600–608.

HAUSDORFF, M., BOUVIER, M., O'DOWD, B.F., IRONS, G.P., CARON, M.G. & LEFKOWITZ, R.J. (1989). Phosphroylation sites on two domains of the beta 2-adrenergic receptor are involved in distinct pathways of receptor desensitization *J. Biol. Chem.*, **264**, 12657–65.

HAUSDORFF, W.P., CARON, M.G. & LEFKOWITZ, R.J. (1990). Turning off the signal: desensitization of beta-adrenergic receptor function. *FASEB. J.*, **4**, 2881–2889.

HILL, S.J. (1990). Distribution, properties, and functional characteristics of three classes of histamine receptor. *Pharmacol. Rev.*, **42**, 45–83.

HUGANIR, R.L. & GREENGARD, P. (1990). Regulation of neurotransmitter receptor desensitization by protein phosphroylation. *Neuron.*, **5**, 555–567.

INGLESE, J., FREEDMAN, N.J., KOCH, W.J. & LEFKOWITZ, R.J. (1993). Structure and mechanism of the G-protein-coupled receptor kinases. *J. Biol. Chem.*, **268**, 23735–23738.

JACOB, R., MERRITT, J.E., HALLAM, T.J. & RINK, T.J. (1988). Repetitive spikes in cytoplasmic calcium evoked by histamine in human endothelial cells. *Nature*, **335**, 40–45.

JAFFE, E.A., NACHMAN, R.L., BECKER, C.G. & MINICK, G.R. (1973). Culture of human endothelial cells derived from umbilical veins. *J. Clin. Invest.*, **52**, 2745–2756.

KASE, H., IWAHASHI, K., NAKANISHI, S., MATSUDA, Y., YAMADA, K., TAKAHASHI, M., MURAKATA, C., SATO, A. & KANEKO, M. (1987). K-252 compounds, novel and potent inhibitors of protein kinase C and cyclic nucleotide-dependent protein kinases. *Biochem. Biophys. Res. Commun.*, **142**, 436–440.

KLUEPPELBERG, U.G., GATES, L.K., GORELICK, F.S. & MILLER, L.J. (1991). Agonist-regulated phosphorylation of the pancreatic cholecystokinin receptor. *J. Biol. Chem.* **266**, 2403–2408.

KOLBILKA, B. (1992). Adrenergic receptors as models for G protein-coupled receptors. *Annu. Rev. Neurosci.*, **15**, 87–114.

LEEB-LUNDBERG, L.M.F., COTECCHIA, S., DEBLASI, A., CARON, M.G. & LEFKOWITZ, R.J. (1987) Regulation of adrenergic receptor function by phosphorylation. Agonist-promoted desensitization and phosphorylation of alpha 1-adrenergic receptors coupled to inositol phospholipid metabolism in DDT1 MF-2 smooth muscle cells. *J. Biol. Chem.*, **262**, 3098–3105.

LEFKOWITZ, R.J. (1993). G-protein-coupled receptor kinases *Cell*, **74**, 409–412.

LEURS, R., SMIT, M.J., BAST, A. & TIMMERMAN, H. (1990). Different profiles of desensitization dynamics in guinea-pig jejunal smooth muscle after stimulation with histamine and methacholine. *Br. J. Pharmacol.*, **101**, 881–888.

LO, W.W.Y. & FAN, T.P.D. (1987). Histamine stimulates inositol phosphate accumulation via the H_1-receptor in cultured human endothelial cells. *Biochem. Biophys Res. Commun.*, **148**, 47–53.

LOHSE, M.J., ANDEXINGER, S., PITCHER, J., TRUKAWINSKI, S. CODINA, J., FAURE, J.-P., CARON, M.G. & LEFKOWITZ, R.J. (1992). Receptor-specific desensitization with purified proteins: Kinase dependence and receptor specificity of β-arrestin and arrestin in the β_2-adrenergic receptor and rhodopsin systems. *J. Biol. Chem.*, **267**, 8558–8564.

LOHSE, M.J., BENOVIC, J.L., CARON, M.G. & LEFKOWITZ, R.J. (1990). Multiple pathways of rapid β_2-adrenergic receptor desensitization. *J. Chem.*, **265**, 3202–3209.

LURIE, K.G., TSUJIMOTO, G. & HOFFMAN, B.B. (1985). Desensitization of alpha-1 adrenergic receptor-mediated vascular smooth muscle contraction. *J. Pharmacol. Exp. Ther.*, **234**, 147–52.

OSTROWSKI, J., KJELSBERG, M.A., CARON, M.G. & LEFKOWITZ, R.J. (1992). Mutagenesis of the β_2-adrenergic receptor: How structure elucidates function. *Annu. Rev. Pharmacol. Toxicol.*, **32**, 167–183.

POLLOCK, E.K., WREGGET, K.A. & IRVINE, R.F. (1988). Inositol phosphate production and calcium mobilization in human umbilical-vein endothelial cells stimulated by thrombin and histamine. *Biochem J.*, **256**, 371–376.

RESINK, T.J., GRIGORIAN, G.Y., MOLDABAEVA, A.K., DANILOV, S.M. & BUHLER, F.R. (1987). Histamine-induced phosphoinositide metabolism in cultured human umbilical vein endothelial cells. Association with thromboxane and prostacyclin release. *Biochem. Biophys. Res. Commun.*, **144**, 438–446.

ROTROSEN, D. & GALLIN, J.I. (1986). Histamine type 1 receptor occupancy increases endothelial cytosolic calcium, reduces F-actin and promotes albumin diffusion across cultured endothelial monolayers. *J. Cell. Biol.*, **103**, 2379–2387.

RUEGG, U.T. & BURGESS, G.M. (1989). Staurosporine, K-252 and UCN-01, potent but nonspecific inhibitors of protein kinases. *Trends Pharmacol. Sci.*, **10**, 162–164.

SCHACHTELE, C., SEIFORT, R. & OSSWALD, H. (1988). Stimulus-dependent inhibition of platelet aggregation by the protein kinase C inhibitors polymixim b, H-7 and staurosporine. *Biochem. Biophys. Res. Commun.* **151**, 542–547.

TAMAOKI, T., NOMOTO, H., TAKAHASHI, I., KATO, Y., MORIMOTO, M. & TOMITA, F. (1986). Staurosporine, a potent inhibitor of phospholipid/Ca^{2+} dependent protein kinase. *Biochem. Biophys. Res. Commun.* **135**, 397–402.

TAYLOR, J.E. & RICHELSON, E. (1979). Desensitization of histamine H_1-receptor-mediated cyclic GMP formation in mouse neuroblastoma cells. *Mol. Pharmacol.*, **15**, 462–471.

TISCHLER, A.S., RUZICKA, L.A. & PERLMAN, R.L. (1990). Mimicry and inhibition of nerve growth factor effects: interactions of staurosporine, forskolin, and K-252a in PC12 cells and normal rat chromaffin cells in vitro. *J. Neurochem.*, **55**, 1159–1165.

TOBIN, A.B., LAMBERT, D.G. & NAHORSKI, S.R. (1993). Rapid desensitization of muscarinic m3 receptor-stimulated polyphosphoinositide responses. *Mol. Parmacol.*, **42**, 1042-1048.

TOBIN, A.B. & NAHORSKI, S.R. (1993). Rapid agonist-mediated phosphorylation of m3-muscarinic receptors revealed by immunoprecipitation. *J. Biol. Chem.*, **268**, 9817–9823.

TOKUMITSU, H., CHIJIWA, T., HAGINARA, M., MIZUTANI, A., TERASAWA, M. & HIDAKA, H. (1990). 1-[N,O-*bis*(S-isoquinolinesulfonyl)-N-methyl-L-tyrosyl]-4-phenylpiperaxine, a specific inhibitor of Ca^{2+}/calmodulin-dependent protein kinase II. *J. Biol. Chem.*, **265**, 4315–4320.

WOJCIKIEWICZ, R.J.H., TOBIN, A.B. & NAHORSKI, S.R. (1983). Desensitization of cell signalling mediated by phosphoinositidase C. *Trends Pharmacol. Sci.*, **14**, 279–285.

YU, S.S., LEFKOWITZ, R.J. & HAUSDORFF, W.P. (1993). β-adrenergic receptor sequestration: A potential mechanism of receptor desensitisation. *J. Biol. Chem.*, **268**, 337–341.

(Received March 23, 1994
Revised June 23, 1994
Accepted July 14, 1994)

Br. J. Pharmacol. (1994), **113**, 831–838 © Macmillan Press Ltd, 1994

Effects of dihydropyridine calcium antagonists on rat midbrain dopaminergic neurones

*[1]Nicola B. Mercuri, *Antonello Bonci, *Paolo Calabresi, *Francesca Stratta, *Alessandro Stefani & *†Giorgio Bernardi

*Clinica Neurologica, Dip. Sanita' Pubblica, Universita' di Roma Tor Vergata, Via O. Raimondo, 00173, Roma, Italy and †IRCCS, Clinica Santa Lucia

1 The effects of the dihydropyridine calcium channel antagonists, nifedipine and nimodipine (300 nM–30 μM) were tested *in vitro* on intracellularly recorded dopaminergic neurones in the rat ventral mesencephalon.

2 Bath applied nifedipine and nimodipine inhibited in a concentration-dependent manner the spontaneous firing discharge of the action potentials, whereas, the dihydropyridine calcium channel agonist, Bay K 8644 increased the firing rate.

3 Pacemaker oscillations and bursts of action potentials were produced by loading the cells with caesium. Nifedipine and nimodipine reduced the rate and the duration of the caesium-induced membrane oscillations and decreased the number of action potentials in a burst. During the blockade of potassium currents the dopaminergic neurones often developed a prolonged (100–800 ms) afterdepolarization that was also inhibited by dihydropyridines.

4 The spontaneous discharge of calcium spikes was also inhibited by both dihydropyridine calcium antagonists. The apparent input resistance and the level of membrane potential were not affected by the dihydropyridine calcium antagonists.

5 If the action potential duration was less than 150 ms the shape of the spike was not clearly influenced by both calcium antagonists. However, when the duration of the action potential was longer than 150–200 ms due to the intracellular injection of caesium ions plus the extracellular application of tetraethylammonium (10–50 mM), both nifedipine and nimodipine reversibly shortened the plateau potential.

6 It is suggested that nifedipine and nimodipine depress the rhythmic and bursting activity of the dopaminergic cells and shorten the calcium action potential by blocking dihydropyridine-sensitive high-threshold calcium currents.

Keywords: Nifedipine; nimodipine; Bay K 8644; substantia nigra; ventral tegmental area; intracellular electrophysiological recordings; calcium

Introduction

The regular pacemaker-like electrical activity of dopaminergic cells in slices of the ventral mesencephalon is highly dependent on a set of intrinsic membrane conductances (Silva & Bunney, 1988; Lacey *et al.*, 1989; Grace, 1991), which should make them capable of rhythmic firing even in the absence of synaptic inputs (Hainsworth *et al.*, 1991). Furthermore, it has recently been reported that the rhythmic pattern of firing in these cells could be transformed in a bursting one under particular conditions (e.g. K^+ channels blockade by the extracellular application of apamin, Shepard & Bunney, 1991).

Several subtypes of calcium channels (L, N, T and P) have already been characterized at neuronal level (Tsien *et al.*, 1991). Among them, it has been clearly demonstrated that the L-type channels are sensitive to agonists and antagonists of the dihydropyridine class (Bellmann *et al.*, 1983; Greenberg *et al.*, 1984; Gahwiler & Brown, 1987; Regan *et al.*, 1991; Sayer *et al.*, 1993), whereas T, N and P type channels are almost unaffected by these agents. The role of the different types of calcium channels in regulating the functioning of the dopaminergic cells has not yet been fully investigated. It is interesting to note that the substantia nigra has a high density of nitrendipine (a dihydropyridine antagonist) binding sites which are reduced in patients with Parkinson's disease (Nishino *et al.*, 1986). In addition, dihydropyridine Ca^{2+}-channel antagonists have recently been reported to inhibit the firing rate of mesencephalic dopaminergic cells (Ugedo *et al.*, 1988; Nedergaard *et al.*, 1993). In order to study further the role of the dihydropyridine-sensitive calcium currents on the spontaneous rhythmic and bursting firing rate and on the shape of the action potentials, we applied the organic Ca^{2+} channel antagonists, nifedipine and nimodipine to midbrain dopaminergic cells intracellularly recorded *in vitro* in a rat brain slice preparation.

[1] Author for correspondence.

Methods

Preparation of the tissue

A detailed description of the methods has been published elsewhere (Lacey *et al.*, 1989; Mercuri *et al.*, 1991). Albino Wistar rats (150–300 g) (Morini, Reggio Emilia) were anaesthetized with ether and killed by a blow to the chest. The brain was removed and horizontal slices (thickness 300 μm) were cut by a vibratome starting from the ventral surface of the midbrain. A single slice containing the substantia nigra and the ventral tegmental area was then transferred to a recording chamber and completely submerged in an artificial cerebrospinal fluid warmed to 35°C. The perfusing solution contained (mM): NaCl 126, KCl 2.5, $MgCl_2$ 1.2, NaH_2PO_4 1.2, $CaCl_2$ 2.4, glucose 11, $NaHCO_3$ 25, gassed with 95% O_2 and 5% CO_2. In low-sodium experiments (20–40% of control) NaCl was replaced by equimolar choline chloride and scopolamine (10 μM) was added to avoid cholinergic effects. Zero calcium solutions were obtained by replacing $CaCl_2$

with $MgCl_2$ (10–30 mM). When $CoCl_2$ was added to the solution NaH_2PO_4 was omitted. The ventral tegmental area (VTA) and the substantia nigra pars compacta (SN) were identified with a dissecting microscope as the regions medial (VTA), rostral and caudal (SN) to the medial terminal nucleus of the accessory optic tract.

Recordings

The recording electrodes (Clark 1.5 mm, thick wall), pulled by a Narishige vertical puller, were filled with 2 M KCl or 2 M CsCl and had a tip resistance of 40–80 MΩ. The signals were obtained by an amplifier (Axoclamp-2A, Axon Instruments) and were displayed on a pen recorder (Gould 2400 S) or saved on a tape recorder (Biologic) for off-line analysis. Data were presented as a mean ± s.e.mean.

Drugs

Drugs were bath-applied via a three-way tap system. Complete exchange of the bath solution occurred in about 1 min. The following drugs were used: dopamine hydrochloride, tetraethylammonium chloride (TEA), tetrodotoxin (TTX), all of which were dissolved in water and were obtained from Sigma. Nifedipine, nimodipine and Bay K 8644 (methyl 1,4-dihydro-2, 6-dimethyl-3-nitro-4-(2-trifluoromethylphenyl)-pyridine-5-carboxylate) were obtained from Bayer. They were dissolved in 100% ethanol before dilution in the external solution. The final ethanol concentration in all test and control solutions ranged between 0.1 and 0.3%. These concentrations of ethanol did not produce *per se* any detectable electrophysiological effect on the dopaminergic cells. The lights were dimmed throughout the experiments to prevent inactivation of the dihydropyridines.

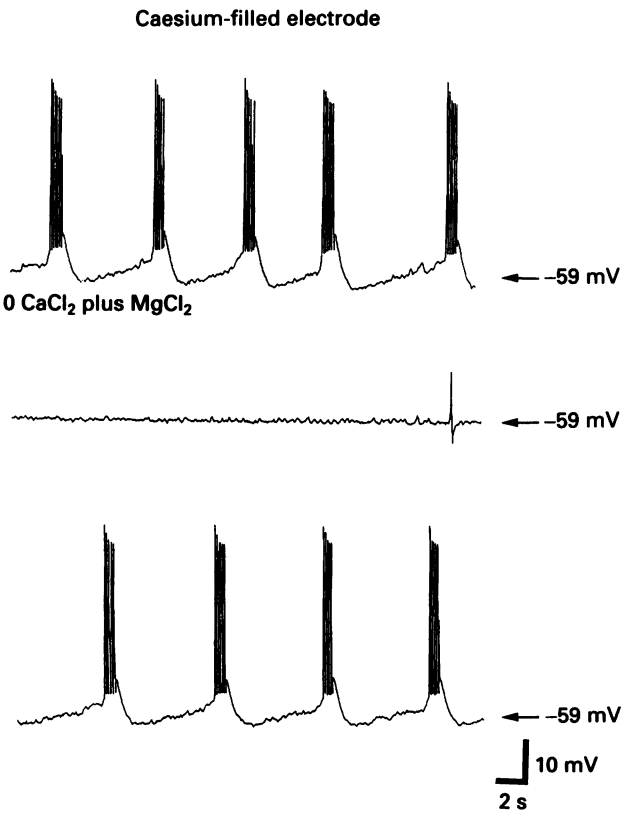


Figure 1 The caesium-induced burst firing is calcium-dependent. Oscillographic traces showing the reversible depressant effect of a solution with nominally no calcium on the bursting activity induced by the intracellular diffusion of caesium ions in a dopaminergic neurone.

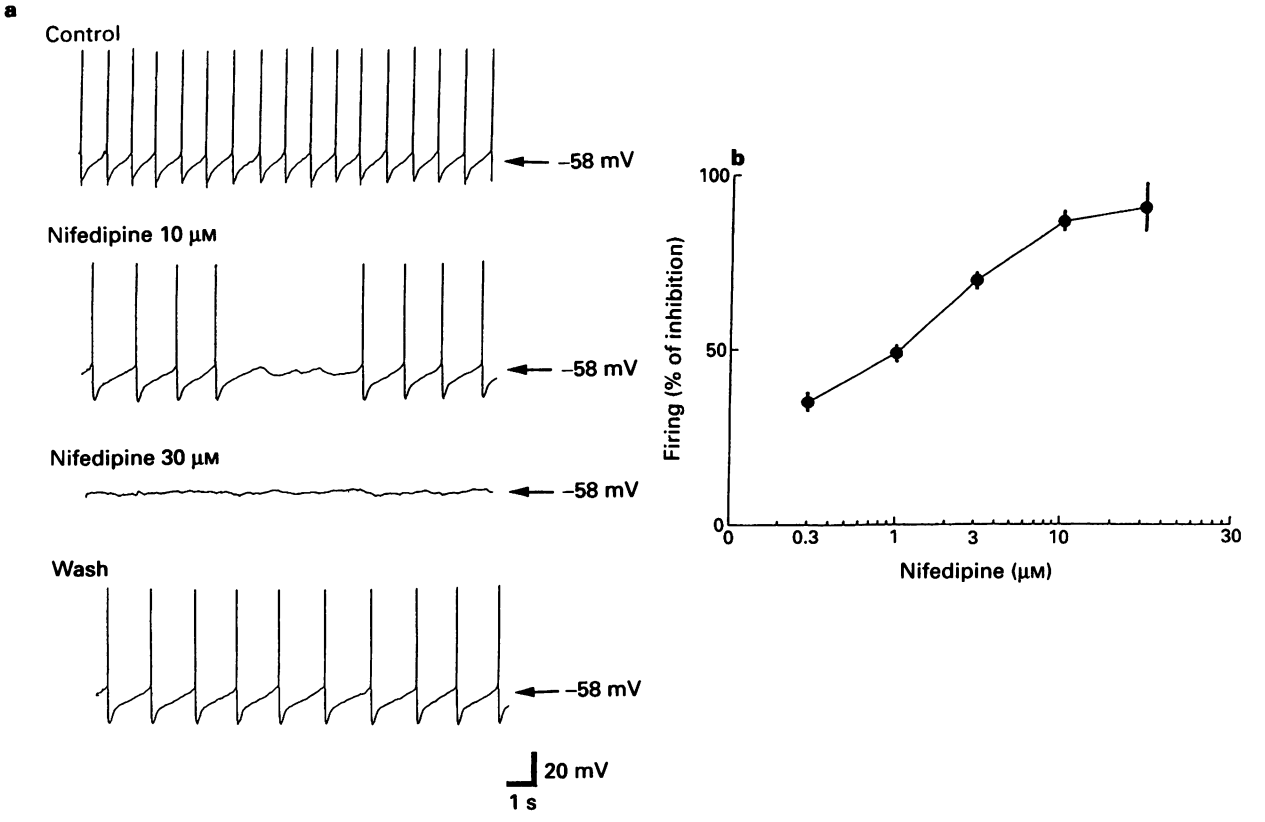


Figure 2 Effects of nifedipine on the spontaneous activity of dopaminergic cells. (a) Oscillographic records showing the concentration-dependent reduction of the spontaneous firing rate caused by nifedipine. (b) Dose-response relation for the inhibitory effects of nifedipine. Each point (4–7 experiments) shows mean effects ± s.e.mean.

Results

The experiments described in this paper are based on a total of 54 dopaminergic cells (30 in the substantia nigra pars compacta and 24 in the ventral tegmental area). The electrophysiological and pharmacological properties of these cells have been widely described (Grace & Onn, 1989; Kita *et al.*, 1986; Lacey *et al.*, 1989; Johnson & North, 1992; Hajos & Greenfield, 1993). All the neurones included in this study fired rhythmically spontaneous action potentials at a frequency of 1.9 ± 0.5 Hz. They showed a pronounced voltage- and time-dependent inward rectification (Ih) and had a hyperpolarizing response to dopamine application. The steady-state input resistance measured by a long hyperpolarizing pulse (1–7 s, 10–15 mV) ranged between 80 and 195 MΩ. Sixteen cells were also impaled with Cs-filled electrodes. They showed a progressive broadening of the action potential (10–80 ms) and eight of them developed a pattern of bursting activity, consisting of pacemaker depolarizations (0.1–0.7 Hz) which gave rise to a plateau-spike and sequence of two to ten action potentials (Figure 3d) (Mercuri *et al.*, 1994). The interspike interval within the burst increased as the burst progressed. In fact, the first, fourth and ninth interspike intervals were 27.9 ms ± 1.4 (30 bursts), 41.6 ms ± 2.5 (24 bursts) and 57.5 ms ± 1.4 (8 bursts) respectively. The average interspike interval between spikes occurring in a burst was 44.5 ± 3.1 ms. The bursting pattern of activity was depressed by 0 mM Ca^{2+} plus 25 mM $MgCl_2$ solutions ($n = 3$) (Figure 1).

Actions of dihydropyridines

Application of nifedipine (300 nM–30 μM) inhibited the spontaneous electrical activity of 32 dopaminergic cells in a concentration-dependent manner (Figure 2). Nifedipine at 1 μM reduced the spontaneous firing by about 50% of control (Figure 2b). This effect had a slow onset (2–4 min) and peaked in 7–12 min. An incomplete recovery was observed upon prolonged washout (more than 2 h). Nifedipine produced neither changes in membrane potential nor in the apparent input resistance (not shown). In cells loaded with caesium the rhythmic spontaneous firing activity was inhibited and the pacemaker oscillations of the membrane potential were depressed and narrowed in the presence of nifedipine (1–30 μM) ($n = 6$) (Figure 3). The narrowing of the pacemaker oscillations was mainly due to a marked inhibition of the depolarizing-after-potential (100–800 ms) that followed the plateau-spike (Figure 3d). The number of action potentials above the depolarizing oscillation was also reduced (Figure 3d).

Bath-applied nimodipine (1–30 μM) also inhibited the spontaneous firing of dopaminergic cells ($n = 11$) (Figure 4) and reduced the number of action potentials when a bursting pattern of activity was generated by the intracellular diffusion of caesium ions ($n = 3$) (not shown). Our experiments did not systematically examine the effects of a wide range of nimodipine concentrations on the dopaminergic cells. However, the effects observed with nimodipine were similar to those seen with the same concentrations of nifedipine. Five dopaminergic cells were also exposed to Bay K 8644 (1 μM); this drug increased the rate of firing of three cells by 20 ± 8% of control and slightly depolarized the membrane (1–3 mV) (Figure 5). In some neurones that were completely inhibited by nifedipine ($n = 4$) the spontaneous firing could be partially restored by superfusing the L-type Ca^{2+} channel agonist.

Actions of dihydropyridine antagonists on the spontaneous activity of calcium-dependent action potentials

The neurones loaded with caesium or treated with TEA (10–30 mM) were able to fire spontaneous calcium potentials even when the cells were treated with TTX (1 μM) or the extracellular concentration of sodium was reduced to 26.2 mM (choline chloride substitution). Under these conditions nifedipine (10–30 μM) ($n = 3$) (Figure 6) and nimodipine (30 μM) ($n = 2$) reduced or blocked the spontaneous activity of the calcium spikes.

Actions of nifedipine and nimodipine on the shape of the spike

In control conditions (KCl-filled electrodes), nifedipine and nimodipine did not change the shape of the action potentials significantly (measured at the midpoint of spike height)

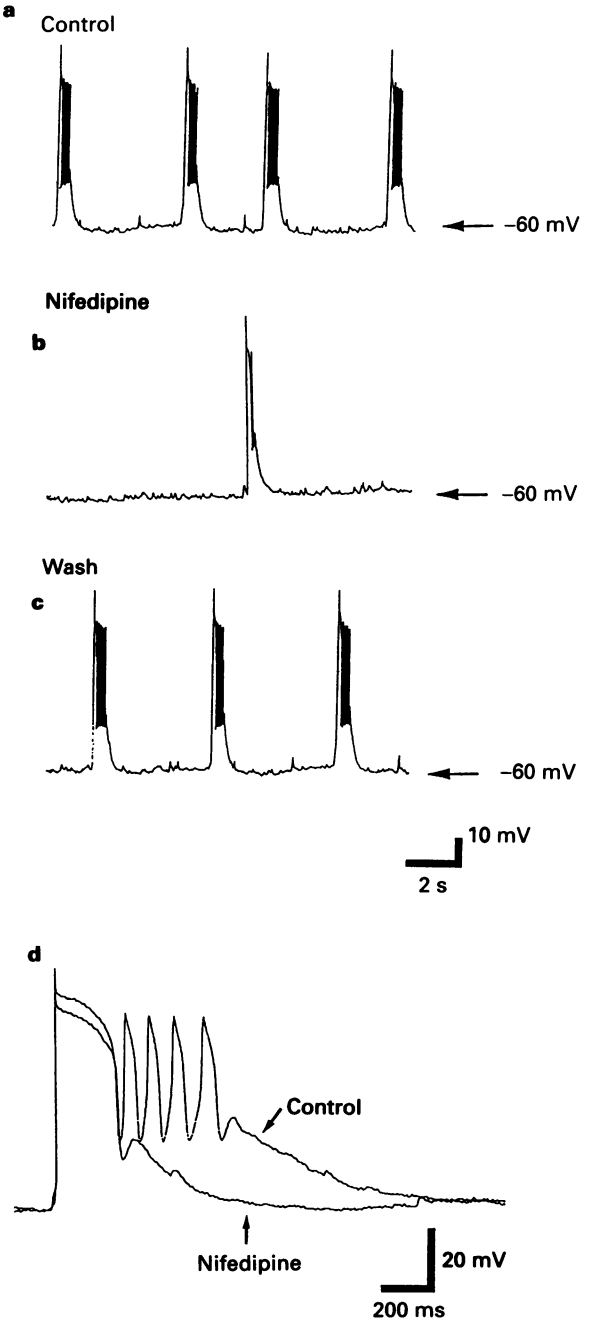


Figure 3 Effects of nifedipine on the spontaneous bursting activity. (a) This cell was impaled with a caesium-filled electrode; later (5 ms) depolarizing membrane oscillations and spontaneous bursts developed. (b) The application of nifedipine (10 μM) decreased the amplitude of depolarization and reduced the number of spikes in the burst. (c) Wash. (d) Superimposed traces to show the depressant effect of nifedipine on the depolarizing envelope which produced burst firing.

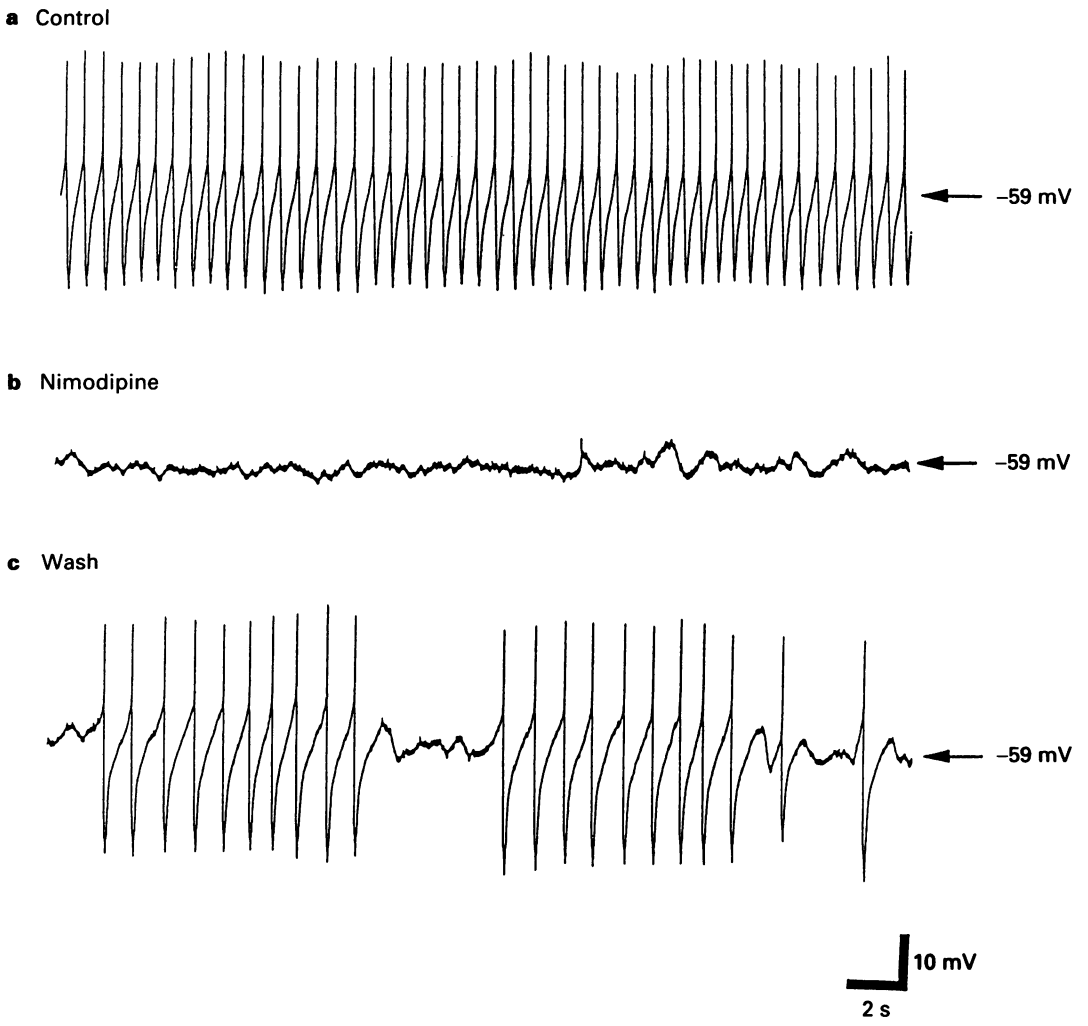


Figure 4 Inhibitory effects of nimodipine on pacemaker firing activity. The spontaneous firing (a) was blocked by nimodipine (10 μM) (b). Note that this is a chart recording. The full amplitude of the action potential is not reproduced because of the low frequency of the pen recorder.

(Figure 7a(i)) ($n = 10$). In addition, the shape of the after-hyperpolarization was not clearly affected by the dihydropyridines (Figure 7a(ii)) ($n = 13$). A lack of effect on the shape of the action potential was also observed even in cells impaled with CsCl-filled electrodes. It has to be pointed out that the maximal duration of the spike obtained with caesium-filled electrodes was around 80 ms. However, when a long-lasting spike (above 150–200 ms) was produced by applying 10–50 mM TEA on the caesium-loaded cells, both calcium antagonists, applied at concentrations (3–30 μM) likely to be maximally effective based on findings in other neurones (Regan *et al.*, 1991; Moyer *et al.*, 1992; Sayer *et al.*, 1993), were able to reduce the duration and the amplitude of the plateau potential. The shortening of the spike caused by the dihydropyridine calcium antagonists was either observed on sodium and calcium-dependent plateau potentials or on calcium plateau spike evoked in the presence of TTX (1 μM) (Figure 7b(i,ii)). Nifedipine (3 μM) reduced the duration and the amplitude of the spike to 66.5 ± 8.4% ($n = 7$) and 84.5 ± 2.7% ($n = 7$) of the respective controls. Nimodipine (3 μM) also shortened the duration of the plateau-spike and depressed its amplitude to 74.2 ± 4.2 ($n = 4$) and 89.5 ± 1.8 ($n = 4$) respectively. A block or a reduction of the amplitude and duration of the spike was also produced by the inorganic calcium channel blocker cobalt (1–3 mM) ($n = 4$) (Figure 7b (iii,iv)). In order to maintain the shape of the long lasting action potential a constant depolarizing pulse was injected intracellularly at a rate of 0.03–0.1 Hz while the neurones were manually clamped at − 70, − 85 mV.

Discussion

The present study suggests that calcium currents sensitive to dihydropyridine antagonists modulate the spontaneous rhythmic and bursting firing in the dopaminergic mesencephalic cells. The rhythmic and bursting activity observed *in vitro* could be compared with the firing properties previously recorded from the dopaminergic cells *in vivo*, which consisted in regular, irregular and burst discharge of action potentials (Grace & Bunney, 1983; 1984). It has to be pointed out that the burst firing evoked in cells loaded with caesium *in vitro* exhibits a shorter interspike interval (about 45 ms) than that observed in bursts occurring *in vivo* (about 70 ms). Although a normal synaptic connectivity between cells is required for the modulation of the discharge patterns typically observed *in vivo* (Shepard & Bunney, 1991), in the light of the ability of the potassium channel blockers (tetraethylammonium, barium, apamin and caesium) to trigger and/or increase bursts either *in vivo* (Grace & Bunney, 1984) or *in vitro* (see also Shepard & Bunney, 1991), it could be hypothesized that an inhibition of potassium-mediated outward currents and an increase of voltage-dependent inward currents play a key role in the bursting behaviour observed in both experimental conditions.

Action of dihydropyridines on firing rate

The rhythmic activity of the dopaminergic neurones is mainly regulated by the interplay of threshold and suprathreshold

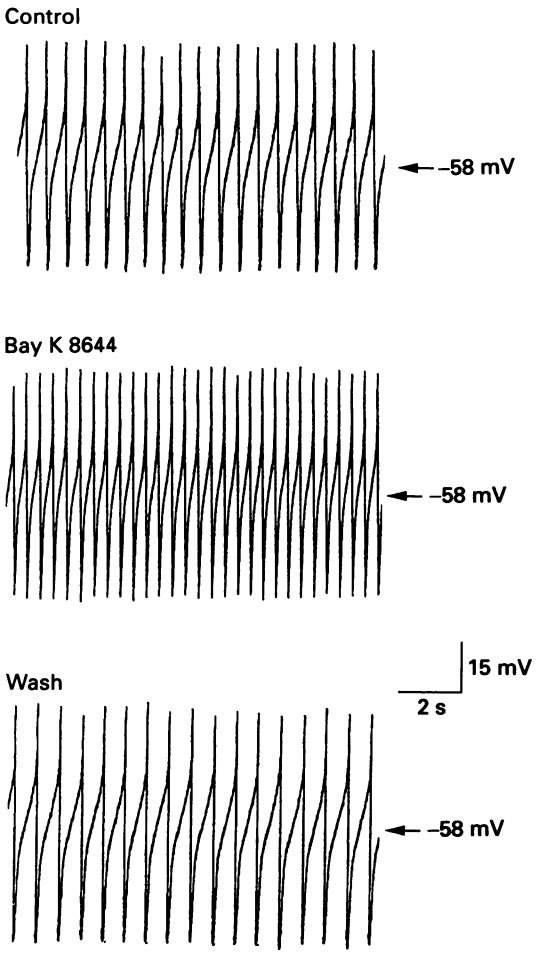


Figure 5 Bay K 8644 increases the spontaneous firing rate. The discharge of the spontaneous action potential in a ventral tegmental area cell is increased in a reversible manner by Bay K 8644 (1 μM). Note that the full amplitude of the spike is not reproduced because of the low frequency of the chart recorder.

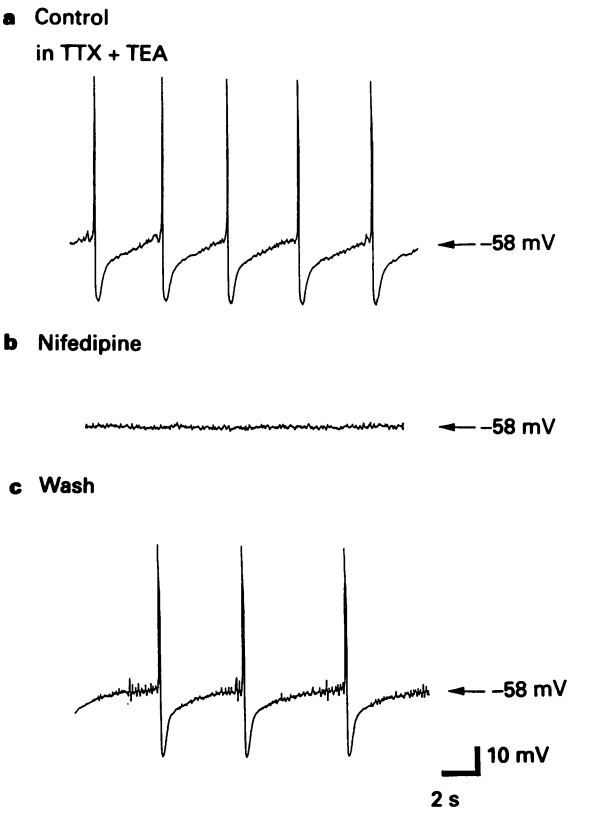


Figure 6 Dihydropyridine calcium channel antagonists depress the spontaneously occurring calcium spikes. Nifedipine (10 μM) inhibited the spontaneous activity of calcium action potentials (b). These spikes occurred in the presence of tetrodotoxin (TTX, 1 μM) and tetraethylammonium (TEA, 30 mM) (a).

currents intrinsic to the membrane (for a review see Connor, 1985). Among these are: (a) the voltage-activated inward current which appears to be carried by Na^+ and Ca^{2+} ions (Grace & Onn, 1989; Grace, 1991), the Na^+-K^+-dependent inwardly rectifying current (Lacey & North, 1987; Silva *et al.*, 1990) and the low- and high-threshold Ca^{2+} currents (Llinas *et al.*, 1984; Kang & Kitai, 1993b); (b) the Ca^{2+}-activated outward potassium current, mainly responsible for the afterhyperpolarization (Grace & Bunney, 1983), and the outwardly rectifying potassium currents (Grace & Onn, 1989; Silva *et al.*, 1990). It has already been demonstrated that calcium currents sustain the spontaneous firing of dopaminergic cells. The treatment of the neurones with inorganic calcium channel blockers and with solutions containing low-calcium depresses the spontaneous firing rate suggesting that calcium inward currents are determinant in generating and maintaining the intrinsic pacemaker (Llinas, 1988; Fujimara & Matsuda, 1989; Grace, 1991; Mercuri *et al.*, 1991; Kang & Kitai, 1993a).

The bursting firing of the dopaminergic cells produced by intracellular caesium loading is also dependent on calcium influx. In fact, it is depressed by lowering the extracellular concentration of calcium. The ability of the dihydropyridine calcium antagonists to affect, in a concentration-dependent manner, not only the rhythmic but also the bursting activity proves that L-type Ca^{2+} channels, sensitive to these agents, contribute to the inward currents underlying the two different patterns of spontaneous cellular discharge. The observation that the dihydropyridine calcium channel agonist, Bay K 8644 (Schramm *et al.*, 1983; Nowycky *et al.*, 1985) increases the spontaneous firing activity also suggests a role of the dihydropyridine-sensitive calcium currents in the regulation of the interval between spikes. In line with the present study, it has already been reported that bath-applied nifedipine decreases the spontaneous activity of guinea-pig dopaminergic neurones in the substantia nigra (Nedergaard *et al.*, 1993) and intravenous application of nimodipine decreases the regular and burst firing discharge of rat dopaminergic neurones in the ventral tegmental area (Ugedo *et al.*, 1988).

To account for the effects of the dihydropyridines on pacemaker firing activity, it could be suggested that a high-threshold dihydropyridine-sensitive Ca^{2+} current, preferentially located in the dendrites (Llinas *et al.*, 1984; Nishino *et al.*, 1986; Grace, 1990), is necessary to trigger either the spikes or the membrane depolarization causing bursting activity. The Na^+/Ca^{2+} spikes generated at the soma might in turn reactivate the dendritic calcium depolarizations, thus contributing to the electrical autorhythmicity of the dopaminergic cells. The importance of the high-threshold calcium currents in sustaining a rhythmic firing is also supported by a computer modelling of cardiac pacemaking in the sinoatrial node (Egan & Noble, 1987). An additional effect of dihydropyridine on low-threshold calcium currents could also account for the slowing of the regenerative rhythmic depolarizations (Nedergaard *et al.*, 1993); however, a recent whole cell patch-clamp study has reported that the calcium current which underlies the pacemaker-like depolarization in dopaminergic cells is not blocked by nifedipine (Kang & Kitai, 1993b).

Effects on the shape of the action potential

An important finding of this study was the shortening of the plateau action potential and of the depolarizing after poten-

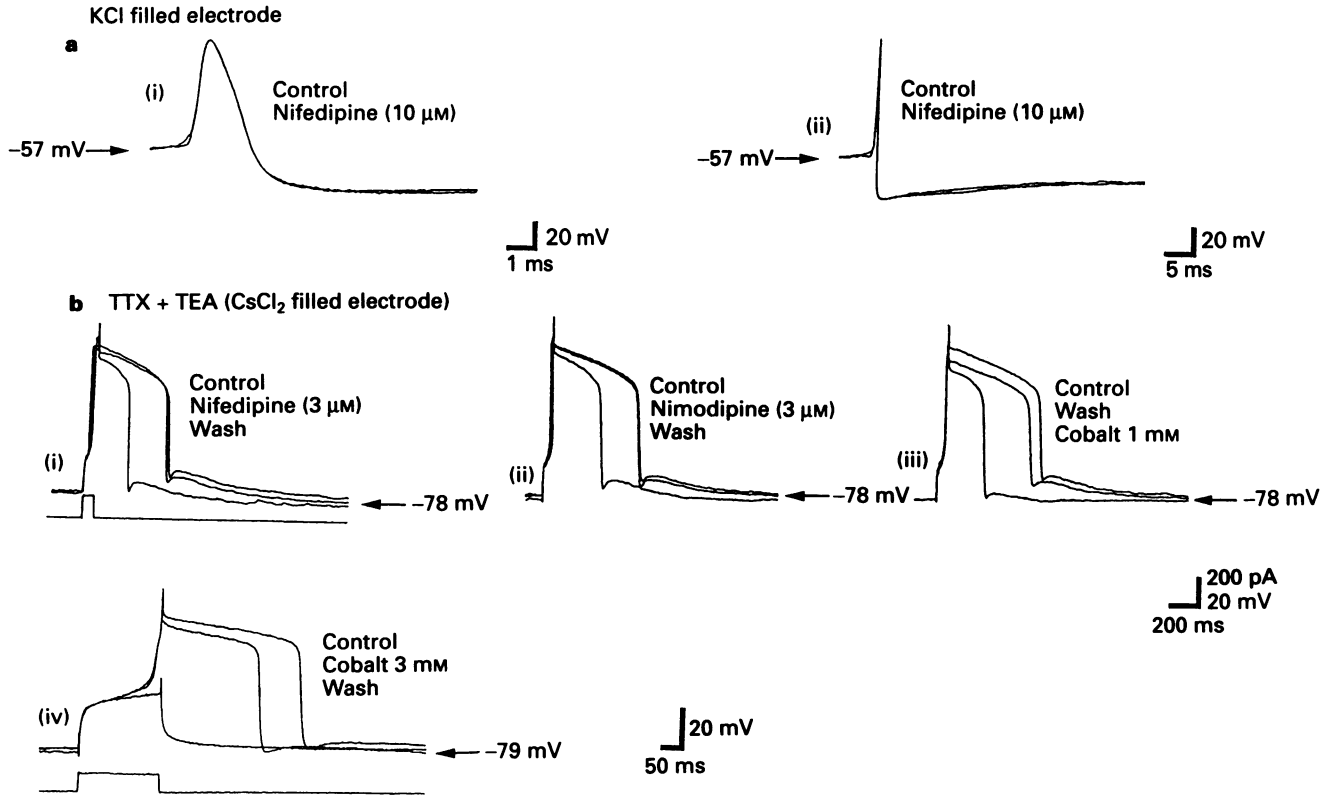


Figure 7 Effects of dihydropyridines on the shape of the action potentials. (a) (i) Nifedipine (10 μM) did not affect the shape of the action potentials recorded from a dopaminergic cell in control conditions (KCl-filled electrodes). (ii) The spike afterhyperpolarization was also unaffected by the dihydropyridine. Note that each trace is an average of four sweeps. (b) (i) Inhibitory effect of nifedipine (3 μM) on the amplitude and duration of the plateau potential in a cell impaled with caesium and treated with tetraethylammonium (TEA, 30 μM) and tetrodotoxin (TTX, 1 μM). The membrane was set to − 78 mV and a small, just threshold, depolarizing pulse was delivered at 0.03 Hz. The pulse elicited a long lasting TTX-insensitive spike that outlasted it. Upper voltage, The three traces in (i), (ii) and (iii) show control, effects of drugs and wash. The lower trace in (a) shows current. (ii) The TTX-insensitive calcium spike was also reversibly inhibited by nimodipine (3 μM). (iii) Depressant effects on the plateau-potential of cobalt (1 mM). (iv) The application of cobalt (3 mM) on this dopaminergic cell completely blocked the calcium spike. Note that (1) all the records in a (i), b (ii) and c (iii) were taken from the same dopaminergic cell; (2) the dihydropyridines reduced the calcium spikes without requiring a further increase of the injected current.

tials by dihydropyridine calcium antagonists. This suggests that a relevant source of calcium influx during a prolonged spike-like and post-spike depolarization is through L-type calcium channels and is consistent with the increased efficacy of the dihydropyridines at depolarized membrane potentials (Bean, 1984; Bean *et al.*, 1986; Jones & Jacobs, 1990). It is also evident that the dihydropyridine-induced shortening of the spike is dependent on the duration of the action potential. The plateau-spike has to be longer than 150 ms to observe the depressant effect of the dihydropyridines.

It has recently been shown that nifedipine blocks the TTX-resistant slow oscillation of the membrane whereas it does not affect the shape of the spike in dopaminergic cells (Nedergaard *et al.*, 1993 but see Fujimara & Matsuda, 1989; Kang & Kitai, 1993a,b). The apparent difference from our study could be explained by the fact that nifedipine was tested on action potentials that were not broad enough to cause the plateau-like depolarization and the post-spike depolarizing potentials which may have dendritic origin. The preferential blocking effects of dihydropyridine antagonists of L-type calcium channels during a maintained depolarization of the membrane could account for this phenomenon (Bean, 1984; Sanguinetti & Kass, 1984; Bean *et al.*, 1986; Hess, 1990; Jones & Jacobs, 1990).

It is interesting to note that Higashi *et al.* (1990) have already shown that organic calcium channel blockers preferentially depress the post-spike prolonged dendritic depolarization in hippocampal neurones.

Relationship between the electrophysiological effects of dihydropyridine and dopamine release

The level of extracellular dopamine is strictly dependent on the rate and the mode of firing of the dopaminergic neurones (Gonon, 1988). Although the contribution of the L-type calcium current in controlling dopamine release is still controversial, in agreement with our electrophysiological data showing an inhibitory effect of dihydropyridine antagonists, it has been reported that L-type Ca^{2+} channels control the influx of calcium (de Erausquin *et al.*, 1992) and the amount of dopamine released from dopaminergic cells in dendrites, and synaptosomes (Woodward & Leslie, 1986; Chaudieu *et al.*, 1992; Brouard *et al.*, 1993).

Therapeutic implications

The reduction of the voltage-dependent calcium influx by dihydropyridine Ca^{2+} antagonists might protect dopaminergic neurones from excessive intracellular loading of calcium ions during an excessive membrane depolarization caused by an ischaemic/anoxic episode (Choi, 1990).

Furthermore, the inhibitory effect of dihydropyridines on the spontaneous firing of the dopaminergic neurones might also be relevant to the control of movements, of drug seeking behaviour and of mental performances. Thus, dihydropyridine calcium antagonists could turn out to be useful

for the treatment of psychiatric and neurological disorders (Scriabine *et al.*, 1989).

We thank Giuseppe Gattoni and Massimo Tolu for their excellent technical assistance.

References

BEAN, B.P. (1984). Nitrendipine block of cardiac calcium channels: high-affinity binding to the inactivated state. *Proc. Natl. Acad. Sci. U.S.A.*, **81**, 6388–6392.

BEAN, B.P., STUREK, M., PUGA, A. & HERMESMEYER, K. (1986). Calcium channels in muscle cells isolated from rat mesenteric arteries: modulation by dihydropyridine drugs. *Circ. Res.*, **59**, 229–235.

BELLMANN, P., SCHADE, A. & TOWART, R. (1983). Dihydropyridine receptor in rat brain labeled with [3H]nimodipine. *Proc. Natl. Acad. Sci. U.S.A.*, **80**, 2356–2360.

BROUARD, A., PELAPRAT, D., VIAL, M., LHIAUBET, A.M. & ROSTENE, W. (1993). Effect of ion channel blockers and alteration of protein kinase C activity on 3H dopamine release and neurotensin action in primary cultures of mesencephalic cells. *J. Neurochem.*, **61**, S201D.

CHAUDIEU, I., ALONSO, R., MOUNT, H., QUIRION, R. & BOKSA, P. (1992). Effects of L- and N-type Ca++ channel antagonists on excitatory amino acid-evoked dopamine release. *Eur. J. Pharmacol.*, **220**, 203–209.

CHOI, D.W. (1990). Cerebral hypoxia: some new approaches and unanswered questions. *J. Neurosci.*, **10**, 2493–2501.

CONNOR, J.A. (1985). Neural pacemakers and rhythmicity. *Annu. Rev. Physiol.*, **47**, 17–28.

DE ERAUSQUIN, G., BROOKER, G. & HANBAUER, I. (1992). K^+-evoked dopamine release depends on a cytosolic Ca++ pool regulated by N-type Ca^{++} channels. *Neurosci. Lett.*, **145**, 121–125.

EGAN, T.M. & NOBLE, S.J. (1987). Acetylcholine and the mammalian 'slow inward' current: a computer investigation. *Proc. R. Soc. B.*, **230**, 315–337.

FUJIMURA, K. & MATSUDA, Y. (1989). Autogenous oscillatory potentials in neurones of the guinea pig substantia nigra pars compacta in vitro. *Neurosci. Lett.*, **104**, 53–57.

GAHWILER, B.H. & BROWN, D.A. (1987). Effects of dihydropyridines on calcium currents in CA3 pyramidal cells in slices cultures of rat hippocampus. *Neuroscience*, **20**, 731–738.

GONON, F.G. (1988). Regulation of dopamine release by impulse flow and by autoreceptors as studied by in vivo voltammetry in the rat striatum. *Neuroscience*, **14**, 765–774.

GRACE, A.A. (1990). Evidence for the functional compartmentalization of spike generating regions of rat midbrain dopamine neurones recorded in vitro. *Brain Res.*, **524**, 31–41.

GRACE, A.A. (1991). Regulation of spontaneous activity and oscillatory spike firing in rat midbrain dopamine neurons recorded in vitro. *Synapse*, **7**, 221–234.

GRACE, A.A. & BUNNEY, B.S. (1983). Intracellular and extracellular electrophysiology of nigral dopaminergic neurons-I. Identification and characterization. *Neuroscience*, **10**, 301–315.

GRACE, A.A. & BUNNEY, B.S. (1984). The control of firing pattern in nigral dopamine neurons: burst firing. *J. Neurosci.*, **4**, 2877–2890.

GRACE, A.A. & ONN, S.P. (1989). Morphology and electrophysiological properties of immunocytochemically identified rat dopamine neurones recorded in vitro. *J. Neurosci.*, **9**, 3463–3481.

GREENBERG, D.A., COOPER, E.X. & CARPENTER, C.L. (1984). Calcium channel 'agonist' Bay K 8644 inhibits calcium antagonist binding to brain and PC12 cell membranes. *Brain Res.*, **305**, 365–368.

HAINSWORTH, A.H., ROPER, J., KAPOOR, R. & ASCHCROFT, F.M. (1991). Identification and electrophysiology of isolated pars compacta neurons from guinea-pig substantia nigra. *Neuroscience*, **43**, 81–93.

HAJOS, M. & GREENFIELD, S.A. (1993). Topographic heterogeneity of substantia nigra neurons: diversity in intrinsic membrane properties and synaptic inputs. *Neuroscience*, **55**, 919–934.

HESS, P. (1990). Calcium channels in vertebrate cells. *Annu. Rev. Neurosci.*, **13**, 337–356.

HIGASHI, H., SUGITA, S., MATSUNARI, S. & NISHI, S. (1990). Calcium-dependent potentials with different sensitivities to calcium agonists and antagonists in guinea-pig hippocampal neurons. *Neuroscience*, **34**, 35–47.

JOHNSON, S.W. & NORTH, R.A. (1992). Two types of neurons in the rat ventral tegmental area and their synaptic inputs. *J. Physiol.*, **450**, 455–468.

JONES, S.W. & JACOBS, S.L. (1990). Dihydropyridine actions on calcium currents of frog sympathetic neurones. *J. Neurosci.*, **10**, 2261–2267.

KANG, Y. & KITAI, S.T. (1993a). Calcium spike underlying rhythmic firing in dopaminergic neurons of rat substantia nigra compacta. *Neurosci. Res.*, **18**, 195–207.

KANG, Y. & KITAI, S.T. (1993b). A whole cell patch-clamp study on the pacemaker potential in dopaminergic neurons of rat substantia nigra compacta. *Neurosci. Res.*, **18**, 209–221.

KITA, T., KITA, H. & KITAI, S.T. (1986). Electrical membrane properties of rat substantia nigra compacta neurons in an in vitro slice preparation. *Brain Res.*, **372**, 21–30.

LACEY, M.G., MERCURI, N.B. & NORTH, R.A. (1989). Two cell types in rat substantia nigra zona compacta distinguished by membrane properties and the action of dopamine and opioids. *J. Neurosci.*, **9**, 1233–1241.

LACEY, M.G. & NORTH, R.A. (1987). An inward current activated by hyperpolarization (Ih) in rat substantia nigra zona compacta neurones in vitro. *J. Physiol.*, **406**, 18P.

LLINAS, R.R. (1988). The intrinsic electrophysiological properties of mammalian neurons: insights into central nervous system functions. *Science*, **242**, 1654–1664.

LLINAS, R.R., GREENFIELD, S.A. & JAHNSEN, H. (1984). Electrophysiology of pars compacta cells in the in vitro substantia nigra a possible mechanism for dendritic release. *Brain Res.*, **294**, 127–132.

MERCURI, N.B., BONCI, A., JOHNSON, S.W., STRATTA, F., CALABRESI, P. & BERNARDI, G. (1994). Effects of anoxia on rat midbrain dopamine neurons. *J. Neurophysiol.*, **71**, 1165–1173.

MERCURI, N.B., STRATTA, F., CALABRESI, P. & BERNARDI, G. (1991). The electrophysiological effects of amineptine on neurones of the rat substantia nigra pars compacta: evidence for an inhibition of the dopamine uptake system. *Br. J. Pharmacol.*, **104**, 700–704.

MOYER, J.R., THOMPSON, L.T., BLACK, J.P. & DISTERHOFT, J.F. (1992). Nimodipine increases excitability of rabbit CA1 pyramidal neurons in an age- and concentration-dependent manner. *J. Neurophysiol.*, **68**, 2100–2109.

NEDERGAARD, S., FLATMANN, J.A. & ENGBERG, I. (1993). Nifedipine and ω-conotoxin-sensitive Ca++ conductances in guinea-pig substantia nigra pars compacta neurones. *J. Physiol.*, **466**, 727–747.

NISHINO, N.N., NOGUCHI-KUNO, S.A., SUGIYAMA, T. & TANAKA, C. (1986). [3H]Nitrendipine binding sites are decreased in the substantial nigra and striatum of the brain from patients with Parkinson's disease. *Brain Res.*, **377**, 186–189.

NOWYCKY, M.C., FOX, A.P. & TSIEN, R.W. (1985). Long opening mode of gating of neuronal calcium channels and its promotion by the dihydropyridine calcium agonist Bay K 8644. *Proc. Natl. Acad. Sci. U.S.A.*, **82**, 2178–2182.

REGAN, L.J., SAH, D.W.Y. & BEAN, B.P. (1991). Ca^{++} channels in rat central and peripheral neurons: high threshold current resistant to dihydropyridine blockers and ω-conotoxin. *Neuron*, **6**, 269–280.

SANGUINETTI, M.C. & KASS, R.S. (1984). Voltage-dependent block of calcium channel current in the calf cardiac Purkinje fiber by dihydropyridine calcium channel antagonists. *Circ. Res.*, **55**, 336–348.

SAYER, R.J., BROWN, A.M., SCHWINDT, P.C. & CRILL, W.E. (1993). Calcium currents in acutely isolated human neocortical neurons. *J. Neurophysiol.*, **69**, 1596–1606.

SCHRAMM, M., THOMAS, G., TOWART, R. & FRANCKOWIAK, G. (1983). Novel dihydropyridines with positive inotropic action through activation of Ca^{++} channels. *Nature*, **303**, 535–537.

SCRIABINE, A., SCUURMANN, T. & TRABER, J. (1989). Pharmacological basis for the use of nimodipine in central nervous system disorders. *FASEB J.*, **3**, 1799–1806.

SHEPARD, P.D. & BUNNEY, B.S. (1991). Repetitive firing properties of putative dopamine-containing neurons in vitro: regulation of apamin-sensitive Ca^{++}-activated K^+ conductance. *Exp. Brain Res.*, **86**, 141–150.

SILVA, N.L. & BUNNEY, B.S. (1988). Intracellular studies of dopamine neurons in vitro: pacemakers modulated by dopamine. *Eur. J. Pharmacol.*, **86**, 141–150.

SILVA, N.L., PECHURA, C.M. & BARKER, J.L. (1990). Postnatal rat nigrostriatal dopaminergic neurons exhibit five types of potassium conductances. *J. Neurophysiol.*, **64,** 262–272.

TSIEN, R.W., ELLINOR, P.T. & HORNE, W.A. (1991). Molecular diversity of voltage-dependent Ca^{++} channels. *Trends Pharmacol. Sci.*, **12,** 349–351.

UGEDO, L., GRENHOFF, J. & SVENSSON, T.H. (1988). Effects of nimodipine on the physiological activity of A10-DA neurons. *Acta Physiol. Scand.*, **134,** P33.

WOODWARD, J.J. & LESLIE, S.W. (1986). Bay K 8644 stimulation of calcium entry and endogenous dopamine release in rat striatal synaptosomes antagonized by nimodipine. *Brain Res.*, **370,** 397–400.

(Received February 7, 1994
Revised May 2, 1994
Accepted May 13, 1994)

Br. J. Pharmacol. (1994), **113**, 839–844 © Macmillan Press Ltd, 1994

The effects of clozapine on behavioural responses to the selective 'D_1-like' dopamine receptor agonist, A 68930, and to the selective 'D_2-like' agonist, RU 24213

Siobhan A. Daly & [1]John L. Waddington

Department of Clinical Pharmacology, Royal College of Surgeons in Ireland, St. Stephen's Green, Dublin 2, Ireland

1 The influence of the atypical antipsychotic clozapine on D_1 dopamine receptor-mediated function was examined in terms of its effects on behavioural responses to the new isochroman selective D_1 agonist, A 68930, and to the selective D_2 agonist, RU 24213.

2 In rat striatal membrane preparations, radioligand binding studies with [^{3}H]-SCH 23390 and [^{3}H]-spiperone confirmed clozapine to show weak and non-selective affinity for both D_1 and D_2 receptors.

3 Using a rapid time-sampling behavioural check list technique, clozapine (4.0–36.0 mg kg^{-1}) exerted only modest antagonism of RU 24213 (15.0 mg kg^{-1})-induced sniffing and locomotion, and weakly released some episodes of myoclonic jerking; such antagonism with release of jerking has been shown previously to occur *only* during concurrent stimulation of D_2 receptors *and* attenuation of D_1 function.

4 Over the same dose-range, clozapine completely blocked A 68930 (0.25 mg kg^{-1})-induced intense grooming but failed to influence the vacuous chewing response; this profile was similar to that demonstrated previously for selective D_1 antagonists.

5 On the basis of complete blockade of typical D_1 agonist-induced grooming and weak release of atypical jerking to D_2 agonism in the face of modest reduction in typical D_2-stimulated behaviours, clozapine apears to exert some preferential but not selective attenuation of D_1 receptor-mediated function. Clozapine may attenuate activity through a classical D_1 receptor at a level beyond the recognition site, for which it has little affinity, or by way of new, putative 'D_1-like' site(s) that subserve distinct elements of dopaminergic behaviour.

Keywords: Dopamine; D_1 and D_2 receptors; clozapine; A 68930; RU 24213; grooming behaviour; vacuous chewing; antipsychotics

Introduction

Renewed interest in the psychopharmacology of the dibenzodiazepine antipsychotic, clozapine, stems from an atypical clinical profile that is, to date, unique; its efficacy encompasses a significant proportion of patients who are refractory to typical neuroleptic agents, with little liability to induce extrapyramidal side effects though with raised liability to induce agranulocytosis (Kane *et al.*, 1988; Waddington, 1994). The search for any specific basis to the advantageous clinical properties of clozapine is made difficult by its very broad range of pharmacological actions (Baldessarini & Frankenburg, 1991; Waddington, 1994), but two proposals have attracted particular attention and study: (i) concurrent antagonism of D_2 and 5-HT_2 receptors (Meltzer *et al.*, 1989), and (ii) preferential blockade of D_1 function (Coward *et al.*, 1989); this latter proposal is the focus of the present investigations.

Despite having relatively low affinity for blockade of both D_1 and D_2 receptors in an essentially non-selective manner, neurochemical studies (Andersen & Braestrup, 1986; Altar *et al.*, 1988; Imperato & Angelucci, 1989) have suggested a disproportionately greater effect on D_1-mediated function. Similarly, in rodents depleted of dopamine by 6-hydroxydopamine (6-OHDA) or reserpine there is behavioural evidence that clozapine can show properties similar to those of the selective D_1 antagonist, SCH 23390 (Arnt & Hyttel, 1986; Chipkin & Latranyi, 1987; Criswell *et al.*, 1989). In intact rodents, we have previously described clozapine as readily blocking grooming behaviour induced by the selective D_1 agonist, SK&F 77434 but not apomorphine-induced stereotypy, while it exerted some attenuation of typical responses to the selective D_2 agonist, quinelorane (LY 163502; Murray & Waddington, 1990) in accordance with cooperative D_1:D_2 interactions that appear to regulate such typical behaviours (Waddington & Daly, 1993); furthermore, in this latter situation clozapine appeared to release an atypical response of myoclonic jerking to quinelorane (Murray & Waddington, 1990), which we have shown to be released only by selective antagonism of D_1 receptors prior to D_2 agonist challenge (Murray & Waddington, 1989a; Daly & Waddington, 1992a) in accordance with oppositional D_1:D_2 interactions that appear to regulate such atypical behaviours (Waddington & Daly, 1993). These findings suggest that clozapine may exert some preferential attenuation of D_1 receptor-mediated function(s).

Over recent years, it has become apparent that the number of dopamine receptors may be considerably larger than envisaged originally, with the classical D_1/D_2 nomenclature (Kebabian & Calne, 1979) now seen to serve as an 'umbrella' for two families of 'D_1-like' (D_{1A}, D_{1B}/D_5) and 'D_2-like' ($D_{2L/S}$, D_3, D_4) receptors identified in molecular biological studies (Sibley & Monsma, 1992; Civelli *et al.*, 1993; Gingrich & Caron, 1993); indeed, clozapine may show some modest preferential affinity for D_4 relative to other dopamine receptors (Van Tol *et al.*, 1991). In the functional domain, we have presented behavioural evidence for 'D_1-like' subtypes; the new high potency, full efficacy isochroman D_1 agonist, A 68930, induced an intense grooming response that was antagonized both by the new isoquinoline D_1 antagonist, BW 737C and by the benzazepine D_1 antagonists, SCH 23390 and NNC 756, while the vacuous chewing response to A 68930 was blocked only by BW 737C and not by either of the benzazepines (Daly & Waddington, 1993). The purpose of the present study was to examine similarly the effects of clozapine on behavioural response to A 68930, in comparison with those to the selective D_2 agonist RU 24213, and thus to

[1] Author for correspondence.

clarify further the nature of its apparently preferential actions on D_1 function.

Methods

Radioligand binding studies

Striata from male Sprague-Dawley rats were homogenized in 30 vol 50 mM Tris-HCl buffer, pH 7.6 at 25°C, and centrifuged at 10000 *g* at 4°C for 5 min as described previously (Daly & Waddington, 1993). The pellet was twice resuspended, diluted and centrifuged as above. The membrane preparation was finally resuspended at 4–8 mg original wet weight ml^{-1} in Tris-HCl buffer containing (mM): NaCl 120, KCl 5, $MgCl_2$ 1, $CaCl_2$ 2, $Na_2S_2O_5$ 0.2 (as antioxidant) and pargyline 10 μM (as monoamine oxidase inhibitor).

The binding of [^{3}H]-SCH 23390 (79 Ci $mmol^{-1}$, Amersham) to 'D_1-like' receptors was determined by incubating 0.5 ml membrane suspension with 0.3 nM ligand and unlabelled drugs at 37°C for 20 min in a total volume of 1 ml. Specific binding was defined as that displaced by 100 nM piflutixol (Lundbeck), and typically represented 91% of total binding. Incubations were stopped by filtration through GF/B filters, followed by two 8 ml washes with ice-cold buffer. Radioactivity trapped on the filters was quantified by liquid scintillation spectroscopy after addition of 5 ml liquiscint (Medlabs) using a LKB 1214 Rackbeta counter with 51% counting efficiency for tritium.

The binding of [^{3}H]-spiperone (28 Ci $mmol^{-1}$, Amersham) to 'D_2-like' receptors was determined in membranes prepared as above. Incubations contained 0.5 ml membrane suspension with 0.2 nM ligand and unlabelled drugs in a total volume of 5 ml. Specific binding was defined as that displaced by 1 μM domperidone (Janssen) and typically represented 79% of total binding. Incubation and filtration were as described above.

Behavioural studies

Young adult male Sprague-Dawley rats (UCD, Dublin) were used in all experiments. The rats were housed in groups of five per cage with food and water available *ad libitum*, and were maintained at 21 ± 1°C on a 12/12 h (6 h 00 min on; 18 h 00 min off) light/dark schedule. On experimental days they were placed individually in perspex cages 52 × 39 × 18 cm and left undisturbed for a habituation period of 2.5 h.

Behavioural assessments were carried out in a manner similar to that described previously (Daly & Waddington, 1993). Immediately before and at intervals after injection of drug or vehicle, animals were assessed by a rapid time-sampling behavioural check list technique. For this procedure, each rat was observed individually for 5 s periods at 1 min intervals over 5 consecutive min using an extended behavioural check list. This allowed the presence or absence of the following individual behaviours (occurring alone or in any combination) to be determined in each 5 s period: stillness (motionless with no behaviour evident); sniffing; locomotion; rearing; grooming (of any form); intense grooming (a characteristic pattern of grooming of the face with the forepaws followed by vigorous grooming of the hind flank with the snout); vacuous chewing (not directed onto any physical material); chewing (directed onto any physical material); jerking (myoclonic movements of the limbs or whole body). After assessment on the behavioural check list, animals were evaluated for 30 s each by use of a conventional 0–6 stereotypy rating scale: 0 = asleep or inactive; 1 = episodes of normal activities; 2 = discontinuous activity with bursts of prominent sniffing or rearing; 3 = continuous stereotyped activity such as sniffing or rearing along a fixed path; 4 = stereotyped sniffing or rearing fixated at one location; 5 = stereotyped behaviour with bursts of licking or gnawing; 6 = continuous licking or gnawing. This cycle was repeated at 10 min intervals. Rats were used on two occasions only, separated by a drug-free interval of at least 1 week; on each occasion rats were randomly allocated to one of the various treatment groups. All assessments were made by an observer unaware of the treatment given to each animal.

Drugs

The following agents were used: A 68930 ([1R,3S]-1-aminomethyl-5,6-dihydroxy-3-phenylisochroman; Abbott, U.S.A.); RU 24213 (N-*n*-propyl-*N*-phenylethyl-*p*-3-hydroxyphenylethylamine; Roussel- UCLAF, France); clozapine (Sandoz, Switzerland). A 68930 was dissolved in dilute acetic acid and made up to volume with distilled water; RU 24213 was dissolved in distilled water; clozapine was dissolved in dilute hydrochloric acid and made up to volume with distilled water; control animals received injections of the appropriate vehicle. All substances were injected s.c. in a volume of 2 ml kg^{-1}, with clozapine or its vehicle given 45 min prior to challenge with agonist or vehicle.

Data analysis

Data from radioligand displacement experiments were analysed by a computer-assisted non-linear iterative curve fitting procedure (Barlow, 1983). The resulting IC_{50} was converted to a K_I value using the Cheng-Prusoff equation, $K_I = IC_{50}/(1 + C/K_D)$, where C is ligand concentration and K_D is the apparent dissociation constant from saturation studies described elsewhere (Daly & Waddington, 1992b).

From the application of the behavioural check list, the total 'counts' for each individual behaviour was determined as the number of 5 s observation 'windows' in which a given behaviour was evident, summed over a 1 h period and expressed as means ± s.e.mean, $n = 8$ per group; stereotypy scores were averaged over the 1 h period and expressed similarly. These data were then analysed using analysis of variance (ANOVA) or the Kruskal-Wallis non-parametric ANOVA, followed by Student's *t* test or Mann-Whitney U test respectively.

Results

Radioligand binding studies

The D_1 and D_2 receptor affinities of A 68930 and RU 24213, together with values for the selective D_1 antagonist, SCH 23390 ([*R*]-7-chloro-8-hydroxy-2, 3, 4, 5-tetrahydro-3-methyl-1-phenyl-1H-3-benzazepine) and the selective D_2 antagonist, YM 09151-2 ([*cis*]-*N*-[1-benzyl-2-methyl-pyrolidin-3-yl]-5-chloro-2-methoxy-4-methylaminobenzamide) as reference compounds (Daly & Waddington, 1992a, 1993), are shown in Table 1; these agonists and antagonists demonstrated appropriate selective affinities, while clozapine dem-

Table 1 Displacement of [^{3}H]-SCH 23390 and of [^{3}H]-spiperone from striatal D_1 and D_2 receptors, respectively, by investigational agents and by clozapine

	K_I (mol l^{-1})		
	[^{3}H]-SCH 23390 (D_1)	*[^{3}H]-spiperone* (D_2)	D_1/D_2
A 68930	2.9	651	0.005
RU 24213	>10,000	244	>41
SCH 23390	0.18	846	0.0002
YM 09151-2	6,884	0.23	29,930
Clozapine	336	271	1.2

Values are geometric means of 3–7 independent determinations, each performed in duplicate.

onstrated only weak, non-selective affinity for both D_1 and D_2 receptors.

Effects of clozapine on behavioural responses to RU 24213

Administration of RU 24213 (15.0 mg kg^{-1}) essentially abolished the stillness evident in well-habituated control animals and induced a typical response of multiple interpolated episodes of sniffing and locomotion (Figure 1); there were also low levels of rearing and chewing, most commonly of cage bedding and faecal pellets (Table 2). No compulsive stereotyped behaviour was evident, with scores on the 0–6 stereotypy scale reflecting only discontinuous bursts of activity [vehicle: 0.2 ± 0.1; RU 24213 15.0 mg kg^{-1}: 1.9 ± 0.1, $P<0.01$].

The sniffing response to challenge with 15.0 mg kg^{-1} RU 24213 was significantly antagonized by 4.0–36.0 mg kg^{-1} clozapine, though this effect was modest (−31%, $P<0.01$) even at the highest clozapine dose; similarly, clozapine exerted only modest antagonism (−41% at 36.0 mg kg^{-1}, $P<0.05$) of RU 24213-induced locomotion (Figure 1). There was little substantive effect of clozapine on the low levels of rearing and chewing induced by RU 24213, but some limited activity of clozapine to release episodes of jerking in response to RU 24213 was apparent; while this failed to attain statistical significance in terms of behavioural counts (Table 2), 8 of 16 animals (50%) receiving RU 24213 following pretreatment with 12.0 or 36.0 mg kg^{-1} clozapine (4 of 8 animals for each dose) showed at least one episode of jerking, while such behaviour was evident in only 5 of a total of 56 animals (9%) receiving RU 24213 alone ($P<0.01$; Fisher exact probability test) which we have examined both here (1 of 8 animals) and previously (4 of 48 animals) in an identical manner (Daly & Waddington, 1992a).

Effects of clozapine on behavioural responses to A 68930

Administration of A 68930 (0.25 mg kg^{-1}) substantially reduced the stillness evident in well-habituated control animals and induced a typical response of multiple interpolated episodes of grooming (particularly intense grooming) and vacuous chewing (Figure 2); there were also numerous episodes of sniffing (Table 3). No compulsive stereotyped behaviour was evident, with scores on the 0–6 stereotypy scale reflecting only discontinuous activation (vehicle: 0.1 ± 0.1; A 68930 0.25 mg kg^{-1}: 0.5 ± 0.1, $P<0.01$).

The intense grooming response to challenge with 0.25 mg kg^{-1} A 68930 was readily and significantly antagonized by 4.0–36.0 mg kg^{-1} clozapine, with essential abolition of this response at the highest dose (−98%, $P<0.01$); conversely, clozapine exerted no significant effect on the vacuous chewing (Figure 2) or sniffing (Table 3) responses to A 68930.

Discussion

It is well recognized that clozapine is a relatively weak antagonist of dopamine-mediated function, in keeping with its

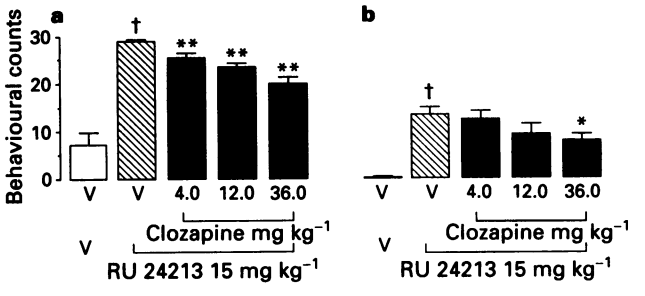


Figure 1 Effect of pretreatment with clozapine, 4.0–36.0 mg kg^{-1}, on (a) sniffing and (b) locomotor responses to the D_2 agonist, RU 24213, 15.0 mg kg^{-1}; data are mean ± s.e.mean of behavioural counts, $n = 8$. †$P<0.01$ vs vehicle (V); **$P<0.01$; *$P<0.05$ vs RU 24213.

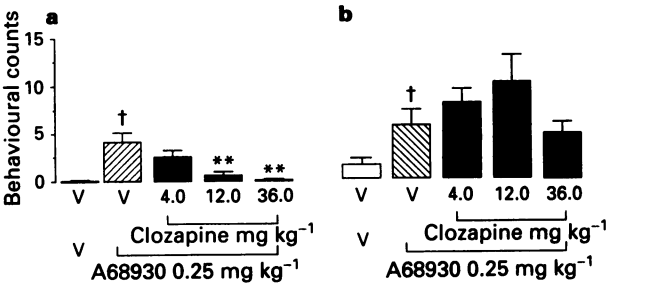


Figure 2 Effect of pretreatment with clozapine, 4.0–36.0 mg kg^{-1}, on (a) intense grooming and (b) vacuous chewing responses to the D_1 agonist, A 68930, 0.25 mg kg^{-1}; data are mean ± s.e.mean of behavioural counts, $n = 8$. †$P<0.01$ vs vehicle (V); **$P<0.01$ vs A 68930.

Table 2 Effect of pretreatment with clozapine on behavioural responses to the D_2 agonist, RU 24213

Drug	mg kg^{-1}	*St*	*Sn*	*R*	*Gr*	*Ch*	*J*
Vehicle	–	19.5 ± 3.4	6.1 ± 2.2	0.0 ± 0.0	1.4 ± 0.8	0.1 ± 0.1	0.0 ± 0.0
RU 24213	15.0	0.4 ± 0.3[a]	29.1 ± 0.4[a]	1.9 ± 0.4[b]	0.1 ± 0.1	0.8 ± 0.3[b]	0.1 ± 0.1
+ clozapine	4.0	4.1 ± 1.1**	25.5 ± 0.9**	1.3 ± 0.4	0.1 ± 0.1	1.0 ± 0.6	0.3 ± 0.2
	12.0	6.3 ± 1.2**	23.6 ± 0.8**	0.9 ± 0.3	0.1 ± 0.1	0.8 ± 0.4	0.8 ± 0.4
	36.0	9.3 ± 1.1**	20.0 ± 1.3**	1.4 ± 0.6	0.0 ± 0.0	0.3 ± 0.2	1.0 ± 0.6

Data are means ± s.e.mean of behavioural counts, $n = 8$, for: St, stillness; Sn, sniffing; R, rearing; Gr, grooming; Ch, chewing; J, jerking. [a]$P<0.01$, [b]$P<0.05$ vs vehicle; **$P<0.01$ vs RU 24213.

Table 3 Effect of pretreatment with clozapine on behavioural responses to the D_1 agonist, A 68930

Drug	mg kg^{-1}	*St*	*Sn*	*R*	*Gr*	*Ch*	*J*
Vehicle	–	22.8 ± 2.0	6.5 ± 1.8	0.8 ± 0.4	0.5 ± 0.3	0.1 ± 0.1	0.0 ± 0.0
A 68930	0.25	7.0 ± 2.3[a]	17.6 ± 2.2[a]	2.3 ± 1.0	6.4 ± 1.4[a]	0.3 ± 0.2	0.0 ± 0.0
+ clozapine	4.0	6.5 ± 0.9	20.6 ± 1.3	0.9 ± 0.4	5.3 ± 0.8	0.4 ± 0.3	0.0 ± 0.0
	12.0	9.1 ± 1.8	18.6 ± 2.1	0.5 ± 0.2	1.6 ± 0.7**	0.3 ± 0.3	0.9 ± 0.0
	36.0	15.6 ± 2.6*	13.1 ± 2.8	0.3 ± 0.3	0.5 ± 0.4**	0.4 ± 0.2	0.0 ± 0.0

Data are means ± s.e.mean of behavioural counts, $n = 8$, for: St, stillness; Sn, sniffing; R, rearing; Gr, grooming; Ch, chewing; J, jerking. *$P<0.01$ vs vehicle; **$P<0.01$; *$P<0.05$ vs A 68930.

relatively low affinity for dopamine receptors (Coward *et al.*, 1989; Baldessarini & Frankenburg, 1991); in an experimental paradigm very similar to that used here, we have confirmed that clozapine exerts little or no antagonism of apomorphine-induced stereotyped behaviour (Murray & Waddington, 1990). In the present study, we report that clozapine exerts at best only modest antagonism of the typical behaviours of locomotion and sniffing induced by the selective D_2 agonist, RU 24213 (Euvrard *et al.*, 1980; Pugh *et al.*, 1985) that might appear consistent with its modest affinity for the D_2 receptor.

However, the modest antagonism by clozapine of such typical D_2 agonist responses was accompanied by some limited release of episodes of atypical myoclonic movements, whereby various combinations of head, upper and lower limb/body regions jerk in a manner which, when severe, can propel the animal upwards into the air from the floor of the cage; this tendency failed to attain statistical significance in terms of behavioural counts but, when analysed in terms of prevalence of jerking as a categorical measure, statistically significant release thereof by clozapine was demonstrable. Critically this atypical behaviour is released *only* when D_2 receptors are stimulated and D_1 function contemporaneously attenuated, for example with selective D_1 antagonists; in this situation, typical locomotor and sniffing responses are reduced (Grabowska-Anden & Anden, 1983; 1987; Murray & Waddington, 1989a; Daly & Waddington, 1992a; Hubbard & Trugman, 1993). These phenomena appear to have their basis in two forms of D_1:D_2 interaction, whereby tonic activity through D_1 receptors both 'enables' the expression of typical D_2-initiated responses such as locomotion in a cooperative/synergistic manner and inhibits the expression of atypical responses such as jerking in an oppositional fashion (Waddington & Daly, 1993); these two forms of D_1:D_2 interaction appear to have physiological counterparts at diverse levels of dopaminergic function (Waddington *et al.*, 1994b). Thus, the present findings extend to RU 24213 our previous report on the effects of clozapine on responsivity to quinelorane (LY 163502; Murray & Waddington, 1990), and indicate further that clozapine modestly reduces typical D_2 agonist responses and weakly releases some atypical jerking primarily via preferential reduction in tonic D_1 function that is interactive with the D_2 system.

Were this to be the case, clozapine would be expected to show particular effectiveness in blocking responses to selective D_1 receptor stimulation. We have shown previously that clozapine, in contrast to its lack of effect on apomorphine-induced stereotypy and modest activity against typical D_2 agonist-induced responses, can readily and completely block grooming induced by the potent benzazepine D_1 agonist SK&F 77434 (Murray & Waddington, 1990). Grooming constitutes the most established behavioural model of D_1 receptor stimulation, while vacuous chewing represents a more controversial model thereof (Rosengarten *et al.*, 1983; 1986) that we have not found to be induced by a range of conventional benzazepine selective D_1 agonists (Murray & Waddington, 1989b; Daly & Waddington, 1992b; Waddington *et al.*, 1994a). However, we have recently reported the novel, high potency isochroman D_1 agonist, A 68930 (DeNinno *et al.*, 1991; Grenader & Healy, 1992) to induce both intense grooming *and* vacuous chewing; unexpectedly, while this grooming response was readily blocked by both benzazepine (SCH 23390, NNC 756) and isoquinoline (BW 737C) selective D_1 antagonists, vacuous chewing was blocked only by BW 737C but not by SCH 23390 or NNC 756 (Daly & Waddington, 1993). We found here that clozapine, like SCH 23390 and NNC 756, readily and completely blocked intense grooming but did not influence the vacuous chewing response to A 68930; this attests the preferential action of clozapine on D_1-mediated function, but indicates that this is confined to specific elements of D_1 agonist-induced behaviour. The action of BW 737C but not of SCH 23390 or NNC 756 in blocking A 68930-induced vacuous chewing suggests that this response is mediated via a subtype of 'D_1-like' receptor distinct from that mediating grooming (Daly & Waddington, 1993); thus, the present data suggest that preferential interaction of clozapine with the D_1 system may be confined to 'D_1-like' receptors mediating grooming and not to generalise to those mediating vacuous chewing.

These 'open field' data are complemented by recent findings at other levels of behavioural examination in the intact adult rodent, including hind limb retraction (Ellenbroek *et al.*, 1991) and prepulse inhibition of acoustic startle (Swerdlow *et al.*, 1991), which indicate similarly some preferential action of clozapine in attenuating D_1-mediated function and sharing of some of the psychopharmacological properties of selective D_1 antagonists; however, they leave open the issue of the basis of this effect. It is well recognised, and confirmed here, that clozapine is a relatively weak and essentially non-selective antagonist of both D_1 and D_2 (more correctly 'D_1-like' and 'D_2-like'; see Introduction) receptors, with affinity for a number of non-dopaminergic sites (Coward *et al.*, 1989; Baldessarini & Frankenburg, 1991; Leysen *et al.*, 1993; Waddington, 1994). However, the lack of selective affinity of clozapine for the classical D_1 vs D_2 receptor or for D_{1A} vs D_{1B} receptors (Pedersen *et al.*, 1994) does not exclude preferential interaction(s) with the D_1 system at other levels of synaptic function.

Furthermore, while recent expansion in dopamine receptor multiplicity is associated primarily with the application of molecular biology/gene cloning techniques, it should not be overlooked that proposals for further dopamine receptor heterogeneity beyond the classical D_1/D_2 schema evolved initially from neurochemical and behavioural considerations; these have included particularly the notion of functionally relevant 'D_1-like' receptors *not* linked to the stimulation of adenylyl cyclase (Mailman *et al.*, 1986; Murray & Waddington, 1989b; Andersen *et al.*, 1990; Johansen *et al.*, 1991; Schoors *et al.*, 1991; Daly & Waddington, 1992b; Downes & Waddington, 1993; Laitinen, 1993), in addition to D_{1A} and D_{1B} receptors which each demonstrate such linkage. On the basis of complete blockade of typical D_1 agonist-induced grooming and weak release of atypical jerking to D_2 agonism in the face of modest reduction in typical D_2-stimulated behaviours, clozapine appears to interact preferentially but not selectively with the classical D_1 system; this action would appear to be at a level beyond the recognition site, for which clozapine has little affinity, or with new, putative 'D_1-like' entities that subserve distinct elements of behaviour. Though D_1 action(s) of clozapine may contribute to its clinical profile (Waddington, 1993; 1994), these considerations leave open the question as to whether properties such as combined D_2/5-HT_2 or preferential D_4 antagonism may play a role in its atypical antipsychotic activity.

These studies were supported by the Wellcome Trust. We thank Abbott, Roussel and Sandoz for gifts of drugs.

References

ALTAR, C.A., BOYAR, W.C., WASLEY, A., GERHARDT, S.C., LIEBMAN, J.M. & WOOD, P.L. (1988). Dopamine neurochemical profile of atypical antipsychotics resembles that of D_1 antagonists. *Naunyn-Schmied. Arch. Pharmacol.*, **338**, 162–168.

ANDERSEN, P.H. & BRAESTRUP, C. (1986). Evidence of different states of the dopamine D_1 receptor: clozapine and fluperlapine may preferentially label an adenylate cyclase-coupled state of the D_1 receptor. *J. Neurochem.*, **47**, 1822–1831.

ANDERSEN, P.H., GINGRICH, J.A., BATES, M.D., DEARRY, A., FALARDEAU, P., SENOGLES, S.E. & CARON, M.G. (1990). Dopamine receptor subtypes: beyond the D-1/D-2 classification. *Trends Pharmacol. Sci.*, **11**, 231–236.

ARNT, J. & HYTTEL, J. (1986). Inhibition of SK&F 38393- and pergolide-induced circling in rats with unilateral 6-OHDA lesion is correlated to dopamine D-1 and D-2 receptor affinities in vitro. *J. Neural Transm.*, **67**, 225–240.

BALDESSARINI, R.J. & FRANKENBURG, F.R. (1991). Clozapine: a novel antipsychotic agent. *New Engl. J. Med.*, **324**, 746–754.

BARLOW, R.B. (1983) *Biodata Handling with Microcomputers*. Amsterdam: Elsevier.

CHIPKIN, R.E. & LATRANYI, M.B. (1987). Similarity of clozapine and SCH 23390 in reserpinized rats suggest a common mechanism of action. *Eur. J. Pharmacol.*, **136**, 371–375.

CIVELLI, O., BUNZOW, J.R. & GRANDY, D.K. (1993). Molecular diversity of the dopamine receptors. *Annu. Rev. Pharmacol. Toxicol.*, **32**, 281–307.

COWARD, D.M., IMPERATO, A., URWYLER, S. & WHITE, T.G. (1989). Biochemical and behavioural properties of clozapine. *Psychopharmacology*, **99** (Supplement), S6–S12.

CRISWELL, H.E., MUELLER, R.A. & BREESE, G.R. (1989). Clozapine antagonism of D_1 and D_2 dopamine receptor-mediated behaviours. *Eur. J Pharmacol.*, **159**, 141–147.

DALY, S.A. & WADDINGTON, J.L. (1992a). Two directions of dopamine D_1/D_2 receptor interaction in studies of behavioural regulation: a finding generic to four new, selective dopamine D_1 receptor antagonists. *Eur. J. Pharmacol.*, **213**, 251–258.

DALY, S.A. & WADDINGTON, J.L. (1992b). D-1 dopamine receptors and the topography of unconditioned motor behaviour: studies with the selective, 'full efficiency' benzazepine D-1 agonist SKF 83189. *J. Psychopharmacol.*, **6**, 50–60.

DALY, S.A. & WADDINGTON, J.L. (1993). Behavioural evidence for 'D-1-like' dopamine receptor subtypes in rat brain using the new isochroman agonist A 68930 and isoquinoline antagonist BW 737C. *Psychopharmacology*, **113**, 45–50.

DENINNO, M.P., SCHOENLEBER, R., MACKENZIE, R., BRITTON, D.R., ASIN, K.E., BRIGGS, C., TRUGMAN, J.M., ACKERMAN, M., ARTMAN, L., BEDNARZ, L., BHATT, R., CURZON, P., GOMEZ, E., KANG, C.H., STITTSWORTH, J. & KEBABIAN, J.W. (1990). A68930: a potent agonist selective for the dopamine D_1 receptor. *Eur. J. Pharmacol.*, **199**, 209–219.

DOWNES, R.P. & WADDINGTON, J.L. (1993). Grooming and vacuous chewing induced by SK&F 83959, an agonist of dopamine 'D_1-like' receptors that inhibit dopamine-sensitive adenylyl cyclase. *Eur. J. Pharmacol.*, **234**, 135–136.

ELLENBROEK, B.A., ARTZ, M.T. & COOLS, A.R. (1991). The involvement of dopamine D_1 and D_2 receptors in the effects of the classical neuroleptic haloperidol and the atypical neuropleptic clozapine. *Eur. J. Pharmacol.*, **196**, 103–108.

EUVRARD, C., FERLAND, L., DI PAULO, T., BEAULIEU, M., LABRIE, F., OBERLANDER, C., RAYNAUD, J.P. & BOSSIER, J.R. (1980). Activity of two new potent dopaminergic agonists at the striatal and anterior pituitary levels. *Neuropharmacology*, **19**, 379–386.

GINGRICH, J.A. & CARON, M.G. (1993). Recent advances in the molecular biology of dopamine receptors. *Annu. Rev. Neurosci.*, **16**, 299–321.

GRABOWSKA-ANDEN, M. & ANDEN, N.-E. (1983). Stimulation of postsynaptic DA-2 receptors produces jerks in reserpine-treated rats. *J. Pharm. Pharmacol.*, **35**, 543–545.

GRABOWSKA-ANDEN, M. & ANDEN, N.-E. (1987). Inhibitory role of D-1 dopamine receptors for the jerks induced by B-HT 920 in rats. *J. Pharm. Pharmacol.*, **39**, 660–661.

GRENADER, A. & HEALY, D.P. (1992). A68930 is a potent, full agonist at dopamine$_1$ (D_1) receptors in renal epithelial LLC-PK_1 cells. *Br. J. Pharmacol.*, **106**, 229–230.

HUBBARD, C.A. & TRUGMAN, J.M. (1993). Reversal of reserpine-induced catalepsy by selective D1 and D2 dopamine agonists. *Mov. Disord.*, **8**, 473–478.

IMPERATO, A. & ANGELUCCI, L. (1989). The effects of clozapine and fluperlapine on the in vivo release and metabolism of dopamine in the striatum and in the prefrontal cortex of freely moving rats. *Psychopharmacol. Bull.*, **25**, 383–389.

JOHANSEN, P.A., HU, X.-T. & WHITE, F.J. (1991). Relationship between D-1 dopamine receptors, adenylate cyclase, and the electrophysiological responses of rat nucleus accumbens neurons. *J. Neural Transm.*, [Gen. Sect.], **86**, 97–113.

KANE, J., HONIGFELD, G., SINGER, J., MELTZER, H. & THE CLOZARIL COLLABORATIVE STUDY GROUP (1988). Clozapine for the treatment-resistant schizophrenic. *Arch. Gen. Psychiat.*, **45**, 789–796.

KEBABIAN, J.W. & CALNE, D.B. (1979). Multiple receptors for dopamine. *Nature*, **277**, 93–96.

LAITINEN, J.T. (1993). Dopamine stimulates K^+ efflux in the chick retina via D_1 receptors independently of adenylyl cyclase activation. *J. Neurochem.*, **61**, 1461–1469.

LEYSEN, J.E., JANSSEN, P.M.F., SCHOTTE, A., LUYTEN, W.H.M.L. & MEGENS, A.A.H.P. (1993). Interaction of antipsychotic drugs with neurotransmitter receptor sites in vitro and in vivo in relation to pharmacological and clinical effects: role of 5-HT_2 receptors. *Psychopharmacology*, **112** (Supplement), S40–S54.

MAILMAN, R.B., SCHULZ, D.W., KILTS, C.D., LEWIS, M.H., ROLLEMA, H. & WYRICK, S. (1986). Multiple forms of the D-1 dopamine receptor: its linkage to adenylate cyclase and psychopharmacological effects. *Psychopharmacol. Bull.*, **22**, 593–598.

MELTZER, H.Y., MATSUBARA, S. & LEE, J.C. (1989). Classification of typical and atypical antipsychotic drugs on the basis of dopamine D-1, D-2 and serotonin$_2$ pK_i values. *J. Pharmacol. Exp. Ther.*, **251**, 238–246.

MURRAY, A.M. & WADDINGTON, J.L. (1989a). Further evidence for two directions of D-1:D-2 dopamine receptor interaction revealed concurrently in distinct elements of typical and atypical behaviour: studies with the new enantioselective D-2 agonist LY 163502. *Psychopharmacology*, **98**, 245–250.

MURRAY, A.M. & WADDINGTON, J.L. (1989b). The induction of grooming and vacuous chewing by a series of selective D_1 dopamine receptor agonists: two directions of D_1:D_2 interaction. *Eur. J. Pharmacol.*, **160**, 377–384.

MURRAY, A.M. & WADDINGTON, J.L. (1990). The interaction of clozapine with dopamine D_1 versus dopamine D_2 receptor-mediated function: behavioural indices. *Eur. J. Pharmacol.*, **186**, 79–86.

PEDERSEN, U.B., NORBY, B., JENSEN, A.A., SCHIODT, M., HANSEN, A., SUHR-JESSEN, P., SCHEIDELER, M., THASTRUP, O. & ANDERSEN, P.H. (1994). Characteristics of stably expressed human dopamine D_{1a} and D_{1b} receptors; atypical behaviour of the dopamine D_{1b} receptor. *Eur. J. Pharmacol.-Mol. Pharmacol. Sect.*, **267**, 85–93.

PUGH, M.T., O'BOYLE, K.M., MOLLOY, A.G. & WADDINGTON, J.L. (1985). Effects of the putative D-1 antagonist SCH 23390 on stereotyped behaviour induced by the D-2 agonist RU 24213. *Psychopharmacology*, **87**, 308–312.

ROSENGARTEN, H., SCHWEITZER, J.W. & FRIEDHOFF, A.J. (1983). Induction of oral dyskinesia in naive rats by D-1 stimulation. *Life Sci.*, **33**, 2479–2482.

ROSENGARTEN, H., SCHWEITZER, J.W. & FRIEDHOFF, A.J. (1986). Selective dopamine D-2 receptor reduction enhances a D-1 mediated oral dyskinesia in rats. *Life Sci.*, **39**, 29–35.

SCHOORS, D.F., VAUQUELIN, G.P., DE VOS, H., SMETS, G., VELKENIERS, B., VANHAELST, L. & DUPONT, A.G. (1991). Identification of a D_1 dopamine receptor, not linked to adenylate cyclase, on lactotroph cells. *Br. J. Pharmacol.*, **103**, 1928–1934.

SIBLEY, D.R. & MONSMA, F.J. (1992). Molecular biology of dopamine receptors. *Trends Pharmacol. Sci.*, **13**, 61–69.

SWERDLOW, N.R., KEITH, V.A., BRAFF, D.L. & GEYER, M.A. (1991). Effects of spiperone, raclopride, SCH 23390 and clozapine on apomorphine inhibition of sensorimotor gating of the startle response in the rat. *J. Pharmacol. Exp. Ther.*, **256**, 530–536.

VAN TOL, H.H.M., BUNZOW, J.R., GUAN, H.-C., SUNAHARA, R.S., SEEMAN, P., NIZNIK, H.B. & CIVELLI, O. (1991). Cloning of the gene for a human dopamine D_4 receptor with high affinity for the antipsychotic clozapine. *Nature*, **350**, 610–614.

WADDINGTON, J.L. (1993). Pre- and postsynaptic D_1 to D_5 dopamine receptor mechanisms in relation to antipsychotic activity. In *Antipsychotic Drugs and their Side Effects*. ed. Barnes, T.R.E. pp. 65–85. London: Academic Press.

WADDINGTON, J.L. (1994). Mechanistic and clinical psychopharmacology of typical neuroleptics and atypical antipsychotic drugs in schizophrenia. In *Schizophrenia*. ed. Hirsch, S.R. & Weinberger, D.R. Oxford: Blackwell (in press).

WADDINGTON, J.L. & DALY, S.A. (1993). Regulation of unconditioned motor behaviour by D_1:D_2 interactions. In *D_1:D_2 Dopamine Receptor Interactions: Neuroscience and Psychopharmacology*. ed. Waddington, J.L. pp. 51–78. London: Academic Press.

WADDINGTON, J.L., DALY, S.A., DOWNES, R.P., DEVENEY, A.M., MCCAULEY, P.G. & O'BOYLE, K.M. (1994a). Behavioural pharmacology of 'D-1-like' dopamine receptors: further subtyping, new pharmacological probes and interactions with 'D-2-like' receptors. *Prog. Neuro-Psychopharmacol. Biol. Psychiat.*, (in press).

WADDINGTON, J.L., DALY, S.A., MCCAULEY, P.G. & O'BOYLE, K.M. (1994b). Levels of functional interaction between 'D-1-like' and D-2-like' dopamine receptor systems. In *Dopamine Receptors and Transporters*. ed. Niznik, H.B. pp. 513–537. New York: Marcel Dekker.

(Received May 9, 1994
Revised July 13, 1994
Accepted July 15, 1994)

Br. J. Pharmacol. (1994), **113**, 845–852 © Macmillan Press Ltd, 1994

Characterization of receptors mediating vascular responses to endothelin-1 in the conscious rat

[1]János G. Filep, *Martine Clozel, †Alain Fournier & Éva Földes-Filep

Research Center, Maisonneuve-Rosemont Hospital, University of Montréal, P.Q., Canada H1T 2M4; *Pharma Division, Preclinical Research, F. Hoffmann-La Roche Ltd., CH-4002 Basel, Switzerland and †Institut National de la Recherche Scientifique-Santé, Montréal, P.Q., Canada H9R 1G6

1 The present study has determined the receptors mediating the vascular responses (pressor and depressor actions and vascular permeability effect) to endothelin-1 (ET-1) in the conscious rat by using the novel non-peptide ET_A/ET_B receptor antagonist, bosentan (Ro 47-0203, 4-*tert*-butyl-N-[6-(2 hydroxyethoxy)-5-(2-methoxy-phenoxy)-2,2'-bipyrimidine-4-yl]benzene-sulphonamide), the ET_A receptor-selective antagonist, FR 139317 and the ET_B receptor-selective peptide agonist, IRL 1620.

2 Bolus injection of ET-1 (1 nmol kg^{-1}, i.v.) resulted in a prolonged pressor effect (maximum increase in mean arterial blood pressure (MABP) was 47 ± 3 mmHg, $n = 6$) preceded by a transient depressor response (maximum decrease in MABP was 17 ± 1 mmHg). Both these responses were inhibited by bosentan (1-20 mg kg^{-1}, i.v. bolus) in a dose-dependent manner. The maximum inhibition of ET-induced depressor and pressor responses did not exceed 53 and 87%, respectively. FR 139317 (2.5 mg kg^{-1}, i.v.) attenuated the pressor response to ET-1 by 75% without affecting the depressor response. Furthermore, FR 139317, but not bosentan, prolonged the depressor action of ET-1. Corresponding to changes in blood pressure, a small transient tachycardia (Δheart rate 15 ± 5 beats min^{-1}) followed by a sustained bradycardia (Δheart rate -48 ± 10 beats min^{-1}, $n = 6$) was observed following injection of 1 nmol kg^{-1} ET-1. FR 139317 and bosentan (10 mg kg^{-1}) inhibited ET-1-induced bradycardia by 79% and 71%, respectively. ET-1-induced tachycardia was significantly attenuated by bosentan, but not FR 139317.

3 The ET_B receptor agonist, IRL 1620 (0.1–2 nmol kg^{-1}, i.v.) produced biphasic dose-dependent changes in MABP with an initial transient fall followed by a prolonged pressor action. The maximum decrease and increase in MABP were 11 ± 2 and 19 ± 3 mmHg, respectively ($n = 5$). These changes in MABP were accompanied by a transient tachycardia (Δheart rate 9 ± 3 beats min^{-1}) and prolonged bradycardia (Δheart rate -17 ± 11 beats min^{-1}), respectively. Pretreatment of the animals with FR 139317 (2.5 mg kg^{-1}, i.v.) did not affect IRL 1620 (1 nmol kg^{-1})-induced changes in MABP and heart rate, whereas both the depressor and pressor actions of IRL 1620 and the accompanying tachycardia and bradycardia were almost completely inhibited by bosentan (10 mg kg^{-1}).

4 ET-1 (1 nmol kg^{-1}) enhanced albumin extravasation in the upper and lower bronchi, spleen, kidney, stomach and duodenum (up to 246%) as measured by the extravasation of Evans blue dye. FR 139317 (2.5 mg kg^{-1}) completely inhibited ET-1-induced protein extravasation in the stomach and duodenum, whereas 40–75% inhibition was observed in the other vascular beds studied. The permeability effect of ET-1 was almost completely inhibited by bosentan (10 mg kg^{-1}) in all vascular beds studied.

5 IRL 1620 (0.4 or 1 nmol kg^{-1}, i.v.) enhanced albumin extravasation (up to 219%) in the upper and lower bronchi, spleen and kidney in a dose-dependent manner. Unlike ET-1, IRL 1620 failed to increase albumin extravasation in the stomach and duodenum.

6 The present study demonstrates in the conscious rat that ET_A and ET_B receptors are responsible for mediating the majority of the pressor response to ET-1 and suggest that a small component of the ET-1 pressor response might be mediated via a non-ET_A, non-ET_B receptor, whereas ET_B and perhaps a non-ET_A, non-ET_B receptor may mediate the depressor action of ET-1. Furthermore, the ET-1 induced albumin extravasation is mediated solely via ET_A receptors in the stomach and duodenum, whereas both ET_A and ET_B receptors are involved in the permeability effect of ET-1 in the bronchial, splenic and renal vascular beds.

Keywords: Endothelin-1; ET_A and ET_B receptors; vascular effects; vascular permeability; bosentan; FR 139317; IRL 1620; airways; gastrointestinal tract; kidney

Introduction

An increasing body of evidence supports a role for endothelin-1 (ET-1) in the regulation of cardiovascular functions including systemic and local vascular tone, cardiac output (see Simonson & Dunn, 1991; Rubanyi & Parker Botelho, 1991) and microvascular permeability (Filep *et al.*, 1991; Zimmerman *et al.*, 1992). Receptor binding studies, functional data and cross-desensitization experiments implied the existence of multiple endothelin receptor subtypes (see Sakurai *et al.*, 1992; Sokolovsky, 1992), which may mediate the cardiovascular actions of ET-1.

To date, two mammalian ET receptor subtypes, designated ET_A and ET_B, have been cloned, sequenced and characterized (Arai *et al.*, 1990; Sakurai *et al.*, 1990). The ET_A receptor is considered isopeptide-selective, since it binds ET-1 and ET-2 more avidly than ET-3. In contrast, the ET_B receptor binds all three ET isopeptides with a similar affinity and is considered non-isopeptide-selective. Recently, an ET-3-specific receptor (termed ET_C) was also cloned from *Xenopus* melanophores (Karne *et al.*, 1993). However, it remains to be established

[1] Author for correspondence.

whether this amphibian ET_C receptor has a mammalian counterpart. Activation of ET_A receptors is implicated in mediating the vasoconstrictor and pressor actions of ET-1, whereas it has been suggested that ET_B receptors mediate vasodilatation and depressor responses to ET-1 (Takayanagi *et al.*, 1991; Ihara *et al.*, 1992). However, these concepts have been challenged as recent studies have demonstrated that complete inhibition of the pressor effect of ET-1 cannot be achieved by the putative ET_A receptor antagonists, BQ-123 (Ihara *et al.*,1992; Filep *et al.*, 1992; 1993b; McMurdo *et al.*, 1993) and FR 139317 (Bird & Waldron, 1993; Sogabe *et al.*, 1993) both in conscious and anaesthetized rats. The pressor effect of the ET_B receptor-selective agonists, sarafotoxin S6c and [$Ala^{1,3,11,15}$]endothelin-1 has also been described in pithed and conscious rats (Gardiner *et al.*, 1990; Douglas & Hiley, 1991; Williams *et al.*, 1991; Clozel *et al.*, 1992). Furthermore, recent studies on isolated blood vessels provided evidence for ET_B-mediated vasoconstriction (Bigaud & Pelton, 1992; Clozel *et al.*, 1992; Moreland *et al.*, 1992; Sumner *et al.*, 1992; LaDouceur *et al.*, 1993) and for the involvement of a novel, non-ET_A, non-ET_B receptor in mediating the coronary vasoconstrictor action of ET-1 (Harrison *et al.*, 1992). We have shown recently that ET-1-induced albumin extravasation can be partially inhibited by BQ-123 in selected vascular beds of conscious rats (Filep *et al.*,1993b). These findings suggest that a component of the permeability effect of ET-1 is not mediated via the ET_A receptor. Recent observations raised the possibility that BQ-123 may also antagonize a non-ET_A, non-ET_B receptor as it has been reported to show a preferential antagonistic effect on the ET-3 over the ET-1 twitch response in the rat vas deferens (Eglezos *et al.*, 1993).

The aim of the present experiments was to characterize the ET receptor subtypes which mediate the vascular (haemodynamic and albumin extravasation) responses to ET-1 in the conscious rat by using a novel, non-peptide ET_A/ET_B receptor antagonist, bosentan (Ro 47-0203, 4-*tert*-butyl-N-[6-(2 hydroxy-ethoxy)-5-(2-methoxy-phenoxy)-2,2'-bipyrimidin-4-yl]-benzene-sulphonamide) (Clozel *et al.*, 1994), the modified tripeptide ET_A receptor-selective antagonist, FR 139317 ((**R**) 2-[(**R**)-2-[(S)-2-1-(hexahydro-1*H*-azepinyl)] carbonyl]amino-4-methylpentanoyl] amino-3-[-3-(1-methy-1*H*-indoyl)] propionyl]amino-3-(2-pyridyl)propionicacid) (Aramori *et al.*, 1993; Sogabe *et al.*, 1993) and the ET_B receptor-selective agonist, IRL 1620 (Suc-[Glu^9, $Ala^{11,15}$]endothelin-1(18–21)) (Takai *et al.*, 1992).

Methods

Preparation of the animals

The experiments were performed on conscious, chronically catheterized male Wistar rats weighing 210–280 g. The animals were housed in individual metabolic cages. During anaesthesia (ketamine, 75 mg kg^{-1} and sodium pentobarbitone, 15 mg kg^{-1}), catheters were implanted into the abdominal aorta and vena cava as described previously (Filep & Fejes-Tóth, 1986). The animals were allowed to recover completely for at least four days following the surgical procedures. During the experiments the animals could move freely and had free access to food and water. Mean arterial blood pressure (MABP) and heart rate were monitored continuously by a blood pressure analyser (Micro-Med, Louisville, KY, U.S.A.) using a COBE CDX III pressure transducer.

Experimental protocols

In the first series of experiments, following an equilibration period of 1 h, animals were given ET-1 or IRL 1620 (0.1, 0.4, 1, 1.3 or 2 nmol kg^{-1}, i.v., bolus) in a volume of 5 µl per 100 g body weight, followed by 30 µl 0.9% w/v NaCl. Some animals were given bosentan (1, 3, 10 or 20 mg kg^{-1}, i.v.) 10 min before injection of ET-1 (1 nmol kg^{-1}). In a separate set of experiments, IRL 1620 (1 nmol kg^{-1}, i.v.) was injected following pretreatment of the animals with FR 139317 (2.5 mg kg^{-1}, i.v.) or bosentan (10 mg kg^{-1}, i.v.) On any one day each animal received only one dose of ET-1 or IRL 1620. At least 2 days were allowed to elapse between different experiments on the same rat. Both the order in which ET-1 or IRL-1620 were injected and the doses within each dose-response curve was randomized. In another set of experiments, the specificity of bosentan as an ET receptor antagonist was assessed by comparing changes in MABP elicited by i.v. bolus injections of noradrenaline (15 nmol kg^{-1}), arginine vasopressin (40 mu kg^{-1}), acetylcholine (8 nmol kg^{-1}) or platelet-activating factor (1.9 nmol kg^{-1}) in the absence and presence of bosentan (10 mg kg^{-1}, i.v., 10 min prior to vasoactive agents.)

In subsequent experiments to measure albumin extravasation, Evans blue dye which binds to plasma albumin (Rawson, 1943) was used as a marker. Previous studies have demonstrated close correlation for the extravasation of Evans blue dye and radioiodinated serum albumin (Udaka *et al.*, 1970; Rogers *et al.*, 1989). Animals were pretreated with FR 139317 (2.5 mg kg^{-1} i.v., bolus) for 5 min, bosentan (10 mg kg^{-1}, i.v., bolus) for 10 min or 0.9% NaCl before injection of ET-1 (1 nmol kg^{-1}, i.v.) and Evans blue dye (20 mg kg^{-1}). In a separate series of experiments IRL 1620 (0.4 or 1 nmol kg^{-1}) was administered i.v. together with Evans blue dye. Ten min after injection of Evans blue with ET-1 or IRL 1620, the animals were anaesthetized with sodium pentobarbitone (50 mg kg^{-1}, i.v.) and perfused with 50 ml 0.9% w/v NaCl solution through a catheter inserted into the abdominal aorta to remove the excess intravascular dye. The perfusion was completed by 5 min. Portions of the trachea, upper bronchi (airways extending from the bifurcation of the trachea to its entry to parenchyma), lower bronchi (defined as major airways surrounded by pulmonary parenchyma that could be easily dissected without magnification), liver, spleen, pancreas, right kidney, stomach and duodenum were then excised and weighed. The tissue content of Evans blue dye was then measured by spectrophotometry following extraction with formamide as described previously (Filep *et al.*, 1991) and expressed as µg dye g^{-1} dry tissue weight, to avoid underestimation of changes due to plasma fluid extravasation.

Drugs and chemicals

ET-1 and IRL 1620 were synthesized in our laboratories by solid-phase methodology (Germain *et al.*, 1993). The purity of the preparations were greater than 97% as measured by high performance liquid chromatography. ET-1 and IRL 1620 were dissolved in distilled water and stored at −20°C. On the day of the experiments an aliquot was removed and diluted further with 0.9% w/v NaCl. Bosentan, (Ro 47-0203 as the sodium salt, Hoffmann-La Roche Ltd, Basel, Switzerland) was dissolved in distilled water containing 300 mM glucose. FR 139317 (Fujisawa Pharmaceutical Co., Osaka, Japan), acetylcholine chloride, noradrenaline hydrochloride, arginine vasopressin (Grade VI, 100 u ml^{-1}, Sigma Chemical Co., St. Louis, MO, U.S.A.) and platelet-activating factor (1-O-hexadecyl-2-O-acetyl-sn-glycero-3-phosphorylcholine, Bachem, Bubendorf, Switzerland) were dissolved in 0.9% w/v NaCl. Evans blue dye was purchased from Sigma Chemical Co.

Statistical analysis

Results are expressed as mean values ± s.e.mean. Statistical evaluation of the data was performed by one-way analysis of variance using ranks (Kruskal-Wallis test) followed by Dunn's multiple contrast hypothesis test (Dunn, 1964), when various treatments were compared to the same control; or by Wilcoxon signed rank test and Mann-Whitney U test, for paired

and unpaired observations, respectively. A P value of <0.05 was considered significant for all tests.

Results

Baseline values for MABP and heart rate in conscious rats were 103 ± 1 mmHg and 340 ± 5 beats min^{-1} ($n = 78$), respectively. These values were unaffected by vehicle, FR 139317 and bosentan at any of the doses employed in this study.

Effects of bosentan on the pressor and depressor responses to endothelin-1

Preliminary experiments showed that bosentan (10 mg kg^{-1}, i.v.) was an effective inhibitor when given 10 min prior to ET-1 (1 nmol kg^{-1}, i.v., bolus, $n = 4$). Since a pretreatment greater than 10 min did not enhance further the inhibitory action of bosentan, this was used in all subsequent experiments.

As well established, ET-1 (1 nmol kg^{-1}) produced a sustained pressor effect preceded by a transient depresser action (Figure 1). The depressor response lasted for 30–50 s. Maximum increases in MABP was observed within 3–4 min after injection of the peptide. Corresponding to the changes in MABP, a small transient tachycardia (Δheart rate: 15 ± 5 beats min^{-1}, $n = 6$) was followed by a sustained bradycardia (Δheart rate -48 ± 10 beats min^{-1}, $n = 6$).

Both the depressor and pressor effects of ET-1 were attenuated by bosentan in a dose-dependent manner (Figure 1). However, complete inhibition of the ET-1-induced depressor and pressor responses after bosentan treatment was not observed. The peak depressor and pressor effects of ET-1 were decreased on average by 53 and 87%, respectively, following bosentan (10 mg kg^{-1}) (Figure 1). ET-1-induced tachycardia and bradycardia were also markedly reduced by bosentan (Δheart rate were 6 ± 2 and -14 ± 7 beats min^{-1}, respectively, $n = 6$, $P < 0.05$ compared to ET-1). Bosentan at a dose of 20 mg kg^{-1} did not cause a significantly greater reduction in either the maximum decrease or maximum increase in MABP elicited by ET-1 (1 nmol kg^{-1}) than 10 mg kg^{-1} (Figure 1). Bosentan, up to a dose of 20 mg kg^{-1}, did not prolong the depressor action of ET-1. For example, the duration of ET-1 (1 nmol kg^{-1})-induced hypotension was 35–60 s in the presence of 10 mg kg^{-1} bosentan.

The inhibitory action of bosentan was qualitatively and quantitatively different from that of FR 139317. The depressor response to 1 mg kg^{-1} ET-1 was unaffected by FR 139317, 2.5 mg kg^{-1} (maximum decreases in MABP were 17 ± 1 mmHg and 20 ± 3 mmHg in the absence and presence of FR 139317, respectively, $n = 6$, $P > 0.05$). On the other hand, the peak pressor response to ET-1 was decreased to 12 ± 2 mmHg ($n = 6$, $P < 0.01$) by 2.5 mg kg^{-1} FR 139317. Increasing the dose of FR 139317 to 10 mg kg^{-1} did not cause further inhibition of the pressor effect of ET-1. The maximum inhibition of the pressor effect of ET-1 that can be achieved with bosentan was greater than that observed following FR 139317 treatment (ET-1 (1 nmol kg^{-1})- induced increases in MABP were 12 ± 2 mmHg ($n = 6$) and 6 ± 1 mmHg ($n = 6$) in FR 139317 and bosentan-treated animals, respectively, $P < 0.02$). FR 139317 did not affect ET-1-induced transient tachycardia (Δheart rate 12 ± 2 beats min^{-1} ($n = 6$) $P > 0.05$ compared to ET-1), whereas it inhibited ET-1-induced bradycardia (Δheart rate -10 ± 3 beats min^{-1} ($n = 6$) $P < 0.05$ compared to ET-1).

Bosentan (10 mg kg^{-1}) neither affected significantly the pressor responses to 15 nmol kg^{-1} noradrenaline (maximum increases in MABP were 41 ± 3 and 41 ± 2 mmHg in the absence and presence of bosentan, respectively, $n = 4$) or 40 mu kg^{-1} arginine vasopressin (ΔMABP 39 ± 3 and 38 ± 2 mmHg in the absence and presence of bosentan, respectively, $n = 4$) nor modified the depressor responses elicited by 8 nmol kg^{-1} acetylcholine (maximum decreases in MABP were 29 ± 2 and 31 ± 1 mmHg in the absence and presence of bosentan, respectively, $n = 3$) or 1.9 nmol kg^{-1} platelet-activating factor (ΔMABP -37 ± 3 and -36 ± 3 mmHg in the absence and presence of bosentan, respectively, $n = 3$).

Effects of bosentan and FR 139317 on IRL 1620-induced changes in blood pressure

Bolus i.v. injection of the ET_B receptor agonist, IRL 1620 (0.1–2 nmol kg^{-1}) produced biphasic, dose-dependent

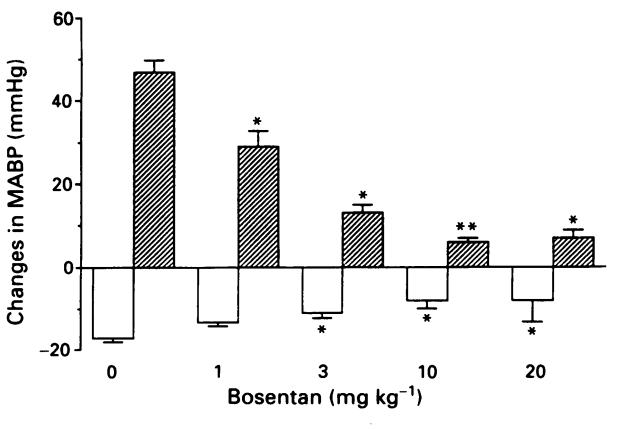


Figure 1 Dose-dependent inhibition by bosentan of the peak depressor (open columns) and pressor responses (hatched columns) to endothelin-1 1 nmol kg^{-1}, in conscious rats. Bosentan or its vehicle (300 mM glucose) was injected i.v. 10 min before administration of ET-1. Baseline MABP was 102 ± 2 mmHg ($n = 6$). Values are means with s.e.mean for 4–6 separate experiments. $^*P<0.05$; $^{**}P<0.01$ (compared to control (vehicle) by Dunn's multiple contrast hypothesis tests).

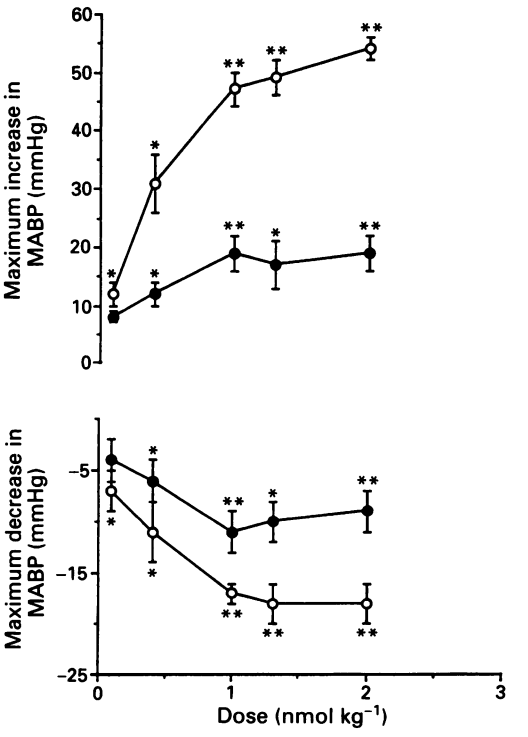


Figure 2 Peak depressor and pressor responses observed following i.v. injection of endothelin-1 (○) or IRL 1620 (●) in conscious rats. Baseline MABP was 103 ± 2 mmHg ($n = 11$). Values are means with s.e.mean for 3–6 separate experiments. $^*P<0.05$; $^{**}P<0.01$ (compared to vehicle by Dunn's multiple contrast hypothesis test).

changes in MABP with a transient fall followed by a prolonged pressor action. The duration of the depressor action of IRL 1620 was longer than that of equimolar doses of ET-1. For example, the depressor response to 1 nmol kg^{-1} IRL 1620 lasted for 50–110 s. Maximum decreases and increases in MABP were observed following 1 nmol kg^{-1} IRL 1620 (Figure 2). Corresponding to the changes in MABP, IRL 1620 (1 nmol kg^{-1}) evoked a slight, transient tachycardia (Δheart rate 9 ± 3 beats min^{-1}, $n = 5$) followed by a prolonged bradycardia (Δheart rate −17 ± 11 beats min^{-1}, $n = 5$). Since at the dose of 2 nmol kg^{-1}, ET-1 caused severe bleeding from the orbital sinus, higher doses were not tested and consequently the maximum effects of ET-1 on MABP were not precisely determined. The apparent maximum decrease in MABP that could be evoked by ET-1 was 2 fold greater than that elicited by IRL 1620 (Figure 2). Similarly, the apparent maximum increase in MABP that can be evoked by ET-1 was 2.8 fold greater than that observed following IRL 1620 (Figure 2). Pretreatment of the animals with FR 139317 (2.5 mg kg^{-1}, i.v. 5 min prior to IRL 1620) did not affect IRL 1620 (1 nmol kg^{-1})-induced changes in MABP, whereas both the depressor and pressor responses to IRL 1620 were almost completely inhibited by bosentan (10 mg kg^{-1}) (Figure 3).

Effects of bosentan and FR 139317 on endothelin-1-induced Evans blue extravasation

ET-1 at 1 nmol kg^{-1} significantly enhanced albumin extravasation in the upper and lower bronchi (Figure 4), spleen, kidney, stomach and duodenum (Figure 5), whereas no significant changes were observed in the trachea, pulmonary parenchyma, liver and pancreas (data not shown). FR 139317 (2.5 mg kg^{-1} i.v. 5 min prior to ET-1) reduced tissue Evans blue content on average by 56, 72, 40, 75, 96 and 100% in the upper and lower bronchi, spleen, kidney, stomach and duodenum, respectively (Figures 4 and 5). Pretreatment of the animals with the ET_A/ET_B receptor antagonist, bosentan (10 mg kg^{-1}, i.v. bolus, 10 min prior to ET-1) also protected against ET-1-induced albumin extravasation in the same vascular beds. ET-1-induced Evans blue accumulation was reduced on average by 88, 96, 89, 91, 100 and 100% in the upper and lower bronchi, spleen, kidney, stomach and duodenum, respectively in the presence of bosentan (Figures 4 and 5). Neither FR 139317 nor bosentan by itself affected significantly extravasation of Evans blue dye in the vascular beds studied (Figures 4 and 5).

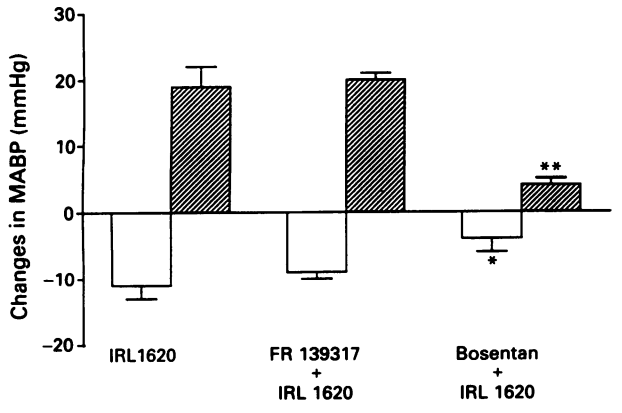


Figure 3 Effects of FR 139317 and bosentan on the peak depressor (open columns) and pressor responses (hatched columns) to IRL 1620 in conscious rats. FR 139317 (2.5 mg kg^{-1}) or bosentan (10 mg kg^{-1}) were injected i.v. 10 or 5 min before administration of IRL 1620 (1 nmol kg^{-1}), respectively. Baseline MABP were 102 ± 2 mmHg ($n = 5$), 101 ± 2 mmHg ($n = 5$) and 98 ± 3 mmHg in control, FR 139317 and bosentan-treated animals, respectively. Values are means with s.e.mean. *$P<0.05$; **$P<0.01$ (compared to IRL 1620 by Mann-Whitney's U test).

IRL 1620-induced albumin extravasation

Injection of 1 nmol kg^{-1} IRL 1620 increased tissue Evans blue content in the upper and lower bronchi on average by 45 and 119%, respectively (Figure 4), whereas no significant changes were observed in the trachea and pulmonary parenchyma (Table 1). IRL 1620 injection also produced increases of 45 and 70% in albumin extravasation in the spleen and kideny (Figure 5). In these vascular beds, the effects of IRL 1620 appeared to be dose-related (Table 1). Unlike ET-1, IRL 1620 failed to increase albumin extravasation in the stomach and duodenum (Figure 5). IRL 1620-induced changes in tissue Evans blue dye content were almost completely prevented by bosentan (10 mg kg^{-1}) in all vascular beds studied (Table 1).

Discussion

It is well documented that injection of ET-1 evokes an initial transient depressor response followed by a prolonged pressor response both in anaesthetized and conscious rats (Yanagisawa *et al.*, 1988; De Nucci *et al.*, 1988; Gardiner *et al.*, 1989; Le Monnier de Gouville *et al.*, 1989), albeit quantitative differences exist in the magnitude of the responses. These changes in MABP are thought to be mediated via at least two different ET receptors. In order to characterize these receptors, we have studied the inhibitory effect of bosentan, a non-peptide, orally active ET_A/ET_B receptor antagonist (Clozel *et al.*, 1994) and the ET_A receptor-selective antagonist FR 139317 (Aramori *et al.*, 1993; Sogabe *et al.*, 1993) on the depressor and pressor actions of ET-1 and the

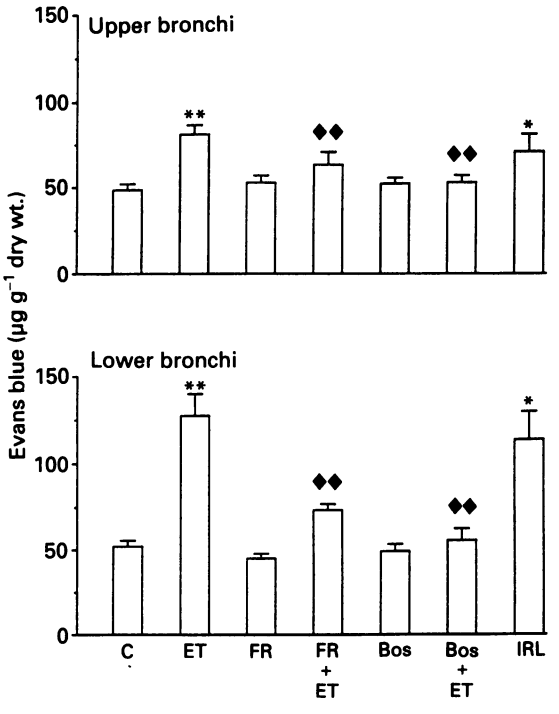


Figure 4 Effects of FR 139317 and bosentan on endothelin-1-induced albumin extravasation in rat airways. The animals were injected i.v. with 0.9% w/v NaCl (C), endothelin-1 (ET, 1 nmol kg^{-1}), FR 139317 (FR, 2.5 mg kg^{-1}), FR 139317 (2.5 mg kg^{-1}, 5 min prior to ET-1) plus ET-1 (1 nmol kg^{-1}), bosentan (Bos, 10 mg kg^{-1}), bosentan (10 mg kg^{-1} 10 min prior to ET-1) plus ET-1 (1 nmol kg^{-1}) or IRL 1620 (1 nmol kg^{-1}) together with Evans blue dye (20 mg kg^{-1}. The rats were anaesthetized and perfused with 0.9% w/v NaCl 10 min after injection of Evans blue dye. The permeability measurement was made 15 min after injection of the dye. Values are means with s.e.mean for 6 experiments. *$P<0.05$; **$P<0.01$ (compared to control); ◆$P<0.05$; ◆◆$P<0.01$ (compared to ET-1).

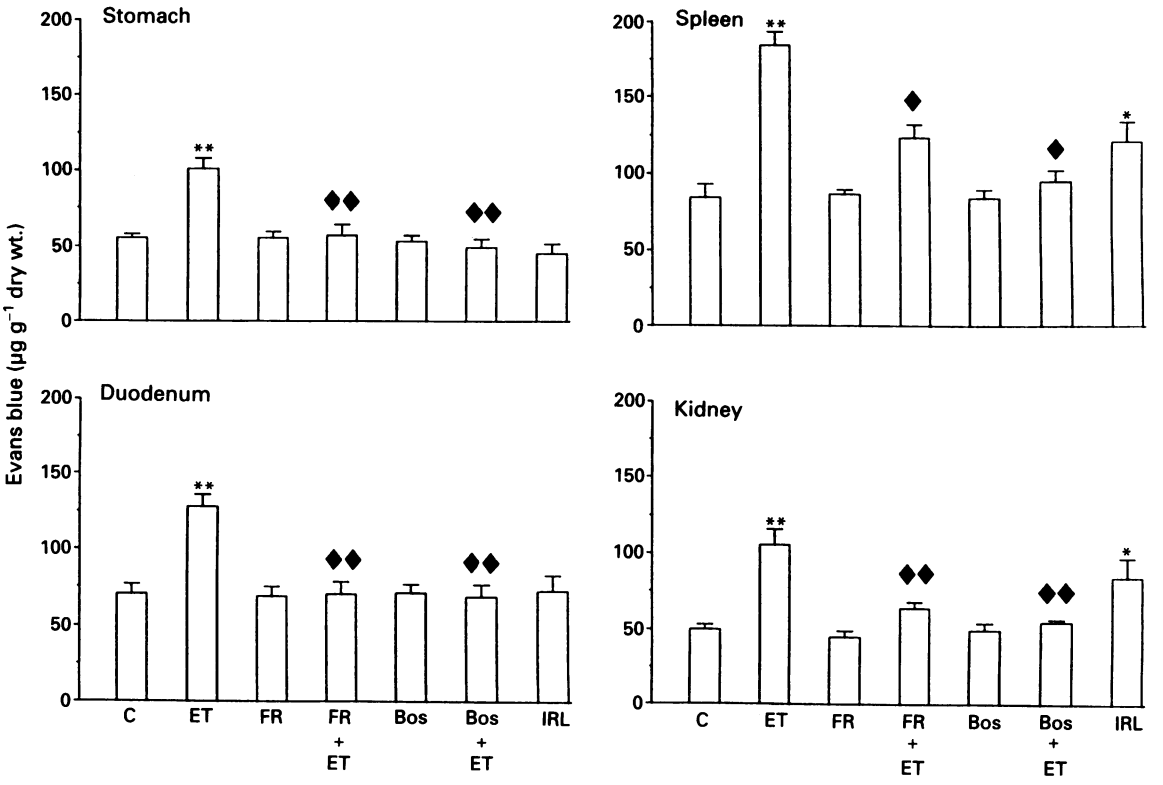


Figure 5 Effects of FR 139317 and bosentan on endothelin-1-induced albumin extravasation in selected vascular beds of conscious rats. The animals were injected i.v. with 0.9% w/v NaCl (C), ET-1 (ET, 1 nmol kg^{-1}), FR 139317 (FR, 2.5 mg kg^{-1}), FR 139317 (2.5 mg kg^{-1}, 5 min prior to ET-1) plus ET-1 (1 nmol kg^{-1}), bosentan (Bos, 10 mg kg^{-1}), bosentan (10 mg kg^{-1}, 10 min prior to ET-1) plus ET-1 (1 nmol kg^{-1}) or IRL 1620 (1 nmol kg^{-1}) together with Evans blue dye (20 mg kg^{-1}). The rats were anaesthetized and perfused with 0.9% w/v NaCl 10 min after injection of the dye. The permeability measurement was made 15 min after injection of the dye. Values are means with s.e.mean for 6 experiments. $*P<0.05$; $**P<0.01$ (compared to control); ◆$P<0.05$; ◆◆$P<0.01$ (compared to ET-1).

Table 1 Effect of bosentan on IRL 1620-induced albumin extravasation in conscious rats

	Control	*IRL 1620* (nmol kg^{-1})		*Bosentan* (10 mg kg^{-1}) *plus*
		0.4	1	*IRL 1620* (1 nmol kg^{-1})
	($n = 6$)	($n = 4$)	(n = 6)	($n = 4$)
Albumin extravasation (μg Evans blue dye per g dry tissue weight)				
Trachea	55 ± 5	51 ± 9	57 ± 8	54 ± 7
Upper bronchi	49 ± 3	61 ± 2*	71 ± 10*	51 ± 3#
Lower bronchi	52 ± 3	71 ± 8*	114 ± 16**	61 ± 3#
Pulmonary parenchyma	73 ± 3	72 ± 9	90 ± 10	76 ± 6
Liver	39 ± 6	40 ± 3	55 ± 11	44 ± 5
Spleen	84 ± 9	113 ± 10	122 ± 12*	78 ± 7#
Pancreas	32 ± 6	53 ± 5	52 ± 9	44 ± 7
Kidney	50 ± 3	74 ± 2*	85 ± 13**	52 ± 2#
Stomach	55 ± 3	44 ± 3	45 ± 6	47 ± 5
Duodenum	70 ± 7	76 ± 6	73 ± 10	73 ± 6

Values are means ± s.e.mean. The animals were given a bolus i.v. injection of bosentan or its vehicle (distilled water containing 300 mM glucose) 10 min before i.v. administration of IRL 1620 or its vehicle (0.9% w/v NaCl) together with Evans blue dye (20 mg kg^{-1}). Ten min later, the rats were anaesthetized and perfused with 0.9% w/v NaCl. The permeability measurement was made 15 min after injection of the dye. $*P<0.05$; $**P<0.01$ (compared to control by Dunn's multiple contrast hypothesis test), $\#P<0.05$ (compared to animals receiving 1 nmol kg^{-1} IRL 1620).

ET_B receptor-selective agonist, IRL 1620 (Takai *et al.*, 1992). Bosentan has been shown to antagonise competitively the specific binding of ET-1 on ET_A receptors (human umbilical vein vascular smooth muscle cells) and on ET_B receptors (microsomal membranes from human placenta) with K_i values of 4.7 nM and 95 nM, respectively (Clozel *et al.*, 1994). The present findings that bosentan neither affected the pressor effect of noradrenaline and arginine vasopressin, nor modified the depressor effect of acetylcholine and platelet-activating factor, indicate that it is a specific ET receptor antagonist *in vivo*. IRL 1620 has K_i values of 1.9 μM and 16 pM for the ET_A and ET_B receptors, respectively (Takai *et al.*, 1992). FR 139317 has been reported to be 7000 times more potent in inhibiting the binding of ET-1 to ET_A than ET_B receptors *in vitro* (Aramori *et al.*, 1993). Since FR 139317 did not affect the depressor action of ET-1 (see below) and failed to modify IRL 1620-induced changes in MABP, it might be assumed that at the dose used, FR 139317 does not interfere with ET_B receptors *in vivo*.

The depressor action of ET-1 is thought to be mediated via

ET_B receptors (Saeki *et al.*, 1991; Douglas & Hiley, 1991). Effects involving ET_B receptors would presumably be resistant to inhibition by an ET_A receptor-selective antagonist. Indeed, FR 139317 did not affect the maximum decrease in MABP elicited by ET-1 (Sogabe *et al.*, 1993; Bird & Waldon, 1993 and the present study), but significantly prolonged the duration of the depressor response. This is most likely the consequence of suppression of the ET_A-mediated vasoconstrictor activity. This prolonged depressor response in the presence of FR 139317 may indicate that ET-1 induces sustained release of endogenous vasodilators, which, in turn, ameliorate the pressor effect of the peptide. One of these vasodilators is likely to be nitric oxide as inhibition of its formation leads to potentiation of the pressor action of ET-1 in conscious rats (Filep *et al.*, 1993a). On the other hand, the ET_A/ET_B antagonist, bosentan attenuated ET-1-induced decreases in MABP in a dose-dependent fashion. However, the maximal inhibition reached a plateau at approximately 50%. Thus, there is a component of the depressor action of ET-1 which cannot be inhibited by bosentan, and, therefore, may not be mediated via the ET_B receptor. The finding that the maximum decrease in MABP that can be achieved with IRL 1620 was about 50% of the apparent peak depressor response to ET-1 would lend further support to this notion. The difference in efficacy of ET-1 and IRL 1620 might reflect the partial agonist activity of IRL 1620 at ET_B vasorelaxant receptors *in vivo*. However, the finding that IRL 1620 at equimolar concentrations to ET-1 caused a more protracted vasodilatation response in perfused lungs of neonatal pigs (Pinheiro & Malik, 1993) would argue against this explanation. Alternatively, it is possible that more than one subtype of ET_B receptor, which is insensitive to bosentan, mediates the depressor action of ET-1. This hypothesis should, however, be tempered by the facts that the two ET_B receptor subtypes yet described have been implicated in mediating vasodilatation and vasoconstriction, respectively (Sokolovsky *et al.*, 1992), and that bosentan has similar K_i values for the ET_B receptors mediating vasoconstriction and endothelium-dependent relaxation *in vitro* (Clozel *et al.*, 1994).

Pretreatment of the animals with FR 139317 markedly inhibited the pressor effect of ET-1. However, the degree of inhibition did not exceed 75% (Sogabe *et al.*, 1993 and the present study). These results are comparable to the 70–75% inhibition of the ET-1-induced pressor response observed after bolus injection of BQ-123 both in anaesthetized (McMurdo *et al.*, 1993) and conscious rats (Ihara *et al.*, 1992; Filep *et al.*, 1992; 1993b). In contrast, complete inhibition of the pressor action of ET-1 has been reported following infusion of BQ-123 in the anaesthetized rats (Pollock & Opgenorth, 1993). However, it is likely that the depressor response observed in this latter study following infusion of BQ-123 to control animals might have contributed to the apparent complete inhibition of the pressor action of ET-1. In the conscious rat, bolus injection of BQ-123 had no effect on blood pressure (Ihara *et al.*, 1992; Filep *et al.*, 1992; 1993b). The present study shows that about 90% inhibition of the ET-1 pressor response could be achieved with bosentan compared to the reduction of only 75% observed following ET_A receptor blockade. The ET_B receptor agonist, IRL 1620 can also evoke pressor responses in the conscious rat (Webb *et al.*, 1992 and the present study). Under our experimental conditions, the maximum increase in MABP that can be achieved with IRL 1620 did not exceed 36% of the apparent maximum increase elicited by ET-1. The pressor response to IRL 1620 was not modified by FR 139317, whereas it can be effectively inhibited by bosentan. These findings provide direct evidence for the notion that a portion of the pressor action of ET-1 is mediated through ET_B receptors. Previous studies have also reported a rise in MABP following injection of the supposedly ET_B receptor-selective agonist, sarafotoxin 6c in the pithed rat (Williams *et al.*, 1991; Clozel *et al.*, 1992). However, BQ-123 has been reported to inhibit the pressor action of sarafotoxin 6c (McMurdo *et al.*, 1993), indicating that the sarafotoxin 6c-induced pressor response is not entirely mediated via the ET_B receptor as suggested previously (Williams *et al.*, 1991). It is noteworthy that ET-1 produced a small, 3–8 mmHg increase in MABP in the presence of bosentan, suggesting the involvement of a third, non-ET_A, non-ET_B receptor subtype in the generation of the pressor response. This receptor may be similar to that which has been described in the pig coronary circulation (Harrison *et al.*, 1992).

The transient fall and prolonged increase in MABP elicited by either ET-1 and IRL 1620 were accompanied by a transient increase (reflex tachycardia) and a prolonged decrease in heart rate (reflex bradycardia). The observations that both FR 139317 and bosentan markedly attenuated, but did not abolish, ET-1-induced bradycardia, coupled with the findings that bosentan, but not FR 139317, significantly reduced, but did not abolish ET-1-induced transient tachycardia suggest that changes in heart rate were secondary to changes in MABP (i.e. attenuation of the ET-1 depressor or pressor responses resulted in amelioration of the accompanying tachycardia or bradycardia, respectively).

Although ET-1 is present in low concentrations in normal rat plasma (Shirakami *et al.*, 1991; Löffler *et al.*, 1992), it is unclear whether circulating ET-1 has physiological functions on its own. As neither FR 139317, nor bosentan alone produced changes in MABP and albumin extravasation, it seems unlikely that circulating ET-1 could influence blood pressure and/or modulate albumin extravasation through ET_A and/or ET_B receptors under physiological conditions.

We have reported previously that BQ-123 completely inhibited ET-1-induced albumin extravasation in the stomach and duodenum, whereas it caused partial inhibition in the upper and lower bronchi, kidney and spleen (Filep *et al.*, 1993b). In the present experiments, qualitatively and quantitatively similar inhibition was achieved with FR 139317. In contrast, bosentan almost completely inhibited accumulation of Evans blue dye in all vascular beds studied. These findings indicate that ET-1-induced albumin extravasation in the stomach and duodenum is mediated via ET_A receptors, whereas activation of both ET_A and ET_B receptors is responsible for the permeability effect of ET-1 in the upper and lower bronchi, spleen and kidney. Additional evidence supporting a role for ET_B receptors in these latter vascular beds is derived from the experiments with IRL 1620. IRL 1620 mimicked the effect of ET-1 on albumin extravasation in the upper and lower bronchi, spleen and kidney, albeit, on a molar basis, it appeared to be less potent than ET-1. On the other hand, unlike ET-1, IRL 1620 did not enhance albumin extravasation in the stomach and duodenum, suggesting regional differences in the expression of ET_B receptors.

Previous studies from our laboratories have demonstrated that the effect of ET-1 on albumin extravasation is not simply a consequence of changes in systemic blood pressure (Filep *et al.*, 1991; 1993a,b), but, as with other mediators, it can be attributed to formation of interendothelial cell gaps in the venules (Grega *et al.*, 1986). ET-1 may induce gap formation directly via ET_A and/or ET_B receptors or through the release of secondary mediators including platelet-activating factor (Filep *et al.*, 1991). Since ET-1-induced accumulation of Evans blue dye in the stomach and duodenum can be completely inhibited by platelet-activating factor receptor antagonists (Filep *et al.*, 1991) as well as by FR 139317, it might be concluded that ET-1 enhances formation of platelet-activating factor via ET_A receptors in the microvasculature. Accordingly, the degree of inhibition of ET-1-induced albumin extravasation observed following ET_A or platelet-activating factor receptor blockade appears to be similar in the large airways, kidney and spleen (Filep *et al.*, 1991 and the present study). The observation that ET-1 is a more potent constrictor of venous than arterial vessels (Yang *et al.*, 1989; Warner, 1990) coupled with the findings that ET_A-like contractile receptors predominate on arterial preparations and ET_B-like contractile receptors on venous

smooth muscle (Moreland *et al.*, 1992) suggest that activation of ET_B receptors may lead to elevation of transcapillary pressure. This would facilitate albumin extravasation provided that interendothelial cell gaps are already formed.

In conclusion, the present study has demonstrated that the majority of the pressor response to ET-1 can be attributed to activation of ET_A and ET_B receptors, and a small component of the ET-1 pressor response might be mediated via activation of a non-ET_A, non-ET_B receptor, whereas ET_B and perhaps a third type of non-ET_A, non-ET_B receptor may mediate the depressor action of ET-1 in conscious rats. The present data also show differences in the ET receptor subtypes mediating the permeability effect of ET-1 in different vascular beds: activation of ET_A receptors appears to be the sole mechanism by which ET-1 enhances albumin extravasation in the stomach and duodenum, whereas both ET_A and ET_B receptors mediate albumin extravasation in the bronchial, splenic and renal vascular beds.

FR 139317 was a generous gift of Fujisawa Pharmaceutical Co., Ltd., Osaka, Japan. This study was supported by the Foundation of the Maisonneuve-Rosemont Hospital. J.G.F. and A.F. are Scholars of the Fonds de la Recherche en Santé du Québec.

References

ARAI, H., HORI, S., ARAMORI, I., OHKUBO, H. & NAKANISHI, S. (1990). Cloning and expression of a cDNA encoding an endothelin receptor. *Nature*, **348**, 730–732.

ARAMORI, I., NIREI, H., SHOUBO, M., SOGABE, K., NAKAMURA, K., KOJO, H., NOTSU, Y., ONO, T. & NAKANISHI, S. (1993). Subtype selectivity of a novel endothelin antagonist, FR 139317, for the endothelin receptors in transfected Chinese hamster ovary cells. *Mol. Pharmacol.*, **43**, 127–131.

BIGAUD, M. & PELTON, J. (1992). Discrimination between ET_A- and ET_B-receptor-mediated effects of endothelin-1 and [$Ala^{1,3,11,15}$]endothelin-1 by BQ-123 in the anaesthetized rats. *Br. J. Pharmacol.*, **107**, 912–918.

BIRD, J.E. & WALDRON, T.L. (1993). Incomplete inhibition of endothelin-1 pressor effects by an endothelin ET_A receptor antagonist. *Eur. J. Pharmacol.*, **240**, 295–298.

CLOZEL, M., BREU, V., GRAY, G.A., KALINA, B., LÖFFLER, B.M., BURRI, K., CASSAL, J.M., HIRTH, G., MÜLLER, M., NEIDHART, W. & RAMUZ, H. (1994). Pharmacological characterization of bosentan, a new potent orally active non-peptide endothelin receptor antagonist. *J. Pharmacol. Exp. Ther.*, (in press).

CLOZEL, M., GRAY, G., BREU, V., LÖFFLER, B.M. & OSTERWALDER, R. (1992). The endothelin ET_B receptor mediates both vasodilation and vasocontriction in vivo. *Biochem. Biophys. Res. Commun.*, **186**, 867–873.

De NUCCI, G., THOMAS, R., D'ORLEANS-JUSTE, P., ANTUNES, E., WALDER, C., WARNER, T. & VANE, J.R. (1988). Pressor effects of circulating endothelin are limited by its removal in the pulmonary circulation and by the release of prostacyclin and endothelium-derived relaxing factor. *Proc. Natl. Acad. Sci. U.S.A.*, **85**, 9797–9800.

DOUGLAS, S.A. & HILEY, C.R. (1991). Endothelium-dependent mesenteric vasorelaxant effects and systemic vascular actions of endothelin(16-21) and other endothelin-related peptides in the rat. *Br. J. Pharmacol.*, **104**, 311–320.

DUNN, O.J. (1964). Multiple comparisons using rank sums. *Technometrics*, **6**, 241–252.

EGLEZOS, A., CUCCHI, P., PATACCHINI, R., QUARTARA, L., MAGGI, C.A. & MIZRAHI, J. (1993). Differential effects of BQ-123 against endothelin-1 and endothelin-3 on the rat vas deferens: evidence for an atypical endothelin receptor. *Br. J. Pharmacol.*, **109**, 736–738.

FILEP, J. & FEJES-TÓTH, G. (1986). Does vasopressin sustain blood pressure in conscious spontaneously hypertensive rats? *Hypertension*, **8**, 514–519.

FILEP, J.G., FÖLDES-FILEP, E., ROUSSEAU, A., FOURNIER, A., SIROIS, P. & YANO, M. (1992). Endothelin-1 enhances vascular permeability in rat heart through the ET_A receptor. *Eur. J. Pharmacol.*, **219**, 343–344.

FILEP, J.G., FÖLDES-FILEP, E., ROUSSEAU, A., SIROIS, P. & FOURNIER, A. (1993a). Vascular responses to endothelin-1 following inhibition of nitric oxide synthesis in the conscious rat. *Br. J. Pharmacol.*, **110**, 1213–1221.

FILEP, J.G., SIROIS, M.G., FÖLDES-FILEP, E., ROUSSEAU, A., PLANTE, G.E., FOURNIER, A., YANO, M. & SIROIS, P. (1993b). Enhancement by endothelin-1 of microvascular permeability via the activation of ET_A receptors. *Br. J. Pharmacol.*, **109**, 880–886.

FILEP, J.G., SIROIS, M.G., ROUSSEAU, A., FOURNIER, A. & SIROIS, P. (1991). Effects of endothelin-1 on vascular permeability in the conscious rat: interactions with platelet-activating factor. *Br. J. Pharmacol.*, **104**, 797–804.

GARDINER, S.M., COMPTON, A.M. & BENNETT, T. (1989). Regional haemodynamic effects of endothelin-1 in conscious, unrestrained, Wistar rats. *J. Cardiovasc. Pharmacol.*, **13** (Suppl. 5), S202-S204.

GARDINER, S.M., COMPTON, A.M. & BENNETT, T. (1990). Regional haemodynamic effects of endothelin-2 and sarafotoxin-S6b in conscious rats. *Am. J. Physiol.*, **258**, R912–R917.

GERMAIN, M., BATTISTINI, B., FILEP, J.G., SIROIS, P. & FOURNIER, A. (1993). Endothelin derivatives showing potent effects in the guinea pig trachea. *Peptides*, **14**, 613–619.

GREGA, G.J., ADAMSKI, S.W. & DOBBINS, D.E. (1986). Physiological and pharmacological evidence for the regulation of permeability. *Fed. Proc.*, **45**, 96–100.

HARRISON, V.J., RANDRIANTSOA, A. & SCHOEFFTER, P. (1992). Heterogeneity of endothelin-sarafotoxin receptors mediating contraction of pig coronary artery. *Br. J. Pharmacol.*, **105**, 511–513.

IHARA, M., NOGUCHI, K., SAEKI, T., FUKURODA, T., TSUCHIDA, S., KIMURA, S., FUKAMI, T., ISHIKAWA, K., NISHIKIBE, M. & YANO, M. (1992). Biological profiles of highly potent novel endothelin antagonists selective for the ET_A receptor. *Life Sci.*, **50**, 247–255.

KARNE, S., JAYAWICKCREME, C.K. & LERNER, M.R. (1993). Cloning and characterization of an endothelin-3 specific receptor (ET_C) from *Xenopus laevis* dermal melanophores. *J. Biol. Chem.*, **268**, 19126–191133.

LA DOUCEUR, D.M., FLYNN, M.A., KEISER, J.A., REYNOLDS, E. & HALEEN, S.J. (1993). ET_A and ET_B receptors coexist on rabbit pulmonary artery vascular smooth muscle mediating contraction. *Biochem. Biophys. Res. Commun.*, **196**, 209–215.

LE MONNIER DE GOUVILLE, A.C., MONDOT, S., LIPPTON, H., HYMAN, A. & CAVERO, I. (1990). Hemodynamic and pharmacological evaluation of the vasodilator and vasoconstrictor effects of endothelin in rats. *J. Pharmacol. Exp. Ther.*, **252**, 300–311.

LÖFFLER, B.M., JACOT-GUILLARMOD, H. & MAIRE, J.P. (1992). Concentrations and ratios of immunoreactive big-endothelin-1 and endothelin-1 in human, rat and rabbit plasma. *Biochem. Int.*, **27**, 755–761.

McMURDO, L., CORDER, R., THIEMERMANN, Ch. & VANE, J.R. (1993). Incomplete inhibition of the pressor effect of endothelin-1 and related peptides in the anaesthetized rat with BQ-123 provides evidence for more than one vasoconstrictor receptor. *Br. J. Pharmacol.*, **108**, 557–561.

MORELAND, S., McMULLEN, D.M., DELANEY, C.L., LEE, V.G. & HUNT, J.T. (1992). Venous smooth muscle contains vasoconstrictor ET_B-like receptors. *Biochem. Biophys. Res. Commun.*, **186**, 100–106.

PINHEIRO, J.M. & MALIK, A.B. (1993). Mechanisms of endothelin-1-induced pulmonary vasodilatation in neonatal pigs. *J. Physiol.*, **469**, 739–752.

POLLOCK, D.M. & OPGENORTH, T.J. (1993). Evidence for endothelin-induced renal vasoconstriction independent of ET_A receptor activation. *Am. J. Physiol.*, **264**, R222–R227.

RAWSON, R.A. (1943). The binding of T-1824 and structurally related diazo dyes by the plasma protein. *Am. J. Physiol.*, **138**, 708–717.

ROGERS, D.F., BOSCHETTO, P. & BARNES, P.J. (1989). Plasma exudation. Correlation between Evans blue dye and radiolabeled albumin in guinea pigs in vivo. *J. Pharmacol. Meth.*, **21**, 309–315.

RUBANYI, G.M. & PARKER BOTELHO, L.H. (1991). Endothelins. *FASEB J.*, **5**, 2713–2720.

SAEKI, T., IHARA, M., FUKURODA, T., YAMAGIWA, M. & YANO, M. (1991). [$Ala^{1,3,11,15}$]endothelin-1 analogs with ET_B agonistic activity. *Biochem. Biophys. Res. Commun.*, **179**, 286–292.

SAKURAI, T., YANAGISAWA, M. & MASAKI, T. (1992). Molecular characterization of endothelin receptors. *Trends Pharmacol. Sci.*, **13**, 103–108.

SAKURAI, T., YANAGISAWA, M., TAKUWA, Y., MIYAZAKI, H., KIMURA, S., GOTO, K. & MASAKI, T. (1990). Cloning of a cDNA encoding a non-isopeptide selective subtype of the endothelin receptor. *Nature*, **348**, 732–735.

SHIRAKAMI, G., NAKAO, K., SAITO, Y., MAGARIBUCHI, T., JOUGASAKI, M., MUKOYAMA, M., ARAI, H., HOSODA, K., SUGA, S., OGAWA, Y., YAMADA, T., MORI, K. & IMURA, H. (1991). Acute pulmonary alveolar hypoxia increases lung and plasma endothelin-1 levels in conscious rats. *Life Sci.*, **48**, 969–972.

SIMONSON, M.S. & DUNN, M.J. (1991). The molecular mechanisms of cardiovascular and renal regulation by endothelin peptides. *J. Lab, Clin. Med.*, **119**, 622–639.

SOGABE, K., NIREI, H., SHOUBO, M., NOMOTO, A., AO, S., NOTSU, Y. & ONO, T. (1993). Pharmacological profile of FR 139317, a novel, potent endothelin ET_A receptor antagonist. *J. Pharmacol. Exp. Ther.*, **264**, 1040–1046.

SOKOLOVSKY, M. (1992). Structure-function relationships of endothelins, sarafotoxins, and their receptor subtypes. *J. Neurochem.*, **59**, 809–821.

SOKOLOVSKY, M., AMBAR, I. & GALRON, A. (1992). A novel subtype of endothelin receptors. *J. Biol. Chem.*, **267**, 20551–20554.

SUMNER, M.J., CANNON, T.R., MUNDIN, J.W., WHITE, D.G. & WATTS, I.S. (1992). Endothelin ET_A and ET_B receptors mediate vascular smooth muscle contraction. *Br. J. Pharmacol.*, **107**, 858–860.

TAKAI, M., UMEMURA, I., YAMASAKI, K., WATAKABE, T., FUJITANI, Y., ODA, K., URADE, Y., INUI, T., YAMAMURA, T. & OKADA, T. (1992). A potent and specific agonist, Suc-[Glu^9, $Ala^{11,15}$]-endothelin-1(18-21), IRL 1620, for the ET_B receptor. *Biochem. Biophys. Res. Commun.*, **184**, 953–959.

TAKAYANAGI, R., KITAZUMI, K., TAKASAKI, C., OHNAKA, K., AIMOTO, S., TASAKA, K. & OHASHI, M. & NAWATA, H. (1991). Presence of non-selective type of endothelin receptor on vascular endothelium and its linkage to vasodilation. *FEBS Lett.*, **282**, 103–106.

UDAKA, K., TAKEUCHI, Y. & MOVAT, H.Z. (1970). Simple method for quantitation of enhanced vascular permeability. *Proc. Soc. Exp. Biol. Med.*, **133**, 1384–1387.

WARNER, T.D. (1990). Simultaneous perfusion of rat isolated superior mesenteric arterial and venous beds: comparison of their vasoconstrictor and vasodilator responses to agonists. *Br. J. Pharmacol.*, **99**, 427–433.

WEBB, R.L., OKADA, T., BARCLAY, B.W. & LAPPE, R.W. (1992). Central and peripheral actions of IRL 1620, and ET_B selective endothelin agonists in conscious rats. *Hypertension*, **20**, 425–431.

WILLIAMS, D.L. Jr., JONES, K.L., PETTIBONE, D.J., LIS, E.V. & CLINESCHMIDT, B.V. (1991). Sarafotoxin S6c: An agonist which distinguishes between endothelin receptor subtypes. *Biochem. Biophys. Res. Commun.*, **175**, 556–561.

YANAGISAWA, M., KURIHARA, H., KIMURA, S., TOMOBE, Y., KOBAYASHI, M., MITSUI, Y., YAZAKI, Y., GOTO, K. & MASAKI, T. (1988). A novel potent vasoconstrictor peptide produced by vascular endothelial cells. *Nature*, **332**, 411–415.

YANG, Z.H., BÜHLER, F.R., DIEDERICH, D. & LÜSCHER, T.F. (1989). Different effects of endothelin-1 on cAMP- and cGMP-mediated vascular relaxation in human arteries and veins: comparison with norepinephrine. *J. Cardiovasc. Pharmacol.*, **13** (Suppl. 5), S129–S131.

ZIMMERMAN, R.S., MARTINEZ, A.J., MAYMIND, M. & BARBEE, R.W. (1992). Effect of endothelin on plasma volume and albumin escape. *Circ. Res.*, **70**, 1027–1034.

(Received March 21, 1994
Revised July 1, 1994
Accepted July 15, 1994)

Br. J. Pharmacol. (1994), **113**, 853–860 © Macmillan Press Ltd, 1994

Characterization of P_2-purinoceptors in the smooth muscle of the rat tail artery: a comparison between contractile and electrophysiological responses

[1]R.J. Evans & [2]C. Kennedy

Department of Physiology and Pharmacology, University of Strathclyde, Royal College, 204 George Street, Glasgow G1 1XW

1 The electrophysiological actions of the P_2-purinoceptor agonists, adenosine 5'-triphosphate (ATP), 2-methylthioATP (2-meSATP), α,β-methyleneATP (α,β-meATP) and uridine 5'-triphosphate (UTP) were studied under concentration and voltage-clamp conditions in acutely dissociated rat tail artery smooth muscle cells. For comparison, their actions as vasoconstrictors were studied in intact ring preparations.

2 Rapid application of ATP (100 nM–1 μM) via a U-tube superfusion system activated concentration-dependent inward currents with a latency to onset of less than 3 ms. The inward current decayed by more than 95% during a 2 s application of 300 nM and 1 μM ATP.

3 2-meSATP (100 nM–1 μM) and α,β-meATP (100 nM–1 μM) also evoked transient inward currents. The agonist order of potency was ATP = 2-meSATP ≥ α,β-meATP. UTP (300 nM–1 μM) did not produce a change in the holding current.

4 A second application of ATP (300 nM and 1 μM) 10 min after the first, evoked currents which were one third of the initial amplitude. This decline was dependent upon activation of the P_2-purinoceptor. Similar results were seen with 2-meSATP and α,β-meATP (both 300 nM and 1 μM). Cross-desensitization was seen between ATP and 2-meSATP or α,β-meATP.

5 Inward currents evoked by ATP, 2-meSATP and α,β-meATP (all 1 μM) were abolished by the P_2-purinoceptor antagonist suramin (100 μM).

6 α,β-meATP (100 nM–30 μM), 2-meSATP (3 μM–100 μM), ATP (3 μM–1 mM) and UTP (3 μM–1 mM) produced concentration-dependent contractions of rat tail artery rings. When measured at a level equal to 50% of the maximum response to noradrenaline, the rank order of agonist potency was α,β-meATP >> 2-meSATP > UTP > ATP.

7 This study shows that the rank order of agonist potency at the P_{2X}-purinoceptor which mediates contractions of the rat isolated tail artery is very different from the potency order for evoking the inward current which initiates the contractions. It is concluded that this difference may be due to the relative absence of breakdown of some of the agonists in the single cell system compared with artery rings.

Keywords: Rat tail artery; smooth muscle; P_2-purinoceptors; ATP; UTP; suramin

Introduction

There is now considerable evidence that adenosine 5'-triphosphate (ATP) acts as a neurotransmitter in vascular (Burnstock, 1990; Evans & Surprenant, 1992; Kennedy, 1993a) and neuronal (Evans *et al.*, 1993; Edwards *et al.*, 1993) preparations. ATP produces its physiological and pharmacological actions through the activation of P_2-purinoceptors (Burnstock, 1978), which have been subdivided into at least five subtypes, P_{2X}, P_{2Y}, P_{2U}, P_{2T} and P_{2Z}, largely on the basis of the relative agonist potencies of ATP and a number of its structural analogues (Burnstock & Kennedy, 1985; Gordon, 1986; Kennedy, 1990; O'Connor *et al.*, 1991). The best characterized of these are the P_{2X}-, P_{2Y}- and P_{2U}-subtypes.

The P_{2Y}- and P_{2U}-purinoceptors were cloned recently and both belong to the G protein-coupled receptor superfamily (Lustig *et al.*, 1993; Webb *et al.*, 1993). In contrast, the P_{2X}-purinoceptor is thought to be a ligand-gated cation channel (Bean & Friel, 1990; Kennedy, 1990). In smooth muscle preparations the opening of this cation channel underlies membrane depolarization and contraction following P_2-purinoceptor activation (Benham *et al.*, 1987; Nakazawa & Matsuki, 1987; Inoue & Brading, 1990; Bean, 1992; Kennedy, 1993b).

The rank order of agonist potency at the P_{2X}-purinoceptor is α,β-methyleneATP (α,β-meATP) >> 2-methylthioATP (2-meSATP) ≥ ATP, while the potency order at the P_{2Y}-purinoceptor is 2-meSATP >> ATP > α,β-meATP (Burnstock & Kennedy, 1985; Kennedy, 1990). Uridine 5'-triphosphate (UTP) has little or no action at these receptors, but is an agonist at the P_{2U}-purinoceptor (O'Connor *et al.*, 1991). ATP is also an agonist at the P_{2U}-purinoceptor, whereas 2-meSATP and α,β-meATP have little or no effect. One weakness with this classification is that it is based on results from whole tissue preparations in which the influence of ectonucleotidase activity could not be determined. ATP and 2-meSATP are susceptible to breakdown by ectonucleotidases, but α,β-meATP is relatively resistant (Gordon, 1986; Welford *et al.*, 1986; 1987).

In several studies where P_2-purinoceptors were examined in single acutely dissociated smooth muscle cells using electrophysiological techniques, the relative potency of ATP and its analogues did not correspond to that described in the whole tissues (Benham & Tsien, 1987; Friel, 1988; Inoue & Brading, 1990; Xiong *et al.*, 1991). The reason for this difference is uncertain, but it could simply reflect different enzymatic breakdown of ATP and its analogues in whole tissues and dissociated cells. However, the pharmacological profile of P_2-purinoceptors in single smooth muscle cells has not been well characterized.

Therefore, the aim of the present study was to compare the agonist order of potency of ATP and a number of its

[1] Present address: Glaxo Institute for Molecular Biology, 14, chemin des Aulx, 1228 Plan-les-Oates, Geneva, Switzerland.
[2] Author for correspondence.

analogues in whole tissue and single cell preparations. Thus, we have determined the relative potency of ATP, 2-meSATP, α,β-meATP and UTP in evoking inward currents in acutely dissociated smooth muscle cells and contractions in isolated rings of the rat tail artery, a vessel in which ATP acts as an excitatory cotransmitter (Sneddon & Burnstock, 1984; Åstrand *et al.*, 1988) and which has a high density of P_{2X}-purinoceptors (Bo & Burnstock, 1993).

Methods

Single cell isolation and electrophysiological experiments

Rat tail artery smooth muscle cells were isolated by a modification of the method of overnight digestion with papain (Clapp & Gurney, 1991). Male Sprague Dawley rats (100–175 g) were killed by exposure to carbon dioxide followed by exsanguination. The tail artery was removed and placed in a 'low calcium' dissociation solution of the following composition (mM): NaCl 140, KCl 5, Na_2HPO_4 0.06, glucose 10, HEPES 10, EGTA 0.5, $MgCl_2$ 1.2, $CaCl_2$ 0.1, titrated to pH 7.3 with NaOH. The connective tissue was removed, the cleaned vessel opened along its longitudinal axis and the endothelial layer removed by gentle rubbing. The artery was then cut into small pieces 1–2 mm long, transferred to 5 ml of dissociation solution containing 5 mg ml^{-1} bovine serum albumin and 8.5 units ml^{-1} papain and incubated overnight (16–18 h) at 4–6°C. The following morning the tail artery pieces and enzyme solution were incubated at 37°C. Gentle trituration with a fire-polished Pasteur pipette (tip diameter 1 mm) 30–40 times at 10, 20 and 25 min yielded single, spindle shaped cells. The supernatant was centrifuged at 150 g for 5 min, the pellet resuspended in 1 ml of dissociation solution and stored at 4–6°C until the cells were plated. Cells were used within 8 h of dissociation.

Smooth muscle cells were plated onto glass coverslips and allowed to settle for 10–20 min before transfer to the recording chamber. Cells were superfused at 3–4 ml min^{-1} at room temperature with 'normal calcium' bathing solution of the following composition (mM): NaCl 140, KCl 5, Na_2HPO_4 0.06, glucose 10, HEPES 10, $MgCl_2$ 1.2, $CaCl_2$ 2.5, titrated to pH 7.3 with NaOH. In some experiments cells were initially bathed in the 'low calcium' dissociation solution, followed by the 'normal calcium' bathing solution once the whole cell recording mode was achieved. Only one cell per coverslip was tested for responses to drugs.

Whole cell currents were recorded by the patch clamp technique with an Axopatch 1D amplifier (Axon Instruments, U.S.A.). The resistance of the patch pipette was 2–5 MΩ when filled with internal solution of the following composition (mM): KCl 160, $MgCl_2$ 2, HEPES 10, EGTA 5, Na_2ATP 2, Na_2GTP 0.1, adjusted to pH 7.3 with KOH. The pipette tips were coated with beeswax to reduce capacitance artefacts. In all experiments the membrane potential was clamped at −60 mV. Data were collected on an IBM compatible PC using WCP software (J. Dempster, University of Strathclyde, Glasgow, Scotland) with a National Instruments Lab PC Plus interface.

Application of agonists

In initial studies, bath superfusion of 10 and 30 μM ATP for 10–20 s evoked small inward currents of 203 ± 63 pA ($n = 6$) and 176 ± 19 pA ($n = 6$) respectively. The currents developed slowly, with a 10–90% rise time of approximately 4–5 s and decayed by more than 95% during the continued application of ATP. A second application of ATP after 10 min washout evoked a current which was usually less than 10% of the initial test response. The inward currents were associated with an increase in membrane conductance in response to brief (200 ms) voltage jumps to +60 mV.

Due to the relatively slow exchange time of the bath solution (about 30 s) cells are exposed to a slow concentration-ramp rather than a rapid concentration-step and if, as seen here, there is desensitization of the inward current during ATP application, then it is very likely that the peak amplitude of the response to ATP is underestimated. Therefore, in order to minimize these problems, throughout this study ATP and other agonists were applied rapidly by use of a solenoid valve-controlled, U-tube superfusion system placed close (100–150 μm) to the cell (Fenwick *et al.*, 1982). The delay to onset of solution change by the U-tube and the equilibration time (calculated as the time between 10–90% of the maximum change) were measured by monitoring the change in resistance of a patch electrode when deionised water was applied from the U-tube. The delay between activation of the solenoid valve and onset of increased resistance was 20–25 ms and the equilibration time was 15–20 ms. The increase in resistance was maintained throughout a 2 s application of deionised water, indicating that the U-tube was providing an effective concentration-clamp. Agonists were routinely applied to cells 5 min after whole cell mode was achieved, in order to standardize any time-dependent effects of cell dialysis on the currents evoked.

Contraction experiments

Rings (5–10 mm) of the proximal tail artery (internal diameter ≈300 μm) from rats (100–175 g) were mounted horizontally under isometric conditions in 10 ml organ baths by inserting two stainless steel wires into the lumen according to the method of Bevan & Osher (1972). The tissues were bathed in the 'normal calcium' bathing solution described above, at 37°C and bubbled with 100% O_2. Preparations were allowed to equilibrate for at least 60 min under a resting tension of 0.5–0.75 g. Contractions of the smooth muscle were recorded with a Grass FT103 transducer. In all preparations the endothelium was removed by gently pulling a 20 mm length of platinum wire (250 μm diameter) through the lumen of the vessel. Following precontraction with 1 μM noradrenaline, 10 μM acetylcholine did not produce vasodilatation, confirming that the mechanical rubbing had successfully removed the endothelium.

ATP, 2-meSATP, α,β-meATP and UTP were added as single concentrations to give the required final bath concentrations, with at least 35 min allowed between additions in order to avoid desensitization. Control experiments showed that no change in sensitivity to the agonists was observed over the time course of the experiments. As a maximum response was not reached for any of the agonists, contractions are expressed as a percentage of the maximum response evoked by noradrenaline in each tissue. Relative agonist potency was measured at a level equal to 50% of the maximum response to noradrenaline.

Statistics

Data are expressed throughout as the mean ± s.e.mean or the mean with 95% confidence limits where indicated. Results were compared by Student's paired and unpaired t tests where appropriate and $P < 0.05$ was considered to be statistically significant.

Drugs

Stock solutions of acetylcholine chloride, adenosine 5'-triphosphate (sodium salt), α,β-methyleneATP (lithium salt), uridine 5'-triphosphate (sodium salt) (all Sigma), 2-methylthio ATP (Research Biochemicals Inc.) and suramin (Bayer, UK) were dissolved in deionised water. (−)-Noradrenaline bitartrate (Sigma) was dissolved in acid saline. All drugs were then diluted in 'normal calcium' bathing solution.

Results

Responses of single rat tail artery smooth muscle cells to rapid application of ATP

Isolated smooth muscle cells of the rat tail artery had a resting membrane potential of -43.8 ± 1.4 mV ($n = 70$), which is in the range of those recorded in other smooth muscle preparations (Nakazawa & Matsuki, 1987; Friel, 1988; Inoue & Brading, 1990; Clapp & Gurney, 1991). When applied rapidly for 2 s, ATP (100 nM–1 μM) evoked inward currents in cells held at −60 mV (Figure 1). The delay between application of ATP and the onset of the rise of the inward current was less than 3 ms, which indicates that the current was due to the direct activation of an ion channel and not through a G protein-coupled mechanism. The peak amplitude and time course of ATP responses were concentration-dependent (Figure 1, Table 1). There was a large variation in the peak current amplitude for a given concentration of ATP, which was not related to cell size and is reflected in the relatively large s.e.mean values.

ATP (100 nM) produced a relatively sustained inward current which decayed by less than 30% during 2 s application. ATP (300 nM and 1 μM) evoked transient inward currents which were larger and which reached a peak and decayed much more rapidly as concentration increased. These currents decayed by more than 95% during the 2 s application. The rise time of the response to 3 μM ATP ($n = 2$) was faster than that for solution changeover and so may underestimate the peak current amplitude. Therefore, concentrations of ATP greater than 1 μM were not applied.

Desensitization by repeated application of ATP

Initial studies showed that there was a marked diminution in peak current amplitude on repeated application of ATP. A second application of ATP (300 nM and 1 μM) 10 min after the first, evoked a response that was significantly smaller ($P < 0.05$), but which had a similar time course (Figure 2, Table 2). In three cells in which ATP was applied a third time, 10 min after the second, a further decrease in peak current amplitude was seen (Figure 2). If ATP was applied for a shorter period (500 ms) a similar degree of desensitization was seen (not shown).

The dialysis of the cell interior which occurs during whole cell recordings can lead to rundown of ionic currents. Therefore, in order to determine if this was involved in the decrease in peak current amplitude seen here, ATP was first applied 15 min after the whole cell recording mode was achieved, rather than 5 min after, as was standard throughout this study. In cells in which ATP (300 nM) was first applied after 15 min, the evoked currents (470 ± 160 pA, $n = 4$) were not significantly different from those recorded in cells where ATP was first applied after 5 min (686 ± 116 pA, $n = 20$). Thus, the decreased response to repeated application of ATP was not simply due to time-dependent rundown, but appears to depend upon ATP-induced activation of the P_2-purinoceptor.

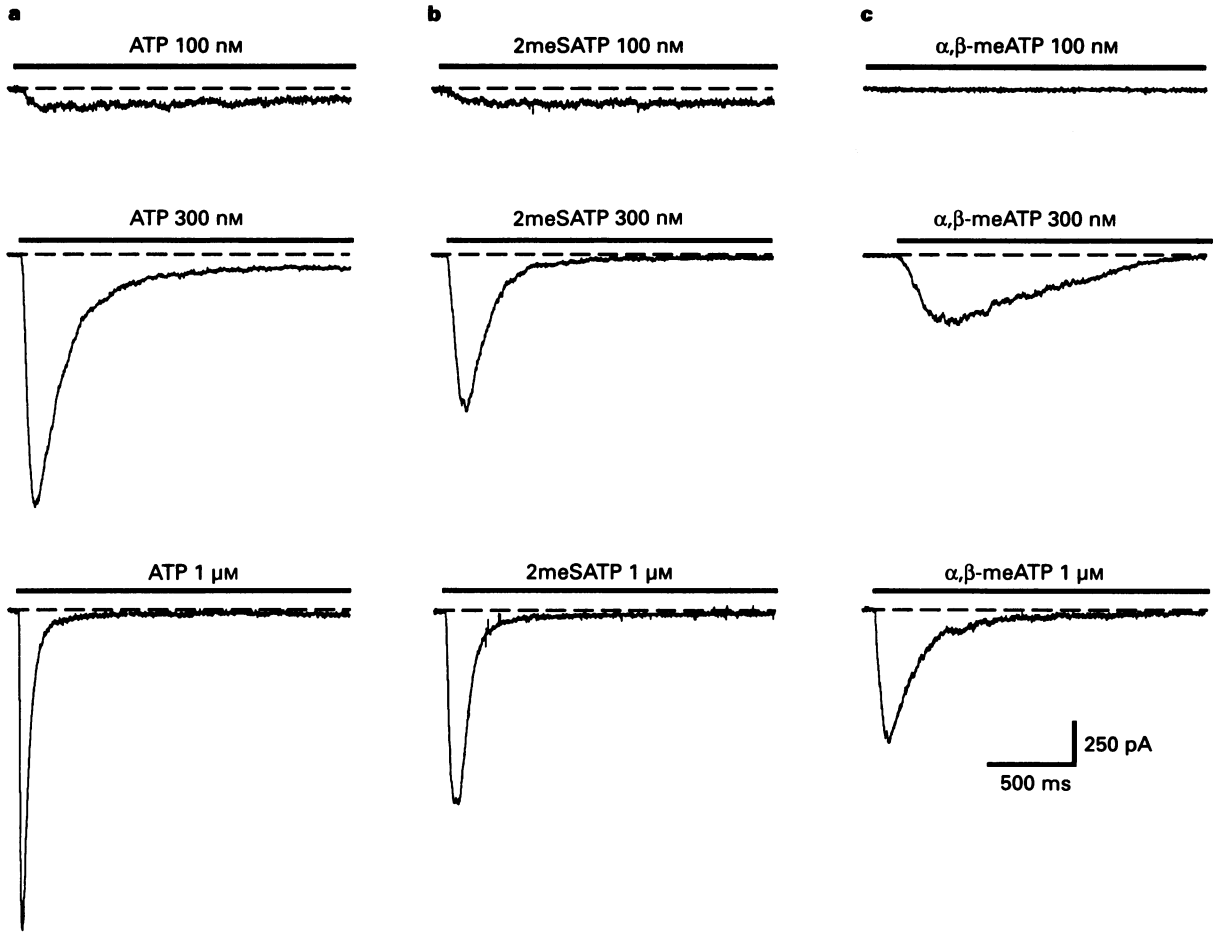


Figure 1 ATP, 2-meSATP and α,β-meATP evoke fast inward currents when rapidly applied to acutely dissociated smooth muscle cells from the rat tail artery: traces show the inward currents evoked by ATP (panel a), 2-meSATP (panel b) and α,β-meATP (panel c) (all 100 nM–1 μM) when applied rapidly for 2 s using a U-tube superfusion system, as indicated by the solid bars. The dashed lines represent zero current levels. The holding potential was −60 mV. Each record is from a different cell.

Responses of rat isolated tail artery smooth muscle cells to 2-meSATP and α,β-meATP

The lack of reproducible responses to ATP in any given cell meant that it was not possible to construct concentration-response curves or to compare the order of potency of ATP and its analogues in a single cell, so the responses were compared in a population of cells. As we were interested in agonist potency relative to ATP, alternate cells from a dissociation were exposed to ATP or to 2-meSATP, α,β-meATP or UTP.

2-meSATP and α,β-meATP evoked inward currents which, like those evoked by ATP, had a delay of less than 3 ms between drug application and onset of the response, indicating that they were due to the direct activation of a ligand-gated ion channel. The peak amplitude, rise time and 50% decay time of inward currents evoked by 2-meSATP (100 nM–1 μM) were concentration-dependent and of similar amplitude and time course to those evoked by ATP (Figure 1, Table 1). A similar degree of desensitization was also seen on repeated application of 2-meSATP (300 nM and 1 μM) (Table 2).

α,β-meATP (100 nM) had no effect on the holding current of rat isolated tail artery smooth muscle cells (Figure 1, Table 1). In these cells, subsequent application of ATP (100 nM) evoked inward currents which were of similar magnitude to those recorded in control cells. Higher concentrations of α,β-meATP (300 nM and 1 μM) evoked inward currents, the peak amplitude, rise time and 50% decay time of which were concentration-dependent. At 300 nM the current was significantly smaller than that evoked by ATP ($P<0.01$), while at both concentrations the rise time and rate of decay were significantly slower ($P<0.05$) (Figure 1, Table 1). When compared at concentrations which evoked a current of similar mean amplitude (300 nM ATP and 2-meSATP, 1 μM α,β-meATP), the time-course of currents to α,β-meATP was similar to those to ATP and 2-meSATP (Table 1). Thus, α,β-meATP has a different interaction with the P_2-purinoceptor, but it not clear if this is due to a difference in affinity or efficacy or both. Desensitization was also seen on repeated application of α,β-meATP (300 nM and 1 μM) (Table 2).

Cross-desensitization

In all cells where ATP was applied 10 min after the same concentration of 2-meSATP ($n=4$) or α,β-meATP ($n=3$) had been applied, the peak current amplitude evoked by ATP was much smaller than the mean response to a single application of ATP in control cells. Similar cross-desensitization was seen when ATP was applied before 2-meSATP ($n=3$). Although cross-desensitization was not studied in detail, this suggests that ATP, 2-meSATP and α,β-meATP act through a common site.

Responses of rat isolated tail artery smooth muscle cells to the pyrimidine UTP

UTP (300 nM, $n=5$ or 1 μM, $n=3$) applied for 2 s, had no effect on the holding current in rat tail artery smooth muscle cells (Figure 3). In many tissues it has been found that only a subpopulation of cells express P_2-purinoceptors (see Bean & Friel, 1990, and references therein). However, in all of the cells in which UTP was ineffective here, subsequent application of ATP (300 nM or 1 μM) evoked inward currents (Figure 3). This suggests that the inability of UTP to evoke currents was not due to the absence of P_2-purinoceptors.

Effects of suramin

In a number of vascular and neuronal preparations suramin has been shown to be an antagonist at P_2-purinoceptors (Kennedy, 1990; Dubyak & El-Moatassim, 1993). However, we could not determine the effects of ATP, 2-meSATP or α,β-meATP before and during application of suramin as we would have been unable to differentiate between an antagonistic effect of suramin and desensitization on the second application of agonist. In order to circumvent this problem we determined the effects of these agonists first in the

Table 1 Characteristics of inward currents evoked by ATP, 2-meSATP and α,β-meATP in acutely dissociated rat tail artery smooth muscle cells

	(n)	*Peak amplitude* (pA)	*10–90% rise time* (ms)	*50% decay time* (ms)
ATP				
100 nM	(9)	89 ± 68	84 ± 14	–
300 nM	(20)	686 ± 116	92 ± 7	199 ± 12
1 μM	(17)	904 ± 128	25 ± 3	79 ± 9
2-meSATP				
100 nM	(5)	45 ± 9	214 ± 74	–
300 nM	(9)	517 ± 129	65 ± 7	177 ± 22
1 μM	(9)	800 ± 368	35 ± 4	96 ± 10
α,β-meATP				
100 nM	(4)	0	–	–
300 nM	(9)	222 ± 40	206 ± 28	692 ± 121
1 μM	(9)	535 ± 160	71 ± 16	208 ± 25

Currents evoked by 100 nM ATP and 2-meSATP decayed by less than 30% during 2 s application.

Table 2 Desensitization evoked by repeated agonist application in acutely dissociated rat tail artery smooth muscle cells

	ATP		*2-meSATP*		*α,β-meATP*	
	300 nM	1 μM	300 nM	1 μM	300 nM	1 μM
% of initial peak amplitude	37 ± 5 (8)	31 ± 6 (7)	31 ± 6 (6)	31 ± 8 (4)	55 ± 7 (6)	36 ± 8 (4)

Values indicate the mean amplitude of the current evoked by a second application of the agonist expressed as a percentage of the response evoked by the initial application.
The number of cells is indicated in parentheses.

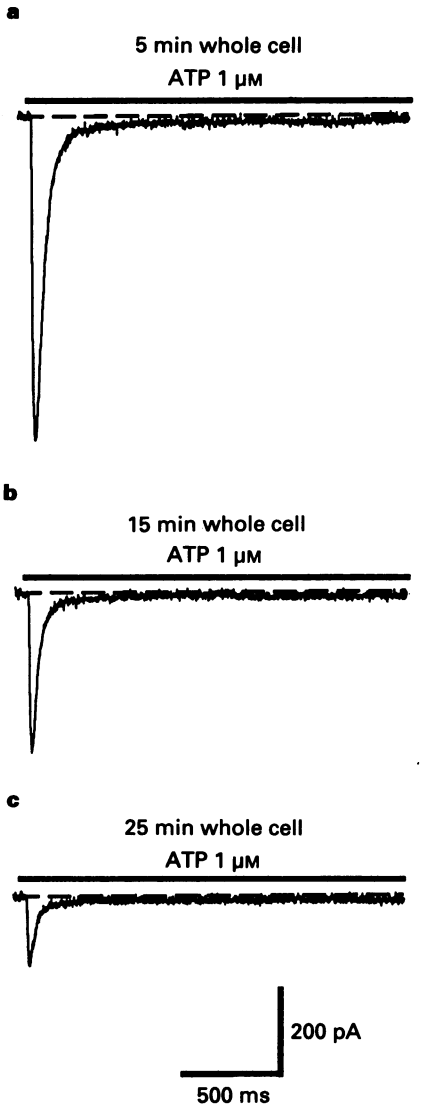


Figure 2 The peak inward current evoked by ATP in acutely dissociated rat tail artery smooth muscle cells decreases on repeated application. The records show the inward currents evoked by ATP (1 μM) in the same cell when applied rapidly for 2 s using a U-tube superfusion system, as indicated by the solid bars at (a) 5, (b) 15 and (c) 25 min after the whole cell mode was achieved. The dashed lines represent zero current levels. The holding potential was − 60 mV.

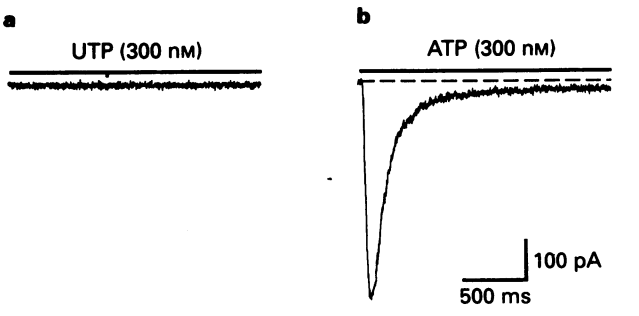


Figure 3 UTP has no effect on the holding current in acutely dissociated rat tail artery smooth muscle cells: (a) UTP (300 nM) has no effect on the holding current. (b) However, a transient inward current was evoked by ATP (300 nM) from the same cell 10 min later. ATP and UTP were applied for 2 s using a U-tube superfusion system as indicated by the solid bars. The dashed line represents the zero current level. The holding potential was − 60 mV.

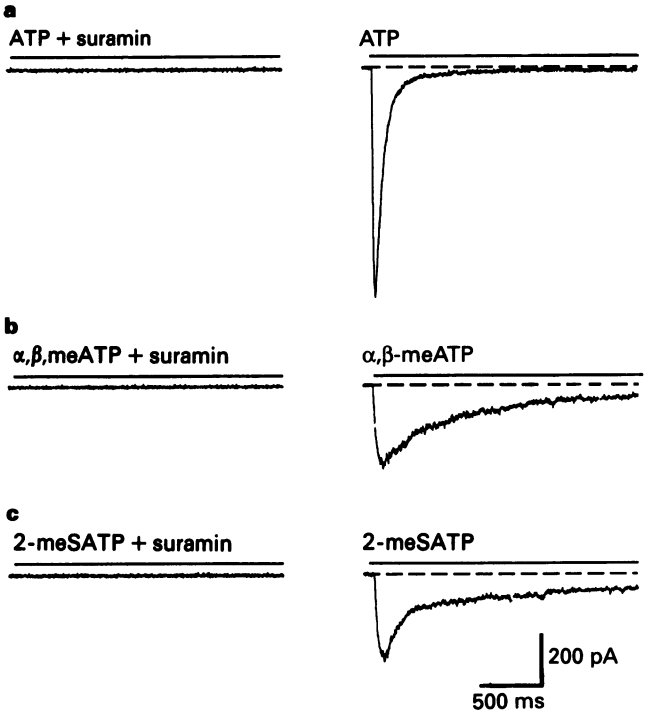


Figure 4 Suramin abolishes inward currents evoked by ATP, 2-meSATP and α,β-meATP in acutely dissociated rat tail artery smooth muscle cells: the left hand panel shows that after 5 min bath superfusion with suramin (100 μM), the concomitant application of (a) ATP (b) 2-meSATP or (c) α,β-meATP (all 1 μM) with suramin (100 μM) had no effect on the holding current. The right hand panel shows that after 10 min washout of suramin, inward currents were evoked by reapplication of these compounds in the same cells. ATP, 2-meSATP and α,β-meATP were applied for 2 s using a U-tube superfusion system as indicated by the solid bars. The dashed lines represent zero current levels. The holding potential was − 60 mV. Paired records in (a), (b) and (c) are from different cells.

presence of suramin and then 10 min later in the same cell in the absence of suramin.

Cells were exposed to suramin (100 μM) for 5 min, before concomitant application of one of the agonists plus suramin for 2 s. Under these conditions ATP, 2-meSATP and α,β-meATP (1 μM, $n = 4$ for each) did not evoke inward currents (Figure 4). Following washout of suramin for 10 min, ATP, 2-meSATP or α,β-meATP (1 μM, $n = 4$ for each) now evoked inward currents in all cells treated. The time course of the decay of the currents evoked by 2-meSATP and α,β-meATP appeared to be prolonged compared to those recorded in untreated cells which may reflect incomplete washout of suramin. This was not investigated further. Thus, it is concluded that ATP, 2-meSATP and α,β-meATP evoke inward currents through the activation of P_2-purinoceptors which are sensitive to suramin.

Contractions evoked by purines and UTP

α,β-meATP (100 nM–30 μM), 2-meSATP (3 μM–100 μM), ATP (3 μM–1 mM) and UTP (3 μM–1 mM) produced reproducible, concentration-dependent contractions of rat tail artery rings (Figure 5a,b,c). Contractions to α,β-meATP, 2-meSATP and ATP usually reached a peak within 1 min, but were not maintained, whereas those to UTP developed more slowly and were maintained during administration of the drug. Contractions reversed rapidly on washout of the drugs and could be inhibited by preincubation with suramin (100 μM) (not shown).

α,β-meATP was the most potent agonist. At a level equal to 50% of the maximum response to noradrenaline, the rank order of agonist potency was α,β-meATP >> 2-meSATP

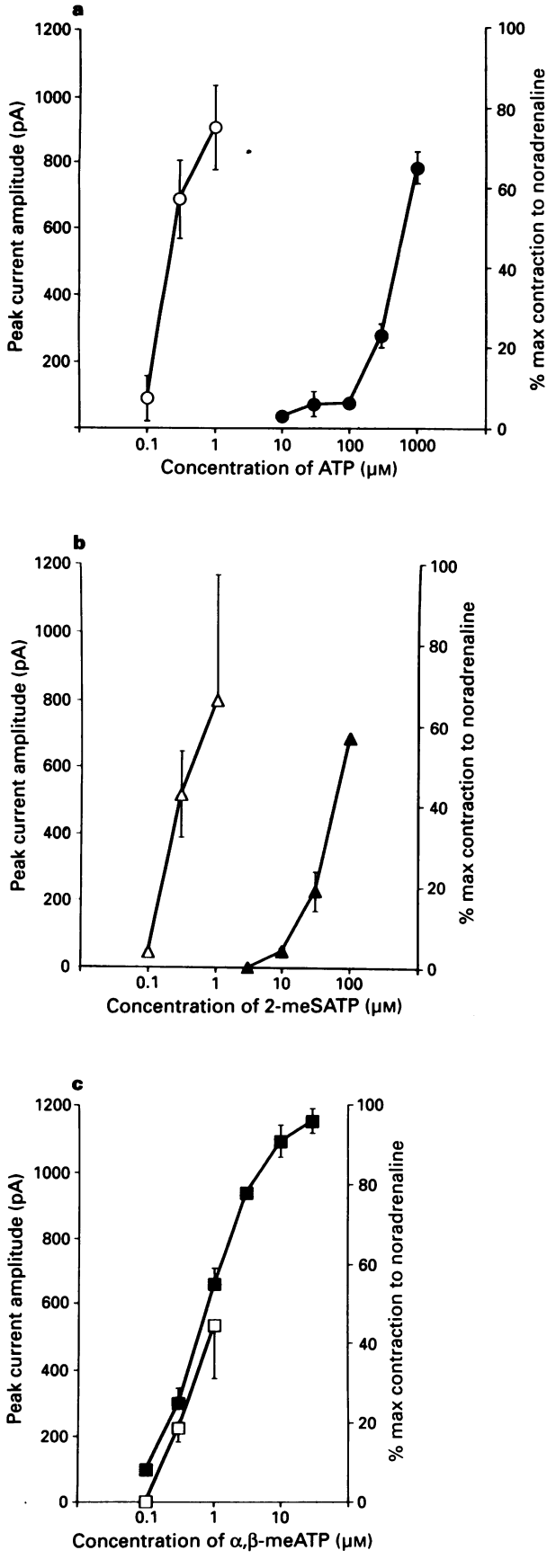


Figure 5 ATP, 2-meSATP and α,β-meATP evoke contractions of rat tail artery rings: comparison of the log concentration-response curves for contractions (solid symbols) ($n = 4$) and inward currents (pA) (open symbols) (n as indicated in Table 1) evoked by (a) ATP, (b) 2-meSATP and (c) α,β-meATP. Contractions are expressed as a percentage of the maximum response to noradrenaline. Mean values ± s.e.mean are shown.

> UTP > ATP (Table 3). This is very different from the rank order of agonist potency for eliciting inward currents in single cells. The concentrations of ATP required to evoke inward currents were three orders of magnitude lower than those required to evoke contraction (Figure 5a) and the difference for 2-meSATP was two orders of magnitude (Figure 5b). In contrast, similar concentrations of α,β-meATP were effective at inducing both responses (Figure 5c). This similar potency of α,β-meATP in the two types of preparation suggests that the dissociation procedure had no effect on the P_{2X}-purinoceptor *per se*.

Discussion

This study shows that the rank order of agonist potency for evoking contraction of the rat isolated tail artery is α,β-meATP >> 2-meSATP > ATP, which is characteristic of the P_{2X}-purinoceptor (Burnstock & Kennedy, 1985; Kennedy, 1990). However, when inward currents were evoked in acutely dissociated smooth muscle cells the potency order was ATP = 2-meSATP ≥ α,β-meATP. This is clearly different and does not correspond pharmacologically to any of the P_2-purinoceptor subtypes identified in whole tissues. The inward currents and contractions were inhibited by the P_2-purinoceptor antagonist, suramin and agonist cross-desensitization was seen in single cells. This is consistent with ATP, 2-meSATP and α,β-meATP acting at a common site, but the possibility cannot be excluded that they acted at more than one suramin-sensitive site or that desensitization was heterologous.

UTP also evoked suramin-sensitive contractions of the rat tail artery, but did not activate an inward current. This suggests that UTP was acting via a P_{2U}-purinoceptor and agrees with a previous report that UTP acts at a different site from ATP to evoke contraction in this vessel (Saïag *et al.*, 1990). The P_{2U}-purinoceptor has been cloned and belongs to the G protein-coupled receptor superfamily (Lustig *et al.*, 1993).

In this study low concentrations of ATP evoked inward currents with a delay to onset of less than 3 ms, supporting the suggestion that the P_{2X}-purinoceptor is a ligand-gated ion channel. This is consistent with ATP acting as an excitatory cotransmitter in sympathetic nerves innervating smooth muscle, as stimulation of these nerves in the rat tail artery evokes excitatory junction potentials (Sneddon & Burnstock, 1984) and currents (Åstrand *et al.*, 1988) with a similar short latency. Responses to ATP showed marked desensitization in the present experiments, yet in the intact rat tail artery, excitatory junction potentials (Sneddon & Burnstock, 1984) and current (Åstrand *et al.*, 1988) can be evoked repetitively without any decrease in amplitude. Desensitization of P_{2X}-purinoceptors may be minimal *in vivo* because neurotransmission at individual sympathetic varicosities in the rat tail artery is brief and intermittent (Åstrand *et al.*, 1988).

One objection to the cotransmission hypothesis is that the concentrations of ATP calculated to be present in the neuroeffector junction during neurotransmission (1–2 μM) (see Sjöblom-Widfelt *et al.*, 1993), are much lower than those of exogenous ATP required to evoke contraction (10 μM–1 mM here). However, in the present study, the concentrations effective in single cells of the rat tail artery under concentration-clamp conditions (100 nM–1 μM), are close to the levels of ATP calculated to be released during sympathetic nerve stimulation.

The marked difference in agonist order of potency in rat tail artery rings and acutely dissociated cells is perhaps surprising, as opening of a ligand-gated cation channel is the initial step by which P_{2X}-purinoceptor agonists act to contract smooth muscle (Benham *et al.*, 1987; Nakazawa & Matsuki, 1987; Inoue & Brading, 1990; Bean, 1992; Kennedy, 1993b). The simplest explanation for this discrepancy is that ATP, 2-meSATP and α,β-meATP act at the same site (the

Table 3 Potency of purines and UTP in contracting rat tail artery rings

	EEC_{50}[1]	95% CL[2]	Potency relative to ATP
α,β-meATP	830 nM	(0.49–1.2 μM)	795 $P<0.01$
2-meSATP	81 μM	(70–91 μM)	8.1 $P<0.05$
UTP	350 μM	(150–550 μM)	1.9 $P<0.05$
ATP	660 μM	(310–1000 μM)	1.0

$n = 4$ for each agonist.
[1]Equi-effective concentrations producing contraction equivalent to 50% of the maximum contraction to noradrenaline.
[2]95% confidence limits.

P_{2X}-purinoceptor) to evoke inward currents and contraction, but their relative potencies are determined by differences in their breakdown in intact muscles and dissociated cells. ATP and 2-meSATP are both susceptible to breakdown by ectonucleotidases, whereas α,β-meATP is relatively resistant (Welford *et al.*, 1986; 1987). In organ bath studies, drug equilibration in the bathing solution is relatively slow, so ectonucleotidases present in blood vessels in high levels (see Gordon, 1986), have more time to break down P_2-purinoceptor agonists which are also enzyme substrates. Furthermore, the enzymes which break down ATP to adenosine appear to be clustered together, allowing preferential delivery of substrates to the enzymes such that ATP is broken down extremely rapidly (Gordon *et al.*, 1989). In contrast, in single cells equilibration time was very short (less than 20 ms) and under concentration-clamp conditions the influence of ectonucleotidases on agonist action is likely to be substantially reduced or abolished. Thus, ATP and 2-meSATP were much more potent in single rat tail artery smooth muscle cells than in ring preparations, whereas α,β-meATP was of a similar potency. The similar potency of α,β-meATP also suggests that the dissociation procedure had no effect on the P_{2X}-purinoceptor *per se*.

To confirm this interpretation of the results it will be necessary to study contractions in ring preparations in the absence of agonist breakdown using the new ectonucleotidase inhibitor FPL 67156 (Leff *et al.*, 1994). However, similar results have been found in the guinea-pig urinary bladder, where α,β-meATP evokes inward currents and contraction over the same concentration-range and is more potent than ATP in contracting muscle strips, but less potent than ATP in evoking inward currents (Inoue & Brading, 1990). A similar shift in the potency of ATP has also been seen in rat mesenteric artery rings when a metabolically-stable compound, caged ATP, was used (Sjöblom-Widfelt *et al.*, 1993). When released rapidly from caged ATP by photolysis, ATP evoked concentration-dependent contractions and was 100 times more potent than when ATP itself was added to the bathing solution.

This explanation of the results means that a rank order of potency of α,β-meATP >> 2-meSATP > ATP can no longer be considered to be the pharmacological profile of the P_{2X}-purinoceptor. This study is not extensive enough to define the P_{2X}-purinoceptor in the absence of breakdown, but it is clear that ATP and 2-meSATP are more potent than α,β-meATP, although the difference in potency here was less than one order of magnitude. Nonetheless, α,β-meATP is still a useful tool for receptor characterization as it is the agonist most effective at producing desensitization of the P_{2X}-purinoceptor in whole tissues. In the present experiments in single cells, α,β-meATP, 2-meSATP and ATP induced a similar degree of desensitization, suggesting that the greater ability of α,β-meATP to produce desensitization in whole tissues is due to its resistance to breakdown.

ATP and 2-meSATP are also more potent than α,β-meATP at the P_{2Y}-purinoceptor, but the differences in potency are much larger, as 2-meSATP is approximately two orders of magnitude more potent than ATP, which in turn is an order of magnitude more potent than α,β-meATP (see Burnstock & Kennedy, 1985; Kennedy, 1990, for reviews). In a number of neuronal preparations, P_2-purinoceptor agonists also evoke a rapidly developing inward current via a ligand-gated cation channel (see Illes & Nörenberg, 1993). Since ATP and 2-meSATP were more potent than α,β-meATP, it was suggested that a P_{2Y}-purinoceptor was involved (Illes & Nörenberg, 1993). In view of the results presented here, it may be premature to characterize a response in single cells as being mediated via a P_{2Y}-purinoceptor simply because 2-meSATP and ATP are more potent than α,β-meATP.

In conclusion, this study shows that the rank order of agonist potency at the P_{2X}-purinoceptor which mediates contraction of the rat isolated tail artery is very different from the potency order for evoking the inward current which initiates the contractions. The difference may be due to greater breakdown of some of the agonists in artery rings compared with the single cell system. This has important consequences for the pharmacological characterization of P_2-purinoceptor subtypes.

This work was supported by a grant from the Wellcome Trust. We are grateful to the Scottish Hospital Endowments Research Trust for refurbishing the laboratories in which these experiments were performed.

References

ÅSTRAND, P., BROCK, J.A. & CUNNANE, T.C. (1988). Time course of transmitter action at the sympathetic neuroeffector junction in rodent vascular and non-vascular smooth muscle. *J. Physiol.*, **401**, 657–670.

BEAN, B.P. (1992). Pharmacology and electrophysiology of ATP-activated ion channels. *Trends Pharmacol. Sci.*, **13**, 87–90.

BEAN, B.P. & FRIEL, D.D. (1990). ATP-activated channels in excitable cells. In *Ion Channels*, Vol. 2. ed. Narahashi, T. pp. 169–203. London/New York: Plenum Press.

BENHAM, C.D., BOLTON, T.B., BYRNE, N.G. LARGE, W.A. (1987). Action of extracellular adenosine triphosphate in single smooth muscle cells dispersed from the rabbit ear artery. *J. Physiol.*, **387**, 473–488.

BENHAM, C.D. & TSIEN, R.W. (1987). A novel receptor-operated Ca^{2+}-permeable channel activated by ATP in smooth muscle. *Nature*, **328**, 275–278.

BEVAN, J.A. & OSHER, J.V. (1972). A direct method for recording tension changes in the wall of small blood vessels *in vitro*. *Agents Actions*, **2**, 257–260.

BO, X. & BURNSTOCK, G. (1993). Heterogeneous distribution of [^{3}H] α,β-methyleneATP binding sites in blood vessels. *J. Vasc. Res.*, **30**, 87–101.

BURNSTOCK, G. (1978). A basis for distinguishing two types of purinergic receptor. In *Cell Membrane Receptors for Drugs and Hormones, A Multidisciplinary Approach*, ed. Straub, R.W. & Bolis, L. pp. 107–118. New York: Raven Press.

BURNSTOCK, G. (1990). Purinergic mechanisms. *Ann N.Y. Acad. Sci.*, **603**, 1–17.

BURNSTOCK, G. & KENNEDY, C. (1985). Is there a basis for distinguishing two types of P_2-purinoceptor? *Gen. Pharmacol.*, **5**, 433–440.

CLAPP, L.H. & GURNEY, A.M. (1991). Outward currents in rabbit pulmonary artery cells dissociated with a new technique. *Exp. Physiol.*, **76**, 677–693.

DUBYAK, G.R. & EL-MOATASSIM, C. (1993). Signal transduction via P_2-purinergic receptors for extracellular ATP and other nucleotides. *Am. J. Physiol.*, **265**, (*Cell Physiol.* **34**), C577–C606.

EDWARDS, F.A., GIBB, A.J. & COLQUHOUN, D. (1993). ATP receptor-mediated synaptic currents in the central nervous system. *Nature*, **359**, 144–146.

EVANS, R.J., DERKACH, V. & SURPRENANT, A. (1993). ATP mediates fast synaptic transmission in mammalian neurones. *Nature*, **357**, 503–505.

EVANS, R.J. & SURPRENANT, A. (1992). Vasoconstriction of guinea-pig submucosal arterioles following sympathetic nerve stimulation is mediated through the release of ATP. *Br. J. Pharmacol.*, **106**, 242–249.

FENWICK, E.M., MARTY, A. & NEHER, E. (1982). A patch-clamp study of bovine chromaffin cells and their sensitivity to acetylcholine. *J. Physiol.*, **331**, 577–597.

FRIEL, D. (1988). An ATP-sensitive conductance in single smooth muscle cells from the rat vas deferens. *J. Physiol.*, **401**, 361–380.

GORDON, E.L., PEARSON, J.D., DICKINSON, E.S., MOREAU, D. & SLAKEY, L.L. (1989). The hydrolysis of extracellular adenine nucleotides by arterial smooth muscle cells. Regulation of adenosine production at the cell surface. *J. Biol. Chem.*, **264**, 18986–18992.

GORDON, J. (1986). Extracellular ATP: effects, sources and fate. *Biochem. J.*, **233**, 309–319.

ILLES, P. & NÖRENBERG, W. (1993). Neuronal ATP receptors and their mechanism of action. *Trends Pharmacol. Sci.*, **14**, 50–54.

INOUE, R. & BRADING, A.F. (1990). The properties of the ATP-induced depolarisation and current in single cells isolated from the guinea-pig urinary bladder. *Br. J. Pharmacol.*, **100**, 619–625.

KENNEDY, C. (1990). P_1- and P_2-purinoceptor subtypes – an update. *Arch. Int. Pharmacol. Ther.*, **303**, 30–50.

KENNEDY, C. (1993a). ATP as a cotransmitter with noradrenaline in sympathetic perivascular nerves. In *Vascular Innervation and Receptor Mechanisms – New Perspectives*. ed. Edvinsson, L. & Uddman, R. pp. 187–199. San Diego: Academic Press.

KENNEDY, C. (1993b). Cellular mechanisms underlying the excitatory actions of ATP in vascular smooth muscle. *Drug Dev. Res.*, **28**, 423–427.

LEFF, P., HUMPHRIES, R.G., CRACK, B.E., POLLARD, C.E. & MCKECHNIE, K. (1994). New ATP analogues: pharmacological tools & potential drugs. *Drug Dev. Res.*, **31**, 290.

LUSTIG, K.D., SHIAU, A.K., BRAKE, A.J. & JULIUS, D. (1993). Expression cloning of an ATP receptor from mouse neuroblastoma cells. *Proc. Natl. Acad. Sci. U.S.A.*, **90**, 5113–5117.

NAKAZAWA, K. & MATSUKI, N. (1987). Adenosine triphosphate-activated inward current in isolated smooth muscle cells from the rat vas deferens. *Pflügers Arch.*, **409**, 644–646.

O'CONNOR, S.E., DAINTY, I. & LEFF, P. (1991). Further subclassification of ATP receptors based on agonist studies. *Trends Pharmacol. Sci.*, **12**, 137–141.

SAÏAG, B., MILON, D., ALLAIN, H., RAULT, B. & VAN DEN DRIESSCHE, J. (1990). Constriction of the smooth muscle of the rat tail and femoral arteries and dog saphenous vein is induced by uridine triphosphate via 'pyrimidinoceptors', and by adenosine triphosphate via P_{2X}-purinoceptors. *Blood Vessels*, **27**, 352–364.

SJÖBLOM-WIDFELDT, N., ARNER, A. & NILSSON, H. (1993). Contraction of small mesenteric arteries induced by micromolar concentrations of ATP released from caged ATP. *J. Vasc. Res.*, **30**, 38–42.

SNEDDON, P. & BURNSTOCK, G. (1984). ATP as a cotransmitter in rat tail artery. *Eur. J. Pharmacol.*, **106**, 149–152.

WEBB, T.E., SIMON, J., KRISHEK, B.J., BATESON, A.N., SMART, T.G., KING, B.F., BURNSTOCK, G. & BARNARD, E.A. (1993). Cloning and functional expression of a brain G-protein-coupled ATP receptor. *FEBS*, **324**, 219–225.

WELFORD, L.A., CUSACK, N.J. & HOURANI, S.M.O. (1986). ATP analogues and the guinea-pig taenia coli: a comparison of the structure-activity relationships of ectonucleotidases with those of the P_2-purinoceptor. *Eur. J. Pharmacol.*, **129**, 217–224.

WELFORD, L.A., CUSACK, N.J & HOURANI, S.M.O. (1987). The structure-activity relationships of ectonucleotidases and of excitatory P_2-purinoceptors: evidence that dephosphorylation of ATP analogues reduces pharmacological potency. *Eur. J. Pharmacol.*, **141**, 123–130.

XIONG, Z., KITAMURA, K. & KURIYAMA, H. (1991). ATP activates cationic currents and modulates the calcium current through GTP-binding protein in rabbit portal vein. *J. Physiol.*, **440**, 143–165.

(Received May 16, 1994
Revised July 8, 1994
Accepted July 18, 1994)

Br. J. Pharmacol. (1994), **113**, 861–868 © Macmillan Press Ltd, 1994

Inhibition by SK&F 96365 of Ca^{2+} current, IL-2 production and activation in T lymphocytes

S. Clare Chung, Thomas V. McDonald & [1]Phyllis Gardner

Department of Molecular Pharmacology and Medicine, Stanford University School of Medicine, Stanford, California 94305-5332, U.S.A.

1 By use of whole cell patch-clamp and Indo-1 fluorescence studies of the Jurkat T leukaemic cell line, we show that the new organic antagonist of receptor-mediated Ca^{2+} entry, SK&F 96365, inhibits the T cell Ca^{2+} current in a dose-dependent fashion, with an IC_{50} of 12 μM.

2 SK&F 96365 also inhibits [^{3}H]-thymidine incorporation and interleukin-2 (IL-2) synthesis in peripheral blood lymphocytes.

3 SK&F 96365 has no effect on Ca^{2+} stores release or K^+ channels.

4 This is the first account of an organic inhibitor of the T cell Ca^{2+} current. The ability of SK&F 96365 to inhibit IL-2 synthesis and cell proliferation suggests that a new class of related Ca^{2+} channel blockers can be developed as immunosuppressive agents.

Keywords: T lymphocytes; Ca^{2+} channels; SK&F 96365

Introduction

The early events of T cell activation include an elevation in intracellular Ca^{2+}, which consists of two phases, a transient release from intracellular stores and a sustained influx across the plasma membrane (Gardner, 1989). The latter phase of Ca^{2+} influx is critical for full T cell activation, since either treatments that reduce Ca^{2+} influx (Jy *et al.*, 1989; Mignery *et al.*, 1992) or T cell receptor (TCR) mutants with submaximal and transient changes in $[Ca^{2+}]_i$ in response to stimulation (Goldsmith *et al.*, 1989) do not produce the autocrine growth factor interleukin-2 (IL-2), as required for progression through the cell cycle (Crabtree, 1989).

The mechanism by which Ca^{2+} traverses the plasma membrane has been the subject of many studies. Plasmalemmal Ca^{2+} channels can be divided into two broad categories; voltage-gated and non-voltage gated. Voltage-gated channels are found in nervous, endocrine, cardiac and skeletal tissue (Nowycky *et al.*, 1985; Tsien *et al.*, 1991). The L-type, or dihydropyridine-sensitive, voltage-gated channels have been well characterized and are the target of the clinically used Ca^{2+} channel blockers such as verapamil, diltiazem, nicardipine and nifedipine (Lee & Tsien, 1983; Brown *et al.*, 1984; Hess & Tsien, 1984) but early patch clamp studies ruled out the presence of classical voltage-gated Ca^{2+} channels in the T cell membrane (DeCoursey *et al.*, 1984; Matteson & Deutsch, 1984). Instead, one or more non-voltage gated Ca^{2+} channels have been found in lymphocytes by means of patch clamp recording (Kuno *et al.*, 1986; Kuno & Gardner, 1987; Lewis & Cahalan, 1989; McDonald *et al.*, 1993). Whole-cell studies suggest that the major source of Ca^{2+} influx flows through a highly Ca^{2+}-selective, inwardly rectifying, Cd^{2+} and Ni^{2+} sensitive channel (Lewis & Cahalan, 1989; McDonald *et al.*, 1993; Zweifach & Lewis, 1993) that is activated either after intracellular generation of $InsP_3$ (Lewis & Cahalan, 1989; McDonald *et al.*, 1993) or after the application of endoplasmic reticulum Ca^{2+} ATPase inhibitors such as thapsigargin (TG) (Zweigach & Lewis, 1993; Premack *et al.*, 1994). The characteristics of the current, as well as its activation by various modalities that deplete intracellular Ca^{2+} stores, suggest that it is in the same category as I_{crac} (for Ca^{2+} release associated current) first described in mast cells (Hoth & Penner, 1992). This current is activated by a 'capacitative' mechanism (Putney, 1990), in which depletion of the endoplasmic reticulum Ca^{2+} stores serves as a trigger for Ca^{2+} influx by an as yet unidentified mechanism. Though current which flows in response to depletion of stores is blocked by inorganic ions including Cd^{2+}, Ni^{2+}, and La^{3+}, there are as yet no reported organic inhibitors of I_{crac}.

We undertook the present study to determine if SK&F 96365 (1-{b- [3-(*p*-methoxyphenyl)-propyloxy-*p*-methoxyphenyethyl}-1H-imidazole hydrochloride), a receptor-mediated Ca^{2+} entry inhibitor in platelets and endothelial cells (Merritt *et al.*, 1990; Mason *et al.*, 1991; Graier *et al.*, 1992) inhibits the I_{crac} type Ca^{2+} current in Jurkat T lymphoblasts. To activate the Ca^{2+} current in Jurkat cells, we used either the mitogen phytohaemagglutinin (PHA), monoclonal antibody to the T cell receptor (mAb C305), carbachol (CCh) stimulation of Jurkat cells transfected with human muscarinic receptor 1 (JHM1 cells; 12), or the microsomal Ca^{2+} ATPase inhibitor thapsigargin (TG). Each of these methods of receptor stimulation have been shown to activate the characteristic, inwardly rectifying, Ca^{2+}-selective whole-cell current (Lewis & Cahalan, 1989; McDonald *et al.*, 1993; Zwiefach & Lewis, 1993; Premack *et al.*, 1994). We also assessed effects of SK&F 96365 on T cell function by monitoring cellular proliferation and IL-2 synthesis. We show here that SK&F 96365 inhibits T cell Ca^{2+} current, mitogen or thapsigargin-induced cellular proliferation, and IL-2 synthesis with a similar concentration-dependence. This suggests that a new class of related Ca^{2+} channel blockers may be developed to inhibit the I_{crac} class of Ca^{2+} channels and that this class of drugs may have therapeutic potential as immunosuppressants.

Methods

Cell lines

Jurkat E6-1 cells of malignant T-lymphocyte cell line were grown at 37°C (5% CO_2) in media RPMI 1640 (Irvine Scientific) supplemented with 10% foetal bovine serum (Hyclone) and L-glutamine. A stable cell line transfected with the human muscarinic receptor type 1 (De Coursey *et al.*, 1984) was kindly provided by Dr A. Weiss (University of California San Francisco Medical Center). Transfected cells were grown in the above media with the addition of G418 (2 mg ml^{-1}) to maintain selection of HM1 + populations.

[1] Author for correspondence.

HT-2 lymphocytes, which are dependent on human IL-2 for growth and which were used in the IL-2 assay, were a gift from Dr C. Clayberger (Stanford University).

Peripheral blood lymphocytes

Peripheral blood lymphocytes were obtained by standard procedures from a healthy volunteer on the day of the experiment. Briefly, blood samples were prepared as follows. First the sample was layered onto Ficoll-Hypaque separation media. This eluent was centrifuged at 2000 r.p.m. for 15 min and peripheral blood lymphocyte fraction was collected. Excess Ficoll was washed from cell fraction and centrifuged at 1200 r.p.m. for 10 min. The pellet was resuspended in PBS buffer and centrifuged at 800 r.p.m. to separate the lymphocytes from the platelets. Cells were washed several times with PBS buffer. The isolated lymphocytes were placed in a media RPMI 1640 with 10% foetal bovine serum.

Materials

SK&F 96365 was a gift from Dr Janet E. Merritt from Smith & Kline and Beecham Pharmaceuticals. MAb C305 was a gift from Dr A. Weiss (University of California at San Francisco). Indo-1/AM and Indo-1/K salt were obtained from Molecular Probes.

Indo-1/AM loading and population $[Ca^{2+}]_i$ measurements

Cells were loaded with 2.5 μM Indo-1/AM in complete growth medium at 30°C for 45 min followed by successive washes to remove unincorporated dye. The cells were then resuspended (5×10^5 cells per 2 ml) in solution of the following composition (mM): NaCl 137, KCl 5.8, $MgCl_2$ 1, $CaCl_2$ 2.5, glucose 5 and HEPES 10, pH = 7.4. Cell suspensions were studied in acrylic cuvettes with constant stirring at 30°C. Fluorescence measurements for the determination of $[Ca^{2+}]_i$ were made in a spectrofluorimeter (SLM 8000/Aminco) with excitation wavelength of 350 nm and dual simultaneous emission fluorescence detection at 405 nm and 464 nm. Agonists were introduced by pipette addition to the cuvettes. Final $[Ca^{2+}]_i$ values were calculated from the emission ratio with the standard equation (Grynkewicz *et al.*, 1985). The R_{max} value was obtained following treatment of cell suspensions with 10 μM ionomycin. The R_{min} value was obtained with a calibration solution (mM): KCl 140, $MgCl_2$ 2, EGTA 10, HEPES 20 calibration solution which contained Indo-1 K salt 1 μM.

Electrophysiology

Cells were placed in a acrylic/polystyrene perfusion chamber mounted on the stage of an inverted microscope (Nikon Diaphot). Initial extracellular solution was mM: Tris-Cl 170, $MgCl_2$ 1, $CaCl_2$ 2.5, glucose 5 and HEPES 10, pH = 7.4, at room temperature (20°C). Intracellular pipette solution contained mM: Cs-glutamate 80 (or Cs-aspartate 80), CsCl 8, $MgCl_2$ 2, EGTA 20 and HEPES 20, pH = 7.3. The estimated $E_{rev\,Cl-} = -71$ mV with these solutions. Carbachol (100–200 μM), thapsigargin (100 nM), and monoclonal antibody to TCR ($1/10^4$ dilution) addition and changes in extracellular ion concentrations were made by use of a perfusion system which exchanged the chamber bath solution within 30–35 s. Solutions for ion substitution experiments were adjusted to avoid changes in osmolarity.

For studies testing the effect of SK&F 96365 on K^+ currents, the extracellular solution was (mM): NaCl 130, $CaCl_2$ 10, $MgCl_2$ 2, KCl 5 and HEPES 10, pH = 7.3. The intracellular pipette solution (mM) was: KCl 140, $MgCl_2$ 2, EGTA 10 and HEPES 10, pH 7.3.

The whole-cell configuration of the patch clamp technique was used to record plasma membrane currents (Hamil *et al.*, 1981). Glass pipettes with a tip resistance of 1–3 MegOhms was used. An Axopatch-1C patch-clamp amplifier (Axon Instruments, Foster City, CA, U.S.A.) and a 80386-based PC computer with a 12-bit AD/DA converter (Scientific solutions) were used for membrane voltage clamp protocols and whole-cell current recording. Data was stored in digital form on floppy diskettes for later analysis with pClamp software (Axon Instruments). Holding potential was maintained at −70 mV and voltage clamp protocols included steps (from −125 mV to +50 mV in 25 mV increments) to monitor steady-state currents and repetitive voltage ramps at 0.75 mV ms^{-1} (from −125 mV to +50 mV) to generate current-voltage ($I-V$) curves. For studies of K^+ current, holding potential was maintained at −70 mV and voltage clamp protocols included steps from −125 mV to +50 mV in 25 mV increments.

Cell proliferation assay

Cells (3×10^5 cells/well) were placed in a 96-well plate and incubated with PHA (20 μg ml^{-1}) or thapsigargin (100 nM) for 24 h: 1 μCi of [^{3}H]-thymidine was then added to each well. Cells were incubated for 24 h and harvested onto a filter paper. The filter papers were placed in a counting vial and counted in a beta radiation counter (1500-TRI-CARB liquid scintillation analyzer by Packard).

IL-2 assay

Peripheral blood lymphocytes (5×10^6 cells ml^{-1}) were incubated with PHA (20 μg ml^{-1}) for 18 h and the supernatant was collected from these cells. The supernatant was then added to 5×10^3 HT-2 cells per well and cells were cultured for 24 h at 37°C. [^{3}H]-thymidine (1 μCi) was then added to each well. Cells were incubated for 4 h and then harvested onto a filter paper. The papers were counted in a beta radiation counter (1500-TRI-CARB liquid scintillation analyzer by Packard). Different concentrations of human interleukin-2 (IL-2; Sigma) were added to HT-2 cells to create a standard curve. Control experiments in which different concentrations of SK&F 96365 were added with IL-2 to HT-2 cells, confirmed that SK&F 96365 had no effect on the bioassay.

Results

Effects of SK&F 96365 on agonist-stimulated $[Ca^{2+}]_i$ responses in Indo-1/AM-loaded Jurkat cells

Figure 1 shows the typical fluorescence traces of Indo-1/AM-loaded Jurkat cells stimulated with monoclonal antibody to the T cell receptor (mAb C305; $1/10^4$ dilution) or PHA (20 μg ml^{-1}). As has been shown by many investigators, these agonists cause a rapid and sustained rise in intracellular $[Ca^{2+}]_i$, which consists of both release of Ca^{2+} from intracellular stores and transmembrane Ca^{2+} influx (Tsien *et al.*, 1982; Nisbet-Brown *et al.*, 1985; Rabinovitch *et al.*, 1986; Gardner, 1989). In a similar fashion, stimulation by carbachol (CCh; 150 μM) of Jurkat cells stably transfected with the human muscarinic receptor 1 (JHM1 cells) also generated a rapid and sustained rise in $[Ca^{2+}]_i$ (Figure 1b). In each case of agonist stimulation, addition of 30 μM SK&F 96365 caused a rapid reduction in the sustained phase of increase intracellular $[Ca^{2+}]_i$ to a level approaching but greater than baseline $[Ca^{2+}]_i$ (Figure 1a,b,c). When external Ca^{2+} is removed by use of the Ca^{2+} chelator EGTA (3 mM) prior to stimulation, a submaximal and transient rise in $[Ca^{2+}]_i$ is seen, representing release from intracellular stores (shown for PHA in Figure 1d). SK&F 96365 has little to no effect on the agonist generated Ca^{2+} signals in Ca^{2+} free media (Figure 1d). Furthermore agonist-generated Ca^{2+} responses after preincubation with SK&F 96365 are roughly equivalent to

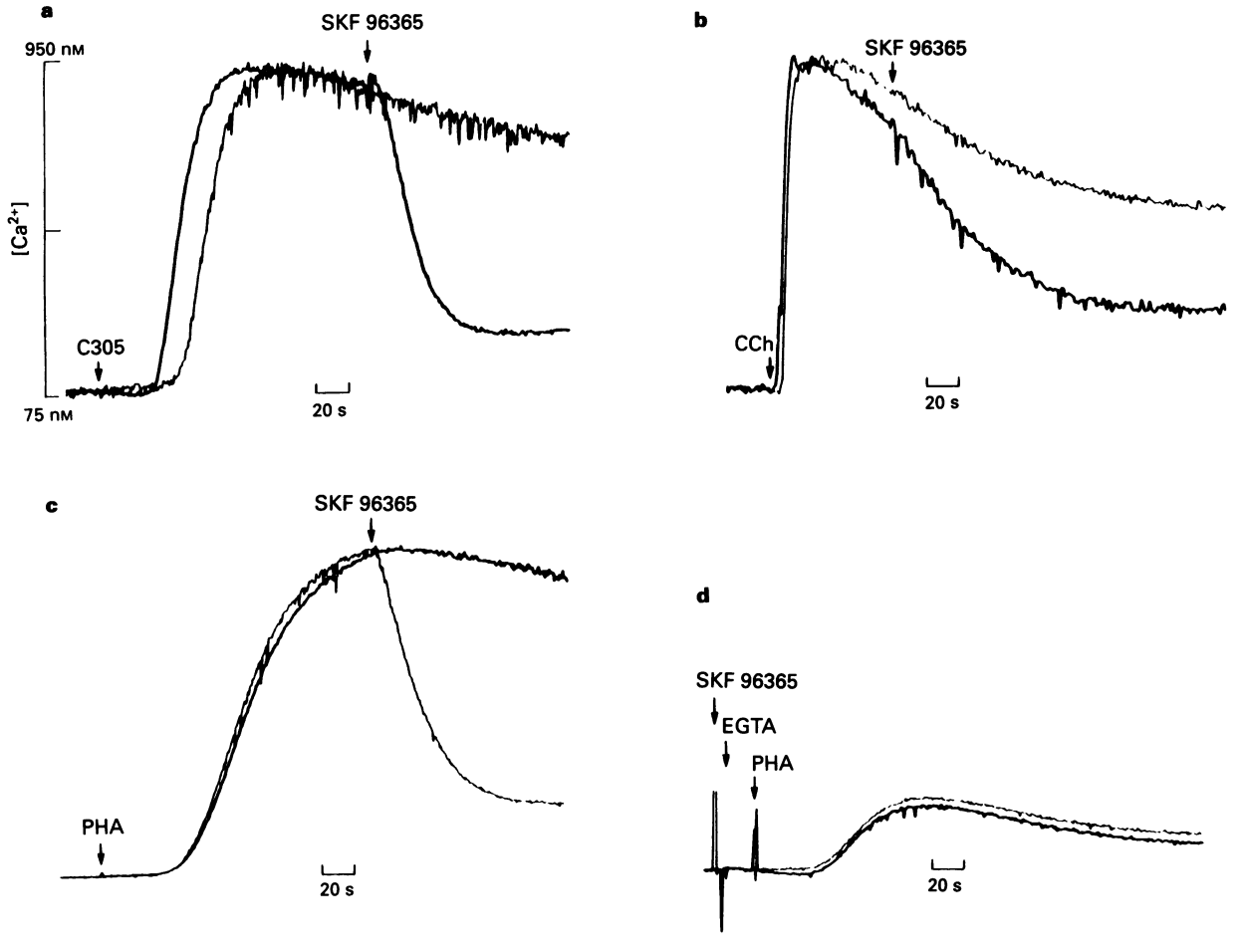


Figure 1 Sustained elevation of $[Ca^{2+}]_i$ following receptor stimulation in Jurkat cells is inhibited by SK&F 96365. (a) $[Ca^{2+}]_i$ measured by Indo-1 fluorescence, as a function of time, in a population of Jurkat cells after addition of mAb C305 ($1/10^4$ dilution) to the T cell receptor, with or without addition of SK&F 96365 (30 μM), to the extracellular solution. (b) $[Ca^{2+}]_i$ in a population of JHM1 cells after addition of carbachol (CCh, 150 μM), with or without addition of SK&F 96365 (30 μM), to extracellular solution. (c) $[Ca^{2+}]_i$ in a population of Jurkat cells after addition of phytohaemagglutinin (PHA) with or without SK&F 9636 (30 μM), to the extracellular solution. (d) Comparison of $[Ca^{2+}]_i$ in two population of Jurkat cells, both of which were suspended in extracellular solution followed by chelation of external Ca^{2+} by EGTA (3 mM) as indicated by the arrow.

the responses seen after depletion of the extracellular Ca^{2+} pool by EGTA (data not shown). These results suggest that SK&F 96365 does not affect the release of Ca^{2+} from intracellular stores but rather selectively inhibits transmembrane Ca^{2+} influx. This agrees with the original observations on the effect of SK&F 96365 on agonist-stimulated $[Ca^{2+}]_i$ responses in quin2-loaded human platelets (Graier *et al.*, 1992). The effect of SK&F 96365 was not due to general cell toxicity, since at all concentrations tested, the viability of cells exposed to the SK&F 96365, as checked by trypan blue exclusion, remained unaltered over a period of 48 h.

Effect of SK&F 96365 on whole-cell Ca^{2+} current

Changes in $[Ca^{2+}]_i$ measured by Indo-1/AM fluorescence represent indirect measurements of transmembrane Ca^{2+} entry, in aggregate with Ca^{2+} stores release, Ca^{2+} stores uptake, and transmembrane Ca^{2+} efflux. A direct assessment of the Ca^{2+} current underlying receptor-mediated Ca^{2+} influx can be attained by the whole cell patch clamp technique. By use of previously described protocols (McDonald *et al.*, 1993), we next tested the effect of SK&F 96365 on whole-cell Ca^{2+} currents after agonist stimulation. We and others have previously shown that stimulation of Jurkat cells by phosphoinositide-linked agonists activates whole-cell Ca^{2+} current (Lewis & Cahalan, 1989; McDonald *et al.*, 1993). The current is characterized by an inwardly rectifying $I-V$ relation which approaches zero current asymptotically at very positive potentials and is carried by a channel selective for divalent cations. In addition TG, a microsomal Ca^{2+}-ATPase inhibitor, activates Ca^{2+} current in T cells by depletion of intracellular Ca^{2+}-stores (Zweifach & Lewis, 1993; Premack *et al.*, 1994). The TG-induced Ca^{2+} current is indistinguishable from that activated by phosphoinositide-linked agonists (Premack *et al.*, 1994). By use of ionic solutions that maximize Ca^{2+} currents relative to other ionic species, we recorded the activation of Ca^{2+} current after stimulation of Jurkat cells with mAb C305 ($1/10^4$ dilution) (Figure 2a), after stimulation of JHM1 cells with 150 μM CCh (Figure 2c) or after stimulation of Jurkat cells with thapsigargin (100 nM) (Figure 2e). Baseline current measured from step protocols prior to stimulation was -0.49 ± 0.3 pA/pF (mean ± s.d.) at -125 mV, $n = 40$. After stimulation, the peak current was -1.3 ± 0.4 pA/pF at -125 mV, $n = 40$. In each case the current was characterized by inward rectification and lack of measurable reversal over the voltage range studied (Figure 2b, 2d and 2f). Bath perfusion of SK&F 96365 (30 μM) decreased (-0.5 ± 0.2 pA/pF, mean ± s.d., at -125 mV, $n = 30$) the mAb C305-induced Ca^{2+} current to approximately baseline over a 30 to 60 s interval (Figure 2a and 2b). Similarly 30 μM SK&F 96365 inhibited CCh-induced Ca^{2+} current in JHM1 cells (Figure 2c and 2d) and TG-induced Ca^{2+} current in Jurkat cells (Figure 2e and 2f) to nearly baseline levels over a similar time course. The similarity of the effect of SK&F 96365 on the different modes current activation indicated that it is a functional antagonist, as was previously found in

other cell types (Merritt et al., 1990). The effect of SK&F 96365 was reversible upon removal of the drug (data not shown) and dose-dependent. The relation between SK&F 96365 concentration and inhibition of Ca^{2+} influx as assessed by both Indo-1/AM fluorescence and whole-cell patch clamp recordings is shown in Figure 3. The IC_{50} for inhibition lies between 12 μM (assessed whole-cell patch clamp) and 20 μM (as assessed by Indo-1 fluorescence), while the maximal effect is seen at drug concentration greater than 30 μM.

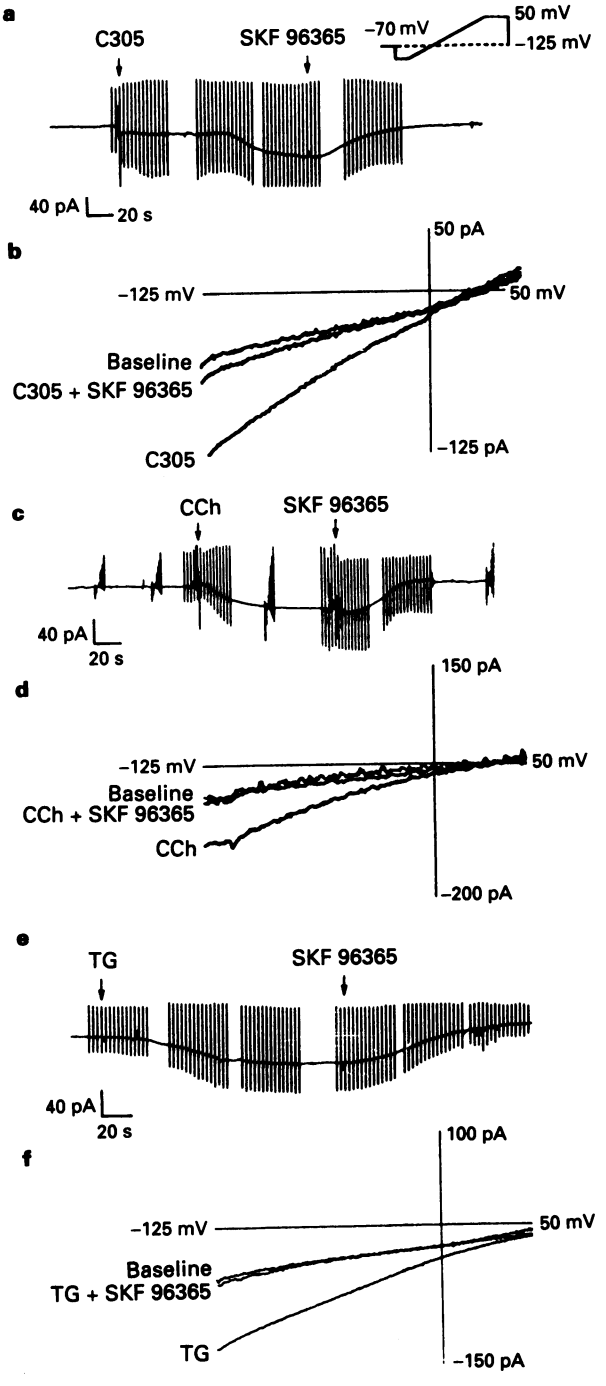


Figure 2 SK&F 96365 inhibits the inward Ca^{2+} current stimulated by mAb C305 in Jurkat cells, by carbachol (CCh) in JHM1 cells, or thapsigargin (TG) in Jurkat cells. (a) Continous whole cell patch clamp current recording of a Jurkat cell during repetitive voltage clamp ramps from − 125 mV to + 50 mV from a holding potential of − 70 mV (protocol shown in insert). (b) Whole cell ramp current is plotted as a function of membrane potential (ramp $I-V$) from the same cell as in (a), at baseline, after stimulation with mAb C305, and after subsequent perfusion with SK&F 96365. (c) Effect of CCh and SK&F 96365 on continous whole cell patch clamp current recording of a JHM1 cell during voltage clamp ramps. (d) Ramp $I-V$ from the same cell as in (c) at baseline after stimulation by CCh, and after subsequent perfusion with SK&F 96365. (e) Effect of TG and SK&F 96365 on continous whole cell patch clamp current recording of a Jurkat cell during voltage clamp ramps; (f) ramp $I-V$ from the same cell as in (e) at baseline, after stimulation by TG, and after subsequent perfusion with SK&F 96365.

For purpose of comparison, the standard L-type voltage-gated Ca^{2+} channel blockers, nicardipine and diltiazem, were assessed for effect on the $[Ca^{2+}]_i$ responses in Indo-1/AM loaded Jurkat cells. Neither nicardipine (up to 50 μM) nor diltiazem (up to 1 mM) affected the fluorescence rise stimulated by mAb C305, PHA, or CCh (data not shown). Higher concentrations of nicardipine could not be tested due to autofluorescence of the drug at concentrations greater than 50 μM. Whole-cell patch clamp recordings confirm that standard Ca^{2+} channel blockers do not inhibit the T cell Ca^{2+} current. Figure 4a shows a representative family of current traces obtained by voltage steps from a holding potential of − 70 mV at baseline, after stimulation by CCh, and after addition of SK&F 96365. As expected, the agonist-activated Ca^{2+} current showed little to no volage- or time-dependent gating, differentiating the T cell Ca^{2+} channel from voltage-gated Ca^{2+} channels. SK&F 96365 blocks the current to nearly baseline levels. By contrast, high concentrations of diltiazem have no effect on the CCh-activated Ca^{2+} current in transfected Jurkat cells (Figure 4b), confirming the results derived from fluorescence studies.

The ability of SK&F 96365 to inhibit Ca^{2+} current is unaffected by changes in the membrane holding potential. When the holding potential was varied over a range from − 70 mV to + 25 mV, no change is seen in the ability of SK&F 96365 to block Ca^{2+} current (at − 70 mV, 87% block, $n = 10$; at − 25 mV, 92% block, $n = 5$; at 0 mV, 98% block, $n = 5$; at + 25 mV, 91% block, $n = 4$). Both the magnitude of the current inhibition and its time course of inactivation kinetics remained the same as the membrane holding potential is made more positive.

Lack of effect of SK&F 96365 on whole-cell K^+ currents

In order to rule out an indirect Ca^{2+} channel blockade via inhibition of K^+ channels, the effect of SK&F 96365 on K^+ currents was studied in Jurkat T cells. Outward K^+ currents

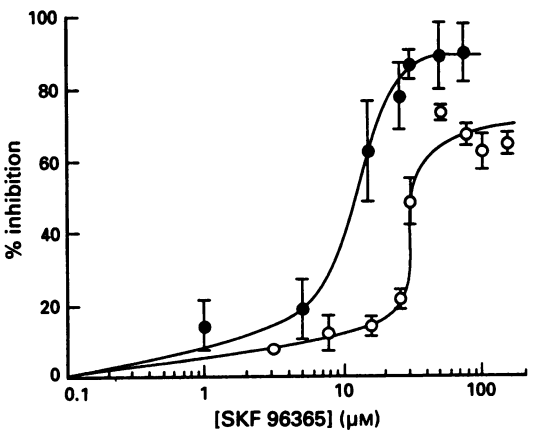


Figure 3 Dose-response curve for inhibition by SK&F 96365 of Ca^{2+} influx: (○) $[Ca^{2+}]_i$, measured by Indo-1 fluorescence after stimulation of Jurkat cells by 20 μg ml^{-1} phytohaemagglutinin (PHA), as a function of SK&F 96365 concentration; (●) Ca^{2+} current, as measured in single JHM1 cells by the whole-cell recording technique after stimulation by 150 μM carbachol (CCh), as function of SK&F 96365 concentration. Inhibition is calculated as the percentage decrease from peak response relative to basline. Data are expressed as mean ± s.e. mean of five experiments (○), or seven cells (●). Where not shown, the error bars are within the symbol size.

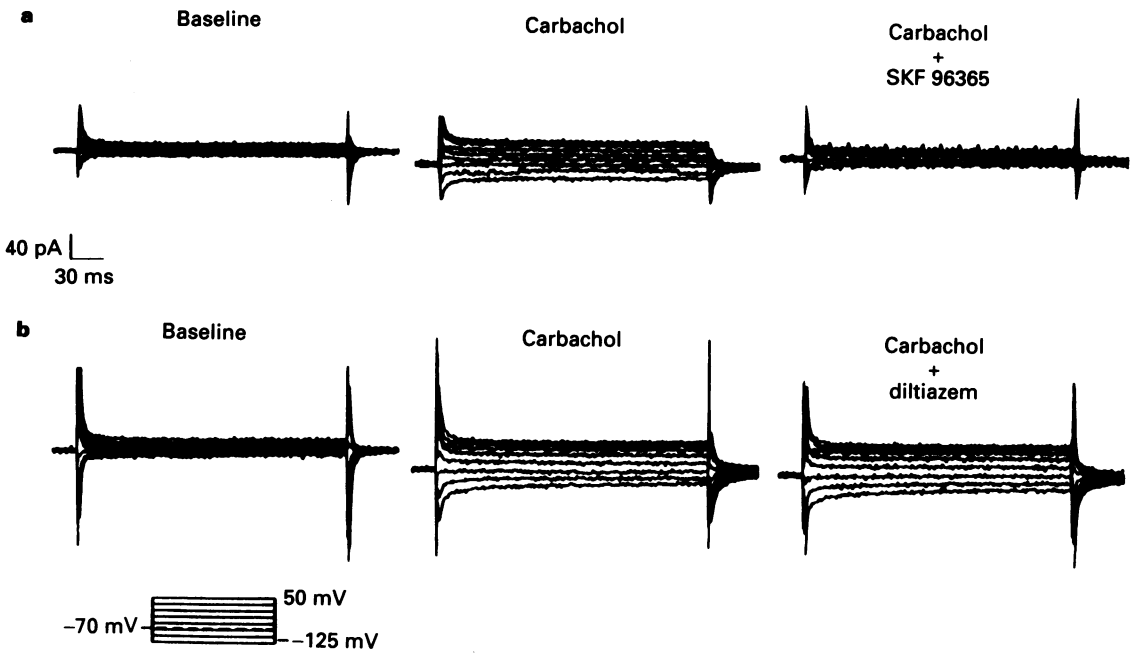


Figure 4 The voltage-gated Ca^{2+} channel blocker diltiazem does not block the Ca^{2+} current in Jurkat cells: (a) whole cell patch clamp record of steady-state currents during voltage steps (protocol demonstrated in the insert) from a JHM1 cell, at baseline, after stimulation by 150 μM carbachol (CCh) and after addition of 30 μM SK&F 96365. (b) Whole cell patch clamp records of steady-state currents during voltage steps form a JHM1 cell, at baseline, after stimulation by 150 μM CCh, and after addition of 30 μM diltiazem. Representative results of four experiments.

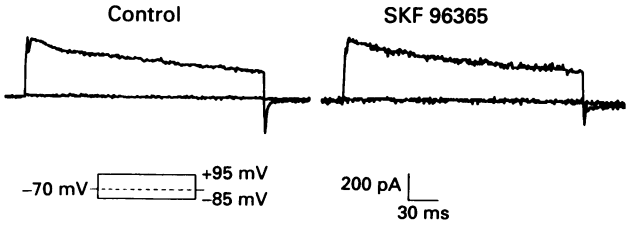


Figure 5 SK&F 96365 does not block K^+ currents in Jurkat cells. Whole cell patch clamp record of K^+ current activated by depolarizing voltage steps (protocol shown in inset), at baseline (left) and after perfusion with 30 μM SK&F 96365. Representative results of five experiments.

evoked by depolarizing voltage steps are demonstrated in Figure 5. Perfusion with 30 μM SK&F 96365 had no apparent effect on either the magnitude of the K^+ current or its inactivation kinetics. Therefore, the action of SK&F 96365 in T cells is apparently specifically directed against agonist-generated Ca^{2+} currents.

Effect of SK&F 96365 on cell growth and on IL-2 synthesis

Having shown that SK&F 96365 inhibits T cell Ca^{2+} currents, we next used SK&F 96365 to see whether this inhibition was of functional importance. In order to assess the effect of SK&F 96365-mediated inhibition of Ca^{2+} currents on mitogen-induced cell proliferation, peripheral blood lymphocytes were stimulated with PHA (20 μg ml^{-1}) or TG (100 nM) for 24 h, in the presence or absence of SK&F 96365. Subsequently cells were pulsed with [^{3}H]-thymidine for an additional 24 h, harvested and incorporated radioactivity was determined. Surprisingly, TG alone induced cell proliferation, but the magnitude of proliferation was ten fold less than with PHA stimulation (Figure 6a). SK&F 96365 inhibited cell proliferation in a concentration-dependent fashion with an IC_{50} of approximately 20 μM for PHA-stimulated cells and 5 μM for thapsigargin-stimulated cells. SK&F 96365 did not affect the viability of peripheral lymphocytes over a 48 h period as assessed by trypan blue exclusion.

IL-2, which expressed at the time T cells become committed to activation, is essential for T lymphocyte cell cycle progression, proliferation and immune function (Crabtree, 1989). Like T cell activation, the expression of IL-2 requires extracellular Ca^{2+} (Mills *et al.*, 1985; Gelfand *et al.*, 1987). We next investigated whether SK&F 96365 inhibited the synthesis of IL-2. As demonstrated in Figure 6b, SK&F 96365 blocks IL-2 synthesis in a concentration-dependent fashion (IC_{50} = 15 μM) with a dose-response relationship close to that obtained for both inhibition of Ca^{2+} current and inhibition of cell proliferation.

Discussion

Using fluorescence measurements of Indo-1 loaded cells and whole-cell patch clamp recording, we have shown that SK&F 96365 inhibits the I_{crac} type Ca^{2+} current stimulated in Jurkat T cells after depletion of Ca^{2+} stores. IL-2 synthesis and [^{3}H]-thymidine incorporation were inhibited in the similar concentration-range, indicating the functional significance of T cell Ca^{2+} channel blockade. This concurs with previous findings in which it has been shown that SK&F 96365 inhibited proliferation of Jurkat cells by interfering with progression through the cell cycle (Nordstrom *et al.*, 1992).

Several early patch clamp studies of human peripheral T lymphocytes revealed that the predominant ion channels present are voltage-gated K^+ channels which closely resemble the delayed rectifier K^+ channels of nerve and muscle (DeCoursey *et al.*, 1984; Matteson & Deutsch, 1984; Deutsch *et al.*, 1986; Grissmer *et al.*, 1992). The lymphocyte K^+ current is blocked not only by K^+ channel blockers, but also by classical Ca^{2+} channel antagonists such as verapamil

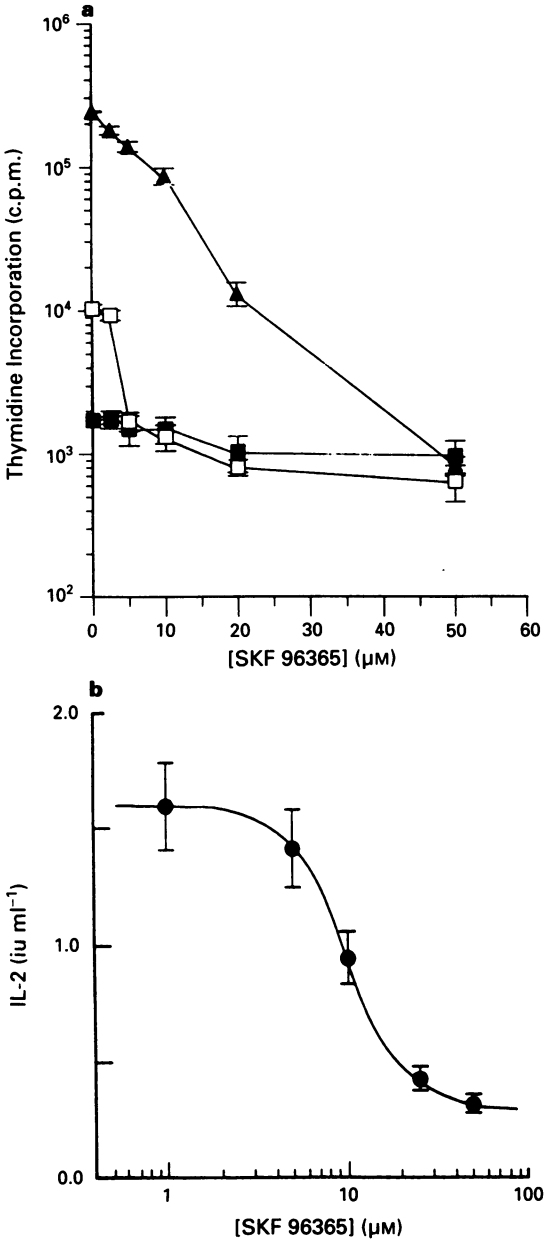


Figure 6 Dose-response curves for inhibition by SK&F 96365 of T cell proliferation and IL-2 synthesis. (a) PBL's were cultured as described with 20 μg ml^{-1} phytohaemagglutinin (▲) or 100 nM thapsigargin (□) plus SK&F 96365 at the indicated concentrations for 24 h. Each well was pulsed with [^{3}H]-thymidine (1 μCi) for 24 h. For control experiment, PBL was treated with SK&F 96365 alone (■). Data are shown as c.p.m. ± s.e.mean of four samples. (b) Dose-response curve for inhibition by SK&F 96365 of the production of IL-2 activity in culture supernatants. Supernatants from PBL's stimulated with PHA (20 μg ml^{-1}) for 24 h were assayed on 5 × 10^3 HT-2 cells/well. Data are shown as mean IL-2 activity ± s.e.mean as determined by a standardized curve generated with recombinant IL-2, from triplicate samples.

(IC_{50} = 6–7 μM) and diltiazem (IC_{50} = 60 μM) (Chandy *et al.*, 1984). The voltage-gated K^+ channel is felt to play a role in maintaining Ca^{2+} influx during T cell activation. By repolarizing the cell toward the Nerstian equilibrium potential for K^+ (about − 80 mV), voltage-gated K^+ channels may maintain the driving force for Ca^{2+}. Thus blockade of K^+ channels may indirectly affect the rise in Ca^{2+} associated with agonist stimulation. At concentrations inhibitory to the Ca^{2+} current, no effect of SK&F 96365 on internal Ca^{2+} stores release or K^+ currents were seen.

In a process comparable to that in T cells, receptor activation in other nonexcitable cell types results in an initial release of internal Ca^{2+} stores followed by sustained Ca^{2+} entry across the plasma membrane. Receptor-mediated Ca^{2+} entry (RCME) is mimicked by Ca^{2+} influx initiated by microsomal ATPase inhibitors, such as TG. These experimental findings provide strong support for the 'capacitative Ca^{2+} entry' model (Putney, 1990), in which emptying of intracellular Ca^{2+} stores activates Ca^{2+} influx across the plasma membrane by an unknown mechanism. RCME is often measured indirectly by monitoring Ca^{2+} or Mn^{2+} entry into cells loaded with fluorescent Ca^{2+} indicator dyes. By use of such techniques, it has been shown that a novel inhibitor, SK&F 96365, which is structurally distinct from known Ca^{2+} channel antagonists, inhibits RCME in platelets, neutrophils and endothelial cells (Merritt *et al.*, 1990; Mason *et al.*, 1991; Graier *et al.*, 1992). The IC_{50} for inhibition of RCME ranged from 8–12 μM. SK&F 96365 showed selectivity in inhibiting RCME compared with internal stores release or Ca^{2+} currents through purinoceptors or NMDA receptors, but not with voltage-gated Ca^{2+} currents (Merritt *et al.*, 1990). Similar concentrations of SK&F 96365 also inhibited platelet aggregation, adhesion, and chemotaxis of neutrophils (Merritt *et al.*, 1990) and the synthesis and release of NO in endothelial cells (Graier *et al.*, 1992), substantiating the functional importance of RCME blockade in these cell types.

Recently, I_{crac}, the Ca^{2+} current activated by depletion of internal Ca^{2+} stores, was described in mast cells (Hoth & Penner, 1992). A Ca^{2+} current with nearly identical properties is also seen in T cells after internal generation of $InsP_3$ (McDonald *et al.*, 1993) or after stores depletion by thapsigargin (Zweifach & Lewis, 1993; Premack *et al.*, 1994). The I_{crac} class of Ca^{2+} currents appears to be partially or wholly responsible for RCME (Clapham, 1993). Our finding that SK&F 96365 inhibits this current in Jurkat T cells is the first report of an organic antagonist for I_{crac}.

The latency with which SK&F 96365 produces full blockade of Jurkat T cell Ca^{2+} current (up to 60 s) raises the question of whether SK&F 96365 works directly through an association with the Ca^{2+} channel versus indirectly by interfering with intermediate biochemical steps. The mechanism by which depletion of Ca^{2+} stores signals activation of I_{crac} is largely unknown (Clapham, 1993), though recent studies suggest the synthesis of a novel, diffusible, phosphorylated second messenger (Parekh *et al.*, 1993; Randriamampita & Tsien, 1993). Suggestions that SK&F 96365 may be working by indirect mechanisms involving the intermediate biosynthetic pathway of a requisite second messenger have been made on the basis that this drug closely resembles the imidazole antimycotics, econozole, miconazole, and clotrimazole, which are thought to be selective antagonists of cytochrome P-450. Importantly the cytochrome P-450 inhibitors have also been noted to inhibit Mn^{2+} entry in rat thymocytes and human neutrophils, raising the possibility that cytochrome P-450 is involved in regulating plasma membrane Ca^{2+} permeability (Alonso *et al.*, 1989; Alvarez *et al.*, 1992; Montero *et al.*, 1991; 1993; Sargeant *et al.*, 1992). In the hepatic microsome, cytochrome P-450 directly inhibits the activity of the endoplasmic reticulum Ca^{2+} ATPase pump through an oxygen-dependent oxidative process, further substantiating a role for this enzyme in Ca^{2+} homeostasis. Two cytochromes (P1-450 or P448) have been found in microsomes of human lymphocytes after mitogen stimulation, where they are responsible for enzymatic activities such as aryl hydrocarbon hydroxylase (Amsbaugh *et al.*, 1986).

Additional suggestion that SK&F 96365 may inhibit Ca^{2+} channels by indirect means is provided by the observation that this drug interacts with the Ca^{2+} binding regulatory protein calmodulin as measured by ^{1}H-nuclear magnetic resonance (n.m.r.) (Reid *et al.*, 1990). Since calmodulin antagonists have been shown to facilitate RCME (Rao, 1987; Alvarez *et al.*, 1992), it remains possible that SK&F blocks I_{crac} through a calmodulin-related action. Histochemical

studies have shown that the endoplasmic reticulum contains significant amounts of calmodulin (Nordstrom *et al.*, 1992). A role for calmodulin in modulating Ca^{2+} influx is suggested by the finding that several calmodulin antagonists (phenothiazine, trifluoperazine, fluphenazine and chlorpromazine) increase the uptake of Mn^{2+} by thymocytes whose Ca^{2+} stores are filled (Alonso *et al.*, 1989; Schleuning *et al.*, 1989).

In conclusion, we present evidence that SK&F 96365 inhibits Ca^{2+} current in T cells and is thus the first reported organic inbibitor of I_{crac} type Ca^{2+} channels. The mechanism by which this drug inhibits I_{crac} is largely unknown, but may involve either direct channel blockade versus interference with a requisite intermediate biochemical step. The low potency ($IC_{50} = 12\ \mu M$), lack of selectivity (also blocks voltage-gated Ca^{2+} channels; Merritt *et al.*, 1990) and lack of knowledge about the precise mechanism by which it works limit this drug to the status of an experimental tool. The functional consequence of Ca^{2+} channel blockade in T cells, however, further emphasizes the potential therapeutic value of higher potency, more selective I_{crac} blockers.

We thank Dr Janet E. Merritt for providing SK&F 96365 (Smith & Kline and Beecham Pharmaceuticals).

This research was supported by American Cancer Society Grant No. DB-26E (to P.G.), National Institute of Health Grants K11-HL02387 (to T.M.) and Predoctoral Pharmacology Training Grant GM07149 (S.C.), and the Burroughs Wellcome Fund Faculty Scholar Award (to P.G.).

References

ALONSO, M.T., SANCHEZ, A. & GARCIA-SANCHO, J. (1989). Monitoring of the activation of receptor-operated Ca^{2+} channel in human platelets. *Biochem. Biophys. Res. Commun.*, **162**, 24–29.

ALVAREZ, J., MONTERO, M. & GARCIA-SANCHO, J. (1992). Cytochrome P450 may regulate plasma membrane Ca^{2+} permeability according to filing states of the intracellular Ca^{2+} stores. *FASEB J.*, **6**, 786–792.

AMSBAUGH, S.C., DING, J., SWAN, D.C., POPESCU, N.C. & CHEN, Y. (1986). Expression and Chromosomal localization of the cytochrome P1-450 gene in human mitogen-stimulated lymphocytes. *Cancer Res.*, **46**, 2423–2427.

BROWN, A.M., KUNZE, D.L. & YATANI, A. (1984). The agonist effect of dihydropyridines on Ca^{2+} channels. *Nature*, **311**, 570–572.

CHANDY, K.G., DECOURSEY, T.E., CAHALAN, M.D., MCLAUGHLIN, C. & GUPTA, S. (1984). Voltage-gated K^+ channels are required for human T lymphocyte activation. *J. Exp. Med.*, **160**, 369–385.

CLAPHAM, D. (1993). A mysterious new influx factor. *Nature*, **364**, 763–764.

CRABTREE, G. (1989). Contigent genetic regulatory events in T lymphocyte activation. *Science*, **243**, 355–361.

DECOURSEY, T.E., CHANDY, K.G., GUPTA, S. & CAHALAN, M.D. (1984). Voltage-gated K^+ channels in human T lymphocytes: a role in mitogenesis? *Nature*, **307**, 465–468.

DEUTSCH, C., KRAUSE, D. & LEE, S.C. (1986). Voltage-gated K^+ conductance in human T lymphocytes stimulated with phorbol ester. *J. Physiol.*, **372**, 405–423.

GARDNER, P. (1989). Ca^{2+} and T lymphocyte activation. *Cell*, **59**, 15–20.

GELFAND, E.W., MILLS, G.B., CHEUNG, R.K., LEE, L.W. & GRINSTEIN, S. (1987). Transmembrane ion fluxes during activation of human T lymphocytes: Role of Ca^{2+}, Na^+/H^+ Exchange and phospholipid turnover. *Immunol. Rev.*, **95**, 59–87.

GOLDSMITH, M.A., DESAI, D.M., SCHULTZ, T. & WEISS, A. (1989). Function of a heterologous muscarinic receptor in T cell antigen receptor signal transduction mutants. *J. Biol. Chem.*, **26**, 17190–17197.

GRAIER, W.F., GROSCHNER, K., SCHMIDT, K. & KUKOVETZ, W.R. (1992). SK&F 96365 inhibits histamine induced formation of endothelium-derived relaxing factor in human endothelial cells. *Biochem. Biophys. Res. Commun.*, **186**, 1539–1545.

GRISSMER, S., LEWIS, R.S. & CAHALAN, M.D. (1992). Ca^{2+} activated K^+ channel in human leukemic T cell. *J. Gen. Physiol.*, **99**, 63–84.

GRYNKEWIZ, G., POENIC, M. & TSIEN, R.Y. (1985). A new generation of Ca^{2+} indicators with greatly improved fluorescence properties. *J. Biol. Chem.*, **260**, 3440–3448.

HAMIL, O.P., MARTY, A., NEHER, E., SAKMANN, B. & SIGWORTH, F.J. (1981). Improved patch-clamp techniques for high resolution current recording from cells and cell-free membrane patches. *Pflügers Arch.*, **391**, 85–100.

HESS, P. & TSIEN, R.W. (1984). Different modes of Ca^{2+} channel gating behavior favored by dihydropyridine Ca^{2+} agonist and antagonist. *Nature*, **311**, 538–544.

HOTH, M. & PENNER, R. (1992). Depletion of Intracellular Ca^{2+} stores activates a Ca^{2+} current in mast cells. *Nature*, **355**, 353–356.

JY, W., FREIGIEN, N., BOURGUIGNON, G.J. & BOURGUIGNON, L.Y.W. (1989). Role of Ca^{2+} during lymphocyte activation. *Biochem. Biophys. Acta.*, **983**, 153–160.

KUNO, M., GORONZY, J., WEYAND, D. & GARDNER, P. (1986). Single-channel and whole cell recordings of mitogen-regulated inward currents in human cloned helper T lymphocytes. *Nature*, **323**, 269–273.

KUNO, M. & GARDNER, P. (1987). Ion channels activated by inositol 1,4,5-trisphosphate in plasma membrane of human T lymphocytes. *Nature*, **326**, 301–304.

LEE, K.S. & TSIEN, R.W. (1983). Mechanism of Ca^{2+} channel blockade by verapamil, D600, diltiazem and nitrendipine in single dialyzed heart cells. *Nature*, **302**, 790–794.

LEWIS, R.S. & CAHALAN, M.D. (1989). Mitogen-induced oscillations of cytosolic Ca^{2+} and transmembrnae Ca^{2+} current in human leukemic T cells. *Cell Regulation*, **1**, 99–112.

MASON, M.J., MAHAUT-SMITH, M.P. & GRINSTEIN, S. (1991). The role of intracellular Ca^{2+} in the regulation of the plasma membrane Ca^{2+} permeability of unstimulated rat lymphocytes. *J. Biol. Chem.*, **266**, 10872–10879.

MATTESON, D.R. & DEUTSCH, C. (1984). K^+ channels in T lymphocytes: a patch clamp study using monoclonal antibody adhesion. *Nature*, **307**, 468–471.

MCDONALD, T.V., PREMACK, B.A. & GARDNER, P. (1993). Flash photolysis of caged inositol 1,4,5-trisphosphate activates plasma membrane Ca^{2+} current in human T cells. *J. Biol. Chem.*, **268**, 3889–3896.

MERRITT, J.E., ARMSTRON, W.P., BENHAM, C.D., HALLAM, T.J., JACOB, R., JAXACHAMIEC, A., LEIGH, B.K., MCCARTHY, S.A., MOORES, K.E. & RINK, T.J. (1990). SK&F 96365, a novel inhibitor of receptor-mediated Ca^{2+} entry. *Biochem. J.*, **271**, 515–522.

MIGNERY, G.A., JOHNSTON, P.A. & SUDHOF, T.C. (1992). Mechanism of Ca^{2+} inhibition of inositol 1,4,5-trisphosphate (IP3) binding to the cellular IP3 receptor. *J. Biol. Chem.*, **267**, 7450–7455.

MILLS, G.B., CHEUNG, R.K., CRAGOE, E., GRINSTEIN, S. & GELFAND, E.W. (1985). Increase in cytosolic free Ca^{2+} concentration is an intracellular messenger for production of IL-2. *J. Immunol.*, **134**, 1640–1643.

MONTERO, M., ALVAREZ, J. & GARCIA-SANCHO, J. (1991). Agonist-induced Ca^{2+} influx in human neutrophils is secondary to the emptying of intracellular Ca^{2+} stores. *Biochem. J.*, **277**, 73–79.

MONTERO, M., GARCIA-SANCHO, J. & ALVAREZ, J. (1993). Comparative effects of cytochrome P450 inhibitors of Ca^{2+} and Mn^{2+} entry. *Biochim. Biophys. Acta.*, **1177**, 127–133.

NISBET-BROWN, E., CHEUNG, R.K., LEE, J. & GELFAND, E.W. (1985). Antigen-dependent increase in cytosolic Ca^{2+} in human T lymphocyte. *Nature*, **316**, 545–547.

NORDSTROM, T., NEVANLINNA, H.A. & ANDERSSON, L.C. (1992). Mitosis-arresting effect of the Ca^{2+} channel inhibitor SK&F 96365 on human leukemia cells. *Exp. Cell Res.*, **202**, 487–494.

NOWYCKY, M.C., FOX, A.P. & TSIEN, R.W. (1985). Three types of neuronal Ca^{2+} channel with different Ca^{2+} agonist sensitivity. *Nature*, **316**, 440–443.

PAREKH, A.G., TERLAU, H. & STUHMER, W. (1993). Depletion of IP_3 stores activates a Ca^{2+} and K^+ current by means of a phosphatase and a diffusible messenger. *Nature*, **364**, 814–818.

PREMACK, B.A., MCDONALD, T.V. & GARDNER, P. (1994). Activation of Ca^{2+} currents in Jurkat T cells following the Depletion of Ca^{2+} stores by microsomal Ca^{2+}-ATPase Inhibitor. *J. Immunol.*, **15**, 5226–5240.

PUTNEY, J.W. Jr. (1990). Capacitative Ca^{2+} entry revisited. *Cell Calcium*, **11**, 611–624.

RABINOVITCH, P., JUNE, C., GROSSMANN, A. & LEDBETTER, J. (1986). Heterogeneith among T cells in intracellular free Ca^{2+} responses after mitogen stimulation with PHA or anti-CD3. *J. Immunol.*, **137**, 952–961.

RANDRIAMAMPITA, C. & TSIEN, R.Y. (1993). Emptying of intracellular Ca^{2+} stores releases a novel small messenger that stimulates Ca^{2+} influx. *Nature*, **364**, 809–814.

RAO, G.H. (1987). Influence of calmodulin antagonist on agonist induce Ca^{2+} mobilization and platelet activation. *Biochem. Biophys. Res. Commun.*, **148**, 768–775.

REID, D.G., MACLACHLAN, L.K., ROBINSON, S.P., CAMILLERI, P., DYKE, C.A. & THORPE, C.J. (1990). Calmodulin discriminates between the two enantiomer of the receptor-operated Ca^{2+} channel blocker SK&F 96365. *Chirality*, **2**, 229–232.

SARGEANT, P., CLARKSON, W.D., SAGE, S.O. & HEEMSKERK, J.W. (1992). Ca^{2+} influx evoked by Ca^{2+} store depletion in human platelets is more susceptible to cytochrome P450 than receptor mediated Ca^{2+} entry. *Cell Calcium*, **13**, 553–564.

SCHLEUNING, M.J., DUGGAN, A. & REEM, G.H. (1989). Inhibition by chlorpromazine of lymphokine-specific mRNA expression in human thymocytes. *Eur. J. Immunol.*, **19**, 1491–1496.

TSIEN, R.W., ELLINOR, P.T. & HOME, W.A. (1991). Molecular Diversity of voltage-dependent Ca^{2+} channels. *Trends Pharmacol. Sci.*, **12**, 349–354.

TSIEN, R.Y., POSSAN, T. & RINK, T.J. (1982). T cell mitogens cause early changes in cytoplasmic-free Ca^{2+} and membrane potential in lymphocytes. *Nature*, **295**, 68–71.

ZWEIFACH, A. & LEWIS, R.S. (1993). Mitogen-regulated Ca^{2+} current of T lymphocytes is activated by depletion of intracellular Ca^{2+} stores. *Proc. Natl. Acad. Sci. U.S.A.*, **90**, 6295–6299.

(Received December 23, 1993
Revised May 3, 1994
Accepted July 18, 1994)

Br. J. Pharmacol. (1994), **113**, 869–876 © Macmillan Press Ltd, 1994

Role of endogenous endothelin in myocardial and coronary endothelial injury after ischaemia and reperfusion in rats: studies with bosentan, a mixed ET_A-ET_B antagonist

[1]Vincent Richard, Nathalie Kaeffer, Manuela Hogie, Christophe Tron, Thierry Blanc & Christian Thuillez

Department of Pharmacology, VACOMED, IFRMP, Rouen University Medical School, 76031 Rouen Cedex, France

1 Previous studies suggested that endothelin-1 (ET-1) may play a role in myocardial ischaemia and reperfusion. This study was designed to test the effect of a new nonpeptide antagonist of endothelin ET_A and ET_B receptors, bosentan, on myocardial infarct size, ventricular arrhythmias, and coronary endothelial dysfunction after ischaemia and reperfusion.

2 Anaesthetized male Wistar rats were subjected to 20 min ischaemia (left coronary artery occlusion) followed by 1 h (for the evaluation of coronary endothelial dysfunction) or 2 h (for the evaluation of infarct size) reperfusion, or 5 min ischaemia followed by 15 min reperfusion (for the evaluation of reperfusion arrhythmias). Vascular studies were performed on 1.5–2 mm coronary segments (internal diameter 250–300 μm) removed distal to the site of occlusion and mounted in wire myographs for isometric tension recording. Area at risk and infarct size were determined by Indian ink injection and triphenyl tetrazolium staining, using computerized analysis of enlarged sections after colour video acquisition.

3 Bosentan, administered at a dose which virtually abolished the pressor response to big ET-1 (3 mg kg^{-1}, i.v. before ischaemia) did not affect heart rate, arterial pressure or the rate pressure product before ischaemia, during ischaemia and during reperfusion. Bosentan did not affect the incidence of reperfusion-induced ventricular fibrillation (controls: 86%, $n = 14$; bosentan: 93%, $n = 15$), and did not modify infarct size (% of area at risk: controls: 63 ± 4, $n = 10$; bosentan: 60 ± 6, $n = 8$). Ischaemia followed by reperfusion markedly reduced the endothelium-dependent relaxations to acetylcholine (maximal response: sham: $59 \pm 4\%$, $n = 9$; ischaemia–reperfusion: $26 \pm 6\%$, $n = 8$; $P < 0.01$), characteristic of reperfusion-induced endothelial dysfunction, and this dysfunction was not prevented by bosentan (maximal response to acetylcholine: $25 \pm 5\%$, $n = 9$; $P < 0.01$ vs sham; P = NS vs ischaemia/reperfusion).

4 These experiments suggest that endogenous endothelin does not contribute to myocyte or coronary endothelial injury in this rat model of ischaemia and reperfusion.

Keywords: reperfusion; endothelin; bosentan; infarct size; coronary circulation; arrhythmias; endothelium

Introduction

Vascular endothelial cells synthesize various vasoactive substances, including endothelin-1 (ET-1), a 21 amino acid vasoconstrictor peptide. Several experiments have suggested that ET-1 is released in basal conditions (Ando *et al.*, 1989; Suzuki *et al.*, 1989), and that this release is increased in various pathophysiological conditions, including myocardial ischaemia or infarction (Miyauchi *et al.*, 1989; 1992; Yasuda *et al.*, 1990; Stewart *et al.*, 1991; Tsuji *et al.*, 1991; Watanabe *et al.*, 1991a; Vemulapalli *et al.*, 1992; Lechleitner *et al.*, 1993; Qiu *et al.*, 1993; Donckier *et al.*, 1994). ET-1 increases cardiac contractility (Shah *et al.*, 1989; Shomisch Moravec *et al.*, 1989) and induces coronary constriction (Tippins *et al.*, 1989), leading to myocardial ischaemia (Ezra *et al.*, 1989; Larkin *et al.*, 1989; Hori *et al.*, 1991) or arrhythmias (Yorikane & Koike, 1990; Salvati *et al.*, 1991). Furthermore, ischaemia can induce an externalization of ET-1 receptors in rat cardiac membranes (Liu *et al.*, 1990), and the response of rat isolated hearts to endothelin is increased during ischaemia and reperfusion (Nebauer *et al.*, 1990; 1991). Thus, based on those data, it is tempting to speculate that endogenous release of ET-1 may aggravate myocardial ischaemia, either through coronary constriction or through direct myocardial effects. This hypothesis has been difficult to test directly, due to the absence of specific antagonists of endothelin receptors. Recent studies, however, have suggested that monoclonal antibodies directed against ET-1, or phosphoramidon (an inhibitor of endothelin converting enzyme) could reduce ischaemic damage in experimental models of myocardial ischaemia and reperfusion in rats (Watanabe *et al.*, 1991a; Grover *et al.*, 1992).

Two receptor subtypes, ET_A and ET_B mediate the biological effects of endothelin (Arai *et al.*, 1990; Sakurai *et al.*, 1990). Although it was initially assumed that ET_A receptors were present on vascular smooth muscle and induced vasoconstriction, whereas ET_B receptors were present on vascular endothelium and mediated the vasodilator effect of endothelin (Sakurai *et al.*, 1992), recent experiments showed that ET_B receptors are in fact also present on smooth muscle cells and contribute to the vasoconstrictor effect of endothelin; indeed, in rats (McMurdo *et al.*, 1993; Bird *et al.*, 1993), as well as in isolated arteries (Seo *et al.*, 1994) the ET_A antagonists BQ-123 and FR-139317 are unable to antagonize fully the vasoconstrictor effect of endothelin-1, suggesting that part of this response could be due to stimulation of smooth muscle cell ET_B receptors. Thus, the physiological and pathophysiological effects of endogenous endothelin can be evaluated best through inhibition of both ET_A and ET_B-mediated responses.

Bosentan (Ro 47-0203) is a novel, non peptide, orally active ET-1 antagonist (Clozel *et al.*, 1994) derived from Ro 46-2005, a previously described ET-1 antagonist (Clozel *et al.*, 1993a,b). *In vitro*, bosentan binds competitively to both human ET_A and ET_B receptors, and inhibits the ET_A and ET_B-mediated responses of isolated arteries (Clozel *et al.*, 1994). *In vivo*, this compound inhibits the pressor and depres-

[1] Author for correspondence.

sor responses induced by intravenous administration of ET-1, big ET-1, or sarafotoxin S6C, also suggestive of antagonism at both ET_A and ET_B receptors (Clozel *et al.*, 1994). Thus, this compound represents a new tool to investigate the role of endogenous endothelin in physiological and pathophysiological situations. Indeed, preliminary data suggest that bosentan decreases arterial pressure in various experimental models of hypertension (Clozel *et al.*, 1993c) and reverses cerebral vasospasm in subarachnoid haemorrhage, a situation associated with a marked increase in endothelin release (Roux *et al.*, 1993).

Thus, the purpose of the present study was to evaluate the effect of bosentan in a rat model of myocardial ischaemia followed by reperfusion. Specifically, the effect of bosentan was investigated on three major aspects of ischaemia/reperfusion injury: infarct size, reperfusion-induced arrhythmias and reperfusion-induced coronary endothelial dysfunction.

Methods

General animal preparation

The experimental protocol was similar to that described previously (Richard *et al.*, 1993; 1994). The study was performed in 96 male Wistar rats (Charles River, Saint Aubin les Elbeuf, France), weighing between 300 and 400 g, which were anaesthetized with sodium pentobarbitone, 40 mg kg^{-1} intraperitoneally. A midline incision was made in the neck and a tracheotomy performed. The rats were mechanically ventilated with room air supplemented with low flow oxygen using small rodent ventilators (Apelex, Massy, France or MDI, Mobile, AL, U.S.A.), at a rate of 60 cycles min^{-1} and a tidal volume of 10 ml kg^{-1} body weight. The respiratory rate and tidal volume were adjusted in order to maintain arterial blood gases within a normal range. Body temperature was maintained at 37°C with a thermostated heating blanket connected to a rectal thermometer. The right jugular vein was cannulated for injection of drugs and of Indian ink for the delineation of area at risk (see below). The left carotid artery was cannulated, and a small Millar Mikrotip catheter (Model SPR407, Millar, Houston, TX, U.S.A.) was inserted in the artery in order to measure arterial blood pressure. An electrocardiogram was also obtained with standard limb electrodes. A left thoracotomy was performed, and the heart exposed. A 7/0 polypropylene suture was passed around the proximal left coronary artery and the ends were passed through a small plastic tube to form a snare. The artery was occluded by pulling the snare, which was kept in place by means of a haemostatic clamp. Myocardial ischaemia was confirmed by visual cyanosis. Reperfusion was induced by releasing the snare.

Effect of bosentan on the pressor response to big endothelin in ganglion-blocked rats

Experiments were performed in 13 rats (7 controls, 6 bosentan). Rats were anaesthetized, ventilated and instrumented as described above, but the chest was not opened. The animals were allowed to rest for 15 min after completion of the surgical preparation, after which they received the ganglion blocking agent, chlorisondamine (2.5 mg kg^{-1}, i.v.). Fifteen min after chlorisondamine, rats received bosentan (Ro 47-0203, 3 mg kg^{-1}) or saline, given as an 0.2 ml i.v. bolus. Fifteen min after bosentan, the animals received increasing doses of big endothelin (0.01–1 nmol kg^{-1}). ECG and heart rate were monitored continuously on a Gould Windowgraph recorder (Gould, Ballainvilliers, France). Pressor effects of big endothelin were assessed 15 min after administration of each dose.

Effect of bosentan on infarct size

Experiments were performed in 20 rats (10 controls and 10 bosentan). Rats were assigned to two groups, which were subjected to a 20 min coronary occlusion followed by 120 min reperfusion. Bosentan was given as an 0.2 ml i.v. bolus (3 mg kg^{-1}) 15 min before ischaemia. In these experiments, ECG and arterial pressure were monitored continuously on a Gould ES2000 recorder. The methods for quantitating infarct size were similar to those used in our previous studies (Richard *et al.*, 1993; 1994). At the end of the 120 min reperfusion period, the artery was briefly reoccluded, and 0.7 ml Indian ink was injected slowly into the jugular catheter, in order to delineate the area at risk of infarction. The heart was excised, the right ventricle and the atria were dissected away with small surgical scissors, and the remaining left ventricle was frozen in cold isopentane and kept in isopentane at − 10°C for 1 h. We have previously verified that this freezing procedure does not affect histochemical determination of necrosis as compared to fresh tissue (Richard *et al.*, 1993). The frozen ventricle was then sliced from apex to base into 7–8 sections. After thawing, the slices were immersed in 1% triphenyletrazolium chloride (TTC, Sigma Chimie) in pH 7.4 phosphate buffer for 20 min at 37°C, in order to delineate the infarcted tissue. The sections were then fixed in 10% phosphate buffered-formalin at room temperature for a minimum of 4 days. After fixation, each section was weighed and placed under a microscopic video camera (Microwatcher VS-30H, Mitsubishi Kasei Corporation, Tokyo, Japan) with a 20 fold enlargement lens. The camera was connected to an electronic colour digitalisation card (Matrox Illuminator 16) coupled to an AST computer. The digitized colour images were enlarged 5 fold (final enlargement 100 fold), and the resulting images were stored as bitmap files for later analysis. These stored images were later displayed on a 1024 × 768 pixel colour screen using a Windows-based image analysis software (Cyberview, Cervus Int., France), and the area (mm^2) of nonischaemic (Indian, ink stained), viable (TTC positive) and infarcted (TTC negative) tissue were determined on each section using the same image analysis software. From these measurements, infarct and area at risk weights were calculated knowing the individual weight of each section. The size of the area at risk was then expressed as a percentage of left ventricular weight, and infarct size was expressed as a percentage of the left ventricle and as a percentage of the area at risk.

Effect of bosentan on reperfusion-induced arrhythmias

Experiments were performed in 29 rats (14 controls and 15 bosentan). Animals were subjected to a 5 min coronary occlusion (corresponding to the duration of ischaemia for which the incidence of reperfusion arrhythmias is the highest) followed by 15 min reperfusion. We verified in pilot experiments that no severe arrhythmias occurred in this model after the first 15 min of reperfusion. Bosentan was given as a 0.2 ml i.v. bolus (3 mg kg^{-1}) 15 min before ischaemia. ECG and heart rate were monitored continuously on a Gould Windowgraph recorder. The occurrence of ventricular tachycardia and fibrillation (reversible and irreversible) during ischaemia and reperfusion was detected on the electrocardiogram and the blood pressure tracing; ventricular tachycardia was detectable on the ECG signal, whereas fibrillation was detectable both on the ECG and as a complete absence of arterial pressure.

Effect of bosentan on reperfusion-induced coronary endothelial dysfunction

Experiment were performed in 34 rats, which were assigned to three groups: group 1 rats (Sham, $n = 10$) were killed after a 100 min open-chest period without occlusion of the artery; group 2 rats (ischaemia/reperfusion, $n = 12$) were subjected

to a 20 min coronary occlusion followed by 60 min reperfusion; group 3 rats (bosentan, $n = 12$) were subjected to the same 20 min coronary occlusion/60 min reperfusion cycle as in group 2, but received bosentan given as a 0.2 ml i.v. bolus (3 mg kg^{-1}) 15 min before ischaemia.

Coronary endothelial dysfunction was assessed as described previously (Richard *et al.*, 1994). At the end of the experiment, the heart was removed and immediately placed in cold, oxygenated physiological saline (control solution) of the following composition (mM): NaCl 118.3, KCl 4.7, $CaCl_2$ 2.5, $NaHCO_3$ 25, $MgSO_4$ 1.2, KH_2PO_4 1.2, EDTA 0.02 and glucose 11.1. The left coronary artery was carefully dissected free under a dissecting microscope. Segments of the artery (length 1.5–2 mm; internal diameter 250–300 μm) were taken distal to the occlusion site and mounted in a small vessel myograph for isometric tension recording (JP Trading, Aarhus, Denmark). For this purpose, the segments were threaded into two 40 μm stainless steel wires; the ends of the wires were then fastened to two stainless steel support blocks (Mulvany & Halpern, 1977). One block was mounted on a tension transducer and the other on a displacement device operated by a micrometer. Care was taken during the dissection procedure to avoid damage to the endothelium. During the mount process, the myograph chamber was filled with cold, oxygenated (95% O_2:5% CO_2, pH 7.4) control solution. Vessel length was measured with a calibrated lens placed in the dissection microscope. After equilibration, the vessel was progressively stretched using the micrometer; the internal circumference of the vessel was calculated from the micrometer reading and the corresponding force was read on the recorder. Wall tension was calculated for each level of stretch by dividing this reading by vessel length. From these measurements, the Laplace law was used to calculate the effective pressure (which corresponds to the pressure that would be necessary to extend the vessel to the measured internal circumference), as: effective pressure = wall tension × 2Π/internal circumference (Mulvany & Halpern, 1977).

The distension was stopped when effective pressure exceeded 100 mmHg. The relation between effective pressure and internal circumference was then fitted to an exponential curve, and the circumference of the vessel corresponding to a transmural pressure of 100 mmHg (IC_{100}) was calculated from the fitted curve. The vessel was then set to a circumference equal to $0.9 \times IC_{100}$, which corresponds to the circumference for which the active concentration is maximal (Mulvany & Halpern, 1977). After mounting, the vessels were allowed to equilibrate for 30 min, during which chamber temperature was progressively increased to 37°C.

After another 60 min equilibration period during which the vessels were washed, segments were exposed to increasing concentrations of 5-hydroxytryptamine (5-HT, 10^{-9}–10^{-5} M), after which concentration-response curves to acetylcholine (10^{-9}–10^{-5} M) or the NO donor SIN-1 (10^{-8}–10^{-4} M) were studied in each ring after precontraction by serotonin.

Drugs

Bosentan was a gift from F. Hoffmann-La Roche Ltd., Basel, Switzerland. SIN-1 (3-morphilinosydronimine) was a gift from Laboratories Hoechst, Paris, France. Chlorisondamine was a gift from Ciba-Geigy, Basel, Switzerland. Triphenyl tetrazolium, acetylcholine, 5-hydroxytryptamine, big endothelin-1 were all purchased from Sigma.

Data analysis

All results are expressed as mean ± s.e.mean. Area at risk and infarct size were compared by Student's unpaired t test. Comparisons of the incidence of arrhythmias were performed using a Pearson chi-square test. In all *in vitro* experiments, n refers to the number of animals from which the arteries were taken. Contractions to 5-HT are expressed as a percentage of maximal contraction, whereas relaxations to acetylcholine or SIN-1 are expressed as a percentage of the contraction to 5-HT. Results from *in vitro* studies were then compared using ANOVA followed when ANOVA was significant by a Tukey's test for multiple comparisons. A P value ≤ 0.05 was considered statistically significant.

Results

Pressor response to big ET-1

The effect of bosentan (3 mg kg^{-1}, i.v.) on the pressor response induced by increasing doses of big ET-1 (0.01–1 nmol kg^{-1}) in ganglion-blocked rats is shown in Figure 1. Bosentan was itself devoid of effect on blood pressure. In the absence of bosentan, big ET-1 induced a dose-dependent increase in blood pressure, the maximal increase in mean blood pressure being 68 ± 11% at the dose of 1 nmol kg^{-1}. The pressor response to big ET-1 was markedly reduced by bosentan (maximal increase in mean blood pressure: 13 ± 6%; $P < 0.01$ vs controls).

Haemodynamics during ischaemia and reperfusion

Table 1 shows the evolution with time of heart rate, systolic and diastolic blood pressure, and rate pressure product (an index of myocardial oxygen consumption) in the animals that entered the infarct size study and survived the entire protocol. Haemodynamic parameters were measured at baseline (i.e. before administration of bosentan), immediately before ischaemia (i.e. 15 min after administration of bosentan), at the end of the 20 min period of ischaemia, and after 120 min of reperfusion. In controls, neither ischaemia nor reperfusion affected heart rate, blood pressure or rate pressure product. Bosentan did not significantly affect the haemodynamic parameters measured at any time during the experiments, although it tended to decrease heart rate, blood pressure and the rate pressure product during reperfusion.

Area at risk and infarct size

Out of the 20 animals which entered the study (10 controls and 10 bosentan), one bosentan-treated rat died of ventricular fibrillation during ischaemia and one had to be excluded because of technical difficulties. Results on infarct size were thus obtained in 18 animals (10 controls and 8 bosentan). Figure 2 summarizes the area at risk and infarct size data for the two groups, and shows that the size of the area at risk, which is a major predictor of infarct size in models of

Table 1 Heart rate (HR, beats min^{-1}), systolic (SAP, mmHg) and diastolic (DAP, mmHg) arterial pressure, and rate pressure product (RPP 10^2 mmHg beats min^{-1}) measured at baseline, before ischaemia (i.e. 15 min after bosentan administration), at the end of the ischaemic period and after 120 min of reperfusion in control rats or in animals treated with bosentan (3 mg kg^{-1})

	Baseline		*Before ischaemia*		*End of ischaemia*		*End of reperfusion*	
	Control	*Bosentan*	*Control*	*Bosentan*	*Control*	*Bosentan*	*Control*	*Bosentan*
HR	421 ± 11	420 ± 11	389 ± 11	376 ± 13	399 ± 9	394 ± 16	393 ± 11	369 ± 13
SAP	124 ± 4	130 ± 11	120 ± 2	124 ± 11	116 ± 4	123 ± 10	122 ± 16	116 ± 8
DAP	102 ± 5	107 ± 7	96 ± 3	103 ± 8	96 ± 4	101 ± 7	97 ± 5	92 ± 7
RPP	597 ± 29	549 ± 54	536 ± 14	504 ± 59	535 ± 25	524 ± 62	556 ± 33	491 ± 41

regional ischaemia, was not significantly different in the two groups (controls: 51 ± 2%; bosentan 49 ± 6% of left ventricle). As compared to controls, bosentan did not affect infarct size, whether expressed as a percentage of left ventricle (controls: 32 ± 2; bosentan 31 ± 6%; Figure 2), or as a percentage of the area at risk (controls: 63 ± 4%; range 48–85%; bosentan 60 ± 6%; range 38–83%; Figure 2).

Reperfusion arrhythmias

Figure 3 shows the incidence of ventricular fibrillation upon reperfusion after a 5 min period of ischaemia in controls or bosentan-treated rats. In controls, reperfusion was associated with the occurrence of ventricular fibrillation in 86% of the animals; fibrillation was irreversible (i.e. no reversion to normal sinus rhythm during the first 15 min of reperfusion) in 21% of the animals. Bosentan did not affect the incidence of reperfusion-induced ventricular fibrillation (93 and 26% of total and irreversible fibrillation, respectively).

Coronary endothelial dysfunction

Out of the 34 rats that entered the study, 5 animals (2 controls and 3 bosentan) died of ventricular fibrillation. Experiments on isolated blood vessels were then performed in arteries taken from the 29 surviving animals (10 sham, 10 ischaemia/reperfusion controls and 9 ischaemia/reperfusion + bosentan). Responses of isolated arteries to increasing concentrations of 5-HT or SIN-1 are shown in Figure 4. As compared to sham-operated animals, neither ischaemia/reperfusion nor its treatment by bosentan affected the contractile responses to 5-HT (Figure 4). Similarly, the endothelium-independent relaxant response to the nitric oxide donor SIN-1 was not affected by ischaemia/reperfusion or by bosentan (Figure 4).

Responses of isolated coronary arteries to the endothelium-dependent vasodilator acetylcholine are shown in Figure 5. In arteries taken from sham-operated animals, acetylcholine induced concentration dependent relaxations which reached 59 ± 4% at the highest concentration (10^{-5} M). This response to acetylcholine was virtually abolished by L-arginine analogues such as N^G-nitro-L-arginine or N^G-nitro-L-arginine methyl ester (data not shown). The response to acetylcholine was markedly reduced after ischaemia and reperfusion (Figure 5; maximal response: 26 ± 6%; $P<0.01$ vs sham). As compared to sham-operated rats, the response to acetylcholine was significantly reduced by ischaemia/reperfuson at all concentrations from 3×10^{-7} M to 10^{-5} M. This ischaemia/reperfusion – induced impairment of endothelium-dependent response to acetylcholine was not affected by bosentan (maximal relaxation: 25 ± 5%; $n=9$; $P<0.01$ vs sham; P = NS vs ischaemia reperfusion).

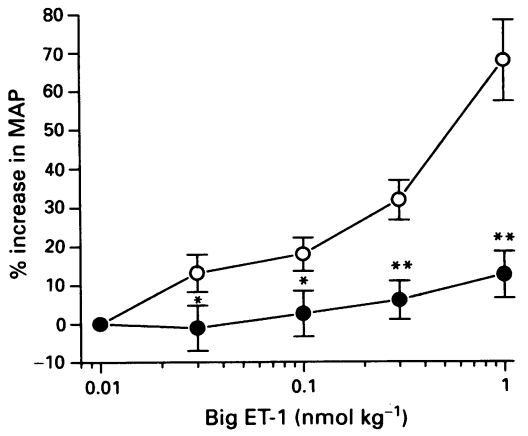


Figure 1 Percentage increase in mean arterial pressure (MAP) induced by increasing doses of big endothelin-1 in control rats (○) and in rats treated with bosentan (3 mg kg^{-1}, ●), in the presence of the ganglionic blocking agent chlorisondamine (2.5 mg kg^{-1}, i.v.). *$P<0.05$ and **$P<0.01$ vs controls.

Discussion

The present study shows that a mixed ET_A-ET_B endothelin antagonist, bosentan, administered at a dose which virtually abolished the pressor response to big ET-1, had no effect of infarct size, reperfusion arrhythmias or reperfusion-induced coronary endothelial dysfunction in a rat model of ischaemia/reperfusion. These results suggest that ET-1 probably does not contribute to the postischaemic myocardial or coronary endothelial injury in this model.

Effect of bosentan on the pressor response to big ET-1

In the present experiments, bosentan (3 mg kg^{-1}) markedly inhibited the pressor response to big ET-1, in agreement with previous results (Clozel *et al.*, 1994). *In vivo*, the major part of the pressor effect of big ET-1 is considered to be ET_A-mediated, but a small component is resistant to inhibition by the ET_A antagonist BQ-123 (McMurdo *et al.*, 1993) and could be the consequence of activation of the ET_B receptor present at the level of the smooth muscle. We chose to assess the effect of bosentan on the response to intravenous administration of big ET-1, rather than ET-1 itself on the basis that big ET-1 mimics better than ET-1 the physiological

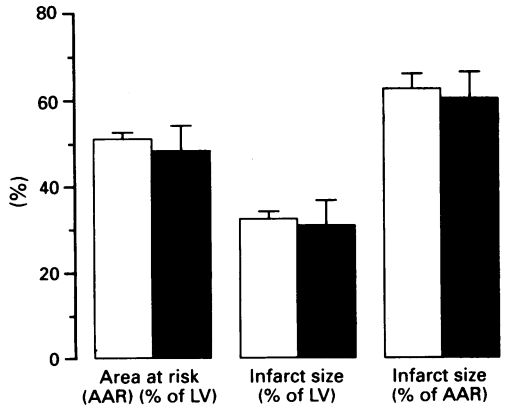


Figure 2 Area at risk (AAR), expressed as % of left ventricle (LV), and infarct size, expressed as % of left ventricle and % of the area at risk, in controls rats (open columns), or in animals treated by bosentan (3 mg kg^{-1}, solid columns).

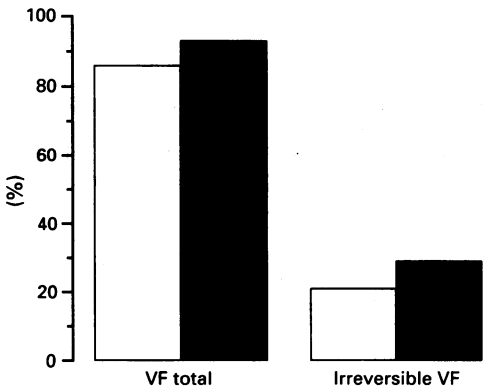


Figure 3 Incidence of total and irreversible ventricular fibrillation (VF) upon reperfusion after a 5 min period of ischaemia in control rats (open columns) or in rats treated by bosentan (3 mg kg^{-1}, solid columns).

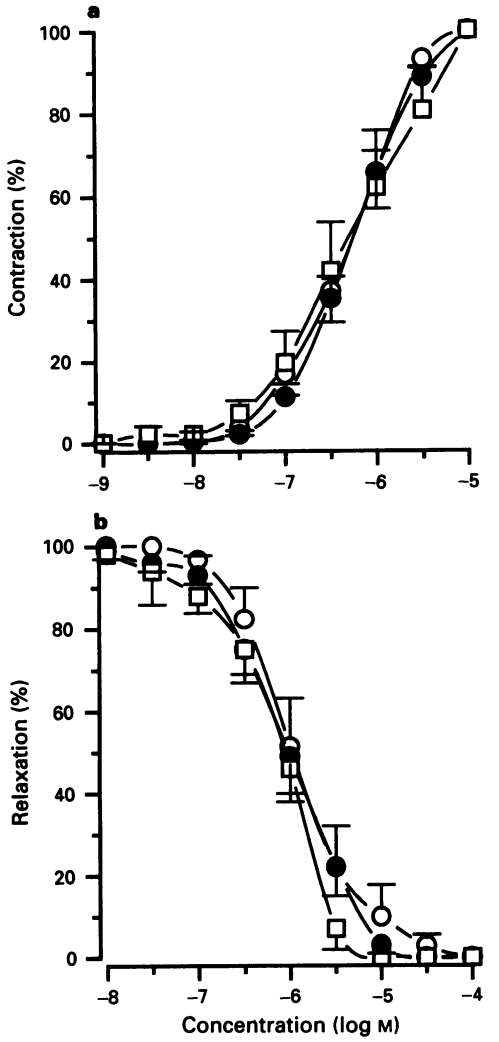


Figure 4 Contracting responses of rat coronary arteries to 5-hydroxytryptamine (5-HT) (a) and relaxant responses to the nitric oxide donor SIN-1 (in 5-HT-precontracted rings; b). Arteries were taken from sham-operated animals (○), or animals subjected to ischaemia followed by reperfusion in the absence (●) or in the presence of bosentan (□). Values for 5-HT are expressed as a percentage of maximal response, and values for SIN-1 are expressed as a percentage of the contraction to 5-HT.

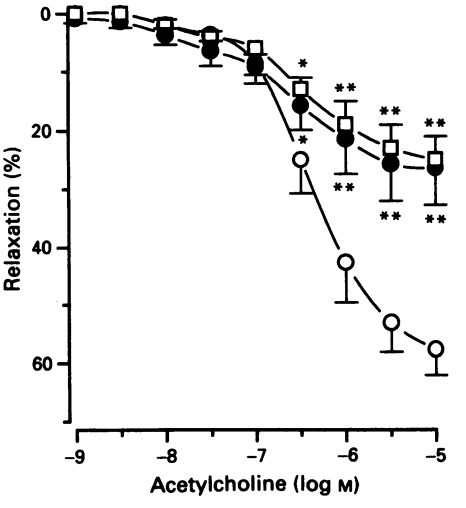


Figure 5 Relaxant responses of rat coronary arteries to acetylcholine. Arteries were taken from sham-operated animals (○), or animals subjected to ischaemia followed by reperfusion in the absence (●) or in the presence of bosentan (□). Values are expressed as a percentage of the contraction to 5-hydroxytryptamine. $*P<0.05$ and $**P<0.01$ vs sham.

release of this peptide from endothelial cells (Clozel *et al.*, 1993b; 1994). Indeed, big ET-1 must be converted to ET-1 for activity (Gardiner *et al.*, 1991). This conversion, which is inhibited by phosphoramidon, seems to take place mainly in the tissues (Watanabe *et al.*, 1991b), and ET-1 is then preferentially released toward the vascular smooth muscle rather than toward the lumen (Wagner *et al.*, 1992). Indeed, the vasoconstrictor effects of big ET-1 can be observed at doses for which no increase in plasma ET-1 can be detected (Teerlink *et al.*, 1993). For this reason, i.v. administration of ET-1 probably leads to an overestimation of the endothelium-mediated depressor response to ET-1, which might not be a physiologically relevant phenomenon if ET-1 is preferentially released toward the vascular smooth muscle *in vivo*.

Effect of bosentan on infarct size

In the present study, we used a rat model of *in vivo* myocardial ischaemia and reperfusion similar to the one used in our previous studies (Richard *et al.*, 1993; 1994). Although the rat offers numerous advantages in terms of cost and reproducibility (especially because of the absence of native collaterals), the small size of the heart may be the cause of various potential difficulties and imprecision during infarct size quantification. In our experiments, necrosis was quantified by computerized image analysis of ventricular sections after a 100 fold enlargement, i.e. on >10 cm diameter images. Thus, despite the small size of the heart, we believe that our quantification of infarct size was highly accurate.

In the present experiments, we used a short (20 min) duration of ischaemia. Nevertheless, such ischaemia still resulted in the development of large myocardial infarcts, averaging 60% of the area at risk, and this is consistent with results from our previous studies (Richard *et al.*, 1993; 1994). It must be noted that this duration of ischaemia is shorter than that used in other infarct size studies performed in rats. However, despite this shorter duration of ischaemia, infarcts in our studies are of similar size or even larger than those obtained by other groups (e.g. Li *et al.*, 1992; Yellon *et al.*, 1992; Liu & Downey, 1992; 1993; Li & Kloner, 1993). The reasons for these differences in the rate of development of necrosis could be due in part to differences in the anaesthetics used or to differences in the strains of rats used (Wistar in the present study vs Sprague-Dawley in other studies). Finally, using the same experimental model, we have been previously able to detect significant limitation of infarct size with ischaemic preconditioning (Richard *et al.*, 1993; 1994), and with calcium antagonists such as verapamil (unpublished data). Thus, despite the development of large infarcts, this model appears adequate to evaluate the efficacy of potential anti-ischaemic drugs.

Our infarct size studies were performed after a short (2 h) period of reperfusion. However, it is unlikely that limiting reperfusion to 2 h affected the outcome of the study or the delineation of the infarcts based on tetrazolium staining. Indeed, in a previous study, we have shown that varying the duration of reperfusion from 1 to 6 h in the same experimental model did not affect the size of the infarcts measured by tetrazolium staining. This suggests that prolonging the reperfusion period does not contribute to the extension of infarct size in this model and that, despite the short duration of reperfusion used in the present experiments, our measurements of infarct size are valid.

In the present experiments, blockade of endothelin receptors with bosentan did not affect infarct size. It is unlikely that this lack of effect of bosentan is due to an insufficient

blockade of the endothelin-induced responses, since we showed that the same dose markedly reduced the pressor response induced by big ET-1 (Figure 1), and we verified in pilot experiments that this inhibitory effect of bosentan on the response to big ET-1 persists for at least 2 h. Furthermore, the half-life of bosentan in these conditions is known to be at least 3 h (M. Clozel, Roche, Basel, personal communication).

Our results are in contrast to those of two other studies in rats which reported a significant limitation of infarct size either with a monoclonal antibody against ET-1 (Watanabe *et al.*, 1991a), or with phosphoramidon (Grover *et al.*, 1992). It should be noted that, in both previous studies (unlike the present study), the area at risk was not quantified, and infarct size was expressed as a percentage of left ventricle. It is now clearly established that the size of the area at risk is a major determinant of infarct size in all models of regional ischaemia (e.g. Reimer *et al.*, 1985). Thus, a study on the effect of a treatment on infarct size should include a measurement of area at risk in order to express infarct size as a percentage of area at risk and eliminate individual variations of infarct size due to variations in the anatomical area at risk (Schaper, 1984). Furthermore, in both previous studies, the duration of reperfusion was 24 h. It has been shown previously that rat infarcts undergo rapid remodelling characteristic of infarct healing, such as wall thinning, increased lumen volume and decreased infarct size secondary to scar formation. Indeed, such an early healing is already markedly evident in 24 h old infarcts, since at this time the anatomical area at risk is reduced by about 30% as compared to early values (Hearse *et al.*, 1988). One consequence of this is that any drug that can influence the rate of early infarct remodelling may give an impression of infarct size limitation when assessed at 24 h (especially when area at risk is not quantified), when in reality no such event may have occurred (Hearse *et al.*, 1988). Thus, differences in the duration of reperfusion or absence of measurements of area at risk may explain the differences between our results and those of the two previously published studies performed in rats.

Another difference between our study and that of Grover *et al.* (1992) relates to the drug used to inhibit the endothelin effects. We used a specific inhibitor of endothelin receptors which does not show any binding inhibitory activity against various eicosanoids, ions or peptides (Clozel *et al.*, 1994). In contrast, the study of Grover *et al.* (1992) was performed using phosphoramidon, a metalloprotease inhibitor that is not specific for endothelin converting enzyme but may inhibit other metalloproteases such as neutral endopeptidase EC.3.4.24.11 (Turner, 1987). Thus, it is possible that the positive results obtained by Grover *et al.* (1992) could be the consequence of nonspecific effects of phosphoramidon, independent of its inhibitory effect on endothelin converting enzyme. Indeed, recent experiments showed that a specific antagonist of ET_A receptors, FR 139317, also did not affect infarct size in a rabbit model of ischaemia–reperfusion (McMurdo *et al.*, 1994). Thus, our results confirm those of McMurdo *et al.* and extend those to ET_B receptors. Taken together, our results and those of McMurdo *et al.* (1994) suggest that endogenous endothelin does not contribute to the extension of infarct size after myocardial ischaemia and reperfusion.

One possible explanation of this lack of effect would be that endothelin is not released in quantities sufficient to induce deleterious effects during ischaemia and reperfusion, or to express its pro-arrhythmic effects. Although we have not measured plasma levels of ET-1 in our model, a previous study showed a fourfold increase in plasma ET-1 10 min into reperfusion after a 1 h episode of *in vivo* ischaemia in rats (Watanabe *et al.*, 1991a). In dogs, a short episode of coronary occlusion (10 min) induces an even less marked increase in plasma ET-1 (from 1.3 to 2.0 pM; Donckier *et al.*, 1994). Although the pro-ischaemic effects of such an increase in plasma endothelin cannot be easily assessed, it is possible that such moderate increases in plasma ET-1 are not sufficient to induce significant myocardial or vascular effects.

Effect of bosentan on coronary endothelial dysfunction

In our experiments, ischaemia followed by reperfusion did not affect the coronary response to 5-HT or to the nitric oxide donor SIN-1, but markedly reduced the response to acetylcholine, confirming our previous results in the same experimental model (Richard *et al.*, 1994). Such an endothelial dysfunction also confirms previous results obtained in other species (Vanbenthuysen *et al.*, 1987; Dauber *et al.*, 1990; Pearson *et al.*, 1990a; Tsao *et al.*, 1990). Moreover, we showed previously that a similar alteration was not observed in arteries obtained from hearts subjected to ischaemia without reperfusion (Richard *et al.*, 1994), suggesting that this coronary endothelial dysfunction is a manifestation of reperfusion injury.

One limitation of the study is that only one endothelium-dependent vasodilator was used (acetylcholine). We attempted to study other potential endothelium-dependent vasodilators, i.e. adenosine di-phosphate, α_2-adrenoceptor agonists, histamine and bradykinin, and found in pilot studies that none of them induced significant endothelium-dependent relaxations. In addition, we found previously that receptor-independent, endothelium-dependent relaxations to the calcium ionophore, A23187, were rather weak in this preparation (Richard *et al.*, 1994). Furthermore, substance P and 5-HT, which induce endothelium-dependent relaxations in other species, also do not relax rat coronary arteries (Nyborg & Mikkelsen, 1990; Prieto *et al.*, 1991). Thus, to our knowledge, acetylcholine is the only endothelium-dependent relaxing agent active on rat isolated coronary arteries. Because of this limitation, we could not determine whether the impairment observed in the present experiment reflects a true defect in nitric oxide synthase activity or a specific impairment of the transduction pathway linking muscarinic receptors to NO-synthase. Such a selective impairment has already been shown to occur in other pathological situations such as hypercholesterolaemia or atherosclerosis, which selectively affect Gi protein-mediated transduction pathways (Flavahan, 1992), and in canine experiments involving chronic reperfusion (Pearson *et al.*, 1990b). In any case, the absence of any effect of bosentan on the response to acetylcholine suggests that this compound was unable to prevent coronary endothelial dysfunction, and thus that endogenous endothelin probably does not contribute to reperfusion-induced coronary endothelial dysfunction in this model.

In conclusion, our results obtained in rats suggest that administration of the mixed ET_A and ET_B endothelin antagonist, bosentan, at a dose which virtually abolished the pressor response to big ET-1, did not have any significant effect of infarct size, reperfusion arrhythmias, and reperfusion-induced coronary endothelial dysfunction. These results suggest that endogenous endothelin probably does not contribute to myocyte or coronary endothelial injury in this model of ischaemia with reperfusion.

This study was supported in part by BQR, Université de Rouen, France. The authors wish to thank Dr Clozel (Hoffman – La Roche, Basel, Switzerland) for the supply of bosentan, Dr Hofbauer (Ciba-Geigy, Basel, Switzerland) for the supply of chlorisondamine, and Dr Winicki (Laboratories Hoechst, Paris, France) for the supply of SIN-1.

References

ANDO, K., HIRATA, Y., SCHICHIRI, M., EMORI, T. & MARUNO, F. (1989). Presence of immunoreactive endothelin in human plasma. *FEBS Lett.*, **245**, 164–166.

ARAI, H., HORI, S., ARAMORI, I., OHKUBO, H. & NAKANISHI, S. (1990). Cloning and expression of a cDNA encoding an endothelin receptor. *Nature*, **348**, 730–732.

BIRD, J.E. & WALDRON, T.L. (1993). Incomplete inhibition of endothelin-1 pressor effects by an endothelin ETA receptor antagonist. *Eur. J. Pharmacol.*, **240**, 295–298.

CLOZEL, M., BREU, V., BURRI, K., CASSAL, J.M., FISCHLI, W., GRAY, G.A., HIRTH, G., LÖFFLER, B.M., MÜLLER, M., NEIDHART, W. & RAMUZ, H. (1993a). Pathophysiological role of endothelin revealed by the first orally active endothelin receptor antagonist. *Nature*, **365**, 759–761.

CLOZEL, M., BREU, V., GRAY, G.A., KALINA, B., LÖFFLER, B,. BURRI, K,. CASSAL, J., HIRTH, G., MÜLLER, M., NEIDHART, W. & RAMUZ, H. (1994). Pharmacological characterization of bosentan, a new potent orally active non-peptide endothelin receptor antagonist. *J. Pharmacol. Exp. Ther.* (in press).

CLOZEL, M., BREU, V., GRAY, G.A. & LÖFFLER, B. (1993b). In vivo pharmacology of Ro 46-2005, the first synthetic nonpeptide endothelin receptor antagonist: implications for endothelin biology. *J. Cardiovasc. Pharmacol.*, **22** (Suppl. 8), S377–S379.

CLOZEL, M., CLOZEL, J.P. & HESS, P. (1993c). Endothelin receptor antagonism: a new therapeutic approach in experimental hypertension. *Circulation*, **88**, I–316 (Abstract).

DAUBER, I.M., VANBENTHUYSEN, K.M., MCMURTRY, I.F., WHEELER, G.S., LESNEFSKY, E.J., HORWITZ, L.D. & WEIL, J.F. (1990). Functional coronary microvascular injury evident as increased permeability due to brief ischemia and reperfusion. *Circ. Res.*, **66**, 986–998.

DONCKIER, J., HANET, C., STOLERU, L., VAN MECHELEN, H.V., GALANTI, L., HAYASHIDA, W., KEYEUX, A., KETELSLEGERS, J.-M. & POULEUR, H. (1994). Effects of endothelin-1 at pathophysiological concentrations on coronary perfusion and mechanical function of normal and postischemic myocardium. *J. Cardiovasc. Pharmacol.*, **23**, 212–219.

EZRA, D., GOLDSTEIN, R.E., CZAJA, J.F. & FEUERSTEIN, G.Z. (1989). Lethal ischemia due to intracoronary endothelin in pigs. *Am. J. Physiol.*, **257**, H339–H343.

FLAVAHAN, N.A. (1992). Atherosclerosis or lipoprotein-induced endothelial dysfunction. Potential mechanisms underlying reduction in EDRF/nitric oxide activity. *Circulation*, **85**, 1927–1938.

FLAVAHAN, N.A. (1992). Atherosclerosis or lipoprotein-induced endothelial dysfunction. Potential mechanisms underlying reduction in EDRF/nitric oxide activity. *Circulation*, **85**, 1927–1938.

GARDINER, S.M., COMPTON, A.M., KEMP, P.A. & BENNETT, T. (1991). The effects of phosphoramidon on the regional haemodynamic responses to human proendothelin [1-38] in conscious rats. *Br. J. Pharmacol.*, **103**, 2009–2015.

GROVER, G.J., SLEPH, P.G., FOX, M. & TRIPPODO, N.C. (1992). Role of endothelin-1 and big endothelin-1 in modulating coronary vascular tone, contractile function and severity of ischemia in rat hearts. *J. Pharmacol. Exp. Ther.*, **263**, 1074–1082.

HEARSE, D.J., RICHARD, V., YELLON, D.M. & KINGMA, J.G. (1988). Evolving myocardial infarction in the rat in vivo: an inappropriate model for the investigation of drug-induced infarct size limitation during regional sustained ischemia. *J. Cardiovasc. Pharmacol.*, **11**, 701–710.

HORI, S., KYOTANI, S., INOUE, S., FUKUDA, K., OHNISHI, Y., KUSUHARA, M., AIKAWA, N., YAMAGUCHI, K., NAKAMURA, Y. & HANDA, S. (1991). Subepicardial microischemia formation induced by epicardial application of endothelin-1. *J. Cardiovasc. Pharmacol.*, **17** Suppl 7, S300–S301.

LARKIN, S.W., CLARKE, J.G., KEOGH, B.E., ARAUJO, L., RHODES, C., DAVIES, G.J., TAYLOR, K.M. & MASERI, A. (1989). Intracoronary endothelin induces myocardial ischemia by small vessel constriction in the dog. *Am. J. Cardiol.*, **64**, 956–958.

LECHLEITNER, P., GENSER, N,. MAIR, J., MAIER, J., ARTNER-DWORZAK, E., DIENSTL, F. & PUSCHENDORF, B. (1993). Plasma immunoreactive endothelin in the acute and subacute phases of myocardial infarction in patients undergoing fibrinolysis. *Clinical Chemistry*, **39**, 955–959.

LI, Y.P., WHITTAKER, P. & KLONER, R.A. (1992). The transient nature of the effect of ischemic preconditioning on myocardial infarct size and ventricular arrhythmia. *Am. Heart. J.*, **123**, 346–353.

LI, Y. & KLONER, R.A. (1993). The cardioprotective effects of ischemic 'preconditioning' are not mediated by adenosine receptors in rat hearts. *Circulation*, **87**, 1642–1648.

LIU, J., CHEN, R., CASLEY, D.J. & NAYLER, W.G. (1990). Ischemia and reperfusion increase 125I-labeled endothelin-1 binding in rat cardiac membranes. *Am. J. Physiol.*, **258**, H829–H835.

LIU, Y. & DOWNEY, J.M. (1992). Ischemic preconditioning protects against infarction in rat heart. *Am. J. Physiol.*, **263**, H1107–H1112.

LIU, Y. & DOWNEY, J.M. (1993). Preconditioning against infarction in the rat heart does not involve a pertussis toxin sensitive G protein. *Cardiovascular Res.*, **27**, 608–611.

MCMURDO, L., CORDER, R., THIEMERMANN, C. & VANE, J.R. (1993). Incomplete inhibition of the pressor effects of endothelin-1 and related peptides in the anaesthetized rat with BQ-123 provides evidence for more than one vasoconstrictor receptor. *Br. J. Pharmacol.*, **108**, 557–561.

MCMURDO, L., THIEMERMANN, C. & VANE, J.R. (1994). The effects of the endothelin ET_A receptor antagonist, FR 139317, on infarct size in a rabbit model of acute myocardial ischaemia and reperfusion. *Br. J. Pharmacol.*, **112**, 75–80.

MIYAUCHI, T., DOI, T., SUZUKI, N., KAKIHANA, M,. YAMAGUCHI, I., SUGISHITA, Y., MITSUI, T., HORI, M., MASAKI, T. & GOTO, K. (1992). Plasma endothelin-1 concentrations in the coronary sinus in dogs with artifically induced myocardial infarction. *Peptides*, **13**, 1013–1015.

MIYAUCHI, T., YANAGISAWA, M,. TOMIZAWA, T., SUGISHITA, Y., SUZUKI, N., FUJINO, M., AJISAKA, R., GOTO, K. & MASAKI, T. (1989). Increased plasma concentrations of endothelin-1 and big endothelin-1 in acute myocardial infarction [letter]. *Lancet*, **ii**, 53–54.

MULVANY, M.J. & HALPERN, W. (1977). Contractile properties of small arterial resistance vessels in spontaneously hypertensive and normotensive rats. *Circ. Res.*, **41**, 19–26.

NEUBAUER, S., ERTL, G., PULZER, F., HAAS, U., HIRSCH, A., ZIMMERMAN, S. & KOCKSIEK, K. (1990). Effects of endothelin-1 in the isolated heart under ischaemic and cardioplegic solutions. *J. Cardiovasc. Pharmacol.*, **16**, 804–811.

NEUBAUER, S., ZIMMERMAN, S ., HIRSCH, A., PULZER, F., TIAN, R., BAUER, W., BAUER, B. & ERTL, G. (1991). Effects of endothelin-1 in the isolated heart in ischemia/reperfusion and hypoxia/reoxygenation injury. *J. Mol. Cell. Cardiol.*, **23**, 1397–1409.

NYBORG, N.C.B. & MIKKELSEN, E.O. (1990). 5-Hydroxytryptamine does not induce release of endothelium-derived relaxing factor in rat coronary arteries. *Eur. J. Pharmacol.*, **186**, 295–300.

PEARSON, P.J., SCHAFF, H.V. & VANHOUTTE, P.M. (1990a). Acute impairment of endothelium-dependent relaxations to aggregating platelets following reperfusion injury in canine coronary arteries. *Circ. Res.*, **67**, 385–393.

PEARSON, P.J., SCHAFF, H.V. & VANHOUTTE, P.M. (1990b). Long-term impairment of endothelium-dependent relaxations to aggregating platelet after reperfusion injury in canine coronary arteries. *Circulation*, **81**, 1921–1927.

PRIETO, D., BENEDITO, S. & NYBORG, N.C.B. (1991). Heterogeneous involvement of endothelium in calcitonin gene-related peptide-induced relaxation in coronary arteries from rats. *Br. J. Pharmacol.*, **103**, 1764–1768.

QIU, S., THEROUX, P., MARCIL, M. & SOLYMOSS, B.C. (1993). Plasma endothelin-1 levels in stable and unstable angina. *Cardiology*, **82**, 12–19.

REIMER, K.A., JENNINGS, R.B., COBB, F.R., MURDOCK, R.H., GREENFIELD, J.C., BECKER, L.C., BULKLEY, B.H., HUTCHINS, G.M., SCHWARTZ, R.P.J., BAILEY, K.R. & PASSAMANI, E.R. (1985). Animal models for protecting ischemic myocardium (AMPIM): results of the NHLBI cooperative study. Comparison of the unconscious and conscious dog models. *Circ. Res.*, **56**, 651–665.

RICHARD, V., TRON, C. & THUILLEZ, C. (1993). Ischaemic preconditioning is not mediated by oxygen-derived free radicals in rats. *Cardiovasc. Res.*, **27**, 2016–2021.

RICHARD, V., KAEFFER, N., TRON, C. & THUILLEZ, C. (1994). Ischemic preconditioning protects against coronary endothelial dysfunction induced by ischemia and reperfusion. *Circulation*, **89**, 1254–1261.

ROUX, S.P., CLOZEL, M., SPRECHER, U., GRAY, G. & CLOZEL, J.P. (1993). Ro 47-0203, a new endothelin receptor antagonist reverses chronic vasospasm in experimental subarachnoid hemorrhage. *Circulation*, **88**, I–170 (Abstract).

SAKURAI, T., YANAGISAWA, M.,TAKUWA, Y., MIYAZAKI, H., KIMURA, S., GOTO, H. & MASAKI, T. (1990). Cloning of a cDNA encoding a non-isopeptide selective subtype of the endothelin receptor. *Nature*, **348**, 732–735.

SAKURAI, T., YANAGISAWA, M., MASAKI, T. (1992). Molecular characterization of endothelin receptors. *Trends Pharmacol. Sci.*, **13**, 103–108.

SALVATI, P., CHIERCHIA, S., DHO, L., FERRARIO, R.G., PARENTI, P., VICEDOMINI, G. & PATRONO, C. (1991). Proarrhythmic activity of intracoronary endothelin in dogs: relation to the site of administration and to changes in regional flow. *J. Cardiovasc. Pharmacol.*, **17**, 1007–1014.

SCHAPER, W. (1984). Experimental infarcts and the microcirculation. In *Therapeutic Approaches to Myocardial Infarct Size Limitation*. ed. Hearse, D.J. & Yellon, D.M. pp. 79–90. New York: Raven Press.

SEO, B., OEMAR, B.S., SIEBENMANN, R., VON SEGESSER, L. & LÜSCHER, T.F. (1994). Both ET_A and ET_B receptors mediate contraction to endothelin-1 in human blood vessel. *Circulation*, **89**, 1203–1208.

SHAH, A.M., LEWIS, M.J. & HENDERSON, A.H. (1989). Inotropic effects of endothelin in ferret ventricular myocardium. *Eur. J. Pharmacol.*, **163**, 365–367.

SHOMISCH MORAVEC, C., REYNOLDS, E.E., STEWART, R.W. & BOND, M. (1989). Endothelin is a positive inotropic agent in human and rat heart in vitro. *Biochem. Biophys. Res. Commun.*, **159**, 14–18.

STEWART, D.J., KUBAC, G., COSTELLO, K.B. & CERNACEK, P. (1991). Increased plasma endothelin-1 in the early hours of acute myocardial infarction. *J. Am. Coll. Cardiol.*, **18**, 38–43.

SUZUKI, N., MATSUMOTO, H. & KITADA, C. (1989). Immunoreactive endothelin-1 in plasma detected by a sandwich-type enzyme immunoassay. *J. Cardiovasc. Pharmacol.*, **13**, 151–153.

TEERLINK, J.R., CARTEAUX, J.-P., LÖFFLER, B.-M., CLOZEL, M. & CLOZEL, J.P. (1993). Big endothelin as a probe for the endothelin paracrine system: dissociation of plasma endothelin levels and hemodynamic effects. *Circulation*, **88**, I–182 (Abstract).

TIPPINS, J.R., ANTONIW, J.W. & MASERI, A. (1989). Endothelin-1 is a potent constrictor in conductive and resistive coronary arteries. *J. Cardiovasc. Pharmacol.*, **13** Suppl 5, S177–S179.

TSAO, P.S., AOKI, N., LEFER, D.J., JOHNSON III, G. LEFER, A.M. (1990). Time course of myocardial injury and endothelial dysfunction during myocardial ischemia and reperfusion in the cat. *Circulation*, **82**, 1402–1412.

TSUJI, S., SAWAMURA, A., WATANABE, H., TAKIHARA, K., PARK, S.E. & AZUMA, J. (1991). Plasma endothelin levels during myocardial ischemia and reperfusion. *Life Sci.*, **48**, 1745–1749.

TURNER, A. (1987). *Neuropeptides and their Peptidases*. ed. Turner, A. pp. 183–201. Chichester, Sussex: Horwood.

VANBENTHUYSEN, K.M., MCMURTRY, I.F. & HORWITZ, L.D. (1987). Reperfusion after coronary occlusion in dogs impairs endothelium-dependent relaxation to acetylcholine and augments contractile reactivity in vitro. *J. Clin. Invest.*, **79**, 265–274.

VEMULAPALLI, S., RIVELLI, M., CHIU, P.J., DEL PRADO, M. & HEY, J.A. (1992). Phosphoramidon abolishes the increases in endothelin-1 release induced by ischemia-hypoxia in isolated perfused guinea-pig lungs. *J. Pharmacol. Exp. Ther.*, **262**, 1062–1069.

WAGNER, O.F., CHRIST, G. & WOJTA, A. (1992). Polar secretion of endothelin-1 by cultured endothelial cells. *J. Biol. Chem.*, **267**, 16066–16068.

WATANABE, T., SUZUKI, N., SHIMAMOTO, N., FUJINO, M. & IMADA, A. (1991a). Contribution of endogenous endothelin to the extension of myocardial infarct size in rats. *Circ. Res.*, **69**, 370–377.

WATANABE, Y., NARUSE, M., MONZEN, C. & *et al.* (1991b). Is big endothelin converted to endothelin-1 in circulating blood? *J. Cardiovasc. Pharmacol.*, **17** (Suppl. 7), S503–S505.

YASUDA, M., KOHNO, M., TAHARA, A., ITAGANE, H., TODA, I., AKIOKA, K., TERAGAKI, M., OKU, H., TAKEUCHI, K. & TAKEDA, T. (1990). Circulating immunoreactive endothelin in ischemic heart disease. *Am. Heart J.*, **119**, 801–806.

YELLON, D.M., ALKHULAIFI, A.M., BROWNE, E.E. & PUGSLEY, W.B. (1992). Ischaemic preconditioning limits infarct size in the rat heart. *Cardiovasc. Res.*, **26**, 983–987.

YORIKANE, R. & KOIKE, H. (1990). The arrhythmogenic action of endothelin in rats. *Jpn. J. Pharmacol.*, **53**, 259–263.

(Received May 16, 1994
Revised July 13, 1994
Accepted July 18, 1994)

Br. J. Pharmacol. (1994), **113**, 877–882 © Macmillan Press Ltd, 1994

Presence of neuropeptide Y in the rat seminal vesicle and its effects on noradrenaline- and nerve-induced contractions

[1]M.M. Iravani & [2]M.A. Zar

The Department of Pharmacological Sciences, The Medical School, Framlington Place, University of Newcastle upon Tyne, Newcastle upon Tyne NE2 4HH

1 Immunohistochemical and functional studies have been performed to localize and determine the effects of neuropeptide Y (NPY) in the rat seminal vesicle.

2 An abundant presence of NPY-immunoreactive nerves, mainly concentrated in the smooth muscle layer of the seminal vesicle was found. Chronic 6-hydroxydopamine treatment (four doses of 50 mg kg^{-1} i.p. on days 1, 2, 4 and 6; rats killed one week after the last injection) led to a large reduction but not abolition of the NPY-immunoreactivity.

3 NPY (1–250 nM) did not affect the resting tone of the seminal vesicle.

4 The seminal vesicle was contracted by electrical field stimulation (EFS) and by exposure to 5 μM noradrenaline (NA). These contractions were abolished by phentolamine (1 μM). Tetrodotoxin (0.5 μM) abolished EFS-evoked contractions but did not affect NA-evoked contractions.

5 Seminal vesicles, from animals chronically-treated with reserpine (5 mg kg^{-1} i.p. on days 1 and 2; rats killed on day 3), were contracted by NA but not by EFS.

6 NPY (0.25–250 nM), concentration-dependently, inhibited EFS-evoked contractions by up to 70% maximum inhibition. Contractions evoked by EFS with short trains of pulses were inhibited by NPY to a greater degree than those with longer trains.

7 NPY had no significant effect on NA-evoked contractions.

8 These data provide strong evidence that the motor transmission in rat seminal vesicle is predominantly if not exclusively, adrenergic. It is further concluded that a rich NPY-containing innervation is present in the smooth muscle layer of rat seminal vesicle. The primary effect of NPY is modulation of adrenergic motor transmission by a prejunctional inhibition of NA release.

Keywords: Rat seminal vesicle; neuropeptide Y; adrenergic motor transmission; neuropeptide Y-immunoreactivity

Introduction

The seminal vesicles are the major sites for the production and storage of seminal fluid in mammals. Each vesicle is composed of many tubuloalveolar glands which consist of mucosal layer and a smooth muscle layer. In rats and guinea-pigs the seminal vesicles are supplied with both sympathetic and parasympathetic innervation (Waddell, 1917; Al-Zuhair *et al.*, 1975). Histochemical, immunohistochemical and electron microscopic techniques have revealed the presence of nerves in seminal vesicles containing acetylcholine, noradrenaline, vasoactive intestinal polypeptide, gastrin releasing peptide and substance P (Alm *et al.*, 1980; Stjernquist *et al.*, 1983). Neuropeptide Y (NPY), a 36 amino acid peptide, has also been shown to be present in the innervation of seminal vesicles of man and rodents (Adrian *et al.*, 1984; Stjernquist *et al.*, 1987; Yuri, 1990). The location of NPY-containing nerve terminals in close proximity to the smooth muscle led Yuri (1990) to suggest that NPY might be involved in contraction of smooth muscle cells. The present investigation was undertaken firstly to confirm the presence of NPY in the innervation of rat seminal vesicle and secondly to explore the physiological role of this neuropeptide in this organ by analysis of its effects on the level of tone and on the responsiveness of the seminal vesicle smooth muscle. A brief account of some of the results has been presented at a Meeting of British Pharmacological Society (Iravani & Zar, 1988).

[1] Present address: Department of Pharmacology, Queen Mary & Westfield College, Mile End Road, London E1 4NS.
[2] Author for correspondence.

Methods

Animals

All experiments were performed on tissues obtained from adult male Wistar rats weighing 200–350 g.

Experimental procedures

Tissue preparation for organ bath studies After the animals were killed by concussion and decapitation, the lower abdomen was opened, both horns of the seminal vesicle were separated from the coagulating gland, excised, and transferred to a Petri dish containing Krebs-Henseleit solution of the following composition (mM): NaCl 113, KCl 4.7, $CaCl_2$ 2.5, $MgSO_4$ 1.2, KH_2PO_4 1.2, $NaHCO_3$ 25 and glucose 11. An oblique cut was made near the proximal end of each horn and the contents were quickly but gently squeezed out. A delay of even a few minutes caused the lumenal contents to coagulate into dense, viscous masses which once formed were difficult to dislodge without causing damage to the tissue. The lumen of each horn was then flushed clean by a jet of Krebs-Henseleit solution directed through a 10 ml syringe into the cut. The distal 1 cm length of each horn was cut and both ends were tied with fine cotton thread and suspended between parallel platinum wire electrodes in a 1 ml jacketed organ bath containing the bathing solution, aerated with 95% O_2:5% CO_2 at 37°C. Whilst one end of the tissue was fixed to a tissue holder, the other end was attached to an isometric transducer. The preparation was placed on a resting tension of 1.0 g and changes in tension were recorded with a potentiometric chart recorder. An equilibration period of 1 h was allowed before experiments were started. During this period the preparation was washed repeatedly with fresh

Krebs-Henseleit solution. At the end of this period, contractions of the smooth muscle in each seminal vesicle horn were evoked either by electrical field stimulation (EFS) or directly by brief exposure to noradrenaline (NA).

Electrical field stimulation (EFS) and noradrenaline-induced contractions EFS was delivered through a square wave stimulator (Bell & Stein, 1971) using trains of 3–90 pulses of 0.1 ms pulse duration at a frequency of 10 Hz and at supramaximal voltage (30 V), repeated once every min or once every 5 min. In order to establish the adrenergic nature of the EFS-induced contractile responses, the preparation was exposed to phentolamine (1 μM) for at least 20 min. Exposure to 0.5 μM tetrodotoxin (TTX) lasted for 10 min before its effect on response to EFS was ascertained.

For assessing the effect of NPY on the response to EFS (delivered once every min), it was introduced into the organ bath fluid either as a single concentration or as cumulatively rising concentrations in the concentration range of 0.75–250 nM. Exposure to each concentration of NPY lasted until the response to EFS had stabilized. In order to determine the effect of NPY on responses to EFS of variable train lengths, the following procedure was adopted: the preparation was stimulated by 3-pulse trains at 5 min intervals until responses became reproducible; 3-pulse trains were then replaced with trains of 3, 10, 30 and 90 pulses, delivered in that sequence at 5 min intervals. After completing the sequence, a period of 10 min was allowed for recovery before repeating the sequence. This cycle was continued until the responses to EFS became reproducible. Once steady levels were obtained, NPY (75 nM) was introduced into the bathing medium and 5 min later the sequence of electrical stimuli was repeated. For evaluating pre- and postjunctional effects of NPY on seminal vesicle, the following protocol was followed: the preparation was contracted by EFS (3-pulse train) once every min until responses were steady. Stimulation was stopped and the preparation was contracted by 5 μM NA. This concentration of NA produced submaximal contractions of approximately equivalent tension to those evoked by EFS of 3-pulse trains (see Results). When NA-evoked contraction reached its peak, NA was washed out and the preparation was washed repeatedly to facilitate its return to the baseline tension. After obtaining at least two reproducible control responses to NA, intermingled with EFS, 75 nM NPY was introduced into the bath. Once the effect of NPY on responses to EFS reached its peak, EFS was suspended and the preparation was exposed to 5 μM NA during the concurrent presence of 75 nM NPY.

Immunohistochemistry Small pieces (2 × 3 mm) from the distal part of the seminal vesicle horn were obtained and fixed by immersion in 0.4% w/v *p*-benzoquinone in 0.01 M phosphate buffered saline (PBS), pH 7.4, for 2 h at 4°C and were then washed for at least 24 h with several changes of 0.01 M PBS containing 10% w/v sucrose and 0.01% w/v sodium azide (NaN_3). The tissues were then frozen in isopentane cooled with liquid nitrogen and frozen section, 10 mm thick, were cut on a cryostat. The sections were placed on glass slides coated with poly-L-lysine, to prevent detachment during further processing and were allowed to air dry for 60 min. The first layer antibody was rabbit anti-NPY IgG, diluted 1:200 with 0.01 M PBS containing 0.1% w/v bovine serum albumin (BSA) and 0.01% w/v NaN_3. This was applied to the sections for 16 h at room temperature in a covered Petri-dish, containing a moist filter paper in order to maintain humidity and thus prevent drying. Before the second layer antibody was applied, slide mounted sections were washed in three changes of 0.01 M PBS at 10 min intervals. The second layer antibody, goat anti-rabbit IgG, conjugated with fluorescein isothiocyanate (FITC), was applied at a dilution of 1:50 in 0.01 M PBS containing 0.1% w/v BSA and 0.01% w/v NaN_3 for 2 h at room temperature. The preparation was washed in three changes of 0.01 M PBS every 10 min and mounted in phosphate buffered glycerol. The sections were visualised under a Leitz Ortholux II microscope with excitation filter KP 490, TK 510 dichroic mirror and a barrier filter K 515. Photomicrographs were taken with Kodak T-MAX P3200 exposed at ASA 3200 and were processed in Kodak T-MAX film developer according to manufacturer's guidelines.

Pretreatment with 6-hydroxydopamine (6-OHDA) Four doses of (50 mg kg^{-1}) freshly made 6-OHDA solution in saline containing 1% w/v ascorbic acid were injected i.p. on days 1, 2, 4 and 6. The animals were killed one week after the last injection.

Pretreatment with reserpine Two rats were injected i.p. with 5 mg kg^{-1} reserpine on two consecutive days and were killed on the third day.

Drugs, chemicals and their sources

The following were used: noradrenaline bitartrate, 6-hydroxydopamine hydrochloride, bovine serum albumin, sodium azide, sodium *para*-benzoquinone, poly-L-lysine and phosphate buffered glycerol (Sigma), phentolamine mesylate and reserpine (Ciba-Geigy), ascorbic acid was obtained from (BDH), neuropeptide Y (Cambrige Research Biochemicals), tetrodotoxin (Sankyo), rabbit anti-porcine NPY serum and goat anti-rabbit serum (Peninsula Europe Ltd.). Drugs were dissolved in distilled water. Solutions of phentolamine and noradrenaline were made fresh on the day of experiment. Tetrodotoxin was dissolved in distilled water and stored as stock solution, frozen at −20°C. NPY was first dissolved in distilled water containing 200 μg ml^{-1} bovine serum albumin (Sigma), aliquoted out into smaller volumes and then freeze dried and stored at −20°C until the day of experiment, when the aliquot was reconstituted with distilled water. Reserpine was in the form of ready-to-inject solution, contained within sealed ampoules (Serpasil, 2.5 mg ml^{-1}). All chemicals were of analytical grade and were obtained from BDH.

Statistics

Results are expressed as arithmetical means ± standard error of means (s.e.mean) of absolute values or percentage change from control values. Statistical significance was assessed with Student's *t* test for paired and unpaired comparisons as appropriate. $P<0.05$ values were considered to be statistically significant.

Results

Immunohistochemistry

The wall of the rat seminal vesicle consists of an outer layer of connective tissue, a middle layer of smooth muscle and an inner mucosal layer. Indirect immunofluorescence staining for NPY revealed an abundance of dense intensely fluorescent network of fine beaded nerve fibres in the muscle layer (Figure 1a,b). Occasionally a few NPY-immunoreactive varicosities could be observed in the mucosa but generally the mucosal layer and the outer adventitial layer were devoid of any NPY-specific fluorescence. In sections of seminal vesicle obtained from 6-OHDA pretreated rats, there was a marked reduction both in the number of NPY-immunoreactive nerves as well as in the intensity of NPY-immunofluorescence (Figure 1c).

Pharmacological studies

The effect of NPY on resting tone NPY (0.25–250 nM) did not exert any contractile or relaxant effect on the level of resting tone of the smooth muscle.

Response of the seminal vesicle to EFS and noradrenaline The isolated preparation of the seminal vesicle responded with contraction to EFS (trains of 3–90 pulses) and to NA (5 μM). The tension generated in response to EFS with trains of 3 pulses and to 5 μM NA were of similar magnitude (mean ± s.e.mean; EFS = 378 ± 101 mg; NA = 402 ± 70 mg; $n = 7$) and were submaximal. EFS with longer trains of pulses (Figure 2) and higher concentrations of NA generated

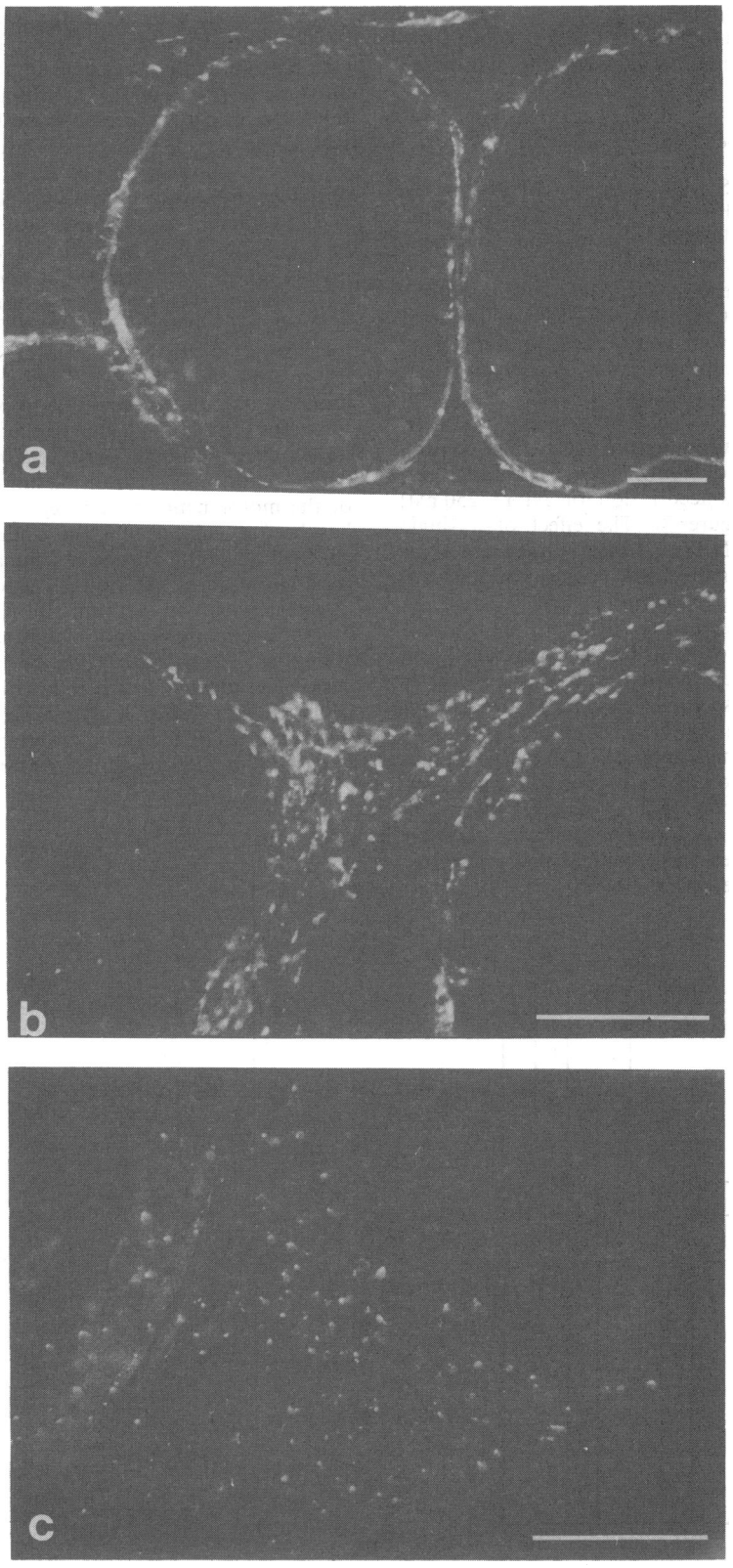


Figure 1 Immunofluorescence micrographs of transverse sections of rat seminal vesicle after incubation with antiserum to neuropeptide Y (NPY) at low (a) and high (b,c) magnification. In (c) the tissue was obtained from a 6-hydroxydopamine (6-OHDA)-treated animal. Note, the dense presence and localization of NPY-immunoreactivity within the smooth muscle layer of the seminal vesicle. Also note the reduction of NPY-immunoreactivity in the section obtained from a 6-OHDA-treated animal (c). Bars represent 50 μm.

greater tension. The response to EFS, was completely blocked by a 10 min exposure to TTX (0.5 μM); TTX was without effect on contractions produced by NA. Exposure for 20 min to phentolamine (1 μM) also abolished the response to EFS. Exposure to NA (5 μM) did not evoke a contractile response in phentolamine-treated preparations. EFS of preparations obtained from reserpine-treated animals either did not evoke any response or produced a very small contractile response (< 5% of the untreated controls). However, NA (5 μM)-induced contractions, were not reduced by reserpine-treatment.

The effect of NPY on EFS-evoked contractions

Contractions evoked by EFS were inhibitied by NPY. The development of inhibition by NPY was rapid and 5 min exposure to NPY was usually sufficient to induce maximal inhibition. The inhibition was reversible and washing out NPY led to complete recovery of the EFS-evoked contractions. There was no apparent tachyphylaxis to the inhibitory action of NPY on EFS-evoked contractions and repeated application of NPY followed by wash outs, produced similar inhibition. The threshold concentration of NPY for inhibition was about 0.25 nM. The inhibitory effect of NPY (0.25–250 nM) was concentration-dependent; a small component of response (30 ± 7% of control, $n = 5$) to EFS persisted even at the highest concentration of NPY (250 nM) employed in this study (Figure 3). The effect of a single constant concentration of NPY (75 mM) on contractions evoked by a variable number of pulses in the stimulus train was also ascertained. There appeared to be a clear correlation between the number of pulses in the stimulus train and the degree of inhibition. Responses evoked by shorter trains were inhibited to a significantly greater extent than those by longer trains (Figure 4). We have also considered the possibility that the inhibition of EFS-evoked contractions by NPY might be caused by an inhibition of the responses to released NA. In experiments in which EFS-evoked contractions were matched with NA-evoked contractions, NPY (75 nM) selectively inhibited electrically-evoked contractions but was without effect on contractions induced by a submaximally effective concentration of NA (Figure 5a,b).

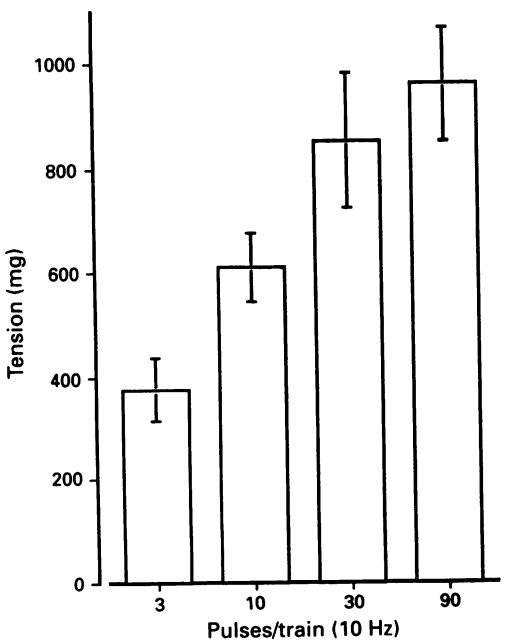


Figure 2 Contractile responses of the rat isolated seminal vesicle preparation to electrical field stimulation (trains of 3, 10, 30 and 90 pulses, 10 Hz, at 5 min intervals). The results of 5 experiments are expressed as mean (columns) ± s.e.mean.

Discussion

The main objectives of the present investigation were to determine whether NPY was present in the innervation of the rat seminal vesicle and to explore its effect on the motor transmission on this preparation. Our immunohistochemical observations have confirmed the original report of Yuri (1990) as to its presence in the innervation of the rat seminal vesicle. Furthermore, our studies have also revealed a reduction both in density and intensity of NPY immunofluorescent nerve fibres by 6-OHDA treatment. This finding could be taken to imply its presence both in adrenergic and non-adrenergic nerves, since if NPY were present only in adrenergic nerves, the fluorescence would be expected to be totally abolished following 6-OHDA treatment.

The seminal vesicle consists of a glandular mucosal layer and a smooth muscle layer. NPY immunofluorescence was almost exclusively located in the nerves of the muscular layer, confirming earlier findings by others (Gu *et al.*, 1983; Carvalho *et al.*, 1986; Yuri, 1990; Properzi *et al.*, 1992). Its localization in the muscular layer suggests the unlikelihood of its involvement in the glandular secretory activity and indicates its physiological role to be related to smooth muscle functions. In assessing this role of NPY, it is important that no ambiguity should exist regarding the nature of motor nerve-smooth muscle transmission in this organ. The identity of the motor neurotransmitter of seminal vesicles in rodents has been a subject of some uncertainty. Thus EFS-evoked contractions of guinea-pig seminal vesicle, although TTX-sensitive, are not affected by atropine, guanethidine, phenoxybenzamine or propranolol and the neurotransmitter involved remains yet to be identified (Stjernquist *et al.*, 1983; Wang & Hakanson, 1992). However, in the rat seminal vesicle the identity of the motor neurotransmitter appears to be much more certain. Our observation that the contractile responses to EFS were blocked by phentolamine and were greatly attenuated by chronic reserpinisation are indicative of

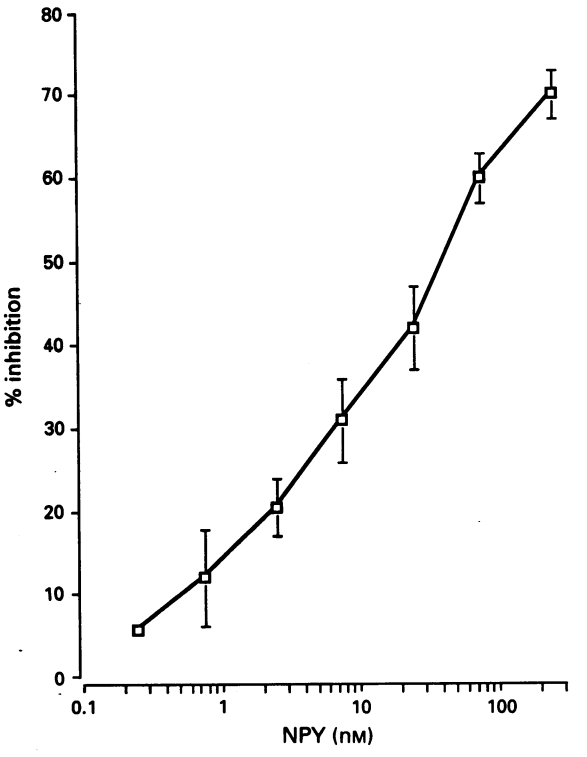


Figure 3 Inhibitory effect of neuropeptide Y (NPY) on contractile responses of rat isolated seminal vesicle to electrical field stimulation (trains of 3 pulses, 10 Hz, once every min). The results from 5 experiments are plotted as mean % inhibition of the contractile response ± s.e.mean ($n = 5$).

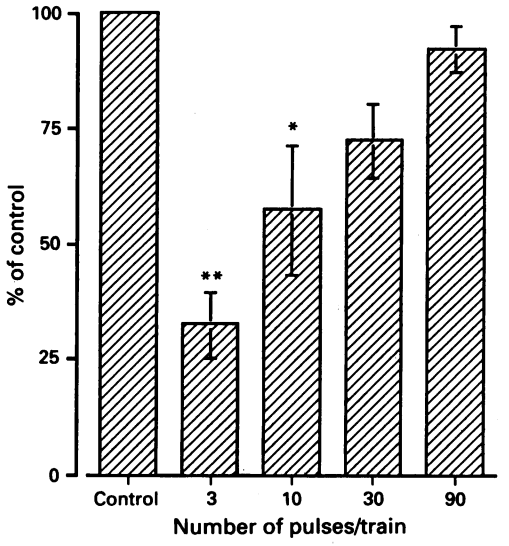


Figure 4 Effect of train-length on the inhibition of electrically-evoked contractions by neuropeptide Y (NPY). Contractions by electrical field stimulation (trains of 3, 10, 30 and 90 pulses, 10 Hz, 5 min intervals) were evoked in the absence and presence of NPY (75 nM). Results from 5 experiments are plotted as columns and the contractions in the presence of NPY are expressed as mean % control contraction before exposure to NPY for each train length. Vertical bars represent standard error of the mean. Significant difference between contractions in the absence (control) and presence of NPY is shown as $*P<0.05$ and $**P<0.005$, Student's paired t test.

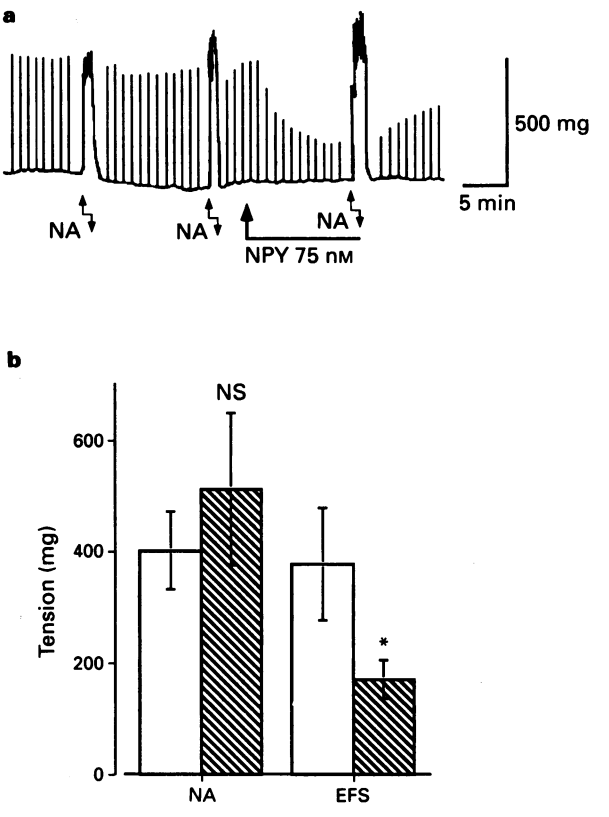


Figure 5 Effect of neuropeptide Y (NPY) on contractions evoked by EFS (trains of 3 pulses, 10 Hz, 1 every min) and by noradrenaline (NA, 5 μM). EFS was interrupted during exposure to NA and lasted until the contractions to NA had peaked (60–90 s). (a) Shows trace of a typical experiment. In (b) each column represents the mean contractile tension in response to NA and EFS (open column = control; hatched column = in the presence of NPY); ± s.e.mean are shown ($n = 5$). Significant difference between contractions in the absence (control) and presence of NPY is shown as $*P<0.05$.

NA being the putative neurotransmitter. This interpretation is consistent with the immunohistochemical findings of Yuri (1990), who had demonstrated an abundant presence of tyrosine hydroxylase immunoreactive nerve fibres, presumably adrenergic, in close proximity of smooth muscle cells in the rat seminal vesicle. The solely adrenergic nature of motor transmission in rat seminal vesicle is also strongly supported by the observations that EFS-evoked contractions of rat seminal vesicle are blocked by guanethidine or phentolamine and are not affected by α,β-methylene ATP desensitization, providing evidence against ATP as a cotransmitter with NA in this organ (Chin & Pennefather, 1988). The effects of reserpine, guanethidine and phentolamine on EFS-evoked contractions, also makes it unlikely that SP serves as a motor neurotransmitter in the rat seminal vesicle. This conclusion is consistent with Stjernquist *et al.* (1983) who found in guinea-pig seminal vesicle that the SP antagonist (D-Pro^2,D-Trp^{7,9})-SP, abolished the contraction elicited by SP but did not affect the response to electrical stimulation.

In the present investigation, NPY did not affect the tone of the smooth muscle of the seminal vesicle suggesting that a direct effect of NPY on the smooth muscle is unlikely to be its main contribution to neuromuscular transmission in this organ. NPY inhibited the contractions evoked by EFS but not that by 5 μM NA, indicating thereby that its main functional role is modulation of adrenergic motor transmission, by a prejunctional mechanism. NPY has been known to inhibit neurotransmitter release including NA, at many neuroeffector junctions (for review see Bleakman *et al.*, 1993) and the present result in the rat seminal vesicle is another example of this phenomenon. Recently, direct evidence has been provided to show that presynaptic inhibition by NPY at sympathetic nerve terminals is associated with a reduction in Ca^{2+} influx and that this is due to the selective inhibition of N-type Ca^{2+} channels located at the nerve terminals (Toth *et al.*, 1993).

A feature of the inhibitory effect of NPY on contractions evoked by EFS in the seminal vesicle was its inverse relationship with the length of stimulus train. Thus whereas with 3-pulse trains the percentage inhibition of EFS-evoked contraction by NPY (75 nM) was about 70% and statistically highly significant, the corresponding value for 90-pulse trains was less than 10% and not statistically significant. This is a feature common to many (but not all, for instance guanethidine) presynaptically acting inhibitors of transmitter release. The explanation which has found most favour is one based upon electrophysiological data and measurement of intracellular free Ca^{2+} concentration in neurones following a stimulus. These studies have shown the existence of a non-linear relationship between Ca^{2+} current and intracellular Ca^{2+} concentration with long stimulus trains (Thayer & Miller, 1990). More efficient buffering at higher intracellular Ca^{2+} levels is said to be responsible for this non-linearity (Duckles & Budai, 1990; Bleakman *et al.*, 1993). According to this explanation, with longer stimulus trains, the reduced Ca^{2+} influx by NPY does not lead to a reduction in intracellular Ca^{2+} concentration because of the concurrent prevention of the enhancement in Ca^{2+} buffering capacity.

In conclusion, the results presented here confirm a rich presence of NPY-containing innervation in the muscular layer of rat seminal vesicle. The motor transmission appears to be solely adrenergic in this organ and the principal function of NPY is modulation of adrenergic motor transmission by a prejunctional mechanism.

References

ADRIAN, T.E., GU, J., ALLEN, J.M., TATEMOTO, K., POLAK, J.M. & BLOOM, S.R. (1984). Neuropeptide Y in the human male genital tract. *Life Sci.*, **35**, 2643–2648.

ALM, P., ALUMET, J., HAKANSON, R., OWMAN, C., SJOBERG, N.-O., SUNDLER, F. & WALLES, B. (1980). Origin and distribution of VIP (Vasoactive intestinal polypeptide)-nerves in the genito-urinary tract. *Cell Tissue Res.*, **205**, 337–347.

AL-ZUHAIR, A., GOSLING, J.A. & DIXON, J.S. (1975). Observations on the structure and autonomic innervation of the guinea-pig seminal vesicle and ductus deferens. *J. Anat.*, **120**, 81–93.

BELL, P.M.G. & STEIN, R.B. (1971). A digital stimulator built on modular principles using integrated circuits. *J. Physiol.*, **218**, 5P.

BLEAKMAN, D., MILLER, R.J. & COLMERS, W.F. (1993). Actions of neuropeptide Y on the electrophysiological properties of nerve cells. In *The Biology of Neuropeptide Y and Related Peptides*. pp. 241–274. Totowa: Humana Press.

CARVALHO, T.L., HODSON, N.P., BLANK, M.A., WATSON, P.F., MULDERRY, P.K., BISHOP, A.E., GU, J., BLOOM, S.R. & POLAK, J.M. (1986). Occurrence, distribution and origin of peptide-containing nerves of guinea-pig and rat male genitalia and the effects of denervation on sperm characteristics. *J. Anat.*, **149**, 121–141.

CHIN, P.F. & PENNEFATHER, J.N. (1988). Evidence that ATP does not act as a cotransmitter with noradrenaline in field stimulated preparations of rat seminal vesicle. *Eur. J. Pharmacol.*, **155**, 309–312.

DUCKLES, S.P. & BUDAI, D. (1990). Stimulation intensity as a critical determinant of presynaptic receptor effectiveness. *Trends Pharmacol. Sci.*, **11**, 440–443.

GU, J., POLAK, J.M., PROBERT, L., ISLAM, K.N., MARANGOS, P.J., MINA, S., ADRIAN, T.E., MCGREGOR, G.P., O'SHAUGHNESSY, D.J. & BLOOM, S.R. (1983). Peptidergic innervation of the human male genital tract. *J. Urol.*, **130**, 386–391.

IRAVANI, M.M. & ZAR, M.A. (1988). The effects of neuropeptide Y (NPY) on the adrenergic neurotransmission in isolated rat seminal vesicle. *Br. J. Pharmacol.*, **93**, 286P.

PROPERZI, G., CORDESCHI, G. & FRANCAVILLA, S. (1992). Post-natal development and distribution of peptide-containing nerves in the genital system of the male rat. An immunohistochemical study. *Histochemistry*, **97**, 61–68.

STJERNQUIST, M., HAKANSON, R., LEANDER, C., OWMAN, C., SUNDLER, F. & UDDMAN, R. (1983). Immunohistochemical localisation of substance P, vasoactive intestinal polypeptide and gastrin-releasing peptide in vas deferens and seminal vesicle, and the effect of these and eight other neuropeptides on resting tension and neurally evoked contractile activity. *Regul. Pept.*, **7**, 67–86.

STJERNQUIST, M., OWMAN, C., SJOBERG, N.O. & SUNDLER, F. (1987). Coexistence and co-operation between neuropeptide Y and norepinephrine in nerve fibres of guinea pig vas deferens and seminal vesicle. *Biol. Reprod.*, **36**, 149–155.

THAYER, S.A. & MILLER, R.J. (1990). Regulation of the intracellular free calcium concentration in single rat dorsal root ganglion neurons *in vitro*. *J. Physiol.*, **425**, 85–115.

TOTH, P.T., BINDOKAS, V.P., BLEAKMAN, D., COLMERS, W.F. & MILLER, R.J. (1993). Mechanism of presynaptic inhibition by neuropeptide Y at sympathetic nerve terminals. *Nature*, **364**, 635–639.

WADDEL, J.A. (1917). The pharmacology of the seminal vesicles. *J. Pharmacol. Exp. Ther.*, **9**, 113–120.

WANG, Z.-Y. & HAKANSON, R. (1992). (±)-CP-96,345 a selective tachykinin NK$_1$ receptor antagonist, has non-specific actions on neurotransmission. *Br. J. Pharmacol.*, **107**, 762–765.

YURI, K. (1990). Immunohistochemical and enzyme histochemical localisation of peptidergic, aminergic and cholinergic nerve fibres in the rat seminal vesicle. *J. Urol.*, **143**, 194–198.

(Received February 25, 1994
Revised July 14, 1994
Accepted July 20, 1994)

Br. J. Pharmacol. (1994), **113**, 883–888 © Macmillan Press Ltd, 1994

Y_2-receptor-mediated selective inhibition of slow, inhibitory postsynaptic potential in submucous neurones of guinea-pig caecum

Shauna M.C. Cunningham, *Satoshi Mihara & [1]Gordon M. Lees

Department of Biomedical Sciences, University of Aberdeen, Marischal College, Aberdeen AB9 1AS and *Department of Physiology, Kurume University School of Medicine, 67 Asahi-machi, Kurume-shi, 830 Japan

1 The subtype of neuropeptide Y receptor mediating the selective inhibition of the slow inhibitory postsynaptic potential (i.p.s.p.) of submucous neurones in guinea-pig caecum was investigated by use of conventional intracellular electrophysiological recording techniques.

2 Neuropeptide Y (NPY) (1–300 nM) was found to depress or abolish reversibly the slow i.p.s.p. evoked by focal stimulation of internodal fibre tracts. At low concentrations (1–30 nM), a reduction in the duration of the slow i.p.s.p. was often apparent before any inhibition of the amplitude of this synaptic potential.

3 These inhibitory effects of NPY were mimicked by peptide YY (PYY; 0.3–100 nM), NPY13–36 (1–300 nM) and NPY22–36 (10–100 nM); [Leu^{31},Pro^{34}]NPY ([Pro^{34}]NPY) and bovine pancreatic polypeptide (bPP) were without pre- or postsynaptic effects at concentrations of up to 300 nM. The IC_{50} ± s.e. mean values for PYY, NPY, and NPY13–36 were 2.7 ± 0.3, 7.8 ± 2.1 and 30 ± 4.8 nM, respectively, and were significantly different from each other. Thus, the apparent rank order of potency was PYY>NPY>NPY13–36>>[Pro^{34}]NPY and bPP.

4 In concentrations of up to 300 nM, NPY and its analogues had no depressant effects on the active and passive properties of the impaled neurone and did not affect the amplitude or duration of either cholinergic fast synaptic potentials or non-cholinergic, slow excitatory postsynaptic potentials (e.p.s.ps). Furthermore, none of these peptides altered the amplitude or time-course of changes in membrane potential induced by focal application of acetylcholine or noradrenaline.

5 It is, therefore, concluded that the selective inhibition of the slow i.p.s.p. is mediated by Y_2-receptors, located presynaptically on noradrenergic nerve terminals.

Keywords: Submucous neurones; slow i.p.s.p.; Y_2-receptors; neuropeptide Y; NPY analogues; neuromodulation

Introduction

Neuropeptide Y (NPY) and the closely related, endogenously-occurring peptide, peptide YY (PYY), modify neuro-effector transmission in a variety of tissues (for reviews see Morris & Gibbins, 1992 and Wahlestedt & Reis, 1993). For example, in the intestine of several species, NPY acts as an anti-secretory neuropeptide (Friel *et al.*, 1986; Cox & Cuthbert, 1990; for review see Cox, 1993) and in the guinea-pig small and large intestine, both PYY and NPY have been shown to inhibit cholinergic neuro-effector transmission (Garzon *et al.*, 1986; Holzer *et al.*, 1987; Wiley & Owyang, 1987). With respect to the guinea-pig enteric nervous system, two other observations were germane to the present investigation. First, in myenteric neurones of the guinea-pig gastric corpus, NPY depresses fast, cholinergic ganglionic transmission by a presynaptic mechanism (Schemann & Tamura, 1992). Secondly, we recently obtained evidence that NPY could depress inhibitory ganglionic transmission in submucous neurones of the caecum (Cunningham *et al.*, 1994a). Further evidence is now presented that, in causing this inhibition, NPY selectivity targets noradrenergic nerve terminals to reduce transmitter release by activation of Y_2-receptors. A preliminary account of part of this study was presented to the British Pharmacological Society, at its Spring Meeting, 1994 (Cunningham *et al.*, 1994b).

Methods

Albino guinea-pigs of either sex and weighing 170–550 g were killed either by stunning and exsanguination or by overdose with anaesthetic ether followed by exsanguination. Full-thickness segments (1.0 × 1.5 cm) of mid-caecum located between the taeniae were isolated and placed in Krebs solution of the following composition (mM): NaCl 118, KCl 4.7, $CaCl_2$ 2.54, $MgSO_4$ 1.12 or $MgCl_2$ 1.1, $NaHPO_4$ 1.2, $NaHCO_3$ 25 and glucose 11.1. The solution (pH 7.43) was gassed with 95% oxygen and 5% carbon dioxide.

The mucosa and all traces of smooth muscle were removed from small, rectangular tissue samples. Such preparations, containing 1–4 ganglia, were pinned to the bottom of a small recording chamber lined with Sylgard (Dow Corning) and superfused (8–13 ml min^{-1}) with Krebs solution at 36 ± 1° C. Ganglia were viewed at a magnification of 250–400 by means of either a Zeiss RA34 or ICM35 (inverted) microscope.

Conventional single microelectrode intracellular recordings were made by means of fine glass microelectrodes (55–125 MΩ) filled with 2 M KCl connected to the headstage of an Axoclamp 2A Preamplifier; the signals were displayed on a digital storage oscilloscope and on either a Gould-Brush 2200 or a Nihon Koden RJG-4124 three-channel pen recorder. In some experiments, the signals were stored on magnetic tape (Racal) for subsequent analysis. For fuller details of the methods used, see Mihara *et al.*, (1985) and Katayama *et al.*, (1986).

Synaptic inputs to individual neurones were traced by means of a roving extracellular microelectrode (tip diameter 5–15 μm), filled with a modified Krebs solution and placed on an internodal fibre strand or directly on the surface of the ganglion from which intracellular recordings were made. Noradrenaline was applied either by superfusion (100 nM for 30–60 s) or by pressure ejection (70–310 kPa) from glass

[1] Author for correspondence.

microelectrodes (tip diameter 5–12 μm) filled with a solution of noradrenaline (0.1–1.0 mM). Micro-ionophoresis of acetylcholine (ACh) was used to induce a depolarization in impaled neurones.

All other drugs were applied by superfusion, without recirculation; in some cells peptide application was cumulative. Unless full recovery from the inhibitory action of a peptide was obtained, the observation was disregarded. No peptidase inhibitors were used in the present experiments. All drugs used in this study were purchased from Sigma Ltd. unless otherwise specified. They included: acetylcholine chloride, idazoxan (gift from Pfizer), noradrenaline bitartrate, neuropeptide Y (Sigma and Peninsula Europe), NPY13–36, NPY22–36 (Peninsula Europe), [Leu^{31},Pro^{34}]-NPY ([Pro^{34}]NPY), peptide Y (PYY), tetrodotoxin, trimetaphan.

Quantitative data are expressed as means (± s.e. mean) of n observations (each in a separate preparation). The Mann-Whitney Two-Tailed Test was used to test for the level of significance of differences in IC_{50} values, $P<0.05$ being considered significant.

Results

Stable intracellular recordings (30–330 min) were made from a total of 107 neurones and 7 glial cells in 84 preparations of submucosa; intracellular recordings were considered to be satisfactory if the resting membrane potential (E_m) was more negative than −45 mV, if the input resistance (R_{in}) was greater than 50 MΩ and action potentials induced by direct soma depolarization or focal stimulation of preganglionic nerves showed unequivocal overshoot. In the vast majority (103/107; E_m −55.7 ± 1.0 mV, $n=66$; R_{in} 256 ± 17 MΩ, $n=49$) of neurones, at least one prominent (mean amplitude 10.3 ± 0.6 mV; $n=46$), subthreshold fast excitatory synaptic potential (e.p.s.p.) could be evoked in response to activation of an internodal fibre strand with single stimuli; occasionally (17/63) there was a 'strong fibre' input, i.e. the resulting fast e.p.s.p. was always suprathreshold. When action potentials were generated in 90/103 neurones, they were not followed by a prolonged period of after-hyperpolarization or fall in input resistance; these cells were, therefore, designated S-neurones. In the remaining 13/103 neurones with fast e.p.s.ps, a long-lasting (4–8 s) hyperpolarization was observed following the generation of a somal action potential; such cells were called S/AH neurones (Mihara, 1993). The amplitude and threshold of action potentials, which were sensitive to tetrodotoxin (TTX; 50–100 nM) in both S and S/AH neurones, were 63.7 ± 1.0 mV ($n=63$) and −36.7 ± 1.2 mV ($n=30$), respectively.

Repetitive stimulation with trains of five pulses at 20 or 40 Hz elicited slow e.p.s.ps (mean amplitude 5.5 ± 0.6 mV; $n=47$) in 85/103 neurones; this non-cholinergic depolarization was associated with an increase in input resistance and was preceded by a slow inhibitory postsynaptic potential (i.p.s.p.) (mean amplitude 24.5 ± 1.1 mV, $n=56$) in 98/103 cells.

Only 4 neurones (E_m −61.0 ± 6.2 mV, R_{in} 166 ± 33 MΩ) were impaled that showed the classic characteristics of AH-neurones, i.e. no fast e.p.s.ps and a prolonged period of after-hyperpolarization or reduction in R_{in} following generation of a somal action potential, which was insensitive to TTX (200 nM).

In confirmation of our previous findings (Cunningham et al., 1994a), NPY (1–300 nM; $n=50$) applied by superfusion for 4–10 min inhibited in a concentration-dependent manner the duration and amplitude of the slow i.p.s.p. (Figure 1) in every cell tested; at concentrations of >30 nM, the slow i.p.s.p. was usually abolished. The inhibition usually commenced within 4 min at lower concentrations and within 2 min at the highest concentration (it took approximately 25–30 s for the drug to reach the recording chamber). The

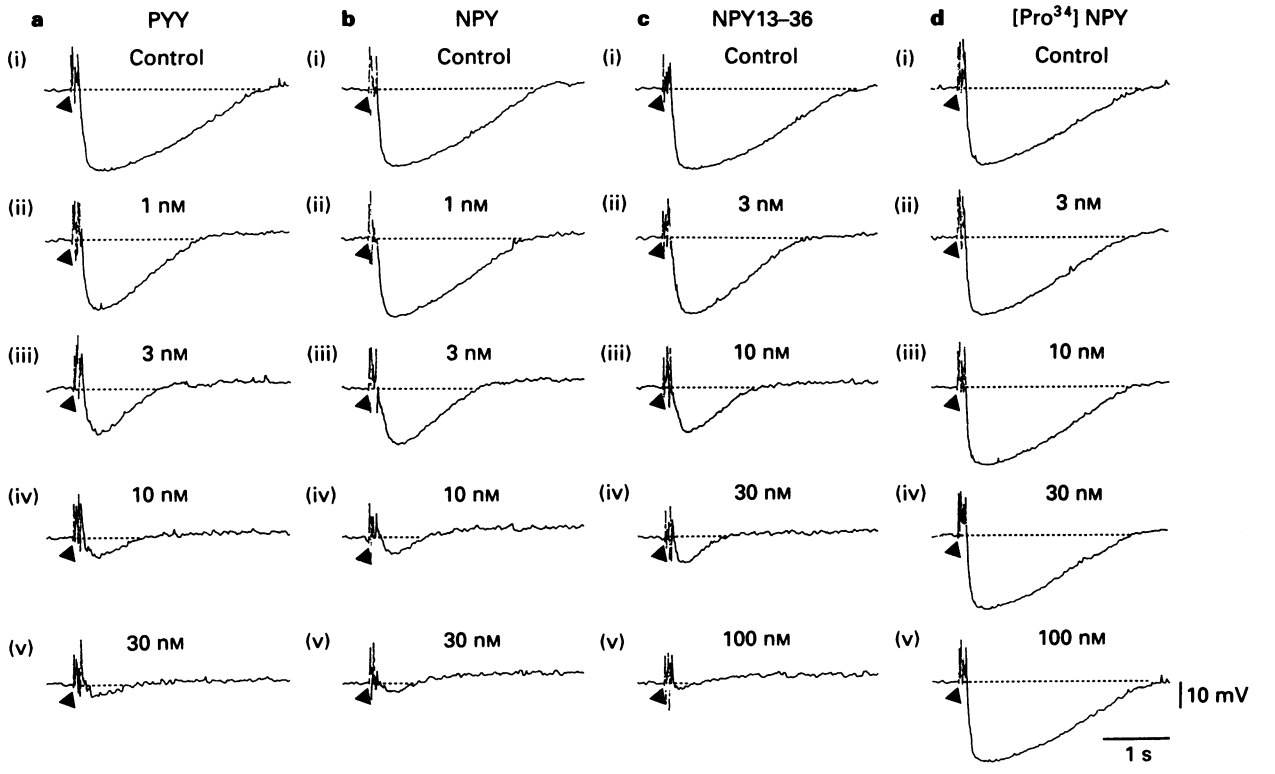


Figure 1 Effects of neuropeptide Y (NPY) and related peptides on slow i.p.s.p. in a single submucous neurone of the guinea-pig caecum. In each case, an individual concentration of a peptide was applied for 8–10 min, followed by a wash-out period of at least 20 min. The order of peptide application was NPY, PYY, NPY13–36 and [Pro^{34}]NPY; the intracellular recording lasted >300 min; the resting/holding potential was −53 mV. Note the lack of an inhibitory effect of [Pro^{34}]NPY, even at a concentration of 100 nM. For graphic representation of these results, see Figure 2.

IC_{50} value ($n = 6$ observations) for the depressant effect of NPY on the amplitude of the slow i.p.s.p. was 7.8 ± 2.1 nM.

PYY (0.3–100 nM; $n = 6$; IC_{50} 2.7 ± 0.3 nM), NPY13–36 (1–300 nM; $n = 3$; IC_{50} 30 ± 4.8 nM) and NPY22–36 (10–100 nM; $n = 2$) also selectively depressed or abolished the slow i.p.s.p. (Figures 1, 2 and 3). The IC_{50} value of NPY was significantly greater than that of PYY ($P<0.003$) and significantly less than that of NPY13–36 ($P<0.03$). [Pro^{34}]NPY ($n = 3$) and bovine pancreatic polypeptide (bPP; $n = 3$) had no detectable pre- or postsynaptic effects at concentrations of up to 300 nM (Figures 2 and 3). Thus, in the absence of a peptidase inhibitor, the apparent rank order of potency was PYY>NPY>NPY13–36>>[Pro^{34}]NPY and bPP (Figures 1, 2 and 3), a finding confirmed by the results of 2 neurones in which it was possible to test the effects of more than one peptide. No evidence was obtained for a desensitization to the peptides and these depressant effects were seen in every neurone tested.

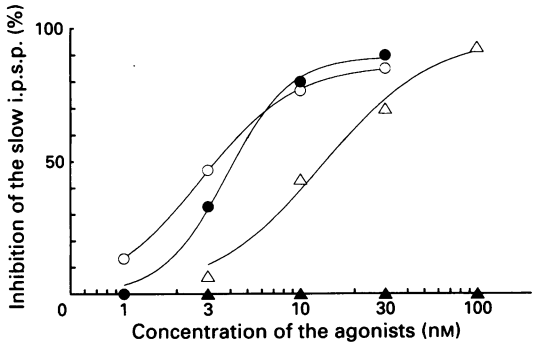


Figure 2 Log concentration-response relationships for neuropeptide Y (NPY) and related peptides in a single submucous neurone of the guinea-pig caecum. Data from Figure 1: (●) NPY; (○) PYY; (△) NPY13–36; (▲) [Pro^{34}]NPY.

Although, in concentrations of up to 300 nM, NPY and the other peptides had no effect on the resting membrane potential, membrane time constant, input resistance, or on action potential amplitude or threshold, the possibility existed that these peptides might have had a postsynaptic depressant effect to attenuate the actions of noradrenaline released during the stimulus train. In each neurone with a slow i.p.s.p. examined, noradrenaline induced a hyperpolarization; noradrenaline application by superfusion or pressure ejection was adjusted to induce a membrane hyperpolarization of approximately 100% or 50% of the amplitude of the slow i.p.s.p. in that neurone. In no case ($n = 25$) did NPY alter the response of the cell to noradrenaline (Figure 4). Likewise, in the concentrations tested, NPY (Figure 5) and its analogues did not affect the amplitude of either the fast or slow e.p.s.ps of S-neurones with slow i.p.s.ps (other neurones were not tested). Furthermore, NPY had no inhibitory effect on ACh-induced depolarizations ($n = 2$).

Discussion

It was interesting to find that the quantitative data concerning the active and passive properties of submucous neurones of the guinea-pig caecum were virtually identical to those previously obtained with quite different experimental set-ups (Mihara *et al.*, 1985; Mihara, 1993). Thus, it seems likely that the characteristics of submucous neurones of the caecum are

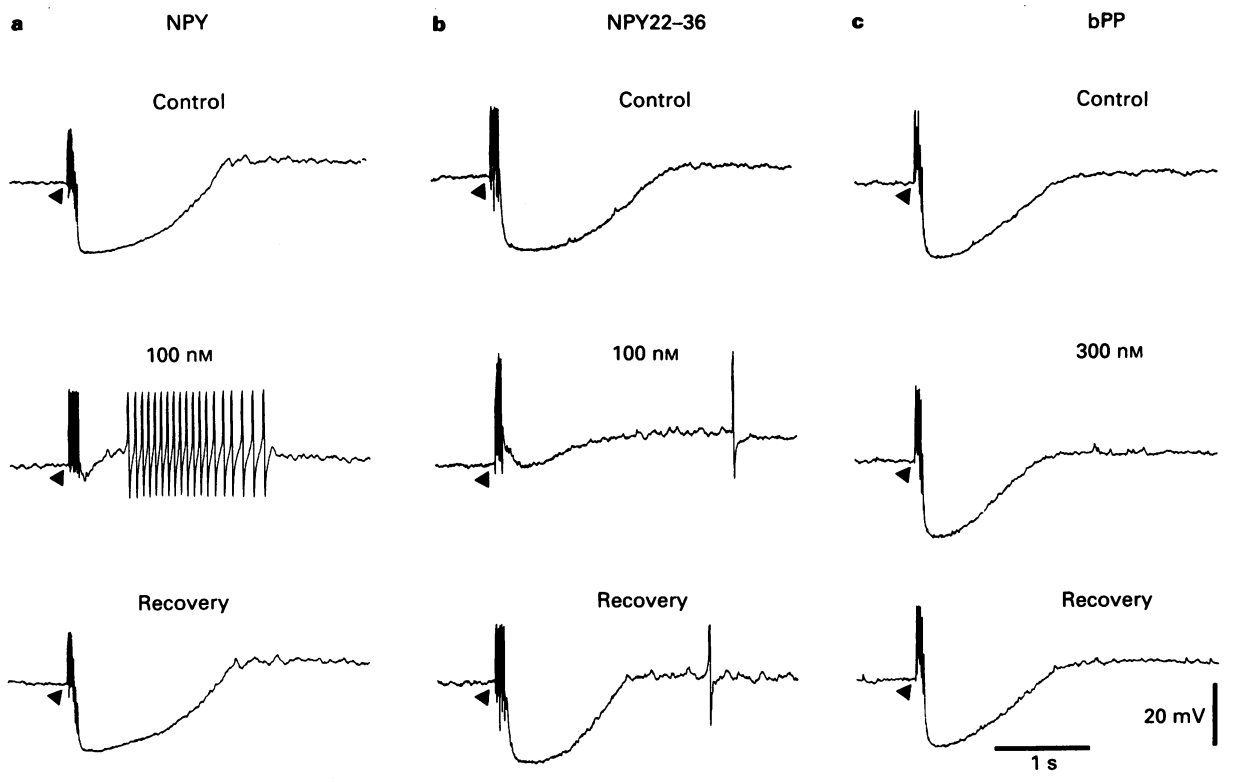


Figure 3 Comparison of the effects of neuropeptide Y (NPY), NPY22–36 and bovine pancreatic polypeptide (bPP) on the slow i.p.s.p. of submucous neurones of guinea-pig caecum evoked by trains of five pulses at 40 Hz. Column (a), inhibitory effect of NPY (100 nM); column b, inhibitory effect of NPY22–36 (100 nM); column c, lack of effect of bPP (300 nM) on slow i.p.s.p. Intracellular recordings from three neurones, the resting potentials being −51 mV, −48 mV and −52 mV, respectively. Upper records, controls; middle records, 3, 3 and 10 min after exposure to the respective peptides; lower records, each approximately 15 min after discontinuation of exposure to peptide. Note the firing of action potentials during the slow e.p.s.p. when the neurones were exposed to NPY or NPY22–36; the increased excitability occurred *pari passu* with the suppression of the slow i.p.s.p. The amplitude of the action potentials was not recorded in full and was reduced by the frequency response of the pen recorder.

fundamentally different from those of the distal colon (Frieling et al., 1991a,b; Cunningham, Hirai, Mihara & Lees, unpublished observations), where, for example, slow i.p.s.ps are rare and very small. This is doubly of interest in view of the differences in the nature and density of NPY-immunoreactive nerve fibres in these and other regions of the large intestine (Messenger & Furness, 1990; Cunningham et al., 1994a; Cunningham & Lees, unpublished observations).

In myenteric neurones of the gastric corpus, a presynaptic inhibition by NPY (50–500 nM), PYY (50–500 nM) or bPP (50–500 nM) of fast, cholinergic ganglionic transmission has been convincingly demonstrated (Schemann & Tamura, 1992) although the inhibition was observed in only 82%, 75% and 67% of cells, respectively. According to these authors, the peptides were virtually equiactive; from Figure 2 of their paper, the IC_{50} values appeared to be approximately 50 nM ($n = 3$). The receptor type responsible was not established and none of the known NPY-, PYY- or PP-preferring receptors has the profile shown in their study. (see Grundemar et al., 1993).

Evidence that this presynaptic mode of action of NPY in caecal submucous neurones may occur physiologically has already been presented and discussed (Cunningham et al., 1994a). Two conclusions from the present experiments may be of relevance: first, since it has been established previously that the slow i.p.s.p. is due to the activation of α_2-

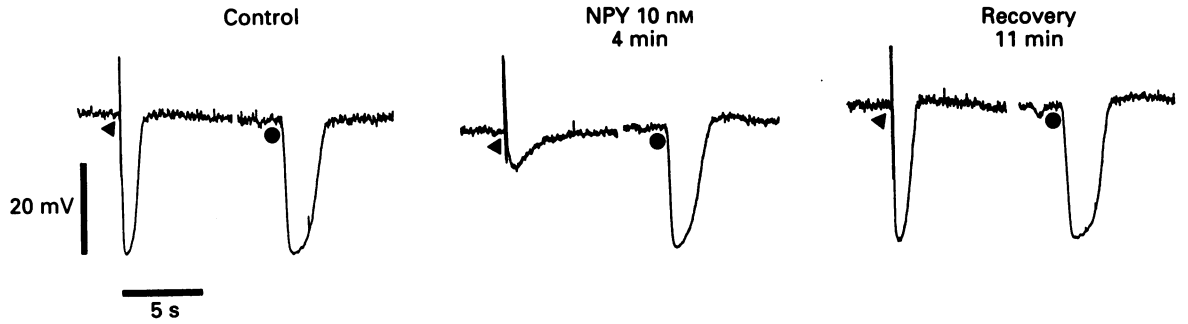


Figure 4 Lack of effect of neuropeptide Y (NPY) on noradrenaline-induced hyperpolarization of a caecal submucous S/AH-neurone in which slow i.p.s.p. was simultaneously suppressed. Slow i.p.s.p. was evoked by a train of five pulses at 40 Hz (▶) applied to an internodal nerve fibre strand. Noradrenaline was applied by pressure ejection (●; 210 kPa for 55 ms) from a microelectrode located approximately 20 μm from the impaled neurone. The resting potential was −55 mV. Note the marked suppression by NPY (10 nM) of the slow i.p.s.p. at a time when the response to noradrenaline was unchanged. In this neurone, facilitation of fast e.p.s.ps evoked by the stimulus train caused some fast e.p.s.ps to become suprathreshold; the after-hyperpolarization (slow AH) and the slow i.p.s.p. were therefore superimposed in control and recovery periods. The hyperpolarization during exposure to 10 nM NPY was mainly due to the presence of the (summated) slow AH associated with the generation of three action potentials during the train. NPY did not affect the amplitude or time-course of the slow AH, the threshold for action potential generation or the facilitation of fast e.p.s.ps.

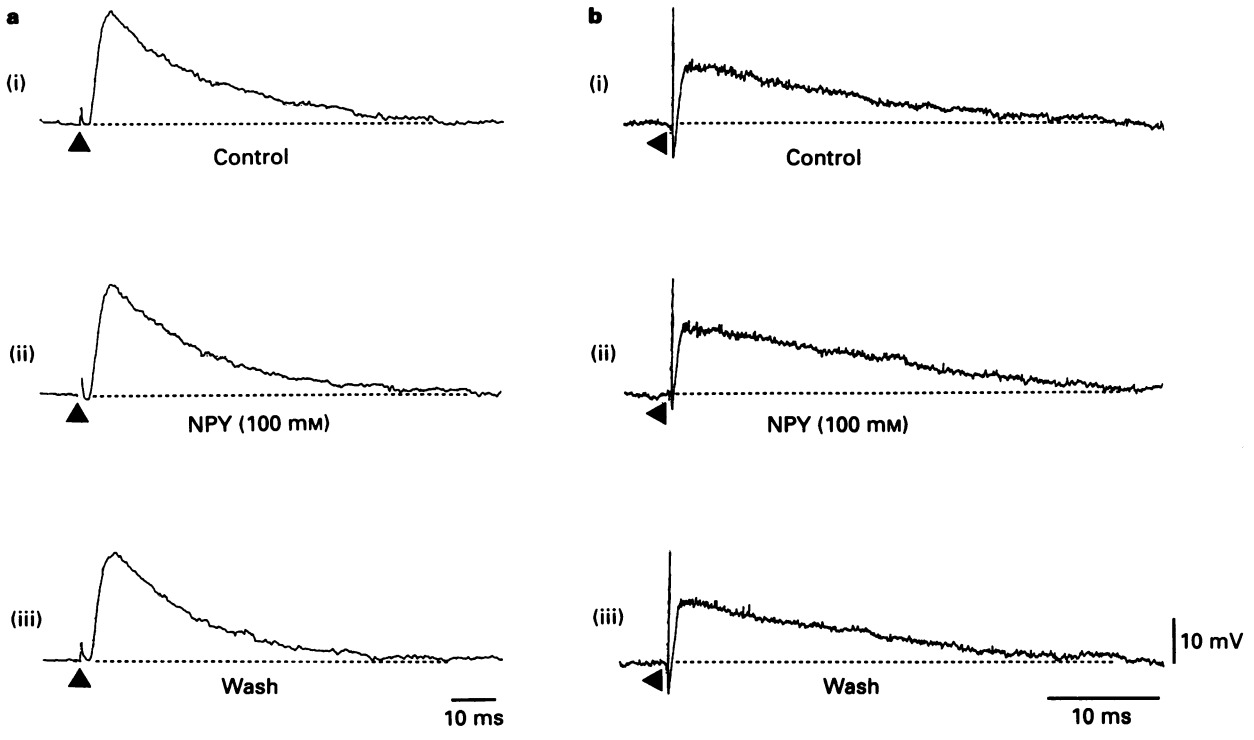


Figure 5 Lack of effect of neuropeptide (NPY, 100 nM) on cholinergic and non-cholinergic synaptic transmission in a submucous neurone of guinea-pig caecum. (a) Fast (cholinergic) e.p.s.p. evoked by a single stimulus applied focally to an internodal fibre tract. (b) Slow (non-cholinergic) e.p.s.p. evoked by a train of five pulses at 40 Hz applied with the same focal electrode at the same location; idazoxan (100 nM) was present to suppress the slow i.p.s.p., which was further reduced by NPY (100 nM). Resting potential throughout b was −57 mV; a holding potential of −85 mV was used throughout (a).

adrenoceptors by noradrenaline released from intraganglionic nerve terminals (Mihara *et al.*, 1985; Mihara, 1993), the presynaptic action of NPY was targeted exclusively for the inhibition of noradrenaline release and not for the release of either ACh or the non-cholinergic neurotransmitter responsible for the fast and slow e.p.s.ps generated in the same cells. Furthermore, the inhibitory action of NPY on ganglionic transmission in neurones of the submucosa of the caecum occurred at a concentration nearly one order of magnitude lower than that required to depress cholinergic synaptic transmission in the gastic corpus (Schemann & Tamura, 1992).

The present experiments were aimed at identifying the Y-receptor subtype mediating this presynaptic inhibition. There are, however, no NPY-preferring receptor antagonists, with suitable receptor-subtype selectivity, available at present. The tetramine disulphide, benextramine, has been proposed as an irreversible NPY-preferring receptor antagonist (Doughty *et al.*, 1990) but this drug is also an irreversible antagonist at α-adrenoceptors (Belleau *et al.*, 1982) probably including the subtype (α_2-) mediating the slow i.p.s.p. (North & Surprenant, 1985). D-*myo*-Inositol-1,2,6-trisphosphate (PP56) has also been proposed as an antagonist (Edvinsson *et al.*, 1990). Despite its structural similarity to inositol-1,4,5-triphosphate (IP_3), PP56 has been suggested to interact directly with NPY-preferring receptors in the 10–1000 nM concentration-range; however, it does not appear to distinguish between subtypes of NPY-preferring receptors and its action is non-competitive.

NPY receptor classification is currently, therefore, based upon the rank order of potency of agonists. It is generally accepted that NPY and PYY are approximately equipotent at Y_1- and that PYY is the preferred agonist at Y_2-receptors; the Y_1-receptor has an absolute requirement for an intact N-terminus, so that N-terminally-truncated fragments, such as NPY13–36 and NPY22–36, are much less potent at Y_1-receptors. In contrast, the Y_2-receptor is more stringent in its demands on the C-terminus of NPY, having an absolute requirement for the last 12 amino acid residues of NPY and PYY. A substitution of isoleucine[31] and glycine[34] with leucine[31] and proline[34] results in an analogue that is inactive at Y_2-receptors but retains full agonist activity at Y_1-receptors, substitution in the 31 position being of only minor importance (Fühlendorff *et al.*, 1990; Michel, 1991; Grundemar *et al.*, 1993; Wahlestedt & Reis, 1993). The only receptor that can readily distinguish between NPY and PYY (NPY $\geqslant$ [Pro[34]]NPY $\geqslant$ NPY(13–36) $>>$ PYY) is the so-called Y_3-receptor. The related endogenous peptide, PP, is inactive at all NPY- and PYY-preferring receptors but is much more potent than either NPY or PYY at its own (PP-preferring) receptor (Inui *et al.*, 1989). Thus, in caecal submucous neurones, the absence of neuromodulatory effects of either bPP or [Pro[34]]NPY, an acknowledged Y_1-receptor agonist, and the finding of an apparent rank order of potency PYY $>$ NPY $>$ NPY13–36 $>>$ [Pro[34]]NPY and PP, are strongly suggestive of an involvement of NPY receptors of the Y_2-receptor subtype in mediating this disinhibition. The true rank order of potency would be different if there were differences in the rates of inactivation of these peptides in this tissue. Obviously, verification of our conclusion and an exploitation of the pharmacological potential of this neuromodulation will have to await the availability of a selective Y_2-receptor antagonist (Grundemar & Håkanson, 1994).

Since there were no effects of the peptides tested on active and passive neuronal properties, nor on ACh- and noradrenaline-induced changes in membrane potential, these Y_2-receptors are presumed to be located presynaptically on noradrenergic nerve terminals. How these receptors are coupled to the mechanisms controlling noradrenaline release and whether, or not, NPY is released endogenously in the guinea-pig caecum remain to be explored, as does the possibility that the small non-adrenergic, non-cholinergic (NANC) slow inhibitory post-synaptic potential (Mihara *et al.*, 1987), believed to be mediated by somatostatin (Shen & Surprenant, 1993), is also affected by NPY.

The generous financial assistance of The Wellcome Trust (G.M.L.), a Grant-in-Aid for Scientific Research, International Scientific Research Program, from the Ministry of Education, Science and Culture of Japan (S.M.) and of the British Pharmacological Society (S.M.C.C.) are gratefully acknowledged.

References

BELLEAU, B., BENFEY, B.G. & MELCHIORRE, C. (1982). Presynaptic effect of clonidine antagonised by the tetramine disulphide, benextramine. *Br. J. Pharmacol.*, **75**, 617–621.

COX, H.M. (1993). The role of NPY and related peptides in the control of gastrointestinal function. In *The Biology of Neuropeptide Y and Related Peptides*. ed. Colmers, W.F. & Wahlestedt, C. & Totowa, N.J: Humana Press Inc.

COX, H.M. & CUTHBERT, A.W. (1990). The effects of neuropeptide Y and its fragments upon basal and electrically stimulated ion secretion in rat jejunum mucosa. *Br. J. Pharmacol.*, **101**, 247–252.

CUNNINGHAM, S.M.C., MIHARA, S. & LEES, G.M. (1994a). Presynaptic inhibition by neuropeptide Y of slow inhibitory synaptic transmission in submucous neurones of guinea-pig caecum. *Exp. Physiol.*, **79**, 261–264.

CUNNINGHAM, S.M.C., MIHARA, S. & LEES, G.M. (1994b). Evidence that presynaptic modulation by neuropeptide Y of inhibitory transmission in submucous ganglia of guinea-pig caecum is mediated by Y_2-receptors. *Br. J. Pharmacol.*, **112**, 528P.

DOUGHTY, M.B., CHU, S.S., MILLER, D.W., LI, K. & TESSEL, R.E. (1990). Benextramine: a long-lasting neuropeptide Y receptor antagonist. *Eur. J. Pharmacol.*, **185**, 113–114.

EDVINSSON, L., ADAMSSON, M. & JANSEN, I. (1990). Neuropeptide Y antagonist properties of D-myo-inositol-1,2,6-triphosphate in guinea-pig basilar arteries. *Neuropeptides*, **17**, 99–105.

FRIEL, D.D., MILLER, R.J. & WALKER, M.W. (1986). Neuropeptide Y: a powerful modulator of epithelial ion transport. *Br. J. Pharmacol.*, **88**, 425–431.

FRIELING, T., COOKE, H.J. & WOOD, J.D. (1991a). Electrophysiological properties of neurones of the submucosal ganglia of the guinea-pig distal colon. *Am. J. Physiol.*, **260**, G835–G841.

FRIELING, T., COOKE, H.J. & WOOD, J.D. (1991b). Synaptic transmission in submucosal ganglia of guinea-pig distal colon. *Am. J. Physiol.*, **260**, G842–G849.

FÜHLENDORFF, J., GETHER, U., AAKERLUND, L., LANGELAND-JOHANSEN, N., THOGERSEN, H., MELBERG, S.T., OLSEN, U.B., THASTRUP, O. & SCHWARTZ, T.W. (1990). [Leu[31],Pro[34]]-Neuropeptide Y: A specific Y_1 receptor agonist. *Proc. Natl. Acad. Sci. U.S.A.*, **87**, 182–186.

GARZON, J., HÖLLT, V. & SCHANCHEZ-BLAZQUES, P. (1986). Neuropeptide Y is an inhibitor of neural function in the myenteric plexus of the guinea-pig ileum. *Peptides*, **7**, 623–629.

GRUNDEMAR, L. & HÅKANSON, R. (1994). Neuropeptide Y effector systems: perspectives for drug development. *Trends Pharmacol. Sci.*, **15**, 153–159.

GRUNDEMAR, L., SHEIKH, H.P. & WAHLESTEDT C. (1993). Characterisation of receptor types for neuropeptide Y and related peptides. In *The Biology of Neuropeptide Y and Related Peptides*. ed. Colmers, W.F. & Wahlestedt, C. Totowa, N.J.: Humana Press Inc.

HOLZER, P., LIPPE, T.H., BARTHO, L. & SARIA, A. (1987). Neuropeptide Y inhibits excitatory and enteric neurons supplying the circular muscle of the guinea-pig small intestine. *Gastroenterology*, **92**, 1944–1950.

INUI, A., OKITA, M., INOUE, T., SAKATANI, N., OYA, M., MORIBKA, H., SHII, K., YOKONO, K., MIZUNO, N. & BABA, S. (1989). Characterisation of peptide YY receptors in the brain. *Endocrinology*, **124,** 402–409.

KATAYAMA, Y., LEES, G.M. & PEARSON, G.T. (1986). Electrophysiology and morphology of vasoactive-intestinal-peptide-immunoreactive neurones of the guinea-pig ileum. *J. Physiol.*, **378,** 1–11.

MESSENGER, J.P. & FURNESS, J.B. (1990). Projections of chemically-specified neurons in the guinea-pig colon. *Arch. Histol. Cytol.*, **53,** 467–495.

MICHEL, M. (1991). Receptors for neuropeptide Y: multiple subtypes and multiple second messengers. *Trends Pharmacol. Sci.*, **12,** 389–394.

MIHARA, S. (1993). Intracellular recording from neurones of the submucous plexus. *Prog. Neurobiol.*, **40,** 529–572.

MIHARA, S., KATAYAMA, Y. & NISHI, S. (1985). Slow synaptic potentials in neurones of submucous plexus of guinea-pig caecum and their mimicry by noradrenaline and various peptides. *Neuroscience*, **16,** 1057–1068.

MIHARA, S., NISHI, S., NORTH, R.A. & SURPRENANT, A. (1987). A non-adrenergic, non-cholinergic slow inhibitory post-synaptic potential in neurones of the guinea-pig submucous plexus. *J. Physiol.*, **390,** 357–365.

MORRIS, J.L. & GIBBINS, I.L. (1992). Cotransmission and neuromodulation. In *Autonomic Neuroeffector Mechanisms*. ed. Burnstock, G. & Hoyle, C.H.V. Chur, Switzerland: Harwood Academic Publishers.

NORTH, R.A. & SURPRENANT, A. (1985). Inhibitory synaptic potentials resulting from α_2-adrenoceptor activation in guinea-pig submucous plexus neurones. *J. Physiol.*, **358,** 17–32.

SCHEMANN, M. & TAMURA, K. (1992). Presynaptic inhibitory effects of the peptides NPY, PYY and PP on nicotinic EPSPs in guinea-pig gastric myenteric neurones. *J. Physiol.*, **451,** 79–89.

SHEN, K.-Z. & SURPRENANT, A. (1993). Somatostatin-mediated inhibitory postsynaptic potential in sympathetically-denervated guinea-pig submucosal neurones. *J. Physiol.*, **470,** 619–635.

WAHLESTEDT, C. & REIS, D.R. (1993). Neuropeptide Y-related peptides and their receptors – are the receptors potential therapeutic drug targets? *Annu. Rev. Pharmacol. Toxicol.*, **32,** 309–352.

WILEY, J. & OWYANG, C. (1987). Neuropeptide Y inhibits cholinergic transmission in the isolated guinea-pig colon: mediation through α-adrenergic receptors. *Proc. Natl. Acad. Sci. U.S.A.*, **84,** 2047–2051.

(Received May 24, 1994
Revised July 8, 1994
Accepted July 26, 1994)

Br. J. Pharmacol. (1994), **113**, 889–897 © Macmillan Press Ltd, 1994

Regional and species differences in glyburide-sensitive K^+ channels in airway smooth muscles as estimated from actions of KC 128 and levcromakalim

[1]Kenshi Kamei, Shohshin Yoshida, Jun-ichi Imagawa, Hiroyuki Nabata & Hirosi Kuriyama

Fuji-Gotemba Research Laboratories, Chugai Pharmaceutical Co. Ltd., 1– 135, Komakado, Gotemba, Shizuoka, 412, Japan

1 The purpose of the present experiments was to elucidate the differences in actions of two K^+ channel openers, KC 128 and levcromakalim, on the carbachol-induced contraction, membrane potential and $^{86}Rb^+$ efflux of the dog tracheal and bronchial smooth muscles. Furthermore, we compared the effects of these agents on guinea-pig and human airway smooth muscles.

2 In the dog tracheal and bronchial smooth muscle tissues, levcromakalim induced a concentration-dependent relaxation of the carbachol-induced contraction. The IC_{50} values were 0.35 μM (pIC_{50}: 6.46 ± 0.10, $n = 9$) and 0.55 μM (pIC_{50}: 6.26 ± 0.07, $n = 5$), respectively. KC 128 relaxed bronchial smooth muscles precontracted by carbachol with an IC_{50} value of 0.19 μM (pIC_{50}: 6.73 ± 0.10, $n = 7$). However, KC 128 had almost no effect on the contraction evoked by carbachol in the trachea ($IC_{50} > 10$ μM). The relaxations induced by levcromakalim and KC 128 were antagonized by glyburide (0.03–1 μM) but not by charybdotoxin (100 nM).

3 Levcromakalim (1 μM) hyperpolarized the membrane of both dog tracheal and bronchial smooth muscle cells, whereas KC 128 (1 μM) hyperpolarized the membrane of bronchial but not of tracheal smooth muscle cells.

4 Levcromakalim (10 μM) increased $^{86}Rb^+$ efflux rate from both tracheal and bronchial smooth muscle tissues but KC 128 (10 μM) increased $^{86}Rb^+$ efflux rate only from bronchial and not tracheal smooth muscle tissues. Glyburide (1 μM) prevented the hyperpolarization and the $^{86}Rb^+$ efflux induced by these agents at the same concentration as observed for mechanical responses.

5 Both KC 128 and levcromakalim relaxed the guinea-pig isolated tracheal smooth muscles precontracted by carbachol (100 nM), histamine (3 μM) or U46619 (10 nM). KC 128 was approximately 10 times more potent than levcromakalim for each agonist.

6 In human bronchial smooth muscles, levcromakalim but not KC 128 induced a concentration-dependent relaxation of the carbachol-induced contraction.

7 It is concluded that KC 128 has relaxant and hyperpolarizing effects in the dog bronchial and guinea-pig tracheal smooth muscles, but not in the dog tracheal and human bronchial smooth muscles. On the other hand, levcromakalim acts consistently on all the above airway smooth muscle tissues. These results indicate that there are regional and species differences in distribution of K^+ channels, and at least two different K^+ channel opener- and glyburide-sensitive K^+ channels are present in the dog airway smooth muscles.

Keywords: Levcromakalim; KC 128; airway smooth muscle; K^+ channel opener (activator); membrane potential; Rb^+ efflux; glyburide

Introduction

Recently many K^+ channel openers have been developed for the treatment of diseases, such as hypertension, asthma and ischaemic heart disease (Edwards & Weston, 1990; 1993; Atwal, 1992; Quast, 1992; Small *et al.*, 1992). These drugs were thought to activate a glyburide- and ATP-sensitive K^+ channel that is not sensitive to charybdotoxin in vascular smooth muscle. However, until now there is no consensus on which K^+ channel is the common target. The target channel has been identified with a large or small conductance and as Ca^{2+}-sensitive or -insensitive in different vascular smooth muscle tissues (see reviews of Kajioka *et al.*, 1991; Edward & Weston, 1993).

For airway smooth muscles, it has also been reported that many ATP-sensitive K^+ channel openers relax the airway smooth muscles including human airway preparations (Taylor *et al.*, 1988; 1992; Black *et al.*, 1990; Black & Barns, 1990; Small *et al.*, 1992). When we examined the relaxant effect of bronchodilators including K^+ channel openers, we have often used guinea-pig tracheal smooth muscle tissues, because they have spontaneous tone that is similar to human airway preparations. However, the differences between guinea-pig and human airway preparations have often been pointed out. Concerning the K^+ channel openers, the relaxant effect of these agents on carbachol-induced contraction is reported to be weaker in guinea-pig than in human preparations (Taylor *et al.*, 1988; 1992; Black *et al.*, 1990; Imagawa *et al.*, 1993). Recently, we have reported that in the dog tracheal smooth muscle tissues, the action of K^+ channel openers shows greater similarity to human bronchi than to guinea-pig tracheal smooth muscle (Kamei *et al.*, 1994).

KC 128 (N-cyano-*N'*,*N''*,2,2-tetramethyl-6-nitro-2*H*-1-benzopyran-4-carboxamidine) has recently been synthesized in our laboratory based on computer-assisted analysis of the pharmacophore model of K^+ channel openers (Koga *et al.*, 1993a,b). We examined the effect of KC 128 and levcromakalim (Figure 1) on the electrical and mechanical properties of the dog tracheal and bronchial smooth muscles. Furthermore, we compared the effects of these compounds on the guinea-pig and human airway smooth muscles.

[1] Author for correspondence.

Methods

Tissue preparation

Dog airway preparations Adult beagle dogs of either sex, (8–15 kg, CSK) were anaesthetized by i.v. administration of pentobarbitone (35 mg kg^{-1}) and exsanguinated. Segments of tracheal smooth muscle were prepared for all experiments as previously described (Kamei *et al.*, 1994). Briefly, circular muscle strips were excised from the cervical part of the trachea and immediately placed in Krebs-Henseleit solution. Tracheal smooth muscle tissues were dissected from both ends of the cartilage, then carefully freed of fat and connective tissue in a dissecting chamber under a binocular microscope. The preparation was cut into segments, 2–3 mm wide and 10 mm long, in the transverse direction. Bronchi were excised from the third or fourth branches (diameter; 1–3 mm) and were cleaned. These ring preparations were used to record the mechanical responses and the preparations, which were cut along the longitudinal axis, were used for measurement of $^{86}Rb^+$ efflux. For electrical response recording, following removal of cartilage and connective tissues the bronchial smooth muscle tissues were prepared and cut into segments, 3–5 mm wide and 5 mm long, in the transverse direction.

Guinea-pig tracheal preparations Male guinea-pigs (500–1000 g, Hartley, CRJ) were killed by a blow to the head and exsanguinated. The trachea was removed and immediately placed in Krebs-Henseleit solution and carefully freed of fat and connective tissue. The trachea was cut along the longitudinal axis directly opposite the smooth muscle layer for tension recording (Imagawa *et al.*, 1993).

Human bronchus preparations Human lung tissues were obtained from patients undergoing surgery for carcinoma of the lung and maintained at 4°C overnight in Krebs-Henseleit solution before use. Bronchi (diameter; 1–5 mm) were dissected free of adhering fat and connective tissue and cut into ring preparations (Imagawa *et al.*, 1993).

Mechanical response recording

Dog airways Dog tracheal smooth muscle tissues were suspended in organ baths containing Krebs-Henseleit solution (35°C) and mounted vertically with the ends tied by silk thread. Ring preparations of dog bronchial smooth muscle were cannulated and fixed by a pair of fine L-shaped needles. One end of each preparation was tied to an isometric mechanotransducer (TB-911T, Nihon Kohden, Tokyo, Japan) and the other end to the bottom of the bath. Resting tension was maintained at 0.5 g in both tissues. Tension recordings were started after repetitively applied 60 mM K^+ produced a consistent amplitude of contraction (about 2–3 h were required after placing the tissues in the bath). For experiments on the inhibitory effects of KC 128 or levcromakalim on precontracted smooth muscles, tracheal and bronchial smooth muscle were exposed to 100 nM and 300 nM carbachol, respectively, which induced about 70% of the maximum contraction of each preparation. When a stable amplitude of tone had been achieved, inhibitory, concentration-response curves were constructed for cumulative doses of KC 128 or levcromakalim. To observe the effects of glyburide, charybdotoxin or RbCl on the KC 128- or levcromakalim-induced relaxation (of the carbachol-induced contraction), these agents were applied 15 min before application of KC 128 or levcromakalim and throughout the experiments. Maximum relaxation was obtained by application of 1 mM aminophylline at the end of each experiment.

Guinea-pig trachealis Guinea-pig tracheal smooth muscle tissues were suspended in organ baths (capacity 10 ml) containing Krebs-Henseleit solution (35°C) and incubated with indomethacin (3 μM) for 60 min to inhibit spontaneous tone generated by prostaglandins (Farmer *et al.*, 1974). The tissues were placed under 1 g initial tension and were connected to TB-911T (Nihon Kohden). Following the 60–90 min stabilization period, tone was generated by the application of carbachol (100 nM), histamine (3 μM) or U46619 (10 nM). These concentrations induced about 70% of the maximum contraction for each agonist. When a stable amplitude of tracheal tone had been achieved, inhibitory concentration-response curves were constructed with cumulative doses of KC 128 or levcromakalim. Maximum relaxation was obtained by application of 1 mM aminophylline given at the end of each experiment.

Human bronchi Ring preparations of human bronchial smooth muscles were suspended in organ baths in a similar way to the dog bronchial smooth muscle preparations and resting tension was maintained at 1 g. After a 90 min stabilization period, the bronchi were exposed to 300 nM carbachol which also induced about 70% of the maximum contraction. When a stable amplitude of the tone had been achieved, inhibitory concentration-response curves were constructed with cumulative doses of KC 128 or levcromakalim. The maximum relaxation was obtained by application of 1 mM aminophylline at the end of each experiment.

Electrophysiological response recording

The membrane potential from single smooth muscle cells was recorded with glass capillary microelectrodes (Glass Filament 1.0X100, 6010, A-M System, Inc. WA, U.S.A.) filled with 3 M KCl and with tip resistance of 30–50 MΩ. The microelectrode was held in an electrode-holder (MEH-1S10, World Precision Instruments, Inc., New Haven, U.S.A.) connected to a high input impedance preamplifier (NEZ-7200, Nihon Kohden). Signals from the preamplifier were recorded on a chart recorder (model VP-6538, Panasonic, Yokohama, Japan). The tissue was pinned onto a rubber plate in a chamber (2 ml bath volume) and superfused with Krebs-Henseleit solution (35°C) at a flow rate of 3 ml min^{-1}. The electrode was inserted into smooth muscle cells from the inner surface of the tracheal tissue and from the outer surface of bronchial tissue. To observe the effect of KC 128 or levcromakalim on the membrane potential in normal Krebs-Henselit solution ($[K^+]_{out}$ = 6.0 mM), the solution containing the agent was superfused for longer than 15 min before measurements of the membrane potential were made. When the effects of KC 128 or levcromakalim on the membrane potential in low K^+ solution were examined, low K^+ solution ($[K^+]_{out}$ = 1.2 mM) was superfused up to 20 min before application of the agent. After a stable level of the membrane potential had been achieved, superfusion of the solution containing the agent was started. To observe the effects of glyburide on the KC 128- or levcromakalim-induced membrane potential changes, glyburide was added to the superfusing fluid 15 min before application of the solution containing KC 128 or levcromakalim with glyburide.

Measurement of $^{86}Rb^+$ efflux rate

Segments of tracheal or bronchial smooth muscles were loaded with $^{86}Rb^+$ (74 MBq ml^{-1}) at 35°C for 180 min in Krebs-Henseleit solution bubbled with 95% O_2 and 5% CO_2. After loading with $^{86}Rb^+$, the tissue was pinned onto a rubber plate in a chamber filled with 2 ml Krebs-Henselit solution, and the solution was replaced with fresh Krebs-Henseleit solution every 3 min. The 8th–13th replacing solutions contained vehicle, KC 128 or levcromakalim. When the effect of glyburide on KC 128- or levcromakalim-induced $^{86}Rb^+$ efflux was examined, a solution containing glyburide (1 μM) was used as all the replacing solutions. The radioactivity of each replacing solution was counted by a liquid scintillation counter. At the end of experiments, the tissues

were solubilized with Soluen 350 (Packard) overnight at 35°C, then the radio activity of $^{86}Rb^+$ remaining in the tissues was measured.

Drugs and solutions

KC 128 (*N*-cyano-*N'*,*N'*,2,2-tetramethyl-6-nitro-2*H*-1-benzopyran-4-carboxamidine) and levcromakalim were synthesized in our laboratory (Fuji-Gotemba research Labs, Gotemba, Japan) (Figure 1). KC 128, levcromakalim and glyburide were dissolved to 10–20 mM in DMSO (dimethylsulphoxide). The maximum final concentration of DMSO was 0.5%. Carbachol (carbamylcholine chloride, Tokyo Kasei Co., Tokyo, Japan), charybdotoxin (Peptide Institute Inc., Osaka, Japan) and aminophylline (Sigma Chemical Co., St. Louis, MO, U.S.A.) were dissolved in Krebs-Henseleit solution. Solutions were freshy prepared before each experiment except for the solution containing 100 μM charybdotoxin which was stored at − 20°C and used within one week.

The Krebs-Henseleit solution used in all experiments had the following composition (mM): Na^+ 143.8, K^+ 6.0, Ca^{2+} 2.5, Mg^{2+} 1.2, Cl^- 128.8, HCO_3^- 24.8, $H_2PO_4^-$ 1.2 and glucose 10.0. Solutions containing various concentrations of K^+ were prepared by replacing NaCl with KCl isosmotically. All these solutions were bubbled with 95% O_2 and 5% CO_2, and their pH maintained at 7.4.

Statistical analysis

The concentration of drug required to produced half-maximum inhibition (IC_{50}) was calculated by linear regression analysis applied to the linear portion of each concentration-response curve. The negative logarithm of the IC_{50} value (pIC_{50}) is expressed as mean ± s.e.mean of the number (n) of observations. The significance of differences between means was assessed by Student's t test. Values of $P<0.05$ were considered statistically significant.

Results

Relaxant effects on dog tracheal and bronchial smooth muscles

Figure 2 shows the relaxant effects of levcromakalim and KC 128 on the dog tracheal and bronchial smooth muscles precontracted by carbachol. Levcromakalim induced concentration-dependent relaxation in both tracheal and bronchial preparations in the same concentration range. The IC_{50} values were 0.35 μM (pIC_{50}; 6.46 ± 0.10, $n=9$) and 0.55 μM (pIC_{50}; 6.26 ± 0.07, $n=5$), and the maximum relaxations were 96.5 ± 0.6% and 93.9 ± 2.1%, respectively. However, KC 128-induced relaxation occurred to a greater extent in bronchial (IC_{50}; 0.19 μM, pIC_{50}; 6.73 ± 0.10, maximum relaxation; 90.9 ± 2.9%, $n=7$) than in tracheal smooth muscle ($IC_{50}>10$ μM). The relaxant effect of KC 128 was observed in epithelial cell-denuded bronchial smooth muscle (data not shown). In the tracheal smooth muscle, high concentration of KC 128 (30 μM) produced only a transient relaxation.

The relaxation induced by levcromakalim in bronchial smooth muscle was antagonized by glyburide (Figure 3a). The IC_{50} values measured in the absence and presence of glyburide (0.03, 0.1, 0.3, 1 μM) were 0.55 μM (pIC_{50}; 6.26 ± 0.04, $n=5$), 0.91 μM (pIC_{50}; 6.04 ± 0.11, $n=4$), 2.34 μM (pIC_{50}; 5.63 ± 0.12, $n=4$), 8.91 μM (pIC_{50}; 5.05 ± 0.09, $n=5$) and 30.9 μM (pIC_{50}; 4.51 ± 0.10, $n=7$), respectively. The maximum relaxations reached 85% of that induced by aminophylline (1 mM). Glyburide produced a rightward parallel shift of the concentration-relaxation curves of levcromakalim on the carbachol-induced contraction in bronchial smooth muscles ($pA_2=7.50$). Glyburide also inhibited the relaxant action of KC 128 in a concentration-dependent manner (Figure 3b). However the inhibitory action was different from that of the levcromakalim-induced relaxation, since the maximum relaxation induced by KC 128 was markedly reduced by glyburide, but the levcromakalim-induced maximum relaxation was not. Charybdotoxin (100 nM), a blocker of the large conductance Ca^{2+}-activated K^+ channel, had no effect on the relaxant actions of either levcromakalim or KC 128. The IC_{50} values of levcromakalim

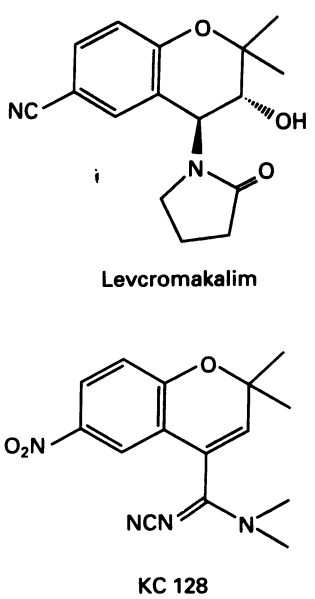


Figure 1 Chemical structures of levcromakalim and KC 128.

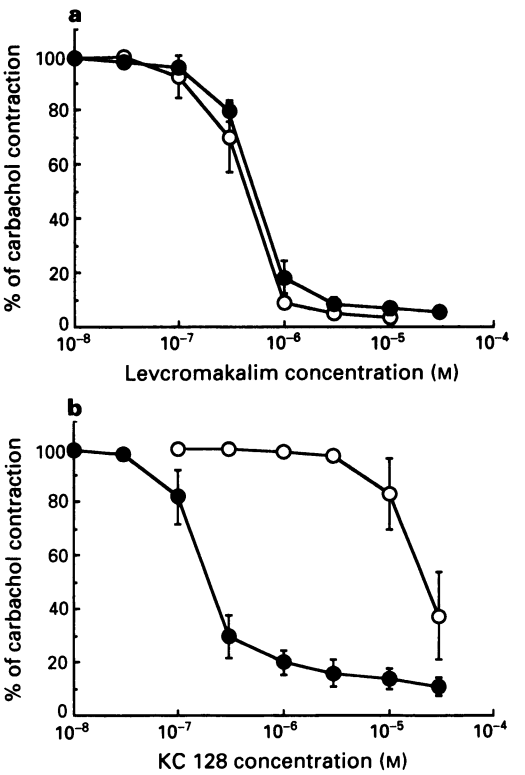


Figure 2 Concentration-dependent relaxation induced by levcromakalim (a) and KC 128 (b) in dog tracheal (○) or bronchial (●) smooth muscle tissues precontracted by carbachol (0.1 μM (tracheal), 0.3 μM (bronchial)). Each point represents the mean ± s.e.mean from 5 to 9 preparations.

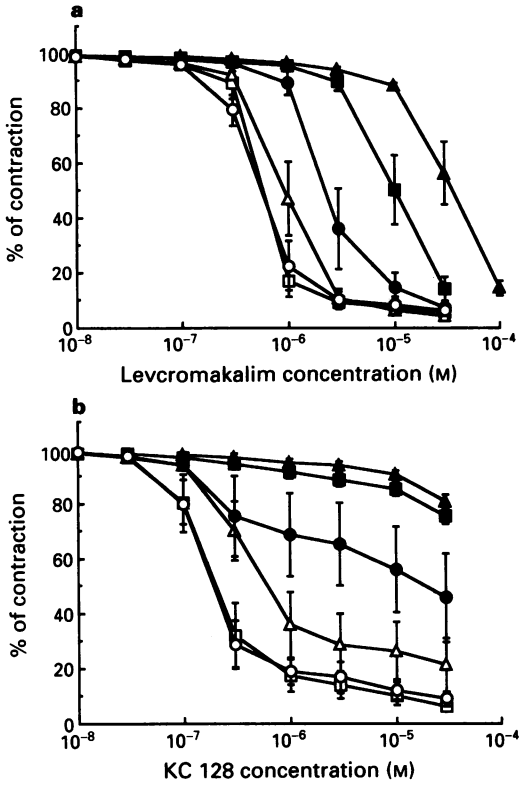


Figure 3 Concentration-dependent relaxation induced by levcromakalim (a) and KC 128 (b) in the dog bronchial smooth muscle tissues precontracted by carbachol (0.3 μM) in the absence (○) or presence of charybdotoxin (□, 0.1 μM) or glyburide (△, 0.03 μM; ●, 0.1 μM; ■, 0.3 μM; ▲, 1 μM). Each point represents the mean ± s.e.mean from 4 to 6 preparations.

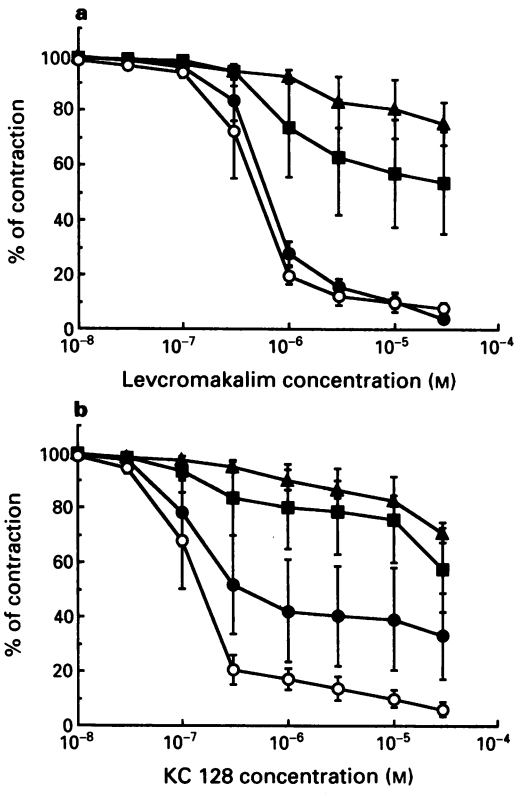


Figure 4 Effects of various concentrations of RbCl (○, vehicle; ●, 1 mM; ■, 3 mM; ▲, 5 mM) on levcromakalim- (a) and KC 128- (b) induced relaxation in dog bronchial smooth muscle precontracted by carbachol (0.3 μM). Each point represents the mean ± s.e.mean from 4 to 6 preparations.

and KC 128 in the presence of charybdotoxin were 0.55 μM (pIC_{50}; 6.26 ± 0.04, $n = 5$) and 0.21 μM (pIC_{50}; 6.67 ± 0.12, $n = 6$), respectively. These IC_{50} values were not significantly different from those observed in the absence of charybdotoxin ($P > 0.05$).

Application of RbCl (1, 3 and 5 mM) to bath solution containing 6.0 mM KCl slightly enhanced the carbachol (300 nM)-induced contraction in dog bronchial smooth muscles (102.6 ± 0.6%; $n = 11$, 106.2 ± 1.2%; $n = 11$ and 107.8 ± 1.4%; $n = 9$, respectively). The concentration-dependent relaxations induced by levcromakalim and KC 128 in dog bronchial smooth muscles were inhibited by application of RbCl in a concentration-dependent manner (Figure 4), but such inhibitions were not observed with application of additional KCl (1–5 mM). The inhibitory effect of RbCl on the concentration-relaxation curves of KC 128 was not different from that of levcromakalim, but the inhibitory effects of RbCl on the KC 128-induced relaxation was more potent than on that of levcromakalim.

Effects on the membrane potential of dog airway smooth muscle cells

The membranes of the dog tracheal and bronchial smooth muscle cells were electrically quiescent. In normal Krebs-Henseleit solution ($[K^+]_{out} = 6.0$ mM), the mean resting membrane potential of tracheal smooth muscle cells was − 60.2 ± 0.8 mV ($n = 21$) and that of bronchial smooth muscle cells was − 70.0 ± 0.7 mV ($n = 16$). The resting membrane potential of bronchi was significantly higher than trachea by about 10 mV ($P < 0.05$). In low K^+ solution ($[K^+]_{out} = 1.2$ mM), the membrane potential did not change in tracheal smooth muscle cells (− 60.8 ± 0.8 mV, $n = 10$). However, a small but significant hyperpolarization was observed (− 75.4 ± 1.7 mV, $n = 8$) in bronchial smooth muscle cells ($P < 0.05$).

In tracheal smooth muscle, levcromakalim (> 0.1 μM) hyperpolarized the membrane in a concentration-dependent manner in both normal and low K^+ solution (Figure 5a and b, closed circle and Figure 6). The levcromakalim-induced hyperpolarization in the low K^+ solution was larger than that in normal K^+ solution. However, in the case of KC 128, hyperpolarization was observed in neither normal nor low K^+ solution (< 10 μM). On the other hand, in bronchial smooth muscles, KC 128 (> 0.3 μM) hyperpolarized the membrane to a small extent in normal K^+ solution and markedly hyperpolarized it in low K^+ solution, and effect similar to that produced by levcromakalim (Figure 5c and d and Figure 6). Glyburide (1 μM) depolarized the membrane of bronchial smooth muscle cell from − 75.4 mV to − 69.5 mV ($n = 2$). The hyperpolarizations induced by KC 128 (1 μM) or levcromakalim (1 μM) were inhibited with application of glyburide (1 μM) (Figure 6b). However, the levcromakalim (1 μM)-induced hyperpolarization was not suppressed by the pretreatment of KC 128 (1, 3 μM, Figure 6).

Effects on $^{86}Rb^+$ efflux from dog airway smooth muscles

Figure 7 shows the effects of KC 128 (10 μM) and levcromakalim (10 μM) on $^{86}Rb^+$ efflux rate in the absence or presence of glyburide (1 μM) from the dog tracheal and bronchial smooth muscles. The efflux rate settled to a low and almost constant value about 20 min after starting to replace the solution. The averages of $^{86}Rb^+$ efflux rate before application of drugs (basal value, 24 min) were 0.65 ± 0.04% min^{-1} ($n = 18$) and 0.99 ± 0.02% min^{-1} ($n = 18$) from tracheal and bronchial smooth muscle tissues, respectively.

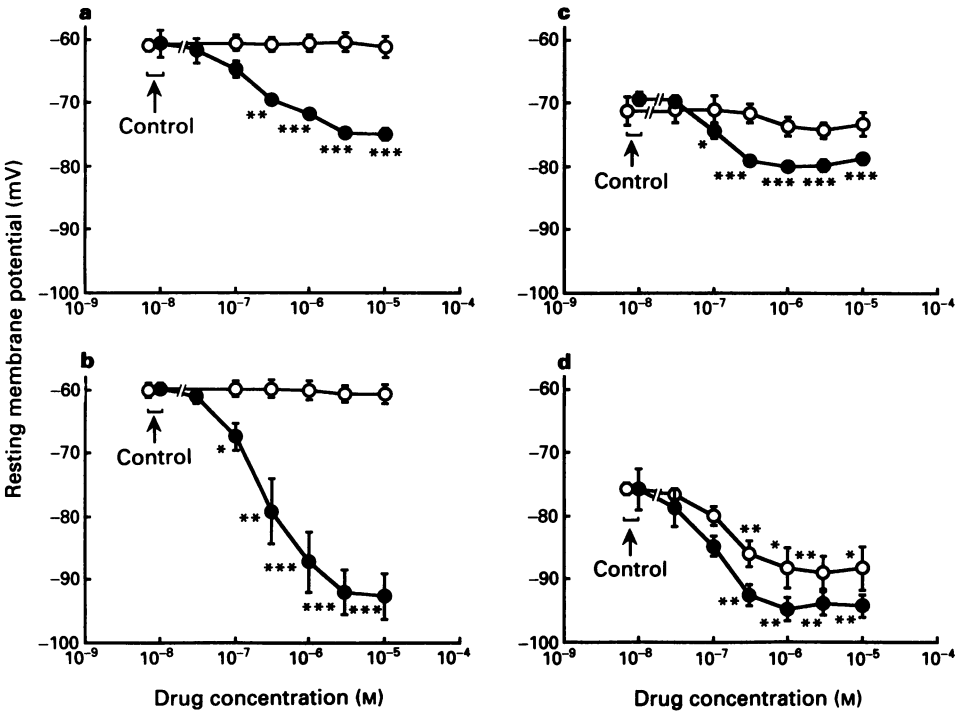


Figure 5 Effects of levcromakalim (●) and KC 128 (○) on the membrane potential of the dog tracheal (a and b) or bronchial smooth muscle cells (c and d) in normal ($[K^+]_{out}$ = 6.0 mM, a and c) or low K^+ ($[K^+]_{out}$ = 1.2 mM, b and d) solution. Each point represents the mean ± s.e.mean from 4 to 6 preparations. Control values represent the membrane potential before treatment with drugs. $^*P<0.05$, $^{**}P<0.01$ and $^{***}P<0.001$ for comparison with the control value.

The basal value of the efflux rate from tracheal smooth muscle tissues was significantly larger than that from bronchial smooth muscle tissues ($P<0.05$).

Levcromakalim caused a significant increase of $^{86}Rb^+$ efflux rate from both tracheal and bronchial smooth muscle tissues (2.16 ± 0.22 and 1.55 ± 0.04 fold respectively at the peak compared to vehicle, $n = 6$) within 6 min of exposure to the drug. However, KC 128 produced a significant increase in efflux only from bronchial smooth muscle tissues (1.33 ± 0.07 fold, $n = 6$) within 9 min of exposure to the drug. This was similar to levcromakalim, but the increase induced by KC 128 was lower than induced by levcromakalim ($P<0.05$). On the other hand, there was no change in the efflux rate in tracheal smooth muscle tissues exposed to KC 128 for 15 min.

In the presence of glyburide (1 μM), the basal values of $^{86}Rb^+$ efflux rate were 0.59 ± 0.04% min^{-1} ($n = 6$) and 0.97 ± 0.04% min^{-1} ($n = 6$) from tracheal and bronchial smooth muscle tissues, respectively. There was no difference between tissues in the absence and presence of glyburide. However, glyburide inhibited the increase of $^{86}Rb^+$ efflux rate induce by KC 128 and levcromakalim in both tissues.

Comparison of the relaxant effects on the guinea-pig and human airway tissues contracted by carbachol

Levcromakalim relaxed the guinea-pig tracheal smooth muscles precontracted by carbachol (100 nM), histamine (3 μM) and U46619 (10 nM) in a concentration-dependent manner with IC_{50} values of 1.58 μM, 0.66 μM and 0.83 μM, respectively (Table 1). KC 128 also relaxed the guinea-pig tracheal smooth muscle with IC_{50} values of 0.19 μM, 0.07 μM and 0.08 μM, respectively (Table 1). The potency of KC 128 was approximately 10 times higher than that of levcromakalim as estimated from the IC_{50} value on any agonist-induced contraction. The maximum relaxations occurring on application of either levcromakalim or KC 128 to tissues contracted by U46619 were roughly the same ($P>0.05$), and were greater than the effects on the carbachol and histaime-induced contractions ($P<0.05$). However, the maximum relaxations induced by KC 128 on the carbachol- and histamine-induced contractions were less than those induced by levcromakalim.

Levcromakalim caused concentration-dependent relaxation in the dog tracheal, bronchial, guinea-pig tracheal and human bronchial smooth muscles contracted with carbachol (Figure 8a). Concentrations of carbachol in each preparation induced about 70% of maximum contraction (see Methods). Both the potency and maximum relaxation of levcromakalim in the dog tracheal smooth muscles were almost equal to those in dog bronchial smooth muscles. In the human bronchial smooth muscles, the potency was similar to that in dog airway preparations. In the guinea-pig tracheal smooth muscles, both the potency and maximum relaxation were significantly weaker than those in dog tracheal and bronchial preparations.

KC 128 caused concentration-dependent relaxation only in the dog bronchial and the guinea-pig tracheal smooth muscle tissues but not in other preparations, but the maximum relaxation was smaller in the guinea-pig tracheal smooth muscle than in the dog bronchial smooth muscle (Figure 8b).

Discussion and conclusions

Differences in electrical properties and action of K^+ channel openers between tracheal and bronchial smooth muscle cells

Although the membranes of both dog tracheal and bronchial smooth mucle cells were electrically quiescent, the resting membrane potential of the bronchial smooth muscle cells was more negative than that of tracheal smooth muscle cells by about 10 mV in normal Krebs-Henseleit solution. Moreover the basal $^{86}Rb^+$ efflux from the bronchial smooth muscle tissues was also larger than that from the tracheal smooth muscle tissues. Xie *et al.* (1992) reported that the resting

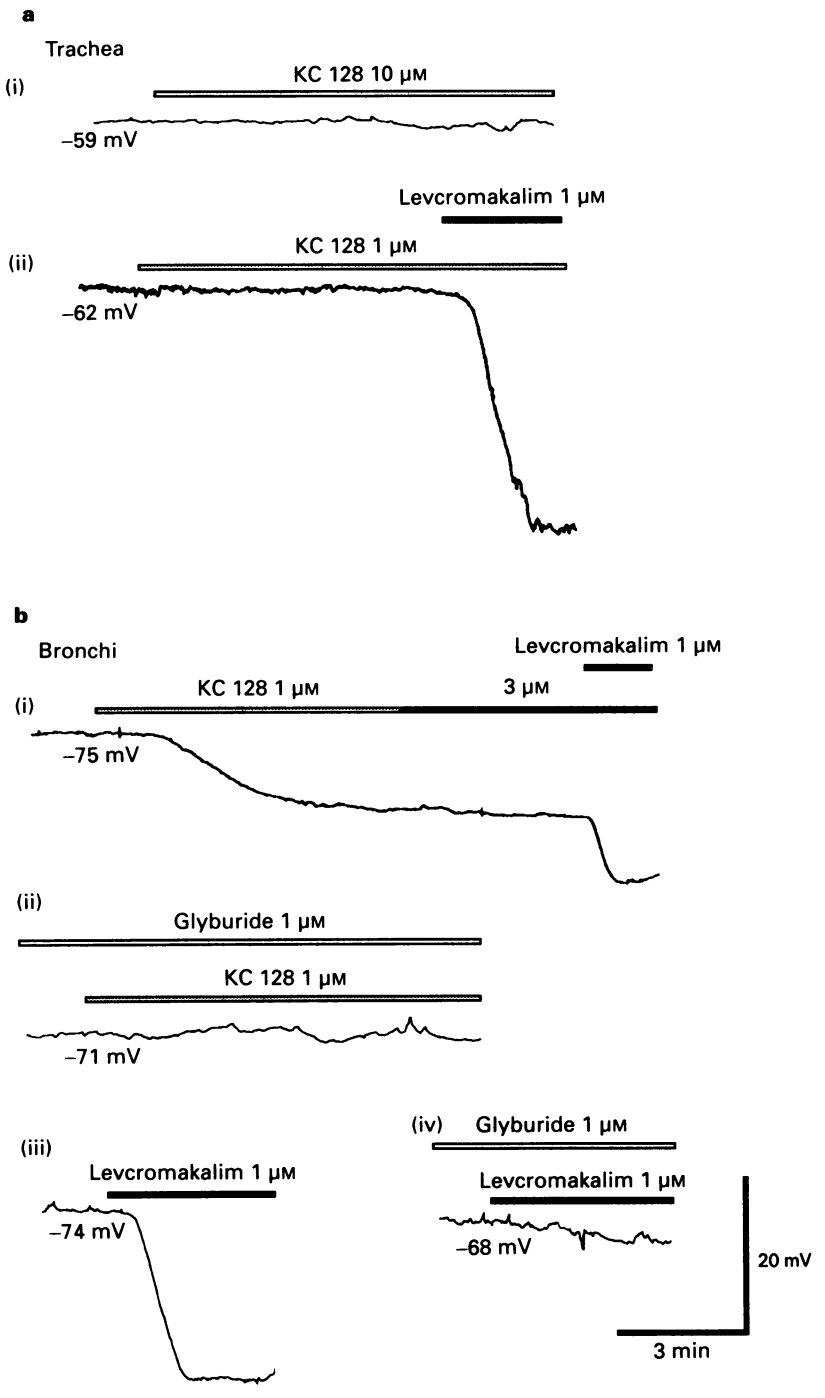


Figure 6 Effects of levcromakalim and KC 128 on the membrane potential of dog tracheal (a) and bronchial (b) smooth muscle cells in low K^+ solution ($[K^+]_{out}$ = 1.2 mM). Bars indicate application of levcromakalim, KC 128 or glyburide. The resting membrane potential before application of levcromakalim or KC 128 is indicated in each trace.

membrane potential of the dog bronchiole with epithelium was higher than that without epithelium, and they postulated that a hyperpolarizing factor is released from the epithelial cells. The bronchial preparation we used in this study also had intact epithelial cells, so the higher resting membrane potential of bronchial smooth muscle cells may be due to an epithelial-drived hyperpolarizing factor that activates the K^+ channels.

Levcromakalim induced concentration-dependent relaxations in the dog tracheal and bronchial preparations precontracted by carbachol in the same concentration-range and was able to relax each preparation almost completely. These effects of levcromakalim on the dog were more potent than on the guinea-pig tracheal smooth muscles. In the dog bronchial smooth muscle, there was a parallel shift of the concentration-relaxation curve to levcromakalim to the right on application of glyburide in a concentration-dependent manner. Furthermore, the levcromakalim-induced hyperpolarization in both tracheal and bronchial tissues occurred in a concentration-dependent manner and this hyperpolarization was enhanced in low K^+ solution. These hyperpolarizing actions were inhibited by glyburide. The increases of $^{86}Rb^+$ efflux rate from both tissues induced by levcromakalim was inhibited by glyburide. These results indicate that dog tracheal and bronchial smooth muscle possess glyburide-sensitive K^+ channels and these are opened by levcromakalim.

In contrast, only in bronchial smooth muscle was the relaxant effect of KC 128 observed in the same

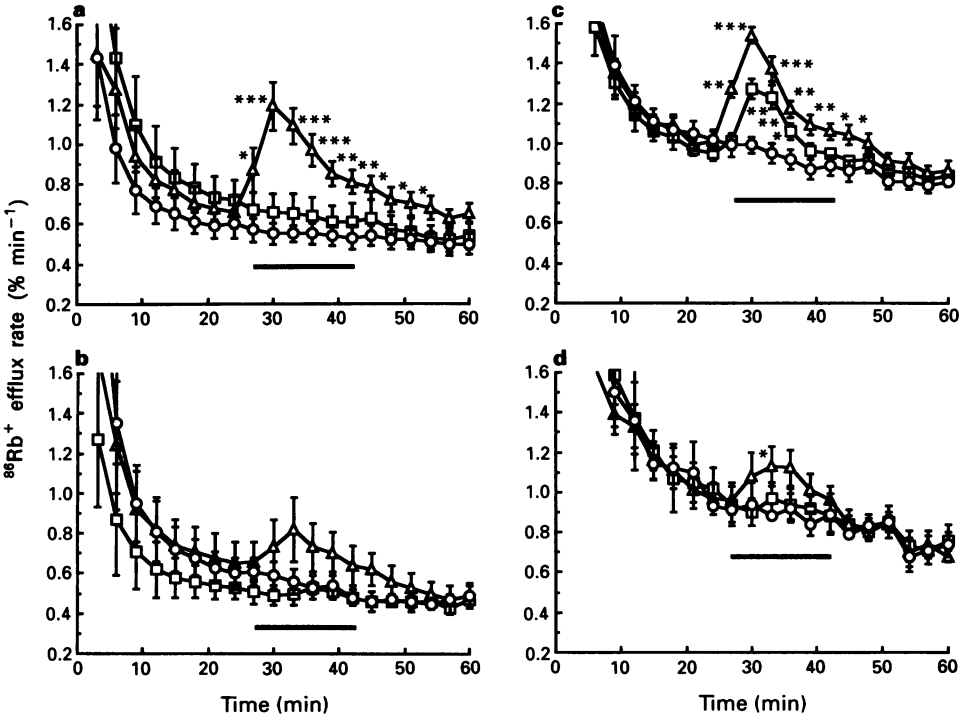


Figure 7 Effects of vehicle (○), levcromakalim (△) and KC 128 (□) on the $^{86}Rb^+$ efflux rate from the dog tracheal (a.b) and bronchial (c,d) smooth muscle cells in the absence (a and c) and presence of glyburide (b and d). Bars indicate application of levcromakalin or KC 128. Each point represents the mean ± s.e.mean from 4 to 6 preparations. $^*P<0.05$, $^{**}P<0.01$ and $^{***}P<0.001$ for comparison with value of vehicle only for each point.

Table 1 The effects of levcromakalim and KC 128 on agonist-induced contraction in guinea pig tracheal smooth muscle

	Levcromakalim			*KC 128*		
Agonist	pIC_{50} (−log[M])	*Max* (%)	(n)	pIC_{50} (−log[M])	*Max* (%)	(n)
Carbachol	−5.80 ± 0.06	69.1 ± 4.5	(7)	−6.73 ± 0.10***	49.8 ± 4.9*	(6)
Histamine	−6.18 ± 0.10	76.0 ± 3.4	(7)	−7.16 ± 0.07***	57.2 ± 3.1*	(6)
U46619	−6.05 ± 0.08	91.5 ± 1.5	(7)	−7.11 ± 0.07***	89.7 ± 3.9	(6)

The concentration of each agonist induced about 70% of maximum contraction. Each pIC_{50} value is the negative logarithm of the IC_{50} value. Maximum relaxation (Max) is expressed as a percentage of relaxation induced by aminophylline (1 mM). Values are expressed as the mean ± s.e.mean of 6 or 7 preparations (*n*). $^*P<0.05$, $^{**}P<0.01$, $^{***}P<0.001$ compared to the response to levcromakalim for each agonist.

concentration-range as in the guinea-pig tracheal smooth muscle. The dog tracheal smooth muscle was less sensitive to KC 128, but high concentrations (10–30 μM) of KC 128 induced a transient relaxation in tracheal smooth muscle precontracted by carbachol. Presumably, high concentrations of KC 128 may be nonspecific relaxing actions. KC 128 hyperpolarized the membrane of bronchial smooth muscle cells but not of tracheal smooth muscle cells. Furthermore, a KC 128-induced increase of $^{86}Rb^+$ efflux was observed only from bronchial smooth muscle tissues. The relaxation, hyperpolarization and increase of $^{86}Rb^+$ efflux rate were all attenuated by the presence of glyburide. These findings suggested that KC 128 relaxed selectively the bronchial smooth muscle mainly by opening the glyburide-sensitive K^+ channel.

The concentration-dependent inhibition by glyburide of the KC 128-induced relaxation differed from the inhibition of the levcromakalim-induced relaxation. The levcromakalim-induced relaxation was antagonized by glyburide apparently in a competitive manner in bronchial smooth muscles, whereas the inhibition by glyburide of the KC 128-induced relaxation was not competitive and the maximum relaxation induced by KC 128 was suppressed by glyburide. KC 128-induced hyperpolarization and increase of $^{86}Rb^+$ efflux rate were smaller than levcromakalim. However, in the dog airway smooth muscle pretreated by KC 128 (1 or 3 μM), the levcromakalim (1 μM)-induced hyperpolarization was observed to the same extent as that in untreated cells in the low K^+ solution (Figure 5 and 6). Furthermore in preliminary experiments, we confirmed that levcromakalim-induced relaxation was not modified by KC 128 (0.3, 1, 3 μM) in tracheal smooth muscles. Thus KC 128 does not antagonize the action of levcromakalim and KC 128 may not be a 'partial K^+ channel opener'.

Recently, it was reported that the K^+ channel opener and glyburide bind to different sites on the ATP-sensitive K^+ channel and were coupled in a negatively allosteric manner (Gopalakrishnan *et al.*, 1991; Bray & Quast, 1992; Schwanstecher *et al.*, 1992). Therefore, it is plausible to postulate that in the dog bronchial smooth muscle, a glyburide-sensitive K^+ channel may have more than one binding site for K^+ channel openers. The glyburide-sensitive K^+ channel in bronchial smooth muscle may differ from that in the dog tracheal smooth muscle. The K^+ channel activated by KC 128 may also be different from that activated by levcromakalim. Both levcromakalim- and KC 128-sensitive and also glyburide-

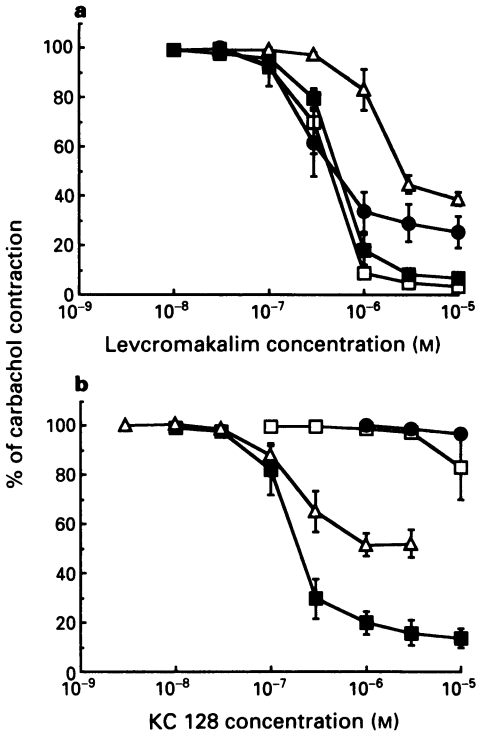


Figure 8 Comparison of the relaxant effects of levcromakalim (a) and KC 128 (b) on the bronchial smooth muscle tissues of dog (■) and human (●), and on the tracheal smooth muscle tissues of dog (□) and guinea-pig (△). Each point represents the mean ± s.e.mean from 3 to 7 preparations.

sensitive K^+ channels may be distributed in bronchial smooth muscle, but in tracheal smooth muscle there may be no KC 128- and glyburide-sensitive K^+ channels.

Foster *et al.* (1992) have reported that cromakalim opens two populations of potassium channels in the guinea-pig tracheal smooth muscle, one of which is susceptible to blockade by Rb^+ and one of which is not. Both KC 128- and levcromakalim-induced relaxations were inhibited by RbCl in a concentration-dependent manner (1–5 mM) in dog bronchial smooth muscle tissues. The inhibition was similar to each, therefore it is difficult to distinguish these two channels by the sensitivity to Rb^+ in the present experiments.

Distribution of KC 128-sensitive K^+ channel in various airway tissues

Generally, ATP-sensitive K^+ channel openers, including levcromakalim, have been reported to be not very effective on cholinoceptor agonist-induced contraction in the guinea-pig tracheal smooth muscle (Allen *et al.*, 1986; Nielsen-Kudsk *et al.*, 1988; Paciorek *et al.*, 1990; Taylor *et al.*, 1992; Imagawa *et al.*, 1993). It has also been reported that the relaxant effects of K^+ channel openers in airway tissues were largely dependent on the concentration of agonist used (Raeburn & Brown, 1991). Therefore in the present experiments the concentration of each agonist used was chosen to induce 70% of the maximum contraction. Under these conditions, we confirmed that the relaxant effects of levcromakalim on the carbachol-induced contraction in the guinea-pig tracheal smooth muscle were less potent that those on the histamine- and U46619-induced contraction.

Glyburide-sensitive K^+ channels have been reported to be widely distributed in airway smooth muscle of many species, including guinea-pig, dog, human, bovine and others (Allen *et al.*, 1986; Black *et al.*, 1990; Longmore *et al.*, 1991; Taylor *et al.*, 1992). Levcromakalim and other K^+ channel openers have been reported to relax almost any airway smooth muscles. In our experiment, levcromakalim relaxed the dog tracheal, bronchial, guinea-pig tracheal and human bronchial smooth muscle tissues precontracted by carbachol. However, KC 128 relaxed only the guinea-pig tracheal and dog bronchial smooth muscles in the same concentration-range. These results suggested that the dog tracheal and human bronchial muscles possess only the levcromakalim-sensitive K^+ channel but not the KC 128-sensitive K^+ channel.

In summary, KC 128 and levcromakalim showed different actions on airway smooth muscles: KC 128 produced relaxation, hyperpolarization and increase in $^{86}Rb^+$ efflux in the dog bronchial smooth muscles but not in tracheal smooth muscles, whereas levcromakalim consistently relaxed both tracheal and bronchial smooth muscles. Furthermore, KC 128 relaxed precontracted guinea-pig tracheal smooth muscles but not human bronchial smooth muscles. In contrast, levcromakalim consistently relaxed both tissues. Thus, it is estimated that at least two different glyburide-sensitive K^+ channels occur in the dog airway smooth muscle.

References

ALLEN, S.L., BOYLE, J.P., CORTIJO, J., FOSTER, R.W., MORGAN, G.P. & SMALL, R.C. (1986). Electrical and mechanical effects of BRL 34195 in guinea-pig isolated trachealis. *Br. J. Pharmacol.*, **89**, 395–405.

ATWAL, K.S. (1992). Modulation of potassium channels by organic molecules. *Med. Res. Rev.*, **12**, 569–591.

BLACK, J.L., ARMOUR, C.J., JOHNSON, P.R.A., ALOUAN, L.A. & BARNS, P.J. (1990). The action of a potassium channel activator, BRL 38227 (lemakalim), on human airway smooth muscle. *Am. Rev. Respir. Dis.*, **142**, 1384–1389.

BLACK, J.L. & BARNS, P.J. (1990). Potassium channels and airway function: new therapeutic prospects. *Thorax*, **45**, 213–218.

BRAY, K.M. & QUAST, U. (1992). A specific binding site for K^+ channel openers in rat aorta. *J. Biol. Chem.*, **267**, 11689–11692.

COOK, N.S. (1988). The pharmacology of potassium channels and their therapeutic potential. *Trends Pharmacol. Sci.*, **9**, 21–28.

EDWARDS, G. & WESTON, A.H. (1990). Structure-activity relationships of K^+ channel openers. *Trends Pharmacol. Sci.*, **11**, 417–422.

EDWARDS, G. & WESTON, A.H. (1993). The pharmacology of ATP-sensitive potassium channels. *Annu. Rev. Pharmacol. Toxicol.*, **33**, 597–637.

FARMER, J.B., FARRAR, D.G. & WILSON, J. (1974). Antagonism of tone and prostaglandin-mediated responses in a tracheal preparation by indomethacin and SC-19220. *Br. J. Pharmacol.*, **52**, 559–565.

FOSTER, K.A., ARCH, J.R.S., NEWSON, P.N., SHAW, D. & TAYLOR, S.G. (1992). Effect of Rb^+ on cromakalim-induced relaxation and ion fluxes in guinea pig trachea. *Eur. J. Pharmacol.*, **222**, 143–151.

GOPALAKRISHNAN, M., JOHNSON, D.E., JANIS, R.A. & TRIGGLE, D.J. (1991). Characterization of binding of the ATP-sensitive potassium channel ligand, [^{3}H] glyburide, to neuronal and muscle preparations. *J. Pharmacol. Exp. Ther.*, **257**, 1162–1171.

IMAGAWA, J., YOSHIDA, S., KOGA, T., KAMEI, K. & NABATA, H. (1993). The effect of a novel benzopyrane derivative, KC 399, on the isolated guinea-pig trachealis and human bronchi. *Gen. Pharmacol.*, **24**, 1505–1512.

KAJIOKA, S., NAKASHIMA, M., KITAMURA, K. & KURIYAMA, H. (1991). Mechanisms of vasodilatation induced by potassium-channel activators. *Clin. Sci.*, **81**, 129–139.

KAMEI, K., NABATA, H. & KURIYAMA, H. (1994). Effects of KC 399, a novel ATP-sensitive K^+ channel opener, on electrical and mechanical responses in dog tracheal smooth muscle. *J. Pharmacol. Exp. Ther.*, **268**, 319–327.

KOGA, H., SATO, H., ISHIZAWA, T., KUROMARU, K., MAKINO, T., TAKA, N., TAKAHASHI, T., SATO, T. & NABATA, H. (1993a). Benzopyran-4-carboxamide K^+ channel openers. *Bioorg. Med. Chem. Lett.*, **3**, 1115–1118.

KOGA, H., SATO, H., ISHIZAWA, T., KUROMARU, K., NABATA, H., IMAGAWA, J., YOSHIDA, S. & SUGO, I. (1993b). *N,N*-disubstituted benzopyrane-4-(*N'*-cyano) carboxamidines, cromakalim analogs with selective activity for guinea pig trachealis. *Bioorg. Med. Chem. Lett.*, **3**, 1111–1114.

LONGMORE, J., BRAY, K.M. & WESTON, A.H. (1991). The contribution of Rb-permeable potassium channels to the relaxant and membrane hyperpolarizing actions of cromakalim, RP46359 and diazoxide in bovine tracheal smooth muscle. *Br. J. Pharmacol.*, **102**, 979–985.

NIELSEN-KUDSK, J.E., MELLEMKJÆR, S., SIGGAARD, C. & NIELSEN, C.B. (1988). Effects of pinacidil on guinea-pig airway smooth muscle contracted by asthma mediators. *Eur. J. Pharmacol.*, **157**, 221–226.

PACIOREK, P.M., COWLRICK, I.S., PERKINS, R.S., TAYLOR, J.C., WILKINSON, G.F. & WATERFALL, J.F. (1990). Evaluation of the bronchodilator properties of Ro 31-6930, a novel potassium channel opener, in the guinea-pig. *Br. J. Pharmacol.*, **100**, 289–294.

QUAST, U. (1992). Potassium channel openers: pharmacological and clinical aspects. *Fundam. Clin. Pharmacol.*, **6**, 279–293.

RAEBURN, D. & BROWN, T.J. (1991). RP 49356 and cromakalim relax airway smooth muscle in vitro by opening a sulfonylurea-sensitive K^+ channel: a comparison with nifedipine. *J. Pharmacol. Exp. Ther.*, **256**, 480–485.

SCHWANSTECHER, M., BRANDT, C., BEHRENDS, S., SCHAUPP, U. & PANTEN, U. (1992). Effect of MgATP on pinacidil-induced displacement of glibenclamide from the sulphonylurea receptor in a pancreatic beta-cell line and rat cerebral cortex. *Br. J. Pharmacol.*, **106**, 295–301.

SMALL, R.C., BERRY, J.L., BURKA, J.F., COOK, S.J., FOSTER, R.W., GREEN, K.A. & MURRAY, M.A. (1992). Potassium channel activators and bronchial asthma. *Clin. Exp. Allergy*, **22**, 11–18.

TAYLOR, S.G., ARCH, J.R.S., BOND, J., BUCKLE, D.R., SHAW, D.J., TAYLOR, J.F. & WARD, J.S. (1992). The inhibitory effects of cromakalim and its active enantiomer BRL 38227 against various agonists in guinea pig and human airways: comparison with pinacidil and verapamil. *J. Pharmacol. Exp. Ther.*, **261**, 429–437.

TAYLOR, S.G., BUMSTEAD, J., MORRIS, J.E.J., SHAW, D.J. & TAYLOR, J.F. (1988). Cromakalim inhibits cholinergic-mediated responses in human isolated bronchioles but not in guinea-pig airways. *Br. J. Pharmacol.*, **95**, 795P.

XIE, Z., HAKODA, H. & ITO, Y. (1992). Airway epithelial cells regulate membrane potential, neurotransmission and muscle tone of the dog airway smooth muscle. *J. Physiol.*, **446**, 619–639.

(Received February 4, 1994
Revised June 16, 1994
Accepted June 22, 1994)

Br. J. Pharmacol. (1994), **113**, 898–902 © Macmillan Press Ltd, 1994

The sensitivity of nicotinic synapses in bullfrog sympathetic ganglia to α-bungarotoxin and neuronal-bungarotoxin

Wei-Xing Shen, Phillip Jobling & [1]John P. Horn

Department of Neurobiology, E1440 Biomedical Science Tower, University of Pittsburgh, School of Medicine, Pittsburgh, Pennsylvania 15261, U.S.A.

1 The sensitivity of nicotinic synapses to α-bungarotoxin (α-Bgt) and neuronal-bungarotoxin (n-Bgt) was measured in the B and C cell systems of bullfrog paravertebral sympathetic ganglia 9 and 10 by recording extracellular compound postganglionic action potentials from the rami communicantes.

2 High concentrations (10 μM) of α-Bgt applied for up to 8 h had no effect upon synaptic transmission in either the B or C cell system. Ganglia pretreated with collagenase were also insensitive to α-Bgt. In control experiments on isolated sartorius muscle preparations, nerve-evoked twitches were fully blocked by 30–100 nM α-Bgt.

3 Nicotinic transmission in the B and C cell systems was reversibly blocked by 30–300 nM n-Bgt. Block appeared within 25–45 min of exposure to toxin and reversed fully with a half-time of 40–80 min. This was indistinguishable from washout times after block by 100 μM (+)-tubocurarine.

4 The results demonstrate close parallels between the bungarotoxin sensitivity of neuronal nicotinic receptors mediating ganglionic transmission in functional subclasses of bullfrog sympathetic neurones and the bungarotoxin sensitivity which has been reported for autonomic neurones in avian and mammalian preparations.

Keywords: Sympathetic neurones; α-bungarotoxin; neuronal-bungarotoxin; neuronal nicotinic receptors; cholinergic synapses

Introduction

Paravertebral sympathetic ganglia 9 and 10 in the bullfrog contain fast B, slow B and C-type neurones that differ in their axonal conduction velocities (Dodd & Horn, 1983). Fast excitatory postsynaptic potentials (e.p.s.p.s) in the ganglia 9 and 10 are mediated by the action of acetylcholine upon postsynaptic nicotinic receptors (Blackman *et al.*, 1963; Horn & Dodd, 1981; Marshall, 1981). A two fold difference between the mean open-channel lifetimes of nicotinic receptors on B and C cells is evident from analysis of excitatory postsynaptic currents and acetylcholine-induced noise (Marshall, 1986). In addition the B and C groups of sympathetic neurones differ in their neuropeptide expression, muscarinic receptor expression, and synaptic connections with preganglionic neurones and peripheral targets (Horn, 1992). Together these findings suggest that phenotypic properties of nicotinic receptors are related to the functional modality of the sympathetic neurones expressing them.

The general significance of differences between nicotonic receptors on B and C cells in the bullfrog is clouded by a more basic question as to whether these receptors are fundamentally different from those in higher vertebrates. This possibility is supported by two pharmacological studies of B cells. In the first, Marshall (1981) reported that high doses of α-bungarotoxin (α-Bgt, 3 μM) reversibly blocked nicotinic transmission. He also found that binding of α-Bgt and of antibodies raised against nicotinic receptors from *Torpedo* electroplax was localized ultrastructurally at synapses. These results are paradoxical because in avian and mammalian ganglia, micromolar concentrations of α-Bgt have no effect on nicotinic transmission while nanomolar α-Bgt will saturate nicotinic binding sites (Fumagalli *et al.*, 1976; Brown & Fumagalli, 1977; Carbonetto *et al.*, 1978), which are localized in extrasynaptic regions (Jacob & Berg, 1983; Loring *et al.*, 1985). In a second study of bullfrog B cells, Lipscombe & Rang (1988) reported that the blocking mechanisms of 4 nicotinic antagonists (other then α-Bgt) more closely resembled effects seen at the neuromuscular junction than in rat submandibular ganglion. They concluded that nicotinic receptors on bullfrog sympathetic neurones are pharmacologically best described as 'muscle-like'.

The present experiments were designed to determine whether α-Bgt also blocks nicotinic synapses on C neurones to measure the sensitivities of B and C neurones to neuronal-bungarotoxin (n-Bgt). In higher vertebrates, n-Bgt selectively binds with high affinity to postsynaptic regions of autonomic neurones and blocks nicotinic transmission (Chiappinelli & Zigmond, 1978; Ravdin & Berg, 1979; Chiappinelli, 1983; Chiappinelli & Dryer, 1984; Loring *et al.*, 1984; Loring & Zigmond, 1987). Our goal was to obtain a more detailed pharmacological profile of the bullfrog receptors that could then be compared with those of nicotinic receptors on other neurones and on muscle.

Methods

Preparations of lumbar paravertebral ganglia 7–10 were isolated from adult bullfrogs of either sex (6–7 inches in length). The methods for dissection, stimulation and recording have been described (Dodd & Horn, 1983). Preganglionic B and C cell pathways were supramaximally stimulated through separate electrodes and compound postganglionic responses were recorded with suction electrodes from individual rami communicantes on ganglion 9 or 10. Presynaptic nerves were stimulated at rates <0.2 Hz in order to eliminate use-dependent components of block that arise from presynaptic depression (Shen & Horn, 1993). Recordings were monitored on an oscilloscope and chart recorder, and were stored on a laboratory computer using Axotape (Axon Instruments). Peak amplitudes of responses were measured with Axotape. Grouped data are expressed as the mean ± s.e. Some data files were transferred to a Macintosh computer for preparation of figures using Igor (Wavemetrics). Experiments were done at room temperature (20–24°C).

In order to minimize diffusion barriers the ganglia were desheathed during dissection. In some experiments, the ganglia were also treated with CLSPA-type collagenase (Wor-

[1] Author for correspondence.

thington) using the method of Marshall (1981). Collagenase treatment had no discernible effect upon the extracellular recordings and they remained stable for 5–36 h, thus permitting the effects of toxins to be monitored for extended periods.

The recording chamber had a volume of ~1.5 ml. In order to conserve α-Bgt which was used in high concentrations and to conserve n-Bgt, the availability of which is very limited, they were both applied by the following procedure. Normal Ringer solution was removed by Pasteur pipette and rapidly replaced twice by volumes of Ringer containing toxin. The preparation was then allowed to sit in a static bath. Periodic replacement of the Ringer solution showed that blockade in n-Bgt was not a consequence of the static bath procedure. For consistency, (+)-tubocurarine was also applied in a static bath. During control periods and washouts, the preparations were superfused at a rate of 1.5 ml min^{-1}.

Isolated preparations of the sartorius muscle were used to test the potency of α-Bgt. Muscles were dissected from small adult bullfrogs (1–3 inches) and pinned out in a Sylgard-coated dish. A suture was tied around the muscle and attached to a force transducer (Cambridge Instruments, model 400A). The nerve was supramaximally stimulated through a suction electrode and twitches were recorded on a Gould Easy-Graf chart recorder.

Three different lots of α-Bgt were obtained from Calbiochem and (+)-tubocurarine was obtained from Sigma. Neuronal bungarotoxin was a gift from Dr Ralph Loring at Northeastern University.

Results

High concentrations of α-Bgt had no effect upon synaptic transmission in either the B or C cell systems ($n = 9$). When 5 preparations of desheathed ganglia were exposed to 3–10 μM α-Bgt for 1–2 h the compound action potential amplitudes remained at 99 ± 7% (B wave) and 93 ± 9% (C wave) of control. In 4 ganglia that were desheathed and then pretreated with collagenase in the hope of reducing any remaining diffusion barriers, the amplitudes of the B and C waves held constant at 99 ± 4% and 109 ± 13% of control after 2 h in 10 μM α-Bgt. Figure 1a illustrates recordings from a collagenase-treated ganglion that was unaffected by 8 h of exposure to 10 μM α-Bgt.

In order to check whether our samples of α-Bgt were active, the two lots that had been used upon collagenase-treated ganglia were tested for their ability to block evoked contractions in sartorius nerve-muscle preparations. Doses of 10–100 nM α-Bgt from both lots inhibited contractions. In 4 experiments, 10 nM α-Bgt produced >50% neuromuscular block ($n = 1$) and contractions were completely blocked within 20–60 min of exposure to 30 nM α-Bgt ($n = 2$) or 100 nM α-Bgt ($n = 2$) (Figure 1b). The effects of α-Bgt were not reversed by washing for 18 h. Cutting of muscle fibres did however cause contractions, thereby indicating that failure of the contractile apparatus was not responsible for the block of transmission.

In contrast to the preceding results, low concentrations of n-Bgt (30–300 nM) reversibly inhibited nicotinic transmission

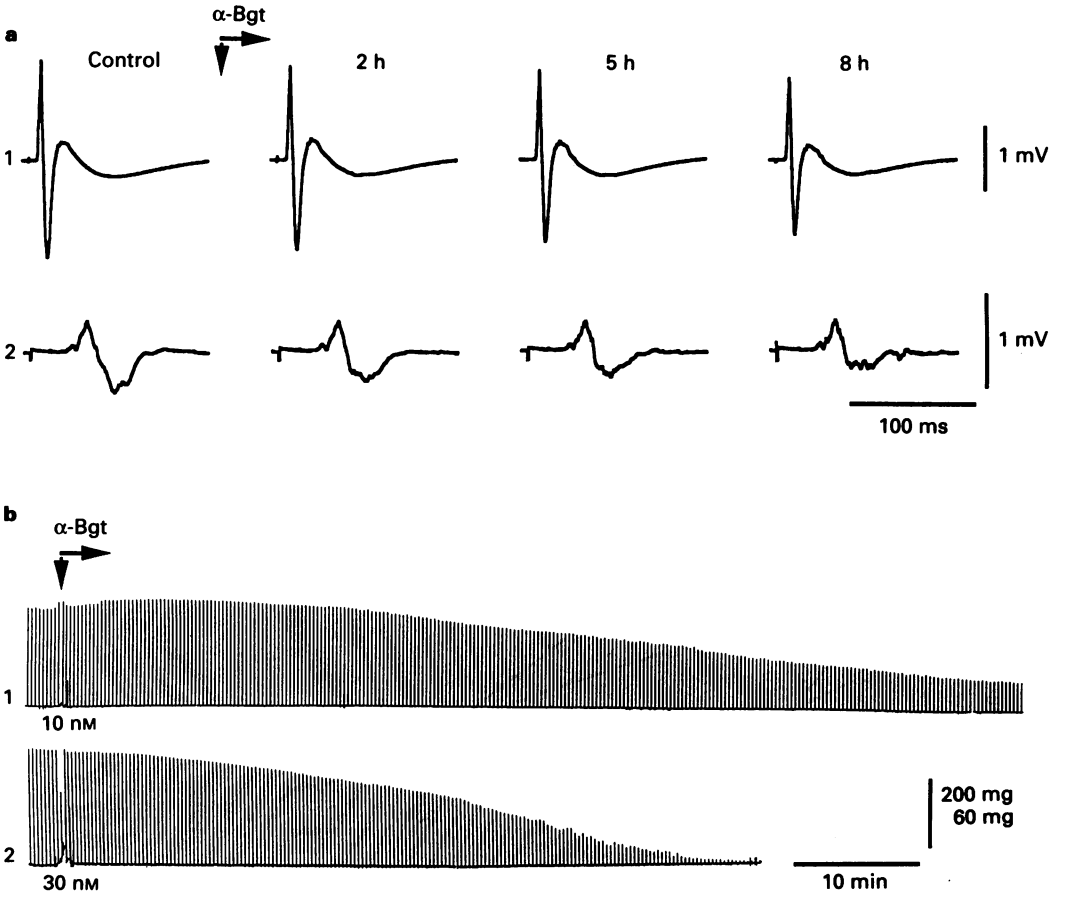


Figure 1 Alpha-bungarotoxin (α-Bgt) sensitivity of bullfrog sympathetic ganglia and sartorius muscle. Compound postganglionic B waves (a1) and C waves (a2) are insensitive to 10 μM α-Bgt after 2, 5, and 8 h of exposure. This preparation had been pretreated with collagenase. (b1) α-Bgt (10 nM) blocks by >50% the amplitude of nerve-evoked twitches in an isolated sartorius muscle preparation. (b2) α-Bgt (30 nM) fully blocks contraction in another muscle.

in both the B and C cell systems (Figure 2). In 6 ganglia that were desheathed and pretreated with collagenase, block appeared within 25–90 min of exposure to n-Bgt, reached a steady-state within 80–150 min, and fully reversed within 2–3 h of washing. In one experiment it was necessary to increase the stimulus frequency above 0.2 Hz in order to observe an effect of 150 nM n-Bgt. In this preparation repetitive stimulation (40 shocks) of the B pathway at 5 Hz of the C pathway at 20 Hz produced use-dependent reductions in the amplitudes of the compound responses. Studies of other antagonists have shown that, in bullfrog ganglia, transmission at higher frequencies is more sensitive to postsynaptic blockade because acetylcholine release is depressed (Shen & Horn, 1993). The extent of the variability in dose-response relations from the other 5 collagenase-treated ganglia is illustrated in Figure 2b which contains data from the most and least sensitive preparations. Differences in sensitivity between ganglia may have arisen in part because some toxin samples were taken through several freeze-thaw cycles. However, within individual experiments there was no difference in the sensitivities of the B and C waves to n-Bgt (Figure 2b).

Collagenase treatment was not a prerequisite for observing effects of n-Bgt. In 3 of 5 ganglia that were desheathed but not treated with enzyme, 100–300 nM n-Bgt caused a partial block (50–90%) of transmission within 40–80 min. The 2 ganglia that did not respond were only exposed to toxin for 40 and 50 min.

Several previous studies have shown that n-Bgt binding sites can be protected by pre-incubation with other nicotinic antagonists (e.g. Chiappinelli, 1983, Sah *et al.*, 1987). In order to test whether synaptic receptors on bullfrog sympathetic neurones could be protected, we compared recovery times from block by (+)-tubocurarine alone, by n-Bgt alone, and by (+)-tubocurarine and n-Bgt together. After pretreatment with collagenase, ganglia were exposed to 100 μM (+)-tubocurarine for 60 min which completely blocked transmission in the B and C cell systems. Upon washout the recovery of action potential amplitude was measured at 5 min intervals. Ganglia were then exposed to 100–300 nM n-Bgt until block reached a steady level (120–180 min) and the recovery was again monitored at 5 min intervals. Finally the ganglia were exposed to (+)-tubocurarine alone for 60 min and then to 100 μM (+)-tubocurarine in combination with n-Bgt. In both the B ($n = 4$) and C ($n = 3$) systems the recovery times for the three treatments were similar with half-times ranging between 40 and 80 min (Figure 3). Although it appeared in two cases that recovery times for block by n-Bgt were decreased by combined exposure to (+)-tubocurarine and n-Bgt, when all the data were considered together there was no consistent evidence of protection.

Discussion

We have compared the potencies of α-Bgt and n-Bgt upon nicotinic synapses on B and C neurones in bullfrog sympathetic ganglia. Based on parallels with autonomic neurones in higher vertebrates, the present data indicate that nicotonic receptors on bullfrog sympathetic B and C cells should be classified as neuronal in type.

A previous study reported that nicotinic synapses on bullfrog sympathetic B neurones were unique in their sensitivity to high concentrations of α-Bgt (Marshall, 1981). In our experiments, α-Bgt failed to alter synaptic transmission in either B or C cells even at concentrations that were comparable to and higher than those used by Marshall (1981). In order to reduce the possibility that diffusion barriers limit the

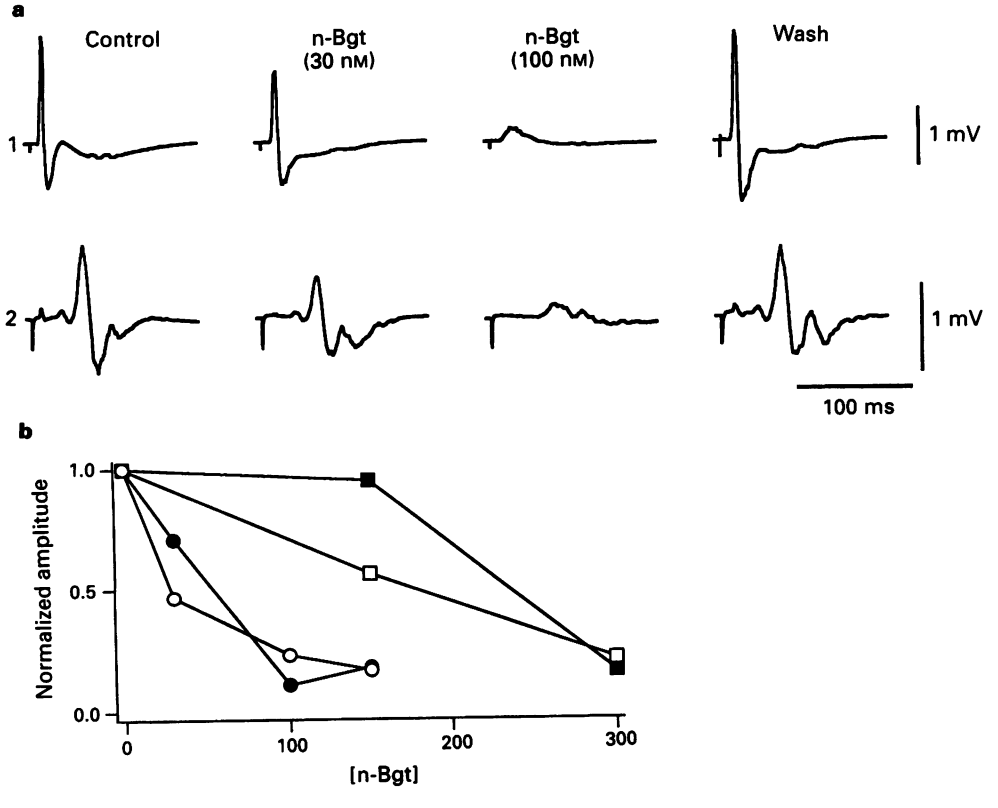


Figure 2 Neuronal-bungarotoxin (n-Bgt) sensitivity of bullfrog ganglia after pretreatment with collagenase. Postganglionic B waves (a1) and postganglionic C waves (a2) are inhibited to a similar extent by exposure to 30 nM n-Bgt for 120 min and to 100 nM n-Bgt for 140 min. Synaptic transmission recovered after washing in normal Ringer for 120 min. (b) Normalized amplitude of B waves (closed symbols) and C waves (open symbols) from the most sensitive (○, ●) and the least sensitive (□, ■) ganglia of 5 preparations. Ganglia were exposed to each concentration of toxin for 90–140 min.

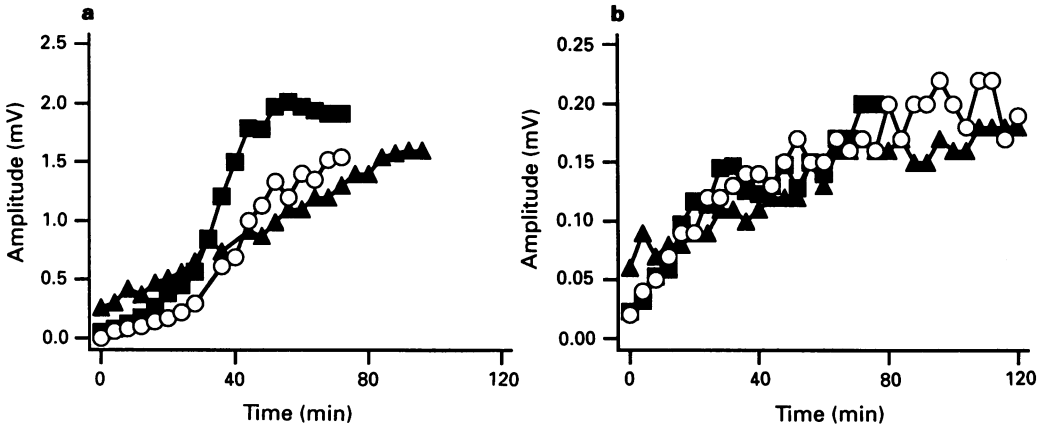


Figure 3 Two experiments illustrating recovery times from postsynaptic nicotinic block in the B (a) and C cell systems (b). Compound response amplitudes are plotted as a function of time. Each experiment included washout of (+)-tubocurarine alone (■), washout of n-bungarotoxin (n-Bgt) alone (▲), and washout of (+)-tubocurarine and n-Bgt (○).

access of α-Bgt (mol. wt. 8,000 D) to synapses and were responsible for our negative results, we replicated Marshall's collagenase procedure. Furthermore, the potency of our α-Bgt samples was checked and found to be normal in experiments on the sartorius muscle. Several explanations may account for the discrepancies between the present and earlier results. The α-Bgt used by Marshall in 1981 most likely contained small amounts of n-Bgt (see Chiappinelli & Zigmond, 1978). It was only after the subsequent purification and sequencing of n-Bgt that the molecular distinctions between α-Bgt and n-Bgt were definitively established (Chiappinelli & Zigmond, 1978; Ravdin & Berg, 1979; Grant & Chiappinelli, 1985; Loring *et al.*, 1986). Contamination of α-Bgt with n-Bgt would also explain the reversibility and synaptic localization of α-Bgt reported by Marshall (1981). Impure toxin does not explain why antibodies to acetylcholine receptors purified from *Torpedo* electrolax also bound specifically to synapses on bullfrog sympathetic neurones (Marshall, 1981). In retrospect, it appears likely that the polyclonal antibodies cross-reacted with amphibian neuronal nicotinic receptors. Examples of such cross-reactivity have been reported for monoclonal and polyclonal antibodies (Patrick & Stallcup, 1977; Watters & Maelicke, 1983; Jacob *et al.*, 1984).

There are strong similarities between the actions of n-Bgt upon bullfrog sympathetic neurones and actions that have been established in autonomic neurones from higher vertebrates. We have shown that nanomolar concentrations of n-Bgt reversibly inhibit nicotinic transmission in bullfrog ganglia. Nicotinic transmission in chick parasympathetic and sympathetic ganglia (Chiappinelli, 1983; Chiappinelli & Dryer, 1984) and rat sympathetic ganglia (Chiappinelli & Dryer, 1984; Sah *et al.*, 1987) are also reversibly blocked by nanomolar n-Bgt. However, receptors in birds, mammals and amphibians differ in their kinetics of recovery from block by n-Bgt. Recovery rates in rat (Chiappinelli & Dryer, 1984; Sah *et al.*, 1987) and bullfrog sympathetic ganglia (Figure 3) are notably faster (half-times ~40–100 min) than those reported in the chick (half times >120 min) (Chiappinelli, 1983; Chiappinelli & Dryer, 1984). In our experiments, the similarity of n-Bgt washout rates in the presence and absence of (+)-tubocurarine suggests either that (+)-tubocurarine does not protect nicotinic receptors or that protection is briefer than the tissue washout of antagonists. The difference between the relatively fast reversal of n-Bgt effects in curarized rat and bullfrog ganglia and their much slower reversal in curarized chicken ganglia remains unexplained. One possibility is heterogeneity in receptor topology. It may therefore prove interesting to investigate homologies and variations between the molecular properties of neuronal nicotinic receptors in these three classes of vertebrates.

This work was supported by a Grant-in-Aid (J.P.H.) and a Postdoctoral Fellowship (P.J.) from the American Heart Association, Pennsylvania Affiliate, and by a Research Career Development Award (KO4 NS01427) to J.P.H. We are grateful to Dr Ralph Loring for supplying a sample of neuronal-bungarotoxin and to Dr Elias Aizenman for many helpful discussions.

References

BLACKMAN, J.G., GINSBORG, B.L. & RAY, C. (1963). Synaptic transmission in the sympathetic ganglion of the frog. *J. Physiol.*, **167**, 355–373.

BROWN, D.A. & FUMAGALLI, L. (1977). Dissociation of α-bungarotoxin binding and receptor block in the rat superior cervical ganglion. *Brain Res.*, **129**, 165–168.

CARBONETTO, S.T., FAMBROUGH, D.M. & MULLER, K.J. (1978). Nonequivalence of α-bungarotoxin receptors and acetylcholine receptors in chick sympathetic neurons. *Proc. Natl. Acad. Sci. U.S.A.*, **75**, 1016–1020.

CHIAPPINELLI, V.A. (1983). Kappa-bungarotoxin: a probe for the neuronal nicotinic receptor in the avian ciliary ganglion. *Brain Res.*, **277**, 9–21.

CHIAPPINELLI, V.A. & DRYER, S.E. (1984). Nicotinic transmission in sympathetic ganglia: blockade by the snake venom neurotoxin kappa-bungarotoxin. *Neurosci. Lett.*, **50**, 239–244.

CHIAPPINELLI, V.A. & ZIGMOND, R.E. (1978). α-Bungarotoxin blocks nicotinic transmission in the avian ciliary ganglion. *Proc. Natl. Acad. Sci. U.S.A.*, **75**, 2999–3003.

DODD, J. & HORN, J.P. (1983). A reclassification of B and C neurones in the ninth and tenth paravertebral sympathetic ganglia of the bullfrog. *J. Physiol.*, **334**, 255–269.

FUMAGALLI, L., RENZIS, G.D. & MIANI, N. (1976). Acetylcholine receptors: number and distribution in intact and deafferented superior cervical ganglion of the rat. *J. Neurochem.*, **27**, 47–52.

GRANT, G.A. & CHIAPPINELLI, V.A. (1985). κ-Bungarotoxin: complete amino acid sequence of a neuronal nicotinic receptor probe. *Biochemistry*, **24**, 1532–1537.

HORN, J.P. (1992). The integrative role of synaptic cotransmission in the bullfrog vasomotor C system: evidence for a synaptic gain hypothesis. *Can. J. Physiol. Pharmacol.*, **70**, S19–S26.

HORN, J.P. & DODD, J. (1981). Monosynaptic muscarinic activation of K+ conductance underlies the slow inhibitory postsynaptic potential in sympathetic ganglia. *Nature*, **292**, 625–627.

JACOB, M.H. & BERG, D.K. (1983). The ultrastructural localization of α-bungarotoxin binding sites in relation to synapses on chick ciliary ganglion neurons. *J. Neurosci.*, **3**, 260–271.

JACOB, M.H., BERG, D.K. & LINDSTROM, J.M. (1984). Shared antigenic determinant between the *Electrophorus* acetylcholine receptor and a synaptic component on chicken ciliary ganglion neurons. *Proc. Natl. Acad. Sci. U.S.A.*, **81**, 3223–3227.

LIPSCOMBE, D. & RANG, H.P. (1988). Nicotinic receptors of frog ganglia resemble pharmacologically those of skeletal muscle. *J. Neurosci.*, **8**, 3258–3265.

LORING, R.H., ANDREWS, D., LANE, W. & ZIGMOND, R.E. (1986). Amino acid sequence of toxin F, a snake venom toxin that blocks neuronal nicotinic receptors. *Brain Res.*, **385**, 30–37.

LORING, R.H., CHIAPPINELLI, V.A., ZIGMOND, R.E. & COHEN, J.B. (1984). Characterization of a snake venom neurotoxin which blocks nicotinic transmission in the avian ciliary ganglion. *Neuroscience*, **11**, 989–999.

LORING, R.H., DAHM, L.M. & ZIGMOND, R.E. (1985). Localization of α-bungarotoxin binding sites in the ciliary ganglion of the embryonic chick: an autoradiographic study at the light and electron microscopic level. *Neuroscience*, **14**, 645–660.

LORING, R.H. & ZIGMOND, R.E. (1987). Ultrastructural distribution of ^{125}I-toxin F binding sites on chick ciliary neurons: synaptic localization of a toxin that blocks ganglionic nicotinic receptors. *J. Neurosci.*, **7**, 2153–2162.

MARSHALL, L.M. (1981). Synaptic localization of α-bungarotoxin binding which blocks nicotinic transmission at frog sympathetic neurons. *Proc. Natl. Acad. Sci. U.S.A.*, **78**, 1948–1952.

MARSHALL, L.M. (1986). Different synaptic channel kinetics in sympathetic B and C neurons of the bullfrog. *J. Neurosci.*, **6**, 590–593.

PATRICK, J. & STALLCUP, W.B. (1977). Immunological distinction between acetylcholine receptor and the α-bungarotoxin-binding component on sympathetic neurons. *Proc. Natl. Acad. Sci. U.S.A.*, **74**, 4689–4692.

RAVDIN, P.M. & BERG, D.K. (1979). Inhibition of neuronal acetylcholine sensitivity by α-toxins from *Bungarus multicinctus* venom. *Proc. Natl. Acad. Sci. U.S.A.*, **76**, 2072–2076.

SAH, D.W.Y., LORING, R.H. & ZIGMOND, R.E. (1987). Long-term blockade by toxin F of nicotinic synaptic potentials in cultured sympathetic neurons. *Neuroscience*, **20**, 867–874.

SHEN, W.X. & HORN, J.P. (1993). Nicotinic antagonists distinguish between synapses on sympathetic B and C neurons in the bullfrog. *Soc. Neurosci. Abstr.*, **19**, 1532.

WATTERS, D. & MAELICKE, A. (1983). Organization of ligand binding sites at the acetylcholine receptor: a study with monoclonal antibodies. *Biochemistry*, **22**, 1811–1819.

(Received April 19, 1994
Revised June 16, 1994
Accepted June 27, 1994)

Br. J. Pharmacol. (1994), **113**, 903–911 © Macmillan Press Ltd, 1994

Location of the sulphonylurea receptor at the cytoplasmic face of the β-cell membrane

Mathias Schwanstecher, Christina Schwanstecher, Corinna Dickel, Franz Chudziak, Ali Moshiri & [1]Uwe Panten

Institute of Pharmacology and Toxicology, University of Göttingen, Robert-Koch-Strasse 40, D-37075 Göttingen, Germany

1 In insulin-secreting cells the location of the sulphonylurea receptor was examined by use of a sulphonylurea derivative representing the glibenclamide molecule devoid of its cyclohexyl moiety (compound III) and a benzenesulphonic acid derivative representing the glibenclamide molecule devoid of its cyclohexylurea moiety (compound IV). At pH 7.4 compound IV is only present in charged form.

2 Lipid solubility declined in the order tolbutamide > compound III > compound IV.

3 The dissociation constant (K_D) for binding of compound IV to the sulphonylurea receptor in HIT-cells (pancreatic β-cell line) was similar to the K_D value for tolbutamide and fourfold higher than the K_D value for compound III.

4 In mouse pancreatic β-cells, drug concentrations inhibiting adenosine 5'-triphosphate-sensitive K^+ channels (K_{ATP}-channels) half-maximally (EC_{50}) were determined by use of the patch-clamp technique. When the drugs were applied to the extracellular side of outside-out or the intracellular side of inside-out membrane patches, the ratio of extracellular to intracellular EC_{50} values was 281 for compound IV, 25.5 for compound III and 1.2 for tolbutamide.

5 In mouse pancreatic β-cells, measurement of K_{ATP}-channel activity in cell-attached patches and recording of insulin release displayed much higher EC_{50} values for compound IV than inside-out patch experiments. A corresponding, but less pronounced difference in EC_{50} values was observed for compound III, whereas the EC_{50} values for tolbutamide did not differ significantly.

6 It is concluded that the sulphonylurea receptor is located at the cytoplasmic face of the β-cell plasma membrane. Receptor activation is induced by the anionic forms of sulphonylureas and their analogues.

Keywords: Sulphonylurea receptor; ATP-sensitive K^+ channel; insulin secretion; pancreatic β-cell; glibenclamide analogues

Introduction

In the plasma membrane of β-cells a K^+ channel has been identified which is inhibited by cytosolic ATP (K_{ATP})-channel) (Cook & Hales, 1984; for reviews see Ashcroft & Rorsman, 1991; Dunne & Petersen, 1991). Activation of β-cell energy metabolism by glucose or other insulin releasing fuels closes K_{ATP}-channels and thereby initiates a chain of events eventually leading to the release of insulin (Ashcroft *et al.*, 1984; Ashcroft & Rorsman, 1991). Sulphonylureas stimulate insulin secretion by inhibiting the K_{ATP}-channel via direct interaction with the β-cell plasma membrane (Sturgess *et al.*, 1985; Trube *et al.*, 1986; for reviews see Ashford, 1990; Edwards & Weston, 1993). In microsomal membranes from insulin secreting cells, a high affinity binding site for sulphonylureas has been found which probably represents the sulphonylurea receptor (Geisen *et al.*, 1985; for reviews see Panten *et al.*, 1992; Ashcroft & Ashcroft, 1992; Edwards & Weston, 1993). However, it is still unclear whether the sulphonylurea receptor is a component of the K_{ATP}-channel or a regulatory protein not permanently associated with the K_{ATP}-channel.

Sulphonylureas and their analogues (e.g. meglitinide) inhibit the K_{ATP}-channel from both sides of the β-cell membrane (Trube *et al.*, 1986; Sturgess *et al.*, 1988). This can be explained by rapid distribution of these drugs within the lipid phase of the cell membrane. Sulphonylureas and their analogues are weak organic acids, and the proportions of their lipophilic undissociated forms decrease with increasing pH. When performing whole-cell clamp experiments and raising the pH value in the extracellular solution at constant total tolbutamide concentration, both the rate of development and the degree of tolbutamide-induced K_{ATP}-channel block is diminished (Zünkler *et al.*, 1989). This finding and additional evidence suggest that the undissociated forms are the effective forms and reach the binding site on the sulphonylurea receptor from the lipid phase of the β-cell membrane. However, the possibility is not ruled out that the binding site is located at the cytoplasmic face of the plasma membrane and that the undissociated forms are only required for transport of externally applied sulphonylureas and related compounds across the membrane.

The aim of the present investigation was to elucidate further the location of the sulphonylurea receptor in the β-cell membrane. We have also sought evidence that the dissociated forms of sulphonylureas and related compounds directly interact with the receptor site. To address these issues we applied glibenclamide analogues (Figure 1) much less lipophilic than the sulphonylureas used so far. The affinities of these compounds for the sulphonylurea receptor were compared with their potencies for K_{ATP}-channel inhibition and stimulation of insulin secretion. Using different configurations of the patch-clamp technique the compounds were applied at the extracellular or intracellular side of the plasma membrane.

Methods

Measurement of [^{3}H]-glibenclamide binding to microsomes

Culture of HIT-cells, preparation of microsomes from these cells and measurement of [^{3}H]-glibenclamide binding to microsomes were performed as previously described (Schwanstecher *et al.*, 1992b).

[1] Author for correspondence.

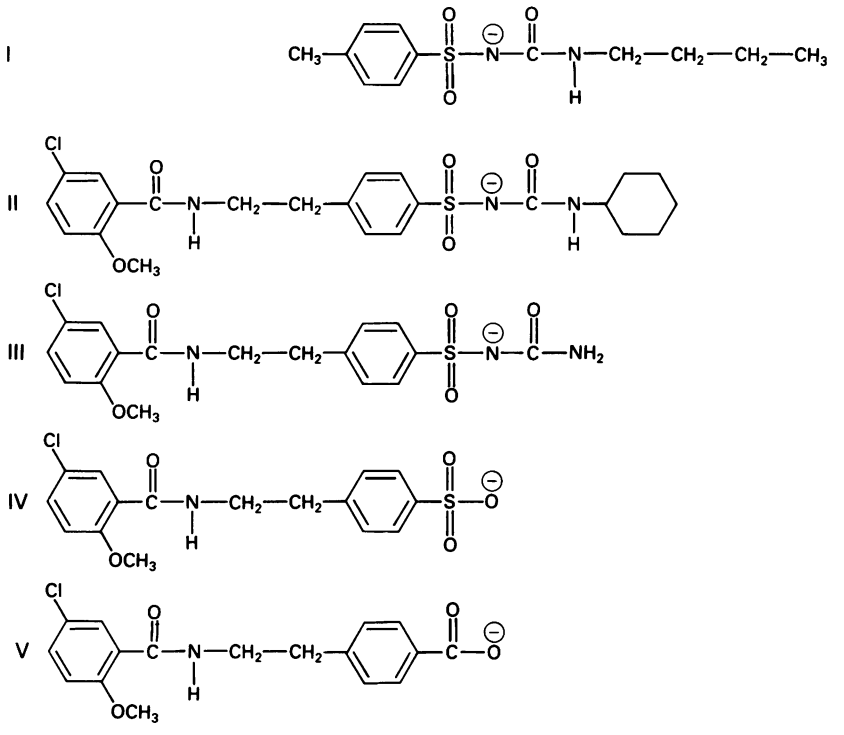


Figure 1 Structures of tolbutamide (I), glibenclamide (II), compound III, compound IV and meglitinide (V). The anionic forms are shown.

Isolation and culture of pancreatic β-cells

Pancreatic islets were isolated from male albino mice (NMRI, 11–15 weeks old, fed *ad libitum*) as previously described (Panten *et al.*, 1989). The islets were dissociated into single cells by shaking in a solution without Ca^{2+} (Lernmark, 1974). The cells were cultured for 1–4 days on Nunc Petri dishes (35 × 10 mm) in RPMI 1640 tissue culture medium containing 10% foetal calf serum, 100 μg ml^{-1} streptomycin, 100 u ml^{-1} penicillin G and 5 mM D-glucose for cell-attached experiments or 10 mM D-glucose for inside-out and outside-out experiments.

Electrophysiological recording and analysis

The cell-attached, inside-out and outside-out configuration of the patch-clamp technique (Hamill *et al.*, 1981) were used to record currents flowing through K_{ATP}-channels as previously described (Panten *et al.*, 1990; Schwanstecher *et al.*, 1992c). All experiments were performed at room temperature (20–22°C). The bath was perfused continuously at 2 ml min^{-1}. Pipettes were pulled from borosilicate glass and had resistances between 3 and 8 MΩ when filled with pipette solution. At the beginning of an experiment the current output signal of the amplifier was set to zero with the pipette being immersed in extracellular solution (cell-attached and outside-out experiments) or in intracellular solution (inside-out experiments). The zero-current potential served as reference for all measurements and no corrections have been made for the liquid junction potential. In cell-attached patch experiments, the pipette potential was held at 0 mV. The membrane potential was clamped at − 50 mV and 0 mV in inside-out and outside-out patch experiments, respectively. Inward and outward membrane K^+ currents are indicated as downward and upward deflections, respectively, in all current traces.

In cell-attached patch experiments data samples of 1–2 min duration were analyzed with the half-amplitude threshold technique (Colquhoun & Sigworth, 1983) using an interactive graphics-based analysis programme (pCLAMP 5.5.1, FETCH series). Amplitude histograms of sampled cell-attached currents were formed to calculate the mean single-channel current amplitudes (i). Channel activity was defined as the product of N, the number of functional channels and P_o, the open state probability and was determined by dividing the total time the channels spent in the open state by the total sample time. In case of superpositions of channels, the channel activity was calculated by summing the activity for each different current level. In addition, the mean of the channel activity during the control periods (presence of 3 mM D-glucose) before and after application of test substance (0.3–10 μM compound III or 1–100 μM compound IV) was set at 1.0 and the channel activity in the presence of test substance was normalized to this value. Data were sampled during the last minute of a test period (4–13 min duration). Data sampling during the control periods was started 1–2 min before and 5–25 min after the test period.

In inside-out patch experiments the cytoplasmic face of the membrane patch was exposed for 45 s periods to intracellular solution which contained Mg^{2+} and 1 mM ATP and was applied directly to the patch from a U-shaped polythene capillary (Fenwick *et al.*, 1982; Ohno-Shosaku *et al.*, 1987). These 45 s periods alternated with 15 s periods of intracellular solution which was supplemented with or without test substances (ADP and/or drugs) and was applied to the patch by bath perfusion (experimental design shown in Figure 3). Before and after application of test substance-containing bath solution, there were periods during which the same solution was applied except that the test substances were omitted. The mean of the amplitudes of the current responses (current amplitudes) during application of test substances was normalized to the mean current amplitude during ADP- and drug-free control periods in each single experiment. The single-channel current amplitudes of the K_{ATP}-channels were not changed by the applied concentrations of compound III, compound IV and meglitinide.

In outside-out patch experiments K^+ currents were measured during the test period (presence of 1–100 μM tolbutamide, 1–100 μM compound III or 1–1000 μM compound

IV) at the extracellular membrane side and during control periods before and after the test period. In each experiment, test periods with 100 μM tolbutamide were included to detect the base-line (all K_{ATP}-channels closed) for the K^+ current measurements. The mean K^+ current during 1 min intervals was measured during the last minute of the control period before drug application and during the new steady states induced by application and removal of test substance. The K^+ current during a test period was normalized to the mean of the K^+ currents during the control periods before and after application of test substance. Changes of the single-channel current amplitudes of the K_{ATP}-channels were not detected after application of tolbutamide and compounds III and IV.

Recordings were made using an LM-EPC7 patch clamp amplifier (List Electronic, Darmstadt, Germany). Current signals were low-pass filtered at 2 kHz (cell-attached currents) or at 0.5 kHz (inside-out and outside-out currents) with a 4-pole Bessel filter (AF 173, Thomatronik, Rosenheim, Germany), digitized using an A/D converter (Instrutech, New York, U.S.A.) and stored on video tape. For analysis, taped data were replayed, digitized at 10 kHz for cell-attached and at 2 kHz for inside-out and outside-out currents using an Axolab 1100 computer interface (Axon Instruments, Foster City, CA, U.S.A.) and stored in a microcomputer. Analysis of the data was performed with the computer programme pCLAMP 5.5.1 (Axon Instruments). For Figures 3(a), 4(a) and 5(a) taped data were replayed into a chart recorder (220, Gould, Cleveland, OH, U.S.A.).

Measurement of insulin secretion

Measurement of insulin secretion from batches of 50 mouse islets (for animals and isolation see above) and data analysis were performed as described previously (Panten *et al.*, 1989). The islets were perifused at 0.9 ml min^{-1} and 37°C for 60 min in the presence of 10 mM D-glucose and then for 60 min in the presence of 10 mM D-glucose + test substance.

Determination of albumin binding

Binding of drugs to albumin in the perifusion media (37°C) was measured by ultrafiltration as described previously (Panten *et al.*, 1989). The concentration of compound III in the ultrafiltrate was determined by measuring inhibition of specific [^{3}H]-glibenclamide binding to HIT-cell microsomes induced by the ultrafiltrate. Albumin-free media containing known concentrations of compound III served as standards. The concentration of compound IV in the ultrafiltrate was determined by analytical high performance liquid chromatography (h.p.l.c.) on a Kontron 325 system (Kontron Instruments, Neufahrn, Germany) equipped with an ODS-Hypersil 5 μm column (250 × 4 mm, Bischoff, Leonberg, Germany).

Determination of partition coefficients

Determination of apparent octanol-water partition coefficients was performed at room temperature as previously described (Panten *et al.*, 1989). The aqueous phase consisted of 50 mM potassium phosphate and 50 mM boric acid, titrated to pH 7.4 with KOH. Drug concentration in the appropriate phase was measured by u.v. spectrophotometry against the appropriate blank.

Chemicals and solutions

Chemicals for organic syntheses were purchased from Aldrich Chemical Co. (Steinheim, Germany) and Fluka Chemie AG (Buchs, Switzerland). [^{3}H]-glibenclamide (51 Ci $mmol^{-1}$, 96% radiochemical purity) was purchased from NEN (Dreieich, Germany). Compound III (known as Hoe 36320; Figure 1) was from Hoechst AG (Frankfurt, Germany). The sodium salt of compound IV (Figure 1) was synthesized as described below and dissolved in the test solutions immediately before use. Stock solutions of compound III, meglitinide and tolbutamide were prepared daily in 50–100 mM NaOH or KOH; if necessary, the pH of the stock solutions was adjusted to 8.5 with HCl. All other chemicals were obtained from sources described elsewhere (Panten *et al.*, 1989; 1990; Schwanstecher *et al.*, 1992a,b).

The solution at the cytoplasmic side of the membrane (intracellular solution) contained (in mM): KCl 140, $CaCl_2$ 2, $MgCl_2$ 1, ethylene glycol *bis*(β-aminoethyl ether)-*N,N,N',N'*-tetraacetic acid (EGTA) 10 and 4-(2-hydroxyethyl)-1-piperazineethane-sulphonic acid (HEPES) 5 (titrated to pH 7.15 with KOH) (free $[Ca^{2+}] = 0.05$ μM). The free Mg^{2+} concentration was held close to 0.7 mM by adding appropriate amounts of $MgCl_2$ to nucleotide-containing solutions. The required amounts of $MgCl_2$ and the composition of the solutions for pH 7.15 were calculated with a computer programme (Fabiato, 1988) except that some stability constants of the programme were exchanged as detailed previously (Schwanstecher *et al.*, 1992d). After addition of 1 mM Na_2-ATP, the intracellular solution was also used for filling the U-shaped polythene capillary of the aforementioned microflow system (Ohno-Shosaku *et al.*, 1987). After addition of 1 mM KADP + 0.1 mM Na_2-ATP, the intracellular solution was used for filling the pipette in outside-out patch experiments. The bath solution in cell-attached and outside-out patch experiments contained (in mM): NaCl 140, KCl 5.6, $CaCl_2$ 2.6, $MgCl_2$ 1.2, HEPES 10 (titrated to pH 7.40 with NaOH). The pipette solution in cell-attached and inside-out patch experiments contained (in mM): KCl 146, $CaCl_2$ 2.6, $MgCl_2$ 1.2, HEPES 10 (titrated to pH 7.40 with KOH). In cell-attached patch experiments 3 mM D-glucose and 10 μM nifedipine were added to bath and pipette solutions. Nifedipine was used to prevent action potentials and opening of Ca^{2+}-dependent K^+ channels. Control experiments with nifedipine-free pipette solution showed that switching from a nifedipine-free bath solution containing 3 mM D-glucose to one containing 3 mM D-glucose + 10 μM nifedipine did not significantly alter K_{ATP}-channel activity in cell-attached patches ($n = 5$).

The pH of all solutions was determined after adding D-glucose, nifedipine, tolbutamide, meglitinide, compound III, compound IV or any nucleotides and was readjusted if necessary. Tolbutamide, meglitinide, compound III and compound IV were completely dissolved at all applied concentrations.

Synthesis of compound IV

Synthesis of 2-(5-chloro-2-methoxybenzamido)-ethylbenzene To 18.66 g (0.1 mol) of 5-chloro-2-methoxybenzoic acid was added, while stirring, 72.76 ml (1 mol) of thionyl chloride. After heating for 1 h under reflux, the excess thionyl chloride was removed by vacuum distillation. The resulting 5-chloro-2-methoxybenzoyl chloride was added slowly, while stirring and cooling with ice, to 100 ml dichloromethane containing 12.56 ml (0.1 mol) 2-phenylethylamine and 13.21 ml (0.1 mol) collidine. After stirring for 30 min at room temperature, most of the solvent was removed by vacuum distillation. The remaining reaction mixture was poured into 100 ml icewater (acidified with HCl). The aqueous phase was extracted three times with 50 ml diethyl ether, and the combined ether extracts were washed sequentially with 1 M HCl, 1 M NaOH and water. After drying over anhydrous sodium sulphate and removal of the diethyl ether *in vacuo*, a pale yellow oil (26.6 g) was obtained.

Synthesis of 4-[2-(5-chloro-2-methoxybenzamido)-ethyl]-benzenesulphonic acid (compound IV) To 5.87 g (0.02 mol) of 2-(5-chloro-2-methoxybenzamido)-ethylbenzene, 1.4 ml (0.02 mol) of chlorosulphonic acid was added dropwise at 90°C while stirring. After stirring for 2 h at 90°C and then cooling to room temperature, the reaction mixture was dissolved in a mixture of 80 ml water and 50 ml diethyl ether. The aqueous

phase was washed three times with 50 ml diethyl ether, neutralized with 2 N NaOH and concentrated *in vacuo* to approximately 5 ml. The residue was purified by column chromatography on silica gel (Kieselgel 60, Merck, Darmstadt, Germany). The column was eluted with a mixture of chloroform, methanol and water (13:8:2). After evaporation to dryness, a pale yellow solid (1.90 g) was obtained. The solid was recrystallized from water.

The structure of compound IV shown in Figure 1 was confirmed by ^{1}H-n.m.r. and ^{13}C-n.m.r. (D_6-DMSO, 200 MHz) on a model VXR-200 spectrometer (Varian, Palo Alto, CA, U.S.A.) and IR spectroscopy on a model 297 spectrometer (Perkin-Elmer Corp., Norwalk, CT, U.S.A.), supported by positive-ion fast atom bombardment mass spectrometry on a Finnigan MAT 95 spectrometer.

Elementary analysis: calculated for $C_{16}H_{15}ClNNaO_5S$: C,49.05; H,3.86; Na,5.87. Found: C,49.18; H,3.95; Na,5.93.

Treatment of results

Values are presented as mean ± s.e.mean. Significances were calculated by the two-tailed U-test of Wilcoxon and of Mann and Whitney, $P < 0.05$ was considered significant. Relations between drug concentration and effects, specific binding or free drug concentration were analysed by fitting the function

$$(1)\quad E = \frac{a-b}{1 + (EC_{50}/[A])^n} + b$$

to the experimental data by a non-linear least-squares routine where E = effect, specific binding or free drug concentration, EC_{50} = half-maximally effective drug concentration, [A] = drug concentration, n = slope parameter (Hill coefficient), a = maximum value for effect, specific binding or free drug concentration and b = additive constant.

Results

Membrane binding studies

Competitive inhibition assays revealed that compound III and compound IV inhibited specific [^{3}H]-glibenclamide binding to HIT-cell microsomes half-maximally at 4.4 μM (Hill coefficient = − 0.93) and 18.6 μM (Hill coefficient = − 0.92), respectively (Figure 2). These half-maximally inhibitory concentrations, the dissociation constant (K_D) for glibenclamide (0.22 nM, Schwanstecher *et al.*, 1992a) and the free [^{3}H]-glibenclamide concentration in the incubations were used to calculate the K_D values for compounds III and IV (1.9 and 7.9 μM, respectively) (Cheng & Prusoff, 1973).

Patch-clamp studies

Figure 3a shows the typical design of our inside-out patch experiments. In order to slow the run-down of channel activity (Ohno-Shosaku *et al.*, 1987), the cytoplasmic face of the membrane patch was exposed for 45 s periods to an intracellular solution containing 0.7 mM free Mg^{2+} and 1 mM ATP, alternating with 15 s periods serving as test or control periods. The example in Figure 3a demonstrates that 1 mM ADP inhibited the K_{ATP}-channel activity in the presence of Mg^{2+} by 32%. Intracellular solution supplemented with Mg^{2+} and ADP contains both the Mg complex of ADP (MgADP) which stimulates the K_{ATP}-channels and free ADP which inhibits the K_{ATP}-channels, but less effectively than free ATP (Ashcroft & Rorsman, 1991). Further addition of 1 μM of compound IV decreased the channel activity to 45% of the activity in control solution (nucleotide- and drug-free). In the presence of Mg^{2+} and 1 mM ADP, compound III (10 μM) and compound IV (100 μM) induced complete block of the K_{ATP}-channels; compound III and compound IV were half-maximally effective at 0.2 μM (Hill coefficient = − 1.20) and 0.8 μM (Hill coefficient = − 1.14), respectively (Figure 3b). However, in the presence of Mg^{2+}, but in the absence of nucleotides, 100 μM concentrations of compound III or compound IV caused only reduction of channel activity to 41 or 33% of the control value (absence of nucleotides and drugs), respectively (Figure 3b). Even 1–3 mM concentrations of compound IV did not lead to closure of all K_{ATP}-channels. As the concentration-response curve showed a turning point at 100 μM compound IV, the additional channel inhibition induced by 1–3 mM compound IV was probably not due to actions at the specific sulphonylurea receptor sites. When curve fitting was restricted to the range of drug concentrations which presumably induced specific effects (up to 100 μM), compound III and compound IV were half-maximally effective in the absence of nucleotides at 0.1 μM (Hill coefficient = − 0.75) and 0.4 μM (Hill coefficient = − 0.85), respectively (Figure 3b).

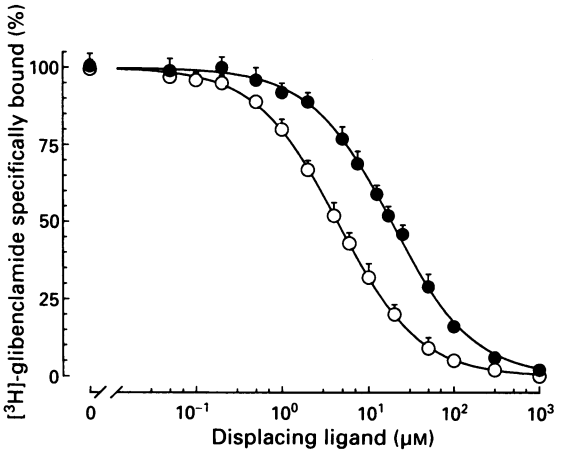


Figure 2 Effects of compounds III and IV on binding of [^{3}H]-glibenclamide to microsomes from HIT-cells. Inhibition of [^{3}H]-glibenclamide binding by compound III (○) or compound IV (●) was measured at room temperature in 1 ml of buffer containing (final concentrations) 0.3 nM [^{3}H]-glibenclamide, 1 mM free Mg^{2+} and the indicated concentrations of inhibiting drug (logarithmic scale). Incubations were started by addition of microsomal protein (200 μg ml^{-1} final concentration) and were terminated after 60 min by filtration. Nonspecific binding was defined by incubations in the presence of 100 nM glibenclamide. Results are presented as percentages of specific binding of [^{3}H]-glibenclamide in the absence of inhibiting drugs. Data analysis was performed as described in the Methods section. Values are given as means (with s.e.mean shown when larger than symbols) for results from four separate experiments using separate membrane preparations.

Using the experimental design shown in Figure 3, the K_{ATP}-channel-inhibiting effect of meglitinide (0.01–10 μM) applied to the cytoplasmic membrane side was examined in the presence of 1 mM ADP at the cytoplasmic membrane side. Meglitinide caused complete channel inhibition at 10 μM and was half-maximally effective at 0.5 μM (Hill coefficient = − 0.97; n = 3–4; data not shown in a figure).

Figure 4a shows the typical design of our outside-out patch experiments with drug application at the extracellular membrane side. Tolbutamide (100 μM) strongly inhibited the K_{ATP}-channel activity. Within 1.5 min after starting the exchange of the bath solution a new steady state was reached. The mean K^+ current measured 4 min after switching to tolbutamide (100 μM) was 3.4% of the mean K^+ current during the control periods (measurements started 1 min before switching to tolbutamide and 4 min after switching back to drug-free solution). Compound IV (100 μM) weakly inhibited the K_{ATP}-channel activity. Within 3 min after switching to compound IV (100 μM) a new steady state was reached. The mean K^+ current measured 5 min after switching to compound IV (100 μM) was 70% of the mean K^+ current during the control periods (measurements started 1 min before switching to compound IV and 4 min after

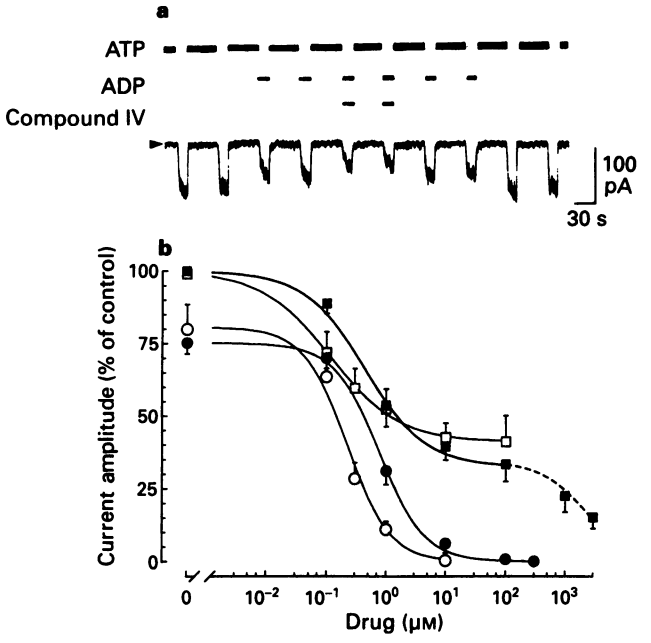


Figure 3 Inhibition of K_{ATP}-channels in inside-out patches of mouse pancreatic β-cells by compounds III and IV applied to the cytoplasmic membrane side. (a) Current trace obtained from an inside-out patch. The uppermost horizontal bars indicate application of intracellular solution containing 0.7 mM free Mg^{2+} and 1 mM ATP for 45 s by the capillary of the microflow system. The other horizontal bars above the current trace indicate application of intracellular solution containing 0.7 mM free Mg^{2+} and 1 mM ADP (with or without 1 μM compound IV) for 15 s by the bath. The 15 s periods of application of nucleotide- and drug-free intracellular solution (with 0.7 mM free Mg^{2+}) by the bath represent the control periods. (b) Relationship between normalized current amplitude and concentration (logarithmic scale) of compound III (open symbols) or compound IV (solid symbols) during 15 s periods of exposure to intracellular solution (with 0.7 mM free Mg^{2+}) containing no nucleotide (squares) or 1 mM ADP (circles). Using the experimental design shown in (a), the mean current amplitude during drug application was normalized to the mean current amplitude during 15 s periods of exposure to control solution (intracellular solution with 0.7 mM free Mg^{2+}) before and after application of drug or ADP alone in each single experiment. Data analysis was performed as described in the Methods section, except that the dashed line was fitted by eye. Symbols indicate the mean of 4–10 experiments (with s.e.mean shown when larger than symbols).

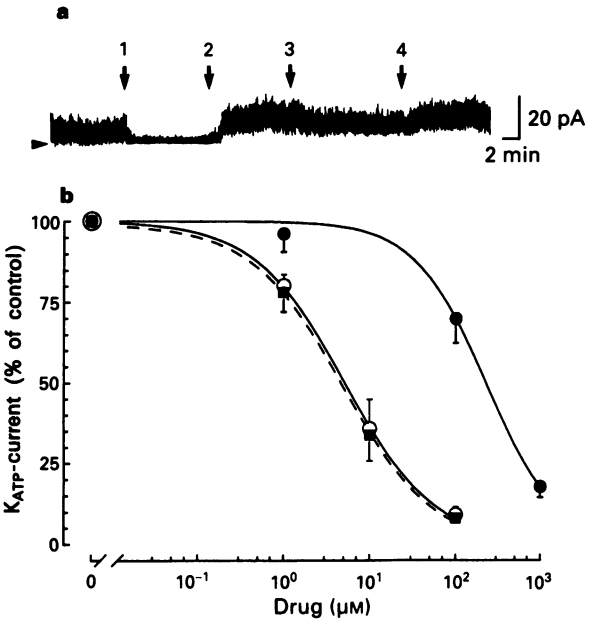


Figure 4 Inhibition of K_{ATP}-channels in outside-out patches of mouse pancreatic β-cells by tolbutamide and compounds III and IV applied to the extracellular membrane side. (a) Continuous chart recorder trace demonstrating the responses of outward K_{ATP}-currents in an outside-out patch when switching from control solution (drug-free bath solution) to a bath solution with 100 μM tolbutamide (arrow 1) and then back to control solution (arrow 2), followed by switching to a bath solution with 100 μM compound IV (arrow 3) and then back to control solution (arrow 4). (b) Relationship between normalized K_{ATP}-current and external concentration (logarithmic scale) of tolbutamide (■—■) compound III (○) or compound IV (●). Using the experimental design shown in (a), the K_{ATP}-current during drug application was normalized to the mean of the K_{ATP}-currents during the control periods before and after drug application in each single experiment. Data analysis was performed as described in the Methods section. Symbols indicate the mean of 3–12 experiments (with s.e.mean shown when larger than symbols).

switching back to drug-free solution). Single-channel current amplitudes ranged between 1.75 and 1.85 pA in the absence of drugs, in the presence of tolbutamide (100 μM) and in the presence of compound IV (100 μM). Tolbutamide, compound III and compound IV were half-maximally effective at 4.8 μM (Hill coefficient = − 0.82), 5.1 μM (Hill coefficient = − 0.83) and 225 μM (Hill coefficient = − 1.02), respectively (Figure 4b).

Figure 5a shows the typical design of our cell-attached patch experiments carried out in the presence of 3 mM D-glucose. On changing to a bath solution containing 30 μM of compound IV (test solution), the K_{ATP}-channel activity slowly decreased from 0.14 (last 1 min interval of the control period before start of bath exchange) to 0.05 during the new steady state (last 1 min interval of the test period). After switching back to drug-free bath solution, it took 12 min until a steady state was reached again (channel activity = 0.15). Single channel current amplitudes were − 4.5 pA during the test period and − 4.7 pA during the control periods before and after the test period, respectively. Compound III and compound IV were half-maximally effective at 0.6 μM (Hill coefficient = − 1.44) and 34 μM (Hill coefficient = − 1.46), respectively (Figure 5b).

Insulin secretion studies

In perifused mouse islets compounds III and IV stimulated a steep increase in insulin release reaching a peak rate at 2.5–3.5 min (compound III) or 2.5–5.5 min (compound IV), then declining rapidly within the next few min and slowly or not at all from 18 to 58 min (Figure 6). This secretory pattern was seen in each single experiment with the indicated concentrations of compounds III and IV. At 58 min, 0.1 mM of compound III and 3 mM of compound IV produced secretory rates which did not differ significantly.

The relationships between total and free drug concentrations in the perifusion media (Figure 7) and the secretory rates shown in Figure 6 were used to establish concentration-response curves for free compound III and IV (Figure 8). Half-maximally effective concentrations of free compound III and IV were 3.5 μM (Hill coefficient = 0.90) and 141 μM (Hill coefficient = 0.76) at min 2.5, respectively, (analysis not shown) and 1.3 μM (Hill coefficient = 0.90) and 68.2 μM (Hill coefficient = 0.76) at min 58, respectively (Figure 8).

Lipophilicity of compounds III and IV

To characterize the lipophilicity of compounds III and IV, the partition of the compounds between octanol and an aqueous phase was measured at pH 7.4. Apparent partition coefficients of 0.6 (compound III) and 0.4 (compound IV) were observed (means of results from two separate experiments).

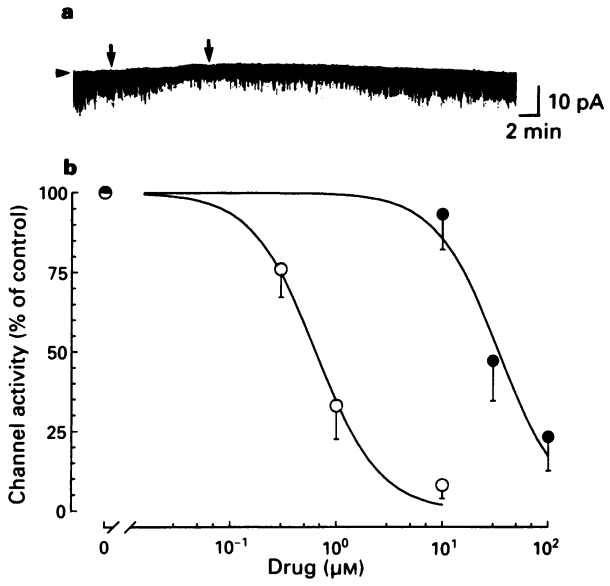


Figure 5 Inhibition of K_{ATP}-channels in cell-attached patches of mouse pancreatic β-cells by compounds III and IV. (a) Continuous chart recorder trace demonstrating the responses of single K_{ATP}-channel currents in a cell-attached patch when switching from control solution (drug-free bath solution) to a solution with 30 μM compound IV (first arrow) and then back to control solution (second arrow). The pipette solution and all bath solutions were supplemented with 3 mM D-glucose and 10 μM nifedipine. The arrowhead indicates the zero current level (all channels closed). (b) Relationship between normalized channel activity and concentration (logarithmic scale) of compound III (○) or compound IV (●). Using the experimental design shown in (a), channel activity during drug application was normalized to the mean channel activity during the control periods before and after drug application in each single experiment. Data analysis was performed as described in the Methods section. Symbols indicate the mean of 4–7 experiments (with s.e.mean shown when larger than symbols).

Discussion

Compound IV can be regarded as a derivative of *p*-toluenesulphonic acid. The pK_a value of compound IV has not been measured, but is probably close to that of *p*-toluenesulphonic acid (1.55; Schawartz & Ladik, 1953). Compound IV is therefore completely dissociated at pH 7.4 and barely dissolves in the lipid phase of cell membranes. The present study shows that this anionic sulphonylurea analogue binds to the sulphonylurea receptor, inhibits the K_{ATP}-channel and stimulates insulin secretion. These findings reflect interaction of compound IV with membrane-bound sulphonylurea receptors and thus argue against direct accessibility of the receptor binding sites from the lipid phase of the β-cell plasma membrane. Furthermore, the receptor binding of compound IV suggests that the anionic forms of hypoglycaemic sulphonylureas bind to the sulphonylurea receptor.

The benzoic acid derivative, meglitinide (Figure 1), represents another sulphonylurea analogue which is effective at the sulphonylurea receptor and initiates insulin release (Ashcroft & Rorsman, 1991). Brown & Foubister (1984) proposed that the COOH group of meglitinide and the SO_2NHCO group of sulphonylureas are isosteres and that these acidic groups are required for hypoglycaemic activity. The effects of compound IV also demonstrate that the urea group of sulphonylureas is not a prerequisite for interaction of these drugs with their receptor. The urea group is mainly a means of attaching a hydrophobic residue to benzenesulphonic acid with conservation of an acidic group. Unlike the urea group, the hydrophobic cyclohexyl group strongly enhances receptor binding. This is reflected in the finding that the binding affinity of compound III is not much higher than that of compound IV (Table 1), whereas the binding affinity of glibenclamide is higher by several orders of magnitude (K_D = 0.2–0.8 nM in HIT-cell microsomes; Gaines *et al.*, 1988; Schwanstecher *et al.*, 1992a).

When compound III or IV is applied to the cytoplasmic face of inside-out patches in the absence of nucleotides, the

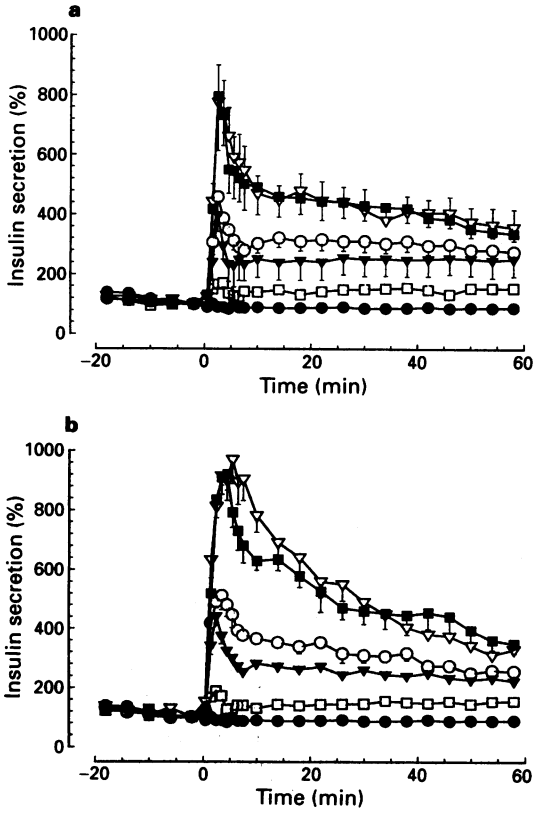


Figure 6 Concentration-dependent effects of compounds III (a) and IV (b) on the kinetic of insulin secretion from mouse pancreatic islets. All media contained 10 mM D-glucose. In addition, from zero time to min 60 the test media contained 0 (●), 1 (□), 3 (▼), 10 (○), 30 (■) or 100 (▽) μM of compound III or 0 (●), 30 (□), 100 (▼), 300 (○), 1000 (■) or 3000 (▽) μM of compound IV. Symbols indicate the mean of results from 4–8 separate experiments (with s.e.mean shown when larger than symbols).

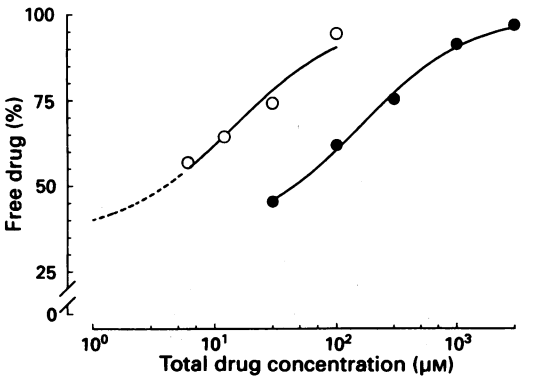


Figure 7 Binding of compounds III (○) and IV (●) to bovine serum albumin in basal perifusion medium (modified Krebs bicarbonate buffer containing 20 mM bicarbonate, 10 mM HEPES and 2 mg ml^{-1} albumin, pH adjusted to 7.4; Panten *et al.*, 1989). The percentages of free drug at the indicated total drug concentrations (logarithmic scale) were measured at 37°C. Symbols indicate the mean of 2–3 separate experiments. Data analysis was performed as described in the Methods section and the calculated constants were used to extrapolate the curve for compound III (------) into the range of concentrations which could not be measured.

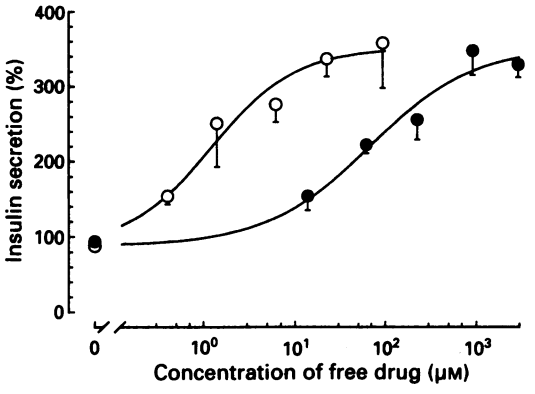


Figure 8 Dependence of insulin secretion from mouse pancreatic islets on the free concentrations (logarithmic scale) of compounds III (○) and IV (●). The secretory rates at 58 min were taken from the experiments shown in Figure 6. The free drug concentrations were calculated using the relations shown in Figure 7. Data analysis was performed as described in the Methods section. Symbols indicate the mean of results from 4–8 separate experiments (with s.e.mean shown when larger than symbols).

effects of millimolar drug concentrations probably result from occupation of both the specific sulphonylurea receptor sites and low affinity binding sites (Figure 3). Occupation of all specific sites by compound III or IV appears to cause only partial inhibition of the K_{ATP}-channels in the absence of nucleotides, but complete channel-block in the presence of Mg^{2+} and 1 mM total ADP (0.5 mM MgADP + 0.5 mM free ADP) (Figure 3). A similar ADP effect has previously been observed for tolbutamide and meglitinide and is due to the simultaneous presence of MgADP which stimulates the channel and free ADP which inhibits the channel (Zünkler *et al.*, 1988b; Panten *et al.*, 1990; Schwanstecher *et al.*, 1992d). Binding of sulphonylureas to their specific receptor increases the potency of inhibitory nucleotides and shifts the competitive interaction between stimulatory and inhibitory nucleotides towards the inhibitory nucleotides (Schwanstecher *et al.*, 1994). The K_D values for binding of tolbutamide, meglitinide, compound III and compound IV to microsomal membranes are 3 to 10 fold higher than the corresponding EC_{50} values for channel inhibition in inside-out patches exposed to ADP (Table 1). This finding is consistent with the previous conclusion that spare receptors for sulphonylureas may exist in the β-cell membrane (Panten *et al.*, 1989). All of these findings indicate that compounds III and IV control the K_{ATP}-channel via the specific sulphonylurea receptor in the same way as more lipophilic sulphonylureas and analogues.

In the outside-out patch experiments of the present study channel run-down was reduced by including 0.09 mM Mg-ATP (0.1 mM total ATP) in the cytosol-like pipette solution. In the inside-out patch experiments, channel run-down was reduced by 0.9 mM MgATP (1 mM total ATP) present in the cytosol-like bath solution except for 15 s test periods. In addition, the cytoplasmic membrane side was exposed to MgADP (0.5 mM) and free ADP (0.5 mM) when comparing the K_{ATP}-channel-inhibiting potencies of drugs applied to the extracellular side of outside-out membrane patches with the potencies of drugs applied to the intracellular side of inside-out membrane patches. Under these conditions the ratio of extracellular to intracellular EC_{50} value was 281 for compound IV, 25.5 for compound III and 1.2 for tolbutamide (Table 1). This finding can be explained by location of the sulphonylurea receptor at the cytoplasmic face of the β-cell plasma membrane and the additional assumption that the externally applied drugs are transported across the plasma membrane at rates increasing in the order compound IV < compound III < tolbutamide. In our outside-out patch experiments the rate of membrane transport controls the drug concentration effective at the internal membrane side, since the drug molecules diffuse rapidly into the recording pipette which represents an effectively infinite volume (Penner *et al.*, 1987; Pusch & Neher, 1988). Compound IV which is only present in charged form does not cross the β-cell membrane by rapid diffusion through the lipid phase of the membrane. There is some partition of compound IV into the octanol phase which is saturated with buffer (Table 1). This partition does not indicate similar affinity of compound IV for the lipid phase of plasma membranes but probably reflects that the partitioning process into octanol is an imperfect model for drug distribution between buffer and natural membranes. Carriers which remain to be characterized for β-cells might mediate the membrane transport of compound IV and the anionic forms of sulphonylureas. These carriers might resemble the transporters for the anionic forms of sulphonylureas detected in the plasma membrane of hepatocytes (Petzinger & Fückel, 1992). Whatever is the system transporting compound IV, its capacity seems to be too low to compete efficiently with the diffusion of compound IV into the pipette. However, a high octanol-water partition coefficient for undissociated tolbutamide (350; Panten *et al.*, 1989) is calculated from the pK_a value and the apparent partition coefficient (P) for tolbutamide suggesting that nonionic diffusion of the undissociated species mediates rapid membrane transport of tolbutamide. Therefore, tolbutamide applied to the external side of outside-out membrane patches appears to cross the β-cell membrane so rapidly that its rate of diffusion into the pipette does not cause a significant decrease in the tolbutamide concentration at the internal membrane side. Hence, similar tolbutamide concent-

Table 1 pK_a values, partition coefficients, binding affinities and β-cytotropic potencies of tolbutamide and glibenclamide analogues

	Tolbutamide	*Meglitinide*	*Compound III*	*Compound IV*
pK_a	5.3[a]	4.4[a]	5.3[a]	1.6[b]
P (octanol-water)	2.9[a]	2.7[a]	0.6	0.4
K_D (binding)	11.9[c]	4.0[a]	1.9	7.9
EC_{50} (inside-out)	4.0[d]	0.5	0.2	0.8
EC_{50} (outside-out)	4.8	ND	5.1	225.0
EC_{50} (whole-cell)	4.1[e]	0.5[e]	ND	ND
EC_{50} (cell-attached)	2.2[f]	ND	0.6	34.0
EC_{50} (secretion)	5.2[a]	1.6[a]	1.3	68.2

The pK_a values for compound III and IV are assumed to be similar to the pK_a values for tolbutamide and *p*-toluenesulphonic acid, respectively. Apparent octanol-water partition coefficients (P) were measured at pH 7.4. The pK_a values, the K_D values for binding to microsomes from insulin-secreting cells, the EC_{50} values for inhibition of K_{ATP}-channels in mouse β-cells (patch-clamp configuration in parentheses) and the EC_{50} values for insulin secretion in mouse pancreatic islets were taken from the Results section or were previously published ([a]Panten *et al.*, 1989; [b]Schawartz & Ladik, 1953; [c]Schwanstecher *et al.*, 1992e; [d]Schwanstecher *et al.*, 1992c; [e]Zünkler *et al.*, 1988a; [f]Panten *et al.*, 1990). The EC_{50} values for drug application to the cytoplasmic membrane side (inside-out configuration) or to the extracellular membrane side (outside-out configuration) were determined in the presence of 1 mM ADP at the cytoplasmic membrane side. K_D and EC_{50} values are given as μM of free drug. ND, not determined.

rations are probably present at the external and internal membrane side. Unlike the apparent partition coefficient (P) for compound IV, the coefficient for compound III reflects not only distribution of the charged form but also distribution of the undissociated form. Since undissociated compound III crosses the cell membrane via non-ionic diffusion, the rate of membrane transport of compound III is probably higher than that of compound IV. In comparison with undissociated tolbutamide, the undissociated form of compound III is much less lipophilic (see P values in Table 1) and its rate of non-ionic diffusion across the cell membrane is therefore much slower. Hence, in excised membrane patches no major deviation of extracellular from intracellular EC_{50} value is expected for tolbutamide whereas pronounced deviations are expected for compound III and in particular for compound IV.

Findings with meglitinide are also in accord with a location of the sulphonylurea receptor at the cytoplasmic membrane side (Table 1). Rapid membrane transport of meglitinide is suggested by the very high partition coefficient of its undissociated form (2500; Panten *et al.*, 1989) and can explain that the EC_{50} value for meglitinide externally applied in whole-cell clamp experiments is identical with the EC_{50} value for meglitinide applied to the cytoplasmic membrane side in inside-out experiments (Table 1). In the whole-cell configuration of the patch-clamp technique small molecules (M_r < 1000) diffuse rapidly from the intracellular space into the recording pipette (Penner *et al.*, 1987; Pusch & Neher, 1988).

Owing to the inside negative membrane potential, passive anion distribution across the plasma membrane leads to free anion concentrations lower at the internal than at the external membrane side of intact cells (Murer & Burckhardt, 1983). In accordance with such a transmembrane concentration gradient and location of the sulphonylurea receptor at the cytoplasmic face of the β-cell plasma membrane, cell-attached patch experiments and recordings of insulin release displayed much higher EC_{50} values for the anionic compound IV than inside-out patch experiments (Table 1). However, much less pronounced differences in EC_{50} values were observed for compound III and particularly for meglitinide and tolbutamide. When an organic acid crosses the plasma membrane of intact cells solely by diffusion of its nonionic undissociated form and not by transport of its anionic form, no transmembrane concentration gradient results for the organic acid. Thus the findings are consistent with the view that nonionic diffusion plays a major role in the transport of compound III and nearly completely controls the flux of meglitinide and tolbutamide.

In conclusion, there is strong evidence for location of the sulphonylurea receptor at the cytoplasmic face of the β-cell plasma membrane and for receptor activation by the anionic forms of sulphonylureas and their analogues.

The paper contains work of the Dr rer.nat. thesis of F. Chudziak and of the Dr med.vet. thesis of A. Moshiri. We are grateful to M. Winkler for excellent assistance. This work was supported by the Deutsche Forschungsgemeinschaft (Pa 229/5-1 and SFB 402,B1).

References

ASHCROFT, F.M., HARRISON, D.E. & ASHCROFT, S.J.H. (1984). Glucose induces closure of single potassium channels in isolated rat pancreatic β-cells. *Nature*, **312**, 446–448.

ASHCROFT, F.M. & RORSMAN, P. (1991). Electrophysiology of the pancreatic β-cell. *Prog. Biophys. Molec. Biol.*, **54**, 87–143.

ASHCROFT, S.J.H. & ASHCROFT, F.M. (1992). The sulfonylurea receptor. *Biochim. Biophys. Acta*, **1175**, 45–59.

ASHFORD, M.L.J. (1990). Potassium channel and modulation of insulin secretion. In *Potassium Channels: Structure, Classification, Function and Therapeutic Potential*. ed. Cook, N.S. pp. 300–325. Chichester: Ellis Horwood.

BROWN, G.R. & FOUBISTER, A.J. (1984). Receptor binding sites of hypoglycemic sulfonylureas and related [(acylamino)alkyl]benzoic acids. *J. Med. Chem.*, **27**, 79–81.

CHENG, Y.-C. & PRUSOFF, W.H. (1973). Relationship between the inhibition constant (K_i) and the concentration of inhibitor which causes 50 per cent inhibition (I_{50}) of an enzymatic reaction. *Biochem. Pharmacol.*, **22**, 3099–3108.

COLQUHOUN, D. & SIGWORTH, F.J. (1983). Fitting and statistical analysis of single-channel records. In *Single-Channel Recording*. ed. Sakmann, B. & Neher, E. pp. 191–193. New York, London: Plenum.

COOK, D.L. & HALES, C.N. (1984). Intracellular ATP directly blocks K^+ channels in pancreatic B-cells. *Nature*, **311**, 271–273.

DUNNE, M.J. & PETERSEN, O.H. (1991). Potassium selective ion channels in insulin-secreting cells: physiology, pharmacology and their role in stimulus-secretion coupling. *Biochim. Biophys. Acta.*, **1071**, 67–82.

EDWARDS, G. & WESTON, A. (1993). The pharmacology of ATP-sensitive potassium channels. *Annu. Rev. Pharmacol. Toxicol.*, **33**, 597–637.

FABIATO, A. (1988). Computer programs for calculating total from specified free or free from specified total ionic concentrations in aqueous solutions containing multiple metals and ligands. In *Methods in Enzymology*, Vol. 157, Part Q. ed. Fleischer, S. & Fleischer, B. pp. 378–417. San Diego: Academic Press.

FENWICK, E.M., MARTY, A. & NEHER, E. (1982). A patch-clamp study of bovine chromaffin cells and of their sensitivity to acetylcholine. *J. Physiol.*, **331**, 577–597.

GAINES, K.L., HAMILTON, S. & BOYD, A.E. III (1988). Characterization of the sulfonylurea receptor on beta-cell membranes. *J. Biol. Chem.*, **263**, 2589–2592.

GEISEN, K., HITZEL, V., ÖKOMONOPOULOS, R., PÜNTER, J., WEYER, R. & SUMM, H.-D. (1985). Inhibition of ^{3}H-glibenclamide binding to sulphonylurea receptors by oral antidiabetics. *Arzneim.-Forsch.*, **35**, 707–712.

HAMILL, O.P., MARTY, A., NEHER, E., SAKMANN, B. & SIGWORTH, F.J. (1981). Improved patch-clamp techniques for high-resolution current recording from cells and cell-free membrane patches. *Pflügers Arch.*, **391**, 85–100.

LERNMARK, Å. (1974). The preparation of, and studies on, free cell suspensions from mouse pancreatic islets. *Diabetologia*, **10**, 431–438.

MURER, H. & BURCKHARDT, G. (1983). Membrane transport of organic anions across epithelia of mammalian small intestine and kidney proximal tubule. *Rev. Physiol. Biochem. Pharmacol.*, **96**, 1–52.

OHNO-SHOSAKU, T., ZÜNKLER, B.J. & TRUBE, G. (1987). Dual effects of ATP on K^+ currents of mouse pancreatic β-cells. *Pflügers Arch.*, **408**, 133–138.

PANTEN, U., BURGFELD, J., GOERKE, F., RENNICKE, M., SCHWANSTECHER, M., WALLASCH, A., ZÜNKLER, B.J. & LENZEN, S. (1989). Control of insulin secretion by sulfonylureas, meglitinide and diazoxide in relation to their binding to the sulfonylurea receptor in pancreatic islets. *Biochem. Pharmacol.*, **38**, 1217–1229.

PANTEN, U., HEIPEL, C., ROSENBERGER, F., SCHEFFER, K., ZÜNKLER, B.J. & SCHWANSTECHER, C. (1990). Tolbutamide-sensitivity of the adenosine 5'-triphosphate-dependent K^+ channel in mouse pancreatic B-cells. *Naunyn-Schmied. Arch. Pharmacol.*, **342**, 566–574.

PANTEN, U., SCHWANSTECHER, M. & SCHWANSTECHER, C. (1992). Pancreatic and extrapancreatic sulfonylurea receptors. *Horm. Metab. Res.*, **24**, 549–554.

PENNER, R., PUSCH, M. & NEHER, E. (1987). Washout phenomena in dialyzed mast cells allow discrimination of different steps in stimulus-secretion coupling. *Biosci. Rep.*, **7**, 313–321.

PETZINGER, E. & FÜCKEL, D. (1992). Evidence for a saturable, energy-dependent and carrier-mediated uptake of oral antidiabetics into rat hepatocytes. *Eur. J. Pharmacol.*, **213**, 381–391.

PUSCH, M. & NEHER, E. (1988). Rates of diffusional exchange between small cells and a measuring patch pipette. *Pflügers Arch.*, **411**, 204–211.

SCHAWARTZ, J. & LADIK, J. (1953). Über das Acylieren von phenolischen Hydroxylgruppen. *Acta Chim. Hung.*, **3**, 305–313.

SCHWANSTECHER, M., BEHRENDS, S., BRANDT, C. & PANTEN, U. (1992a). The binding properties of the solubilized sulfonylurea receptor from a pancreatic B-cell line are modulated by the Mg^{++}-complex of ATP. *J. Pharmacol. Exp. Ther.*, **262**, 495–502.

SCHWANSTECHER, M., BRANDT, C., BEHRENDS, S., SCHAUPP, U. & PANTEN, U. (1992b). Effects of MgATP on pinacidil-induced displacement of glibenclamide from the sulphonylurea receptor in a pancreatic β-cell line and rat cerebral cortex. *Br. J. Pharmacol,*. **106,** 295–301.

SCHWANSTECHER, C., DICKEL, C., EBERS, I., LINS, S., ZÜNKLER, B.J. & PANTEN, U. (1992c). Diazoxide-sensitivity of the adenosine 5′-triphosphate-dependent K^+ channel in mouse pancreatic β-cells. *Br. J. Pharmacol.*, **107,** 87–94.

SCHWANSTECHER, C., DICKEL, C. & PANTEN, U. (1992d). Cytosolic nucleotides enhance the tolbutamide-sensitivity of the ATP-dependent K^+ channel in mouse pancreatic B-cells by their combined actions at inhibitory and stimulatory receptors. *Mol. Pharmacol.*, **41,** 480–486.

SCHWANSTECHER, C., DICKEL, C. & PANTEN, U. (1994). Interaction of tolbutamide and cytosolic nucleotides in controlling the ATP-sensitive K^+ channel in mouse β-cells. *Br. J. Pharmacol.*, **111,** 302–310.

SCHWANSTECHER, M., LÖSER, S., BRANDT, C., SCHEFFER, K., ROSENBERGER, F. & PANTEN, U. (1992e). Adenine nucleotide-induced inhibition of binding of sulphonylureas to their receptor in pancreatic islets. *Br. J. Pharmacol.*, **105,** 531–534.

STURGESS, N.C., ASHFORD, M.L.J., COOK, D.L. & HALES, C.N. (1985). The sulphonylurea receptor may be an ATP-sensitive potassium channel. *Lancet*, **ii,** 474–475.

STURGESS, N.C., KOZLOWSKI, R.Z., CARRINGTON, C.A., HALES, C.N. & ASHFORD, M.L.J. (1988). Effects of sulphonylureas and diazoxide on insulin secretion and nucleotide-sensitive channels in an insulin-secreting cell line. *Br. J. Pharmacol.*, **95,** 83–94.

TRUBE, G., RORSMAN, P. & OHNO-SHOSAKU, T. (1986). Opposite effects of tolbutamide and diazoxide on the ATP-dependent K^+ channel in mouse pancreatic β-cells. *Pflügers Arch.*, **407,** 493–499.

ZÜNKLER, B.J., LENZEN, S., MÄNNER, K., PANTEN, U. & TRUBE, G. (1988a). Concentration-dependent effects of tolbutamide, meglitinide, glipizide, glibenclamide and diazoxide on ATP-regulated K^+ currents in pancreatic B-cells. *Naunyn-Schmied. Arch. Pharmacol.*, **337,** 225–230.

ZÜNKLER, B.J., LINS, S., OHNO-SHOSAKU, T., TRUBE, G. & PANTEN, U. (1988b). Cytosolic ADP enhances the sensitivity to tolbutamide of ATP-dependent K^+ channels from pancreatic B-cells. *FEBS Lett.*, **239,** 241–244.

ZÜNKLER, B.J., TRUBE, G. & PANTEN, U. (1989). How do sulfonylureas approach their receptor in the B-cell plasma membrane? *Naunyn-Schmied. Arch. Pharmacol.*, **340,** 328–332.

(Received March 9, 1994
Revised June 22, 1994
Accepted June 27, 1994)

Br. J. Pharmacol. (1994), 113, 912–916 © Macmillan Press Ltd, 1994

Contribution of intercellular adhesion molecule 1 (ICAM-1) to the pathogenesis of splanchnic artery occlusion shock in the rat

[1]Francesco Squadrito, Domenica Altavilla, Patrizia Canale, MariaPatrizia Ioculano, Giuseppe M. Campo, Letteria Ammendolia, *Giovanni Squadrito, *Antonino Saitta, Gioacchino Calapai & Achille P. Caputi

Institute of Pharmacology and *Department of Internal Medicine, School of Medicine, University of Messina, Italy

1 It has been suggested that leukocytes play a key role in the pathogenesis of splanchnic artery occlusion shock. Intercellular adhesion molecule 1 (ICAM-1) is an adhesion molecule of crucial importance in the phenomenon of leukocyte accumulation.

2 We investigated the involvement of ICAM-1 in the pathogenesis of splanchnic artery occlusion shock. Splanchnic artery occlusion (SAO) shock was induced in anaesthetized rats by clamping splanchnic arteries for 45 min. Sham-operated animals were used as controls. Survival time, serum tumour necrosis factor-α (TNF-α), white blood cell (WBC) count, mean arterial blood pressure, myeloperoxidase activity (MPO; studied as a quantitative means to assess leukocyte accumulation) and the responsiveness to acetylcholine of aortic rings were investigated. SAO shocked rats had a decreased survival time (90 ± 9.5 min, while sham-shocked rats survived more than 4 h), reduced mean arterial blood pressure, increased serum levels of TNF-α (201 ± 10 u ml^{-1}) and MPO activity in the ileum (0.15 ± 0.03 u × 10^{-3} per g tissue) and in the lung (1.9 ± 0.8 u × 10^{-3} per g tissue), leukopenia and reduced responsiveness to acetylcholine (ACh, 10 nM–10 μM) of aortic rings.

3 Administration of monoclonal antibody raised against rat ICAM-1 significantly increased survival time (225 ± 9 min), reduced leukopenia and MPO activity both in the ileum (0.031 ± 0.003 u × 10^{-3} per g tissue) and in the lung 0.23 ± 0.03 u × 10^{-3} per g tissue), improved the cardiovascular changes and restored the responsiveness to ACh of aortic rings.

4 Our findings are consistent with an involvement of adhesion mechanisms *in vivo* in the pathogenesis of SAO shock and suggest that specific adhesion mechanisms, which support leukocyte accumulation, may represent potentially important therapeutic targets in circulatory shock.

Keywords: ICAM-1; splanchnic artery occlusion shock; leukocyte accumulation

Introduction

Splanchnic artery occlusion (SAO) shock is a lethal form of experimental shock that causes animal death within 80–95 min after the occlusive clamps have been released. It is due to prolonged ischaemia of the splanchnic region followed by reperfusion (Sturniolo *et al.*, 1988; Squadrito *et al.*, 1991) and it is also characterized by a profound fall in mean arterial blood pressure (Squadrito *et al.*, 1989), impairment in the activity of the reticuloendothelial system (Sturniolo *et al.*, 1989), enhanced macrophage and plasma levels of thromboxane B_2 (Squadrito *et al.*, 1992b), increased plasma concentration of myocardial depressant factor (MDF) and platelet activating factor (Zingarelli *et al.*, 1992b) and elevated macrophage and serum levels of tumour necrosis factor (TNF-α) (Squadrito *et al.*, 1992a). In addition we have shown that polymorphonuclear leukocytes play a key role in the pathogenesis of SAO shock: indeed leukopenia induced by administering vinblastine protects against the pathological sequelae of this experimental type of circulatory shock (Canale *et al.*, 1993).

Intercellular adherence seems to be important for leukocyte accumulation at sites of inflammation (Osborn, 1990), but recent evidence from our laboratory has suggested that adhesion mechanisms supporting leukocyte adhesion and accumulation are present in ischaemic states (Altavilla *et al.*, 1994).

It has been suggested that in endotoxin shock the administration of monoclonal antibodies against the CD11/CD18 complex reduces neutrophil accumulation (Arfors *et al.*, 1987; Harlan *et al.*, 1991). However, leukocyte accumulation is a complex phenomenon which also involves endothelium-based adhesion molecules.

In fact, endothelial adhesion molecules are considered to play a pivotal role in the localization and development of an inflammatory reaction (Butcher, 1990). Intercellular adhesion molecule 1 (ICAM-1) is an adhesion molecule normally expressed at a low basal level on endothelial cells, but its expression can be enhanced by various inflammatory mediators such as interleukin-1 (IL-1) and TNF-α (Wetheimer *et al.*, 1992). Structurally ICAM-1 is a member of the Ig supergene family with five extracellular IG-like domains, a single transmembrane region and a short cytoplasmic tail (Simmons *et al.*, 1988). It is a ligand for at least two members of the CD 18 family of leukocyte adhesion molecules: LFA-1 or CD11a/CD18 and Mac-1 CD11b/CD18 (Marlin & Springer, 1987; Diamond *et al.*, 1990).

In the present study we investigated the involvement of ICAM-1 in the pathogenesis of SAO shock. Administration of monoclonal antibody raised against rat ICAM-1 was found to increase the resistance of rats to experimental shock, to reduce leukocyte accumulation and finally to restore impaired vascular reactivity.

Methods

Surgical procedures

Male Sprague-Dawley rats weighing 250–300 g were permitted access to food and water *ad libitum*. The rats were anaesthetized with urethane (1.3 g kg^{-1}, i.v.). After anaes-

[1] Author for correspondence at: Institute of Pharmacology Piazza XX Settembre 4, 98122 Messina, Italy.

thesia, catheters were placed in the carotid artery and jugular vein. For monitoring blood pressure a cannula (PE 50) was inserted into the left common carotid artery as described elsewhere (Caputi *et al.*, 1980). The arterial catheter was connected to a pressure transducer. The pressure pulse triggered a cardiotachometer, and arterial blood pressure was displayed on a polygraph. Arterial blood pressure is reported as mean arterial pressure (MAP) in mmHg. After midline laparotomy, the coeliac and superior mesenteric arteries were isolated near their aortic origins. During this procedure, the intestinal tract was maintained at 37°C by placing it between gauze pads soaked with warmed 0.9% NaCl solution.

Rats were given heparin (1000 u kg^{-1}, i.v.) and were observed for a 30 min stabilization period prior to either splanchnic ischaemia or sham ischaemia. SAO shock was induced by clamping both the superior mesenteric artery and the coeliac trunk resulting in total occlusion of these arteries for 45 min. After this period of occlusion the clamps were removed. Following reperfusion the rats were observed for 240 min. Sham shocked rats were subjected to all the same surgical procedures as SAO shocked rats except that arteries were not occluded.

Survival evaluation

Three hours before the splanchic artery occlusion shock procedures, treated rats received intravenously anti-rat ICAM-1 monoclonal antibody (1 mg kg^{-1}) dissolved in 0.3 ml of a phosphate-buffered solution at pH 7.4 and control rats received the carrier vehicle. Survival was evaluated for 4 h.

Biological assay for tumour necrosis factor-α activity

Killing of L929 mouse tumour cells was used to measure TNF-α levels in serum on the basis of a standard assay (Ruff & Gifford, 1980). L929 cells in RPMI 1640 medium containing 5% foetal calf serum were seeded at 3×10^4 cells per well in 96-well microdilution plates and incubated overnight at 37°C in an atmosphere of 5% CO_2 in air. Serial dilutions of serum (drawn at different time intervals) were made in a medium containing actinomycin D 1 μg ml^{-1} and 100 μl of each dilution was added to the wells. On the next day, cell survival was assessed by fixing and staining the cells with crystal violet (0.2% methanol) and 0.1 ml of 1% sodium dodecyl sulphate was added to each well to solubilize the stained cells. The absorbance of each well was read at 490 nm with a model BT-100 Microelisa Autoreader. The percentage of cytotoxicity was calculated as [1 − (A490 of sample/A490 of control)] × 100. One unit of TNF-α was defined as the amount producing 50% cell cytotoxicity. TNF-α content in the sample was calculated by comparison with a calibration curve performed with recombinant murine TNF-α (Nuclear Laser Medicine, Italy). To verify if the cytotoxicity tested was due to the presence of TNF-α or to other factors, we preincubated our samples for 2 h at 37°C with an excess of rabbit antirecombinant murine TNF-α polyclonal antibody (Nuclear Laser Medicine, Milan, Italy) or with control rabbit serum. Our results showed that cytotoxicity against L929 cells was completely neutralized by rabbit anti-recombinant TNF-α polyclonal antibody but not by control rabbit serum.

Myeloperoxidase activity

Leukocyte accumulation was investigated using the activity of myeloperoxidase (MPO). MPO activity was determined in intestinal mucosa and in the left lung, as previously described (Squadrito *et al.*, 1993). The samples were obtained at 0 and 45 min before reperfusion (release of the arterial clamp) and at 80 min after reperfusion. The samples were first homogenized in a solution containing 20 mM potassium phosphate buffer (pH 7.4), 0.01 M EDTA, 50 u ml^{-1} of a protease inhibitor (aprotinin) in proportions of 1:10 (W:v) and then centrifuged for 30 min at 20,000 *g* at 4°C. The supernatant of each sample was then discarded and the pellet was immediately frozen on dry ice; freezing was continued for 14 h before sonication. After thawing, the resulting pellet was added to a buffer solution consisting of 0.5% hexacyltrimethylammonium bromide (Sigma Chemical Co., St. Louis, MO, U.S.A.) dissolved in 50 nM potassium phosphate buffered solution (pH 6) containing 30 u ml^{-1} of protease inhibitor. Each sample was then sonicated for 1 min at intensity 2 and at a temperature of 4°C. After the sonication the samples were allowed to chill on ice for approximately 30 min, and then centrifuged for 30 min at 40,000 *g* at 4°C. An aliquot of the supernatant was then allowed to react with 0.167 mg ml^{-1} *ó*-dianisidine dihydrochloride (Sigma Chemical Co.) and 0.001% H_2O_2, and the rate of change in absorbance was measured at 405 nm in a microtitre plate reader. MPO activity was defined as the quantity of enzyme degrading 1 μmol of peroxide min^{-1} at 25°C and was expressed in milliunits per gram weight ($u \times 10^{-3}$) of tissue.

Leukocyte count

Tail vein blood samples for the leukocyte count (Squadrito *et al.*, 1992a) were taken at different time intervals (0 and 45 min before occlusion, and 80 min after reperfusion). The numbner of leukocytes (WBC × $10^3/mm^3$) is shown as mean ± s.d.

Isolated aortic rings

Animals were killed 80 min after the start of reperfusion. Thoracic aortae were removed and placed in cold Krebs solution of the following composition (nM): NaCl 118.4, KCl 4.7, $MgSO_4$ 1.2, $CaCl_2$ 2.5, KH_2PO_4 1.2, $NaHCO_3$ 25.0 and glucose 11.7. Then aortae were cleaned of adherent connective and fat tissue and cut into rings of approximately 2 mm in length. Rings were then placed under 1 g of tension in an organ bath containing 10 ml Krebs solution at 37°C and bubbled with 95% O_2 and 5% CO_2 (pH 7.4). All experiments were carried out in the presence of indomethacin (10 μM) in order to exclude the involvement of eicosanoids and their metabolites. Developed tension was measured with an isometric force transducer and recorded on a polygraph (Ugo Basile, Torino, Italy). After an equilibration period of 60 min during which time the rings were washed with fresh Krebs solution at 15–20 min intervals and basal tension was readjusted to 1 g, the tissue was exposed to phenylephrine (PE, 100 nM). When the contraction was stable, the functional integrity of endothelium was assessed by a relaxant response to acetylcholine (ACh, 100 nM). The tissues were then washed occasionally for 30 min.

Endothelium-dependent relaxation was evaluated with cumulative concentrations of ACh (10 nM–1 μM) in aortic rings precontracted with PE (100 nM). Relaxation of the rings was calculated as percentage decrease of contractile force.

Drugs

Acetylcholine chloride, phenylephrine hydrochloride and indomethacin were obtained from Sigma.

Monoclonal mouse antibody raised against rat ICAM-1 (clone IA 29, subclass: IgG_1) was purchased from British Biotechnology Products Ltd (Abingdon, UK). This antibody was found to inhibit rat neutrophil adherence to rat ICAM-1. Control rats were injected with a non-immune mouse serum dissolved in the carrier vehicle (0.3 ml of phosphate-buffered saline solution at pH 7.4). Testing for the presence of endotoxin (chromogenic *Limulus* amoebocyte lysate assay) revealed < 1 pg ml^{-1} endotoxin in both the immune and non-immune serum.

Statistical analysis

The difference between the means of two groups was evaluated with an ANOVA followed by Bonferroni's test and was considered significant when $P<0.05$.

Results

Survival

Sham-shocked rats, treated either with the carrier vehicle or with anti ICAM-1 antibody, survived the entire 4 h observation period. In contrast, in rats treated with vehicle, SAO shock produced a profound shock state characterized by a high lethality and no rats survived at 2 h (survival time = 90 ± 9.5 min; $n = 8$). Administration of monoclonal antibody raised against ICAM-1 significantly protected rats from the lethality induced by splanchnic artery occlusion shock: in fact survival time in these animals was 225 ± 9 min ($n = 8$; $P<0.001$).

Arterial blood pressure

Occlusion of the splanchnic arteries produced a marked increase in mean arterial blood pressure. Subsequently pressure decreased upon release of the occlusion (Figure 1). The administration of monoclonal antibody raised against ICAM-1 significantly blunted the reduction in mean arterial blood pressure (Figure 1).

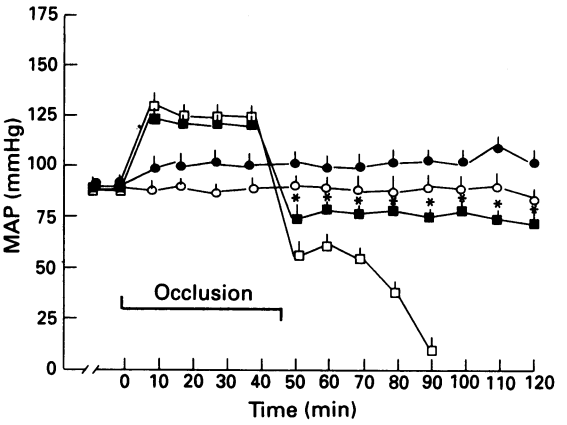


Figure 1 Effects of anti ICAM-1 antibody (1 mg kg/i.v.) or non immune serum administration (0.3 ml/i.v. dissolved in a phosphate-buffered saline solution at pH 7.4) on mean arterial blood pressure (MAP) in rats subjected to splanchnic artery occlusion (SAO) shock or sham operated. Open circles = sham operated animals + non immune serum; closed circles = sham operated animals + anti ICAM-1 antibody; open squares = SAO shocked rats + non immune serum; closed squares = SAO shocked rats + anti ICAM-1 antibody. Each point represents the mean ± s.d. of eight experiments. *$P<0.001$ vs SAO + non immune serum.

Serum TNF-α

Serum levels of TNF-α were undetectable in sham-shocked rats treated either with the immune or non-immune serum. TNF-α was also undetectable during the occlusion period. In contrast, serum TNF-α was significantly enhanced at the end of the reperfusion period in SAO shocked rats (201 ± 10 u ml^{-1}). Treatment with anti ICAM-1 antibody did not modify TNF-α levels during reperfusion (209 ± 19 u ml^{-1}).

Myeloperoxidase activity

The kinetics of ileal and pulmonary leukocyte infiltration in SAO-shocked rats were determined by measurement of the myeloperoxidase (MPO) activity content in rats at different times: 0 and 45 min after occlusion and 80 min post superfusion. MPO levels were significantly increased in the ileum (0.15 ± 0.03 u × 10^{-3} per g tissue) and in the lung (1.9 ± 0.8 u × 10^{-3}per g tissue) at 80 min after reperfusion (Table 1) in shocked rats pretreated with the non-immune serum.

Administration of monoclonal antibody raised against ICAM-1 significantly lowered the increase in ileal and pulmonary MPO activity (Table 1).

Leukocyte count

The administration of either the immune or non-immune serum did not modify the leukocyte count in sham-shocked rats. In contrast, SAO shock produced a marked leukopenia. Our data show that the leukocyte count was markedly decreased at the end (80 min) of reperfusion. The administration of monoclonal anti ICAM-1 antibody significantly ameliorated leukopenia (Table 1).

Table 1 Effects of anti ICAM-1 or non immune serum on myeloperoxidase (MPO) activity of ileum and lung and on white blood cell count (WBC) of rats subjected to splanchnic artery occlusion (SAO) shock

	Time (min)		
	Basal 0	*Ischaemia* 45	*Reperfusion* 80
MPO activity in ileum (U × 10^{-3} g^{-1} tissue)			
Sham + non-immune serum	0.018 ± 0.03	0.02 ± 0.05	0.02 ± 0.04
Sham + Ab anti-ICAM-1 (1 mg kg^{-1} i.v.)	0.021 ± 0.02	0.023 ± 0.05	0.023 ± 0.06
SAO + non-immune serum	0.035 ± 0.01	0.05 ± 0.02	0.15 ± 0.03
SAO + Ab anti-ICAM-1 (1 mg kg^{-1} i.v.)	0.033 ± 0.02	0.047 ± 0.01	0.031 ± 0.03*
MPO activity in lung (U × 10^{-3} g^{-1} tissue)			
Sham + non-immune serum	0.22 ± 0.7	0.2 ± 0.8	0.2 ± 0.5
Sham + Ab anti-ICAM-1 (1 mg kg^{-1} i.v.)	0.27 ± 0.5	0.25 ± 0.9	0.28 ± 0.8
SAO + non-immune serum	0.36 ± 0.4	0.65 ± 0.5	1.9 ± 0.8
SAO + Ab anti-ICAM-1 (1 mg kg^{-1} i.v.)	0.32 ± 0.3	0.5 ± 0.6	0.23 ± 0.3*
Circulating white cells (× 10^{-3} mm^{-3})			
Sham + non-immune serum	11.2 ± 1.2	11.5 ± 1.0	11.0 ± 1.0
Sham + Ab anti-ICAM-1 (1 mg kg^{-1} i.v.)	11.1 ± 1.1	11.3 ± 1.2	11.1 ± 1.0
SAO + non-immune serum	11.4 ± 1.0	8.0 ± 0.5	3.5 ± 0.6
SAO + Ab anti-ICAM-1 (1 mg kg^{-1} i.v.)	11.0 ± 0.4	7.8 ± 0.3	8.3 ± 0.4*

Each point represents the mean ± s.d. of seven experiments. *$P<0.001$ vs SAO + non immune serum.

Relaxant response to acetylcholine

Addition of PE (100 nM) to the organ bath contracted intact aortic rings (80–90% of the maximum response). These rings were relaxed in a concentration-dependent manner by ACh (10 nM–1 μM). The maximum relaxation by 1 μM ACh in aortic rings from shocked rats was significantly lower (Figure 2; 38 ± 3.2%) in SAO shocked rats than in sham-shocked rats (Figure 2; 80 ± 4%). Administration of monoclonal antibody raised against ICAM-1 significantly improved responsiveness to ACh (Figure 2; 90 ± 5% after 1 μM ACh).

Discussion

It has been shown that leukocytes as well as endothelium express adhesion molecules and their expression is considered to play a pivotal role in the localization and development of an inflammatory reaction (Mackay & Imhof, 1993). The first step in leukocyte-endothelium interaction is the 'rolling' of the leukocytes, a signalling event that, by altering the conformation of the extracellular binding domain of these molecules, produces the activation of other adhesion molecules belonging to the integrin family and the immunoglobulin superfamily (Butcher, 1990; Mackay & Imhof, 1993). This second interaction results in the strong adhesion of leukocytes to the endothelium and provokes the transendothelial migration of leukocytes. This second event in leukocyte-endothelium interaction seems to be mediated by the adhesion molecule ICAM-1.

ICAM-1 has a molecular weight of 95 kD (Marlin & Springer, 1987). The binding molecules for ICAM-1 in neutrophils and monocytes are the integrin ligands LFA-1 and Mac-1 (Marlin & Springer, 1987; Diamond *et al.*, 1990).

De novo expression of ICAM-1 has been described on different cell types in inflammatory lesions, during rejection and on melanoma cells (Vejlsgaard *et al.*, 1989; Johnson *et al.*, 1989; Adams *et al.*, 1989). Experimental studies have also shown that antibodies against ICAM-1 inhibit leukocyte adhesion to endothelial cells, granulocyte migration through endothelium and mixed lymphocyte reactions *in vitro* (Dougherty *et al.*, 1987; Boyd *et al.*, 1988; Merluzzi *et al.*, 1989). In addition, *in vivo* administration of antibodies raised against ICAM-1 reduces neutrophil infiltration into inflamed lungs in the rabbit, non-human primate kidney and heart allograft rejection and it blunts Ag-induced airway eosinophil influx and airway hyperresponsiveness (Barton *et al.*, 1989; Cosimi *et al.*, 1990; Flavin *et al.*, 1990; Wegner *et al.*, 1990).

Besides inflammation, recent evidence has suggested that the phenomenon of leukocyte adhesion and accumulation is involved in the mediation of myocardial reperfusion injury (Altavilla *et al.*, 1994), thus suggesting that adhesion molecules may also be important in ischaemic and/or low-flow states.

Circulatory shock is a low-flow state where leukocyte-endothelium interaction might play a key role. In fact we have previously sugested that leukocytes are deeply involved in the pathogenesis of SAO shock. Leukopenia, induced by administering vinblastine, dramatically increased the resistance of experimental animals to SAO shock (Canale *et al.*, 1993).

We therefore investigated whether ICAM-1 might be involved *in vivo* in mediating leukocyte accumulation in SAO shock, Our results shown that leukocytes significantly accumulate in the ileum and in the lung of SAO-shocked rats at the end of reperfusion. The kinetics of leukopenia and TNF-α appearance in the serum demonstrated that both pathological events occur at the end of reperfusion. Indeed a good relationship was noted between peak leukopenia, peak levels of TNF-α and maximum increase in leukocyte accumulation. Furthermore SAO shocked rats had high mortality.

Administration of monoclonal antibody raised against ICAM-1 increased the resistance of rats to the experimental procedures of SAO shock. Survival time in the group of rats given the non-immune serum was 90 ± 9.5 min, whereas rats given monoclonal anti ICAM-1 antibody showed enhanced survival (225 ± 9 min). Furthermore, the passive immunization with specific anti ICAM-1 antibodies reduced leukopenia and leukocyte accumulation in the ileum and in the lung. These data, taken together, strongly suggest that ICAM-1 is involved in the pathogenesis of SAO shock and, moreover, that this adhesion molecule significantly contributes, *in vivo*, to the mechanisms underlying leukocyte accumulation.

The mechanisms underlying the irreversible circulatory failure observed in shock are not yet well known. The involvment of the L-arginine/nitric oxide (NO) pathway in the vascular dysfunction that occurs in experimental shock has been proposed (Zingarelli *et al.*, 1992a; Nava *et al.*, 1992). As far as SAO shock is concerned, experimental pieces of evidence have pointed out that NO donors exert beneficial effects in feline SAO shock (Aoki *et al.*, 1990), thus suggesting that a dysfunction in the L-arginine/nitric oxide pathway (i.e. a decrease in NO production) might also be present in this type of experimental shock. In accordance with this hypothesis our present data show that aortic rings from SAO shocked rats had a markedly reduced responsiveness to vasorelaxant effects of ACh. Indeed this result indicates that NO generated by the endothelial constitutive NO synthase is blunted in SAO shocked rats. Adherence of leukocytes to the endothelium, by releasing cytokines such as TNF-α or oxygen-derived free radicals, may impair the release of NO from endothelial cells (Aoki *et al.*, 1989). Therefore therapeutic approaches that reduce leukocyte adherence to the endothelial cells are expected to restore the impairment in NO dysfunction. In agreement with this hypothesis, administration of monoclonal antibody raised against ICAM-1 markedly improved the responsiveness to ACh of aortic rings from SAO shocked rats by inhibiting leukocyte-endothelium interaction.

In conclusion, our study would suggest that the mechanism supporting the strong adhesion of leukocytes to endothelium (which is ICAM-1 dependent) is likely to be involved in the pathogenesis of SAO shock.

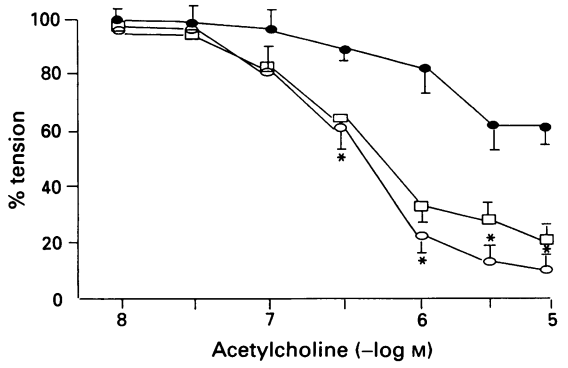


Figure 2 Relaxant effect of acetylcholine in aortic rings (contracted with phenylephrine, 100 nM) of sham operated rats (open squares), or splanchnic artery occlusion (SAO) shocked rats given either specific anti ICAM-1 antibody (1 mg/kg, i.v.) (open circles) or a non immune serum (0.3 ml/i.v. dissolved in a phosphate-buffered saline solution at pH 7.4) (closed circles). Bar heights represent the mean ± s.d. from seven experiments. *$P<0.001$ vs SAO + non immune serum.

This work was supported by Ministero Pubblica Istruzione, Fondi 40% and 60%. We gratefully acknowledge the skilful technical assistance of Carole Campbell in the preparation of the manuscript.

References

ADAMS, D.H., HUBSCHER, S.G., SHAW, J. ROTHLEIN, R. & NEURBERGER, J.M. (1989). Intercellular adhesion molecule 1 on liver allograft during rejection. *Lancet*, **ii**, 1122–1138.

ALTAVILLA, D., SQUADRITO, F., IOCULANO, M., CANALE, P., CAMPO, G.M., ZINGARELLI, B. & CAPUTI, A.P. (1994). E-selectin in the pathogenesis of experimental myocardial ischemia-reperfusion injury. *Eur. J. Pharmacol.*, **270**, 45–51.

AOKI, N., SIEGFRIED, M. & LEFER, A.M. (1989). Anti-EDRF effect of tumor necrosis factor in isolated perfused cat carotid arteries. *Am. J. Physiol.*, **256**, H1509–H1512.

AOKI, N., JOHNSON III, G. & LEFER, A.M. (1990). Beneficial effects of two forms of NO administration in feline splanchnic artery occlusion shock. *Am. J. Physiol.*, **321**, G275–G281.

ARFORS, K.-E., LUNDBERG, C., LINDBOM, L., LUNDBERG, K., BEATTY, P.G. & HARLAN, J.M. (1987). A monoclonal antibody to the membrane glycoprotein complex CD18 inhibits polymorphonuclear leukocyte (neutrophil) adherence to microvascular endothelium as well as plasma leakage in vivo and tissue accumulation of neutrophils in response to a localized source of endotoxin in rabbits. *Blood*, **69**, 338–340.

BARTON, R.W., ROTHLEIN, R., KSIAZEK, J. & KENNEDY, C. (1989). The effect of anti-intercellular adhesion molecule-1 on phorbol-ester-induced rabbit lung inflammation. *J. Immunol.*, **143**, 1278–1285.

BOYD, A.W., WAWRYK, S.O., BURNS, G.F. & FECONDO, J.V. (1988). Intercellular adhesion molecule-1 (ICAM-1) has a central role in cell-cell contact-mediated immune mechanism. *Proc. Natl. Acad. Sci. U.S.A.*, **85**, 3095–3103.

BUTCHER, E.C. (1990). Cellular and molecular mechanisms that direct leukocyte traffic. *Am. J. Pathol.*, **136**, 3–11.

CANALE, P., SQUADRITO, F., ZINGARELLI, B., ALTAVILLA, D., IOCULANO, M., CAMPO, G.M. & CAPUTI, A.P. (1993). Splanchnic artery occlusion shock: vinblastine induced leukopenia reduces tumor necrosis factor and thromboxane A_2 formation and increases survival rate. *Pharmacol. Res.*, **27**, 61–71.

CAPUTI, A.P., ROSSI, F., CARNEY, K. & BREZENOFF, H.E. (1980). Modulatory effect of brain acetylcholine on reflex-induced bradycardia and tachycardia in conscious rats. *J. Pharmacol. Exp. Ther.*, **215**, 309–316.

COSIMI, A.B., CONTI, D., DELMONICO, F.L., PREFFER, F.I., WEE, S.L., ROTHLEIN, R., FAANES, R. & COLVIN, R.B. (1990). In vivo effects of monoclonal antibody to ICAM-1 (CD54) in non human primates with renal allografts. *J. Immunol.*, **144**, 4604–4610.

DIAMOND, M.S., STAUNTON, D.E., DE FOURGEROLLES, A.R., STACKER, S.A., GARCIA-AGUILAR, J., HIBBS, M.L. & SHAW, S. (1990). ICAM-1 (CD54): a counter receptor for Mac-1 (CD11b/CD18). *J. Cell. Biol.*, **111**, 3129–3133.

DOUGHERTY, G.M., MURDOCH, S. & HOGGS, N. (1987). The function of human intercellular adhesion molecule-1 (ICAM-1) in the generation of an immune response. *Eur. J. Immunol.*, **180**, 35–41.

FLAVIN, T., ROTHLEIN, R., FAANES, R., IVENS, K. & STARNES, V. (1990). Monoclonal antibody against intercellular adhesion molecule (ICAM-1) prolongs cardiac allograft survival in cynomologous monkeys. *Transplant Proc.*, **23**, 533–540.

HARLAN, J.M., WINN, R.K., VEDDER, N.B., DOERSCHUK, C.M. & RICE, C.L. (1991). In vivo models of leukocyte adherence to endothelium. In *Adhesion: Its Role in Inflammatory Disease*. ed. Harlan J.M. & Liu D.Y. pp. 117–150. New York: W.H. Freeman and Company.

JOHNSON, J.P., STADE, B.G., HOLZMANN, B., SCHWABLE, W. & RIETHMULLER, G. (1989). De novo expression of intercellular adhesion molecule 1 in a melanoma correlates with increased risk of metastasis. *Proc. Natl. Acad. Sci. U.S.A.*, **86**, 641–650.

MACKAY, C.R. & IMHOF, B.A. (1993). Cell adhesion in the immune system. *Immunol. Today*, **14**, 99–102.

MARLIN, S.D. & SPRINGER, T.A. (1987). Purified intercellular adhesion molecule-1 (ICAM-1) is a ligand for lymphocyte function-associated antigen-1 (LFA-1). *Cell*, **51**, 813–818.

MERLUZZI, V.J., ROTHLEIN, R., WOOD, C., STEARNS, C.D., FAANES, R.B. & LAST-BARNEY, K. (1989). Inhibition of human mixed lymphocyte reactions by monoclonal antibodies to intercellular adhesion molecule-1 (ICAM-1). In *Leukocyte Adhesion Molecules*. ed. Springer, T.A., Anderson, D.C., Rosenthal, A.S. & Rothlein, R. p. 244. New York: Springer-Verlag.

NAVA, E., PALMER, R.M.J. & MONCADA, S. (1992). The role of nitric oxide in endotoxin shock. In *The Biology of Nitric Oxide, I Physiological and Clinical Aspects*. ed. Moncada S., Marletta M.A., Hibbs J.B. & Higgs, E.A. pp. 231–233. London: Portland Press.

OSBORN, L. (1990). Leukocyte adhesion to endothelium in inflammation. *Cell*, **62**, 48–51.

RUFF, M.R. & GIFFORD, G.E. (1980). Purification and physicochemical characterization of rabbit tumor necrosis factor. *J. Immunol.*, **125**, 1671–1675.

SIMMONS, D., MAKGOBA, M.W. & SEED, B. (1988). ICAM-1, an adhesion ligand of LFA-1, is homologous to the neural cell adhesion molecule NCAM. *Nature*, **331**, 624–630.

SQUADRITO, F., ALTAVILLA, D., IOCULANO, M., CALAPAI, G., ZINGARELLI, B., SAITTA, A., CAMPO, G.M., RIZZO, A. & CAPUTI, A.P. (1992a). Passive immunization with antibodies against tumor necrosis factor (TNF-α) protects from the lethality of splanchnic artery occlusion shock. *Cir. Shock*, **37**, 236–244.

SQUADRITO, F., ALTAVILLA, D., ZINGARELLI, B., IOCULANO, M., CALAPAI, G., CAMPO, G.M., MICELI, A. & CAPUTI, A.P. (1993). Tumor necrosis factor involvement in myocardial ischaemia-reperfusion injury. *Eur. J. Pharmacol.*, **237**, 223–230.

SQUADRITO, F., ALTAVILLA, D., ZINGARELLI, B., IOCULANO, M., CAMPO, G.M., SAITTA, A., URNA, G., SPIGNOLI, G. & CAPUTI, A.P. (1992b). Protective effects of G 619, a dual thromboxane synthase inhibitor and thromboxane A_2 receptor antagonist, in splanchnic artery occlusion shock. *J. Cardiovasc. Pharmacol.*, **19**, 115–119.

SQUADRITO, F., STURNIOLO, R., ALTAVILLA, D., CAMPO, G.M., TRIMARCHI, G.R., SCURI, R. & CAPUTI, A.P. (1989). Effects of fructose 1,6 diphosphate on splanchnic artery occlusion shock in the rat. *Resuscitation*, **18**, 299–307.

SQUADRITO, F., STURNIOLO, R., ALTAVILLA, D., SANTORO, G., CAMPO, G.M., ARENA, A. & CAPUTI, A.P. (1991). Platelet activating factor involvement in splanchnic artery occlusion shock in rats. *Eur. J. Pharmacol.*, **192**, 47–53.

STURNIOLO, R., ALTAVILLA, D., BERLINGHIERI, M.C., SQUADRITO, F. & CAPUTTI, A.P. (1988). Splanchnic artery occlusion shock in the rat: effects of calcium entry blockers nimodipine and verapamil. *Circ. Shock*, **24**, 43–53.

STURNIOLO, R., SQUADRITO, F., ALTAVILLA, D., TRIMARCHI, G.R., PROSDOCIMI, M. & CAPUTI, A.P. (1989). Cloricromene improves survival rate and macrophage function in splanchnic artery occlusion shock in rats. *Circ. Shock*, **28**, 267–277.

VEJLSGAARD, G.L., RALFKIAER, E., AVNSTORP, C., CZAJKOWSKI, M., MARLIN, S.D. & ROTHLEIN, R. (1989). Kinetics and characterization of intercellular adhesion molecule-1 (ICAM-1) expression on keratinocytes in various inflammatory skin lesions and malignant cutaneous lymphomas. *J. Am. Acad. Dermatol.*, **20**, 782–788.

WEGNER, C.D., GUNDEL, P., REILLY, N. & HAYNES, L.G. (1990). Intracellular adhesion molecule-1 (ICAM-1) in the pathogenesis of asthma. *Science*, **247**, 456–460.

WETHEIMER, S.J., MYERS, C.L., WALLACE, R.W. & PARKS, T.P. (1992). Intercellular adhesion molecule-1 gene expression in human endothelial cells. *J. Biol. Chem.*, **267**, 12030–12035.

ZINGARELLI, B., SQUADRITO, F., ALTAVILLA, D., CALAPAI, G., CAMPO, G.M., SAITTA, A. & CAPUTI, A.P. (1992a). Evidence for a role of nitric oxide in hypovolemic hemorrhagic shock. *J. Cardiovasc. Pharmacol.*, **19**, 982–986.

ZINGARELLI, B., SQUADRITO, F., IOCULANO, M., ALTAVILLA, D., BUSSOLINO, F., CAMPO, G.M. & CAPUTI, A.P. (1992b). Platelet activating factor interaction with tumor necrosis factor and myocardial depressant factor in splanchnic artery occlusion shock. *Eur. J. Pharmacol.*, **222**, 13–19.

(Received February 23, 1994
Revised June 27, 1994
Accepted June 28, 1994)

Br. J. Pharmacol. (1994), **113**, 917–925 © Macmillan Press Ltd, 1994

Regulation of nicotinic receptors in rat brain following quasi-irreversible nicotinic blockade by chlorisondamine and chronic treatment with nicotine

H. El-Bizri & [1]P.B.S. Clarke

Department of Pharmacology and Therapeutics, McGill University, 3655 Drummond St, Montreal, Canada H3G 1Y6

1 Chronic administration of nicotinic agonists *in vivo* increases the density of brain nicotinic binding sites. It has been proposed that this up-regulation results from agonist-induced functional blockade of nicotinic receptors. This hypothesis was tested by examining post mortem [^{3}H]-nicotine and [^{125}I]-α-bungarotoxin ([^{125}I]-αBTX) binding following treatment *in vivo* with the quasi-irreversible and insurmountable CNS nicotinic blocker chlorisondamine, given either alone or in combination with chronic nicotine administration.

2 In rats that had not received chlorisondamine pretreatment, chronic nicotine administration (0.6 mg kg^{-1} s.c., twice daily for 12 days) increased [^{3}H]-nicotine binding density (B_{max}) in forebrain tissue sections by 19%, with no change in the apparent dissociation constant (K_D). Chlorisondamine (10 mg kg^{-1}, s.c.), given once prior to the chronic treatment phase, neither increased [^{3}H]-nicotine binding by itself, nor altered the extent of nicotine-induced up-regulation. Nevertheless, chlorisondamine pretreatment resulted in a persistent blockade of CNS nicotinic receptors, as demonstrated by complete block of acute locomotor responses to nicotine.

3 In a second experiment, [^{3}H]-nicotine and [^{125}I]-αBTX binding was measured in tissue homogenates prepared from several brain regions. In the absence of chlorisondamine pretreatment, chronic nicotine administration (1 mg kg^{-1} s.c., twice daily for 12 days) increased the B_{max} of [^{3}H]-nicotine binding in the cerebral cortex (by 34%), striatum (by 28%), midbrain (by 16%) and hippocampus (by 36%); K_D was unchanged. As before, this up-regulation was neither mimicked nor blocked by chlorisondamine pretreatment (10 mg kg^{-1}, s.c., given twice), despite persistent blockade of acute locomotor responses to nicotine. Chronic nicotine treatment also increased the B_{max} (but not K_D) of [^{125}I]-αBTX binding in cerebral cortex (by 35%), hippocampus (by 46%) and midbrain (by 35%). Chlorisondamine altered neither B_{max} nor K_D when given alone, but significantly attenuated the nicotine-induced up-regulation of toxin binding sites in midbrain, with a similar trend in the other two regions.

4 The finding that chronic receptor blockade neither mimicked nor blocked the agonist-induced up-regulation of [^{3}H]-nicotine binding sites suggests that up-regulation of these receptors is not determined by their functional status. In contrast, it appears that chronic nicotine-induced up-regulation of [^{125}I]-αBTX binding sites may result from receptor activation.

Keywords: Nicotine; chlorisondamine; locomotor activity; nicotinic receptors; α-bungarotoxin; receptor regulation

Introduction

Chronic *in vivo* treatment with nicotine and other nicotinic agonists increases the density of high-affinity binding sites for [^{3}H]-nicotinic agonists in rodent brain (e.g. Marks *et al.*, 1983; Schwartz & Kellar, 1983; Morrow *et al.*, 1985; Lapchak *et al.*, 1989; Collins *et al.*, 1990a; Rowell & Wonnacott, 1990; Sanderson *et al.*, 1993). An analogous finding has been reported in the brains of human smokers *post mortem* (Benwell *et al.*, 1988). Nicotine-induced receptor up-regulation is regarded as paradoxical because nicotine is classed as an agonist. However, nicotine can cause CNS nicotinic receptor desensitization, and it has been proposed that chronic treatment with nicotine may thus functionally block its own receptors, leading to a compensatory receptor up-regulation (Marks *et al.*, 1983; Schwartz & Kellar, 1985).

If long-term functional block of nicotinic receptors is sufficient to produce up-regulation, the latter should also occur after chronic treatment with a centrally-active nicotinic antagonist. However, Schwartz & Kellar (1985) reported that subcutaneous injections of mecamylamine or dihydro-β-erythroidine did not alter cortical nicotinic [^{3}H]-acetylcholine ([^{3}H]-ACh) binding in rats, whereas subjects treated in parallel with nicotine did show such an up-regulation. Subsequently, Collins *et al.* (1990a) reported that chronic infusion with mecamylamine increased [^{3}H]-nicotine binding in mouse brain. Thus, the mechanisms underlying chronic nicotine-induced up-regulation remain unclear.

Recently, CNS nicotinic receptor up-regulation was re-examined in an initial study employing the nicotinic antagonist chlorisondamine (CHL) (Clarke *et al.*, 1994). This drug has an unusually persistent action; whereas acute blockade by mecamylamine or dihydro-β-erythroidine lasts for a few hours at most, a single administration of CHL produces a blockade of CNS nicotinic receptor-mediated responses which persists for several weeks at least (Clarke & Kumar, 1983; Clarke, 1984; Kumar *et al.*, 1987; El-Bizri & Clarke, 1994b). Blockade by CHL appears pharmacologically selective (Clarke, 1984; Reavill *et al.*, 1986; Kumar *et al.*, 1987; Corrigall *et al.*, 1992; Clarke *et al.*, 1994; El-Bizri & Clarke, 1994b). Like mecamylamine, but in contrast to dihydro-β-erythroidine, CHL has been shown to produce an insurmountable antagonism of central nicotinic responses (El-Bizri & Clarke, 1994a). We and others recently observed that nicotinic blockade resulting from a single administration of CHL was not accompanied by a change in the density of [^{3}H]-nicotine binding in rat brain (Clarke *et al.*, 1994; Decker *et al.*, 1994).

A second major population of CNS nicotinic receptors is labelled with high affinity by [^{125}I]-α-bungarotoxin ([^{125}I]-

[1] Author for correspondence.

αBTX); these receptors are not identified in standard assays using [^{3}H]-nicotine or [^{3}H]-ACh (Marks & Collins, 1982; Schwartz *et al.*, 1982; Clarke *et al.*, 1985). In mice, chronic treatment with nicotine consistently increases the density of brain [^{125}I]-αBTX binding sites (Collins *et al.*, 1990a), whereas in rats, both increases (Morley, 1989; Collins *et al.*, 1990b) and no change (Marks *et al.*, 1986; Sanderson *et al.*, 1993) have been reported. In a preliminary report, the administration of mecamylamine alone did not alter [^{125}I]-αBTX binding to rat cerebral cortex, but enhanced nicotine-induced up-regulation (Morley, 1989).

The principal aim of the present study was to test whether chronic *in vivo* blockade of nicotinic receptors could account for the ability of nicotine to up-regulate nicotinic binding sites in the brain. Continuous nicotinic receptor blockade was assured through the use of the quasi-irreversible antagonist CHL, and the persistence of central nicotinic blockade was directly confirmed in behavioural tests (Clarke & Kumar, 1983). Several brain regions were examined, since nicotinic cholinergic tone may be region-dependent. In addition, since the possibility has not been excluded that the paradoxical nicotine-induced up-regulation results from receptor activation, it was of interest to test whether CHL pretreatment could prevent nicotine-induced up-regulation. Finally, observations were extended to the effects of chronic drug treatment on nicotinic receptors that bind with high affinity to [^{125}I]-αBTX.

Methods

Male Sprague-Dawley rats (Charles River, St. Constant, Quebec, Canada), weighing 230–300 g, were maintained on a 12 h light/12 h dark cycle. Rats were housed four per cage and were allowed 3 days for acclimatization before use. Food and water were available *ad libitum*.

Locomotor activity tests

The 12 test cages (approximate dimensions in cm: 42 × 25 × 31 high) were made of clear perspex with perforated lids to permit ventilation. The floor was coated with a thin layer of sawdust. Parallel infra-red photobeams, 34 cm apart, were projected 3 cm above the floor and 4 cm away from the two short sides of the chamber. Photobeam interruptions were registered by an in-house computer programme and locomotor activity was measured by the number of times a rat moved from one beam to the other. Sessions were of 120 min duration, starting immediately after injection. Locomotor testing was carried out between 9 h 00 min and 14 h 00 min. Rats were permitted to habituate to the behavioural room for 30 min prior to testing.

[^{3}H]-nicotine binding to forebrain sections

Slide-mounted rat brain sections were prepared as described previously (Clarke *et al.*, 1984). Briefly, coronal forebrain sections (20 μm thick, $n = 24$ per rat) were cut at −16°C in a cryostat (Frigocut model 2700; Reichert-Jung, Nubloch, Germany). Sections were thaw-mounted on pre-cleaned gelatin-coated glass microscope slides, 2 sections per slide, dried under partial vacuum at 4°C for 12 h, and stored at −40°C until use. Thawed slide-mounted brain sections were placed in racks and incubated in 250 ml capacity glass dishes containing [^{3}H]-nicotine in 50 mM Tris buffer/8 mM Ca^{2+} buffer (pH 7.4), for 30 min at RT. [^{3}H]-nicotine incubations were conducted in a nitrogen atmosphere and protected from light. Sections were then gently agitated in four consecutive washes of 30 s each, in Tris/Ca^{2+} buffer (composition as above), pH 7.4 at 4°C. Sections were then immediately dried under a stream of cold air. Non-displaceable binding was defined by the addition of 10^{-5} M (−)-nicotine bitartrate. Sections were scraped into glass scintillation vials (Fisher Scientific, Montreal, Canada) and vortexed in 1 ml distilled water. Scintillation cocktail (4 ml; Hi-Safe, Fisher Scientific) was added and vortexed, and radioactivity was measured in a liquid scintillation counter (Wallac 1410; Pharmacia LKB Biotech, Sweden). Free concentrations of [^{3}H]-nicotine were determined after each incubation.

Saturation analysis of [^{3}H]-nicotine binding was initially performed using sections from a drug-naive rat (16 concentrations: 0.1–24 nM). This initial assay revealed a single high affinity binding component ($K_D = 2.58$ nM, $r = 0.91$). Subsequent assays were performed using 7 concentrations of [^{3}H]-nicotine (0.24–16 nM).

Preparation of tissue homogenates

Animals were decapitated, and cerebral cortex (left or right, randomly selected), hippocampus, striatum, midbrain and cerebellum were dissected on ice. Tissues were immediately weighed and stored at −40°C. Binding assays were prepared according to the method of Marks *et al.* (1986) with minor modifications suggested by the authors. Briefly, thawed brain tissues were homogenized (15 ml polypropylene tubes; Sarstedt, St. Laurent, Canada) in 10 volumes of incubation buffer (concentrations in mM: NaCl 118, KCl 4.8, $CaCl_2$ 2.5, $MgSO_4$ $(H_2O)_7$ 1.2, HEPES 20, NaOH 10), by 12 up and 12 down strokes at 850 r.p.m. Tissue homogenates were incubated in buffer at 37°C for 5 min, and centrifuged at 12000 *g* for 20 min. The supernatant was discarded and the pellet resuspended in an equal volume of distilled H_2O, incubated at 4°C for 30 min then at 37°C for 5 min. The centrifugation, pellet resuspension and incubation (at 4°C and 37°C) steps were repeated once. The homogenate was centrifuged once more and the pellet was resuspended in incubation buffer to a final dilution of 40 mg original tissue ml^{-1} (cerebral cortex, midbrain, cerebellum) or 30 mg original tissue ml^{-1} (hippocampus, striatum). Each homogenate sample was divided into 4 aliquots, centrifuged at 15,000 or 17,000 *g* for 15 min and stored at −40°C until use. On the day of the assay, thawed tissue was resuspended, incubated at 37°C for 5 min, centrifuged at 15,000 *g* for 20 min then resuspended in an equal volume of fresh incubation buffer.

[^{3}H]-nicotine binding to tissue homogenates

Tissue incubation was performed in uncoated polystyrene, U-bottom 96 multiwell plates (Dynatech Laboratories, Chantilly, VA, U.S.A.). The final volume of incubation in each well was 100 μl. Non-displaceable binding was determined in the presence of 10^{-5} M nicotine bitartrate. Determinations were made in quadruplicate (cerebral cortex, midbrain and cerebellum) or triplicate (hippocampus and striatum). Tissue membranes were incubated at 4°C for 120 min. Subsequent washing and filtration steps were performed using a Inotech cell harvester (Biosystems International Inc., Lansing, MI, U.S.A.) at 4°C. Filter (A/E glass fibre filter; Gelman Sciences, Ann Arbor, MI, U.S.A.) and prefilter (borosilicate microfibre filter; Micro Filtration Systems, Dublin, CA, U.S.A.) were presoaked in incubation buffer containing 0.05% polyethyleneimine (PEI) overnight. Homogenates received 6 washes with incubation buffer (as above except containing HEPES 5 mM). Filters were vortexed in 0.5 ml distilled H_2O in polyethylene vials (Fisher Scientific) and vortexed again with 7 ml of scintillation cocktail (Hi-Safe; Fisher Scientific). Radioactivity was measured in a liquid scintillation counter (Wallac 1410; Pharmacia LKB Biotech, Sweden).

Saturation analysis of [^{3}H]-nicotine binding was initially performed on cerebral cortex homogenate from a drug-naive rat (16 concentrations: 0.24–30 nM). Scatchard analysis revealed a single high affinity binding site ($K_D = 0.90$ nM, $r = 0.97$). Subsequent binding assays were performed using 3 concentrations of [^{3}H]-nicotine (0.24, 2 and 16 nM). It should be noted that the lower K_D values obtained with tissue

homogenates than with tissue sections is attributable to the lower incubation temperature (unpublished observations).

[^{125}I]-αBTX binding to tissue homogenates

The procedure was as for the [^{3}H]-nicotine binding with the following modifications: incubations were at 37°C for 4 h; non-displaceable binding was determined in the presence of 10^{-3} M nicotine; prefilters were presoaked in incubation buffer containing 0.05% PEI and 0.5% w/v powdered milk (Carnation, Nestlé, Ont., Canada) at 4°C, 1 h before use; filters were counted in a gamma counter (COBRA II; Canberra Packard Canada, Montreal, Canada).

Initial tests were conducted using brain homogenates from drug-naive rats in order to characterize [^{125}I]-αBTX binding. These experiments confirmed that [^{125}I]-αBTX bound to brain homogenates with a single high-affinity component and that *in vitro* administration of CHL did not appreciably alter [^{125}I]-αBTX binding (see Results). Since displaceable binding was barely detectable in the striatum and the cerebellum, these regions were not examined further. Subsequently, saturation analysis was performed on cerebral cortex, midbrain and hippocampus from all chronically treated animals, using 6 concentrations of [^{125}I]-αBTX (0.08–8 nM). Since the results with [^{125}I]-αBTX binding were inconclusive, 4 more rats per group were added to this part of the experiment.

Data analysis

Binding isotherms were analysed for each individual rat by non-linear regression analysis (LIGAND, Elsevier Biosoft, Cambridge, UK) (Munson & Rodbard, 1980). The effects of CHL pretreatment and chronic nicotine treatment on B_{max} and K_D were examined by analysis of variance, using commerical software (Systat, Evanston, IL, U.S.A.). Selected between-group comparisons of B_{max} values were made for each brain region and for each ligand by Student's t test, as follows: effect of nicotine alone (group 1 vs 2), effect of CHL alone (group 1 vs 3), and effect of nicotine after CHL pretreatment (group 3 vs 4). In locomotor activity tests, the effects of acute administration of nicotine were defined by subtracting the saline photocell scores from the corresponding nicotine scores for each individual rat; within a given group, a significant nicotine effect refers to a Student's t test comparison between nicotine-saline difference scores and zero. Throughout this study, t tests were subjected to Bonferroni's correction (Glantz, 1992). Probability values were 2-tailed.

Drugs

Chemicals were as follows: [^{3}H]-nicotine (nicotine, -(−)-[N-methyl-^{3}H]-, specific activity 71.3–85 Ci mmol^{-1}; New England Nuclear, Boston, MA, U.S.A.); [^{125}I]-α-bungarotoxin ([^{125}I]Tyr^{54}-α-bungarotoxin, specific activity 111.2–131.2 Ci mmol^{-1}; New England Nuclear, Boston, MA, U.S.A.); (−)-nicotine hydrogen tartrate, Tris base (Sigma Chemical Corp., St. Louis, MO, U.S.A.); polyethyleneimine (PEI) (ICN Biomedicals Canada, St. Laurent, Canada); and chlorisondamine chloride (CHL) (gift of Ciba-Geigy, Summit, NJ, U.S.A.). Other chemicals were purchased from commerical sources. For *in vivo* administration, drugs were dissolved in saline (0.9% NaCl solution) and given as 1 ml kg^{-1} s.c. The nicotine tartrate solutions were neutralized with NaOH to pH 7.3 ± 0.1 prior to administration. Doses of nicotine and CHL refer to the free base. The [^{3}H]-nicotine was purified by thin layer chromatography (Uniplate, Analtech, Newark, U.S.A.) (Romm *et al.*, 1990).

Procedures

Experiment 1: Effects of chloridondamine and nicotine on locomotor activity and [^{3}H]-nicotine binding to forebrain sections Rats were randomly allocated to 4 groups (n = 12 per group), corresponding to all possible combinations of pretreatment (saline vs CHL) and chronic treatment (saline vs nicotine). Each group was divided into two subgroups, whose treatments were staggered two days apart. Rats received a subcutaneous injection of saline (groups 1 and 2) or CHL (10 mg kg^{-1}: groups 3 and 4) at 9 h 00 min on the first day, and three days later were subjected to a first set of locomotor activity tests in order to test for central nicotinic blockade by CHL. Each rat received one test with saline and one with nicotine (0.6 mg kg^{-1}, s.c.), given on two consecutive days. The order of drug administration was counterbalanced within each group.

The following day, chronic treatment with saline (groups 1 and 3) or nicotine (0.6 mg kg^{-1}, s.c.) (groups 2 and 4) was initiated. Injections were given twice daily, at 8 h 00 min and 18 h 00 min, for 10 days. This was followed by a second set of locomotion tests, given as before except that the chronic treatment was maintained during the first day of locomotor activity tests; rats from group 2 and 4 which were scheduled to receive locomotor tests after saline injection, received their nicotine injection after the session. Final chronic injections with nicotine were given on the second test day immediately after the locomotor activity session. Animals were decapitated 24 h later, and their brains were rapidly frozen in isopentane (−50°C) and stored at −40°C. Subsequently, forebrain sections of these rats were prepared for [^{3}H]-nicotine binding.

Experiment 2: Effects of chlorisondamine and nicotine on locomotion and on [^{3}H]-nicotine and [^{125}I]-αBTX binding in microdissected brain regions The *in vivo* procedure was the same as in Experiment 1 with the following modifications. Given the lack of observed effect by CHL on [^{3}H]-nicotine binding, the pretreatment was increased to two s.c. injections of either saline (groups 1 and 2) or CHL (10 mg kg^{-1}, s.c.) (groups 3 and 4). The first injection was given at 9 h 00 min, and the second at 17 h 00 min the following day. Locomotor activity tests were given after but not prior to chronic treatment. A higher nicotine dose (1 mg kg^{-1}) was used both for the chronic treatment and the locomotor testing in order to increase the extent of nicotine-induced up-regulation. Following decapitation, brains were immediately dissected on ice as described above.

Results

Experiment 1: Effects of chlorisondamine and nicotine on locomotor activity and [^{3}H]-nicotine binding in the forebrain sections

CHL pretreatment resulted in a small (23%) reduction in saline test locomotor scores prior to the chronic treatment with nicotine (t test: $P<0.05$). In animals that had not received CHL, nicotine decreased locomotor activity in the first 20 min after injection (t test: $P<0.02$) (Figure 1a). In rats pretreated with CHL, nicotine did not produce a depressant effect (t test: $P>0.05$) (Figure 1a). In the remainder of the session (20–120 min after injection), nicotine stimulated locomotor activity in the groups that had not received CHL (t test: $P<0.02$), and this stimulant effect was also completely blocked by pretreatment with CHL (Figure 1a).

In the second set of locomotor activity tests (given after chronic treatment), the initial depressant effect of nicotine was absent in all four groups. Therefore, only total session scores (0–120 min) were subsequently analysed. Neither CHL pretreatment nor chronic treatment with nicotine significantly altered saline test scores (ANOVA: $P>0.05$ for each). In rats that had not been pretreated with CHL, acute administration of nicotine tended to stimulate locomotor activity, but this effect was only significant in the group that had received chronic treatment with nicotine (t test: group 1,

$P>0.05$; group 2: $P<0.0005$) (Figure 1b). The locomotor stimulant effect of nicotine was completely absent in both groups pretreated with CHL (t test: group 3, $P>0.5$; group 4: $P>0.05$).

The saturation analysis of [^{3}H]-nicotine binding to forebrain sections revealed no significant drug-induced change in the apparent dissociation constant (K_D) (ANOVA: main effects of nicotine, CHL and interaction, $P>0.05$, for each), and K_D values were very similar across groups (K_D values in nM: group 1, 2.1 ± 0.3; group 2, 2.4 ± 0.2; group 3, 2.1 ± 0.3; group 4, 2.1 ± 0.15). In the absence of CHL pretreatment, chronic treatment with nicotine produced a small (19%) but significant increase in the binding site density (B_{max}) (t test: $P<0.005$) (Figure 2). CHL pretreatment neither altered B_{max} when given alone (t test: groups 1 vs 3: $P>0.5$), nor altered the increase in B_{max} resulting from the chronic administration of nicotine (Nic) (ANOVA: Nic × CHL interaction: $P>0.5$). B_{max} values (mean ± s.e.mean) for groups 1, 2, 3 and 4 were 13.0 ± 0.5, 15.4 ± 0.5, 12.9 ± 0.4 and 15.2 ± 0.7 fmol per section, respectively.

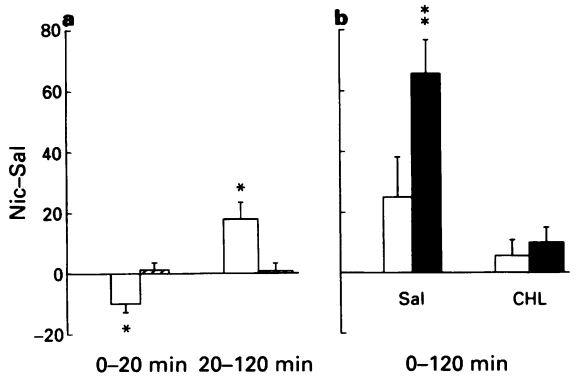


Figure 1 The effects of acute nicotine on locomotor activity in rats pretreated with chlorisondamine (CHL, 10 mg kg^{-1}, s.c.) or saline (Sal), before (a) and after (b) 10 days of chronic treatment with nicotine (0.6 mg kg^{-1}, s.c.) or saline (Expt 1). (a) After pretreatment with chlorisondamine (widely hatched columns) or saline (open columns). (b) After chronic treatment with nicotine (narrowly hatched columns) or saline (open columns). Each rat served as its own control, receiving one locomotor test after nicotine injection (0.6 mg kg^{-1}, s.c.) and one locomotor test after saline, given on consecutive days in a counterbalanced order. The vertical axis represents the mean nicotine effect (± s.e.mean), determined by subtracting saline test scores from nicotine test scores (0.6 mg kg^{-1}, s.c.) (n = 12 rats per group). *$P<0.02$; **$P<0.0005$ (Student/Bonferroni t test) denotes a significant effect of nicotine.

Experiment 2: Effects of chlorisondamine and nicotine on locomotor activity and on [^{3}H]-nicotine and [^{125}I]-αBTX binding in microdissected brain regions

In the locomotor activity tests, saline session scores were increased by 44.6% by CHL pretreatment (ANOVA: $P<0.05$), but were unaffected by prior chronic treatment with nicotine (ANOVA: main effect, $P>0.5$; CHL × Nic interaction, $P>0.1$). In the first 20 min after injection (Figure 3a), nicotine depressed activity in drug-naive rats (group 1: $P<0.05$) but tended to increase activity in subjects that had received chronic nicotine treatment (group 2: $P>0.05$). In groups pretreated with CHL, nicotine produced neither an increase nor a decrease in locomotor activity during this period (t test, groups 3 and 4: $P>0.5$ for both) (Figure 3a). In the remainder of the session (20–120 min), nicotine stimulated locomotor activity in CHL-naive rats (groups 1 and 2; t test: $P<0.005$ for each). This acute locomotor stimulant effect by nicotine appeared to be more marked in group 2, which had previously received chronic nicotine, than in group 1 (Figure 3b). In both groups

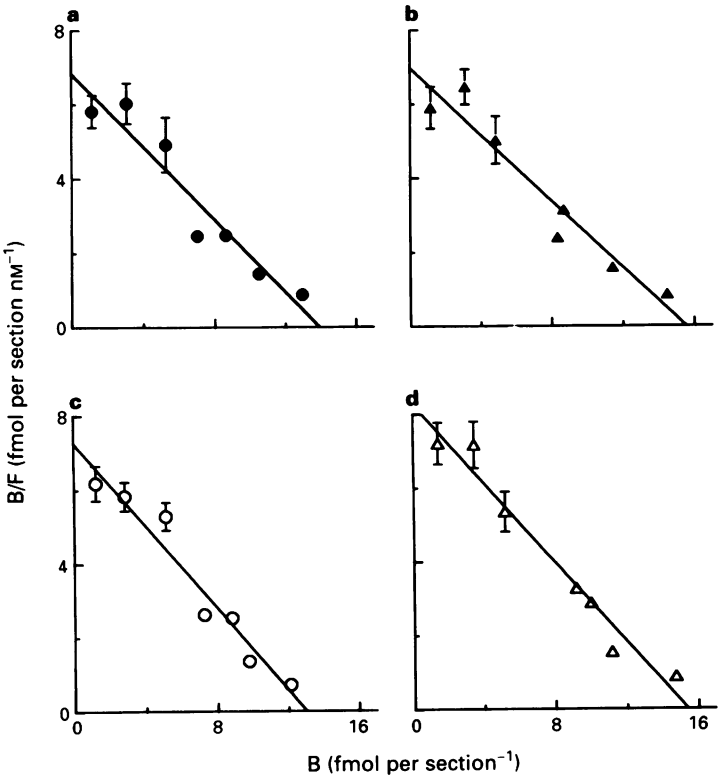


Figure 2 Scatchard plots of [^{3}H]-nicotine binding (concentrations: 0.24–16 nM) to coronal forebrain sections (Expt 1). Groups of rats were pretreated with saline (a,b) or chlorisondamine (10 mg kg^{-1}, s.c.) (c,d), and 3 days later were treated for 10 days with saline (a,c) or nicotine (0.6 mg kg^{-1}, s.c. twice daily) (b,d). Data points represent group mean values of bound/free (± s.e.mean; vertical axis) and bound (horizontal axis) (n = 10–11 rats per group).

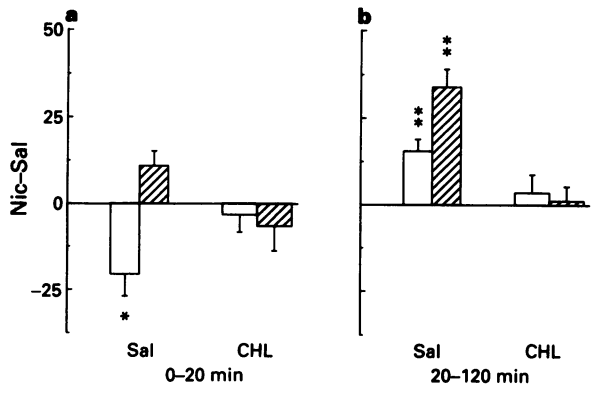


Figure 3 The acute effects of nicotine on locomotor activity in rats which had received two injections of chlorisondamine (CHL, 10 mg kg^{-1}, s.c.) or saline, followed by 10 days of twice-daily treatment with nicotine 1 mg kg^{-1}, s.c. (hatched columns) or saline (open columns) (Expt 2). Each rat served as its own control, receiving one locomotor test after nicotine (1 mg kg^{-1}, s.c.) and one locomotor test after saline, given on consecutive days in a counterbalanced order. The vertical axis represents the mean nicotine effect (± s.e.mean), determined by subtracting saline test scores from nicotine test scores, 0–20 min (a) and 20–120 min (b) post injection ($n = 12$ rats per group). *$P<0.05$; **$P<0.005$ (Student/Bonferroni t test) denotes a significant effect of nicotine.

pretreated with CHL, the locomotor stimulant effect of nicotine was absent (t test; groups 3 and 4: $P>0.5$ for each).

Analysis of [^{3}H]-nicotine binding revealed no significant change in K_D (Table 1) occurring after either pretreatment with CHL or chronic treatment with nicotine (ANOVA: main effects, $P>0.1$; interaction, $P>0.05$ for each brain region) (Table 1). In the absence of CHL pretreatment, chronic treatment with nicotine increased the B_{max} of [^{3}H]-nicotine binding in cerebral cortex (34%; t test: $P<0.0005$), midbrain (16%; t test: $P<0.01$), striatum (28%; t test: $P<0.005$), and hippocampus (36%; t test: $P=0.06$), but not in cerebellum (2%) (Figure 4). Pretreatment with CHL alone did not alter the B_{max} in any of the regions examined (t test: $P>0.05$, for each brain region). In subjects pretreated with CHL, nicotine significantly increased B_{max} in cerebral cortex, striatum and hippocampus (t test: $P<0.05$ for each). CHL pretreatment did not significantly alter nicotine-induced up-regulation (ANOVA interaction term, $P>0.05$, for each brain region) (Figure 4). In midbrain tissue from subjects pretreated with CHL, nicotine did not produce a significant increase in B_{max} (t test: $P>0.5$). However, there was no significant interaction between CHL and nicotine treatments ($P>0.05$).

In initial experiments, saturation analysis of [^{125}I]-αBTX binding (12 concentrations: 0.06–6 nM) to brain homogenates of drug-naive rats revealed a single high-affinity binding component (in cerebral cortex, hippocampus and midbrain: $K_D = 0.83$, 1.28, 0.69 nM respectively), reflected in linear Scatchard plots ($r = 0.93$, 0.94 and 0.86, respectively). Additional tests showed that [^{125}I]-αBTX binding (0.6 nM) was not appreciably affected by the prior addition of CHL *in vitro*, in concentrations that might conceivably be attained *in vivo*. Thus, binding (mean ± s.e.mean) in the presence of CHL (0.001, 0.01, 0.1, 1, 10, 100 μM) was 97 ± 3, 94 ± 11, 99 ± 5, 98 ± 5, 102 ± 9 and 95 ± 6% of control values respectively. Only at the highest concentration of CHL tested (1 mM) was binding significantly reduced (58 ± 4% of control).

Analysis of [^{125}I]-αBTX binding revealed no change in the K_D, either after CHL pretreatment or chronic nicotine treatment (ANOVA: main effects, $P>0.1$; interaction term, $P>0.05$ for each region) (Table 1). In the absence of CHL, chronic treatment with nicotine increased the density of toxin binding sites in all three regions examined: cerebral cortex (35%, t test: $P<0.01$), hippocampus (46%, t test: $P<0.005$) and midbrain (35%, t test: $P<0.05$) (Figure 5). Pretreatment with CHL alone did not increase the B_{max} of [^{125}I]-αBTX binding in any of the regions examined (t test: $P>0.1$ for each region). In CHL-pretreated rats, chronic nicotine treatment did not significantly increase B_{max} in any of the regions examined (t test: $P>0.5$ for each region). CHL blockade of nicotine-induced up-regulation was confirmed by a significant ANOVA interaction term in midbrain ($P<0.005$), with a similar trend in cerebral cortex and hippocampus ($P<0.08$ for each) (Figure 5).

Table 1 Apparent dissociation constants (K_D)* of [^{3}H]-nicotine and [^{125}I]-α-bungarotoxin ([^{125}I]-αBTX) to brain tissue homogenates

	[^{3}H]-nicotine			
	Group 1 Sal/Sal	*Group 2 Sal/Nic*	*Group 3 CHL/Sal*	*Group 4 CHL/Nic*
CC	0.73 ± 0.06	0.66 ± 0.04	0.71 ± 0.05	0.89 ± 0.13
MB	0.82 ± 0.08	1.16 ± 0.15	0.88 ± 0.08	0.76 ± 0.10
HC	0.69 ± 0.10	0.57 ± 0.06	0.75 ± 0.11	0.62 ± 0.10
ST	0.75 ± 0.08	0.67 ± 0.10	0.66 ± 0.10	0.67 ± 0.08
CM	0.61 ± 0.05	0.67 ± 0.07	0.70 ± 0.05	0.57 ± 0.06
	[^{125}I]-αBTX			
	Group 1 Sal/Sal	*Group 2 Sal/Nic*	*Group 3 CHL/Sal*	*Group 4 CHL/Nic*
CC	0.82 ± 0.05	0.92 ± 0.07	0.85 ± 0.06	0.89 ± 0.13
MB	1.04 ± 0.08	1.21 ± 0.05	1.10 ± 0.07	1.05 ± 0.06
HC	1.10 ± 0.13	1.13 ± 0.09	1.10 ± 0.12	1.23 ± 0.09

Rats received two injections of chlorisondamine (10 mg kg^{-1}, s.c.) (CHL: groups 3 and 4) or saline (Sal: groups 1 and 2), followed by 10 days of treatment with nicotine 1 mg kg^{-1}, s.c. twice daily (Nic: groups 2 and 4) or saline (Sal: groups 1 and 3). CC, cerebral cortex; MB, midbrain; HC, hippocampus; ST, striatum; CM, cerebellum. *Mean (± s.e.mean) K_D ($n = 9$–12 and 14–16 for [^{3}H]-nicotine and [^{125}I]-αBTX, respectively).

Discussion

CHL pretreatment did not alter [^{3}H]-nicotine binding

In the present study, pretreatment with CHL resulted in a complete and continuous central nicotinic blockade (as assessed by locomotor tests) but failed to alter either the affinity or density of [^{3}H]-nicotine binding sites in any of the brain regions examined. The lack of effect on binding density is consistent with previous reports from our laboratory and from others (Clarke *et al.*, 1994; Decker *et al.*, 1994).

Our observation that *in vivo* treatment with CHL did not alter the K_D of [^{3}H]-nicotine binding stands in contrast to certain previous findings (Clarke *et al.*, 1994; Decker *et al.*, 1994). We initially reported a decrease in K_D following CHL treatment, albeit in only one of two forebrain levels sampled (Clarke *et al.*, 1994). However, when this finding was re-evaluated both in forebrain sections (Expt 1) and regional homogenates (Expt 2), a shift of the K_D was clearly absent. Recently, Decker *et al.* (1994) reported a substantial CHL-associated decrease in K_D in homogenates of whole rat brain. There is no obvious explanation for these divergent results. However, it should be noted that K_D values for [^{3}H]-nicotine binding tend to vary somewhat between individual assays, and that in the present study, all drug treatments and binding assays were strictly randomized.

Nicotine-induced receptor up-regulation of [^{3}H]-nicotine binding

The effects of centrally-active nicotinic antagonists on nicotinic [^{3}H]-ACh and [^{3}H]-nicotine high affinity binding

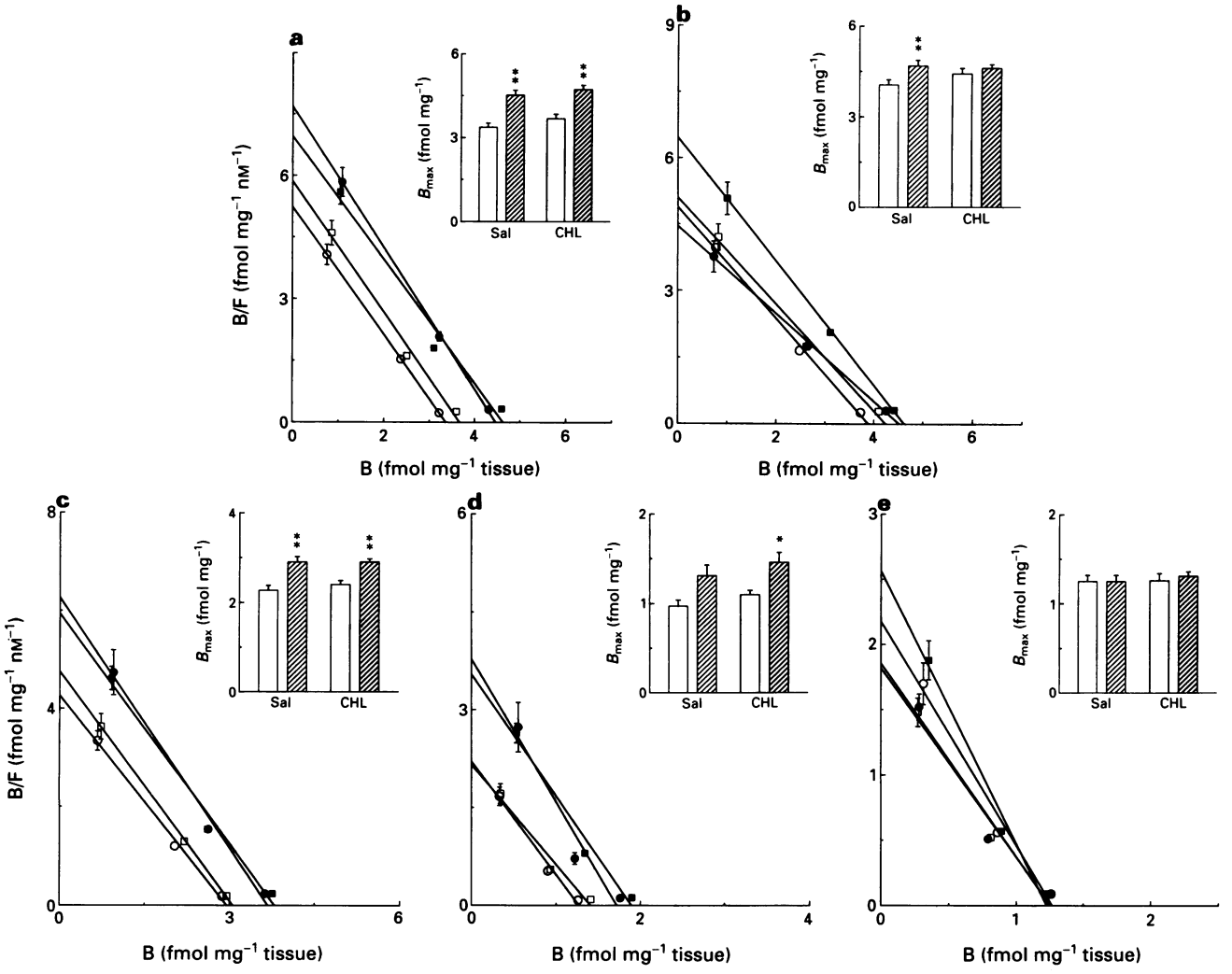


Figure 4 Scatchard plots of [^{3}H]-nicotine binding (0.24, 2, and 16 nM) to tissue homogenate prepared from cerebral cortex (a), midbrain (b), hippocampus (c), striatum (d), and cerebellum (e). Insets represent group mean (± s.e.mean), B_{max} values obtained by non-linear regression analysis of individual rats. Rats received two injections of chlorisondamine (CHL, 10 mg kg^{-1}, s.c.) (squares) or saline (circles), followed by 10 days of treatment with nicotine 1 mg kg^{-1}, s.c. twice daily (solid symbols, hatched columns) or saline (open symbols, open columns). Data points represent group mean values of bound/free (± s.e.mean; vertical axis) and bound (horizontal axis) ($n = 9-12$ rats per group). $*P<0.05$; $**P<0.01-0.001$ (Student/Bonferroni t test) denotes a significant effect of nicotine.

have been previously examined, but with inconsistent results. Schwartz & Kellar (1985) reported that neither mecamylamine (1 or 3 mg kg^{-1}, s.c. twice daily for 10 days) nor dihydro-β-erythroidine (1 mg kg^{-1}, s.c. twice daily for 10 days) altered nicotinic [^{3}H]-ACh binding in rat cerebral cortex. In addition, the increase in [^{3}H]-ACh binding density that resulted from chronic nicotine treatment was not altered by co-administration of either antagonist. However, the presence, degree and duration of CNS nicotinic receptor block after antagonist administration were not examined in this study. In contrast, Collins *et al.* (1990a) reported that in mice, chronic infusion with mecamylamine *increased* [^{3}H]-nicotine binding density in the areas examined (cerebral cortex and hippocampus). This group also found that chronic nicotine-induced [^{3}H]-nicotine up-regulation was increased by co-infusion with mecamylamine. However, in the absence of pharmacokinetic measurements, it is conceivable that at the dose of mecamylamine administered (3 mg kg^{-1} h^{-1}) high levels of the drug were attained over the ten day treatment period. Thus, the possibility cannot be ruled out that in this study, mecamylamine exerted additional non-nicotinic effects (see Snell & Johnson, 1989; Clarke *et al.*, 1994).

In the present study, central nicotinic blockade was confirmed by testing locomotor responses to nicotine (Clarke, 1984). Behavioural and *in vitro* studies conducted to date suggest that pharmacological blockade associated with CHL administration is selective for nicotinic receptors (Clarke, 1984; Reavill *et al.*, 1986; Kumar *et al.*, 1987; Corrigall *et al.*, 1992; Clarke *et al.*, 1994; El-Bizri & Clarke, 1994b). It is not clear why central nicotinic blockade produced by CHL and mecamylamine should differ in terms of receptor up-regulation. Both drugs have been found to block the same neuropharmacological and centrally-mediated behavioural actions of nicotine (Clarke & Kumar, 1983; Kumar *et al.*, 1987; Mundy & Iwamoto, 1988; Izenwasser *et al.*, 1991; Corrigall *et al.*, 1992; Brioni *et al.*, 1993; Marks *et al.*, 1993; El-Bizri & Clarke, 1994a) with one possible exception (Decker & Majchrzak, 1993). In addition, both antagonists fail to inhibit *in vitro* [^{3}H]-nicotine binding to brain tissue (Schwartz *et al.*, 1982; Clarke *et al.*, 1984; Marks *et al.*, 1993), and both have been shown to produce an insurmountable central nicotinic blockade (El-Bizri & Clarke, 1994a).

Possible mechanisms underlying nicotine-induced receptor up-regulation of [^{3}H]-nicotine binding

The present paper demonstrates a clear dissociation between the effects of CHL on nicotine-induced receptor up-

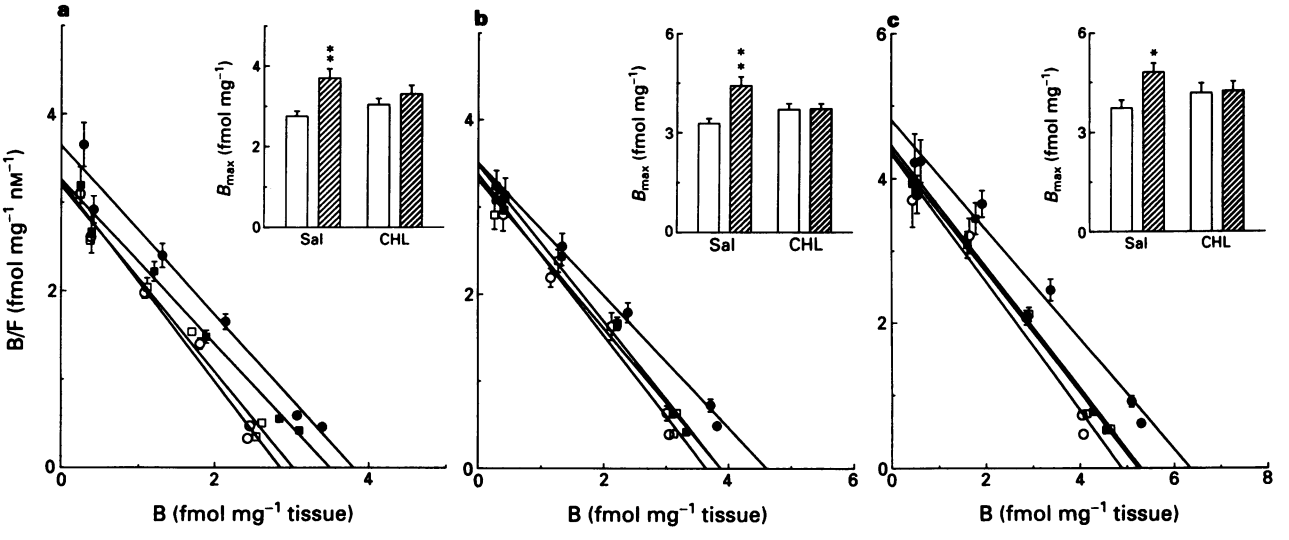


Figure 5 Scatchard plots of [^{125}I]-α-bungarotoxin ([^{125}I]-αBTX) binding (0.08–8 nM) to tissue homogenate prepared from cerebral cortex (a), midbrain (b), and hippocampus (c). Insets represent group mean (± s.e.mean), B_{max} values obtained by non-linear regression analysis of individual rats. Rats received two injections of chlorisondamine (10 mg kg^{-1}, s.c.) (squares) or saline (circles), followed by 10 days of treatment with nicotine 1 mg kg^{-1}, s.c. twice daily (solid symbols, hatched columns) or saline (open symbols, open columns). Data points represent group mean values of bound/free (± s.e.mean; vertical axis) and bound (horizontal axis) (n = 14–16 rats per group). $^{*}P<0.05$; $^{**}P<0.01$ (Student/Bonferroni t test) denotes a significant effect of nicotine.

regulation and behavioural responses. This finding prompts a reconsideration of the notion that these effects of nicotine are mediated by the same receptors. The available data, albeit incomplete, suggest that CNS nicotinic receptors which *in vitro* bind ^{3}H-labelled agonists with nanomolar affinity, do indeed represent targets mediating the neuropharmacological and behavioural responses to micromolar concentrations of nicotine (Schwartz & Kellar, 1983; 1985; London *et al.*, 1990; Stolerman, 1990; Wonnacott, 1991; Grady *et al.*, 1992). Since CHL has been found to block every behavioural effect of nicotine tested to date that is known to be centrally-mediated (Clarke & Kumar, 1983; Clarke, 1984; Reavill *et al.*, 1986; Fudala & Iwamoto, 1987; Kumar *et al.*, 1987; Munday & Iwamoto, 1988; Corrigall *et al.*, 1992; Clarke *et al.*, 1994; El-Bizri & Clarke, 1994b), it appears likely that in the present study, the receptors that possess high-affinity binding sites for [^{3}H]-nicotine were indeed blocked *in vivo* by CHL. This assumption underlies the following discussion.

It was originally proposed that chronic nicotine-induced up-regulation of ^{3}H-labelled agonist binding sites was due to agonist-induced functional blockade (Marks *et al.*, 1983; Schwartz & Kellar, 1985). This proposal is consistent with a variety of neuronal systems in which a compensatory receptor up-regulation has been observed in response to chronic antagonism (Creese & Sibley, 1981). However, in the present study, chronic CNS nicotinic blockade failed to increase [^{3}H]-nicotine binding density. This suggests that receptor blockade was not a sufficient stimulus to effect an up-regulation of this receptor population. The additional observation that pretreatment with the antagonist CHL did not affect chronic *nicotine-induced* up-regulation of this receptor population further suggests that this form of up-regulation may not depend on receptor activation. Since CHL does not act directly at the agonist recognition site, but may instead block the receptor ionophore (Schwartz *et al.*, 1982; Clarke *et al.*, 1984; Marks *et al.*, 1993), it appears that occupation of the agonist binding site is necessary for up-regulation to occur. This notion is consistent with reports that other nicotinic agonists, which are not all chemically related to nicotine, can produce ^{3}H-agonist binding site up-regulation when they are administered chronically *in vivo* (Schwartz & Kellar, 1985; Collins *et al.*, 1990a; Rowell & Wonnacott, 1990). Whether binding to the agonist site is a *sufficient* stimulus for up-regulation is unclear. Chronic administration of dihydro-β-erythroidine, which is a competitive antagonist (Schwartz & Kellar, 1983; El-Bizri & Clarke, 1994a), did not trigger up-regulation of ^{3}H-agonist binding (Schwartz & Kellar, 1985). However, it is not clear whether appreciable central receptor occupation was obtained in this study, since no nicotinic response was measured *in vivo*. This is a particular concern, since this competitive antagonist did not prevent nicotine-induced up-regulation from occurring.

If the functional status of the receptors does not determine whether receptor density will be increased, a more discrete signal may be involved. This would be, presumably, mediated by some form of agonist-induced conformational change occurring at the receptor level. Such a conformational change, being unaltered by CHL administration, may represent a signal transduction pathway operating in parallel to ligand-gated ion flux.

Does chronic nicotine regulate [^{125}I]-αBTX and [^{3}H]-nicotine binding sites in the same manner?

Chronic treatment with nicotine resulted in a significant increase in [^{125}I]-αBTX binding density in all three regions examined. Whilst this phenomenon has been consistently observed in mice (Collins *et al.*, 1990a), results with rats have been variable. Thus, two reports described an increase in binding following chronic administration of nicotine in rats (Morley, 1989; Collins *et al.*, 1990b). In contrast, there are two other reports of no change (Marks *et al.*, 1986; Sanderson *et al.*, 1993). Although the negative results of Sanderson *et al.* (1993) might reflect the low dose of nicotine used, it is not clear why the findings of Marks *et al.* (1986) are also divergent.

Administration of CHL did not increase the density of [^{125}I]-αBTX binding, and hence did not mimic the effects of chronic nicotine administration. However, CHL did significantly block nicotine-induced [^{125}I]-αBTX binding up-regulation in the midbrain, with a similar trend in the remaining two regions. Morley (1989) reported that in rats, the antagonist mecamylamine administered alone did not increase the density of [^{125}I]-αBTX binding. Nevertheless, an ineffective dose of mecamylamine given with a sub-effective dose of nicotine did produce nicotinic receptor up-regulation. The reasons for this difference was not clear.

The present finding that CHL attenuated nicotine-induced [^{125}I]-αBTX binding up-regulation suggests that the up-regulation of the central [^{125}I]-αBTX binding site may require receptor activation. Thus, the results of the present paper indicate that [^{3}H]-nicotine and [^{125}I]-αBTX labelled receptors may be regulated by different mechanisms.

We thank Dr Brian Collier for his valuable comments, Dr Michael Marks for technical advice, Mr Guy Isabel for computer programming and Ms Melanie Reuben for excellent technical assistance. Ciba-Geigy generously donated samples of chlorisondamine. Supported by the Medical Research Council of Canada. H.E.B. was a Hydro-Quebec Fellow and holds an MRC (Canada) Studentship. P.B.S.C. holds a Senior I Scholarship of the Fonds de la Recherche en Santé du Québec.

References

BENWELL, M.E., BALFOUR, D.J. & ANDERSON, J.M. (1988). Evidence that tobacco smoking increases the density of (−)-[^{3}H]nicotine binding sites in human brain. *J. Neurochem.*, **50**, 1243–1247.

BRIONI, J.D., O'NEILL, A.B., KIM, D.J.B. & DECKER, M.W. (1993). Nicotinic receptor agonists exhibit anxiolytic-like effects on the elevated plus-maze test. *Eur. J. Pharmacol.*, **238**, 1–8.

CLARKE, P.B.S. (1984). Chronic central nicotinic blockade after a single administration of the bisquaternary ganglion-blocking drug chlorisondamine. *Br. J. Pharmacol.*, **83**, 527–535.

CLARKE, P.B.S., CHAUDIEU, I., EL-BIZRI, H., BOKSA, P., QUIK, M., ESPLIN, B.A. & CAPEK, R. (1994). The pharmacology of the nicotinic antagonist, chlorisondamine, investigated in rat brain and autonomic ganglion. *Br. J. Pharmacol.*, **111**, 397–405.

CLARKE, P.B.S. & KUMAR, R. (1983). Characterization of the locomotor stimulant action of nicotine in tolerant rats. *Br. J. Pharmacol.*, **80**, 587–594.

CLARKE, P.B.S., PERT, C.B. & PERT, A. (1984). Autoradiographic distribution of nicotine receptors in rat brain. *Brain Res.*, **323**, 390–395.

CLARKE, P.B.S., SCHWARTZ, R.D., PAUL, S.M., PERT, C.B. & PERT, A. (1985). Nicotinic binding in rat brain: autoradiographic comparison of ^{3}H-acetylcholine, ^{3}H-nicotine, and ^{125}I-alpha-bungarotoxin. *J. Neurosci.*, **5**, 1307–1315.

COLLINS, A.C., BHAT, R.V., PAULY, J.R. & MARKS, M.J. (1990a). Modulation of nicotine receptors by chronic exposure to nicotinic agonists and antagonists. *CIBA Foundation Symposia*, **152**, 68–82.

COLLINS, A.C., ROMM, E. & WEHNER, J.M. (1990b). Dissociation of the apparent relationship between nicotine tolerance and up-regulation of nicotinic receptors. *Brain Res. Bull.*, **25**, 373–379.

CORRIGALL, W.A., FRANKLIN, K.B.J., COEN, K.M. & CLARKE, P.B.S. (1992). The mesolimbic dopaminergic system is implicated in the reinforcing effects of nicotine. *Psychopharmacology (Berlin)*, **107**, 285–289.

CREESE, I. & SIBLEY, D.R. (1981). Receptor adaptations to centrally acting drugs. *Annu. Rev. Pharmacol. Toxicol.*, **21**, 357–391.

DECKER, M.W. & MAJCHRZAK, M.J. (1993). Effects of central nicotinic cholinergic receptor blockade produced by chlorisondamine on learning and memory performance in rats. *Behav. Neural Biol.*, **60**, 163–171.

DECKER, M.W., MAJCHRZAK, M.J., CADMAN, E.D. & ARNERIC, S.P. (1994). Effects of chlorisondamine on nicotinic receptor binding in whole brain and nicotine-induced changes in locomotor activity in rats. *Drug Dev. Res.*, **31**, 89–94.

EL-BIZRI, H. & CLARKE, P.B.S. (1994a). Blockade of nicotinic receptor-mediated release of dopamine from striatal synaptosomes by chlorisondamine and other nicotinic antagonists administered *in vitro*. *Br. J. Pharmacol.*, **111**, 406–413.

EL-BIZRI, H. & CLARKE, P.B.S. (1994b). Blockade of nicotinic receptor-mediated release of dopamine from striatal synaptosomes by chlorisondamine administered *in vivo*. *Br. J. Pharmacol.*, **111**, 414–418.

FUDALA, P.J. & IWAMOTO, E.T. (1987). Conditioned aversion after delay place conditioning with nicotine. *Psychopharmacology*, **92**, 376–381.

GLANTZ, S.A. (1992). *Primer of Biostatistics*. 3rd edn. New York: McGraw-Hill.

GRADY, S., MARKS, M.J., WONNACOTT, S. & COLLINS, A.C. (1992). Characterization of nicotinic receptor-mediated [^{3}H]dopamine release from synaptosomes prepared from mouse striatum. *J. Neurochem.*, **59**, 848–856.

IZENWASSER, S., JACOCKS, H.M., ROSENBERGER, J.G. & COX, B.M. (1991). Nicotine indirectly inhibits [^{3}H]dopamine uptake at concentrations that do not directly promote [^{3}H]dopamine release in rat striatum. *J. Neurochem.*, **56**, 603–610.

KUMAR, R., REAVILL, C. & STOLERMAN, I.P. (1987). Nicotine cue in rats: effects of central administration of ganglion-blocking drugs. *Br. J. Pharmacol.*, **90**, 239–246.

LAPCHAK, P.A., ARAUJO, D.M., QUIRION, R. & COLLIER, B. (1989). Effect of chronic nicotine treatment on nicotinic autoreceptor function and N-3Hmethylcarbamylcholine binding sites in the rat brain. *J. Neurochem.*, **52**, 483–491.

LONDON, E.D., FANELLI, R.J., KIMES, A.S. & MOSES, R.L. (1990). Effects of chronic nicotine on cerebral glucose utilization in the rat. *Brain Res.*, **520**, 208–214.

MARKS, M.J., BURCH, J.B. & COLLINS, A.C. (1983). Effects of chronic nicotine infusion on tolerance development and nicotinic receptors. *J. Pharmacol. Exp. Ther.*, **226**, 817–825.

MARKS, M.J. & COLLINS, A.C. (1982). Characterization of nicotine binding in mouse brain and comparison with the binding of alpha-bungarotoxin and quinuclidinyl benzilate. *Mol. Pharmacol.*, **22**, 554–564.

MARKS, M.J., STITZEL, J.A., ROMM, E., WEHNER, J.M. & COLLINS, A.C. (1986). Nicotinic binding sites in rat and mouse brain: comparison of acetylcholine, nicotine, and alpha-bungarotoxin. *Mol. Pharmacol.*, **30**, 427–436.

MARKS, M.J., FARNHAM, D.A., GRADY, S.R. & COLLINS, A.C. (1993). Nicotinic receptor function determined by stimulation of rubidium efflux from mouse brain synaptosomes. *J. Pharmacol. Exp. Ther.*, **264**, 542–552.

MORLEY, B.J. (1989). Alpha-bungarotoxin receptors in the CNS. *Prog. Brain Res.*, **79**, 101–108.

MORROW, A.L., LOY, R. & CREESE, I. (1985). Alteration of nicotinic cholinergic agonist binding sites in hippocampus after fimbria transection. *Brain Res.*, **334**, 309–314.

MUNDY, W.R. & IWAMOTO, E.T. (1988). Actions of nicotine on the acquisition of an autoshaped lever-touch response in rats. *Psychopharmacology (Berlin)*, **94**, 267–274.

MUNSON, P.J. & RODBARD, D. (1980). LIGAND: a versatile computerized approach for characterization of ligand-binding systems. *Anal. Biochem.*, **107**, 220–239.

REAVILL, C., STOLERMAN, I.P., KUMAR, R. & GARCHA, H.S. (1986). Chlorisondamine blocks acquisition of the conditioned taste aversion produced by (−)-nicotine. *Neuropharmacology*, **25**, 1067–1069.

ROMM, E., LIPPIELLO, P.M., MARKS, M.J. & COLLINS, A.C. (1990). Purification of L-[^{3}H]nicotine eliminates low affinity binding. *Life Sci.*, **46**, 935–943.

ROWELL, P.P. & WONNACOTT, S. (1990). Evidence for functional activity of up-regulated nicotine binding sites in rat striatal synaptosomes. *J. Neurochem.*, **55**, 2105–2110.

SANDERSON, E.M., DRASDO, A.L., McCREA, K. & WONNACOTT, S. (1993). Upregulation of nicotinic receptors following continuous infusion of nicotine is brain-region-specific. *Brain Res.*, **617**, 349–352.

SCHWARTZ, R.D., McGEE, R., Jr. & KELLAR, K.J. (1982). Nicotinic cholinergic receptors labeled by ^{3}H-acetylcholine in rat brain. *Mol. Pharmacol.*, **22**, 56–62.

SCHWARTZ, R.D. & KELLAR, K.J. (1983). Nicotinic cholinergic receptor binding sites in the brain: regulation in vivo. *Science*, **220**, 214–216.

SCHWARTZ, R.D. & KELLAR, K.J. (1985). In vivo regulation of ^{3}H-acetylcholine recognition sites in brain by nicotinic cholinergic drugs. *J. Neurochem.*, **45**, 427–433.

SNELL, L.D. & JOHNSON, K.M. (1989). Effects of nicotinic agonists and antagonists on N-methyl-D-aspartate-induced 3H-norepinephrine release and 3H-(1-1-(2-thienyl)cyclohexyl-piperidine) binding in rat hippocampus. *Synapse*, **3**, 129–135.

STOLERMAN, I.P. (1990). Behavioural pharmacology of nicotine: implications for multiple brain nicotinic receptors. *CIBA Foundation Symposia*, **152**, 3–22.

WONNACOTT, S. (1991). Neuronal nicotinic receptors: functional correlates of ligand binding sites. *Biochem. Soc. Trans.*, **19**, 121–124.

(Received March 11, 1994
Revised June 20, 1994
Accepted July 4, 1994)

Br. J. Pharmacol. (1994), **113**, 926–930 © Macmillan Press Ltd, 1994

Effect of cytoplasmic pH on Ca^{2+}-stimulated eicosanoid biosynthesis in human platelets

Jacqueline S. Edwards & [1]James M. Ritter

Department of Clinical Pharmacology, United Medical and Dental Schools of Guy's and St. Thomas' Hospitals, London

1 We have investigated the effect of cytoplasmic pH (pH_i) on the relationship between platelet cytoplasmic Ca^{2+} concentration ($[Ca^{2+}]_i$) and eicosanoid biosynthesis. Stirred gel-filtered human platelets loaded with fluorescent indicators of Ca^{2+} and H^+ were suspended in balanced salt solutions at 37°C. $[Ca^{2+}]_i$ was controlled by calcium ionophore (ionomycin). Increased $[Ca^{2+}]_i$ was associated with increased production of thromboxane A_2 (TXA_2) as determined by radioimmunoassay of its stable hydrolysis product TXB_2, and of 12-hydroxy eicosatetraenoic acid (12-HETE) measured by high performance liquid chromatography.

2 Varying pH_i with a K^+/H^+ ionophore (nigericin) in platelets suspended in K^+ rich solutions of pH 6.8, 7.4 or 7.8 with subsequent resuspension in solution of pH 7.4 containing albumin (1 g l^{-1}) and Ca^{2+} (1 mM) resulted in pH_i of 6.72 ± 0.05, 7.31 ± 0.02 and 7.71 ± 0.04 (mean ± s.e.mean, $n = 5$). Ionomycin (1.2 μM) increased $[Ca^{2+}]_i$ by 97.1 ± 17.6, 191.9 ± 48.7 and 322.8 ± 55.7 nM at the different values of pH_i respectively; TXB_2 production was 0.7 ± 0.2, 2.1 ± 0.4 and 10.7 ± 3.3 ng μg^{-1} protein, and 12-HETE production was 150.9 ± 68.2, 184.4 ± 77.9 and 302.3 ± 62.8 ng μg^{-1} protein.

3 Ammonium chloride (50 mM) caused a small reduction in pH_o while increasing pH_i from 7.32 ± 0.04 to 7.89 ± 0.05 and increasing ionomycin (1.2 μM)-induced $[Ca^{2+}]_i$ responses from 94.1 ± 67.3 to 721.6 ± 288.3 nM. TXB_2 production increased from 3.1 ± 2.1 to 17.3 ± 8.2 and 12-HETE production increased from 100.5 ± 26.7 to 203.2 ± 36.4 ng μg^{-1} protein. Responses of $[Ca^{2+}]_i$ and TXB_2 production to epoxymethano prostaglandin H_2 (U46619, an endoperoxide-thromboxane receptor agonist) increased significantly in the presence of NH_4Cl.

4 Alterations of pH_i (such as may occur under pathological conditions) influence $[Ca^{2+}]_i$ responses and eicosanoid synthesis in human platelets.

Keywords: Platelets; intracellular Ca^{2+}; intracellular pH; thromboxane; 12-HETE; signal transduction

Introduction

Thromboxane A_2 (TXA_2) is synthesized by platelets during aggregation (Hamberg *et al.*, 1975). Therapeutic and prophylactic effects of aspirin, which inhibits TXA_2 synthesis, suggest that this eicosanoid is important in the pathogenesis of myocardial infarction (Oates *et al.*, 1988). Biosynthesis of TXA_2 and other eicosanoids is determined by availability of free arachidonic acid which is controlled by cellular phospholipases (Irvine, 1982). Most of these enzymes are Ca^{2+} dependent and many agonists cause a rapid increase in cytosolic Ca^{2+} ($[Ca^{2+}]_i$). There is evidence that while $[Ca^{2+}]_i$ plays a central role in controlling platelet TXA_2 biosynthesis it is not sufficient to account for phospholipase A_2 activation under all circumstances (Rink & Sage, 1990).

Purified phospholipase A_2 has an alkaline pH optimum (Jesse & Fransom, 1979), suggesting that pH could modify the effects of $[Ca^{2+}]_i$ on TXA_2 synthesis. Stimulus-evoked changes in platelet cytosolic pH (pH_i) have been reported (Horne *et al.*, 1981; Zavoico *et al.*, 1986) and it was suggested that cytosolic alkalinisation is an essential step in agonist-induced platelet activation (Siffert & Akkerman, 1987). There is convincing evidence that this is not the case (Simpson & Rink, 1987; Zavoico & Cragoe, 1988). It is, however, possible that changes in pH_i caused not by agonists but by the prevailing biological conditions will alter either the $[Ca^{2+}]_i$ response to agonists or the effects of $[Ca^{2+}]_i$ on eicosanoid biosynthesis. This could be important in the setting of thrombosis when TXA_2 production occurs in a local millieu that is subject to marked metabolic acidosis, and to other pathological states associated with local or generalized acidosis or alkalosis, but the influence of pH_i on $[Ca^{2+}]_i$ responses or TXA_2 biosynthesis is incompletely understood. The object of the present study was to investigate these relationships. We measured pH_i and $[Ca^{2+}]_i$ with ion-selective fluorescent dyes. pH_i was controlled with either nigericin, a K^+/H^+ ionophore, (Ng & Dudley, 1989) or NH_4 Cl (Roos & Boron, 1981). Ionomycin, (a Ca^{2+} ionophore) was used to alter $[Ca^{2+}]_i$. TXA_2 biosynthesis was measured by determining its stable hydrolysis product TXA_2. 12-Hydroxy eicosatetraenoic acid (12-HETE) is the main lipoxygenase product of platelets (Hamberg & Samuelsson, 1974). Its biological role is less well understood than is that of TXA_2. 12-HETE was measured in some experiments to determine whether effects of pH_i were similar on cyclo-oxygenase and lipoxygenase pathways of eicosanoid synthesis in platelets.

Methods

Preparation of platelet suspensions

Venous blood was collected from healthy volunteers (11 men aged 22–49 years and 10 women aged, 22–30 years who had not taken aspirin or any other medication for 14 days) using a 19 G Butterfly needle (Abbot, Sligo, Ireland). The blood was anti-coagulated with trisodium citrate (final concentration 0.31% w/v) and spun at 150 *g* for 8 min at room temperature. Platelet rich plasma was aspirated with a plastic pipette (LIP, Shipley, UK) added to a column packed with Sepharose (CL-2B Pharmacia, Milton Keynes, UK) and eluted with Tyrode solution (composition, mM: sodium chloride 140, glucose 5.6, HEPES 5, potassium chloride 2.8, potassium dihydrogen orthophosphate 0.8, and magnesium chloride 0.4) to produce gel filtered platelets.

[1] Author for correspondence at: Department of Clinical Pharmacology, UMDS, Medical School Building, Guy's Hospital, London, SE1 9RT.

Measurement of $[Ca^{2+}]_i$ and pH_i

$[Ca^{2+}]_i$ was measured with the fluorescent dye, fura 2 (Grynkiewicz *et al.*, 1985). The dye was loaded by incubating its acetoxymethylester (fura 2-AM, 2 μM) with gel filtered platelets for 45 min at 37°C, following which the platelets were refiltered through Sepharose to remove free fura 2-AM. Cytoplasmic pH was measured in all experiments in a separate portion of platelets using *bis* carboxyethyl carboxyfluoroscein (BCECF, Rink *et al.*, 1986). The dye was loaded by incubating BCECF-AM (5 μM) with platelet rich plasma for 30 min at 37°C. The loaded platelets were then eluted through Sepharose as described above.

Portions of fura 2- or BCECF-loaded platelet suspensions (2 ml) were transferred to a quartz cuvette with a magnetic stirring bar in a thermostatically controlled holder at 37°C in a dual excitation wavelength spectrofluorimeter (Deltascan, Photon Technology International, Princeton, NJ, U.S.A.). For Ca^{2+} measurements, excitation wavelengths were set at 340 and 380 nm and the emission wavelength set at 505 nm. F_{max} and F_{min} were obtained at the end of each measurement by sequential additions of 5% Triton X-100 and 5 mM EGTA. For pH_i measurements excitation wavelengths were 430 and 500 nm and emission wavelengths was 530 nm. The BCECF fluorescence signal was calibrated separately in each experiment by treating a portion of platelets suspended in 140 mM K^+ Tyrode solution (composition as above but with KCl substituted for NaCl) with nigericin followed by sequential additions of NaOH and HCl (Thomas *et al.*, 1979). pH in the cuvette after each addition was measured with a pH electrode (CE2: Phillips Analytical, Cambridge, UK).

To determine whether pH over the range 6.8–7.8 has an effect on K_d of fura 2 for Ca^{2+}, we prepared a series of EGTA solutions of known Ca^{2+} concentration using a Ca^{2+}-electrode (Fry, 1990). Fura 2 (5 μM fluorescence was measured and excesses of Ca^{2+} (1 mM) and EGTA (5 mM) used to obtain F_{max} and F_{min}. K_d was calculated from the equation of Grynkiewicz *et al.* (1985):

$$[Ca^{2+}] = K_d\ (R-R_{min})/(R_{max}-R) \times F380_{min}/F380_{max}$$

At pH 6.8 K_d was 230 ± 4.9, pH 7.4 K_d was 240 ± 3.7 and at pH 7.8 K_d was 236 ± 6.5 nM.

Measurement of TXA_2 and 12-HETE biosynthesis

Samples (200 μl) of platelet suspensions were added to ice cold tubes containing indomethacin (final concentration 10 μM). Samples were then spun at 800 *g* for 12 min and the supernatant removed and assayed for TXB_2 by radioimmunoassay using a previously described antibody (Burch *et al.*, 1979), and a rabbit antibody prepared in our department and validated against both the other antibody and by gas chromatography/mass spectrometry (Barrow *et al.*, 1989). 12-HETE was measured by reverse phase high performance liquid chromatography (Powell, 1987). Briefly, supernatant was spiked with prostaglandins B_2 (100 ng) as standard, eicosanoids extracted with C_{18} Sep-Pak cartridges (Millipore/Waters, Waterford, UK) and separated on a 5 μm ultrasphere ODS column (Beckman, RIIC Ltd.) using a Beckman System Gold high performance liquid chromatograph as described by Pettit and colleagues (1991). Platelet pellets were dissolved in 0.1 M NaOH, and protein determined by the method of Lowry *et al.* (1951). Eicosanoid production was expressed per μg protein.

Alteration of pH

pH_0 was varied by use of HEPES buffered Tyrode solutions at pH 6.8, 7.4 and 7.8. pH_i was controlled with nigericin (Ng & Dudley, 1989). Aliquots of fura 2- or BCECF-loaded platelets were treated with forskolin (5 μM) and spun at 800 *g* for 10 min. The supernatant was removed and the platelet pellet resuspended in 140 mM potassium Tyrode solution buffered at pH 6.8, 7.4 or 7.8. Nigericin (2.7 μM) was added to set pH_i to pH_o followed by centrifugation and resuspension of the platelet pellet in Tyrode solution at pH 7.4 containing human serum albumin (Sigma, essentially fatty acid free, 1 gl^{-1}). pH_i was also changed using ammonium chloride (Roos & Boron, 1981).

Materials

Salts were of Analar grade and were obtained from British Drug Houses (Poole, Dorset). All drugs were from Sigma (Poole, Dorset) apart from ionomycin, fura 2-AM and BCECF-AM which were from Calbiochem (La Jolla, CA, U.S.A.).

Statistics

Data are presented as means ± s.e.mean. Statistical analysis was performed using Student's two-tailed *t* test for paired data. Where indicated, $[Ca^{2+}]_i$ and TXB_2 responses to a number of concentrations of agonist in the test and control (pH 7.4) groups were compared by repeated measures of analysis of variance. Differences were considered significant if $P<0.05$.

Results

Platelets were incubated in Tyrode solution containing 5 μM extracellular Ca^{2+} and stimulated with various concentrations of ionomycin to determine the time course of $[Ca^{2+}]_i$ responses and TXB_2 production. Figure 1 shows representative traces of $[Ca^{2+}]_i$ which rises to a plateau 60–100 s after addition of ionomycin (50–1200 nM). The time course of TXB_2 biosynthesis is similar to that for $[Ca^{2+}]_i$ (Figure 2), with a plateau at 60–120 s. Measurements were made at 60 s in subsequent experiments. Changing pH_o (6.8–7.8) did not influence $[Ca^{2+}]_i$ or TXB_2 responses to ionomycin significantly (data not shown).

Figure 3 illustrates effects of nigericin on pH_i in platelets suspended in K^+ Tyrode solution at pH 6.8, 7.4 and 7.8. Mean pH_i after resuspension of platelets in Tyrode solution at pH 7.4 containing albumin (1 gl^{-1}) and total Ca^{2+} 1 mM, was 6.72 ± 0.05, 7.31 ± 0.02 and 7.71 ± 0.04 ($n = 5$ at each pH). The effect of ionomycin (1.2 μM) on $[Ca^{2+}]_i$ and eicosanoid biosynthesis was measured at each pH_i (Figure 4). Responses were reduced in acid and increased in alkaline cytoplasm. Further similar experiments were performed in

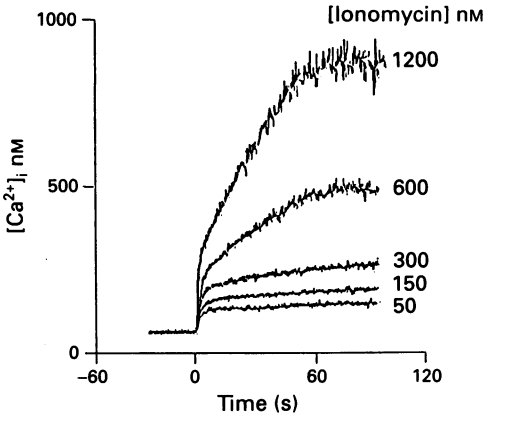


Figure 1 Representative traces showing responses to ionomycin in fura-2 loaded platelets. Gel filtered platelets loaded with fura-2 were suspended in Tyrode solution at 37°C in the presence of 5 μM extracellular Ca^{2+} before addition of ionomycin. Traces are representative of evaluations on nine subjects.

the absence and presence of added extracellular Ca^{2+} (1 mM). In the absence of extracellular Ca^{2+}, alteration of pH_i had no significant effect on ionomycin induced $[Ca^{2+}]$ response (Figure 5).

NH_4Cl (50 mM) increased pH_i from 7.32 ± 0.04 to 7.89 ± 0.05 and decreased pH_o from 7.37 ± 0.05 to 7.22 ± 0.05. Effects of ionomycin (0.15–1.2 μM) on $[Ca^{2+}]_i$ and TXB_2 production (Figure 6) were increased (each $P<0.05$). 12-HETE production in response to ionomycin 1.2 μM increased from 100.5 ± 26.7 (control) to 203.2 ± 36.4 ng μg^{-1} protein in the presence of NH_4Cl. Cytoplasmic alkalinisation with NH_4Cl also increased $[Ca^{2+}]_i$ responses and increased TXB_2 production in response to epoxymethano prostaglandin H_2 (U46619) (Figure 7).

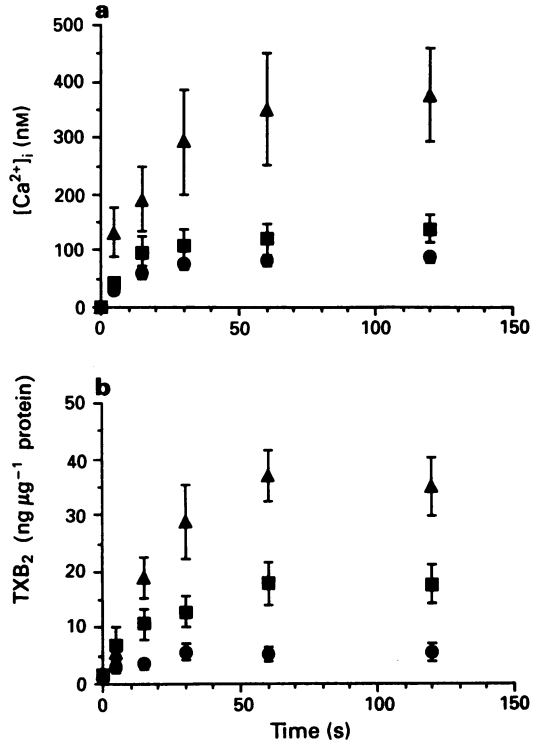


Figure 2 Time course of the effects of ionomycin (50 (●), 300 (■), or 600 nM (▲)) on $[Ca^{2+}]_i$ (a) and thromboxane B_2 (TXB_2) biosynthesis (b). Fura-2 loaded, gel filtered platelets were suspended in Tyrode solution at 37°C in the presence of 5 μM $[Ca^{2+}]_o$. The platelets were then stimulated with ionomycin and the changes in $[Ca^{2+}]_i$ monitored. In identical experiments samples were taken at various times for radioimmunoassay of TXB_2. The results are the means ± s.e.mean, $n = 4$.

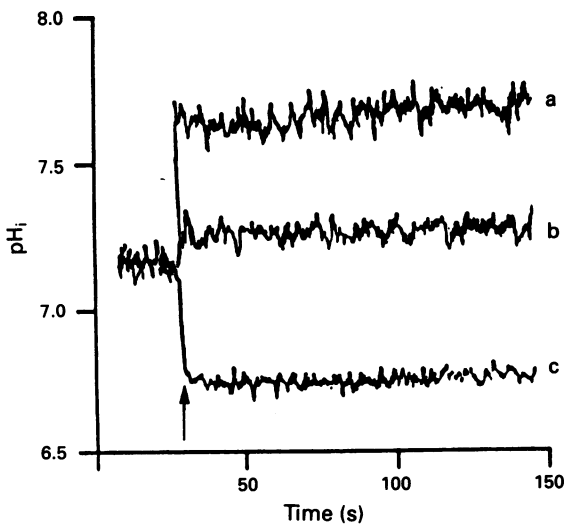


Figure 3 Representative traces depicting the effect of the K^+/H^+ ionophore nigericin (2.7 μM) on the cytoplasmic pH of BCECF loaded platelets suspended in Tyrode solution containing 140 mM K^+ in place of Na^+, at 37°C at pH 7.8 (a), 7.4 (b) or 6.8 (c). Nigericin was added as indicated by the arrow.

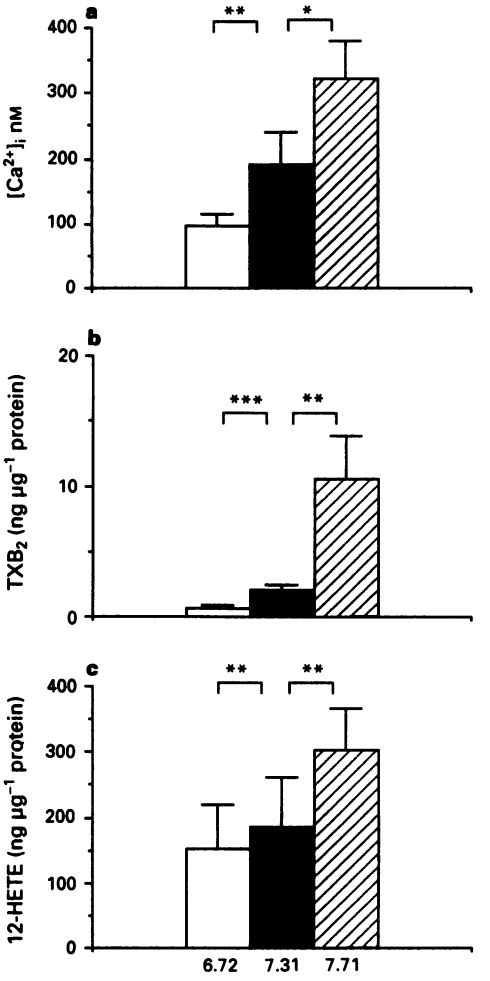


Figure 4 Effect of ionomycin (1.2 μM) on $[Ca^{2+}]_i$ (a), thromboxane B_2 (TXB_2) (b) and 12-HETE (c) when pH_i is 6.72 ± 0.05 (open columns), 7.31 ± 0.02 (solid columns) and 7.71 ± 0.04 (cross hatched columns). pH_i was controlled by the nigericin method. Means ± s.e.mean, $n = 5$. (P values: * = <0.05; ** = <0.01; *** = < 0.001).

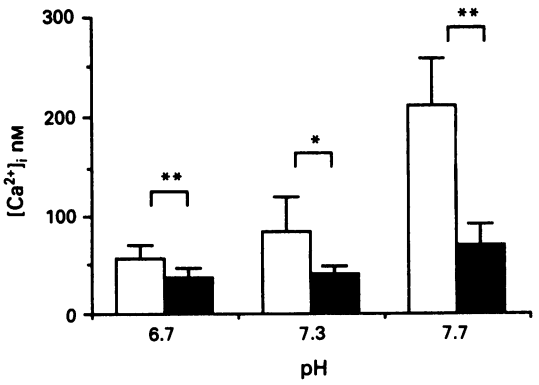


Figure 5 Effect of $[Ca^{2+}]_o$ on ionomycin-stimulated Ca^{2+} influx at pH_i 6.7–7.7. pH_i was changed in fura-2 loaded platelets by the nigericin method. The platelets were stimulated with ionomycin (1.2 μM) in the presence (open columns) and absence (solid columns) of extracellular Ca^{2+} (1 mM). Values are mean ± s.e.mean for four experiments. (P values: * = <0.05; ** = <0.01, *** = <0.001).

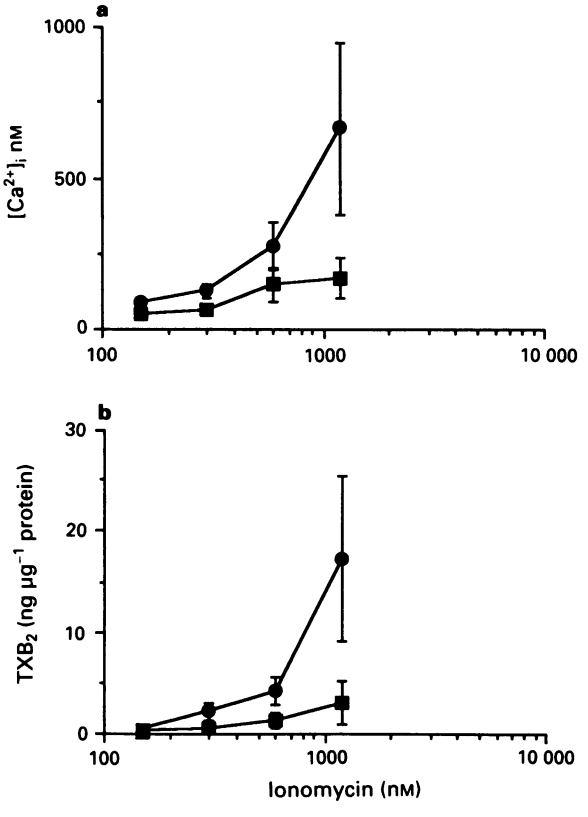


Figure 6 The effect of alkaline pH_i caused by NH_4Cl on response to ionomycin. The panels show dose-response relationships between ionomycin (150–1200 nM) and Ca^{2+} increase (a) and thromboxane B_2 (TXB_2) biosynthesis (lower panel) in fura-2 loaded platelets. NH_4Cl (50 mM) changed pH_i from 7.32 ± 0.04 to 7.89 ± 0.05. (●) NH_4Cl-treated; (■) control. Experiments were performed in the presence of 5 µM extracellular Ca^{2+} and measurements made 60 s after addition of ionomycin. Values are means ± s.e.mean for six experiments ($P = <0.05$ by ANOVA).

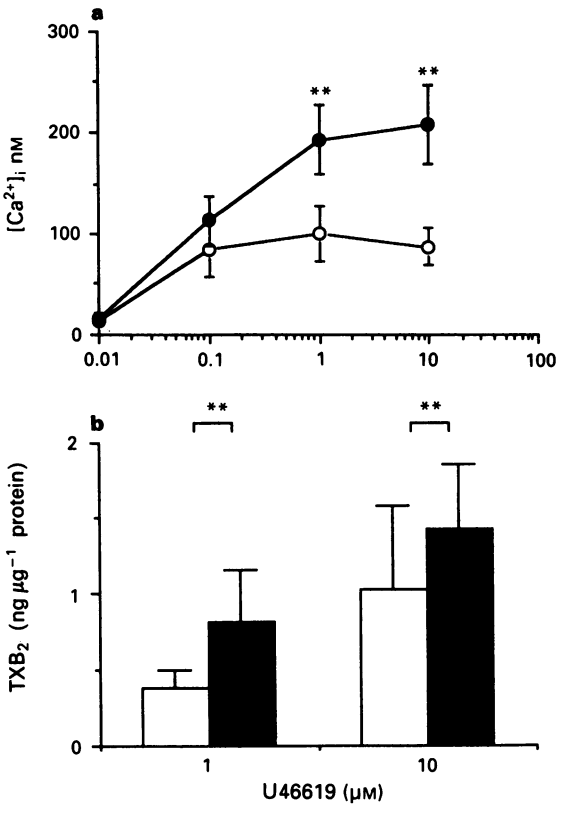


Figure 7 The effect of ammonium chloride on U46619-stimulated thromboxane B_2 (TXB_2) production (b) and cytosolic $[Ca^{2+}]$ (a). Platelets were suspended in Na^+ Tyrode solution containing 1 mM Ca^{2+} and stimulated with U46619 in the presence (●) or absence (○) of 50 mM NH_4Cl. Values are means ± s.e.mean for seven experiments. (*P* values: * = <0.05; ** = <0.01; *** = <0.001).

Discussion

Determination of effects of pH_i on $[Ca^{2+}]_i$ responses with fluorescent dyes demands a Ca^{2+} indicator that is not influenced by changes in pH. Grinstein *et al.* (1987) found that the K_d of fura 2 for Ca^{2+} is unaffected by pH, and we confirmed this over the pH range 6.8–7.8 used in the present experiments. Reducing pH_i by the nigericin method (Ng & Dudley, 1989) reduces both $[Ca^{2+}]_i$ responses and eicosanoid biosynthesis, whereas alkaline pH_i has opposite effects. The finding that effects of pH_i on Ca^{2+}-stimulated TXB_2 and 12-HETE production are qualitatively similar is consistent with an action of cytoplasmic pH on $[Ca^{2+}]_i$ which in turn influences phospholipase activity, rather than an action on more distal enzymes in cyclo-oxygenase of lipoxygenase pathways. Increased $[Ca^{2+}]_i$ responses and eicosanoid biosynthesis in platelets with alkaline pH_i also occurred in parallel when cytoplasmic alkalinisation was achieved with NH_4Cl, so these findings do not appear to be due to an artefact of the nigericin method. Furthermore, qualitatively similar effects of pH_i on $[Ca^{2+}]_i$ and prostanoid release have been described upon hypoxia-reoxygenation of hepatic Kupffer cells (Gyenes & de Groot, 1993).

Omission of Ca^{2+} from the medium abolishes the pH_i-dependency of platelet $[Ca^{2+}]_i$ responses to ionomycin, suggesting that this is secondary to changes in Ca^{2+} influx rather than to altered release from intracellular stores. The parallel between $[Ca^{2+}]_i$ responses and eicosanoid production at different pH, argues for the effects of pH_i on eicosanoid biosynthesis being mediated via effects on Ca^{2+} influx rather than any effect of pH on the Ca^{2+}-dependent phospholipases that are rate-limiting in TXA_2 biosynthesis. This relationship between $[Ca^{2+}]_i$ and TXB_2 synthesis also accords with findings in permeabilised platelets (Authi *et al.*, 1986).

Use of platelets prepared with nigericin and forskolin severely attenuates responses to receptor-mediated agonists, so we also used platelets treated with NH_4Cl to determine whether cytoplasmic alkalinisation influences the $[Ca^{2+}]_i$ response and TXB_2 production in response to a receptor-mediated agonist (U46619) as well as to inomycin. The finding that cytoplasmic alkalinisation with NH_4Cl affects responses to U46619 to a similar extent as it affects responses to ionomycin suggests that alterations to pH_i under pathological conditions might influence platelet function *in vivo*. The functional role of platelet-derived 12-HETE is not known, but there is evidence that it is chemotactic for vascular smooth muscle cells and recently it has been proposed that it also has a central role in the regulation of platelet activation (Sekiya *et al.*, 1991). Effects of pH_i on eicosanoid synthesis in human platelets may be relevant in pathological conditions, such as myocardial infarction and arterial restenosis following balloon angioplasty, characterized by platelet activation and/or vascular proliferation in an ischaemic local environment, and under other pathological conditions associated with abnormal acid-base metabolism.

We are very grateful to Dr C. Fry (Department of Physiology, St. Thomas' Hospital) for help with the Ca^{2+} electrodes and to Dr A. Rowley (Department of Biological Sciences, University of Swansea) for supervising the measurements of 12-HETE.

References

AUTHI, K.S., EVENDEN, B.J. & CRAWFORD, N. (1986). Metabolic and functional consequences of introducing inositol 1,4,5-trisphosphate into saponin-permeabilized human platelets. *Biochem. J.*, **233**, 709–718.

BARROW, S.E., WARD, P.S., SLEIGHTHOLM, M.A., RITTER, J.M. & DOLLERY, C.T. (1989). Cigarette smoking: profiles of thromboxane- and prostacyclin-derived products in human urine. *Biochim. Biophys. Acta*, **993**, 121–127.

BURCH, R.M., KNAPP, D.R. & HALUSHKA, P.V. (1979). Vasopressin stimulates thromboxane synthesis in the toad urinary bladder: effects of imidazole. *J. Pharmacol. Exp. Ther.*, **210**, 344–348.

FRY, C.H. (1990). Ion-selective electrodes: manufacture and use in biological system. *Methods in Experimental Physiology and Pharmacology Biological Measurement Techniques VII*. March: Biomesstechnik-Verlag.

GRINSTEIN, S., GOETZ-SMITH, J.D. & COHEN, S. (1987). Cytoplasmic free Ca^{2+} and the intracellular pH of lymphocytes. In *Cell Calcium and the Control of Membrane Transport*. ed. Mandel, L.J. & Eaton, D.C. pp. 215–228. New York: Rockefeller University Press.

GRYNKIEWICZ, G., POENIE, M. & TSIEN, R.Y. (1985). A new generation of Ca^{2+} indicators with greatly improved fluorescence properties. *J. Biol. Chem.*, **260**, 3440–3450.

GYENES, M. & DE GROOT, H. (1993). Prostanoid release by Kupffer cells upon hypoxia-reoxygenation: role of pH_i and Ca_i^{2+} . *Am. J. Physiol.*, **27**, G535–G540.

HAMBERG, M. & SAMUELSSON, B. (1974). Prostaglandin endoperoxides. Novel transformations of arachidonic acid in human platelets. *Proc. Natl. Acad. Sci. U.S.A.*, **71**, 3400–3404.

HAMBERG, M., SVENSSON, J. & SAMUELSSON, B. (1975). Thromboxanes: a new group of biologically active compounds derived from prostaglandin endoperoxides. *Proc. Natl. Acad. Sci. U.S.A.*, **72**, 2994–2998.

HORNE, W.C., NORMAN, N.E., SCHWARZ, D.B. & SIMONS, E.R. (1981). Changes in cytoplasmic pH and in membrane potential in thrombin stimulated human platelets. *Eur. J. Biochem.*, **120**, 295–302.

IRVINE, R.F. (1982). How is the level of free arachidonic acid controlled in mammalian cells? *Biochem. J.*, **204**, 3–16.

JESSE, P.T. & FRANSON, R.C. (1979). Modulation of purified phospholipase A2 activity from human platelets by calcium and indomethacin. *Biochim. Biophys. Acta*, **575**, 467–470.

LOWRY, O.H., ROSEBROUGH, N.J., FARR, A.L. & RANDALL, R.J. (1951). Protein measurement with the Folin phenol reagent. *J. Biol. Chem.*, **193**, 265–275.

NG, L.L. & DUDLEY, C. (1989). Intracellular pH clamping of human leucocytes: a technique for determination of cellular buffering power and Na^+/H^+ antiport characteristics. *Clin. Sci.*, **77**, 417–423.

OATES, J.A., FITZGERALD, G.A., BRANCH, R.A., JACKSON, E.K., KNAPP, H.R. & ROBERTS, L.J. II (1988). Clinical implications of prostaglandin and thromboxane A_2 formation. *N. Engl. J. Med.*, **319**, 689–698.

PETTITT, T.R., ROWLEY, A.F., BARROW, S.E., MALLET, A.I. & SECOMBES, C.J. (1991). Synthesis of lipoxins and other lipoxygenase products by macrophages from the rainbow trout, oncorhynchus mykiss. *J. Biol. Chem.*, **266**, 8720–8726.

POWELL, W.S. (1987). High pressure liquid chromatography in the analysis of arachidonic acid metabolites. In *Prostaglandins and Related Substances*. ed. Bennedetto, C., McDonald, R.G., Nigam, S. & Slater, T.F. pp. 75–88. Oxford: IRL Press.

RINK, T.J. & SAGE, S.O. (1990). Calcium signalling in human platelets. *Annu. Rev. Physiol.*, **52**, 431–449.

RINK, T.J., TSIEN, R.Y. & POZZAN, T. (1986). Cytoplasmic pH and free Mg^{2+} in lymphocytes. *J. Cell Biol.*, **95**, 189–196.

ROOS, A. & BORON, W.F. (1981). Intracellular pH. *Physiol. Rev.*, **61**, 296–434.

SEKIYA, F., TAKAGI, J., USUI, T., KAWAJIRI, K., KOBAYASHI, Y., SATA, F. & SAITO, J. (1991). 12S-Hydroxyeicosatetraenoic acid plays a central role in the regulation of platelet activation. *Biochem. Biophys. Res. Commun.*, **179**, 345–351.

SIFFERT W. & AKKERMAN, J.W.N. (1987). Activation of sodium-proton exchange is a prerequisite for Ca^{2+} mobilization in human platelets. *Nature*, **325**, 456–458.

SIMPSON, A.W.M. & RINK, T.J. (1987). Elevation of pH_i is not an essential step in calcium mobilisation in fura2 loaded human platelets. *FEBS Letts*, **222**, 144–148.

THOMAS, J.A., BUCHSBAUM, R.N., ZIMNIAK, A. & RACKER, E. (1979). Intracellular pH measurements in Ehrlich ascites tumour cells utilising spectroscopic probes generated in situ. *Biochemistry*, **18**, 2210–2218.

ZAVOICO, G.B. & CRAGOE, E.J. (1988). Ca^{2+} mobilisation can occur independent of Na^+/H^+ exchange in thrombin stimulated human platelets. *J. Biol. Chem.*, **263**, 9635–9639.

ZAVOICO, G.B., CRAGOE, E.J. & FEINSTEIN, M.B. (1986). Regulation of intracellular pH in human platelets. *J. Biol. Chem.*, **261**, 13160–13167.

(Received May 23, 1994
Accepted July 4, 1994)

Br. J. Pharmacol. (1994), **113**, 931–939 © Macmillan Press Ltd, 1994

Identification of renal natriuretic peptide receptor subpopulations by use of the non-peptide antagonist, HS-142-1

Richard A.D. Rutherford, †Yuzuru Matsuda, *Martin R. Wilkins, Julia M. Polak & [1]John Wharton

Departments of Histochemistry and *Clinical Pharmacology, Royal Postgraduate Medical School, Hammersmith Hospital, London W12 0NN and †Tokyo Research Laboratories, Kyowa Hakko Kogyo Co., Ltd., Tokyo 194, Japan

1 The renal actions of natriuretic peptides are dictated by the distribution of guanylyl cyclase-linked (NPR_A and NPR_B) and non-guanylyl cyclase-linked (NPR_C) receptors. Natriuretic peptide receptors have previously been distinguished on the basis of their differential affinity for peptide fragments and analogues; however, most of the available ligands are not fully selective. We have used the specific guanylyl cyclase-linked receptor antagonist, HS-142-1, to investigate the differential distribution of natriuretic peptide receptor subtypes in the human, bovine and rat kidney.

2 Specific, high affinity 3-([^{125}I]-iodotyrosyl)-rat-ANP-(1-28)([^{125}I]-rANP1-28) binding sites were identified in all three species, localized to glomeruli, inner medulla, intrarenal arteries and regions in the outer medulla corresponding to vasa recta bundles. Binding sites were also identified in the smooth muscle lining of the hilar region in the bovine and rat kidney.

3 In the rat, [^{125}I]-rANP1-28 binding was inhibited by unlabelled peptide sequences with a rank order of potency (rANP1-28 > pCNP1-22 > C-ANP4-23). The glomeruli exhibited a heterogeneous population of binding sites, C-ANP4-23 and pCNP1-22 producing a significantly better fit to a two component inhibition curve compared to the single component curve for rANP1-28.

4 Competitive inhibition experiments with the receptor selective ligands, C-ANP4-23 and HS-142-1, suggested that, like the rat, human and bovine glomeruli possessed a heterogeneous population of binding sites, whilst those in the inner medulla and intrarenal arteries of all three species represented a homogeneous population. Rat glomeruli exhibited a high proportion (>80%) of the NPR_C receptor subtype whereas in human and bovine glomeruli this receptor represented less than 20% of the total population, the majority of binding sites being HS-142-1-sensitive.

5 C-ANP4-23 exhibited a significantly higher inhibitory potency for binding sites in rat glomeruli compared to those in human and bovine kidney whilst HS-142-1 was significantly more potent in the rat and bovine kidney compared to man. No evidence was found to suggest the presence of a renal NPR_B receptor subtype.

6 The relative density, affinity and proportion of natriuretic receptor subtypes in the kidney exhibit significant species differences. HS-142-1 may be a valuable tool in further elucidating the localization and function of these receptors, but heterogeneity between species should be considered when selecting experimental models.

Keywords: atrial natriuretic peptide; natriuretic peptide receptors; kidney; autoradiography

Introduction

The natriuretic peptide family is considered to have a significant role in maintaining cardiovascular homeostasis and consists of atrial natriuretic peptide (ANP), brain natriuretic peptide (BNP), C-type natriuretic peptide (CNP) and urodilatin (Wilkins *et al.*, 1993). The biological effects of these peptides are mediated by two classes of receptor, one of which comprises a monomeric transmembrane protein possessing an intracellular guanylyl cyclase domain and an extracellular domain displaying rigorous criteria for ligand binding and activity (De Léan *et al.*, 1985; Chinkers *et al.*, 1989). Two subtypes of this receptor class have been identified, so-called A and B natriuretic peptide receptors (NPR_A and NPR_B), which exhibit different rank orders of potency for guanosine 3':5'-cyclic monophosphate (cyclic GMP) production (Bennett *et al.*, 1991; Suga *et al.*, 1992). The NPR_B subtype is selectively activated by CNP, displaying an affinity 10 to 50 fold greater than either ANP or BNP (Koller *et al.*, 1991; Komatsu *et al.*, 1991).

The other high-affinity receptor class (NPR_C) is a dimeric protein, composed of two disulphide-linked subunits which lacks the guanylyl cyclase domain (Porter *et al.*, 1990). It is generally thought that these receptors have a clearance role (Maack *et al.*, 1987); however, receptor subtypes may exist which are linked to other second-messenger systems (Hirata *et al.*, 1989; Isales *et al.*, 1992). NPR_C receptors are much less demanding than NPR_A and NPR_B receptors in their structural requirements for ligand binding and display high affinity for D-amino acid substitutions and ring-deleted analogues of ANP1-28 such as des[Gln^{18},Ser^{19},Gly^{20},Leu^{21},Gly^{22}]-rANP4-23 (C-ANP4-23) (Scarborough *et al.*, 1988). This analogue is ineffective in eliciting natriuretic and diuretic responses in the isolated perfused kidney (Maack *et al.*, 1987) and has been used in autoradiographic studies as a selective ligand to distinguish NPR_C receptors in organs such as the kidney and heart (Brown *et al.*, 1990; Rutherford *et al.*, 1991; 1992). In contrast, the investigation of guanylyl cyclase-linked NPR_A and NPR_B receptors has been hampered by the lack of selective antagonists. For example, it is unclear whether both subtypes are present in the kidney and recent binding studies have produced either negative or equivocal findings regarding the possible presence and localization of renal NPR_B receptors (Brown & Zuo, 1992; Konrad *et al.*, 1992). A number of peptide sequences have recently been synthesized which are selective for the guanylyl cyclase-linked ($NPR_{A/B}$) receptor subtypes (Weber *et al.*, 1991; Delporte *et*

[1] Author for correspondence.

al., 1992; Mimeault et al., 1993); however, the best characterized receptor antagonist to date is a novel microbial polysaccharide, HS-142-1, which selectively binds to guanylyl cyclase-linked natriuretic peptide receptors in rat, rabbit, bovine and porcine tissues inhibiting ANP-induced responses in the kidney, cultured neuronal cells, lung and adrenocortical membranes (Morishita et al., 1991; 1992; Toki et al., 1992; Oda et al., 1992; Ohyama et al., 1993). In contrast to other ligands, HS-142-1 exhibits no apparent affinity for non-guanylyl cyclase-linked natriuretic receptors (Morishita et al., 1992; Tanaka et al., 1992) and thus provides a significant new tool with which to determine the differential distribution of natriuretic peptide receptor subtypes in heterogeneous tissues such as the kidney. The majority of binding studies to date have employed experimental animals to examine renal natriuretic peptide receptors. However, their relevance to man is uncertain as there may be significant species differences in the distribution of these receptors (Féthière & De Léan, 1991). We have used quantitative *in vitro* autoradiography and receptor selective ligands to investigate the differential distribution, relative proportion and affinity of natriuretic receptor subtypes in the rat, bovine and human kidney.

Methods

Tissues

Rat ($n = 6$) and bovine ($n = 6$) kidney samples were obtained immediately after death caused by pentobarbitone overdose or exsanguination respectively. Non-involved regions of cortex and medulla were also obtained at nephrectomy from six male patients aged 40–66 years. Tissue blocks were placed on cork mats, surrounded in mounting medium (Tissue-Tek, Miles Inc., Elkhart, Indiana, U.S.A.) and frozen in melting dichlorodifluoromethane (Arcton'12, ICI, Cheshire) suspended in liquid nitrogen.

In vitro *autoradiography*

Cryostat sections (10 μm) were thaw mounted onto chromalum gelatin coated glass slides and stored at −20°C. Sections were preincubated at 20°C for 15 min in 30 mM phosphate buffer (comprising 20 mM $Na_2HPO_4.H_2O$, 10 mM $NaH_2PO_4.(2H_2O)$, 123 mM NaCl, pH 7.4) and then incubated in fresh buffer containing 0.5% bovine serum albumin, 0.18 mM bacitracin and 250 pM [^{125}I]-rANP1-28 at room temperature for up to 90 min. [^{125}I]-rANP1-28 was used as pilot studies had previously demonstrated an identical distribution and density of binding for ^{125}I-labelled rat and human ANP1-28 on sections of rat, human and bovine kidney. We have also previously shown that the inclusion of 0.18 mM bacitracin in the incubation buffer is sufficient to inhibit significantly degradation of the radioligand over the incubation period used, without having a detrimental effect on the specific binding of [^{125}I]-rANP1-28 (Wharton et al., 1994). Following incubation, the slides were washed twice in buffer at 4°C for 5 min, rinsed in distilled water at 4°C and dried under a stream of cold air. The NPR_C subpopulation was distinguished from the NPR_A and NPR_B subpopulations by co-incubation of 250 pM [^{125}I]-rANP1-28 with an excess of either HS-142-1 (2 mg ml^{-1}) or the NPR_C selective sequence, C-ANP4-23 (1 μM). Autoradiographic images were produced by exposing dry, labelled sections to Hyperfilm ^{3}H (Amersham, Bucks.) for 36 h at 4°C. The resulting autoradiographic film was developed in Kodak D-19 developer for 4–5 min, fixed in Amfix and rinsed in running water.

Microautoradiographs provided a higher degree of anatomical resolution of the binding sites and were obtained following exposure of labelled sections to Hyperfilm ^{3}H. Sections were fixed in Bouin's solution for 1 h at 20°C, washed twice in phosphate buffer (2–3 min) at 4°C, rinsed in cold distilled water, dried under a stream of cold air and dipped in liquid emulsion (LM-1, Amersham, Bucks) at 43°C. The dried slides were then stored in the dark at 4°C for up to 6 days, developed in Kodak D-19 for 2.5 min at 20°C, fixed and stained with haematoxylin and eosin.

Quantification and characterization of binding sites

An IBAS 386 Image Analysis System (Kontron Elektronic, Watford) was used to quantify ligand binding to specific tissue structures in autoradiographic film images. Specific binding (amol mm^{-2}) was determined by subtracting the non-specific binding from the total binding obtained by incubating adjacent sections with 250 pM [^{125}I]-rANP1-28 either alone or in the presence of 1 μM unlabelled rANP1-28.

Association binding kinetics were examined by incubating sections of rat kidney with 250 pM [^{125}I]-rANP1-28 for up to 90 min at 20°C. Dissociation kinetics were determined following the addition of 1 μM unlabelled rANP1-28 to sections at equilibrium and incubating for a further 150 min. Competitive inhibition of specific [^{125}I]-rANP1-28 (250 pM) binding to human, bovine and rat kidneys was examined in the presence of increasing concentrations (10^{-12}–10^{-5} M) of unlabelled rANP1-28, pCNP1-22, C-ANP4-23 or HS-142-1 (0.1–2000 μg ml^{-1}), with or without concomitant blockade of the NPR_C receptor subpopulation by C-ANP4-23 (10 μM). Further investigation of the guanylyl cyclase-linked subpopulation was afforded by co-incubation of serial sections with [^{125}I]-rANP1-28 and C-ANP4-23 (1 μM), either alone or in the presence of pCNP1-22 (0.1 μM), the selective agonist for the NPR_B receptor subtype. Binding data were analysed by the non-linear curve fitting programme, GraphPad InPlot version 4.0 (GraphPad Software, San Diego, U.S.A.). A four parameter logistic equation was used to describe the relationship between the percentage of [^{125}I]-rANP1-28 bound and the concentration of rANP1-28, pCNP1-22, C-ANP4-23 and HS-142-1 in competitive inhibition experiments. Data from inhibition of [^{125}I]-rANP1-28 was fitted to one or two site models and the 'best-fit' sums of squares compared statistically by an F-test. The concentration of peptide which inhibited 50% of the specific ligand binding (IC_{50}) was calculated for each competing peptide and expressed as a geometric mean with 95% confidence interval (95% CI), being derived from logarithmically transformed data.

Statistics

Binding data were analysed by one way or repeated analysis of variance, differences being considered significant if the P value was less than 0.05. To reduce the probability of significant differences arising by chance, a Bonferroni correction was applied to the data (Wallenstein et al., 1980). The IC_{50} values of competitive inhibition data for glomeruli, inner medulla and intrarenal blood vessels were used as three separate dependent variables and the competing peptides as within subject factors.

Drugs

Drugs used were 3-([^{125}I]-iodotyrosyl)-rat ANP1-28 (~2000 Ci mmol^{-1}; Amersham, Bucks.), bacitracin, bovine serum albumin (fraction V)(Sigma Chemical Co., UK) and HS-142-1 (Tokyo Research Laboratories, Kyowa Hakko Kogyo Co. Ltd., Japan). Rat ANP1-28, human ANP1-28, porcine CNP1-22 and C-ANP4-23 were obtained from Peninsula Laboratories, St. Helens.

Results

The distribution of [^{125}I]-rANP1-28 binding sites was similar in human, bovine and rat renal tissues. Specific binding sites were localized to glomeruli, non-glomerular cortex, inner

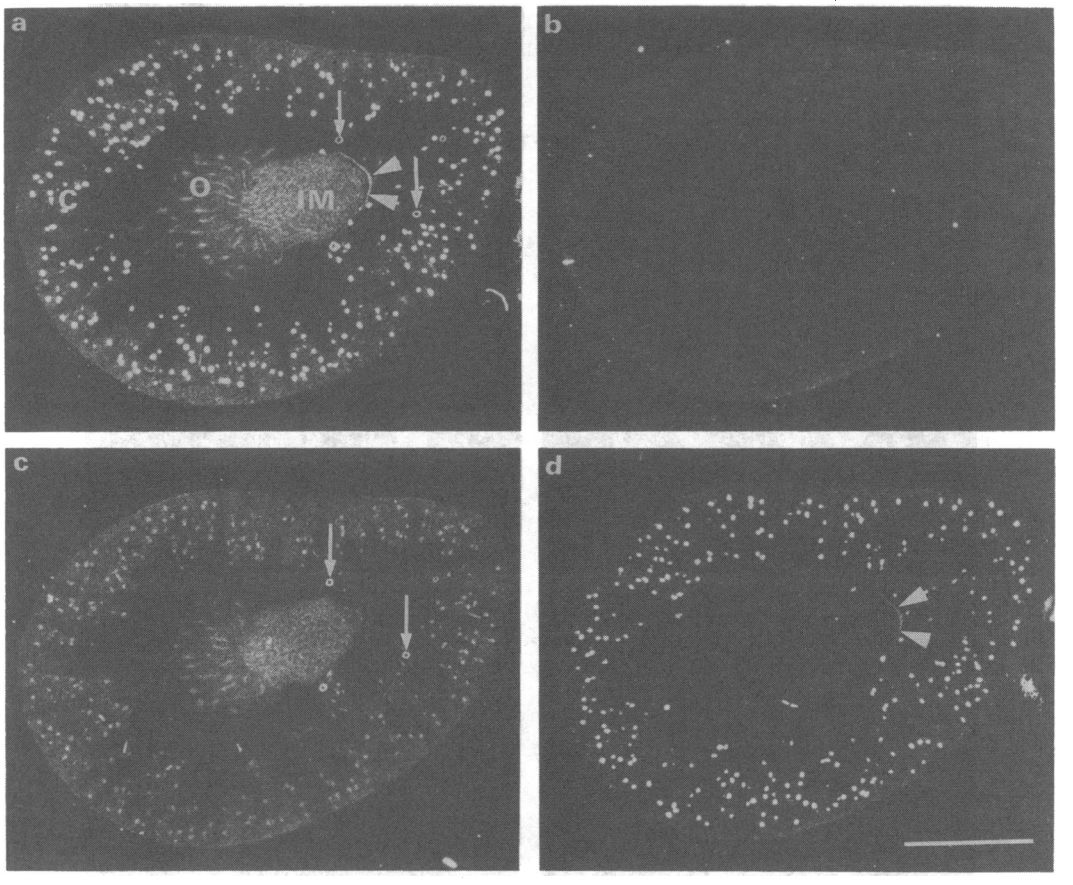


Figure 1 Autoradiographic localization of [^{125}I]-rANP1-28 binding sites in the rat kidney. Serial cryostat sections were incubated with 250 pM [^{125}I]-rANP1-28 in the absence (a) or presence of 1 μM rANP1-28 (b), C-ANP4-23 (c) or 2 mg ml^{-1} HS-142-1 (d). Binding sites are localized to glomeruli in the cortex (C), the inner medulla (IM), vasa recta bundles in the inner stripe of the outer medulla (O), intrarenal arteries (arrows) and smooth muscle in the hilar region of the kidney (arrowheads). Bar = 3 mm.

medulla, intrarenal arteries and regions in the outer medulla corresponding to vasa recta bundles. Binding sites were also observed in the hilar region of the bovine and rat kidney (Figures 1 and 2). Co-incubation of [^{125}I]-rANP1-28 with an excess (1 μM) of unlabelled ANP1-28 inhibited specific binding to all renal sites whereas co-incubation with receptor-selective ligands produced a differential inhibition of ligand binding (Figures 1 and 2). Microscopic examination demonstrated a high density of [^{125}I]-rANP1-28 binding to glomeruli and cortical radial, arcuate and interlobar arteries in all species, as well as non-vascular smooth muscle in the hilar region of rat and bovine kidney (Figure 3). The possibility of distinct binding to vascular endothelium could not be established due to the high density of binding sites on the medial layer and limited resolution of the autoradiographic images obtained with [^{125}I]-rANP1-28. Silver grains were also diffusely distributed in the inner medulla, non-glomerular cortex and medullary stripes. Of the three species examined, the rat exhibited the highest density of renal natriuretic peptide binding sites in all of the regions examined, the relative binding density of 250 pM [^{125}I]-rANP1-28 binding being 3–5 fold higher than in bovine and human kidney (Table 1). In the glomeruli and intrarenal arteries of all three species, non-specific binding was low (<10%), however, the human medulla exhibited a relatively high level of non-specific binding corresponding to 40% of the total compared to less than 10% in the bovine and rat medulla.

Specific [^{125}I]-rANP1-28 binding to rat kidney was high affinity, time-dependent and reversible, reaching apparent steady-state conditions by 30 min at 20°C (Figure 4, Table 2). Binding was inhibited by unlabelled peptide sequences with a rank order of potency rANP1-28 >pCNP1-22 >C-ANP4-23 (Figure 5, Table 3). The inhibition curve for unlabelled rANP1-28 was best described by a single site model whereas the inhibition curves for pCNP1-22 and C-ANP4-23 were best described by a two site model ($P<0.01$) (Figure 5, Table 3). Non-linear regression analysis of these two site models suggested that in the rat glomeruli 58.9% (51.4–66.0) of the binding sites corresponded to the clearance receptor subtype (NPR_C). Unlabelled pCNP1-22 and C-ANP4-23 both displayed a high affinity for NPR_C binding sites; however, at high concentrations pCNP1-22 (>0.1 μM) and C-ANP4-23 (>1 μM) also appeared to bind, albeit with lower affinity, to another population of [^{125}I]-rANP1-28 binding sites (Figure 5, Table 3). Unlike the inhibition of binding to glomeruli both rANP1-28 and pCNP1-22 displayed a monophasic inhibition of [^{125}I]-rANP1-28 binding in the inner medulla and intrarenal arteries whereas C-ANP4-23 had no apparent affinity for these sites at concentrations up to 10^{-6} M (Figure 5, Table 3).

The differential distribution and relative affinity of natriuretic peptide receptors in the human, rat and bovine kidney were also examined by competitive inhibition studies, using the receptor selective ligands C-ANP4-23 and HS-142-1 (Figures 6 and 7). As in the rat, bovine and human glomeruli exhibited a heterogeneous population of [^{125}I]-rANP1-28 binding sites with high affinity for both C-ANP4-23 (Figure 6) and HS-142-1 (Figure 7). In the presence of excess (10 μM) C-ANP4-23, 70.5% (63.8–77.2) of the binding to rat glomeruli was inhibited whereas 58.9% (54.0–63.8) and 61.0% (42.5–79.5) of glomerular binding was inhibited in the bovine and human kidney respectively. C-ANP4-23 exhibited significantly higher affinity ($P<0.001$) for binding sites in rat glomeruli (IC_{50} 38.2 nM (19.9–72.4)) compared with those

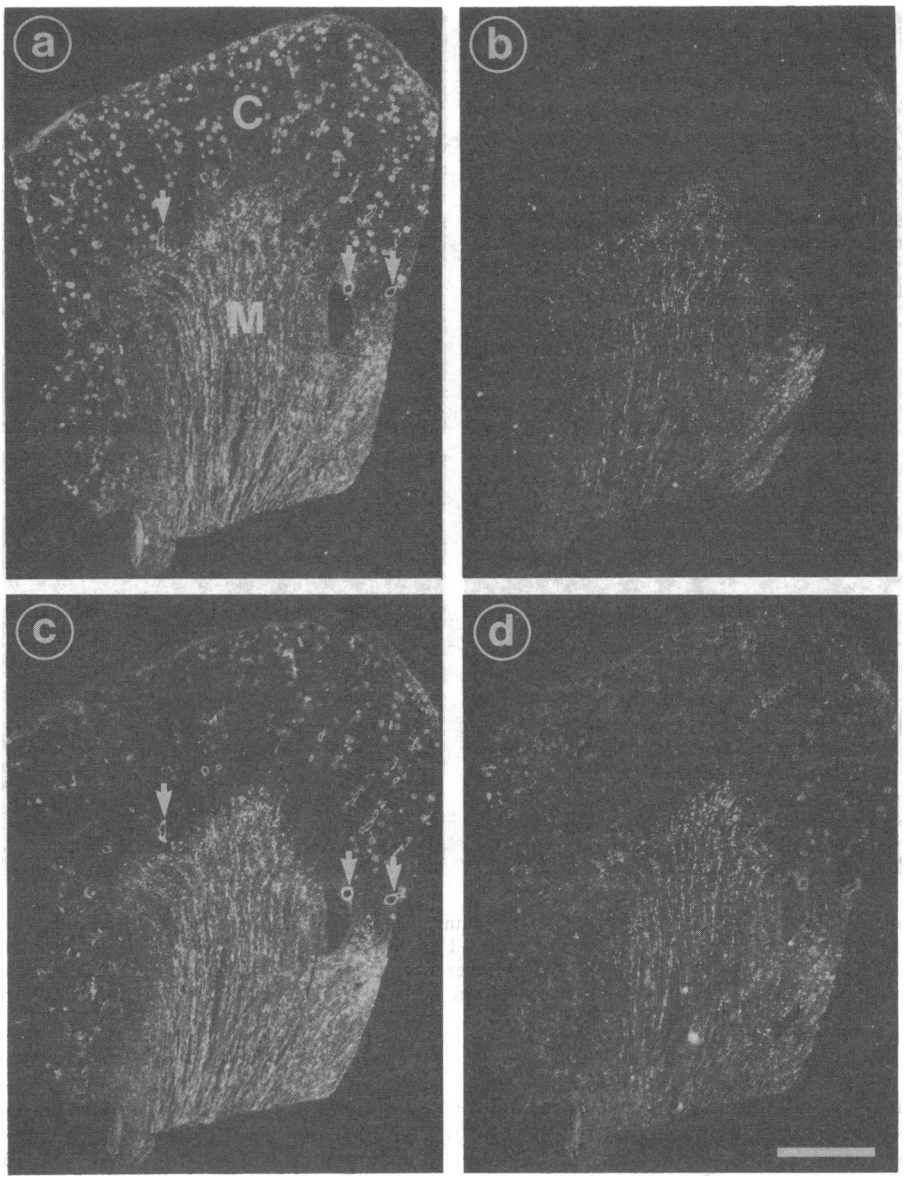


Figure 2 Autoradiographic localization of [^{125}I]-rANP1-28 binding sites in the human kidney. Serial cryostat sections were incubated with 250 pM [^{125}I]-rANP1-28 in the absence (a) or presence of 1 μM rANP1-28 (b), C-ANP4-23 (c) or 2 mg ml^{-1} HS-142-1 (d). Binding sites are localized to glomeruli in the cortex (C), the medulla (M) and intrarenal arteries (arrows). Bar = 3 mm.

identified in human (IC_{50} 182 nM (96–345)) and bovine glomeruli (IC_{50} 5058 nM (3048–8395)) (Figure 6).

Co-incubation of [^{125}I]-rANP1-28 (250 pM) with excess HS-142-1 (2 mg ml^{-1}) inhibited 17.1% (7.7–33.9) of the specific binding in rat glomeruli; however, in the human and bovine glomeruli, as many as 80.7% (69.9–88.2) and 88.0% (84.6–90.7) of the binding sites were HS-142-1-sensitive respectively. In addition, HS-142-1 inhibited 94–100% of the specific binding to the inner medulla and intrarenal arteries in all three species. Co-incubation of serial sections with [^{125}I]-rANP1-28 and C-ANP4-23 (1 μM), either alone or in the presence of pCNP1-22 (0.1 μM), exhibited no significant differences in the relative ligand binding density between sections of either the rat, bovine or human kidney. Under conditions of concomitant NPR_C receptor blockade with C-ANP4-23 (10 μM), HS-142-1 exhibited significant inter-species differences in its inhibitory potency of [^{125}I]-rANP1-28 binding to kidney structures (Table 4). HS-142-1 was significantly more potent in inhibiting ligand binding to sites in the rat and bovine kidney than in man, and exhibited a 2.5–3.6 fold greater inhibitory potency for binding to bovine glomeruli and intrarenal arteries than in the rat kidney (Figure 7, Table 4).

Discussion

[^{125}I]-rANP1-28 binds to a heterogeneous population of receptors in rat, human and bovine kidney displaying both regional and species differences in their affinity and distribution. The localization and affinity of specific binding sites are consistent with our previous studies in the rat kidney (Rutherford *et al.*, 1991) as well as those of other autoradiographic and immunohistochemical studies which have demonstrated natriuretic peptide receptors in the kidney of all three species studies, localized to glomeruli, medulla, intrarenal arteries and ureter smooth muscle (Mantyh *et al.*, 1986; Ishikawa *et al.*, 1987; Shimonaka *et al.*, 1987; Brucksch *et al.*, 1988; Kawaguchi *et al.*, 1989; Brown *et al.*, 1990). Non-linear regression analysis of the biphasic inhibition curves produced by pCNP1-22 and C-ANP4-23 indicated that 40–60% of the binding to glomeruli in all three species was to the NPR_C receptor subtype and the remainder to the guanylyl cyclase-linked $NPR_{A/B}$ receptor subtypes. This is consistent with our previous estimates of the proportion of guanylyl cyclase-linked and non-guanylyl cyclase-linked natriuretic peptide receptors in the rat kidney, obtained from binding studies in the presence of C-ANP4-23 (Brown *et al.*, 1990; Rutherford

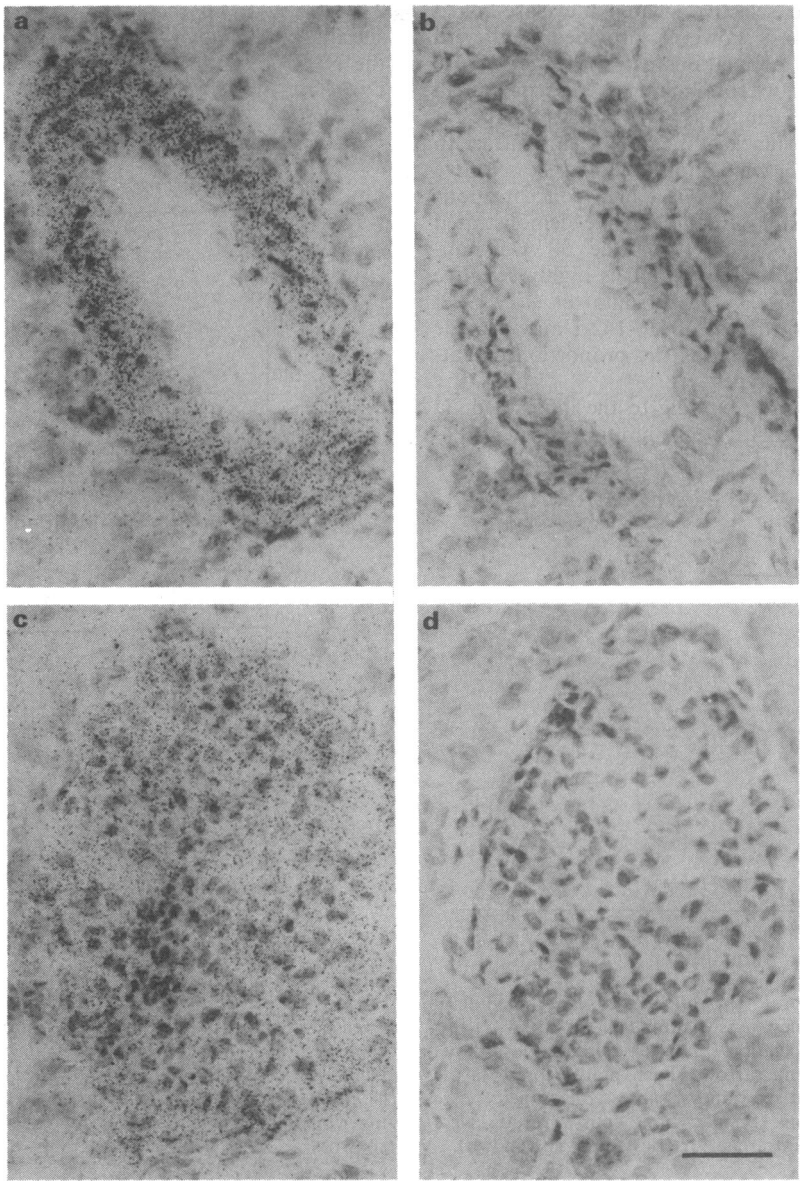


Figure 3 Microautoradiographic localization of [^{125}I]-rANP1-28 binding sites in human kidney. Sections were incubated in the absence (a,c) and presence (b,d) of 1 μM unlabelled rANP1-28. Specific binding sites are demonstrated by silver grains in the emulsion overlying the media of an intrarenal artery (a) and a glomerulus in the cortex (c). Bar = 50 μm.

Table 1 Relative binding density of [^{125}I]-rANP1-28 to human, bovine and rat kidney

	[^{125}I]-rANP1-28 bound (amol mm^{-2})		
	Glomeruli	*Medulla*	*Intrarenal arteries*
Human	71.0 (45.5–96.5)**	29.8 (1.40–57.2)*	79.8 (46.3–113.3)**
Bovine	113 (86.2–140.2)**	16.7 (13.0–20.4)**	55.2 (37.3–73.1)**
Rat	313.6 (245.1–382.1)	61.0 (44.7–77.3)	184.6 (149.2–220.0)

Specific binding of 250 pM [^{125}I]-rANP1-28 for 30 min at 20°C expressed as the mean and 95% confidence interval for six separate human, bovine and rat kidneys. Significantly lower (*$P<0.05$; **$P<0.001$) binding density compared to the rat.

Table 2 Association and dissociation constants for [^{125}I]-rANP1-28 binding to rat kidney

	k_{+1} ($\times 10^{-8}$ M^{-1} min^{-1})	k_{-1} ($\times 10^{-2}$ min^{-1})	K_d (nM)
Glomeruli	3.88 (3.43–4.30)	2.42 (1.72–3.11)	0.08 (0.03–0.17)
Inner medulla	1.85 (1.20–2.49)	3.54 (0.81–6.28)	0.17 (0.06–0.45)
Intrarenal arteries	1.98 (0.91–3.04)	2.60 (1.14–4.07)	0.12 (0.03–0.47)

Association (k_{+1}), dissociation (k_{-1}) and apparent equilibrium dissociation constant (K_d) values derived from non-linear regression analysis of time course studies of 250 pM [^{125}I]-rANP1-28 binding at 20°C. Values expressed as the mean and 95% confidence interval for six separate kidneys.

et al., 1991). Use of the selective guanylyl cyclase-linked receptor antagonist HS-142-1, however, provided a different estimate of the receptor populations which reflects more closely the results of affinity cross-linking studies in human glomeruli (Féthière & De Léan, 1991) and studies on the rat isolated perfused kidney (Maack et al., 1987). In contrast to pCNP1-22 and C-ANP4-23, which appear not to be selective for glomerular NPR_C receptors when at high concentrations ($\geqslant 10^{-6}$ M), affinity cross-linking studies have demonstrated that HS-142-1 displays no affinity for the 60 kDa non-guanylyl cyclase-linked ANP receptor and is highly selective for particulate guanylyl cyclase (Morishita et al., 1992; Tanaka et al., 1992). Thus, the use of HS-142-1 may provide a more accurate means of estimating the proportion of natriuretic peptide receptor subtypes.

In contrast to the glomeruli, binding to the inner medulla of all three species was insensitive to inhibition by C-ANP4-23. HS-142-1, on the other hand, completely inhibited the specific binding of [^{125}I]-rANP1-28 indicating an absence of the NPR_C receptor subtype from renal medullary sites. This

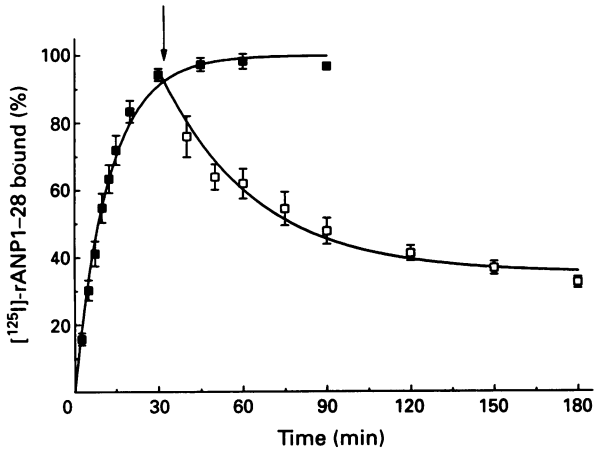


Figure 4 Specific binding of [^{125}I]-rANP1-28 to inner medullary binding sites in the rat kidney. Association (■) of 250 pM [^{125}I]-rANP1-28, at 20°C, and dissociation (□) after the addition of 1 μM unlabelled rANP1-28 at 30 min (arrow). Each point represents the mean ± s.e.mean derived from six kidneys, expressed as a percentage of maximum specific binding. Similar time course results were observed for glomeruli and intrarenal arteries (data not shown).

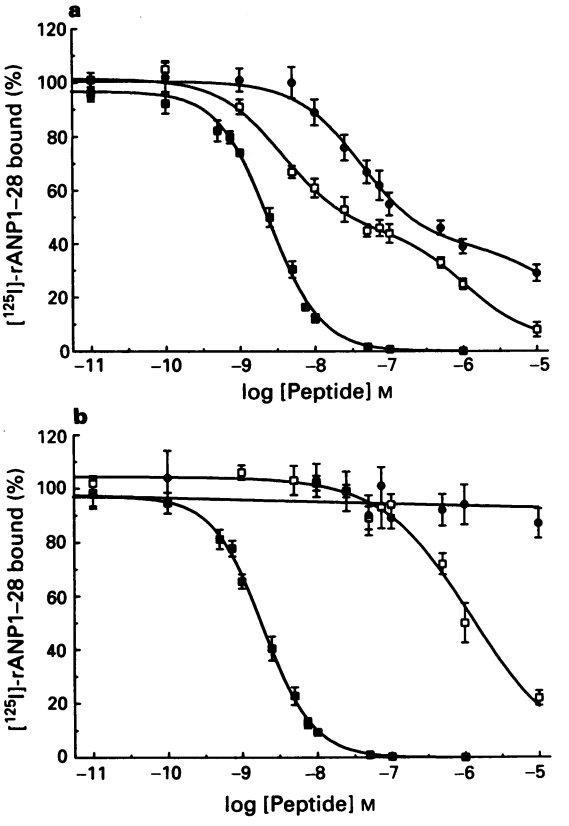


Figure 5 Competitive inhibition curves of specific [^{125}I]-rANP1-28 binding to gomeruli (a) and intrarenal arteries (b) in rat kidney. Each point represents the mean ± s.e.mean derived from six kidneys, expressed as a percentage of ligand binding in the presence of increasing concentrations of unlabelled rANP1-28 (■), pCNP1-22 (□) and C-ANP4-23 (●). Competitive inhibition of binding to the inner medulla gave very similar curves to intrarenal arteries (data not shown).

Table 3 Competitive inhibition of specific [^{125}I]-rANP1-28 binding to rat kidney by unlabelled peptide sequences

	rANP1-28 IC_{50} (nM)	*nH*	pCNP1-22 IC_{50} (nM)	*nH*	C-ANP4-23 IC_{50} (nM)
Glomeruli	2.31 (1.87–2.86)	1.15 (0.96–1.34)	3.67 (2.14–6.17)	–	38.2* (19.9–72.4)
			1514* (912–2512)	–	17179* (4786–60256)
Inner medulla	1.03 (0.77–1.37)	0.99 (0.65–1.34)	676* (407–1122)	0.83 (0.59–1.07)	>> 10 μM
Intrarenal arteries	1.82 (1.41–2.36)	1.33 (1.05–1.61)	1202* (631–2291)	0.91 (0.52–1.29)	>> 10 μM

IC_{50} values and Hill coefficients (nH) derived from non-linear regression analysis of the inhibition of 250 pM [^{125}I]-rANP1-28 binding to rat kidney. Data are expressed as the geometric mean and 95% confidence interval for six separate kidneys. *Significantly lower ($P<0.001$) inhibitory potency of pCNP1-22 and C-ANP4-23 compared with rANP1-28.

Table 4 Competitive inhibition of specific renal [^{125}I]-rANP1-28 binding by the antagonist, HS-142-1

	Human	*Bovine*	*Rat*
Glomeruli	57.1 (43.1–75.7)**	0.54 (0.31–0.95)*	1.95 (1.25–2.66)
Medulla	216 (83.0–562.3)**	1.73 (0.71–4.25)	1.54 (1.07–2.22)
Intrarenal arteries	93.8 (54.6–160.7)**	0.73 (0.27–2.06)*	1.82 (1.13–2.92)

IC_{50} values (μg ml^{-1}) derived from non-linear regression analysis of [^{125}I]-rANP1-28 binding to human, bovine and rat kidney. Data are expressed as the geometric mean and 95% confidence interval for six separate kidneys. Significant differences (*$P<0.05$; **$P<0.001$) in the inhibitory potency of the functional antagonist, HS-142-1, for sites in human and bovine kidney compared to those in the rat.

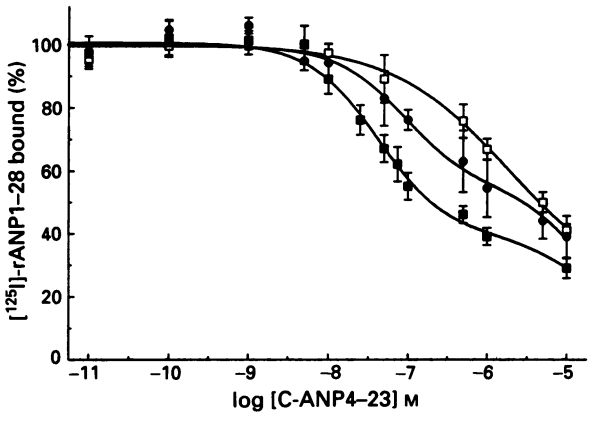


Figure 6 Competitive inhibition curves of specific [^{125}I]-rANP1-28 binding to glomeruli in the rat (■), human (●) and bovine (□) kidney. Each point represents the mean ± s.e.mean derived from six kidneys, expressed as a percentage of ligand binding in the presence of increasing concentrations of C-ANP4-23.

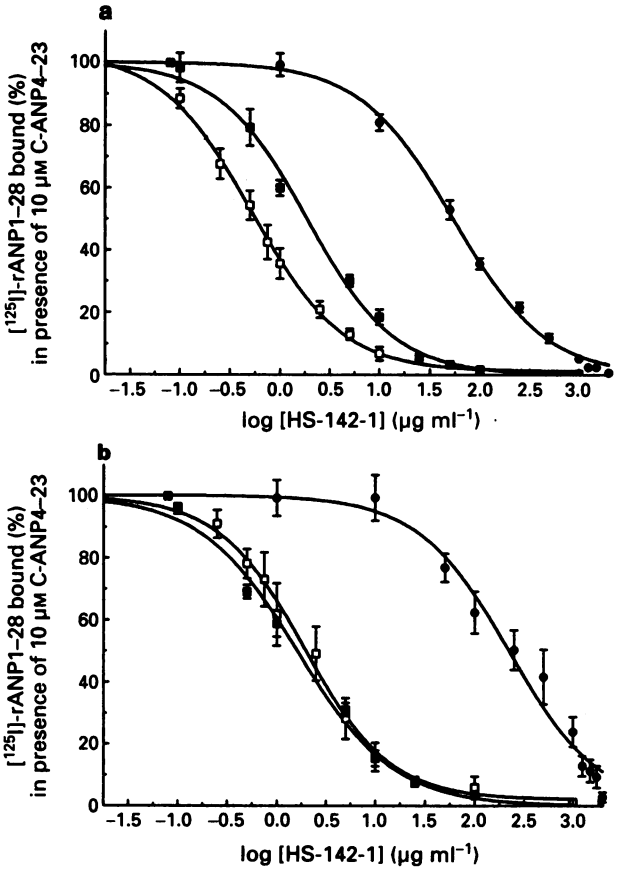


Figure 7 Competitive inhibition curves of specific [^{125}I]-rANP1-28 binding to gomeruli (a) and inner medulla (b) in the presence of increasing concentrations of HS-142-1. Incubations were carried out in the presence of excess (10 μM) C-ANP4-23, blocking the NPR_C receptor subpopulation. Each point represents the mean ± s.e.mean derived from six kidneys expressed as a percentage of ligand binding in bovine (□), rat (■) and human (●) kidney. Competitive inhibition of binding to intrarenal arteries gave very similar inhibition curves to glomeruli (data not shown).

is supported by studies demonstrating that papillary membranes, collecting duct cells and interstitial cells express only a 130–140 kDa, guanylyl cyclase-linked receptor subtype (Gunning *et al.*, 1988; Martin *et al.*, 1989; Fontoura *et al.*, 1990). The similarity between the binding profiles in the inner medulla and intrarenal arteries indicates that, like the inner medulla, $NPR_{A/B}$ subtypes also predominate in the interlobar and arcuate arteries of rat, human and bovine kidney. Activation of these receptors by natriuretic peptides has been shown to induce a selective relaxation of rat arcuate arteries, mediated by an increase in guanylyl cyclase activity (Aalkjaer *et al.*, 1985; Ohishi *et al.*, 1988; Veldkamp *et al.*, 1988).

Clearance of ANP from the circulation is achieved both via NPR_C receptors and the enzyme endopeptidase 24.11 (EC.3.4.24.11). This enzyme has been identified on human vascular endothelial cells and, in the kidney, on brush border cells of the proximal tubule (Schulz *et al.*, 1989; Llorens-Cortes *et al.*, 1992). It is likely that endopeptidase 24.11 and NPR_C receptors may act in concert to regulate plasma ANP levels (Barclay *et al.*, 1992); however, species differences in the relative density of renal NPR_C receptors may indicate that this pathway is less influential in the human and bovine kidney than in the rat. The highest density of natriuretic peptide binding sites was found in the rat kidney. Despite the homology which exists between mammalian ANP sequences, it was considered that the lower binding density observed in the human and bovine kidney may be due to the use of species-specific ligands. Studies using both [^{125}I]-rANP1-28 and [^{125}I]-hANP1-28, however, demonstrated an identical localization and density of binding on glomeruli, inner medulla and intrarenal arteries in all three species indicating that the differential binding was not due to use of the rat ligand.

In the present study, [^{125}I]-rANP1-28 binding was inhibited by HS-142-1 in the rat and bovine kidney with an inhibitory potency similar to that previously found in rabbit kidney cortex and bovine adrenocortical membrane preparations (Morishita *et al.*, 1991). *In vivo*, HS-142-1 has been shown to inhibit the natriuresis and diuresis induced by acute volume expansion in rats (Sano *et al.*, 1992b) whilst *in vitro* it inhibits ANP binding to its guanylyl cyclase-linked receptor, ANP-stimulated cyclic GMP accumulation and binding of [^{125}I]-rANP1-28 to isolated rat glomeruli (Morishita *et al.*, 1991; Sano *et al.*, 1992a), suggesting that the inhibition of natriuresis and diuresis is due in part to the direct antagonism by HS-142-1 of guanylyl cyclase-linked receptors in renal glomeruli. The differences in affinity which HS-142-1 displayed for [^{125}I]-rANP1-28 binding sites, in rat, bovine and human kidney suggest a significant species heterogeneity in the guanylyl cyclase-linked receptor subtype, an observation supported by pharmacological investigation in membrane preparations of rat, human and bovine glomeruli and papillae (Féthière & De Léan, 1991).

No evidence was obtained for the presence of a renal NPR_B subtype although recent reports have indicated expression of this receptor in human kidney, following PCR amplification (Canaan-Kühl, 1992), and by the autoradiographic demonstration of low level [^{125}I]-Tyr^{0}CNP1-22 binding to rat kidney sections (Konrad *et al.*, 1992). This apparent discrepancy may reflect the relatively low level expression of the NPR_B receptor in the kidney and the lack of a specific antagonist for binding studies. HS-142-1 does not appear to distinguish between NPR_A and NPR_B receptor subtypes (Toki *et al.*, 1992) while CNP1-22, the proposed endogenous ligand for the NPR_B subtype (Koller *et al.*, 1991; Suga *et al.*, 1992), is non-selective and has a high affinity for both NPR_B and NPR_C subtypes (Brown & Zuo, 1992; 1993). The present findings suggest that although CNP1-22 may produce a vasodilatation *in vivo* via activation of NPR_B receptors (Wong & Garbers, 1992) this subtype is not involved in the renal response to natriuretic peptides.

Studies investigating the functional significance of the natriuretic peptide family have to date been hindered by the lack of specific receptor antagonists. Although a number of peptide sequences have been synthesized which are selective for the NPR_C receptor (Maack *et al.*, 1987; Koepke *et al.*, 1989) and more recently for the guanylyl cyclase-linked NPR_A

receptor (Delporte *et al.*, 1992; Mimeault *et al.*, 1993), the discovery and characterization of the non-peptide guanylyl cyclase-linked receptor antagonist, HS-142-1, may help to elucidate further the physiological and pathophysiological roles of the natriuretic peptides. The apparent differences displayed in the affinity for competing sequences implies the existence of a significant interspecies heterogeneity in natriuretic peptide receptors which may be of importance in the interpretation of results obtained using animal models to study peptide receptor-ligand interactions and their relevance to man.

The authors would like to thank Patricia Harley for excellent technical assistance and the staff of the Histopathology Department, Royal Marsden Hospital, London, for providing tissue samples. The work was supported in part by the British Heart Foundation and the Council for Tobacco Research, U.S.A.

References

AALKJAER, C., MULVANY, M.J. & NYBORG, N.C.B. (1985). Atrial natriuretic factor causes specific relaxation of rat renal arcuate arteries. *Br. J. Pharmacol.*, **86**, 447–453.

BARCLAY, P.L., BENNETT, J.A., GREENGRASS, P.M., GRIFFIN, A., SAMUEL, G.M.R. & SHEPPERSON, N.B. (1992). The pharmacokinetics of ^{125}I-atrial natriuretic factor in anaesthetized rats. Effects of neutral endopeptidase inhibition with candoxatrilat and of ANF-C receptor blockade. *Biochem. Pharmacol.*, **44**, 1013–1022.

BENNETT, B.D., BENNETT, G.L., VITANGCOL, R.V., JEWETT, J.R., BURNIER, J., HENZEL, W. & LOWE, D.G. (1991). Extracellular domain IgG fusion proteins for three human natriuretic peptide receptors. Hormone pharmacology and application to solid phase screening of synthetic peptide antisera. *J. Biol. Chem.*, **266**, 23060–23067.

BROWN, J., SALAS, S.P., SINGLETON, A., POLAK, J.M. & DOLLERY, C.T. (1990). Autoradiographic localization of atrial natriuretic peptide receptor subtypes in rat kidney. *Am. J. Physiol.*, **259**, F26–F39.

BROWN, J. & ZUO, Z. (1992). Renal receptors for atrial and C-type natriuretic peptides in the rat. *Am. J. Physiol.*, **263**, F89–F96.

BROWN, J. & ZUO, Z. (1993). C-type natriuretic peptide and atrial natriuretic peptide receptors of rat brain. *Am. J. Physiol.*, **264**, R513–R523.

BRUCKSCH, A., GRÖNE, H.J., TALARTSCHIK, J. & FUCHS, E. (1988). Bindings sites of atrial natriuretic peptide in human renal tissue-quantification by in vitro receptor autoradiography. *Klin. Wochenschr.*, **66**, 303–307.

CANAAN-KÜHL, S., JAMISON, R.L., MYERS, B.D. & PRATT, R.E. (1992). Identification of 'B' receptor for natriuretic peptide in human kidney. *Endocrinol.*, **130**, 550–552.

CHINKERS, M., GARBERS, D.L., CHANG, M., LOWE, D.G., CHIN, H., GOEDDEL, D.V. & SCHULZ, S. (1989). A membrane form of guanylate cyclase is an atrial natriuretic peptide receptor. *Nature*, **338**, 78–83.

DE LÉAN, A.G., THIBAULT, N.G., SEIDAH, C., LAZURE, J., GUTKOWSKA, M., CHRÉTIEN, M., GENEST, J. & CANTIN, M. (1985). Structure-activity relationships of atrial natriuretic factor (ANF) III. Correlation of receptor affinity with relative potency on aldosterone production in zona glomerulosa cells. *Biochem. Biophys. Res. Commun.*, **132**, 360–367.

DELPORTE, C., WINAND, J., POLOCZEK, P., VON GELDERN, T. & CHRISTOPHE, J. (1992). Discovery of a potent atrial natriuretic peptide antagonist for ANP_A receptors in the human neuroblastoma NB-OK-1 cell line. *Eur. J. Pharmacol.*, **224**, 183–188.

FÉTHIÈRE, J. & DELÉAN, A. (1991). Pharmacological evidence for the heterogeneity of atrial natriuetic factor-R_1 receptor subtype. *Mol. Pharmacol.*, **40**, 915–922.

FONTOURA, B.M.A., NUSSENZVEIG, D.R., FELTON, K.M. & MAACK, T. (1990). Atrial natriuretic factor receptors in cultured renomedullary interstitial cells. *Am. J. Physiol.*, **258**, C692–C699.

GUNNING, M., BALLERMANN, B.J., SILVA, P., BRENNER, B.M. & ZEIDEL, M.L. (1988). Characterization of ANP receptors in rabbit inner medullary collecting duct cells. *Am. J. Physiol.*, **258**, F467–F472.

HIRATA, M., CHANG, C.H. & MURAD, F. (1989). Stimulatory effects of atrial natriuretic factor on phosphoinositide hydrolysis in cultured bovine aortic smooth muscle cells. *Biochim. Biophys. Acta*, **1010**, 346–351.

ISALES, C.M., LEWICKI, J.A., NEE, J.J. & BARRETT, P.Q. (1992). ANP-(7-23) stimulates a DHP-sensitive Ca^{2+} conductance and reduces cellular cAMP via a cGMP-independent mechanism. *Am. J. Physiol.*, **263**, C334–C342.

ISHIKAWA, Y., UMEMURA, S., YASUDA, G., UCHINO, K., SHINDOU, T., MINAMIZAWA, K., TOYA, Y. & KANEKO, Y. (1987). Identification of an atrial natriuretic peptide specific receptor in human kidney. *Biochem. Biophys. Res. Commun.*, **147**, 135–139.

KAWAGUCHI, S., UCHIDA, K., ITO, T., KOZUKA, M., SHIMONAKA, M., MIZUNO, T. & HIROSE, S. (1989). Immunohistochemical localization of atrial natriuretic peptide receptor in bovine kidney and lung. *J. Histochem. Cytochem.*, **37**, 1739–1742.

KOEPKE, J.P., TYLER, L.D., TRAPANI, A.J., BOVY, P.R., SPEAR, K.L., OLINS, G.M. & BLAINE, E.H. (1989). Interaction of non-guanylate cyclase-linked atriopeptin receptor ligand and endopeptidase inhibitor in conscious rats. *J. Pharmacol. Exp. Ther.*, **249**, 172–176.

KOLLER, K.J., LOWE, D.G., BENNETT, G.L., MINAMINO, N., KANGAWA, K., MATSUO, H. & GOEDDEL, D.V. (1991). Selective activation of the B natriuretic peptide receptor by C-type natriuretic peptide (CNP). *Science*, **252**, 120–123.

KOMATSU, Y., NAKAO, K., SUGA, S., OGAWA, Y., MUKOYAMA, M., ARAI, H., SHIRAKAMI, G., HOSODA, K., NAKAGAWA, O., HAMA, N., KISHIMOTO, I. & IMURA, H. (1991). C-type natriuretic peptide (CNP) in rats and humans. *Endocrinol.*, **129**, 1104–1106.

KONRAD, E.M., THIBAULT, G. & SCHIFFRIN, E.L. (1992). Autoradiographic visualization of the natriuretic peptide receptor-B in rat tissues. *Regul. Pept.*, **39**, 177–189.

LLORENS-CORTES, C., HUANG, H., VICAR, P., GASC, J.-M., PAULIN, D. & CORVOL, P. (1992). Identification and characterization of neutral endopeptidase in endothelial cells from venous or arterial origins. *J. Biol. Chem.*, **267**, 14012–14018.

MAACK, T., SUZUKI, M., ALMEIDA, F.A., NUSSENZVEIG, D., SCARBOROUGH, R.M., MCENROE, G.A. & LEWICKI, J.A. (1987). Physiological role of silent receptors of atrial natriuretic factor. *Science*, **238**, 675–678.

MANTYH, C.R., KRUGER, L., BRECHA, N.C. & MANTYH, P.W. (1986). Localization of specific binding sites for atrial natriuretic factor in peripheral tissues of the guinea-pig, rat and human. *Hypertens*, **8**, 712–721.

MARTIN, E.R., LEWICKI, J.A., SCARBOROUGH, R.M. & BALLERMANN, B.L. (1989). Expression and regulation of ANP receptor subtypes in rat renal glomeruli and papillae. *Am. J. Physiol.*, **257**, F649–F657.

MIMEAULT, M., FOURNIER, A., FÉTHIÈRE, J. & DE LÉAN, A. (1993). Development of natriuretic peptide analogs selective for the atrial natriuretic factor-R_{1A} receptor subtype. *Mol. Pharmacol.*, **43**, 775–782.

MORISHITA, Y., SANO, T., ANDO, K., SAITOH, Y., KASE, H., YAMADA, K. & MATSUDA, Y. (1991). Microbial polysaccharide, HS-142-1, competitively and selectively inhibits ANP binding to its guanylyl cyclase-containing receptor. *Biochim. Biophys. Res. Commun.*, **176**, 949–957.

MORISHITA, Y., SANO, T., KASE, H., YAMADA, K., INAGAMI, T. & MATSUDA, Y. (1992). HS-142-1, a novel nonpeptide atrial natriuretic peptide (ANP) antagonist, blocks ANP-induced renal responses through a specific interaction with guanylyl cyclase-linked receptors. *Eur. J. Pharmacol.*, **225**, 203–207.

ODA, S., SANO, T., MORISHITA, Y. & MATSUDA, Y. (1992). Pharmacological profile of HS-142-1, a novel nonpeptide atrial natriuretic peptide (ANP) antagonist of microbial origin. II. Restoration by HS-142-1 of ANP-induced inhibition of aldosterone production in adrenal glomerulosa cells. *J. Pharmacol. Exp. Ther.*, **263**, 241–245.

OHISHI, K., HISHIDA, A. & HONDA, N. (1988). Direct vasodilatory action of atrial natriuretic factor on canine glomerular afferent arterioles. *Am. J. Physiol.*, **255**, F415–F420.

OHYAMA, Y., MIYAMOTO, K., MATSUDA, Y., KOJIMA, M., MINAMINO, N., KANGAWA, K. & MATSUO, H. (1993). HS-142-1, a novel antagonist for natriuretic peptides, has no effect on the third member of membrane bound guanylate cyclases (GC-C) in T84 cells. *Life Sci.*, **52**, PL153–157.

PORTER, J.G., ARFSTEN, A., FULLER, F., MILLER, J.A., GREGORY, L.C. & LEWICKI, J.A. (1990). Isolation and functional expression of the human atrial natriuretic peptide clearance receptor cDNA. *Biochem. Biophys. Res. Commun.*, **171**, 796–803.

RUTHERFORD, R.A.D., WHARTON, J., GORDON, L., MOSCOSO, G, YACOUB, M.H. & POLAK, J.M. (1992). Endocardial localization of natriuretic peptide binding sites in human fetal and adult heart. *Eur. J. Pharmacol.*, **212**, 1–7.

RUTHERFORD, R.A.D., WHARTON, J., NEEDLEMAN, P. & POLAK, J.M. (1991). Autoradiographic discrimination of brain and atrial natriuretic peptide binding sites in rat kidney. *J. Biol. Chem.*, **266**, 5819–5826.

SANO, T., IMURA, R., MORISHITA, Y., MATSUDA, Y. & YAMADA, K. (1992a). HS-142-1, a novel polysaccharide of microbial origin, specifically recognizes guanylyl cyclase-linked ANP receptor in rat glomeruli. *Life Sci.*, **51**, 1445–1451.

SANO, T., MORISHITA, Y., YAMADA, K. & MATSUDA, Y. (1992b). Effects of HS-142-1, a novel non-peptide ANP antagonist, on diuresis and natriuresis induced by acute volume expansion in anaesthetized rats. *Biochem. Biophys. Res. Commun.*, **182**, 824–829.

SCARBOROUGH, R.M., MCENROE, G.A., ARFSTEN, A., KANG, L.-L., SCHWARTZ, K. & LEWICKI, J.A. (1988). D-amino acid-substituted atrial natriuretic peptide analogs reveal novel receptor recognition requirements. *J. Biol. Chem.*, **263**, 16818–16822.

SCHULZ, W.W., HAGLER, H.K., BUJA, L.M. & ERDOS, E.G. (1988). Ultrastructural localization of angiotensin 1-converting enzyme (E.C.3.4.15.1) and neutral metalloendopeptidase (E.C.3.4.24.11) in the proximal tubule of the human kidney. *Lab. Invest.*, **59**, 789–797.

SHIMONAKA, M., SAHEKI, T., HAGIWARA, H., HAGIWARA, Y., SONO, H. & HIROSE, S. (1987). Visualization of ANP receptor on glomeruli of bovine kidney by use of a specific antiserum. *Am. J. Physiol.*, **253**, F1058–F1062.

SUGA, S., NAKAO, K., HOSODA, K., MUKOYAMA, M., OGAWA, Y., SHIRAKAMI, G., ARAI, H., SAITO, Y., KAMBAYASHI, Y., INOUYE, K. & IMURA, H. (1992). Receptor selectivity of natriuretic peptide family, atrial natriuretic peptide, brain natriuretic peptide, and C-type natriuretic peptide. *Endocrinol.*, **130**, 229–239.

TANAKA, T., ICHIMURA, M., NAKAJO, S., SNAJDAR, R.M., MORISHITA, Y., SANO, T., YAMADA, K., INAGAMI, T. & MATSUDA, Y. (1992). HS-142-1, a novel non-peptide antagonist for atrial natriuretic peptide receptor, selectively inhibits particulate guanylyl cyclase and lowers cyclic GMP in LLC-PK1 cells. *Biosci. Biotech. Biochem.*, **56**, 1041–1045.

TOKI, S., MORISHITA, Y., SANO, T. & MATSUDA, Y. (1992). HS-142-1, a novel non-peptide ANP antagonist, blocks the cyclic GMP production elicited by natriuretic peptides in PC12 and NG108-15 cells. *Neurosci. Lett.*, **135**, 117–120.

VELDKAMP, P.J., CARMINES, P.K., INSCHO, E.W. & NAVAR, L.G. (1988). Direct evaluation of the microvascular actions of ANP in juxtamedullary nephrons. *Am. J. Physiol.*, **254**, F440–F444.

WALLENSTEIN, S., ZUCKER, C.L. & FLEISS, J.L. (1980). Some statistical methods useful in circulation research. *Circ. Res.*, **47**, 1–9.

WEBER, W., FISCHLI, W., HOCHULI, E., KUPFER, E. & WEIBEL, E.K. (1991). Anantin – a peptide antagonist of the atrial natriuretic factor (ANF). *J. Antibiot. Tokyo*, **44**, 164–171.

WILKINS, M.R., NUNEZ, D.J. & WHARTON, J. (1993). The natriuretic peptide family: turning hormones into drugs. *J. Endocrinol.*, **137**, 347–359.

WHARTON, J., WALSH, D.A., RUTHERFORD, R.A.D., KNOCK, G.A. & POLAK, J.M. (1994). *In vitro* autoradiographic localization and characterization of binding sites. In *Receptor Autoradiography: Principles and Practice*. ed. Wharton, J. & Polak, J.M. pp. 79–105. Oxford: Oxford University Press.

WONG, S.K.F. & GARBERS, D.L. (1992). Receptor guanylyl cyclases. *J. Clin. Invest.*, **90**, 299–305.

(Received November 22, 1993
Revised April 18, 1994
Accepted July 6, 1994)

Br. J. Pharmacol. (1994), **113**, 940–944 © Macmillan Press Ltd, 1994

The role of bradykinin B_1 receptors in the maintenance of intra-articular plasma extravasation in chronic antigen-induced arthritis

S.C. Cruwys, †N.E. Garrett, *M.N. Perkins, D.R. Blake & [1]B.L. Kidd

The Inflammation Group, ARC Building, London Hospital Medical College, London E1 2AD, †Department of Pharmacology, Queen Mary and Westfield College, London E1 4NS and *Sandoz Institute for Medical Research, Gower Place, London WC1E 6BN

1 The role of bradykinin B_1 and B_2 receptors in bradykinin- and des-Arg^9-bradykinin-induced plasma extravasation in normal and inflamed rat knee joints was investigated by use of an antigen-induced model of chronic arthritis. A modification of an Evans blue extraction technique allowed the unstimulated (basal) plasma extravasation to be assessed in this model. The contributions of bradykinin B_1 and B_2 receptors towards basal synovial plasma extravasation were determined.

2 In normal knees, intra-articular injection of bradykinin (BK) induced plasma extravasation in a potent, dose-dependent manner with a threshold of 0.01 nmol and an ED_{50} of 0.1 nmol. In day 5 arthritic knees, basal plasma extravasation was substantially enhanced. Lower doses of BK had no demonstrable effect and increases above basal extravasation were first observed at 0.1 nmol. Thereafter the dose-response mirrored the response in normal knees and the maximal response was unaltered.

3 The B_1 agonist, des-Arg^9-BK, induced slight but significant plasma extravasation in normal knees but was less potent than bradykinin. This response was inhibited by the B_1 receptor antagonist, des-Arg^9, [Leu^8]-BK. Lower doses of des-Arg^9-BK bradykinin did not significantly increase basal extravasation in day 5 arthritic knees but, in contrast to BK, the maximal response was significantly enhanced.

4 The B_2 antagonist, Hoe 140, inhibited BK-induced plasma extravasation in normal joints over a dose-range of 0.1–1.0 nmol but was relatively inactive in day 5 inflamed knees. The B_1 receptor antagonist, des-Arg^9, [Leu^8]-BK, was relatively inactive in normal joints but showed increased potency against BK-induced plasma extravasation in day 5 arthritic joints.

5 Hoe 140 and des-Arg^9,[Leu^8]-BK both inhibited basal extravasation in arthritic joints on days 1 and 5 post-challenge in a dose-dependent fashion. Whilst Hoe 140 was the more potent inhibitor on day 1, it was less potent than des-Arg^9,[Leu^8]-BK on day 5.

6 Although the majority of responses to BK in normal tissue are mediated via B_2 receptors, a small population of B_1 receptors may exist in normal joint tissues. The data presented in this study suggest an evolving role for B_1 receptors in the mediation of plasma extravasation in inflamed joint tissues. A role for BK antagonists in the treatment of arthritis is also suggested.

Keywords: Bradykinin; bradykinin receptors; chronic arthritis; plasma extravasation; joint inflammation

Introduction

Bradykinin (BK) is a pro-inflammatory nonapeptide which is synthesized *de novo* at sites of tissue damage producing many of the cardinal signs of inflammation (Proud & Kaplan, 1988). In both acute and chronic arthritis BK has been implicated as a potent mediator of pain and swelling and may play a role in cell proliferation, bone resorption and the secondary release of various cytokines from leucocytes (Bhoola *et al.*, 1992a; Sharma, 1992).

BK is produced in damaged tissues from kininogen substrates present in the circulation and degranulating neutrophils (Bhoola *et al.*, 1992b). Elevated levels of BK have been reported in animal models of inflammation and in patients with inflammatory joint diseases (Steranka *et al.*, 1987; Hargreaves *et al.*, 1988). It is inactivated by proteolytic enzymes, including kininase I and II, forming a variety of metabolites which include the active fragments des-Arg^9-BK and Lys-des-Arg^9-BK.

Two types of bradykinin receptor, B_1 and B_2, have been characterized to date (Regoli & Barabé, 1980). Most actions of BK have been reported to be mediated via the B_2 receptor (Steranka *et al.*, 1988; Dray *et al.*, 1992) which is optimally stimulated by BK and kallidin (Lys-BK). In normal uninflamed tissues selective B_1 agonists, which include des-Arg^9-BK and Lys-des-Arg^9-BK (Dray & Perkins, 1993), are largely inactive possibly due to lack of expression or masking of the B_1 receptors. In contrast, increased expression of B_1 receptors has recently been reported in pathological states, particularly in inflammation or after exposure to noxious stimuli (Farmer *et al.*, 1991; Bhoola *et al.*, 1992a; Perkins *et al.*, 1993).

Plasma extravasation in arthritis has important consequences leading to joint swelling and facilitating many secondary and potentially damaging intra-articular events. Although the effects of BK on acute joint swelling are relatively well established, its role in maintenance of chronic joint swelling is less clear (Bhoola *et al.*, 1992a). We have therefore compared the actions of BK on plasma extravasation in normal and chronically inflamed joints using an antigen-induced model of chronic arthritis. In light of the evidence supporting a role for B_1 receptors in chronic inflammation we have also examined the relative actions of B_1 and B_2 agonists and antagonists on plasma extravasation in the same inflammatory model.

Methods

The experiments were performed on male Wistar rats (200–250 g) which were deeply anaesthetized with sodium pentobarbitone (65 mg kg^{-1}). Evans blue (100 mg kg^{-1}) was

[1] Author for correspondence.

injected into the penile vein. The right knee was then injected with either 0.1 ml BK (0.01–10 nmol per knee) or sterile saline (control). The contralateral knee was left uninjected and provided an internal control. Anaesthesia was maintained for 2 h after which the animals were exsanguinated. A 2 h period was chosen we have previously found bradykinin-induced plasma extravasation to plateau between 1.5 and 3 h using this technique. The synovium was dissected from each joint, weighed and the Evans blue extracted by a modification of the dye extraction technique described by Lam & Ferrell (1989).

The synovium was mixed with 2 ml of extraction medium (acetone and a 1% aqueous solution of sodium sulphate; ratio 7:3) and then left at room temperature for 24 h. The concentration of Evans blue recovered was determined by comparing the absorbance of 620 nm with a standard curve prepared with known concentrations of Evans blue. As Evans blue binds to plasma proteins, which are largely retained within the vasculature, its increased presence within the synovium is indicative of plasma extravasation into the synovial tissues. Data are presented as mean difference in plasma extravasation (± s.e.) between the test knees and the uninjected contralateral controls.

In further studies the ability of the B_1 agonist, des-Arg^9-BK, to induce plasma extravasation was assessed. The effects of B_1 and B_2 antagonists on BK-induced plasma extravasation were also investigated.

Antigen-induced arthritis

Chronic monoarticular arthritis was induced in male Wistar rats by a modification of the method described by Brackertz *et al.* (1977). The animals were sensitized on two occasions (days 0 and 7) with 5 mg methylated bovine serum albumin (mBSA; Sigma). The mBSA (10 mg ml^{-1}) was dissolved in 0.9% saline and then emulsified in an equal volume of Freund's complete adjuvant (Sigma). The emulsion (0.5 ml) was then injected into multiple intradermal sites on the animals back. On day 21 the animals were challenged by the intra-articular injection of 100 µl mBSA (5 mg ml^{-1} in sterile saline) into the right knee. The progress of the arthritis was monitored by daily measurement of joint diameter. The response to BK and des-Arg^9-BK was assessed on day 5 post-challenge by the method described above.

Basal plasma extravasation

Antigen-induced arthritis is a model of a chronic monoarthritis (Brackertz *et al.*, 1977) and allowed the investigation of basal (i.e. unstimulated) plasma extravasation into the arthritic knee whilst using the contralateral joint as a control. Basal plasma extravasation into the arthritic knees was assessed on days 1, 3, 5 and 21 post-challenge. The arthritic rats were anaesthetized and injected with Evans blue. After 2 h the rats were exsanguinated, the synovium dissected and the Evans blue content determined. The difference between the Evans blue content of the two knees was a measure of inflammation-induced plasma extravasation into the arthritic joint.

In further experiments the effects of BK antagonists on basal plasma extravasation were investigated on days 1 and 5 post-challenge. Prior to the injection of Evans blue the arthritic rats were given an intravenous injection of the test antagonist and the experimental protocol was then as stated above. Control animals were treated with an equivalent volume of sterile saline.

Statistics

Data were expressed as means ± s.e.mean and analyzed for statistical significance by Student's t test. $P<0.05$ was considered significant. Correlation analysis was by the Pearson product-moment method.

Results

Basal plasma extravasation in arthritic knees

Chronic monoarticular arthritis was induced in the right knee. Callipers were used to measure knee diameter on days 1, 3, 5 and 21 post-challenge. The diameters of the arthritic knee were greatly increased on day 1 (mean increase 4.8 ± 0.24 mm, $n=5$, $P<0.01$) and then slowly decreased during the course of the experiment (Figure 1a). A significant increase in arthritic knee diameter compared to the control knees was observed at all four time points ($P<0.05$).

Basal plasma extravasation was assessed in different groups of animals on days 1, 3, 5 and 21 post-challenge. Basal plasma extravasation into the arthritic joints was found to dramatically increase on day 1 and then fall slowly during the course of the experiment (Figure 1b). The increase in basal plasma extravasation correlated with the increase in joint diameter (Correlation coefficient $r=0.82$). No change was noted in the control knees throughout the study.

BK-induced plasma extravasation into normal and arthritic knee joints

When injected into the synovial cavity of normal knees, BK induced plasma extravasation in a dose-dependent manner (Figure 2a). The threshold for this response was 0.01 nmol BK and the ED_{50} was approximately 0.1 nmol.

BK-induced plasma extravasation in arthritic knees 5 days after the mBSA challenge was then assessed (Figure 2a). As shown above, there was significant basal plasma extravasation into the arthritic knees compared to normal control joints. Plasma extravasation in the arthritic knees injected with lower doses of BK (0.01 and 0.03 nmol) was not significantly different from basal (unstimulated) plasma extravasation. At higher doses (0.1–10 nmol) the BK-induced plasma extravasation was significantly greater than the basal

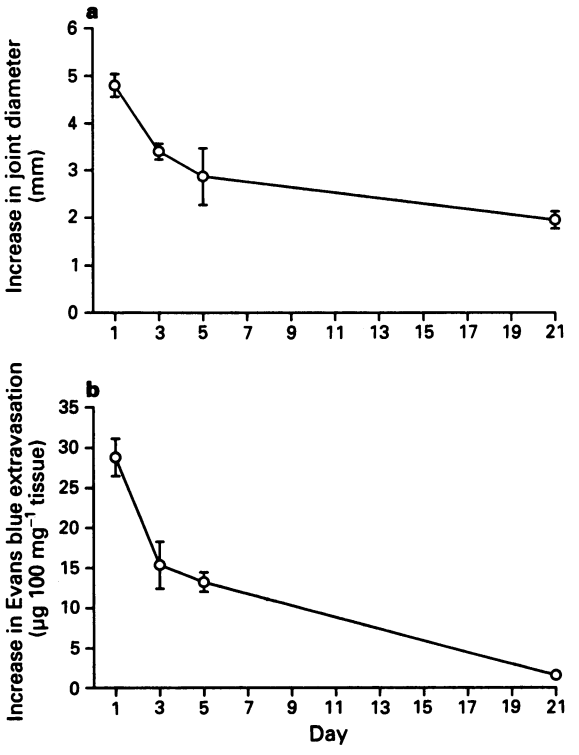


Figure 1 Increase in (a) joint diameter and (b) basal plasma extravasation following induction of antigen-induced arthritis. A significant increase was observed in both parameters at all time points ($P<0.05$). Points represent means ± s.e.mean ($n=4$ per group).

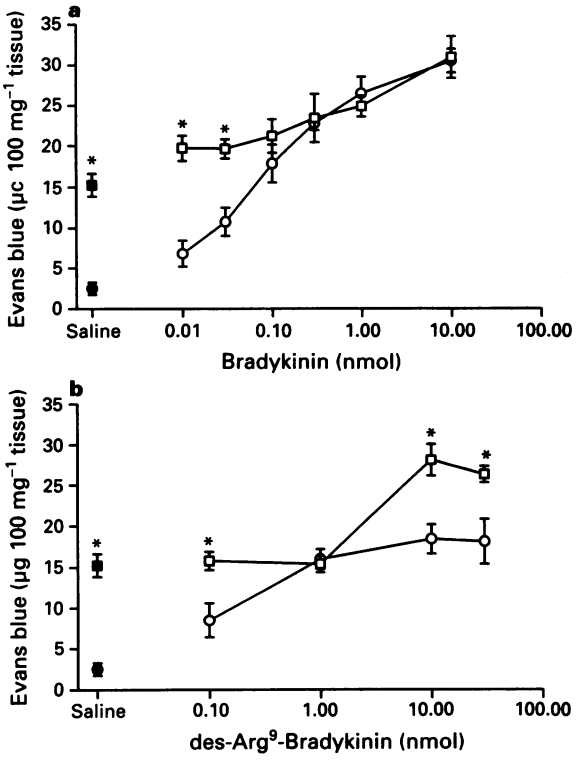


Figure 2 Dose-response curves for (a) bradykinin- and (b) des-Arg^9-Bradykinin-induced plasma extravasation into normal (○) and arthritic (□) rat knee joints. Values for unstimulated (basal) plasma extravasation in normal (●) and arthritic (■) joints are given. Points represent the means ± s.e.mean ($n = 4-6$ per group). *$P <$ 0.05 vs response in normal controls.

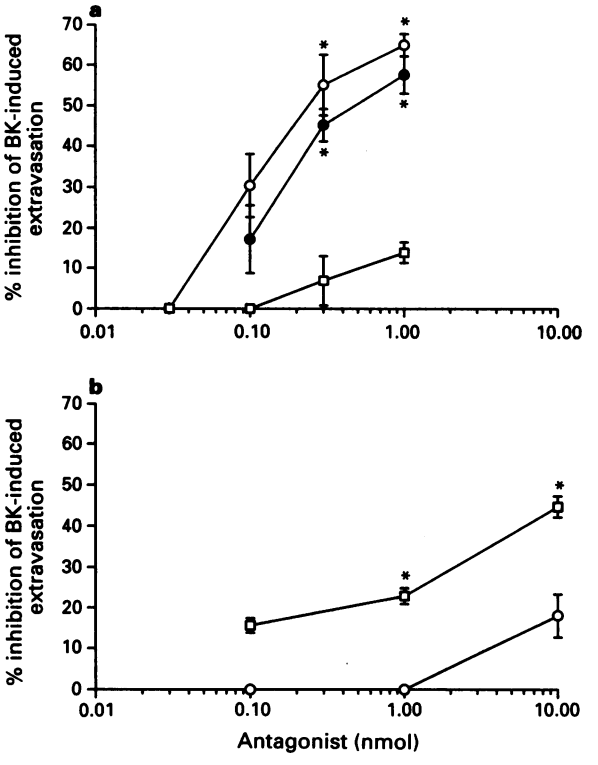


Figure 3 Inhibition of bradykinin (BK)-induced plasma extravasation by co-injection of Hoe 140 (○) and des-Arg^9,[Leu^8]-BK (□) with ED_{50} doses of BK in (a) normal and (b) arthritic knee joints. Hoe 140 was also co-injected with 1.0 nmol BK in normal joints (●). Points represent the means ± s.e.mean ($n = 3-6$ per group). *$P <$ 0.05 vs response to bradykinin alone.

extravasation. Plasma extravasation at the higher doses was similar in the arthritic and non-arthritic animals as was the maximum response (Figure 2a). The ED_{50} for plasma extravasation induced in arthritic knees by exogenous BK was 1.0 nmol and the threshold for this response was 0.1 nmol.

B_1-agonist induced plasma extravasation in normal and arthritic knees

The B_1 agonist, des-Arg^9-BK, dose-dependently induced plasma extravasation into the knee joint (Figure 2b); however, this response was less potent than that induced by BK (maximum responses 30.51 ± 1.49 BK vs 18.4 ± 1.76 des-Arg^9-BK; $P < 0.05$). In the arthritic joints, plasma extravasation in joints injected with lower dose of des-Arg^9-BK was not significantly different from the basal plasma extravasation. In contrast to BK, the responses to the higher doses of des-Arg^9-BK were greater in the arthritic joints than in the naïve controls with the maximum response in day 5 arthritic joints being 28.08 ± 1.96 μg Evans blue 100 mg^{-1} tissue compared to 18.4 ± 1.76 μg Evans blue 100 mg^{-1} tissue in the naïve controls ($P < 0.05$). The ED_{50} was raised from 0.1 nmol to 2.0 nmol (Figure 2b).

Effect of BK antagonists on BK-induced plasma extravasation in normal knees

The effects of the co-injection of BK antagonists with BK (0.1 nmol) were investigated. Hoe 140 (D-Arg[Hyp3,Thi5,D-Tic7,Oic8]-BK) inhibited BK-induced plasma extravasation over a dose range of 0.1–1.0 nmol; no inhibition was observed with 0.03 nmol (Figure 3a). BK-induced plasma extravasation was not significantly inhibited by any dose of des-Arg^9,[Leu^8]-BK (Figure 3a). This same antagonist at a dose of 1.0 nmol significantly inhibited plasma extravasation induced by the B_1 agonist des-Arg^9-BK (0.1 nmol) by 61% ($P < 0.02$), whereas Hoe 140 had no effect. With the lower doses of des-Arg^9,[Leu^8]-BK (0.03–0.3 nmol) a potentiation of the BK-induced plasma extravasation of between 5 and 13% was observed suggesting that des-Arg^9,[Leu^8]-BK may exhibit partial agonist activity.

Effect of BK antagonists on BK-induced plasma extravasation in arthritic rats

The effects of the co-injection of BK antagonists with BK (1.0 nmol) were investigated. In contrast to the antagonist effects observed in normal joints, Hoe 140 over the dose range 0.1–1.0 nmol failed to inhibit BK-induced plasma extravasation in the arthritic joints (Figure 3b). At a higher dose (10 nmol) Hoe 140 slightly inhibited the response. In normal animals, the ability of Hoe 140 to inhibit the bradykinin-induced plasma extravasation was not compromised by the higher dose of BK (1.0 nmol) used in the arthritic rats (Figure 3a). By comparison, des-Arg^9,[Leu^8]-BK, was a more potent inhibitor in the arthritic knees than in the normal joints and inhibited the response to a greater degree than Hoe 140 (Figure 3b).

Effect of BK antagonists on basal plasma extravasation in arthritic rats

On days 1 and 5 post-challenge either Hoe 140 or des-Arg^9,[Leu^8]-BK was injected (3–30 nmol kg^{-1}, i.v.) prior to the administration of Evans blue and the basal plasma extravasation was assessed over the next 2 h. There was no significant difference between basal plasma extravasation in the untreated arthritic animals and those injected with saline (data not shown). Basal plasma extravasation was significantly inhibited in a dose-dependent fashion by Hoe 140 on

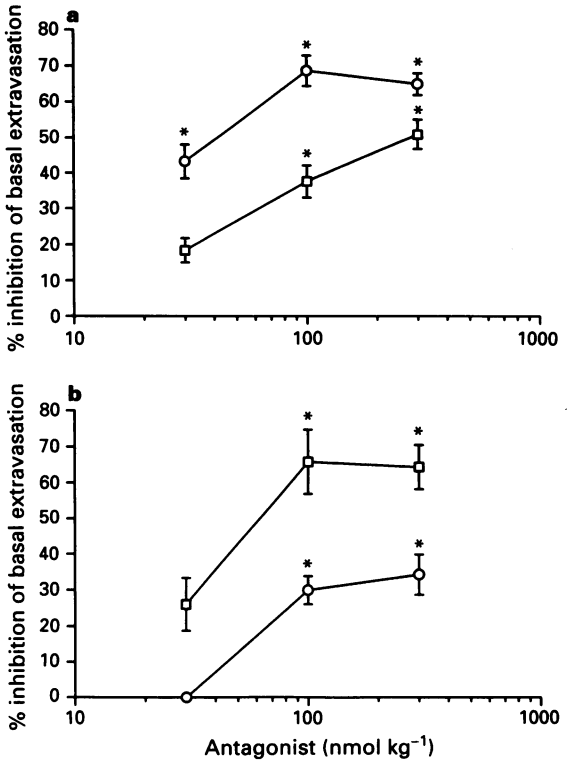


Figure 4 Effect of Hoe 140 (○) and des-Arg^9,[Leu^8]-BK (□) on basal plasma extravasation on (a) day 1 and (b) day 5 post-challenge. Points represent the means ± s.e.mean ($n = 3-6$ per group). *$P < 0.05$ vs saline treated controls.

day 1 (maximum inhibition 68.6 ± 4.2%, $n = 4$, $P < 0.002$; Figure 4a) and to a lesser extent on day 5 (maximum inhibition 34.3 ± 5.6%, $n = 6$, $P < 0.02$; Figure 4b). The results for des-Arg^9,[Leu^8]-BK showed a significant inhibition of basal plasma extravasation on day 1 (maximum 50.9 ± 4.2%, $n = 3$, $P < 0.005$; Figure 4a) and a greater inhibition on day 5 (65.9 ± 8.9%, $n = 5$, $P < 0.001$; Figure 4b).

Discussion

The present study shows that while BK and related peptides are potent mediators of intra-articular oedema in both normal and inflamed joints, the functional role of BK receptors may change with time. The relative inability of the B_1 agonist, des-Arg^9-BK, to induce plasma extravasation in the normal joint combined with the greater potency of Hoe 140 in the inhibition of BK-induced plasma extravasation suggests that, in normal joints, BK acts predominantly via B_2 receptors. These observations are in keeping with those made in other normal tissues (Steranka *et al.*, 1988; Dray *et al.*, 1992). The B_1 antagonist, des-Arg^9,[Leu^8]-BK, had only a small effect on the BK-induced plasma extravasation in normal joints. However, the observation that des-Arg^9-BK was able to induce some degree of extravasation and the ability of des-Arg^9,[Leu^8]-BK to inhibit this response, suggests that a small population of B_1 receptors may exist within the normal joint. The possibility that B_1 receptors might have been unmasked or expressed during the 2 h time-course of the experiment cannot be excluded.

Chronic joint inflammation was induced with the mBSA model of arthritis as it mirrors some of the features of chronic human arthritis, particularly rheumatoid arthritis (Brackertz *et al.*, 1977). Following prior sensitization with mBSA, a single intra-articular injection of mBSA causes an inflammatory response with a initial vascular phase (plasma extravasation and hyperaemia) followed by cellular infiltration and resultant tissue breakdown. The Evans blue extraction technique allowed for estimation of both stimulated and underlying unstimulated, basal, extravasation. The contralateral joint was not used for the saline control as recent studies have raised the possibility of contralateral sensitization following an inflammatory insult (Cruwys *et al.*, 1991; Perkins & Kelly, 1993).

In chronically inflamed joints the response to intra-articular injections of BK was unaltered although at lower doses the response appeared to be masked by increased basal plasma extravasation. In contrast, plasma extravasation in response to higher doses of des-Arg^9-BK was enhanced. This observation, together with the enhanced inhibition of BK-induced plasma extravasation by the B_1 antagonist, des-Arg^9,[Leu^8]-BK, suggested a functional role for B_1 receptors in persistant arthritis.

Further evidence of a role for B_1 receptors in chronic joint disease was evident from the basal extravasation studies. Comparison of the relative abilities of Hoe 140 and des-Arg^9,[Leu^8]-BK to inhibit basal plasma extravasation on days 1 and 5 of joint inflammation showed that whereas Hoe 140 became less potent, des-Arg^9,[Leu^8]-BK became more potent as the model progressed. Whilst it is possible that this inhibition might have been due to the antagonists having vascular effects, Wirth *et al.* (1991) demonstrated that at similar doses to those used in this study, Hoe 140 had no effect on blood pressure or heart rate.

Our results relating to changes of receptor expression in arthritis are in keeping with observations from other inflamed tissues. These show that acute oedema appears to be mediated via B_2 receptors (Burch & De Haas, 1990; Neppl *et al.*, 1991) but that the B_2 receptor antagonists, including Hoe 140, become less effective in longer duration models such as carrageenin-induced paw oedema (Beresford & Birch, 1992). Increased expression of B_1 receptors has recently been reported in aortic smooth muscle following induction of chronic inflammation (Farmer *et al.*, 1991) and B_1 receptors may be involved in the hyperalgesia accompanying inflammatory conditions (Perkins *et al.*, 1993).

BK is metabolized to des-Arg^9-BK and thereafter to a variety of other metabolites by kininases which we have recently demonstrated in inflamed but not normal joint tissues (Map *et al.*, 1992). The conversion of BK to des-Arg^9-BK has been shown to be much faster in rheumatoid arthritis than in osteoarthritis or normal individuals (Sheikh & Kaplan 1987) and levels of both BK and des-Arg^9-BK are increased in inflammatory conditions (Steranka *et al.*, 1987; Hargreaves *et al.*, 1988). In view of the probable changes to BK receptors in chronic arthritis it follows that formation of specific kinin metabolites, including des-Arg^9-BK, could result in an altered inflammatory response in these disorders (Bhoola *et al.*, 1992).

In vitro studies have demonstrated a role for inflammatory mediators known to be present in inflamed joints, particularly the cytokines interleukin-1 (IL-1) and IL-2, in the induction of B_1 receptors (De Blois *et al.*, 1988; 1989). Similarly, agents which stimulate macrophages have been shown to increase responses to des-Arg^9-BK (De Blois *et al.*, 1989). It follows that the components required for the expression and activation of B_1 receptors are present within an inflamed joint. des-Arg^9-BK is a potent stimulator of IL-1 release from macrophages (Burch *et al.*, 1989; Tiffany & Burch, 1989) and the potential exists for arthritis to be exacerbated by a positive feedback loop whereby des-Arg^9-BK stimulates the release of IL-1 from macrophages and the IL-1 in turn acts to stimulate the induction of B_1 receptors.

The clinical use of BK receptor antagonists has been proposed for the treatment of inflammatory diseases including rheumatoid arthritis (Sharma, 1992). The data presented here support this proposal and indicate that selective B_1 receptor antagonists may reduce joint swelling in inflammatory arthritis. Perkins *et al.* (1993) demonstrated that B_1 receptors are involved in the hyperalgesia which accompanies inflamma-

tion. By implication, B_1 receptors on sensory nerves may also be involved in the release of vasoactive peptides as a result of the axon reflex response. These peptides serve to modify many aspects of the inflammatory cascade (Cruwys *et al.*, 1992) and inhibition of this process may well serve to modify the outcome of chronic disease (Hakanson *et al.*, 1987; Kidd *et al.*, 1990).

In conclusion, the present study shows that BK contributes significantly to the formation and maintenance of plasma extravasation in arthritis. Whilst the majority of responses to BK in normal and acutely inflamed joints are mediated via B_2 receptors, an increasingly dominant role appears to be played by B_1 receptors in the chronic and potentially more deleterious phases of the disease. This may reflect an important role for the BK metabolite, des-Arg^9-BK, in the maintenance of arthritis and suggests that selective B_1 receptor antagonists may be of therapeutic benefit in chronic disease.

References

BERESFORD, I.J.M. & BIRCH, P.J. (1992). Antinociceptive activity of the bradykinin antagonist HOE 140 in rat and mouse. *Br. J. Pharmacol.*, **105**, 135P.

BHOOLA, K.D., ELSON, C.J. & DIEPPE, P.A. (1992a). Kinins – key mediators in inflammatory arthritis? *Br. J. Rheum.*, **31**, 509–518.

BHOOLA, K.D., FIGUEROA, C.D. & WORTHY, K. (1992b). Regulation of kinins: kallikreins, kininogens and kinase. *Pharmacol. Rev.*, **44**, 1–80.

BRACKERTZ, D., MITCHELL, G.F. & MACKAY, I.R. (1977). Antigen-induced arthritis in mice. I. Induction of arthritis in various strains of mice. *Arth. Rheum.*, **20**, 841–850.

BURCH, R.M., CONNOR, J.R. & TIFFANY, C.W. (1989). The kallikrein-kininogen-kinin system in chronic inflammation. *Agents Actions*, **27**, 258–260.

BURCH, R.M. & DE HAAS, C. (1990). A bradykinin antagonist inhibits carrrageenin edema in rats. *Arch. Pharmacol.*, **342**, 189–193.

CRUWYS, S.C., KIDD, B.L., MAPP, P.I., WALSH, D.A. & BLAKE, D.R. (1991). Arthritis in one knee enhances the vascular response to bradykinin in the opposite knee. *Br. J. Rheumatol.*, **30**, 284.

CRUWYS, S.C., KIDD, B.L., MAPP, P.I., WALSH, D.A. & BLAKE, D.R. (1992). The effects of calcitonin gene-related peptide on formation of intra-articular oedema by inflammatory mediators. *Br. J. Pharmacol.*, **107**, 116–119.

DE BLOIS, D., BOUTHILLIER J. & MARCEAU, F. (1988). Effect of glucocorticoids, monoamines and growth factors on the spontaneously developing responses of the rabbit isolated aorta to des-Arg^9-bradykinin. *Br. J. Pharmacol.*, **93**, 969–977.

DE BLOIS, D., BOUTHILLIER, J. & MARCEAU F. (1989). Pharmacological modulation of the up-regulated responses to des-Arg^9-bradykinin in vivo and in vitro. *Immunopharmacol.*, **17**, 187–198.

DRAY, A., PATEL, I.A., PERKINS, M.N. & RUEFF, A. (1992). Bradykinin-induced activation of nociceptors: receptor and mechanistic studies on the neonatal rat spinal cord-tail preparation *in vitro*. *Br. J. Pharmacol.*, **107**, 1129–1134.

DRAY, A. & PERKINS, M. (1993). Bradykinin and inflammatory pain. *Trends Neurosci.*, **16**, 99–104.

FARMER, S.G., MCMILLAN, B.A., MEEKER, S.N. & BURCH, R.M. (1991). Induction of vascular smooth muscle bradykinin B_1 receptors in vivo during antigen arthritis. *Agents Actions*, **34**, 191–193.

HAKANSON, R., BEDING, B., EKMAN, R., HEILIG, M., WAHLESTEDT, C. & SUNDLER, F. (1987). Multiple tachykinin pools in sensory nerve fibres in the rabbit iris. *Neuroscience*, **21**, 943–950.

HARGREAVES, K.M., TROULLOS, E.S., DIONNE, R.A., SCHMIDT, E.A., SCHAFER, S.C. & JORIS, J.L. (1988). Bradykinin is increased during acute and chronic inflammation: therapeutic implications. *Clin. Pharmacol. Ther.*, **44**, 613–621.

KIDD, B.L., MAPP, P.I., BLAKE, D.R., GIBSON, S.J. & POLAK, J.M. (1990). Neurogenic influences in arthritis. *Ann. Rheum. Dis.*, **49**, 649–652.

LAM, F.Y. & FERRELL, W.R. (1989). Inhibition of carrageenin induced inflammation in the rat knee joint by substance P antagonist. *Ann. Rheum. Dis.*, **48**, 928–932.

MAPP, P.I., WALSH, D.A., CRUWYS, S.C., KIDD, B.L., POLAK, J.M. & BLAKE, D.R. (1992). Localisation of neutral endopeptidase to the human synovium. *J. Rheumatol.*, **19**, 1838–1844.

NEPPL, N., NEUHOF, H., AFFLERBACH, F., LLACH, J., NEPPL, P. & BREGHOFER, A. (1991). Bradykinin-induced oedema formation proceeds from B_2 receptor stimulation and is potentiated by concomitantly released prostaglandins. *Acta Physiol. Scand.*, **142**, 141–147.

PERKINS, M.N., CAMPBELL, E. & DRAY, A. (1993). Antinociceptive activity of the bradykinin B_1 and B_2 receptor antagonists, des-Arg^9,[Leu^8]-BK and HOE 140, in two models of persistent hyperalgesia in the rat. *Pain*, **53**, 191–197.

PERKINS, M.N. & KELLY, D. (1993). Induction of bradykinin B_1 receptors *in vivo* in a model of ultra-violet irradiation-induced thermal hyperalgesia in the rat. *Br. J. Pharmacol.*, **110**, 1441–1444.

PROUD, D. & KAPLAN, A.P. (1988). Kinin formation: Mechanisms and role in inflammatory disorders. *Ann. Rev. Immunol.*, **6**, 49–83.

REGOLI, D. & BARABE, J. (1980). Pharmacology of bradykinin and related kinins. *Pharmacol. Rev.*, **32**, 1–46.

SHARMA, J.N. (1992). Involvement of the kinin-forming system in the physiopatholog of rheumatoid inflammation. *Agents Actions*, **38**, 343–361.

SHEIKH, I.A. & KAPLAN, A.P. (1987). Assessment of kininases in rheumatic disease and the effects of therapeutic agents. *Arthritis Rheum.*, **30**, 138–145.

STERANKA, L.R., DE HAAS, C.J., VAVREK, R.J., STEWART, J.M., ENNA, S.J. & SNYDER, S.H. (1987). Antinociceptive effects of bradykinin antagonists. *Eur. J. Pharmacol.*, **136**, 261–262.

STERANKA, L.R., MANNING, D.C., DE HAAS, C.J., FERKANY, J.W., BOROSKY, S.A., CONNOR, J.R., VAVREK, R.J., STEWART, J.M. & SNYDER, S.H. (1988). Bradykinin as a pain mediator: Receptors are localised to sensory neurones, and antagonists have analgesic actions. *Proc. Natl. Acad. Sci. U.S.A.*, **85**, 3245–3249.

TIFFANY, C.W. & BURCH, R.M. (1989). Bradykinin stimulates tumour necrosis factor and interleukin 1 release from macrophages. *FEBS Lett.*, **247**, 189–192.

WIRTH, K., HOCK, F.J., ALBUS, U., LINZ, W., ALPERMANN, H.G., ANAGNOSTOPOULOS, H., HENKE, St., BREIPHOL, G., KONIG, W., KNOLLE, J. & SCHOLKENS, B.A. (1991). Hoe 140 a new potent and long acting bradykinin-antagonist: *in vivo* studies. *Br. J. Pharmacol.*, **102**, 774–777.

(Received January 21, 1994
Revised May 16, 1994
Accepted July 18, 1994)

Br. J. Pharmacol. (1994), **113**, 945–953 © Macmillan Press Ltd, 1994

Inhibition by gomisin C (a lignan from *Schizandra chinensis*) of the respiratory burst of rat neutrophils

[1]Jih P. Wang, Shue L. Raung, *Mei F. Hsu & †Chien C. Chen

Department of Medical Research, Taichung Veterans General Hospital, Taichung, Taiwan; *Department of Biochemistry, China Medical College, Taichung, Taiwan and †National Research Institute of Chinese Medicine, Taipei, Taiwan

1 The possible mechanisms of action of the inhibitory effect of gomisin C on the respiratory burst of rat neutrophils *in vitro* was investigated.

2 The peptide formyl-Met-Leu-Phe (FMLP) induced superoxide anion ($O_2^{\cdot-}$) formation and O_2 consumption, which was inhibited by gomisin C in a concentration-dependent manner (IC_{50} 21.5 ± 4.2 μg ml^{-1} for $O_2^{\cdot-}$ formation). Gomisin C also suppressed $O_2^{\cdot-}$ formation and O_2 consumption at low concentrations of phorbol myristate acetate (PMA) with an IC_{50} value of 26.9 ± 2.1 μg ml^{-1} for $O_2^{\cdot-}$ formation. However, gomisin C did not affect the responses induced by a high concentration of PMA.

3 Gomisin C had no effect on $O_2^{\cdot-}$ generation and uric acid formation in the xanthine-xanthine oxidase system, and failed to alter $O_2^{\cdot-}$ generation during dihydroxyfumaric acid (DHF) autoxidation, indicating that it does not scavenge superoxide.

4 Like trifluoperazine (TFP), gomisin C attenuated the activity of PMA-activated neutrophil particulate NADPH oxidase in a concentration-dependent manner.

5 Gomisin C reduced the elevations of cytosolic free Ca^{2+} in neutrophils stimulated by FMLP in the presence or absence of EDTA. Cyclopiazonic acid (CPA) induced the release of Ca^{2+} from intracellular stores and this was also reduced by gomisin C. However, the Ca^{2+} influx pathway activated by CPA was not affected by gomisin C.

6 The cellular cyclic AMP level was markedly increased by forskolin, but not by gomisin C. Moreover, the inositol phosphate levels in FMLP-activated neutrophils were not affected by gomisin C.

7 These results show that the inhibitory action of gomisin C on the respiratory burst is not mediated by changes in cellular cyclic AMP or in inositol phosphates, or by scavenging $O_2^{\cdot-}$ released from neutrophils, but may be mediated partly by the suppression of NADPH oxidase and partly by the decrease of cytosolic Ca^{2+} released from an agonist-sensitive intracellular store.

Keywords: Gomisin C; neutrophil; superoxide anion; NADPH oxidase; xanthine-xanthine oxidase; cyclic AMP; inositol phosphates; intracellular calcium concentration

Introduction

Wu-Wei-Zi, the dry fruit of *Schizandra chinensis* BAILL (*Schisandraceae*), has for centuries been used in Chinese medicine as an antitussive and as a tonic for the treatment of cough, bronchitis and asthma. Chemical investigations of Wu-Wei-Zi have led to the isolation of several constituents: sesquiterpenoids (chamigrene, sesquicarene, etc.), and dibenzocyclooctadiene lignans (schizandrin, deoxyschizandrin, gomisins, etc.) (Ohta & Hirose, 1968; Ikeya *et al.*, 1979; Nakajima *et al.*, 1983). Pharmacological studies have revealed that gomisin A possesses choleretic action in CCl_4-treated animals and prevents the development of acute hepatic failure (Maeda *et al.*, 1985; Mizoguchi *et al.*, 1991), and gomisin J relaxes trachea, ileum and mesenteric artery probably by behaving as a calcium antagonist (Suekawa *et al.*, 1987). Recently, gomisin A and J were found to inhibit phorbol myristate acetate (PMA)-induced inflammation in mouse skin (Yasukawa *et al.*, 1992).

The neutrophil is an important inflammatory cell. The primary physiological function of neutrophils is to protect the host from infections by effective killing and digestion of pathogens. For this purpose, they are equipped for chemotaxis, phagocytosis, degranulation and generation of toxic oxygen metabolites (Baggiolini & Dewald, 1985; Borregaard, 1988). Neutrophils can be triggered by a variety of inflammatory stimuli to produce highly reactive oxygen species, including superoxide anion, hydrogen peroxide, hydroxyl radical and hypochlorous acid (Babior, 1978; Tauber & Babior, 1985), which have potent microbicidal and inflammatory effects. However, if these processes are uncontrolled, neutrophils may deleteriously affect adjacent cells or structural matrix components of tissue by extensive release of toxic oxygen metabolites. This is probably involved in the pathogenesis of many diseases including emphysema, glomerulonephritis, rheumatoid arthritis and tissue damage in ischaemia-reperfusion states (Johnson *et al.*, 1981; Lefer *et al.*, 1981; Halliwell & Gutteridge, 1990; Sibille & Reynolds, 1990).

In this study, we investigated the inhibitory effect of gomisin C (Figure 1), a lignan isolated from the fruits of *Schizandra chinensis*, on the respiratory burst in rat peripheral neutrophils and assessed the underlying mechanism. The present data provide evidence that the attenuation of the respiratory burst by gomisin C is mediated partly by the suppression of NADPH oxidase and partly by the inhibition of cytosolic Ca^{2+} release from an intracellular store.

Methods

Isolation of neutrophils

Rat peripheral neutrophils were isolated by a modification of the procedure described by Böyum (1968). EDTA-mixed fresh blood was obtained from the abdominal aorta of pentobarbitone (60 mg kg^{-1}, i.p.) anaesthetized rats (Sprague Dawley, 300–350 g). Neutrophils were separated from other blood cells by dextran sedimentation and centrifugation on a Ficoll-hypaque density gradient. Erythrocytes in the pellets

[1] Author for correspondence.

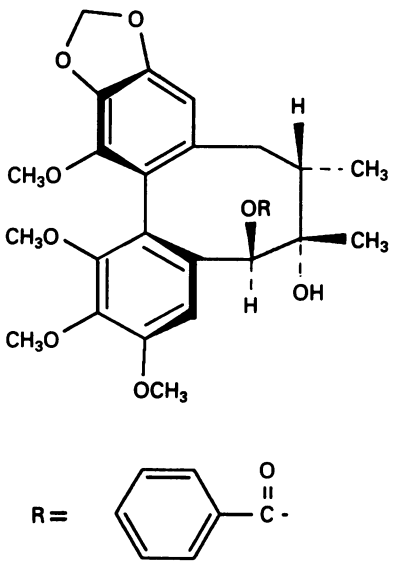


Figure 1 Chemical structure of gomisin C.

were lysed by suspending the cells in 0.05% saline for 15 s followed by washing with 1.75% saline containing 0.25% bovine serum albumin (BSA). Cells were resuspended in Hanks' balanced salt solution containing 4 mM $NaHCO_3$ and 10 mM N-[2-hydroxyethyl]piperazine-N'-[2-ethanesulphonic acid] (HEPES), pH 7.4 (HBSS) to a final concentration of 2×10^6 cells ml^{-1}. For measurement of oxygen consumption, cells were resuspended in HBSS at 1×10^7 cells ml^{-1}. The cell preparations consisted of 90–95% neutrophils (viability approximately 95% by trypan blue exclusion).

Measurement of superoxide anion production

Superoxide anion ($O_2^{\cdot-}$) production was determined by a continuous assay in which superoxide dismutase (SOD)-inhibitable ferricytochrome c reduction was followed with time as previously described (Cohen & Chovaniec, 1978) with modifications. Assay mixtures contained 0.7 ml cell suspension and 0.5 mg ml^{-1} of ferricytochrome c in a final volume of 1.5 ml. The reference cuvette also received 6.6 μg ml^{-1} of SOD. Both reference and sample cuvettes were placed in the thermostatted and stirred cell compartments of a double beam spectrophotometer (Hitachi, U-3210) and the absorbance at 550 nm was followed for 3 min. The reactions were then started by adding activating agent. The amount of $O_2^{\cdot-}$ in the reaction mixture was calculated from the formula: $O_2^{\cdot-}$ (nmol) = 71.55 × absorbance (Markert *et al.*, 1984).

Measurement of oxygen consumption

O_2 consumption by neutrophils was measured with a Clark-type oxygen electrode using a YSI oxygen monitor (Model 5300). Assays were conducted at 37°C with 6×10^6 cells which were preincubated for 5 min with stirring to permit temperature equilibration. Reaction was started by injection of the activating agent into the chamber so that the final total volume was 0.6 ml. O_2 consumption was determined by a continuous assay as described by Ingraham *et al.* (1982).

Superoxide anion production in xanthine-xanthine oxidase system and in dihydroxyfumaric acid autoxidation

The SOD-inhibitable ferricytochrome c reduction was determined in the xanthine-xanthine oxidase system. Assay mixtures contained 3.3 mu xanthine oxidase, 0.5 mg ml^{-1} of ferricytochrome c in a final volume of 1.5 ml. The reference cuvette also received SOD, 6.6 μg ml^{-1}. After addition of 0.15 mM xanthine, the ferricytochrome c reduction was continuously recorded at 550 nm, and $O_2^{\cdot-}$ production was calculated as above.

In the experiments to assess the xanthine oxidase activity, ferricytochrome c was omitted from the reaction mixture. The amount of uric acid formation was monitored continuously at 292 nm and calculated by using absorbance-uric acid standard curve.

$O_2^{\cdot-}$ production during the autoxidation of dihydroxyfumaric acid (DHF) was determined as previously described (Goldberg & Stern, 1977). Briefly, the reaction mixture contained 0.891 mM DHF and 0.274 mM nitroblue tetrazolium (NBT) in 10 mM HEPES buffer pH 7.4. Reduction of NBT during the autoxidation of DHF was continuously monitored at 560 nm.

Determination of NADPH oxidase activity

Particulate NADPH oxidase was isolated as described (Markert *et al.*, 1984) with certain modifications. Cells (5×10^7 cells ml^{-1}) in HBSS containing 1 mM NaN_3 were preincubated at 37°C for 20 min in the presence of 2 μM PMA. A 5 fold excess volume of ice-cold HBSS was added and the tubes were then immediately placed in a melting ice bath. After centrifugation at 500 *g* for 8 min, the pellets were resuspended in cold 0.34 M sucrose buffered with 10 mM tris[hydroxymethyl]aminomethane (Tris), pH 7.0 to 2.5×10^7 cells ml^{-1}, and sonicated in an ice-water bath for 30 s in the presence of 2 mM phenylmethylsulphonyl fluoride (PMSF). Sonicates were centrifuged at 300 *g* for 8 min, supernatants were then centrifuged at 50,000 *g* for 45 min at 4°C. Final pellets were resuspended in 0.34 M sucrose to yield a protein concentration of 2–3 mg ml^{-1} and were stored at −70°C until time of assay. NADPH oxidase activity was measured spectrophotometrically at 28°C by detecting the consumption of β-nicotinamide adenine dinucleotide reduced form (NADPH). The assay mixture contained 0.04% sodium deoxycholate, 12.5 μM flavin adenine dinucleotide (FAD), 0.2 ml of particulate protein solution and 62.5 μM NADPH in a final volume of 1.6 ml. The oxidation of NADPH to NADP was continuously monitored at 340 mm. The amount of NADP production was calculated by reference to a NADP standard curve.

Measurement of cytosolic Ca^{2+} concentration

Neutrophils (1×10^7 cells ml^{-1}) were suspended in HEPES buffer of the following composition: 145 mM NaCl, 5 mM KCl, 10 mM HEPES, pH 7.4, and loaded with 5 μM fura 2-AM at 37°C for 15 min. The cells were then diluted 5 fold with HEPES buffer and incubated at 37°C for an additional 15 min. Cell suspensions were then centrifuged at 200 *g* for 10 min at 4°C, and the pellets resuspended in HEPES buffer with 1 mM $CaCl_2$, 1 mM $MgCl_2$, 5.56 mM dextrose and 1 mg ml^{-1} BSA to a final concentration of 5×10^6 cells ml^{-1}. Cell suspensions was placed in a double wavelength fluorescence spectrophotometer (PTI, Deltascan 4000) equipped with a thermostatted cuvette holder and stirrer. The fluorescence was monitored at 510 nm with excitation wavelengths of 340 and 380 nm in the ratio mode. Calibration of the excitation ratio in terms of Ca^{2+} concentration was performed by using fura 2-Ca^{2+} standards according to a previously described method (Grynkiewicz *et al.*, 1985).

Entry of Mn^{2+} into cells was measured by the fura 2 fluorescence quenching technique (Demaurex *et al.*, 1992). Briefly, fluorescence monitored in fura 2-loaded cells in the Ca^{2+}-containing medium at excitation 360 nm and emission 510 nm. Mn^{2+} (0.5 mM) was added following the preincubation of the leukocytes with 3 μM cyclopiazonic acid (CPA) for 1 min. Diethylenetriamine pentaacetic acid (DTPA) 2 mM was added at the end of an experiment, which indicated that less than 5% of the total fluorescence quenched by Mn^{2+} was due to leakage of fura 2.

Determination of inositol phosphates level

Intracellular levels of inositol phosphates were measured as described (Downes & Michell, 1981) with modification. Cells (3×10^7 cells ml^{-1}) in HBSS with 0.1 mM $CaCl_2$ were incubated with 100 μCi ml^{-1} of *myo*-[^{3}H]-inositol at 37°C for 2 h. Cells were then washed twice with HBSS containing 10 mM LiCl, and divided into 0.2 ml aliquots on ice. After preincubation at 37°C for 3 min, cells were exposed to activating agent for 10 s, and the reaction was then stopped by the addition of 1.8 ml of $CHCl_3$:CH_3OH (1:1, v/v) mixture and 0.5 ml of 2.4 M HCl. The aqueous phase was removed and neutralized by 0.4 M NaOH, and then applied to column containing 0.6 ml of AG 1-X8 resin (formate) which had been equilibrated with 50 mM ammonium formate. Inositol, inositol-1-phosphate (IP), inositol bisphosphate (IP_2) and inositol trisphosphate (IP_3) were eluted sequentially using 2 ml of 0.05, 0.2, 0.4 and 1.0 M ammonium formate in 0.1 M formic acid, respectively, as eluents. Each of the column fractions were collected and counted in a liquid scintillation counter.

Determination of cyclic AMP levels

Adenosine 3':5'-cyclic monophosphate (cyclic AMP) content was determined as described by Verghese *et al.* (1985). Cells (2×10^6 cells ml^{-1}) in HBSS were preincubated with test drugs for 9.5 min at 30°C. Thirty seconds after addition of activating agent, the reaction mixture was immediately added to 1.0 ml of 0.05 M acetate buffer, pH 6.2 containing 0.05 mM 3-isobutyl-1-methylxanthine (IBMX). After boiling for 5 min, the suspension was kept on ice and sonicated for 45 s, followed by centrifugation at 8,000 *g* at 4°C for 5 min. The supernatants were acetylated by the addition of 0.025 volume of triethylamine:acetic anhydride (2:1,v/v). The cyclic AMP content of the aliquot was assayed by the enzyme immunoassay methods (Amersham International).

Drugs

Gomisin C (M_r 536) was isolated and purified as previously described by Ikeya *et al.* (1979). All chemicals were purchased from Sigma Chemical Co., St. Louis, U.S.A. except for the following: dextran T500 (Pharmacia LKB, Taipei, R.O.C.). LiCl, $LaCl_3$ and $MnCl_2$ (Merck Taiwan Ltd.); Hank's balanced salt solution (Gibco Lab., Grand Island, U.S.A.); xanthine oxidase (Boehringer Mannheim, Germany); fura 2-AM (Molecular Probes Inc., Eugene, U.S.A.); cyclic AMP EIA kit and *myo*-[^{3}H]-inositol (Amersham International plc., Buckinghamshire).

Statistical analysis

Data are given as mean ± s.e.mean. Statistical evaluation of the data was performed by one-way analysis of variance to determine any significant variance (ANOVA) among groups. If a significant variance was found, a Newman-Keuls test was used to test for significant differences between individual groups. A P value less than 0.05 was considered significant for all tests. Analysis of the regression line test was used to calculate IC_{50} values.

Results

Effect of gomisin C on superoxide anion release from neutrophils

When FMLP (0.1 μM) or PMA (3 nM) was added to rat neutrophil suspensions, O_2^- production was observed by detecting the reduction of ferricytochrome c in the reaction mixture. Like SOD (0.3–1 μg ml^{-1}) and TFP (3–10 μM), gomisin C (3–30 μg ml^{-1}) evoked a concentration-dependent inhibition of FMLP-induced responses with an IC_{50} value of 21.5 ± 4.2 μg ml^{-1} (57.6–22.6 μM, 95% confidence interval). Statistically significant inhibition was observed with gomisin C 30 μg ml^{-1} ($P<0.05$) (Figure 2a). NaF-induced O_2^- formation was also reduced by gomisin C with an apparent IC_{50} value of 19.7 ± 2.4 μg ml^{-1} (51.2–22.2 μM, 95% confidence interval). However, unlike SOD and TFP, gomisin C at concentrations up to 30 μg ml^{-1} did not significantly affect the PMA (3 nM)-induced response (Figure 2b).

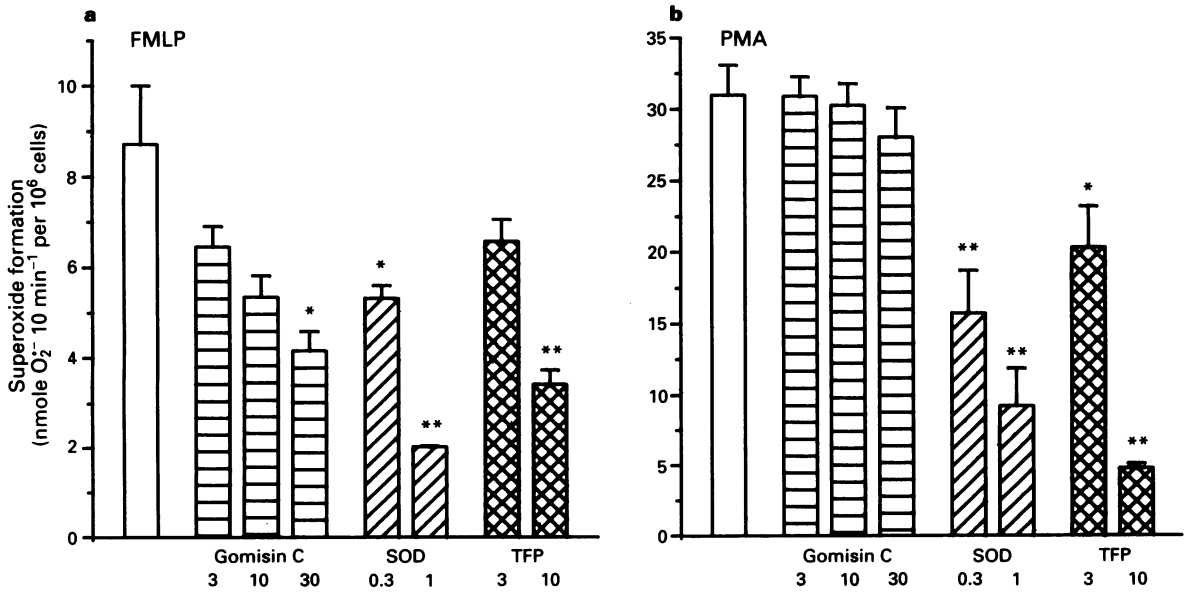


Figure 2 Effect of gomisin C, superoxide dismutase (SOD) and trifluoperazine (TFP) on (a) formayl-Met-Leu-Phe (FMLP)- and (b) phorbol myristate acetate (PMA)-induced O_2^- release from rat neutrophils. Control (open column); gomisin C 3–30 μg ml^{-1} (horizontally hatched column); SOD 0.3–1 μg ml^{-1} (hatched column); TFP 3–10 μM (cross hatched column); were incubated with cell suspension at 37°C for 3 min before addition of 0.1 μM FMLP with 5 μg ml^{-1} of dihydrocytochalasin B, or 3 nM PMA. Results are expressed as the mean O_2^- release ± s.e.mean of 4–5 experiments. *$P<0.05$, **$P<0.01$ compared to the corresponding control values.

Table 1 Effect of gomisin C, superoxide dismutase (SOD) and trifluoperazine (TFP) on formyl-Met-Leu-Phe (FMLP)- and phorbol myristate acetate (PMA)-induced O_2 consumption in rat neutrophils

		FMLP (0.3 μM)	*PMA* (10 nM)
		(nmol O_2 consumed in 5 min per 6×10^6 cells)	
Control		27.4 ± 2.9	55.7 ± 2.0
Gomisin C	3 μg ml^{-1}	27.9 ± 4.4	54.8 ± 5.7
	10 μg ml^{-1}	21.8 ± 2.5	49.8 ± 4.1
	30 μg ml^{-1}	17.9 ± 2.6*	53.4 ± 3.6
SOD	3 μg ml^{-1}	29.1 ± 2.3	48.3 ± 1.7
	10 μg ml^{-1}	27.5 ± 4.0	50.9 ± 3.4
TFP	3 μM	23.7 ± 1.5	50.8 ± 5.1
	10 μM	17.4 ± 0.8*	40.6 ± 3.1**
	30 μM	10.4 ± 1.7**	24.4 ± 3.7**

Values are expressed as mean O_2 consumed ± s.e.mean of 4–5 separate experiments.
*$P<0.05$, **$P<0.01$ compared to the control values.

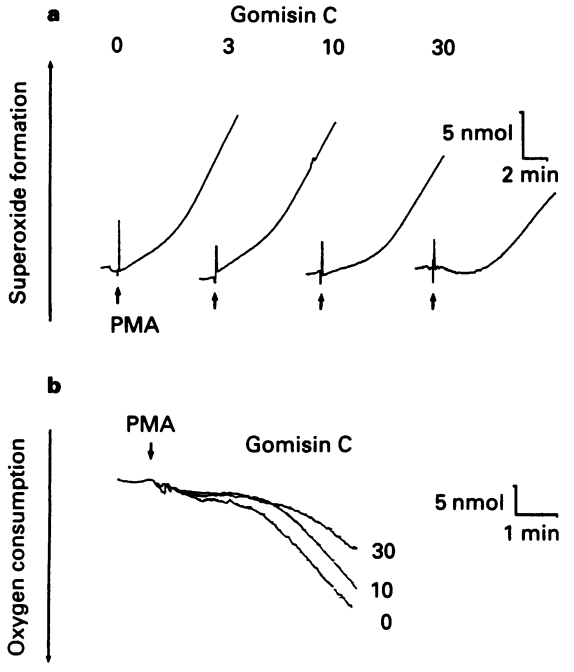


Figure 3 Effect of gomisin C on O_2^- release (a) and O_2 consumption (b) in neutrophils challenged by phorbol myristate acetate (PMA) 1 nM and 3 nM, respectively. Gomisin C (3–30 μg ml^{-1}) was incubated with cell suspension at 37°C for 3 min before addition of PMA.

Table 2 Effect of gomisin C, superoxide dismutase (SOD) and allopurinol on O_2^- generation and uric acid formation in xanthine (0.15 mM)-xanthine oxidase (3.3 mu) system

			O_2^- (nmol in 10 min)	*Uric acid* (nmol in 10 min)
A	Control		5.88 ± 0.30	14.1 ± 0.6
	Gomisin C	3 μg ml^{-1}	5.71 ± 0.39	14.9 ± 0.1
		10 μg ml^{-1}	5.88 ± 0.45	14.8 ± 0.7
		30 μg ml^{-1}	6.34 ± 0.23	13.9 ± 0.5
B	Control		8.14 ± 0.32	11.6 ± 0.3
	SOD	1 μg ml^{-1}	3.91 ± 0.38**	14.3 ± 0.8
		10 μg ml^{-1}	1.65 ± 0.05**	14.8 ± 1.1
	Allopurinol	0.3 μg ml^{-1}	4.74 ± 0.21**	8.6 ± 0.6**
		3 μg ml^{-1}	0.64 ± 0.24**	1.2 ± 0.3**

Values are expresed as mean ± s.e.mean of 4–5 separate experiments.
**$P<0.01$ compared to corresponding control values.

Effect of gomisin C on oxygen consumption of neutrophils

The results displayed in Table 1 demonstrate that gomisin C suppressed the FMLP (0.3 μM)-induced O_2 consumption, with a significant effect observed at 30 μg ml^{-1} ($P<0.05$) but did not reduce the PMA (10 nM)-induced response. This profile closely resembles that previously shown in Figure 2. TFP (3–30 μM) produced a concentration-dependent inhibition of both FMLP- and PMA-induced O_2 consumption in neutrophils, whereas SOD at 10 μg ml^{-1} had no significant effect on these responses.

However, when studying the respiratory burst induced by a low concentration of PMA, we observed that gomisin C reduced both O_2 consumption and O_2^- release in the neutrophil suspensions in a concentration-dependent manner when challenged by 3 nM and 1 nM PMA, respectively, and statistically significant inhibitions were observed at 30 μg ml^{-1} (38.6 ± 5.3% inhibition for O_2 consumption, $P<0.05$, $n=5$; 54.5 ± 3.0% inhibition for O_2^- release, $P<0.01$, $n=6$) (Figure 3), with an IC_{50} value of 26.9 ± 2.1 μg ml^{-1} (62.7–37.5 μM, 95% confidence interval) for O_2^- release.

Effect of gomisin C on superoxide generation in xanthine-xanthine oxidase system

Table 2 shows that both SOD and allopurinol significantly inhibited the O_2^- generation in the xanthine-xanthine oxidase system (Table 2B), while there were no significant differences in O_2^- generation between control and gomisin C-treated groups (Table 2A). In addition, uric acid formation

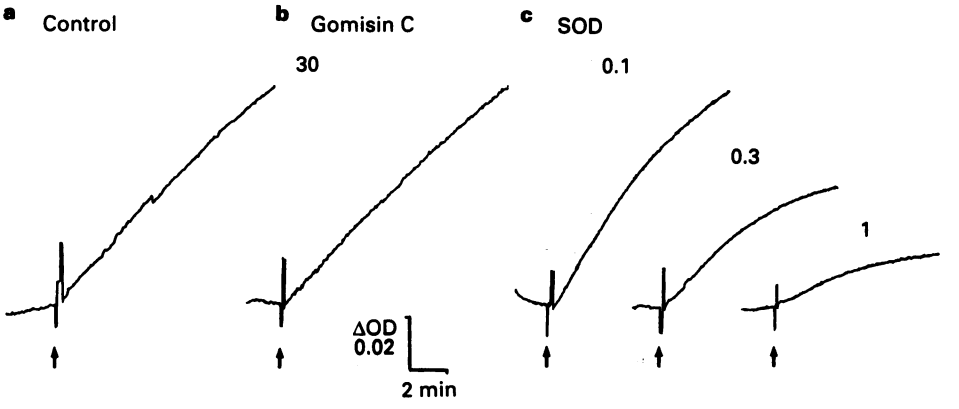


Figure 4 Effect of gomisin C and superoxide dismutase (SOD) on dihydroxyfumaric acid (DHF) autoxidation. Control (a) gomisin C 30 μg ml^{-1} (b); or SOD 0.1–1 μg ml^{-1} (c); was added into the reaction mixture at 37°C for 3 min before addition of 0.891 mM DHF.

in the xanthine-xanthine oxidase system was significantly reduced ($P<0.01$) by allopurinol, whereas neither SOD nor gomisin C reduced it (Table 2).

Effect of gomisin C on dihydroxyfumaric acid autoxidation

In the DHF autoxidation experiments, generation of $O_2^{\cdot-}$ was demonstrated by the time-dependent reduction of NBT. Reaction mixtures pretreated with SOD showed a concentration-dependent inhibition with an apparent IC_{50} value of $0.45 \pm 0.04\ \mu g\ ml^{-1}$ ($0.58-0.32\ \mu g\ ml^{-1}$, 95% confidence interval). However, gomisin C up to $30\ \mu g\ ml^{-1}$ failed to alter DHF autoxidation significantly (Figure 4).

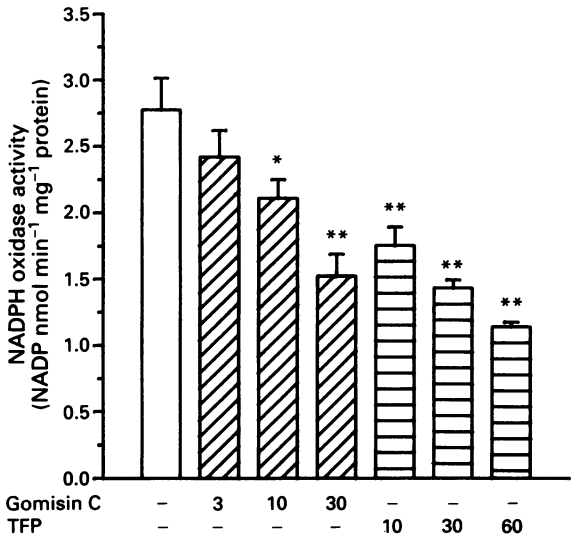


Figure 5 Effect of gomisin C and trifluoperazine (TFP) on NADPH oxidase activity. Control (open column); gomisin C $3-30\ \mu g\ ml^{-1}$ (right hatched column); TFP $10-60\ \mu M$ (horizontal hatched column); were preincubated with phorbol myristate acetate (PMA)-activated particulate NADPH oxidase at 28°C for 3 min before addition of $62.5\ \mu M$ NADPH to the reaction mixture. Values are expressed as the mean NADP formation ± s.e.mean for 4–5 separate experiments. $^*P<0.05$, $^{**}P<0.01$ compared to the control value.

Effect of gomisin C on particulate NADPH oxidase activity

NADPH oxidase activity was examined by detecting the rate of NADPH oxidation in PMA-activated neutrophil particulate NADPH oxidase. As shown in Figure 5 NADPH oxidase activity was suppressed significantly by gomisin C ($39.2 \pm 8.0\%$ inhibition at $30\ \mu g\ ml^{-1}$, $P<0.01$) and by TFP ($23.1 \pm 6.5\%$ inhibition at $10\ \mu M$, $P<0.01$; $53.4 \pm 3.9\%$ inhibition at $60\ \mu M$, $P<0.01$).

Effect of gomisin C on intracellular Ca^{2+} concentration

As shown in Figure 6, following addition of FMLP ($0.1\ \mu M$) into the fura 2-loaded cell suspensions in the absence or the presence of EDTA, the intracellular Ca^{2+} concentration was elevated by $0.131 \pm 0.016\ \mu M$ and $0.090 \pm 0.010\ \mu M$, respectively. These FMLP-induced responses were partially inhibited by gomisin C, statistically significant inhibitions being observed at $50\ \mu g\ ml^{-1}$ ($36.1 \pm 4.3\%$ inhibition in the absence of EDTA, $P<0.05$, $n=6$; $39.7 \pm 7.2\%$ inhibition in the presence of EDTA, $P<0.05$, $n=5$).

Effect of gomisin C on cytosolic inositol phosphates and cyclic AMP levels

Addition of FMLP ($0.3\ \mu M$) to cell suspensions loaded with *myo*-[^{3}H]-inositol significantly increased the IP_3 levels but not the IP and IP_2 levels (Figure 7). Unlike neomycin, which significantly reduced ($P<0.05$) the IP_3 levels, gomisin C up to $50\ \mu g\ ml^{-1}$ had no effect. Analysis of the cyclic AMP levels in the neutrophils showed that forskolin caused a large increase ($P<0.01$), whereas no changes in cyclic AMP levels were observed in gomisin C-treated cell suspensions (Table 3).

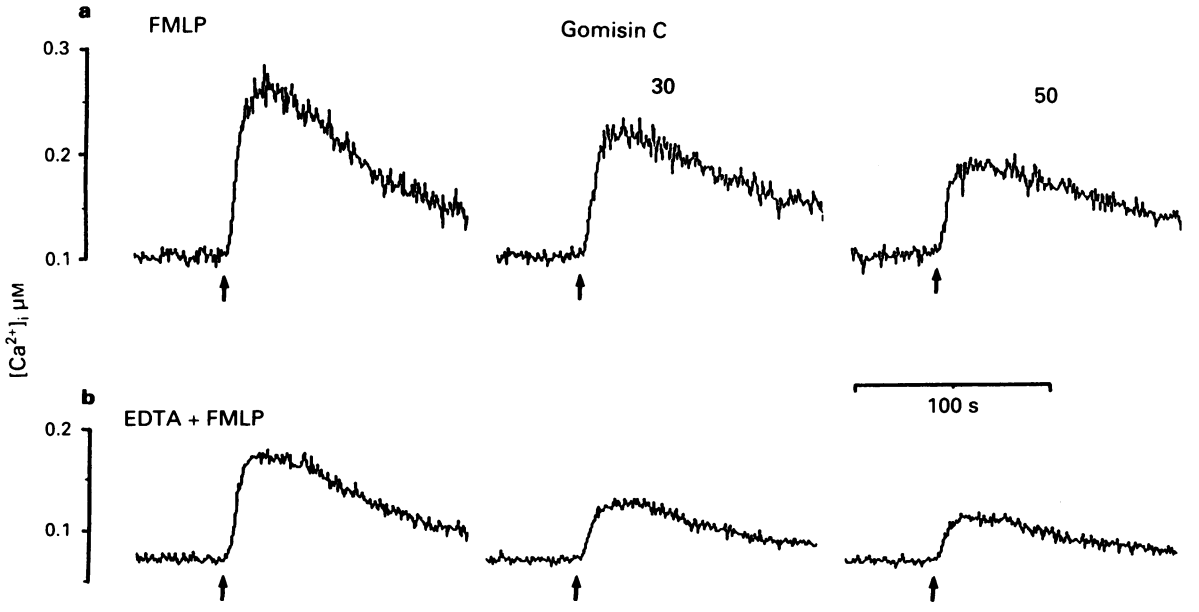


Figure 6 Effect of gomisin C on intracellular Ca^{2+} concentrations in neutrophils challenged by formyl-Met-Leu-Phe (FMLP) in (a) the presence or (b) the absence of EDTA. The fura 2-loaded cell suspension was preincubated with dimethylsulphoxide (as control) or gomisin C $30-50\ \mu g\ ml^{-1}$ in the presence or absence of 1 mM EDTA 37°C for 3 min before addition of $0.1\ \mu M$ FMLP with $5\ \mu g\ ml^{-1}$ of dihydrocytochalasin B. Intracellular Ca^{2+} concentrations were monitored in the excitation ratio 340/380 nm mode with emission wavelength at 510 nm.

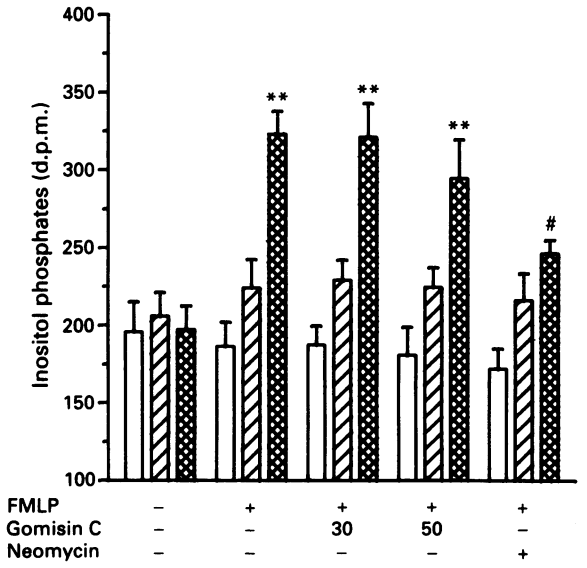


Figure 7 Effect of gomisin C and neomycin on formyl-Met-Leu-Phe (FMLP)-induced inositol phosphates generation in neutrophils. Gomisin C 30, 50 $\mu g\ ml^{-1}$, or neomycin 6 mM was added to the *myo*-[^{3}H]-inositol-loaded cell suspension in the presence of 10 mM LiCl at 37°C for 3 min before addition of 0.3 μM FMLP with 5 $\mu g\ ml^{-1}$ of dihydrocytochalasin B to start the reaction. After extraction and separation, the levels of inositol phosphates including inositol-1-phosphate (IP, open column), inositol bisphosphate (IP_2, hatched column) and inositol triphosphate (IP_3, cross hatched column) were counted. The resting levels of inositol phosphates were also determined. Values are expressed as mean d.p.m. ± s.e.mean of 6–7 separate experimetns. $^{**}P<0.01$ compared to the corresponding resting values. $\#P<0.01$ compared to the corresponding values in the group treated with FMLP alone.

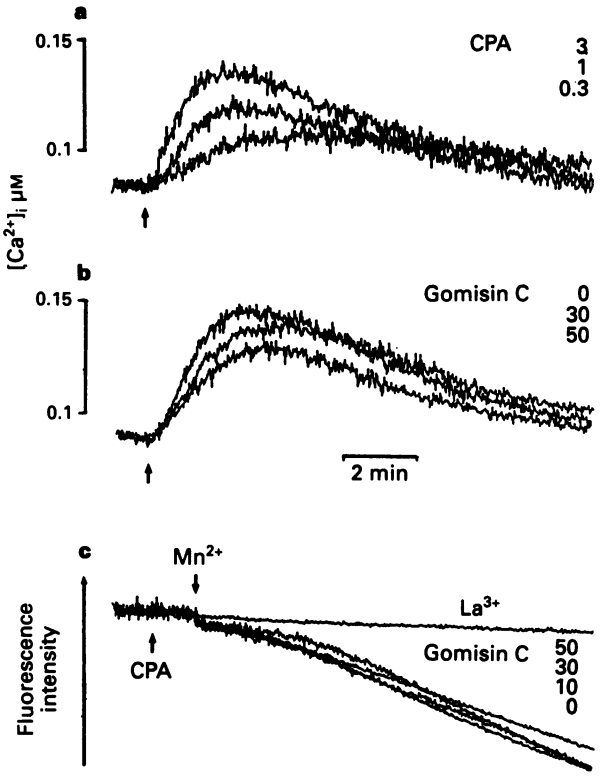


Figure 8 Effect of gomisin C on Mn^{2+} influx and cyclopiazonic acid (CPA)-induced Ca^{2+} release from intracellular Ca^{2+} stores. Ca^{2+} concentration was monitored in the ratio mode following the addition of CPA (0.3–3 μM) to the fura 2-loaded cell suspension in the presence of 1 mM EGTA (a), or addition of CPA (3 μM) in the presence of EGTA (1 mM) and gomisin C (30, 50 $\mu g\ ml^{-1}$) (b). Fura 2-loaded cell suspension was preincubated with 0.1 mM $LaCl_3$ or gomisin C (10–50 $\mu g\ ml^{-1}$) at 37°C for 3 min prior to the addition of CPA 3 μM (c). One minute later, 0.5 mM $MnCl_2$ was added and fura 2-quenching was monitored.

Effect of gomisin C on Ca^{2+} influx and release from intracellular Ca^{2+} store

In fura 2-loaded cell suspensions, CPA evoked a concentration-dependent increase of cytosolic free Ca^{2+} in the presence of EGTA (Figure 8a). At 3 μM CPA, the cytosolic free Ca^{2+} concentration was elevated by 0.016 ± 0.001 μM. In cell suspensions preincubated with gomisin C at 50 $\mu g\ ml^{-1}$, a slight but significant reduction of the cytosolic Ca^{2+} level in response to CPA was observed (24.4 ± 4.0% inhibition, $P<0.05$, $n=5$) (Figure 8b). Gomisin C at concentrations up to 50 $\mu g\ ml^{-1}$ did not affect Mn^{2+} influx in CPA-treated cell suspensions. However, this Mn^{2+} influx was abolished in the presence of 0.1 mM La^{3+} (Figure 8c).

Table 3 Effect of gomisin C and forskolin (10 μM) on the cyclic AMP levels of neutrophils

		Cyclic AMP (pmol per 10^7 cells)
Control		2.81 ± 0.44
FMLP		5.87 ± 0.95
FMLP + gomisin C	3 $\mu g\ ml^{-1}$	5.95 ± 1.25
	30 $\mu g\ ml^{-1}$	4.28 ± 0.64
Forskolin		26.95 ± 5.44**

Values are expressed as mean ± s.e.mean of 5–6 separate experiments.
$^{**}P<0.01$ compared to the FMLP (1 μM) alone treated group.

Discussion

It has been proposed that FMLP, PMA and other soluble stimuli elicit the respiratory burst by activating the same NADPH oxidase in neutrophils, but that they utilize different transduction mechanisms and are regulated differently (McPhail & Snyderman, 1983; Morel *et al.*, 1991; Segal & Abo, 1993). FMLP activates neutrophils by binding to a specific G-protein linked receptor on the membrane (Ohta *et al.*, 1985), whilst NaF and PMA bypass the membrane receptor and directly activate the G-protein and protein kinase C (PKC) (Castagna *et al.*, 1982; Hartfield & Robinson, 1990), respectively. The present study shows that gomisin C, a lignan isolated from *Schizandra chinensis*, reduces the FMLP-, NaF- and PMA-induced $O_2^{\cdot-}$ formation and O_2 consumption in rat peripheral neutrophils *in vitro*. These results indicate that the inhibitory effect of gomisin C, like SOD, an $O_2^{\cdot-}$ scavenger, and TFP, a calmodulin and NADPH oxidase inhibitor (Jones *et al.*, 1982; Bellavite *et al.*, 1983; Rao, 1987), may arise from the suppression of a common pathway.

In order to find out if the inhibitory effect of gomisin C on the respiratory burst can be attributed in part to $O_2^{\cdot-}$-scavenging activity, $O_2^{\cdot-}$ formation in the xanthine-xanthine oxidase system and by DHF autoxidation were also determined. It is unlikely that gomisin C acts as a pure $O_2^{\cdot-}$ scavenger, because gomisin C decreased the O_2 consumption of the neutrophils, whereas SOD had no effect on this response. Unlike SOD and allopurinol, a xanthine oxidase inhibitor (Kelley & Beardmore, 1970), gomisin C did not affect $O_2^{\cdot-}$ and uric acid formation in the xanthine-xanthine oxidase system. Furthermore, gomisin C did not alter the

SOD-inhibitable reduction of NBT during DHF autoxidation, used to measure $O_2^{\cdot-}$-scavenging potential (Goldberg & Stern, 1977; Yue *et al.*, 1992). These results exclude the possibility that $O_2^{\cdot-}$-scavenging activity contributes to the inhibitory effect of gomisin C on the respiratory burst in neutrophils. Therefore the direct effect of gomisin C on the activity of NADPH oxidase, an enzyme which occupies a prominent position in the final common pathway of the respiratory burst, was determined.

In the unstimulated neutrophil, the NADPH oxidase is normally dormant and the membrane component (cytochrome b_{558}) and cytosolic factors ($p47^{phox}$, $p67^{phox}$ and $p21^{rac}$) are not assembled (Segal & Abo, 1993). When the neutrophil is challenged by appropriate stimuli, the activation of the NADPH oxidase is associated with the formation of an active complex of three cytosolic factors, and is then assembled with the membrane component flavocytochrome, favourable to electron transport, thereby proceeding to the univalent reduction of oxygen (Segal & Abo, 1993). Like TFP, gomisin C produced a concentration-dependent inhibition of the activity of NADPH oxidase in cell-free incubations. These findings suggest that the inhibitory effect of gomisin C on the respiratory burst is likely due to the reduction of oxidase activity.

It has been reported that FMLP-mediated activation of NADPH oxidase is immediate, peaks and declines within 2 min. In contrast, activation by PMA has a slow onset, continuously increases and is sustained for more than an hour (Lehmeyer *et al.*, 1979; McPhail & Snyderman, 1983). Since the PKC route is predominant in oxidase activation (Tauber, 1987) and there is a correlation between the magnitude of the increase in intracellular diacylglycerol, a natural PKC-activator, and $O_2^{\cdot-}$ production in neutrophils exposed to a variety of agonists (Honeycutt & Niedel, 1986; Truett *et al.*, 1988; Tyagi *et al.*, 1989), a persistent activation of PKC by PMA and consequent prolonged stimulation of oxidase may account for the pronounced respiratory response caused by PMA. The present study indicates that gomisin C is a weak inhibitor of NADPH oxidase, this might explain the observations that gomisin C reduced the respiratory burst in neutrophils challenged by FMLP, and by PMA at low concentrations but not at higher concentrations. However, TFP at a concentration which produced a similar degree of inhibition of oxidase as that observed with gomisin C, markedly attenuated the high concentration of PMA-induced respiratory burst. These results makes it most likely that gomisin C and TFP suppressed respiratory burst through different mechanisms of action.

A common mechanism for neutrophil activation involves the binding of different agonists to specific receptors. This mechanism involves activation of phospholipase D (PLD)/phosphatidate phosphohydrolase pathway resulting in the production of phosphatidic acid/diradylglycerol (Agwu *et al.*, 1989; Billah *et al.*, 1989), and activation of the turnover of phosphoinositides with formation of inositol phosphates and diacylglycerol and the release of Ca^{2+} from intracellular stores (Rossi, 1986). $O_2^{\cdot-}$ production evoked by FMLP but not by PMA is dependent on the Ca^{2+} concentration in the external medium (Lehmeyer *et al.*, 1979; Simchowitz & Spilberg, 1979). Therefore, we also determined the effect of gomisin C on $[Ca^{2+}]_i$ changes in response to FMLP in order to evaluate whether or not this effect contributed to the suppression of the FMLP-induced respiratory burst. Gomisin C attenuated the increase of cytosolic free Ca^{2+} caused by FMLP in the presence or absence of EDTA. The rise of cytosolic Ca^{2+} in activated neutrophils results partly from Ca^{2+} influx and partly from the release of bound Ca^{2+} (Von Tscharner *et al.*, 1986). IP_3, through a specific receptor, induces rapid release of Ca^{2+} from intracellular Ca^{2+} stores (Spät *et al.*, 1986). Unlike neomycin, which inhibits the phosphoinositide turnover and generation of IP_3 via high affinity binding to phosphatidylinositol bisphosphate (PIP_2) (Gabev *et al.*, 1989), gomisin C did not affect the IP_3 formation.

Elevation of the cytosolic cyclic AMP level has been proposed as an inhibitor of phosphoinositide turnover and NADPH oxidase (De Togni *et al.*, 1984; Della Bianca *et al.*, 1986). Unlike forskolin, which stimulates adenylate cyclase (Seamon & Daly, 1986), gomisin C did not alter the cytosolic cyclic AMP level.

CPA, an inhibitor of a Ca^{2+}-ATPase of intracellular Ca^{2+} stores (Seidler *et al.*, 1989), releases Ca^{2+} through an IP_3-independent mechanism, resulting in depletion of agonist-sensitive Ca^{2+} stores (Demaurex *et al.*, 1992). Gomisin C reduced the increase of cytosolic free Ca^{2+} in neutrophils challenged by CPA. However, the Mn^{2+} influx in CPA-treated neutrophils was abolished by La^{3+} but not by gomisin C. Mn^{2+} has been shown to permeate through the neutrophil Ca^{2+} influx pathway activated by chemotactic peptides, and the influx of Mn^{2+} and Ca^{2+} can be inhibited by La^{3+} (Andersson *et al.*, 1986). Our results indicate that when gomisin C reduced the cytosolic free Ca^{2+}, it was probably not through the inhibition of Ca^{2+} influx but through the suppression of Ca^{2+} release from an agonist-sensitive Ca^{2+} store. Activation of PLD has been suggested to play an important, but probably not predominant, role in the activation of the neutrophil respiratory burst (Kessels *et al.*, 1992). Since PLD activation is predominantly dependent on the rapid initial rise in $[Ca^{2+}]_i$ (Kessels *et al.*, 1991) and gomisin C attenuates the rise of $[Ca^{2+}]_i$, it is proposed that the activation of PLD by FMLP in neutrophils is probably also reduced by gomisin C.

In conclusion, gomisin C attenuated the O_2 consumption and $O_2^{\cdot-}$ formation in rat neutrophils during activation and this can be attributed partly to inhibition of the activity of NADPH oxidase and partly to a reduction in the release of Ca^{2+} from an intracellular Ca^{2+} store. Furthermore, gomisin C did not function via scavenging of $O_2^{\cdot-}$, or by altering the cellular levels of cyclic AMP or inositol phosphates.

This study was supported by the National Science Council of the Republic of China (NSC-81-0420-B-075A-513 and NSC-81-0204-B-075A-514).

References

AGWU, D.E., MCPHAIL, L.C., CHABOT, M.C., DANIEL, L.W., WYKLE, R.L. & MCCALL, C.E. (1989). Choline-linked phosphoglycerides: a source of phosphatidic acid and diglycerides in stimulated neutrophils. *J. Biol. Chem.*, **264**, 1405–1413.

ANDERSSON, T., DAHLGREN, C., POZZAN, T., STENDAHL, O. & LEW, P.D. (1986). Characterization of fMet-Leu-Phe receptor-mediated Ca^{2+} influx across the plasma membrane of human neutrophils. *Mol. Pharmacol.*, **30**, 437–443.

BABIOR, B.M. (1978). Oxygen-dependent microbial killing by phagocytes. *New Engl. J. Med.*, **298**, 659–668.

BAGGIOLINI, M. & DEWALD, B. (1985). The neutrophil. *Int. Arch. Allergy Appl. Immunol.*, **76** Suppl 1, 13–20.

BELLAVITE, P., SERRA, M.C., DAVOLI, A., BANNISTER, J.V. & ROSSI, F. (1983). The NADPH oxidase of guinea pig polymorphonuclear leucocytes; properties of the deoxycholate extracted enzyme. *Mol. Cell. Biochem.*, **52**, 17–25.

BILLAH, M.M., ECKEL, S., MULLMANN, T.J., EGAN, R.W. & SIEGEL, M.I. (1989). Phosphatidylcholine hydrolysis by phospholipase D determines phosphatidate and diglyceride levels in chemotactic peptide-stimulated human neutrophils. Involvement of phosphatidate phosphohydrolase in signal transduction. *J. Biol. Chem.*, **264**, 17069–17077.

BORREGAARD, N. (1988). The human neutrophil. Function and dysfunction. *Eur. J. Haematol.*, **41**, 401–413.

BÖYUM, A. (1968). Isolation of mononuclear cells and granulocytes from blood. *Scand. J. Clin. Invest.*, **97** Suppl, 77–89.

CASTAGNA, M., TAKAI, Y., KAIBUCHI, K., SANO, K., KIKKAWA, U. & NISHIZUKA, Y. (1982). Direct activation of calcium-activated, phospholipid-dependent protein kinase by tumor-promoting phorbol esters. *J. Biol. Chem.*, **257**, 7847–7851.

COHEN, H.J. & CHOVANIEC, M.E. (1978). Superoxide production by digitonin-stimulated guinea pig granulocytes. The effect of N-ethylmaleimide, divalent cations; and glycolytic and mitochondria inhibitors on the activation of the superoxide generating system. *J. Clin. Invest.*, **61**, 1088–1096.

DELLA BIANCA, V., DE TOGNI, P., GRZESKOWIAK, M., VICENTINI, L.M. & DI VIRGILIO, F. (1986). Cyclic AMP inhibition of phophoinositide turnover in human neutrophils. *Biochim. Biophys. Acta*, **886**, 441–447.

DEMAUREX, N., LEW, D.P. & KRAUSE, K.H. (1992). Cyclopiazonic acid depletes intracellular Ca^{2+} stores and activates an influx pathway for divalent cations in HL-60 cells. *J. Biol. Chem.*, **267**, 2318–2324.

DE TOGNI, P., CABRINI, G. & DI VIRGILIO, F. (1984). Cyclic AMP inhibition of fMet-Leu-Phe-dependent metabolic responses in human neutrophils is not due to its effects on cytosolic Ca^{2+}. *Biochem. J.*, **224**, 629–635.

DOWNES, C.P. & MICHELL, R.H. (1981). The polyphophoinositide phosphodiesterase of erythrocyte membranes. *Biochem. J.*, **198**, 133–140.

GABEV, E., KASIANOWICZ, J., ABOTT, T. & MCLANGHLIN, S. (1989). Binding of neomycin to phosphatidylinositol-4,5-bisphosphate (PIP_2). *Biochem. Biophys. Acta*, **979**, 105–112.

GOLDBERG, B. & STERN, A. (1977). The role of the superoxide anion as a toxic species in the erythrocyte. *Arch. Biochem. Biophys.*, **178**, 218–225.

GRYNKIEWICZ, G., POENIE, M. & TSIEN, R.Y. (1985). A new generation of calcium indicators with greatly improved fluorescence properties. *J. Biol. Chem.*, **260**, 3440–3450.

HALLIWELL, B. & GUTTERIDGE, J.M.C. (1990). Role of free radicals and catalytic metal ions in human disease: an overview. *Methods Enzymol.*, **186**, 1–85.

HARTFIELD, P.J. & ROBINSON, J.M. (1990). Fluoride-mediated activation of the respiratory burst in electropermeabilized neutrophils. *Biochim. Biophys. Acta*, **1054**, 176–180.

HONEYCUTT, P.J. & NIEDEL, J.E. (1986). Cytochalasin B enhancement of the diacylglycerol response in formyl peptide-stimulated neutrophils. *J. Biol. Chem.*, **261**, 15900–15905.

IKEYA, Y., TAGUCHI, H., YOSIOKA, I. & KOBAYASHI, H. (1979). The constituents of *Schizandra chinensis* BAILL I. Isolation and structure determination of five new lignans gomisin A, B, C, F and G, and the absolute structure of schizandrin. *Chem. Pharmacol. Bull.*, **27**, 1383–1394.

INGRAHAM, L.M., COATES, T.D., ALLEN, J.M., HIGGINS, C.P., BAEHNER, R.L. & BOXER, L.A. (1982). Metabolic, membrane, and functional response of human polymorphonuclear leukocytes to platelet-activating factor. *Blood*, **59**, 1259–1266.

JOHNSON, K.J., FANTONE, J.C., KAPLAN, J. & WARD, P.A. (1981). *In vivo* damage of rat lungs by oxygen metabolites. *J. Clin. Invest.*, **67**, 983–993.

JONES, H.P., GHAI, G., PETRONE, W.F. & MCCORD, J.M. (1982). Calmodulin-dependent stimulation of the NADPH oxidase of human neutrophils. *Biochim. Biophys. Acta*, **714**, 152–156.

KELLEY, W.N. & BEARDMORE, T.D. (1970). Allopurinol: alteration in pyrimidine metabolism in man. *Science*, **169**, 388–390.

KESSELS, G.C.R., KRAUSE, K.H. & VERHOEVEN, A.J. (1993). Protein kinase C activity is not involved in N-formylmethionyl-leucyl-phenylalanine-induced phospholipase D activation in human neutrophils, but is essential for concomitant NADPH oxidase activation: studies with a staurosporine analogue with improved selectivity for protein kinase C. *Biochem. J.*, **292**, 781–785.

KESSELS, G.C.R., ROOS, D. & VERHOEVEN, A.J. (1991). fMet-Leu-Phe-induced activation of phospholipase D in human neutrophils. Dependence on changes in cytosolic free Ca^{2+} concentration and relation with respiratory burst activation. *J. Biol. Chem.*, **266**, 23152–23156.

LEFER, A.M., ARAKI, H. & OKAMATSU, S. (1981). Beneficial actions of a free radical scavenger in traumatic shock and myocardial ischemia. *Circ. Shock*, **8**, 273–282.

LEHMEYER, J.E., SNYDERMAN, R. & JOHNSTON, R.B. Jr. (1979). Stimulation of neutrophil oxidative metabolism by chemotactic peptides: influence of calcium ion concentration and cytochalasin B and comparison with stimulation by phorbol myristate acetate. *Blood*, **54**, 35–45.

MAEDA, S., TAKEDA, S., MIYAMOTO, Y., ABURADA, M. & HARADA, M. (1985). Effects of gomisin A on liver functions in hepatotoxic chemicals-treated rats. *Jpn. J. Pharmacol.*, **38**, 347–353.

MARKERT, M., ANDREWS, P.C. & BABIOR, B.M. (1984). Measurement of O_2^- production by human neutrophils. The preparation and assay of NADPH oxidase-containing particles from human neutrophils. *Methods Enzymol.*, **105**, 358–365.

MCPHAIL, L.C. & SNYDERMAN, R. (1983). Activation of the respiratory burst enzyme in human polymorphonuclear leukocytes by chemoattractants and other soluble stimuli. Evidence that the same oxidase is activated by different transductional mechanisms. *J. Clin. Invest.*, **72**, 192–200.

MIZOGUCHI, Y., KAWADA, N., ICHIKAWA, Y. & TSUTSUI, H. (1991). Effects of gomisin A in the prevention of acute hepatic failure induction. *Planta Med.*, **57**, 320–324.

MOREL, F., DOUSSIERE, J. & VIGNAIS, P.V. (1991). The superoxide-generating oxidase of phagocytic cells. Physiological, molecular and pathological aspects. *Eur. J. Biochem.*, **210**, 523–546.

NAKAJIMA, K., TAGUCHI, H., IKEYA, Y., ENDO, T. & YOSIOKA, I. (1983). The constituents of *Schizandra chinensis* BAIL XIII. Quantitative analysis of lignans in the fruits of *Schizandra chinensis* BAILL by high performance liquid chromatography. *Yakugaku Zasshi*, **103**, 743–749.

OHTA, Y. & HIROSE, Y. (1968). New sesquiterpenoids from *Schizandra chinensis*. *Tetrahedron Lett.*, **12**, 2483–2485.

OHTA, H., OKAJIMA, F. & UI, M. (1985). Inhibition by islet-activating protein of chemotactic peptide-induced early breakdown of insotiol phospholipids and Ca^{2+} mobilization in guinea pig neutrophils. *J. Biol. Chem.*, **260**, 15771–15780.

RAO, G.H. (1987). Influence of calmodulin antagonist (stelazine) on agonist-induced calcium mobilization and platelet activation. *Biochem. Biophys. Res. Commun.*, **148**, 768–775.

ROSSI, F. (1986). The O_2^--forming NADPH oxidase of the phagocytosis: nature, mechanisms of action and function. *Biochim. Biophys. Acta*, **853**, 65–89.

SEAMON, K.B. & DALY, J.W. (1986). Forskolin: its biological and chemical properties. *Adv. Cyclic Nucleotide Protein Phosphorylation Res.*, **20**, 1–150.

SEGAL, A.W. & ABO, A. (1993). The biochemical basis of the NADPH oxidase of phagocytes. *Trends Biochem. Sci.*, **18**, 43–47.

SEIDLER, N.W., JONA, I., VEGH, M. & MARTONOSI, A. (1989). Cyclopiazonic acid is a specific inhibitor of the Ca^{2+}-ATPase of sarcoplasmic reticulum. *J. Biol. Chem.*, **264**, 17816–17823.

SIBILLE, Y. & REYNOLDS, H.Y. (1990). Macrophages and polymorphonuclear neutrophils in lung defense and injury. *Am. Rev. Respir. Dis.*, **141**, 471–501.

SIMCHOWITZ, L. & SPILBERG, I. (1979). Generation of superoxide radicals by human peripheral neutrophils activated by chemotactic factor. Evidence for the role of calcium. *J. Lab. Clin. Med.*, **93**, 583–593.

SPÄT, A., BRADFORD, P.G., MCKINNEY, J.S., RUBIN, R.P. & PUTNEY, J.W. (1986). A saturable receptor for ^{32}P-inositol-1,4,5-triphosphate in hepatocytes and neutrophils. *Nature*, **319**, 514–516.

SUEKAWA, M., SHIGA, T., SONE, H., IKEYA, Y., TAGUCHI, H., ABURADA, M. & HOSOYA, E. (1987). Effects of gomisin J and analogous lignan compounds in Schisandra fruits on isolated smooth muscle. *Yakugaku Zasshi*, **107**, 720–726.

TAUBER, A.I. (1987). Protein kinase C and the activation of the human neutrophil NADPH-oxidase. *Blood*, **69**, 711–720.

TAUBER, A.I. & BABIOR, B.M. (1985). Neutrophil oxygen reduction: the enzymes and the products. *Free Radic. Biol. Med.*, **1**, 265–307.

TRUETT, A.P., VERGHESE, M.W., DILLON, S.B. & SNYDERMAN, R. (1988). Calcium influx stimulates a second pathway for sustained diacylglycerol production in leukocytes activated by chemoattractants. *Proc. Natl. Acad. Sci. U.S.A.*, **85**, 1549–1553.

TYAGI, S.R., BURNHAM, D.N. & LAMBETH, J.D. (1989). On the biological occurrence and regulation of 1-acyl and 1-o-alkyl-diacylglycerols in human neutrophils. Selective destruction of diacyl species using Rhizopus lipase. *J. Biol. Chem.*, **204**, 12977–12982.

VERGHESE, M.W., FOX, K., MCPHAIL, L.C. & SNYDERMAN, R. (1985). Chemoattractant-elicited alterations of cAMP levels in human polymorphonuclear leukocytes require a Ca^{2+}-dependent mechanism which is independent of transmembrane activation of adenylate cyclase. *J. Biol. Chem.*, **260**, 6769–6775.

VON TSCHARNER, V., DERANLEAU, D.A. & BAGGIOLINI, M. (1986). Calcium fluxes and calcium buffering in human neutrophils. *J. Biol. Chem.*, **261**, 10163–10168.

YASUKAWA, K., IKEYA, Y., MITSUHASHI, H., IWASAKI, M., ABURADA, M., NAKAGAWA, S., TAKEUCHI, M. & TAKIDO, M. (1992). Gomisin A inhibits tumor promotion by 12-o-tetradecanoylphorbol-13-acetate in two-stage carcinogenesis in mouse skin. *Oncology*, **49**, 68–71.

YUE, T.L., MCKENNA, P.J., RUFFOLO, R.R. Jr. & FEUERSTEIN, G. (1992). Carvediol, a new β-adrenoceptor antagonist and vasodilator antihypertensive drug, inhibits superoxide release from human neutrophils. *Eur. J. Pharmacol.*, **214**, 277–280.

(Received January 27, 1994
Revised June 20, 1994
Accepted July 8, 1994)

Br. J. Pharmacol. (1994), **113**, 954–958 © Macmillan Press Ltd, 1994

Role of K^+ channels in the vasodilator response to bradykinin in the rat heart

David Fulton, John C. McGiff & [1]John Quilley*

Department of Pharmacology, Basic Science Building, New York Medical College, Valhalla, New York 10595, U.S.A.

1 The role of K^+ channels in the nitric oxide (NO)-independent coronary vasodilator efffect of bradykinin was examined in the Langendorff heart preparation in which nitroarginine was used to inhibit NO synthesis and elevate perfusion pressure; cyclo-oxygenase was inhibited with indomethacin.

2 The K^+ channel inhibitors, tetraethylammonium, procaine and charybdotoxin, but not glibenclamide, further increased perfusion pressure suggesting a role for K^+ channels, other than ATP-sensitive K^+ channels, in the regulation of coronary vascular tone under the experimental conditions adopted here.

3 The non-specific K^+ channel inhibitors, tetraethylammonium and procaine, reduced vasodilator responses to bradykinin and cromakalim but not those to nitroprusside in the perfused heart treated with nitroarginine and indomethacin.

4 Glibenclamide, an inhibitor of ATP-sensitive K^+ channels, reduced vasodilator responses to cromakalim but did not affect those to bradykinin or nitroprusside.

5 Charybdotoxin, an antagonist of Ca^{2+}-activated K^+ channels, inhibited responses to bradykinin but did not affect those to cromakalim or nitroprusside.

6 Nifedipine inhibited vasodilator responses to bradykinin and cromakalim without affecting those to nitroprusside.

7 Inhibition of cytochrome P450 with clotrimazole reduced responses to bradykinin but did not modify those to cromakalim or nitroprusside.

8 These results suggest that bradykinin utilizes a Ca^{2+}-activated K^+ channel to produce vasodilatation in the rat heart.

Keywords: Langendorff heart; bradykinin-induced vasodilatation; K^+ channels

Introduction

We have provided pharmacological evidence that cytochrome P450-derived metabolites of arachidonic acid play a role in both the renal and coronary vasodilator actions of bradykinin in the rat (Fulton *et al.*, 1992; Quilley *et al.*, 1993). In the kidney, responses to bradykinin are subserved by two major components, nitric oxide (NO) and cytochrome P450, and a minor prostaglandin component. In the heart the response, which is a kinin B_2-receptor mediated event (Baydoun & Woodward, 1991), is independent of NO and prostaglandins (Baydoun & Woodward, 1991) but highly dependent on cytochrome P450, presumably via arachidonic acid metabolism as 17-ODYA, a mechanism based inhibitor of fatty acid metabolism by cytochrome P450 (Zou *et al.*, 1994), also reduces the effect of bradykinin (Quilley *et al.*, 1994). As NO-independent, but endothelium-dependent, vasodilatation to bradykinin in human, porcine and canine coronary vessels is reported to result from the release of a hyperpolarizing factor (Richard *et al.*, 1990; Tschudi *et al.*, 1991; Nakashima *et al.*, 1993), it is possible that this factor is a metabolite of arachidonic acid, a contention that is supported by two recent reports that vasodilatation elicited by epoxides is associated with increased K^+ conductance (Gebremedhedin *et al.*, 1993; Hu & Kim, 1993).

Consequently, the present study was undertaken to determine the role of K^+ channels in the vasodilator response to bradykinin in hearts treated with nitroarginine and indomethacin to inhibit synthesis of NO and prostaglandins, respectively. Tetraethylammonium and procaine were used as non-specific inhibitors of K^+ channels, while glibenclamide and charybdotoxin were used to investigate the role of ATP-sensitive K^+ channels and Ca^{2+}-activated K^+ channels, respectively. Nifedipine was used to inhibit voltage-regulated Ca^{2+} channels, which are reportedly absent from the endothelium (Luckoff & Busse, 1990), to block the effects of hyperpolarization at the level of vascular smooth muscle. As we have previously shown that inhibition of cytochrome P450 mono-oxygenases reduces the vasodilator effect of bradykinin, we also determined whether the inhibitory effect of clotrimazole resulted from inhibition of K^+ channels rather than cytochrome P450. Thus, clotrimazole (an imidazole antifungal agent like miconazole which inhibits cytochrome P450 mono-oxygenases, Zou *et al.*, 1994), has also been reported to inhibit K^+ channels (Alvarez *et al.*, 1992; Brugnara *et al.*, 1993).

Our results demonstrate that the NO-independent, coronary vasodilator effect of bradykinin is dependent on stimulation of a Ca^{2+}-activated K^+ channel.

Methods

Male Wistar rats, 300–400 g, were used in these studies. Following pentobarbitone anaesthesia (65 mg kg^{-1}, i.p.) and thoracotomy, the heart with attached aorta was excised, flushed with Krebs buffer and immersed in buffer at 0°C. The aorta was cannulated and the heart perfused at constant flow (8–9 ml min^{-1}) with oxygenated Krebs buffer at 37°C according to the method of Langendorff, (1895), as modified by Broadley, (1979). Initial perfusion pressure was between 30–40 mmHg. The perfusate contained indomethacin (2.8 μM) to inhibit prostaglandin formation and nitroarginine (50 μM) to inhibit NO synthesis and increase vascular tone in order to amplify vasodilator responses. Once a stable, elevated perfusion pressure (130–135 mmHg) was obtained, changes in perfusion pressure in response to bradykinin

[1] Author for correspondence.

(10–1000 ng), nitroprusside (1000 ng) and cromakalim (1–10 μg) were determined in the presence and absence of tetraethylammonium (10 mM), procaine (1 mM), glibenclamide (10 μM), nifedipine (5 nM) and clotrimazole (1 μM). These agents were added to the perfusate once a stable, elevated pressure was attained in response to nitroarginine. Three to four preparations/day were completed where at least one served as a control ($n = 9$), while the others were randomly assigned to one of the treatment groups ($n = 4–5$ for each). Therefore, the control group was the same for each of these interventions. In a separate series of experiments, we compared the coronary vasodilator responses to bradykinin, nitroprusside and cromakalim in the absence ($n = 5$) or presence ($n = 4$) of charybdotoxin (10 nM).

In all experiments nitroprusside was used as a reference vasodilator to assess any non-specific effects of the pharmacological inhibitors that were used. Responses to cromakalim, an ATP-sensitive K^+ channel activator, were used as an index of the effectiveness of the K^+ channel blocking agents, excepting charybdotoxin.

Drugs

The following drugs were obtained from Sigma Chemical Co., St. Louis, MO, U.S.A.: tetraethylammonium, procaine, nitroarginine, bradykinin, cromakalim, clotrimazole, nifedipine, sodium nitroprusside and glibenclamide. Charybdotoxin was obtained from Peptides International, Louisville, KY, U.S.A. and U46619 (11, 9 epoxy methano-protaglandin H_2), an endoperoxide analogue, was obtained from the Upjohn Com., Kalamazoo, MI, U.S.A. Indomethacin was a gift from Merck, Sharpe and Dohme.

Statistical analysis

Data from the various treatment groups and respective control groups were compared by analysis of variance and individual data points were compared by Newman-Keuls test (Pharmacologic Calculation System based on Manual of Pharmacologic Calculations with Computer Programmes, 2nd Edition, by Tallarida & Murray, Springer-Verlag, New York, 1987). $P < 0.05$ was considered statistically significant.

Results

In nitroarginine- and indomethacin-treated hearts, perfusion pressure stabilized at approximately 130–140 mmHg. Addition of the K^+ channel inhibitors, tetraethylammonium and procaine, further increased perfusion pressure by approximately 20 mmHg indicating a role for K^+ channels in the regulation of coronary vascular tone. The perfusion pressure for the control group was 134 ± 3 mmHg compared to 153 ± 3 and 152 ± 4 mmHg for the tetraethylammonium and procaine groups, respectively. In contrast, glibenclamide did not alter perfusion pressure (131 ± 5 mmHg) compared to the control group. Nifedipine caused a marked reduction in perfusion pressure which was elevated to its original level with U46619 (8–14 nM), 147 ± 9 mmHg. Clotrimazole had no effect on elevated perfusion pressure (130 ± 7 mmHg). In the charybdotoxin group, perfusion pressure was 150 ± 6 mmHg compared to 130 ± 5 mmHg for the control group.

Procaine abolished responses to cromakalim and tetraethylammonium caused substantial reductions (Figure 1). Both tetraethylammonium and procaine also reduced vasodilator responses to bradykinin (Figure 2) signifying a role for K^+ channels. Tetraethylammonium did not affect responses to nitroprusside whereas procaine caused a significant reduction (Figure 2) indicating that it has effects other than inhibition of K^+ channels.

Inhibition of ATP-sensitive K^+ channels with glibenclamide inhibited vasodilator responses to cromakalim (Figure 3) but was without effect on responses to bradykinin or nitroprusside (Figure 4). In contrast, inhibition of voltage-regulated Ca^{2+} channels with nifedipine greatly reduced vasodilator responses to bradykinin (Figure 4) and cromakalim without modifying responses to nitroprusside. At higher concentrations (10–20 nM), nifedipine eliminated vasodilatation induced by bradykinin and cromakalim.

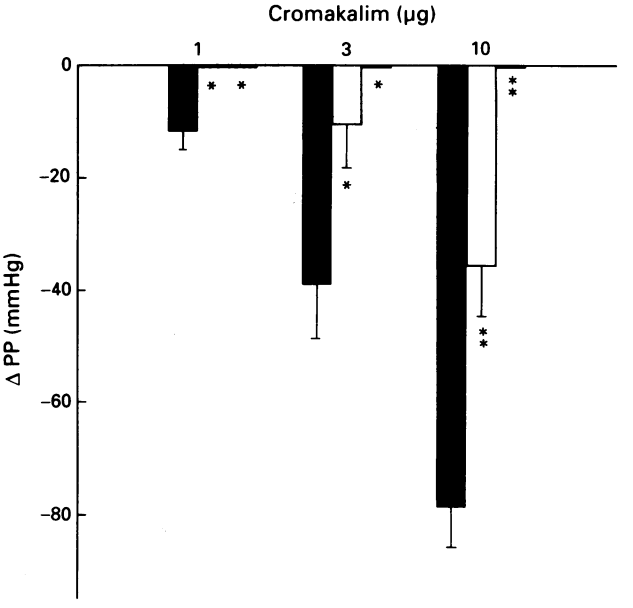


Figure 1 Effects of tetraethylammonium (TEA) and procaine on coronary vasodilator responses to cromakalim in perfused hearts treated with nitroarginine (50 μM) to inhibit NO and indomethacin (2.8 μM) to inhibit prostaglandin synthesis. Nitroarginine resulted in elevation of perfusion pressure to 130–140 mmHg from an initial basal value of 30–40 mmHg. Solid columns, control ($n = 9$); open columns, TEA 10 mM ($n = 5$); hatched columns, procaine 1 mM ($n = 4$). $^*P<0.05$; $^{**}P<0.01$.

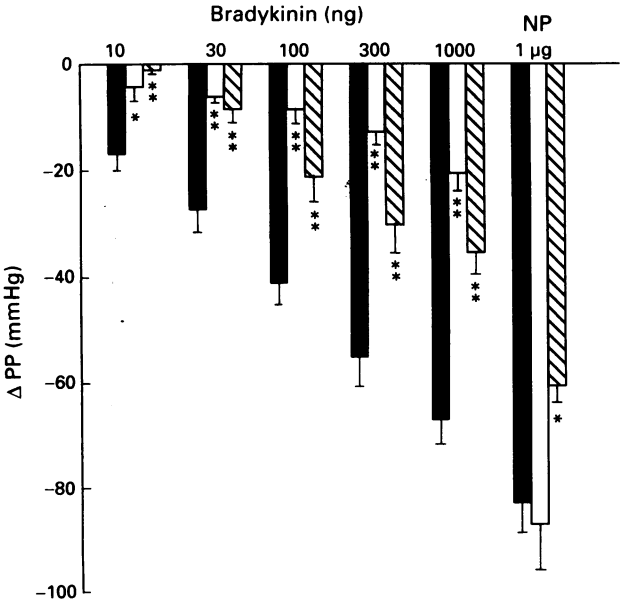


Figure 2 Effects of tetraethylammonium (TEA) and procaine on vasodilator responses to bradykinin and sodium nitroprusside (NP) in hearts treated with nitroarginine (50 μM) and indomethacin (2.8 μM) to inhibit NO and prostaglandin synthesis, respectively. Nitroarginine was also used to elevate perfusion pressure to 130–140 mmHg to amplify vasodilator responses. Solid columns, control ($n = 9$); open columns, TEA 10 mM ($n = 5$); hatched columns, procaine 1 mM ($n = 4$). $^*P<0.05$; $^{**}P<0.01$.

Inhibition of Ca^{2+}-activated K^+ channels with charybdotoxin also reduced the coronary vasodilator effect of bradykinin (Figure 5) but was without effect on responses to nitroprusside or cromakalim (Figure 5).

As reported previously, clotrimazole reduced coronary vasodilator responses to bradykinin by approximately 60% (Figure 6) without affecting those to nitroprusside or cromakalim (Figure 6).

Discussion

In hearts perfused with buffer containing nitroarginine and indomethacin to inhibit NO and prostaglandin synthesis, respectively, bradykinin produced dose-dependent decreases in perfusion pressure which were dependent on activation of K^+ channels. Thus, tetraethylammonium and procaine, in concentrations that inhibited vasodilator effects of K^+ chan-

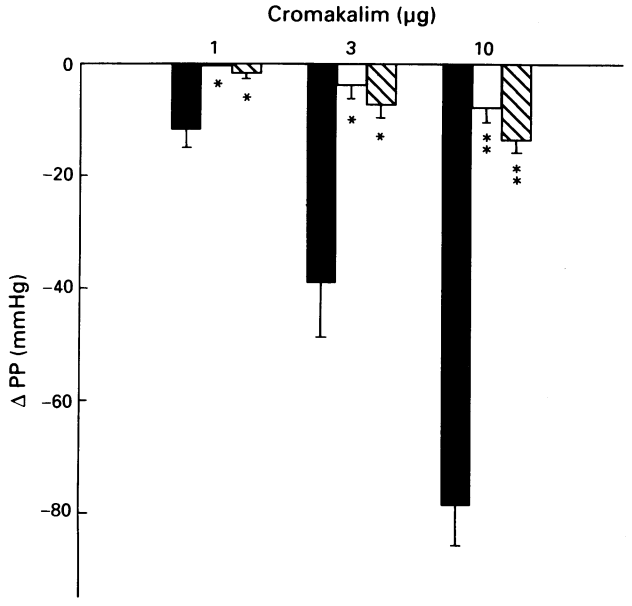


Figure 3 Vasodilator responses to cromakalim and the effects of nifedipine and glibenclamide in hearts in which NO synthase and cyclo-oxygenase were inhibited with nitroarginine (50 μM) and indomethacin (2.8 μM), respectively. Perfusion pressure was 130–140 mmHg. Solid columns, control ($n = 9$); open columns, nifedipine 5 nM ($n = 4$); hatched columns, glibenclamide 10 μM ($n = 4$). $^*P<0.05$; $^{**}P<0.01$.

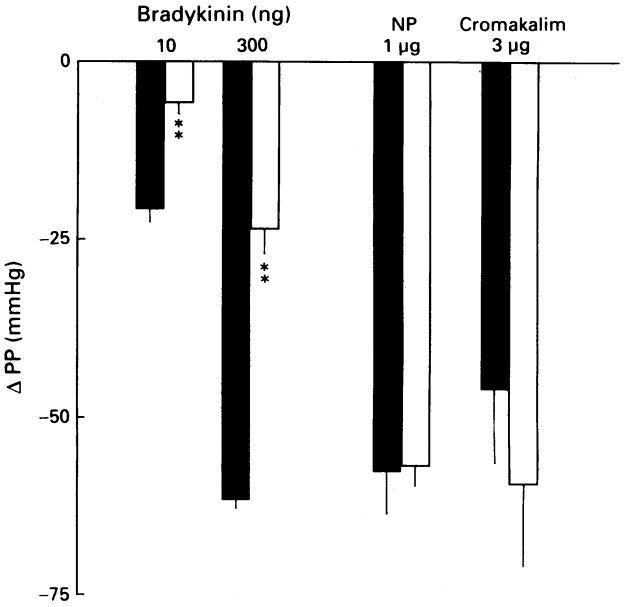


Figure 5 Vasodilator responses to bradykinin, sodium nitroprusside (NP) and cromakalim in the absence and presence of charybdotoxin in hearts treated with nitroarginine (50 μM) and indomethacin (2.8 μM). Nitroarginine was also used to elevate perfusion pressure which was 130–140 mmHg. Solid columns, control ($n = 5$); open columns, charybdotoxin 10 nM ($n = 4$). $^{**}P<0.01$.

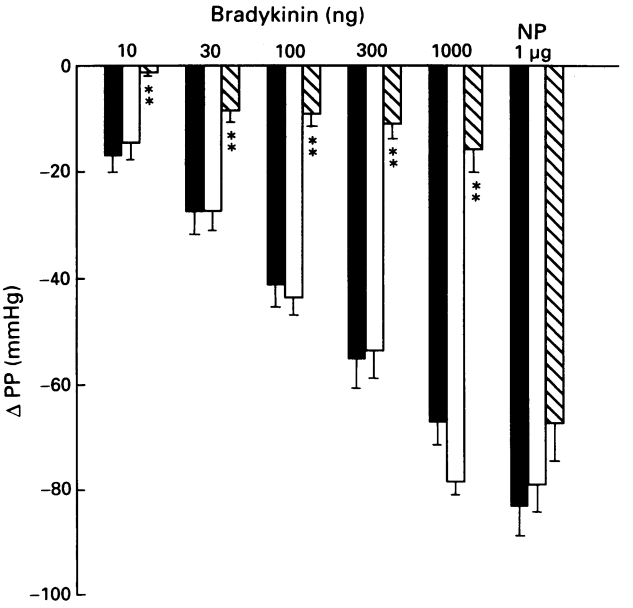


Figure 4 Effects of nifedipine and glibenclamide on vasodilator responses to bradykinin and sodium nitroprusside (NP) in hearts constricted with nitroarginine (50 μM) to inhibit NO synthesis and treated with indomethacin (2.8 μM) to inhibit cyclo-oxygenase. Perfusion pressure was 130–140 mmHg. Solid columns, control ($n = 9$); open columns, glibenclamide 10 μM ($n = 4$); hatched columns, nifedipine 5 nM ($n = 4$). $^{**}P<0.01$.

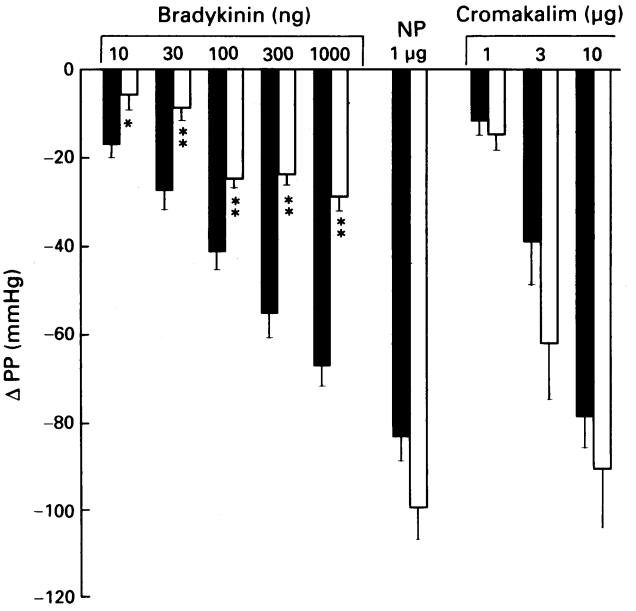


Figure 6 Vasodilator responses to bradykinin, sodium nitroprusside (NP) and cromakalim in the absence and presence of clotrimazole in hearts constricted with nitroarginine (50 μM) and treated with indomethacin (2.8 μM). Perfusion pressure was 130–140 mmHg. Solid columns, control ($n = 9$); open columns, clotrimazole 1 μM ($n = 4$). $^*P<0.05$; $^{**}P<0.01$.

nel activation, reduced the vasodilator response to bradykinin. Part of the inhibitory effect of procaine could be attributed to a non-specific effect as this agent also reduced responses to nitroprusside. The lack of effect of glibenclamide, at a concentration that reduced responses to cromakalim by approximately 90%, on vasodilator responses to bradykinin excluded a role for ATP-sensitive K^+ channels. In contrast, the inhibitory effect of charybdotoxin is presumptive evidence that bradykinin-induced vasodilatation in the heart is dependent on stimulation of a Ca^{2+}-activated K^+ channel. This is a specific effect as charybdotoxin did not affect responses to nitroprusside or cromakalim, results which also demonstrate that, in the coronary vasculature of the rat, the effect of cromakalim is independent of Ca^{2+}-activated K^+ channels but solely dependent on ATP-sensitive K^+ channels. All of the K^+ channel inhibitors, except glibenclamide, further elevated perfusion pressure in hearts preconstricted by nitroarginine suggesting that, under these experimental conditions, tonic activation of K^+ channels contributed to the regulation of vascular tone. The results with glibenclamide excluded a role for ATP-sensitive K^+ channels under these conditions whereas the results with charybdotoxin implicated Ca^{2+}-activated K^+ channels in the regulation of vascular tone. However, other investigators have reported that inhibition of ATP-sensitive K^+ channels elevates perfusion in isolated perfused heart preparations (Wolleben *et al.*, 1989; Tweedie *et al.*, 1993). The lack of effect of glibenclamide in our studies could relate to two factors. First, we used indomethacin to inhibit cyclooxygenase and, thereby, prevent formation of prostacyclin which has been reported to activate ATP-sensitive K^+ channels (Jackson *et al.*, 1993). Second, the perfusion pressure in our preparations was higher than that used in the previously cited studies, 135 mmHg vs 70 mmHg, which could have masked any further effect of glibenclamide. However, this is less likely considering that the other K^+ channel inhibitors all caused further elevations in perfusion pressure.

The results of this study, coupled with those showing a role of cytochrome P450 in the coronary vasodilator effect of bradykinin (Quilley *et al.*, 1993), are consistent with the interpretation that bradykinin stimulates the release of a cytochrome P450-dependent arachidonic acid metabolite that elicits vasorelaxation by stimulating Ca^{2+}-activated K^+ channels, particulary as the epoxides have been reported to increase K^+ conductance (Gebremedhin *et al.*, 1992; Hu & Kim, 1993). However, there are other possible interpretations of our data, e.g. bradykinin may stimulate endothelial K^+ channels which, in turn, may result in the release of a relaxant factor that may or may not increase K^+ conductance of vascular smooth muscle. The results with nifedipine, however, argue against this possibility as voltage-regulated Ca^{2+} channels are apparently absent from the endothelium and, therefore, the inhibitory effects of nifedipine on responses to bradykinin and cromakalim could be attributed to an effect on smooth muscle (Revest & Abbott, 1992), i.e., nifedipine is preventing the effects of a vasorelaxant factor rather than affecting its release. However, the results with nifedipine should be interpreted cautiously as there are reports of voltage-regulated Ca^{2+} channels in microvascular endothelial cells (Revest & Abbott, 1992). Moreover, we still cannot exclude a role for hyperpolarization in releasing the vasorelaxant mediator. Future studies comparing the effects of the more selective inhibitor of large Ca^{2+}-activated K^+ channels, ibereotoxin, with charybdotoxin should resolve this issue as the endothelial Ca^{2+}-activated K^+ channel is an intermediate sized channel which may be susceptible to charybdotoxin but not ibereotoxin.

Finally, we addressed whether the previously reported attenuating effect of cytochrome P450 inhibitors on bradykinin vasodilator responses related to a possible effect on K^+ or Ca^{2+} channels rather than cytochrome P450. Thus, imidazole antifungal agents have been reported to inhibit K^+ channels at concentrations lower than that required to inhibit cytochrome P450 (Alvarez *et al.*, 1992; Brugnara *et al.*, 1993) as well as to inhibit both receptor-operated and voltage-gated Ca^{2+} channels (Montero *et al.*, 1991; Villabos *et al.*, 1992). Clotrimazole inhibited responses to bradykinin without affecting those to nitroprusside or cromakalim, suggesting that this was a specific effect and that clotrimazole does not affect ATP-sensitive K^+ channels although it is possible that clotrimazole inhibits vascular Ca^{2+}-activated K^+ channels, particularly in light of the reports by Alvarez *et al.* (1992) and Brugnara *et al.* (1993). However, we also reported that 17-ODYA and 7-ethoxyresorufin, structurally distinct inhibitors of cytochrome P450, also reduced coronary vasodilator responses to bradykinin (Quilley *et al.*, 1994), implicating cytochrome P450 rather than effects of these agents on K^+ channels. Nonetheless, it is possible that K^+ channels are modulated, in some way, by cytochrome P450. The possibility that the inhibitory effects of clotrimazole on bradykinin-induced vasodilatation can be accounted for by an effect on Ca^{2+} channels can be excluded by comparing the results obtained with nifedipine and clotrimazole. As noted, inhibition of voltage-regulated Ca^{2+} channels should prevent the vasodilatation associated with hyperpolarization and exemplified by nifedipine which blocked vasodilator responses to both cromakalim and bradykinin. If the inhibitory effects of clotrimazole on bradykinin responses were due to inhibition of voltage-regulated Ca^{2+} channels, then the effects of clotrimazole and nifedipine should be essentially the same. This was not the case as clotrimazole, unlike nifedipine, did not affect the coronary vasodilator response to cromakalim. However, a possibility which cannot be excluded by the present studies is that clotrimazole is a bradykinin receptor antagonist although the observations that 17-ODYA and 7-ethoxyresorufin also reduced coronary vasodilator responses to bradykinin are consistent with a role for cytochrome P450 (Quilley *et al.*, 1994).

In summary, we have shown that the coronary vasodilator response to bradykinin that is independent of NO is dependent on activation of K^+ channels, specifically Ca^{2+}-activated K^+ channels.

This work was supported by NIH grants 5RO1 HL25394 and 5 PO1 HL 34300. We thank Jennifer Brown for secretarial assistance.

References

ALVAREZ, J., MONTERO, M. & GARCIA-SANCHO, J. (1992). High affinity inhibition of Ca^{2+}-dependent K^+ channels by cytochrome P450 inhibitors. *J. Biol. Chem.*, **267**, 11789–11793.

BAYDOUN, A.R. & WOODWARD, B. (1991). Effects of bradykinin in the rat isolated perfused heart: role of kinin receptors and endothelium-derived relaxing factor. *Br. J. Pharmacol.*, **103**, 1829–1833.

BROADLEY, K.J. (1979). The Langendorff heart preparation – reappraisal of its role as a research and teaching model for coronary vasoactive drugs. *J. Pharmacol. Methods*, **2**, 143–156.

BRUGNARA, C., DE FRANCHESHI, L. & ALPER, S.L. (1993). Inhibition of Ca^{2+}-dependent K^+ transport and cell dehydration in sickle erythrocytes by clotrimazole and other imidazole derivatives. *J. Clin. Invest.*, **92**, 520–526.

FULTON, D., MCGIFF, J.C. & QUILLEY, J. (1992). Contribution of NO and cytochrome P450 to the vasodilator effect of bradykinin in the rat kidney. *Br. J. Pharmacol.*, **107**, 722–725.

GEBREMEDHIN, D., MA, Y.H., FALCK, J.R., ROMAN, R.J., VANROLLINS, M. & HARDER, D.R. (1992). Mechanisms of action of cerebal epoxyeicosatrienoic acids in cerebal arterial smooth muscle. *Am. J. Physiol.*, **263**, H519–H525.

HU, S. & KIM, H.S. (1993). Activation of K^+ channels in vascular smooth muscles by cytochrome P450 metabolites of arachidonic acid. *Eur. J. Pharmacol.*, **230**, 215–221.

JACKSON, W.F., KONIG, A., DAMBACHER, T. & BUSSE, R. (1993). Prostaglandin-induced vasodilation in rabbit heart is mediated by ATP-sensitive K^+ channels. *Am. J. Physiol.*, **264**, H238–H243.

LANGENDORFF, O. (1895). Untersuchargen am iiberlebender Saugethierherzer. *Pflügers Arch. Ges. Physiol.*, **61**, 295–303.

LUCKOFF, A. & BUSSE, R. (1990). Calcium influx into endothelial cells and formation of endothelium-derived relaxing factor is controlled by the membrane potential. *Pflügers Arch.*, **416**, 305–311.

MONTERO, M., ALVAREZ, J. & GARCIA-SANCHO, J. (1991). Agonist-induced Ca^{2+} influx in human neutrophils is secondary to emptying of intra-cellular calcium stores. *Biochem. J.*, **277**, 73–79.

NAKASHIMA, M., MOMBOULI, J.-V., TAYLOR, A.A. & VANHOUTTE, P.M. (1993). Endothelium-dependent hyperpolarization caused by bradykinin in human coronary arteries. *J. Clin. Invest.*, **92**, 2867–2871.

QUILLEY, J. MCGIFF, J.C., FULTON, D., BALAZY, M. & MAHBOUBI, K. (1993). Nitric oxide-independent coronary vasodilator effect of bradykinin. *Hypertension*, **22**, 429 Abstr.

QUILLEY, J., MCGIFF, J.C., MAHBOUBI, K. & FULTON, D. (1994). Coronary vasodilator response to bradykinin: role of cytochrome P450 and K^+ conductance. *Blood Vessels*, (In press). Abstr.

REVEST, P.A. & ABBOTT, N.J. (1992). Membrane ion channels of endothelial cells. *Trends Pharmacol. Sci.*, **13**, 404–407.

RICHARD, V., TANNER, F.C., TSCHUDI, M. & LUSCHER, T.F. (1990). Different activation of L-arginine pathway by bradykinin, serotonin and clonidine in coronary arteries. *Am. J. Physiol.*, **259**, H1433–H1439.

TALLARIDA, R.J. & MURRAY, R.B. (1987). *Manual of Pharmacologic Calculations with Computer Programs*. 2nd edn. New York: Springer.

TSCHUDI, M., RICHARD, V., BUHLER, F.R. & LUSCHER, T.F. (1991). Importance of endothelium-derived nitric oxide in porcine coronary resistance arteries. *Am. J. Physiol.*, **260**, H13–H20.

TWEEDIE, D., HENDERSON, C. & KANE, K. (1993). Glibenclamide, but not class III drugs, prevents ischemic shortening of the refractory period in guinea-pig hearts. *Eur. J. Pharmacol.*, **240**, 252–257.

VILLABOS, C., FONTERIZ, R., LOPEZ, M.G., GARCIA, A.G. & GARCIA-SANCHO, J. (1992). Inhibition of voltage-gated $Ca^{\beta+}$ entry into GH_3 and chromaffin cells by imidazole antimycotics and other cytochrome P450 blockers. *FASEB J.*, **6**, 2742–2747.

WOLLEBEN, C.D., SANGUINETTI, M.C. & SIEGL, P.K.S. (1989). Influence of ATP-sensitive potassium channel modulators on ischemia-induced fibrillation in isolated rat hearts. *J. Mol. Cell. Cardiol.*, **21**, 783–788.

ZOU, A.-P., MA, Y.-H., ZUI, Z.-H., ORTIZ DE MONTELLANO, P.R., CLARK, J.E., MASTER, B.S. & ROMAN, R.J. (1994). Effects of 17-octadecynoic acid, a suicide substrate inhibitor of cytochrome P450 fatty acid ω-hydroxylases on renal function in rats. *J. Pharmacol. Exp. Ther.*, **268**, 474–480.

(Received April 14, 1994
Revised July 20, 1994
Accepted July 22, 1994)

Br. J. Pharmacol. (1994), **113**, 959–967 © Macmillan Press Ltd, 1994

Blockade by dendrotoxin homologues of voltage-dependent K^+ currents in cultured sensory neurones from neonatal rats

Adam Hall, *John Stow, †Roger Sorensen, J. Oliver Dolly & [1]*David Owen

Department of Biochemistry, Imperial College of Science, Technology and Medicine, London, SW7 2AZ; *Wyeth Research (UK) Ltd., Taplow, Berkshire SL6 0PH and †Jefferson Medical College, Thomas Jefferson University, Philadelphia, PA 19107, U.S.A.

1 Homologues of dendrotoxin (Dtx) were isolated from the crude venom of Green and Black Mamba snakes and examined for K^+ channel blocking activity in neonatal rat dorsal root ganglion cells (DRGs) by whole-cell patch clamp recording.

2 Outward potassium current activated by depolarization was composed of two major components: a slowly inactivating current (SIC, $\tau_{decay} \approx 50$ ms, 200 ms and 2 s), and a non-inactivating current (NIC, $\tau_{decay} > 2$ min). Tail current analysis revealed two time constants of deactivation of total outward current, 3–12 ms and 50–150 ms (at −80 mV) which corresponded to SIC and NIC, respectively.

3 All the homologues (α-, β-, γ- and δ-Dtx and toxins I and K) blocked outward current activated by depolarization in a dose-dependent manner. The most potent in blocking *total* outward current was δ-Dtx (EC_{50} of 0.5 ± 0.2 nM), although there were no statistically significant differences in potency between any of the homologues.

4 Qualitative differences in the nature of the block were noted between homologues. In particular, the block by δ-Dtx was time-dependent, whereas that by α-Dtx was not.

5 α-Dtx was a much better blocker of SIC ($EC_{50} = 1.0 \pm 0.4$ nM) than was δ-Dtx ($EC_{50} = 17.6 \pm 5.8$ nM). Furthermore, δ-Dtx was selective for NIC ($EC_{50} \pm 0.24 \pm 0.03$ nM) over SIC and reduced the slow component of tail currents (NIC), preferentially. On the other hand, α-Dtx did not significantly distinguish between SIC and NIC although tail current analysis showed that α-Dtx preferentially reduced the fast component of tail currents (SIC).

6 The results confirm, using direct electrophysiological methods, that homologues of dendrotoxins from Mamba snake venom block K^+ channels in rat sensory neurones. Furthermore, α-Dtx and δ-Dtx distinguish between sub-types of K^+ channels in these cells and may thus be useful pharmacological tools in other neuronal K^+ channel studies.

Keywords: Dendrotoxins; potassium currents, dorsal root ganglion cells; neonatal rat

Introduction

The discovery of the naturally-occuring toxin, dendrotoxin (Harvey & Karlsson, 1980), in the venom of the Green Mamba snake (*Dendroaspis angusticeps*) provided a valuable tool for characterizing voltage-activated K^+ channels in neurones. Its usefulness arises from the fact that it is both highly potent and selective for a subset of voltage-activated K^+ channels. Since the initial separation of dendrotoxin (α-dendrotoxin or α-Dtx) from venom of the Green Mamba, a number of homologues, β_1-Dtx, β_2-Dtx, γ-Dtx and δ-Dtx, have also been isolated (Benishin *et al.*, 1988). In addition, closely-related peptides, Toxin I and K, have been purified from the Black Mamba (*Dendroaspis polylepis polylepis*) venom (Strydom, 1976). They are all basic polypeptides, containing ~60 amino acid residues that also show homology to Kunitz protease inhibitors (which are not themselves ion channel modulators) and to the smaller chain of β-bungarotoxin, a synaptically-active peptide from Krait venom (see Dolly, 1992). Most reports, to date, have indicated that α-Dtx is selective for delayed-rectifier-like K^+ currents, e.g. delayed rectifier K^+ currents in frog nerve fibres (Benoit & Dubois, 1986; Bräu *et al.*, 1990) and slowly- or non-inactivating outward K^+ conductances in sensory neurones of guinea-pigs and rats (Penner *et al.*, 1986; Stansfeld *et al.*, 1986; Stansfeld & Feltz, 1988). However, a Dtx-sensitive 'A-current' has been described in central CA1 neurones from rat and guinea-pig hippocampal slices (Halliwell *et al.*, 1986), although much higher concentrations and prolonged incubation times were required for an effect in this preparation.

Receptors for the dendrotoxins have been localized in the central nervous system (Pelchen-Matthews & Dolly, 1989) and purified from bovine brain (Parcej & Dolly, 1989). These are large sialoglyco-proteins containing α and β subunits of 65 kDa (after *N*-glycosylation) and 39 kDa, respectively. Microsequencing, by one group, of the N-terminus of the Dtx-purified α-subunit (Scott *et al.*, 1990), together with gene cloning (Reid *et al.*, 1992) has shown that this protein is homologous with a rat brain cloned K^+ channel, rKv1.2 (also known as RCK5), which is sensitive to α-Dtx when expressed in *Xenopus* oocytes (Stühmer *et al.*, 1989). Other microsequencing studies together with the use of specific antibodies suggest that Kv1.1 (also known as MK1, RCK1 and RBK1) channels also contribute to purified brain Dtx-binding protein (Rehm *et al.*, 1989). Kv1.1 cRNA + cDNA also gives rise to 'delayed-rectifier-like', Dtx-sensitive currents when expressed in *Xenopus* oocytes (Stühmer *et al.*, 1989) and mammalian cells (Owen *et al.*, 1992; Robertson & Owen, 1993; Bosma *et al.*, 1993).

It has been suggested that Dtx homologues can select for K^+ channel sub-types, although these conclusions were reached on the basis of indirect measurements (^{86}Rb efflux from synaptosomes) which lacked good temporal resolution (Benishin *et al.*, 1988). Other evidence in support of homologue-specific receptors has also been obtained from binding studies in synaptosomes (Muniz *et al.*, 1990) and autoradiographically in rat brain (Awan & Dolly, 1991). The present study is the first to examine directly, by electrophysiological methods, the actions of Dtx homologues on K^+ currents in mammalian neurones; namely rat dorsal root ganglion cells (DRGs). Two components of current were

[1] Author for correspondence.

characterized in these cells, a slowly-inactivating K^+ current (SIC) and a non-inactivating current (NIC). All the toxin homologues reduced the amplitude of the total outward K^+ current and evidence was found for selective block of the two components of K^+ current by α-Dtx and δ-Dtx, in particular. Some of the results of the present study have already been reported in preliminary form (Owen *et al.*, 1990; Hall *et al.*, 1991).

Methods

DRG cells were isolated from neonatal rats (1–3 days) and cultured for up to 5 days in accordance with previous methods (Wood *et al.*, 1988). In some cases, cells were replated in order to remove neurites thus facilitating whole-cell voltage-clamp. The bathing medium contained (mM): NaCl 124, KCl 2.5, $MgCl_2$ 4, HEPES 5, glucose 10, sucrose 20, pH 7.4; Tetrodotoxin (TTX) 1 μM was included to eliminate voltage-activated Na^+ currents and calcium omitted in order to minimize contaminating Ca^{2+} and Ca^{2+}-activated currents. Deactivation of outward K^+ currents was studied in a medium containing elevated K^+ (25 mM) in order to enhance the amplitude of tail currents recorded following repolarization.

Electrophysiological recordings were made by the whole-cell patch-clamp method with an Axoclamp 2A amplifier (Axon Instruments) in switch-clamp mode (5–7 kHz). Patch electrodes were prepared with a two-stage pull (Brown and Flaming), fire-polished and dipped in silane (Sigma) to reduce capacitance. Electrode resistance was typically 4–8 MΩ when filled with an intracellular medium consisting of (mM): Kgluconate 140, $MgCl_2$ 2, EGTA 1.1, HEPES 5, Glucose 16, pH 7.2. Individual cells were continually superperfused with bathing medium (30–40 μl min^{-1}) via a micro-perfusion system through which drugs were also applied. Raw data were acquired and analysed by M2-Lab (Instrutech Corp.) with an ITC-16 interface and Atari Mega ST4 computer. Currents were filtered at 1 kHz and sampled at between 0.1 ms and 0.5 ms per point. Data were subsequently analysed using REVIEW (Instrutech Corp.). Exponential analysis was carried out with REVIEW and other curve-fitting performed using IGOR (Wavemetrics) and NonLinII (Stephen Ikeda) on a Macintosh IIx. In some cases currents were digitally subtracted to isolate the inactivating components. Otherwise no leak subtraction of currents was carried out (leak $<5\%$ of non-inactivating outward current activated at +60 mV).

α-, β-, γ- and δ-Dtx were isolated from crude venom of *D. angusticeps* according to published methods (Benishin *et al.*, 1988; Dolly, 1992). The β-Dtx fraction was found to consist of a mixture of β_1- and β_2-Dtx by capillary electrophoresis. Toxins I and K were purified from the venom of *D. polylepis polylepis* by ultra-filtration, cation exchange chromatography, followed by reverse-phase high performance liquid chromatography (h.p.l.c.).

Results

Electrophysiological characterization of outward K^+ currents

Voltage-clamp experiments revealed that the total outward current was composed of at least two components. Depolarizing voltage steps from a holding potential of −40 mV elicited a non-inactivating current (NIC), whilst an additional slowly-inactivating current (SIC) was recruited with a hyperpolarizing pre-pulse to −100 mV (Figure 1a: inset). This was reflected in the current-voltage (*I-V*) relationships obtained under the two conditions (Figure 1a).

In some cells there was an initial inward current (within the first 50 ms) which was attributed to a TTX-resistant Na^+ current (Kostyuk *et al.*, 1981; Roy & Narahashi, 1992) since it was abolished by replacement of Na^+ by $Tris^+$ ions (not shown). The reversal potential (*ca.* −80 mV) of the outward current was consistent with that expected for a K^+ conductance. Typically a 1s test pulse yielded 5–10 nA of outward current (peak) which normally inactivated slowly (30–50%) over the time course of the step (Figure 1).

Activation and inactivation properties

The inactivating current (SIC) evoked by a depolarizing voltage step from −100 mV was isolated from the total outward current by subtracting NIC. Thereby, a series of such

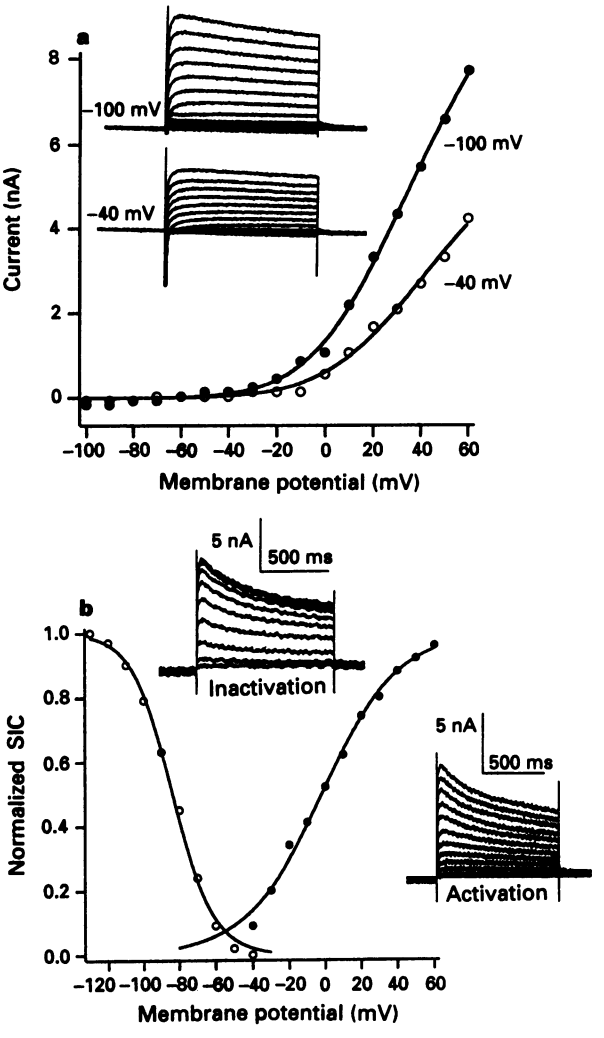


Figure 1 Inactivating and non-inactivating voltage-activated outward currents in dorsal root ganglia. (a) *Inset*: Raw current evoked with depolarizing voltage steps from holding potentiala of −100 mV (top panel) and −40 mV (lower panel). Tetrodotoxin (TTX)-resistant Na^+ currents are evident at the beginning of current records (truncated in upper traces). Current-voltage relationships constructed from the raw data: (○) −40 mV; (●) −100 mV. Additional current recruited by holding the cell at the more negative membrane potential. (b) activation and inactivation parameters of the slowly-inactivating current (SIC). The steady-state activation and inactivation curves were constructed from the peak values of difference currents (*insets*) which were obtained by subtracting the appropriate non-inactivating current (NIC) from the total outward currents measured at each voltage, as described in the Methods. The continuous lines drawn through the data points represent Boltzmann functions fitted to the raw data (inactivation: $V_h = -83.7$ mV, slope factor = 11.4 mV; activation: $V_h = -1.6$ mV, slope factor = 21.0 mV).

voltage steps were used to construct the steady-state activation- and inactivation-voltage relationships for SIC (Figure 1b). In the majority of cells, SIC was completely inactivated at between − 30 and − 40 mV. From the *I–V* curve for SIC, the threshold for activation of SIC was between − 50 mV and − 40 mV and a comparison of the *I-V* curves derived for SIC and total outward current suggested that NIC activated at more hyperpolarized potentials (− 70 mV to − 60 mV) (not shown).

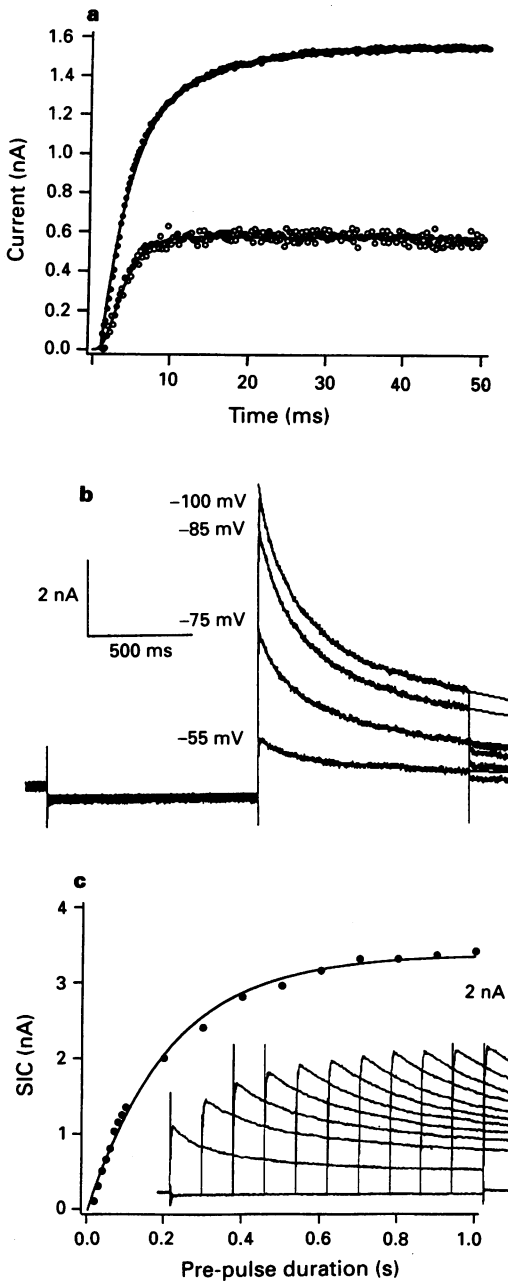


Figure 2 Kinetics of activation, inactivation and recovery from inactivation. (a) Currents were activated from a holding potential of − 30 mV or − 100 mV with a step to + 40 mV. Slowly inactivating current (SIC) was obtained by digital subtraction of current activated from − 30 mV (●). The non-inactivating current (NIC, ○), activated from − 30 mV, was leak subtracted (by scaling a − 10 mV hyperpolarizing pulse from − 60 mV). SIC (●) was fitted with a double exponential ($\tau_1 = 3.7$ ms, $\tau_2 = 14.6$ ms) with an offset of 2 ms. NIC (○) was fitted with a Hodgkin-Huxley function ($\tau = 0.5$ ms, $n = 4$). (b) SIC (obtained by subtraction) activated with a voltage step to + 60 mV following a pre-pulse (1 s) to membrane potentials indicated on the left. All the currents are fitted with a three component exponential function, the majority of the current in each case being described by the second and third components: − 55 mV (69 ms, 262 ms, 1.6 s); − 70 mV (47 ms, 239 ms, 1.8 s); − 85 mV (61 ms, 206 ms, 2.0 s); − 100 mV (53 ms, 203 ms, 2.1 s). (c) Recovery from inactivation at − 100 mV follows single exponential function ($\tau = 220$ ms). *Inset*: raw difference currents (*i.e.* difference between currents activated with and without prepulse to − 100 mV) vary with pre-pulse durations. Currents were activated at + 60 mV.

Activation kinetics

The time course of activation of SIC by a depolarizing step was best described by a double exponential function ($\tau_1 = 4$ ms, $\tau_2 = 15$ ms) following a brief delay (1.5 ms), whereas activation of NIC followed a sigmoidal time course which was well fitted by the Hodgkin-Huxley equation ($n = 4$ and $\tau = 0.5$ ms) (Figure 2a).

Inactivation

Inactivation of SIC was in most cases adequately described by the sum of three exponential components ($\tau_1 = 20$–80 ms,

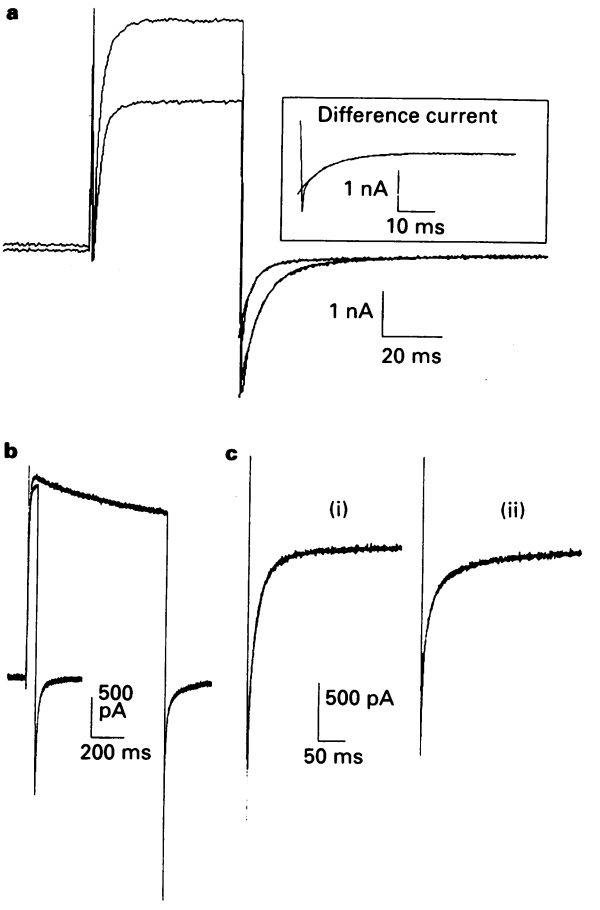


Figure 3 Inactivating current deactivates according to a single exponential. (a) Currents activated at + 40 mV either from − 80 mV (upper trace) or − 30 mV (lower trace). Tail currents measured following repolarization to − 80 mV decay according to a double or single exponential process, respectively. The tail currents have been fitted (fitted curve superimposed upon raw data) and parameters of 3.5 ms, 1.9 nA and 49 ms, 0.3 nA obtained for current activated from − 30 mV, whereas tail currents following current activated from − 80 mV gave parameters of: 6 ms, 3.2 nA and 99 ms, 0.3 nA. Tail current of the difference current (corresponding to the inactivating component of outward current) was fitted with a single exponential function ($\tau = 6.8$ ms). (b) Tail currents measured at 50 ms or 750 ms after activation of outward current at + 40 mV. (c) Tail currents as in (b) but shown on a faster sweep, (i) t = 50 ms, (ii) t = 750 ms. Double exponential fits are superimposed on the raw data. Parameters: 11.0 ms, 1.40 nA and 130 ms, 0.11 nA (t = 50 ms); 10.5 ms, 0.88 nA and 135 ms, 0.26 nA (t = 750 ms).

τ_2 = 200–300 ms and τ_3 = 1–3 s). The time-course of inactivation was not influenced by pre-pulse potential, between − 50 and − 100 mV, indicating that no additional currents were recruited over this range of membrane potentials (Figure 2b).

Recovery from inactivation of SIC followed a single exponential function (τ = 220 ms at − 100 mV, Figure 2c, the rate of which was voltage-sensitive (*eg.* at − 20 mV recovery was complete only after *ca.* 10 s; not shown). An anomalous decrease in amplitude of the activated current following

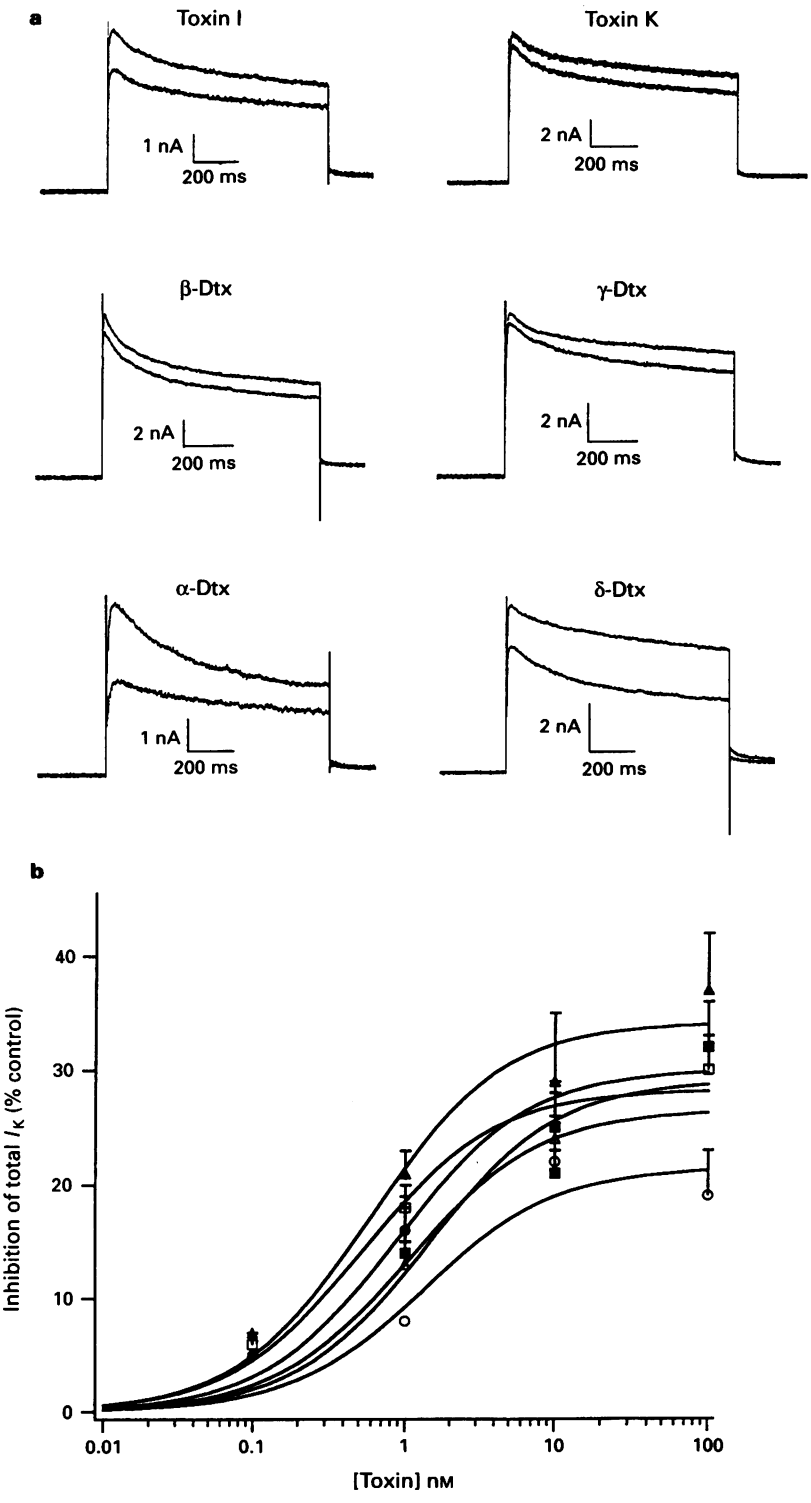


Figure 4 Block of voltage-activated currents in dorsal root ganglia cells by dendrotoxin homologues. (a) Dendrotoxin homologues from Black and Green Mamba venom applied by local perfusion at a concentration of 10 nM in each case. All homologues blocked voltage-activated K^+ current to some degree with variation in the extent of inhibition. In each panel two current records are shown overlaid, a control and one taken in the presence of a dendrotoxin homologue. All currents were activated with a voltage step to + 60 mV from a conditioning potential of − 100 mV. (b) Dose-response relationships constructed using the amount of inhibition of current at the end of voltage-steps by toxin. Data have been fitted with the logistic function and EC_{50}s derived from the equation: $y = y_{max}/1 + (EC_{50}/[toxin])^n$. EC_{50}s were: α-Dtx (●), 0.87 ± 0.35 nM; β-Dtx (○), 1.33 ± 1.11 nM; γ-Dtx (■), 1.39 ± 1.29 nM; δ-Dtx (□), 0.52 ± 0.18 nM; Toxin I (▲), 0.59 ± 0.27 nM; Toxin K (△), 1.04 ± 0.60 nM. S.e.means shown for n = 4–6. Bars represent s.e.mean, n = 4–6.

hyperpolarizations of up to 30 ms in duration occurred before subsequently increasing with more prolonged conditioning steps (not shown). In subsequent experiments, in order that inactivation be removed fully, a 1 s hyperpolarizing pre-pulse was employed.

Deactivation

The tail currents recorded at − 80 mV, following activation of outward currents at + 40 mV, decayed according to the sum of two exponential functions ($\tau_1 = 3-12$ ms and ($\tau_2 = 50-150$ ms: Figure 3a). The fast component was preferentially reduced when the holding potential was depolarized (*e.g.* − 30 mV) and indeed difference currents obtained under these circumstances could be fitted quite well by a single exponential function with time constant of 6.8 ms (Figure 3a: inset). Similarly, the fast component of the tail current was preferentially reduced following longer steps (Figure 3b and c). Thus tail current analyses indicated that SIC and NIC deactivate according to the fast and slow time constants, respectively.

Inhibition of voltage-activated K^+ currents by Dtx homologues

α-, β-, γ- and δ-Dtx homologues from *D. angusticeps* venom, and Toxins I and K from *D. polylepis polylepis* venom, exhibited a spectrum of activities on the outward K^+ current activated from − 100 mV (Figure 4). All the homologues were found to block outward current in a dose-dependent fashion and to varying degrees. The onset of inhibition by toxins was relatively quick, taking 1–2 min to reach steady-state. However, recovery from block by toxins was rarely complete. Typically 80–90% of the total outward current remained although the actual extent of washout and time taken to recover was dependent upon length of exposure and

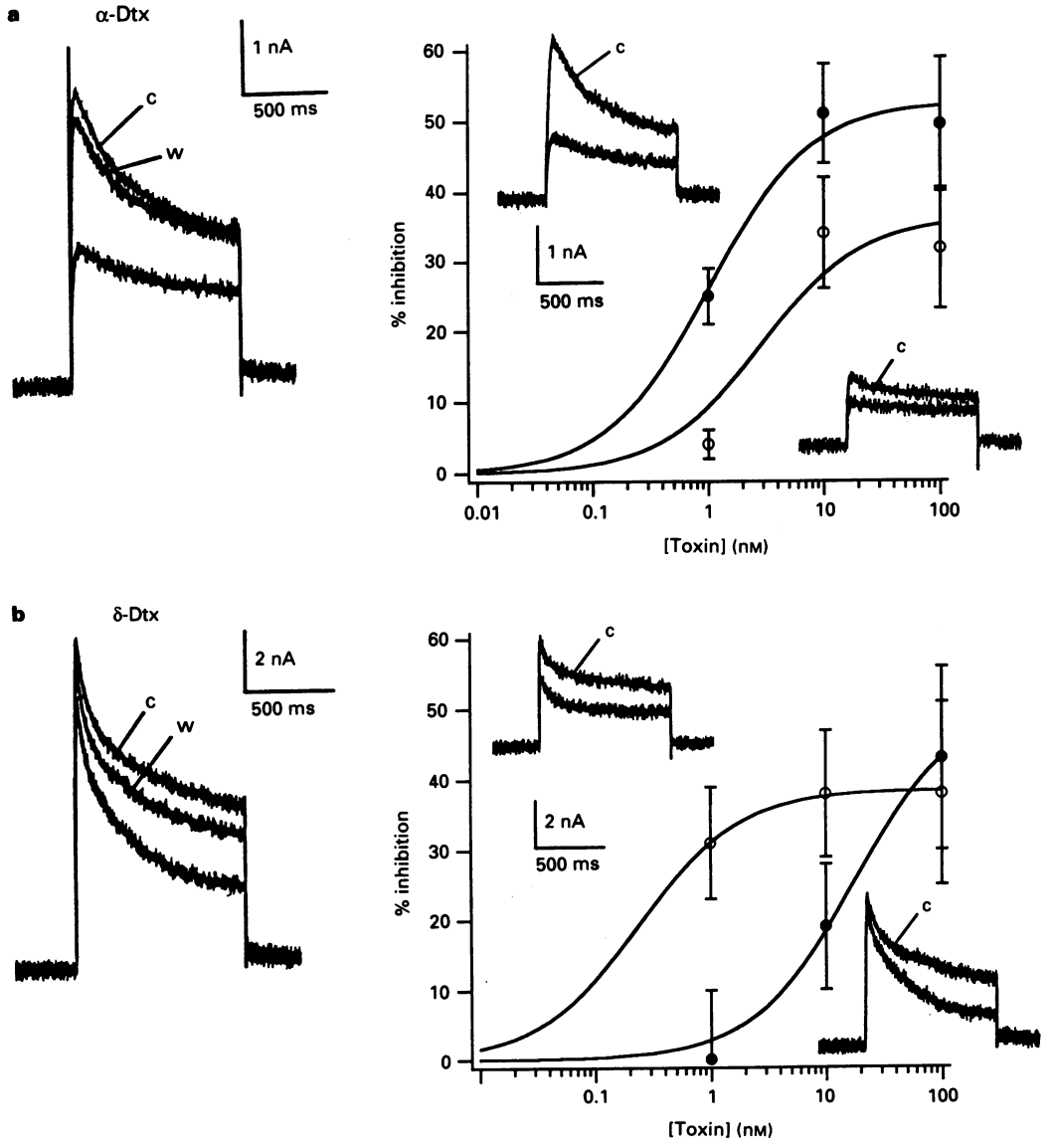


Figure 5 Differential block of slowly inactivating currents (SIC) and non-inactivating currents (NIC) by α-Dtx and δ-Dtx. Dose-response relationships for block of NIC and SIC by α-Dtx (a) and δ-Dtx (b). *Left*: whereas α-Dtx (10 nM) blocks a similar proportion of current at the beginning and end of the step, δ-Dtx (10 nM) shows time-dependent block. *Right*: Dose-response relationships for block of NIC (○) and SIC (●) components of current determined from difference currents (Methods). In each panel, insets are juxtaposed with the relevant dose-response curve *e.g.* top panel: top left insets are SIC currents (● in graph) and bottom right insets are NIC currents (○ in graph). In each case 'c' indicates the control current and 'w' the current after washout. Current amplitudes were measured at the end of voltage-steps and curves drawn according to the logistic function, from which EC_{50}s were derived: α-Dtx, 1.0 ± 0.4 nM and 2.9 ± 3.5 nM for SIC and NIC respectively; δ-Dtx, 17.6 ± 5.8 nM and 0.24 ± 0.03 nM for SIC and NIC, respectively. Bars represent s.e.mean, $n = 3-4$.

degree of block. For example, for a 1–3 min application of 10 nM α-Dtx, washout took *ca.* 5 min, whereas further irreversible inhibition was obtained by continued application of toxin for up to 10 min. Interestingly, the maximum amount of block achievable was *ca.* 30–40% of the control peak current (see graph, Figure 4b), although in some cells subjected to a more prolonged exposure (up to 10 min), the steady-state block by 10 nM α-Dtx reached *ca.* 50–70% of total current. In these cases only partial recovery was observed and an underlying rundown of the K^+ current, seen in other cells (10–20% over *ca.* 30 min), may have contributed to the observation.

Dose-reponse curves to each of the toxin homologues were fitted with the logistic function and EC_{50}s were thus derived (Figure 4b). δ-Dtx had the lowest EC_{50} (0.52 ± 0.18 nM), however although a factor of about 2.7 separated the EC_{50}s of the most and least active homologues, there were in fact no statistically-significant differences in the apparent potency in blocking the total outward currents.

Qualitative differences in the nature of block were observed in some cases. For example, the proportion of current blocked by 10 nM α-Dtx and Toxin I was constant throughout the duration of the step, whereas the effect of δ-Dtx was time-dependent, resulting in more inhibition at the end of the step than immediately after the depolarizing voltage jump (Figure 4a). A tendency for Toxin K and β- and γ-Dtx to behave in this way was also seen, although in these cases the response was much less clear-cut and was not studied further. The qualitative difference in the mode of block seen with α-Dtx and δ-Dtx, prompted an examination of whether it could be ascribed to a selective action on different components of K^+ current or, alternatively, differences in the mechanism of block.

Selective blockade of K^+ currents by dendrotoxin homologues

Difference currents In order to isolate the inactivating (SIC) and non-inactivating (NIC) currents, cells were held at − 30 mV or − 40 mV and currents activated with depolarizations to + 60 mV with or without a one second hyperpolarizing pre-pulse to − 100 mV (*e.g.* Figure 3a).

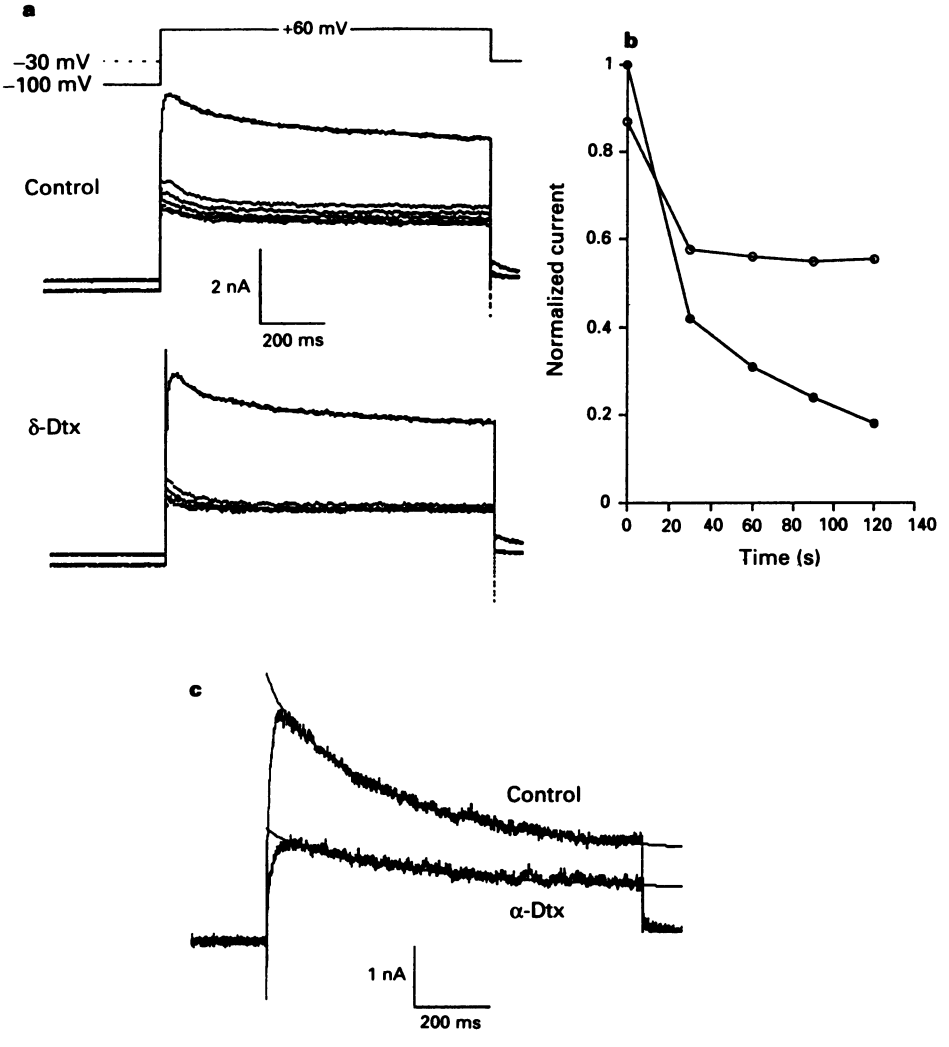


Figure 6 Effects of δ-Dtx and α-Dtx on inactivation of slowly inactivating current (SIC). (a) Series of currents evoked with a voltage step to + 60 mV before and during application of 3 nM δ-Dtx. First current in each series (largest) evoked following a condition step to − 100 mV. Current then declined with successive test depolarizations, the residual current representing non-inactivating current (NIC). (b) SIC (●) (normalized with respect to maximum amplitude) *vs* time to illustrate slow inactivation; (○) ratio of currents obtained *following* the conditioning pulse (to − 100 mV), in the presence and absence of δ-Dtx. The ratio decreases during the first 30 s but remains constant thereafter even though slow inactivation of SIC is not complete. (c) Two difference currents (SIC), superimposed, in the presence and absence of 10 nM α-Dtx. Although αDtx blocks *ca.* 50% of the current, there is no effect on the rate of decay. The two currents have been fitted with a three component exponential in each case having the parameters: control, 0.27 nA, $\tau_1 = 22.5$ ms; 1.97 nA, $\tau_2 = 238.0$ ms; 1.95 nA, $\tau_3 = 4.15$s; α-Dtx, 0.08 nA, $\tau_1 = 24.1$ ms; 0.69 nA, $\tau_2 = 269.0$ ms; 1.14 nA, $\tau_3 = 4.01$ s.

At low concentrations (*e.g.* 1 nM), α-Dtx was virtually selective for SIC and even at higher concentrations blocked SIC in preference to NIC. For example, in Figure 5a, 10 nM α-Dtx reduced SIC by *ca.* 60% compared with *ca.* 30% inhibition of NIC (leak current *ca.* 2% of control). Toxin I (1 nM) showed a similar selectivity of action (not shown). In contrast to α-Dtx, the overall effect of δ-Dtx on total outward current was very time-dependent (Figure 5b). Low concentrations of δ-Dtx (*e.g.* 1 nM) selectively blocked NIC although higher concentrations also blocked SIC to a variable degree (Figure 5b: inset). The voltage-dependence that gave rise to the observed time-dependent block, on occasion gave rise to an apparent *increase* in the amount of SIC, although evidently there was an *overall decrease* in total outward current (not shown). This selectivity for SIC and NIC by α-Dtx and δ-Dtx respectively, was reflected in the *I-V* relationships for α-Dtx and δ-Dtx-sensitive currents, which revealed δ-Dtx-sensitive current at more negative potentials (not shown).

These relationships indicate an equipotent molar ratio (e.p.m.r.) for α-Dtx over δ-Dtx of *ca.* 0.06, with respect to SIC, and 12.25 with respect to NIC. Although α-Dtx was apparently selective for SIC over NIC e.p.m.r. = 0.35), this was not statistically significant. On the other hand, δ-Dtx was selective for NIC over SIC (e.p.m.r. *ca.* 0.01). The maximum amount of block of SIC and NIC was similar for α-Dtx (53% and 36%, respectively) and δ-Dtx (51% and 38%, respectively).

Block by α-Dtx was not voltage-dependent having a negligible effect on the conductance-voltage relationship ($V_{1/2}$ shifted from + 5 mV to + 1 mV) (not shown). Furthermore, there was no effect of α-Dtx on the rate of inactivation of SIC (Figure 6c).. δ-Dtx (3 nM), on the other hand, clearly accelerated the decay of the total outward current (Figure 5b). This did not result from an acceleration of slow inactivation as indicated by the fact that the ratio of currents in the absence and presence of δ-Dtx reached a minimum within 30 s and was constant thereafter. In contrast slow inactivation was not complete until 2–3 min had elapsed (Figure 6b). Rather, it is likely that the time-dependent action of δ-Dtx reflects an open-channel type of block which is relieved at negative potentials.

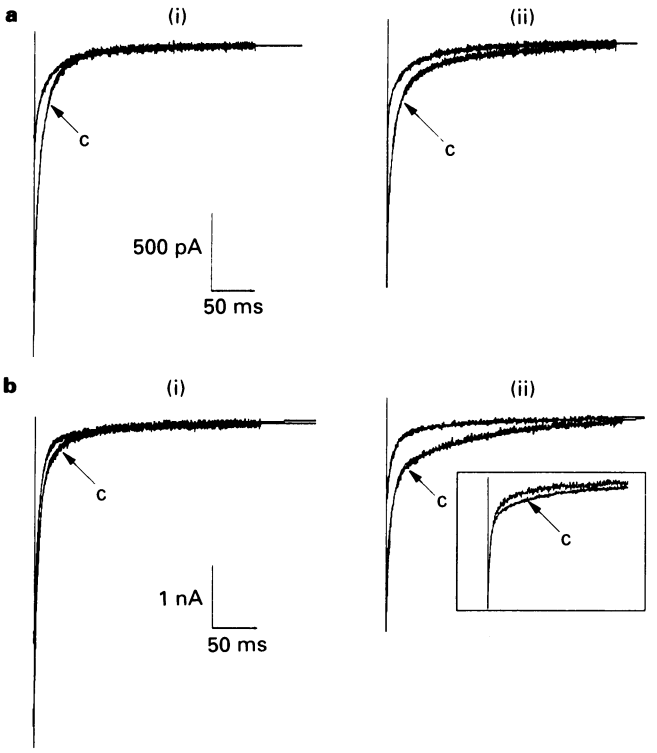


Figure 7 α-Dtx and δ-Dtx block different components of tail currents. Tail currents recorded in presence and absence of 3 nM α-Dtx (a) and 3 nM δ-Dtx (b). Tail currents were measured 50 ms (*i*) or 750 ms (*ii*) after activation (at + 40 mV) of outward current at a reference potential of − 80 mV. In each case (*c*) indicates the control current. Tail currents are fitted with double exponential functions: (a) (i) control: 0.18 nA, $\tau_1 = 63$ ms, 1.44 nA, $\tau_2 = 8.9$ ms; α-Dtx: 0.2 nA, $\tau_1 = 46.8$ ms, 0.38 nA, $\tau_2 = 9.8$ ms; (a) (ii) control: 0.28 nA, $\tau_1 = 128$ ms, 1.04 nA, $\tau_2 = 8.3$ ms; α-Dtx: 0.18 nA, $\tau_1 = 161$ ms, 0.33 nA, $\tau_2 = 11.1$ ms; (b) (i) control: 0.66 nA, $\tau_1 = 59.2$ ms, 4.2 nA, $\tau_2 = 5.1$ ms; δ-Dtx; 0.3 nA, $\tau_1 = 115$ ms, 3.2 nA, $\tau_2 = 5.6$ ms; (b) (ii) control: 0.91 nA, $\tau_1 = 141$ ms, 1.8 nA, $\tau_2 = 5.9$ ms; δ-Dtx: 0.31 nA, $\tau_1 = 234$ ms, 1.1 nA, $\tau_2 = 7.7$ ms. *Insert*: tail current in δ-Dtx scaled (× 2.4) to match peak of control tail current.

Tail currents

As shown by difference current analysis, α-Dtx and δ-Dtx were apparently selective for SIC and NIC, respectively. This conclusion was supported by the observation that the fast component of the tail current, which was associated with SIC (see above), was more sensitive to inhibition by α-Dtx than the slow component (Figure 7a). In contrast, the slow component of the tail current, which was attributed to deactivation of NIC, was preferentially reduced by δ-Dtx (Figure 7b).

For example, following activation to + 40 mV for 50 ms, α-Dtx (3 nM) reduced the fast component of deactivation ($\tau = 8.9–9.8$ ms) by 74%, whereas the amplitude of the slow component ($\tau = 47–62$ ms) remained relatively unaffected. Curiously, α-Dtx decreased the amplitude of the slow tail current, measured at $t = 750$ ms, although this was not as substantial an effect as the block of the fast component. In contrast, the principle effect of δ-Dtx (3 nM) was to decrease the amplitude of the slow component (55%, compared with a 24% reduction in the fast component). This effect was time-dependent, being more evident after longer voltage steps (Figure 7b). Interestingly, both α-Dtx and δ-Dtx appeared to slow the decay of the slow component of tail currents.

Discussion

Receptors for the K^+ channel toxins, α-Dtx, δ-Dtx and Toxin I, have been extensively characterized in neuronal tissue (Black *et al.*, 1988; Rehm & Lazdunski, 1988; Muniz *et al.*, 1990). With the exception of α-Dtx and Toxin I, functional activity of other Dtx homologues has so far only been studied against cloned K^+ channels (Kavanaugh *et al.*, 1990; Owen *et al.*, 1992) or indirectly, by monitoring ^{86}Rb efflux from rat brain synaptosomes (Benishin *et al.*, 1988; Sorensen *et al.*, 1990). The results of the latter experiments were interpreted as evidence of homologue selectivity for subtypes of voltage-activated K^+ channel (Benishin *et al.*, 1988). The results of the present study also suggest specificity of various homologues for sub-types of K^+ channel, although the details differ markedly from those of the above study.

We have identified two distinct components of voltage-activated K^+ current, a slowly-inactivating current (SIC) and a non-activating current (NIC). This was deduced from the following observations: (1) depolarized holding potentials inactivated a proportion of the total outward current activated by depolarizing voltage steps; (2) kinetic analysis showed that the activation of SIC and NIC were different; (3) tail current analysis revealed two exponential processes, consistent with the deactivation of two types of K^+ channel.

All the homologues blocked a fraction of the total voltage-activated K^+ current in these cells at concentrations in the range 1 nM–1 μM. The most potent of the homologues was δ-Dtx (EC_{50} *ca.* 0.5 nM) although the apparent differences between homologues in their ability to block *total* outward currents were not statistically significant. In all cases the toxin homologues blocked at most only *ca.* 35% of the total K^+ current, even at concentrations up to 1 μM (not shown). Furthermore, even with subtracted currents the maximum

amount of block was only *ca.* 50% (*e.g.* α-Dtx *vs.* SIC). This inability of dendrotoxins to block all of SIC or NIC might reflect an inherent property of the toxin-channel interaction. This seems unlikely since Dtx homologues cause almost complete block (up to 90%) of heterologously- (and singly-) expressed cloned K^+ α-subunits, such as mKv1.1 (Owen *et al.*, 1992). However, combinations of K^+ channel α-subunit sub-types into hetero-oligomeric structures may occur in the DRG, as has been found in various other neuronal preparations (Sheng *et al.*, 1993; Wang *et al.*, 1993; Scott *et al.*, 1994). Indeed at least four members of the Kv1 class K^+ channels are expressed in rat DRGs, including the Dtx-sensitive α-subunits: rKv1.1 (RCK1) and rKv1.2 (RCK5) and the Dtx-insensitive channels: rKv1.3 (RCK3) and rKv1.4 (RCK4) (Beckh & Pongs, 1990). *In vitro*, mixing and matching of subunits results in mixed properties although not in a predictable manner (Po *et al.*, 1993) and it is conceivable that the ceiling on block results from such a combination. An alternative explanation for this observation is that at a molecular level, SIC (*e.g.*) may comprise more than one species of inactivating channel which have varying sensitivity to dendrotoxins but are nevertheless isolated together on the basis of similar electrophysiological characteristics. Note, however that the association of single tail currents with SIC does not support this idea.

α- and δ-Dtx had qualitatively distinct blocking characteristics which implied different mechanisms of action. In particular, the block by δ-Dtx was voltage- and time-dependent, whereas the block by α-Dtx was neither. Furthermore as shown by both difference current and tail current analyses, α-Dtx and δ-Dtx selectively blocked SIC and NIC, respectively. The time-dependence of the block by δ-Dtx is consistent with an open-channel blocking mechanism and relief at hyperpolarized potentials in the continued presence of the toxin. The 'slow inactivation' of SIC (time course *ca.* 2.5 to 3 min) was unaffected by δ-Dtx since normalized (ratioed) currents remained constant after the initial 30 s. No growth phase was seen in the tail currents which could be ascribed to unblocking of channels, although there *was* an increase in the amplitude and time constant of decay of the slow component of the tail current in the presence of 3 nM δ-Dtx which could reflect such a phenomenon. The lack of time-dependence to the block by δ-Dtx of currents activated from −30 mV may reflect the fact that NIC is already at least partially activated at this potential.

These electrophysiological results suggest that α-Dtx and δ-Dtx have specificity for distinct subtypes of K^+ currents, although single channel recording is required to confirm such an interpretation. Support for this notion does come, however, from biochemical studies on toxin binding sites (Dolly, 1992) which suggest that δ-Dtx can distinguish between two α-Dtx receptors from bovine brain. At low concentrations (*e.g.* 1 nM, as used in this study), only one of these sites was labelled by δ-Dtx. Co-distribution of α-Dtx and δ-Dtx sites and mutual antagonism of their binding has been described in rat brain sections (Awan & Dolly, 1991) and it is tempting to speculate that this common acceptor might correspond to NIC. The weak affinity of δ-Dtx for the second population of α-Dtx acceptor, suggests that this site may reside on SIC channels, in view of the relatively weak block of this current by δ-Dtx. Additional support for the existence of distinct sites of action of α-Dtx and δ-Dtx is lent by the observation that α-Dtx, but not δ-Dtx, enhances electrically evoked noradrenaline release in rat hippocampus (Hu *et al.*, 1991). Furthermore, cloned rat brain K^+ channels from the *Shaker* sub-family (rKv1.1, rKv1.2 & rKv1.6), exhibit differential sensitivity to dendrotoxin homologues, when expressed in *Xenopus* oocytes: specifically, δ-Dtx is the more potent blocker of rKv1.1 (Kavanaugh *et al.*, 1990; Wittka & Pongs, personal communication) whereas against rKv1.2, the rank order is reversed and α-Dtx is more potent (Wittka & Pongs, personal communication). We therefore, tentatively suggest that NIC and SIC may represent rKv1.1 and rKv1.2, respectively.

The dendrotoxins share considerable sequence homology (Dufton, 1985; Harvey & Karlsson, 1982). Whereas the C-terminus is highly conserved (including the electrophysiologically-inactive protease-inhibitors). (Joubert & Taljaard, 1980; Dufton, 1985), the N-terminus of α-Dtx, Toxin I, δ-Dtx, Toxin K, β-Dtx and γ-Dtx varies significantly (Benishin *et al.*, 1988) and thus may be important in determining channel specificity. Several clusters of positively-charged residues are represented in all the homologues but with subtle variations. For example, δ-Dtx has three consecutive lysines at positions 17, 18 and 19, whereas Toxin K has two ($Lys^{17\ \&\ 19}$) and α-Dtx and Toxin I have only a one (Lys^{19}) in this region. Other regions of possible significance include a triplet of lysines in α-Dtx and Toxin I ($Lys^{28,\ 29\ \&\ 30}$) which lie on a protruding loop connecting two β-sheets in the tertiary structure (Skarzynski, 1992) and which is represented by only Lys^{28} & Lys^{30} in δ-Dtx and Toxin K. In addition, α-Dtx has three positively-charged residues (Arg^3, Arg^4 and Lys^5) at the N-terminus, whereas δ-Dtx has only one, Lys^5. Chemical modification of dendrotoxin also indicates that a positively charged residue at position 3 and residues around position 17 are important for biological activity (Hollecker *et al.*, 1993). The results obtained in the present study suggest that dendrotoxin homologues, in particular α-Dtx and δ-Dtx, may be useful pharmacological tools in the study of neuronal subtypes of voltage-activated K^+ channels. Further studies of the interactions of Dtx homologues with cloned K^+ channels, together with single channel recording in neurones, will be needed to determine the precise mechanisms underlying the different properties of α-Dtx and δ-Dtx observed here.

This study was funded in part by the Medical Research Council. A.H. was in receipt of an SERC-Wyeth Research (UK), CASE-studentship. We wish to thank David Parcej (Imperial College) and Zilda Muniz (Imperial College) for providing us with purified α-Dtx and purified δ-Dtx, respectively and Nadine Bissue (Wyeth Research) and Janette Scott (Wyeth Research) for the isolation and maintenance of DRGs in tissue culture.

References

AWAN, K.A. & DOLLY, J.O. (1991). K^+ channel sub-types in rat brain: characteristic locations revealed using β-bungarotoxin, α- and δ-dendrotoxins. *Neurosci.*, **40**, 29–39.

BECKH, S. & PONGS, O. (1990). Members of the RCK potassium channel family are differentially expressed in the rat nervous system. *EMBO. J.*, **9**, 777–782.

BENISHIN, C.G., SORENSEN, R.G., BROWN, W.E., KRUEGER, B.K. & BLAUSTEIN, M.P. (1988). Four polypeptide components of green mamba venom selectively block certain potassium channels in rat brain synaptosomes. *Mol. Pharmacol.*, **34**, 152–159.

BENOIT, E. & DUBOIS, J.-M. (1986). Toxin I from the snake *Dendroaspis polylepis polylepis*: a highly specific blocker of one type of potassium channel in myelinated nerve fiber. *Brain Res.*, **377**, 374–377.

BLACK, A.R., DONEGAN, C.M., DENNY, B.J. & DOLLY, J.O. (1988). Solubilization and physical characterisation of acceptors for dendrotoxin and β-bungarotoxin from synaptic membranes of rat brain. *Biochem.*, **27**, 6814–6820.

BOSMA, M.M., ALLEN, M.L., MARTIN, T.M. & TEMPEL, B.L. (1993). PKA-dependent regulation of mKv1.1, a mouse *Shaker*-like potassium channel gene, when stably expressed in CHO cells. *J. Neurosci.*, **13**, 5242–5250.

BRÄU, M.E., DREYER, F., JONAS, P., REPP, H. & VOGEL, W. (1990). A K^+ channel in *Xenopus* nerve fibres selectively blocked by bee and snake toxins: binding and voltage-clamp experiments. *J. Physiol.*, **420**, 365–385.

DOLLY, J.O., PARCEJ, D.N., SCOTT, V.E., MUNIZ, Z.M., SEWING, S. & PONGS, O. (1992). Molecular architecture of K^+ channels. *Neurochem. Int.*, (in press).

DUFTON, M.J. (1985). Proteinase inhibitors and dendrotoxins. *Eur. J. Biochem.*, **153**, 647–654.

HALL, A., STOW, J., DOLLY, O. & OWEN, D.G. (1991). Dendrotoxin homologues block voltage-dependent potassium currents in cultured rat dorsal root ganglion cells by different mechanisms. *10th World Congress on Animal, Plant & Microbial Toxins*, Abstr. 371.

HALLIWELL, J.V., OTHMAN, I.B., PELCHEN-MATTHEWS, A. & DOLLY, J.O. (1986). Central action of dendrotoxin: selective reduction of a transient K^+ conductance in hippocampus and binding to localised acceptors. *Proc. Natl. Acad. Sci. U.S.A.*, **83**, 493–497.

HARVEY, A.L. & KARLSSON, E. (1980). Dendrotoxin from the venom of the green mamba, *Dendroaspis angusticeps*. A neurotoxin that enhances the acetylcholine release at neuromuscular junctions. *Naunyn-Schmied. Arch. Pharmacol.*, **312**, 1–6.

HARVEY, A.L. & KARLSSON, E. (1982). Protease inhibitor homologues from mamba venoms: facilitation of acetylcholine release and interactions with prejunctional blocking toxins. *Br. J. Pharmacol.*, **77**, 153–161.

HOLLECKER, M., MARSHALL, D.L. & HARVEY, A.L. (1993). Structural features important for the biological activity of the potassium channel blocking dendrotoxins. *Br. J. Pharmacol.*, **110**, 790–794.

HU, P.S., BENISHIN, C. & FREDHOLM, B.B. (1991). Comparison of the effects of four dendrotoxin peptides, 4-aminopyridine and tetraethylammonium on the electrically-evoked [^{3}H]noradrenaline release from rat hippocampus. *Eur. J. Pharmacol.*, **209**, 87–93.

JOUBERT, F.J. & TALJAARD, N. (1980). The amino acid sequence of two proteinase inhibitor homologues from *Dendroaspis angusticeps* venom. *Hoppe-Seyler's Z. Physiol. Chem.*, **361**, 661–674.

KAVANAUGH, M.P., OSBORNE, P.B., CHRISTIE, M.J., BUSCH, A.E., HARTSHORNE, R.P., NORTH, R.A. & ADELMAN, J.P. (1990). Sensitivity to blocking agents of cloned potassium channels expressed in *Xenopus* oocytes. *Soc. Neurosci. Abstr.*, **16**, Abstr. 281.14.

KOSTYUK, P.G., VESELOVSKY, N.S. & TSYNDRENKO, A.Y. (1981). Ionic currents in the somatic membrane of rat dorsal root ganglion neurons-I. Sodium currents. *Neurosci.*, **6**, 2423–2430.

MUNIZ, Z.M., DINIZ, C.R. & DOLLY, J.O. (1990). Characterization of binding sites for δ-dendrotoxin in guinea-pig synaptosomes: relationship to acceptors for the K^+-channel probe α-dendrotoxin. *J. Neurochem.*, **54**, 343–346.

OWEN, D.G., HALL, A., SORENSEN, R.G. & STOW, J. (1990). Inhibition of outward currents in dorsal root ganglion cells by dendrotoxin homologues. *Soc. Neurosci. Abstr.*, **16**, Abstr. 156.8.

OWEN, D.G., ROBERTSON, B., HALL, A. & SCOTT, J.A. (1992). Blockade by peptidic toxins of MK1 potassium currents in CHO cells. *Soc. Neurosci. Abstr.*, **18**, Abstr. 335.1.

PARCEJ, D.N. & DOLLY, J.O. (1989). Dendrotoxin acceptor from bovine synaptic plasma membranes: binding properties, purification and subunit composition of a putative constituent of certain voltage-activated K^+ channels. *Biochem. J.*, **257**, 899–903.

PELCHEN-MATTHEWS, A. & DOLLY, J.O. (1989). Distribution in the rat central nervous system of acceptor sub-types for dendrotoxin, a K^+ channel probe. *Neuroscience*, **29**, 347–361.

PENNER, R., PETERSEN, M., PIERAU, F.-K. & DREYER, F. (1986). Dendrotoxin: a selective blocker of a non-inactivating potassium current in guinea-pig doral root ganglion neurones. *Pflüger's Arch.*, **407**, 365–369.

PO, S., ROBERDS, S., SYNDERS, D.J., TAMKUN, M.M. & BENNETT, P.B. (1993). Heteromultimeric assembly of human potassium channels. Molecular basis of a transient outward current? *Circ. Res.*, **72**, 1326–1336.

REHM, H. & LAZDUNSKI, M. (1988). Purification and subunit structure of a putative K^+ channel protein identified by its binding properties for dendrotoxin I. *Proc. Natl. Acad. Sci. USA*, **85**, 4919–4923.

REHM, H., NEWITT, R.A. & TEMPEL, B.L. (1989). Immunological evidence for a relationship between the dendrotoxin-binding protein and the mammalian homologue of the *Drosophila Shaker* K^+ channel. *FEBS Lett.*, **249**, 224–228.

REID, P.F., PONGS, O. & DOLLY, J.O. (1992). Cloning of a bovine voltage-gated K^+ channel gene utilising partial amino acid sequence of a dendrotoxin-binding protein from brain cortex. *FEBS Lett.*, **302**, 31–34.

ROBERTSON, B. & OWEN, D.G. (1993). Pharmacology of a cloned potassium channel from mouse brain (MK-1) expressed in CHO cells: effects of blockers and an inactivation peptide. *Br. J. Pharmacol.*, **109**, 725–735.

ROY, M.L. & NARAHASHI, T. (1992). Differential properties of tetrodotoxin-sensitive and tetrodotoxin-resistant sodium channels in rat dorsal root ganglion neurons. *J. Neurosci.*, **12**, 2104–2111.

SCOTT, V.E.S., PARCEJ, D.N., KEEN, J.N., FINDLAY, J.B.C. & DOLLY, J.O. (1990). α-dendrotoxin acceptor from bovine brain is a K^+ channel protein: evidence from the N-terminal sequence of its larger subunit. *J. Biol. Chem.*, **265**, 20094–20097.

SCOTT, V.E.S., MUNIZ, Z.M., SEWING, S., LICHTINGHAGEN, R., PARCEJ, D.N., PONGS, O. & DOLLY, J.O. (1994). Antibodies specific for distinct K_v subunits unveil a heterooligomeric basis for subtypes of α-dendrotoxin-sensitive K^+ channels in bovine brain. *Biochemistry*, **33**, 1617–1623.

SHENG, M., LIAO, Y.J., JAN, Y.N. & JAN, L.Y. (1993). Presynaptic A-current based on heteromultimeric K^+ channels detected *in vivo*. *Nature*, **365**, 72–75.

SKARZYNSKI, T. (1992). Crystal structure of α-dendrotoxin from the green mamba venom and its comparison with the structure of bovine pancreatic trypsin inhibitor. *J. Mol. Biol.*, **224**, 671–683.

SORENSEN, R.G., SCHNEIDER, M.J., ROGOWSKI, R.S. & BLAUSTEIN, M.P. (1990). Snake and scorpion neurotoxins as probes of rat brain synaptosomal potassium channels. *Prog. Clin. Biol. Res.*, **334**, 279–301.

STANSFELD, C.E., MARSH, S.J., HALLIWELL, J.V. & BROWN, D.A. (1986). 4-aminopyridine and dendrotoxin induce repetitive firing in rat visceral sensory neurones by blocking a slowly inactivating outward current. *Neurosci. Lett.*, **64**, 299–304.

STANSFELD, C. & FELTZ, A. (1988). Dendrotoxin-sensitive K^+ channels in dorsal root ganglion cells. *Neurosci. Lett.*, **93**, 49–55.

STRYDOM, D.J. (1976). Snake venom toxins. Purification and properties of low-molecular weight polypeptides of *Dendroaspis polylepis* (Black Mamba) venom. *Eur. J. Biochem.*, **69**, 169–176.

STÜHMER, W., RUPPERSBERG, J.P., SCHRÖTER, K.H., SAKMANN, B., STOCKER, M., GIESE, K.P., PERSCHKE, A., BAUMANN, A. & PONGS, O. (1989). Molecular basis of functional diversity of voltage-gated potassium channels in mammalian brain. *EMBO J.*, **8**, 3235–3244.

WANG, H., KUNKEL, D.D., MARTIN, T.M., SCHWARTZKROIN, P.A. & TEMPEL, B.L. (1993). Heteromultimeric K^+ channels in terminal and juxtaparanodal regions of neurons. *Nature*, **365**, 75–79.

WOOD, J.N., WINTER, J., JAMES, I.F., RANG, H.P., YEATS, J. & BEVAN, S. (1988). Capsaicin-induced ion fluxes in dorsal root ganglion cells in culture. *J. Neurosci.*, **8**, 3208–3220.

(Received February 24, 1994
Revised July 1, 1994
Accepted July 11, 1994)

Br. J. Pharmacol. (1994), **113**, 968–972 © Macmillan Press Ltd, 1994

Role of 5-HT_3 receptors in basal and K^+-evoked dopamine release from rat olfactory tubercle and striatal slices

A. Zazpe, I. Artaiz & J. [1]Del Río

Department of Pharmacology, School of Medicine, University of Navarra, 31080-Pamplona, Spain

1 The present study was aimed at examining the role of 5-HT_3 receptors in basal and depolarization-evoked dopamine release from rat olfactory tubercle and striatal slices. [^{3}H]-dopamine ([^{3}H]-DA) release was measured in both brain regions and endogenous dopamine release from striatal slices was also studied.

2 The selective 5-HT_3 receptor agonist 2-methyl-5-HT (0.5–10 μM) produced a concentration-dependent increase in [^{3}H]-DA efflux evoked by K^+ (20 mM) from slices of rat olfactory tubercle. 1-Phenylbiguanide (PBG) and 5-HT also increased K^+-evoked [^{3}H]-DA efflux.

3 5-HT (1–100 μM) increased in a concentration-dependent manner basal [^{3}H]-DA release from olfactory tubercle and striatal slices as well as endogenous DA release from striatal slices. The selective 5-HT_3 receptor agonists 2-methyl-5-HT and 1-phenylbiguanide were weaker releasing agents. In all cases, the release was Ca^{2+} independent and tetrodotoxin insensitive.

4 5-HT_3 receptor antagonists such as ondansetron, granisetron and tropisetron (0.2 μM) significantly blocked the enhanced K^+-evoked [^{3}H]-DA efflux from rat olfactory tubercle slices induced by 2-methyl-5-HT. A ten fold higher concentration of the 5-HT_2 receptor antagonist ketanserin was ineffective.

5 Much higher concentrations, up to 50 μM, of the same 5-HT_3 receptor antagonists did not block the increase in basal [^{3}H]-DA release from striatal or olfactory tubercle slices induced by 5-HT or the release of endogenous DA induced by 5-HT from striatal slices.

6 The DA uptake blocker nomifensine (10 μM) did not modify the enhancement in K^+-evoked [^{3}H]-DA efflux from rat olfactory tubercle slices induced by 2-methyl-5-HT. However, both nomifensine and cocaine significantly blocked the increase in basal dopamine release, either tritiated or endogenous, induced by 5-HT.

7 These results indicate that 5-HT_3 receptors only modulate DA release when the terminal fields of dopaminergic systems have been activated. In basal conditions, 5-HT_3 receptor agonists enhance DA release through a carrier-mediated mechanism. This may be of therapeutic relevance for the possible use of 5-HT_3 receptor antagonists under conditions of abnormal activation of the dopaminergic system.

Keywords: Dopamine release; 5-hydroxytryptamine; 5-HT_3 receptors; olfactory tubercle; striatum; 2-methyl-5-hydroxytryptamine; 1-phenylbiguanide; ondansetron; granisetron; tropisetron

Introduction

It has been suggested that antagonists at 5-hydroxytryptamine$_3$ (5-HT_3) receptors may be of value in the treatment of withdrawal reactions to drugs of abuse such as cocaine, morphine or ethanol (see reviews in Palfreyman *et al.*, 1993; Hagan *et al.*, 1993) and also in the treatment of schizophrenia (Hagan *et al.*, 1993). One of the mechanisms involved in these hypothetical therapeutic effects would be a blockade of the mesolimbic dopamine system activation induced by 5-HT_3 receptor stimulation (Costall *et al.*, 1987; Hagan *et al.*, 1987). It is known that agonists at this 5-HT receptor subtype are able to release dopamine from striatal and limbic regions both *in vitro* (Blandina *et al.*, 1989; Schmidt & Black, 1989; Yi *et al.*, 1991; Benuck & Reith, 1992; Jacocks & Cox, 1992) and *in vivo* (Jiang *et al.*, 1990; Chen *et al.*, 1991). Some *in vitro* experiments suggest that dopamine release by 5-HT_3 agonists is a receptor-mediated effect (Blandina *et al.*, 1989), while many other studies indicate that the release is carrier mediated (Schmidt & Black, 1989; Yi *et al.*, 1991; Benuck & Reith, 1992; Jacocks & Cox, 1992).

There is much behavioural, electrophysiological and neurochemical evidence suggesting that the 5-HT system may modulate the dopaminergic system, especially when the latter has been activated. In this regard, particular attention has been paid to 5-HT_3 receptors found in moderately high levels in terminal regions of the mesolimbic dopaminergic system, such as the nucleus accumbens, olfactory tubercle and amygdala (Kilpatrick *et al.*, 1988; Waeber *et al.*, 1989; Barnes *et al.*, 1990). Ondansetron, a typical 5-HT_3 receptor antagonist, is able to block the behavioural effects of amphetamine, a dopamine-releasing drug, when amphetamine is injected into the nucleus accumbens but not when given systemically (Costall *et al.*, 1987). Ondansetron also attenuates the increase in dopamine turnover induced by injection of the neurokinin agonist DiMe-C7 into the ventral tegmental area (Hagan *et al.*, 1987). Chronic administration of another 5-HT_3 antagonist, MDL-73147EF, decreases the number of spontaneously active dopaminergic neurones in the ventral tegmental area (A10) (Sorensen *et al.*, 1989), which have been associated with the rewarding effect of drugs of abuse (Koob & Bloom, 1988). Tropisetron reverses the increase in dopamine release resulting from stress (Imperato *et al.*, 1990) or from the administration of morphine, nicotine and ethanol (Carboni *et al.*, 1989).

The present study was aimed at examining the role of 5-HT_3 receptors in basal and depolarization-evoked dopamine release from slices of rat olfactory tubercle, a terminal field of the mesolimbic dopaminergic system. Tritium efflux was measured after loading the slices with [^{3}H]-dopamine both under basal conditions and after stimulation with KCl. Slices from rat striatum were comparatively studied. In this region, endogenous dopamine release was also studied. A preliminary report of this study has been presented elsewhere (Del Río & Zazpe, 1993).

[1] Author for correspondence.

Methods

Preparation of brain slices

Olfactory tubercles or corpora striata from male Wistar rats (200–250 g) were dissected and cut sagitally into 350 μm sections with a McIlwain tissue slicer. Each superfusion chamber contained tissue from two rats. The cut tissue was washed three times in gassed (95% O_2/5% CO_2) Krebs solution (NaCl 113; $NaHCO_3$ 25; KCl 4.75; NaH_2PO_4 1.18; $CaCl_2$ 2.52; $MgSO_4$ 1.19; glucose 10 and pargyline 0.01 mM).

Release of endogenous dopamine

The slices were placed in 1 ml chambers and superfused in an overflow manner at a rate of 0.5 ml min^{-1} with gassed Krebs solution at 37°C. After a 75 min equilibration period, 1.5 ml samples were collected into tubes containing 166 μl of a solution of 1 N $HClO_4$, 0.1% ascorbic acid and 20.8 ng of dihydroxybenzylamine as an internal standard. At selected times, slices were exposed to the 5-HT agonist for 12 min by transferring the chamber inflow tubing to reservoirs containing medium of appropriate composition. When the interaction of a given compound with the 5-HT agonist was studied, slices were perfused with the compound 30 min before adding the 5-HT agonist. Dopamine (DA) release was calculated as percentage increase over basal release. The concentration of DA was determined by high-pressure liquid chromatography with electrochemical detection as previously described (Pérez-Otaño *et al.*, 1991).

Release of [^{3}H]-dopamine

Slices were incubated with agitation in 5 ml of gassed Krebs solution with 0.1 μM [^{3}H]-dopamine (35 Ci mmol^{-1}, Amersham). After this time the tissue was washed three times with normal Krebs and the superfusion procedure was initiated as above. The equilibration period was 90 min. Samples were collected and 80 μl aliquots were added to 4 ml of scintillation fluid (Biogreen no. 3) for radioactivity counting. Under the present experimental conditions, it is generally accepted that the radioactivity released from slices is predominantly [^{3}H]-DA (e.g. Werling *et al.*, 1988).

K$^+$-evoked release of [^{3}H]-dopamine

Slices were placed in a Krebs solution containing 39.75 mM KCl (tonicity maintained by reducing the NaCl concentration) and the flasks were shaken at 37°C for 20 min. After being washed the slices were incubated at 37°C for 30 min in normal Krebs buffer containing 0.1 μM [^{3}H]-dopamine (35 Ci mmol^{-1}). Washed slices were placed into 1 ml superfusion chambers and superfused with Krebs solution (0.5 ml min^{-1}) at 37°C. After a 35 min washout period, 3 min samples of perfusate were collected. At 12 min (S_1) and 42 min (S_2) the slices were depolarized by changing the superfusion fluid for 6 min to a Krebs solution containing 20 mM KCl. All test drugs were added 15 min before S_2. The superfusate samples were collected over a 60 min period. S_2 and S_1 were calculated as K$^+$-stimulated tritium increase on basal efflux.

Drugs and chemicals

The following drugs were used: [^{3}H]-dopamine (Amersham), 5-hydroxytryptamine, creatinine sulphate, cocaine and pargyline (Sigma), 2-methyl-5-HT, 1-phenylbiguanide and nomifensine (RBI), tropisetron (Sandoz), granisetron (SmithKline Beecham) and ondansetron (Glaxo). Inorganic salts and all other reagents were from Merck.

Results

Effect of 5-HT agoniss on K$^+$-evoked [^{3}H]-DA release from olfactory tubercle slices

Tritium efflux was practically the same after the two K$^+$ pulses (S_2/S_1 ratio = 1.07 ± 0.07; n = 7). The selective 5-HT$_3$ receptor agonist 2-methyl-5-HT (2-Me-5-HT) produced a concentration-dependent increase in K$^+$-evoked [^{3}H]-DA efflux (S_2/S_1 ratio) from slices of rat olfactory tubercle preloaded with [^{3}H]-DA (Figure 1). Phenylbiguanide (PBG) produced substantially the same effect and 5-HT was not significantly more potent than the selective 5-HT$_3$ agonists (Figure 1). The K$^+$-evoked [^{3}H]-DA efflux was virtually absent in the absence of Ca^{2+} in the superfusion medium (not shown). Tetrodotoxin (TTX, 1 μM) partially blocked the K$^+$-evoked tritium overflow. S_2/S_1 for control and TTX was 1.07 ± 0.07 and 0.83 ± 0.07 respectively (n = 5; $P<0.05$). A similar percentage blockade was observed in slices stimulated with K$^+$ and 2-Me-5-HT (2-Me-5-HT, 1.69 ± 0.07; TTX + 2-Me-5-HT, 1.35 ± 0.09).

Effect of 5-HT agonists on basal DA release from olfactory tubercle or striatal slices

The percentage release from striatal slices produced by 5-HT on either tritiated or endogenous DA was practically identical. The percentage release of [^{3}H]-DA obtained from olfactory tubercle slices was slightly higher (Figure 2). Selective 5-HT$_3$ receptor agonists produced a weaker effect on DA

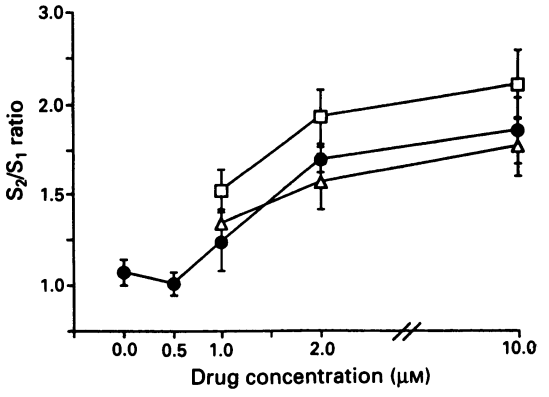


Figure 1 Concentration-dependent increase induced by 2-methyl-5-HT (●), 1-phenylbiguanide (△) and 5-HT (□) in K$^+$-evoked [^{3}H]-dopamine efflux from rat olfactory tubercle slices preloaded with [^{3}H]-dopamine. Data are means (± s.e.mean) of 4–10 experiments.

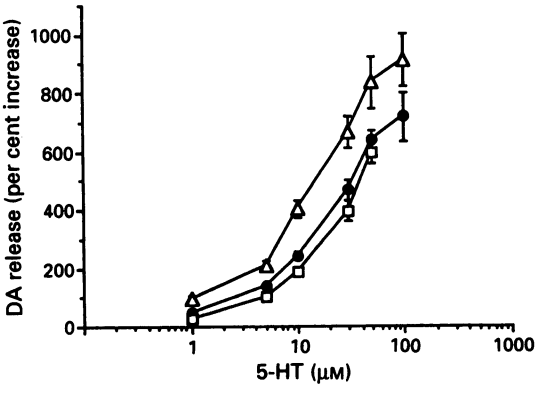


Figure 2 Effect of 5-HT on dopamine release from rat brain slices (per cent increase over basal values). Data are means (± s.e.mean) of at least five separate experiments (△---△) [^{3}H]-dopamine, olfactory tubercle; (●---●) [^{3}H]-dopamine, striatum (□---□) endogenous dopamine, striatum.

Table 1 Effect of 5-HT and 5-HT_3 receptor agonists on release of tritiated or endogenous dopamine from rat striatal (str.) and olfactory tubercle (o.t.) slices

5-HT agonist (μM)	*[^{3}H]-DA (o.t.)*	*[^{3}H]-DA (str.)*	*DA (str.)*
5-HT (10)	405 ± 28	242 ± 12	188 ± 10
PBG (10)	241 ± 23	166 ± 14	118 ± 18
PBG (30)	438 ± 32	256 ± 20	238 ± 52
2-Me-5-HT (100)	122 ± 18	53 ± 7	n.d.

Data (means ± s.e.; $n = 4-6$) are expressed as per cent increase over basal release. PBG, 1 phenylbiguanide; n.d., not determined.

release (Table 1). The releasing effect of 2-Me-5-HT on endogenous dopamine was not determined because of interference of the chromatographic peak of this drug with dopamine. In all cases, the release was not modified by omission of Ca^{2+} in the superfusion medium and was tetrodotoxin insensitive (not shown).

Basal [^{3}H]-DA release was also studied in olfactory tubercle slices pre-exposed for 20 min to a high-K^+ solution, as in the above experiments on K^+-evoked [^{3}H]-DA efflux, and no difference in percentage release was apparent after this previous exposure. Using these experimental conditions, the percentage increase in basal [^{3}H]-DA release induced by 5 μM 5-HT was 188.7 ± 19.3 (mean ± s.e.mean of five experiments), and 2-Me-5-HT (10–50 μM) did not show any significant effect on basal [^{3}H]-DA release. Endogenous DA release was not studied in striatal slices pre-exposed to a high level of K^+ since the rise in DA induced by 5-HT in the subsequent experiments was not high enough for accurate chromatographic quantification.

Effect of 5-HT_3 receptor antagonists on K^+-evoked [^{3}H]-DA release from olfactory tubercle slices

All of the studied 5-HT_3 receptor antagonists lacked any intrinsic effect on K^+-stimulated release. For example, S_2/S_1 ratio after 2 μM ondansetron was 1.12 ± 0.10 ($n = 4$). Ondansetron (0.05–2 μM) produced a concentration-dependent blockade of the increased K^+-evoked [^{3}H]-DA efflux induced by 2-Me-5-HT in rat olfactory tubercle slices (Figure 3). Other 5-HT_3 receptor antagonists such as granisetron and tropisetron (0.2 μM) also blocked the effect of 2-Me-5-HT (Figure 3). A ten fold higher concentration (2 μM) of ketanserin, a 5-HT_2 receptor antagonist, did not modify the effect of 2-Me-5-HT (Figure 4). The increased K^+-evoked [^{3}H]-DA efflux induced by 5-HT was again blocked by ondansetron and not by ketanserin, 2 μM each. S_2/S_1 ratio was 1.96 ± 0.15, 1.31 ± 0.14 and 1.72 ± 0.24 for 5-HT, 5-HT + ondansetron and 5-HT + ketanserin respectively ($n = 4-6$).

Effect of 5-HT_3 receptor antagonists on basal DA release

At variance with the above results, much higher concentrations (10 or 50 μM) of the 5-HT_3 receptor antagonists ondansetron, granisetron or tropisetron did not block the increase in basal [^{3}H]-DA release from olfactory tubercle or striatal slices induced by 5–10 μM 5-HT or the release of endogenous DA induced by 10 μM 5-HT in striatal slices. Control release (per cent increase over basal) was essentially the same in all cases: [^{3}H]-DA (olfactory tubercle), 213 ± 21; endogenous DA (striatum), 182 ± 23; [^{3}H]-DA (striatum), 229 ± 25. The results obtained in the presence of 5-HT_3 receptor antagonists were practically identical (not shown). The increase in [^{3}H]-DA induced by the 5-HT_3 receptor agonist PBG was not blocked by either ondansetron or tropisetron, 50 μM each (not shown).

In olfactory tubercle slices pre-exposed to a high level of K^+, 5-HT_3 receptor antagonists did not block the increase in basal [^{3}H]-DA release induced by 5-HT. For example, 2 μM 5-HT produced a percentage increase over basal values of 77.3 ± 11.7 and 70.3 ± 9.4 ($n = 5$) when tested alone and in the presence of 2 μM ondansetron respectively. A higher ondansetron concentration (10 μM) was also unable to block the enhanced release after 10 μM 5-HT; percentage increases were 378 ± 29 and 358 ± 22 for 5-HT and 5-HT + ondansetron respectively.

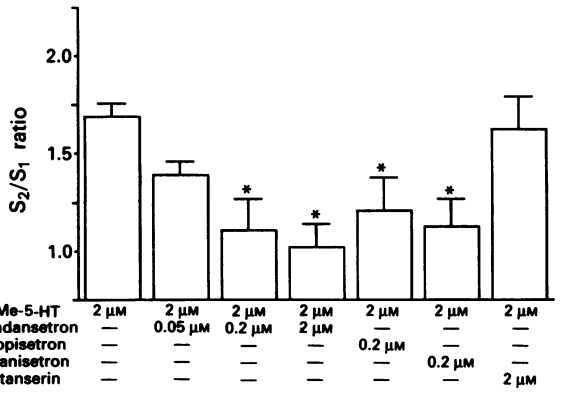


Figure 3 Effect of 5-HT_3 and 5-HT_2 receptor antagonists on the enhanced K^+-evoked [^{3}H]-dopamine efflux from rat olfactory tubercle slices induced by 2-methyl-5-HT. Data are means (± s.e.mean) of at least five separate experiments. *$P < 0.01$ *vs* 2-Me-5-HT (Student's *t* test).

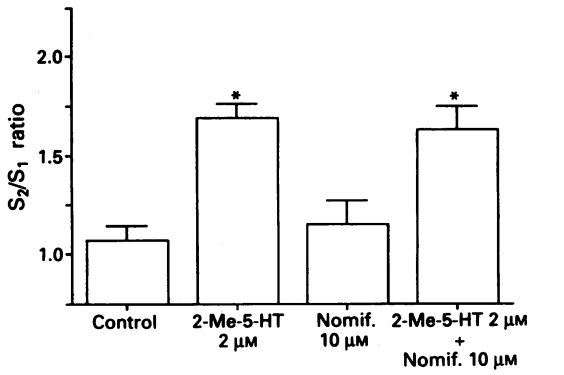


Figure 4 Lack of effect of nomifensine (nomif.) on the enhanced K^+-evoked [^{3}H]-dopamine efflux from rat olfactory tubercle slices induced by 2-methyl-5-HT. Data are means (± s.e.mean) of five separate experiments. *$P < 0.01$ *vs* control (Student's *t* test).

Effect of DA uptake blockers on K^+-evoked and basal DA release from olfactory tubercle and striatal slices

Nomifensine (10 μM) did not show an intrinsic effect on K^+-evoked [^{3}H]-DA efflux from rat olfactory tubercle slices. The same concentration of nomifensine did not modify the enhancing effect of 2-Me-5-HT on K^+-evoked tritium efflux (Figure 4).

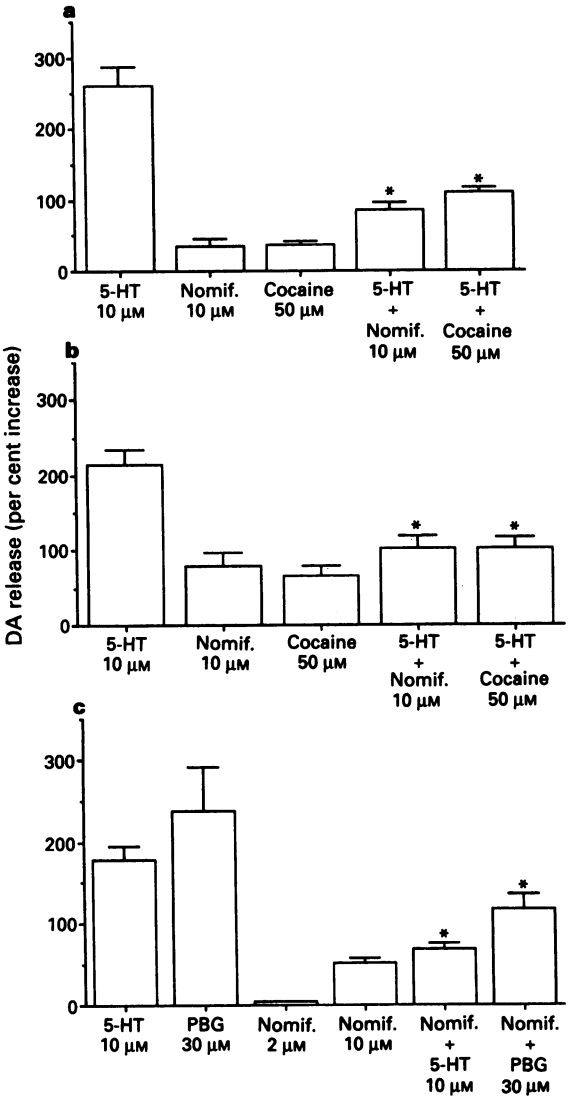


Figure 5 Blockade by nomifensine (nomif.) and cocaine of dopamine release from rat brain slices (per cent increase over basal values) induced by 5-HT or 1-phenylbiguanide (PBG). Data are means (± s.e.mean); $n = 4-7$. (a) [^{3}H]-dopamine, striatum; (b) [^{3}H]-dopamine, olfactory tubercle; (c) endogenous dopamine, striatum. *$P < 0.01$ *vs* 5-HT (Student's *t* test).

Basal [^{3}H]-DA release was not modified by 2 μM nomifensine or 10 μM cocaine and was enhanced by five fold higher concentrations of the DA uptake blockers (Figure 5a and b). Both nomifensine (10 μM) and cocaine (50 μM) were able to significantly block the much larger increase in basal [^{3}H]-DA release from striatal or olfactory tubercle slices induced by 5-HT (Figure 5a and b). The lower concentrations of nomifensine and cocaine, 2 and 10 μM respectively, also produced a small but significant decrease in 5-HT-induced [^{3}H]-DA release (not shown). Nomifensine also blocked the increase in endogenous DA release from striatal slices produced by 5-HT or PBG (Figure 5c).

Discussion

The present results provide evidence for the modulation by 5-HT$_3$ receptors of K^+-evoked dopamine release from slices of rat olfactory tubercle. Conversely, when terminal fields of the mesolimbic or nigrostriatal dopaminergic system are not activated with K^+, 5-HT and 5-HT$_3$ receptor stimulants enhance dopamine release through a carrier-mediated mechanism.

Previous studies have addressed the role of 5-HT$_3$ receptors in dopamine release by using either slices (Blandina *et al.*, 1989; Benuck & Reith, 1992; Jacocks & Cox, 1992) or synaptosome preparations (Yi *et al.*, 1991) from rat brain regions and measuring either endogenous dopamine release or tritium efflux after preloading the preparation with [^{3}H]-DA. In the present study, all experiments were carried out in brain slices, which allow the detection of effects mediated by receptors located not only on nerve terminals but also on interneurones. As to the interest in measuring tritium efflux or endogenous dopamine release, previous studies indicate that tritium efflux closely mimics endogenous dopamine release (Herdon *et al.*, 1985; Werling *et al.*, 1988). The almost identical results obtained with striatal slices in the present study (Figure 3) corroborate this assumption.

In keeping with several previous studies (Nurse *et al.*, 1988; Schmidt & Black, 1989; Yi *et al.*, 1991; Benuck & Reith, 1992; Jacocks & Cox, 1992), 5-HT-enhanced [^{3}H]-DA release was prevented by DA uptake blockers and not by 5-HT$_3$ receptor antagonists. Partial depletion of endogenous DA stores by pre-exposure of the slices to a high level of K^+ did not modify the effect of 5-HT or 2-Me-5-HT on basal [^{3}H]-DA release and, likewise, 5-HT$_3$ receptor antagonists were unable to block the enhancement in basal [^{3}H]-DA efflux induced by 5-HT. This is consonant with the ability of PBG to promote [^{3}H]-DA efflux in striatal slices from rats pretreated with reserpine (Benuck & Reith, 1992): not only are endogenous DA stores markedly reduced but DA storage mechanisms are also affected. Release of either endogenous or tritiated dopamine by 5-HT or 5-HT$_3$ receptor agonists was not dependent on Ca^{2+} and was also tetrodotoxin insensitive, thus supporting the notion of a carrier-mediated release of the neurotransmitter (see Levi & Raiteri, 1993). However, our results are not in accordance with those reported by Blandina *et al.* (1989), who found that 5-HT$_3$ receptor antagonists are able to prevent endogenous DA release from striatal slices. Since in their study all experiments were carried out in the presence of nomifensine, it is possible that other mechanisms may still be operative in such an experimental condition. The comparatively low density of 5-HT$_3$ receptors in the striatum compared with limbic and cortical areas (Kilpatrick *et al.*, 1988) raises some doubt about their physiological significance in this brain region.

K^+-stimulated dopamine release from the olfactory tubercle showed a strong Ca^{2+} dependence, consistent with an exocytotic mechanism. At a 20 mM K^+ concentration, the neuronal firing would be activated and this would activate in turn Ca^{2+} influx (Illes, 1986). However, K^+-evoked dopamine release was only partially tetrodotoxin sensitive, indicating that only a part of the K^+-stimulated release is dependent on excitatory input from sites distal to the terminal (Jacocks & Cox, 1992). Tetrodotoxin blocked to approximately the same extent the enhancement by 2-Me-5-HT of the K^+-stimulated release, suggesting that 5-HT$_3$ receptor activation potentiates the K^+ effect, probably by contributing to a greater ionic influx through opening of the associated 5-HT-gated channel (Derkach *et al.*, 1989).

Forebrain 5-HT$_3$ receptors are concentrated in terminal fields of the mesolimbic dopaminergic system, such as the olfactory tubercle (Kilpatrick *et al.*, 1988) so their role at this level should be more relevant than at the striatum. Interestingly, it seems that these receptors are only operative in the control of dopamine release when dopaminergic terminals have been depolarized by a high potassium concentration. Under these experimental conditions, there is not a marked difference in potency between the specific 5-HT$_3$ receptor agonists 2-Me-5-HT or PBG and 5-HT, as is the case when their effects on basal dopamine release are compared. It is possible that under conditions of K^+-stimulated exocytotic release 5-HT may act also on presynaptic receptors inhibiting dopamine release (see Levi & Raiteri, 1993). The enhancement of K^+-evoked dopamine release by 5-HT seems to be dependent on 5-HT$_3$ receptor stimulation and not on activa-

tion of any other 5-HT receptor subtype. The lack of blockade by ketanserin of the 5-HT effect argues against the involvement of 5-HT_2 receptors, which rather appear to control carrier-mediated release of dopamine (Nash, 1990; Huang & Nichols, 1993).

The results of the present study showing that 5-HT_3 receptor antagonists are only able to prevent the effect of serotonergic stimulation on terminal fields of the mesolimbic dopaminergic system when this system has been previously activated by K^+ offer parallelism with many *in vivo* studies and stress the potential psychiatric interest of a class of drugs that would only be affecting the dopaminergic system under conditions of abnormal activation.

We thank Gobierno de Navarra (Spain) for a fellowship to one of us (I.A.). The generous gift of drugs by pharmaceutical companies is gratefully acknowledged.

References

BARNES, J.M., BARNES, N.M., CHAMPANERIA, S., COSTALL, B. & NAYLOR, R.J. (1990). Characterization and autoradiographic localization of 5-HT_3 receptor recognition sites identified with [^{3}H]-(S)-zacopride. *Neuropharmacology*, **29**, 1037–1045.

BENUCK, M. & REITH, M.E.A. (1992). Dopamine releasing effect of phenylbiguanide in rat striatal slices. *Naunyn-Schmied. Arch. Pharmacol.*, **345**, 666–672.

BLANDINA, P., GOLDFARB, J., CRADDOCK-ROYAL, B. & GREEN, J.P. (1989). Release of endogenous dopamine by stimulation of 5-hydroxytryptamine$_3$ receptors in rat striatum. *J. Pharmacol. Exp. Ther.*, **251**, 803–809.

CARBONI, E., ACQUAS, E., FRAU, R. & DI CHIARA, G. (1989). Differential inhibitory effects of a 5-HT_3 antagonist on drug-induced stimulation of dopamine release. *Eur. J. Pharmacol.*, **164**, 515–519.

COSTALL, B., DOMENEY, A.M., NAYLOR, R.J. & TYERS, M.B. (1987). Effects of the 5-HT_3 receptor antagonist, GR 38032F, on raised dopaminergic activity in the mesolimbic system of rat and marmoset brain. *Br. J. Pharmacol.*, **92**, 881–894.

CHEN, J., VAN PRAAG, H.M. & GARDNER, E.L. (1991). Activation of 5-HT_3 receptor by 1-phenylbiguanide increases dopamine release in the rat nucleus accumbens. *Brain Res.*, **543**, 354–357.

DEL RIO, J. & ZAZPE, A. (1993). Release of dopamine from rat olfactory tubercle is mediated by activation of 5-HT_3 receptors. *Soc. Neurosci. Abstr.*, **23**, 1380.

DERKACH, V., SUPRENANT, A. & NORTH, R.A. (1989). 5-HT3 receptors are membrane ion-channels. *Nature*, **339**, 706–709.

HAGAN, R.M., BUTLER, A., HILL, J.M., JORDAN, C.C., IRELAND, S.J. & TYERS, M.B. (1987). Effect of the 5-HT_3 receptor antagonist, GR 38032F, on responses to injection of a neurokinin agonist into the ventral tegmental area of the brain. *Eur. J. Pharmacol.*, **138**, 303–305.

HAGAN, R.M., KILPATRICK, G.J. & TYERS, M.B. (1993). Interactions between 5-HT_3 receptors and cerebral dopamine function: implications for the treatment of schizophrenia and psychoactive substance abuse. *Psychopharmacology*, **112**, S68–S75.

HERDON, H., STRUPISH, J. & NAHORSKI, S.R. (1985). Differences between the release of radiolabelled and endogenous dopamine from superfused rat brain slices: effect of depolarizing stimuli, amphetamine and synthesis inhibition. *Brain Res.*, **348**, 309–320.

HUANG, X. & NICHOLS, D.E. (1993). 5-HT_2 receptor-mediated potentiation of dopamine synthesis and central serotonergic deficits. *Eur. J. Pharmacol.*, **238**, 291–296.

ILLES, P. (1986). Mechanisms of receptor-mediated modulation of transmitter release in noradrenergic, cholinergic and sensory neurons. *Neuroscience*, **17**, 909–928.

IMPERATO, A., PUGLISI-ALLERGRA, S., ZOCCHI, A., SCROCCO, M.G., CASOLINI, P. & ANGELUCCI, L. (1990). Stress activation of limbic and cortical dopamine release is prevented by ICS205-930 but not diazepam. *Eur. J. Pharmacol.*, **175**, 211–214.

JACOCKS, H.M. & COX, B.M. (1992). Serotonin-stimulated release of [^{3}H]dopamine via reversal of the dopamine transporter in rat striatum and nucleus accumbens: a comparison with release elicited by potassium, N-methyl-D-aspartic acid, glutamic acid and D-amphetamine. *J. Pharmacol. Exp. Ther.*, **262**, 356–364.

JIANG, L.H., ASHBY, Jr. C.R., KASSER, R.J & WANG, R.Y. (1990). The effect of intraventricular administration of the 5-HT_3 receptor agonist 2-methyl-serotonin on the release of dopamine in the nucleus accumbens: an in vivo chronocoulometric study. *Brain Res.*, **513**, 156–160.

KILPATRICK, G.J., JONES, B.J. & TYERS, M.B. (1988). The distribution of specific binding of the 5-HT_3 receptor ligand [^{3}H] GR 65630 in rat brain using quantitative autoradiography. *Neurosci. Lett.*, **94**, 156–160.

KOOB, G.F. & BLOOM, F.E. (1988). Cellular and molecular mechanisms of drug dependence. *Science*, **242**, 715–722.

LEVI, G. & RAITERI, M. (1993). Carrier-mediated release of neurotransmitters. *Trends Neurosci.*, **16**, 415–419.

NASH, J.F. (1990). Ketanserin pretreatment attenuates MDMA-induced dopamine release in the striatum as measured by in vivo microdialysis. *Life Sci.*, **47**, 2401–2408.

NURSE, B., RUSSELL, V.A. & TALJAARD, J.J.F. (1988). Characterization of the effects of serotonin on the release of [^{3}H]dopamine from rat nucleus accumbens and striatal slices. *Neurochem. Res.*, **13**, 403–407.

PALFREYMAN, M.G., SCHMIDT, C.J., SORENSEN, S.M., DUDLEY, M.W., KEHNE, J.H., MOSER, P., GITTOS, M.W. & CARR, A.A. (1993). Electrophysiological, biochemical and behavioural evidence for 5-HT2 and 5-HT3 mediated control of dopaminergic function. *Psychopharmacology*, **112**, S60–S67.

PEREZ-OTAÑO, I., HERRERO, M.T., OSET, C., DE CEBALLOS, M.L., LUQUIN, M.R., OBESO, J.A. & DEL RIO, J. (1991). Extensive loss of brain dopamine and serotonin induced by chronic administration of MPTP in the marmoset. *Brain Res.*, **567**, 127–132.

SCHMIDT, C.J. & BLACK, C.K. (1989). The putative 5-HT_3 agonist phenylbiguanide induces carrier-mediated release of [^{3}H]dopamine. *Eur. J. Pharmacol.*, **167**, 309–310.

SORENSEN, S., HUMPHREYS, T.M. & PALFREYMAN, M.G. (1989). Effect of acute and chronic MDL 73,147EF, a 5-HT_3 receptor antagonist, on A9 and A10 dopamine neurones. *Eur. J. Pharmacol.*, **163**, 115–118.

WAEBER, C., HOYER, D. & PALACIOS, J.M. (1989). 5-Hydroxytryptamine receptors in the human brain, autoradiographic visualization using [^{3}H]ICS 205-930. *Neuroscience*, **31**, 393–400.

WERLING, L.L., FRATTALI, P., PORTOGHESE, P.S., TAKEMORI, A.E. & COX, B.M. (1988). Kappa receptor regulation of dopamine release from striatum and cortex of rats and guinea-pigs. *J. Pharmacol. Exp. Ther.*, **246**, 282–286.

YI, S.-J., GIFFORD, A.N. & JOHNSON, K.M. (1991). Effect of cocaine and 5-HT_3 receptor antagonists on 5-HT-induced [^{3}H]dopamine release from rat striatal synaptosomes. *Eur. J. Pharmacol.*, **199**, 185–189.

(Received March 3, 1994
Revised July 28, 1994
Accepted August 2, 1994)

Br. J. Pharmacol. (1994), **113**, 973–981 © Macmillan Press Ltd, 1994

Modulatory effect of neuropeptide Y on acetylcholine-induced oedema and vasoconstriction in isolated perfused lungs of rabbit

Annie Delaunois, [1]Pascal Gustin, [2]Cécile Dessy-Doize & Michel Ansay

Department of Pharmacology & Toxicology, Faculty of Veterinary Medicine, University of Liège, Bd de Colonster B41, B4000 Liège, Belgium

1 The modulatory role of neuropeptide Y (NPY) on pulmonary oedema induced by acetylcholine and capsaicin was investigated. The effects of NPY on the haemodynamic response to acetylcholine, phenylephrine and substance P were also investigated.

2 Isolated, ventilated, exsanguinated lungs of the rabbit were perfused with a constant flow of recirculating blood-free perfusate. The double/arterial/venous occlusion method was used to partition the total pressure gradient (ΔPt) into four components: the arterial gradient (ΔPa), the pre- and post-capillary gradients (respectively $\Delta Pa'$ and $\Delta Pv'$) and the venous pressure gradient (ΔPv). Endothelial permeability was evaluated by measuring the capillary filtration coefficient (Kf,c).

3 Acetylcholine (10^{-8} M to 10^{-4} M) and substance P (SP, 10^{-10} M to 10^{-6} M) induced a concentration-dependent increase in the Kf,c. Capsaicin (10^{-4} M) and 5-hydroxytryptamine (5-HT) (10^{-4} M) also increased this parameter. NPY (10^{-8} M) completely inhibited the effects of acetylcholine and capsaicin on the Kf,c, without preventing the effects of substance P and 5-HT.

4 Acetylcholine induced concentration-dependent vasoconstriction in the precapillary segment. The effect was inhibited by NPY and aspirin, an inhibitor of cyclo-oxygenase, while ketanserin, a 5-HT_2 receptor antagonist, and SR140333, a new NK_1 antagonist, had no protective effect. Phenylephrine increased ΔPa at high concentration, an effect also inhibited by NPY and aspirin. Substance P had no significant haemodynamic effect. When injected together with NPY, substance P (10^{-6} M) induced a significant increase in the total pressure gradient.

5 It was concluded that NPY can protect the lung against acetylcholine- and capsaicin-induced oedema via a prejunctional modulatory effect on the C-fibres. NPY also inhibits acetylcholine-evoked precapillary and phenylephrine-induced arterial vasoconstriction, probably by interfering with cyclo-oxygenase products synthesis.

Keywords: Neuropeptide Y; acetylcholine; C-fibres; rabbit lungs; vasoconstriction; permeability oedema

Introduction

Neuropeptide Y (NPY) is a 36-amino acid peptide. It is widely distributed through the central and peripheral nervous systems. It is co-localized and released together with noradrenaline (NA) at some sympathetic nerve endings (Lundberg *et al.*, 1982). Nonadrenergic NPY-containing fibres have also been identified in some species. In the airways, such fibres are located around blood vessels, exocrine glands and tracheobronchial smooth muscle (Uddman *et al.*, 1984). NPY interacts both pre- and postsynaptically with NA. The prejunctional effect is mediated by Y_2-receptors and involves inhibition of NA release from sympathetic nerves (Lundberg *et al.*, 1985). NPY also inhibits parasympathetic and non adrenergic, non cholinergic (NANC) transmissions via prejunctional receptors (Stretton & Barnes, 1988; Grundemar *et al.*, 1990). At the postsynaptic level, activation of Y_1-receptors on target cells produces a moderate contractile response. However, NPY can nonspecifically potentiate the effects of spasmogens such as histamine, NA, and prostaglandins on rabbit systemic arteries (Edvinsson *et al.*, 1984; Han & Abel, 1987), while inhibiting acetylcholine (ACh)-triggered relaxation (Grundemar & Högestätt, 1992). A few studies have focused on how NPY affects pulmonary blood vessels.

In an earlier study on rabbit isolated perfused lungs, we have shown that ACh can induce pulmonary oedema by increasing endothelial permeability (Delaunois *et al.*, 1993a). The effect involves stimulation of afferent capsaicin-sensitive fibres (C-fibres) with subsequent release of substance P (SP) and calcitonin gene-related peptide (CGRP) (Delaunois *et al.*, 1994). The latter substances trigger a cascade of events. These involve arachidonic acid derivates and 5-hydroxytryptamine (5-HT) and lead ultimately to oedema (Delaunois *et al.*, 1993a). We have also investigated the haemodynamic effects of ACh, which induces vasoconstriction, as previously demonstrated by Catravas *et al.* (1984) in the rabbit. The latter authors speculated that cyclo-oxygenase products might be involved in this contractile response, but were not clear as to whether mediators responsible for endothelial permeability changes, such as 5-HT or neuropeptides, might also play a role in the process.

Accordingly, the aim of the present study was to verify whether NPY can modulate ACh- and capsaicin-induced permeability changes, to identify the pharmacological mechanisms underlying the vasoconstrictor effects of ACh and finally to investigate the possible modulatory effect of NPY on this haemodynamic response.

Methods

General procedure

New Zealand White rabbits (male and female) weighing 2.5–3 kg were deeply anaesthetized with a single intramuscular injection of fentanyl (0.2 mg kg^{-1}) plus fluanisone

[1] Author for correspondence.
[2] Present address: Department of Histology, Faculty of Veterinary Medicine, University of Liège, Bd de Colonster B41, B4000, Liège, Belgium.

(10 mg kg^{-1}) (Hypnorm, Janssen Pharmaceutica, Beerse, Belgium). The trachea of each animal was isolated and cannulated. Pancuronium (0.2 mg kg^{-1}) was administered into the marginal ear vein to prevent sudden reflex movements of the chest due to anoxia during midsternal incision. The animals were ventilated with a small animal respirator (Palmer; Analis; Namur; Belgium). The chest was opened by midsternal incision and heparin (2000 u kg^{-1}; Liquémine, Roche, Brussels, Belgium) was injected into the right ventricle before exsanguination. The heart-lung block was rapidly removed from the chest and weighed. Both ventricles were opened and glass cannulae (length 15 mm; i.d. 3 mm) secured in the pulmonary artery and left atrium via the corresponding ventricles. The surrounding tissues were included in the ligature of the pulmonary artery and left atrium, so as to decrease the compliance of these structures (Wangensteen *et al.*, 1977; Kern *et al.*, 1984).

The isolated heart-lungs were suspended on one side of a beam balance. The lung weight was counterbalanced and further weight changes occurring during the experiments were measured by an isometric force transducer (Palmer; Analis; Namur; Belgium) attached to the lever of the balance. This system was calibrated before each experiment by suspending weights in place of the lung. The heart-lungs were connected to a recirculating perfusion circuit and perfused with a constant perfusate flow (20 ml min^{-1} kg^{-1}). The circuit included an open venous reservoir, an electronic roller pump (NY-7550-62 Masterflex, Bioblock, Illkirch, France) indicating the perfusate flow, a heat exchanger, and a bubble trap. Care was taken to avoid introducing air into the circuit. The lungs were first flushed until the remainder of blood in the vascular bed was completely removed, then perfused with 200 ml of artificial blood-free perfusate (Krebs-Ringer-bicarbonate buffer containing 2.5% bovine albumin: Sigma Chemical Co, St Louis, U.S.A.). The pH and temperature of the perfusate were continually monitored and maintained within physiological ranges (pH = 7.4–7.5; t° = 37–38°C). The pH was controlled by adding 1 N $NaHCO_3$ or by aerating the liquid in the venous reservoir with 95% CO_2 and 5% O_2. The Po_2 and Pco_2 of the perfusion liquid were checked at the beginning and at the end of each experiment. These parameters remained within physiological ranges in all experiments (Po_2 = 128–160.4 mmHg; Pco_2 = 17.4–31.6 mmHg). The lungs were ventilated with humidified room air at a frequency of 45 breaths per minute, a tidal volume of 5 ml kg^{-1} and an end-expiratory pressure (*Pe*) of 2 cmH_2O. They were periodically hyperinflated to avoid atelectasis and covered with a plastic bag to prevent evaporative fluid loss.

Arterial (*Pa*) and venous (*Pv*) pressures were measured by means of two thin catheters connected to side ports of the cannulae secured in the pulmonary artery and left atrium, and to pressure transducers (P23 ID and P50, Gould; Brussels, Belgium). The pressures were zero-referenced at the level of the lung hilus. Equilibration, obtained after 10–15 min, was characterized by an isogravimetric state, i.e. one in which no gain or loss of weight was observed, and by stability of arterial and left atrium pressures in zone III conditions ($Pa > Pv > Pe$). All parameters were recorded on a Gould recorder (TA 2000; Brussels, Belgium). Lungs which developed high arterial pressure ($Pa > 20$ cmH_2O) at the onset of perfusion were rejected from the study.

Experimental measurements

The total pressure gradient across the vascular bed (ΔPt) was partitioned into four components (arterial, pre-capillary, post-capillary, and venous segments) by application of the double, arterial/venous occlusion method used by Hakim *et al.* (1982) in dogs and by Gustin *et al.* (1994) in pigs. Briefly, inflow and outflow occlusions were successively performed by use of two electromagnetic valves placed around the arterial and venous tubes, near the cannulae, for a brief period (2–3 s) at the end of expiration. When inflow was stopped, the *Pa* first dropped rapidly by an amount equal to the pressure gradient through the large arteries ($\Delta Pa = Pa - Pa'$), then more slowly, due to lung compliance. Clamping the outflow induced an abrupt increase in *Pv* equal to the pressure gradient through the large veins ($\Delta Pv = Pv' - Pv$), followed by a slow rise in *Pv* due to progressive filling of the vascular bed with perfusion liquid. *Pa'* and *Pv'* are respectively defined as the pressures at the distal end of the arterial segment and the proximal end of the venous segment. Detailed plots of pressure variations obtained in dogs and pigs after arterial and venous occlusions have been published by Hakim (1988) and Gustin *et al.* (1994). The segment including the capillaries, the small arteries, and the small veins, all highly distensible vessels, was divided into pre- and post-capillary components by measuring capillary pressure (*Pc*) by means of the double occlusion method (Dawson *et al.*, 1982). Simultaneous occlusion of both inflow and outflow (for a few seconds) induces an increase in *Pv* and a decrease in *Pa* until *Pa* and *Pv* equilibrate at the same pressure, providing a good estimate of capillary pressure. The pressure gradients across the pre-($\Delta Pa' = Pa' - Pc$) and post-($\Delta Pv' = Pv' - Pc$) capillary segments were calculated. As the perfusate flow was constant, the vascular resistances across the four segments of the pulmonary circulation are directly proportional to the pressure gradient measurements (ΔPt; ΔPa; $\Delta Pa'$; $\Delta Pv'$; ΔPv).

The capillary filtration coefficient (Kf,c) was measured by increasing *Pa* and *Pv*, usually by 10–15 cmH_2O for 2 to 4 min. *Pc* was estimated before and at the end of this period in order to determine the hydrostatic pressure difference (ΔPc) inducing fluid filtration across the endothelium. The amount of fluid filtering across was calculated from the weight-gain plot. At first, due to congestion, the lungs gained weight rapidly for 30 to 60 s following the vascular pressure increases. Thereafter, lung weight increased more slowly due to subsequent fluid filtration out of the vessels and accumulation in the lung tissue. The slopes of the slow phase of the weight increase ($\Delta W/\Delta t$) were plotted on a semi-logarithmic scale as a function of time and extrapolated to zero-time. The value obtained was divided by ΔPc and by lung weight to yield the Kf,c expressed in ml (the fluid filtered was assumed to have a density of 1.0) per minute per cmH_2O per 100 g wet lung weight. Details of this method have been published (Drake & Gabel, 1981; Sumita *et al.*, 1989; Delaunois *et al.*, 1992; Gustin *et al.*, 1994).

Experimental design

In each group of rabbit lungs, baseline values of the parameters were measured after the equilibration period of the lung, ranging from 10 to 15 min. All drug concentrations given in the text are final concentrations in the perfusate (200 ml).

To investigate haemodynamic effects, we established cumulative concentration-response curves for ACh (10^{-8} M to 10^{-5} M), phenylephrine (10^{-8} M to 10^{-3} M) and SP (10^{-10} M to 10^{-6} M) by adding increasing concentrations of the drug to the venous reservoir. After the first concentration, subsequent concentrations were injected when the vascular response reached a plateau. Under these conditions, the haemodynamic parameters were measured at 10–15 min intervals. Control values were obtained by measuring the vascular pressures every 10–15 min in lungs receiving no drug. The Kf,c was not determined for these groups. In order to determine the pharmacological mechanisms involved in vascular response to ACh, other groups of lungs were pretreated with NPY, aspirin, an inhibitor of cyclo-oxygenase, ketanserin, a 5-HT_2 receptor antagonist, or a new NK_1 receptor antagonist, SR140333 ((*S*)]-{2-[3-(3,4-dichlorophenyl)-1-(3-isopropoxyphenyl-acetyl)piperidin-3-yl]ethyl}-4-phenyl-1-azoniabi-cyclo [2.2.2]octane chloride) (Emonds-Alt *et al.*, 1993), before recording the concentration-response curve. We also pretreated some lungs with NPY or aspirin before recording the concentration-response curves for phenylephrine and SP.

To determine Kf,c changes, we prevented the vasoconstrictor effects of ACh, SP and 5-HT with a single dose of papaverine (3×10^{-4} M). This pretreatment enabled us to measure permeability changes without interfering with the vascular response (Delaunois *et al.*, 1993a). Graded concentrations of ACh (10^{-8} M to 10^{-4} M) and SP (10^{-10} M to 10^{-6} M) were added in the circuit and the Kf,c was determined after each concentration, at 20 min intervals. In other groups, the effects of a single dose of capsaicin (10^{-4} M) or 5-HT (10^{-4} M) were investigated. Control values were calculated by measuring the Kf,c value at 20 min intervals for 2 h in lungs not receiving any drug.

To test the protective effects of NPY, a single dose of this drug (10^{-8} M) was used to pretreat four groups of lungs, just before addition of ACh, SP, capsaicin or 5-HT.

Drugs

Acetylcholine chloride (Roche; Brussels; Belgium), substance P (Sigma Chemical Co; St Louis; U.S.A.), 5-hydroxytryptamine (Sigma Chemical Co; St Louis; U.S.A.), phenylephrine (Sigma Chemical Co; St Louis; U.S.A.) and neuropeptide Y (Sigma Chemical Co; St Louis; U.S.A.) were dissolved and diluted in NaCl 9%. Acetylsalicylic acid (Sigma Chemical Co; St Louis; U.S.A.) were dissolved in NaCl 9% with $NaHCO_3$ 5%. Papaverine chlorhydrate (Roche; Brussels; Belgium) and ketanserin (Sigma Chemical Co; St Louis; U.S.A.) were diluted in the perfusion liquid, to which was added HCl 1 N to facilitate dilution. SR 140333 (gift from Pr Ch. Advenier; Faculty of Medicine; Paris; France) and capsaicin (Sigma Chemical Co; St Louis; U.S.A.) were dissolved in ethanol (0.3 ml) and then diluted in the perfusion liquid. Reagents and solvents used to prepare the drugs had no effect on any measurement made.

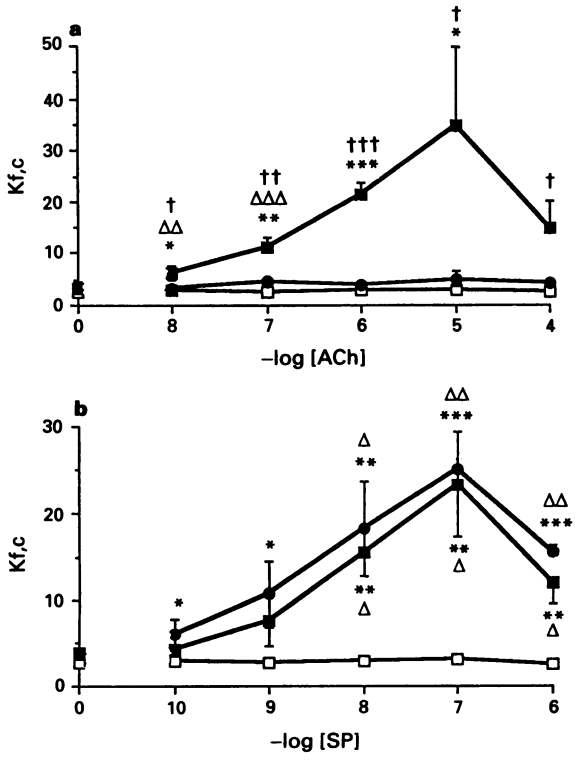


Figure 1 Values of the capillary filtration coefficent (Kf,c), expressed as ml min^{-1} cmH_2O^{-1} 100 g^{-1}, after addition of graded concentrations of acetylcholine (ACh) (a) or substance P (SP) (b) in control lungs (□) ($n = 8$), agonist-treated lungs (■) ($n = 9-5$) and in neuropeptide Y (NPY) plus agonist-treated lungs (●) ($n = 5-4$). S.e.means are shown. Values differing from controls are denoted: $^{*}P<0.05$, $^{**}P<0.01$ and $^{***}P<0.001$. Values differing from baseline are $^{\Delta}P<0.05$, $^{\Delta\Delta}P<0.01$ and $^{\Delta\Delta\Delta}P<0.001$. Values differing from NPY group are $^{\dagger}P<0.05$, $^{\dagger\dagger}P<0.01$ and $^{\dagger\dagger\dagger}P<0.001$.

Electron mieroscopy studies

At the end of experiment, the lungs were hyperinflated. Specimens were divided, fixed in 4% Millonig's phosphate buffered glutaraldehyde, pH 7, and postfixed in 2% aqueous osmium tetroxide. Tissue blocks were embedded in Epon. Thin sections were contrasted with uranyl acetate followed by lead citrate. Sections were examined with a Zeiss 910 electron microscope.

Statistics and calculations

Data are expressed as means ± standard error of the mean (s.e.mean). Data were subjected to two-way analysis of variance (ANOVA 2). When the ANOVA was significant, Student's paired or unpaired t test was used for comparison of two means. When necessary, the P values for significance were corrected by Bonferroni's method to allow multiple comparisons (Wallenstein *et al.*, 1980). Differences were considered significant when $P<0.05$.

In response to ACh and SP, each lung exhibited a concentration-dependent increase in the Kf,c, followed by a decrease (see Results). This decrease was due to an artifact, explained by the overflow of the lung. Accumulation of fluid in the interstitial tissue can induce an increase in the hydrostatic tissue pressure, which opposes new fluid filtration across the endothelium. For each lung, the Kf,c value obtained just before the decrease was taken as the maximum effect (E_{max}). E_{max} is the highest value the Kf,c can reach under such experimental conditions, limited by this mechanical factor. The EC_{50}, i.e. the molar concentration of agonist producing a Kf,c increase equivalent to 50% of the E_{max}, was calculated for each lung from the linear regression equation obtained with the values ranging from 10% to 90% of E_{max} and with the logarithm of the concentration. At least three values were considered. A mean EC_{50} was then calculated in each group. The pD_2 value was defined as the negative logarithm of the EC_{50}. In this preparation, pD_2 value reflects the sensitivity of the preparation to an agonist rather than the real affinity of this agonist for its receptor.

Results

Effects of NPY on the permeability changes induced by ACh, capsaicin SP and 5-HT

Figure 1a illustrates the effects of ACh on the Kf,c. ACh induced a concentration-dependent increase in this parameter. The mean pD_2 was 6.59 ± 0.32. The effect was maximal (34.61 ± 15.88 ml min^{-1} cmH_2O^{-1} 100 g^{-1}) at 10^{-5} M, lower values being recorded at higher concentrations. Lung volume increased considerably and pulmonary oedema was observed. Electron photomicrographs of tissue samples from control lung (Figure 2) and ACh-treated lung (Figure 3) reveal damage in the latter. The control lung tissue appears intact. Capillary endothelium is separated from the alveolar epithelium by a continuous basement membrane. The integrity of the endothelial cells and of their nucleus is maintained. By contrast, the photomicrograph from the treated lung shows irreversible lesions. The basement membrane is completely destroyed and the capillary endothelium shows a great number of transcytotic vacuoles. The alveolar epithelium is discontinuous and presents abnormal swellings. No significant change was observed in the vascular pressures (Table 1) since these lungs were pretreated with papaverine.

NPY (10^{-8} M) had no direct effect on the Kf,c. The value of this parameter measured 15 min after administration of NPY (4.19 ± 0.84 ml min^{-1} cmH_2O^{-1} 100 g^{-1}) did not differ significantly from the baseline value (3.74 ± 0.83 ml min^{-1} cmH_2O^{-1} 100 g^{-1}). By comparison, NPY (10^{-8} M) completely inhibited the ACh-induced Kf,c increase at all concentrations (Figure 1a).



Figure 2 Electron micrograph of tissue from a control lung. BL = basal lamina, AE = alveolar epithelium, CE = capillary endothelium, A = alveolus, C = capillary. Scale bar = 0.58 µm.

Capsaicin (10^{-4} M), like ACh, caused the Kf,c to increase, to 271 ± 48% of baseline (Figure 4). Pretreatment with NPY completely prevented this reaction ($P<0.01$). Similarly, SP increased the Kf,c in a concentration-dependent manner (Figure 1b) with a pD_2 of 8.65 ± 0.08 and a E_{max} of 23.62 ± 6.04 ml min^{-1} cmH_2O^{-1} 100 g^{-1}. However, NPY did not significantly affect this SP-evoked response. NPY, likewise, did not significantly change the 5-HT-induced Kf,c increase (676 ± 147% of baseline without NPY ($n = 4$) vs 693 ± 208% with NPY ($n = 4$)).

Pharmacological modulation of the haemodynamic effects of ACh

Vascular pressure values in each segment of the pulmonary circulation are presented in Table 2. At ACh concentrations ranging from 3×10^{-7} M to 3×10^{-6} M, an abrupt increase in *Pa* and *Pa'* was recorded, followed by a slower rise at higher concentrations. Due to the interindividual variability in the sensitivity of the preparations, the mean responses to *Pa* and *Pa'* were significant only at concentrations exceeding 10^{-6} M and 3×10^{-7} M, respectively. *Pc*, *Pv'* and *Pv* did not change significantly.

Since the contractile response to ACh caused only *Pa* and *Pa'* to increase, Table 3 shows only changes in these two parameters in lungs pretreated with several drugs. Aspirin completely prevented the increase in *Pa* and *Pa'*, while ketanserin and SR 140333 did not significantly inhibit vasoconstriction induced by ACh at any concentration.

Figure 5 illustrates ACh-induced changes in the pressure gradients at the different levels of the vascular bed. A significant concentration-related increase in ΔPt was observed. The same profile was recorded for $\Delta Pa'$. The pressures gradients in the other vascular segments were not significantly modified. NPY (10^{-8} M), when given alone, had no direct effect on the haemodynamics. The values of the vascular pressures measured 5 min after NPY administration did not significantly differ from the baseline values. However, the ACh-induced increases in ΔPt and $\Delta Pa'$ were partly inhibited by pretreatment with NPY (10^{-8} M) and, at all concentrations of ACh, completely prevented by aspirin (10^{-3} M) (Figure 5).

Phenylephrine at concentrations below 10^{-3} M did not significantly alter the pulmonary haemodynamics. At 10^{-3} M, it produced an increase in ΔPa from 1.94 ± 0.68 to 4.62 ± 1.07 cmH_2O ($P<0.05$), explaining the increased value of ΔPt (from 11.12 ± 0.59 to 19.45 ± 4.75 cmH_2O) ($P<0.01$). Pressure gradients in the other vascular segments did not change significantly. The increase in ΔPa was completely prevented by NPY (1.81 ± 0.49 cmH_2O) ($P<0.05$) and by aspirin (1.12 ± 0.12 cmH_2O) ($P<0.05$).

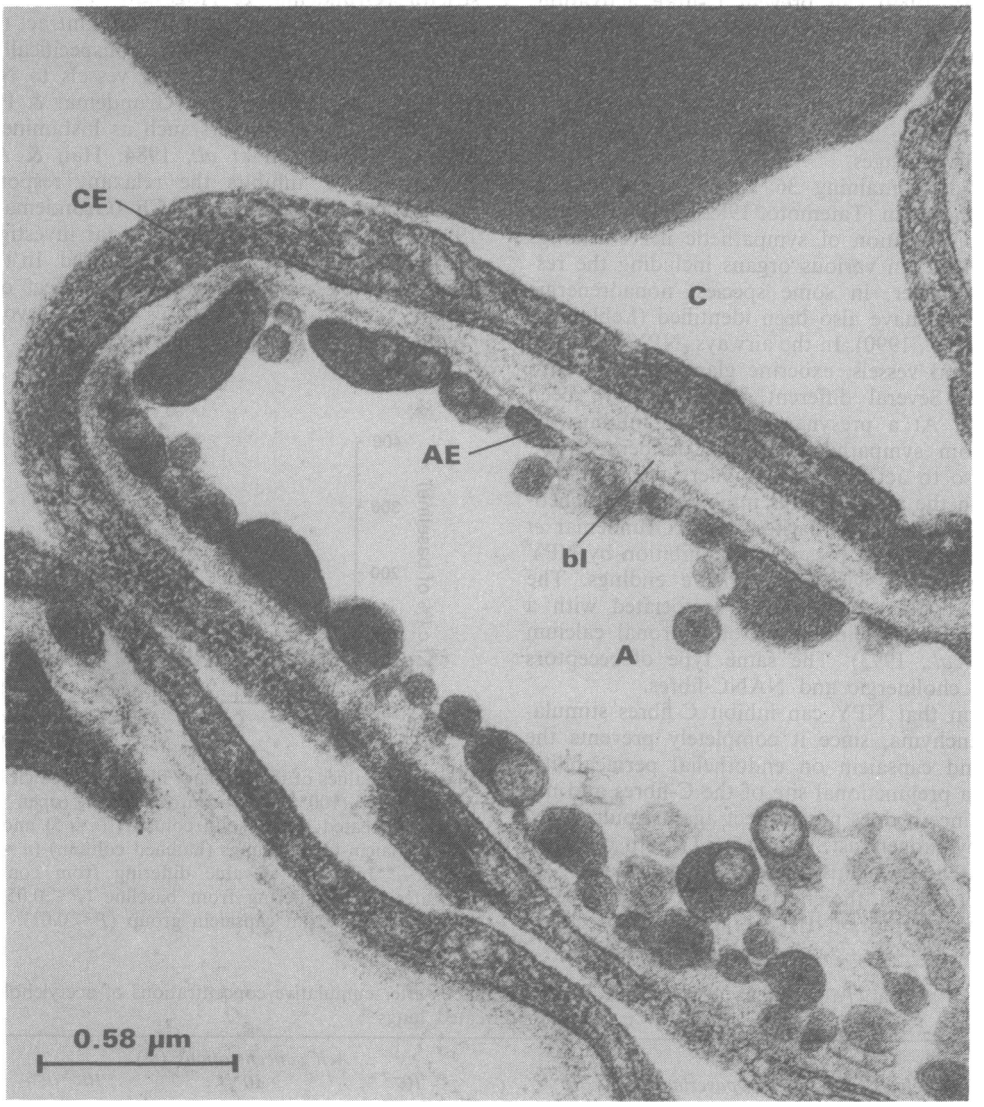


Figure 3 Electron micrograph of tissue from an acetylcholine-treated lung after the dose-response curve was recorded. BL = basal lamina, AE = alveolar epithelium, CE = capillary endothelium, A = alveolar, C = capillary. Scale bar = 0.58 μm.

SP did not significantly alter the pressure gradients in any segment of the vascular bed, although ΔPt was somewhat higher at the highest concentration (17.37 ± 2.17 cmH_2O at 10^{-6} M vs 10.17 ± 0.76 cmH_2O for baseline) (not significant). Pretreatment with NPY enhanced SP-induced vasoconstriction enough to render the total resistance increase significant ($P<0.05$) (22.17 ± 6.20 cmH_2O). Pretreatment with aspirin did not significantly change the SP concentration-response curve.

Discussion

This study demonstrates that NPY can prevent the ACh- and capsaicin-induced pulmonary oedema by inhibiting the increase in endothelial permeability. NPY also protects the lung against acetylcholine- or phenylephrine-evoked vasoconstriction, while it potentiates the vascular effects of SP.

The role of the NANC nervous system in controlling vascular and airway smooth muscle or glandular secretions is now well recognized in many species, including man (Lundberg *et al.*, 1984). Afferent nerve endings, also called C-fibres, are located in the upper airway as well as in the lower respiratory tract (Joos *et al.*, 1988). These fibres contain neuropeptides such as SP, calcitonin gene-related peptide (CGRP) and neurokinins A and B which act as neurotransmitters. These substances can be released locally upon various stimuli such as cigarette smoke or administration of capsaicin (Lundberg *et al.*, 1983). In a previous study, we showed that ACh induces pulmonary oedema in the rabbit by increasing endothelial permeability (Delaunois *et al.*, 1993a). The mechanisms involved in this reaction have been investigated. ACh activates muscarinic receptors located on C-fibres, which subsequently release neuropeptides such as SP or CGRP (Delaunois *et al.*, 1994). These substances trigger a cascade of events involving 5-HT, released from mast cells, and arachidonic acid derivates. Capsaicin, by activating the same cascade of events, also induces pulmonary oedema (Delaunois *et al.*, 1993b). The data in Figures 1 and 4 confirm these previous findings. Furthermore, the electron micrographs shown in Figure 2 and 3 illustrate the irreversible damage caused by high concentrations of ACh. The numerous, large, transcytotic vacuoles contained in the endothelial cells, the presence of swellings and perforations in the alveolar epithelium and the disappearance of the basal lamina could explain the changes in the permeability of the endothelial-epithelial barrier and the filtration of fluid from the capillary lumen to the alveolus.

Various drugs can interfere with C-fibres at a prejunctional level. α_2-Adrenoceptor (Grundstrom & Andersson, 1985), opiate (Frossard & Barnes, 1987) and histamine H_3 agonists

(Ichinose & Barnes, 1989) can prevent C-fibre activation, thus inhibiting the release of neuropeptides. Such substances probably act on their respective receptors, located on the nerve fibres. The aim of the present study was to see whether NPY, a known inhibitor of C-fibre stimulation (Matran et al., 1989), can protect the lung against capsaicin- and ACh-induced permeability changes.

NPY is a peptide containing 36 amino acids, initially isolated from porcine brain (Tatemoto, 1982). It is co-located with NA in a subpopulation of sympathetic nerve endings (Lundberg et al., 1982) in various organs including the respiratory tract. Moreover, in some species, nonadrenergic NPY-containing fibres have also been identified (Leblanc et al., 1987; Lacroix et al., 1990). In the airways, NPY-fibres are present around blood vessels, exocrine glands and beneath surface epithelium. Several different functions have been attributed to NPY. At a presynaptic level, it inhibits the release of NA from sympathetic fibres (Lundberg et al., 1985). It seems also to act on both cholinergic and NANC excitatory nerves in the airways, thus inhibiting the tracheobronchial response (Stretton & Barnes, 1988; Grundemar et al., 1990). The mechanism of presynaptic inhibition by NPY has been investigated in sympathetic nerve endings. The effect is mediated by Y_2 receptors and associated with a reduced calcium influx and inhibition of neuronal calcium channels (Toth et al., 1993). The same type of receptors probably exist on cholinergic and NANC-fibres.

Our data confirm that NPY can inhibit C-fibres stimulation in lung parenchyma, since it completely prevents the effects of ACh and capsaicin on endothelial permeability. NPY must act at a prejunctional site of the C-fibres and not postsynaptically, since it does not protect against pulmonary oedema induced by exogenous SP and 5-HT, both of which are involved in ACh- and capsaicin-evoked oedema.

At a postjunctional level, the effects of NPY are related to the activation of Y_1 receptors. NPY acts as a weak vasoconstrictor (Grundemar & Högestätt, 1992), but it can cause tracheobronchial smooth muscle to contract (T-Benchekroun et al., 1992). Moreover, NPY nonspecifically enhances the contractile response of systemic vessels to NA (Fallgren et al., 1993) or phenylephrine (Grundemar & Högestätt, 1992) and other vasoconstrictors such as histamine or prostaglandins $F_{2\alpha}$ (Edvinsson et al., 1984; Han & Abel, 1987). In contrast, NPY inhibits the relaxant response of the rat isolated femoral artery to ACh (Grundemar & Högestätt, 1992). Only a few studies have so far investigated the effects of NPY on the pulmonary vascular bed. In the rabbit, NPY seems to have no direct constrictor effect on isolated pulmonary artery but potentiates the NA-evoked vasospasm (Wahlestedt et al., 1985). In the present work, we have

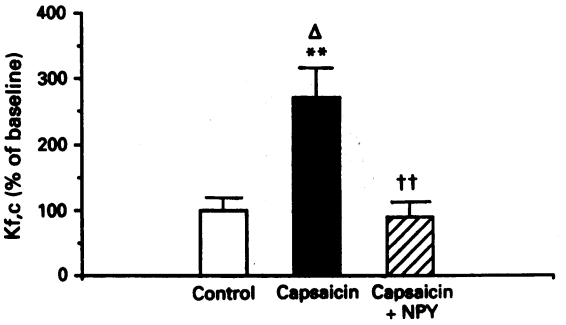


Figure 4 Values of the capillary filtration coefficient, expressed as % of baseline (100%), in control lungs (open column) ($n = 5$), capsaicin-treated lungs (solid column) ($n = 5$) and neuropeptide Y-plus-capsaicin-treated lungs (hatched column) ($n = 4$). S.e.means are shown. **Indicates a value differing from control ($P < 0.01$), $^{\Delta}$ indicates value differing from baseline ($P < 0.05$) and †† denotes value differing from capsaicin group ($P < 0.01$).

Table 1 Values of arterial (*Pa*), capillary (*Pc*) and venous (*Pv*) pressures after cumulative concentrations of acetylcholine (ACh) in papaverine-pretreated lungs

	Baseline	*After papaverine*	*Ach concentrations* (M) 10^{-8}	10^{-7}	10^{-6}	10^{-5}	10^{-4}
Pa (cmH_2O)	13.80 ± 0.62	12.93 ± 0.43	12.55 ± 0.30	12.39 ± 0.78	11.87 ± 0.93	14.42 ± 0.86	13.62 ± 1.37
Pc (cmH_2O)	9.06 ± 1.02	8.09 ± 0.88	9.52 ± 1.08	7.64 ± 1.06	7.57 ± 1.00	9.08 ± 1.10	7.87 ± 0.87
Pv (cmH_2O)	3.67 ± 0.61	3.91 ± 0.73	4.58 ± 0.46	2.94 ± 0.25	3.28 ± 0.47	4.21 ± 0.63	3.50 ± 0.05

All values are mean ± s.e.mean. $n = 9$.

Table 2 Values of arterial (*Pa*), pre-capillary (*Pa'*), capillary (*Pc*), post-capillary (*Pv'*) and venous (*Pv*) pressures and of blood flow (Q) in control group ($n = 8$) and after cumulative concentrations of acetylcholine (ACh)

	Baseline	*ACh concentrations* (M) 10^{-8}	10^{-7}	3×10^{-7}	10^{-6}	3×10^{-6}	6×10^{-6}	10^{-5}
Pa (cmH_2O)								
Control	15.21 ± 0.60	14.60 ± 0.57	14.70 ± 0.83	14.85 ± 1.17	15.05 ± 1.09	14.06 ± 0.66	13.95 ± 0.75	14.00 ± 0.60
ACh	13.95 ± 0.54	14.02 ± 0.41	15.97 ± 1.44	16.61 ± 0.82	27.75 ± 6.68[a]	28.36 ± 6.21[a,b]	29.82 ± 7.20[a,b]	29.97 ± 8.89[a,b]
Pa' (cmH_2O)								
Control	12.90 ± 0.70	12.55 ± 0.39	12.15 ± 0.40	12.40 ± 0.53	12.50 ± 0.49	12.22 ± 0.28	12.06 ± 0.34	12.13 ± 0.24
ACh	12.29 ± 0.47	12.92 ± 0.31	13.89 ± 0.80	15.33 ± 0.94[b]	24.64 ± 5.90[a]	25.71 ± 5.32[a,b]	27.30 ± 6.18[a,b]	27.35 ± 7.12[a,b]
Pc (cmH_2O)								9.56 ± 0.55
Control	9.85 ± 0.70	9.55 ± 0.58	9.45 ± 0.55	9.72 ± 0.62	9.55 ± 0.61	9.69 ± 0.60	9.75 ± 0.61	9.85 ± 1.52
ACh	8.39 ± 0.48	8.54 ± 0.30	9.28 ± 0.81	8.70 ± 0.24	9.87 ± 0.88	9.47 ± 0.72	9.92 ± 1.16	
Pv' (cmH_2O)								7.14 ± 1.16
Control	7.17 ± 1.06	7.45 ± 0.72	7.15 ± 0.86	7.17 ± 0.94	7.30 ± 0.96	7.06 ± 1.25	7.03 ± 1.22	4.57 ± 0.87
ACh	6.15 ± 0.80	5.00 ± 0.33	6.17 ± 1.03	5.00 ± 0.48	5.13 ± 0.57	4.70 ± 0.29	4.56 ± 0.33	
Pv (cmH_2O)								4.44 ± 0.86
Control	4.90 ± 0.88	5.00 ± 0.92	4.60 ± 0.87	4.70 ± 0.99	4.64 ± 0.91	4.24 ± 1.07	4.24 ± 1.07	2.95 ± 0.20
ACh	3.83 ± 0.62	3.25 ± 0.44	3.96 ± 0.70	3.31 ± 0.30	2.96 ± 0.18	2.85 ± 0.16	2.95 ± 0.20	
Q ($ml\ min^{-1}$)								61.43 ± 1.43
Control	61.43 ± 1.43	61.43 ± 1.43	61.43 ± 1.43	61.43 ± 1.43	61.43 ± 1.43	61.43 ± 1.43	61.43 ± 1.43	79.00 ± 1.79
ACh	79.00 ± 1.79	79.00 ± 1.79	79.00 ± 1.79	79.00 ± 1.79	79.00 ± 1.79	79.00 ± 1.79	79.00 ± 1.79	

All values are mean ± s.e.mean. $n = 8$.

[a] $P < 0.05$ (Student's t test) compared to base-line value in the same group.

[b] $P < 0.05$ (Student's t test) compared to value measured in the control group.

Table 3 Values of arterial (*Pa*) and precapillary pressure (*Pa'*) (cmH_2O) after cumulative concentrations of acetylcholine (ACh) in lungs with or without (ACh group; $n = 8$) pretreatment with ketanserin (10^{-8} M, $n = 3$), SR140333 (10^{-7} M, $n = 4$) or aspirin (10^{-3} M, $n = 3$)

		ACh concentrations (M)					
	Baseline	10^{-8}	10^{-7}	3×10^{-7}	10^{-6}	3×10^{-6}	6×10^{-6}	10^{-5}
Pa								
Control group	15.21 ± 0.60	14.60 ± 0.57	14.70 ± 0.83	14.85 ± 1.17	15.05 ± 1.09	14.06 ± 0.66	13.95 ± 0.75	14.00 ± 0.60
ACh group	13.95 ± 0.54	14.02 ± 0.41	15.97 ± 1.44	16.61 ± 0.82	27.75 ± 6.68[a]	28.36 ± 6.21[a,b]	29.82 ± 7.20[a,b]	29.97 ± 8.89[a,b]
Ketanserin group	13.50 ± 1.53	11.67 ± 1.01	19.12 ± 4.37	23.58 ± 4.17[b]	28.75 ± 7.07[b]	34.00 ± 8.02[b]	29.83 ± 7.65[b]	28.00 ± 7.94
SR 140333 group	12.56 ± 0.66	12.37 ± 0.68	14.62 ± 0.12	16.08 ± 1.08	17.92 ± 2.92	19.17 ± 3.30	23.68 ± 5.25[b]	25.50 ± 5.05[a]
Aspirin group	13.25 ± 0.75	11.75 ± 0.50	12.37 ± 1.12	13.25 ± 1.75	13.37 ± 1.62[c]	13.75 ± 1.75[c]	13.25 ± 1.25[c]	13.75 ± 1.25[c]
Pa'								
Control group	12.90 ± 0.70	12.55 ± 0.39	12.15 ± 0.40	12.40 ± 0.53	12.50 ± 0.49	12.22 ± 0.28	12.06 ± 0.34	12.13 ± 0.24
ACh group	12.29 ± 0.47	12.92 ± 0.31	13.89 ± 0.80	15.33 ± 0.94[b]	24.64 ± 5.90[a]	25.71 ± 5.32[a,b]	27.30 ± 6.18[a,b]	27.35 ± 7.12[a]
Ketanserin group	11.42 ± 2.06	10.00 ± 1.44	17.75 ± 5.25[b]	21.92 ± 4.61[b]	27.12 ± 7.43[b]	30.17 ± 7.36[b]	27.00 ± 7.30[b]	25.75 ± 7.56
SR 140333 group	11.25 ± 1.19	11.06 ± 0.99	13.75 ± 0.50	14.92 ± 1.31[b]	16.58 ± 3.36	17.83 ± 3.61[b]	21.87 ± 4.94	17.25 ± 2.40[b]
Aspirin group	11.62 ± 0.62	10.50 ± 1.00	10.87 ± 1.12	11.62 ± 1.62[c]	11.87 ± 1.37[c]	11.87 ± 0.62[c]	11.87 ± 0.87[c]	12.12 ± 1.12[c]

Control group ($n = 8$) are lungs without ACh treatment. All values are mean ± s.e.mean.
[a] $P < 0.05$ (Student's paired t test) compared to base-line measured value in the same group.
[b] $P < 0.05$ (Student's unpaired t test) compared to the value measured in the control group.
[c] $P < 0.05$ (Student's t test) compared to value measured in ACh group.

assessed the possible interactions of NPY with different constrictor agents at the level of the different segments of the pulmonary vascular bed.

The effects of ACh on pulmonary circulation depend strongly on the animal species, the drug dosage, the route of administration and the type of preparation. *In vivo* studies have revealed both depressor or vasoconstrictor action in various species. In dogs (Hofman *et al.*, 1985) and rabbits (Lazaris *et al.*, 1969), ACh increase the pulmonary blood flow resistance, while it induces vasodilatation in cats (Nandiwada *et al.*, 1983) and calves (MacMurtry *et al.*, 1976). Both reactions can occur in the same species, as shown by Ni (1990) who observed depressor and pressor responses in rabbits. Isolated precontracted pulmonary arteries of rabbits (Altiere *et al.*, 1986) and dogs (Chand & Altura, 1981) relax with ACh. The vasodilator effect of ACh has been linked with the release of nitric oxide from the endothelium (Palmer *et al.*, 1987). Mechanisms underlying the contractile response are less certain.

The vasoconstrictor response observed in our study is in agreement with the findings of Catravas *et al.* (1984), who reported arterial vasoconstriction in isolated perfused rabbit lungs due to activation of muscarinic M_1 receptors (El-Kashef & Catravas, 1991). However, these authors did not locate the site of the contractile response. They demonstrated the involvement of arachidonic acid derivates in the vasospasm but did not speculate as to the possible role of other excitatory mediators, like neuropeptides or 5-HT, involved in ACh-evoked permeability changes in the same preparation. Our data show that the precapillary segment is the main site of ACh-triggered pulmonary vasoconstriction. The inhibitory effect of aspirin confirms the role of cyclo-oxygenase products in this reaction, while the inability of ketanserin and NK_1 antagonists to act as protectors precludes the involvement of SP and 5-HT in the contractile response to ACh. Accordingly, we conclude that the mechanisms responsible for vasoconstriction differ from those involved in the permeability changes. ACh seems to act directly on vascular smooth muscle where it probably interferes with cyclo-oxygenase derivates synthesis. As previously demonstrated with papaverine (Delaunois *et al.*, 1993a), the absence of a depressor action of ACh on this preparation is probably due to the low basal tone.

In our preparation, NPY inhibits the precapillary contractile response to exogenous ACh. This postjunctional inhibitory effect appears non specific, since NPY also prevented phenylephrine-induced vasoconstriction. Phenylephrine, well known for its systemic vasoconstrictor properties (Grundemar & Högestätt, 1992), is a poor spasmogen agent in the rabbit pulmonary circulation. The increase in total resistance produced by concentrations as high as 10^{-3} M were only 60% of the ACh-induced response. Moreover, the site of the vasospasm is in the arterial segment, i.e. the large arteries and not the precapillary vessels, as with ACh. Since NPY and aspirin inhibit the vascular responses to both ACh and phenylephrine, and since these responses affect different levels of the circulation, it seems likely that the cyclo-oxygenase cascade is the target of NPY action. Interference of NPY with prostaglandin synthesis has been speculatively suggested by T-Benchekroun *et al.* (1992), who showed that the inhibitory action of NPY on agonist-evoked tracheal responses is restricted to agents for which prostaglandins are important determinants.

The difference between our data and those of Wahlestedt *et al.* (1985), who observed a potentiation of NA-evoked vasoconstriction by NPY, should be explained by some differences in the reactivity of each vascular segment. The contractile response of an isolated pulmonary artery, recorded *in vitro*, is not representative of the response of the other vascular segments in the whole organ.

In the present work, we have also investigated the vascular effects of SP, involved in the ACh-triggered permeability changes, in order to see whether this peptide also plays a role

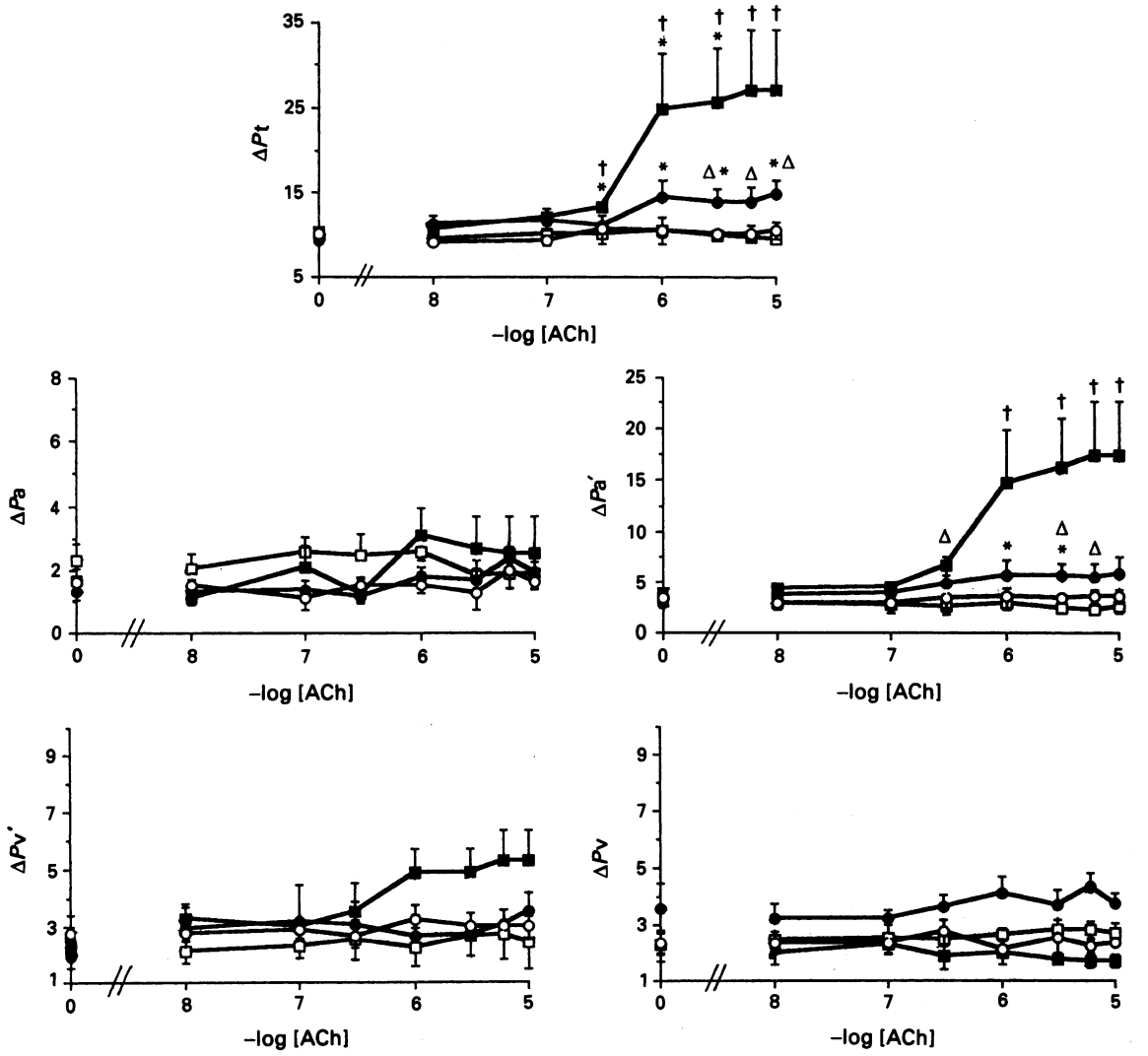


Figure 5 Concentration-response curves for acetylcholine (ACh): responses of the total (ΔPt), arterial (ΔPa), precapillary ($\Delta Pa'$), postcapillary ($\Delta Pv'$) and venous (ΔPv) pressure gradients expressed as cmH_2O. Data are expressed as mean and s.e.mean. Control group ($n = 8$) (○), ACh group ($n = 8$) (■), NPY-pretreated group ($n = 6$) (●) and aspirin-pretreated group ($n = 3$) (○). A value differing from baseline in the same group is denoted *, values differing from values in control group are indicated as $^{\Delta}$. † indicates a value differing from baseline and from the control value, and also from the values obtained in the NPY- and aspirin-treated groups.

in the haemodynamic response to ACh. The insignificant effect of SP in our preparation and the inability of the NK_1 antagonist to inhibit the vascular response to ACh (Table 3), suggests that SP plays no role in ACh-induced vasoconstriction. Although there are some differences between species or with the type of preparation, the main effect of SP on systemic or pulmonary vascular smooth muscle is hypotensive. In the rabbit, two opposite haemodynamic effects were observed. Intravenous injection of SP produced systemic vasodilatation and pulmonary vasoconstriction (Whorthen *et al.*, 1985), while low doses of SP elicited dilatation of precontracted pulmonary arteries. Our data show that SP administered alone does not significantly alter the pulmonary haemodynamics of rabbit isolated perfused lung. However, in combination with NPY, it does increase the total resistance. This enhancing effect of NPY is probably nonspecific, since this peptide has been shown to potentiate the effects of various constrictor agents in other preparations. The dose-response curve for SP was not influenced by aspirin.

We conclude that NPY can prevent ACh- and capsaicin-induced pulmonary oedema. It acts at the prejunctional level, modulating the release of neuropeptides from the C-fibres. NPY can also inhibit ACh-induced precapillary and phenylephrine-triggered arterial vasoconstriction, probably by acting on the arachidonic acid cascade.

The authors thank S. Bloden and J.-F. Bradfer for their technical assistance. They also thank Pr C. Advenier for his valuable advice on the protocol.

This work was supported by the National Funds for Scientific Research (FNRS).

References

ALTIERE, R.J., KIRITSY-ROY, J.A. & CATRAVAS, J.D. (1986). Acetylcholine-induced contractions in isolated rabbit pulmonary arteries: role of thromboxane A2. *J. Pharmacol. Exp. Ther.*, **236**, 535–541.

CATRAVAS, J.D., BUCCAFUSCO, J.J. & EL-KASHEF, H. (1984). Effects of acetylcholine in the pulmonary circulation of rabbits. *J. Pharmacol. Exp. Ther.*, **231**, 236–241.

CHAND, N. & ALTURA, B.M. (1981). Acetylcholine and bradykinin relax intrapulmonary arteries by acting on endothelial cells: role in lung vascular diseases. *Science*, **213**, 1376–1379.

DAWSON, C.A., LINEHAN, J.H. & RICKABY, D.A. (1982). Pulmonary microcirculatory hemodynamics. *Ann. N.Y. Acad. Sci.*, **384**, 90–106.

DELAUNOIS, A., GUSTIN, P. & ANSAY, M. (1992). Altered capillary filtration coefficient in parathion- and paraoxon-induced pulmonary edema in isolated and perfused rabbit lungs. *Toxicol. Appl. Pharmacol.*, **116**, 161–169.

DELAUNOIS, A., GUSTIN, P. & ANSAY, M. (1993a). Role of neuropeptides in acetylcholine-induced oedema in isolated and perfused rabbit lungs. *J. Pharmacol. Exp. Ther.*, **266**, 483–491.

DELAUNOIS, A., GUSTIN, P. & ANSAY, M. (1993b). Effects of capsaicin on the endothelial permeability in isolated and perfused rabbit lungs. *Fundam. Clin. Pharmacol.*, **7**, 81–91.

DELAUNOIS, A., GUSTIN, P. & ANSAY, M. (1994). Modulation of the acetylcholine- and substance P-induced pulmonary oedema by calcitonin gene-related peptide in the rabbit. *J. Pharmacol. Exp. Ther.*, **270**, 30–36.

DRAKE, R.E. & GABEL, J.C. (1981). Comparison of technic to measure pulmonary capillary filtration coefficient in dogs. *Microvasc. Res.*, **21**, 133–141.

EDVINSSON, L., EKBLAD, E., HAKANSON, R. & WAHLESTEDT, C. (1984). Neuropeptide Y potentiates the effect of various vasoconstrictor agents in rabbit blood vessels. *Br. J. Pharmacol.*, **83**, 519–525.

EL-KASHEF, H. & CATRAVAS, J.D. (1991) The nature of muscarinic receptor subtypes mediating pulmonary vasoconstriction in the rabbit. *Pulm. Pharmacol.*, **4**, 18–19.

EMONDS-ALT, X., DOUTREMEPUICH, J.-D., HEAULME, M., NELIAT, G., SANTUCCI, V., STEINBERG, R., VILAIN, P., BIHON, D., DUCOUX, J.-P., PROIETTO, V., VAN BROECK, D., SOUBRIE, P., LE FUR, G. & BRELIERE, J.-C. (1993). In vitro and in vivo biological activities of SR140333, a novel potent non-peptide tachykinin NK1 receptor antagonist. *Eur. J. Pharmacol.*, **250**, 403–413.

FALLGREN, B., ARLOCK, P. & EDVINSSON, L. (1993). Neuropeptide Y potentiates noradrenaline-evoked vasoconstriction by an intracellular calcium-dependent mechanism. *J. Autonom. Nerv. System*, **44**, 151–159.

FROSSARD, N. & BARNES, P.J. (1987). m-opioid receptors modulate non-cholinergic constrictor nerves in guinea-pig airways. *Eur. J. Pharmacol.*, **141**, 519–522.

GRUNDEMAR, L., GRUNDSTRÖM, N., JOHANSSON, I.G.M., ANDERSSON, R.G.G. & HAKANSON, R. (1990). Suppression by neuropeptide Y of capsaicin-sensitive sensory nerve-mediated contraction in guinea pig airways. *Br. J. Pharmacol.*, **99**, 473–476.

GRUNDEMAR, L. & HÖGESTÄTT, E.D. (1992). Unmasking the vasoconstrictor response to neuropeptide Y and its interaction with vasodilating agents in vitro. *Eur. J. Pharmacol.*, **221**, 71–76.

GRUNDSTROM, N. & ANDERSSON, R.G.G. (1985). In vivo demonstration of alpha-2 adrenoceptor-mediated inhibition of the excitatory non-cholinergic neurotransmission in guinea pig airways. *Naunyn-Schmied. Arch. Pharmacol.*, **328**, 236–240.

GUSTIN, P., URBAIN, B., PROUVOST, J.-F. & ANSAY, M. (1994). Effects of ammonia on pulmonary hemodynamics and vascular permeability in pigs: interaction with endotoxins. *Toxicol. Appl. Pharmacol.*, **125**, 17–26.

HAKIM, T.S. (1988). Identification of constriction in large versus small vessels using the arterial-venous and double-occlusion techniques in isolated canine lungs. *Respiration*, **54**, 61–69.

HAKIM, T.S., MICHEL, R.P. & CHANG, H.K. (1982). Partitioning of pulmonary vascular resistance in dogs by arterial and venous occlusion. *J. Appl. Physiol.*, **52**, 710–715.

HAN, C. & ABEL, P.W. (1987). Neuropeptide Y potentiates contraction and inhibits relaxation of rabbit coronary arteries. *J. Cardiovasc. Pharmacol.*, **9**, 675–681.

HOFMAN, W.F., EHRHART, I.C. & CATRAVAS, J.D. (1985). Prostanoid inhibition potentiates the vasoconstrictive response to acetylcholine in dog lung. *Fed. Proc.*, **44**, 1755.

ICHINOSE, M. & BARNES, P.J. (1989). Histamine H_3-receptors modulate nonadrenergic noncholinergic bronchoconstriction in guinea-pig *in vivo*. *Eur. J. Pharmacol.*, **174**, 49–55.

JOOS, G.F.P., PAUWELS, R.A.R. & VAN DER STRAETEN, M.E.R.P. (1988). The role of neuropeptides as neurotransmitters of non-adrenergic, non-cholinergic nerves in bronchial asthma. *Bull. Eur. Physiopathol. Respir.*, **23**, 619–637.

KERN, D.F., KIVLEN, C. & MALIK, A.G. (1984). Pulmonary capillary filtration coefficient (Kf,c): blood vs Albumin-Ringer's. *Microvasc. Res.*, **27**, 248.

LACROIX, J.-S., ANGGAARD, A., HÖKFELT, T., O'HARE, M.M., FAHRENKRUG, J. & LUNDBERG, J.M. (1990). Neuropeptide Y: presence in sympathetic and parasympathetic innervation of the nasal mucosa. *Cell. Tissue Res.*, **259**, 119–128.

LAZARIS, Y.A., SEREBROVSKAYA, I.A. & CHEREPANOVA, A.G. (1969). Study of reaction of pulmonary vascular bed to some vasoactive agents using serial contrast roetgenovasography. *Cor Vasa*, **11**, 21–28.

LEBLANC, G.G., TRIMMER, B.A. & LANDIS, S.C. (1987). Neuropeptide Y-like immunoreactivity in rat cranial parasympathetic neurons: coexistence with vasoactive intestinal peptide and choline acetyltransferase. *Proc. Natl. Acad. Sci. U.S.A.*, **84**, 3511–3515.

LUNDBERG, J.M., FAHRENKRUG, J., HÖKFELT, T., MARTLING, C.R., LARSSON, O., TATEMOTO, K. & ANGGARD, A. (1984). Coexistence of peptide HI and VIP in nerves regulating blood flow and bronchial smooth muscle tone in various mammals including man. *Peptides*, **235**, 593–606.

LUNDBERG, J.M., MARTLING, C.R., SARIA, A., FOLKERS, K. & ROSELL, S. (1983). Cigarette smoke induced oedema due to activation of capsaicin-sensitive vagal afferents and substance P release. *Neurosci.*, **10**, 1361–1368.

LUNDBERG, J.M., PERNOW, J., TATEMOTO, K. & DAHLOF, C. (1985). Pre- and post-junctional effects of NPY on sympathetic control of rat femoral artery. *Acta Physiol. Scand.*, **123**, 511–517.

LUNDBERG, J.M., TERENIUS, L., HÖKFELT, T., MARTLING, C.R., TATEMOTO, K., MUTT, V., POLAK, J., BLOOM, S.R. & GOLDSTEIN, M. (1982). Neuropeptide Y (NPY)-like immunoreactivity in peripheral noradrenergic neurons and effects of NPY on sympathetic function. *Acta Physiol. Scand.*, **116**, 477–480.

MACMURTRY, I.F.E., WEIR, E.K., REEVES, J.T., WILL, D.H. & GROVER, R.F. (1976). Prostaglandin synthesis does not mediate the pulmonary vasodilatory effect of acetylcholine. *Prostaglandins*, **11**, 63–69.

MATRAN, R., MARTLING, C.-R. & LUNDBERG, J.M. (1989). Inhibition of cholinergic and non-adrenergic, non-cholinergic bronchoconstriction in the guinea pig mediated by neuropeptide Y and alpha 2-adrenoceptors and opiate receptors. *Eur. J. Pharmacol.*, **163**, 15–23.

NANDIWADA, P.A., HYMAN, A.L. & KADOWITZ, P.J. (1983). Pulmonary vasodilator responses to vagal stimulation and acetylcholine in the cat. *Circ. Res.*, **53**, 86–95.

NI, H. (1990). The pulmonary vascular responses to peripheral and central applications of acetylcholine. *Eur. J. Pharmacol.*, **181**, 167–174.

PALMER, R.J.M., FERRIGE, A.G. & MONCADA, S. (1987). Nitric oxide release accounts for the biological activity of endothelial derived relaxing factor. *Nature*, **327**, 524–526.

STRETTON, C.D. & BARNES, P.J. (1988). Modulation of cholinergic neurotransmission in guinea pig trachea by neuropeptide Y. *Br. J. Pharmacol.*, **93**, 672–678.

SUMITA, T., ISHIKAWA, N., HASHIBA, Y., TAKAGI, K. & SATAKE, T. (1989). 5-Hydroxytryptamine receptor subtypes participating in pulmonary edema in dogs. *Eur. J. Pharmacol.*, **164**, 69–75.

TATEMOTO, K. (1982). Neuropeptide Y: complete amino acid sequence of the brain peptide. *Proc. Natl. Acad. Sci. U.S.A.*, **79**, 5485–5489.

T-BENCHEKROUN, M., FOURNIER, A., ST-PIERRE, S. & CADIEUX, A. (1992). Inhibitory action of neuropeptide Y on agonist-induced responses in isolated guinea pig trachea. *Eur. J. Pharmacol.*, **216**, 421–428.

TOTH, P.T., BINDOKAS, V.P., BLEAKMAN, D., COLMERS, W.F. & MILLER, R.J. (1993). Mechanism of presynaptic inhibition by neuropeptide Y at sympathetic nerve terminals. *Nature*, **364**, 635–638.

UDDMAN, R., SUNDLER, F. & EMSON, P. (1984). Occurrence and distribution of neuropeptide Y-immunoreactive nerves in the respiratory tract and middle ear. *Cell. Tiss. Res.*, **237**, 321–327.

WAHLESTEDT, C., EDVINSSON, L., EKBLAD, E. & HAKANSON, R. (1985). Neuropeptide Y potentiates noradrenaline-evoked vasoconstriction: mode of action. *J. Pharmacol. Exp. Ther.*, **234**, 735–741.

WALLENSTEIN, S., ZUCKER, C.L. & FLEISS, J.L. (1980). Some statistical methods useful in circulation research. *Circ. Res.*, **47**, 1–9.

WANGENSTEEN, O.D., LYSAKER, E. & DAVARYN, P. (1977). Pulmonary capillary filtration and flexion coefficients in the adult rabbit. *Microvasc. Res.*, **14**, 81–87.

WHORTEN, G.S., GUMBAY, R.S., TANAKA, D.T. & GRUNSTEIN, M.M. (1985). Opposing hemodynamic effects of substance P on pulmonary vasculature in rabbits. *J. Appl. Physiol.*, **59**, 1098–1103.

(Received April 5, 1994
Revised June 17, 1994
Accepted July 15, 1994)

Br. J. Pharmacol. (1994), 113, 982–986 © Macmillan Press Ltd, 1994

Pharmacological profile of the ATP-mediated increase in L-type calcium current amplitude and activation of a non-specific cationic current in rat ventricular cells

[1]Frédérique Scamps & Guy Vassort

Laboratoire de Physiopathologie Cardiovasculaire, INSERM U-390, CHU Arnaud de Villeneuve, 32495 Montpellier Cedex OS, France

1 The pharmacological profile of the ATP-induced increase in I_{Ca} amplitude and of ATP activation of a non-specific cationic current, I_{ATP}, was investigated in rat ventricular cells.

2 The EC_{50} values for I_{Ca} increase and I_{ATP} activation were 0.36 μM and 0.76 μM respectively. Suramin (10 μM) and cibacron blue (1 μM) competitively antagonized both effects of ATP.

3 The rank order of efficacy and potency of ATP analogues in increasing I_{Ca} amplitude was 2-methylthio-ATP ≈ATP≈ATPγS. The derivatives α,β-methylene-ATP, β,γ-methylene-ATP and β,γ-imido-ATP up to 500 μM had no significant effects.

4 The rank order of efficacy of ATP analogues in activating a non-specific cationic current, I_{ATP}, was 2-methylthio-ATP >ATP >>ATPγS. The rank order of potency was 2-methylthio-ATP≈ATP. The EC_{50} of ATPγS could not be determined owing to its very low efficacy.

5 The ATP analogues α,β-methylene-ATP, β,γ-methylene-ATP and β,γ-imido-ATP at 500 μM did not activate I_{ATP} but acted as antagonists of activation of I_{ATP} by ATP.

6 The results suggest that the increase in I_{Ca} amplitude induced by external ATP is due to activation of P_{2Y}-purinoceptors.

7 The mechanism of I_{ATP} activation remains to be determined before the receptor subtype involved can be deduced.

Keywords: Adenosine 5'-triphosphate; P_{2Y}-purinoceptor; suramin; cibacron blue 3GA; calcium current; non-specific cationic current; rat ventricular myocyte

Introduction

It is now well established that extracellular adenosine 5'-triphosphate (ATP) exerts physiological effects in many different tissues through P_2-purinoceptors, and at least five subtypes of P_2-purinoceptors are proposed: P_{2T}, P_{2X}, P_{2Y} and P_{2U} (Dubyak & El-Moatassim, 1993). In rat cardiac preparations, ATP is reported to have positive inotropic effects and to increase the Ca^{2+} transients of electrically stimulated cells (Danziger *et al.*, 1988; Legssyer *et al.*, 1988). It has also been reported that ATP transiently increases the intracellular Ca^{2+} concentration, Ca_i, of quiescent cells (De Young & Scarpa, 1987; Danziger *et al.*, 1988; Björnsson *et al.*, 1989; Pucéat *et al.*, 1991a; Hirano *et al.*, 1991). In addition, electrophysiological studies have shown that ATP activates a non-specific cationic current in frog, rat and guinea pig cardiac cells (Friel & Bean, 1988; Scamps & Vassort, 1990; Matsuura & Ehara, 1992), an inwardly rectifying K^+ channel in frog (Friel & Bean, 1990) and a chloride current in guinea pig (Matsuura & Ehara, 1992), increases the L-type calcium current amplitude in rat (Scamps *et al.*, 1990; 1992; Zheng *et al.*, 1993) and increases both the L- and T-type in frog cells (Alvarez & Vassort, 1992). However, in ferret ventricular myocytes, ATP decreases both Ca_i and I_{Ca} amplitude and does not induce the non-specific cationic current (Qu *et al.*, 1993a). This decrease in I_{Ca} has been attributed to occupancy of P_{2Y}-purinoceptors, with 2-methylthio-ATP being more potent than α,β-methylene-ATP (Qu *et al.*, 1993b). The transient increase in Ca_i (in rat) and the positive inotropism (in rat and guinea pig) induced by ATP have also been attributed to P_{2Y} purinoceptors (Björnsson *et al.*, 1989; Mantelli *et al.*, 1993; Wang *et al.*, 1993). In the present study we have investigated the pharmacological profile of ATP-activated non-specific cationic current and the increase in I_{Ca} in rat ventricular myocytes, which are supposed to be largely responsible for the changes in Ca_i and the positive inotropism.

[1] Author for correspondence.

Methods

Cell isolation

Adult male Wistar rats (200–300 g) were anaesthetized with ethylcarbamate prior to excision of the hearts. The procedure for dissociating ventricular myocytes has been previously described (Scamps *et al.*, 1990).

Electrophysiological study

Membrane currents were recorded with the whole-cell patch-clamp (Hamill *et al.*, 1981). For routine monitoring of L-type Ca current, I_{Ca}, and of non-specific cationic current induced by external ATP, I_{ATP}, a ventricular cell was depolarized from −70 mV holding potential to 0 mV for 200 ms every 4 s. The cells were superfused with solution containing (mM) CsCl 20, NaCl 117, $CaCl_2$ 1.8, $MgCl_2$ 1.7, glucose 10 and HEPES 10; pH was adjusted to 7.4 with NaOH and 50 μM tetrodotoxin was added to block the sodium current. No T-type Ca current was observed in the rat ventricular cell. The internal solution in the patch electrode contained (mM) CsCl 120, $MgCl_2$ 4, Na_2ATP 5, Na_2-creatine phosphate 5, Na_2GTP 0.4, Cs_2EGTA 5, $CaCl_2$ 0.062 (intracellular free $Ca^{2+} = 2 \times 10^{-9}$ M) and HEPES 20; pH was adjusted to 7.2 with CsOH. Experiments were conducted at room temperature (20 ± 1°C).

Drugs

ATP and cibacron blue 3GA (cibacron blue) were from Sigma. Adenosine 5'-*O*-3-thiotriphosphate (ATPγS), 2-methylthio-ATP, α,β-methylene-ATP, β,γ-methylene-ATP and β,γ-amido-ATP were from Boehringer Mannheim (France). Suramin was a gift from Dr Kazda, Bayer Leverkusen (Germany).

Statistical analysis

Data are given as means ± s.e.mean. Statistical analyses were based on a paired *t*-test or on a Student's *t*-test. The differences were significant when $P<0.05$. To determine the concentration–response curves, no more than two concentrations of ATP, one low and one high, were used for each cell.

Results

Effects of inhibitors

Figure 1 shows typical effects of external application of ATP on I_{Ca} amplitude and on holding current for a holding potential of −70 mV in rat ventricular cells. The first effect of external application of 1 μM ATP was to induce a transitory inward current at −70 mV which peaked more or less rapidly depending on the ATP concentration and then decreased (upper part of Figure 1 for current traces; lower part of Figure 1 and Figure 6 for kinetics of activation). This change in holding current has been attributed to the activation of a non-specific cationic current, I_{ATP} (Scamps & Vassort, 1990). In addition, application of 1 μM ATP induced a progressive increase of I_{Ca} amplitude up to a steady-state value reached after 2–3 min of ATP application (upper part of Figure 1 for current traces; lower part shows the kinetics of effects). The increase in I_{Ca} amplitude under ATP application has also been characterized (Scamps *et al.*, 1990; 1992). In 80% of cells ATP induced both effects, while in 20% ATP induced only the non-specific cationic current. The 20% of cells have not been analysed.

In the presence of 10 μM suramin, a non-specific blocker of P_2-purinoceptors, 3 μM ATP had no effects on both currents (Figure 2a). Increasing the ATP concentration to 100 μM could overcome the blocking effect of suramin (not shown). In the presence of 1 μM cibacron blue (reactive blue 2), a reported selective inhibitor of P_{2Y}-purinoceptors, ATP at 1 μM hardly increased I_{Ca} and activated a small but significant I_{ATP}, as shown in Figure 2b. A full response developed when 20 μM ATP was applied.

Figure 3 shows the concentration–response curves of the ATP-induced I_{Ca} increase in control cells and in the presence of the inhibitors. Under control conditions, the concentration of ATP giving half-maximal effect, EC_{50}, was 0.36 μM. This value was shifted to 2.2 μM and 12.4 μM in the presence of 1 μM cibacron blue or 10 μM suramin respectively. The Hill factor, n_H, was 1.9, 1.8 and 2.2, respectively, in control and cibacron blue- and suramin-treated cells. The concentration–response curves of ATP activation of a non-specific cationic current, I_{ATP}, are illustrated in Figure 4. Under control conditions, the EC_{50} was 0.76 μM. This value was shifted to 4.1 μM and 16.5 μM in the presence of 1 μM cibacron blue and 10 μM suramin respectively. n_H was 1.9, 2.6 and 3.1, respectively, in control and cibacron blue- and suramin-treated cells. At 10 μM, cibacron blue completely inhibited the effects of 10 μM ATP on I_{Ca} and I_{ATP} ($n=3$, not shown) and thus appears to be a more potent inhibitor of ATP effects than suramin.

Agonist efficacy and potency

To determine whether the I_{Ca} increase and I_{ATP} activation are due to occupation of the same subtype of purinergic receptor,

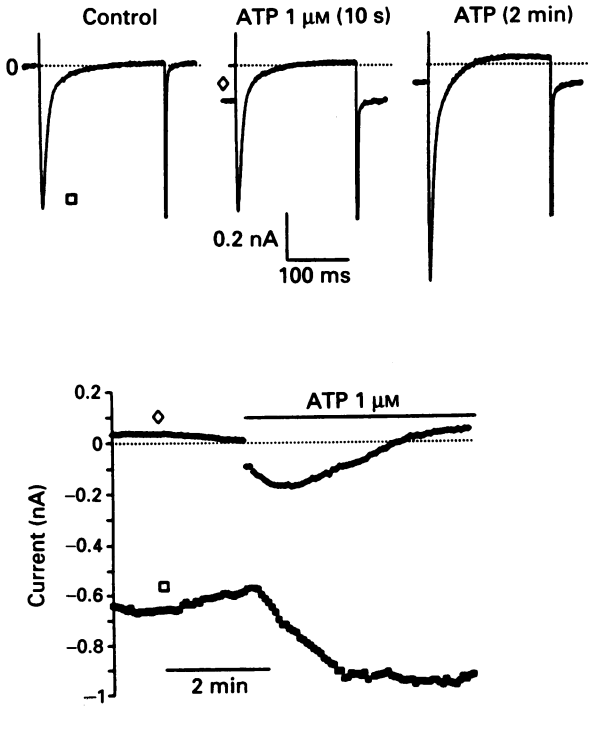


Figure 1 Effects of ATP on calcium current amplitude measured at 0 mV test pulse and on holding current flowing at −70 mV, every 4 s. In a control cell, 1 μM ATP increased I_{Ca} amplitude (□, measured as the difference between peak inward current and the current at the end of the 200 ms pulse) and the current measured at −70 mV became transiently more inward (◇, measured relative to the zero current). The upper part of figure shows current traces and the lower part of the kinetics of ATP effects.

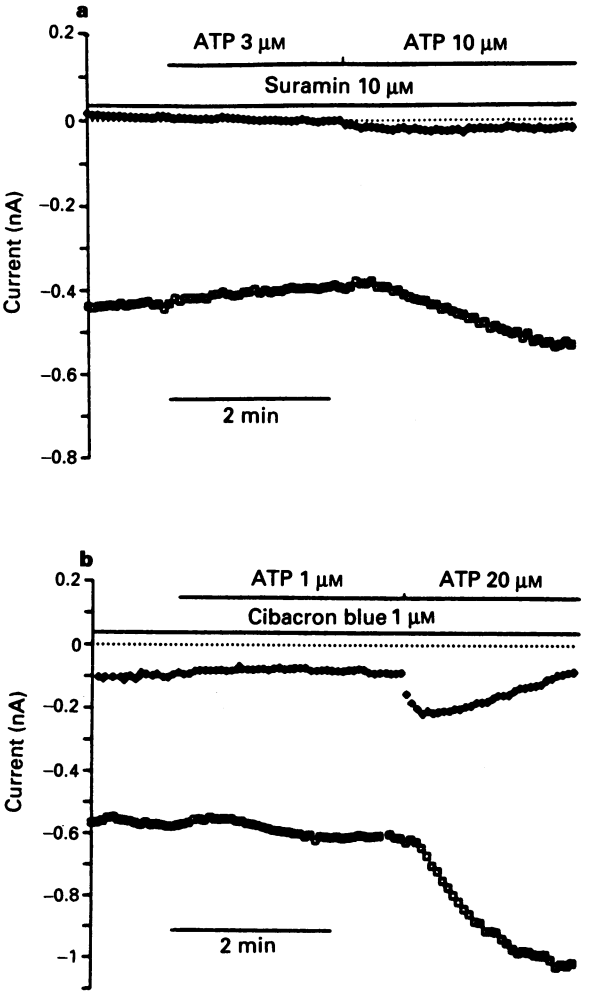


Figure 2 Effects of ATP on I_{Ca} amplitude and on holding current on a cell superfused with (a) 10 μM suramin and (b) 1 μM cibacron blue (same protocol as in Figure 1).

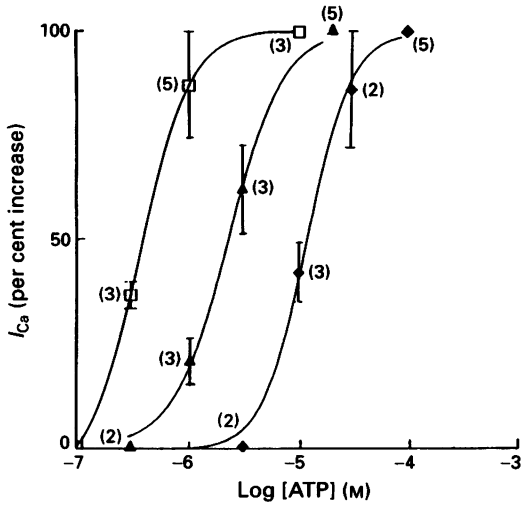


Figure 3 Concentration–response curves of ATP-induced I_{Ca} increase in control (□) cells and in the presence of 1 μM cibacron blue (▲) 10 μM suramin (◆). Curves were fitted according to a sigmoid shape: $y = EC_{max} \times [ATP]^{nH}/([ATP] + EC_{50}^{nH})$. The curves were normalized to EC_{max} (concentration giving maximal effect). Number of cells in brackets (as for the other figures).

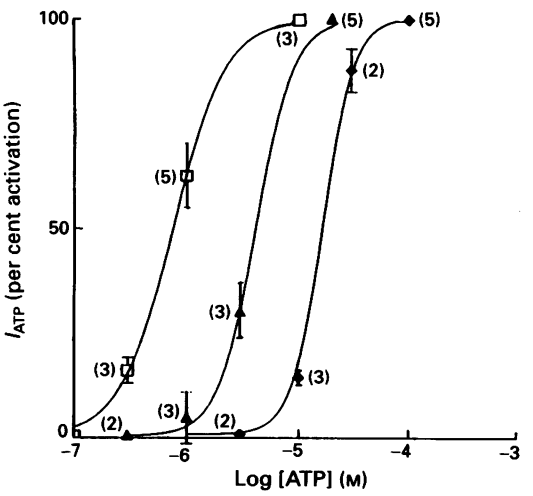


Figure 4 Concentration–response curves of ATP-activated non-specific cationic current in control (□), in the presence of 1 μM cibacron blue (▲) or 10 μM suramin (◆). Curves were fitted according to $y = EC_{max} \times [ATP]^{nH}/([ATP] + EC_{50}^{nH})$ and normalized to EC_{max}.

the rank orders of ATP analogues efficacy and potency were evaluated. Figure 5 gives the maximal percentage of I_{Ca} increase and the maximal amplitude of I_{ATP} elicited by applying various ATP analogues. For I_{Ca} increase, the rank order of efficacy was 2-methylthio-ATP≈ATP≈ATPγS. The ATP derivatives of α,β-methylene-ATP, β,γ-methylene-ATP and β,γ-imido-ATP were without significant effects (Figure 5a). The EC_{50} observed was 0.23 μM and 0.41 μM for 2-methylthio-ATP and ATPγS respectively. Thus the rank order of potency for I_{Ca} increase was 2-methylthio-ATP≈ATP≈ATPγS. For I_{ATP} activation the rank order of efficacy was 2-methylthio-ATP > ATP >> ATPγS (Figure 5b). Similarly to the case of the I_{Ca} increase, α,β-methylene-ATP, β,γ-methylene-ATP and β,γ-imido-ATP at 500 μM did not activate I_{ATP}. The EC_{50} for 2-methylthio-ATP was 0.71 μM. The EC_{50} for ATPγS could not be determined because of the small amplitude of the maximal effect. Thus the rank order of potency for activation of I_{ATP} was 2-methylthio-ATP≈ATP.

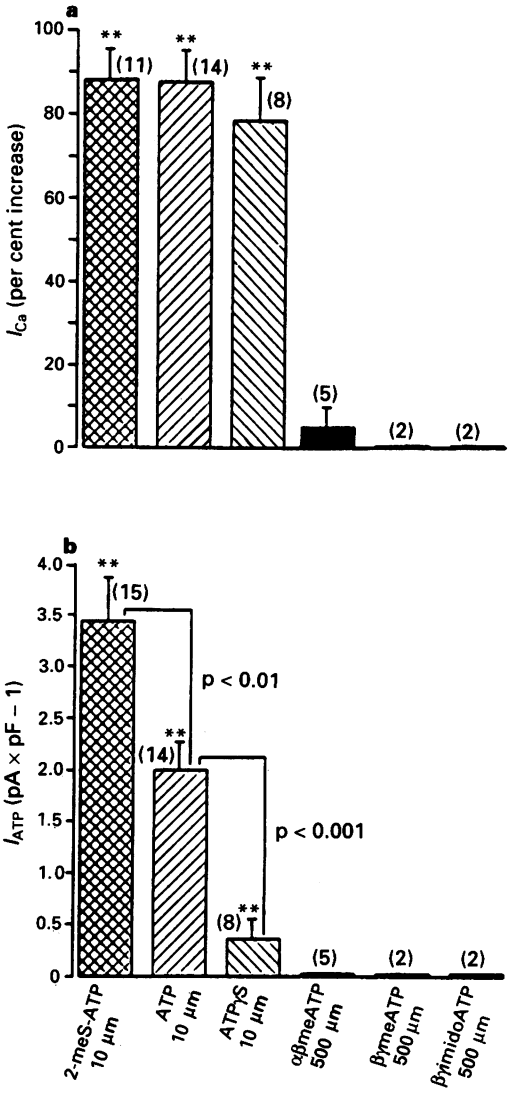


Figure 5 Rank order of agonist efficacy on the percentage of I_{Ca} increase (a) and the density of I_{ATP} (b). The values of I_{ATP} are normalized to the cell capacitance and thus given in density. $^{**}P < 0.01$ (paired test). In (b) a Student's *t*-test was used to compare 2-methylthio-ATP and ATPγS with ATP; *P*-values are given in the figure.

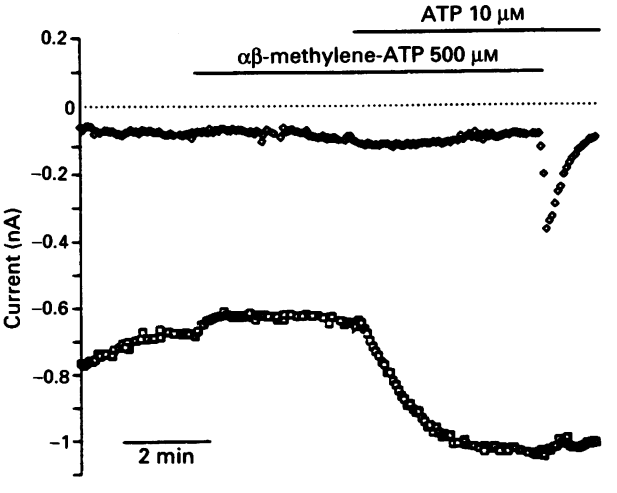


Figure 6 Antagonism of α,β-methylene-ATP on ATP activation of a non-specific cationic current. α,β-Methylene-ATP by itself did not activate I_{ATP} nor did it increase I_{Ca} amplitude (same protocol as in Figure 1).

As stated above, the analogues α,β-methylene-ATP, β,γ-methylene ATP and β,γ-imido-ATP did not increase I_{Ca} amplitude, even at 500 μM, and did not prevent the increase in I_{Ca} induced by adding 10 μM ATP in their presence (Figure 6). Furthermore, these analogues, which also did not activate I_{ATP}, prevented the activation of I_{ATP} with the further addition of 10 μM ATP. Note that on washout of these analogues, I_{ATP} instantaneously appeared. Figure 6 illustrates such an effect for α,β-methylene-ATP. Similar results were obtained with the three analogues mentioned above ($n = 6$, for two experiments in each condition). α,β-methylene-ATP, used at 100 μM, did not prevent the activation of I_{ATP} (not shown), which suggested a competitive antagonism. Superfusion of the cell for a longer period of time (10 min) with 500 μM α,β-methylene-ATP did not desensitize the ATP effects (two cells).

Discussion

In the present study, it is shown that the external application of ATP triggers an increase in I_{Ca} amplitude and activates a non-specific cationic current, I_{ATP}, with similar EC_{50}. Both currents are inhibited by the P_2-purinoceptor antagonists suramin and cibacron blue. However, the subtypes of purinoceptors involved should be different, as suggested by the variations in rank order of efficacy of ATP analogues and the observation that some of these analogues exert an antagonistic effect only on the ATP-activated non-specific cationic current.

Based on the rank order of efficacy and potency of ATP analogues, 2-methylthio≈ATP≈ATPγS>>α,β-methylene-ATP, the increase in I_{Ca} amplitude indicates activation of a P_{2Y}-purinoceptor. In support of this proposal, α,β-methylene-ATP (a potent P_{2X}-purinoceptor agonist) not only had no effect by itself, but it also did not induce desensitization of the receptor. The increase in I_{Ca} amplitude is probably responsible for part of the sustained positive inotropism reported for purinergic compounds in rat papillary muscle (Legssyer *et al.*, 1988; Scamps *et al.*, 1990). In agreement with this suggestion, a P_{2Y}-purinoceptor was recently proposed to mediate the positive inotropism induced by ATP in rat and guinea pig hearts (Wang *et al.*, 1993; Mantelli *et al.*, 1993). A discrepancy remains concerning the effect of α,β-methylene-ATP, which on the one hand did not significantly increase I_{Ca} amplitude (this study) and on the other hand had clear positive inotropic effects (Legssyer *et al.*, 1988; Mantelli *et al.*, 1993). A possible alternative is that α,β-methylene-ATP acts through another type of receptor, the P_{2X}-purinoceptor being a good candidate. Occupation of this receptor subtype could involve different intracellular events, such as an increase in phosphoinositide turnover, as reported by Legssyer *et al.* (1988), and expected to lead to a positive inotropism. Consequently, the positive inotropism induced by purinergic compounds should be related to occupation of different purinoceptors subtypes. One of them is linked to the increase in I_{Ca} amplitude and identified in the present study as a P_{2Y}-purinoceptor with an EC_{50} of around 1 μM, in the range of values usually reported for the effects of ATP. The best concentration–response curve fittings were obtained by assuming two binding sites. The same Hill coefficient was obtained for the inhibition of I_{Ca} of chromaffin cells by ATP (Gandia *et al.*, 1993), while for I_{Ca} inhibition in ferret ventricular cells a 1:1 binding of ligand to receptor was suggested (Qu *et al.*, 1993b). Suramin and cibacron blue were competitive antagonists, which suggests that they act at the ATP binding site. It should be mentioned that the concentration of antagonists required in rat ventricular cells (1 μM for cibacron blue and 10 μM suramin) used in this study was much lower than those reported to achieve inhibition in other cell types (usually in the 100–500 μM range).

In the present study, the EC_{50} values obtained for I_{Ca} increase and I_{ATP} activation during ATP application were not significantly different under control conditions or in the presence of suramin or cibacron blue, which rather suggests a common receptor for both effects. As for the I_{Ca} increase, two binding sites gave the best concentration–response curves fitting for I_{ATP} activation. Two binding sites were also reported for I_{ATP} in bullfrog atrial cells (Friel & Bean, 1988). However, the rank order of efficacy of the agonists is not identical for the I_{Ca} increase and I_{ATP} activation. While 2-methylthio-ATP, ATP and ATPγS are roughly equipotent in increasing I_{Ca}, there is a clear sequence of agonist efficacy in activating I_{ATP}, with 2-methylthio-ATP being the most efficient and ATPγS the least. Importantly, while high concentrations of the non-hydrolysable analogues prevented I_{ATP}, they did not prevent the increase in I_{Ca} amplitude and thus are not antagonists of this response. Such an antagonistic effect of α,β-methylene-ATP on I_{ATP} activation has been previously reported by Friel & Bean (1988) in bullfrog atrial cells. In addition, we show that the lack of ATP effect in the presence of these analogues was not due to a slow desensitization of the receptor since a full effect of ATP was observed on washout of these analogues. Consequently, α,β-, β,γ-methylene-ATP and β,γ-imido-ATP act as rather specific antagonists of I_{ATP}. We should point out that the activation of I_{ATP} that we report in this study and which was determined to be a non-specific cationic current as previously described, and not a chloride current, seems inconsistent with the hypothesis we initially proposed (Scamps & Vassort, 1990), i.e. I_{ATP} is the consequence of an internal acidosis, with α,β-methylene-ATP, β,γ-methylene-ATP and β,γ-imido-ATP being less potent but as efficient as ATP in inducing acidosis (Pucéat *et al.*, 1991b). However, it should be noted that in parallel experiments the cells did not show clear acidosis on applying ATP. Thus these results do not rule out the possibility that acidosis can activate an I_{ATP}, the nature of which (non-specific cationic current or chloride current) should be checked by applying the ATP analogues.

In view of the present results, two theories can be proposed concerning the type of receptors involved. First, the receptors involved in the I_{Ca} increase and in I_{ATP} activation are of two different subtypes of P_2-purinoceptors, which, however, share a close pharmacological profile. The presence of two types of P_2-purinoceptors on the same preparation has been reported previously based on photoaffinity labelling (Giannattasio *et al.*, 1992). Second, both types of effects are mediated by a common P_{2Y}-purinoceptor, but the effector involved in I_{ATP} is blocked by the non-hydrolysable analogues. A strong argument against the latter hypothesis of a common receptor is that the increase in I_{Ca} amplitude is mediated by a G-protein, while the activation of I_{ATP} is not (Scamps *et al.*, 1992; Zheng *et al.*, 1993). Indeed, it has been shown that internal perfusion of the cell with non-hydrolysable analogues of GTP modifies the ATP-induced I_{Ca} increase in a way that would be expected from involvement of a G-protein while having no effect on the I_{ATP} response. It has been proposed that P_{2Y}-purinoceptors can be subdivided in two subtypes (Illes & Nörenberg, 1993). The subtype $P_{2Y\alpha}$ (also called P_{2X}, see Edwards & Gibb, 1993) would be the ligand-activated channel while the $P_{2Y\beta}$ would be G-protein linked. Until now, cloning of G-protein-coupled receptors has demonstrated three types of P_{2Y}-purinoceptors, classified as P_{2Y1}, P_{2Y2} and P_{2Y3}, with P_{2Y1} having the closest pharmacological profile to the P_2-purinoceptor that induces I_{Ca} increase (Barnard *et al.*, 1994). However, P_{2X}-purinoceptor has been solubilized and found to have a pharmacology rather different from I_{ATP} (Bo *et al.*, 1992). A complementary hypothesis initially suggested by Björnsson *et al.* (1989) and developed by Christie *et al.* (1992) would be that I_{ATP} is the result of an external phosphorylation. According to this scheme, a kinase would be close to the P_{2Y}-purinoceptor and would utilize the appropriate substrate. This hypothesis would both meet the pharmacological profile and explain the competitive antagonism of the poorly hydrolysable analogues through a mass action law on the kinase reaction. However,

in that case ATPγS would be as efficient as ATP. Obviously, further experiments are required to understand the nature of I_{ATP} activation.

In conclusion, the increase in I_{Ca} amplitude caused by ATP application relates to occupancy of a P_{2Y}-purinoceptor. Despite a close pharmacological profile and antagonistic effects of suramin and cibacron blue, the activation of I_{ATP} cannot be attributed to simple P_{2Y}-purinoceptor occupancy. A better understanding of the mechanism of activation of I_{ATP} should help to clarify the receptor subtype involved.

We thank Jaime Requena for reading the manuscript and Catherine Vannier and Michel Pucéat for cell preparation.

References

ALVAREZ, J. & VASSORT, G. (1992). Properties of the low threshold Ca current in single frog atrial cardiomyocytes. *J. Gen. Physiol.*, **100**, 519–545.

BARNARD, E.A., BURNSTOCK, G. & WEBB, T.E. (1994). G protein-coupled receptors for ATP and other nucleotides: a new receptor family. *Trends Pharmacol. Sci.*, **15**, 67–70.

BJÖRNSSON, O.G., MONCK, J.R. & WILLIAMSON, J.R. (1989). Identification of P_{2Y} purinoceptors associated with voltage-activated cation channels in cardiac ventricular myocytes of the rat. *Eur. J. Biochem.*, **186**, 395–404.

BO, X., SIMON, J., BURNSTOCK, G. & BARNARD, E.A. (1992). Solubilization and molecular size determination of the P_{2X} purinoceptor from rat vas deferens. *J. Biol. Chem.*, **267**, 17581–17587.

CHRISTIE, A., SHARMA, V.K. & SHEU, S.-S. (1992). Mechanism of extracellular ATP-induced increase of cytosolic Ca^{2+} concentration in isolated rat ventricular myocytes. *J. Physiol.*, **445**, 369–388.

DANZIGER, R.S., RAFFAELI, S., MORENO-SANCHEZ, R., SAKAI, M., CAPOGROSSI, M.C., SPURGEON, H.A., HANSFORD, R.G. & LAKATTA, E.G. (1988). Extracellular ATP has a potent effect to enhance cystolic calcium and contractility in single ventricular myocytes. *Cell Calcium*, **9**, 193–199.

DE YOUNG, M.B. & SCARPA, A. (1987). Extracellular ATP induces Ca^{2+} transients in cardiac myocytes which are potentiated by norepinephrine. *FEBS Lett.*, **223**, 53–58.

DUBYAK, G.R. & EL-MOATASSIM, C. (1993). Signal transduction via P_2-purinergic receptors for extracellular ATP and other nucleotides. *Am. J. Physiol.*, **265**, C577–C606.

EDWARDS, F.A. & GIBB, A.J. (1993). ATP – a fast neurotransmitter. *FEBS Lett.*, **325**, 86–89.

FRIEL, D.D. & BEAN, B.P. (1989). Two ATP-activated conductances in bullfrog atrial cells. *J. Gen. Physiol.*, **91**, 1–27.

FRIEL, D.D. & BEAN, B.P. (1990). Dual control by ATP and acetylcholine of inwardly rectifying K^+ channels in bovine atrial cells. *Pflügers Arch.*, **415**, 651–657.

GANDIA, L., GARCIA, A.G. & MORAD, M. (1993). ATP modulation of calcium channels in chromaffin cells. *J. Physiol.*, **470**, 55–72.

GIANNATTASIO, B., POWERS, K. & SCARPA, A. (1992). Characterization of myocardial extracellular ATP receptors by photoaffinity labelling and functional assays. *FEBS Lett.*, **304**, 27–31.

HAMILL, O.P., MARTY, A., NEHER, E., SAKMANN, B. & SIGWORTH, F.J. (1981). Improved patch-clamp techniques for high resolution current recording from cells and cell free membrane patches. *Pflügers Arch.*, **391**, 85–100.

HIRANO, Y., ABE, S., SAWANOBORI, T. & HIRAOKA, M. (1991). External ATP-induced changes in $[Ca^{2+}]_i$ and membrane currents in mammalian atrial myocytes. *Am. J. Physiol.*, **260**, C673–C680.

ILLES, P. & NÖRENBERG, W. (1993). Neuronal ATP receptors and their mechanism of action. *Trends Pharmacol. Sci.*, **14**, 50–54.

LEGSSYER, A., POGGIOLI, J., RENARD, D. & VASSORT, G. (1988). ATP and other adenine compounds increase mechanical activity and inositol triphosphate production in rat heart. *J. Physiol.*, **401**, 185–199.

MANTELLI, L., AMERINI, S., FILIPPI, S. & LEDDA, F. (1993). Blockade of adenosine receptors unmasks a stimulatory effect of ATP on cardiac contractility. *Br. J. Pharmacol.*, **109**, 1268–1271.

MATSUURA, H. & EHARA, T. (1992). Activation of chloride current by purinergic stimulation in guinea pig heart cells. *Circ. Res.*, **70**, 851–855.

PUCEAT, M., CLEMENT, O., SCAMPS, F. & VASSORT, G. (1991a). Extracellular ATP-induced acidification leads to cytosolic calcium transient rise in single rat cardiac myocytes. *Biochem. J.*, **274**, 55–62.

PUCEAT, M., CLEMENT, O. & VASSORT, G. (1991b). Extracellular MgATP activates the Cl^-/HCO_3^- exchanger in single rat cardiac cells. *J. Physiol.*, **444**, 241–256.

QU, Y., HIMMEL, H.M., CAMPBELL, D.L. & STRAUSS, H.C. (1993a). Effects of extracellular ATP on I_{Ca}, $[Ca^{2+}]_i$ and contraction in isolated ferret ventricular myocytes. *Am. J. Physiol.*, **264**, C702–C708.

QU, Y., CAMPBELL, D.L. & STRAUSS, H.C. (1993b). Modulation of L-type Ca^{2+} current by extracellular ATP in ferret isolated right ventricular myocytes. *J. Physiol.*, **471**, 295–317.

SCAMPS, F. & VASSORT, G. (1990). Mechanism of extracellular ATP-induced depolarization in rat isolated ventricular cardiomyocytes. *Pflügers Arch.*, **417**, 309–316.

SCAMPS, F., LEGSSYER, A., MAYOUX, E. & VASSORT, G. (1990). The mechanism of positive inotropy induced by adenosine triphosphate in rat heart. *Circ. Res.*, **67**, 1007–1016.

SCAMPS, F., RYBIN, V., PUCEAT, M., TKACHUK, V. & VASSORT, G. (1992). A Gs protein couples P_2-purinergic stimulation to cardiac Ca channels without cyclic AMP production. *J. Gen. Physiol.*, **100**, 675–701.

WANG, D.S., CUSACK, N.J. & BELARDINELLI, L. (1993). Identification of P_2-purinoceptor subtype responsible for the extracellular effects of ATP in rat ventricular myocytes. *Circulation*, **88**, 1–434.

ZHENG, J.-S., CHRISTIE, A., LEVY, M.N. & SCARPA, A. (1993). Modulation by extracellular ATP of two distinct currents in rat myocytes. *Am. J. Physiol.*, **264**, C1411–C1417.

(Received March 14, 1994
Accepted August 2, 1994)

Br. J. Pharmacol. (1994), **113**, 987–993 © Macmillan Press Ltd, 1994

The transhepatic action of ATP on the hepatic arterial and portal venous vascular beds of the rabbit: the role of nitric oxide

Dominic J. Browse, *Robert T. Mathie, Irving S. Benjamin & [1]Barry Alexander

Department of Surgery, King's College School of Medicine and Dentistry, Rayne Institute, 123 Coldharbour Lane, London SE5 9NU and *Department of Surgery, Royal Postgraduate Medical School, 150 Du Cane Road, London W12 0NN

1 The effect of bolus administration of adenosine 5'-triphosphate (ATP) into the portal vein on hepatic arterial pressure (the transhepatic action of ATP) and portal venous pressure, and the contribution of nitric oxide towards these responses, was studied in the *in vitro* dual-perfused rabbit liver.

2 At basal tone, hepatic arterial and portal venous vasoconstriction followed ATP injection, while at a tone raised with methoxamine (10^{-6}–10^{-5} M) ATP caused hepatic arterial vasodilatation, and a phasic vasodilatation followed by vasoconstriction in the portal venous vascular bed.

3 To determine whether the transhepatic arterial dilatation was due to the diffusion of nitric oxide (NO) from the portal venous vasculature, N^G-nitro-L-arginine methyl ester (L-NAME, 100 μM), an inhibitor of NO synthesis, was infused selectively into the portal vein. L-NAME infusion potentiated portal venous vasoconstriction to ATP ($-\log$ M ED_{50} 5.32 ± 0.31 to 6.51 ± 0.43, $P<0.05$, Student's paired t test) indicating the possible inhibition of a NO-mediated vasodilator component of the portal venous response to ATP. There was, however, no demonstrable difference in the transhepatic arterial vasodilatation induced by ATP during this infusion.

4 Simultaneous perfusion of both the hepatic arterial and portal venous inflows with L-NAME (100 μM) resulted in a significant decrease in the amplitude of hepatic arterial responses to ATP demonstrating that these responses were ultimately mediated by an NO-dependent mechanism.

5 This study has thus demonstrated a vasodilator component of the portal venous response to ATP that is NO-mediated. It also provides evidence that it is not portally-derived NO, but NO released from the hepatic arterial vascular bed, that accounts for the hepatic arterial vasodilatation to intra-portal administration of ATP. This implies that ATP itself, and not a second messenger, diffuses from the portal venous to hepatic arterial vascular bed to elicit the hepatic arterial response.

Keywords: Hepatic circulation; vasodilatation; vasoconstriction; L-NAME

Introduction

It is widely accepted that adenosine 5'-triphosphate (ATP) has a role in the control of systemic (Su, 1985; Burnstock, 1986) and hepatic vascular tone (Mathie *et al.*, 1991). It has been shown to act as a co-transmitter with noradrenaline in the sympathetic nervous system in the hepatic artery of the rabbit (Brizzolara & Burnstock, 1990), and perhaps with nitric oxide (NO) in the non-adrenergic, non-cholinergic nerves of the longitudinal muscle of the rabbit portal vein (Brizzolara *et al.*, 1993). ATP also affects the spontaneous electrical and mechanical activity of the longitudinal muscle of the rat portal vein (Reilly & Burnstock, 1987). ATP may act directly on the vessel wall to cause either vasoconstriction as in the rabbit's perfused liver (Ralevic *et al.*, 1991) and rat liver (Lee & Filkins, 1988) via P_{2x} receptors on the smooth muscle of the vessel (Kennedy & Burnstock, 1985), or vasodilatation via P_{2Y} receptors located either on the endothelium in the hepatic arterial vascular bed (Mathie *et al.*, 1991) or on the smooth muscle in the isolated hepatic artery (Brizzolara & Burnstock, 1991).

It has been recognized for a long time that a complex interrelationship occurs in the liver between the hepatic arterial and portal venous blood flows (Burton-Opitz, 1911). In particular the 'hepatic arterial buffer response' (Lautt, 1985), hepatic arterial dilatation in response to a reduction in portal venous flow, has been shown to be in some way dependent on adenosine (Lautt *et al.*, 1985) although the exact mechanism in not clear. Adenosine may not be the only participant in the control of the buffer response (Mathie & Alexander, 1990) and it is possible that ATP is also involved, although an extrinsic neural regulation has been excluded (Mathie *et al.*, 1980). Injection of vasoactive agents into either the hepatic artery or the portal vein affects vascular tone in both inflow vessels by a 'transhepatic effect' (Withrington & Richardson, 1990), or 'transvascular' route of action (Lautt *et al.*, 1984). It seems that tissue diffusion is the most likely mechanism for the transfer of action from one vessel to the other, although a direct intraluminal transfer through a portal to arterial communicating vessel has not been completely excluded. The transhepatic effect may be important in the generation of the buffer response because purines, including ATP, may be released from blood constituents (Bergfeld & Forrester, 1992) and endothelium (Palmer *et al.*, 1987; Bodin *et al.*, 1991), during conditions such as hypoxia (Belloni *et al.*, 1985) or altered flow (Ralevic *et al.*, 1992).

Recently Falcone & Bohlen (1990) showed that perivenular injection of acetylcholine (ACh) caused dilatation of the paired arteriole and that this was not due to diffusion of ACh but of NO, following release of NO by the venule. The present study was designed to test the hypothesis that the hepatic arterial vasodilator action of portally injected ATP was due to diffusion of NO, released from the portal vascular bed and acting on the hepatic arterial resistance sites, rather than transfer of the primary agent itself. ATP was chosen as the prime agent because of its importance in the regulation of hepatic arterial vascular tone. This investigation, therefore, studied the effect of portally administered N^G-nitro-L-arginine methyl ester (L-NAME), an NO synthesis inhibitor (Moore *et al.*, 1990), on the hepatic arterial vasodilator res-

[1] Author for correspondence.

ponses to intraportal injections of ATP. The results further characterize hepatic arterial vasodilatation and portal venous vasoconstriction to ATP and provide evidence which suggests that it is ATP itself, and not NO, that diffuses from the portal vein to the hepatic arterial resistance sites to produce the transhepatic effect of ATP.

Methods

Operative procedures

Male New Zealand White rabbits, weighing 2.2–2.9 kg, were initially sedated with subcutaneous fentanyl-fluanisone (Hypnorm, 0.3 ml kg^{-1}), and 15 min later anaesthetized with intravenous midazolam (Hypnovel, 1.5 mg kg^{-1}) through a cannulated marginal ear vein. A further 0.3 ml kg^{-1} Hypnorm was injected i.m. for continued analgesia during the 40 min operative period. The operative technique has been described elsewhere (Alexander *et al.*, 1992) but will be outlined in brief here.

The abdomen was opened through a mid-line incision, and the common bile duct cannulated. After administration of heparin i.v. (300 units kg^{-1}) the common hepatic artery, and the gastroduodenal artery when present, were cannulated (Portex 3FG) and the gastroduodenal vein ligated. Heparinised saline, 10 ml of a 20 units ml^{-1} solution, was infused into the catheters to prevent blood coagulation in the intrahepatic hepatic arterial vasculature. The portal vein was then cannulated and 40 ml of heparinised saline were flushed through the portal venous system. The liver was then rapidly excised from the animal, weighed and placed in an organ bath.

Liver perfusion

Livers were perfused via the hepatic arterial and portal venous cannulae at constant flow rates of 25 and 75 ml min^{-1} 100 g^{-1} respectively. The perfusate used was Krebs-Bülbring buffer solution (composition mM: NaCl 133, KCl 4.7, NaH_2PO_4 1.35, $NaHCO_3$ 20.0, $MgSO_4$ 0.61, glucose 7.8 and $CaCl_2$ 2.52) at 37°C, from a common oxygenated reservoir (95% O_2:5% CO_2). Homogeneous liver perfusion was indicated by all sections of the liver changing to an even beige colour. Perfusion pressures were measured with Spectramed (Statham) P23XL physiological pressure transducers from side arms of the perfusion circuit and from the gastroduodenal cannula. Recordings were made on a Grass 79F polygraph (Grass Instrument Co., Quincy, Mass., U.S.A.). Perfusion under these conditions has been shown to maintain liver viability for 5 h (Browse *et al.*, 1994a).

Drug administration

Methoxamine (hydrochloride), ATP (disodium salt) and L-NAME (hydrochloride) were obtained from Sigma Chemical Company. All were dissolved in distilled water. Methoxamine was added to the perfusate at a $-\log$ M dose of 5.31 ± 0.06 (mean ± s.e.mean) to raise the tone in the hepatic vascular bed. ATP was injected into the hepatic artery and portal vein as a 0.1 ml bolus to give doses over the range 10^{-10} to 10^{-4} mol 100 g $liver^{-1}$ (doses were adjusted for liver weight), further injections being given when the pressures had returned to normal. L-NAME was administered either as an infusion into the portal inflow via a syringe pump to a portal venous perfusate concentration of 100 μM, or was added to the perfusate reservoir to enter both inflow circuits (arterial and venous) at the same perfusate concentration (100 μM). A 30 min equilibration period followed any addition of L-NAME.

Statistics and presentation of data

Responses were recorded as changes in perfusion pressure (mmHg). All results are presented as mean ± s.e. Student's paired or unpaired t test was used, as appropriate, to test for differences between responses, $P<0.05$ being taken as significant.

Comparison between the direct responses (injection and response in same vascular bed) and transhepatic responses (injection and response in opposite vascular beds) to ATP was made by the method described by Withrington (1992). A 'transhepatic' ratio was calculated by dividing the arterial molar ED_{50} by the molar portal dose required to give a response equivalent to that seen with the arterial molar ED_{50}. In practice this was performed by subtracting the logarithms of these doses to give a log-transhepatic ratio.

Experimental protocol

Experiments were divided into three groups, with five rabbits in each.

Group 1 To define the dose-related responses of the hepatic arterial and portal venous vascular beds to ATP, injected via the hepatic artery and the portal vein, at both basal and raised tone.

Group 2(a) To demonstrate the effect of L-NAME administration via the portal vein on the hepatic arterial and portal venous responses to portally injected ATP at raised tone. First, dose response curves to ATP for portal venous injection were constructed (phase 1); L-NAME was then infused into the portal venous circuit and the dose-response curves to ATP repeated (phase 2); finally, further dose-response curves were obtained after addition of L-NAME to the perfusate reservoir, common to both hepatic arterial and portal venous inflows (phase 3). Single hepatic arterial doses of 10^{-7} mol 100 g^{-1} liver ATP and adenosine were also given into the hepatic artery at regular intervals throughout the experiment to monitor the effect of portal venous L-NAME on direct responses of the hepatic vascular bed, and to confirm the stability of hepatic arterial responses with time.

Group 2(b) To act as control experiments to allow for the changes seen during a long duration of perfusion and for changes associated with the vehicle for L-NAME. Three ATP dose-response curves were constructed following portal venous injection. These experiments were time-matched with those in group 2a and used the vehicle for L-NAME (distilled water) as a control portal venous infusion during phase 2, and as an addition to the reservoir in phase 3. Single hepatic arterial doses of ATP and adenosine were given at intervals similar to those in group 2(a).

Results

Perfusion indices

Group 1 Five rabbits (2.65 ± 0.10 kg), with liver weight 80.4 ± 5.7 g, were perfused at basal pressure (hepatic arterial and portal venous pressures were 33.6 ± 2.5, and 0.8 ± 0.6 mmHg respectively) while dose-response curves to ATP were constructed for both hepatic arterial and portal venous injection. After addition of methoxamine, further dose-response curves were obtained at raised pressure (hepatic arterial pressure = 142.0 ± 10.4, portal venous pressure = 3.0 ± 1.3 mmHg).

Group 2a and 2b In group 2a, 5 rabbits (2.58 ± 0.10 kg), liver weight 96.0 ± 0.2 g, were perfused at raised tone (hepatic arterial pressure = 158.8 ± 5.2, portal venous pressure = 2.7 ± 0.8 mmHg) for the duration of the experiment.

In group 2b, 5 rabbits (2.59 ± 0.12 kg), liver weight 89.8 ± 4.1 g, were perfused in the same manner (hepatic arterial pressure = 152.0 ± 4.9, portal venous pressure = 1.9 ± 0.7 mmHg). There were no significant differences in perfusion pressure between these groups.

The rate of bile production fell during the perfusion period in all groups (group 2a, 7.0 ± 2.2 to 2.9 ± 0.7, group 2b, 7.5 ± 1.2 to 3.7 ± 0.8 ml h^{-1}), consistent with interruption of the entero-hepatic circulation of bile salts. This fall was not correlated with the administration of L-NAME and was not investigated further.

ATP responses

Group 1 Hepatic arterial and portal venous dose-response curves at basal and raised tone The hepatic arterial and portal venous responses to ATP, following hepatic arterial and portal venous injection, at basal tone are shown in Figure 1a and 2a respectively. In all cases vasoconstriction was the demonstrated response. There was a significant difference between direct and indirect hepatic arterial responses to ATP above 10^{-7} mol 100 g^{-1} liver. Although the responses were small, hepatic arterial vasoconstriction was seen at high intraportal doses with a threshold to elicit a measurable response of 5.40 ± 0.37 − log mol 100 g^{-1} liver (maximal transmitted response = 3.2 ± 0.5 mmHg, resolution limit approximately = 1 mmHg pressure change). The portal venous responses were comparable following direct and indirect injection of ATP, differing significantly only at low doses (3×10^{-7}–3×10^{-6} mol 100 g^{-1} $liver^{-1}$, threshold 6.40 ± 0.25 and 5.50 ± 0.16 − log mol 100 g^{-1} $liver^{-1}$ for direct and indirect injection respectively, $P<0.05$). Maximal responses were not attained at the doses administered.

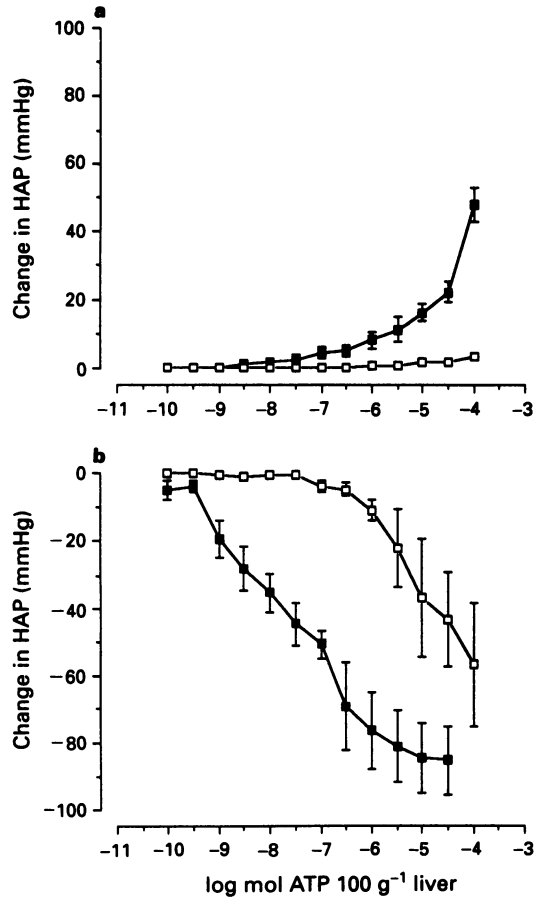


Figure 1 Responses of hepatic arterial pressure (HAP) to increasing doses of ATP injected direct (into the hepatic artery) and indirectly (into the portal vein) at basal tone (a) and at a tone raised with methoxamine (b). There is a significant difference between direct (■) and indirect (□) injections above 10^{-7} and 3×10^{-10} mol 100 g^{-1} liver in (a) and (b) respectively. (Group 1).

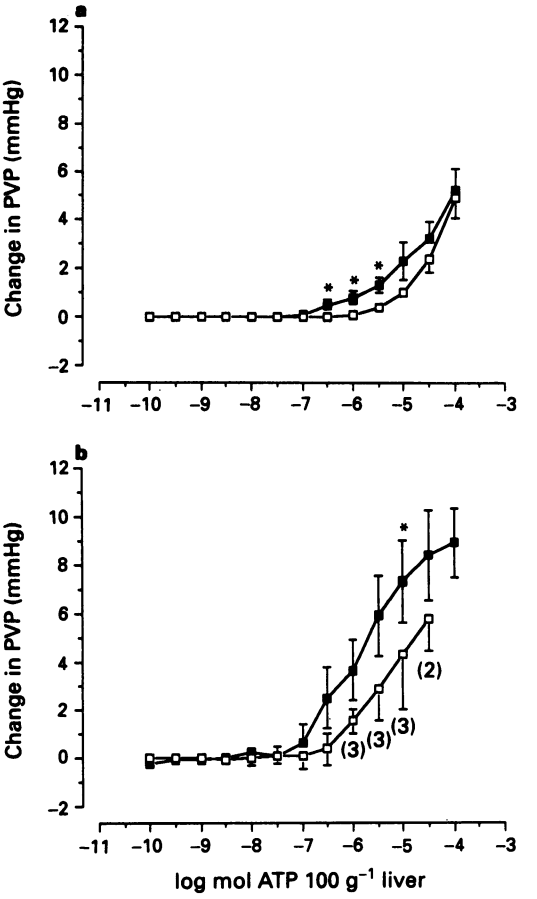


Figure 2 Responses of portal venous pressure to increasing doses of ATP injected direct (into the portal vein ■) and indirectly (into the hepatic artery □) at basal tone (a) and at a tone raised with methoxamine (b). There is a significantly lower threshold for vasoconstriction following direct injection at basal tone. *$P<0.05$ between direct and indirect responses. Numbers in parentheses = n; these decrease as the dose injected increases due to duration of hepatic arterial response following supramaximal injection. (Group 1).

At raised tone, dilatation was the predominant response to ATP in the hepatic arterial vascular bed (Figure 1b) with a − log molar ED_{50} of 7.72 ± 0.27 for direct hepatic arterial injection and 4.06 ± 0.58 for indirect portal venous injection, giving a log-transhepatic ratio of 3.66 ± 0.56. In the portal venous bed constriction remained the dominant response (Figure 2b). The venous constriction to indirect (hepatic arterial) injection was similar to that at basal tone although the responses to direct injection were of greater amplitude than at the lower tone ($P<0.05$ for doses 3×10^{-5}–3×10^{-4} mol 100 g^{-1} liver). A modest degree of vasodilatation to ATP was seen at raised tone in the portal bed and had a much lower threshold than vasoconstriction (8.90 ± 0.50 and 7.30 ± 0.30 − log mol 100 g^{-1} liver for vasodilation and vasoconstriction respectively, $P<0.05$). It was, however, overriden by the strong constrictor response at higher doses (above 7.11 ± 0.29 − log mol 100 g $liver^{-1}$, Figure 2b). Lag times between injection and the initiation of response were of short duration (<5 s) for ATP although this was not the case for hepatic arterial responses to portal venous injection. In this latter situation the lag time was prolonged to 10–20 s, with a slow gradual rise to the maximal response (cf. direct hepatic arterial responses) (Figure 3).

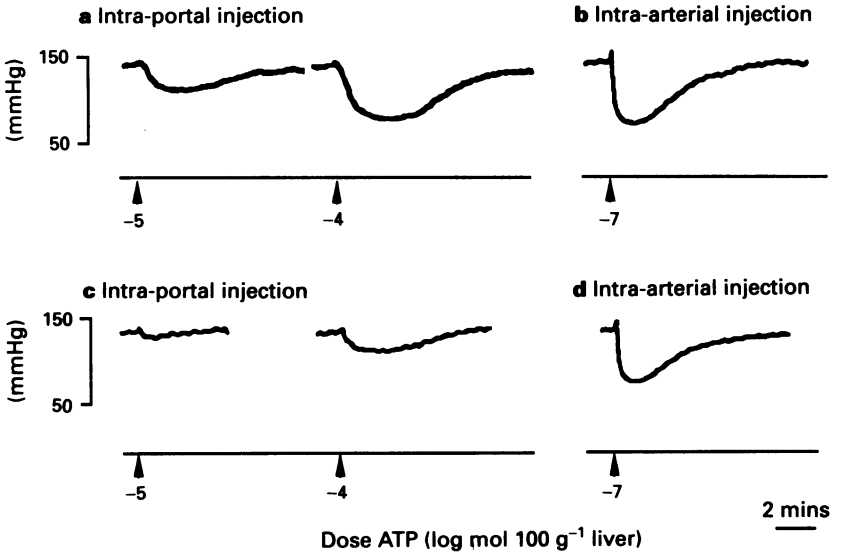


Figure 3 Hepatic arterial pressure responses to ATP following intraportal (a) and intra-arterial injection (b). The effect of 100 mM N^G-nitro-L-arginine methyl ester in the perfusate is shown in (c) and (d). (Group 2).

Group 2. The effect of L-NAME on transhepatic responses

Hepatic arterial responses to portal venous injection of ATP Hepatic arterial perfusion pressure was unaffected by the addition of 100 μM L-NAME, or its vehicle.

The arterial responses to intra-portal ATP (phase 1) were unaffected by portal venous L-NAME (phase 2); however, the addition of L-NAME to the perfusate reservoir (phase 3) significantly reduced responses at most doses (Figure 3 and 4a). The vehicle for L-NAME had no effect on the hepatic arterial responses (Figure 4b).

Portal venous responses to direct injection of ATP The addition of 100 μM L-NAME to the portal circulation resulted in an increase in portal venous pressure (by 3.9 ± 0.8 mmHg, $P<0.001$). Subsequent addition of L-NAME to the perfusate reservoir did not alter portal perfusion pressure further.

L-NAME, 100 μM, in the portal venous circulation, enhanced vasoconstriction and caused a left shift of the direct portal venous dose-response curve to ATP, (Figure 5a) (− log molar ED_{50} from 5.32 ± 0.37 to 6.51 ± 0.43 for phase 1 and 2 respectively, $P = 0.014$). This value was calculated by assuming that the response at maximal dose was the maximal responsible possible. It was possible that a similar maximal response to that in phase 2 and 3 could have been reached at higher doses but this would have only increased the ED_{50} further and subsequently increase the left shift of the curve between phase 1 and 2. However, when this change in ED_{50} was compared to control results (− log molar ED_{50} changing from 5.32 ± 0.31 to 5.75 ± 0.27 for phase 1 and phase 2 respectively, $P = 0.13$, (Figure 5b) the left shift did not reach significance ($P = 0.068$). However, analysis of responses to individual ATP doses, with L-NAME in the portal circulation, against controls showed a significant difference in response at the doses of 10^{-7} and 3×10^{-7} mol 100 g^{-1} liver. These results confirmed that L-NAME did have an effect over and above the changes seen during control experiments.

The substitution of portal L-NAME with L-NAME in both inflows did not alter the ED_{50} of the portal dose-response curve further (− log molar $ED_{50} = 6.25 \pm 0.39$ and 5.78 ± 0.30 for addition of L-NAME and vehicle control respectively).

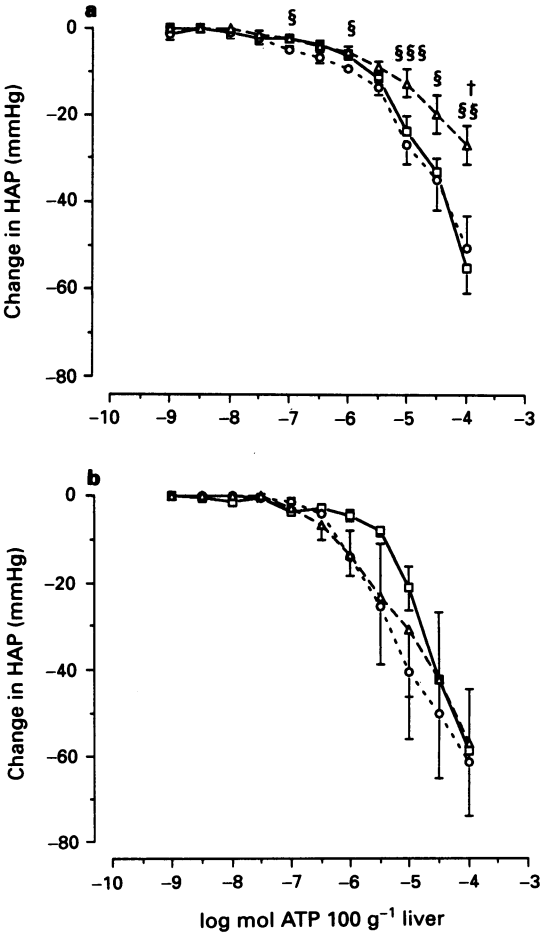


Figure 4 Responses of hepatic arterial pressure (HAP) to increasing intraportal doses of ATP, before (phase 1, □), during infusion alone (phase 2, ○) and during arterial and portal perfusion (phase 3, △) of 100 μM N^G-nitro-L-arginine methyl ester (a) and (b) vehicle. Statistical significance is denoted by †$P<0.05$ for phase 1 vs phase 3; §$P<0.05$, §§$P<0.01$, §§§$P<0.001$ for phase 2 vs phase 3 respectively. (Group 2).

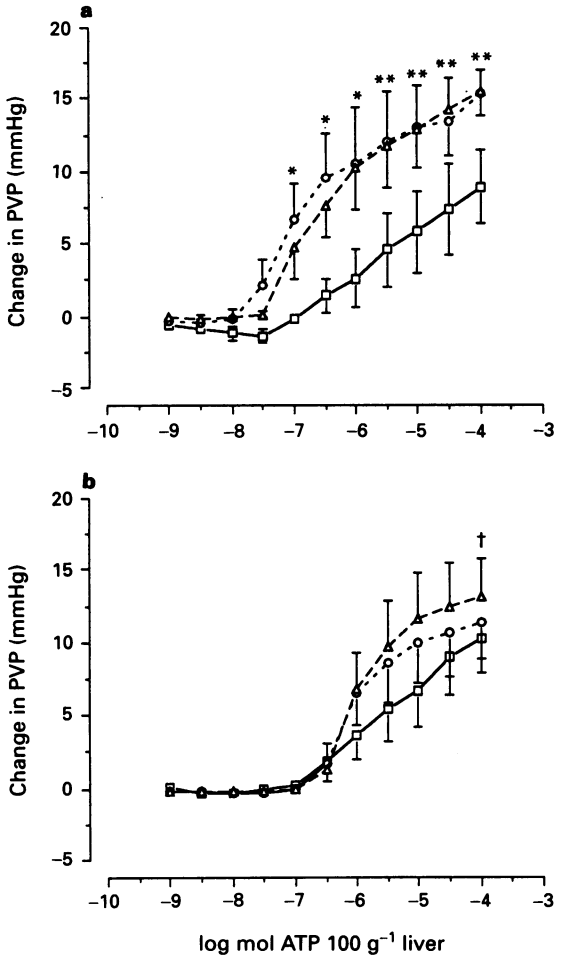


Figure 5 Responses of portal venous pressure (PVP) to increasing intraportal doses of ATP, before (phase 1, □), during portal infusion alone (phase 2, ○) and during arterial and portal perfusion (phase 3, △) of 100 mM N^G-nitro-L-arginine methyl ester (a) and vehicle (b). Statistical significance is denoted by $*P<0.05$, $**P<0.01$ for phase 1 vs. phase 2; and $\dagger P<0.05$ for phase 1 vs. phase 3. (Group 2).

Hepatic arterial and portal venous responses to hepatic arterial injection of ATP

The direct hepatic arterial vasodilator responses to intra-arterial injection of ATP, 10^{-7} mol 100 g^{-1} liver, were unaffected by portal venous administration of L-NAME, but were reduced with L-NAME in the hepatic arterial and portal venous inflows ($P = 0.058$). The responses to adenosine were not affected by L-NAME. The amplitude of portal venous responses to arterially injected doses of ATP and adenosine (vasoconstriction and vasodilatation respectively) tended to increase in the presence of L-NAME but not in the control experiments.

Discussion

L-NAME perfusion of the portal circulation did not affect the transhepatic arterial vasodilator responses to ATP. It did, however, enhance portal venous vasoconstriction to ATP, presumably by inhibiting a co-existing NO-mediated vasodilatation of the portal venous vascular bed. The subsequent infusion of L-NAME into both portal and arterial inflows inhibited hepatic arterial dilatation to portal venous injections of ATP, demonstrating that intra-portally administered ATP was ultimately acting through a NO-mediated mechanism in the artery. L-NAME would have been expected to inhibit the transhepatic action of ATP during portal venous infusion of L-NAME if the arterial response was due to NO released by ATP in the portal venous bed. The lack of effect of L-NAME on arterial responses during this phase of the experiment also indicated that L-NAME did not reach the arterial resistance sites in sufficient concentration to block the action of ATP. These results therefore do not substantiate the hypothesis that NO diffuses to the hepatic arterial resistance sites to elicit the transhepatic action of ATP.

Falcone & Bohlen (1990) produced substantial evidence, in the mesentery and skeletal muscle of the rat, that NO could act as a diffusible secondary messenger in the transfer of vasodilatation from a venule to its paired arteriole. Injection of acetylcholine (ACh) into a venular wall caused dilatation of the paired arteriole, but injection into the parenchyma at a similar distance from the arteriole did not result in dilatation. Therefore, a second messenger produced by the venule, which could be blocked by the addition of L-NAME, caused the arteriole to react. Some possible differences between this study and the present one which may explain the difference in results are: (1) The liver may have better diffusion characteristics than the tissues used by Falcone & Bohlen, perhaps as a result of endothelial fenestration of the sinusoids; (2) ACh and ATP differ in their size and electrical charge (ATP is a molecule approximately three times larger than ACh with a greater electrical charge). We chose to use ATP because of its apparent importance in the hepatic circulation and also because of recent evidence that L-NAME acted as a muscarinic receptor antagonist (Buxton *et al.*, 1993); (3) the anatomical distance between the vessels in the inflow tract of the liver may be significantly different from those in the rat mesentery/trapezius muscle, although this seems unlikely. The distance between the ACh injection site and the arteriole in Falcone & Bohlen's work was approx. 200 μm; in the liver the distance between the pre-sinusoidal vessels in the inflow tract is of the same order (approx. 100 μm) (Grisham & Nopanitaya, 1981); (4) the extra-venular injection used by Falcone & Bohlen may behave differently from the intravascular injection of an agent, perhaps due to the release of NO from tissues other than the endothelium. Alternatively, the ability to metabolize NO in tissues outside the vessel wall may be less than that in the smooth muscle layer, thereby allowing more NO to diffuse away.

The ability of ATP to diffuse to the artery was further substantiated by the transmission of a vasoconstrictor hepatic arterial response to ATP at a basal tone in this series and the more substantial transmitted vasoconstrictor response to noradrenaline which has been shown to be dependent on the magnitude of the arterioportal pressure gradient (Browse *et al.*, 1994b). Consequently, the threshold for bolus doses of noradrenaline to elicit an hepatic arterial responses was 500–1000 times greater if injection was into the portal vein. At raised tone the arterioportal pressure gradient and the transhepatic ratio for hepatic arterial responses was increased. However, transmission of responses could still be detected although at raised tone, in the current experiments with ATP, the predominant response was vasodilatation. In the present experiments L-NAME infusion into the portal vein did not affect hepatic arterial responses to portal venous injection or hepatic arterial injection of ATP. This implies that either L-NAME diffusion is poor in the liver or more likely that diffusion against the hepatic arterial to portal venous pressure gradient allows too small a concentration to reach the hepatic arterial vascular bed.

This work only excludes NO as a diffusible secondary messenger in the transmission of responses to ATP. ATP has also been shown to release prostacyclin (PGI_2) from the endothelium of rabbit aorta and pulmonary artery (Boeynaems & Galand, 1983) although it is not known whether this happens in the venous system. ATP is also rapidly taken up or metabolized to adenosine by ecto-enzymes (Pearson *et al.*, 1978; 1980). This is so effective that in the guinea-pig heart only 1% of injected ATP was found in the venous

effluent (Paddle & Burnstock, 1974). It may be that another metabolite of ATP is responsible for its transhepatic arterial vasodilatation; however, the agent(s) in question must act, to a large extent, through NO because the hepatic arterial responses to intra-portal ATP were reduced by the addition of L-NAME to the perfusate.

These experiments have also further characterized the responses of the hepatic vascular bed to ATP. ATP is known to be present as a neurotransmitter in the hepatic artery (Brizzolara & Burnstock, 1990) and portal vein (Reilly *et al.*, 1987; Brizzolara *et al.*, 1993). It acts in the vascular bed through smooth muscle P_{2X} receptors mediating arterial constriction and P_{2Y} receptors mediating arterial vasodilatation (Ralevic *et al.*, 1991) although these may be endothelial or on the smooth muscle (Brizzolara & Burnstock, 1991). At basal tone, we have reaffirmed the vasoconstrictor arterial responses showing a similar threshold for direct injection as shown previously (Ralevic *et al.*, 1991) but by using higher doses we have demonstrated that only the lower portion of the dose-dependent response curve had been characterized. It seems therefore that the $-\log$ molar ED_{50} value for P_{2X} receptors is unlikely to be greater than 4.5, a factor of 100 different from that previously reported (Ralevic *et al.*, 1991). We have shown that the artery does constrict to intra-portal administration of high doses of ATP, although a maximal response was not obtained. At raised tone the vasodilator effect of ATP compares well with that seen previously (pD_2 8.3 ± 0.1 (Ralevic *et al.*, 1991) vs 7.72 ± 0.27 in these experiments) although the amplitude of responses and the smaller dose of pre-constriction agent required would suggest that our preparation is more sensitive. The transhepatic action of ATP on the hepatic arterial vascular bed has not been demonstrated before in the *in vitro* perfused rabbit liver and it shows that there is a comparable arterial response threshold (10^{-7} mol $100\,g^{-1}$ liver) to that seen *in vivo* in our laboratory (unpublished observation).

The effect of ATP on the portal venous bed has not been well documented before, although the constrictor effect of an infusion of ATP at basal tone has been demonstrated in the perfused rat liver (Lee & Filkins, 1988). In our experiments the portal venous responses to direct injection, at basal or raised tone, are similar to the transhepatic responses following hepatic arterial injection, but direct injections have a lower threshold. This suggests that either more ATP is metabolized during passage through the hepatic arterial vascular bed than through the portal system, or that portal venous resistance sites are, at least partly, pre-sinusoidal. In addition the hepatic arterial and portal venous vascular beds are perfused at different flow rates. This could ultimately result in different quantities of drug arriving at the receptors (per unit time) and could contribute to the difference in responses between the 2 vascular beds.

At raised tone, the dominant portal venous response was, again, vasoconstriction with a threshold level similar to that at basal tone. There was, however, a larger amplitude of response at raised tone. This difference can be explained by the order of construction of the dose-response curves in these experiments. Increasing duration of liver perfusion was shown to potentiate venous vasoconstriction in the control experiments, and dose-response curves were constructed at basal and then raised tone. It is also possible that vasoconstriction was facilitated by an increased tone. At lower doses of ATP there was obvious, although small, portal vasodilatation, a feature not noted previously in the portal venous bed. This vasodilatation had a lower threshold than constriction (8.9 vs 7.3 $-\log$ mol $100\,g^{-1}$ liver) but was overcome by constriction at higher doses. There was a marked lag time before constriction and often there was a noticeable dilatation even after the portal pressure/resistance had risen. Certain features of the preparation employed in these experiments, in particular free-flotation of the liver, and the use of methoxamine in preference to noradrenaline as a pre-constriction agent, tend to produce a low portal perfusion pressure, which probably results in an underestimate of the amplitude of the portal vasodilatation. It is quite clear, however, that using L-NAME causes a left shift of the portal venous vasoconstriction-response curve suggesting that a marked vasodilator element, dependent on NO (probably acting via P_{2Y} purinoceptors) has been inhibited. Further physiological limitations in this model include the use of the same perfusate for the portal venous and hepatic arterial vascular beds but this has not been shown to alter the vascular responses to ATP over those using more acidic (hypercapnic) portal venous perfusates (Browse and Alexander, unpublished obervation). Experiments on the transhepatic effects of drugs have also been hampered, particularly *in vivo* by the presence of the buffer response (hepatic arterial vasodilatation in response to reductions in portal venous blood flow) which may alter vascular resistance; this preparation does not exhibit a demonstrable buffer response.

The role of NO in the portal venous response to arterial injection of ATP is unclear. Following the addition of intra-portal L-NAME, portal vasoconstriction in response to 10^{-7} mol ATP injected into the artery did not increase significantly; however, the tendency for greater responses was apparent and may be due to an inhibition of the same NO-mediated vasodilatation in the portal venous bed, although the potentiating effect of the increasing duration of perfusion cannot be excluded. Further examination/characterization of these vasodilator responses would require inhibition of P_{2X} receptors and the increase of portal venous pressure. The introduction of L-NAME into the portal circulation also caused a significant increase in portal venous pressure suggesting that there is a basal NO release, a feature which has been noted before in a rabbit isolated portal vein preparation (Brizzolara *et al.*, 1993). This was not seen in the hepatic arterial vascular bed. It may well be that the more important physiological response of the portal circulation to raised ATP levels, which may reach as high as 200 μM in shock (Gordon, 1986), is vasodilatation.

In summary, we have further characterized the hepatic arterial and portal venous vascular responses to ATP, in particular demonstrating that the portal venous bed exhibits basal NO release, and that portal responses at raised tone are a mixture of vasodilatation and vasoconstriction. The vasoconstrictor response is enhanced by L-NAME, presumably by inhibiting NO-mediated vasodilatation. The lack of effect of portal venous L-NAME on the vasodilator hepatic arterial responses to ATP suggests that NO from the portal venous vascular bed does not have a role in the transhepatic action of ATP, implying that ATP itself is probably responsible for this action. This mechanism of action may contribute to the fine control of hepatic arterial tone by portally-borne intestinal vasoactive agents, and may play a role in the production of the hepatic arterial 'buffer response'.

The authors wish to thank Dr Vera Ralevic for her invaluable suggestions in the preparation of this manuscript. This work was funded by the Joint Research Committee of King's College London.

References

ALEXANDER, B., MATHIE, R.T., RALEVIC, V. & BURNSTOCK, G. (1992). An isolated dual-perfused rabbit liver preparation for the study of hepatic blood flow regulation. *J. Pharmacol. Methods*, **27**, 17–22.

BELLONI, F.L., ELKIN, P.L. & GIANNOTTO, B. (1985). The mechanism of adenosine release from hypoxic rat liver cells. *Br. J. Pharmacol.*, **85**, 441–446.

BERGFELD, G.R. & FORRESTER, T. (1992). Release of ATP from human erythrocytes in response to a brief period of hypoxia and hypercapnia. *Cardiovasc. Res.*, **26**, 40–47.

BODIN, P., BAILEY, D. & BURNSTOCK, G. (1991). Increased flow-induced ATP release from isolated vascular endothelial cells but not smooth muscle cells. *Br. J. Pharmacol.*, **103**, 1203–1205.

BOEYNAEMS, J.M. & GALAND, N. (1983). Stimulation of vascular prostacyclin synthesis by extracellular ADP and ATP. *Biochem. Biophys. Res. Commun.*, **112**, 290–295.

BRIZZOLARA, A.L. & BURNSTOCK, G. (1990). Evidence for noradrenergic-purinergic cotransmission in the hepatic artery of the rabbit. *Br. J. Pharmacol.*, **99**, 835–839.

BRIZZOLARA, A.L. & BURNSTOCK, G. (1991). Endothelium-dependent and endothelium-independent vasodilatation of the hepatic artery of the rabbit. *Br. J. Pharmacol.*, **103**, 1206–1212.

BRIZZOLARA, A.L., CROWE, R. & BURNSTOCK, G. (1993). Evidence for the involvement of both ATP and nitric oxide in non-adrenergic, non-cholinergic inhibitory neurotransmission in the rabbit portal vein. *Br. J. Pharmacol.*, **109**, 606–608.

BROWSE, D.J., BENJAMIN, I.S. & ALEXANDER, B. (1994a). Dose-related responses to vasoactive agents in the hepatic artery and portal vein of the isolated dual-perfused rabbit liver: effects of prolonged perfusion. *Br. J. Pharmacol.*, **112**, 195P.

BROWSE, D.J., BENJAMIN, I.S. & ALEXANDER, B. (1994b). The transhepatic response to noradrenaline in the rabbit liver: the influence of the arterioportal pressure gradient. *J. Physiol.*, **475**, 118P.

BURNSTOCK, G. (1985). Local control of blood pressure by purines. Neurohumoral control of blood vessel tone. Proc. Int. Symp., Springfield, Ill, 1986. *Blood Vessels*, **24**, 156–160.

BURTON-OPITZ, R. (1911). The vascularity of the liver: the influence of the portal blood flow upon the flow in the hepatic artery. *Q. J. Exp. Physiol.*, **4**, 93–102.

BUXTON, I.L.O., CHEEK, D.J., ECKMAN, D., WESTFALL, D.P., SANDERS, K.M. & KEEF, K.D. (1993). N^G-nitro-L-arginine methyl ester and other alkyl esters of arginine are muscarinic receptor antagonists. *Circ. Res.*, **72**, 387–395.

FALCONE, J.C. & BOHLEN, H.G. (1990). EDRF from rat intestine and skeletal muscle venules causes dilation of arterioles. *Am. J. Physiol.*, **258**, H1515–H1523.

GORDON, J.L. (1986). Extracellular ATP: effects, sources and fate. *Biochem. J.*, **233**, 309–319.

GRISHAM, J.W. & NOPANITAYA, W. (1981). Scanning electron microscopy of casts of hepatic microvessels; review of methods and results. In *Hepatic Circulation in Health and Disease*. ed. Lautt, W.W. pp. 87–105. New York: Raven Press.

KENNEDY, C. & BURNSTOCK, G. (1985). Evidence for two types of P_2-purinoceptors in longitudinal muscle of the rabbit portal vein. *Eur. J. Pharmacol.*, **111**, 49–56.

LAUTT, W.W. (1985). Mechanism and role of intrinsic regulation of hepatic arterial blood flow: hepatic arterial buffer response. *Am. J. Physiol.*, **249**, G549–G556.

LAUTT, W.W., LEGARE, D.J. & D'ALMEIDA, M.S. (1985). Adenosine as a putative regulator of hepatic arterial flow (the buffer response). *Am. J. Physiol.*, **248**, H331–H338.

LAUTT, W.W., LEGARE, D.J. & DANIELS, T.R. (1984). The comparative effect of administration of substances via the hepatic artery or the portal vein on hepatic artery resistance, liver blood volume and hepatic extraction in cats. *Hepatology*, **4**, 927–932.

LEE, J.W. & FILKINS, J.P. (1988). Exogenous ATP and hepatic haemodynamics in the perfused rat liver. *Circ. Shock*, **24**, 99–110.

MATHIE, R.T. & ALEXANDER, B. (1990). The role of adenosine in the hyperaemic response of the hepatic artery to portal vein occlusion (the 'buffer response'). *Br. J. Pharmacol.*, **100**, 626–630.

MATHIE, R.T., LAM, P.H.M., HARPER, A.M. & BLUMGART, L.H. (1980). The hepatic arterial blood flow response to portal vein occlusion in the dog. The effect of hepatic denervation. *Pflügers Arch.*, **386**, 77–83.

MATHIE, R.T., RALEVIC, V., ALEXANDER, B. & BURNSTOCK, G. (1991). Nitric oxide is the mediator of ATP-induced dilatation of the rabbit hepatic arterial vascular bed. *Br. J. Pharmacol.*, **103**, 1602–1606.

MOORE, P.K., AL-SWAYEH, O.A., CHONG, N.W.S., EVANS, R.A. & GIBSON, A. (1990). L-N^G-nitro-arginine (L-NOARG), a novel L-arginine-reversible inhibitor of endothelium-dependent vasodilatation *in vitro*. *Br. J. Pharmacol.*, **99**, 408–412.

PADDLE, B.M. & BURNSTOCK, G. (1974). Release of ATP from perfused heart during coronary vasodilatation. *Blood Vessels*, **11**, 110–119.

PALMER, R.M.J., FERRIGE, A.G. & MONCADA, S. (1987). Nitric oxide release accounts for the biological activity of endothelium-derived relaxing factor. *Nature*, **327**, 524–526.

PEARSON, J.D., CARLETON, J.S. & GORDON, J.L. (1980). Metabolism of adenine nucleotides by ecto-enzymes of vascular endothelial and smooth muscle cells in culture. *Biochem. J.*, **190**, 421–429.

PEARSON, J.D., CARLETON, J.S., HUTCHINGS, A. & GORDON, J.L. (1978). Uptake and metabolism of adenosine by pig aortic endothelial and smooth muscle cells in culture. *Biochem. J.*, **170**, 265–271.

RALEVIC, V., MATHIE, R.T., ALEXANDER, B. & BURNSTOCK, G. (1991). Characterisation of P_{2X} and P_{2Y}-purinoceptors in the rabbit hepatic arterial vasculature. *Br. J. Pharmacol.*, **103**, 1108–1113.

RALEVIC, V., MILNER, P., KIRKPATRICK, K.A. & BURNSTOCK, G. (1992). Flow-induced release of adenosine 5'-triphosphate from endothelial cells of the rat mesenteric arterial bed. *Experientia*, **48**, 31–34.

REILLY, W.M. & BURNSTOCK, G. (1987). The effect of ATP analogues on the spontaneous electrical and mechanical activity of rat portal vein longitudinal muscle. *Eur. J. Pharmacol.*, **138**, 319–325.

REILLY, W.M., SAVILLE, V.L. & BURNSTOCK, G. (1987). An assesment of the antagonist activity of reactive blue 2 at P_1 and P_2-purinoceptors: supporting evidence for purinergic innervation of the rabbit portal vein. *Eur. J. Pharmacol.*, **140**, 47–53.

SU, C. (1985). Extracellular functions of nucleotides in heart and blood vessels. *Annu. Rev. Physiol.*, **47**, 665–676.

WITHRINGTON, P.G. (1992). The actions of two sensory neuropeptides, Substance P and Calcitonin gene-related peptide, on the canine hepatic arterial and portal venous beds. *Br. J. Pharmacol.*, **107**, 296–302.

WITHRINGTON, P.G. & RICHARDSON, P.D.I. (1990). Liver blood flow. In *Hepatology, a Textbook of Liver Disease*. ed. Zakim, D. & Boyer, T.D. Vol. 1: pp. 30–48. Philadelphia: W.B. Saunders Company.

(Received January 12, 1994
Revised June 22, 1994
Accepted June 23, 1994)

Br. J. Pharmacol. (1994), **113**, 994–1000 © Macmillan Press Ltd, 1994

Long-lasting inhibitory activity of the hetrazepinic BN 50730 on exudation and cellular alterations evoked by PAF and LPS

Ana L.A. Pires, Patricia M.R. e Silva, Claudia Pasquale, Hugo C. Castro-Faria-Neto, Patricia T. Bozza, Renato S.B. Cordeiro, *Giles A. Rae, **Pierre Braquet, †Vincent Lagente & [1]Marco A. Martins

Departamento de Fisiologia e Farmacodinâmica, Instituto Oswaldo Cruz/FIOCRUZ; Av. Brasil 4365, 21045-900 – Caixa Postal 926, Rio de Janeiro, Brazil; *Universidade Federal de Santa Catarina, Florianópolis, **Institut Henri Beaufour, 17 avenue Descartes, 92230 Le Plessis-Robinson, France and †Université de Rennes 1, 2 avenue du Professeur Léon Bernard, 35043 Rennes, France

1 Inhibitory effects of the hetrazepinic derivative BN 50730 on the rat pleural inflammatory response, triggered by PAF or lipopolysaccharides (LPS), were examined. The type of pharmacological blockade exerted by this antagonist in *in vitro* assays of eosinophil chemotaxis and platelet aggregation were also investigated.

2 Intrathoracic injection of PAF (1 μg per cavity) caused a 4 fold increase in the extravasated protein within 15 min and led to a marked eosinophil accumulation 24 h post-challenge. BN 50730 (0.5–10 μg per cavity) inhibited exudation by PAF dose-dependently without modifying the response induced by histamine, bradykinin or 5-hydroxytryptamine (5-HT).

3 The kinetics of the inhibitory effect on exudation revealed that the actions of WEB 2086 and BN 52021 (10 μg per cavity) were over within 2 and 4 h respectively, whereas BN 50730 (10 μg per cavity) retained 80% of its inhibitory activity for 4 days.

4 Oral treatment with BN 50730 (10–20 mg kg^{-1}, 1 h beforehand) suppressed the leucocyte accumulation and late eosinophilia observed 6 and 24 h after PAF respectively, but did not modify the eosinophilia induced by leukotriene B_4 (LTB_4) or bradykinin. BN 50730 also failed to reduce the eosinophil accumulation induced by LPS but drastically inhibited the neutrophil influx.

5 The pre-incubation of rat peritoneal eosinophils for 10 min with BN 50730 (30 nM–1 μM) dose-dependently inhibited the chemotaxis induced by PAF (0.1 μM) *in vitro*. The IC_{50} values for BN 52021, WEB 2086 and BN 50730 in this system were 5, 5 and 0.05 μM respectively.

6 In separate assays, rat peritoneal eosinophils and rabbit washed platelets were preincubated with BN 50730 or WEB 2086 (1 μM) then subjected to a series of at least two consecutive washings in order to remove the antagonist from the receptor environment. Under such conditions, only the cells pretreated with WEB 2086 recovered the sensitivity to the lipid.

7 We conclude that BN 50730 is a potent, specific and long-acting PAF antagonist and its effect seems to result from a high affinity and non-competitive interaction of the drug with the PAF receptor.

Keywords: Inflammation; PAF, eosinophils; BN 50730; lipopolysaccharide

Introduction

Platelet activating factor (PAF) (1-*O*-alkyl-2-acetyl-sn-glycero-3-phosphoryl choline) is a potent endogenous phospholipid mediator, firstly described by Benveniste *et al.* in 1972, which exhibits many different biological effects *in vivo* and *in vitro*. For instance, PAF causes platelet aggregation and degranulation, increases plasma leakage, induces bronchoconstriction and airway hyper-responsiveness and stimulates adherence, migration and/or activation of a range of cells, including neutrophils, eosinophils, macrophages, lymphocytes and endothelial cells, which are involved in the sequential biological response from inflammation to immunity (reviewed in Braquet *et al.*, 1987; Zimmerman *et al.*, 1992). Despite exhibiting a great nonspecific binding to cell membranes, it is recognized that PAF exerts its actions via specific high affinity receptors expressed on the external membrane of the responsive cells. PAF binding proteins belonging to the G protein-coupled receptor superfamily have recently been identified and cloned from guinea-pig lung (Honda *et al.*, 1991), human leucocytes (Nakamura *et al.*, 1992) and human heart (Sugimoto *et al.*, 1992).

Specific inhibitors of the various biological activities of PAF have been described since 1983 (reviewed in Hwang, 1990). In general, these antagonists are competitive in nature and they can be divided into at least three distinct groups: PAF-related compounds like CV 3988 (Terashita *et al.*, 1985); synthetic PAF-unrelated compounds like WEB 2086 (Casals-Stenzel *et al.*, 1987), PCA 4248 (Sunkel *et al.*, 1990) and SR 27417 (Herbert *et al.*, 1991); and nature products including kadsurenone (Shen *et al.*, 1985), BN 52021 (Braquet *et al.*, 1987) and epiyamgambine (Castro-Faria-Neto *et al.*, 1993). The hetrazepine, BN 50730 {tetrahydro-4,7,8,10 methyl-1(choro-2 phenyl)-6 (methoxy-4 phenyl-carbamoyl)-9 pyrido [4'-3'-4,5] thieno [3,2-f] triazolo-1,2,4[4,3-a] diazepine-1,4)} is a novel PAF receptor antagonist (Braquet *et al.*, 1990) which has been reported to be markedly effective against several pharmacological actions of this lipid, including bronchoconstriction in the cat (Dyson *et al.*, 1990), human monocyte Fc_eRII/CD 23 expression (Paul-Eugéne *et al.*, 1990) and peribronchial eosinophil recruitment in guinea-pigs (Lagente *et al.*, 1993). Nevertheless, its mode of action has not been clearly elucidated.

In the present study, we have investigated the effect of BN 50730 on the pleural inflammatory response evoked by PAF or lipopolysaccharides (LPS). We have measured protein and

[1] Author for correspondence.

leucocyte accumulation in the rat pleural fluid at different times following treatment with BN 50730, and used other PAF receptor antagonists for comparison. Furthermore, *in vitro* assays, involving PAF-induced platelet aggregation and eosinophil chemotaxis, were carried out in order to investigate the type of pharmacological blockade exhibited by BN 50730. The findings are consistent with the interpretation that BN 50730 is a specific, long-acting and non-competitive PAF receptor antagonist.

Methods

Animals

Wistar rats (150–200 g) and New Zealand White rabbits (2–3.5 kg) of either sex obtained from the Oswaldo Cruz Foundation breeding colony were used.

Induction of pleurisy

Pleurisy was induced as previously reported (Martins *et al.*, 1992). Briefly, ether-anaesthetized rats were injected intrathoracically (0.1 ml) with either PAF (1 μg per cavity), histamine (200 μg per cavity), bradykinin (50 μg per cavity), 5-hydroxytrypatmine (5-HT, 100 μg per cavity), LTB_4 (0.5 μg per cavity) or LPS (250 ng per cavity). Control animals were injected with 0.1 ml of vehicle. PAF and LTB_4 (LTB_4) were diluted with sterile 0.9% NaCl solution (saline) containing 0.01% bovine serum albumin (BSA), whereas all other agents were dissolved in saline. The animals were killed with an overdose of ether and the pleural cavity was opened and rinsed with 3 ml of heparinized saline (5 i.u. ml^{-1}). Unless otherwise stated, animals were killed 15 min post-challenge for the exudatory response assays, and at 6 and 24 h for the cellular analysis. In case of exudation caused by histamine, 5-HT or bradykinin, the animals were killed 60 min post-challenge. The pleural washing was recovered in a graduated syringe for further analyses of volume, protein content and leucocyte population. In the rare case of haemorrhage noted in the pleural cavity, the animal was not included in subsequent analysis.

Total protein quantification

The fluid recovered from the pleural cavity was centrifuged for 10 min at 770 *g* and the total protein content was quantified from the supernatant in a spectrophotometer (Shimadzu corporation) by the Biuret technique (Gornall *et al.*, 1949).

Total and differential leucocyte counts

Total leucocytes were counted in a Coulter counter ZM and expressed as millions of cells per cavity. Differential analyses were performed in cytocentrifuged smears stained with May-Grunwald-Giemsa dye under oil immersion objective, by means of a light microscope.

Treatment

BN 50730 (0.5 to 10 μg per cavity), WEB 2086 (2.5 to 10 μg per cavity) (Casals-Stenzel *et al.*, 1987) and BN 52021 (2.5 to 10 μg per cavity) (Braquet *et al.*, 1987) were locally administered into the pleural cavity of ether-anaesthetized rats at different periods of time, ranging from 5 min to 7 days, before the agonist. In some experiments BN 50730 (10 to 20 mg kg^{-1}) was orally administered 1 h before stimulation. ID_{50} value (dose of the drug that inhibits 50% of the agonistic effect) for BN 50730 was calculated from the Hill plot (Hill, 1910). This is a plot of log[(% of inhibition)/(100 – % of inhibition)] versus log[drug].

In control groups the antagonists were replaced by their vehicles. BN 50730 was dissolved in a small volume of 25% ethanol (50 μl for 1 mg) and diluted 100 fold to the final concentration with saline. WEB 2086 was dissolved in saline with 0.1 N HCl. BN 52021 was dissolved in a small volume of 0.5 N NaOH, diluted with saline to an intermediate concentration, neutralized with 0.5 N HCl and finally made up to the final concentration with saline. All drug solutions were prepared immediately before use.

In vitro *eosinophil chemotaxis assay*

Eosinophils were obtained from the peritoneal cavity of normal rats and were 'purified' (80–90%) by means of a discontinuous gradient of metrizamide, according to Martins *et al.* (1989a). The *in vitro* migration experiments were carried out in a 48-well chemotaxis microchamber (Neuroprobe, Inc., U.S.A.) and with Toyo cellulose nitrate filters (3 μm pore). To test the effect of BN 50730 on the eosinophil chemotaxis induced by increasing concentrations of PAF (10^{-9} to 10^{-5} M), cells were pre-incubated (10 min at 37°C) with 3×10^{-8} to 10^{-6} M BN 50730, or its vehicle, and transferred to the upper part of the chemotaxis chamber. BN 52021 and WEB 2086 (10^{-6} to 10^{-4} M) were also tested for comparison. This procedure consistently did not modify the cell viability (greater than 95%) as attested by trypan blue dye exclusion. In another set of experiments, eosinophils incubated with BN 50730 (10^{-6} M) or WEB 2086 (10^{-4} M) were subjected to 2 consecutive washings before the challenge with PAF (10^{-7} M). In the washing procedure, eosinophils were centrifuged at 1200 *g* for 10 min and resuspended in RPMI medium, pH 7.2, prepared with RPMI 1640, 30 mM HEPES buffer, 2 mg ml^{-1} sodium bicarbonate and 4 mg ml^{-1} ovalbumin. In all protocols, chambers were incubated for 2 h at 37°C in a 5% CO_2:95% O_2 atmosphere. Then, the filters were fixed and stained as previously reported (Richards & McCullough, 1984). The results are given as number of eosinophils per 15 consecutive high-power fields on the immersion objective 40 μm from the upper filter surface.

Rabbit platelet aggregation

The blood was obtained from normal ether anaesthetized rabbits through a cardiac puncture and mixed with 2% sodium citrate (1 vol for 9 vol of blood). Platelet rich plasma (PRP) was prepared by blood centrifugation at 200 *g* for 15 min and platelet-poor plasma (PPP) was obtained by the centrifugation of the remaining blood for 20 min at 2500 *g*. The final concentration of platelets in PRP was adjusted to 6×10^5 μl^{-1} with PPP, and the platelet aggregation was monitored by measuring the changes in turbidity of a 0.3 ml PRP aliquot at 37°C, according to Born (1962). To test the effect of BN 50730 on the platelet aggregation induced by increasing concentrations of PAF (10^{-9} to 10^{-5} M), cells were pre-incubated with 5×10^{-7} to 10^{-6} M BN 50730, or its vehicle, for 2 min at 37°C.

In another set of experiments, PRP was further washed twice by centrifugation at 1700 *g* for 15 min in Tyrode buffer (composition, mM: NaCl 137, KCl 2.7, NaH_2PO_4 0.42, $MgCl_2$ 2, $NaHCO_3$ 12, glycose 5.5 and BSA 0.35%, pH 6.5) containing iloprost (10^{-8} M). The platelets were resuspended to a final concentration of 6×10^5 μl^{-1} in Tyrode solution (pH 7.4, without iloprost) and BN 50730 or WEB 2086 (10^{-6} M) was incubated with washed platelets for 2 min before PAF stimulation (10^{-9} M). In order to wash the drug from the platelets, cells incubated with each of these antagonists were subjected to 4 consecutive washings, as previously stated, before the challenge with PAF (10^{-9} M). In all protocols, platelet aggregation was recorded as percentage change in light transmission.

Materials

PAF (1-*O*-hexadecyl-2-acetyl-sn-glyceryl-3-phosphorylcholine) was purchased from Bachem (Feinchemikalien AG, Switzer-

land); histamine, 5-hydroxytryptamine, bradykinin, LPS (lipopolysaccharide from *E. coli* serotype 0127:B8), metrizamide, HEPES buffer, ovalbumin and RPMI medium were purchased from Sigma (St Louis, MO, U.S.A.); Iloprost from Schering (Berlin, Germany); BN 50730 (tetrahydro-4,7,8,10 methyl-1 (chloro-2 phenyl)-6 (methoxy-4 phenyl-carbamoyl)-9 pyrido [4',3'-4,5] thieno [3,2-f] triazolo-1,2,4[4,3-a] diazepine-1,4) and BN 52021 (3-(1,1-dimethylethyl) hexahydro-1,4,7b-trihydroxy-8-α methyl-9H-1,7α (epoxymethanol) 1H, 6H-cyclopenta (c)furo (2,3-b)furo(3', 2':3,4) cyclopenta(1,2-d) furan-5,9,12 (4H)-trione) from Institute Henri Beaufour (Le Plessis Robinson, France); and WEB 2086 (3-(4-(2-chlorophenyl)-9-methyl-6H-thieno2,2-f-(1,2,4) triazolo (4,3-a)(1,4)-diazepin-2-yl-1-(4-morpholinyl-1-propanone) was kindly provided by Dr H. Heuer, Boehringer-Ingelheim (Ingelheim am Rhein, Germany).

Statistical analysis

The data were statistically examined by means of analysis of variance (ANOVA), followed by Newman-Keuls Student's test. P values of 0.05 or less were considered significant.

Results

Effect of BN 50730 on the pleural exudation

As reported (Silva *et al.*, 1991), the injection of PAF into the rat pleural cavity leads to an early exudation (15–30 min) followed by a marked increase in the number of eosinophils, neutrophils and mononuclear cells 6 h post challenge. Within 24 h, neutrophils and mononuclear cell counts return to control values, whereas the eosinophila peaks and persists up to 96 h. In the first series of experiments, the effectiveness of BN 50730 on the pleural exudation induced by PAF was evaluated. Administered at 0.5 to 10 μg per cavity, 5 min before the agonist, BN 50730 dose-dependently inhibited the protein extravasation noted within 15 min following PAF stimulation (1 μg per cavity), presenting an ID_{50} value of 1.4 nmol per cavity (Figure 1). In contrast, BN 50730 failed to modify the exudation induced by other vasoactive substances, including histamine, 5-HT and bradykinin (Table 1). The comparative analysis with the classical PAF receptor antagonists, BN 52021 and WEB 2086, revealed that BN 50730 was the most potent since at 2.5 μg per cavity it inhibited 86% of the exudatory response to PAF (1 μg per cavity) under conditions where the former substance inhibited only 50% (Figure 2). At 10 μg per cavity BN 50730 completely abolished the exudation caused by PAF, whereas BN 52021 and WEB 2086 inhibited the response by about 85%. Analysis of the time of action of these drugs indicated that the effects of WEB 2086 and BN 52021 were over within 2 and 4 h respectively, whereas BN 50730 was able to inhibit PAF-induced exudation significantly for 7 days (Figure 3).

Table 1 Lack of effect of BN 50730 on the pleural exudation induced by histamine (200 μg per cavity), 5-hydroxyltryptamine (5-HT, 100 μg per cavity) or bradykinin (50 μg per cavity)

Stimuli	*Protein* (mg per cavity) *Untreated*	*Treated*
Saline	5.10 ± 0.41	4.86 ± 0.23
Histamine	16.94 ± 1.62*	16.08 ± 2.80
5-HT	14.38 ± 1.84*	14.14 ± 1.85
Bradykinin	17.49 ± 1.53*	16.35 ± 2.79

BN 50730 (10 μg per cavity) was injected 5 min before the agonist. The analysis was performed 1 h after stimulation and the values represent the mean ± s.e.mean from at least 7 rats. *$P<0.001$ as compared to the saline group.

PAF-induced exudation was also significantly sensitive to oral pretreatment with BN 50730. Based on the response to saline, which did not affect the pleural basal level of protein (4.8 ± 0.6 mg per cavity, mean ± s.e. mean, $n = 7$), the exudation evoked by PAF (1 μg per cavity) was 26.2 ± 2.3 mg per cavity ($n = 7$), in untreated animals and 17.6 ± 1.4 mg per cavity ($P<0.05$, $n = 7$) in rats pretreated 1 h before with BN 50730 (10 mg kg^{-1}).

Effect of BN 50730 on leucocyte mobilization in vivo

Oral pretreatment with BN 50730 (10 to 20 mg kg^{-1}), 1 h before PAF, also prevented the pleural leucocyte influx (Figure 4a) and the late eosinophil accumulation (Figure 4b) noted at 6 and 24 h following PAF administration, respec-

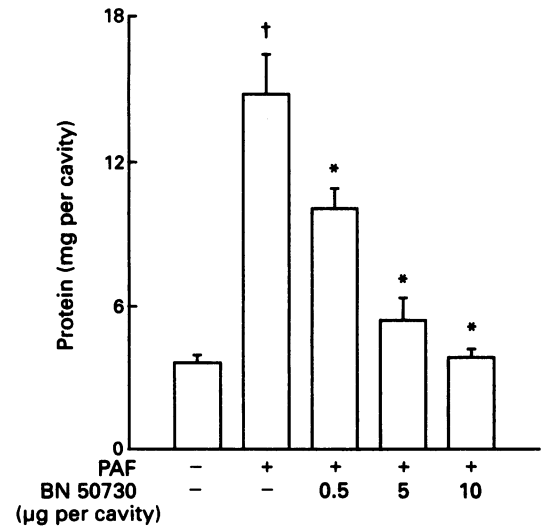


Figure 1 Effect of the intrathoracic treatment with BN 50730 (0.5–10 μg per cavity) on the pleural protein extravasation noted within 15 min following PAF (1 μg per cavity). Columns represent the mean (with s.e.mean) from at least 6 animals. †$P<0.05$ from the PAF-vehicle group by Newman-Keuls-Student's test. *$P<0.05$ from the untreated group by Newman-Keuls-Student's test.

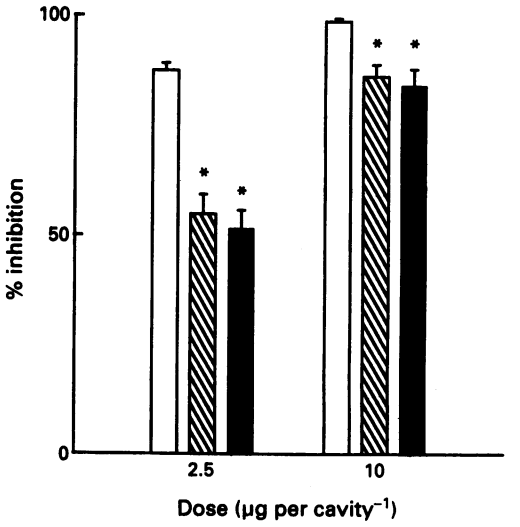


Figure 2 Comparative effect of intrathoracic treatment with either BN 50730 (open column), BN 52021 (hatched column) or WEB 2086 (solid column) (2.5 and 10 μg per cavity), administered 5 min before challenge, on the pleural protein extravasation noted within 15 min following PAF (1 μg per cavity). Columns represent the mean (with s.e.mean) from at least 6 animals. *$P<0.05$ from the BN 50730 treated group by Newman-Keuls-Student's test.

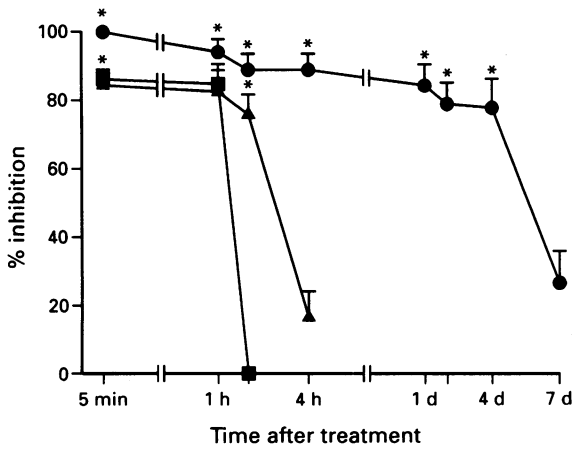


Figure 3 Kinetics of the anti-exudatory effect exhibited by BN 50730 (●) BN 52021 (Δ) and WEB 2086 (■) at 10 μg per cavity. Treatments were performed at different times ranging from 5 min to 7 days before the intrathoracic injection of PAF (1 μg per cavity) and plasma leakage evaluated within 15 min. The values are expressed as the mean (with s.e.mean) from at least 6 animals. $*P<0.001$ from the untreated group by Newman-Keuls-Student's test.

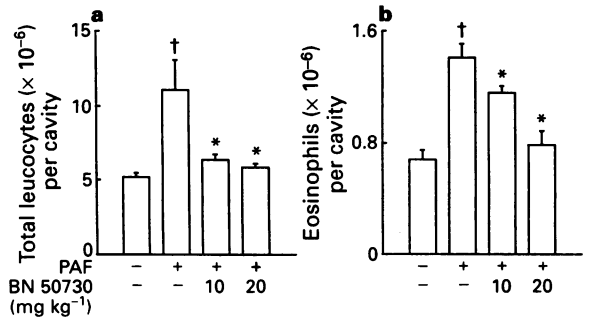


Figure 4 Effect of BN 50730 (10–20 mg kg^{-1}, i.p.) on the total leucocyte infiltration noted at 6 h (a) and on the eosinophil infiltration noted at 24 h (b) following PAF stimulation. The values are expressed as the mean (with s.e.mean) from at least 7 animals. $\dagger P<0.05$ from the saline-stimulated group by Newman-Keuls-Student's test. $*P<0.05$ from the untreated group by Newman-Keuls-Student's test.

tively. Compared to saline, which did not affect the pleural basal level of free eosinophils ($0.92 \pm 0.07 \times 10^6$ per cavity, $n = 7$), LTB_4 (0.5 μg per cavity) and bradykinin (50 μg per cavity) induced eosinophil accumulation which was unaffected by BN 50730. The responses to LTB_4 and bradykinin in these experiments were $2.20 \pm 0.16 \times 10^6$ per cavity ($n = 6$) and $2.18 \pm 0.12 \times 10^6$ per cavity, ($n = 5$) respectively, and after the pretreatment with BN 50730 the values were $1.90 \pm 0.14 \times 10^6$ per cavity ($n = 6$) and $2.36 \pm 0.19 \times 10^6$ per cavity ($n = 6$) respectively. In addition, BN 50730 failed to inhibit eosinophil accumulation caused by the intrathoracic injection of LPS, but drastically reduced the neutrophil infiltration elicited by the same stimulus (Table 2).

Effect of BN 50730 on eosinophil chemotaxis and platelet aggregation

We observed that PAF (10^{-9} to 10^{-5} M) induced a dose-dependent eosinophil mobilization in the 48-microwell Boyden chamber. Preincubation of the cells with BN 50730 (30 nM to 1 μM for 10 min) drastically inhibited the eosinophil migration, under conditions where the highest concentration abolished the effects of all doses of PAF (Figure 5). The comparison with other PAF antagonists

Table 2 Effect of the oral pretreatment with BN 50730 (20 mg kg^{-1}) on the eosinophil and neutrophil infiltration induced by the intrathoracic injection of lipopolysaccharide (LPS, 250 ng per cavity)

Cell type	*Cells* ($\times 10^6$ per cavity) *Untreated*	*Treated*
Eosinophils	3.10 ± 0.18	2.50 ± 0.26
Neutrophils	18.98 ± 1.56	8.95 ± 1.44*

The basal levels for neutrophils and eosinophils in the pleural cavity were 0.0 ± 0.0 and $0.95 \pm 0.18 \times 10^6$ cells per cavity respectively. Neutrophil and eosinophil counts were performed 4 and 24 h after LPS respectively, and the values represent the mean ± s.e.mean from at least 6 rats. $*P<0.001$ as compared to the untreated control groups.

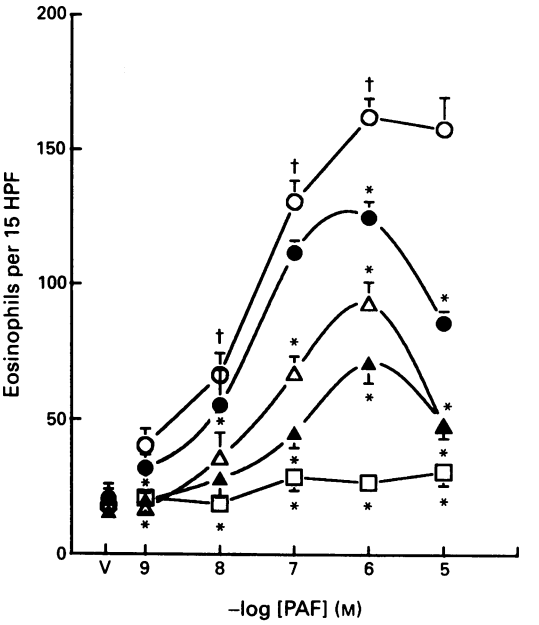


Figure 5 Effect of BN 50730 at 30 nM (●), 60 nM (▲), 90 nM (Δ) and 1 μM (□) on the eosinophil chemotaxis *in vitro* caused by PAF (1 nM–10 μM) (○). The values are expressed as the mean (with s.e.mean) from at least 3 distinct assays. Cells were pre-incubated with drug or vehicle for 10 min prior to stimulation with PAF or its vehicle, remaining in contact with the drug throughout the experiment. $\dagger P<0.05$ from the vehicle-stimulating cells by Newman-Keuls-Student's test. $*P<0.05$ from the untreated group of Newman-Keuls-Student's test.

showed that BN 50730 is two orders of magnitude more potent than WEB 2086 and BN 52021 (Figure 6).

In another set of experiments, PAF (10^{-9} to 10^{-5} M) led to a dose-dependent aggregation of rabbit platelets suspended in plasma. As indicated in Figure 7, the co-incubation of PRP with BN 50730 (0.5, 0.8 and 1 μM for 2 min) dose-dependently inhibited the platelet aggregation. As in eosinophil chemotaxis, the highest concentration abolished the effects of all doses of PAF.

Inhibitory effect of eosinophil chemotaxis and washed platelet aggregation induced by PAF before and after the withdrawal of BN 50730

As indicated in Figure 8, the co-incubation of washed platelets with BN 50730 or WEB 2086 (10^{-6} M) during 2 min abolished the platelet aggregation triggered by PAF (10^{-9} M). Following 4 consecutive washings, only platelets incubated with WEB 2086 recovered the sensitivity to PAF. Similar

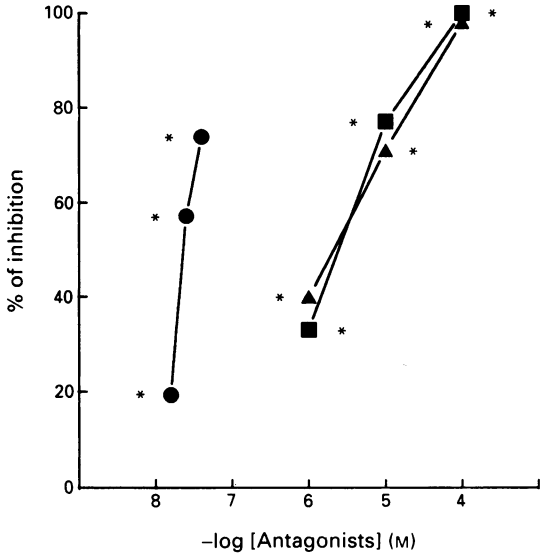


Figure 6 Comparative effect of BN 50730 (●), BN 52021 (△) and WEB 2086 (■) on the eosinophil chemotaxis *in vitro* caused by PAF (0.1 μM). Cells were pre-incubated with drug or vehicle for 10 min prior to stimulation with PAF or its vehicle, remaining in contact with the drug throughout the experiment. The values are expressed as the mean from at least 4 independent assays. $*P<0.001$ from the untreated group by Newman-Keuls-Student's test.

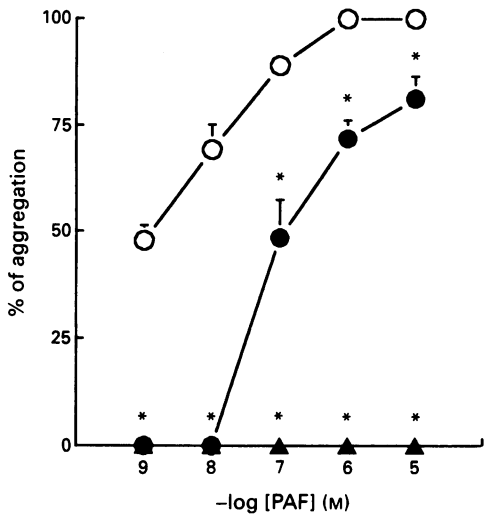


Figure 7 Effect of BN 50730 at 5×10^{-7} M (●), 10^{-6} M (▲) on rabbit platelet aggregation *in vitro* caused by PAF (1 nM–10 μM) (○). The values are expressed as the mean (with s.e.mean) from at least 3 distinct assays. Cells were pre-incubated with drug or vehicle for 2 min prior to stimulation with PAF, remaining in contact with the drug throughout the experiment. $*P<0.05$ from the untreated group by Newman-Keuls-Student's test.

results were obtained when rat isolated eosinophils were used as target cells. Pretreatment with BN 50730 (10^{-6} M) or WEB 2086 (10^{-4} M), during 10 min, impaired the eosinophil chemotaxis caused by PAF (10^{-7} M) but, in contrast to what was observed with WEB 2086, we were not able to wash off the effect from eosinophils exposed to BN 50730 (Table 3).

Discussion

In this study we have evaluated the effect of the new PAF receptor antagonist BN 50730 (Braquet *et al.*, 1990) on the

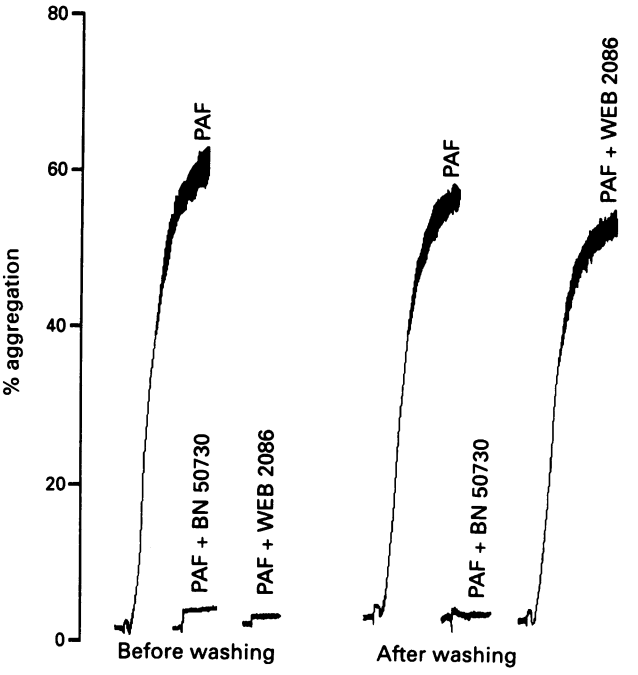


Figure 8 Effect of BN 50730 or WEB 2086 (10^{-6} M) on the rabbit washed platelet aggregation induced by PAF (10^{-8} M) before and after a set of 4 consecutive platelet washings performed as indicated in Methods. Platelets were pre-incubated with drug or vehicle for 2 min prior to stimulation with PAF and the tracings are representative of 3 independent paired assays.

Table 3 Inhibitory effect upon eosinophil chemotaxis induced by PAF before and after withdrawal of BN 50730 and WEB 2086

		% inhibition			
Treatment	Dose (M)	*Before washing*	n	*After washing*	n
BN 50730	10^{-6}	92.8 ± 3.5	5	92.6 ± 4.5	4
WEB 2086	10^{-4}	98.4 ± 1.2	6	12.0 ± 4.7*	4

Values represent the mean ± s.e.mean from at least 4 experiments. $*P<0.001$ as compared to the assay before washing.

exudatory and cellular response elicited by PAF and other inflammatory stimuli. As previously reported, rat pleural stimulation with PAF caused an acute increase in the vascular permeability followed by neutrophil, eosinophil and mononuclear cell infiltration (Martins *et al.*, 1989b; Silva *et al.*, 1991). We verified that the local administration of the hetrazepine, BN 50730, into the rat pleural space did not induce agonistic activity but dose-dependently inhibited the exudation induced by PAF (2 nmol per cavity), presenting an ID_{50} value of 1.4 nmol per cavity. However, it failed to modify the response to either histamine, bradykinin or 5-HT, indicating that BN 50730 is a specific PAF receptor antagonist. The inhibition by BN 50730 in the present study represents a further demonstration of the specificity of this drug since, in the cat airway, BN 50730 inhibited the bronchoconstrictor response to PAF whereas the effect of other agonists, including U-46619, prostaglandin $F_{2\alpha}$ ($PGF_{2\alpha}$), PGD_2 and 5-HT, was not affected (Dyson *et al.*, 1990).

The comparison with other PAF receptor antagonists revealed that BN 50730 is about 4 fold more potent than BN 52021 and WEB 2086. Nevertheless, the major difference in the pharmacological properties of these compounds is related to their duration of action. The kinetics of the inhibitory

effect on pleural exudation revealed that the actions of WEB 2086 and BN 52021 (10 μg per cavity) were over within 2 and 4 h, respectively. In contrast, BN 50730 exhibited a long-lasting effect sustained 80% of its inhibitory activity for at least 4 days. The suppressive effect reduced thereafter but was still noted within 7 days.

Orally administered BN 50730 prevented exudation assessed within 15 min, the increase in the total leucocyte counts observed at 6 h and also abolished the pleural eosinophil accumulation noted 24 h after PAF stimulation. However, this treatment failed to modify the pleural eosinophilia triggered by LTB_4 or bradykinin, adding support to the concept that in the cellular system, BN 50730 is also a specific PAF receptor antagonist. The findings are in line with those reported by Lagente *et al.* (1993), who demonstrated that the guinea-pig peribronchial eosinophil accumulation triggered by aerosol administration of PAF, but not of LTB_4, is suppressed by BN 50730. In this study, BN 50730 was also used to investigate the potential contribution of endogenous PAF to the rat pleural leucocyte infiltration triggered by LPS. We observed that pretreatment with BN 50730 drastically attenuated the neutrophil mobilization observed within 4 h, whereas the subsequent eosinophil accumulation noted 24 h post-LPS was not affected. The same profile of interference was seen with two other PAF receptor antagonists (WEB 2086 and PCA 4248) as previously reported (Bozza *et al.*, 1993). In addtion, lung and alveolar macrophages produce remarkable quantities of PAF in response to LPS stimulation (Chang *et al.*, 1987; Rylander & Beijer, 1987), which is in line with the interpretation that the local generation of PAF is largely implicated in the LPS-induced tissue neutrophil mobilization.

As a single local injection of BN 50730 (10 μg per cavity) was able to prevent PAF-induced exudation for 4 days, we performed a second series of *in vitro* experiments in an attempt to clarify the nature of this pharmacological blockade. It was demonstrated that the pre-incubation of rat isolated peritoneal eosinophils with increasing concentrations of BN 50730 did not modify the viability of these cells (data not shown) but dose-dependently prevented the eosinophil migration caused by PAF in the Boyden chamber, presenting an IC_{50} value of 50 nM. Under the same experimental conditions, the reference compounds BN 52021 and WEB 2086 were shown to be 100 fold less potent than BN 50730, presenting IC_{50} values of 5 μM. It is of interest to emphasize that the dose-response curves performed in the presence of BN 50730 exhibited a marked suppression of the maximal effect, suggesting an antagonism of the non-competitive (unsurmountable) type. In addition eosinophils preincubated with BN 50730 then subjected to a series of 2 washings, in order to remove the antagonist from the receptor environment, failed to restore the sensitivity to the lipid. The inability to wash off the effect from eosinophils indicated a high stability of the binding between BN 50730 and the PAF receptor.

It is noteworthy that BN 50730 is not the only specific antagonist supposed to express high affinity for the PAF receptor. Recently, Herbert and coworkers (1992) have demonstrated that the oral administration of SR 27417 in rabbits selectively abolished the *ex vivo* platelet aggregation induced by PAF during 2–3 days, a blockade which was not overcome by high concentrations of PAF, suggesting a tight drug-receptor association. Furthermore, based on the Scatchard analysis of the specific binding of [^{3}H]-PAF, they reported that the nature of the SR 27417 inhibition changes from a competitive (when the blood was withdrawn 5 min after treatment) to a non-competitive type of blockade (noted when the blood was obtained 3 to 24 h after drug administration) which may be due either to the generation of a drug metabolite with an irreversible affinity for PAF receptors, or to a progressive tight SR 27417-receptor association which becomes irreversible with time (Herbert *et al.*, 1992).

In vitro, BN 50730 inhibited rabbit platelet aggregation induced by PAF dose-dependently and showed a reduction of the maximal response as it was also observed in the eosinophil chemotaxis assay. In an attempt to test the stability of the drug-receptor complex, washed platelets were preincubated with BN 50730 or WEB 2086 for 2 min and then subjected to a series of 4 successive washings in order to discard the antagonist from the receptor environment. In fact, we observed that platelets preincubated with BN 50730 remained selectively blocked to the PAF stimulation even after the washing procedure, under conditions where platelets pretreated with WEB 2086 recovered their responsiveness to the lipid. These findings suggest that, in contrast to WEB 2086, BN 50730 may be regarded as a non-competitive antagonist, which is consistent with the impossibility of surmounting its effect with high concentrations of PAF, as observed in the eosinophil chemotaxis assay. In addition, the inability to wash off the effect of BN 50730 also from platelets reinforce the interpretation that the dissociation kinetics of this drug from the PAF receptor is indeed slow, resulting in a high affinity binding. Studies concerning the potential irreversibility of the BN 50730 blockade are now underway.

In conclusion, our findings indicate that BN 50730 is a potent long-acting and specific PAF receptor antagonist. Its pharmacological profile on platelet aggregation and eosinophil chemotaxis assays suggests that BN 50730 causes a non-competitive inhibition of PAF receptors and that the drug-receptor complex is quite stable.

We are indebted to Dr F. Nöel for his helpful suggestions, Mr F.A. Violante and Mr H.N. Cruz for their technical assistance and Mrs A.M.R.e Silva for the language revision. This work was supported by grants from CNPq (Brazil).

References

BENVENISTE, J., HENSON, P.M. & COCHRANE, C.G. (1972). Leukocyte dependent histamine release from rabbit platelets: The role of IgE, basophils and a platelet activating factor. *J. Exp. Med.*, **136**, 1356–1377.

BORN, G.V.R. (1962). Aggregation of blood platelet by adenosine diphosphate and its reversal. *Nature*, **194**, 927–929.

BOZZA, P.T., CASTRO-FARIA-NETO, H.C., MARTINS, M.A., LARANJEIRA, A.P., PERALES, J.E., SILVA, P.M.R. & CORDEIRO, R.S.B. (1993). Pharmacological modulation of lipopolysaccharide-induced pleural eosinophila in the rat. A role for new generated protein. *Eur. J. Pharmacol.*, **248**, 41–47.

BRAQUET, P., LAURENT, J.P., ROLLAND, A., MARTIN, C., POMMIER, J., HOSFORD, D. & ESANU, A. (1990). From ginkgolides to N-substituted piperidinothieno diazepines, a new series of highly potent dual antagonists. *Adv. Prostaglandin Thromboxane Leukot. Res.*, **21**, 929–937.

BRAQUET, P., TOUQUI, I., SHEN, T.Y. & VARGAFTIG, B.B. (1987). Perspectives in platelet-activating research. *Pharmacol. Rev.*, **39**, 97–145.

CASALS-STENZEL, J., MUACEVIN, G. & WEBER, K.H. (1987). Pharmacological actions of WEW 2086, a new specific antagonist of platelet-activating factor. *J. Pharmacol. Exp. Ther.*, **241**, 974–981.

CASTRO-FARIA-NETO, H.C., MARTINS, M.A., SILVA, P.M.R., BOZZA, P.T., CRUZ, H.N., QUEIROZ-PAULO, M., KAPLAN, M.A.C. & CORDEIRO, R.S.B. (1993). Pharmacological profile of epiyangambin: a furofuran lignan with PAF antagonist activity. *J. Lipid Mediat.*, **7**, 1–9.

CHANG, S.-W., FEDDERSEN, C.O., HENSON, P.M. & VOELKEL, N. (1987). Platelet-activating factor mediates hemodynamic changes and lung injury in endotoxin-treated rats. *J. Clin. Invest.*, **79**, 1498–1509.

DYSON, M.C., BELLAN, J.A., MINKES, R.K., BECKERMAN, R.C., WEGMANN, M.J., BRAQUET, P., MCNAMARA, D.B. & KADOWITZ, P.J. (1990). Influence of SK&F 95587 and BN 50730 on bronchoconstrictor responses in the cat. *J. Pharmacol. Exp. Ther.*, **255**, 1320–1327.

GORNALL, A.G., BARDAWILL, C.J. & DAVID, M.M. (1949). Determination of serum proteins by means of the Biuret reaction. *J. Biol. Chem.*, **177**, 751–766.

HERBERT, J.M., BERNAT, A., VALETTE, G., GIGO, V., LALE, A., LAPLACE, M.-C.L., LESPY, L., SAVI, P., MAFFRAND, J.P. & LE FUR, G. (1991). Biochemical and pharmacological activities of SR 27417, a highly potent, long acting PAF receptor antagonist. *J. Pharmacol. Exp. Ther.*, **259**, 44–51.

HERBERT, J.M., LAPLACE, M.C. & MAFFRAND, J.P. (1992). Ex vivo effects of SR 27417, a novel PAF antagonist, on rabbit platelet aggregation and [^{3}H]-PAF binding. *J. Lipid Mediat.*, **5**, 1–12.

HILL, A.V. (1910). The possible effects of the aggregation of the molecules of haemoglobin on its dissociation curves. *J. Physiol.*, **40**, 4–6.

HONDA, Z., NAKAMURA, M., MIKI, I., MINAMI, M., WATANABE, T., SEYAMA, Y., OKADO, H., TOH, H., ITO, K., MIYAMOTO, T. & SHIMIZU, T. (1991). Cloning by functional expression of platelet-activating factor receptor from guinea-pig lung. *Nature*, **349**, 342–346.

HWANG, S.-B. (1990). Specific receptors of platelet-activating factor, receptor heterogeneity, and signal transduction mechanisms. *J. Lipid Mediat.*, **2**, 123–158.

LAGENTE, V., BOICHOT, E., CARRE, C., MENCIA-HUERTA, J.-M. & BRAQUET, P. (1993). Effects of the platelet activating factor antagonists BN 52021 and BN 50730 on antigen-induced bronchial hyper-responsiveness and eosinophil infiltrating in lung from sensitized guinea-pigs. *Clin. Exp. Allergy*, **23**, 1002–1010.

MARTINS, M.A., ETIENNE, A., SOULARD, C., DOMINGO, M.T. & BRAQUET, P. (1989a). Chemotactic effect of PAF on peritoneal eosinophil from normal rats. *Braz. J. Med. Biol. Res.*, **22**, 1151–1154.

MARTINS, M.A., SILVA, P.M.R., CASTRO-FARIA-NETO, H.C., BOZZA, P.T., DIAS, P.M.F.L., LIMA, M.C.R., CORDEIRO, R.S.B. & VARGAFTIG, B.B. (1989b). Pharmacological modulation of PAF-induced rat pleurisy and its role in inflammation by zymosan. *Br. J. Pharmacol.*, **96**, 363–371.

MARTINS, M.A., PASQUALE, C.P., SILVA, P.M.R., PIRES, A.L.A., RUFFIÉ, C., RIHOUX, J.P., CORDEIRO, R.S.B. & VARGAFTIG, B.B. (1992). Interference of cetirizine with the late eosinophil accumulation induced by either PAF and compound 48/80. *Br. J. Pharmacol.*, **105**, 176–180.

NAKAMURA, M., HONDA, Z., IZUMI, T., SAKANAKA, C., MUTOH, H., MINAMI, M., BITO, H., SEYAMA, Y., MATSUMOTO, T., NOMA, M. & SHIMIZU, T. (1992). Molecular cloning and expression of platelet-activating factor receptor from human leukocytes. *J. Biol. Chem.*, **266**, 20400–20405.

PAUL-EUGÈNE, N., DUGAS, B., PICQUOT, S., LAGENTE, V., MENCIA-HUERTA, J.-M. & BRAQUET, P. (1990). Influence of interleukin-4 and platelet-activating factor on the FC_ϵ RII/CD23 expression on human monocytes. *J. Lipid Mediat.*, **2**, 95–101.

RICHARDS, K.L. & MCCULLOUGH, J. (1984). A modified microchamber method for chemotaxis and chemokinesis. *Immunol. Commun.*, **13**, 49–62.

RYLANDER, R. & BEIJER, L. (1987). Inhalation of endotoxin stimulates alveolar macrophage production of platelet-activation factor. *Am. Rev. Respir. Dis.*, **135**, 83–86.

SHEN, T.Y., HWANG, S.B., CHANG, M.N., DOEBBER, T.W., LAM, M.H., WU, M.S., XAN, G.C. & LI, R.Z. (1985). Characterization of a platelet-activating factor receptor antagonist isolated from haifenteng (*Piper futokadsura*): a specific inhibition of *in vitro* and *in vivo* platelet-activating factor-induced effects. *Proc. Natl. Acad. Sci. U.S.A.*, **82**, 672–676.

SILVA, P.M.R., MARTINS, M.A., CASTRO-FARIA-NETO, H.C., CORDEIRO, R.S.B. & VARGAFTIG, B.B. (1991). Generation of an eosinophilotatic activity in the pleural cavity of platelet-activating factor-injected rats. *J. Pharmacol. Exp. Ther.*, **257**, 1039–1044.

SUGIMOTO, T., TSUCHIMOCHI, H., MCGREGOR, C.G.A., MUTOH, H., SHIMIZU, T. & KURACHI, Y. (1992). Molecular cloning and characterization of the platelet-activating factor receptor gene expressed in the human heart. *Biochem. Biophys. Res. Commun.*, **189**, 617–624.

SUNKEL, C.E., FAU DE CASA-JUANA, SANTO, L., GÓMEZ, M.M., VILLARROYA, M., GONZÁLES-MORALES, M.A., PRIEGO, J.G. & ORTEGA, M.P. (1990). 4-Alkyl-1,4-dihydropyridine derivatives as specific PAF-acether antagonists. *J. Med. Chem.*, **33**, 3205–3210.

TERASHITA, Z., IMURA, Y., NISHIKAWA, K. & SUMIDA, S. (1985). Is platelet-activating factor (PAF) a mediator of endotoxin shock? *Eur. J. Pharmacol.*, **109**, 257–261.

ZIMMERMAN, G.A., PRESCOTT, S.M. & MCINTYRE, T.M. (1992). Platelet-activating factor. A fluid-phase and cell-associated mediator of inflammation. In: *Inflammation: Basic Principles and Clinical Correlates*. ed. Gallin, J.I., Goldstein, I.M. & Snyderman, R. pp. 149–176. New York: Raven Press.

(Received November 9, 1993
Revised June 13, 1994
Accepted June 29, 1994)

Br. J. Pharmacol. (1994), **113**, 1001–1007 © Macmillan Press Ltd, 1994

Effect of cyclopiazonic acid, an inhibitor of sarcoplasmic reticulum Ca^{2+}-ATPase, on the frequency-dependence of the contraction-relaxation cycle of the guinea-pig isolated atrium

Nicola J. Yard, Michele Chiesi & [1]Howard A. Ball

Cardiovascular Biology Research Department, Ciba-Geigy Ltd., CH-4002 Basel, Switzerland

1 The relevance of a functional sarcoplasmic reticulum (SR) membrane system to the contraction-relaxation cycle and to the force-frequency relationship of guinea-pig atrial tissue was investigated. Cyclopiazonic acid (CPA) was used to inhibit selectively the activity of the SR Ca^{2+}-ATPase. IC_{50} values of 0.2 μM or 1.0 μM were measured in guinea-pig isolated SR membranes in the absence or presence of millimolar ATP, respectively. CPA (0.3–30 μM) did not inhibit the activity of the sarcolemmal Na^+-Ca^{2+}-exchanger as measured in isolated cardiac cell membrane preparations.

2 In guinea-pig isolated left atrium paced at 2.5 Hz (30°C), CPA (1–100 μM) produced a concentration-dependent reduction in developed tension and a fall in the maximum rate of tension increase ($+dT/dt_{max}$) and decrease ($-dT/dt_{max}$). The twitch duration was markedly increased due to a prolongation of the time to peak tension, and in particular, the relaxation phase.

3 The contraction-relaxation cycle of the left atrium showed a marked dependence on the frequency of stimulation. The developed tension and $+dT/dt_{max}$ showed a progressive increase from 0.5 Hz, reaching peak values at a stimulation rate of 1.5–2.5 Hz, the positive staircase phenomenon. Higher frequencies of stimulation caused a fall in these parameters. Resting tension was unaffected. The time-course of the contraction-relaxation cycle was also frequency-dependent, with both time to peak tension and relaxation time showing a progressive fall from 2.0–3.5 Hz.

4 The addition of CPA (30 μM) caused marked alterations in the frequency-dependence of the contraction-relaxation cycle. The frequency-dependence of developed tension, $+dT/dt_{max}$ and $-dT/dt_{max}$, was shifted downwards, particularly at higher frequencies, and the frequency at which peak values of $+dT/dt_{max}$ and $-dT/dt_{max}$ were reached was shifted leftwards. The resting tension of the tissues in the presence of 30 μM CPA was increased markedly at frequencies greater than 2 Hz. The time-course of the contraction-relaxation cycle was markedly prolonged between 1.0 and 3.5 Hz, due to an effect on both time to peak tension and relaxation time.

5 In conclusion, these results show that CPA is a highly selective inhibitor of the cardiac SR Ca^{2+}-ATPase, without effect on the sarcolemmal Na^+-Ca^{2+}-exchanger, and suggest that a functional SR Ca^{2+}-ATPase is necessary for the normal contraction-relaxation cycle of guinea-pig cardiac tissue. Additionally, the results suggest an increasing dependence of tension development on SR Ca^{2+}-ATPase with increasing frequency, which may reflect either a frequency-dependent activation of this enzyme or the diminished contribution of the Na^+-Ca^{2+} exchanger. These results also provide novel support for the mechanism of the depressed force-frequency relation found in cardiac tissue of heart failure patients, in which there is a reduced expression of Ca^{2+}-ATPase.

Keywords: Ca^{2+}-ATPase; force-frequency relation; cyclopiazonic acid; contraction-relaxation cycle; sarcoplasmic reticulum

Introduction

The developed tension and time-course of the contraction-relaxation cycle of the isolated myocardium of the majority of mammalian species is dependent on the frequency of stimulation (Buckley *et al.*, 1972). For example, the developed tension of human myocardium increases with the increase in stimulation frequency (positive staircase or treppe effect), while twitch duration decreases (Gwathmey *et al.*, 1990; Mulieri *et al.*, 1992). These changes have been directly related to an increase in the magnitude of the cytosolic calcium transient as well as a shortening of its duration (Wier & Yue, 1986; Gwathmey *et al.*, 1990). In adult mammalian myocardium the peak concentration of cytosolic calcium is principally determined by the amount of calcium released from the sarcoplasmic reticulum (SR) which in turn is related to the amount of calcium present in the SR (Hilgemann & Noble, 1987; Lewartowski & Pytkowski, 1987). One possible explanation for the staircase phenomemon is that there is a frequency-dependent activation of calcium uptake by the SR, but this has so far been difficult to test due to the lack of a selective and specific inhibitor of the Ca^{2+}-ATPase.

Cyclopiazonic acid, a mycotoxin produced by *Aspergillus penicillium*, was originally described as an inhibitor of the SR Ca^{2+}-ATPase expressed in fast twitch muscle from the rabbit (Seidler *et al.*, 1989) and the rat (Goeger & Riley, 1989) and of smooth muscle (Deng & Kwan, 1991; Bourreau *et al.*, 1991; Suzuki *et al.*, 1992). It is reported to be without effect on F-type ATPases, such as the mitochondrial H^+-ATPase and on several other P-type ATPases, such as the gastric H^+,K^+ ATPase, the kidney and brain Na^+,K^+-ATPases, and the Ca^{2+}-ATPase of the plasma membrane (Seidler *et al.*, 1989). In the present paper CPA is shown to be a potent inhibitor also of the slow-twitch muscle isoform of the SR Ca^{2+}-ATPase expressed in guinea-pig heart without effect on the Na^+-Ca^{2+} exchanger. The effects of this selective SR inhibitor on the twitches and on the frequency-dependence of the contraction-relaxation cycle of the guinea-pig isolated left atria were therefore examined. Guinea-pig left atrial tissue was chosen for the present investigation because of the similarity of its response (Reiter, 1966; Penefsky *et al.*, 1972;

[1] Author for correspondence.

Lewartowski & Pytkowski, 1987), to that of human ventricular tissue (Feldman *et al.*, 1988; Mulieri *et al.*, 1992) with increasing frequency. A preliminary account of these results has recently been presented to the British Pharmacological Society (Yard & Ball, 1993).

Methods

SR preparation

Guinea-pig SR vesicles were prepared from the left ventricle as previously described for canine ventricular SR (Chamberlain *et al.*, 1983). The SR fraction was suspended in 250 mM sucrose, 10 mM imidazole, pH 7.0, 0.5 mM dithiothreitol, and 0.1 mM phenylmethyl-sulphony fluoride at a protein concentration of 15 mg ml^{-1}. Aliquots were quickly frozen in liquid nitrogen and stored at − 70°C.

Preparation of cardiac sarcolemmal (SL) vesicles

SL vesicles were prepared from calf ventricle by the sucrose gradient centrifugation method of Jones (1988) except that 50 μM PMSF was added to all solutions. The final vesicle pellet was suspended in 10 mM histidine, pH 7.0, 0.25 mM sucrose, 50 μM PMSF. Aliquots were stored at − 70°C until used. Protein concentration was determined by the method of Lowry *et al.* (1951), using bovine serum albumin as a standard.

Ca^{2+}-uptake measurements

Calcium uptake by SR membranes was measured at 37°C by using the Millipore filtration technique (0.22 μm filters type GS) and ^{45}Ca basically according to Chiesi & Inesi (1979). The initial rate of Ca-uptake was determined in a medium containing (in mM); KCl 100, sucrose 100, MOPS (pH 6.8) 50, $MgCl_2$ 5, NaN_3 5, potassium oxalate 3, ATP 2, EGTA 0.5, and $CaCl_2$ 0.15 (free Ca concentration was 0.47 μM). SR membranes were preincubated with various concentrations of CPA for 10 min with the uptake medium lacking either ATP or $CaCl_2$. Accordingly, the uptake reaction was then started by adding either $CaCl_2$ or ATP.

Measurement of Na^+-Ca^{2+} exchange activity

Na_i^+-dependent Ca^{2+} uptake activity was measured essentially as described by Seiler & Fleischer (1988). The sarcolemmal vesicles were incubated 4 h on ice in 160 mM NaCl, 40 mM 3-(N-morpholino)propanesulphonic acid (MOPS), pH 7.4 at a concentration of 0.2 mg ml^{-1}, sedimented at 70000 *g* for 1 h and suspended in a small volume of the same buffer; 3 μl of vesicles were than rapidly diluted into 60 μl of a buffer containing 160 mM KCl, 40 mM MOPS-Tris pH 7.4, 1 μM valinomycin, 0.3 μCi of $^{45}CaCl_2$ ml^{-1}, 0.2 mM EGTA and 0.188 mM $CaCl_2$ (yielding an approximate free Ca^{2+} concentration of 1 μM). The uptake reaction was stopped by rapid filtration of the sample and extensive washing of the filters (4 times with 2 ml portions of quenching buffer containing 160 mM KCl, 40 mM MOPS, pH 7.4, 1 mM $LaCl_3$). The control samples were diluted into a buffer containing 160 mM NaCl instead of 160 mM KCl.

Tension measurements

Male guinea-pigs (300–450 g) were anaesthetized with Pentothal (100 mg kg^{-1}, i.p.). The heart was rapidly removed and placed in Krebs-Henseleit solution continuously gassed with 95% O_2 and 5% CO_2. The composition was as follows (in mM): NaCl 120, KCl 4.7, $MgSO_4$ 1.2, $CaCl_2$ 2.53, $NaHCO_3$ 25; KH_2PO_4 1.17 and glucose 10. The left atrium was dissected and mounted between plastic micro tissue clamps in a 100 ml tissue bath containing Krebs-Henseleit solution at 30°C, pH 7.45, and gassed as above. (−)-Propranolol hydrochloride (1 μM) was present in the bathing solution throughout the experiment.

The tissue was directly stimulated by unipolar square wave pulses of 5 ms duration with a voltage 15–20% greater than threshold by a Grass stimulator (Grass Instruments, Quincey, MA, U.S.A.) Isometric force was measured by a force transducer (Hugo Sachs Electronic, March-Hugstetten, Germany) The tissues were stretched to a length (l_{max}) at which the developed tension was maximal, by application of a resting tension of approximately 0.5 g.

Concentration-dependent effects, and time-course, of CPA on the contraction-relaxation cycle

The left atria were stimulated continuously at a rate of 2.5 Hz for a 2 h stabilization period. Cumulative concentration-response relationships were constructed for cyclopiazonic acid, 1–100 μM (0.007–0.7% dimethylsulphoxide (DMSO) allowing an equilibration time of 1 h at each concentration. The time-course of effect of 30 μM CPA or vehicle (0.2% DMSO) was examined in a further set of preparations over a 120 min period.

Effect of CPA on the frequency-dependence of the contraction-relaxation cycle

Left atria were stimulated continuously at a rate of 1 Hz for a 2 h equilibration period. Baseline parameter-frequency relations were obtained following stimulation at each frequency for 4 min (pilot experiments showing this to be sufficient time for stable values) starting at 0.5 Hz and increasing in 0.5 Hz increments to 3.5 Hz (data not shown). Then either CPA (final concentration of 30 μM) or an equivalent volume of the vehicle (0.2% DMSO) was added. Following a 1 h equilibrium period a further parameter-frequency relation was obtained.

Drugs and chemicals

CPA and (−)-propranolol hydrochloride were obtained from Sigma Chemical Co. (St. Louis, MO, U.S.A.), Pentothal from Abbott (Cham, Switzerland). CPA was prepared in DMSO immediately prior to use. All other chemicals were of the highest analytical grade commerically available.

Data analysis

All isolated tissue parameters were recorded on a commercially available data-acquisition software computer package (PT-1; Po-Ne-Mah, Storrs, CT, U.S.A.). The developed tension (total tension − resting tension), resting tension, time to peak tension, time to 50% or 95% relaxation (time from peak tension to point of 50% or 95% of change in developed tension, respectively), $+dT/dt_{max}$ (maximum rate of increase of developed tension), $-dT/dt_{max}$ (maximum rate of decrease of developed tension), and twitch duration (time to peak tension + time to 95% relaxation) were automatically computed. All data are expressed as mean ± standard error of the mean (s.e.mean). Parameter-frequency relations following DMSO or CPA were compared by analysis of covariance, the baseline relations being used as the covariate.

Results

Effects of CPA on the Ca^{2+}-uptake activity of cardiac SR and on the Na^+-Ca^{2+}-exchanger of cardiac sarcolemma

Cyclopiazonic acid has been reported to be a potent and selective inhibitor of the Ca^{2+}-ATPase activity of the skeletal muscle SR (Seidler *et al.*, 1989; Goeger & Riley, 1989) and of smooth muscle (Deng & Kwan, 1991, Bourreau *et al.*, 1991;

Suzuki *et al.*, 1992). In the present study we investigated the compound on SR membranes isolated from guinea-pig ventricle and observed that it completely inhibited the Ca^{2+}-uptake activity with an IC_{50} value of 0.2 μM (Figure 1, filled squares). Interestingly, the presence of millimolar ATP protected ATPase from inhibition and shifted the IC_{50} value up to 1.0 μM (see Figure 1, open squares).

The lack of activity of CPA on various other ATPase systems has already been reported (Seidler *et al.*, 1989). Because of the potential importance of the cardiac sarcolemmal Na^+-Ca^{2+} exchanger, in the present study the effect of CPA was determined. No significant inhibition of the Na^+-Ca^{2+}-exchanger was observed with CPA at concentrations as high as 30 μM (Table 1).

Effect of CPA on the contractile activity of guinea-pig atria paced at 2.5 Hz

CPA caused a marked and concentration-dependent reduction in developed tension, $+dT/dt_{max}$ and $-dT/dt_{max}$ (Figure 2a and Table 2). With 30 μM CPA, for example, there was a 40% reduction in developed tension. The duration of the contraction-relaxation cycle was clearly prolonged by CPA as shown in Figure 2b where all traces have been normalized to 100% to clarify this effect. This prolongation was principally due to a marked increase in the relaxation time (eg., 42% prolongation of 95% relaxation time, with 30 μM CPA). There was less prolongation of the contractile phase (Table 2, time to peak tension), with the maximum effect occurring at 30 μM. At a frequency of 2.5 Hz there was no effect on the resting tension even at the highest CPA concentration (100 μM) tested (Figure 2a and Table 2).

The time-course of action of 30 μM CPA was investigated in further detail (Figure 3): All parameters reached equilibrium within 1 h, defining the equilibrium time used for the parameter-frequency relations.

Frequency-dependence of the contraction-relaxation cycle

Several parameters of the contraction-relaxation cycle showed a marked dependence on the frequency of stimulation. Developed tension (Figure 4a, open symbols) showed a progressive increase from 0.5 to 1.5 Hz reaching a peak tension of 216% (as a percent of the value at 0.5 Hz). Between 2–3.5 Hz the developed tension decreased slightly. The maximum rate of developed tension, $+dT/dt_{max}$ (Figure 4b, open symbols), showed a similar frequency-dependence to that of developed tension, peaking at 2.0 Hz. This was in contrast to $-dT/dt_{max}$ which continued to increase over the frequency-range 0.5–3.5 Hz. Resting tension (Figure 4d, open symbols) was unaffected even at the highest frequency of 3.5 Hz. The time-course of the contraction-relaxation cycle was also frequency-dependent, with both time to peak tension (Figure 4e, open symbols) and 95% relaxation time (Figure 4f, open squares) showing a progressive shortening from 1.0 to 3.5 Hz, such that the calculated total twitch

Table 1 Effect of cyclopiazonic acid (CPA) on the Na^+-Ca^{2+} exchange activity of isolated cardiac cell membranes

	CPA [μM]			
	Control	0.3	3	30
Na^+-Ca^{2+} exchange activity (%)	100	91 ± 7	98 ± 11	93 ± 3

The Na^+-dependent Ca^{2+}-uptake reaction was carried out as described in the methods section. The values (mean ± s.e.mean of 3 preparations) are expressed relative to the activity of the control reaction which was set to 100%.

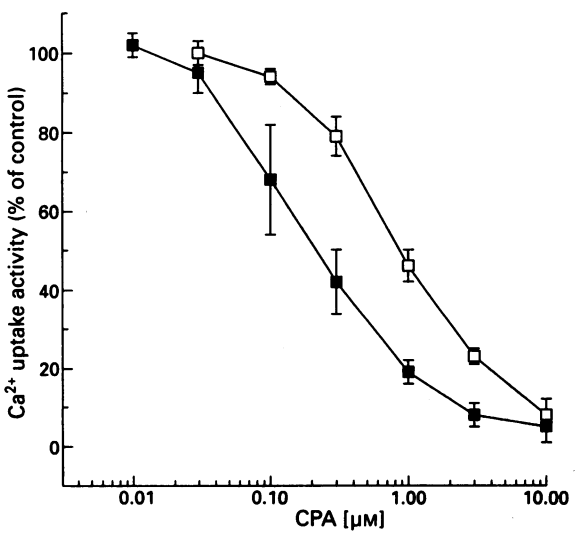


Figure 1 Effect of cyclopiazonic acid (CPA) on the Ca^{2+}-uptake activity of guinea-pig isolated myocardial SR membranes. The uptake reactions were started either by the addition of ATP (■) or $CaCl_2$ (□), details of which are given in the Methods section. Data are represented as mean ± s.e.mean of 5 preparations.

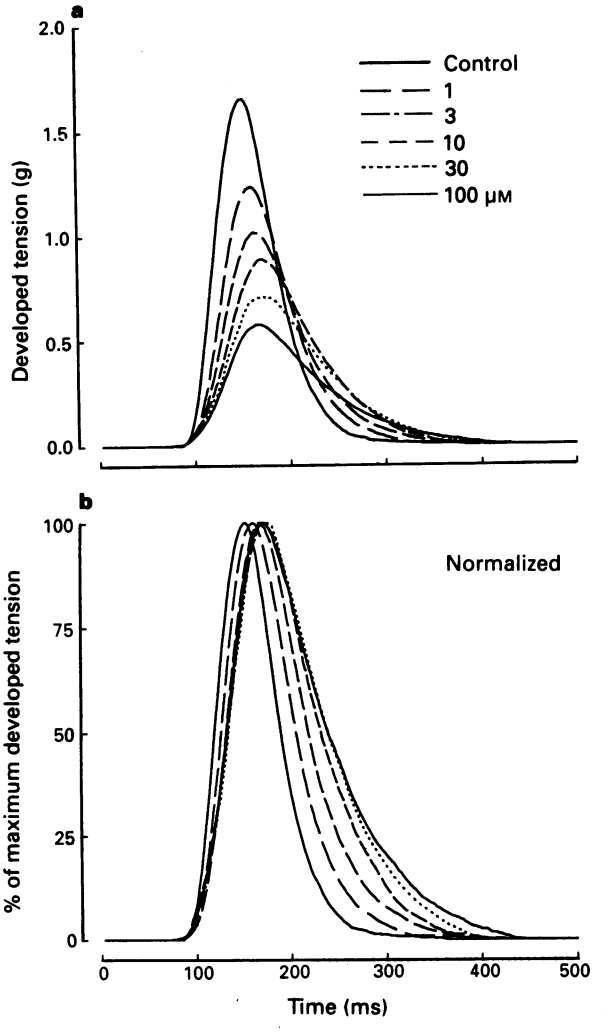


Figure 2 Representative trace (a) showing the concentration-dependent effects of cyclopiazonic acid (CPA) on the contraction-relaxation cycle of the guinea-pig left atrium measured at 2.5 Hz. Data shown in the lower panel (b) have been normalized for developed tension to clarify the effects of CPA on relaxation.

Table 2 Concentration-dependent effects of cyclopiazonic acid (CPA) on guinea-pig isolated left atria stimulated at 2.5 Hz

CPA (μM)	*Developed tension* (g)	*Resting tension* (g)	*Time to peak* (ms)	*Time to 50% relaxation* (ms)	*Time to 95% relaxation* (ms)	$+dT/dt_{max}$ (g s^{-1})	$+dT/dt_{max}$ (g s^{-1})	*Twitch duration* (ms)
0	1.82 ± 0.28	0.53 ± 0.02	81 ± 3	52 ± 2	151 ± 10	42.2 ± 8.0	25.0 ± 3.8	232 ± 12
10	1.28 ± 0.16	0.56 ± 0.02	101 ± 3	70 ± 4	201 ± 5	24.0 ± 2.7	13.3 ± 0.8	303 ± 5
30	1.08 ± 0.16	0.57 ± 0.02	103 ± 4	73 ± 5	215 ± 7	20.0 ± 2.8	11.0 ± 0.8	319 ± 5
100	0.68 ± 0.16	0.59 ± 0.05	96 ± 7	76 ± 7	223 ± 5	13.6 ± 2.8	8.3 ± 1.2	320 ± 4

Data are presented as mean ± s.e.mean ($n = 6$).

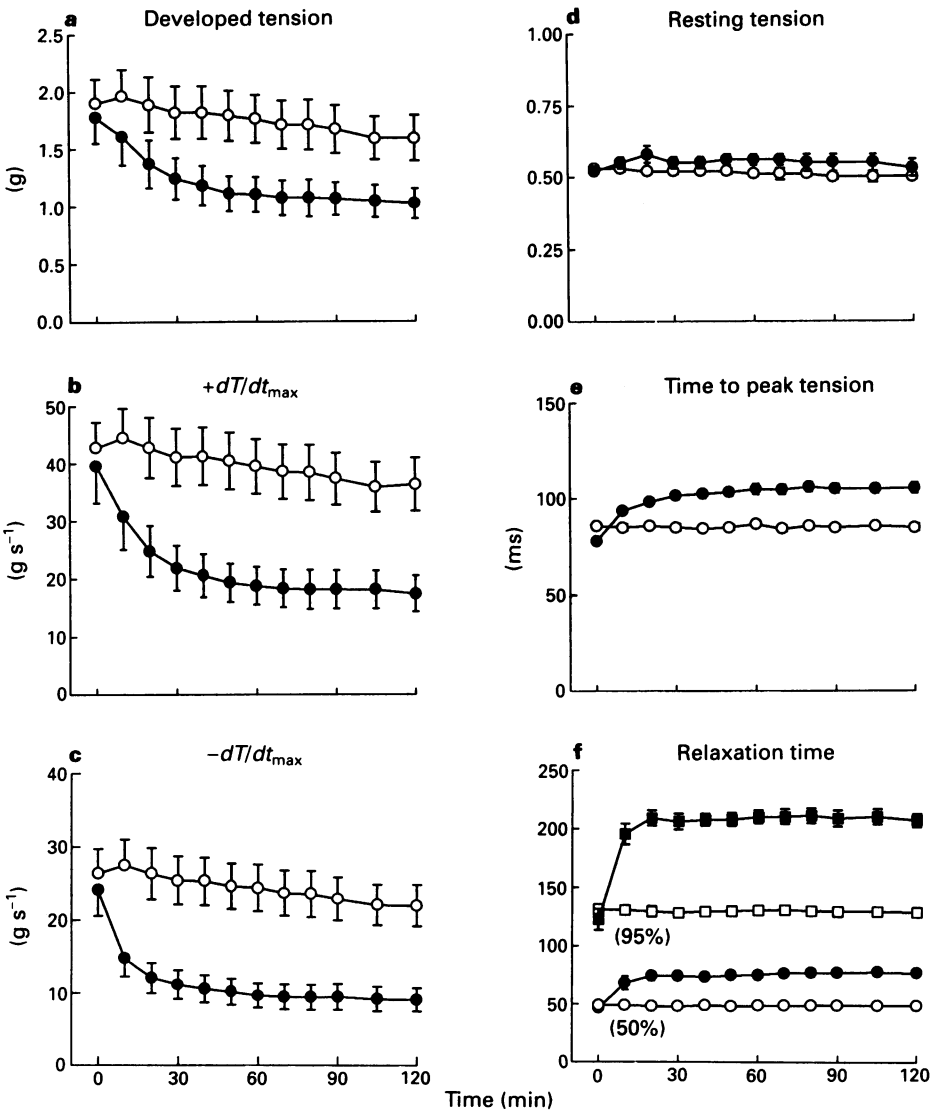


Figure 3 Time-course of the effects of 30 μM cyclopiazonic acid CPA on the contraction-relaxation cycle of the guinea-pig left atria measured at 2.5 Hz: (a) developed tension, (b) $+dT/dt_{max}$, (c) $-dT/dt_{max}$, (d) resting tension, (e) time to peak tension, and (f) time to 50% (circle) and 95% (squares) relaxation. The control group (0.2% DMSO) are represented by open symbols and those in the presence of 30 μM CPA by closed symbols. Each point is the mean ± s.e.mean of 6 tissues.

duration decreased from 247 ± 14 to 186 ± 14 ms ($P < 0.001$).

Effect of CPA on the frequency-dependence of the contraction-relaxation cycle

The addition of CPA (30 μM) caused marked alterations in the frequency-dependence of the contraction-relaxation cycle (Figure 4, closed symbols). The developed tension-frequency relation (Figure 4a) was shifted downwards, particularly at the higher frequencies (e.g., 63% reduction at 3.5 Hz, $P < 0.001$). The frequency-dependence of both $+dT/dt_{max}$ and $-dT/dt_{max}$ (Figure 4b,c) were similarly affected, with a marked reduction particularly at the higher frequencies (e.g., $+dT/dt_{max}$ being reduced by 70% at 3.5 Hz ($P < 0.001$) compared to 40% at 1.5 Hz ($P < 0.001$). In addition, the frequency at which the peak values of these parameters occurred displayed a clear leftward shift (e.g., from 2.0 to 1.5 Hz for $+dT/dt_{max}$).

The resting tension of the tissues in the presence of 30 μM CPA (Figure 4d, closed symbols) was significantly increased at frequencies greater than 2 Hz (e.g., 34% increase at 3.5 Hz; $P < 0.05$) in contrast to those tissues not treated.

The time-course of the contraction-relaxation cycle was

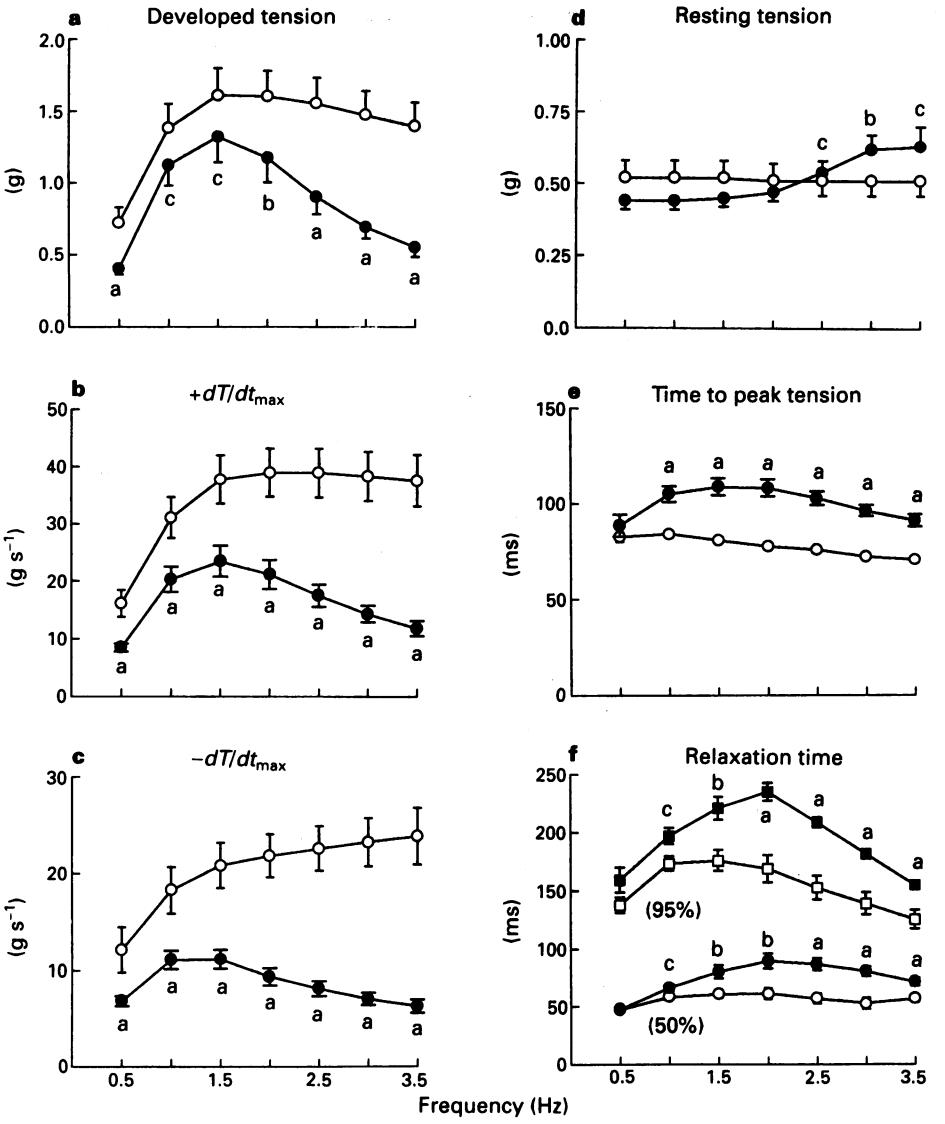


Figure 4 Effect of 30 μM cyclopiazonic acid (CPA) on the frequency-dependence of the contraction-relaxation cycle of the guinea-pig isolated atria: (a) developed tension, (b) $+dT/dt_{max}$, (c) $-dT/dt_{max}$, (d) resting tension, (e) time to peak tension, and (f) time to 50% (○, ●) and 95% (□, ■) relaxation. The control group (0.2% DMSO) are represented by open symbols and those in the presence of 30 μM CPA by closed symbols. Each point is the mean ± s.e.mean of 11 tissues. Statistically significant differences from the control group at the corresponding frequency are denoted by: $^aP<0.001$; $^bP<0.01$; and $^cP<0.05$.

also markedly affected by CPA. Specifically there was a marked prolongation of the twitch duration of the contraction-relaxation cycle between 1.0 and 3.5 Hz, due to a prolongation of time to peak tension (Figure 4e, closed symbols), as well as relaxation time (Figure 4f, closed symbols).

There was no significant effect of a 1 h equilibration with DMSO (0.2%) on the frequency-dependent relations of any of the measured parameters (data not shown).

Discussion

Role of calcium and the SR pump in contraction-relaxation cycle

The rapid cycling of the free Ca^{2+} concentration in adult mammalian cardiac cells is mainly under the control of the activity of the SR membranal system. The cisternal compartments of the SR are the source of most of the excitatory Ca^{2+} ions and the Ca^{2+}-pumping ATPase of the SR is the major mechanism concerned in lowering the free Ca^{2+} concentration to resting levels. Other Ca^{2+}-translocating entities, however, are required to ensure the contractile function of the myocardium. During each contraction-relaxation cycle there is a specific amount of Ca^{2+} entering the cell which is necessary for contraction. This Ca^{2+} of extracellular origin must be ejected during the recovery phase to avoid a Ca^{2+}-overload. Ca^{2+} ions entering the cell via the activation of the voltage-dependent Ca^{2+}-channels are necessary to induce the massive Ca^{2+} release from the SR cisternal compartments. The Na^+-Ca^{2+} exchange activity of the plasma membrane also plays a significant role and could contribute to Ca^{2+}-entry during the plateau phase of the action potential (Nuss & Houser, 1992). These Ca^{2+} ions could either participate directly in the stimulation of the myofilaments or could be used to refill rapidly the SR compartment. Another major role of the Na^+-Ca^{2+} exchanger is to extrude Ca^{2+} ions from the cytosol thus contributing to the relaxation phase (Carafoli, 1987; Philipson, 1990).

CPA has been reported to be a fairly specific inhibitor of the SR Ca^{2+}-ATPase activity (Seidler *et al.*, 1989 and this study). The effects of CPA on the contractile characteristics of guinea-pig atria can most simply be explained by this inhibitory mechanism. Even though SR preparations from

guinea-pig ventricle have been utilized in this study, the same Ca^{2+}-ATPase isoform is also expressed in the atria (Brandl *et al.*, 1986). Therefore, the assumption is made that the atrial SR Ca^{2+} -ATPase is equally affected by CPA. An inhibited SR Ca^{2+}-ATPase would result in a slower removal of intracellular free Ca^{2+} ions, leading to slower relaxation rates (see Figure 2 and Table 2). The slower relaxation kinetics could eventually lead to an increase in resting tension, in particular at the higher frequencies of stimulation (Figure 4d). Inhibition of the SR Ca^{2+} pump would lead to a gradual emptying of the SR compartment and thus to a reduced amount of Ca^{2+} being available for release with the next action potential, decreasing the developed tension (Figures 2, 3a and 4a).

CPA had only a minor, and non dose-related, effect on the contractile phase (time to peak, Table 2), the explanation for which is not clear. The effects of CPA on contractility become clearly evident only at relatively high concentrations (above 10 μM, see Figure 2), while, on the isolated SR system, Ca^{2+}-ATPase inhibition can already be detected in the submicromolar range (see Figure 1). The higher concentration required in the tissue system could be due to compartmentalisation problems (the target of CPA is intracellular) and, in particular, to the presence in the cytosol of the myocytes of millimolar concentrations of ATP, which protect the ATPase from inhibition in a competitive manner (see Figure 1). A similar effect has been previously reported (Seidler *et al.*, 1989) using fast twitch muscle preparations, where ATP protected the Ca^{2+}-ATPase against CPA inhibition in a competitive fashion.

Due to its complex involvement in the contraction-relaxation cycle, a reduction of the Na^+-Ca^{2+} exchange activity could also result in negative inotropic and lusitropic effects on the myocardium. It was therefore mandatory to exclude a possible involvement of the Na^+-Ca^{2+} exchanger in the action of CPA. No inhibition of the exchange reaction of calf heart plasma membrane could be detected. Calf hearts (ventricle) were chosen as the biological material since large amounts of tissue were needed to obtain a sufficient amount of acceptably pure plasma membranes. So far, cardiac Na^+-Ca^{2+} exchanger has been cloned from dog (Nicoll *et al.*, 1990) and calf (Aceto *et al.*, 1992) and found to be highly homologous. Therefore, it is likely that the results obtained with the calf Na^+-Ca^{2+} exchanger can be extrapolated to the guinea-pig atria. Based on such an assumption, the inhibitory effects of CPA on the contractile performance of intact guinea-pig atria could not have resulted from an inhibition of the Na^+-Ca^{2+}-exchanger (Table 1).

Frequency-dependence of contraction-relaxation cycle and effects of CPA

The developed tension and time-course of the contraction-relaxation cycle of the guinea-pig cardiac tissue, like the majority of other mammalian species, is highly dependent on the frequency of stimulation (Figure 4) as has been described for other mammalian cardiac tissues (Buckley *et al.*, 1972). For example, the developed tension of human ventricular myocardium increases with increasing stimulation frequency (positive staircase or treppe effect), while twitch duration decreases (Gwathmey *et al.*, 1990; Mulieri *et al.*, 1992). Such changes have been directly related to an increase in the magnitude of the cytosolic calcium transient as well as a shortening of its duration (Wier & Yue, 1986; Gwathmey *et al.*, 1990). The present findings of a shortening of twitch duration (due to a reduction in both time to peak tension and relaxation time) are consistent with the explanation of a frequency dependent activation of calcium uptake (leading to a reduction in relaxation time) and subsequent release (increase in developed tension) by the SR. The finding that attenuation of the force-frequency relation by CPA is more marked at higher frequencies further supports this hypothesis: because of the limiting contribution of the Na^+-Ca^{2+} exchanger to the *rapid* regulation of intracellular Ca^{2+}, the contraction-relaxation cycle becomes increasingly dependent on the performance of the SR system at higher frequencies.

Potential significance of altered force-frequency relation following Ca^{2+}-ATPase inhibition and that of the failing myocardium

The present results bear several points of similarity to findings obtained with cardiac tissue from heart failure patients where the force-frequency relation is either attenuated (Feldman *et al.*, 1988) or reversed (Mulieri *et al.*, 1992). It has been suggested that this is due to abnormalities in calcium handling with prolongation of Ca^{2+} transients (Gwathmey *et al.*, 1987; Morgan *et al.*, 1990; Beuckelmann *et al.*, 1992) due to an estimated 50% reduction in calcium uptake function (Hasenfuss *et al.*, 1992). The reduction in the number of calcium pumps was shown to be due to a reduced expression of mRNA for Ca^{2+}-ATPase (Mercadier *et al.*, 1990; Arai *et al.*, 1993).

The similarity between the force-frequency relation reported here with CPA and that found in failing heart tissue is of particular interest since both a chronic decrease in Ca^{2+}-ATPase pump expression (heart failure) or acute pump inhibition (CPA), lead to impaired calcium uptake and release, i.e., they are *functionally equivalent*. In this respect, the present results provide novel support for the role of the SR Ca^{2+}-ATPase in the attenuated force-frequency relation of cardiac tissue obtained from heart failure patients. One potential difference however lies in the effects on relaxation. While there was a marked prolongation of relaxation following CPA, the relaxation of failing heart tissue is reported to be prolonged in some cases (Gwathmey *et al.*, 1990) but not in others (Mulieri *et al.*, 1992). However, the recent finding that the expression of the Na^+-Ca^{2+} exchanger is increased in myopathic tissue of at least some patients (Reinecke *et al.*, 1992) might explain the discrepancy: an increased Na^+-Ca^{2+} exchange activity would be expected to improve relaxation and therefore compensate, at least in part, for the down-regulation of the SR Ca^{2+}-ATPase. A further implication of these studies is that agents which could directly stimulate the remaining Ca^{2+}-ATPase of failing cardiac tissue would be expected to normalize the force-frequency relation, and improve cardiac pump function.

In summary, these results suggest that a functional SR Ca^{2+}-ATPase is necessary for the normal contraction-relaxation cycle. Additionally, the results suggest an increasing dependence of tension development on SR Ca^{2+}-ATPase at increasing frequency, which may reflect either a frequency-dependent activation of this enzyme or the diminished contribution of the Na^+-Ca^{2+} exchanger. These results also provide novel support for the mechanism of the depressed force-frequency relation found in cardiac tissue of heart failure patients, in which there is a reduced expression of Ca^{2+}-ATPase.

The authors gratefully acknowledge the assitance of Dr W. Kremers of the Statistical department, Ciba-Geigy.

References

ACETO, J.F., CONDRESCU, M., KROUPIS, C., NELSON, H., NELSON, N., NICOLL, D., PHILIPSON, K.D., REEVES, J.P. (1992). Cloning and expression of the bovine cardiac sodium-calcium exchanger. *Arch. Biochem. Biophys.*, **298**, 553–560.

ARAI, M., ALPERT, N.R., MACLENNAN, D.H., BARTON, P. & PERIASAMY, M. (1993). Alterations in sarcoplasmic reticulum gene expression in human heart failure: a possible mechanism for alterations in systolic and diastolic properties of the failing myocardium. *Circ. Res.*, **72**, 463–469.

BEUCKELMANN, D.J., NÄBAUER, M. & ERDMANN, E. (1992). Intracellular calcium handling in isolated ventricular myocytes from patients with terminal heart failure. *Circulation*, **85**, 1046–1055.

BOURREAU, J.P., ABELA, A.P., KWAN, C.Y. & DANIEL, E.E. (1991). Acetylcholine Ca^{2+} stores refilling directly involves a dihydropyridine-sensitive channel in dog trachea. *Am. J. Physiol.*, **261**, C497–C505.

BRANDL, C.J., GREEN, N.M., KORCZAK, B., MACLENNAN, D.H. (1986). Two Ca^{2+} -ATPase genes: Homologies and mechanistic implications of deduced amino acid sequences. *Cell*, **44**, 597–607.

BUCKLEY, N.M., PENEFSKY, Z.J. & LITWAK, R.S. (1972). Comparative force-frequency relationships in human and other mammalian ventricular myocardium. *Pflügers Arch.*, **332**, 259–270.

CARAFOLI, E. (1987). Intracellular Ca^{2+} homeostasis. *Annu. Rev. Biochem.*, **56**, 395–433.

CHAMBERLAIN, B.K., LEVITSKY, D.O. & FLEISCHER, S. (1983). Isolation and characterisation of canine cardiac sarcoplasmic reticulum with improved Ca^{2+} transport properties. *J. Biol. Chem.*, **258**, 6602–6609.

CHIESI, M. & INESI, G. (1979). The use of quench reagents for resolution of single transport cycles in sarcoplasmic reticulum. *J. Biol. Chem.*, **254**, 10370–10377.

DENG, H.W. & KWAN, C.Y. (1991). Cyclopiazonic acid is a sarcoplasmic reticulum $Ca^{(2+)}$-pump inhibitor of rat aortic muscle. *Chung. Kuo, Yao. Li. Hsueh. Pao.*, **12**, 53–58.

FELDMAN, M.D., GWATHMEY, J.K., PHILLIPS, P., SCHOEN, F. & MORGAN, J.P. (1988). Reversal of the force-frequency relationship in working myocardium from patients with end-stage heart failure. *J. Appl. Cardiol.*, **3**, 273–283.

GOEGER, D.E. & RILEY, R.T. (1989). Interaction of cyclopiazonic acid with rat skeletal muscle sarcoplasmic reticulum vesicles. Effect on Ca^{2+} binding and Ca^{2+} permeability. *Biochem. Pharmacol.*, **38**, 3995–4003.

GWATHMEY, J.K., COPELAS, L., MACKINNON, R., SCHOEN, F.J., FELDMAN, M.D., GROSSMAN, W. & MORGAN, J.P. (1987). Abnormal intracellular calcium handling in myocardium from patients end-stage heart failure. *Circ. Res.*, **61**, 70–76.

GWATHMEY, J.K., SLAWSKY, M.T., HAJJAR, R.J., BRIGGS, M. & MORGAN, J.P. (1990). Role of intra cellular calcium handling in force-interval relationships of human ventricular myocardium. *J. Clin. Invest.*, **85**, 1599–1613.

HASENFUSS, G., MULIERI, L.A., LEAVITT, B.J., ALLEN, P.D., HABERLE, J.R. & ALPERT, N.R. (1992). Alteration of contractile function and excitation-contraction coupling in dilated cardiomyopathy. *Circ. Res.*, **70**, 1225–1232.

HILGEMANN, D.W. & NOBLE, D. (1987). Excitation-contraction coupling and extracellular calcium transients in rabbit atrium: reconstruction of basic cellular mechanisms. *Proc. R. Soc. B.*, **230**, 163–205.

JONES, L.R. (1988). Rapid preparation of canine cardiac sarcolemmal vesicles by sucrose flotation. *Methods Enzymol.*, **157**, 85–91.

LEWARTOWSKI, B. & PYTKOWSKI, B. (1987). Cellular mechanisms of the relationship between myocardial force and frequency of contractions. *Prog. Biophys. Mol. Biol.*, **50**, 97–120.

LOWRY, O.H., ROSEBROUGH, N.J., FARR, A.L. & RANDALL, R.J. (1951). Protein measurements with the folin phenol reagent. *J. Biol. Chem.*, **193**, 265–275.

MERCADIER, J.-J., LOMPRÉ, A.-M., DUC, P., BOHELER, K.R., FRAYSSE, J.-B., WISNEWSKY, C., ALLEN, P.D., KOMAJDA, M. & SCHWARTZ, K. (1990). Altered sarcoplasmic reticulum Ca^{2+}-ATPase gene expression in the human ventricle during end-stage heart failure. *J. Clin. Invest.*, **85**, 305–309.

MORGAN, P.J., ERNY, E.R., ALLEN, D.P., GROSSMAN, W. & GWATHMEY, J.K. (1990). Abnormal intracellular calcium handling, a major cause of systolic and diastolic dysfunction in ventricular myocardium from patients with heart failure. *Circulation*, **81**, III-21-III-32.

MULIERI, L.A., HASENFUSS, G., LEAVITT, B., ALLEN, P.D. & ALPERT, N.R. (1992). Altered myocardial force-frequency relation in human heart failure. *Circulation*, **85**, 1743–1750.

NICOLL, D.A., LONGONI, S. & PHILIPSON, K.D. (1990). Molecular cloning and functional expression of the cardiac sarcolemmal Na-Ca exchanger. *Science*, **250**, 562–565.

NUSS, B.H. & HOUSER, S.R. (1992). Na^+-Ca^{2+} exchange-mediated contractions in feline ventricular myocytes. *Am. J. Physiol.*, **263**, H1161–H1169.

PENEFSKY, Z.J., BUCKLEY, N.M. & LITWAK, R.S. (1972). Effect of temperature and calcium on force-frequency relationships in mammalian ventricular myocardium. *Pflügers Arch.*, **332**, 271–282.

PHILIPSON, K.D. (1990). The cardiac Na^+-Ca^{2+} exchanger. In *Calcium and the Heart*. Langer, G.A. pp. 85–108. New York: Raven Press.

REINECKE, H., STUDER, R., PHILIPSON, K.D., BILGER, J., ESCHENHAGEN, T., BÖHM, M., JUST, H.J., HOLTZ, J. & DREXLER, H. (1992). Myocardial gene expression of Na^+/Ca^{2+} exchanger and sarcoplasmic reticulum Ca^{2+}-ATPase in human heart failure. *Circulation*, **86**, I-860.

REITER, M. (1966). Der Einfluss der Natriumionen auf die Bezeihung zwischen Frequenz und Kraft der Kontraktion des isolierten Meerschweinchenmyocards. *Naunyn Schmied. Arch. Pharmacol. Exp. Path.*, **254**, 261–286.

SEIDLER, N.W., JONA, I., VEGH, M. & MARTONOSI, A. (1989). Cyclopiazonic acid is a specific inhibitor of the Ca^{2+}-ATPase of sarcoplasmic reticulum. *J. Biol. Chem.*, **264**, 17816–17823.

SEILER, S. & FLEISCHER, S. (1988). Isolation and characterisation of sarcolemmal vesicles from rabbit fast skeletal muscle. *Methods in Enzymol.*, **157**, 26–36.

SUZUKI, M., MURAKI, K., IMAIZUMI, Y. & WATANABE, M. (1992). Cyclopiazonic acid, an inhibitor of the sarcoplasmic reticulum $Ca^{(2+)}$-pump, reduces $Ca^{(2+)}$-dependent K^+ currents in guinea-pig smooth muscle cells. *Br. J. Pharmacol.*, **107**, 134–140.

WIER, W.G. & YUE, D.T. (1986). Intracellular calcium transients underlying the short-term force-interval relationship in ferret ventricular myocardium. *J. Physiol.*, **376**, 507–530.

YARD, N. & BALL, H.A. (1993). Effect of cyclopiazonic acid, an inhibitor of sarcoplasmic Ca^{2+}-ATPase, on the force-frequency relation of guinea-pig isolated atria. *Br. J. Pharmacol.*, **110**, 53P.

(Received February 14, 1994
Revised May 5, 1994
Accepted July 6, 1994)

Br. J. Pharmacol. (1994), **113**, 1008–1014 © Macmillan Press Ltd, 1994

Induction of cyclo-oxygenase-2 by cytokines in human pulmonary epithelial cells: regulation by dexamethasone

[1]Jane A. Mitchell, *Maria G. Belvisi, †Pravit Akarasereenont, *Richard A. Robbins, *O.-Jung Kwon, †Jamie Croxtall, J., *Peter J. Barnes & †John R. Vane

Departments of Applied Pharmacology and *Thoracic Medicine, The National Heart and Lung Institute, Dovehouse Street, London SW3 6LD and †The William Harvey Research Institute, Saint Bartholomew's Hospital Medical College, Charterhouse Square, London EC1M 6BQ

1 Cyclo-oxygenase metabolizes arachidonic acid to prostaglandin H_2 (PGH_2) and exists in at least two isoforms. Cyclo-oxygenase-1 (COX-1) is expressed constitutively whereas COX-2 is induced by lipopolysaccharide (LPS) and some cytokines *in vitro* and at the site of inflammation *in vivo*. Epithelial cells may be an important source of prostaglandins in the airways and we have, therefore, investigated the expression of COX-1 or COX-2 isoforms in primary cultures of human airway epithelial cells or in a human pulmonary epithelial cell line (A549).

2 COX-1 or COX-2 protein was measured by western blot analysis using specific antibodies to COX-2 and selective antibodies to COX-1. The activity of COX was assessed by the conversion of either endogenous or exogenous arachidonic acid to four metabolites, PGE_2, $PGF_{2\alpha}$, thromboxane B_2 or 6-oxo $PGF_{1\alpha}$ measured by radioimmunoassay. Thus, COX-1 or COX-2 activity was measured under two conditions; initially the accumulation of the COX metabolites formed from endogenous arachidonic acid was measured after 24 h. In other experiments designed to measure COX activity directly, cells were treated with cytokines for 12 h before fresh culture medium was added containing exogenous arachidonic acid (30 μM) for 15 min after which COX metabolites were measured.

3 Untreated primary cells or A549 cells contained low amounts of COX-1 or COX-2 protein. Bacterial LPS (1 $\mu g\ ml^{-1}$ for 24 h) induced COX-2 protein in the primary cells, a process which was enhanced by interferon-γ, with no further increase in the presence of a mixture of cytokines (interleukin-1β, tumour necrosis factor-α and interferon-γ, 10 $ng\ ml^{-1}$ for all). In contrast, A549 cells contained only low levels of COX-2 protein after exposure to LPS or LPS plus interferon-γ, but contained large amounts of COX-2 protein after exposure to the mixture of cytokines.

4 Untreated human pulmonary primary cells or A549 cells released low levels of all COX metabolites measured over a 24 h incubation period. This release was enhanced by treatment of either cell type with the mixture of cytokines (interleukin-1β, tumour necrosis factor-α and interferon-γ, 10 $ng\ ml^{-1}$ for all). PGE_2 was the principal COX metabolite released by cytokine-activated epithelial cells. The release of PGE_2 induced by cytokines occurred after a lag period of more than 6 h.

5 The glucocorticosteroid, dexamethasone (1 μM; 30 min prior to cytokines) completely suppressed the cytokine-induced expression of COX-2 protein and activity in both primary cells and A549 cells.

6 In experiments where COX-2 activity was supported by endogenous stores of arachidonic acid, treatment of A549 cells with interleukin-1β but not tumour necrosis factor-α or interferon-γ alone caused a similar release of PGE_2 to that seen when the cytokines were given in combination. However, both interleukin-1β and necrosis factor-α alone produced similar increases in COX-2 activity (measured in the presence of exogenous arachidonic acid) as seen when the mixture of interleukin-1β, tumour necrosis factor-α and interferon-γ were used to stimulate the cells.

7 These findings show that COX-2 expression correlates with the exaggerated release of prostaglandins from cytokine-activated human pulmonary epithelial cells and that the induction of the enzyme is suppressed by a glucocorticosteroid. These findings may be relevant to inflammatory diseases of the lung, such as asthma.

Keywords: Prostaglandins; inflammation; cytokines; endotoxin; nitric oxide; asthma; steroid; cyclo-oxygenase; cytokines; pulmonary epithelium

Introduction

Cyclo-oxygenase (COX) converts arachidonic acid to prostaglandin H_2 (PGH_2) (Hamberg *et al.*, 1974) which is then further metabolised to various prostaglandins, prostacyclin and thromboxane A_2. COX exists in at least two isoforms (Xie *et al.*, 1991). COX-1 is expressed constitutively in endothelial cells (Mitchell *et al.*, 1993a) and is probably responsible for the production of prostaglandins under physiological conditions (Vane, 1994). COX-2 is induced by pro-inflammatory stimuli, including mitogens (O'Banion *et al.*, 1992), cytokines (Maier *et al.*, 1990) and bacterial lipopolysaccharide (LPS; Lee *et al.*, 1992; Mitchell *et al.*, 1993a) in cells *in vitro* and in inflamed sites *in vivo* (Vane *et al.*, 1994). COX-1 shares approximately 60% homology with COX-2 (Xie *et al.*, 1991; Hla & Neilson, 1992). COX-1 and COX-2 are inhibited by nonsteroid anti-inflammatory drugs such as aspirin and indomethacin, with some selectivity towards COX-1 (Meade *et al.*, 1993; Mitchell *et al.*, 1993a).

The role of the lung in prostaglandin metabolism has been extensively studied. Indeed, COX preparations from the lung were used to demonstrate the mechanism of action of non-steroid anti-inflammatory drugs (Vane, 1971). Perfused lungs from different species release large amounts of prostaglandins

[1] Author for correspondence at Department of Applied Pharmacology.

from both the vasculature and airways in response to agonists, such as bradykinin, angiotensin and endothelins (Piper & Vane, 1969; Dawson *et al.*, 1976; Bakhle *et al.*, 1985; de Nucci *et al.*, 1988). Pulmonary epithelial cells are at the interface between the environment and the delicate structures of the lung. The airway epithelium acts as a physical barrier but is increasingly recognised as a source of lipid and peptide mediators that may modulate pulmonary inflammation. Indeed epithelial cells from the airways produce PGE_2 and $PGF_{2\alpha}$ in response to bradykinin and the calcium ionophore, A23187 (Churchill *et al.*, 1989).

The regulation of the different isoforms of COX in pulmonary tissue is not known, although human pulmonary macrophages express COX-2 after stimulation with LPS (Hempel *et al.*, 1994). This may be of particular importance in the understanding of pulmonary inflammatory conditions such as asthma. Cytokines influence pulmonary epithelial cell function via an action on specific receptors (see Barnes, 1994) and airway epithelial cells express a number of inflammatory cytokines (Devalia & Davies, 1993; see Barnes, 1994), some of which are known to cause the induction of COX-2 in other cell types (Thiemerman *et al.*, 1993). We have, therefore, used human pulmonary epithelial cells exposed to different pro-inflammatory cytokines to study changes in COX isoforms. We have used a mixture of cytokines previously demonstrated to induce nitric oxide synthase in airway cells (Robbins *et al.*, 1994). In addition we have assessed the effects of the anti-inflammatory steroid, dexamethasone on changes in both the release of COX metabolites and the expression of COX-2 protein. Some of these results have been published in abstract form (Mitchell *et al.*, 1994).

Methods

Tissue culture

Isolation of human airway epithelial cells Trachea or main bronchi were obtained from either heart or heart and lung transplantation donors. These tissues were immersed in cold Hank's balanced salt solution (HBSS) and immediately transported on ice. The cartilaginous parts of trachea or main bronchi were excised, trimmed, washed and incubated overnight at 4°C in 0.1% protease (type 14) prepared in calcium/magnesium free HBSS.

Tracheal-bronchial epithelial cells were isolated by flushing the luminal side with HBSS containing 10% heat inactivated foetal calf serum (FCS). The cells were centrifuged at 270 *g* for 10 min, resuspended in HBSS containing 10% FCS, filtered through sterile 100 μm mesh, and centrifuged again the resulting pellet was resuspended in serum-free, hormone supplemented Ham's F12 medium (complete F12) containing penicillin (100 u ml^{-1}) streptomycin (100 μg ml^{-1}), amphotericin B (2 μg ml^{-1}), L-glutamine (2 mM), insulin (5 μg ml^{-1}), transferrin (5 μg ml^{-1}), epidermal growth factor (25 ng ml^{-1}), endothelial cell growth supplement (15 μg ml^{-1}), hydrocortisone (1 μM), cholera toxin (10 ng ml^{-1}) and retinoic acid (0.1 μM). The cell suspension was again centrifuged and resuspended in complete F12 medium. Cell counts were performed with a Neuubauer haemocytometer; cell viability was assessed by trypan blue dye exclusion and was greater than 95%.

Primary culture of human tracheo-bronchial airway epithelial (HTBE) cells Dissociated HTBE cells were cultured as previously described (Churchill *et al.*, 1989; Kwon *et al.*, 1994a). Cells were plated at a density of $1-3 \times 10^4$ cm^{-2} onto the culture plates (6-well) coated with collagen gel (Vitrogen 100). The culture medium was changed after 24 h and every 2–3 days thereafter. Cultured epithelial cells were nearly confluent after 10 days of culture and showed the typical cobblestone appearance of bronchial epithelial cells (Churchill *et al.*, 1989). When the cells were nearly confluent fresh F12 medium (Ham's F12) containing only L-glutamine and antibiotic was added together with test compounds.

Culture of A549 cells The human pulmonary epithelial cancer cell line (A549), derived from lung alveolar carcinoma and representative of epithelial cells, was purchased from American Type Culture Collection (Rockville, MD). A549 cells spontaneously produce PGE_2 which acts as an autocrine growth regulator (Croxtall & Flower, 1992). Furthermore, this release is enhanced by exposure to growth factors (Croxtall *et al.*, 1993). Glucocorticoid treatment results in a complete suppression of PGE_2 release (Croxtall & Flower, 1992). In previous studies comparing A549 with primary HTBE cells, both cell types were shown to be epithelial in origin (Kwon *et al.*, 1994b). The A549 cell line, therefore, is a convenient model for the investigation of COX expression. A549 cells were grown on 35 mm 6-well culture plates in Dulbecco's modified Eagle's medium (DMEM) containing 10% FCS, L-glutamine (2 mM), penicillin (100 u ml^{-1}) and streptomycin (100 μg ml^{-1}). When the A549 cells were confluent, they were washed and incubated in DMEM without FCS together with test compounds.

Measurement of COX activity

COX metabolites were measured by radioimmunoassay (Salmon, 1978) for 6-oxo $PGF_{1\alpha}$, PGE_2, $PGF_{2\alpha}$ and thromboxane B_2. Antibodies to PGE_2, $PGF_{2\alpha}$ and thromboxane B_2 had less than 5% cross reactivity with all other prostaglandins measured. Antibody to 6-oxo-$PGF_{1\alpha}$ had less than 5% cross reactivity to prostaglandin $F_{2\alpha}$ and thromboxane B_2 and 17% cross reactivity to PGE_2. For experiments designed to measure the release of COX metabolites from endogenous arachidonic acid, cells were treated with either LPS (1 μg ml^{-1}), tumour necrosis factor-α (TNFα; 10 ng ml^{-1}), interleukin 1β (IL-1β; 10 ng ml^{-1}), interferon-γ (IFNγ; 10 ng ml^{-1}) or LPS together with IFNγ (1 μg ml^{-1} and 10 ng ml^{-1}) or a mixture of IL-1β, TNFα and IFNγ (10 ng ml^{-1} for all) for 3, 6, 12 or 24 h and the medium removed for radioimmunoassay. In separate experiments designed to measure COX 'activity', cells were treated with different cytokines for 12 h after which time fresh medium was added containing arachidonic acid (30 μM) for 15 min at 37°C and then removed for radioimmunoassay. In some experiments, dexamethasone (1 μM) was added 30 min before the addition of LPS, IL-1β, TNFα or IFNγ for 24 h and the predominant COX metabolite (PGE_2) measured.

Western blot analysis

In separate experiments HTBE cells or A549 cells were grown in 6-well plates as above. After exposure to test compounds the medium culture was removed and the cells incubated with extraction buffer (Tris, 50 mM; EDTA, 10 mM; Triton X-100, 1% v/v; phenylmethylsulphonyl fluoride, 1 mM; pepstatin A, 0.05 mM and leupeptin, 0.2 mM) with gentle shaking. The cell extract was then boiled (10 min) in a ratio of 1:1 with gel loading buffer (Tris, 50 mM; SDS, 10% w/v; glycerol, 10% v/v; 2-mercaptoethanol 10% v/v and bromphenol blue, 2 mg ml^{-1}). Samples were centrifuged at 10,000 *g* for 2 min before being loaded onto gradient gels (4–12% Tris-glycine; Novex) and subjected to electrophoresis (1.5 h at 125 V). The separated proteins were transferred to nitrocellulose (BIORAD; 1 h at 200 V). After transfer to nitrocellulose, the blot was incubated in blocking solution (dried minimal-fat milk 25 g and Tween-20 1.25 ml in PBS solutions 500 ml) for 1 h and then primed with rabbit antibody raised to murine COX-2 (Cayman Chemical Company, MI, U.S.A.) for 1 h. There was no detectable cross reactivity of the COX-2 antibody with COX-1 (Mitchell *et al.*, 1993a). In some experiments blots were primed with rabbit antibody raised to ovine COX-1 (a generous gift from

K. Wu, Houston, TX, U.S.A.) for 1 h. The COX-1 antibody has approximately 10% cross reactivity with COX-2 (Mitchell *et al.*, 1993a). The blot was then incubated with an anti-rabbit IgG developed in sheep, linked to alkaline phosphatase conjugate for 1 h. Finally, the blot was developed for approximately 5 min with premixed solution containing 5-bromo-4-chloro-3-indeolyl phosphate (0.56 mM), nitroblue tetrazolium, (0.48 mM), Tris (10 mM) and $MgCl_2$ (59.3 mM) at pH 9.2. The detection limit of protein in cell extract was 1–10 ng. The band, which was visualised at approximately 70 kDa was quantified using a laser densitometer with Quantity-One software (PDI, New York, NY, U.S.A.). Individual band density values for each point were expressed in arbitrary OD units.

Statistical analysis

Results are shown as mean ± s.e.mean from n determinations (wells) from at least three separate plates. Unpaired two tailed tests or one way analysis of variance were used as appropriate to determine the significant differences between means and P values of less than 0.05 were taken as statistically significant.

Materials

Recombinant human TNFα was purchased from British Biotechnology (Oxford, UK), Vitrogen 100 from Collagen Co, Ham's F12 medium, DMEM, pre-mixed penicillin-streptomycin and L-glutamine from ICN Flow (High Wycome, UK); FCS from Sera Lab (Crawley Down, UK). All other materials were purchased from Sigma Chemical Company (Poole, Dorset, UK), unless otherwise stated.

Results

Characterization of the isoforms of COX present in human pulmonary epithelial cells

Untreated HTBE or A549 cells contained low or undetectable levels of COX-1 ($n = 3-6$; data not shown) or COX-2 (Figure 1 and 2 respectively). However, after exposure of either cell type to a mixture of cytokines, IL-1β, TNFα plus IFNγ (all at 10 ng ml^{-1}) for 24 h there was an induction of COX-2 protein (Figure 1 and Figure 2; $n = 3-6$). The levels of COX-2 protein induced in A549 cells was greater than that induced in the HTBE cells. Treatment of either cell type with LPS (1 μg ml^{-1}) alone did not induce the expression of COX-2 protein. However, HTBE cells, but not A549 cells, contained detectable levels of COX-2 protein after treatment with LPS together with IFNγ (Figure 1). Pretreatment of A549 cells with dexamethasone (1 μM; 30 min prior to the cytokine mix) almost abolished the induction of COX-2 (Figure 3).

Release of COX metabolites by HTBE or A549 cells from endogenous stores of arachidonic acid

Untreated HTBE or A549 cells released low levels of all COX metabolites measured (6-oxo $PGF_{1\alpha}$, PGE_2, thromboxane B_2 or $PGF_{2\alpha}$ <0.1 ng ml^{-1} for A549 or primary cells, $n = 15$; Figure 4). Incubation of A549 cells or HTBE cells with either LPS (1 μg ml^{-1}) alone or together with IFNγ (10 ng ml^{-1}) did not cause detectable release of COX metabolites (data not shown; $n = 3$). However, incubation of either cell type for 24 h with a mixture of IL-1β, TNFα and IFNγ (10 ng ml^{-1} for all) caused the accumulation of PGE_2 (10.09 ± 0.63 ng ml^{-1} for A549 cells and 0.23 ± 0.04 ng ml^{-1} for HTBE cells, $n = 6-15$) $PGF_{2\alpha}$ (4.03 ± 0.16 ng ml^{-1} for A549 cells and undetectable levels for HTBE cells), 6-oxo $PGF_{1\alpha}$ (3.07 ± 0.12 ng ml^{-1} for A549 cells and undetectable HTBE cells). Thromboxane B_2 was not formed in detectable amounts by either cell type (Figure 4). The treatment of A549 cells with a combination of IL-1β, TFNα and IFNγ (10 ng ml^{-1} for all) for 3, 6, and 24 h resulted in a time-dependent release of PGE_2, which was first significant at 6 h after the addition of the cytokines (Figure 5; $n = 3-15$).

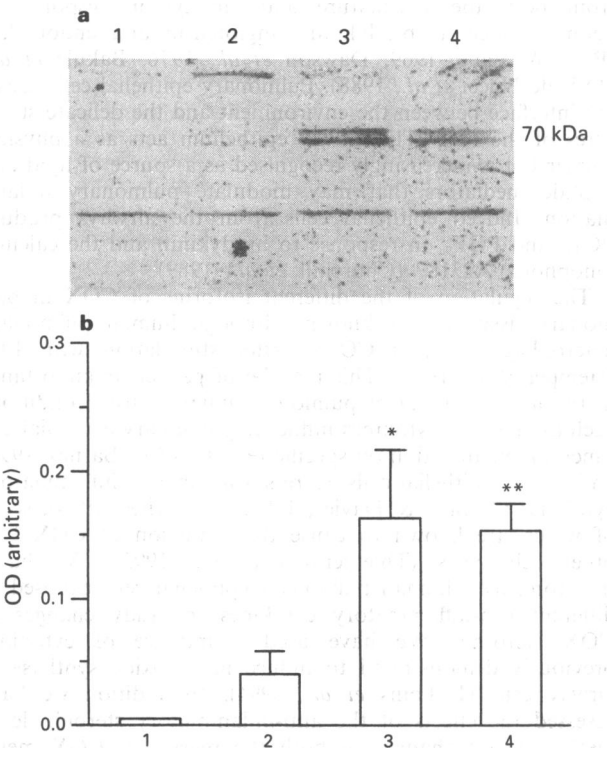


Figure 1 The expression of COX-2 protein in HTBE cells after treatment with cytokines for 24 h. (A) Shows a Western blot using a specific antibody to COX-2 which recognised a doublet of approximately 70 kDa. Each lane was loaded with 1 μg of protein. Lane 1 shows extracts from untreated cells, lane 2 cells treated with LPS (1 μg ml^{-1}) lane 3 treated with LPS and IFN-γ (10 ng ml^{-1}), lane 4 treated with a mixture of cytokines (IL-1β, TNFα, IFNγ all at 10 ng ml^{-1}; lane 4); (b) shows the means ± s.e.mean of the optical density (OD) of COX-2 bands from 3 separate experiments. P values are calculated between treated and untreated groups by unpaired two-tailed t test (*$P<0.05$; **$P<0.01$). In separate experiments, no COX-1 was detected in cell extracts from any of the above treatments ($n = 3$; data not shown). For abbreviations, see text.

Characterization of the regulation by cytokines of the release of COX metabolites from endogenous arachidonic acid

A549 cells treated with a mixture of cytokines released larger amounts of COX metabolites and expressed greater amounts of COX-2 protein than HTBE cells, A549 cells were used, therefore, to characterize further the regulation of COX-2 in human pulmonary epithelial cells by specific cytokines. A549 cells treated with IL-1β (10 ng ml^{-1}) for 24 h showed a more than 30 fold increase in the release of the major COX metabolite, PGE_2 (from 0.27 ± 0.05 ng ml^{-1} to 10.84 ± 0.43 ng ml^{-1}; $n = 3$; Figure 6). However, TNFα (10 ng ml^{-1}) or IFNγ (10 ng ml^{-1}) had no significant effect on the release of PGE_2 by A549 cells ($n = 3$). The release of PGE_2 in response to IL-1β or the cytokine mixture was significantly reduced by pretreatment of the cells with dexamethasone (to 0.3 ± 0.03 ng ml^{-1} or 0.15 ± 0.01 ng ml^{-1} respectively; $n = 3-6$; Figure 6).

In A549 cells COX activity (measured in the presence of exogenous arachidonic acid; 30 μM; 15 min) was elevated at

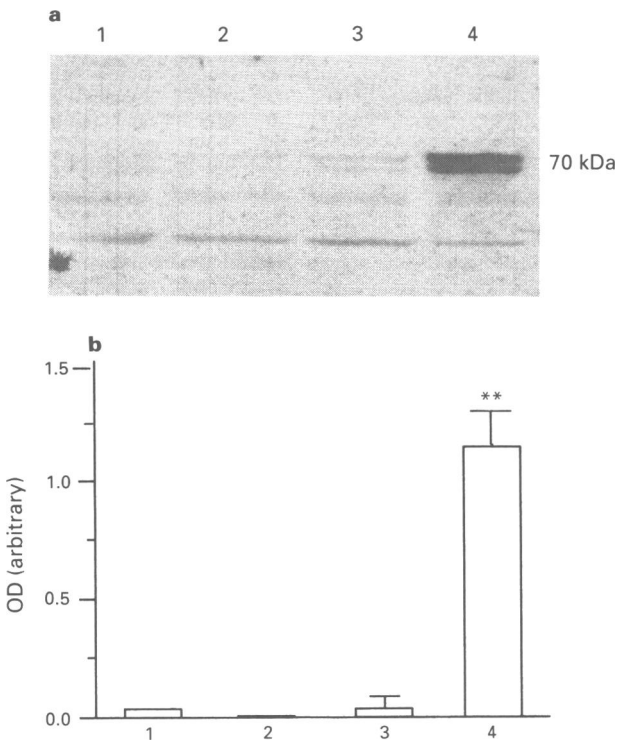


Figure 2 The expression of COX-2 protein in A549 cells after treatment with cytokines for 24 h. (A) Shows a Western blot using a specific antibody to COX-2 which recognised a doublet of approximately 70 kDa. Each lane was loaded with 1 μg of protein. Lane 1 shows extracts from untreated cells, lane 2 cells treated with LPS (1 μg ml^{-1}), lane 3 treated with LPS and IFN-γ (10 ng ml^{-1}), lane 4 treated with a mixture of cytokines (IL-1β, TNFα, IFNγ all at 10 ng ml^{-1}; lane 4); (b) shows the means ± s.e.mean of the optical density (OD) of COX-2 bands from 3 separate experiments. *P* values are calculated between treated and untreated groups using unpaired two-tailed *t* test (**$P<0.01$). In separate experiments no COX-1 was detected in cell extracts from any of the above treatments ($n=3$; data not shown). For abbreviations, see text.

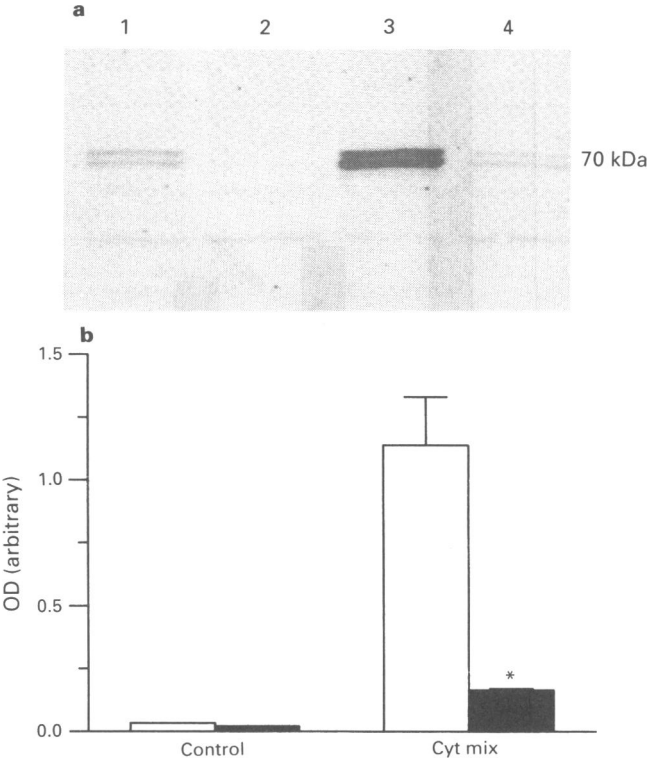


Figure 3 The effect of dexamethasone on the induction of COX-2 in A549 cells. (a) Shows a typical Western blot using a primary antibody to COX-2. Each lane was loaded with 1 μg of protein. Lane 1 contains extract from untreated cell, lane 2 from cells treated with dexamethasone (1 μM; for 24 h), lane 3 cells treated with cytokine mixture (Cyt mix; IL-1β, TNFα and IFNγ all at 10 ng ml^{-1} for all, for 24 h) and lane 4 cells treated with dexamethasone 30 min prior to treatment with the cytokine mixture; (b) shows the means ± s.e.mean of the OD of COX-2 bands from 3 separate determinations, where the open columns represent cells treated with saline and the solid columns cells treated with dexamethasone. *P* values are calculated between dexamethasone and vehicle-treated cells (**$P<0.01$ by unpaired two-tailed *t* test). For abbreviations, see text.

12 h after the addition of either a combination of IL1-β, TNFα and IFN-γ, or IL1-β alone ($n=3$; Figure 7). In contrast to the lack of effect of TNFα on the release of PGE_2 from endogenous stores of arachidonic acid, TNFα caused a significant induction of COX-2 activity as measured in the presence of exogenous arachidonic acid (Figure 7).

Discussion

Pro-inflammatory cytokines, such as TNFα or IL-1β regulate the release of several inflammatory mediators by inducing the expression of synthesizing enzymes. Thus, a mixture of IL-1β, TNFα and IFNγ induces pulmonary epithelial cells to express nitric oxide synthase (Robbins *et al.*, 1994) and LPS causes the co-induction of nitric oxide synthase and COX-2 in murine macrophages (Mitchell *et al.*, 1993b). We have extended these studies and demonstrated that pro-inflammatory cytokines stimulate human pulmonary epithelial cells to release COX metabolites, to express increased COX activity and to express COX-2 protein. No detectable COX-1 was present in either untreated or stimulated cells. In previous studies, a low release of PGE_2 was detected in unstimulated cells (Croxtall & Flower, 1992). However, these authors used a lower ratio of culture medium to cells leading to a greater concentration of metabolites. We found that cytokine-activated HTBE released lower levels of COX metabolites and contained less COX-2 protein than the human pulmonary cell line, A549. In addition, HTBE cells but not A549 cells expressed COX-2 protein after exposure to LPS and IFNγ. In primary cell cultures it was necessary to include the steroid hydrocortisone, which discourages the growth of contaminating fibroblasts. Dexamethasone abolishes the induction of COX-2 and the necessary inclusion of hydrocortisone may, therefore, explain the relative low level of induction in primary cells. In addition, the growth of HTBE cells, but not A549 cells, is suppressed by serum (Barnes & Robbins, unpublished observations). For this reason HTBE cells were serum-deprived at the time of the addition of cytokines. A lack of serum greatly reduces the ability of pulmonary epithelial cells to release prostaglandins (Churchill *et al.*, 1989) so this could be an additional reason for the differences seen between HTBE cells and A549 cells. However, our studies clearly demonstrate that human airway epithelium expresses COX-2 in response to pro-inflammatory cytokines. Others have demonstrated that extracts of human lung contain messenger RNA for COX-2, although the cellular origin was not identified (Neil & Ford-Hutchinson, 1993).

Human pulmonary epithelial cells released predominantly PGE_2 when induced to express COX-2. This finding is in agreement with previous studies, showing that PGE_2 is a major metabolite released from human epithelial cells stimulated with bradykinin or calcium ionophore (Churchill *et al.*, 1989). The induction of COX-2 in other cell types, such as endothelial cells, macrophages (Mitchell *et al.*, 1993a,b; Akarasereenont *et al.*, 1994) and fibroblasts (Kujubu *et al.*,

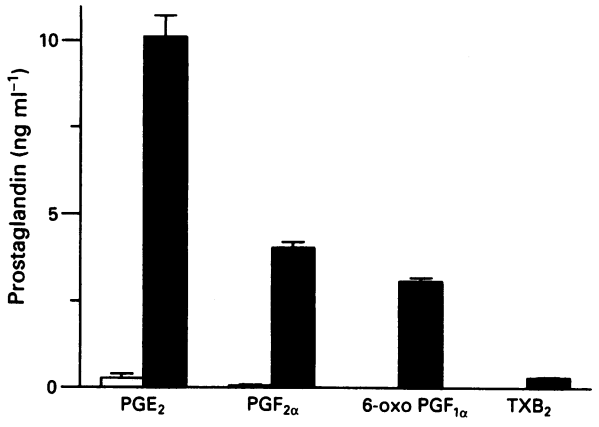


Figure 4 Release of different COX metabolites by HTBE (open columns) or A459 cells (solid columns) after treatment with a mixture of cytokines (IL-1β, TNFα, IFNγ all at 10 ng ml^{-1} for 24 h). Untreated cells released undetectable amounts of COX metabolites. The data represent the mean ± s.e.mean for 3–9 determinations. For abbreviations, see text.

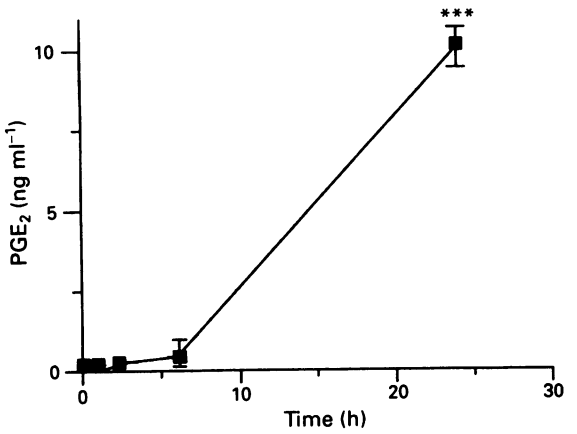


Figure 5 Time-dependent release of PGE_2 from A549 cells after the addition of a mixture of cytokines (IL-1β, TNFα, IFNγ all at 10 ng ml^{-1}). Culture medium was removed at 1, 3, 6 and 24 h after the addition of cytokines (■). No PGE_2 was detected in culture medium removed from cells 24 h after the addition of vehicle. The data represent the mean ± s.e.mean for 3–9 determinations. A significant increase (***$P<0.001$) in the amount of PGE_2 released by cells treated with cytokines compared to cells treated with vehicle (for 24 h) was calculated by one way analysis of variance. For abbreviations, see text.

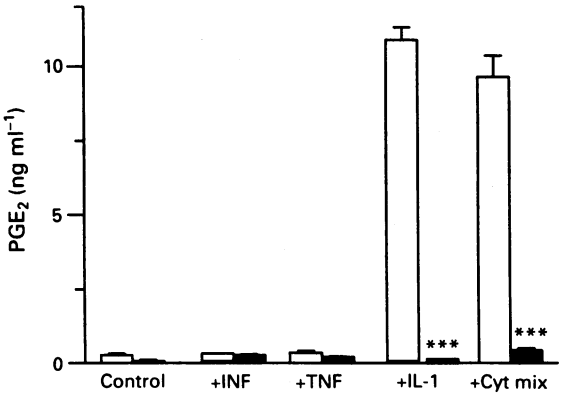


Figure 6 The figure shows the release of PGE_2 by A549 cells treated with either vehicle (Control), IL-1β, TNFα, IFNγ or a mixture of cytokines (Cytmix, IL-1β, TNFα, IFNγ all at 10 ng ml^{-1}) for 24 h (open columns). The solid columns shows the release of PGE_2 by A549 cells treated with dexamethasone (1 μM) 30 min prior to the addition of cytokines. The data represent the mean ± s.e.mean for 3–9 determinations. Significant differences in the release of PGE_2 by cells treated with dexamethasone or vehicle were calculated by an unpaired two-tailed t test (***$P<0.001$). For abbreviations, see text.

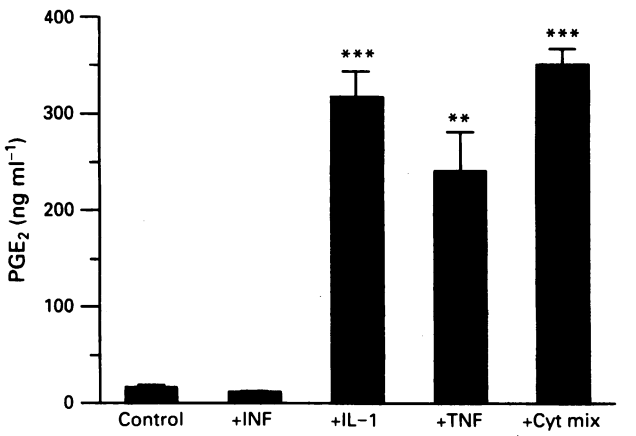


Figure 7 Induction of COX activity (measured in the presence of exogenous arachidonic acid; 30 μM) in A549 cells by different cytokines. Cells were treated with either vehicle (Control) IFNγ, IL-1β, TNFα or a mixture of IFNγ, IL-1β and TNFα (Cytmix, 10 ng ml^{-1} for all) for 12 h. The culture medium was then replaced with fresh medium containing arachidonic acid (30 μM) and incubated for 15 min. The formation of PGE_2 by the cells was then measured as an index of COX-2 activity. The data represent the mean ± s.e.mean for 3 determinations. Significant differences in the release of PGE_2 by cells treated with cytokines or vehicle were calculated by an unpaired two-tailed t test (***$P<0.001$). For abbreviations, see text.

1991) by pro-inflammatory cytokines *in vitro* and in inflamed sites *in vivo* (Vane *et al.*, 1994) supports the hypothesis (Vane, 1994) that it is this isoform of COX which is responsible for the production of prostaglandins under inflammatory conditions. The potential therapeutic benefits of inhibiting COX activity in the airways is complicated by the possibility that there is a resultant shunt of arachidonic acid to the lipoxygenase pathway (Israel *et al.*, 1993), which may be exaggerated in inflammatory conditions where phospholipase A_2 is induced (Glaser *et al.*, 1993).

There may be both deleterious and/or beneficial consequences of COX-2 induction in pulmonary epithelial cells. For instance PGE_2 increases capsaicin-induced cough in human subjects (Choudry *et al.*, 1989). However, PGE_2 dilates airway smooth muscle, inhibits the release of acetylcholine from canine bronchi (Deckers *et al.*, 1989) and inhibits mucus secretion (Marom *et al.*, 1981). PGE_2 also inhibits the release of pro-inflammatory cytokines, such as IL-1β (Monick *et al.*, 1987) and inhibits collagen synthesis by fibroblasts (Rennard *et al.*, 1986). It is, therefore, tempting to speculate that the expression of COX-2 and the subsequent release of PGE_2 may represent a natural defence mechanism of the airways to inflammation and the consequential hyperreactivity which occurs. In addition, the lipoxygenase pathway does not appear to be induced by pro-inflammatory cytokines (Masferrer *et al.*, 1990). Thus the induction of COX-2 in airway epithelial cells may result in a shunt of arachidonic acid away from the potent constrictor leukotrienes towards the production of dilator prostaglandins. However, the pro-inflammatory effects of prostaglandins released due to the induction of COX-2 in other airway cells may ultimately outweigh any beneficial effects in epithelial cells.

Both IL-1β and TNFα induced COX-2 activity, measured in the presence of excess exogenous arachidonic acid but

IFNγ alone had no effect. Interestingly, in the absence of exogenous arachidonic acid, IL-1β, but not TNFα, caused the release of COX-2 metabolites. This finding suggests that the induction of COX-2 without a concomitant induction of phospholipase A_2, results in a depletion of endogenous arachidonic acid. An interpretation of our results is that IL-1β induces both COX-2 and phospholipase A_2 whereas TNFα causes the induction of COX-2 alone. In HTBE cells, LPS plus INFγ caused a similar induction of COX-2 protein as did the cytokine mix, although detectable metabolites were released only with the latter treatment. Similarly this suggests that LPS plus INFγ induces COX-2 without sufficient induction of phospholipase A_2 whereas the cytokine mix causes the induction of both enzymes. Whether such cytokines cause the induction of COX-2 directly or via the release of other cytokines remains the subject of investigation. Interestingly cytokines such as IL-1β and TNFα are released from activated airway macrophages and may act upon the epithelium to cause the induction of COX-2 (see Barnes, 1994). Alternatively epithelial cells may generate such cytokines which then act in an autocrine manner, resulting in the induction of COX-2 (Devalia & Davies, 1993).

The therapeutic benefits of steroids in inflammatory airway disease such as asthma are well described (Barnes & Pedersen, 1993). We found that both the induction of COX-2 protein and activity were greatly reduced by dexamethasone. In addition to the dramatic suppressive effects of dexamethasone on COX-2 induction reported here, dexamethasone also limits the induction of other enyzmes which produce inflammatory mediators. Dexamethasone inhibits the induction of nitric oxide synthase in endothelial cells (Radomski *et al.*, 1990), macrophages and vascular smooth muscle (Rees *et al.*, 1990; Mitchell *et al.*, 1992). In addition dexamethasone inhibits the induction of nitric oxide synthase in human airway epithelial cells (Robbins *et al.*, 1994). Dexamethasone also inhibits the cytokine regulated induction of phospholipase A_2 (Lin *et al.*, 1992). Thus, the therapeutic benefits of dexamethasone resulting from prostaglandin suppression may be partly explained by its ability to inhibit the induction of COX-2 (this paper) and the coupled induction of phospholipase A_2 (Lin *et al.*, 1992).

Interestingly, β_2-adrenoceptor agonists, another important therapy in pulmonary inflammatory diseases, suppress the release of pro-inflammatory cytokines induced by LPS from human peripheral blood monocytes (Seldon *et al.*, 1994). Thus, glucocorticoids or β_2-agonists may inhibit the induction of enzymes such as COX-2 by modulating the release of pro-inflammatory cytokines. The continued study of the mechanisms regulating the induction of COX-2 in airway cells may provide insight into the mode of action of pro-inflammatory cytokines in diseases such as asthma and cystic fibrosis. Nonsteroid anti-inflammatory drugs such as aspirin or indomethacin are potent inhibitors of COX-1, but have less inhibitory effect on COX-2 (Mitchell *et al.*, 1993a; Meade *et al.*, 1993). These drugs have no beneficial effect in asthma suggesting that COX-1 is not important for the pathology of this disease. However, the development of selective inhibitors of COX-2 may have therapeutic potential in inflammatory pulmonary disease.

References

AKARASEREENONT, P., MITCHELL, J.A., THIEMERMANN, C. & VANE, J.R. (1994). Lipopolysaccharide induces bovine aortic endothelial cells to synthesize COX, but not nitric oxide synthase: a comparison with macrophages. *Br. J. Pharmacol.*, **111**, 33P.

BAKHLE, Y.S., MONCADA, S., DENUCCI, G. & SALMON, J.A. (1985). Differential release of eicosanoids by bradykinin, arachidonic acid and calcium ionophore A23187 in guinea-pig isolated lung. *Br. J. Pharmacol.*, **86**, 55–62.

BARNES, P.J. (1994). Airway epithelial receptors. *Eur. Resp. J.* (in press).

BARNES, P.S. & PEDERSEN, A. (1993). Ethics and Safety of inhibitor corticosteroids in asthma. *Am. Rev. Respir. Dis.*, **148**, 21–26.

CHOUDRY, N.B., FULLER, R.W. & PRIDE, N.B. (1989). Sensitivity of the human cough reflex: effect of inflammatory mediators prostaglandin E_2, bradykinin and histamine. *Am. Rev. Resp. Dis.*, **140**, 137–141.

CHURCHILL, L., CHILTON, F.H., RESAU, J.H., BASCOM, R., HUBBARD, W.C. & PROUD, D. (1989). Cyclooxygenase metabolism of endogenous arachidonic acid by cultured human tracheal epithelial cells. *Am. Rev. Respir. Dis.*, **140**, 449–459.

CROXTALL, J.D. & FLOWER, R.J. (1992). Lipocortin-1 mediates dexamethasone-induced growth arrest of the A549 lung adenocarcinoma cell line. *Proc. Natl. Acad. Sci. U.S.A.*, **89**, 3571–3575.

CROXTALL, J.D., WAHEED, S., CHOUDHURY, Q., ANAND, R. & FLOWER, R.J. (1993). N-Terminal peptide fragments of lipocortin-1 inhibit A549 cell growth and block EGF-induced stimulation of proliferation. *Int. J. Cancer*, **54**, 153–158.

DAWSON, W., BOOT, J.R., COCKERIL, A.F., MALLEN, D.N.B. & OSBORNE, D.J. (1976). Release of novel prostaglandins and thromboxanes after immunological challenge of guinea-pig lung. *Nature*, **262**, 699–702.

DECKERS, I.A., RAMPART, M., BULT, H. & HERMAN, A.G. (1989). Evidence for the involvement of prostaglandins in modulation of acetylcholine release from canine bronchial tissue. *Eur. J. Pharmacol.*, **167**, 415–418.

DE NUCCI, G., THOMAS, R., D'ORLEANS-JUSTE, P., ANTUNES, E., WALDER, C., WARNER, T.D. & VANE, J.R. (1988). Pressor effects of circulating endothelin are limited by its removal in the pulmonary circulation and by the release of prostacyclin and endothelium-derived relaxing factor. *Proc. Natl. Acad. Sci. U.S.A.*, **85**, 9797–9800.

DEVALIA, J.L. & DAVIES, R.J. (1993). Airway epithelial cells and mediators of inflammation. *Resp. Medicine*, **87**, 405–407.

GLASER, K.B., MOBILIO, D., CHANNG, J.Y. & SENKO, N. (1993). Phospholipase A_2 enzymes: regulation and inhibition. *Trends Pharmacol. Sci.*, **14**, 92–98.

HAMBERG, M., SVENSSON, J. & SAMUELSSON, B. (1974). Novel transformation of arachidonic acid in human platelets. *Proc. Natl. Acad. Sci. U.S.A.*, **71**, 3400–3404.

HEMPEL, S., MONICK, M.M. & HUNNINGHAKE, G.W. (1994). Lipopolysaccharide induces prostaglandin H synthase-2 protein and mRNA in human alveolar macrophages and blood monocytes. *J. Clin. Invest.*, **93**, 391–396.

HLA, T. & NEILSON, K. (1992). Human cyclo-oxygenase-2 cDNA. *Proc. Natl. Acad. Sci., U.S.A.*, **89**, 7384–7388.

ISRAEL, E., FISCHER, A.R., ROSENBERG, M.A., LILLY, C.M., CALLERY, J.C., SHAPIRO, J, COHN, J., RUBIN, P. & DRAZEN, J.M. (1993). The pivotal role of 5-lipoxygenase products in the reaction of aspirin-sensitive asthmatics to aspirin. *Am. Rev. Respir. Dis.*, **148**, 1447–1451.

KUJUBU, D.A., FLETCHER, B.S., VARNUM, B.C., LIM, R.W. & HERSCHMAN, H.R. (1991). TIS10, a phorbol ester tumor promoter-inducible mRNA from swiss 3T3 cells, encodes a novel prostaglandin synthase/cyclo-oxyenase homologue. *J. Biol. Chem.*, **266**, 12866–12872.

KWON, O.J., COLLINS, P.D., BARANIUK, J.N., ADCOCK, I.M. & BARNES, P.J. (1994a). Inhibition of interleukin-8 expression by dexamethasone in human cultured epithelial cells. *Immunology*, **81**, 389–394.

KWON, O.J., ROBBINS, R.A., AU, B.T., COLLINS, P.D., MAK, J.K., CHUNG, K.F. & BARNES, P.J. (1994b). Glucocorticoid inhibition of TNFα-induced interleukin-8 expression in primary cultured human airway epithelial cells. *Am. J. Physiol.*, (in press).

LEE, S.H., SOYOOLA, E., CHANMUGAM, P., HART, S., SUN, W., ZHONG, H., LIOU, S., SIMMONS, D. & HWANG, D. (1992). Selective expression of mitogen-inducible cyclo-oxygenase in macrophages stimulated with lipopolysaccharide. *J. Biol. Chem.*, **267**, 25934–25938.

LIN, L.-L., LIN, A.Y. & DE WITT, D.L. (1992). Inhibition of phospholipase A_2 expression by dexamethasone. *J. Biol. Chem.*, **267**, 23451–23454.

MAIER, J.A., HLA, T. & MACIAG, T. (1990). Cyclo-oxygenase is an immediate early gene induced by interleukin-1 in human endothelial cells. *J. Biol. Chem.*, **265**, 10805–10808.

MAROM, Z., SHELHAMER, J.H & KALINER, M. (1981). Effects of arachidonic acid, monohydroxyeicosatertraenoic acid and prostaglandins on the release of mucous glycoproteins from human airways *in vitro*. *J. Clin. Invest.*, **67**, 1695–1702.

MASFERRER, J.L., ZWEIFEL, B.S., SEIBERT, K. & NEEDLEMAN, P. (1990). Selective regulation of cellular cyclooxygenase by dexamethasone and LPS. *J. Clin. Invest.*, **86**, 1375–1379.

MEADE, E.A., SMITH, W.L. & DE WITT, D.L. (1993). Differential inhibition of prostaglandin endoperoxide synthase (cyclo-oxygenase) isozymes by aspirin and other non-steroidal anti-inflammatory drugs. *J. Biol. Chem.*, **268**, 6610–6614.

MITCHELL, J.A., AKARASEREENONT, P., THIEMERMANN, T., FLOWER, R.J. & VANE, J.R. (1993a). Selectivity of nonsteroid anti inflammatory drugs as inhibitors of constitutive and inducible cyclo-oxygenase. *Proc. Natl. Acad. Sci. U.S.A.*, **90**, 11693–11697.

MITCHELL, J.A., BELVISI, M.G., AKARASEREENONT, P., ROBBINS, R.A., KWON, O.-J., BARNES, P.J. & VANE, J.R. (1994). Induction of cyclo-oxygenase-2 in human pulmonary epithelial cells. *Br. J. Pharmacol.*, **112**, 78P.

MITCHELL, J.A., KOHLHASS, K.L., MATSUMOTO, T., POLLOCK, J.S., FORSTERMANN, U., WARNER, T.D., SCHMIDT, H.H.H.W. & MURAD, F. (1992). Induction of NADPH-dependent diaphorase and nitric oxide synthase activity in aortic smooth muscle and cultured macrophages. *Mol. Pharmacol.*, **104**, 189–219.

MITCHELL, J.A., SWIERKOSZ, T.A., WARNER, T.D., GROSS, S.S., THIEMERMANN, C. & VANE, J.R. (1993b). Regulation of prostacyclin synthesis by endogenous nitric oxide in response to bacterial lipopolysaccharide. *Br. J. Pharmacol.*, **109**, 4P.

MONICK, M., GLAZIER, J. & HUNNINGHAKE, G.W. (1987). Human alveolar macrophages suppress interleukin-1 (IL-1) activity via the secretion of prostaglandin E_2. *Am. Rev. Respir. Dis.*, **135**, 72–77.

NEIL, G.P. & FORD-HUTCHINSON, A.W. (1993). Expression of mRNA for cyclo-oxygenase-1 and cyclo-oxygenase-2 in human tissue. *FEBS*, **330**, 156–160.

O'BANION, M.K., WINN, V.D. & YOUNG, D.A. (1992). cDNA cloning and functional activity of glucocorticoid-regulated inflammatory cyclo-oxygenase. *Proc. Natl. Acad. Sci. U.S.A.*, **89**, 4888–4892.

PIPER, P.J. & VANE, J.R. (1969). The release of prostaglandins from lung and other tissues. *Ann. N.Y. Acad. Sci.*, **180**, 363–385.

RADOMSKI, M.W., PALMER, R.M.J. & MONCADA, S. (1990). Glucorticoids inhibit the expression of inducible but not constitutive nitric oxide synthase in vascular endothelial cells. *Proc. Natl. Acad. Sci. U.S.A.*, **87**, 10043–10047.

REES, D.D., CELLEK, S., PALMER, R.M.J. & MONCADA, S. (1990). Dexamethasone prevents the induction of nitric oxide synthase and the associated effects on vascular tone: An insight into endotoxic shock. *Biochem. Biophys. Res. Commun.*, **173**, 541–547.

RENNARD, S.I., MOSS, J., OBERPRILLER, J., HORN, B., STIER, L., OZAKI, T. & CRYSTAL, R.G. (1986). Fibroblasts: important producers and targets of inflammatory prostaglandins in the lungs. *Chest*, **83**, 92S–93S.

ROBBINS, R.A., SPRINGALL, D.R., WARREN, J.B., KWON, O.J., BUTTERY, L.K.D., WILSON, A.J., ADCOCK, I.M., RIVEROS-MORENO, V., MONCADA, S., POLAK, J. & BARNES, P.J. (1994). Inducible nitric oxide synthase is increased in murine lung epithelial cells by cytokine stimulation. *Biochem. Biophys. Res. Commun.*, **198**, 835–843.

SALMON, J.A. (1978). A radioimmunoassay for 6-keto-prostaglandins $F_{1\alpha}$. *Prostaglandins*, **5**, 383–397.

SELDON, P.M., BARNES, P.J. & GIEMBYCZ, M.A. (1994). Phosphodiesterase IV inhibitors and β-adrenoceptor agonists suppress lipopolysaccharide-induced tumour necrosis factor-α generation by human peripheral blood monocytes. *Br. J. Pharmacol.*, **112**, 215P.

THIEMERMANN, C., MITCHELL, J.A. & FERNS, G.A.A. (1993). Eicosanoids and atherosclerosis. *Curr. Opin. Lipidol.*, **4**, 401–406.

VANE, J.R. (1971). Inhibition of prostaglandin synthesis as a mechanism of action of aspirin-like drugs. *Nature*, **231**, 232–235.

VANE, J.R. (1994). Pharmacology: towards a better aspirin. *Nature*, **367**, 215.

VANE, J.R., MITCHELL, J.A., APPLETON, I., TOMLINSON, A., BISHHOP-BAILY, D., CROXTALL, J. & WILLOUGHBY, D. (1994). Inducible isoforms of cyclo-oxygenase and nitric oxide synthase in inflammation. *Proc. Natl. Acad. Sci. U.S.A.*, **91**, 2046–2050.

XIE, W.L., CHIPMAN, J.G., ROBERTSON, D.L., ERIKSON, R.L. & SIMMONS, D.L. (1991). Expression of a mitogen-responsive gene encoding prostaglandin synthase is regulated by mRNA splicing. *Proc. Natl. Acad. Sci. U.S.A.*, **88**, 2692–2696.

(Received May 11, 1994
Revised June 28, 1994
Accepted July 6, 1994)

Br. J. Pharmacol. (1994), **113**, 1015–1021 © Macmillan Press Ltd, 1994

Vasoconstrictor and vasodilator responses to various agonists in the rat perfused mesenteric arterial bed: selective inhibition by PPADS of contractions mediated via P_{2x}-purinoceptors

*†Ursula Windscheif, *Vera Ralevic, **Hans G. Bäumert, †Ernst Mutschler, †Günter Lambrecht & *[1]Geoffrey Burnstock

*Department of Anatomy and Developmental Biology and Centre for Neuroscience, University College London, Gower Street, London WC1E 6BT; Departments of †Pharmacology and **Biochemistry, Biocentre Niederursel, University of Frankfurt, Marie-Curie-Straße, 9, D-60439 Frankfurt, Germany

1 The effect of pyridoxalphosphate-6-azophenyl-2',4'-disulphonic acid (PPADS) on vasoconstrictor and/or vasodilator responses to various agonists and electrical field stimulation was investigated in the rat mesenteric arterial bed at basal tone and at tone raised by methoxamine (15–50 μM).

2 At basal tone, nucleotides produced vasoconstriction with the following rank order of potency: α,β-methylene ATP≫2-methylthio ATP≥ATP = UTP. PPADS (0.3–10 μM) concentration-dependently antagonized α,β-methylene ATP-, 2-methylthio ATP- and ATP-induced responses. UTP-, noradrenaline- and nerve-mediated (4–32 Hz) increases in perfusion pressure remained unaffected by 10 μM PPADS.

3 In raised tone preparations, nucleotides produced vasodilations, their rank order of potency being 2-methylthio ATP>ATP>UTP. Responses to 2-methylthio ATP were slightly antagonized, whereas ATP- and UTP-induced responses remained unaffected by 10 μM PPADS. In addition, acetylcholine- and adenosine-elicited relaxations were not influenced by 10 μM PPADS.

4 The present results confirm the previously described selective P_{2x} antagonism by PPADS, this compound being ineffective at muscarinic M_3- and adenosine P_1-receptors as well as at α_1-adrenoceptors. There was some inhibition of P_{2y}-purinoceptors but at a much higher concentration than required for inhibition of P_{2x}-purinoceptors.

5 In addition, this study provides evidence for the ineffectiveness of PPADS at both vasoconstriction- and vasodilatation-mediating P_{2u}-purinoceptors.

Keywords: PPADS; 2-methylthio ATP; ATP; α,β-methylene ATP; UTP; P_{2x}-purinoceptor; P_{2y}-purinoceptor; P_{2u}-purinoceptor; rat mesenteric arterial bed

Introduction

Since the first subclassification of P_2-purinoceptors into P_{2x}- and P_{2y}-subtypes, mainly based on the different rank order of agonist potency of structural ATP analogues (Burnstock & Kennedy, 1985), a more subtle classification of P_2-purinoceptor subtypes continued to be hindered by the lack of potent, highly selective and competitive antagonists. Compounds like suramin (Dunn & Blakeley, 1988; Hoyle *et al.*, 1990; Hoyle & Edwards, 1992), the desensitizing agent α,β-methylene ATP (α,β-mATP; Ralevic & Burnstock, 1988; O'Connor *et al.*, 1990), reactive blue 2 (Burnstock & Warland, 1987) and the photoaffinity label arylazidoaminopropionyl ATP (ANAPP$_3$; Hogaboom *et al.*, 1980) have been used to eliminate either P_{2x}- or P_{2y}-mediated responses. Their use, however, is limited for the following reasons: suramin does not discriminate between the P_{2x}- and the P_{2y}-subtype; α,β-mATP and ANAPP$_3$ irreversibly block P_{2x}-purinoceptor-mediated responses and reactive blue 2 can only be used within a narrow concentration-range to block selectively P_{2y}-purinoceptors.

Recently, the novel compound, pyridoxalphosphate-6-azophenyl-2',4'-disulphonic acid (PPADS), has been described as a functionally selective antagonist of P_{2x}-receptor-mediated responses in rabbit vas deferens. No interaction of PPADS with α_1-adrenoceptors, muscarinic M_1-(M_4-), M_2- and M_3-receptors, histamine H_1- or adenosine A_1-receptors was found (Lambrecht *et al.*, 1992; Grimm *et al.*, 1994). Subsequent studies on guinea-pig ileum resistance vessels (Bungardt *et al.*, 1992), guinea-pig vas deferens (McLaren *et al.*, 1993; 1994), rabbit urinary bladder (Ziganshin *et al.*, 1993) and various rabbit isolated blood vessels (Ziganshin *et al.*, 1994) have confirmed a selective P_{2x}-antagonism by PPADS. However, recent studies in our laboratories showed that PPADS antagonized P_{2y}-receptor-mediated relaxations in the guinea-pig taenia coli and rat duodenum (Ziyal *et al.*, 1994), although higher concentrations of PPADS were needed in these preparations compared to tissues where P_{2x}-receptor-mediated effects are antagonized by PPADS.

The aim of the present study was to investigate further the selectivity of PPADS for coexisting P_2-purinoceptor subtypes in the rat mesenteric arterial bed. This tissue is endowed with P_{2x}- and P_{2y}-purinoceptors as well as with P_{2u}-purinoceptors, which are located on the smooth muscle and on endothelial cells, mediating vasoconstriction and vasodilatation, respectively (Ralevic & Burnstock, 1988; 1991a). It should be noted that purinoceptor subclassification is currently under review. In a unifying receptor proposal the terms 'P_{2x}' and 'P_{2y}' will comprise extended families of receptors and it has been proposed that the P_{2u}-purinoceptor will be reclassified as a member of these families (Abbracchio & Burnstock, 1994). Vasoconstriction to α,β-mATP, 2-methylthio ATP (2-MeSATP), ATP, UTP and electrical field stimulation (EFS), and vasodilatation to 2-MeSATP, ATP and UTP were compared in the absence and in the presence of PPADS. The selectivity of PPADS was further characterized by investigating its effects on noradrenaline (NA)-induced increases in perfusion pressure (mediated via α_1-adrenoceptors; Pipili, 1986; Han *et al.*, 1990) and on acetylcholine (ACh)-(M_3-receptor-mediated; Pinardi *et al.*, 1992; Hendriks *et al.*, 1992)

[1] Author for correspondence.

and adenosine-induced (P_1-purinoceptor-mediated; Jackson, 1987) relaxations, respectively.

A preliminary account of these results has been presented elsewhere (Windscheif et al., 1994).

Methods

General procedures

Male Wistar rats (300–400 g) were killed by asphyxiation with carbon dioxide. A midline abdominal incision was made, and the superior mesenteric artery was exposed and cannulated (monoject cannula 0.8 × 40 mm). The superior mesenteric vein was severed before the bed was perfused with about 1 ml Krebs solution containing (mM): NaCl 133, KCl 4.7, NaH_2PO_4 1.35, $NaHCO_3$ 16.3, $MgSO_4$ 0.61, glucose 7.8 and $CaCl_2$ 2.52. The mesentery was dissected by cutting along the gut as closely as possible, and then was transferred to a heated chamber which was covered with a lid. The cannula was connected with a rubber tubing, serving as an injection port (see below), and perfusion (single-pass, non-recirculating system) with Krebs solution, gassed with 95% O_2/5% CO_2 and kept at 37°C, was adjusted to a constant flow rate of 5 ml min^{-1} (peristaltic pump, Cole Parmer Instruments). Special care was taken to move the cannula gently throughout the whole procedure. Preparations were allowed to equilibrate for 30 min.

Vasoconstrictor and vasodilator responses to exogenous agonists or EFS were measured as changes in perfusion pressure (mmHg) with a Spectramed Statham pressure transducer on a side arm of the perfusion cannula and were recorded on a Grass 79D polygraph. In order to construct dose-response curves, doses of agonists (mol) were administered as 50 µl bolus injections via the injection port close to the tissue. PPADS (0.3–10 µM) added to the perfusate at a given concentration was allowed to equilibrate for 30 min. Only one PPADS concentration was examined in one preparation.

In those cases where PPADS affected the dose-response curves of exogenous agonists, control experiments (same protocol, no incubation of PPADS) were carried out on at least four preparations. These experiments were considered as time-matched controls. For α,β-mATP only one dose-response curve was constructed per preparation.

Experiments at basal tone

The vasoconstrictor responses to NA and the purine nucleotides ATP and 2-MeSATP were investigated in that sequence on a given preparation in the absence and in the presence of 0.3, 1, 3 and 10 µM PPADS; 1.5 min was the minimum time interval between consecutive bolus injections. In order to avoid desensitization, the pressor responses to α,β-mATP in the absence or in the presence of 0.3, 1 and 3 µM PPADS were investigated on separate tissues. Furthermore, the time interval between bolus injections varied from 3 min (lower doses) up to 20 min at higher doses of α,β-mATP. The pyrimidine nucleotide UTP was investigated for its pressor responses on a given tissue before and after incubation of 10 µM PPADS, the highest concentration used in this study. On the same preparations, prior to the respective dose-response curves of UTP, EFS (90 V, 30 s, 1 ms pulse width, at 4–32 Hz) of perivascular sympathetic nerves was applied after one conditioning stimulation at 16 Hz. The two electrodes were represented by: (a) the needle which was used to cannulate the artery and (b) the stainless steel grid upon which the bed was placed in the heated chamber.

Experiments at raised tone

The α_1-adrenoceptor agonist, methoxamine (15–50 µM), was added stepwise to the Krebs reservoir (starting with 5 µM) in order to reach an increase of basal tone by about 50 mmHg. Occasionally, it was necessary to readjust vascular tone during the experiments by further addition of methoxamine. Consecutive doses of exogenous relaxant agonists were applied as soon as tone was regained.

Vasodilator responses to ACh, 2-MeSATP and ATP were registered in that order before and after incubation of 10 µM PPADS on the same preparation. In another set of mesenteries, UTP and adenosine were investigated for their vasodilator activities in the absence and in the presence of 10 µM PPADS, the highest concentration used in this study.

Drugs used

(−)-Noradrenaline bitartrate (NA), adenosine 5′-triphosphate sodium salt (ATP), α,β-methylene ATP lithium salt (α,β-mATP), uridine 5′-triphosphate sodium salt (UTP), (±)-methoxamine hydrochloride, acetylcholine chloride (ACh) and adenosine hemisulphate were all purchased from Sigma Chemical Co., U.K. 2-Methylthio ATP sodium salt (2-MeSATP) was obtained from Research Biochemicals, Inc. (U.S.A.). Pyridoxalphosphate-6-azophenyl-2′,4′-disulphonic acid (PPADS) was synthesized in one of our laboratories. NA was dissolved in 0.1 mM ascorbic acid. The other drug solutions were made up in distilled water.

Analysis of results

Vasoconstrictor and/or vasodilator responses to exogenous agonists and EFS were registered as changes in perfusion pressure (mmHg). In raised tone preparations, vasodilator responses were expressed as % decrease of methoxamine-induced tone. For the dose-response curves of agonists, data were plotted as mean ± s.e.mean of replicate responses at each dose. Statistical significance was evaluated by paired or unpaired Student's t test as appropriate ($P<0.05$ was considered significant). Potencies of agonists were determined graphically from semi-logarithmic dose-response curves as $-\log ED_{50}$ values (mol). Values in the text refer to means ± s.e.mean.

Results

Experiments at basal tone

At a constant flow rate of 5 ml min^{-1}, the mean basal perfusion pressure of the rat isolated mesenteric beds was 36.3 ± 0.8 mmHg ($n = 61$), and this remained constant over the duration of the experiment (also in the presence of PPADS). NA, serving as a control compound, as well as the purine and pyrimidine nucleotides produced dose-dependent instantaneously developing vasoconstrictor responses which declined within seconds. The reproducibility of these responses was checked in control experiments (see below). The rank order of potency of the nucleotides was: α,β-mATP ≫ 2-MeSATP ≥ ATP = UTP (Figure 1). By far the most efficacious compound investigated at basal tone was NA (0.15 nmol–0.5 µmol) with a maximum pressor response of about 160 mmHg at the highest dose tested.

In time-matched control experiments the second dose-response curve for NA was shifted to the left to some degree: the dose producing an increase of perfusion pressure of 80 mmHg ($= -\log ED_{80}$) was 7.65 ± 0.10 (23) for the first and 8.39 ± 0.15 (5) for the second dose-response curve. In preparations incubated with PPADS (0.3, 1, 3 and 10 µM), there was no effect that did not occur with time in any case: $-\log ED_{80}$ = 8.13 ± 0.01 (4), 8.26 ± 0.05 (6), 8.38 ± 0.10 (6) and 8.18 ± 0.14 (7), respectively. Hence, PPADS itself was without effect on NA responses.

In the case of ATP and 2-MeSATP, time-matched control experiments showed that pressor responses only to the highest dose of agonist (5 µmol and 0.5 µmol, respectively)

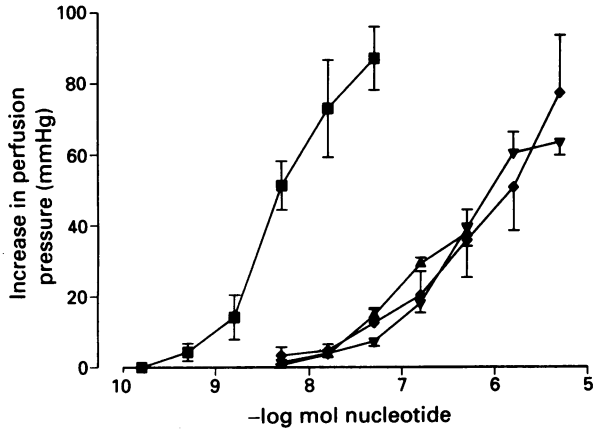


Figure 1 Dose-response curves for the contractile responses to α,β-mATP (■, $n = 7$), ATP (▼, $n = 24$), 2-MeSATP (▲, $n = 23$) and UTP (◆, $n = 4$) in the perfused rat mesenteric bed at basal tone. The bolus volume of individual doses was 50 μl. Data shown are means ± s.e.mean. Error bars falling within the area covered by a symbol are not shown.

were reduced in the second curve by 16% and 28% ($P<0.05$), respectively. PPADS (0.3, 1, 3 and 10 μM) concentration-dependently decreased pressor responses to ATP (Figure 2a) and 2-MeSATP (Figure 2b). Whereas in the presence of PPADS responses to 2-MeSATP levelled off, those to ATP did not. Furthermore, 10 μM PPADS more or less abolished responses to 2-MeSATP, whereas there was still a residual response to ATP (Figure 2a, b and Figure 3). PPADS, 0.3 μM, attenuated the vasoconstrictor response only to the highest dose of α,β-mATP (Figure 2c), which was significant ($P<0.05$). However, 1 and 3 μM PPADS, potently inhibited α,β-mATP-produced responses in an insurmountable fashion.

PPADS (10 μM) failed to affect responses either to the pyrimidine nucleotide UTP, which exerted increases in perfusion pressure similar to ATP, or the monophasic, gradually developing responses following perivascular sympathetic nerve stimulation (data not shown).

Experiments at raised tone

The mean methoxamine-raised (15–50 μM) perfusion pressure was 85.3 ± 3.6 mmHg ($n = 11$) before and 94.5 ± 5.6 mmHg ($n = 11$) after incubation of 10 μM PPADS, which was a slight but significant ($P<0.05$) increase in tone. Depending on the actual tone, PPADS transiently increased methoxamine-induced tone, the extent of which was more pronounced (e.g. up to more than 100%) at moderate tone (i.e. when vasodilator responses to the last dose of agonist before PPADS incubation had not yet recovered), and it was less pronounced at higher tone. The augmentation by PPADS of methoxamine-induced tone diminished during equilibration time until a new level was reached (94.5 mmHg).

ACh, serving as a control compound, 2-MeSATP and ATP dose-dependently elicited vasodilator responses (Figures 4 and 5a), which were reproducible in time-matched control experiments (data not shown). A similar apparent efficacy (84–91% decrease in vascular tone) was seen for ACh, 2-MeSATP and ATP. Also, the pyrimidine nucleotide UTP and the nucleoside adenosine produced decreases in perfusion pressure (Figure 4). Except for adenosine (at the concentrations tested), a maximum effect was reached by each of the other agonists, thus it was possible to calculate $-\log ED_{50}$ values referring to the respective maxima. ACh yielded a $-\log ED_{50}$ value of 10.73 ± 0.08 ($n = 5$); the dose-response curves before and after incubation of PPADS were identical

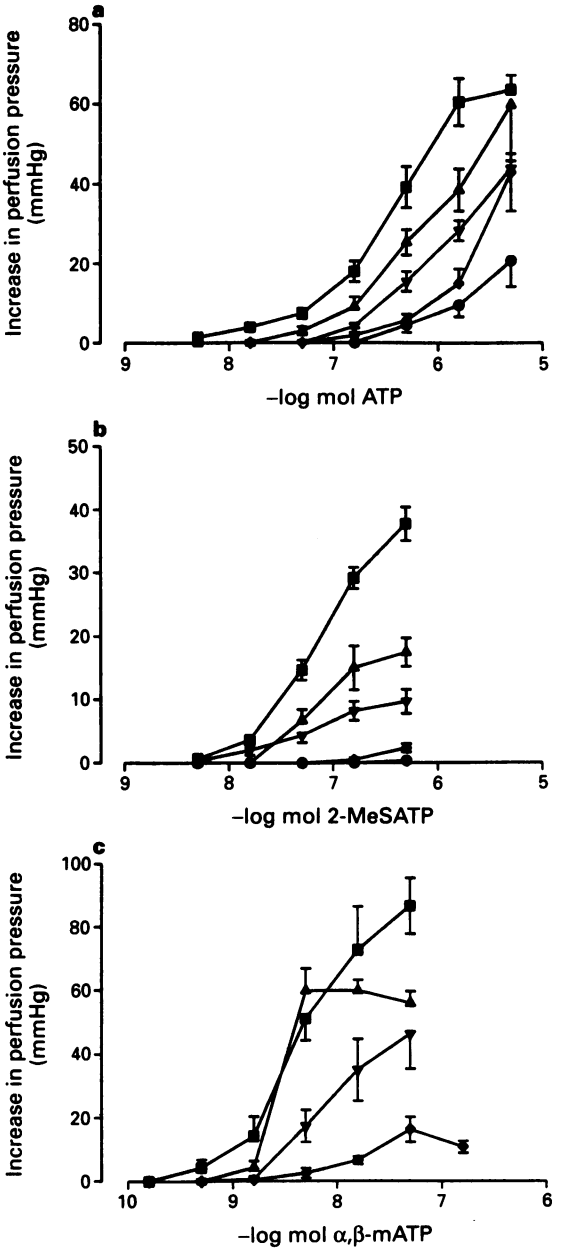


Figure 2 Dose-response curves for the pressor responses to (a) ATP in the absence (■, $n = 24$) and in the presence of 0.3 μM (▲, $n = 4$), 1 μM (▼, $n = 6$), 3 μM (◆, $n = 6$) and 10 μM (●, $n = 6$) PPADS, (b) 2-MeSATP in the absence (■, $n = 23$) and in the presence of 0.3 μM (▲, $n = 4$), 1 μM (▼, $n = 6$), 3 μM (◆, $n = 6$) and 10 μM (●, $n = 6$) PPADS and to (c) α,β-mATP in the absence (■, $n = 7$) and in the presence of 0.3 μM (▲, $n = 4$), 1 μM (▼, $n = 6$) and 3 μM (◆, $n = 6$) PPADS in the perfused rat mesenteric bed. Doses were applied at basal tone as 50 μl bolus injections. Data are means ± s.e.mean. Error bars falling within the area covered by a symbol are not shown.

(Figure 5a). 2-MeSATP ($-\log ED_{50} = 10.62 \pm 0.07$; $n = 7$) was approximately 10 times more potent than ATP ($-\log ED_{50} = 9.93 \pm 0.14$; $n = 6$). Responses to 2-MeSATP were slightly antagonized by PPADS (10 μM; Figure 5b); the $-\log ED_{50}$ value obtained in the presence of PPADS was 10.03 ± 0.14 (6). By contrast, ATP-mediated relaxations remained unaffected by PPADS (10 μM; Figure 5c).

UTP ($-\log ED_{50} = 9.29 \pm 0.07$; $n = 5$) was considerably less potent than ATP ($-\log ED_{50} = 9.93$) and slightly less efficacious (Figure 4). Adenosine was the poorest vasodilator (Figure 4). The responses to both UTP and adenosine remained unaffected by PPADS (10 μM; Figure 6).

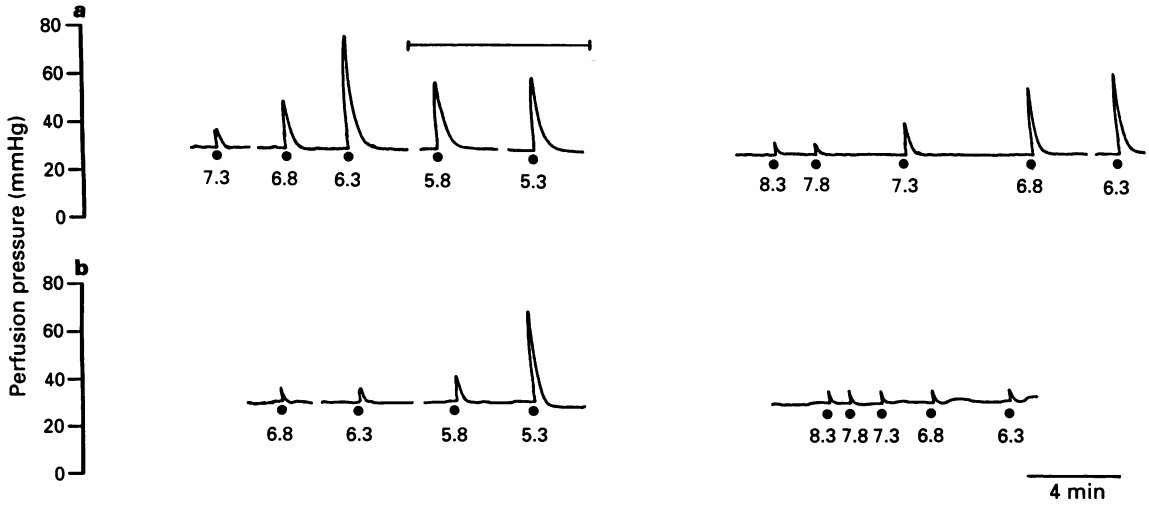


Figure 3 Single traces demonstrating the effect of 10 μM PPADS (b) on the dose-dependent pressor responses to ATP (left hand side) and 2-MeSATP (right hand side) in the perfused rat mesenteric bed preparation at basal tone. Dots indicate drug application (50 μl bolus volume). Doses are expressed as −log mol. The horizontal line in (a) left panel denotes a change of recorder sensitivity (2.5 fold decrease). In the presence of PPADS, ATP showed a residual response, whereas responses to 2-MeSATP were abolished.

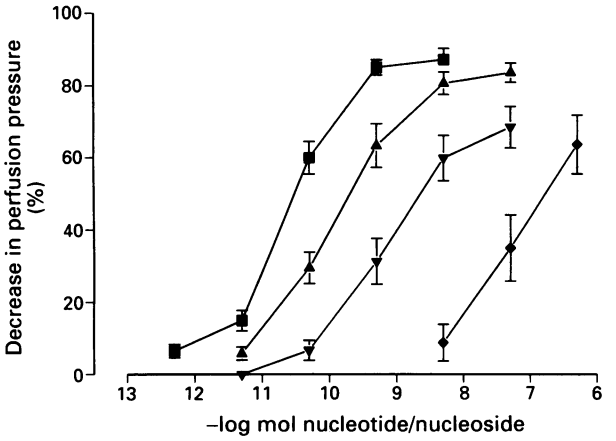


Figure 4 Isolated mesenteric bed preparation of rat with tone raised by methoxamine (15–50 μM), added to the perfusate. Responses are expressed as % decrease of methoxamine-induced tone. Dose-response curves are shown for the relaxant responses to 2-MeSATP (■, $n = 7$), ATP (▲, $n = 7$), UTP (▼, $n = 6$) and adenosine (◆, $n = 4$). Doses were applied as 50 μl bolus injections. Data shown are means ± s.e.mean. Error bars falling within the area covered by a symbol are not shown.

Discussion

The results of this study show that PPADS selectively inhibits P_{2x}-purinoceptor-mediated responses in the rat mesenteric arterial bed.

Experiments at basal tone

Pressor responses to NA, which are mediated via α_1-adrenoceptors located on the smooth muscle of the rat mesentery (Pipili, 1986; Han *et al.*, 1990), remained unaffected by PPADS (up to 10 μM). Thus, any interaction of PPADS with α_1-adrenoceptors could be excluded.

The rank order of potency of the purine nucleotides for eliciting vasoconstriction (α,β-mATP≫ 2-MeSATP ≥ ATP) confirmed the existence of functional P_{2x}-purinoceptors, which have been shown to be present on the smooth muscle in the rat mesenteric bed (Ralevic & Burnstock, 1988). PPADS (0.3–10 μM) concentration-dependently antagonized increases in perfusion pressure elicited by either of the purines. The depression of the maximum response by PPADS might be explained by a non-competitive or a pseudoirreversible antagonism. These results are consistent with recent reports, which describe PPADS as a selective inhibitor of P_{2x}-receptor-mediated effects (Lambrecht *et al.*, 1992; Bungardt *et al.*, 1992; McLaren *et al.*, 1993; 1994; Ziganshin *et al.*, 1993; 1994). However, compared to α,β-mATP and 2-MeSATP, ATP was less prone to be antagonized by PPADS. Even at 10 μM PPADS, there was a residual response to ATP. This result might indicate that ATP is acting both at P_{2x}-purinoceptors which are susceptible to antagonism by PPADS and on PPADS-resistant P_{2u}-purinoceptors (see below). The dose-response curves of UTP and ATP for eliciting vasoconstriction were almost superimposable (present study). Similar potencies of UTP and ATP have already been described for other tissues, e.g. in the rabbit ear artery (von Kügelgen *et al.*, 1987; for review see Seifert & Schultz, 1989; O'Connor *et al.*, 1991; O'Connor, 1992). In the rat mesenteric bed, Ralevic & Burnstock (1991a) have been able to demonstrate the presence of a vasoconstriction-mediating P_{2u}-purinoceptor on the smooth muscle, although UTP appeared to be less potent than ATP in this study. In contrast to ATP, UTP-induced vasoconstriction remained unaffected by PPADS.

Numerous studies on blood vessels provide evidence for sympathetic cotransmission of NA and ATP (Ramme *et al.*, 1987; for review see Burnstock & Kennedy, 1986; Burnstock, 1988; Ralevic & Burnstock, 1991b). Depending on the species, the type of blood vessel, the stimulation pattern (frequency, duration of stimulation) and the temperature at which experiments are carried out, the one or other transmitter dominates (Burnstock, 1988; Starke *et al.*, 1991; Yamamoto *et al.*, 1992). Cotransmission of NA and ATP has been shown in isolated small mesenteric arteries (Sjöblom-Widfeldt, 1990; Sjöblom-Wildfeldt *et al.*, 1990) and under certain conditions in the isolated whole mesenteric arterial bed preparation (Yamamoto *et al.*, 1988; 1992). In the present study, pressor responses to perivascular sympathetic nerve stimulation of the rat mesenteric bed were not attenuated by PPADS (10 μM), but prazosin (1 μM) totally blocked the vasoconstrictor responses produced by EFS (unpublished results). This is likely to be a reflection of the differential contribution of cotransmitters to the response according to the parameters of stimulaton used; single pulses of high-frequency stimulation which are optimal for ATP

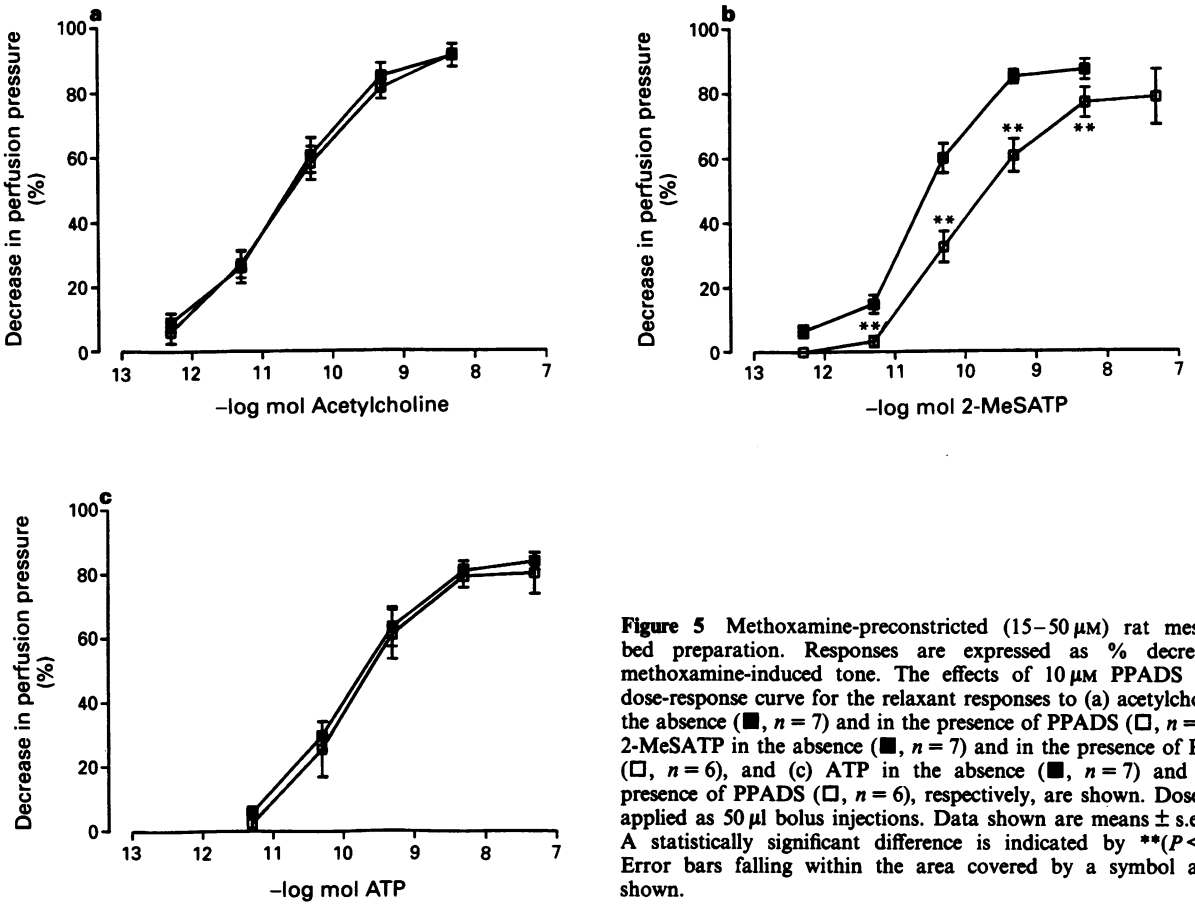


Figure 5 Methoxamine-preconstricted (15–50 μM) rat mesenteric bed preparation. Responses are expressed as % decrease of methoxamine-induced tone. The effects of 10 μM PPADS on the dose-response curve for the relaxant responses to (a) acetylcholine in the absence (■, $n = 7$) and in the presence of PPADS (□, $n = 7$), (b) 2-MeSATP in the absence (■, $n = 7$) and in the presence of PPADS (□, $n = 6$), and (c) ATP in the absence (■, $n = 7$) and in the presence of PPADS (□, $n = 6$), respectively, are shown. Doses were applied as 50 μl bolus injections. Data shown are means ± s.e.mean. A statistically significant difference is indicated by **($P < 0.01$). Error bars falling within the area covered by a symbol are not shown.

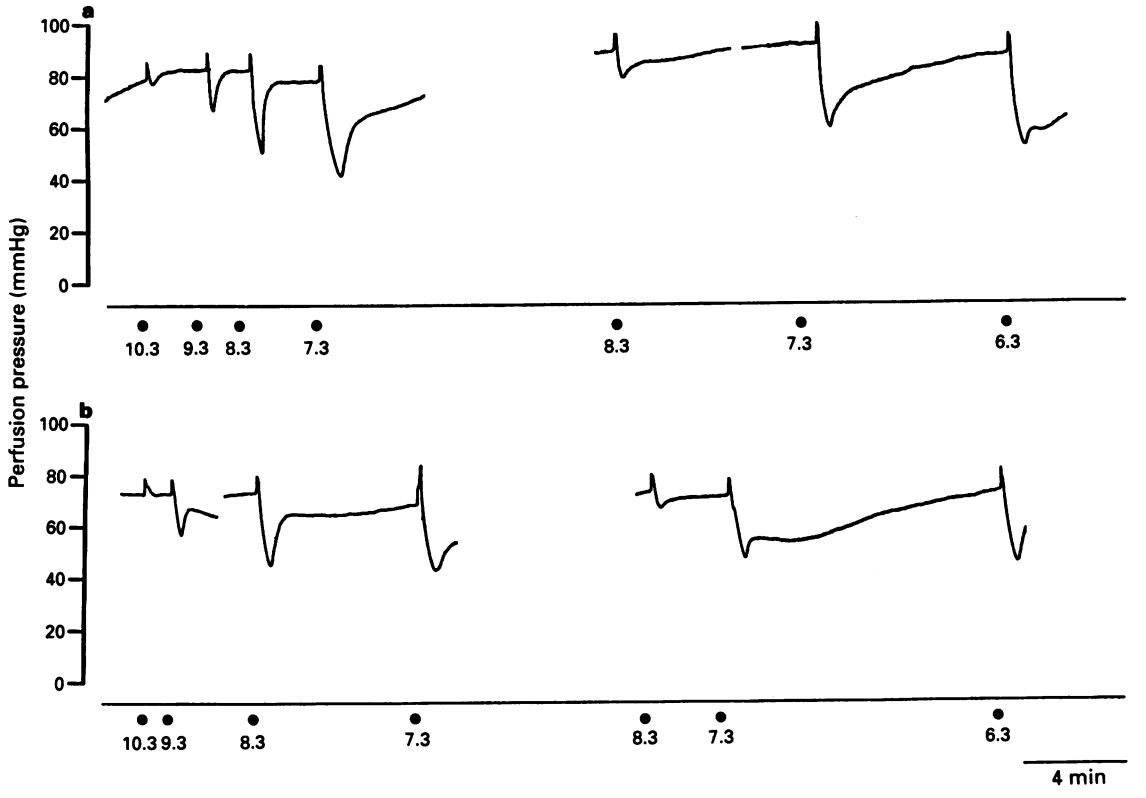


Figure 6 Rat mesenteric vascular bed preparation at methoxamine-raised tone (30–50 μM). Typical traces of the dose-dependent relaxant responses to UTP (left hand side) and adenosine (right hand side) in the absence (a) and in the presence of 10 μM PPADS (b). Dots indicate drug application (50 μl bolus volume). Doses are expressed as −log mol. Responses to either of the agonists remained unchanged in the presence of PPADS.

release are not sufficient to produce a response in the whole bed preparation where the relatively long duration of stimulation (30 s) and high frequencies (4–32 Hz) required to elicit a mechanical response favour NA transmission. These results indicate that under the conditions used, NA is the predominant component of the response to EFS, which explains the lack of effect on these responses by PPADS.

Experiments at raised tone

2-MeSATP was more potent than ATP in reducing perfusion pressure, confirming the presence of a functional P_{2y}-purinoceptor, which is located on the endothelium (Ralevic & Burnstock, 1988). ATP-induced relaxations were not antagonized by PPADS (10 μM), whereas vasodilator responses to 2-MeSATP were slightly inhibited by 10 μM PPADS, a concentration which virtually abolished P_{2x}-purinoceptor-mediated vasoconstriction to exogenous 2-MeSATP. These results demonstrate that PPADS selectively antagonized P_{2x}-purinoceptor-mediated responses in the rat mesenteric arterial bed. It is interesting that vasodilator responses to ATP and 2-MeSATP were affected differently by PPADS. ATP might have elicited its vasodilator activity to a considerable extent via relaxation-mediating P_{2u}-purinoceptors which are not susceptible to antagonism by PPADS (see below).

It is noteworthy that PPADS (10 μM) antagonized P_{2y}-purinoceptor-mediated relaxations to 2-MeSATP in guinea-pig taenia coli and rat duodenum in a reversible and surmountable manner (Ziyal *et al.*, 1994). In contrast, Ziganshin *et al.* (1994) found PPADS (30 μM) to be ineffective at vascular P_{2y}-purinoceptors in rabbit isolated blood vessels.

UTP proved to be less potent that ATP ($-\log ED_{50} = 9.29$ vs. 9.93) in inducing relaxation of the preconstricted rat mesenteric bed preparation. These UTP-induced responses remained unaffected by 10 μM PPADS. UTP might have exhibited its vasodilator effects via relaxation-mediating P_{2u}-purinoceptors, the existence of which has been postulated for the rat mesenteric vascular bed (Ralevic & Burnstock, 1991a). Similar to the vasoconstriction-mediating P_{2u}-purinoceptor, the P_{2u}-purinoceptor mediating vasodilatation did not interact with PPADS.

Vasodilator responses to adenosine, which are mediated via P_1-purinoceptors (Jackson, 1987) were not influenced by PPADS (10 μM). This result is consistent with recent studies documenting that PPADS does not interact with A_1- (Lambrecht *et al.*, 1992) and A_2-purinoceptors (Windscheif *et al.*, unpublished results) in guinea-pig atria and taenia coli, respectively.

The vasodilator action of ACh in the preconstricted rat mesenteric bed preparation involves muscarinic M_3-receptors (Pinardi *et al.*, 1992; Hendriks *et al.*, 1992). PPADS (10 μM) failed to inhibit relaxations to ACh in this study. This lack of antimuscarinic activity of PPADS is in agreement with recent reports for other tissues (Lambrecht *et al.*, 1992; McLaren *et al.*, 1993; 1994; Ziganshin *et al.*, 1993; Grimm *et al.*, 1994).

It is difficult to interpret the observed augmentation by PPADS of methoxamine-induced tone. In the guinea-pig ileum resistance vessels, Bungardt *et al.* (1992) did not observe any effect of PPADS on NA-induced tone. Regarding the synergism between α_1-adrenoceptor- and P_{2x}-purinoceptor mediated responses (Ralevic & Burnstock, 1990) and assuming an endogenous tone of ATP, sources of which may be endothelial (Ralevic *et al.*, 1992) and smooth muscle cells (Gordon, 1986), one would rather expect a decrease of tone, since the P_{2x}-component of the vascular tone induced by endogenous ATP was eliminated in the presence of PPADS. Possibly, a recently reported depolarizing effect of PPADS in the guinea-pig vas deferens (McLaren *et al.*, 1993; 1994) could account for this phenomenon.

In conclusion, the present results clearly demonstrate that PPADS is a selective antagonist of vascular P_{2x}-purinoceptors in the rat mesenteric arterial bed, having no effect at α_1-adrenoceptors, muscarinic M_3-receptors or P_1-purinoceptors, which is in line with previous observations in other tissues. There was only a slight antagonism by PPADS at P_{2y}-purinoceptors. In addition, this study demonstrates the ineffectiveness of PPADS at both vasoconstriction- and vasodilatation-mediating P_{2u}-purinoceptors.

The authors thank the Fonds der Chemischen Industrie (Germany; G.L., E.M.) and the Deutsche Forshungsgemeinschaft (H.G.B., SFB 169) for financial support.

References

ABBRACCHIO, M.P. & BURNSTOCK, G. (1994). Purinoceptors: are there families of P_{2x} and P_{2y} purinoceptors? *Pharmacol. Ther.*, (in press).

BUNGARDT, E., MOSER, U., SPATZ-KÜMBEL, G., BÄUMERT, H.G., LAMBRECHT, G. & MUTSCHLER, E. (1992). Characterization of purinoceptors in guinea-pig ileum resistance vessels by the use of computer-assisted videomicroscopy. *Int. J. Purine Pyrimidine Res.*, **3**, 66.

BURNSTOCK, G. (1988). Sympathetic purinergic transmission in small blood vessels. *Trends Pharmacol. Sci.*, **9**, 116–117.

BURNSTOCK, G. & KENNEDY, C. (1985). Is there a basis for distinguishing two types of P_2-purinoceptor? *Gen. Pharmacol.*, **16**, 433–440.

BURNSTOCK, G. & KENNEDY, C. (1986). Purinergic receptors in the cardiovascular system. *Prog. Pharmacol.*, **6**, 111–132.

BURNSTOCK, G. & WARLAND, J.J.I. (1987). P_2-purinoceptors of two subtypes in the rabbit mesenteric artery: reactive blue 2 selectively inhibits responses mediated via the P_{2y}- but not the P_{2x}-purinoceptor. *Br. J. Pharmacol.*, **90**, 383–391.

DUNN, P.M. & BLAKELEY, A.G.H. (1988). Suramin: a reversible P_2-purinoceptor antagonist in the mouse vas deferens. *Br. J. Pharmacol.*, **93**, 243–245.

GORDON, J.L. (1986). Extracellular ATP: effects, sources and fate. *Biochem. J.*, **233**, 309–319.

GRIMM, U., FUDER, H., MOSER, U., BÄUMERT, H.G., MUTSCHLER, E. & LAMBRECHT, G. (1994). Characterization of the prejunctional muscarinic receptors mediating inhibition of evoked release of endogenous noradrenaline in rabbit isolated vas deferens. *Naunyn-Schmied. Arch. Pharmacol.*, **349**, 1–10.

HAN, C., LI, J. & MINNEMAN, K.P. (1990). Subtypes of α_1-adrenoceptors in rat blood vessels. *Eur. J. Pharmacol.*, **190**, 97–104.

HENDRIKS, M.G.C., PFAFFENDORF, M. & VAN ZWIETEN, P.A. (1992). Characterization of the muscarinic receptor subtype mediating vasodilation in the rat perfused mesenteric vascular bed preparation. *J. Auton. Pharmacol.*, **12**, 411–420.

HOGABOOM, G.K., O'DONNELL, J.P. & FEDAN, J.S. (1980). Purinergic receptors: photoaffinity analog of adenosine triphosphate is a specific adenosine triphosphate antagonist. *Science*, **208**, 1273–1276.

HOYLE, C.H.V. & EDWARDS, G.A. (1992). Activation of P_1- and P_{2y}-purinoceptors by ADP-ribose in the guinea-pig taenia coli, but not of P_{2x}-purinoceptors in the vas deferens. *Br. J. Pharmacol.*, **107**, 367–374.

HOYLE, C.H.V., KNIGHT, G.E. & BURNSTOCK, G. (1990). Suramin antagonizes responses to P_2-purinoceptor agonists and purinergic nerve stimulation in the guinea-pig urinary bladder and taenia coli. *Br. J. Pharmacol.*, **99**, 617–621.

JACKSON, E.K. (1987). Role of adenosine in noradrenergic neurotransmission in spontaneously hypertensive rats. *Am. J. Physiol.*, **253**, H909–H918.

LAMBRECHT, G., FRIEBE, TH., GRIMM, U., WINDSCHEIF, U., BUNGARDT, E., HILDEBRANDT, C., BÄUMERT, H.G., SPATZ-KÜMBEL, G. & MUTSCHLER, E. (1992). PPADS, a novel functionally selective antagonist of P_2-purinoceptor-mediated responses. *Eur. J. Pharmacol.*, **217**, 217–219.

MCLAREN, G.J., LAMBRECHT, G., MUTSCHLER, E., BÄUMERT, H.G., SNEDDON, P. & KENNEDY, C. (1994). Investigation of the actions of PPADS, a novel P_{2x}-purinoceptor antagonist, in the guinea-pig isolated vas deferens. *Br. J. Pharmacol.*, **111**, 913–917.

MCLAREN, G.J., SNEDDON, P., KENNEDY, C., LAMBRECHT, G., BURNSTOCK, G., MUTSCHLER, E., BÄUMERT, H.G. & HOYLE, C.H.V. (1993). Investigation of a putative P_{2x}-purinoceptor antagonist in the guinea-pig vas deferens. *Br. J. Pharmacol.*, **109**, 109P.

O'CONNOR, S.E. (1992). Recent developments in the classification and functional significance of receptors for ATP and UTP, evidence for nucleotide receptors. *Life Sci.*, **50**, 1657–1664.

O'CONNOR, S.E., DAINTY, I.A. & LEFF, P. (1991). Further subclassification of ATP receptors based on agonist studies. *Trends Pharmacol. Sci.*, **12**, 137–141.

O'CONNOR, S.E., WOOD, B.E. & LEFF, P. (1990). Characterization of P_{2x}-receptors in rabbit isolated ear artery. *Br. J. Pharmacol.*, **101**, 640–644.

PINARDI, G., PELISSIER, T., FERNANDEZ, E., BUSTAMANTE, D. & MIRANDA, H.F. (1992). Pharmacological characterization of muscarinic receptors in the rat mesenteric vascular bed. *Neurosci. Res. Commun.*, **11**, 57–64.

PIPILI, E. (1986). A study on the postjunctional excitatory α-adrenoceptor subtypes in the mesenteric arterial bed of the rat. *J. Auton. Pharmacol.*, **6**, 125–132.

RALEVIC, V. & BURNSTOCK, G. (1988). Actions mediated by P_2-purinoceptor subtypes in the isolated perfused mesenteric bed of the rat. *Br. J. Pharmacol.*, **95**, 637–645.

RALEVIC, V. & BURNSTOCK, G. (1990). Postjunctional synergism of noradrenaline and adenosine 5'-triphosphate in the mesenteric arterial bed of the rat. *Eur. J. Pharmacol.*, **175**, 291–299.

RALEVIC, V. & BURNSTOCK, G. (1991a). Effects of purines and pyrimidines on the rat mesenteric arterial bed. *Circ. Res.*, **69**, 1583–1590.

RALEVIC, V. & BURNSTOCK, G. (1991b). Roles of P_2-purinoceptors in the cardiovascular system. *Circulation*, **84**, 1–14.

RALEVIC, V., MILNER, P., KIRKPATRICK, K.A. & BURNSTOCK, G. (1992). Flow-induced release of adenosine 5'-triphosphate from endothelial cells of the rat mesenteric arterial bed. *Experientia*, **48**, 31–34.

RAMME, D., REGENOLD, J.T., STARKE, K., BUSSE, R. & ILLES, P. (1987). Identification of the neuroeffector transmitter in jejunal branches of the rabbit mesenteric artery. *Naunyn-Schmied. Arch. Pharmacol.*, **336**, 267–273.

SEIFERT, R. & SCHULTZ, G. (1989). Involvement of the pyrimidinoceptors in the regulation of cell functions by uridine and by uracil nucleotides. *Trends Pharmacol. Sci.*, **10**, 365–369.

SJÖBLOM-WIDFELDT, N. (1990). Neuro-muscular transmission in blood vessels: phasic and tonic components. *Acta Physiol. Scand.*, **138** (Suppl. 587), 1–52.

SJÖBLOM-WIDFELDT, N., GUSTAFSSON, H. & NILSSON, H. (1990). Transmitter characteristics of small mesenteric arteries from the rat. *Acta Physiol. Scand.*, **138**, 203–212.

STARKE, K., VON KÜGELGEN, I., BULLOCH, J.M. & ILLES, P. (1991). Nucleotides as cotransmitters in vascular sympathetic neuroeffector transmission. *Blood Vessels*, **28**, 19–26.

VON KÜGELGEN, I., HÄUSSINGER, D. & STARKE, K. (1987). Evidence for a vasoconstriction-mediating receptor for UTP, distinct from the P_2 purinoceptor, in rabbit ear artery. *Naunyn-Schmied. Arch. Pharmacol.*, **336**, 556–560.

WINDSCHEIF, U., RALEVIC, V., HOYLE, C.H.V., BÄUMERT, H.G., MUTSCHLER, E., LAMBRECHT, G. & BURNSTOCK, G. (1994). Functional studies on the P_2-purinoceptor subtype selectivity of pyridoxalphosphate-6-azophenyl-2',4'-disulphonic acid. *Drug Dev. Res.*, **31**, 334.

YAMAMOTO, R., CLINE Jr, W.H. & TAKASAKI, K. (1988). Reassessment of the blocking activity of prazosin at low and high concentrations on sympathetic neurotransmission in the isolated mesenteric vasculature of rats. *J. Auton. Pharmacol.*, **8**, 303–309.

YAMAMOTO, R., TAKASAKI, K. & NICKOLS, G.A. (1992). Purinergic vasoconstrictor component revealed by moderate cooling in the isolated mesenteric vasculature of Sprague-Dawley rats. *J. Pharmacol. Exp. Ther.*, **262**, 1133–1138.

ZIGANSHIN, A.U., HOYLE, C.H.V., BO, X., LAMBRECHT, G., MUTSCHLER, E., BÄUMERT, H.G. & BURNSTOCK, G. (1993). PPADS selectively antagonizes P_{2x}-purinoceptor-mediated responses in the rabbit urinary bladder. *Br. J. Pharmacol.*, **110**, 1491–1495.

ZIGANSHIN, A.U., HOYLE, C.H.V., LAMBRECHT, G., MUTSCHLER, E., BÄUMERT, H.G. & BURNSTOCK, G. (1994). Selective antagonism by PPADS in rabbit isolated blood vessels. *Br. J. Pharmacol.*, **111**, 923–929.

ZIYAL, R., PFAFF, O., WINDSCHEIF, U., BO, X., NICKEL, P., ARDANUY, U., BURNSTOCK, G., MUTSCHLER, E. & LAMBRECHT, G. (1994). A novel P_2-purinoceptor ligand which displays selectivity for the P_{2x}-subtype. *Drug Dev. Res.*, **31**, 336.

(Received February 4, 1994
Revised June 22, 1994
Accepted July 6, 1994)

Br. J. Pharmacol. (1994), **113**, 1022–1028 © Macmillan Press Ltd, 1994

Role of Ca^+-dependent K-channels in the membrane potential and contractility of aorta from spontaneously hypertensive rats

Eneida G. Silva, Eugenio Frediani-Neto, Alice T. Ferreira, Antonio C.M. Paiva & [1]Therezinha B. Paiva

Department of Biophysics, Escola Paulista de Medicina, 04023-062 São Paulo, SP, Brazil

1 Contractile responses to KCl and membrane potentials were determined in aortic rings from spontaneously hypertensive rats (SHR), normotensive Wistar rats (NWR) and Wistar Kyoto rats (WKY) both in the absence and in the presence of the Ca^{2+}-dependent K-channel blockers, apamin and tetraethylammonium (TEA).

2 Compared to NWR, aortic rings from WKY and SHR were less reactive and their Ca^{2+} uptake after stimulation with K^+ was decreased.

3 Smooth muscle cell membrane potentials were higher in aortae from SHR and WKY than in NWR aortae, whereas SHR had higher K^+ and lower Na^+ intracellular activities than WKY and NWR, suggesting overactivity of the Na^+/K^+ pump in the hypertensive animals.

4 Treatment with apamin caused depolarization of WKY and SHR aortae, and increased their contractile responses to the same level as those of the NWR. Treatment with TEA also caused depolarization of aortae from WKY and SHR, but in the SHR the depolarization induced by TEA was smaller than that produced by apamin and the contractile responses to KCl did not reach the level of those of aortae from NWR.

5 It is concluded that overactivity of Ca^{2+}-dependent K-channels in aortae of WKY and SHR contributes to their higher membrane potentials and lower responsiveness to vasoconstrictor stimuli. In SHR, an overactive Na^+/K^+ pump is also present, and the contribution of apamin-sensitive Ca^{2+}-dependent K-channels to the membrane potential and reactivity appears to be more relevant than that of TEA-sensitive channels.

Keywords: Aorta; Ca^{2+}-dependent K-channels; hypertension; membrane potential; smooth muscle contraction; spontaneously hypertensive rats

Introduction

In order to understand the mechanisms underlying hypertension, several studies on vascular reactivity have been conducted in hypertensive animals. In conductance vessels, such as the aorta, preparations from spontaneously hypertensive rats (SHR) show decreased contractility when compared to those of normotensive Wistar rats (NWR) (Spector *et al.*, 1969; Shibata *et al.*, 1973).

Control of the membrane potential is critical for determining vascular contractility (Harder & Hermsmeyer, 1983; Nelson *et al.*, 1990), and in aortic smooth muscle Ca^{2+}-dependent K-channels seem to make an important contribution to the membrane potential (Sadoshima *et al.*, 1988; Shoemaker & Worrel, 1991) and therefore to Ca^{2+}-influx and vascular contractility. Single channel measurements (Shoemaker & Worrel, 1991; England *et al.*, 1993) showed that Ca^{2+}-dependent K^+ currents are increased in the SHR aorta when compared to those of normotensive controls.

In the present work we have explored the contributions of membrane potential, calcium influx and Ca^{2+}-dependent K-channels to the reported decreased contractility of SHR aortae. Thus, we attempted to characterize further the Ca^{2+}-dependent K-channels involved, by measuring the effects of tetraethylammonium (TEA) and apamin on the membrane potential and contractility of aortae from SHR, from their normotensive Wistar Kyoto controls (WKY) and from NWR. We also measured the intracellular concentrations of sodium and potassium, as well as the K^+-induced Ca^{2+} influx, in aortic smooth muscle cells from these three animal strains. Our results suggest that the low contractility of SHR aortae may be ascribed to hyperpolarization of the smooth muscle cell membrane, which is due, at least in part, to an overactive Na^+/K^+ pump, to stimulated Ca^{2+}-dependent K-channels (particularly those of the apamin-sensitive type) and to decreased voltage-dependent Ca^{2+} influx.

[1] Author for correspondence.

Methods

Animals

The Okamoto-Aoki strain of female SHR (170–190 g body weight) and their Wistar-Kyoto normotensive controls (WKY, 210–230 g body weight) were derived from an original colony supplied by the National Institutes of Health, Bethesda, MD, U.S.A. Normotensive Wistar rats (NWR, 190–215 g body weight) were from a colony inbred at the Escola Paulista de Medicina. The animals were of similar age (20–30 weeks).

Tension measurements

The animals were decapitated and bled, the thoracic aorta was removed and placed in Krebs-bicarbonate solution of the following composition (in mM): NaCl 118, KCl 4.7, $CaCl_2$ 2.5, KH_2PO_4 1.18, $MgSO_4$ 1.18, $NaHCO_3$ 25, glucose 10 (pH 7.40). Rings of 1-cm length were cut and everted. A plastic rod was inserted through the lumen and the edge of the blood vessel was pulled with the help of a pair of tweezers, thus inverting the ring. The endothelium was removed by rubbing with a thin plastic rod wrapped in cotton. The presence or absence of a functional endothelium was tested in all preparations by checking whether acetylcholine induced relaxation of the preparations, a response

which is characteristic for vessels with an intact endothelium (Furchgott, 1981). The preparations were mounted in chambers containing 6.0 ml of Krebs-bicarbonate solution under the optimum passive tension of 1 g, previously determined as described by Gleason *et al.* (1985). The temperature was kept at 37 ± 0.5°C and the solution was bubbled with a gas mixture of 95% O_2 and 5% CO_2. After an equilibration period of 2 h the isometric contractile responses were recorded.

Cumulative dose-response curves were obtained by stepwise increase of the concentration of KCl, performed in the presence of 10^{-6} M phentolamine to exclude a possible influence of endogenous catecholamine release. These experiments were done both in the absence and in the presence of TEA (1 mM) or apamin (100 nM) added to the bath 20 or 7 min before the addition of KCl, respectively.

Measurement of cellular Na^+ content

Aortae from SHR, WKY and NWR were mounted on small plates and kept under tension in a bath containing Krebs-bicarbonate solution to which ^{99m}Tc-diethyleneaminepentaacetic acid was added in a final concentration of 2.5 μCi ml^{-1}. The tissues were equilibrated for 20 min in this medium and then transferred to tubes containing non-radioactive solution. The radioactivity in the tissues was counted in a gamma counter (Nucleopan-Siemens), after which they were dried by blotting with filter paper, and the wet weight was determined. The dry weight was also measured after the tissues were kept for 20 h in an oven at 100°C. The tissues were then ashed in beakers containing 0.5 ml of a mixture of equal amounts of HNO_3 (61 g per 100 ml H_2O) and $HClO_4$ (60 g per 100 ml H_2O), then dissolved in 0.01 N HCl, and the electrolytes were analyzed by atomic emission spectroscopy.

The extracellular space was calculated from the ratio of the radioactivities in the tissue and in the experimental solution (McAfee *et al.*, 1979). The intracellular Na^+ concentration (in mmol kg^{-1}) was calculated by subtracting from the total Na^+ content (in mmol kg^{-1}) the product of the extracellular Na^+ concentrtation (in mmol l^{-1}) and the extracellular space (in $l.kg^{-1}$).

Measurements of cell membrane potential (V_m) intracellular potassium activity (a^i_K) and intracellular sodium activity (a^i_{Na})

Microelectrodes were constructed as previously described (Harvey & Kernan, 1984) by pulling double-barrelled capillaries in a horizontal puller (Narishige model PN3). The thicker barrel was siliconized, its tip was filled with either potassium or sodium ion exchanger and the volume was completed respectively with either 0.1 M KCl or 0.5 M NaCl solution. The reference barrels (narrower) were filled with either a 1:3 (v:v) mixture of 1 M NaCl and 1 M sodium acetate solutions (potassium microelectrode) or with 1 M KCl (sodium microelectrode) and were used to measure membrane potential. The resistance of the reference barrels ranged between 150 and 200 × 10^6 Ω and their tip potential was less then 5 mV.

The properties of the potassium electrodes were tested in solutions containing 10, 50, 100 and 150 mM KCl, and in isotonic solutions containing mixtures of KCl and NaCl in different proportions. The resistance of the selective barrel averaged 3.75 ± 0.48 × 10^9 Ω and a potential change of 59.8 ± 0.8 mV ($n = 20$) was found for a decade change in a_K. The selectivity coefficients of the electrodes ($K_{K/Na}$) averaged 0.016 ± 0.007, indicating that the interference from Na^+, and hence the possible error in the a^i_K, was small. Therefore, a^i_K was calculated by means of the following equation:

$$a^i_K = a^e_K \times 10^{(\Delta V s^{-1})}$$

where a^e_K is the extracellular potassium activity, ΔV is the difference between the voltages recorded in the selective barrel and in the reference barrel and S is the slope of the selective electrode's calibration curve.

The sodium electrodes were tested in pure NaCl solutions (5, 10, 35 and 70 mM) and in isotonic solutions prepared with KCl in different proportions. Their resistances averaged 1.2 ± 0.1 × 10^{11} Ω, and a potential change of 53.0 ± 1.5 mV ($n = 40$) was found for a decade change in Na^+ activity. Their selectivity coefficient ($K_{Na/K}$) averaged 0.020 ± 0.004, and consequently, no correction for interferent ion (K^+) was necessary. a^i_{Na} was calculated by means of the following equation:

$$a^i_{Na} = a^e_{Na} \times 10^{(\Delta V s^{-1})}$$

The electrodes were mounted in Ag/AgCl half-cells on a micromanipulator (Leitz) and connected to the two channels of an electrometer (WP Instruments, model FD223). The signals from the reference and differential channels were also recorded on a potentiometric chart recorder (ECB, model RB102).

The preparations were placed in a 2-ml chamber and superfused at a rate of 3 ml min^{-1} with Krebs-bicarbonate solution at 37°C, bubbled with a gas mixture containing 5% CO_2 and 95% O_2. As the microelectrode was inserted into the cell from the intimal side, everted rings were used. The experiments were performed in preparations that had been previously mounted under a tension of 1 g during the 2 h that preceded the impalements. Some measurements of membrane potential were also carried out in rings that had been incubated for 7 min with 100 nM apamin or for 20 min with 1 mM TEA before the impalements.

The criteria for accepting an impalement were: (a) abrupt change in the potential recorded with microelectrodes upon entry and withdrawal from the cell; (b) stable potential (± 3 mV) for at least 1 min after impalement; (c) minimal changes in microelectrode tip potential (<20%) and resistance (<10%) after impalement; (d) reproducible calibration curves of the ion-selective barrel before and after experiments. According to the electrical characteristics (Firth & De Felice, 1971), the average diameter of the electrode tip was estimated to be ca. 0.2 μm.

Cell culture

Primary cultures of smooth muscle cells were obtained from the tunica media of NWR, WKY and SHR thoracic aorta as previously described (Yamamoto *et al.*, 1983; Chamley *et al.*, 1985). The cells were dispersed by incubating the tissue with solution containing 1 mg ml^{-1} collagenase type I, 12 u ml^{-1} elastase type I and 1% bovine serum albumin at 37°C for 2 h in humidified atmosphere of 5% CO_2 and 95% air. The cells were seeded in 35-mm Falcon tissue culture dishes (10^5 cells/dish) and grown in Dulbecco's Modified Eagle Medium containing 10% foetal bovine serum, 100 u ml^{-1} penicillin and 100 μg ml^{-1} streptomycin. Every three days the medium was renewed, and the cells were confluent after approximately 10 days, when they were subcultured. The identity and homogeneity of the cells were indicated by positive fluorescence with antibodies against myosin and actin (Yamamoto *et al.*, 1983). The viability of the cells was determined by the trypan blue exclusion method and was found to be greater than 90%. Cultures seeded at the same time were used in each experiment.

Ca^{2+} uptake

The culture medium was removed and the cells were rinsed and incubated for 1 h at 37°C in a physiological salt solution (PSS) of the following composition (in mM): NaCl 137, KCl 2.7, $MgCl_2$ 0.49, $CaCl_2$ 1.36, glucose 5.5 and HEPES 10. After this period of equilibration, 1 ml of the PSS and 2 μCi

of $^{45}Ca^{2+}$ were added to the plates in the absence (controls) or presence of 50 mM KCl. After 120 s, the assay medium was siphoned off and the cells were quickly rinsed twice with 1 ml of ice-cold 0.1 M $MgCl_2$ solution containing 10 mM HEPES and 10 mM $LaCl_3$. The plates were then quickly rinsed by successively dipping in three beakers containing 500 ml of ice-cold 0.1 M $MgCl_2$ (with 10 mM HEPES). Intracellular $^{45}Ca^{2+}$ was extracted with 1 ml of 0.1 N NaOH and the radioactivity was measured by liquid scintillation counting. The Ca^{2+} uptake in the controls was defined as 100% in each strain and after exposure to KCl stimulation the uptake was calculated as a percentage of the controls.

Drugs

Apamin, tetraethylammonium and phentolamine were from Sigma. ^{99m}Tc-diethyleneaminepentaacetic acid was from IPEN (São Paulo, Brazil).

Statistics

Mean values of individual data points from the concentration-response curves were analyzed by one-way analysis of variance followed by the Newman-Keuls test (Snedecor & Cohran, 1976) to compare results in NWR, WKY and SHR aortae, or employing Student's t test for paired data to compare results in treated and untreated aortae from each strain. The measurements of membrane potentials, intracellular K^+ and Na^+ activities and Ca^{2+} uptake were compared by using one-way analysis of variance followed by the Newman-Keuls test. A probability of $P<0.05$ was considered significant.

Results

Mechanical responses to high K^+

Dose-response curves to K^+ were obtained in aortic rings under hyperosmotic conditions in which KCl was simply added to the medium to attain the desired concentration. Figures 1a and 2a show that the contractile responses to K^+ were significantly higher for NWR than for WKY and SHR. Some experiments were also performed under isosmotic conditions, by the replacement of NaCl in the Krebs solution, and similar results were obtained (data not shown).

Incubation with apamin (100 nM) did not affect the responses of aortic rings from NWR, but caused a marked enhancement in the WKY and SHR responses, which reached the same level of the NWR responses (Figure 1b).

When the preparations were incubated with 1 mM TEA (Figure 2b) the responses of the NWR aortae were unaltered, whereas those of the WKY aortae increased significantly, up to the level of the NWR responses. The responses of the SHR aortae were little affected by TEA, with only the lower portion of the dose-response curve being significantly raised.

The TEA and apamin concentrations used in these experiments (1 mM and 100 nM, respectively) did not produce contraction in the aortic preparations from any of the three strains. Preparations which were previously treated with TEA (1 mM) showed contractile responses to apamin concentrations in the range from 200 to 700 nM (data not shown), indicating that 1 mM TEA was not inhibiting apamin-sensitive channels.

Membrane potential

Measurements of the membrane potentials of aortic rings from the three strains showed that the SHR preparations were hyperpolarized in relation to those from the two normotensive controls. The membrane potential of aortic rings from WKY had an intermediate value between those of SHR and NWR (Figure 3).

After incubation with apamin (100 nM), a significant depolarization was observed in aortic rings from WKY and SHR but not in those from NWR. Treatment with TEA (1 mM) also caused a significant depolarization in WKY and SHR. The depolarization induced by TEA in SHR aortae, however, was smaller than that induced by apamin. Some original records of membrane potential both in the absence and in the presence of apamin are shown in Figure 4.

Intracellular K^+ and Na^+

Intracellular K^+ and Na^+ activities were measured by impaling aortic smooth muscle cells from rings that were previously stretched under the same conditions that occurred in the preparations used for the tension measurement experiments (1 g for 2 h).

Table 1 shows that the K^+ activity was higher and the Na^+ activity was lower in aortic rings from SHR than in those from NWR and WKY, which did not differ from each

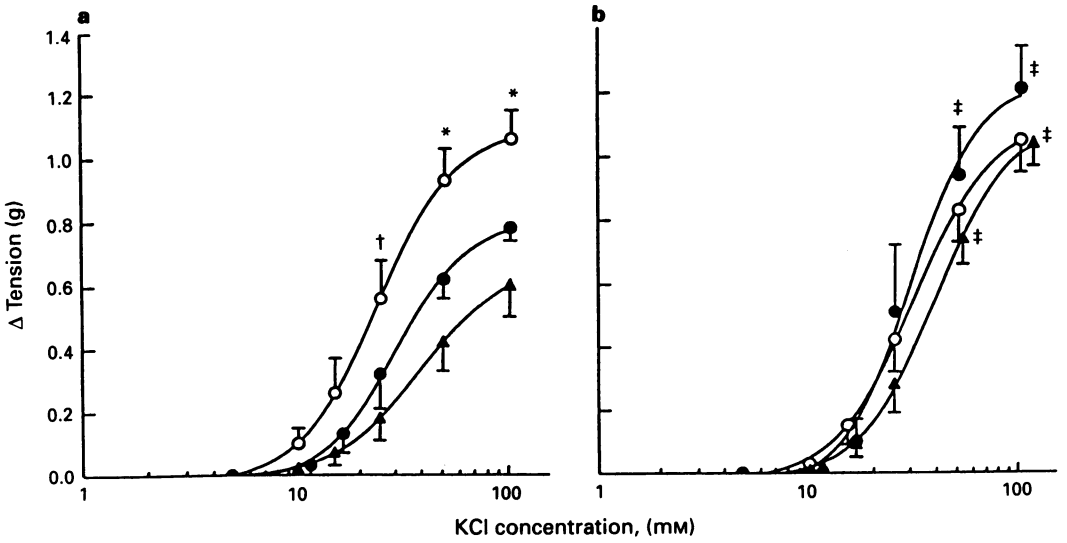


Figure 1 Responses of aortic rings from NWR (○, $n = 8$), WKY (●, $n = 5$) and SHR (▲, $n = 8$) to cumulative increases in KCl concentration in the absence (a) and in the presence (b) of apamin (100 nM). Data are means with s.e.means. *Significantly different from WKY and SHR. †Significantly different from SHR. ‡Significantly different from the respective controls without apamin ($P<0.05$).

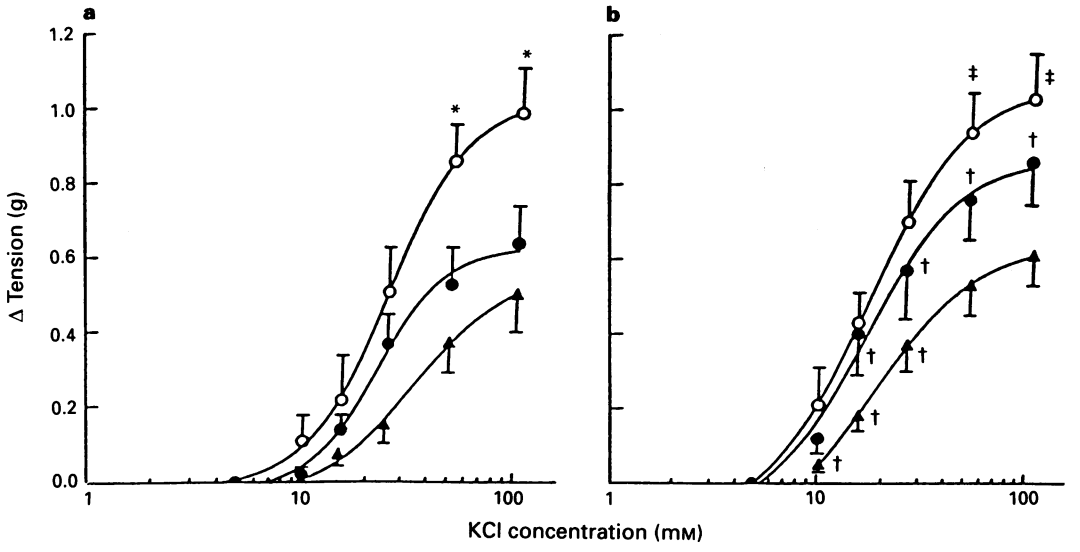


Figure 2 Responses of aortic rings from NWR (○, $n = 5$), WKY (●, $n = 6$) and SHR (▲, $n = 7$) to cumulative increases in KCl concentration in the absence (a) and in the presence (b) of TEA (1 mM). Data are means with s.e.means. *Significantly different from WKY and SHR. †Significantly different from the respective controls without TEA. ‡Significantly different from SHR ($P < 0.05$).

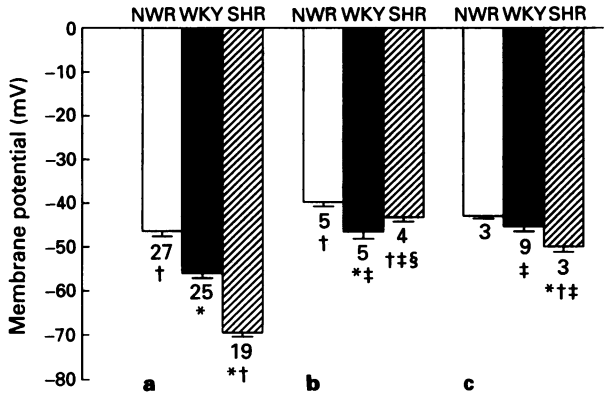


Figure 3 Membrane potentials of aortic rings from NWR, WKY and SHR in the absence (a) and in the presence of 100 nM apamin (b) or TEA 1 mM (c). Values are means and the s.e.means of the number of experiments are given below the columns. *Significantly different from NWR. †Significantly different from WKY. ‡Significantly different from the respective controls without apamin or TEA. §Significantly different from the respective measurements in the presence of TEA ($P < 0.05$).

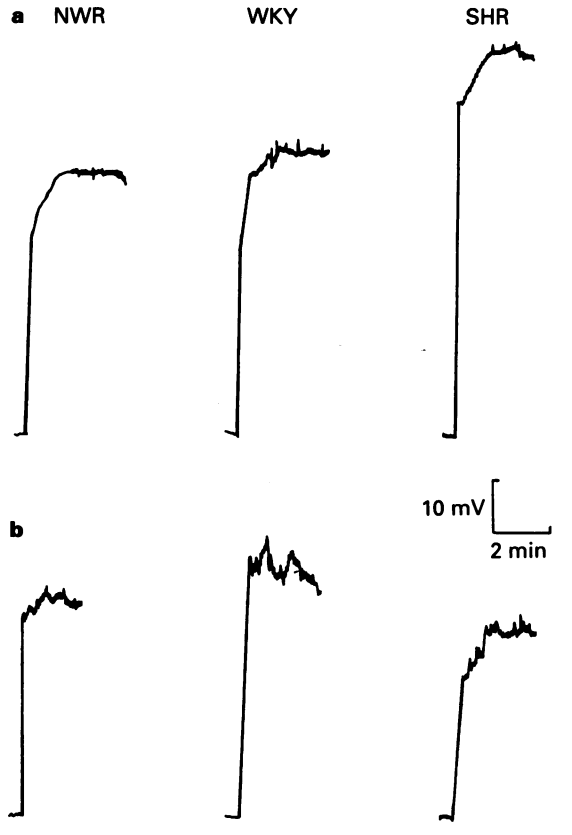


Figure 4 Original records of measurements of membrane potential obtained from aortae of NWR, WKY and SHR in the absence (a) and in the presence of 100 nM apamin (b).

other. These results were corroborated by the measurements of the intracellular Na^+ content performed by chemical analysis, which showed significantly lower values in SHR than in either NWR or WKY (Table 1).

Equilibrium potential for potassium

The values of equilibrium potential for potassium (E_K) were calculated from the values of the intracellular K^+ activity (a^i_K) measured in aortae from NWR, WKY and SHR, by using the Nernst equation. Table 2 shows that, although the E_K values differed from the respective membrane potentials in aortic preparations from WKY and SHR, the difference was significantly more pronounced in preparations from NWR.

Ca^{2+} uptake

The results of the measurements of Ca^{2+} uptake in cultured aortic cells from NWR, WKY and SHR in response to KCl (50 mM) are shown in Figure 5. The stimulation of the cells with KCl for 120 s induced an uptake of Ca^{2+} which was significantly higher in NWR (74.3 ± 7.3% in relation to the control without KCl) than in WKY (29.5 ± 11.5%) and SHR (11.5 ± 1.5%) cells. The basal values of Ca^{2+} uptake in a representative triplicate were 0.52 ± 0.03, 0.65 ± 0.09 and 0.65 ± 0.17 nmol/10^6 cells. 120 s in aortic cells from NWR, WKY and SHR, respectively.

Table 1 Potassium activity, sodium activity and sodium content values for rings of NWR, WKY and SHR aortae

Preparation	*Potassium activity* (mM)	*Sodium activity* (mM)	*Sodium content* (mmol kg^{-1})
NWR	62.1 ± 5.8 (11)	16.4 ± 1.2 (15)	36.3 ± 3.4 (10)
WKY	53.5 ± 5.1 (10)	14.0 ± 0.7 (15)	37.4 ± 4.4 (11)
SHR	79.7 ± 3.7 (9)*	9.0 ± 0.5 (10)*	23.6 ± 4.3 (10)*

Intracellular potassium and sodium activities were measured with potassium and sodium-sensitive microelectrodes, and sodium content was measured by atomic emission spectroscopy. Values are means and the s.e.means of the number of experiments are shown in parentheses. *Significantly different from NWR and WKY ($P<0.05$).

Table 2 Membrane potential (V_m) and equilibrium potential for potassium (E_K) in aortae from NWR, WKY and SHR

Preparation	V_m (mV)	E_K (mV)
NWR	−46.9 ± 1.2 (27)*	−68.9 ± 2.3 (11)
WKY	−56.0 ± 1.1 (15)*	−65.1 ± 2.1 (10)
SHR	−69.5 ± 0.9 (19)*	−76.3 ± 1.2 (9)

Membrane potentials were measured with microelectrodes and the K^+ equilibrium potentials were determined from the intracellular potassium activities by using the Nernst equation. Values are means and s.e.mean of the number of experiments shown in parentheses. *Significantly different from the respective values of E_K ($P<0.05$).

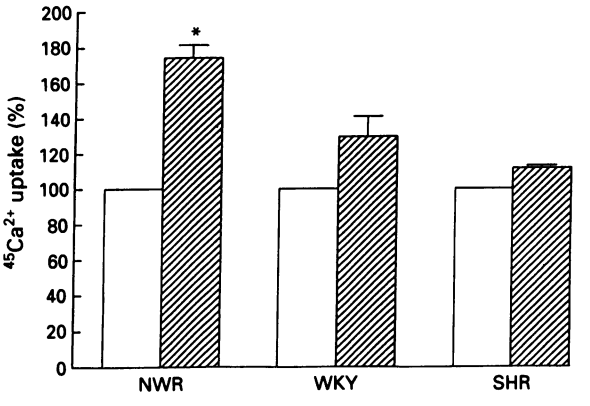


Figure 5 Ca^{2+} uptake in aortic cells of NWR ($n = 3$), WKY ($n = 2$) and SHR ($n = 2$) in response to the stimulation with KCl (50 mM) for 120 s. Ca^{2+} uptake after KCl stimulation was calculated as a percentage of the controls. Each experiment was made in triplicate and the values are means with s.e.means. *Significantly different from WKY and SHR ($P<0.05$).

Discussion

Previous work has shown that preparations from SHR have decreased contractility when compard to those of normotensive Wistar rats (Spector *et al.*, 1969; Shibata *et al.*, 1973). We have observed, however, that WKY aortae are also less reactive than those of NWR to stimulation with potassium (Figures 1a and 2a). Apparently, some properties of smooth muscles from WKY may be closer to those of the SHR than to those of NWR, and therefore may not be pertinent to the hypertensive state. Thus, previous work from our laboratory showed that duodenum preparations from both WKY and SHR develop contractile responses to bradykinin, which are not observed in those from NWR (Feres *et al.*, 1992a).

The lower reactivity of SHR and WKY aortae may be due to the fact that their smooth muscle cell membranes are hyperpolarized in relation to those of NWR. In fact, Figure 3 shows that the membrane potential mesured in aortic smooth muscle cells is larger in WKY than in NWR and larger in SHR than in WKY aortae. This finding differs from that of England *et al.* (1993), who reported comparable membrane potentials in current clamped cells of WKY and SHR. However, these authors recognized that membrane potential values obtained by current clamp methods are somewhat less reliable than those measured with microelectrode methods. Tomobe *et al.* (1992), however, used microelectrode measurements and found SHR aortae to be less polarized than those of WKY. This divergence from our results might be related to the fact that these authors used aortic strips, which were shown to be depolarized in comparison to aortic rings, possibly because of Na^+ leakage into the cells due to lesions made during preparation of the strips (Frediani-Neto *et al.*, 1991).

To obtain further information on the status of our cells, we also measured the intracellular Na^+ and K^+ activities by using ion-selective microelectrodes, a technique not previously employed in aortae from hypertensive rats. Table 1 shows that the intracellular activity of K^+ is higher and that of Na^+ is lower in aortic preparations of SHR than in those of WKY and NWR. The lower intracellular content of Na^+ in SHR aortae was also evidenced through measurements done by chemical analysis. These findings indicate that the sodium pump is more active in aortae from SHR than in those of WKY and NWR, and are in agreement with the previous findings that SHR aortae are more responsive to ouabain and to K^+-free solutions, when compared with WKY (Moreland *et al.*, 1986). Moreover, an overactive sodium pump may explain the hyperpolarized membrane potential that we observed in SHR aortae.

It is known that the contractile responses to potassium are dependent on the influx of calcium from the extracellular medium through voltage-dependent calcium channels (Van Breemen *et al.*, 1972). Since we found that the cellular membranes of aortae from WKY and SHR were more polarized than those of NWR aortae, it is possible that a smaller number of calcium channels is activated during stimulation by potassium, resulting in reduced Ca^{2+} influx and decreased responses of the WKY and SHR aortae in relation to those of NWR. The smaller Ca^{2+} uptake observed in K^+-stimulted aortae from WKY and SHR in relation to those from NWR (Figure 4) supports this idea.

We have also investigated further the hypothesis that Ca^{2+}-dependent K-channels are involved in the differences observed in the behaviour of aortae from SHR, WKY and NWR. Three basic types of Ca^{2+}-dependent K-channels have been reported in muscle cells: (a) a large-conductance (135–250 pS) voltage-dependent channel which is inhibited by concentrations of TEA below 1 mM, described in a variety of non-vascular and vascular smooth muscle cells (Sadoshima *et al.*, 1988; Nelson *et al.*, 1990; Brayden *et al.*, 1992); (b) a weakly voltage-dependent channel with intermediate conductance (55 pS), described in vascular smooth muscle cells (Shoemaker & Worrel, 1991); (c) a small-conductance (10–14 pS) channel which is voltage-independent and is specifically blocked by apamin, described in many tissues (Romey & Lazdunski, 1984; Blatz & Magleby, 1986; Feres *et al.*, 1992b), although not as yet in vascular smooth muscle cells. An increase in the activity of any of these channels would lead to the augmented K^+ permeability described in aortae from hypertensive rats (Jones, 1973; Tamura *et al.*, 1986; Nakamura *et al.*, 1988) and could also result in alterations of vascular membrane potential and contractility.

We have studied the effect of the two Ca^{2+}-dependent K-channel blockers, apamin and TEA, on the contractile responses to K^+ and on the membrane potential of aortae from the three rat strains. In tension measurement experiments (Figure 1), we found that the contractile responses to K^+, which were relatively impaired in SHR and

WKY, were enhanced by treatment with apamin, reaching the level of the responses of the NWR aortae. Treatment with TEA also increased the responses of WKY and SHR aortae, but those of the WKY were significantly more enhanced than those of the SHR (Figure 2). This suggests that either the inhibition by 1 mM TEA was not specific, affecting also apamin-sensitive channels, or that both apamin-sensitive and TEA-sensitive channels may be involved in the lower reactivity of WKY and SHR aortae to K^+. In any case, the impaired SHR responses to K^+ are more dependent than those of WKY on apamin-sensitive channels.

The hypothesis that an increased activity of Ca^{2+}-dependent K-channels may contribute to the hyperpolarized state of smooth muscle membranes of aortae from WKY and SHR was also investigated by studying the effect of apamin and TEA on the membrane potentials. When the aortic rings from NWR were incubated with TEA or apamin, no changes in the membrane potential were observed in relation to the non-treated controls, but preparations from WKY and SHR were significantly depolarized (Figure 3), indicating that the activities of apamin- and TEA-sensitive Ca^{2+}-dependent K^+ channels are enhanced in aortae from both WKY and SHR. However, as the depolarization induced by both Ca^{2+}-dependent K^+ channel blockers was higher in aortae from SHR than in those from WKY, the activity of these channels is probably higher in the SHR than in WKY. In addition, whereas WKY aortae were equally depolarized by TEA and apamin, the depolarization induced by apamin in the SHR was greater than that induced by TEA. These results, together with those of the tension measurements discussed above, suggest that the contribution of the apamin-sensitive channels may be more important in SHR aortae than that of TEA-sensitive Ca^{2+}-dependent K^+ channels to the maintenance of an increased membrane potential and decreased reactivity.

Our results are partly in agreement with recent observations obtained from single channel measurements. Rusch *et al.* (1992) have established a link between K-channel modulation and Ca-channel activation in SHR aorta. Shoemaker & Worrel (1991) described intermediate conductance channels the open probability of which was higher in SHR than in WKY aortae and also higher in WKY than in NWR aortae. England *et al.* (1993) found that high conductance Ca^{2+}-dependent K^+ channels were more active in SHR than in WKY aortic cells. However, these reports do not mention the low-conductance apamin-sensitive channels, the existence of which is suggested by our present results.

The activity of the Ca^{2+}-dependent K-channels of smooth muscles (Singer & Walsh, 1984; Cecchi *et al.*, 1986) and other kinds of cells (French & Wells, 1977; Yellen, 1984) can be reduced by internal Na^+ ions. Thus, besides the intrinsic overactivity of these channels in hypertensive animals reported by Shoemaker & Worrel (1991) and England *et al.* (1993), they may also be activated by a lower intracellular Na^+ concentration due to the increased activity of the Na^+/K^+ pump that we have observed in aortae from SHR. Moreover, it has been demonstrated that the intracellular Ca^{2+} concentration is increased in SHR vascular smooth muscles (Bohr & Webb, 1988), including the aorta (Sada *et al.*, 1990), and this could also result in the increased activity of Ca^{2+}-dependent K-channels.

Thus, our results suggest that the higher membrane potential and the lower contractility observed in WKY and SHR in relation to NWR aortae could rather be attributed to an increased activation of Ca^{2+}-dependent K-channels related both to the rat strain and to hypertension. In SHR and WKY, but not in NWR aortae, the values for E_K are very close to the respective calculated values of membrane potential (Table 2) which could indicate that the permeability for potassium is increased in aortae from these animals. However, in SHR, but not in WKY, an increased activity of the Na^+/K^+ pump and the consequent decrease in the intracellular Na^+ concentration could favour the activation of the Ca^{2+}-dependent K^+ channels, contributing to the more polarized state of the SHR aorta.

This work was supported by a grant from Financiadora de Estudos e Projetos (FINEP) and the technical assistance of Nelson A. Mora is gratefully acknowledged.

References

BLATZ, A.L. & MAGLEBY, K.L. (1986). Single apamin-blocked Ca^{2+}-activated K-channels of small conductance in cultured rat skeletal muscle. *Nature*, **323**, 718–720.

BOHR, D.F. & WEBB, R.C. (1988). Vascular smooth muscle membrane in hypertension. *Annu. Rev. Pharmacol. Toxicol.*, **28**, 389–400.

BRAYDEN, J.E. & NELSON, M.T. (1992). Regulation of artrial tone by activation of calcium-dependent potassium channels. *Science*, **256**, 532–535.

CECCHI, X., ALVAREZ, O. & WOLFF, D. (1986). Characterization of a calium-activated potassium channel from rabbit intestinal smooth muscle incorporated into planar bilayers. *J. Membrane Biol.*, **91**, 11–18.

CHAMLEY, J.H., CAMPBELL, G.R., McCONNELL, J.D. & GROSCHEZ. V. (1985). Comparison of vascular smooth muscle cells: effects of angiotension II and vasopressin. *J. Biol. Chem.*, **260**, 7836–7842.

ENGLAND, S., WOOLDRIDGE, T.A., STEKIEL, W.J. & RUSCH, N.J. (1993). Enhanced single-channel K^+ current in arterial membranes from genetically hypertensive rats. *Am. J. Physiol.*, **264**, H1337–H1345.

FERES, T., PAIVA, A.C.M. & PAIVA, T.B. (1992a). BK_1 and BK_2 bradykinin receptors in the rat duodenum smooth muscle. *Br. J. Pharmacol.*, **107**, 991–995.

FERES, T., VIANA, L.M., PAIVA, A.C.M. & PAIVA, T.B. (1992b). Effect of treatment with vitamin D_3 on the response of spontaneously hypertensive rats to bradykinin and to potassium. *Br. J. Pharmacol.*, **105**, 881–884.

FIRTH, D.R. & DE FELICE, L.J. (1971). Electrical resistance and volume flow in glass microelectrodes. *Can. J. Physiol Pharmacol.*, **49**, 436–447.

FREDIANI-NETO, E., SILVA, E.G., PAIVA, T.B. & PAIVA, A.C.M. (1991). Increased intracellular Na^+ and depolarization favor angiotensin tachyphylaxis in rabbit aorta. *Am. J. Physiol.*, **260**, H373–H378.

FRENCH, R.J. & WELLS, J.B. (1977). Sodium ions as blocking agents and charge carriers in the potassium channel of the squid giant axon. *J. Gen. Physiol.*, **70**, 707–724.

FURCHGOTT, R.F. (1981). The requirement for endothelial cells in relaxation of arteries by acetylcholine and some other vasodilators. *Trends Pharmacol. Sci.*, **2**, 173–176.

GLEASON, M.M., RATZ, P.H. & FLAIM, S.F. (1985). Measurement of calcium flux in tethered rings of rabbit aorta under tension. *Am. J. Physiol.*, **249**, H470–H476.

HARDER, D.R. & HERMSMEYER, K. (1983). Membrane mechanisms in arterial hypertension. *Hypertension*, **5**, 404–408.

HARVEY, B.J. & KERNAN, P. (1984). Intracellular ion activities in frog skin in relation to external sodium and effects of amiloride and/or ouabain. *J. Physiol.*, **349**, 501–517.

JONES, A.W. (1973). Altered ion transport in vascular smooth muscle from spontaneously hypertensive rats. *Circ. Res.*, **33**, 563–572.

MCAFEE, J.G., GAGNE, G., ATKINS, H.L., KIRSCHNER, P.T., REBA, R.C., BLAUFOX, M.D. & SMITH, E.M. (1979). Biological distribution and excretion of DTPA labeled with Tc-99m and In-111. *J. Nucl. Med.*, **20**, 1273.

MORELAND, R.S., MAJOR, T.C. & WEBB, R.C. (1986). Contractile responses to ouabain and K^+-free solution in aorta from hypertensive rats. *Am. J. Physiol.*, **250**, H612–H619.

NAKAMURA, M., NAKAMURA, A., FINE, B. & AVIV, A. (1988). Blunted cGMP response to ANF in vascular smooth cells of SHR. *Am. J. Physiol.*, **255**, C573–C580.

NELSON, M.T., PATLAK, J.B., WORLEY, J.F. & STANDEN, N.B. (1990). Calcium channels, potassium channels and voltage dependence of arterial smooth muscle tone. *Am. J. Physiol.*, **259**, C3–C18.

ROMEY, G. & LAZDUNSKI, M. (1984). The coexistence in rat muscle cells of two distinct classes of Ca^{2+}-dependent K-channels with different pharmacological properties and different physiological functions. *Bioch. Biophys. Res. Commun.*, **118**, 669–674.

RUSCH, N.J., DE LUCENA, R.W., WOOLDRIDGE, T.A., ENGLAND, S.K. & COWLEY Jr, A.W. (1992). A Ca^{2+}-dependent K^+ current is enhanced in arterial membranes of hypertensive rats. *Hypertension*, **19**, 301–307.

SADA, T., KOIKE, H., IKEDA, M., SATO, K., OZAKI, H. & KARAKI, H. (1990). Cytosolic free calcium in aorta in hypertensive rats. *Hypertension*, **16**, 245–251.

SADOSHIMA, J., AKAIKE, N., TOMOIKE, H., KANAIDE, H. & NAKAMURA, M. (1988). Ca-activated K-channel in cultured smooth muscle cells of rat aortic media. *Am. J. Physiol.*, **255**, H410–H418.

SHIBATA, S., KURAHASHI, K. & KUSHII, M. (1973). A possible etiology of contractility impairment of vascular smooth muscle from spontaneously hypertensive rats. *J. Pharmacol. Exp. Ther.*, **185**, 406–417.

SHOEMAKER, R.L. & WORREL, R.T. (1991). Ca^{2+}-sensitive K-channel in aortic smooth muscle of rats. *Proc. Soc. Exp. Biol. Med.*, **196**, 325–332.

SINGER, J.J. & WALSH, J.V. (1984). Large conductance Ca^{++}-activated K-channels in smooth muscle cell membrane. Reduction in unitary currents due to internal Na^+ ions. *Biophys. J.*, **45**, 68–70.

SNEDECOR, G.W. & COCHRAN, W.G. (1976). *Statistical Methods.* Ames, Iowa; Iowa State University Press.

SPECTOR, S., FLEICH, J.H., MALING, H.M. & BRODIE, B.B. (1969). Vascular smooth muscle reactivity in normotensive and hypertensive rats. *Science*, **166**, 1300–1301.

TAMURA, H., HOPP, L., KINO, M., TOKUSHIGE, A., SEARLE, B.M., KHALIL, F. & AVIV, A. (1986). Na^+-K^+ regulation in cultured vascular smooth muscle cells of the spontaneously hypertensive rat. *Am. J. Physiol.*, **250**, C939–C947.

TOMOBE, Y., ISHIKAWA, T., YANAGISAWA, M., KIMURA, S., MAKASI, T. & GOTO, K. (1991). Mechanisms of altered sensitivity to endothelin-1 between aortic smooth muscles of spontaneously hypertensive and Wistar-Kyoto rats. *J. Pharmacol. Exp. Ther.*, **257**, 555–561.

VAN BREEMEN, C., FARINAS, B.R. & GERBA, P. (1972). Excitation-contraction coupling in rabbit aorta studied by the lanthanium method for measuring cellular calcium influx. *Circ. Res.*, **30**, 44–54.

YAMAMOTO, H., KANAIDE, H. & NAKAMURA, M. (1983). Metabolism of glycosaminoglycans of cultured rat aortic smooth mucle cells altered during subculture. *Br. J. Exp. Pathol.*, **64**, 156–165.

YELLEN, G. (1984). Relief of Na^+ block of Ca^{2+}-activated K-channels by external cations. *J. Gen. Physiol.*, **84**, 187–199.

(Received January 18, 1994
Revised July 4, 1994
Accepted July 8, 1994)

Br. J. Pharmacol. (1994), **113**, 1029–1035 © Macmillan Press Ltd, 1994

Paired-pulse depression of the N-methyl-D-aspartate receptor-mediated synaptic potentials in the amygdala

Chiung-Chun Huang & [1]Po-Wu Gean

Department of Pharmacology, College of Medicine, National Cheng-Kung University, Tainan City, Taiwan

1 An *in vitro* slice preparation of rat amygdala was used to study the paired-pulse depression of the N-methyl-D-aspartate (NMDA) receptor-mediated synaptic potential e.p.s.p.$_{NMDA}$.

2 The e.p.s.p.$_{NMDA}$ was isolated pharmacologically by applying a solution containing the non-NMDA receptor antagonist, 6-cyano-7-nitroquinoxaline-2,3-dione (CNQX) and the γ-aminobutyric acid$_A$ ($GABA_A$) blocker picrotoxin and increasing the stimulus intensity.

3 When two stimuli of identical strength were applied in close succession, the second e.p.s.p.$_{NMDA}$ was depressed. This paired-pulse depression was seen with interstimulus intervals of between 100 ms and 2000 ms; the maximal depression was observed at interval of 200 ms.

4 Superfusion of phaclofen or 2-hydroxy-saclofen inhibited the paired-pulse depression indicating the involvement of $GABA_B$ receptors.

5 Bath applications of Ba^{2+} or intracellular injection of Cs^+ to block post- but not presynaptic $GABA_B$ receptors failed to inhibit the paired-pulse depression (PPD).

6 Incubation of slices with pertussis toxin prevented the postsynaptic hyperpolarization induced by baclofen. The PPD of e.p.s.p.$_{NMDA}$, however, was not affected by pertussis toxin treatment.

7 These results suggest that GABA released by the first stimulus acts on $GABA_B$ receptors to suppress the second e.p.s.p.$_{NMDA}$ via mechanisms other than activation of a postsynaptic $GABA_B$ receptor-coupled K^+ conductance.

Keywords: N-methyl-D-aspartate receptor; $GABA_B$ receptor; paired-pulse depression

Introduction

Electrophysiological and immunohistochemical studies have established that γ-aminobutyric acid (GABA) is a major inhibitory neurotransmitter in the amygdala (Le Gal La Salle, 1976; Takagi & Yamamoto, 1981; McDonald, 1985). Synaptic release of GABA from inhibitory interneurones produced a dual component inhibitory postsynaptic potential (i.p.s.p.) in the basolateral amygdala (BLA): a fast, bicuculline-sensitive increase in Cl^- conductance mediated by $GABA_A$ receptors (f-i.p.s.p.), and a late, phaclofen-sensitive increase in K^+ conductance mediated by $GABA_B$ receptors (l-i.p.s.p.) (Rainnie *et al.*, 1991; Gean & Chang, 1992; Washburn & Moises, 1992). The functional role of f-i.p.s.p. is thought to maintain normal levels of amygdalar excitability; blockade of f-i.p.s.p. with bicuculline or picrotoxin invariably leads to the development of epileptiform activity (Gean & Shinnick-Gallagher, 1987). The role of $GABA_B$ receptors is, however, not well understood in this area of the brain.

Recently, it has been demonstrated that the sensitivity of presynaptic $GABA_B$ receptors is reduced in amygdala kindled animals (Asprodini *et al.*, 1992). This suggests that the reduction in $GABA_B$-mediated presynaptic inhibition at excitatory terminals may contribute to the enhancement of glutamatergic transmission (Gean *et al.*, 1989; Rainnie *et al.*, 1992). On the other hand, Hosford *et al.* (1992) have shown that the receptor number but not the equilibrium dissociation constant of $GABA_B$ is increased in neocortical membranes of lethargic mice, a mutant strain with spontaneous seizures. In addition, both proepileptic and antiepileptic effects of baclofen, a $GABA_B$ receptor agonist, have been reported in various *in vivo* and *in vitro* models (Ault & Nadler, 1983; Swartzwelder *et al.*, 1986; Mott *et al.*, 1989; Karlsson *et al.*, 1992). Therefore, it is likely that $GABA_B$ receptors may play both inhibitory and disinhibitory roles in the expression of epileptiform activity, depending on the sites of action.

In the present study, we isolated the N-methyl-D-aspartate (NMDA) receptor-mediated synaptic potential (e.p.s.p.$_{NMDA}$) pharmacologically and found that its amplitude was markedly decreased for a period following the conditioning stimulation. This paired-pulse depression (PPD) of e.p.s.p.$_{NMDA}$ could be reversed by phaclofen or 2-hydroxy-saclofen indicating the involvement of $GABA_B$ receptors. $GABA_B$ receptors are present on the pre- as well as postsynaptic neurones and activation of both sites of $GABA_B$ receptors could be responsible for the paired-pulse inhibition of e.p.s.p.$_{NMDA}$. To determine the site of action, we applied various pharmacological agents known to block the postsynaptic $GABA_B$ receptor-activated K^+ conductance. We found that external Ba^{2+} or internal Cs^+ did not block the PPD. Furthermore, the PPD was unaffected by pertussis toxin pretreatment. These results suggest that the PPD of e.p.s.p.$_{NMDA}$ in the amygdala is produced by activating $GABA_B$ receptors that are not coupled to a Ba^{2+}-sensitive K^+ conductance.

Methods

Brain slices (500 μm in thickness) of the amygdala were prepared from male Sprague-Dawley rats weighing 125–200 g. The rats were decapitated and the brains were quickly removed and submerged in chilled (0–4°C) artificial cerebral spinal fluid (ACSF) of the following composition (in mM): NaCl 117, KCl 4.7, $CaCl_2$ 2.5, $MgCl_2$ 1.2, $NaHCO_3$ 25, NaH_2PO_4 1.2 and glucose 11. The brain was subsequently hemisected and cut transversely. A block of tissue containing the amygdala was dissected from the right hemisphere. Two or three transverse amygdalar slices were obtained with a Vibroslice (Campden Inst.) and placed in a beaker of ACSF oxygenated with 95% O_2:5% CO_2.

The slices were kept at room temperature for at least 1 h before recording. A single slice was then transferred to the

[1] Author for correspondence.

recording chamber where it was held submerged between two nylon nets and maintained at 32 ± 1°C. The chamber consisted of a circular well of a low volume (1–2 ml) and was constantly perfused at a rate of 2–3 ml min^{-1}. A bipolar stimulating electrode was placed in the ventral endopyriform nucleus and stimulated with monophasic constant voltage pulses. The NMDA receptor-mediated synaptic component (e.p.s.p.$_{NMDA}$) was pharmacologically isolated with 6-cyano-7-nitroquinoxaline-2,3-dione (CNQX, 10 μM) and picrotoxin (50 μM). In experiments involving pertussis toxin treatment, slices were incubated in ACSF solution containing pertussis toxin (5 μg ml^{-1}) for at least 7 h before recording. Control preparations were treated with the same protocol in a pertussis toxin-free solution. Previous study on septal neurones has shown that adenosine- and baclofen-induced hyperpolarizing effects were blocked in slices pretreated with pertussis toxin *in vitro* (Hasuo *et al.*, 1992).

Intracellular recordings were made from basolateral amygdala (BAL) neurones by use of glass microelectrodes filled with 3 M KCl (60–120 MΩ). In some experiments, the microelectrodes were filled with 3 M CsCl in order to block postsynaptic $GABA_B$ receptor-mediated K^+ conductance. Electrical signals were amplified using an Axoclamp-2A amplifier and connected to a Data-6100 digital oscilloscope (Data Precision Co.) for data analysis and subsequent plotting of fast transient potentials. All data were expressed as mean ± s.e. Statistical analysis was performed using Student's *t* test, and a *P* value of less than 0.05 was considered to be statistically significant.

All drugs were freshly prepared from stock solutions, dissolved in ACSF and applied by superfusion. DL-2-amino-5-phosphonovalerate (DL-APV), picrotoxin and pertussis toxin were obtained from Sigma Chemicals; 6-cyano-7-nitroquinoxaline-2,3-dione, phaclofen and 2-hydroxy-saclofen from Research Biochemicals Inc.

Results

Stable intracellular recordings were obtained from 63 neurones of control slices and 11 neurones of pertussis toxin-pretreated slices. Twenty out of 63 neurones from control slices were recorded with CsCl-filled microelectrodes. Cells have resting membrane potentials more negative than −55 mV and action potential amplitude greater than 70 mV. The resting membrane potential and neuronal input resistance were −65.7 ± 0.6 mV and 43.5 ± 1.7 MΩ ($n = 43$), respectively. The NMDA receptor-mediated synaptic potential (e.p.s.p.$_{NMDA}$) was isolated pharmacologically by the method of Bashir *et al.* (1991), in which afferent fibres were stimulated in the presence of CNQX (10 μM) and picrotoxin (50 μM) and increasing the stimulus intensity (Bashir *et al.*, 1991). In this study, the e.p.s.p.$_{NMDA}$ has a time to peak of 44.5 ± 1.6 ms with 10–90% duration of 96.7 ± 2.2 ms ($n = 43$).

When two stimuli of identical strength were applied in close succession, the second e.p.s.p.$_{NMDA}$ was depressed in every neurone tested. This paired-pulse depression (PPD) was seen with interstimulus intervals of between 100 ms and 2000 ms; the maximal depression was observed at interval of 200 ms. A representative experiment is illustrated in Figure 1a and the pooled data from 14 cells are shown in Figure 1b. The extent of PPD was dependent on the stimulus strength used; greater depression occurred when higher stimulus intensities were used ($n = 6$). However, higher stimulus intensities appeared to increase the extent of PPD not by reducing the amplitude of second e.p.s.p.$_{NMDA}$, but largely by increasing the amplitude of first e.p.s.p.$_{NMDA}$. Therefore, PPD is not due to a depletion of neurotransmitter stores.

We examined whether $GABA_B$ receptors are involved in PPD by application of $GABA_B$ antagonists. Figure 2a showed that in control medium the amplitude of the second e.p.s.p.$_{NMDA}$ was depressed relative to that of the first.

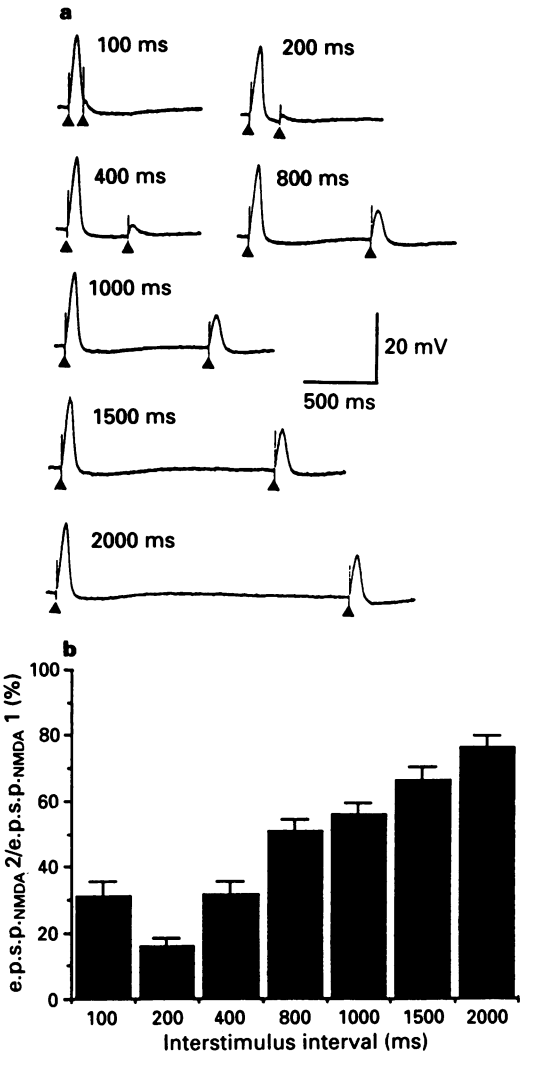


Figure 1 Time course of the paired-pulse depression of e.p.s.p.$_{NMDA}$. (a) Pairs of e.p.s.p.$_{NMDA}$ evoked in the presence of CNQX (10 μM) and picrotoxin (50 μM) by two identical stimuli delivered at intervals of between 100 ms and 2000 ms. The resting membrane potential was −67 mV. (b) Graph of the peak amplitude of the second e.p.s.p.$_{NMDA}$ as a percentage of the first, against interstimulus interval for 14 cells. For abbreviations in this and subsequent legends, see text.

Superfusion with 1 mM phaclofen caused a reduction in e.p.s.p.$_{NMDA}$ (68.0 ± 3.9%, $n = 8$). To quantify the effect, the amplitude of the first e.p.s.p.$_{NMDA}$ in the presence of 1 mM phaclofen was matched to its control level by increasing the stimulus intensity. As illustrated in Figure 2b, phaclofen reduced the percentage depression in 9 of 9 slices. The percentage depressions, at an interstimulus interval of 200 ms, were 84.0 ± 3.3% for control, 23.8 ± 7.5% in the presence of 1 mM phaclofen ($P < 0.001$, $n = 9$) and 86.9 ± 2.4% after washout of phaclofen. We also tested the more potent analogue 2-hydroxy-saclofen (2-OH-saclofen, 200 μM) (Kerr *et al.*, 1988; Bowery, 1989). This agent reversibly reduced the paired-pulse depression in a similar manner. The percentage depressions, at an interstimulus interval of 200 ms, were 88.4 ± 2.4% for control, 35.7 ± 4.1% in the presence of 200 μM 2-hydroxy-saclofen ($P < 0.001$, $n = 7$) and 82.1 ± 4.5% following washout of the 2-hydroxy-saclofen (Figure 3).

Phaclofen (1 mM) and 2-OH-saclofen (200 μM) both depressed the amplitude of the first e.p.s.p.$_{NMDA}$ by 68.0 ± 3.9% ($n = 8$) and 69.7 ± 4.0% ($n = 7$) respectively. However, in the presence of baclofen (5 μM), 2-OH-saclofen did not cause a further suppression of e.p.s.p.$_{NMDA}$. On the

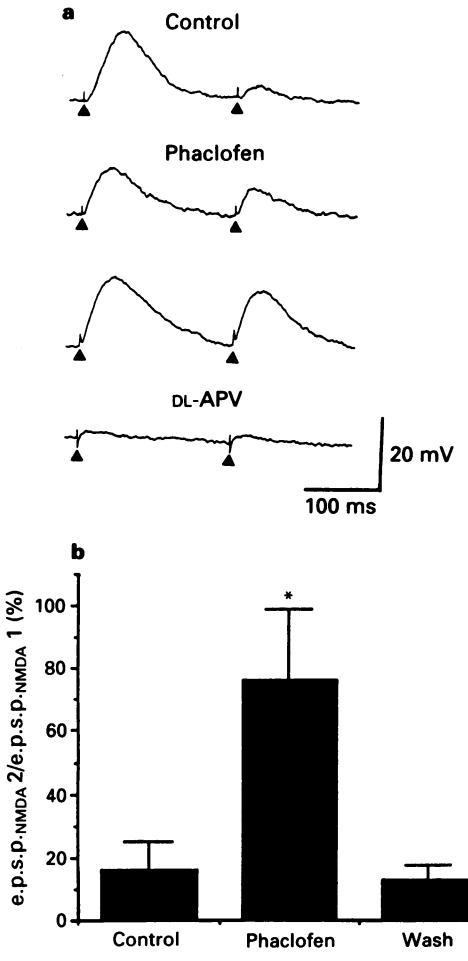


Figure 2 Phaclofen blocks the paired pulse depression (PPD). (a) Intracellular recordings of paired e.p.s.p.$_{NMDA}$s with interstimulus interval of 200 ms. Top tracing: PPD of e.p.s.p.$_{NMDA}$. Second tracing shows that phaclofen (1 mM) blocked the PPD. The amplitude of e.p.s.p.$_{NMDA}$ was substantially depressed by phaclofen. To compensate for this the size of the first e.p.s.p.$_{NMDA}$ of the pairs in the presence of phaclofen was matched to the control by increasing the stimulus intensity. Fourth tracing demonstrates that the e.p.s.p.$_{NMDA}$ could be blocked by DL-APV (50 μM). Resting membrane potential = − 63 mV. (b) Mean percentage depressions in control, during perfusion of phaclofen (1 mM) and after washout of this drug. $n = 9$. $^*P < 0.001$ vs. control.

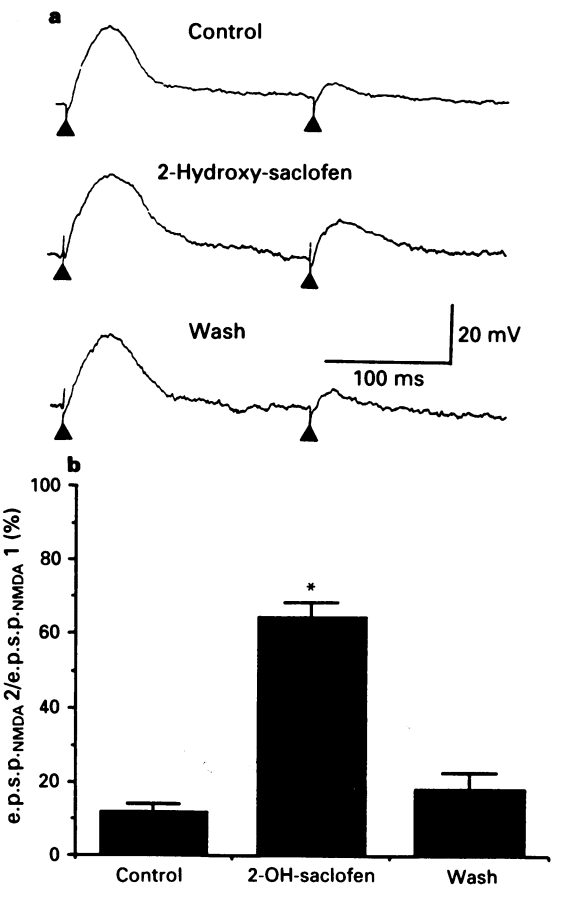


Figure 3 2-Hydroxy-saclofen blocks the paired pulse depression (PPD). (a) PPD of e.p.s.p.$_{NMDA}$ evoked at interstimulus interval of 200 ms under control conditions (top tracing), in the presence of 2-OH-saclofen (200 μM, middle tracing) and after washout of the drug (lower tracing). The amplitude of the first e.p.s.p.$_{NMDA}$ in the presence of 2-OH-saclofen was depressed and was subsequently matched to its initial level by increasing the stimulus intensity. Resting membrane potential = − 68 mV. (b) Mean percentage depressions in control, during perfusion of 2-OH-saclofen (0.2 mM) and after washout of the drug; $n = 7$. $^*P < 0.001$ vs. control.

other hand, 2-OH-saclofen reversed the baclofen-induced presynaptic inhibition (Figure 5d). Similar results were obtained with phaclofen (1 mM, $n = 3$, data not shown). The reduction of the e.p.s.p.$_{NMDA}$ by phaclofen and 2-OH-saclofen and the occluding effect of baclofen on 2-OH-saclofen response are consistent with a partial agonist action of these compounds at presynaptic $GABA_B$ receptors (Kerr *et al.*, 1990).

Phaclofen and 2-OH-saclofen could act as partial agonists, rather than as antagonists, at the presynaptic $GABA_B$ receptors to reduce transmitter release and thereby dininish the PPD observed. We therefore tested if baclofen produced a similar effect on the PPD. We found that application of baclofen (10 nM) mainly decreased the amplitude of first e.p.s.p.$_{NMDA}$ with little effect on the second e.p.s.p.$_{NMDA}$; consequently the extent of PPD was reduced. However, when the amplitude of first e.p.s.p.$_{NMDA}$ was increased by increasing the stimulus intensity to obtain the comparable amplitude in the pre-baclofen condition, the degree of PPD was little affected ($n = 6$, data not shown).

The block of paired-pulse inhibition by phaclofen and 2-OH-saclofen suggests that $GABA_B$ receptors are responsible for suppression of second e.p.s.p.$_{NMDA}$. Since an increase in postsynaptic K^+ conductance induced by the $GABA_B$ receptor activation is known to be blocked by Ba^{2+} (Thomson & Gahwiler, 1992), we therefore tested the effects of Ba^{2+} on the paired-pulse depression. Superfusion with Ba^{2+} (0.5 mM) depolarized the membrane potential by 3–8 mV and increased neuronal input resistance (85 ± 12%, $n = 7$). Figure 4a shows that, in the presence of Ba^{2+} (0.5 mM), baclofen (10 μM) induced little, if any, hyperpolarizing response. In 6 cells, superfusion with 10 μM caused a −7.3 ± 0.5 mV membrane hyperpolarization. In the presence of Ba^{2+} (0.5 mM), baclofen produced little hyperpolarization (−0.4 ± 0.3 mV, $n = 6$). The difference is significant at $P < 0.001$ (unpaired t test).

In 7 out of 7 cells examined, Ba^{2+} produced a large depolarizing wave with several action potentials atop it. The amplitude of the depolarizing wave was then reduced by partially blocking NMDA receptors with 10 μM DL-APV to match the control levels. The e.p.s.ps remaining under these conditions were apparently mediated by NMDA receptors because they could be blocked completely by further increasing the concentration of DL-APV to 50 μM. Under these conditions, the e.p.s.p.$_{NMDA}$ still exhibited paired-pulse depression (Figure 4b) which was not significantly different from the corresponding controls (percentage depressions at interstimulus interval of 200 ms, control: 76.7 ± 3.3%, in the

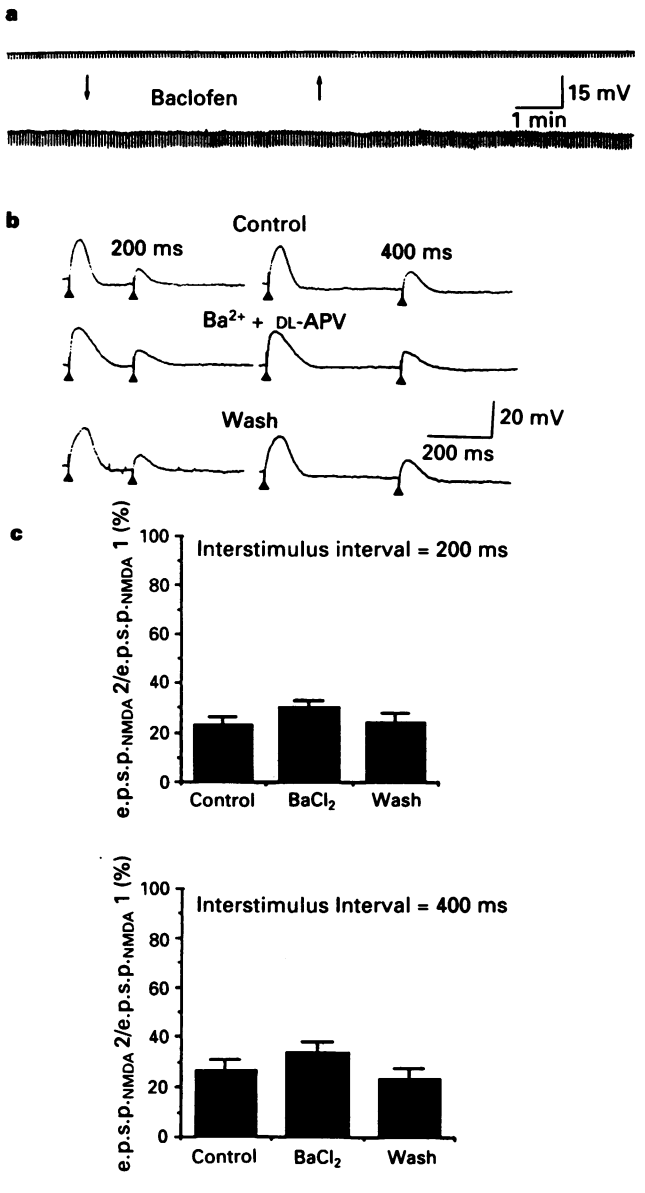


Figure 4 Barium fails to block the paired pulse depression (PPD). (a) Chart record illustrating the effect of baclofen (10 μM) on a basolateral amygdala neurone in the presence of Ba^{2+} (0.5 mM). During the experiment, −0.1 nA hyperpolarizing current pulses (upper trace) were injected intracellularly to monitor the neuronal input resistance. (b) (1) PPD of $e.p.s.p._{NMDA}$ at interstimulus intervals of 200 ms and 400 ms. (b) (2) Application of Ba^{2+} (0.5 mM) produces a large depolarizing wave with several action potentials atop it. The amplitude of the depolarizing wave was subsequently reduced by partially blocking NMDA receptors with 10 μM DL-APV to match the control level. (b) (3) Thirty minutes after washout of Ba^{2+}. (c) Graphic analysis of the effect of barium on the PPD at interstimulus intervals of 200 ms ($n = 7$) and 400 ms ($n = 8$).

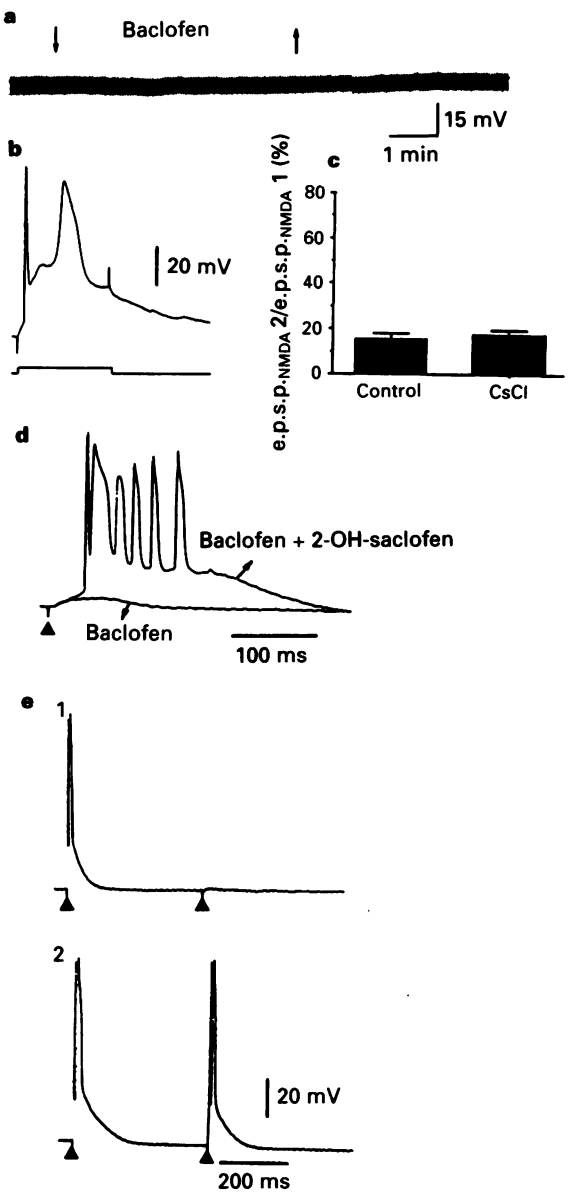


Figure 5 Lack of effect of intracellular Cs^+ on the paired pulse depression (PPD). (a) Chart record showing that baclofen failed to affect the membrane potential and input resistance in a basolateral amygdala neurone impaled with a 3 M CsCl-filled microelectrode. (b) Action potentials elicited by intracellular current injection (+0.3 nA, 100 ms) in the same neurone as in (a). (c) Graphic analysis of the effect of intracellular Cs^+ on the PPD. The percentage depressions, at an interstimulus interval of 200 ms, were 15.7 ± 2.5% for control ($n = 14$) and 17.6 ± 2.1% ($n = 13$, $P = 0.55$) for neurones recorded with CsCl-filled microelectrodes. (d) 2-OH-saclofen (200 μM) reversed the baclofen (5 μM)-induced presynaptic inhibition of $e.p.s.p._{NMDA}$. (e) (1) $e.p.s.p._{NMDA}$s evoked at interval of 400 ms in the presence of baclofen (5 μM). Baclofen reduced the amplitude of $e.p.s.p._{NMDA}$s. The amplitude of first $e.p.s.p._{NMDA}$ was increased by increasing the stimulus intensity; however, the $e.p.s.p._{NMDA}$s still exhibited PPD in the presence of baclofen. (e) (2) Application of 2-OH-saclofen (200 μM) reversed the PPD.

presence of Ba^{2+}: 69.7 ± 2.5%, $P = 0.12$; at interstimulus interval of 400 ms, control: 73.4 ± 4.2%, in the presence of Ba^{2+}: 66.1 ± 4.2%, $P = 0.24$) (Figure 4c) and application of phaclofen (1 mM) reduced the extent of depression (data not shown).

We recorded neurones using CsCl-filled microelectrodes since the postsynaptic $GABA_B$ receptor-activated K^+ current was blocked by internal Cs^+ (Gahwiler & Brown, 1985). A progressive increase in spike duration was observed over 15–40 min after penetration of neurones with a Cs^+-containing electrode (Figure 5b). In addition, as depicted in Figure 5a, baclofen failed to affect the membrane potential or neuronal input resistance in the same neurone. However, paired stimulation at an interval of 200 ms evoked $e.p.s.p._{NMDA}$s that displayed PPD. The second $e.p.s.p._{NMDA}$ was depressed by an average of 82.4 ± 2.1% ($n = 13$), which was not significantly different from the control PPD (84.3 ± 2.5%, $n = 14$, $P = 0.55$) (Figure 5c). Moreover, superfusion of 2-OH-saclofen reversed the PPD in neurones recorded with CsCl (Figure 5e).

Previous study in the amygdala has shown that pre- and

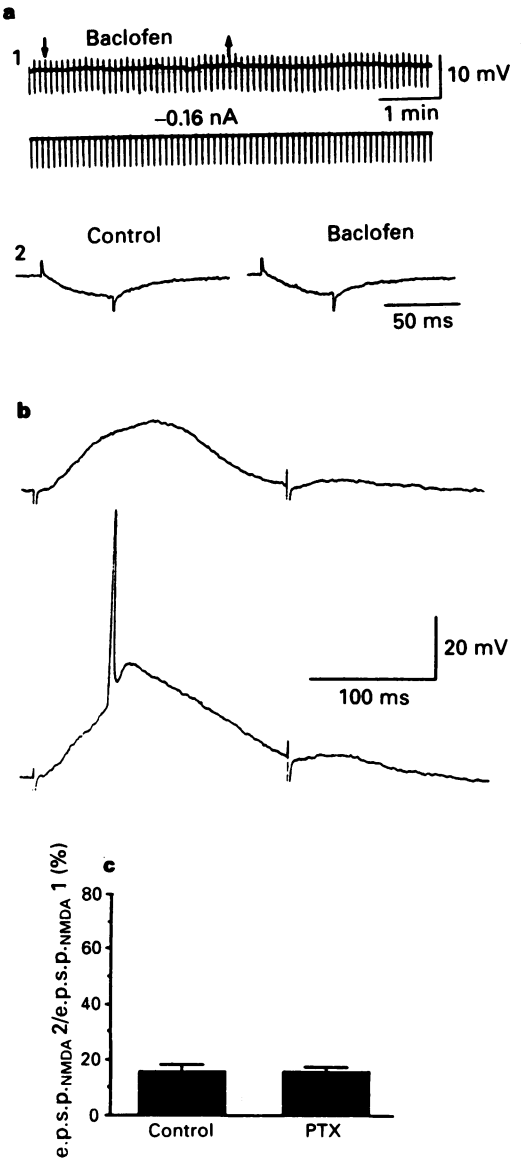


Figure 6 Pertussis toxin treatment blocks the postsynaptic action of baclofen but does not affect the paired pulse depression (PPD). (a) (1) Chart record illustrating the effect of baclofen (10 μM) on a basolateral amygdala neurone which was exposed to PTX 5 μg ml^{-1} for 7 h. During application of baclofen, −0.16 nA hyperpolarizing current pulses were injected to monitor membrane input resistance. (a) (2) Sample traces from (a) (i) were expanded on the oscilloscope to illustrate that baclofen does not affect the input resistance in neurones pretreated with PTX. (b) PPD of e.p.s.p.$_{NMDA}$ evoked with different stimulus intensities. (a) and (b) were taken from the same cell. Graphic analysis of the effect of PTX on the PPD. The percentage depressions, at interstimulus interval of 200 ms, were 15.7 ± 2.5% for control (n = 14) and 15.7 ± 1.8% (n = 11, P = 0.97) in neurones pretreated with PTX.

postsynaptic $GABA_B$ receptors can be distinguished on the basis of their sensitivity to pertussis toxin treatment (Asprodini *et al.*, 1992). We incubated the slices in pertussis toxin-containing ACSF (5 μg ml^{-1}) for 7 h and examined its effect on the PPD. As shown in Figure 6a, both membrane hyperpolarizing and resistance decreasing effects normally produced by baclofen were blocked in basolateral amygdala neurones of pertussis toxin-pretreated slices. Superfusion of 10 μM baclofen which caused a −7.3 ± 0.5 mV (n = 6) hyperpolarization in neurones from untreated slices produced no hyperpolarization in neurones from PTX-treated slices (−1.0 ± 0.4 mV, n = 6, P<0.005). In contrast, the PPD of e.p.s.p.$_{NMDA}$ was not significantly different between neurones obtained from control and PTX-treated slices (Figure 6b). The percentage depressions, at an interstimulus interval of 200 ms, were 84.3 ± 2.5% for control (n = 14) and 84.2 ± 1.8% (n = 11, P = 0.97) in neurones pretreated with PTX (Figure 6c).

Discussion

The present study demonstrates that the e.p.s.p.$_{NMDA}$ isolated with CNQX/picrotoxin exhibits PPD at interstimulus intervals of 100–2000 ms. The mechanism underlying PPD appeared to involve the $GABA_B$ receptors because phaclofen and 2-hydroxy-saclofen reduced or blocked the depression. However, the lack of a significant difference in the external Ba^{2+}, internal Cs^+ or PTX-treated compared to control neurones suggests that GABA released by the first stimulus reduced the second e.p.s.p.$_{NMDA}$ by an action other than that of opening a postsynaptic $GABA_B$ receptor-mediated K^+ conductance.

The involvement of $GABA_B$ receptors in activity-dependent decrease of synaptic potentials evoked by repetitive activation of afferent pathways has been demonstrated recently (Deisz & Prince, 1989; Davies *et al.*, 1990; Calabresi *et al.*, 1991). In the hippocampus, the mechanism underlying paired-pulse depression of i.p.s.ps can be explained by a negative feedback phenomenon which involves GABA acting on presynaptic $GABA_B$ receptors to inhibit its own release (Davies *et al.*, 1990; Otis *et al.*, 1993; Davies & Collingridge, 1993). On the contrary, activation of postsynaptic $GABA_B$ receptors resulting in an increase in K^+ conductance which hyperpolarizes neurones in a region where NMDA receptor-operated channels are blocked by Mg^{2+} is responsible for paired-pulse inhibition of e.p.s.p.$_{NMDA}$ (Morrisett *et al.*, 1991). Baclofen-induced postsynaptic hyperpolarizing responses are known to be blocked by 0.5 mM Ba^{2+} (Washburn & Moises, 1992 and the present study) or internal Cs^+ (Gahwiler & Brown, 1985 and the present study). The inability of external Ba^{2+} or internal Cs^+ to reverse PPD in the present study suggests that $GABA_B$-mediated postsynaptic activation of K^+ conductance is unlikely to be the underlying mechanism. Since the stimulus intensity was increased in order to evoke the e.p.s.p.$_{NMDA}$ in the presence of CNQX, we speculate that the released GABA by the first stimulus spills out from GABAergic synapses to act on glutamatergic fibre terminals and reduces the transmitter release. A recent demonstration that a brief tetanus but not a single conditioning stimulus releases enough GABA to diffuse to the presynaptic receptors on excitatory nerve terminals (Isaacson *et al.*, 1993) is consistent with this hypothesis.

The observation that phaclofen or 2-OH-saclofen suppressed the amplitude of e.p.s.p.$_{NMDA}$ is in accord with previous reports in the amygdala and hippocampus (Asprodini *et al.*, 1992; Hosford *et al.*, 1992) and reflects that these acidic analogues of GABA are in fact partial agonists rather than true antagonists (Kerr *et al.*, 1990). In the present study, we also demonstrate that the degree of PPD is reduced under conditions where transmitter release is decreased by baclofen. Furthermore, 2-OH-saclofen and phaclofen, but not baclofen, are able to reverse the PPD. These results suggest that presynaptic mechanism involving $GABA_B$ receptors is the major contributor to the PPD.

In the basolateral amygdala, it has previously been shown that 2-OH-saclofen and phaclofen block the late i.p.s.p. and reduce the hyperpolarizing effect of baclofen, both of which are mediated by postsynaptic $GABA_B$ receptors. In the present study, we observed that 2-OH-saclofen and phaclofen also reversed the baclofen-induced presynaptic inhibition of e.p.s.p.$_{NMDA}$ and paired-pulse depression. These data suggest that pre- and postsynaptic $GABA_B$ receptors share a similar pharmacological profile on the basis of antagonist sensitivity in the amygdala. However, the lack of an antagonistic effect

of Ba^{2+} and Cs^+ on the PPD suggests that pre- and postsynaptic receptors are coupled to different effectors.

It has been previously established that the $GABA_B$ receptor directly activates postsynaptic K^+ channels via a pertussis toxin-sensitive G-protein (Dutar & Nicoll, 1988). In agreement with previous reports, the hyperpolarizing action of baclofen was abolished in the PTX-treated slices. However, paired-pulse stimulation caused a $84.2 \pm 1.8\%$ depression of the second e.p.s.p.$_{NMDA}$. This result suggests hyperpolarizing membrane potential through the activation of postsynaptic $GABA_B$ receptors could not account for the PPD. Stimulation of Ca^{2+}-phospholipid-dependent protein kinase C (PKC) (Ben-Ari *et al.*, 1992; Chen & Huang, 1991) and cyclic AMP-dependent protein kinase A (PKA) (McVaugh & Waxham, 1992; Huang *et al.*, 1993; Cerne *et al.*, 1993) has recently been shown to modulate positively NMDA responses. Postsynaptic $GABA_B$ receptors may depress e.p.s.p.$_{NMDA}$ by activating G-proteins that interfere with the functions of these kinases. However, in the present study, PTX treatment did not block the PPD, suggesting it is unlikely that $GABA_B$ receptors act through postsynaptic G-proteins to suppress e.p.s.p.$_{NMDA}$.

The mechanism(s) by which activation of $GABA_B$ receptors on excitatory axon terminals inhibits transmitter release has not yet been established. An activation of Ba^{2+}-sensitive K^+ current resulting in hyperpolarization of the presynaptic nerve terminals could lead to reduced transmitter release. However, our data indicate the PPD could not be explained by such a presynaptic hyperpolarization since Ba^{2+} failed to affect it. Considering the long duration (>2 s) of PPD, it is nevertheless possible that a Ba^{2+}-insensitive K^+ current (Wagner & Dekin, 1993) with slow inactivation time constant might underlie the presynaptic hyperpolarization. Other possibilities include a direct inhibition of presynaptic Ca^{2+} current by $GABA_B$ receptors (Dolphin & Scott, 1986; Scholz & Miller, 1991; Pfrieger *et al.*, 1994) or an inhibition of transmitter release subsequent to Ca^{2+} influx (Scanziani *et al.*, 1992).

Interestingly, we observed that there is no stimulus strength-response relationship i.e. irrespective of the stimulus intensities applied, the amplitude of second e.p.s.p.$_{NMDA}$ was constant. In addition, baclofen mainly decreased the amplitude of first e.p.s.p.$_{NMDA}$ with little effect on the second one, suggesting presynaptic $GABA_B$ receptors may be maximally activated at low stimulus intensities. These results are consistent with a previous report that the EC_{50} of baclofen for the presynaptic action was 5 nM representing a 200 fold difference for its postsynaptic action ($EC_{50} = 1\ \mu M$) in the amygdala.

In the mammalian brain, the NMDA subtype of glutamate receptor is thought to play an important role in many forms of neuronal plasticity such as epilepsy, learning and memory (Collingridge & Singer, 1990; Meldrum & Garthwaite, 1990). In the amygdala, an enhancement in NMDA receptor-mediated responses has been demonstrated in both acute and chronic models of epilepsy (Gean *et al.*, 1989; 1990; Rainnie *et al.*, 1992). Furthermore, activation of NMDA receptors is required for the induction of long-term potentiation (LTP) in this region of the brain (Gean *et al.*, 1993). The present study shows that $GABA_B$ receptor antagonists reverse the PPD of e.p.s.p.$_{NMDA}$ suggesting that $GABA_B$ receptors play an important role in the regulation of amygdala neuronal excitability. Indeed, a recent study by Asprodini *et al.* (1992) indicated that a reduced sensitivity of $GABA_B$ receptors located on the nerve terminal of glutamate afferents underlies the kindling-induced epileptogenesis.

In summary, we have shown that $GABA_B$ receptor activation plays an important role in paired-pulse depression of e.p.s.p.$_{NMDA}$ in the amygdala. We have also demonstrated that PPD is not blocked by external Ba^{2+} or internal Cs^+. Furthermore, pretreating the slices with pertussis toxin, which blocked the hyperpolarizing action of baclofen, did not alter the PPD. Taken together, these results suggest that GABA released by the first stimulus acting on $GABA_B$ receptors to suppress the second e.p.s.p.$_{NMDA}$ is via mechanisms other than activation of a postsynaptic $GABA_B$ receptor-coupled K^+ conductance. The present study is therefore in contrast to a previous report where the reduction of the second e.p.s.p.$_{NMDA}$ in the hippocampus is thought to result from activation of postsynaptic K^+ conductance (Morrisett *et al.*, 1991).

This study was supported by the National Science Council of Taiwan (NSC82-0420-B006-012-M10).

References

ASPRODINI, E.K., RAINNIE, D.G. & SHINNICK-GALLAGHER, P. (1992). Epileptogenesis reduces the sensitivity of presynaptic γ-aminobutyric acid$_B$ receptors on glutamatergic afferents in the amygdala. *J. Pharmacol. Exp. Ther.*, **262**, 1011–1021.

AULT, B. & NADLER, J.V. (1983). Anticonvulsant-like actions of baclofen in the rat hippocampal slice. *Br. J. Pharmacol.*, **78**, 701–708.

BASHIR, Z.I., ALFORD, S., DAVIES, S.N., RANDALL, A.D. & COLLINGRIDGE, G.L. (1991). Long-term potentiation of NMDA receptor-mediated synaptic transmission in the hippocampus. *Nature*, **349**, 156–158.

BEN-ARI, Y., ANIKSZTEJN, L. & BREGESTOVSKI, P. (1992). Protein kinase C modulation of NMDA currents: an important link for LTP induction. *Trends Neurosci.*, **15**, 333–339.

BOWERY, N. (1989). $GABA_B$ receptors and their significance in mammalian pharmacology. *Trends Pharmacol. Sci.*, **10**, 401–407.

CALABRESI, P., MERCURI, N.B., DEMURTAS, M. & BERNARDI, G. (1991). Involvement of GABA systems in feedback regulation of glutamate- and GABA-mediated synaptic potentials in rat neostriatum. *J. Physiol.*, **440**, 581–599.

CERNE, R., RUSIN, K.I. & RANDIC, M. (1993). Enhancement of the N-methyl-D-aspartate response by cAMP-dependent protein kinase. *Neurosci. Lett.*, **161**, 124–128.

CHEN, L. & HUANG, L.-Y.M. (1992). Sustained potentiation of NMDA receptor-mediated glutamate responses through activation of protein kinase C by a μ opioid. *Neuron*, **7**, 319–326.

COLLINGRIDGE, G.L. & SINGER, W. (1990). Excitatory amino acid receptors and synaptic plasticity. *Trends Pharmacol. Sci.*, **11**, 290–296.

DAVIES, C.H. & COLLINGRIDGE, G.L. (1993). The physiological regulation of synaptic inhibition by $GABA_B$ autoreceptors in rat hippocampus. *J. Physiol.*, **472**, 245–265.

DAVIES, C.H., DAVIES, S.N. & COLLINGRIDGE, G.L. (1990). Paired-pulse depression of monosynaptic GABA-mediated inhibitory postsynaptic responses in rat hippocampus. *J. Physiol.*, **424**, 513–531.

DEISZ, R.A. & PRINCE, D.A. (1989). Frequency-dependent depression of inhibition in guinea-pig neocortex in vitro by $GABA_B$ receptor feed-back on GABA release. *J. Physiol.*, **412**, 513–541.

DOLPHIN, A.C. & SCOTT, R.H. (1986). Inhibition of calcium currents in cultured rat dorsal root ganglion neurons by (−)-baclofen. *Br. J. Pharmacol.*, **88**, 213–220.

DUTAR, P. & NICOLL, R.A. (1988). Pre- and postsynaptic $GABA_B$ receptors in the hippocampus have different pharmacological properties. *Neuron*, **1**, 585–591.

GAHWILER, B.H. & BROWN, D.A. (1985). $GABA_B$-receptor-activated K^+ current in voltage-clamped CA_3 pyramidal cells in hippocampal cultures. *Proc. Natl. Acad. Sci. U.S.A.*, **82**, 1558–1562.

GEAN, P.W. & CHANG, F.C. (1992). Pharmacological characterisation of excitatory synaptic potentials in rat basolateral amygdaloid neurons. *Synapse*, **11**, 1–9.

GEAN, P.W., CHANG, F.C., HUANG, C.C., LIN, J.H. & WAY, L.T. (1993). Long-term enhancement of EPSP and NMDA receptor-mediated synaptic transmission in the amygdala. *Brain Res. Bull.*, **31**, 7–11.

GEAN, P.W., CHOU, S.M. & CHANG, F.C. (1990). Epileptiform activity induced by 4-aminopyridine in rat amygdala neurons: the involvement of N-methyl-D-aspartate receptors. *Eur. J. Pharmacol.*, **184**, 213–222.

GEAN, P.W. & SHINNICK-GALLAGHER, P. (1987). Picrotoxin induced epileptiform activity in amygdaloid neurons. *Neurosci. Lett.*, **73**, 149–154.

GEAN, P.W., SHINNICK-GALLAGHER, P. & ANDERSON, A.C. (1989). Spontaneous epileptiform activity and alteration of GABA- and of NMDA-mediated neurotransmission in amygdala neurons kindled in vivo. *Brain Res.*, **494**, 177–181.

HASUO, H., SHOJI, S., GALLAGHER, J.P. & AKASU, T. (1992). Adenosine inhibits the synaptic potentials in rat septal nucleus neurons mediated through pre- and postsynaptic A_1-adenosine receptors. *Neurosci. Res.*, **13**, 281–299.

HOSFORD, D.A., CLARK, S., CAO, Z., WILSON, W.A., LIN, F.H., MORRISETT, R.A. & HUIN, A. (1992). The role of $GABA_B$ receptor activation in absence seizures of lethargic (lh/lh) mice. *Science*, **257**, 398–401.

HUANG, C.C., TSAI, J.J. & GEAN, P.W. (1993). Enhancement of NMDA receptor-mediated synaptic potential by isoproterenol is blocked by Rp-adenosine-3′,5′-cyclic monophosphothioate. *Neurosci. Lett.*, **161**, 207–210.

ISAACSON, J.S., SOLIS, J.M. & NICOLL, R.A. (1993). Local and diffuse synaptic actions of GABA in the hippocampus. *Neuron*, **10**, 165–175.

KARLSSON, G., KOLB, C., HAUSDORF, A., PORTET, C., SCHMUTZ, M. & OLPE, H.-R. (1992). $GABA_B$ receptors in various in vitro and in vivo models of epilepsy: a study with the $GABA_B$ receptor blocker CGP 35348. *Neuroscience*, **47**, 63–68.

KERR, D.I., ONG, J., JOHNSON, G.A., ABBENANTE, J. & PRAGER, R.H. (1988). 2-Hydroxy-saclofen: an improved antagonist at central and peripheral $GABA_B$ receptors. *Neurosci. Lett.*, **92**, 92–96.

KERR, D.I., ONG, J. & PRAGER, R.H. (1990). $GABA_B$ receptor agonists and antagonists. In *$GABA_B$ Receptors in Mammalian Function*. ed. Bowery, N.G., Bittiger, H. & Olpe, H.-R. pp. 29–45. Chichester: John Wiley & Sons Ltd.

LE GAL LA SALLE, G. (1976). Unitary responses in the amygdaloid complex following stimulation of various diencephalic structures. *Brain Res.*, **118**, 475–478.

MCDONALD, A.J. (1985). Immunohistochemical identification of gamma-aminobutyric acid-containing neurons in the rat basolateral amygdala. *Neurosci. Lett.*, **53**, 203–207.

MCVAUGH, W.B. & WAXHAM, M.N. (1992). Augment of NMDA currents by cyclic AMP and forskolin. *Soc. Neurosci. Abstr.*, **18**, 651.

MELDRUM, B. & GARTHWAITE, J. (1990). Excitatory amino acid neurotoxicity and neurodegenerative disease. *Trends Pharmacol. Sci.*, **11**, 379–387.

MORRISETT, R.A., MOTT, D.D., LEWIS, D.V., SWARTZWEIDER, H.S. & WILSON, W.A. (1991). $GABA_B$-receptor-mediated inhibition of the N-methyl-D-aspartate component of synaptic transmission in the rat hippocampus. *J. Neurosci.*, **11**, 203–209.

MOTT, D.D., BRAGDON, A.C., LEWIS, D.V. & WILSON, W.A. (1989). Baclofen has a proepileptic effect in the rat dentate gyrus. *J. Pharmacol. Exp. Ther.*, **249**, 721–725.

OTIS, T.S., DE KONINCK, Y. & MODY, I. (1993). Characterization of synaptically elicited $GABA_B$ responses using patch-clamp recordings in rat hippocampal slices. *J. Physiol.*, **463**, 391–407.

PFRIEGER, F.W., GOTTMANN, K. & LUX, H.D. (1994). Kinetics of $GABA_B$ receptor-mediated inhibition of calcium currents and exictatory synaptic transmission in hippocampal neurons in vitro. *Neuron*, **12**, 97–107.

RAINNIE, D.G., ASPRODINI, E.K. & SHINNICK-GALLAGHER, P. (1991). Inhibitory transmission in the basolateral amygdala. *J. Neurophysiol.*, **66**, 999–1009.

RAINNIE, D.G., ASPRODINI, E.K. & SHINNICK-GALLAGHER, P. (1992). Kindled-induced long-lasting changes in synaptic transmission in the basolateral amygdala. *J. Neurophysiol.*, **67**, 443–454.

SCANZIANI, M., CAPOGNA, M., GAHWILER, B.H. & THOMPSON, S.M. (1992). Presynaptic inhibition of miniature excitatory synaptic currents by baclofen and adenosine in the hippocampus. *Neuron*, **9**, 919–927.

SCHOLZ, K.P. & MILLER, R.J. (1991). $GABA_B$ receptor-mediated inhibition of Ca^{++} currents and synaptic transmission in cultured rat hippocampal neurons. *J. Physiol.*, **444**, 669–686.

SWARTZWELDER, H.S., BRAGDON, A.C., SUTCH, C.P., AULT, B. & WILSON, W.A. (1986). Baclofen suppresses hippocampal epileptiform activity at low concentrations without suppressing synaptic transmission. *J. Pharmacol. Exp. Ther.*, **237**, 881–887.

TAKAGI, M. & YAMAMOTO, C. (1981). The long-lasting inhibition recorded in vitro from the lateral nucleus of the amygdala. *Brain Res.*, **206**, 474–478.

THOMSON, S.M. & GAHWILER, B.H. (1992). Comparison of the actions of baclofen at pre- and postsynaptic receptors in the rat hippocampus in vitro. *J. Physiol.*, **451**, 329–345.

WAGNER, P.G. & DEKIN, M.S. (1993). $GABA_B$ receptors are coupled to a barium-insensitive outward rectifying potassium conductance in premotor respiratory neurons. *J. Neurophysiol.*, **69**, 286–289.

WASHBURN, M.S. & MOISES, H.C. (1992). Inhibitory responses of rat basolateral amygdaloid neurons recorded in vitro. *Neuroscience*, **50**, 811–830.

(Received November 1, 1993
Revised July 4, 1994
Accepted July 14, 1994)

Br. J. Pharmacol. (1994), **113**, 1036–1042 © Macmillan Press Ltd, 1994

Role of bradykinin in the hyperaemia following acid challenge of the rat gastric mucosa

†Gábor Pethö, *Milana Jocič & [1]*Peter Holzer

*Department of Experimental and Clinical Pharmacology, University of Graz, A-8010 Graz, Austria and †Department of Pharmacology, Medical University of Pécs, H-7643 Pécs, Hungary

1 This study examined whether the hyperaemia following acid challenge of the rat gastric mucosa involves bradykinin, a peptide formed in response to tissue injury.

2 Gastric mucosal blood flow in urethane-anaesthetized rats was assessed by the hydrogen gas clearance method. Infusion of a bradykinin solution (10 μM) into the gastric wall augmented gastric mucosal blood flow by a factor of 2.3, an effect that was prevented by the bradykinin B_2 antagonist Hoe-140 (icatibant; 100 μmol kg^{-1}, i.v.).

3 I.v. injection of bradykinin (20–60 nmol kg^{-1}) caused a 2.3–3.5 fold increase in blood flow through the left gastric artery as measured by the ultrasonic transit time shift technique. The hyperaemic effect of bradykinin in this gastric artery was also prevented by Hoe-140 (100 μmol kg^{-1}, i.v.).

4 Gastric acid backdiffusion was evoked by perfusing the stomach with 15% ethanol, to break the gastric mucosal barrier, in the presence of luminal acid. Depending on the concentration of acid (0.05 and 0.15 M HCl), this procedure increased gastric mucosal blood flow by a factor of 1.6–2.8 and caused formation of gross damage in 1.5–3% of the glandular mucosa. Hoe-140 (100 μmol kg^{-1}, i.v.) failed to alter the moderate vasodilatation seen in the presence of 0.05 M HCl but significantly ($P<0.05$) attenuated the marked hyperaemia and enhanced the gross mucosal damage observed in the presence of 0.15 M HCl.

5 These data show that bradykinin is able to enhance gastric mucosal blood flow via activation of B_2 receptors. It appears as if this kinin is formed during severe acid challenge of the rat gastric mucosa and participates in the hyperaemic reaction to gastric acid backdiffusion.

Keywords: Bradykinin; bradykinin antagonist; Hoe-140 (icatibant); bradykinin B_2 receptors; gastric blood flow; acid-evoked gastric hyperaemia; gastric mucosal damage

Introduction

Acid backdiffusion through a disrupted gastric mucosal barrier leads to a rise of gastric mucosal blood flow, a reaction that limits acid damage to the surface of the mucosa (Whittle, 1977; Bruggeman *et al.*, 1979; Holzer *et al.*, 1991). The hyperaemic reaction to acid back-diffusion in the rat gastric mucosa is to a large extent mediated by sensory neurones (Holzer *et al.*, 1991; Raybould *et al.*, 1992) that cause arteriolar dilatation via release of calcitonin gene-related peptide (Li *et al.*, 1992) and formation of nitric oxide (Lippe & Holzer, 1992). It is not yet known, however, how acid influx into the gastric mucosa activates this neurogenic vasodilator mechanism. Histamine, which has been implicated in the acid-evoked hyperaemia of the canine gastric mucosa (Bruggeman *et al.*, 1979), does not seem to play a role in the acid-challenged mucosa of the rat stomach (Holzer *et al.*, 1991). Although hydrogen ions themselves can stimulate sensory neurones in the gastric mucosa (Geppetti *et al.*, 1991), other mediators generated during tissue damage need also to be taken into account.

Tissue injury, ischaemia and low pH are known to activate tissue and plasma kallikreins to form bradykinin and other kinins (Hall, 1992; Dray & Perkins, 1993). Newly formed bradykinin acts locally close to its site of production on a wide variety of tissues including blood vessels and sensory nerve fibres. Thus, the kinin has been found to dilate the coeliac and mesenteric arteries *in vitro* (Ritter *et al.*, 1989; Santiago *et al.*, 1993), to augment blood flow through the superior mesenteric artery of the rat (Berguer *et al.*, 1993) and to excite visceral afferents in several species (Longhurst *et al.*, 1984; Stein *et al.*, 1986; Holzer, 1992; Holzer-Petsche, 1992; Geppetti, 1993; Griesbacher, 1994). Both the splanchnic vasodilator and sensory nerve stimulant actions of bradykinin are mediated by bradykinin B_2 receptors as revealed by the use of receptor subtype-selective antagonists (Holzer, 1992; Holzer-Petsche, 1992; Berguer *et al.*, 1993; Santiago *et al.*, 1993; Griesbacher, 1994). The aim of the present study was to test whether bradykinin participates in the gastric hyperaemic reaction to mucosal acid challenge. This question was addressed in two stages. Firstly, we examined whether bradykinin is able to enhance blood flow in the rat stomach. Secondly, we tested whether Hoe-140 (icatibant), a potent, selective and long-acting bradykinin B_2 antagonist (Hock *et al.*, 1991; Lembeck *et al.*, 1991; Wirth *et al.*, 1991) modifies the rise of gastric mucosal blood flow in response to acid backdiffusion.

Methods

Animal preparation

All experiments of this study were approved by the Ministry of Science and Research of the Federal Republic of Austria. Female Sprague-Dawley rats, weighing 180–220 g, were fasted for 20 h but had free access to water. After the induction of anaesthesia with urethane (1.5 g kg^{-1}, s.c.) the rats were fitted with a tracheal cannula to facilitate spontaneous respiration and to allow for the administration of hydrogen. Mean arterial blood pressure was recorded from a cannula in the right carotid artery by means of a pressure transducer (model ISOTEC; HSE, March-Hugstetten, Germany) and displayed on a chart recorder (model SERVOGOR 464; ABB-GOERZ, Vienna, Austria). In some experiments the blood pressure signal was fed into a heart ratemeter (model MINO; HSE, March-Hugstetten, Germany) with digital

[1] Author for correspondence.

readout of the heart rate. A catheter in the left jugular vein was used for the continuous infusion of saline (1.5 ml h^{-1}), to avoid dehydration, and for the i.v. injection of drugs. The stomach, exposed by a midline laparotomy, was fitted with an inflow cannula placed in the forestomach and an outflow cannula inserted through the pylorus (Holzer *et al.*, 1991). The experimental media (kept at room temperature) were perfused through the stomach at a rate of 0.7–0.8 ml min^{-1}. The body temperature of the animals was kept at 37°C by means of a heated table.

Blood flow measurements

Gastric mucosal blood flow was measured with the hydrogen clearance technique. The washout of hydrogen gas was estimated by a needle-type platinum electrode inserted from the serosa into the basal portion of the gastric corpus mucosa and positioned at the submucosal border of the muscularis mucosae (Holzer *et al.*, 1991). The method is based on the principle that the oxidation of molecular hydrogen at the surface of a platinum electrode generates electrons and that the resulting current is proportional to the hydrogen concentration at the site of the electrode (Leung *et al.*, 1984). In the present experiments, hydrogen (3%) was added to the air which the rats were breathing until the current tracing reached a plateau. When 15 min later the external hydrogen source was removed, the current gradually fell due to removal of hydrogen by blood flow. The rate of hydrogen clearance from the tissue is related to the magnitude of tissue blood flow (Leung *et al.*, 1994) which was calculated with a computer programme (Livingston *et al.*, 1989) and expressed as ml min^{-1} 100 g^{-1}. It is evident that the measurement of blood flow with this method was discontinuous, as the experimental protocol involved alternating 15 min periods of saturation, and desaturation, of the tissue with hydrogen gas.

Blood flow in the left gastric artery was recorded continuously with the ultrasonic transit time shift technique which measures the net volume of blood flow with a factory-calibrated sensor (Barnes *et al.*, 1983; Burton & Gorewit, 1984). To this end, the terminal segment of the left gastric artery close to its entry into the stomach was separated from the surrounding tissue over a length of 4–5 mm under a binocular microscope. A perivascular ultrasonic flow probe (model 1RB, Transonic, Ithaca, New York, U.S.A.) was placed around the left gastric artery and connected to a small animal flowmeter (model T106, Transonic) which calculated the volume of blood flow (ml min^{-1}) and fed the signal into a chart recorder (Holzer *et al.*, 1993).

Determination of gross mucosal damage

Gross damage to the gastric glandular mucosa was determined from photographs of the stomachs pinned flat on a board and quantified by computerized planimetry. The area covered by visible haemorrhagic lesions (defined as gross injury) was measured with a digitizing tablet and the software SigmaScan (Jandel, Corte Madera, California, U.S.A.). Gross injury was evaluated by an observer unaware of the experimental treatment. The area covered by gross injury was expressed as a percentage of the total area of the glandular mucosa of the rat stomach.

Experimental protocols

An equilibration period of 45 min was allowed before the experiments were initiated. Three studies were conducted. In Study 1, the effect of local administration of bradykinin on gastric mucosal blood flow was examined. To this end an injection needle (outer diameter 0.3 mm) was inserted in the gastric corpus wall and positioned at the submucosal border of the muscularis mucosae at a distance of 0.5–1 mm from the platinum electrode. The needle, which was connected to an infusion pump, was placed in the gastric wall 1 h before application of the test substances. Bradykinin was administered by intramural infusion (3 µl min^{-1}) of a 10 µM solution for a period of 5 min immediately before a hydrogen desaturation curve was recorded. The vasodilator effect of bradykinin was determined by comparison of the bradykinin-evoked hyperaemia with that induced by the vehicle (saline) infused at a rate of 3 µl min^{-1}.

The effect of bradykinin, injected i.v. at 15 min intervals, on blood flow in the left gastric artery was investigated in Study 2. The experiments were started by priming the animals with i.v. injections of bradykinin (20 nmol kg^{-1}) until the hyperaemic response to the kinin became stable (Holzer *et al.*, 1993). Then the dose-dependency of the haemodynamic effect of bradykinin was tested by recording the responses to 20 and 60 nmol kg^{-1} bradykinin. Thereafter the bradykinin antagonist Hoe-140 (100 µmol kg^{-1}) was administered i.v. followed by further injections of 60 nmol kg^{-1} bradykinin. All drugs were given at a volume of 1 ml kg^{-1}, the vehicle being saline.

Study 3 was carried out to investigate the influence of Hoe-140 (100 µmol kg^{-1}) on the increase in gastric mucosal blood flow caused by gastric acid backdiffusion. The basic experimental protocol used for this purpose was evaluated in previous studies (Holzer *et al.*, 1991; Holzer & Lippe, 1992). The experiments were begun by perfusing the stomach with 0.05 M hydrochloric acid (HCl) in 0.1 M saline (first set of experiments) or with 0.15 M HCl in water (second set of experiments). Saline and water, respectively, were used for preparing the gastric perfusion media in order to achieve solutions of comparable ionic strength and osmolarity (0.15 M). After perfusion of the stomach with these media for 1 h, acid backdiffusion was induced by adding ethanol (15%, wt/wt) to the acid media and continuing the gastric perfusion for another hour. Measurements of gastric mucosal blood flow were taken during the periods 45–30 min and 15–0 min before, and 15–30 min and 45–60 min after, the induction of gastric acid backdiffusion. Hoe-140 or its vehicle (saline, 1 ml kg^{-1}) was injected i.v. 30 min before the gastric perfusion with ethanol in acid was begun.

Substances

The saline solution used here was 0.15 M NaCl. Urethane (Fluka, Buchs, Switzerland) was dissolved in water at a concentration of 25% (wt/wt). Bradykinin (Bachem, Bubendorf, Switzerland) and Hoe-140 (icatibant; Hoechst, Frankfurt am Main, Germany) were dissolved in saline (1 mM). Further dilutions, if necessary, were also made with saline. HCl (1 M) and ethanol (100%) were obtained from Merck (Darmstadt, Germany).

Statistics

All data are presented as mean ± s.e.mean. Statistical evaluation of the results was performed with the Kruskal-Wallis H test or the Mann-Whitney U test, where applicable. Probability values $P<0.05$ were regarded as significant.

Results

Effect of intramural bradykinin on gastric mucosal blood flow (Study 1)

Since it was found that intramural infusion of 1 µM bradykinin failed to augment gastric mucosal blood flow consistently ($n = 3$), a ten fold higher concentration of the kinin (10 µM) was used in this study. This concentration of bradykinin resulted in a 2.3 fold increase in blood flow through the gastric mucosa, whereas the vehicle (saline) infused intramurally at a rate of 3 µl min^{-1} failed to enhance gastric mucosal blood flow significantly (Figure 1). The hyperaemic response to bradykinin was transient and seen

only during the gastric mucosal blood flow measurement period immediately following the intramural infusion of the kinin. Mean arterial blood pressure (88 ± 3 mmHg, $n = 10$) did not change in response to intramural vehicle or bradykinin (data not shown).

I.v. injection of Hoe-140 (100 μmol kg^{-1}, 30 min before the kinin) virtually abolished the vasodilator effect of intramural bradykinin (10 μM), and the bradykinin-induced hyperaemia observed after Hoe-140 was indistinguishable from the insignificant hyperaemia caused by intramural saline (Figure 1). Neither basal gastric mucosal blood flow (Figure 1) nor mean arterial blood pressure (91 ± 2 mmHg, $n = 7$) was significantly altered by Hoe-140. I.v. injection of saline (1 ml kg^{-1}), the vehicle for Hoe-140, had no effect on these parameters and failed to influence the rise of gastric mucosal blood flow elicited by intramural bradykinin (Figure 1).

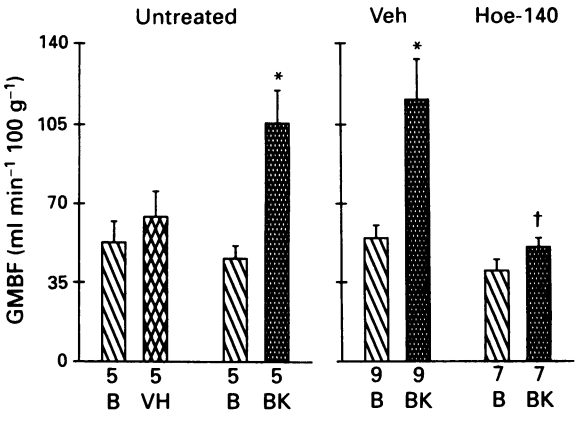


Figure 1 Effect of intramural bradykinin (BK, 10 μM) or its vehicle (VH, saline, infused at a rate of 3 μl min^{-1}) on gastric mucosal blood flow (GMBF) in untreated rats and in rats that had received an i.v. injection of Hoe-140 (100 μmol kg^{-1}) or its vehicle (Veh, saline, 1 ml kg^{-1}) 30 min before the administration of bradykinin. Bradykinin or its vehicle was infused for a period of 5 min immediately before a measurement of gastric mucosal blood flow was taken. The graphs show the basal (B) values of gastric mucosal blood flow that were recorded 15 min before, and the gastric mucosal blood flow values recorded immediately after, the intramural infusion of bradykinin or its vehicle. The values shown are mean with the s.e.mean and the number of rats (n) indicated at the base of the columns. *$P < 0.01$ versus respective basal values; †$P < 0.05$ versus respective value in the vehicle-treated rats.

Effect of i.v. bradykinin on blood flow in the left gastric artery (Study 2)

I.v. injection of bradykinin (20 and 60 nmol kg^{-1}) led to a dose-related increase in blood flow through the left gastric artery, a dose-related increase in heart rate, and a dose-related decrease in mean arterial blood pressure (Figure 2 and Table 1). These cardiovascular effects of bradykinin were transient and abated within 3–5 min (Figure 2). After injection of Hoe-140 (100 μmol kg^{-1}, i.v.) the effects of bradykinin (60 nmol kg^{-1}) on blood flow in the left gastric artery, mean arterial blood pressure and heart rate were practically abolished (Figure 2 and Table 1) for a period of 1 h, the longest period examined. Injection of saline (1 ml kg^{-1}, i.v.), the vehicle for Hoe-140, did not affect any of the cardiovascular responses to bradykinin under study ($n = 3$).

Effect of Hoe-140 on the rise of gastric mucosal blood flow due to acid backdiffusion (Study 3)

Hoe-140 was tested in two series of experiments in which the stomachs were perfused with either 0.05 or 0.15 M HCl. The hyperaemia ensuing after the induction of acid backdiffusion by adding ethanol (15%) to the acid perfusion medium depended on the concentration of HCl. Acid backdiffusion from a medium with 0.15 M HCl caused a 4 fold ($P < 0.01$) higher increase in gastric mucosal blood flow than acid backdiffusion from a medium with 0.05 M HCl (Figures 3 and 4). In contrast, the formation of gross haemorrhagic lesions in the gastric corpus mucosa was not significantly related to the HCl concentration in the perfusion medium, although on average the injury seen after acid backdiffusion

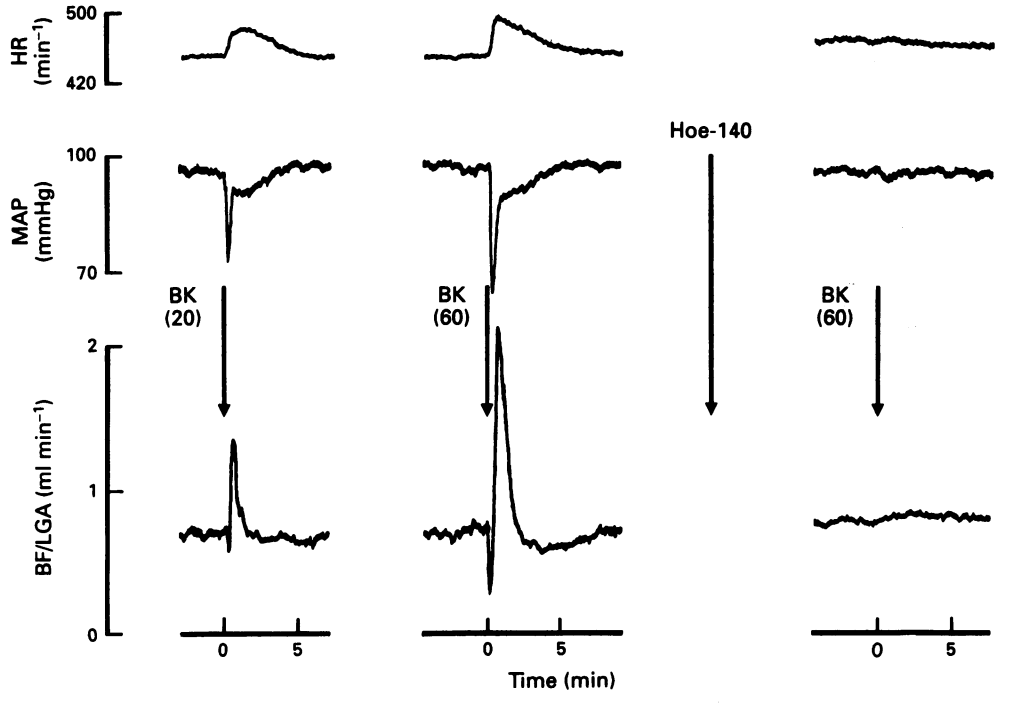


Figure 2 Recording of the effect of i.v. injected bradykinin (BK, doses in nmol kg^{-1} indicated in parentheses) on heart rate (HR), mean arterial blood pressure (MAP) and blood flow in the left gastric artery (BF/LGA) before, and 30 min after, the i.v. injection of Hoe-140 (100 μmol kg^{-1}).

Table 1 Effect of i.v. bradykinin (BK) on blood flow in the left gastric artery (BF/LGA), mean arterial blood pressure (MAP) and heart rate (HR): dose-dependency and antagonism by Hoe-140 (100 μmol kg^{-1})

Agonist	*Antagonist*	*BF/LGA* (ml min^{-1})	*MAP* (mmHg)	*HR* (min^{-1})
None (basal parameters)	None	0.54 ± 0.04 (17)	99 ± 1.7 (17)	465 ± 5.0 (13)
BK (20 nmol kg^{-1})	None	+0.71 ± 0.12 (9)	−34.8 ± 2.7 (9)	+22.3 ± 3.2 (7)
BK (60 nmol kg^{-1})	None	+1.33 ± 0.20 (8)	−42.0 ± 2.0 (8)	+33.0 ± 2.9 (6)
BK (60 nmol kg^{-1})	Hoe-140	+0.14 ± 0.05 (6)*	− 0.4 ± 0.3 (6)*	+ 1.4 ± 1.1 (6)*

The basal parameters were recorded immediately before the i.v. injection of bradykinin. The effects of bradykinin are expressed as increments (labelled with +) or decrements (labelled with −) of the parameters under study (peak values minus basal values). Hoe-140 (100 μmol kg^{-1}) was injected i.v. 30 min before the effect of bradykinin was tested. The figures shown are mean ± s.e.mean, with the number of rats (*n*) indicated in parentheses. *$P<0.01$ versus the effect of bradykinin (60 nmol kg^{-1}) measured in the absence of Hoe-140.

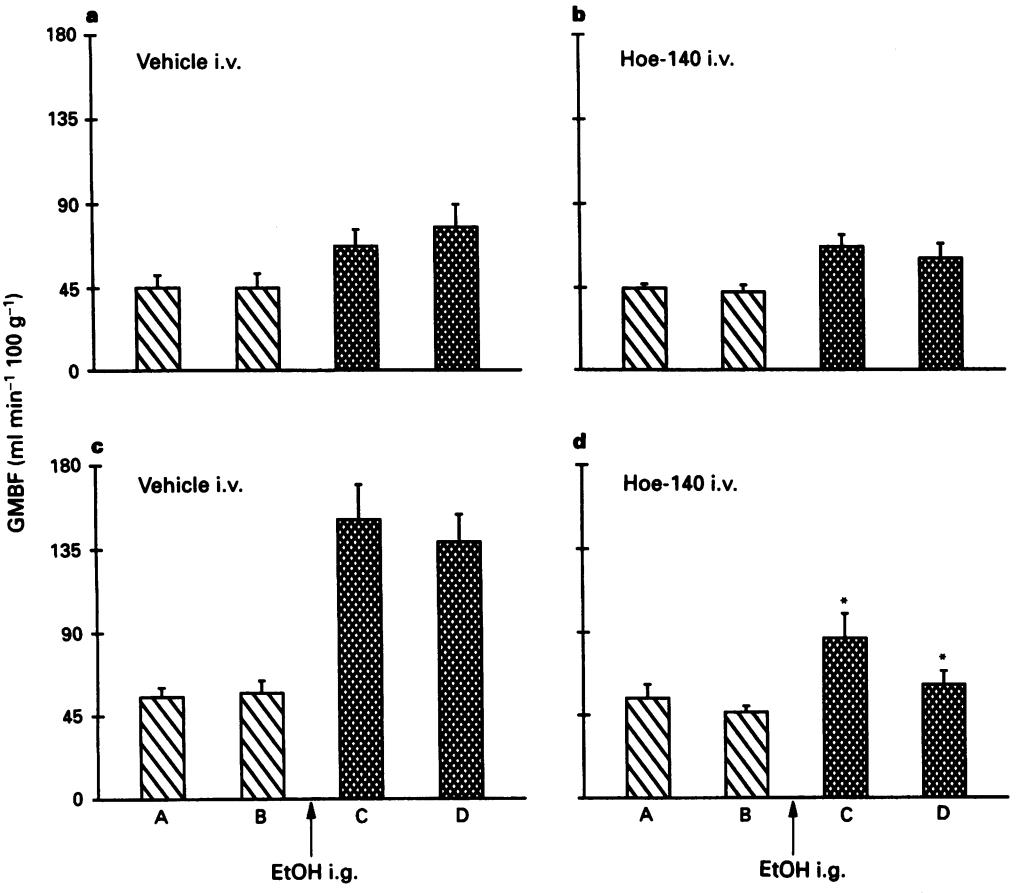


Figure 3 Effect of gastric acid backdiffusion in the presence of 0.05 (a,b) or 0.15 M (c,d) HCl on gastric mucosal blood flow (GMBF) in rats treated either with Hoe-140 (100 μmol kg^{-1}) or its vehicle (saline, 1 ml kg^{-1}). Hoe-140 or its vehicle was injected i.v. 30 min before acid backdiffusion was induced by adding ethanol (EtOH, i.g. = intragastrically, 15%) to the acidified gastric perfusion media. The 4 columns in each graph show gastric mucosal blood flow measured 45–30 min (A) and 15–0 min (B) before, and 15–30 min (C) and 45–60 min (D) after, induction of gastric acid backdiffusion. The values shown are mean with the s.e.mean. The number of rats (*n*) in each group was 8–10. *$P<0.01$ versus respective values in the vehicle-treated rats.

from 0.15 M HCl was double the injury seen after exposure to 0.05 M HCl (Figure 4). Mean arterial blood pressure was not affected by the HCl concentration in the gastric perfusion medium and did not change after induction of gastric acid backdiffusion (data not shown).

The effect of Hoe-140 (100 μmol kg^{-1} injected i.v. 30 min before the induction of acid backdiffusion) on the acid-evoked hyperaemia in the gastric mucosa depended on the HCl concentration in the gastric perfusion medium. At a concentration of 0.05 M HCl, Hoe-140 failed to alter significantly the hyperaemia and the formation of gross mucosal damage induced by gastric acid backdiffusion (Figures 3 and 4). Conversely, the rise of gastric mucosal blood flow elicited in the presence of 0.15 M HCl was significantly attenuated by Hoe-140 as compared with the acid-evoked hyperaemia seen in rats injected with the vehicle (saline). The inhibitory effect of Hoe-140 on the hyperaemic response to acid backdiffusion in the presence of 0.15 M HCl was associated with enhanced formation of gross mucosal damage (Figure 4). Basal gastric mucosal blood flow as well as mean arterial blood pressure before and after gastric acid backdiffusion were not influenced by Hoe-140 (data not shown).

Discussion

The present data demonstrate that bradykinin increases blood flow in the rat stomach and plays a role in the gastric hyperaemic response to backdiffusing acid. The evidence for

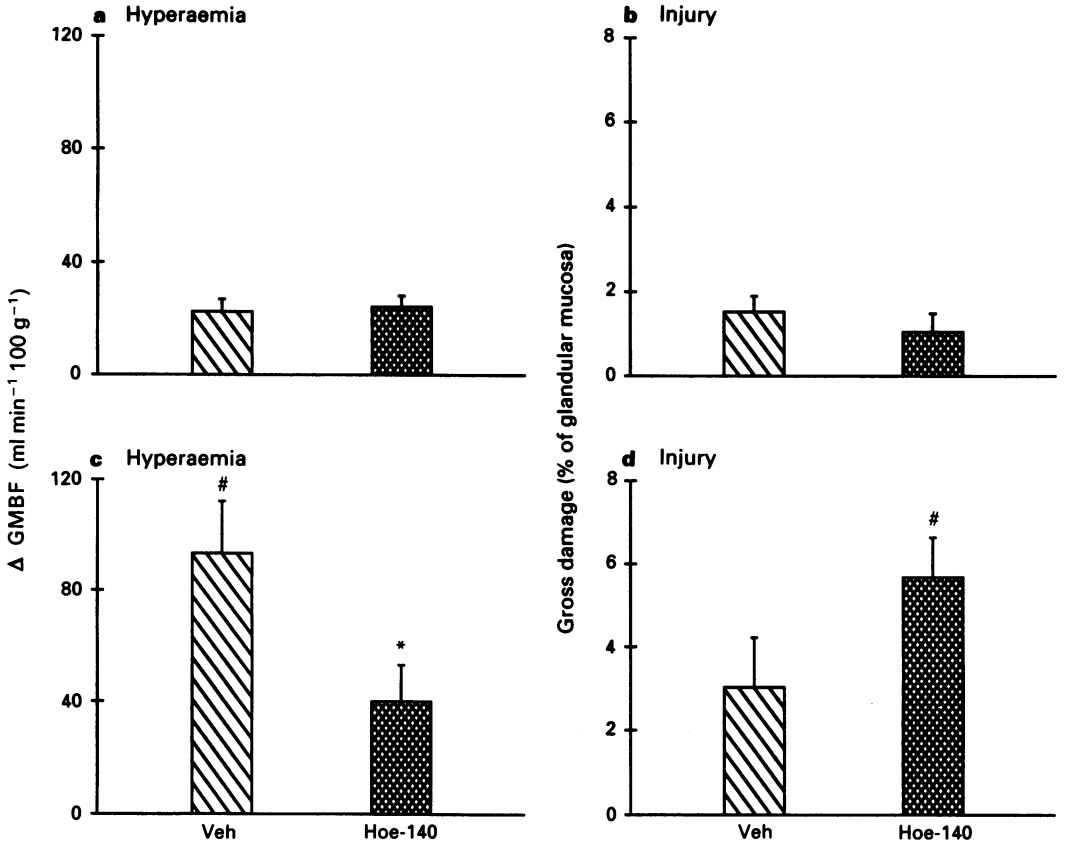


Figure 4 Increment of gastric mucosal blood flow (Δ GMBF) and formation of gross mucosal damage in response to gastric acid backdiffusion in the presence of 0.05 (a,b) or 0.15 M (c,d) HCl in rats treated either with Hoe-140 (100 μmol kg^{-1}) or its vehicle (saline, 1 ml kg^{-1}). Hoe-140 or its vehicle (Veh) was injected i.v. 30 min before gastric acid backdiffusion was induced by adding ethanol (15%) to the acidified gastric perfusion media. The increment of gastric mucosal blood flow was measured during the period 15–30 min, and gross damage was quantified 60 min, after the induction of gastric acid backdiffusion. The values shown are mean with the s.e.mean. The number of rats (n) in each group was 8–10. *$P<0.01$ versus respective values in the vehicle-treated rats; #$P<0.01$ versus respective values in rats whose stomachs were perfused with 0.05 M HCl.

this conjecture was obtained in three experimental stages. In the first study it was shown that bradykinin administered by local infusion into the gastric wall is able to enhance gastric mucosal blood flow. The vasodilator effect of intramural bradykinin implies that formation of this kinin in the gastric tissue is expected to facilitate blood flow through the gastric mucosa. The concentration of intramural bradykinin (10 μM) required to augment gastic mucosal blood flow may seem high, but it is necessary to take into account the fact that the kinin was infused at a rate of 3 μl min^{-1} (30 pmol min^{-1}) in order to avoid the infusate volume affecting blood flow. It is possible that small amounts of bradykinin may be degraded rapidly within the gastric wall.

In the second study it was found that bradykinin given i.v. increases blood flow in the left gastric artery, one of the major arteries supplying the stomach, in spite of an appreciable decrease in mean arterial blood pressure. Bradykinin thus can facilitate gastric blood flow independently of whether it is administered extra- or intravascularly, an issue that was of interest to know in view of the possible extra- and intravascular formation of bradykinin in the injured gastric mucosa. The vasodilator effects of both intramural and i.v. bradykinin were short-lived, which is indicative of a rapid breakdown of the kinin by proteolytic enzymes (Hall, 1992; Geppetti, 1993). Another property common to the bradykinin-induced increases of blood flow in the left gastric artery and gastric mucosa was their susceptibility to blockade by Hoe-140. Since this compound is a selective bradykinin B_2 receptor antagonist (Hock *et al.*, 1991; Wirth *et al.*, 1991) it follows that the dilator effect of bradykinin in the gastric vascular system is exclusively mediated by this type of bradykinin receptor. This conclusion is in keeping with the finding that the dilator response of the mesenteric artery to bradykinin is also brought about by activation of B_2 receptors (Berguer *et al.*, 1993; Santiago *et al.*, 1993).

Unlike the vasodilator effect of intramurally infused bradykinin, the gastric hyperaemic response to i.v. injected bradykinin was associated with transient hypotension and tachycardia. It is unlikely that the rise of blood flow through the left gastric artery was secondary to the effects of bradykinin on blood pressure and heart rate, because hypotension occurring in the absence of gastric vasodilatation is expected to lower blood flow through the stomach. This is the case with another hypotensive peptide, substance P, which fails to increase gastric mucosal blood flow (Holzer & Guth, 1991) and after i.v. injection decreases both blood pressure and blood flow through the left gastric artery (Holzer *et al.*, 1994).

In the third study Hoe-140 was used to examine a possible role of bradykinin in the gastric mucosal hyperaemia evoked by acid backdiffusion. The action of this drug is long-lasting (Hock *et al.*, 1991; Lembeck *et al.*, 1991; Wirth *et al.*, 1991; Holzer, 1992; Santiago *et al.*, 1993), which makes this compound a suitable tool for studying the pathophysiological implications of bradykinin acting via B_2 receptors. The dose of Hoe-140 used here (100 μmol kg^{-1}) has previously been established as effective and specific in antagonizing various responses to bradykinin (Lembeck *et al.*, 1991; Holzer, 1992; Holzer-Petsche, 1992). Its specificity (Hock *et al.*, 1991; Lembeck *et al.*, 1991; Wirth *et al.*, 1991; Holzer, 1992; Holzer-Petsche, 1992; Santiago *et al.*, 1993) was therefore not tested further, especially after it was found to be without

influence on the rise of gastric mucosal blood flow induced by gastric perfusion with 15% ethanol in 0.05 M HCl.

When, however, the intraluminal concentration of HCl was raised to 0.15 M, Hoe-140 was able to reduce significantly the hyperaemia evoked by exposure of the gastric mucosa to ethanol. It has previously been shown that the gastric mucosal hyperaemia seen under these conditions results from acid backdiffusion into the mucosal tissue (Holzer *et al.*, 1991). Ethanol is used to disrupt the gastric mucosal barrier and it is only after exposure to combined ethanol and HCl that gastric mucosal blood flow increases to a significant extent (Holzer *et al.*, 1991). The present study provided further support for this reasoning by showing that the gastric vasodilatation is closely related to the intraluminal concentration of acid. The acid-evoked hyperaemia plays a physiological role in preventing deep mucosal erosions which present themselves as haemorrhagic lesions at the macroscopic level (Holzer *et al.*, 1991).

The inhibitory effect of Hoe-140 on the hyperaemia seen after barrier disruption in the presence of 0.15 M HCl, but not 0.05 M HCl, indicates that endogenous bradykinin contributes to the acid-evoked rise of blood flow through the gastric mucosa only under conditions of severe acid challenge. The relevance of hyperaemia for gastric mucosal protection is reflected by the finding that attenuation of the acid-evoked vasodilatation by Hoe-140 resulted in enhanced lesion formation. The increase in gastric mucosal blood flow seen after acid backdiffusion is accomplished by a reflex-like neural mechanism (Holzer *et al.*, 1991; Holzer & Lippe, 1992; Raybould *et al.*, 1992), and further studies are necessary to establish whether bradykinin itself acts as a vasodilator mediator or whether it acts by stimulating neurones involved in the hyperaemic response. Either mechanism is conceivable, given that the kinin is able to dilate splanchnic blood vessels directly. (Ritter *et al.*, 1989; Berguer *et al.*, 1993; Santiago *et al.*, 1993) and to stimulate visceral afferent neurones (Longhurst *et al.*, 1984; Stein *et al.*, 1986; Holzer, 1992; Holzer-Petsche, 1992; Geppetti, 1993; Griesbacher, 1984).

This work was supported by the Austrian-Hungarian Foundation, the Jubiläumsfonds of the Austrian National Bank (grants 4207 and 4905) and the Austrian Science Foundation (grant P9473-MED). The authors are grateful to Professor B.A. Schölkens, Hoechst AG, Frankfurt am Main, Germany, for the kind donation of Hoe-140 and to Wolfgang Schluet for organizational assistance.

References

BARNES, R.J., COMLINE, R.S., DOBSON, A. & DROST, C.J. (1983). An implantable transit time ultrasonic blood flow meter. *J. Physiol.*, **345**, 2P–3P.

BERGUER, R., HOTTENSTEIN, O.D., PALEN, T.E., STEWART, J.M. & JACOBSON, E.D. (1993). Bradykinin-induced mesenteric vasodilation is mediated by B_2-subtype receptors and nitric oxide. *Am. J. Physiol.*, **264**, G492–G496.

BRUGGEMAN, T.M., WOOD, J.G. & DAVENPORT, H.W. (1979). Local control of blood flow in the dog's stomach: vasodilatation caused by acid back-diffusion following topical application of salicylic acid. *Gastroenterology*, **77**, 736–744.

BURTON, R.G. & GOREWIT, R.C. (1984). Ultrasonic flowmeter uses wide beam transit-time technique. *Med. Electron.*, **15**, 68–73.

DRAY, A. & PERKINS, M. (1993). Bradykinin and inflammatory pain. *Trends Neurosci.*, **16**, 99–104.

GEPPETTI, P. (1993). Sensory neuropeptide release by bradykinin: mechanisms and pathophysiological implications. *Regul. Pept.*, **47**, 1–23.

GEPPETTI, P., TRAMONTANA, M., EVANGELISTA, S., RENZI, D., MAGGI, C.A., FUSCO, B.M. & DEL BIANCO, E. (1991). Differential effect on neuropeptide release of different concentrations of hydrogen ions on afferent and intrinsic neurons of the rat stomach. *Gastroenterology*, **101**, 1505–1511.

GRIESBACHER, T. (1994). Blood pressure reflexes following activation of capsaicin-sensitive afferent neurones in the biliopancreatic duct of rats. *Br. J. Pharmacol.*, **111**, 547–554.

HALL, J.M. (1992). Bradykinin receptors: pharmacological properties and biological roles. *Pharmacol. Ther.*, **56**, 131–190.

HOCK, F.J., WIRTH, K., ALBUS, U., LINZ, W., GERHARDS, H.J., WIEMER, G., HENKE, S., BREIPOHL, G., KÖNIG, W., KNOLLE, J. & SCHÖLKENS, B.A. (1991). Hoe 140 a new potent and long-acting bradykinin-antagonist: *in vitro* studies. *Br. J. Pharmacol.*, **102**, 769–773.

HOLZER, P. (1992). Reflex gastric motor inhibition caused by intraperitoneal bradykinin: antagonism by Hoe 140, a bradykinin antagonist. *Peptides*, **13**, 1073–1077.

HOLZER, P. & GUTH, P.H. (1991). Neuropeptide control of rat gastric mucosal blood flow. Increase by calcitonin gene-related peptide and vasoactive intestinal polypeptide, but not substance P and neurokinin A. *Circ. Res.*, **68**, 100–105.

HOLZER, P., LIPPE, I.TH. (1992). Gastric mucosal hyperaemia due to acid back-diffusion depends on splanchnic nerve activity. *Am. J. Physiol.*, **262**, G505–G509.

HOLZER, P., LIPPE, I.TH., JOCIC, M., WACHTER, CH., ERB, R. & HEINEMANN, A. (1993). Nitric oxide-dependent and -independent hyperaemia due to calcitonin gene-related peptide in the rat stomach. *Br. J. Pharmacol.*, **110**, 404–410.

HOLZER, P., LIVINGSTON, E.H. & GUTH, P.H. (1991). Sensory neurons signal for an increase in rat gastric mucosal blood flow in the face of pending acid injury. *Gastroenterology*, **101**, 416–423.

HOLZER, P., WACHTER, CH., JOCIC, M. & HEINEMANN, A. (1994). Vascular bed-dependent roles of the peptide CGRP and nitric oxide in acid-evoked hyperaemia of the rat stomach. *J. Physiol.* (in press).

HOLZER-PETSCHE, U. (1992). Blood pressure and gastric motor responses to bradykinin and hydrochloric acid injected into somatic or visceral tissues. *Naunyn-Schmied. Arch. Pharmacol.*, **346**, 219–225.

LEMBECK, F., GRIESBACHER, T., ECKHARDT, M., HENKE, S., BREIPOHL, G. & KNOLLE, J. (1991). New, long-acting, potent bradykinin antagonists. *Br. J. Pharmacol.*, **102**, 297–304.

LEUNG, F.W., GUTH, P.H., SCREMIN, O.U., GOLANSKA, E.M. & KAUFFMAN, G.L. (1984). Regional gastric mucosal blood flow measurements by hydrogen gas clearance in the anesthetized rat and rabbit. *Gastroenterology*, **87**, 28–36.

LI, D.-S., RAYBOULD, H.E., QUINTERO, E. & GUTH, P.H. (1992). Calcitonin gene-related peptide mediates the gastric hyperaemic response to acid back-diffusion. *Gastroenterology*, **102**, 1124–1128.

LIPPE, I.TH. & HOLZER, P. (1992). Participation of endothelium-derived nitric oxide but not prostacyclin in the gastric mucosal hyperaemia due to acid back-diffusion. *Br. J. Pharmacol.*, **105**, 708–714.

LIVINGSTON, E.H., REEDY, T., LEUNG, F.W. & GUTH, P.H. (1989). Computerized curve fitting in the analysis of hydrogen gas clearance curves. *Am. J. Physiol.*, **257**, G668–G675.

LONGHURST, J.C., KAUFMAN, M.P., ORDWAY, G.A. & MUSCH, T.I. (1984). Effects of bradykinin and capsaicin on endings of afferent fibers from adbominal visceral organs. *Am. J. Physiol.*, **247**, R552–R559.

RAYBOULD, H.E., STERNINI, C., EYSSELEIN, V.E., YONEDA, M. & HOLZER, P. (1992). Selective ablation of spinal afferent neurons containing CGRP attenuates gastric hyperemic response to acid. *Peptides*, **13**, 249–254.

RITTER, J.M., DOKTOR, H.S. & CRAGOE, E.J. (1989). Actions of bradykinin and related peptides on rabbit coeliac artery rings. *Br. J. Pharmacol.*, **96**, 23–28.

SANTIAGO, J.A., OSEI, S.Y. & KADOWITZ, P.J. (1993). Inhibitory effects of Hoe 140 on vasodilator responses to bradykinin in the mesenteric vascular bed of the cat. *Eur. J. Pharmacol.*, **236**, 315–318.

STEIN, R.D., GENOVESI, S., DEMAREST, K.T. & WEAVER, L.C. (1986). Capsaicin treatment attenuates the reflex excitation of sympathetic activity caused by chemical stimulation of intestinal afferent nerves. *Brain Res.*, **397**, 145–151.

WHITTLE, B.J.R. (1977). Mechanisms underlying gastric mucosal damage induced by indomethacin and bile salts, and the actions of prostaglandins. *Br. J. Pharmacol.*, **60**, 455–460.

WIRTH, K., HOCK, F.J., ALBUS, U., LINZ, W., ALPERMANN, H.G., ANAGNOSTOPOULOS, H., HENKE, S., BREIPOHL, G., KÖNIG, W., KNOLLE, J. & SCHÖLKENS, B.A. (1991). Hoe 140, a new potent and longacting bradykinin-antagonist: *in vivo* studies. *Br. J. Pharmacol.*, **102**, 774–777.

(Received May 5, 1994
Revised June 13, 1994
Accepted July 15, 1994)

Br. J. Pharmacol. (1994), **113**, 1043–1049 © Macmillan Press Ltd, 1994

Pharmacological actions of the selective and non-selective β-adrenoceptor antagonists celiprolol, bisoprolol and propranolol on human bronchi

[1]R.W. Hauck, Ch. Schulz, H.P. Emslander & *M. Böhm

Medizinische Klinik, Klinikum rechts der Isar, Technische Universität München and *Medizinische Klinik 3, Universität zu Köln, Germany

1 The pharmacological actions of the β-adrenoceptor antagonists, celiprolol, bisoprolol and propranolol were investigated in human lung tissue by radioligand binding experiments as well as in human isolated bronchi by functional experiments in organ baths.

2 Data from lung tissue were compared to those obtained from myocardial membranes.

3 Lung tissue was obtained from 10 patients having undergone lung resection for bronchial carcinoma and myocardial tissue from a patient who had received a heart transplantation.

4 In radioligand binding experiments, celiprolol exhibited a high affinity binding to β_1-adrenoceptors in heart and a low affinity binding to β_2-adrenoceptors in lung tissue. The selectivity obtained for the β_1-adrenoceptor was calculated to a factor of eleven.

5 Compared to bisoprolol and propranolol, celiprolol elicited the lowest affinity for the β-adrenoceptor, as judged from the K_I-values.

6 In the absence and presence of the guanine nucleotide Gpp(NH)p celiprolol did not affect receptor binding.

7 In functional experiments on intact bronchi, celiprolol, bisoprolol and propranolol failed to produce relaxation (± forskolin) or a significant difference in efficacy in antagonizing the relaxant effects of isoprenaline. However, a rank order of potencies was revealed (propranolol:bisoprolol:celiprolol = 46:12:1).

8 Plasma concentrations for celiprolol and bisoprolol usually achieved *in vivo* were below the IC_{50} value obtained *in vitro*. In contrast, for propranolol, plasma concentrations were nearly identical with the IC_{50} value.

9 It is concluded that celiprolol is a selective β_1-adrenoceptor antagonist on human heart and has no agonistic properties on intact human bronchi. Compounds such as celiprolol and bisoprolol may in comparison to propranolol, possess reasonable therapeutic advantages in the treatment of patients with obstructive lung disease due to their low affinity for β_2-adrenoceptors.

Keywords: Human bronchi; human lung; β-adrenoceptor antagonists; cardioselectivity; intrinsic sympathomimetic activity; celiprolol; bisoprolol; propranolol; forskolin; asthma

Introduction

β_2-Adrenoceptor antagonists are potentially harmful to patients with airway obstruction and chronic bronchitis (Tattersfield, 1986; Dorow, 1988a); therefore, β-adrenoceptor antagonists should be avoided in these patients (Dorow, 1988b). However, it has been suggested that some newer β-adrenoceptor antagonists, e.g. celiprolol, possess certain properties, such as cardioselectivity and intrinsic sympathomimetic activity or both, which could make them potentially suitable for patients with obstructive lung disease. Clinical studies have shown that celiprolol can elicit some bronchodilator effects (Doshan *et al.*, 1986b; Pruss *et al.*, 1986). Although it has been suggested that β_2-adrenoceptor agonist properties may play a role in this context, pharmacological characterization of the compounds using human tissue and based upon rigorous criteria, i.e. measurement of the affinity of binding to β_2-adrenoceptors, potency and efficacy in antagonizing the isoprenaline effect, investigation of partial agonist and relaxant activity, have not been carried out. Therefore, the pharmacological properties of celiprolol were studied in human lung tissue using radioligand binding experiments. The data obtained were subsequently compared to those collected from human cardiac membranes. To determine whether the biochemical results are relevant for the bronchoconstrictor and bronchodilator responses of bronchial smooth muscles, celiprolol, a β_1-selective adrenoceptor antagonist with intrinsic sympathomimetic activity (ISA), bisoprolol a β_1-selective adrenoceptor antagonist without ISA, and propranolol a non-selective β-adrenoceptor antagonist were investigated in human isolated bronchial rings.

[1] Author for correspondence at: 1. Medizinische Klinik, Technische Universität München, Klinikum rechts der Isar, Ismaninger Straße 22, D-81675 München, Germany.

Methods

Patients

Informed consent was obtained from a total of 10 patients chosen for this study (2 females, 8 males) requiring pneumonectomy or lobectomy for the treatment of bronchial carcinoma (Table 1). All of the patients were subjected to preoperative lung function testing whereby airway obstruction was excluded. Every one of the ten patients were current smokers with an average intake of 10–20 cigarettes per day for over a period of at least 15 years. Age ranged between 34 and 83 (mean ± s.e.mean: 59.2 ± 4.4). None of the patients was taking any medication which interferred with the sympathetic or parasympathetic nervous system. All were administered anaesthesia according to the same regimen: Flunitrazepam, thiopental, pancuronium and isoflurane.

Table 1 Biographical and lung function data of the patients

Initials	*Sex*	*Age*	*FEV_1* (%VC)	*Resistance* (kPa(1 s^{-1})$^{-1}$)
S.W.	m	83	64	0.31
H.O.	m	57	68	0.23
H.A.	m	71	72	0.27
R.M.	m	64	72	0.23
F.K.	m	69	65	0.22
S.A.	f	34	58	0.27
M.D.	m	50	77	0.17
K.W.	f	45	90	0.27
S.G.	m	63	75	0.19
D.R.	m	56	72	0.18
Mean ±		59.2	71.3	0.23
s.e.mean		4.4	2.74	0.01

FEV_1 = forced exspiratory volume in 1 s.
VC = vital capacity.

Human lung tissue

Approximately 100 g (wet weight) tumour-free lung parenchyma was obtained during thoracic surgery and suspended in preaerated ice cold Tyrode-solution (composition see below) as described recently (Hauck *et al.*, 1990; Böhm *et al.*, 1991). The hypoxic delay was kept to a minimum, usually less than 1 min. After rapid transportation to the laboratory, bronchi with an inner diameter between 4–6 mm were prepared from the resected lung tissue. Approximately 10 g (wet weight) of lung tissues were frozen in liquid nitrogen and stored at − 80°C until use. For radioligand binding experiments, frozen tissue was allowed to thaw to 4°C within approximately 2 h. In all subsequent steps, temperature was kept at 4–8°C. Storage did not alter β-adrenoceptor density. The tissue was minced with scissors, homogenized twice for 1 min with an Ultra Turrax (Jahnke & Kunkel, Staufen, Germany) at 15,000 r.p.m. and then once for 2 min at 1500 r.p.m. with an electric glass-Teflon homogenizer (Jahnke & Kunkel, Staufen, Germany). The homogenate was filtered through a layer of gauze and centrifuged in a Beckman centrifuge I-218 (Beckman, Palo Alto, USA) for 10 min to remove undisrupted and fibrous tissue. The supernatant was then recentrifuged at 100,000 *g* for 45 min. The pellet was resuspended in incubation buffer (composition see below), homogenized by hand with a glass-glass homogenizer and recentrifuged (100,000 *g*/45 min). The final pellet was suspended in 10 volumes of the incubation buffer and the protein concentration determined according to Lowry *et al.* (1951).

Human myocardium

Myocardium was obtained from a 60 year old male patient with terminal heart failure due to dilated cardiomyopathy who had undergone heart transplant surgery. The tissue was chilled in 30 ml of ice-cold homogenization buffer (Tris HCl 10 mmol l^{-1}, EDTA 1 mmol l^{-1} pH 7.4) and was disrupted with an Ultra Turrax agitator (see above). The homogenate was spun at 2,000 *g* for 10 min. The supernatant was retained and the pellet was discarded. This homogenate was diluted with an equal volume of ice-cold KCl 1 mol l^{-1} and stored on ice for 10 min. The supernatant was centrifuged at 100,000 *g* for 45 min. The pellet was resuspended in 50 volumes of incubation buffer, homogenized for 1 min in a glass-glass flask and recentrifuged at 100,000 *g* for 45 min. The final pellet was resuspended in incubation buffer (50 vol). The homogenate was then stored as previously described (Böhm *et al.*, 1992). Radioligand binding experiments were subsequently performed in accordance to the undermentioned experiments with lung parenchyma.

Radioligand binding experiments

In order to quantify the affinity constants and potential partial agonist properties of β-adrenoceptor antagonists at β_1- and β_2-adrenoceptors, competitive experiments for binding of [^{125}I]-iodocyanopindolol (specific activity 2000 Ci $mmol^{-1}$) to β-adrenoceptors were performed. Specific binding was defined as the difference in binding in the absence and in the presence of propranolol (3 μmol l^{-1}). Propranolol, celiprolol and bisoprolol at increasing concentrations (0.0001 – 100 μmol l^{-1}) were used for binding experiments with lung, and celiprolol with myocardial tissue. The experiments were performed in the presence and absence of Gpp(NH)p to evaluate agonist properties of the β-adrenoceptor antagonists by changing the agonist affinity state of the binding site in the presence of the metabolically stable guanine nucleotide. Usually, the non-hydrolysable guanine-nucleotide leads to a reduction in binding that results in a steeper and rightward shift of the competitive curve if there is agonist activity of the compound studied at the β-adrenoceptors (Mattera *et al.*, 1985; Jasper *et al.*, 1988; Jasper & Insel, 1992). Lung membrane studies were performed with 30 μg of protein/tube. Each result represents four experiments in triplicate determinations. To block potentially existing β_2-adrenoceptors in the myocardial membranes, the β_2-adrenoceptor antagonist ICI 118.551 (50 nmol l^{-1}) was present in the reaction medium. To block potentially existing β_1-adrenoceptors in the lung membranes, CGP 20,712A (300 nmol l^{-1}) was added to the reaction medium. The binding data of celiprolol obtained in human lung tissue were compared to those from the experiments in human myocardium.

Human isolated bronchi

For the functional investigations, bronchi were cut into rings, 2–3 mm thick and stored overnight in Tyrode solution at 4°C containing tobramycin (5 mg l^{-1}) and penicillin (0.03 mg l^{-1}; de Jongste *et al.*, 1985). The solution was aerated with a slow continuous flow of 95% O_2 and 5% CO_2. This step assured a complete washout of blood compounds and narcotics. After 12 h the bronchial rings were suspended in 75 ml organ chambers, filled with preaerated Tyrode solution at pH 7.4 and maintained at 37°C. Isometric tension was measured with an inductive Fleck force transducer attached to a Hellige Helco Scriptor recorder. Following an equilibration period of 90 min, during which the bathing solution was changed at 30 min intervals, the bronchial rings were mounted under an isometric load of 2 g. Cumulative concentration-response curves were subsequently constructed. All drugs were freshly prepared immediately prior to the experiment and maintained on ice until use. For construction of concentration-response curves, the compounds were added in a cumulative manner. For contraction experiments, the concentrations of the different β-adrenoceptor antagonists ranged from 0.01 μmol l^{-1} to 100 μmol l^{-1}, and for relaxation experiments from 0.001 μmol l^{-1} to 1000 μmol l^{-1}. In relaxation experiments, bronchial rings were first precontracted with carbachol at 0.4 μmol l^{-1} (EC_{50}). This concentration has been shown in former experiments to evoke the half maximal contraction (not shown). In the experiments designed to evaluate the contractile response of the β-adrenoceptor antagonists, bronchial rings were first relaxed with isoprenaline 0.3 μmol l^{-1}, a concentration which results in the half maximal relaxation (IC_{50}) with this substance. In order to unmask the agonist properties of the β-adrenoceptor antagonists via facilitation of β-adrenoceptor-G-protein coupling, relaxation experiments were repeated using the diterpene derivative, forskolin at a concentration of 0.01 μmol l^{-1}.

Substances and buffers

[^{125}I]-CYP ((−)-3-[^{125}I]-iodocyanopindolol) as the radiolabelled ligand (specific activity 2000 Ci $mmol^{-1}$) was obtained

from Amersham-Buchler (Braunschweig, Germany) and the selective β_1-adrenoceptor antagonist CGP 20,712A {2-hydroxy-5- [2-(hydroxy-3-{4-[(1-methyl-4-trifluoromethyl)-1-H-imidazol-2-yl]-phenoxy} propyl) aminoethoxyl] benzamide} from Ciba-Geigy AG (Basel, Switzerland). The selective β_2-adrenoceptor antagonist ICI 118.551 [erythro-(±)-1-(7-methylindian-4-yloxy) -3-isopropyl- aminobutan-2-ol-hydrochloride] was obtained from Zeneca Pharmaceuticals (Macclesfield, U.K.). Celiprolol was from Upjohn, (±)-isoprenaline HCl from Boehringer Ingelheim (Ingelheim, Germany). Forskolin was donated by Dr Metzger, Hoechst AG (Frankfurt, Germany). The Tyrode solution consisted of (mmol l^{-1}): NaCl 119.8, KCl 5.4, $CaCl_2$ 1.8, $MgCl_2$ 1.05, NaH_2PO_4 0.42, $NaHCO_3$ 22.6, Na_2EDTA 0.05, ascorbic acid 0.28 and glucose 5.0. The incubation buffer contained (mmol l^{-1}) Tris 50, $MgCl_2$ 10.

Statistics

In functional studies EC_{50} and IC_{50} values were estimated graphically as the concentrations producing half maximal tension or half maximal relaxation attained with bronchi. Data shown for contraction experiments are mean ± s.e. mean. Statistical significance was estimated with Student's *t* test for unpaired observations. A *P*-value of less than 0.05 was considered to be significant. K_I-values in competition experiments were calculated according to Cheng & Prusoff (1973). Agonist competitive curves were analysed with the SCTFIT-programme (de Lean *et al.*, 1982). Curve fits assuming one, two and three affinity states were compared with an *F*-test. The significantly ($P<0.005$) best fit was accepted.

Results

Radioligand binding experiments

With celiprolol, a monophasic antagonism to [^{125}I]-CYP binding was achieved in human lung and myocardial membranes. This effect occurred with a high affinity for β_1-adrenoceptors in heart and with low affinity for β_2-adrenoceptors in lung membranes (Table 2).

Competition experiments have shown that celiprolol exhibits, neither at lung β_2-adrenoceptors nor at heart β_1-adrenoceptors, partial agonistic activity. From the K_I values, a β_1-adrenoceptor selectivity of celiprolol of a factor of eight (in the absence of Gpp(NH)p) or eleven (in the presence of Gpp(NH)p) was determined (Table 2).

Next the full β-adrenoceptor agonist, isoprenaline, was studied for comparison, as to whether guanine-nucleotide-sensitive high and low affinity binding of agonists could be detected within lung or cardiac membranes (Figure 1). Isoprenaline showed biphasic competition for lung β_2-adrenoceptors. The concentration-binding curve was shifted to the right by Gpp(NH)p, resulting in a fit to one low affinity binding site. This demonstrates that the technique used was sensitive to separate high and low affinity states for agonist binding.

The same experiments were also performed with propranolol and bisoprolol in comparison to celiprolol. As summarized in Figure 2, none of the three β-adrenoceptor antagonists elicited agonist characteristics. Table 2 sum-

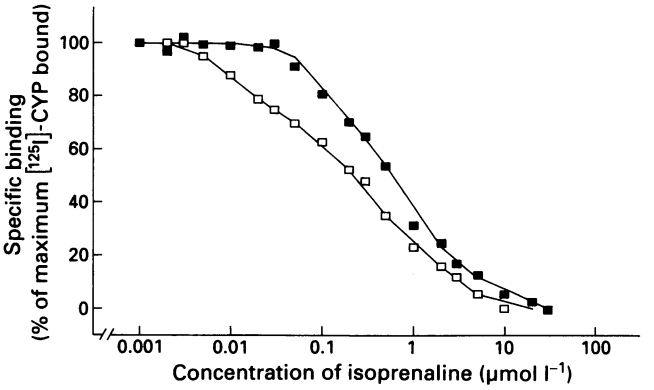


Figure 1 Inhibition of [^{125}I]-iodocyanopindolol ([^{125}I]-CYP) binding to lung β_2-adrenoceptors by isoprenaline in the absence (□) and presence (■) of Gpp(NH)p (100 μmol l^{-1}). Ordinate scale: specific binding as percentage of [^{125}I]-CYP specifically bound. Abscissa scale: concentration of isoprenaline in μmol l^{-1}. Note that with Gpp(NH)p a low affinity binding site was observed.

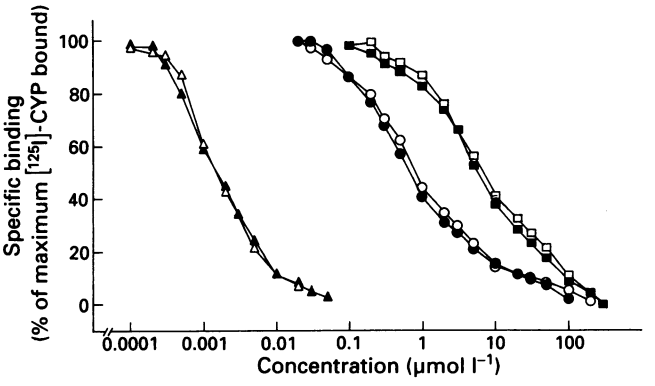


Figure 2 Inhibition of [^{125}I]-iodocyanopindolol ([^{125}I]-CYP) binding to lung β_2-adrenoceptors by isoprenaline (▲, △), bisoprolol (●, ○) and celiprolol (■, □) in the absence (open symbols) and presence (solid symbols) of Gpp(NH)p (100 μmol l^{-1}). Ordinate scale: specific binding as percentage of [^{125}I]-CYP specifically bound. Abscissa scale: concentrations of the different β-adrenoceptor antagonists. Note that propranolol demonstrated the highest affinity for the β_2-adrenoceptors, followed by bisoprolol and celiprolol. No influence was observed of the presence of Gpp(NH)p.

Table 2 Equilibrium dissociation constants K_I for competing β-adrenoceptor antagonists in membranes from human peripheral lung and human heart

	− *Gpp(NH)p* (μmol l^{-1})	+ *Gpp(NH)p* (μmol l^{-1})
Human lung (+ CGP 207.12A)		
Propranolol	0.0006 (0.00045–0.0009)	0.00075 (0.00036–0.0016)
Bisoprolol	0.4 (0.25–0.65)	0.45 (0.25–0.85)
Celiprolol	2.8 (1.35–5.85)	3.55 (1.05–10.7)
Human heart (+ ICI 118.551)		
Celiprolol	0.35 (0.28–0.4)	0.31 (0.23–0.43)

K_I values are given with 95% confidence limits.

marizes the K_I-values of the β-adrenoceptor antagonists with and without Gpp(NH)p. With the β-adrenoceptor antagonists, a difference in the K_I-values within the 95% confidence limits was measured in the presence and absence of 100 μmol l^{-1} Gpp(NH)p (Table 2, Figure 2). Comparison of the compounds studied showed that the β-adrenoceptor affinity of propranolol was significantly higher (K_I: 0.0006 μmol l^{-1}), than that of bisoprolol (K_I: 0.4 μmol l^{-1}) and celiprolol (K_I: 2.8 μmol l^{-1}). Therefore, the rank order of affinity is propranolol > bisoprolol > celiprolol resulting in relative affinities of 4667: 7: 1.

Functional studies

In order to study the bronchoconstrictor and bronchodilator effects of the β-adrenoceptor antagonists, functional experiments with bronchial rings were performed. In Figure 3, original recordings illustrate the effect of isoprenaline and celiprolol in human bronchial rings. At 0.4 μmol l^{-1} carbachol (i.e. the concentration producing half maximal effect on tension development) the evoked tension increased to 9.6 mN. Isoprenaline, added at a half maximal concentration, led to relaxation below the resting tension. After equilibration under these conditions, celiprolol produced an increase in tension which was maximal at a concentration of 100 μmol l^{-1}. The maximal relaxant effect of papaverine at 100 μmol l^{-1} is also illustrated.

In order to evaluate efficacy and potency of the potential bronchoconstrictor action, bronchi were concentration-dependently contracted with the β-adrenoceptor antagonists. A similar efficacy (judged from the maximal effects) of propranolol, bisoprolol and celiprolol in evoking contraction in the human bronchi was observed (not shown).

In order to evaluate the potency of these compounds, the IC_{50}-values (cf. Table 3) were calculated from concentration-response curves (Figure 4). The half maximal effects of propranolol occurred at 0.1 μmol l^{-1}, for bisoprolol at 1.2 μmol l^{-1} and for celiprolol at 4.6 μmol l^{-1} (Table 3). Thus, the rank order of potency is propranolol > bisoprolol > celiprolol, resulting in relative potencies of 46: 12: 1.

In order to evaluate the potential clinical relevance of the bronchoconstrictor response, the IC_{50} values *in vitro* were compared with the therapeutic drug concentrations *in vivo*. As shown in Table 3, the reported plasma concentrations of propranolol subsequent to an oral dose of 80 mg, were within the range which evoked the half maximal bronchial constriction (IC_{50}) *in vitro*. In contrast, the plasma concentrations following an oral application of 10 mg bisoprolol, and 200 mg celiprolol, respectively, were below the range which led to a half maximal contraction at bronchial rings *in vitro*. The therapeutic range of 80 mg propranolol (plasma concentration: 0.289 ± 0.006 μmol l^{-1}, Naline *et al.*, 1990) inhibited the isoprenaline effect on human bronchi by about 58%; 10 mg bisoprolol (plasma concentration: 0.15 ± 0.006 μmol l^{-1}; Naline *et al.*, 1990) antagonized the isoprenaline effect by about 5% and 200 mg celiprolol (plasma concentration: 1.35 ± 0.56 μmol l^{-1}; Schmidt *et al.*, 1985) diminished the isoprenaline effect by around 20% (Figure 4).

Further experiments were designed to determine whether the compounds were capable of producing direct bronchorelaxant effects. As shown in Figure 5 (concentration-response curves), with isoprenaline full relaxation of the

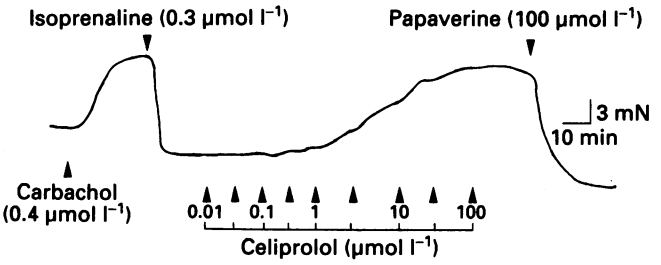


Figure 3 Original recording which illustrates the effect of celiprolol on tension development in human bronchial rings. Note that celiprolol maximally antagonizes the isoprenaline effect at 100 μmol l^{-1}. This was completely reversed by papaverine, 100 μmol l^{-1}.

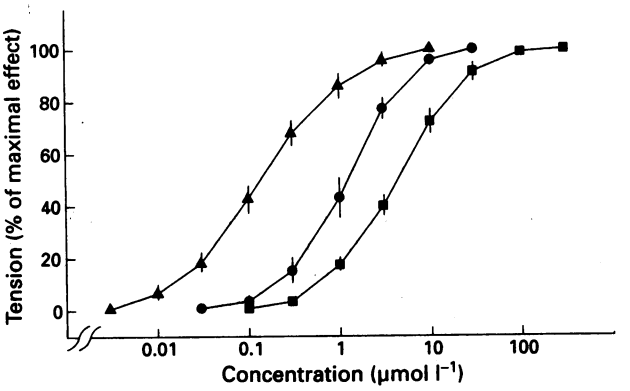


Figure 4 Concentration-response curves for the effect on force of contraction of propranolol (▲), bisoprolol (●) and celiprolol (■) on carbachol (0.4 μmol l^{-1}) precontracted and isoprenaline (0.3 μmol l^{-1}) relaxed human bronchi. Ordinate scale: increase in tension development as percentage of the maximal effect. Abscissa scale: concentration of the different β-adrenoceptor antagonists. Note the rank order of potency was: propranolol > bisoprolol > celiprolol.

Table 3 IC_{50} and EC_{50} concentrations of agonists and antagonists in human bronchi calculated from functional investigations *in vitro*

Substance	n	*IC_{50} EC_{50}* (μmol l^{-1})	*Maximal effect* (mN)	*Plasma level* (μmol l^{-1})
Isoprenaline[1]	7	0.3 (0.2–0.4)	–	–
Isoprenaline[2]	5	0.016 (0.007–0.04)	–	–
Propranolol[3]	4	0.1 (0.074–0.3)	9.15 ± 2.2	0.289 ± 0.006[4]
Bisoprolol[3]	6	1.2 (0.7–2.1)	9.54 ± 3.5	0.15 ± 0.006[5]
Celiprolol[3]	5	4.6 (3.1–6.8)	7.78 ± 0.5	1.35 ± 0.56[6]

Values are mean with 95% confidence limits. Plasma levels *in vivo* of the investigated compounds are shown for comparison. Values are mean ± s.e.mean.

[1]Precontraction with EC_{50} carbachol; [2]precontraction with EC_{50} carbachol and EC_{20} forskolin; [3]after precontraction with EC_{50} carbachol and EC_{50} isoprenaline relaxation.

[4]After 80 mg propranolol p.o. (Naline *et al.*, 1990); [5]After 10 mg bisoprolol p.o. (Naline *et al.*, 1990); [6]After 200 mg celiprolol p.o. (Schmidt *et al.*, 1985).

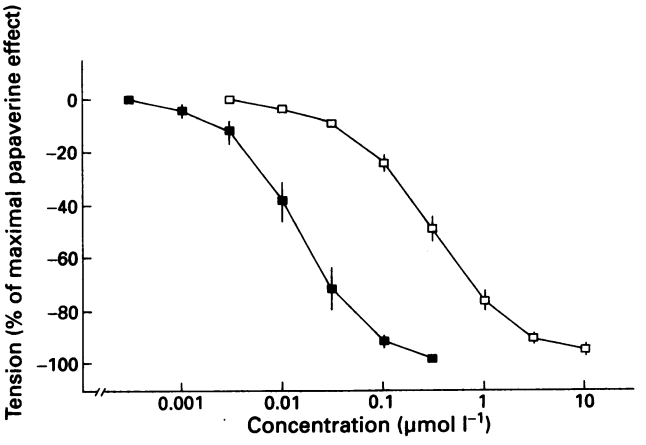


Figure 5 Concentration-response curves for the effect of isoprenaline in the absence (□) and presence (■) of forskolin (0.01 μmol l^{-1}) on carbachol (0.4 μmol l^{-1})- precontracted bronchi. Ordinate scale: tension of bronchi as percentage of the maximal relaxant effect of papaverine. Abscissa scale: concentration of isoprenaline. Note that forskolin led to an increase in potency of isoprenaline in relaxing human bronchi by a factor of 18.

precontracted bronchi could be achieved. The threshold concentration for relaxation was 0.01 μmol l^{-1} and the maximum relaxation was achieved at 10 μmol l^{-1} without an additional effect of papaverine. After forskolin (0.01 μmol l^{-1}) was added, the half maximal relaxation occurred at lower concentrations, i.e. 0.016 (0.007–0.04) μmol l^{-1}, compared to 0.3 (0.2–0.4) μmol l^{-1} in the absence of forskolin. This indicated an increase in potency evoked by forskolin by a factor 18.7. Since forskolin facilitates the coupling of β-adrenoceptors to adenylate cyclase (Böhm *et al.*, 1992), experiments with celiprolol were performed in the absence and presence of forskolin in order to sensitize the β-adrenoceptor-G-protein system towards stimulation by partial agonists. Celiprolol did not elicit a significant bronchorelaxant response at concentrations below 100 μmol l^{-1}. The same experiments with forskolin did not lead to an increase in potency of the relaxant activity of celiprolol which occurred only at concentrations higher than 100 μmol l^{-1}.

Discussion

In the present study, the pharmacological properties of celiprolol, bisoprolol and propranolol on human lung tissue as well as human bronchi were investigated. Because of its high affinity for β_1-adrenoceptors (van Inwegen *et al.*, 1984), often termed cardioselectivity, celiprolol is frequently used in the treatment of such cardiovascular diseases as coronary heart disease and hypertension (Prichard & Tomlinson, 1986; Clauzel *et al.*, 1988). Since in the human lung, the β_2-adrenoceptor subtype predominates (Barnes *et al.*, 1983; Carstairs *et al.*, 1985), it has been suggested that in the treatment of patients with obstructive airway disease the β_1-adrenoceptor selectivity of celiprolol, together with its supposed partial agonist activity on β_2-adrenoceptors, could provide some advantages by evoking bronchodilator effects (Doshan *et al.*, 1986b; Matthys *et al.*, 1986).

The results of this study show that within myocardial membranes, celiprolol exhibited high affinity antagonist binding to β_1-adrenoceptors. Its binding to β_2-adrenoceptors was studied in lung tissue with radioligand binding experiments performed on membranes from lung tissue. It could be demonstrated that for celiprolol, there is only one low affinity binding site of the β_2-adrenoceptor subtype. The use of Gpp(NH)p provided no evidence for agonist properties.

Since bisoprolol should exhibit a similar β_1-adrenoceptor selectivity (Schliep & Frey, 1984), a comparative investigation of these compounds and the non-selective β-adrenoceptor antagonist, propranolol was carried out. Celiprolol demonstrated the lowest β_2-adrenoceptor affinity as judged from the K_I-values, followed by bisoprolol and propranolol. These data reveal celiprolol to be a highly selective compound at β_1-adrenoceptors but without β-adrenoceptor agonist properties at the β_2-adrenoceptor subtype.

Dhein *et al.* (1992) reported a β_2-adrenoceptor-mediated sympathomimetic activity of celiprolol, as shown by its vasodilator effect. These findings raised the question as to whether these agonist effects could also be demonstrated to activate β_2-adrenoceptors within the human lung. Such effects could possibly provide support for cyclic AMP formation in bronchial smooth muscles, with initiation of bronchodilator effects (Jasper & Insel, 1992). In competition radioligand binding experiments with 100 μmol l^{-1} of the non-hydrolysable guanine-nucleotide Gpp(NH)p, no alteration in the affinity state of celiprolol binding was measured (Mattera *et al.*, 1985; Jasper *et al.*, 1988). Hence, no evidence for partial agonist activity was detected. In this respect, the effect of celiprolol did not differ from the effect of the other β-adrenoceptor antagonists. In contrast, guanine-nucleotide-sensitive high- and low-affinity binding was observed with the full β-adrenoceptor agonist, isoprenaline. Thus, with this technique, celiprolol was classified as an antagonist at β_2-adrenoceptors of peripheral lung tissue. Because at this stage the question remained open as to whether the pharmacological properties (e.g. β-adrenoceptor-G-protein coupling) could be different in intact human bronchi, the effects of celiprolol on tension development were studied. In contrast to the β-adrenoceptor agonist, isoprenaline, celiprolol failed to relax isolated intact human bronchi *in vitro*.

Similar results were obtained in the presence of the diterpene derivative forskolin (Seamon & Daly, 1989), which has been reported to unmask increases in cyclic AMP-formation by partial β-adrenoceptor agonists in human lymphocytes via facilitation of β-adrenoceptor-G-protein coupling (Jasper *et al.*, 1989). Even under these conditions, celiprolol did not evoke bronchodilator effects, which would have served as evidence of a β-adrenoceptor agonist action.

In the case of celiprolol, clinical studies (Rosenthal *et al.*, 1985; Schindl *et al.*, 1986; van Zyl *et al.*, 1989) have shown that during treatment, the FEV_1 will not be adversely affected in patients with obstructive lung disease. In addition, it has been demonstrated that after application of celiprolol no decline in the bronchodilator activity of β_2-sympathomimetic drugs occurs. In a study (Carnathan *et al.*, 1988) on cats infused with 5-hydroxytryptamine it was shown that after infusion of celiprolol (35 μg kg^{-1} min^{-1}), a reduction of airway resistance was induced. In contrast, clinical studies (Matthys *et al.*, 1986) indicate that after pretreatment with propranolol a marked antagonism to the bronchodilator response of a β_2-adrenoceptor agonist treatment was observed.

Thus, there is an obvious discrepancy between the beneficial findings concerning the bronchodilator effects of celiprolol in patients *in vivo* (Rosenthal *et al.*, 1985; Matthys *et al.*, 1986; Schindl *et al.*, 1986; van Zyl *et al.*, 1989) and the lack of β_2-adrenoceptor agonist activities of the compound *in vitro* (this study). The tone of the bronchial smooth muscles is under constant regulatory control of the sympathetic nervous system (Tattersfield, 1986). Therefore, it is conceivable that a portion of the β-adrenoceptors are continuously stimulated by endogenous catecholamines (Barnes *et al.*, 1981; Ind *et al.*, 1985; Tattersfield, 1986). From this point of view, an alternative explanation for the beneficial effect of celiprolol (with low incidence and severity of adverse reactions in patients) would be a low antagonist affinity for β_2-adrenoceptors. This low affinity was established in our radioligand binding experiments, in comparison with the other compounds. The pharmacological properties of celiprolol would result only in a small antagonism to the stimulation of β_2-adrenoceptors by endogenous catechola-

mines resulting in less adverse effects on bronchial tone. Since attacks of asthma, associated with dyspnoea and tachycardia, are presumably accompanied by sympathetic activation, this mechanism might become increasingly relevant in severe cases of this disease.

To examine this latter hypothesis experimentally, the situation was mimicked *in vitro* by testing the effects of celiprolol and the other β-adrenoceptor antagonists in the presence of an isoprenaline-induced half maximal bronchodilator response. All the antagonists produced complete antagonism of the bronchial relaxant response to isoprenaline. However, it is worth noting that the drug concentrations necessary to evoke the maximal and half-maximal bronchoconstrictor effects were quite different. This difference in potency amounted for propranolol to a factor 12 and 46 respectively, in comparison to bisoprolol and celiprolol, i.e. propranolol antagonized the bronchorelaxant effects of isoprenaline at the lowest concentration (IC_{50}: 0.1 μmol l^{-1}).

It remained unclear as to whether the latter findings could be influenced by non-specific effects of the β-adrenoceptor antagonists. However, a close correspondence between the affinity of the compounds for the β-adrenoceptor obtained in radioligand binding studies and the IC_{50}-values for their bronchoconstrictor actions was observed. Thus, the results presented favour the suggestion that the different effects of the β-adrenoceptor antagonists on intact preparations are based upon their individual pharmacological profiles of interaction with the β-adrenoceptor.

In order to evaluate further the clinical relevance of these data, the plasma concentrations resulting from oral doses of propranolol, 80 mg (Naline *et al.*, 1990), bisoprolol, 10 mg (Naline *et al.*, 1990) and celiprolol, 200 mg (Schmidt *et al.*, 1985) were compared with the functional effects which had been evoked at those concentrations on intact preparations of human bronchi *in vitro*. This approach allowed the detection of an apparent difference between the β_1-selective and the non-selective β-adrenoceptor antagonists. It was to be expected that celiprolol and bisoprolol would exert smaller bronchoconstriction at therapeutic drug levels than does propranolol. Propranolol evokes half maximal contraction in human bronchi at therapeutic concentrations, whereas bisoprolol, at therapeutic concentrations, antagonizes the isoprenaline relaxed bronchi only by some 5% and celiprolol by just 20%. These *in vitro* data explain the results of clinical studies in which celiprolol was found to be at a lesser disadvantage in the adverse influencing of bronchial resistance. For propranolol, bronchoconstrictor action is reported at oral doses of 40, 100 and 200 mg *in vivo* (Doshan *et al.*, 1986a; Schindl *et al.*, 1986; Bruschi *et al.*, 1988).

It is concluded that celiprolol has a relevant β_1-adrenoceptor selectivity which amounts to a factor of 8–11 in comparison to β_2-adrenoceptors. Agonist properties could not be demonstrated on intact human bronchi or lung membranes even though the β-adrenoceptor-G-protein coupling was facilitated by forskolin. The lack of agonist effects emphasizes the importance of β-adrenoceptor selectivity in the evaluation of undesirable drug effects. The suggested effects of celiprolol on the bronchial tone observed in patients might be due to a low affinity for the β_2-adrenoceptor resulting in weak or no antagonism of bronchodilatation evoked by endogenous catecholamines rather than to relevant partial agonist activities. Evaluation of *in vitro* responses at therapeutically active drug-concentrations revealed reasonable therapeutic indices for celiprolol and bisoprolol. Thus, no obvious advantage for celiprolol could be substantiated. The combined interpretation of data from biochemical, functional and pharmacological investigations might provide valuable tools in the investigation of novel drugs for the treatment of pulmonary and cardiovascular disorders which are limited by their adverse effects exerted upon other systems.

Experimental work was supported by grants from the Deutsche Forschungsgemeinschaft and Upjohn Co. to M.B.

The authors wish to thank Prof. Dr Dienemann, Chirurgische Klinik, Klinikum Grosshadern, Universität München for the supply of bronchi and lung parenchyma.

References

BARNES, P.J., BROWN, M.J., SILVERMAN, M. & DOLLERY, C.T. (1981). Circulating catecholamines in exercise and hyperventilation induced asthma. *Thorax*, **36**, 435–440.

BARNES, P.J., BASBAUM, C.B. & NADEL, J.A. (1983). Autoradiographic localization of autonomic receptors in airway smooth muscles. *Am. Rev. Respir. Dis.*, **127**, 758–762.

BÖHM, M., GENGENBACH, S., HAUCK, R.W., SUNDER-PLASSMANN, L. & ERDMANN, E. (1991). Beta-adrenergic receptor and m-cholinoceptors in human lung. *Chest*, **100**, 1246–1253.

BÖHM, M., SCHULZ, C.H., SCHWINGER, R.H.G. & ERDMANN, E. (1992). Positive inotropic effects due to partial agonistic activity of the β-adrenoceptor antagonist celiprolol following amplification of cAMP formation in failing human myocardium. *J. Cardiovasc. Pharmacol.*, **20**, 479–489.

BRUSCHI, C., CASALI, L., CERVERI, I., PEONA, V. & ZOIA, M.C. (1988). Effects of celiprolol on the bronchial reactivity in asthma. *Am. J. Cardiol.*, **61**, 52C–54C.

CARNATHAN, G.W., SWEENEY, D.M., GORDON, R. & PRUSS, T.P. (1988). Cardiopulmonary effects of celiprolol and bisoprolol in serotinin-infused cats. *Eur. J. Pharmacol.*, **151**, 337–340.

CARSTAIRS, J.R., NIMMO, A.J. & BARNES, P.J. (1985). Autoradiographic visualization of beta-adrenoceptor subtypes in human lung. *Am. Rev. Respir. Dis.*, **132**, 541–547.

CHENG, Y.C. & PRUSOFF, W.H. (1973). Relationship between the inhibition constant (K_i) and the concentration of inhibitor which causes 50% inhibition (IC_{50}) of an enzymatic reaction. *Biochem. Pharmacol.*, **22**, 3099–3108.

CLAUZEL, A.M., JEAN, T., ETIENNE, R., VISIER, S. & MICHEL, F. (1988). Effect of long-term treatment with celiprolol on pulmonary function in a group of mild hypertensive asthmatics. *J. Int. Med. Res.*, **16** (Suppl 1), 27A–33A.

DHEIN, S., TITZER, S., WALLSTEIN, M., MÜLLER, A., GERWIN, R., PANZNER, B. & KLAUS, W. (1992). Celiprolol exerts microvascular dilatation by activation of β_2-adrenoceptors. *Naunyn-Schmied. Arch. Pharmacol.*, **346**, 27–31.

DOROW, P. (1988a). Celiprolol – review of airway studies. *Am. J. Cardiol.*, **61**, 23–26.

DOROW, P. (1988b). Bronchoneutral effects in hypertensive asthmatics – celiprolol versus chlorthalidone. *J. Int. Med. Res.*, **16** (Suppl 1), 23A–26A.

DOSHAN, D.H., BROWN, R., APPLIN, W.J., KAPOOR, M. & CARUSO, F.S. (1986a). Effects of high doses of celiprolol in asthmatic patients. *J. Cardiovasc. Pharmacol.*, **8** (Suppl 4), 109–111.

DOSHAN, D.H., ROSENTHAL, R.R., BROWN, R., SLUTSKY, A., APPLIN, W.J. & CARUSO, F.S. (1986b). Celiprolol, atenolol and propranolol: a comparison of pulmonary effects in asthmatic patients. *J. Cardiovasc. Pharmacol.*, **8** (Suppl 4), 105–108.

HAUCK, R.W., BÖHM, M., GENGENBACH, S., SUNDER-PLASSMANN, L., FRUHMANN, G. & ERDMANN, E. (1990). β_2-Adrenoceptors in human lung and peripheral mononuclear leukocytes of untreated and terbutaline-treated patients. *Chest*, **98**, 376–381.

IND, P.W., CAUSON, R.C., BROWN, M.J. & BARNES, P.J. (1985). Circulating catecholamines in acute asthma. *Br. Med. J.*, **290**, 267–269.

VAN INWEGEN, R.G., KHANDWALA, A., WEINRYB, I., PRUSS, T.P., NEISS, E. & SUTHERLAND, C.A. (1984). Effects of celiprolol (REV 5320), a new cardioselective beta-adrenoceptor antagonist, or in vitro adenylate cyclase, alpha- and beta-adrenergic receptor binding and lipolysis. *Arch. Int. Pharmacodyn.*, **272**, 40–55.

JASPER, J.R. & INSEL, P.A. (1992). Evolving concepts of partial agonism. The β-adrenergic receptor as a paradigm. *Biochem. Pharmacol.*, **43**, 119–130.

JASPER, J.R., MOTULSKY, H.J. & INSEL, P.A. (1988). Characterization of a bromoacetylated derivative of pindolol as a high affinity, irreversible beta-adrenergic antagonist in cultured cells. *J. Pharmacol. Exp. Ther.*, **244**, 820–824.

JASPER, J.R., MICHEL, M.C. & INSEL, P.A. (1989). Amplification of cyclic AMP generation reveals agonistic effects of certain β-adrenergic antagonists. *Mol. Pharmacol.*, **37**, 44–49.

DE JONGSTE, J.C., VAN STRIK, R., BONTA, I.L. & KERREBIJN, K.F. (1985). Measurement of human small airway smooth muscle function in vitro with the bronchiolar strip preparation. *J. Pharmacol. Methods*, **14**, 111–118.

DE LEAN, A., HANCOCK, A.A. & LEFKOWITZ, R.J. (1982). Validation and statistical analysis of a computer modeling for quantitative analysis of radioligand binding data for mixtures of pharmacological receptor subtypes. *Mol. Pharmacol.*, **21**, 5–16.

LOWRY, O.H., ROSEBROUGH, N.J., FARR, N.J. & RANDALL, R.J. (1951). Protein measurements with the folin phenol reagent. *J. Biol. Chem.*, **193**, 265–275.

MATTERA, R., PITTS, B.J.R., ENTMAN, M.L. & BIRNBAUMER, L. (1985). Guanine nucleotide regulation of a mammalian myocardial muscarinic receptor system. Evidence for homo- and heterotropic cooperatively in ligand binding analyzed by computer-assisted curve fitting. *J. Biol. Chem.*, **260**, 7410–7421.

MATTHYS, H., DOSHAN, H.D., RÜHLE, K.H., APPLIN, W.J., BRAIG, H. & POHL, M. (1986). Bronchosparing properties of celiprolol, a new β_1, a_2-blocker, in propranolol-sensitive asthmatic patients. *J. Cardiovasc. Pharmacol.*, **8** (Suppl 4), 40–42.

NALINE, E., SARRIA, B., ERTZBISCHOFF, O., OZANNE, P. & ADVENIER, C. (1990). Comparative β-adrenoceptor blocking effects of propranolol, bisoprolol, atenolol, acebutolol and diacetolol on the human isolated bronchus. *Br. J. Clin. Pharmacol.*, **330**, 135–139.

PRICHARD, B.N.C. & TOMLINSON, B. (1986). The additional properties of beta adrenoceptor blocking drugs. *J. Cardiovasc. Pharmacol.*, **8** (Suppl 4), 1–15.

PRUSS, T.P., KHANDWALA, A., WOLF, P.S., GREBOW, P. & WONG, L. (1986). Celiprolol: a new beta adrenoceptor antagonist with novel ancillary properties. *J. Cardiovasc. Pharmacol.*, **8** (Suppl 4), 29–32.

ROSENTHAL, R.R., DOSHAN, H.D., APPLIN, W.J. & CARUSO, F.S. (1985). Celiprolol: an investigation of a new $beta_1$-, $alpha_2$-adrenoceptor antagonist in asthmatic patients. *Br. J. Clin. Pract.*, **39** (Suppl 40), 34–36.

SCHINDL, R., WÜRTZ, J. & HOFFMANN, H. (1986). The effect of the cardioselective beta blocker celiprolol on pulmonary function in asthmatic patients. *J. Cardiovasc. Pharmacol.*, **8** (Suppl 4), 99–101.

SCHLIEP, H.J. & FREY, H.H. (1984). β_1-Selectively of bisoprolol, a newer β-adrenoceptor antagonist, in anesthetized dogs and guinea pigs. *J. Cardiovasc. Pharmacol.*, **6**, 1156.

SCHMIDT, P., TAKACS, F., PITTNER, H., MINAR, E., BALCKE, P., ZAZGORNIK, P. & DEUTSCH, E. (1985). Vergleichende Pharmakokinetik des beta 1-Rezeptoren-Blockers Celiprolol nach oraler Einzelgabe an Nierengesunde und an Patienten mit eingeschränkter Nierenfunktion. *Wien. Klin. Wochenschr.*, **18**, 729–732.

SEAMON, K.B. & DALY, J.W. (1989). Forskolin: its biological and chemical properties. *Adv. Cyclic Nucleotide Protein Phosphorylation Res.*, **20**, 1–150.

TATTERSFIELD, A.E. (1986). Beta adrenoceptor antagonists and respiratory disease. *J. Cardiovasc. Pharmacol.*, **8**, 35–39.

VAN ZYL, A.I., JENNINGS, A.A., BATEMAN, E.D. & OPIE, L.H. (1989). Comparison of respiratory effects of two cardioselective beta-blockers, celiprolol and atenolol, in asthmatics with mild to moderate hypertension. *Chest*, **95**, 209–213.

(Received April 6, 1994
Revised June 20, 1994
Accepted July 20, 1994)

Br. J. Pharmacol. (1994), **113**, 1050–1056 © Macmillan Press Ltd, 1994

Substrate specificity of the di/tripeptide transporter in human intestinal epithelia (Caco-2): identification of substrates that undergo H^+-coupled absorption

[1]David T. Thwaites, Barry H. Hirst & Nicholas L. Simmons

Gastrointestinal Drug Delivery Research Centre, Department of Physiological Sciences, University of Newcastle upon Tyne, Medical School, Framlington Place, Newcastle upon Tyne, NE2 4HH

1 pH-dependent transepithelial transport and intracellular accumulation of the hydrolysis-resistant dipeptide glycylsarcosine (Gly-Sar) have been demonstrated in the model human intestinal epithelial cell line, Caco-2.

2 Experiments with BCECF (2',7'-*bis*(2-carboxyethyl)-5(6)-carboxyfluorescein)-loaded Caco-2 cells demonstrated that dipeptide (Gly-Sar) transport across the apical membrane is coupled to proton flow into the cell.

3 A range of postulated substrates for the intestinal di/tripeptide carrier were tested for their abilities to: (a) inhibit pH-dependent [^{14}C]Gly-Sar apical-to-basal transport and intracellular accumulation and (b) stimulate H^+ flow across the apical surface of BCECF-loaded Caco-2 cell monolayers.

4 A range of compounds (including Gly-Gly, Leu-Leu, Gly-Gly-Gly, cefadroxil and cephalexin) caused marked acidification of intracellular pH when perfused at the apical surface of Caco-2 cell monolayers. In contrast leucine and D-Leu-D-Leu failed to induce proton flow. The ability to induce proton-flow across the apical surface by these compounds, in this intestinal epithelium, was directly correlated to the relative inhibitory effects on [^{14}C]-Gly-Sar transport and accumulation.

5 The determination of substrate-induced intracellular pH change in the Caco-2 cell system may provide a useful rapid screen for candidate substrates for absorption via H^+-coupled transport mechanisms such as the intestinal di/tripeptide carrier in an appropriate physiological context.

Keywords: Proton-coupled transport; dipeptide; intestine; epithelium; Caco-2 cells; cell culture; cephalosporin; intracellular pH

Introduction

The initial barrier to drug delivery via the oral route is the relative ability of drug molecules to cross the intestinal epithelial cell wall. Absorption may occur by both passive (paracellular and transcellular) and active (transcellular) processes. An important membrane transporter involved in absorption via the transcellular route is the intestinal di/tripeptide carrier which plays a significant role in protein absorption (Matthews, 1975; Matthews & Adibi, 1976). This H^+-gradient driven carrier (Ganapathy & Leibach, 1985) is also thought to be primarily responsible for the oral absorption of a number of pharmaceuticals including some aminocephalosporin antibiotics (Nakashima *et al.*, 1984; Humphrey, 1986; Smith *et al.*, 1992). The driving force for this H^+-gradient driven absorptive mechanism is the acid microclimate (an area of low pH lying adjacent to the apical surface of the intestinal epithelium) which has been identified at the mucosal surface of the human jejunum both *in vivo* (Rawling *et al.*, 1987) and *in vitro* (Lucas *et al.*, 1978). Experiments aimed at identifying substrates that can access this H^+-driven transcellular transport route have generally utilized either whole tissue preparations (i.e. the hamster jejunum *in vitro*: Sleisenger *et al.*, 1976; Matthews & Burston, 1983) or brush-border membrane vesicles (BBMV) prepared from rat or rabbit small intestine (Ganapathy *et al.*, 1984; Ganapathy & Leibach, 1985; Okano *et al.*, 1986a,b; Thwaites *et al.*, 1993h). Until recently there had been relatively few studies at the cellular level (Dantzig & Bergin, 1990; Inui *et al.*, 1992; Thwaites *et al.*, 1993a,b,c).

The human intestinal epithelial cell line, Caco-2, expresses functional H^+-coupled dipeptide carriers at both apical and basolateral membranes (Thwaites *et al.*, 1993a,b). Transepithelial transport of the non-hydrolysable dipeptide Gly-Sar has been extensively characterized (Thwaites *et al.*, 1993a), whilst pH-dependent transport of the orally-absorbed cephalosporin, cephradine (Inui *et al.*, 1992), and the anti-cancer agent, bestatin (Saitǫ & Inui, 1993) across epithelial monolayers of Caco-2 cells have been demonstrated. In addition, to expression of H^+-linked dipeptide transport, Caco-2 cells express a number of solute transporters including those for sugars (Blais *et al.*, 1987), amino acids (Hidalgo & Borchardt, 1990a) and bile acids (Hidalgo & Borchardt, 1990b) confirming the suitability of this human model system as an *in vitro* model of the human intestine.

Recently we have related the ability of a substrate to access the dipeptide transporter with its ability to induce H^+ flow across the apical surface of Caco-2 cell monolayers, as detected by changes in intracellular pH monitored using the pH-sensitive fluorescent dye, 2',7',-*bis*(2-carboxyethyl)-5(6)-carboxyfluorescein BCECF (Thwaites *et al.*, 1993a,b,c). Such a measure provides a novel method to discriminate between a non-transported inhibitor from a true substrate and allows assessment of the substrate-specificity of certain peptides, including those likely to undergo degradation at the epithelial surface (Thwaites *et al.*, 1993c). In addition, by comparison of the relative abilities of substrates to inhibit pH-dependent transepithelial transport (and cellular accumulation) of the dipeptide [^{14}C]-Gly-Sar with substrate-stimulated H^+-flow, it is possible to define potential inhibitors and to identify substrates accessing alternative H^+-linked carriers. Therefore, the aim of this investigation was to identify, by use of two complementary techniques, the range of substrates that access the human H^+-coupled small peptide transporter expressed in an appropriate physiological context, namely the human intestinal epithelial cell line, Caco-2.

[1] Author for correspondence.

Methods

Cell culture

Caco-2 cells (passage number 94–116) were cultured in DMEM (with 4.5 g l^{-1} glucose), with 1% non-essential amino acids, 2 mM L-glutamine, 10% (v/v) foetal calf serum and gentamicin (60 μg ml^{-1}). Cell monolayers were prepared by seeding at high density ($4.4–5.0 \times 10^5$ cells cm^{-2}) onto tissue culture inserts [Transwell (0.4 μm pore) polycarbonate filters (Costar), 24 mm (cat. no. 3412) or 12 mm (cat. no. 3401) in diameter]. Cell monolayers were maintained at 37°C in a humidified atmosphere of 5% CO_2 in air. Media was replaced every 2–3 days. Cell confluence was estimated by microscopy and determination of transepithelial electrical resistance (R_T) using EVOM chopstick electrode STX-2 (WPI), measured at 37°C.

Transport experiments

Uptake and transport experiments with Gly-Sar and mannitol were performed 16–28 days after seeding and 18–24 h after media replacement. Transepithelial flux measurements were performed as described previously (Thwaites *et al.*, 1993a,b). Briefly, the cell monolayers (24 mm in diameter) were washed in 4 × 500 ml of modified Krebs buffer (all mM): NaCl 137, KCl 5.4, $CaCl_2$ 2.8, $MgSO_4$ 1.0, NaH_2PO_4 0.3, KH_2PO_4 0.3, glucose 10, HEPES/Tris 10 (pH 7.4) and were then placed in 6-well plates, each well containing 2 ml of modified Krebs (pH 7.4, 37°C). The pH 6.0/6.5 buffers were identical except that 10 mM MES replaced 10 mM HEPES. Aliquots of Krebs buffer (pH 7.4) were placed in the upper filter cup (apical solution) and the filters were incubated for 10 min at 37°C. The solutions in both apical and basal chambers were then replaced with the experimental buffers. The experimental composition of the buffers in the apical and basal chambers were identical except where stated otherwise. Radiolabelled Gly-Sar and mannitol (0.5 μCi ml^{-1}, 36 μM) were added to the apical chamber. In experiments involving high (10–20 mM) concentrations of substrates isoosmolarity was maintained by addition of mannitol to controls samples. Fluxes in the absorptive (apical-to-basal, J_{a-b}) direction were determined. Fluxes across the monolayers into the contralateral chamber are expressed as pmol.cm^{-2}. h^{-1} or (when stated) after subtraction of the paracellular (passive) component (as determined by mannitol flux) as % control (in the absence of inhibition) so that the stated values represent an estimate of the proportion of transcellular Gly-Sar transport only. However, since [^{3}H]-mannitol is used to estimated paracellular transport, it is likely that the passive component of transport is overestimated. Hence some dipeptides apparently reduce [^{14}C]-Gly-Sar transport to below zero. At the end of the incubation period, cell monolayers were washed in 4 × 500 ml volumes of Krebs buffer (pH 7.4) to remove any extracellular radiolabel, and removed from the insert. Cell monolayer-associated radiolabel was determined by scintillation counting. Cellular accumulation of Gly-Sar is expressed as μM or (after subtraction of filter-associated mannitol values) as % control (in the absence of inhibition). Cell height was determined by confocal microscopy and this value was used in the determination of intracellular volume (Thwaites *et al.*, 1993g).

Intracellular pH measurements

For intracellular pH (pH_i) measurements (Thwaites *et al.*, 1993a), Caco-2 cells grown to confluence (14–23 days after seeding) on 12 mm diameter Transwell polycarbonate filters (Costar) were loaded by incubation with BCECF-AM (5 μM), in both apical and basal chambers, for 40 min at 37°C. After loading, the inserts were placed in a 24 mm diameter perfusion chamber mounted on the stage of an inverted fluorescence microscope (Nikon Diaphot). Perfusion of the apical and basolateral chambers was accomplished by a compressed air-driven system (flow rate 5 ml min^{-1}). All solutions were preheated to 37°C. For Na^+-free conditions the Krebs buffer was modified by replacement of NaCl with choline chloride and omission of NaH_2PO_4. Intracellular H^+ concentration was quantified by fluorescence (excitation at 440/490 nm and emission at 520 nm) from a small group of cells (5–10) using a photon counting system (Newcastle Photometric Systems). Intracellular BCECF fluorescence was converted to pH_i by comparison with values from an intracellular calibration curve using nigericin (10 μM) and high K^+ solutions (Thomas *et al.*, 1979; Watson *et al.*, 1991). Results are expressed as ΔpH_i or ΔpH_i min^{-1} (mean ± s.e.mean, *n*). The rate of change of intracellular pH (ΔpH_i min^{-1}) was calculated by linear regression using Photon Counter System 4.7 (Newcastle Photometric Systems). Changes in ΔpH_i min^{-1} (due to a change in the composition of the superfusate) were determined by linear regression, by comparison of the linear portions of the trace over 30–50 s (15–25 data points) periods before and after the change in composition. The specific change in ΔpH_i min^{-1} due to addition of a particular substrate can be obtained by subtraction of the ΔpH_i min^{-1} in the presence of apical acidity alone from the total ΔpH_i min^{-1} determined upon addition of a particular substrate to the superfusate.

Materials

[^{3}H]-mannitol (specific activity, 30 Ci $mmol^{-1}$) was obtained from NEN. [^{14}C]-Gly-Sar (L-glycyl[1-^{14}C]-sarcosine (specific activity, 14 mCi $mmol^{-1}$)) was from Amersham. Thyrotropin releasing hormone (TRH) was from Bachem (UK). Carnosine (β-alanine-L-histidine) was from Peptide Inst. Inc. (Japan). All other peptides and cephalosporins were from Sigma. BCECF, cell culture media, supplements and plastic were supplied by Life Technologies. All other chemicals were from Merck. All amino acids were the L-isomer unless stated otherwise.

Statistics

Results are expressed as mean ± s.e.mean (*n*). Statistical analysis was performed with Student's paired *t* test.

Results

It has been demonstrated previously that the transepithelial transport of [^{14}C]-Gly-Sar across Caco-2 cell monolayers is pH-dependent (Thwaites *et al.*, 1993a,b,c). In this study, apical-to-basal [^{14}C]-Gly-Sar transport in the presence of a pH gradient (apical pH 6.0, basolateral pH 7.4) was 479.6 ± 18.1 pmol cm^{-2} h^{-1} ($n = 27$), and was increased compared to mannitol transport (134.5 ± 8.8 pmol cm^{-2} h^{-1} ($n = 27$), $P < 0.001$). The dipeptide Gly-Sar showed marked intracellular accumulation above medium levels (36 μM) at apical pH 6.0 (266.6 ± 14.2 μM, $n = 33$). Residual cell-associated mannitol (28.1 ± 2.9 μM ($n = 33$), $P < 0.001$ compared to Gly-Sar) showed no apparent accumulation. In separate experiments, inclusion of 20 mM unlabelled Gly-Sar at the apical surface significantly reduced apical-to-basal [^{14}C]-Gly-Sar transport from 513.0 ± 23.3 pmol cm^{-2} h^{-1} ($n = 13$) to 142.0 ± 10.8 pmol cm^{-2} h^{-1} ($n = 13$, $P < 0.001$). Under these conditions the [^{14}C]-Gly-Sar transport was not significantly different ($P > 0.05$) from the paracellular flux estimated by mannitol transport. [^{14}C]-Gly-Sar intracellular accumulation was reduced by unlabelled Gly-Sar (20 mM) from 270.1 ± 23.5 μM ($n = 14$) to 92.3 ± 3.7 μM ($n = 15$, $P < 0.001$).

Table 1 shows the effects of a wide range of substrates (each at 20 mM) on the pH-dependent apical-to-basal transport and intracellular accumulation of the model compound [^{14}C]-Gly-Sar. A variety of dipeptides (containing L-amino

Table 1 Effect of substrates (20 mM) on pH-dependent [^{14}C]-Gly-Sar transcellular transport and intracellular accumulation

Control	*Transport* 100%	*Uptake* 100%
Amino acid		
Leu	94.5 ± 8.2 (4) NS	92.9 ± 6.3 (4) NS
Dipeptides		
Gly-Gly	− 23.3 ± 1.5 (5)***	2.6 ± 0.3 (5)***
Gly-Phe	− 9.8 ± 0.2 (3)***	6.3 ± 0.3 (3)***
Gly-Pro	− 8.7 ± 0.4 (3)***	9.4 ± 0.3 (3)***
Pro-Gly	19.8 ± 5.6 (7)***	41.4 ± 6.1 (8)***
Gly-Leu	10.3 ± 5.8 (6)***	6.6 ± 1.1 (6)***
Leu-Gly	− 19.9 ± 4.2 (6)***	14.2 ± 0.7 (6)***
Leu-Leu	− 12.2 ± 0.7 (4)***	7.1 ± 0.2 (4)***
Ala-Ala	− 12.4 ± 1.3 (3)***	5.7 ± 0.2 (3)***
Carnosine	− 7.3 ± 1.2 (4)***	28.0 ± 4.0 (4)***
DAA-containing dipeptides		
Gly-D-Leu	22.1 ± 1.3 (4)***	60.3 ± 1.9 (5)***
D-Leu-Gly	42.9 ± 3.2 (4)***	61.5 ± 3.3 (4)***
D-Leu-D-Leu	87.5 ± 9.0 (4) NS	105.5 ± 9.9 (4) NS
D-Ala-D-Ala	90.9 ± 1.0 (3) NS	101.1 ± 14.2 (4) NS
Tripeptides		
3Gly	2.0 ± 1.4 (4)***	19.0 ± 0.9 (4)***
TRH	98.4 ± 1.5 (3) NS	109.2 ± 5.3 (3) NS
Tetrapeptides		
4Gly	–	84.8 ± 2.9 (4) NS
4Ala	− 15.9 ± 1.8 (5)***	6.8 ± 0.4 (5)***
Cephalosporins		
Cefadroxil	− 3.2 ± 0.9 (4)***	33.9 ± 0.7 (4)***
Cephalexin	26.5 ± 0.5 (4)***	63.3 ± 1.9 (4)***
Cephradine	21.4 ± 2.0 (4)***	63.7 ± 2.9 (4)***
Cefazolin	61.0 ± 5.5 (6)**	96.0 ± 6.6 (7) NS

Results are expressed as a percentage of the transcellular transport/accumulation observed in the absence of any competing substrates (20 mM), after subtraction of the paracellular (passive) component (estimated from mannitol flux).
***$P<0.001$ compared with control
**$P<0.01$
*$P<0.05$
NS $P<0.05$

acids in both N and C terminal positions) all significantly inhibited [^{14}C]-Gly-Sar transcellular transport and intracellular accumulation. For instance, the dipeptide, Leu-Leu, significantly reduced both [^{14}C]-Gly-Sar transport and accumulation (Table 1) whereas its constituent amino acid, leucine (20 mM) failed to inhibit either [^{14}C]-Gly-Sar transport or intracellular accumulation (Table 1). The position of the amino acids in the peptide is also important. The inhibitory effects of Pro-Gly on [^{14}C]-Gly-Sar transport and accumulation were significantly reduced compared to Gly-Pro ($P<0.05$ for transport, $P<0.01$ for uptake). Dipeptides containing one D-amino acid had a reduced effect, while dipeptides containing two D-amino acids had no significant effect on [^{14}C]-Gly-Sar transport and accumulation (Table 1). The tripeptide Gly-Gly-Gly significantly reduced transport and accumulation of [^{14}C]-Gly-Sar although a second tripeptide, the orally-active thyrotropin-releasing hormone (TRH; pGlu-His-Pro-NH_2), was without effect. The tetrapeptide tetraglycine caused no significant reduction although a second tetrapeptide (tetra-alanine) did significantly reduce both [^{14}C]-Gly-Sar transport and accumulation.

Dipeptide (Gly-Sar) transport across the apical membrane is associated with the movement of protons across the plasma membrane that can be detected by the resultant acidification of the intracellular environment (Thwaites *et al.*, 1993a). Figure 1 clearly indicates that after apical exposure to the dipeptide Gly-Sar at 20 mM (apical pH 6.5, basolateral pH 7.4) the rate of intracellular acidification ($\Delta pH_i\ min^{-1}$ 0.127 ± 0.021, $n = 3$) due to substrate-induced H^+ flow into the cells is significantly greater ($P<0.001$) than in the presence of apical pH 6.5 alone (0.013 ± 0.010, $n = 3$). A number of dipeptides including Gly-Pro, Gly-Leu, Gly-Phe, Gly-Gln, carnosine (not shown) and Val-Val (Thwaites *et al.*, 1993c) gave similar responses. The Gly-Pro induced intracellular acidification was significantly greater than that observed with Pro-Gly ($P<0.01$). Dipeptides containing D-amino acids (at both N and C terminals) such as D-Leu-D-Leu (Figure 1) and D-Ala-D-Ala (not shown) did not induce intracellular acidification when perfused (at 20 mM) at the apical membrane of Caco-2 cell monolayers. D-Leu-D-Leu ($\Delta pH_i\ min^{-1}$ 0.030 ± 0.007, $n = 6$) failed to increase significantly ($P>0.05$) the rate of intracellular acidification observ-

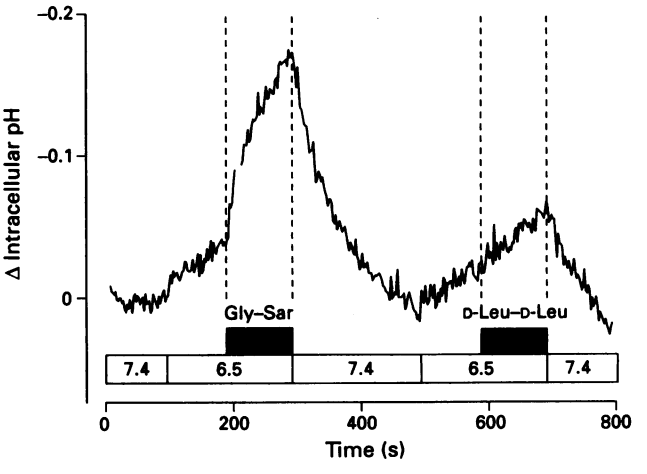


Figure 1 Intracellular pH measured in BCECF-loaded Caco-2 cell monolayers. The relative change in pH_i induced by apical superfusion of either 20 mM Gly-Sar or 20 mM D-Leu-D-Leu at apical pH 6.5 (basolateral pH 7.4). This figure is representative of four separate experiments.

ed with apical acidity alone (0.022 ± 0.004, $n = 7$), whilst the substrate-specific change with D-Leu-D-Leu (0.012 ± 0.004, $n = 6$) was minor compared to Gly-Sar (0.115 ± 0.018 ($n = 3$), $P < 0.001$).

Figure 2 demonstrates that intracellular acidification results from the action of the intact dipeptide (Leu-Leu) since the product of hydrolysis (leucine) does not produce cytosolic acidification. Leu-Leu significantly increased ($P < 0.01$) the rate of acidification (0.083 ± 0.018, $n = 7$) above the levels noted with apical acidity alone (0.016 ± 0.005, $n = 7$). This effect of Leu-Leu (0.068 ± 0.016, $n = 7$, above apical acidity alone) was significantly greater than the specific effects of leucine (0.014 ± 0.007, $n = 4$, $P < 0.05$) or D-Leu-D-Leu (0.012 ± 0.004, $n = 6$, $P < 0.05$). This confirms a previous study with the dipeptide Val-Val and its constituent amino acid valine (Thwaites *et al.*, 1993c).

Figure 3 indicates that tetrapeptides are relatively poor subtrates compared to di and tripeptides. The perfusion of either Gly-Gly or Gly-Gly-Gly at the apical surface of Caco-2 cell monolayers was associated with a significant increase in the rate of intracellular acidification compared with apical acidity alone (an increase above the rate with apical acidity alone of 0.123 ± 0.025 ($n = 5$) with Gly-Gly and 0.079 ± 0.018 ($n = 5$) with Gly-Gly-Gly, both $P < 0.001$ compared to apical acidity alone). Although an intracellular acidification is observed in the presence of tetraglycine (Figure 3; 0.028 ± 0.009, $n = 5$), the rate of acidification is significantly reduced compared to Gly-Gly and Gly-Gly-Gly (both $P < 0.01$). The relative magnitude of excursions in pH_i associated with each peptide are similar in nature to their relative inhibitory effects on [^{14}C]-Gly-Sar transport and accumulation (Table 1). Figure 3 demonstrates that, in contrast to leucine and valine, apical perfusion of glycine (the constituent amino acid of the three peptides used in Figure 3) is associated with intracellular acidification (0.121 ± 0.023, $n = 5$, $P < 0.001$ compared to apical acidity alone), of similar magnitude to that observed with the peptides Gly-Gly and Gly-Gly-Gly (both $P > 0.05$ compared to glycine). Glycine (20 mM) also caused a significant reduction in both [^{14}C]-Gly-Sar transport (49.9 ± 6.7% of control, $n = 14$, $P < 0.001$) and intracellular accumulation (52.4 ± 5.8% of control, $n = 14$, $P < 0.001$). However, the inhibitory effects of glycine on [^{14}C]-Gly-Sar transport and accumulation were significantly reduced compared to the effects of Gly-Gly ($P < 0.001$ for transport and uptake) and Gly-Gly-Gly ($P < 0.01$ for transport, $P < 0.05$ for uptake).

Three orally-active aminocephalosporin antibiotics (cephalexin, cefadroxil and cephradine) that have previously been identified as substrates for transport by the intestinal di/tripeptide carrier inhibited both transport and accumulation (Table 1). However, cefazolin had a reduced effect on [^{14}C]-Gly-Sar transport ($P < 0.01$) and no effect on intracellular accumulation ($P < 0.05$). Figure 4 compares the effects on pH_i of the orally-available cephalosporin antibiotic, cephalexin with the parenterally-administered, cefazolin. Both substrates (20 mM) were perfused at the apical surface of the Caco-2 cell monolayers in the presence of apical acidity. Clearly there is a difference in the responses to the two substrates. Cephalexin (CEX) significantly ($P < 0.05$) increases the rate of acidification (0.123 ± 0.029, $n = 5$ above apical acidity alone) and the intracellular environment is continuing to acidify at the end of the 100 s pulse (0.135 ± 0.20, $n = 5$). In contrast although there is also a rapid initial acidification when cefazolin (CEZ) is perfused at the apical surface (0.030 ± 0.021 ($n = 5$) above apical acidity alone) the response is significantly lower ($P < 0.05$) compared to the cephalexin-induced response, and reaches a plateau after approximately 20 s. At the end of the 100 s pulse the rate of acidification due to cefazolin (0.010 ± 0.038, $n = 5$) is significantly reduced compared to cephalexin ($P < 0.05$). When perfused at apical pH 6.5 (basolateral pH 7.4) at 20 mM both

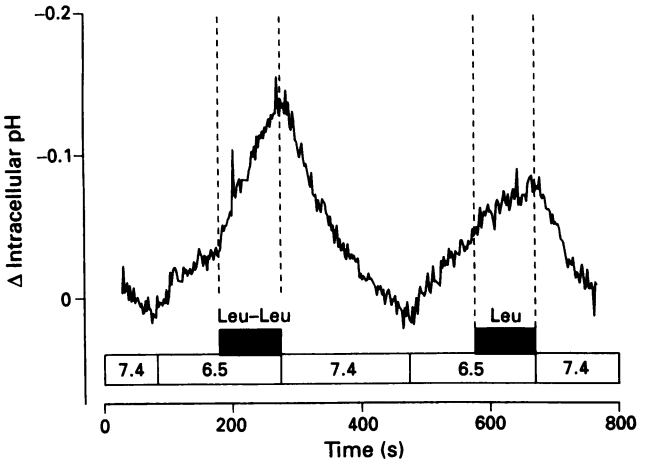


Figure 2 Intracellular pH measured in BCECF-loaded Caco-2 cell monolayers. The effect on intracellular pH of apical exposure to either 20 mM Leu-Leu or 20 mM leucine. Both substrates were superfused across the apical surface at pH 6.5. Basolateral pH was maintained at pH 7.4. The figure is a representative trace of three separate experiments.

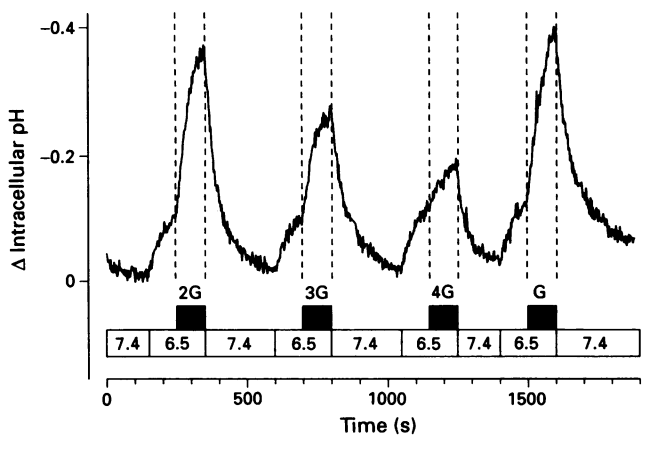


Figure 3 Intracellular pH measured in BCECF-loaded Caco-2 monolayers. The effects of apical exposure (all 10 mM, pH 6.5) to Gly-Gly (2G), Gly-Gly-Gly (3G), Gly-Gly-Gly-Gly (4G) and glycine (G). Basolateral pH was maintained at pH 7.4. The trace is representative of three separate experiments.

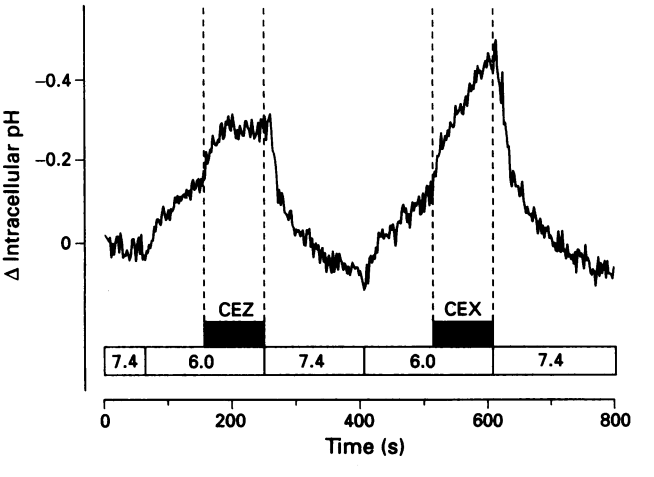


Figure 4 Intracellular pH measured in BCECF-loaded Caco-2 monolayers. The effect of 20 mM cephalexin (CEX) or 20 mM cefazolin (CEZ) on pH_i after exposure at the apical surface at pH 6.0. The basolateral pH was maintained at pH 7.4. This experiment is representative of four others.

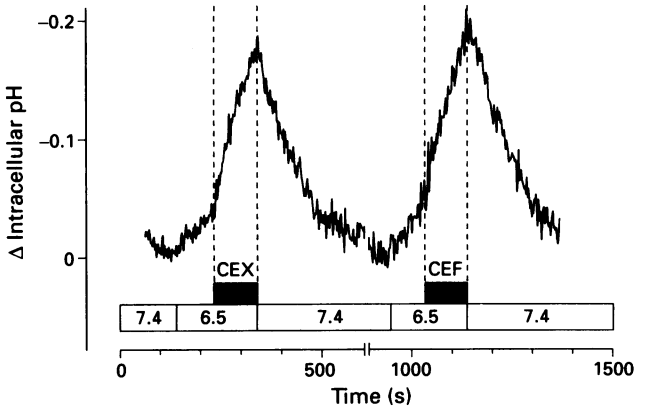


Figure 5 Intracellular pH changes in BCECF-loaded Caco-2 monolayers. The effect of cephalexin (CEX) and cefadroxil (CEF), when superfused (at 20 mM) at the apical surface at pH 6.5 (basolateral pH 7.4).

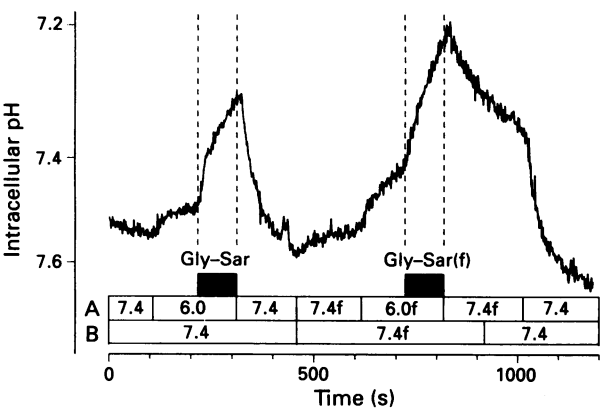


Figure 6 Intracellular pH changes in BCECF-loaded Caco-2 monolayers. The effect of Gly-Sar (20 mM) superfused at the apical surface (at pH 6.0) of Caco-2 cell monolayers in both Na^+-containing and Na^+-free conditions. (f) denotes Na^+-free conditions. Note that the Na^+-containing solutions are re-introduced sequentially to the basolateral (B) then apical (A) membranes.

cephalexin (CEX) and cefadroxil (CEF) are associated with intracellular acidification which is reversible upon removal of the two substrates from the apical chamber (Figure 5).

The experiment illustrated in Figure 6 demonstrates the Na^+-independent nature of the dipeptide-induced intracellular acidification. In a separate series of experiments the relative rates of dipeptide-induced acidification and the nature of the pH_i recovery mechanisms were determined in Na^+ and Na^+-free conditions. The cells were perfused for approximately 200 s until a relatively steady baseline was maintained (rate of acidification 0.001 ± 0.001, $n = 5$). When Na^+-free (pH 7.4) solutions were added to both apical and basal chambers the rate of acidification was 0.006 ± 0.004 ($n = 5$) which increased with apical pH 6.0 (Na^+-free) to 0.049 ± 0.009 ($n = 5$), and was further increased in the presence of apical Gly-Sar (0.158 ± 0.009, $n = 5$). When Gly-Sar was removed from the apical chamber but the transepithelial pH gradient maintained (apical pH 6.0 and basolateral pH 7.4, both Na^+-free) the rate of acidification decreased to 0.017 ± 0.012 ($n = 5$). When Na^+-free pH 7.4 buffer was returned to the apical chamber the intracellular pH recovery from the dipeptide-induced acid load was at a rate of 0.037 ± 0.011 ($n = 5$). Addition of Na^+ to the basolateral chamber had no effect (rate of recovery 0.029 ± 0.010, $n = 5$) whereas addition of Na^+ to the apical chamber markedly increased the rate of recovery (0.109 ± 0.024, $n = 5$). These data demonstrate that a Na^+/H^+ exchange mechanism is localized at the apical surface and confirms observations with the dipeptide Val-Val (Thwaites *et al.*, 1993c).

Discussion

The present study was designed to investigate the specificity of H^+-coupled transport in an epithelial context through the use of the human intestinal Caco-2 cell line. This cell line is known to express pH-dependent accumulation (Dantzig & Bergin, 1990) and transport of the orally-absorbed cephalosporins, cephalexin and cephradine (Inui *et al.*, 1992). These studies confirm earlier observations of pH-dependent aminocephalosporin uptake in rabbit brush-border membrane vesicle preparations (Okano *et al.*, 1986a). More recently our own studies have revealed the pH-dependent nature of dipeptide (Gly-Sar) transport and accumulation in this cell line (Thwaites *et al.*, 1993a). These data complement previous studies with the dipeptide Gly-Sar using rabbit intestinal brush border membrane vesicles (BBMV) (Ganapathy *et al.*, 1984; Ganapthy & Leibach, 1985; Thwaites *et al.*, 1993f). Importantly, we have demonstrated direct coupling of H^+ flow to dipeptide transport across the apical brush-border of these intestinal epithelial cells (Thwaites *et al.*, 1993a). This H^+-coupled dipeptide transport is electrogenic, stimulating inward I_{sc} in voltage-clamped Caco-2 cell monolayers (Thwaites *et al.*, 1993g) and is subject to regulation (inhibition) by protein kinase C (Brandsch *et al.*, 1994). Recently the cDNA encoding for a 707-amino-acid peptide transporter (PepT1) has been isolated from rabbit small intestine by expression cloning in *Xenopus laevis* oocytes (Fei *et al.*, 1994). *Xenopus* oocytes injected with PepT1 cRNA showed a 63 fold increase in [^{14}C]-Gly-Sar uptake when compared with control oocytes (Fei *et al.*, 1994). Furthermore, experiments in voltage-clamped oocytes (Fei *et al.*, 1994) indicate that transport of Gly-Sar is electrogenic, as demonstrated previously in Caco-2 cells (Thwaites *et al.*, 1993g). The Gly-Sar-evoked inward current in PepT1 cRNA-injected oocytes was associated with intracellular acidification (Fei *et al.*, 1994), demonstrating H^+/dipeptide symport, as had previously been demonstrated in Caco-2 cells (Thwaites *et al.*, 1993a,b,c).

Transepithelial transport and accumulation of the dipeptide Gly-Sar are inhibited by a range of other dipeptides including Gly-Pro, carnosine, Gly-Leu and Pro-Gly. Experiments with rabbit intestinal BBMV (Ganapathy *et al.*, 1984) show a similar inhibition pattern to that described here in Caco-2 cell monolayers. In both preparations Pro-Gly has the lowest inhibitory effect on Gly-Sar uptake/transport (Ganapathy *et al.*, 1984; Table 1). The ability of these compounds to inhibit Gly-Sar transport appears directly related to their ability to induce H^+ flow into the cells as determined by changes in intracellular pH (Figures 1–2). Gly-Pro, Gly-Leu, Gly-Phe, Gly-Gln, carnosine, Leu-Leu (Figure 2) and Val-Val (Thwaites *et al.*, 1993c) are all associated with intracellular acidification. Comparison of the effect on pH_i of Leu-Leu and its constituent amino acid (Figure 2) shows that the action is a dipeptide-specific effect. Leucine also failed to inhibit pH-stimulated [^{14}C]-Gly-Sar transport or accumulation (Table 1). This confirms a previous study in Caco-2 cells with the dipeptide Val-Val and the amino acid valine (Thwaites *et al.*, 1993c). Early experiments in the hamster jejunum *in vitro* demonstrated that the mucosal uptake of the dipeptide Leu-Leu was pH-dependent with a maximal uptake at apical pH 6.0 (Matthews & Burston, 1983).

The inhibitory effect of the tripeptide Gly-Gly-Gly suggests that tripeptides may also access this H^+-coupled transporter in Caco-2 epithelia, as demonstrated in other intestinal preparations (Matthews & Adibi, 1976). However, TRH (pGlu-His-Pro-NH_2) failed to inhibit Gly-Sar transport/accumulation. This confirms our previous studies of TRH transport in both rabbit and rat intestinal BBMV (Thwaites

et al., 1993h) and Caco-2 cell monolayers (Thwaites *et al.*, 1993d). It is thus likely that a passive paracellular route is the major pathway for the oral absorption of certain peptides such as TRH. The tetrapeptide, tetraglycine, failed to inhibit Gly-Sar accumulation confirming previous observations in the hamster jejunum *in vitro* (Matthews & Adibi, 1976; Sleisenger *et al.*, 1976) that transport by the intestinal small peptide carrier is restricted to substrates 2–3 amino acids in length. Adibi & Moore (1977) demonstrated (in studies in perfused human jejunum) that the rate of disappearance (and, therefore, absorption) of tetraglycine was slow when compared to Gly-Gly and Gly-Gly-Gly, linear up to 50 mM, and not inhibited by the dipeptide Gly-Leu, although Gly-Leu did inhibit Gly-Gly-Gly absorption. Gly-Leu also inhibits [^{14}C]-Gly-Sar transport in this study (Table 1). Several substrates that inhibit [^{14}C]-Gly-Sar transport (Table 1) and cause intracellular acidification in Caco-2 cells (including cefadroxil, cephalexin, Gly-Leu, Leu-Leu, carnosine, Gly-Gly and Gly-Gly-Gly) also evoked inward currents in PepT1 cRNA-injected oocytes whereas tetraglycine was without effect (Fei *et al.*, 1994). The amino acid glycine did not evoke inward current nor cause intracellular acidification in PepT1 cRNA-injected oocytes (Fei *et al.*, 1994). This observation (when considered with the relative magnitude of the pH_i changes in the presence of glycine, Gly-Gly and Gly-Gly-Gly in Caco-2 cells (Figure 3)), strengthens our hypothesis that the inhibitory effects of glycine on [^{14}C]-Gly-Sar transport are due to non-specific effects on the transepithelial pH gradient and that glycine transport is likely to be via another H^+-coupled carrier, most probably the H^+-coupled amino acid transporter in Caco-2 cells that plays a role in β-alanine (Thwaites *et al.*, 1993e), L-proline (Thwaites *et al.*, 1993f) and L-alanine (Thwaites *et al.*, 1994) transport. The inhibitory effects of tetra-alanine on [^{14}C]-Gly-Sar transport may suggest that the peptide carrier transports some tetrapeptides. However, this inhibitory effect could result from rapid hydrolysis to Ala-Ala (which also significantly reduces [^{14}C]-Gly-Sar transport; Table 1) or to L-alanine (Thwaites *et al.*, 1994) which could inhibit dipeptide transport by an effect on the driving force (the pH gradient) as suggested with glycine (see Discussion above). Thus the ability of peptide substrates (whose metabolism may yield true substrates for the dipeptide carrier or substrates for an alternative H^+-coupled transporter) to access the H^+/dipeptide carrier cannot be distinguished unequivocally in the Caco-2 cell system. In rabbit renal BBMV preparations, 1 mM tetra-alanine was completely hydrolysed to Ala-Ala in 5 s (Daniel *et al.*, 1992) whereas tetraglycine did not undergo hydrolysis.

The stereoselectivity (Matthews, 1975) of the transporter is indicated by the absence of inhibitory effects of D-Ala-D-Ala and D-Leu-D-Leu, and the reduced effects of Gly-D-Leu and D-Leu-Gly (Table 1). D-Leu-D-Leu (Figure 1) and D-Ala-D-Ala (not shown) also failed to affect intracellular pH when perfused at the apical surface of Caco-2 cells. These observations of stereoselectivity are consisent with previous studies in both human and rat intestine (Matthews, 1975). It is thought that introduction of D-amino acids into a dipeptide reduces affinity for the entry mechanism (Matthews, 1975).

Table 1 indicates that the inhibition profiles from this study and those with cephradine (Inui *et al.*, 1992) show a broadly similar pattern. In Caco-2 cell monolayers, pH-dependent cephradine transport and accumulation are inhibited by the dipeptides carnosine, Gly-Leu and Gly-Pro, and the cephalosporin cephalexin. Most recently pH-dependent transport of the anti-cancer agent, bestatin, has been demonstrated in Caco-2 cells and attributed to transport via the di/tripeptide carrier (Saito & Inui, 1993). The pH-dependent accumulation of bestatin across the apical surface of Caco-2 cells was inhibited by the dipeptides Gly-Sar, Gly-Leu, Gly-Pro and carnosine, and the cephalosporin, cephradine (Saito & Inui, 1993). Similar patterns of inhibition are indicated in Table 1. In studies with rabbit intestinal BBMV, uptake of cephradine, cephalexin and cefadroxil were enhanced by an inwardly-directed pH gradient whereas cefazolin uptake was low in comparison and was not stimulated by lowering extravesicular pH (Okano *et al.*, 1986a). This pH-dependent uptake of cephradine in rat intestinal BBMV was reduced in the presence of di and tripeptides (Okano *et al.*, 1986b). The orally-absorbed cephalosporins (cephradine, cefadroxil and cephalexin) all inhibit pH-stimulated [^{14}C]-Gly-Sar transport and intracellular accumulation in Caco-2 cell monolayers. In comparison cefazolin had a reduced effect which is reflected in its reduced effect on intracellular pH (Figure 4). This reduced affinity for the intestinal di/tripeptide transporter may account for the poorer oral absorption of this compound (Bergan, 1984). Cephalexin and cefadroxil both stimulated H^+ flow (Figure 4–5).

An additional feature of transport across an intact epithelial preparation is that it is also dependent upon dipeptide exit across the basolateral membrane. Although the majority of studies discussed above have concentrated on the role of the apical membrane in transepithelial transport, the importance of the basolateral membrane should not be underestimated. It is likely that this is the rate-limiting step in Gly-Sar transport (Thwaites *et al.*, 1993b). Gly-Sar and cephalexin have similar effects on pH_i when perfused at the apical surface of Caco-2 cells but show clear differences when perfused at the basolateral membrane (Thwaites *et al.*, 1993b). At basolateral pH 7.4, cephalexin caused a marked cytosolic acidification whereas Gly-Sar was without effect (Thwaites *et al.*, 1993b). Estimates of Gly-Sar and cephradine efflux in Caco-2 cell monolayers show that Gly-Sar leaves the cells predominantly across the apical surface (Thwaites *et al.*, 1993b) whereas cephradine leaves across the basolateral membrane (Inui *et al.*, 1992). These observations suggest that dipeptide and aminocephalosporin transport across the basolateral membrane of intestinal enterocytes may be via more than one mechanism.

There are likely to be several transport mechanisms in the gastrointestinal tract allowing nutrient absorption energized by the proton gradient present across the apical membrane of intestinal enterocyte. This area of acidity close to the apical surface has been demonstrated both *in vivo* (Rawlings *et al.*, 1987) and *in vitro* (Lucas *et al.*, 1978). The model proposed by Ganapathy & Leibach (1985) suggests that the pH gradient across the apical membrane of the intestinal enterocyte is maintained during H^+-coupled dipeptide transport by Na^+/H^+ exchange at the apical surface and Na^+ extrusion via the Na^+,K^+-ATPase at the basolateral membrane. The present data confirm the role of an apically-localized Na^+/H^+ exchanger in H^+-coupled dipeptide absorption.

The selectivity of the H^+-coupled small peptide carrier expressed at the apical surface of human intestinal epithelial Caco-2 cells has been established by competition studies with [^{14}C]-Gly-Sar and intracellular pH measurements with the pH-sensitive fluorescent dye BECEF. The carrier transports a range of di/tripeptides and cephalosporin antibiotics with an α-amino group. Affinity for the transporter is significantly reduced with peptides greater than three amino acids in length, peptides containing D-amino acids (at both N and C terminals) and cephalosporins without the α-amino group (cefazolin) as well as peptides with blocked N- and C-termini such as TRH. This specificity profile is similar to that observed in experiments with *Xenopus laevis* oocytes expressing the rabbit intestinal oligopeptide transporter (PepT1). A major advantage of the Caco-2 cell system (over oocytes expressing PepT1) is that alternative transport pathways (either H^+-linked transporters, Na^+-dependent transporters or the paracellular pathway) may be studied within the same cell system in an appropriate physiological context. Finally, the use of intracellular pH measurements to determine H^+ flow across either the apical or basolateral membranes provides a simple and rapid method for assessing the potential of novel drug compounds to undergo H^+-coupled intestinal absorption.

Charlotte Ward provided excellent technical assistance. We thank Dr M.J. Humphrey (Pfizer Central Research) for the supply of [^{14}C]-Gly-Sar. This work was supported by the Wellcome Trust (to D.T.T.) and the LINK Programme in Selective Drug Delivery and Targeting (funded by SERC/MRC/DTI and Industry).

References

ADIBI, S.A. & MORSE, E.L. (1977). The number of glycine residues which limits intact absorption of glycine oligopeptides in human jejunum. *J. Clin. Invest.*, **60**, 1008–1016.

BERGAN, T. (1984). Pharmacokinetics of beta-lactam antibiotics. *Scand. J. Infect. Dis.*, **42** (suppl.), 83–98.

BLAIS, A., BISSONNETTE, A. & BERTELOOT, A. (1987). Common characteristics for Na^+-dependent sugar transport in Caco-2 cells and human fetal colon. *J. Membr. Biol.*, **99**, 113–125.

BRANDSCH, M., MIYAMOTO, Y., GANAPATHY, V. & LEIBACH, F.H. (1994). Expression and protein kinase C-dependent regulation of peptide/H^+ co-transport system in the Caco-2 human colon carcinoma cell line. *Biochem. J.*, **299**, 253–260.

DANIEL, H., MORSE, E.L. & ADIBI, S.A. (1992). Determinants of substrate affinity for the oligopeptide H^+ symporter in the renal brush-border membrane. *J. Biol. Chem.*, **267**, 9565–9573.

DANTZIG, A. & BERGIN, L. (1990). Uptake of the cephalosporin, cephalexin, by a dipeptide transport carrier in the human intestinal cell line, Caco-2. *Biochim. Biophys. Acta*, **1027**, 211–217.

FEI, Y.J., KANAI, Y., NUSSBERGER, S., GANAPATHY, V., LEIBACH, F.H., ROMERO, M.F., SINGH, S.K., BORON, W. & HEDIGER, M.A. (1994). Expression cloning of a mammalian proton-coupled oligopeptide transporter. *Nature*, **368**, 563–566.

GANAPATHY, V., BURCKHARDT, G. & LEIBACH, F.H. (1984). Characteristics of glycylsarcosine transport in rabbit intestinal brush-border membrane vesicles. *J. Biol. Chem.*, **259**, 8954–8959.

GANAPATHY, V. & LEIBACH, F.H. (1985). Is intestinal peptide transport energized by a proton gradient? *Am. J. Physiol.*, **249**, G153–G160.

HIDALGO, I.J. & BORCHARDT, R.T. (1990a). Transport of a large neutral amino acid (phenylalanine) in a human intestinal epithelial cell line: Caco-2. *Biochim. Biophys. Acta.*, **1028**, 25–30.

HIDALGO, I.J. & BORCHARDT, R.T. (1990b). Transport of bile acids in the human intestinal epithelial cell line, Caco-2. *Biochim. Biophys. Acta*, **1035**, 97–103.

HUMPHREY, M.J. (1986). The oral bioavailability of peptides and related drugs. In *Delivery Systems for Peptide Drugs*. ed. Davis, S.S., Ilum, L. & Tomlinson, E. pp. 139–151. NATO ASI Series 125, New York: Plenum.

INUI, K.I., YAMAMOTO, Y. & SAITO, H. (1992). Transepithelial transport of oral cephalosporins by monolayers of intestinal epithelial cell line Caco-2: specific transport systems in apical and basolateral membranes. *J. Pharmacol. Exp. Ther.*, **261**, 195–201.

LUCAS, M.L., COOPER, B.T., LEI, F.H., JOHNSON, I.T., HOLMES, G.K.T., BLAIR, J.A. & COOKE, W.T. (1978). Acid microclimate in coeliac and Crohn's disease: a model for folate malabsorption. *Gut*, **19**, 735–742.

MATTHEWS, D.M. (1975). Absorption of peptides by mammalian intestine. In *Peptide Transport in Protein Nutrition*, ed Matthews, D.M. & Payne, J.W. Research monographs, Frontiers of Biology Vol. 37, pp. 61–146. Amsterdam: North-Holland.

MATTHEWS, D.M. & ADIBI, S.A. (1976). Peptide absorption. *Gastroenterology*, **71**, 151–161.

MATTHEWS, D.M. & BURSTON, D. (1983). Uptake of L-leucyl-L-leucine and glycylsarcosine by hamster jejunum *in vitro*. *Clin. Sci.*, **65**, 177–184.

NAKASHIMA, E., TSUJI, A., MIZUO, H. & YAMANA, T. (1984). Kinetics and mechanism of *in vitro* uptake of amino-β-lactam antibodies by rat small intestine and relation to the intact-peptide transport system. *Biochem. Pharmacol.*, **33**, 2245–2252.

OKANO, T., INUI, K.I., MAEGAWA, H., TAKANO, M. & HORI, R. (1986a). H^+ coupled uphill transport of aminocephalosporins via the dipeptide transport system in rabbit intestinal brush-border membranes. *J. Biol. Chem.*, **261**, 14130–14134.

OKANO, T., INUI, K.I., TAKANO, M.& HORI, R. (1986). H^+ gradient-dependent transport of aminocephalosporins in rat intestinal brush-border membrane vesicles. *Biochem. Pharmacol.*, **35**, 1781–1786.

RAWLINGS, J.M., LUCAS, M.L. & RUSSEL, R.I. (1987). Measurement of jejunal surface pH *in situ* by plastic pH electrode in patients with coeliac disease. *Scand. J. Gastroenterol.*, **22**, 377–384.

SAITO, H. & INUI, K.I. (1993). Dipeptide transporters in apical and basolateral membranes of the human intestinal cell line Caco-2. *Am. J. Physiol.*, **265**, G289–G294.

SLEISENGER, M.H., BURSTON, D., DALRYMPLE, J.A., WILKINSON, S. & MATTHEWS, D.M. (1976). Evidence for a single common carrier for uptake of a dipeptide and a tripeptide by hamster jejunum *in vitro*. *Gastroenterology*, **71**, 76–81.

SMITH, P.L., WALL, D.A., GOCHOCO, C.H. & WILSON, G. (1992). Oral absorption of peptides and proteins. *Adv. Drug Dev. Rev.*, **8**, 253–290.

THOMAS, J.A., BUSHBAUM, R.N., ZIMNIAK, A. & RACKER, E. (1979). Intracellular pH measurements in Ehrlich ascites tumor cells utilizing spectroscopic probes generated *in situ*. *Biochemistry*, **18**, 2230–2238.

THWAITES, D.T., BROWN, C.D.A., HIRST, B.H. & SIMMONS, N.L. (1993a). Transepithelial glycylsarcosine transport in intestinal Caco-2 cells mediated by expression of H^+-coupled carriers at both apical and basal membranes. *J. Biol. Chem.*, **268**, 7640–7642.

THWAITES, D.T., BROWN, C.D.A., HIRST, B.H. & SIMMONS, N.L. (1993b). H^+-coupled dipeptide (glycylsarcosine) transport across apical and basal borders of human intestinal Caco-2 cell monolayers display distinctive characteristics. *Biochim. Biophys. Acta*, **1151**, 237–245.

THWAITES, D.T., HIRST, B.H. & SIMMONS, N.L. (1993c). Direct assessment of dipeptide/H^+ symport in intact human intestinal (Caco-2) epithelium: a novel method utilising continuous intracellular pH measurement. *Biochem. Biophys. Res. Commun.*, **194**, 432–438.

THWAITES, D.T., HIRST, B.H. & SIMMONS, N.L. (1993d). Passive transepithelial absorption of thyrotropin-releasing hormone (TRH) via a paracellular route in cultured intestinal and renal epithelial cell lines. *Pharmaceut. Res.*, **10**, 674–681.

THWAITES, D.T., MCEWAN, G.T.A., BROWN, C.D.A., HIRST, B.H. & SIMMONS, N.L. (1993e). Na^+-independent, H^+-coupled transepithelial β-alanine absorption by human intestinal Caco-2 cell monolayers. *J. Biol. Chem.*, **268**, 18438–18441.

THWAITES, D.T., MCEWAN, G.T.A., BROWN, C.D.A., HIRST, B.H. & SIMMONS, N.L. (1994). L-Alanine absorption in human intestinal Caco-2 cells driven by the proton electrochemical gradient. *J. Membr. Biol.*, **140**, 143–151.

THWAITES, D.T., MCEWAN, G.T.A., COOK, M.J., HIRST, B.H. & SIMMONS, N.L. (1993f). H^+-coupled (Na^+-independent) proline transport in human intestinal (Caco-2) epithelial cell monolayers. *FEBS Lett*, **333**, 78–82.

THWAITES, D.T., MCEWAN, G.T.A., HIRST, B.H & SIMMONS, N.L. (1993g). Transepithelial dipeptide (glycylsarcosine) transport across epithelial monolayers of human Caco-2 cells is rheogenic. *Pflügers Arch.*, **425**, 178–180.

THWAITES, D.T., SIMMONS, N.L. & HIRST, B.H. (1993h). Thyrotropin-releasing hormone (TRH) uptake in intestinal brush-border membrane vesicles: comparison with proton-coupled dipeptide and Na^+-coupled glucose transport. *Pharmaceut. Res.*, **10**, 667–673.

WATSON, A.J.M., LEVINE, S., DONOWITZ, M. & MONTROSE, M.H. (1991). Kinetics and regulation of a polarized Na^+-H^+ exchanger from Caco-2 cells, a human intestinal cell line. *Am. J. Physiol.*, **261**, G229–G238.

(Received May 24, 1994
Revised July 11, 1994
Accepted July 15, 1994)

Br. J. Pharmacol. (1994), **113**, 1057–1063 © Macmillan Press Ltd, 1994

FPL 66096: a novel, highly potent and selective antagonist at human platelet P_{2T}-purinoceptors

[1]R.G. Humphries, W. Tomlinson, *A.H. Ingall, *P.A. Cage & P. Leff

Departments of Pharmacology & *Medicinal Chemistry, Fisons plc, Pharmaceutical Division, Research & Development Laboratories, Bakewell Road, Loughborough, Leics, LE11 0RH

1 ADP-dependent platelet aggregation is mediated by the P_{2T}-purinoceptor and is specifically inhibited by ATP, which is a competitive P_{2T}-purinoceptor antagonist. However, ATP functions as an agonist at other P_2-purinoceptor subtypes in other tissues and is, therefore, non-selective. This paper describes the effects of the novel ATP analogue, FPL 66096 (2-propylthio-D-β,γ-difluoromethylene ATP), on ADP-induced and ADP-independent aggregation of human washed platelets and in standard preparations containing P_{2X}- (rabbit ear artery) and P_{2Y}-purinoceptors (guinea-pig aorta).

2 In suspensions of human washed platelets, FPL 66096 (1–100 nM) produced concentration-dependent rightward displacement of concentration-effect (E/[A]) curves obtained for ADP-induced platelet aggregation. Logistic fitting of E/[A] data indicated that the effect of FPL 66096 was consistent with simple competition with a pK_B value of 8.66. FPL 66096 (10–1000 nM) had no effect on aggregation produced by the thromboxane A_2-mimetic, U46619 (0.1–10 μM) when the response to this agent was rendered ADP-independent by inclusion of the non-selective P_2-purinoceptor antagonist, suramin (100 μM).

3 The anti-aggregatory potency of FPL 66096 was not influenced by increasing the incubation time from 2 to 15 min nor by inclusion of the P_1-purinoceptor antagonist 8-sulphophenyltheophylline at a concentration (300 μM) that produced a 68 fold rightward displacement of the anti-aggregatory E/[A] curve for the P_1-purinoceptor agonist, 5'-N-ethylcarboxamidoadenosine (0.1–1000 μM).

4 FLP 66096 behaved as a weak (pA_{50} 3.68) but full P_{2X}-purinoceptor agonist in preparations of the rabbit isolated ear artery and as a weak, competitive antagonist (apparent pK_B 4.71) at P_{2Y}-purinoceptors in the guinea-pig isolated aorta, indicating a selectivity of at least 9000 fold for the P_{2T}-subtype. In the latter preparation, non-specific relaxations were produced by concentrations of FPL 66096 $\geqslant$ 10 μM.

5 These results indicate that FPL 66096 is a P_{2T}-purinoceptor antagonist of unprecedented potency and selectivity and that its effects are consistent with simple competition at the P_{2T}-purinoceptor. Therefore, FPL 66096 represents a novel pharmacological tool in the classification of P_2-purinoceptors and in the elucidation of the mechanisms involved in activation of platelets by ADP.

Keywords: FPL 66096; P_{2T}-purinoceptor antagonist; ADP; platelet aggregation; human washed platelets; suramin; receptor classification; α,β-methylene ATP; 2-methylthio ATP; 8-sulphophenyltheophylline

Introduction

The purine nucleotides adenosine 5'-triphosphate (ATP) and adenosine 5'-diphosphate (ADP) produce extracellular effects by acting either directly at P_2-purinoceptors or indirectly at P_1-purinoceptors following metabolic breakdown to adenosine (Burnstock, 1978). Further sub-classification of P_1-purinoceptors has been facilitated by the availability of potent, selective antagonists (Williams, 1989). However, in the case of P_2-purinoceptors, quantitative pharmacological classification has been hampered by the lack of such pharmacological tools. Identification of receptor subtypes has relied primarily on differences in agonist potency orders obtained for the ATP analogues 2-methylthio ATP (2-MeSATP), D-β,γ-methylene ATP (β,γ-meATP) and D-α,β-methylene ATP (α,β-meATP). Both ATP and ADP are agonists at P_{2X}- (α,β-meATP > β,γ-meATP > 2-MeSATP) and P_{2Y}- (2-MeSATP > β,γ-meATP > α,β-meATP) purinoceptors as defined by Burnstock & Kennedy (1985). However, the P_{2T}-purinoceptor, which mediates ADP-induced platelet aggregation (Gordon, 1986), is unique in that, while ADP is an agonist, ATP is a competitive antagonist (Macfarlane & Mills, 1975) but with low affinity and, by definition, no selectivity as a P_2-purinoceptor ligand. The trypanocidal agent, suramin, has also been shown to function as an apparently competitive P_{2T}-purinoceptor antagonist in human washed platelets but with an affinity similar to that observed in tissues containing P_{2X}- and P_{2Y}-purinoceptors (Hourani *et al.*, 1992). A number of structural analogues of ATP, including those with 2-alkylthio substituents on the adenine ring, show increased affinity for the P_{2T}-purinoceptor but, as with the endogenous ligand, demonstrate little or no selectivity for this subtype (Cusack & Hourani, 1982a,b; 1990). However, these analogues provided a starting point for the design of novel P_{2T}-purinoceptor antagonists with improved potency and selectivity. In this paper, we report the discovery of a new compound of this general class, FPL 66096 (2-propylthio-D-β,γ-difluoromethylene ATP) and describe studies which demonstrate its value as a pharmacological probe for the P_{2T}-purinoceptor.

A preliminary communication of some of this work has been presented to the British Pharmacological Society (Humphries *et al.*, 1993).

Methods

Human washed platelets

Suspensions of human washed platelets were prepared by a modification of the method of Giles and co-workers (1989). Venous blood was obtained from healthy male and female volunteers and anti-coagulated with 1/10 volume, 3.2%

[1] Author for correspondence.

trisodium citrate. The blood was centrifuged for 15 min at 240 g to obtain platelet-rich plasma (PRP) to which 300 ng ml^{-1} prostacyclin (PGI_2) was added to stabilize platelets during the washing procedure. Red cell-free PRP was obtained by centrifugation for 10 min at 125 g and, following further centrifugation for 15 min at 640 g, the supernatant was discarded and the platelet pellet resuspended in 10 ml calcium-free Tyrode solution (CFT, composition (mM): NaCl 137.00, $NaHCO_3$ 11.90, NaH_2PO_4 0.38, KCl 2.68, $MgCl_2$ 1.05, D-glucose 5.55) gassed with 95% O_2/5% CO_2 and maintained at 37°C. Following addition of a further 300 ng ml^{-1} PGI_2, the suspension was centrifuged once more for 15 min at 640 g. The supernatant was discarded and the platelets resuspended initially in 10 ml CFT with further CFT added to adjust the final platelet count to 2×10^5 μl^{-1}. This final suspension was stored in a 60 ml syringe at 4°C with air excluded. To allow recovery from PGI_2-inhibition of normal function, platelets were used in aggregation studies no sooner than 2 h after final re-suspension.

Rabbit ear artery

Isolated ear artery preparations were obtained from male New-Zealand White rabbits (Froxfield, 2.5–3.5 kg) as described previously (O'Connor *et al.*, 1990). Endothelium-denuded arterial rings (5 mm) were mounted horizontally, under isometric conditions, on fine tungsten wire hooks in 20 ml organ baths containing modified Krebs' buffer of the following composition: (mM) NaCl 117.56, NaH_2PO_4 0.89, $NaHCO_3$ 25.00, $MgSO_4$ 1.18, KCl 5.36, $CaCl_2$ 2.55 and D-glucose 11.10. Tissues were maintained at 37°C and gassed continually with 95% O_2/5% CO_2. Indomethacin (2.8 μM) was included in the bathing solution to exclude the possible contribution of effects mediated by by-products of cyclo-oxygenase. Tissues were subjected to an initial force of 1.0 g and allowed to equilibrate for 1 h, during which time the resting force was adjusted to achieve a final value of 0.5–1.0 g. Responses were recorded as changes in force using isometric transducers (Ormed) and displayed on Advance Bryan chart recorders.

Guinea-pig aorta

The use of this preparation for assessment of P_{2Y}-agonist and antagonist activity has been outlined previously (Dainty *et al.*, 1992). Male Dunkin-Hartley guinea-pigs (Charles-River, 300–350 g) were killed by cervical dislocation. The thoracic aorta was carefully removed and cleared of all connective tissue. Rings (3 mm) with intact endothelium were then cut and mounted horizontally, under isometric conditions, on fine tungsten wire hooks in 10 ml organ baths, containing modified Krebs' solution of the following composition mM: NaCl 117.56, NaH_2PO_4 0.89, $NaHCO_3$ 25.00, $MgSO_4$ 1.18, KCl 5.36, $CaCl_2$ 2.55 and D-glucose 11.10. Tissues were maintained at 37°C and gassed continually with 95% O_2/5% CO_2. Indomethacin (2.8 μM) was included in the bathing solution to exclude the possible contribution of effects mediated by by-products of cyclo-oxygenase. Tissues were subjected to an initial force of 2 g and allowed to equilibrate for 15 min. After this time, resting force was adjusted to 2 g at 0, 3, 6 and 9 min and the bathing solution exchanged at these times. The tissues were then allowed to equilibrate for a further 15 min prior to use. Responses were recorded as changes in force using isometric transducers (Ormed) and displayed on Advance Bryan chart recorders.

Experimental protocols

Human washed platelets Aliquots (440 μl) of platelet suspension were added to siliconized aggregation cuvettes containing 10 μl $CaCl_2$ solution (final concentration 1 mM), maintained at 37°C and stirred at 900 r.p.m. in a Biodata PAP4 aggregometer. Human fibrinogen (10 μl) was then added to give a final concentration of 0.2 mg ml^{-1} of clottable protein. Recording of aggregation was then started and baseline light transmission monitored for 20 min prior to addition of ADP (1–300 μM) in a volume of 10 μl. Aggregation responses were recorded as the maximum increase in light transmission through the platelet suspension following addition of ADP. FPL 66096 (1–100 nM) or 30 μl vehicle was added 2 min before ADP. Although only a single concentration of agonist and antagonist was added to each cuvette, use of 8-aggregometer channels enabled construction of 4, time-matched, concentration-effect (E/[A]) curves for ADP-induced aggregation, with duplicate measurements for each point. Thus, in each experiment, a complete analysis of antagonism was conducted.

In a separate series of experiments, the anti-aggregatory potency of FPL 66096 (1–100 nM) was assessed against aggregation produced by a single sub-maximal concentration of ADP (30 or 100 μM) using antagonist incubation times of 2 and 15 min. In addition, the effect of 8-sulphophenyltheophylline (8-SPT, 300 μM, 20 min incubation) on the anti-aggregatory potency of FPL 66096 (2 and 15 min incubation) was investigated. Again, inhibitory E/[A] curves for FPL 66096 under these four test conditions were constructed in a time-matched manner, with each point obtained in duplicate. Inhibition curves for the P_1-purinoceptor agonist, 5'-N-ethylcarboxamidoadenosine (NECA, 0.1–1000 μM) were also obtained in the absence and presence of 8-SPT (300 μM, 20 min incubation) to confirm the effectiveness of the P_1-antagonist.

P_{2T}-specificity of the anti-aggregatory effect of FPL 66096 (10–1000 nM, 2 min incubation) was tested against responses to the thromboxane A_2-mimetic, U46619 (0.1–10 μM), rendered ADP-independent by inclusion of the non-selective P_2-purinoceptor antagonist, suramin (100 μM). E/[A] curves for U46619 were constructed as described for ADP. Suramin was added 1 min prior to FPL 66096 in a volume of 10 μl. The ability of this assay system to detect non-specific inhibition of platelet aggregation was tested with NECA (0.1–10 μM) in place of FPL 66096.

Rabbit ear artery Tissues were initially contracted with KCl (80 mM) to establish viability, followed by addition of acetylcholine (1 μM) to confirm denudation of the endothelium. After washing, tissues were allowed to equilibrate for 45 min prior to construction of a cumulative E/[A] curve for the standard P_{2X}-agonist, α,β-meATP (0.03–10 μM). The tissues were then washed and, after a further 70 min equilibration period, a cumulative E/[A] curve was obtained for FPL 66096 (1–1000 μM). Following subsequent washing, a further E/[A] curve to FPL 66096 (10–1000 μM) was obtained following desensitization of receptors by α,β-meATP (30 μM) added 15 min prior to the first concentration of FPL 66096. All E/[A] curves were constructed in the presence of 8-SPT (300 μM), added 45 min before the agonist, to exclude the possible contribution of P_1-mediated effects.

Guinea-pig aorta Tissues were contracted to a plateau with phenylephrine (Phe, 10 μM) and the standard P_{2Y}-agonist, 2-MeSATP (10 μM) added to confirm the presence of functional endothelium. After washing, tissues were again contracted with Phe (10 μM) and, when the induced tone had stabilized (at least 15 min), cumulative E/[A] curves were constructed to 2-MeSATP (1–3000 nM). After washing, and a 35 min stabilization period, tissues were again pre-contracted with Phe and an E/[A] curve constructed for FPL 66096 (10–1000 μM), with each concentration left in contact with the tissue for at least 3 min or until any relaxant response had plateaued. Beyond this stage, two different protocols were pursued. To determine if any observed relaxations were P_{2Y}-mediated, two tissues were washed and allowed to equilibrate for 35 min prior to pre-contraction with Phe and construction of a second curve to FPL 66096 (10–1000 μM) in the presence of 2-MeSATP (10 μM). This concentration of

2-MeSATP abolishes, or produces at least two orders of magnitude rightward shift and significant depression of, the 2-MeSATP E/[A] curve in this preparation. In five separate preparations, to determine whether FPL 66096 showed any P_{2Y}-purinoceptor antagonist activity, the highest concentration of FPL 66096 (100 or 1000 μM) was left in contact with the tissues for 15 min, after which time an E/[A] curve was constructed to 2-MeSATP (0.03–100 μM) without washing the preparations. All E/[A] curves were constructed in the presence of 8-SPT (300 μM), added 35 min prior to Phe, to exclude the possible contribution of P_1-mediated effects.

Analysis of data

Curve fitting With the exception of data obtained for U46619 in human washed platelets, E/[A] curve data were fitted to a logistic function (i) of the form:

$$E = \frac{\alpha[A]^m}{[A_{50}]^m + [A]^m} \qquad (i)$$

in which α, $[A_{50}]$ and m are, respectively, the asymptote, location and slope paramaters. $[A_{50}]$ values were assumed to be log-normally distributed and they were estimated as such and quoted as $p[A_{50}]$ ($-\log[A_{50}]$) values.

Analysis of antagonism Initially, E/[A] curve data obtained for ADP-induced platelet aggregation in the absence and presence of FPL 66096 were combined from all experiments and fitted to equation (i). Parallelism was tested by one-way analysis of variance on the computed estimates of α and m and, if FPL 66096 had not significantly modified these parameters, E/[A] data describing the four curves obtained in individual experiments were then fitted to the logistic function (ii), incorporating a function describing competitive antagonism:

$$E = \frac{\alpha[A]^m}{[A_{50}]^m(1 + [B]^n/K_B)^m + [A]^m} \qquad (ii)$$

where [B] is the concentration of FPL 66096, K_B is its dissociation equilibrium constant and n is the Schild plot slope. Other parameters are as defined for equation (i). Thus, a value for n and an apparent K_B was obtained from each experiment. If, upon statistical analysis of the values obtained in replicate experiments, n was found to not differ significantly from unity, indicating simple competition, individual estimates of K_B were re-calculated with n constrained to that value and quoted as pK_B ($-\log_{10} K_B$).

When FPL 66096 was tested against E/[A] curves to 2-MeSATP in the guinea-pig aorta, a full quantification of antagonism was not possible because only a single concentration of FPL 66096 (100 or 1000 μM) was employed. In this case, the effect of FPL 66096 was quantified as an apparent pK_B, applying the equation of Arunlakshana & Schild (1959):

$$\log_{10}(r-1) = n\log_{10}[B] + pK_B$$

in which r is the ratio of the $[A_{50}]$ values obtained for 2-MeSATP in the absence and presence of FPL 66096 (100 or 1000 μM). Other terms are as for equation (i) and (ii) with n assumed to be equal to unity.

E/[A] parameters (α and $p[A_{50}]$) for U46619-induced platelet aggregation were calculated from manual plots of the E/[A] data and the effect of NECA and FPL 66096 on these parameters was tested using the non-parametric Kruskal-Wallis test followed by Dunn's multiple comparison test where appropriate.

Effects of incubation time and 8-SPT The effect of alteration of incubation time and of 8-SPT (300 μM) on the anti-aggregatory potency of FLP 66096 was tested by applying Student's unpaired *t* test to comparisons of pIC_{50} values obtained under the different conditions.

Data are presented as mean ± s.e. of results obtained from individual human blood donors or from individual tissues. All fitting procedures used BMDP Statistical Software installed on a VAX mainframe computer. Other statistical analyses used InStat software.

Drugs and solutions

Drugs were obtained from the following sources: U46619 (9,11-dideoxy-9α, 11α-methanoepoxy-$PGF_{2\alpha}$), indomethacin, acetylcholine bromide, phenylephrine hydrochloride, PGI_2, human fibrinogen, NECA and the disodium salts of ADP, β,γ-meATP and α,β-meATP, Sigma Chemical Co., Poole, U.K.; 8-SPT and 2-MeSATP, Research Biochemicals Inc., St. Albans, U.K.; suramin was a gift from Bayer plc, UK.

The tetrasodium salt of FPL 66096 was synthesized by P.A. Cage, Department of Medicinal Chemistry, Fisons plc, R & D Laboratories, Loughborough, UK, extending previously described methodology for the preparation of 2-alkylthio, β,γ-dihalomethylene analogues of ATP (Yoshikawa *et al.*, 1967; Blackburn *et al.*, 1984).

Indomethacin was dissolved in 10% w/v Na_2CO_3 at 10 mg ml^{-1} with subsequent dilutions in Krebs' buffer. A working dilution of PGI_2 (0.1 mg ml^{-1}) was made in saline from a stock solution of 1 mg ml^{-1} in ethanol, no more than 1 min before use. 8-SPT was dissolved at the working concentration (5.6 mg ml^{-1}) in 6% glucose. All other drugs were dissolved in distilled water or saline.

Results

Antagonism of ADP-induced aggregation of human washed platelets by FPL 66096

ADP produced concentration-dependent aggregation of human washed platelets with a $p[A_{50}]$ value of 4.90 ± 0.08 (s.e., $n = 6$, Figure 1). FPL 66096 (1–100 nM) produced concentration-dependent rightward displacement of the ADP E/[A]

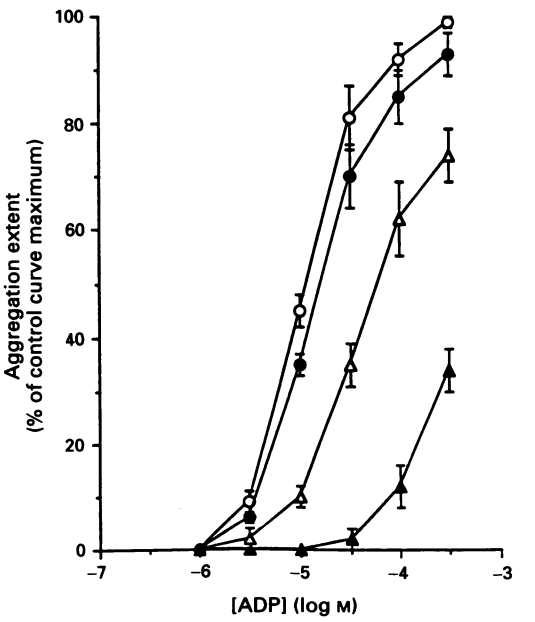


Figure 1 E/[A] curves obtained for ADP-induced aggregation of human washed platelets following 2 min incubation with either FPL 66096 (● 1, Δ 10 or ▲ 100 nM) or vehicle (○). Results are presented as mean responses (± s.e., $n = 6$), expressed as a % of the maximum response to ADP in the control curve.

curve in an apparently parallel manner, indicative of simple competition. We have found that use of concentrations of ADP in excess of 300 μM results in biphasic control E/[A] curves, complicating quantitative analysis of antagonist effects. Therefore, in this study, only data up to and including this concentration are reported. For this reason, the E/[A] curve obtained in the presence of the highest concentration of FPL 66096 is incomplete. However, statistical analysis of the E/[A] parameters (Table 1) obtained from combined, unconstrained logistic fitting of the first three curves shown in Figure 1, indicates that, over the concentration-range 1–10 nM, the rightward displacements produced by FPL 66096 did not deviate significantly from parallelism: there were no statistically significant differences in values of α and m. Therefore, to permit estimation of a pK_B for FPL 66096, it was assumed that the incomplete fourth curve would also have achieved the same asymptote and data sets from individual experiments, including the fourth curve in each case, were fitted to the logistic function (ii), assuming common values of α and m: an assumption of simple competition. This enabled calculation of a predicted value of E for each [A] in each curve. In Figure 2 (a–d), E/[A] curves, plotted through the means ($n = 6$) of these predicted values, are shown superimposed on individual observed datum points obtained from the six replicate experiments under control conditions and in the presence of FPL 66096. The goodness of fit parameter obtained ($R^2 = 0.97 \pm 0.01$, s.e., $n = 6$), indicates that the effect of FPL 66096 was consistent with simple competition and that Schild analysis was valid. Each individual experiment provided a computed estimate of the Schild slope parameter, n and an apparent pK_B. The mean value for n (1.01 ± 0.01), obtained from six replicate experiments, did not differ significantly from unity, indicating that the antagonism was consistent with simple competition. The computed pK_B estimate, using equation (ii), with n constrained to unity was 8.66 ± 0.07 (s.e., $n = 6$). The Schild plot derived from this analysis is presented for display purposes in Figure 2e.

Table 1 E/[A] curve parameters for ADP-induced aggregation of human washed platelets in the absence and presence of FPL 66096

FPL 66096 (nM)	*Parameter* p[A_{50}]	α (%)	m
0	4.90 ± 0.08	99.4 ± 2.2	1.77 ± 0.23
1	4.81 ± 0.04	93.0 ± 3.6	1.65 ± 0.27
10	4.39 ± 0.13	80.2 ± 11.4	1.34 ± 0.10

Values are means (± s.e.) of parameter estimates made by fitting the logistic function (i) (see text) to the combined E/[A] data obtained from six replicate experiments.

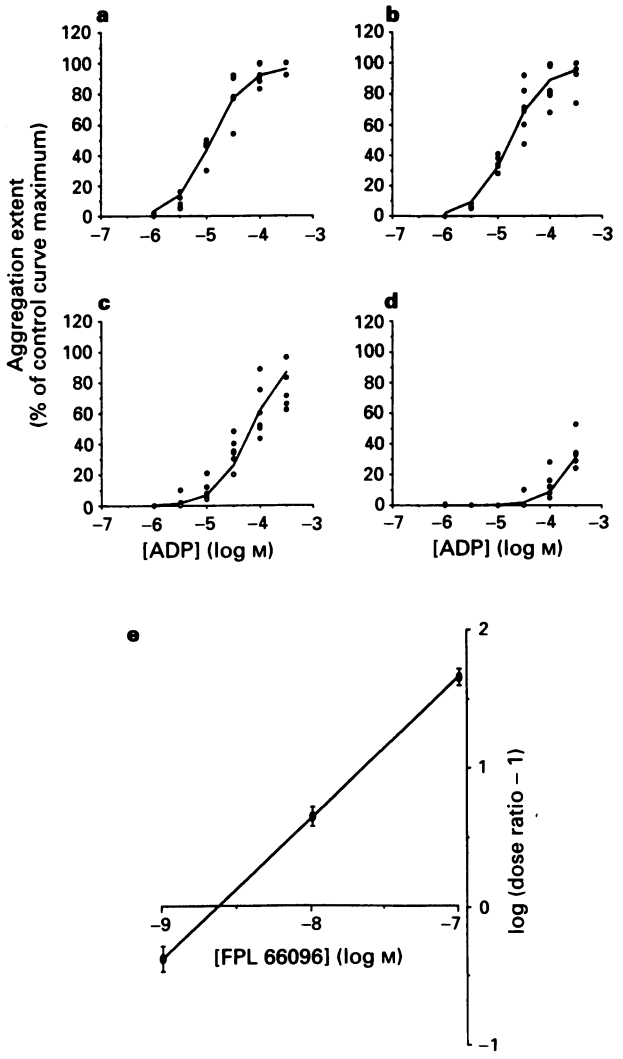


Figure 2 Analysis of antagonism by FPL 66096 of ADP-induced aggregation of human washed platelets. Predicted E/[A] curves, plotted through computer-generated points obtained using the logistic function (ii) (see text), are shown superimposed on individual datum points, from six replicate experiments, describing E/[A] curves obtained for ADP following 2 min incubation with either FPL 66096 ((b) 1, (c) 10 or (d) 100 nM) or vehicle (a). Results are expressed as a % of the maximum response to ADP in the control curve. (e) Corresponding Schild plot of the effect of FPL 66096 on E/[A] curves for ADP. Points show mean (dose ratio – 1) values (± s.e.mean) for six replicate experiments.

The effect of incubation time and 8-SPT on inhibition of ADP-induced aggregation of human washed platelets by FPL 66096

The pK_B estimate for FPL 66096 was obtained using an incubation period of 2 min in the absence of the P_1-purinoceptor antagonist, 8-SPT. When quantified in terms of inhibition of aggregation induced by a standard submaximal concentration of ADP (30 or 100 μM), the pIC_{50} for FPL 66096 under these conditions was 7.95 ± 0.18 (s.e., $n = 4$). Inclusion of 8-SPT, at a concentration (300 μM) that reduced the potency of NECA by 68 fold, increasing the incubation time to 15 min or a combination of these manoeuvres had no significant effect on the anti-aggregatory potency of FPL 66096 (Table 2).

The effect of FPL 66096 on U46619-induced aggregation of human washed platelets

The effect of FPL 66096 on platelet aggregation produced by the thromboxane A_2-mimetic, U46619, is summarized in Figure 3. Under control conditions (Figure 3a), FPL 66096 (0.1 and 1 μM, $n = 4$) significantly ($P < 0.05$) depressed the maximum response to U46619 and produced a small (2 fold) but significant ($P < 0.01$) rightward shift in the p[A_{50}] at 0.1 μM. When repeated in the presence of suramin (100 μM), added 1 min prior to FPL 66096, no significant change in the position or asymptote of the U46619 curve was observed (Figure 3b). However, under the same test conditions, the P_1-purinoceptor agonist, NECA produced marked, concentration-related inhibition of platelet aggregation produced by U46619. (Figure 3c).

Selectivity of FPL 66096

In the rabbit isolated ear artery, FPL 66096 was a very weak but full agonist (α 124 ± 9%, s.e., $n = 5$) with a p[A_{50}] value of 3.68 ± 0.18. Agonist E/[A] curves for both FPL 66096 and

Table 2 The effect of 8-sulphophenyltheophylline (8-SPT) and variation in incubation time on inhibition of ADP-induced aggregation of human washed platelets by FPL 66096 and 5'-N-ethylcarboxamidoadenosine (NECA)

	2 min incubation		*15 min incubation*	
Inhibitor	− 8-SPT	+ 8-SPT	− 8-SPT	+ 8-SPT
FPL 66096	7.95 ± 0.18	7.77 ± 0.11	8.27 ± 0.34	8.15 ± 0.19
NECA	6.24 ± 0.08	4.41 ± 0.08*	not tested	not tested

Results are presented as mean (± s.e., $n = 4$) pIC_{50} values for inhibition of ADP-induced platelet aggregation. *$P < 0.0001$ compared to potency in the absence of 8-SPT (Student's unpaired t test).

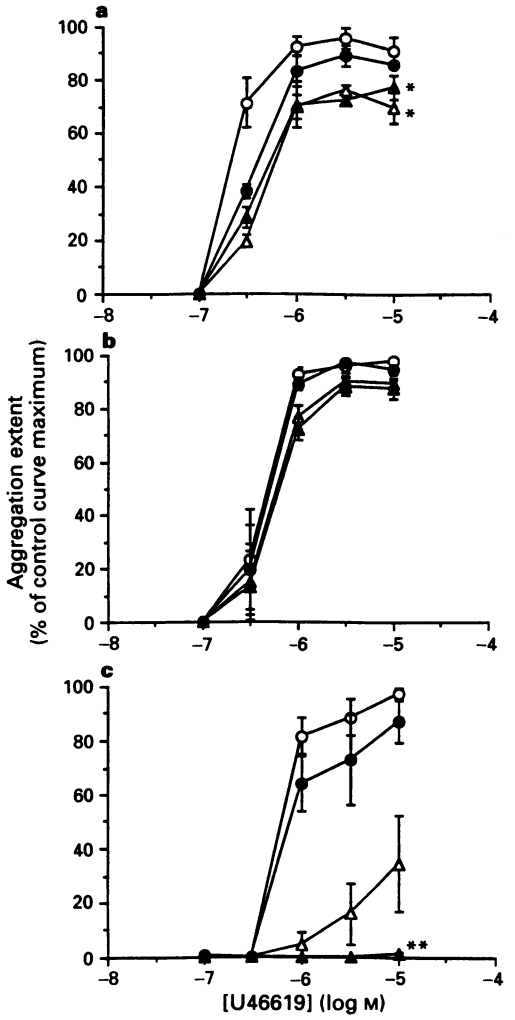


Figure 3 E/[A] curves obtained for U46619-induced aggregation of human washed platelets. Results are presented as mean responses (± s.e., $n = 4$), expressed as a % of the maximum response to U46619 in the control curve. Responses were obtained following 2 min incubation with either FPL 66096 (a,b) (● 10, Δ 100 or ▲ 1000 nM), or NECA (c) (● 0.1, Δ 1 or ▲ 10 μM) or vehicle (○) in the absence (a) or presence (b,c) of suramin (100 μM) added 1 min prior to FPL 66096 or NECA. *$P < 0.05$ and **$P < 0.01$ with respect to maximum response in control E/[A] curve (Dunn's multiple comparison test).

the standard P_{2X}-purinoceptor agonist α,β-meATP, were completely or near abolished in the presence of a desensitizing concentration of α,β-meATP (30 μM) (Figure 4).

In isolated preparations of the guinea-pig aorta, FPL 66096 demonstrated no agonist or antagonist activity at concentrations up to 3 μM. FPL 66096 (10–1000 μM) caused concentration-related relaxation of the tissue. Curves were incomplete (~60% tissue maximum) at 100–1000 μM ($n = 7$) and, in two tissues where a second curve was constructed, the

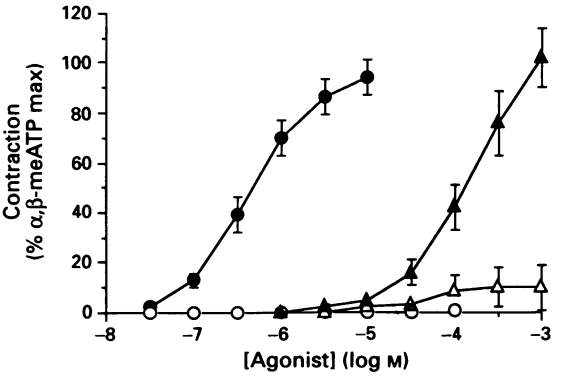


Figure 4 E/[A] curves obtained for contractions of the rabbit isolated ear artery produced by either α,β-meATP (●, ○) or FPL 66096 (▲, Δ), under control conditions (solid symbols) or following desensitization with α,β-meATP (30 μM) (open symbols). Results are presented as mean responses (± s.e., $n = 5$), expressed as a % of the maximum response to α,β-meATP in the control curve.

relaxation was not reliably inhibited by pre-exposure to 2-MeSATP at a concentration (10 μM) that produced marked rightward displacement and depression of the E/[A] curve for the standard P_{2Y} agonist, 2-MeSATP. In the other five tissues, E/[A] curves for 2-MeSATP were constructed in the continued presence of the highest concentration of FPL 66096 (100 or 1000 μM) and were displaced to the right with no depression of the maximum response. The apparent pK_B for FPL 66096 estimated from these data was 4.71 ± 0.18 (s.e., $n = 5$). Examples of results obtained in the guinea-pig aorta using either the occupation-desensitization or antagonist protocols described above are presented for display purposes in Figure 5.

Discussion

In this study, we have demonstrated that FPL 66096 is a highly potent (pK_B 8.66) antagonist of ADP-induced aggregation of human washed platelets. Inhibition of aggregation was characterized by a concentration-dependent rightward displacement of the ADP E/[A] relationship, with a Schild slope parameter that did not differ significantly from unity. Since platelet aggregation produced by ADP is mediated by a purinoceptor classified as the P_{2T}-subtype (Gordon, 1986), the observed effect of FPL 66096 is consistent with it functioning as a competitive P_{2T}-purinoceptor antagonist. In previous studies, the most potent, competitive P_{2T}-purinoceptor antagonist described has been the S_p diastereoisomer of ATP-α-S, with a pK_B of 5.44 in preparations of human PRP (Cusack & Hourani, 1982a). Thus, FPL 66096 represents the most potent P_{2T}-antagonist described to date in any assay system.

Confidence in any claim that an agent represents a potent and selective probe for a particular receptor subtype requires that the test system and protocol are designed to permit exclusion of alternative interpretations of results. Historically,

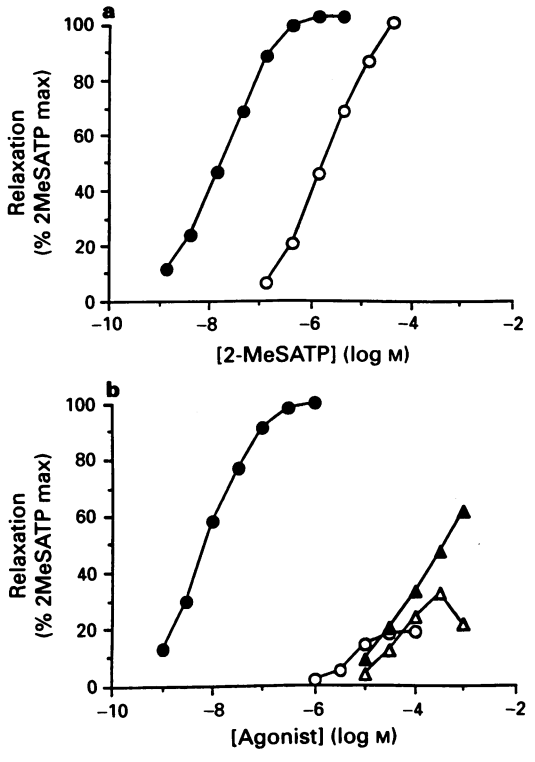


Figure 5 Representative effects of FPL 66096 in the guinea-pig isolated aorta: (a) E/[A] curves for 2-MeSATP-induced relaxation in the absence (●) and presence (○) of FPL 66096 (1 mM); (b) E/[A] curves for either 2-MeSATP (●, ○) or FPL 66096 (▲, △), under control conditions (closed symbols) or following occupation-desensitization with 2-MeSATP (10 μM) (open symbols). In each case, results from a single experiment are expressed as a % of the maximum response to 2-MeSATP in the control curve.

results obtained in the evaluation of ATP analogues as potential P_{2T}-purinoceptor antagonists have often been equivocal because mechanisms other than P_{2T}-purinoceptor antagonism could not be confidently excluded (Haslam & Cusack, 1981). Specifically, it is possible that P_1-purinoceptor-mediated inhibition of platelet aggregation following chemical or metabolic breakdown of the ATP analogue to the corresponding nucleoside may have contributed to the overall pharmacological effect observed in a number of studies. This is a real concern in the preliminary testing of novel ATP analogues with unknown chemical and metabolic stability. In addition, when platelet-rich plasma (PRP) is used as the assay system, plasma protein binding may complicate quantification of antagonist activity, as has been demonstrated recently in the case of suramin (Hourani *et al.*, 1992). Thus, to minimize these potential confounding influences, in the present study, P_{2T}-antagonist activity was determined in suspensions of human washed platelets rather than in PRP and the P_1-purinoceptor antagonist, 8-SPT (Collis *et al.*, 1987) was used to abrogate possible P_1-purinoceptor-mediated effects. Under these conditions, we believe that we were able to make the most appropriate quantitative analysis of the antagonist effects of FPL 66096.

In deriving the pK_B value for FPL 66096, the assumption was made that the incomplete ADP E/[A] curve, obtained in the presence of the highest concentration of FPL 66096, would have achieved the asymptote common to the other E/[A] curves. This assumption appeared justified given the non-deviation of the previous three curves from parallelism and a satisfactory goodness of fit for individual data sets when this assumption was built into the logistic fit. Strictly, while these current data support our conclusion that FPL 66096 represents the most P_{2T}-purinoceptor antagonist yet described, the incompleteness of the data precludes the definitive description of FPL 66096 as a competitive antagonist. Equally, these data do not disprove simple competition. Thus, until a more potent P_{2T}-purinoceptor agonist is used to allow fuller characterization of antagonist activity than has proved possible using ADP, it would seem reasonable to describe the effect of FPL 66096 in human washed platelets as being consistent with simple competition. A contributory factor to the inability to complete the fourth ADP E/[A] curve was the relatively low potency of ADP (A_{50}, 12.5 μM) in this washed platelet system compared to that normally described in PRP (~1 μM). This drop in potency is likely to be a consequence of the 2-stage washing procedure employed. A tendency for the potency of ADP to decline when platelets are washed has also been observed elsewhere (Hourani *et al.*, 1992). We routinely use the 2-stage washing procedure described in the present study because, during method development, we found that a single stage protocol was associated with an unacceptably high failure rate, due to spontaneous aggregation of platelet suspensions in the measuring cuvettes.

A pre-incubation protocol for testing P_{2T}-purinoceptor antagonists in PRP has been suggested as inappropriate because of the potential for metabolic breakdown of ATP-analogues to yield metabolites with agonist activity at P_1-purinoceptors (Cusack & Hourani, 1982a). In the present study, we have shown that the potency of FPL 66096 is statistically unaltered by increasing incubation time from 2 to 15 min. Furthermore, inclusion of the P_1-purinoceptor antagonist, 8-SPT at a concentration that markedly inhibited the anti-aggregatory effect of the P_1-agonist, NECA had no effect on the potency of FPL 66096. Thus, in the human washed platelet system used in this study, a pre-incubation protocol does not complicate analysis of P_{2T}-antagonist activity and, in many cases, pre-incubation may be desirable particularly if slowly-equilibrating antagonists are being tested.

The anti-aggregatory effect of FPL 66096 was specific to P_{2T}-purinoceptors. At a concentration 500 fold in excess of its K_B, FPL 66096 had no effect on responses produced by the thromboxane A_2-mimetic, U46619, when rendered ADP-independent by inclusion of the non-selective P_2-purinoceptor antagonist, suramin, at a concentration (100 μM) that produces a 10 fold rightward shift of the ADP E/[A] curve in human washed platelets (Hourani *et al.*, 1992). In this respect, the profile of FPL 66096 in human washed platelets is similar to that reported for other 2-alkylthio-substituted ATP analogues: in human PRP, 2-MeSATP, 2-ethylthio ATP and 2-methylthio-β,γ-methylene ATP inhibit ADP- but not U46619-induced aggregation (Cusack & Hourani, 1982b; Hourani *et al.*, 1986). However, these analogues behaved as non-competitive inhibitors of ADP-induced aggregation and were of limited efficacy, producing maximum inhibition of only 50–60% at 100 μM. In human washed platelets, this concentration of FPL 66096 abolished aggregation induced by ADP (100 μM). In preliminary experiments, we have observed that, when tested in the washed platelet system, 2-methylthio-β,γ-methylene ATP (100 μM) also abolishes ADP-induced aggregation (pIC_{50} ~5.5, unpublished observation). The reason for the different behaviour of 2-alkylthio analogues of ATP in human PRP and washed platelets requires further investigation, but protein binding or differences in the ionic environment could be contributory factors.

FPL 66096 was highly selective for the P_{2T}-purinoceptor subtype, showing no agonist or antagonist activity at P_{2X}- or P_{2Y}-purinoceptors at a concentration (3 μM) 1400 fold higher than its K_B against ADP-induced platelet aggregation. At still higher concentrations, FPL 66096 produced concentration-related contractions of the rabbit isolated ear artery which were prevented by desensitization with α,β-meATP, confirming that the contractions were mediated by a P_{2X} mechanism. In preparations of the rat isolated aorta, occupation-desensitization by 2-MeSATP has been shown to be selective for P_{2Y}-mediated relaxations (Dainty *et al.*, 1991). In the

present study, in the guinea-pig aorta, concentration-related relaxations produced by 2-MeSATP, but not those produced by FPL 66096 ($\geqslant 10\,\mu M$), were inhibited in the presence of a high concentration of 2-MeSATP. In a separate group of tissues, FPL 66096 (100 or $1000\,\mu M$) behaved as a competitive antagonist of relaxations produced by 2-MeSATP. Thus, in the guinea-pig aorta, at concentrations that produce relaxations by an as yet undefined mechanism, FPL 66096 functions as an apparently competitive P_{2Y}-purinoceptor antagonist. The apparent affinity for P_{2Y}-purinoceptors (apparent pK_B 4.71) and potency at P_{2X}-purinoceptors (pA_{50} 3.68) indicates that FPL 66096 has an approximately 9,000 fold selectivity for the P_{2T}-purinoceptor (pK_B 8.66). This degree of selectivity is particularly interesting in the light of the known structure-activity relationships for ligands at P_{2T}- and P_{2Y}-purinoceptors. In general, 2-alkylthio substitution on ATP analogues has been shown to increase affinity for P_{2T}- and potency at P_{2Y}-purinoceptors, and 2-methylthio-β,γ-difluoromethylene ATP acts as a potent P_{2Y}-agonist in isolated preparations of the guinea-pig taenia coli (Cusack *et al.*, 1987; Cusack & Hourani, 1990). Thus, the observation that FPL 66096 functions as a competitive P_{2Y}-antagonist indicates that 2-propylthio substitution has a profound effect on efficacy at P_{2Y}-purinoceptors.

Activation of platelets by ADP has been suggested to involve two different receptors: one linked to shape change and aggregation and a second receptor linked to inhibition of adenylate cyclase. The evidence for subtypes of receptors for ADP is based largely on binding studies and on the differential effects of 5'-fluorosulphonylbenzoyladenosine and *p*-chloromercuribenzenesulphonate on the various functional responses (Colman & Figures, 1984; Macfarlane, 1987). However, these agents cannot be considered satisfactory probes for use in receptor classification due to their non-specific effects. Using a group of competitive P_{2T}-antagonists, Hourani and co-workers have obtained similar pK_B values for inhibition of ADP-induced increases in intra-platelet calcium concentrations, ADP-induced platelet aggregation, and inhibition of adenylate cyclase (Cusack & Hourani, 1982a; Hall & Hourani, 1993). This provides strong evidence for the existence of a single type of ADP-receptor on platelets.

Identification of FPL 66096, a P_{2T}-purinoceptor antagonist of unprecedented potency and selectivity provides a novel pharmacological tool to clarify this issue further, to investigate the role of ADP in platelet aggregation produced by other agents and for use in the classification of P_2-purinoceptors in general.

The authors would like to thank Dr B.E. Crack and Dr I.A. Dainty for permission to quote data obtained in the rabbit ear artery and guinea-pig aorta preparations.

References

ARUNLAKSHANA, O. & SCHILD, H.O. (1959). Some quantitative uses of drug antagonists. *Br. J. Pharmacol. Chemother.*, **14**, 48–58.

BLACKBURN, G.M., KENT, D.E. & KOLKMANN, F. (1984). The synthesis and metal binding characteristics of novel, isopolar phosphonate analogues of nucleotides. *J. Chem. Soc. Perkin. Trans*, **I**, 1119–1125.

BURNSTOCK, G. (1978). A basis for distinguishing two types of purinergic receptor. In *Cell Membrane Receptors for Drugs and Hormones: A Multidisciplinary Approach*. ed. Straub, R.W. & Bolis, L. pp. 107–118. New York: Raven Press.

BURNSTOCK, G. & KENNEDY, C. (1985). Is there a basis for distinguishing two types of P_2-purinoceptor? *Gen. Pharmacol.*, **16**, 433–440.

COLLIS, M.G., JACOBSON, K.A. & TOMKINS, D.M. (1987). Apparent affinity of some 8-phenyl-substituted xanthines at adenosine receptors in guinea pig aorta and atria. *Br. J. Pharmacol.*, **92**, 69–75.

COLMAN, R.W. & FIGURES, W.R. (1984). Characteristics of an ADP receptor mediating platelet activation. *Mol. Cell. Biochem.*, **59**, 101–111.

CUSACK, N.J. & HOURANI, S.M.O. (1982a). Adenosine 5'-diphosphate antagonists and human platelets: no evidence that aggregation and inhibition of stimulated adenylate cyclase are mediated by different receptors. *Br. J. Pharmacol.*, **76**, 221–227.

CUSACK, N.J & HOURANI, S.M.O. (1982b). Specific but non-competitive inhibition by 2-alkylthio analogues of adenosine 5'-monophosphate and adenosine 5'-triphosphate of human platelet aggregation induced by adenosine 5'-diphosphate. *Br. J. Pharmacol.*, **75**, 397–400.

CUSACK, N.J. & HOURANI, S.M.O. (1990). Subtypes of P_2-purinoceptors. Studies using analogues of ATP. *Ann. N.Y. Acad. Sci.*, **603**, 172–181.

CUSACK, N.J., HOURANI, S.M.O., LOIZOU, G.D. & WELFORD, L.A. (1987). Pharmacological effects of isopolar phosphonate analogues of ATP on P_2-purinoceptors in guinea-pig taenia coli and urinary bladder. *Br. J. Pharmacol.*, **90**, 791–795.

DAINTY, I.A., LEFF, P., MCKECHNIE, K. & O'CONNOR, S.E. (1992). Endothelium-dependent relaxations to ATP in the guinea-pig but not rat aorta are mediated predominantly through P_{2Y}-purinoceptors. *Int. J. Purine Pyrimidine Res.*, **3**, 162P.

DAINTY, I.A., O'CONNOR, S.E. & LEFF, P. (1991). Endothelium-dependent relaxations to UTP in the rat aorta are not mediated by P_{2Y}-purinoceptors. *Fundam. Clin. Pharmacol.*, **5**, 387.

GILES, H., LEFF, P., BOLOFO, M.L., KELLY, M.G. & ROBERTSON, A.D. (1989). The classification of prostaglandin DP-receptors in platelets and vasculature using BW A868C, a novel, selective and potent competitive antagonist. *Br. J. Pharmacol.*, **96**, 291–300.

GORDON, J.L. (1986). Extracellular ATP: effects, sources and fate. *Biochem. J.*, **233**, 309–319.

HALL, D.A. & HOURANI, S.M.O. (1993). Effects of analogues of adenine nucleotides on increases in intracellular calcium mediated by P_{2T}-purinoceptors on human blood platelets. *Br. J. Pharmacol.*, **108**, 728–733.

HASLAM, R.J. & CUSACK, N.J. (1981). Blood platelet receptors for ADP and for adenosine. In *Purinergic Receptors: Receptors and Recognition Series B*, Volume 12. ed. Burnstock, G. pp 221–285. London: Chapman & Hall.

HOURANI, S.M.O., HALL, D.A. & NIEMAN, C.J. (1992). Effects of the P_2-purinoceptor antagonist, suramin, on human platelet aggregation induced by adenosine 5'-diphosphate. *Br. J. Pharmacol.*, **105**, 453–457.

HOURANI, S.M.O., WELFORD, L.A. & CUSACK, N.J. (1986). 2-MeS-AMP-PCP and human platelets: implications for the role of adenylate cyclase in ADP-induced aggregation? *Br. J. Pharmacol.*, **87**, 84P.

HUMPHRIES, R.G., TOMLINSON, W., INGALL, A.H., KINDON, N.D. & LEFF, P. (1993). FPL 66096: A novel, highly potent and selective antagonist at human platelet P_{2T}-purinoceptors. *Br. J. Pharmacol.*, **110**, 42P.

MACFARLANE, D.E. (1987). Agonists and receptors: adenosine diphosphate. In *Platelet Responses and Metabolism Vol II. Receptors and Metabolism*. ed. Holmsen, H. pp. 19–35. Florida: CRC Press.

MACFARLANE, D.E. & MILLS, D.C.B. (1975). The effects of ATP on platelets: evidence against the central role of released ADP in primary aggregation. *Blood*, **46**, 309–320.

O'CONNOR, S.E., WOOD, B.E. & LEFF, P. (1990). Characterization of P_{2X}-receptors in rabbit isolated ear artery. *Br. J. Pharmacol.*, **101**, 640–644.

WILLIAMS, M. (1989). Adenosine antagonists. *Med. Res. Rev.*, **9 (2)**, 219–243.

YOSHIKAWA, M., KATO, T. & TAKENISHI, T. (1967). A novel method for phosphorylation of nucleosides to 5'-nucleotides. *Tetrahedron Lett.*, **50**, 5065–5068.

(Received May 5, 1994
Revised July 6, 1994
Accepted July 21, 1994)

Br. J. Pharmacol (1994), **113**, 1064–1070 © Macmillan Press Ltd, 1994

Haemodynamic actions of a novel sino-atrial node function modulator, ZENECA ZD7288, in the anaesthetized dog: a comparison with zatebradine, atenolol and nitrendipine

[1]W. Rouse & I.R. Johnson

Vascular Inflammatory and Musculoskeletal Research Dept., ZENECA Pharmaceuticals, Alderley Park, Macclesfield, Cheshire SK10 4TG

1 ZENECA ZD7288 (4-(*N*-ethyl-*N*-phenylamino)-1,2-dimethyl-6-(methylamino) pyrimidinium chloride, formerly ICI D7288) is a novel sino-atrial node function modulator which selectively slows sinus node rate. Its effects on haemodynamic function have been studied in pentobarbitone anaesthetized dogs, in comparison with zatebradine, atenolol and nitrendipine.

2 ZD7288 lowered heart rate in the dose-range 0.02 to 1.0 mg kg^{-1} i.v. from 152 to 77 beats min^{-1}. Myocardial contractile function (measured as both dP_{LV}/dt_{max} and right ventricular free wall developed force) decreased along with rate. Stroke volume increased as rate decreased. Cardiac output decreased at doses in excess of 0.2 mg kg^{-1}, i.v.

3 These haemodynamic changes were reversed when heart rate reduction was reversed by atrial pacing and are, therefore, considered to be indirect consequences of heart rate changes induced by ZD7288.

4 The effects of zatebradine paralleled those of ZD7288 (heart rate reduced from 149 to 60.5 beats min^{-1} over the dose-range 0.02 to 1.0 mg kg^{-1}, i.v.), except that dP_{LV}/dt_{max} did not decrease with heart rate and increased during arial pacing.

5 Neither ZD7288 nor zatebradine had significant effects on atrio-ventricular conduction at intrinsic heart rates, but both significantly and dose-dependently prolonged the atrio-ventricular conduction interval during atrial pacing at 180 beats min^{-1}.

6 The observed effects of atenolol were commensurate with removal of β-sympathetic cardiac drive. Atrial pacing was found not to restore the pre-atenolol haemodynamic state completely.

7 Nitrendipine up to 0.2 mg kg^{-1} i.v. induced changes indicative of direct vasodilatation accompanied by reflex compensation, followed by cardiac depression at higher doses. Atrial pacing failed to compensate for the effects of vasodilatation, but caused atrio-ventricular conduction block at doses above 0.5 mg kg^{-1}, i.v.

8 The data show ZD7288 has marked heart rate slowing properties and that accompanying haemodynamic changes appear to be secondary to the rate changes, being reversed by atrial pacing even in the continued presence of the drug. Heart rate slowing without depression of contractile function should prove to be of benefit in the treatment of myocardial ischaemia, particularly in the presence of myocardial dysfunction.

Keywords: Haemodynamics; anaesthetized dog; heart rate; sino-atrial node; specific bradycardic agent; ZD7288; zatebradine; atenolol; nitrendipine

Introduction

Angina pectoris in patients suffering from myocardial ischaemia is a consequence of the imbalance between myocardial oxygen demand and supply. Supply adequacy can become supply deficit if heart work requirement outstrips coronary blood flow and oxygen supply. Heart work, in turn, is determined by pressure development, wall stress and heart rate. Under emotional stress or during exericse, heart rate and blood pressure will increase, contributing to myocardial ischaemia. Of the determinants of cardiac work load, rate is the most crucial; not only does it influence myocardial work (demand), but by affecting diastolic interval, it influences myocardial blood supply, particularly influencing that to the endocardium (Gross & Dämmgen, 1987). Drugs employed to treat angina pectoris include those which are aimed at influencing myocardial blood supply, such as nitrates and calcium channel blockers; and those which cause reduction in heart rate, such as β-adrenoceptor antagonists and some calcium channel blockers. Calcium channel blockers and β-adrenoceptor antagonists also influence contractile function, the former being directly depressant and the latter antagonizing sympathetically-mediated positive inotropic drive, and in certain instances, also being directly depressant.

In recent years, a class of compounds generally referred to as 'specific bradycardic agents' or 'sinus node inhibitors', has been introduced (Kobinger & Lillie, 1984; 1987; Lillie, 1991). These compounds have been found to affect the sino-atrial node pacemaking current, I_f, (BoSmith *et al.*, 1993) and therefore can reduce heart rate without necessarily affecting contractile function.

In this paper we present results from investigations in anaesthetized dogs to elucidate haemodynamic effects of a novel sino-atrial node function modulating compound, ZD7288 (4-(*N*-ethyl-*N*-phenylamino)-1,2-dimethyl-6-(methylamino) pyrimidinium chloride, known as ICI D7288 in previous publications) (Hargreaves *et al.*, 1992; Marshall *et al.*, 1993) with sinus node I_f blocking activity (BoSmith *et al.*, 1993). The results are compared with results from comparable experiments into the effects of an example of a recently-developed 'specific bradycardic agent' zatebradine (UL-FS 49) which, currently under clinical trial, has been shown to have clinical efficacy (Baiker *et al.*, 1991); and with the β-adrenoceptor antagonist atenolol (Tenormin) and the calcium channel blocker, nitrendipine.

[1] Author for correspondence.

Some of the data presented here have previously been published in abstract form (Rouse & Johnson, 1992).

Methods

Beagles of the Alderley Park strain in the weight range 14 to 18 kg, were anaesthetized with pentobarbitone ('Sagatal'), 40 mg kg^{-1}, i.v.. The trachea was intubated with a cuffed endotracheal tube. A double lumen catheter was inserted into the left jugular vein: one lumen was used for compound administration, the other for infusion of anaesthetic maintenance dose throughout the experiment ('Sagatal', 4 mg kg^{-1} min^{-1}, i.v.). Cautery was used throughout preparation to limit bleeding.

Respiration by intermittent positive pressure was commenced (Harvard pump), and a right fourth intercostal space thoractomy was performed. Arterial blood Po_2, Pco_2 and pH were monitored at intervals (Corning 178 pH/Blood Gas Analyser), and the respiration pump was altered to keep values within physiological limits. Lead II electrocardiogram was monitored from needle electrodes inserted subcutaneously.

The heart was suspended in a pericardial cradle, and the aortic root was cleared of fat just sufficiently to allow a close-fitting electromagnetic flow probe ('Skalar', Delft, The Netherlands) to be placed around the ascending aorta.

Platinum electrodes, embedded 1.5 mm apart in acrylic plaques, were sutured to the right atrial appendage and the interventricular sulcus to permit atrial pacing and to record atrial and ventricular epicardiograms.

A Walton-Brodie type strain gauge arch was attached to the free wall of the right ventricle by sutures which passed completely through the thickness of the ventricular wall. Stretch was applied to the myocardium between the sutures sufficient to prevent slackening of the arch during an experiment.

Left ventricular pressure was recorded with Millar 'Mikrotip' catheter tip transducers: either a Type SPC 470 introduced before thoracotomy via the right carotid artery and aortic valve, or a Type MPC 500 introduced after thoracotomy, directly via the left ventricular apical dimple. In the former case, aortic arch pressure was recorded through a 2 mm internal diameter, 600 mm long Teflon tube inserted (before thoracotomy) via a femoral artery; in the latter case, using a similar 200 mm long tube inserted via the right carotid artery. In either case, Transamerican Instruments type 4-422-0001, or Spectramed disposable strain gauge pressure transducers were employed to measure aortic arch pressure.

Signal conditioning employed pressure bridge and electrocardiogram amplifiers which were part of an analogue computing system constructed by the first author. The system was reset every heart beat by a logic pulse triggered by the ventricular epicardial ECG. Haemodynamic variables computed by the system were delivered as analogue peak-read outputs for recording on a 16-channel Gould TA4000 thermal-array recorder. The peak voltage levels were also sampled via an 8-channel analogue-to-digital converter, clocked by the ventricular-driven logic pulse, for data-logging into an IBM PC286 digital computer. The ADC was multiplexed to read up to 16 channels of information as two groups of eight for each heart beat.

From the transducer inputs the following variables were derived by the analogue computing system: systolic, diastolic and true mean aortic pressures; $dP_{LV}dt_{max}$ and cardiac contractile force developed during systole as indices of contractile function; instantaneous heart rate from the epicardial ventricular electrocardiogram; atrio-ventricular conduction interval; and stroke volume, by integration of the ascending aortic arch flow velocity with respect to time. Cardiac output and total peripheral resistance were calculated after data transfer to the digital computer by dedicated software written by the second author. The programme enabled on-line display of drug induced responses of any recorded variable against either time of dosing or logarithm of dose administered. The programme also permitted changes in any two chosen recorded variable to be plotted against one another, as well as enabling acquired data to be filed on magnetic discs.

Protocol

After stabilization of the preparation over a period of at least 30 min, data samples of 10 s duration were acquired on the PC at 10 min intervals, firstly at intrinsic heart rate then directly afterwards when stable conditions had been attained during atrial pacing at 180 beats min^{-1} (this usually took about 30 s). Pacing at 180 beats min^{-1} enabled the intrinsic heart rates of all dogs used in the study to be over-ridden and permitted paced results to be compared directly one with another. In retrospect, a second pacing interval at the control rate of each individual animal would have been useful for comparative purposes. After each paced data sample, the compound under study was administered cumulatively by the intravenous route. Data samples were accepted only if no irregular events occurred during sampling. Otherwise, the sample was replaced by a further sample.

Doses

Doses of drugs were used which, from previous experimental experience, were expected to produce significant changes in heart rate (in the case of ZD7288, zatebradine and atenolol) or atrio-ventricular conduction time (nitrendipine). Thus, the cumulative intravenous doses used were as follows: ZD7288 and nitrendipine; 0.02, 0.05, 0.1, 0.2, 0.5 and 1.0 mg kg^{-1}; zatebradine, 0.01, 0.02, 0.05, 0.1, 0.2, 0.5, and 1.0 mg kg^{-1}; and atenolol, 0.01, 0.02, 0.05, 0.1, 0.2 and 0.5 mg kg^{-1}.

Results

Experiments described here were of approximately 2 h duration. For comparison, in saline-dosed control experiments of 2 h duration in similar preparations (unpublished data), mean heart rate over the 2 h period was 185, ranging between 178 and 190. Similarly, mean values (and ranges) for other variables were as follows: dP_{LV}/dt, 3209 (3120–3339); mean aortic pressure, 129 (123–134); stroke volume, 9.0 (7.9–9.9); cardiac output, 1.66 (1.47–1.75); and systemic vascular resistance, 6107 (5640–6980).

Haemodynamic measurements appertaining to ZD7288 are illustrated in Figures 1 and 2, and are listed in full in Table 1. Results at selected dose levels from experiments on other compounds are shown in Table 2.

ZD7288

Intrinsic heart rate showed statistically significant dose-dependent decreases at all dose levels in excess of 0.02 mg kg^{-1} ZD7288 i.v.; 0.2 mg kg^{-1} caused a mean decrease in heart rate of 57.3 beats min^{-1}. There was a concomitant rate-related increase in stroke volume, but, statistically, cardiac output was not maintained constant at doses greater than 0.2 mg kg^{-1}. Contractile function as indexed by dP_{LV}/dt_{max} was also depressed above 0.5 mg kg^{-1}, though directly measured right ventricular contractile force decreased rate-dependently above 0.05 mg kg^{-1}. Systolic blood pressure remained constant, but diastolic pressure decreased with heart rate, even though systemic resistance increased.

Despite the presence of ZD7288, atrial pacing restored all variables to control-pacing levels with the exception of atrio-ventricular conduction interval, which increased significantly in a dose-dependent manner.

Zatebradine

Heart rate decreased significantly at doses greater than 0.1 mg kg^{-1} i.v. (by 47.3 beats min^{-1} after 0.2 mg kg^{-1} zatebradine). Stroke volume increased significantly at doses above 0.05 mg kg^{-1}, i.v., and systemic vascular resistance tended to increase whilst cardiac output decreased (significantly at doses in excess of 0.5 mg kg^{-1}, i.v.) as heart rate was reduced.

During right atrial pacing there was a dose related increase in dP_{LV}/dt_{max}, with a tendency for stroke volume, cardiac output and aortic pressures to increase. Pacing induced atrio-ventricular conduction interval increases at dose levels above 0.5 mg kg^{-1} i.v.; the magnitudes of these changes were similar to those seen after ZD7288.

Atenolol

Atenolol reduced heart rate significantly at all but the lowest dose studied (0.01 mg kg^{-1} i.v.). At 0.2 mg kg^{-1}, i.v., heart rate was decreased by 40.4 beats min^{-1} on average. There was a significant depression of contractile function by 24% and 22% for dP_{LV}/dt_{max} and right ventricular contractile force respectively. Atrio-ventricular conduction was significantly depressed at doses above 0.05 mg kg^{-1}, i.v.

Whereas atrial pacing to 180 beats min^{-1} maintained con-

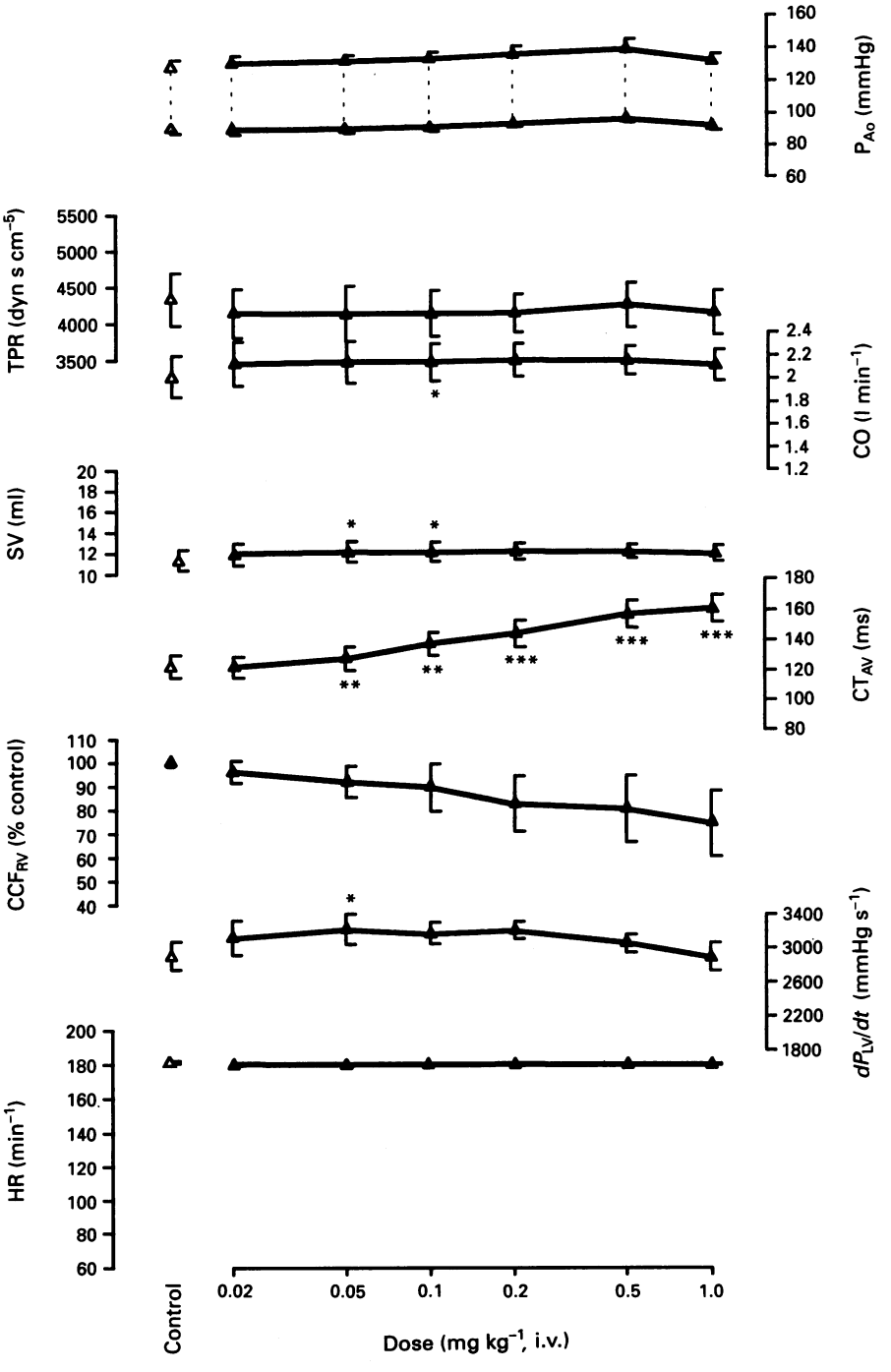


Figure 1 Dose-response relationship between ZD7288 and measured and calculated haemodynamic variables at intrinsic sinus rates in pentobarbitone anaesthetized beagles. Means ± s.e. mean, $n = 6$. (P_{Ao}: systolic and diastolic aortic pressures; TPR: total peripheral resistance; CO: cardiac output; SV: stroke volume; CT_{AV}: atrio-ventricular conduction interval; CCF_{RV}: right ventricular free-wall developed cardiac contractile force; dP_{LV}/dt: maximal rate of left ventricular.isovolumic pressure development; HR: heart rate).

tractile function at constant levels in the presence of ZD7288, both dP_{LV}/dt_{max} and right ventricular contractile force during pacing decreased in the presence of increasing dose levels of atenolol. Cardiac output decreased significantly, and atrio-ventricular conduction interval was significantly prolonged during pacing.

Nitrendipine

Heart rate reductions were minimal for doses of nitrendipine up to 0.2 mg kg^{-1}, i.v., there being a fall of only 3.5 beats min^{-1} on average and both stroke volume and cardiac output increased. At the highest dose administered, 1.0 mg kg^{-1}, i.v., heart rate was approximately halved to 64.7 ± 11.3 beats min^{-1}, comparable to heart rates following ZD7288 or zatebradine at the same dose. Stroke volume decreased to near-control value, while cardiac output decreased to 60% of control. Contractile function decreased to 69% (dP_{LV}/dt_{max}) and 80.7% (CCF_{RV}) of control. Both systolic and diastolic aortic pressures were reduced, despite a marked peripheral vasoconstriction, as indicated by systemic peripheral resistance increase. Atrio-ventricular conduction interval increased markedly in three of the four experiments with nitrendipine (to a mean of 728 ± 210 ms, $n = 4$).

It was not possible to pace the heart rate to 180 beats min^{-1} at doses greater than 0.5 mg kg^{-1} i.v. without inducing complete atrio-ventricular block. Maximum attainable paced rates were 132.5 and 59.5 at 0.5 and 1.0 mg kg^{-1} i.v., respectively. Diastolic aortic pressure decreased significantly by 72.4%.

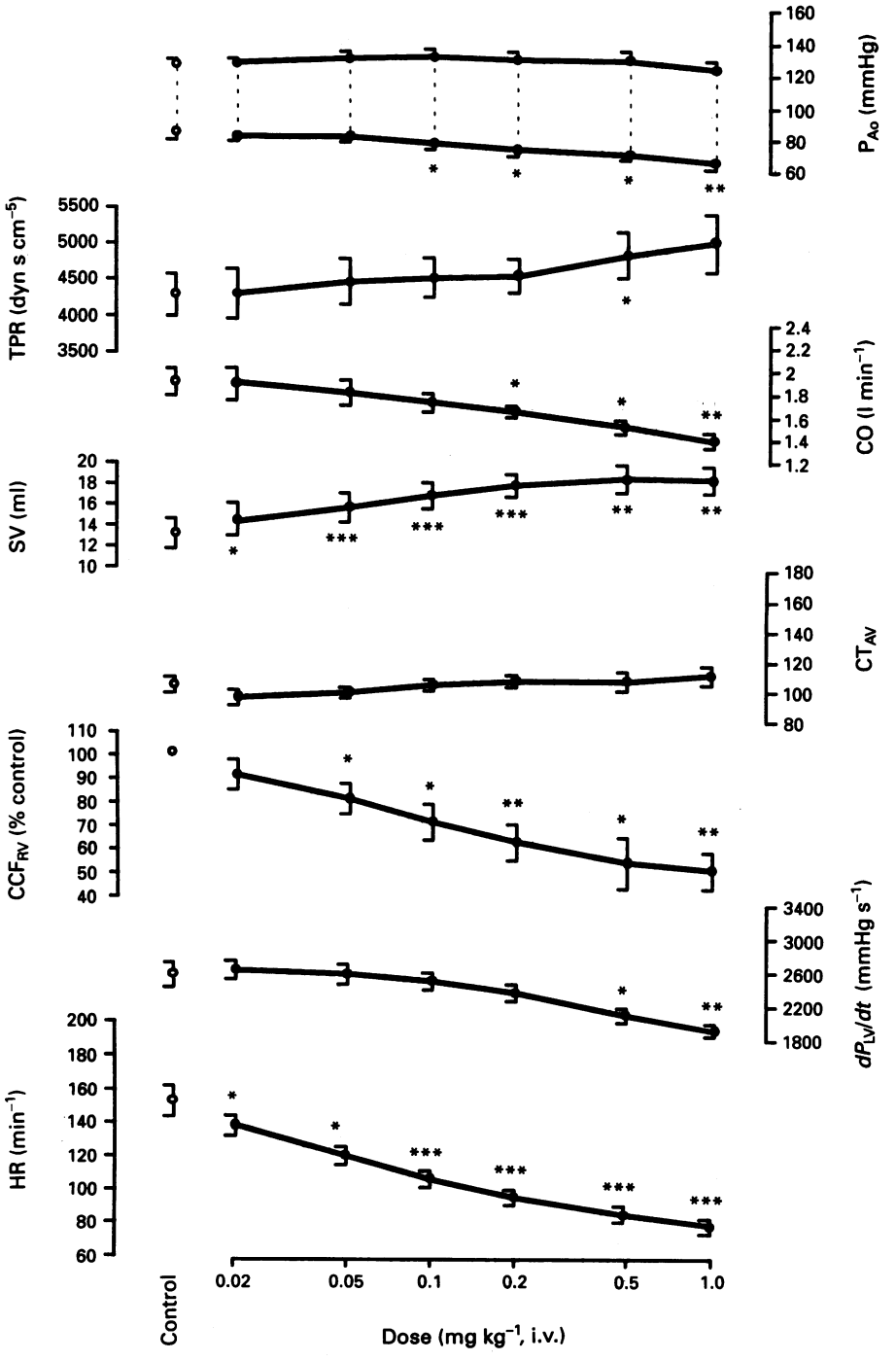


Figure 2 Dose-response relationships between ZD7288 and measured and calculated haemodynamic variables during right atrial pacing at 180 beats min^{-1} in pentobarbitone anaesthetized beagles. Means ± s.e. mean; same experiments as shown in Figure 1.

Discussion

The results presented in this paper confirm that ZD7288 had a dose-dependent action in reducing heart rate in the anaesthetized dog. Despite the considerable difference in chemical structure, its haemodynamic effects were comparable to the effects of zatebradine at doses up to those resulting in approximately 30% reduction in heart rate (0.1 mg kg^{-1} for ZD7288 and 0.2 mg kg^{-1} in the case of zatebradine). In essence, neither compound caused any significant perturbation of haemodynamics apart from a reduction in heart rate and an accompanying compensatory stroke volume increase at those doses, so that cardiac output was maintained constant.

At higher doses, dP_{LV}/dt_{max} fell with decreasing heart rate in the case of ZD7288, but did not in the case of zatebradine. Reports of the effects of zatebradine on contractile function are somewhat varied; zatebradine has been reported to have either some positive inotropic effect (Raberger *et al.*, 1987a) or no effect on the inotropic state of the heart (van Woerkens *et al.*, 1992; Raberger *et al.*, 1987b; Johnston *et al.*, 1991), depending on conditions and species. In our experiments, zatebradine appears to have had a positive inotropic action, in that, though it was not statistically significant, there was a tendency for dP_{LV}/dt_{max} to increase in comparison to initial control dP_{LV}/dt_{max} as heart rate decreased. A rate related decrease in dP_{LV}/dt_{max} might have been expected (Furnival *et al.*, 1970).

However, the second contractile function index employed, the force developed by a segment of right ventricular free-wall (Falotico *et al.*, 1989), indicated that higher doses of either ZD7288 or zatebradine induced cardiac function decreases of remarkably similar magnitudes at intrinsic heart rates. Restoration of rate by atrial pacing indicated that changes in contractile function were rate-related in the case of ZD7288, whether judged by dP_{LV}/dt_{max} measurements or by right ventricular contractile force, and the compound had little or no contractile depressant action.

During constant rate atrial pacing after zatebradine there was more evidence of positive inotropism as both dP_{LV}/dt_{max} and right ventricular free wall developed force increased with increasing dose levels, although only the observed increases in dP_{LV}/dt_{max} reached statistical significance.

It is debatable whether it is desirable to impose inotropic stimulation upon the myocardium in patients with angina of effort. It could be argued that such an action would be likely partially to offset any advantage gained in reducing myocardial oxygen consumption by decreasing heart rate. In addition, neither of the sino-atrial node function modulators used in these experiments has been shown to antagonize the influence of the sympathetic nervous system on myocardial contractile function (unpublished observations in the anaesthetised dog), so that the heart should still respond to altered sympathetic drive, and could rely upon sympathetic drive to support the myocardium. This would be in contrast to the situation where β-adrenoceptor antagonists are used to treat angina pectoris.

In experiments with atenolol, decreases in heart rate, myocardial contractile function, cardiac output and atrioventricular conduction velocity tended to plateau at about 0.1 mg kg^{-1}, i.v., as β-sympathetic drive was removed from the heart. There was seemingly little direct myocardial depression above 0.1 mg kg^{-1}, i.v., but atrial pacing failed to restore contractile function to pre-atenolol levels. Heart rate reduction was limited to that attained by removal of β-sympathetic drive and rates comparable to those seen after either ZD7288 or zatebradine could not be reached.

Nitrendipine induced positive inotropic actions both without and with pacing of heart rate, as well as marked increase in stroke volume even though heart rate did not decrease

Table 1 Haemodynamic effects of ZD7288 at intrinsic heart rates and when paced at 180 beats min^{-1}

Drug	*Dose* (mg kg^{-1}, i.v.)	*HR* (min^{-1})	*dP_{LV}/dt* (mmHg s^{-1})	*CCF_{RV}* (%)	*SV* (ml)	*CO* (l min^{-1})	*P_{Aos}* (mmHg)	*P_{Aod}* (mmHg)	*SVR* (dyn s cm^{-5})	*CT_{AV}* (ms)
ZD7288										
Unpaced:	Pre-dose	151.7	2572	100.0	13.0	1.90	128.5	85.8	4288	104.8
$n = 6$		± 9.1	± 151	± 0.0	± 1.5	± 0.11	± 3.5	± 4.3	± 324	± 5.4
	0.02	137.3[1]	2617	92.1	14.2[1]	1.90	129.9	83.8	4312	96.5
		± 5.8	± 105	± 6.1	± 1.6	± 0.14	± 2.8	± 4.6	± 373	± 5.1
	0.05	119.1[2]	2570	82.5[1]	15.5[3]	1.81	132.3	83.6	4495	99.9
		± 5.6	± 114	± 6.3	± 1.4	± 0.11	± 3.7	± 3.6	± 342	± 3.6
	0.1	105.1[3]	2484	72.6[1]	16.8[3]	1.73	133.3	79.5[1]	4550	105.1
		± 5.2	± 103	± 7.7	± 1.3	± 0.08	± 4.5	± 4.0	± 307	± 3.8
	0.2	94.4[3]	2350	65.5[2]	17.7[3]	1.65[1]	131.7	75.5[1]	4589	107.7
		± 4.7	± 100	± 7.6	± 1.1	± 0.05	± 5.3	± 4.3	± 263	± 4.1
	0.5	83.9[3]	2084[1]	56.8[1]	18.4[2]	1.51[1]	131.2	72.6[1]	4907	107.6
		± 4.8	± 84	± 10.7	± 1.4	± 0.06	± 5.5	± 4.0	± 334	± 6.5
	1	77.2[3]	1901[2]	54.0[2]	18.3[2]	1.39[2]	126.1	67.4[2]	5093	111.6
		± 4.5	± 75	± 7.8	± 1.3	± 0.07	± 5.1	± 4.8	± 438	± 6.4
Paced:	Pre-dose	180.9	2915	111.9	11.3	2.04	130.9	93.0	4296	122.5
		± 1.1	± 163	± 5.2	± 1.0	± 0.18	± 4.2	± 3.2	± 377	± 7.7
	0.02	180.3	3145	109.1	12.0	2.16	133.9	92.5	4089	121.8
		± 0.5	± 203	± 8.5	± 1.0	± 0.19	± 3.4	± 3.6	± 342	± 7.0
	0.05	180.1	3248[1]	105.3	12.1[1]	2.17	134.6	92.7	4084	127.5[2]
		± 0.6	± 175	± 9.4	± 1.0	± 0.18	± 3.4	± 2.5	± 394	± 7.9
	0.1	180.2	3194	104.3	12.1[1]	2.17[1]	135.7	93.8	4080	137.1[2]
		± 0.5	± 122	± 12.7	± 0.9	± 0.16	± 3.8	± 2.3	± 317	± 7.8
	0.2	180.4	3233	98.7	12.1	2.19	137.7	95.7	4092	143.6[3]
		± 0.5	± 101	± 14.4	± 0.7	± 0.14	± 4.1	± 2.0	± 272	± 8.7
	0.5	180.2	3089	96.2	12.1	2.18	141.0	98.5	4210	156.6[3]
		± 0.5	± 104	± 15.8	± 0.6	± 0.12	± 5.2	± 2.7	± 318	± 8.8
	1	180.2	2922	91.3	11.9	2.14	133.5	94.5	4095	160.5[3]
		± 0.6	± 161	± 16.3	± 0.7	± 0.14	± 4.1	± 2.9	± 308	± 9.0

Means ± s.e.mean shown beneath values; [1]$P < 0.05$; [2]$P < 0.01$; [3]$P < 0.001$; Student's paired t test with respect to pre-drug controls. (HR, heart rate; dP_{LV}/dt_{max}, maximum rate of isovolumic left ventricular pressure change: CCF_{RV}, right ventricular free wall contractile force: SV, stroke volume: CO, cardiac output: P_{Ao}, aortic pressure, systolic and diastolic: SVR, systemic vascular resistance: CT_{AV}, atrioventricular conduction interval).

Table 2 Haemodynamic effects of zatebradine, atenolol and nitrendipine at intrinsic heart rates and during pacing at 180 beats per min

Drug	*Dose* (mg kg^{-1}, i.v.)	*HR* (min^{-1})	dP_{LV}/dt (mmHg s^{-1})	CCF_{RV} (%)	*SV* (ml)	*CO* (l min^{-1})	P_{Aos} (mmHg)	P_{Aod} (mmHg)	*SVR* (dyn s cm^{-5})	CT_{AV} (ms)
Zatebradine										
Unpaced:	Pre-dose	148.8	3221	100.0	18.9	2.77	124.8	94.4	3045	115.7
$n=4$		± 9.6	± 73	± 0.0	± 1.65	± 0.10	± 6.6	± 5.6	± 284	± 6.2
	0.02	140.5	3254	97.6	19.5	2.72	123.6	91.8	3035	116.3
		± 6.3	± 23	± 1.4	± 1.4	± 0.13	± 7.2	± 4.9	± 334	± 4.4
	0.1	119.1[1]	3317	89.0[1]	22.5[2]	2.67	124.5	87.2	3045	114.0
		± 5.3	± 57	± 2.8	± 1.4	± 0.16	± 7.8	± 5.7	± 383	± 3.8
	0.5	75.9[2]	3464	61.5[2]	29.3[3]	2.23[1]	132.4	75.0[1]	3493	116.9
		± 3.6	± 223	± 3.3	± 1.8	± 0.20	± 11.4	± 8.1	± 593	± 3.6
Paced:	Pre-dose	179.5	3387	110.3	15.9	2.85	124.1	96.2	2989	125.4
		± 0.8	± 34	± 4.2	± 0.7	± 0.13	± 5.4	± 4.8	± 269	± 1.9
	0.02	180.0	3563	112.5	16.0	2.89	123.1	94.4	2911	127.0
		± 0.7	± 48	± 3.5	± 0.7	± 0.13	± 5.6	± 5.0	± 283	± 2.0
	0.1	180.1	3719	113.7	16.4	2.96	125.1	95.9	2897	130.6
		± 0.8	± 41	± 2.9	± 0.8	± 0.15	± 7.1	± 6.9	± 349	± 0.7
	0.5	180.2	4283[1]	116.0	17.2	3.10	133.1	100.4	2940	148.2[1]
		± 0.9	± 226	± 1.8	± 1.1	± 0.21	± 9.4	± 9.0	± 440	± 3.2
Atenolol										
Unpaced	Pre-dose	167.2	2687	100.0	13.7	2.29	123.0	92.7	3629	100.4
$n=4$		± 1.6	± 308	± 0.0	± 1.0	± 0.14	± 5.0	± 4.5	± 300	± 2.7
	0.02	143.7[1]	2664[1]	85.2	15.4	2.20	123.8	94.4	3794	109.9
		± 4.6	± 350	± 3.6	± 1.1	± 0.11	± 7.8	± 7.3	± 278	± 4.5
	0.1	128.0[3]	2221[1]	83.4[2]	16.7	2.13	112.1[1]	81.4[1]	3483	120.6[1]
		± 3.9	± 253	± 1.8	± 1.3	± 0.13	± 4.7	± 5.1	± 298	± 5.5
	0.5	123.3[3]	2052[1]	75.4[2]	15.7	1.93[1]	111.3	83.0	4158	121.6[1]
		± 4.3	± 181	± 2.8	± 1.5	± 0.14	± 6.4	± 6.9	± 454	± 6.5
Paced	Pre-dose	178.7	2698	108.4	12.8	2.29	121.6	92.9	3605	121.5
		± 0.4	± 260	± 3.1	± 0.6	± 0.11	± 4.7	± 4.7	± 261	± 10.4
	0.02	178.3	2784	99.8	13.0	2.32	120.8	95.5	3595	142.2
		± 0.2	± 313	± 3.3	± 0.7	± 0.13	± 6.1	± 3.5	± 208	± 10.2
	0.1	177.1	2425	100.8[1]	13.0	2.30	113.0	86.5	3352	142.6[1]
		± 1.9	± 224	± 4.5	± 0.6	± 0.13	± 3.5	± 5.1	± 276	± 10.4
	0.5	176.9	2279	95.4[2]	12.0[1]	2.13[1]	110.4	86.3	3790	147.0[1]
		± 2.0	± 148	± 5.4	± 0.7	± 0.14	± 5.1	± 6.8	± 423	± 10.5
Nitrendipine										
Unpaced	Pre-dose	122.7	2087	100.0	11.1	1.36	94.5	62.3	4315	134.0
$n=4$		± 4.2	± 296	± 0.0	± 1.1	± 0.12	± 7.4	± 5.9	± 289	± 10.1
	0.02	124.4	2546	106.4	12.5	1.55	94.4	57.2	3649	128.0
		± 5.7	± 383	± 5.4	± 1.7	± 0.22	± 11.6	± 4.9	± 212	± 10.9
	0.1	122.0	3163	110.9[1]	15.3	1.88	106.0	49.8	2974	120.7
		± 4.7	± 582	± 2.8	± 2.5	± 0.36	± 13.3	± 8.5	± 193	± 10.5
	0.5	96.5	2640	103.4	16.3[1]	1.57	104.9	41.2[1]	3276	294.7
		± 15.8	± 612	± 11.6	± 1.5	± 0.30	± 12.0	± 8.0	± 196	± 146.6
Paced	Pre-dose	178.3	2066	106.1	7.5	1.33	91.0	64.6	4528	167.5
		± 0.9	± 402	± 4.4	± 1.0	± 0.18	± 9.6	± 7.0	± 448	± 14.3
	0.02	178.2	2455	115.6	8.1	1.45	88.5	58.6	3961	165.1
		± 0.9	± 569	± 9.6	± 1.5	± 0.27	± 14.1	± 6.1	± 372	± 12.7
	0.1	178.2	3168	135.9[1]	10.5	1.87	99.5	52.0[2]	2984	166.2
		± 0.8	± 751	± 8.5	± 2.1	± 0.38	± 15.8	± 7.9	± 222	± 12.5
	0.5	132.0	2427	111.8	12.8	1.50	91.6	43.5[2]	3238	A-V
		± 27.4	± 637	± 11.1	± 3.0	± 0.3	± 16.2	± 7.0	± 259	BLOCK

Means ± s.e.mean shown; [1]$P<0.05$; [2]$P<0.01$; [3]$P<0.001$; Student's paired t test with respect to pre-drug controls. Abbreviations as in Table 1).

significantly until dose levels greater than 0.2 mg kg^{-1}, i.v. were achieved. These changes were most likely an indication of activation of sympathetic reflexes in response to the direct vasodilator effect of nitrendipine (as evidenced by decreased systemic vascular resistance), though no experimental steps were adopted to confirm this conjecture. At doses greater than 0.2 mg kg^{-1}, i.v., the depressant properties of nitrendipine became evident, and contractile function and cardiac output decreased. Above this dose, nitrendipine had most pronounced effects on atrioventricular conduction at intrinsic heart rates but because of the considerable variation in magnitude between experiments these effects did not reach statistical significance: depression of conduction prevented conduction during atrial pacing.

During atrial pacing at 180 beats min^{-1}, atrio-ventricular conduction interval showed significant dose-related changes after either ZD7288 or zatebradine, although neither compound had significant effects at intrinsic heart rates. The exact nature of these effects on atrio-ventricular conduction seen with these compounds are not yet clear, and further experimental investigations will be needed to elucidate the mechanisms concerned.

In summary, ZD7288 appears to have direct effects on heart rate in pentobarbitone anaesthetized dogs, similar in all respects to those seen with zatebradine. Concomitant haemodynamic effects appear to be direct consequences of lowering heart rate by atrial pacing. The profile of action of ZD7288, being devoid of direct contractile influences, sug-

gests that ZD7288 may be of benefit in the treatment of ischaemic heart disease, particularly in instances where myocardial dysfunction would preclude the use of β-adrenoceptor antagonists.

Haemodynamic effects in the absence of anaesthesia, when autonomic reflexes are fully active, have been studied in conscious dogs trained to run on a motor-driven treadmill, and are described in the following paper (Rouse *et al.*, 1994).

References

BAIKER, E., VON CZAKO, E., KECK, M. & NEHMIZ, G. (1991). Efficacy and duration of action of three doses of Zatebradine (ULFS 49 CL) in patients with chronic angina pectoris compared to placebo. In *Sinus Node Inhibitors: a New Concept in Angina Pectoris*. ed. Hjalmarson, Å. & Remme, W. pp. 55–63. Darmstadt: Steinkopff; New York: Springer.

BOSMITH, R.E., BRIGGS, I. & STURGESS, N.C. (1993). Inhibitory actions of ZENECA ZD7288 on whole-cell hyperpolarization activated inward current (I_f) in guinea pig dissociated sinoatrial node cells. *Br. J. Pharmacol.*, **110**, 343–349.

FALOTICO, R., HAERTLEIN, B.J., LAKAS-WEISS, C.S., SALATA, J.J. & TOBIA, A.J. (1989). Positive inotropic and haemodynamic properties of flosequinan, a new vasodilator, and a sulphone metabolite. *J. Cardiovasc. Pharmacol.*, **14**, 412–418.

FURNIVAL, C.M., LINDEN, R.J. & SNOW, H.M. (1970). Inotropic changes in the left ventricle: the effect of changes in heart rate, aortic pressure and end diastolic pressure. *J. Physiol.*, **214**, 15–28.

GROSS, G.J. & DÄMMGEN, J.W. (1987). Effects of bradycardic agents on ischaemic myocardium and perfusion in anaesthetized dogs. *Eur. Ht. J.*, **8**, (Suppl. L), 69–74.

HARGREAVES, R.B., MILLS, S.D., MCLOUGHLIN, B.J. & MARSHALL, P.W. (1992). ICI D7288, a novel sino-atrial node modulator: synthesis and pharmacological activity. *23rd National Medicinal Chemistry Symposium, American Chemical Society*. Buffalo, June 1992: abstract 21.

JOHNSTON, W.E., VINTEN-JOHANSEN, J., TOMMASI, E. & LITTLE, W.C. (1991). ULFS-49 causes bradycardia without decreasing right ventricular systolic and diastolic performance. *J. Cardiovasc. Pharmacol.*, **18**, 528–534.

KOBINGER, W. & LILLIE, C. (1984). Cardiovascular characterization of UL-FS 49, 1,3,4,5,-tetrahydro-7,8-dimethoxy-3-[3-[[2-(3,4-dimethoxyphenyl)ethyl]methylimino]propyl]-2H-3-benzazepine-2-on hydrochloride, a new 'Specific Bradycardic Agent'. *Eur. J. Pharmacol.*, **104**, 9–18.

KOBINGER, W. & LILLIE, C. (1987). Specific bradycardic agents – a novel pharmacological class? *Eur. Heart Journal*, **8**, (Suppl. L), 7–15.

LILLIE, C. (1991). ULFS 49 CL, a prototype of a novel pharmacological concept. In *Sinus Node Inhibitors: a New Concept in Angina Pectoris*. ed Hjalmarson, Å. & Remme, W. pp. 9–21. Darmstadt; Steinkopff; New York: Springer.

MARSHALL, P.W., ROUSE, W., BRIGGS, I., HARGREAVES, R.B., MILLS, S.D. & MCLOUGHLIN, B.J. (1993). ICI D7288, a novel sinoatrial node modulator. *J. Cardiovasc. Phamacol.*, **21**, 902–906.

RABERGER, G., KRUMPL, G., SCHNEIDER, W. & MAYER, N. (1987a). Effects of specific bradycardic agents on exercise-induced regional myocardial dysfunction in dogs. *Eur. Heart. J.*, **8** (Suppl L), 53–59.

RABERGER, G., KRUMPL, G. & SCHNEIDER, W. (1987b). Effects of specific bradycardic agents on exercise-induced regional myocardial dysfunction in dogs. *Int. J. Cardiol.*, **14**, 343–354.

ROUSE, W. & JOHNSON, I.R. (1992). Haemodynamic actions of ICI D7288, a novel sino-atrial node modulator. *Br. J. Pharmacol.*, **107**, 383P.

ROUSE, W., STAFFORD, P.J. & JOHNSON, I.R. (1994). The haemodynamic actions of ZENECA ZD7288, a novel sino-atrial function modulator, in the exercising beagle: a comparison with zatebradine and propranolol. *Br. J. Pharmacol.*, (accompanying paper 94-128 -to be published in same issue).

VAN WOERKENS, L.J., VAN DER GIESSEN, W.J. & VERDOUW, P.D. (1992). The selective bradycardic effects of zatebradine (UL-FS 49) do not adversely affect left ventricular function in conscious pigs with chronic coronary artery occlusion. *Cardiovasc. Drugs Therapy*, **6**, 59–65.

(Received January 31, 1994
Revised June 12, 1994
Accepted July 22, 1994)

Br. J. Pharmacol. (1994), **113**, 1071–1077 © Macmillan Press Ltd, 1994

The haemodynamic actions of ZENECA ZD7288, a novel sino-atrial node function modulator, in the exercising beagle: a comparison with zatebradine and propranolol

[1]W. Rouse, P.J. Stafford & I.R. Johnson

Vascular Inflammatory and Musculoskeletal Research Department, ZENECA Pharmaceuticals, Alderley Park, Macclesfield, Cheshire SK10 4TG

1 ZENECA ZD7288 (4-(*N*-ethyl-*N*-phenylamino)-1,2-dimethyl-6-(methylamino) pyrimidinium chloride, formerly ICI D7288) is a novel sino-atrial node function modulator which selectively slows heart rate.

2 The haemodynamic effects of ZD7288 (0.1, 0.3 and 1.0 mg kg^{-1}, i.v.) have been evaluated and compared with those of placebo (physiological saline), zatebradine (ULFS 49, 0.1, 0.3 and 1.0 mg kg^{-1}, i.v.) and propanolol (0.03, 0.1, and 0.3 mg kg^{-1}, i.v.) in beagles chronically instrumented for measurement of heart rate, aortic pressure, aortic flow and dP_{LV}/dt_{max}. The dogs were trained to run at 6.5 k h^{-1} on a level treadmill for 5 min at half hourly intervals over a period of 4 h. Drugs were dosed cumulatively after the second, fourth and sixth exercise periods.

3 Control experiments demonstrated a degree of accommodation to repeated exercise over a period of 4 h. Resting heart rate decreased by 21 beats min^{-1}, but heart rate response to exercise was maintained, whereas dP_{LV}/dt_{max} at rest remained steady while the response to exercise decreased significantly (by 25% after 2 h, $P<0.05$).

4 ZD7288 and zatebradine both decreased heart rate during exercise in a dose-dependent manner, whilst heart rate at rest did not differ from resting heart rates in saline dosed control animals. In contrast, heart rate at rest and during exercise were lowered equally by the lowest doses of propranolol (approximately by 30 beats min^{-1}), and additional doses caused only minor additional decreases. The exercise-induced tachycardia was maintained within 12% of pre-dose levels, presumably by withdrawal of vagal tone.

5 Cardiac inotropism, as indicated by dP_{LV}/dt_{max}, was not affected by ZD7288 or zatebradine at rest, although the inotropic response to exercise decreased in proportion to the decreases in exercise-induced tachycardia. Propranolol caused a marked dose-dependent decrease in the exercise-induced inotropic response (by 85% at 0.3 mg kg^{-1}).

6 Whilst the sino-atrial node modulators increased stroke volume at rest, and augmented increases in response to exercise, propranolol did not affect resting stroke volume and decreased the responses to exercise.

7 Cardiac output at rest and cardiac output increases during exercise were well maintained in the presence of ZD7288 and zatebradine in contrast to propranolol which induced a significant depression of cardiac output, both at rest and during exercise. Propranolol also caused significant systemic vasoconstriction.

8 In conclusion, ZD7288 has haemodynamic actions comparable to those of zatebradine despite their chemical dissimilarity. ZD7288 may be of benefit in the treatment of ischaemic heart disease by reducing heart rate without impairing cardiac function.

Keywords: Sino-atrial node; selective bradycardic agent; heart rate; exercise; haemodynamics; ZD7288; zatebradine; propranolol

Introduction

β-Adrenoceptor antagonists, first introduced with the expressed purpose of reducing the increases in myocardial oxygen consumption consequent upon sympathetically mediated reflex responses to the demands of physical exercise or emotional stress (Shanks, 1966) in myocardial ischaemia, can, as a consequence of their mode of action, interfere with inotropic support of compromised myocardium in the instance of myocardial dysfunction. Calcium channel blockers aimed at influencing myocardial blood flow and peripheral resistance in the treatment of ischaemic heart disease, can also influence contractile function in an adverse fashion.

The so-called 'specific bradycardic agents' have been developed in recent years as an alternative approach to combating the effects of myocardial ischaemia. By selectively influencing sino-atrial pacemaker diastolic depolarization rate, these compounds lower heart rate, reducing myocardial oxygen demand whilst improving endocardial blood supply (Gross & Dämmgen, 1987) by prolonging diastolic coronary perfusion interval. They cause little depression of contractile function or interference with sympathetic nervous control (Lillie, 1991).

Recently, the novel sino-atrial node function modulator, ZENECA ZD7288 (Hargreaves *et al.*, 1992), with potential usefulness in the treatment of *angina pectoris*, has been described, along with its actions in a variety of biological preparations (Rouse & Johnson, 1992; Marshall *et al.*, 1993; BoSmith *et al.*, 1993). An account of the haemodynamic effects of ZD7288 in anaesthetized dogs is described in detail in the preceding paper (Rouse & Johnson, 1994) in this issue.

[1] Author for correspondence.

Raberger *et al.* (1987) and Guth *et al.* (1987) have each modelled exercise-induced regional contractile dysfunction in dogs trained to run on a treadmill, thus mimicking the main features of exercise-induced *angina pectoris* as seen in man. They demonstrated that heart rate reduction by zatebradine was of distinct benefit in their models.

Since it seems reasonable to suppose that the demonstration of heart rate reduction alone, both at rest and during exercise, even in the absence of myocardial dysfunction, would be indicative of comparable benefits, the actions of ZD7288 on haemodynamics were investigated at rest and during treadmill exercise in conscious beagle dogs without coronary flow restrictions. In this paper, the actions of ZD7288 are compared with those of zatebradine, and the β-adrenoceptor antagonist, propranolol.

Methods

Beagles of the Alderley Park strain were selected for their ability to run at 6.5 km h^{-1} on a treadmill (Cambridge model XT 1000). After completion of treadmill training, transducers were implanted in selected animals for measurement of haemodynamic responses to exercise.

Premedication consisted of acepromazine maleate 30 μg kg^{-1} with Temgesic 10 μg kg^{-1}. Anaesthesia was induced with propofol (Diprivan), 8 to 10 ml (1% w/v) given into a foreleg vein. The trachea was intubated with a cuffed endotracheal tube. The neck region and thorax were clipped and sites of incision were shaved and swabbed liberally with cetrimide in 70% alcohol:water solution. Maintenance anaesthesia was a mixture of 'Fluothane' (halothane) 1.5% approximately, and nitrous oxide (4 l min^{-1}) with a supplement of oxygen (3 to 4 l min^{-1}). Using full aseptic precautions, the right scalenius muscle was resected rostrally, and a right fourth intercostal thoracotomy was performed. The sensors to be implanted, which had been sterilized by immersion in 10% cetrimide in 70% alcohol:water solution for 1 h, were then inserted into the thoracic cavity *via* a separate small incision behind the scalenius muscle through the second intercostal space, and the pericardium was opened.

The sensors implanted were as follows: a Königsberg P7 pressure transducer inserted into the left ventricular cavity via the apical dimple and secured with a purse string suture, a 'Skalar' electromagnetic flow probe positioned around the aortic root after careful resection of the aortic fat pad and a tripolar silver recording electrode (including 'earth'), over the interventricular sulcus.

During positioning of sensors, it was important that signals were monitored to ensure correct positioning and function of the transducers.

The cut edges of the pericardium were juxtaposed with a single suture, and the thoracotomy was closed by approximating the ribs with three Dacron sutures. The intercostal muscles were carefully sutured together to seal the incision. The scalenus muscle was carefully re-positioned, sealing the exit of the transducer leads. The latter were tunnelled subcutaneously out through a small incision over the right shoulder. The terminating 'neck button' connectors were tunnelled from there to circular, tight fitting exit incisions in the dorsal surface of the neck.

All incisions were closed in layers. Animals were allowed to recover with analgesic and antibiotic cover under the care of qualified veterinarians for at least two weeks, until sinus arrythmia, which is normally observed in healthy dogs at rest, was again in evidence, thereby indicating that alterations in autonomic balance in response to surgery were restored to normal.

Ten days after thoracotomy, under halothane anaesthesia with intravenous propofol induction, two 1mm internal diameter polyethylene catheters were implanted, one via the right jugular vein to the level of the right atrium for drug administration, and the other into the aortic root via the right carotid artery for measurement of blood pressure. These catheters were exteriorized on the dorsal surface of the neck. They were flushed regularly with sterile heparinized physiological saline to prevent blockage.

Measurements

Dogs were connected to recording equipment by extended leads carried by a counter-balanced arm pivoted on the back of the treadmill, and attached at the free end to an ordinary dog collar worn by the experimental subject, so that the animal had complete freedom of movement within the confines of the treadmill. Aortic pressure was measured with a Statham Spectramed P10EZ transducer attached at shoulder level to the dog collar.

Employing a purpose-built analogue computing system clocked from the ventricular epicardiogram, voltages indicative of heart rate, rate of increase of left ventricular pressure during the isovolumic period of contraction (dP_{LV}/dt_{max}), systolic, true mean and diastolic aortic pressure were derived on a beat by beat basis. In addition, aortic flow velocity was integrated with respect to time as an index of

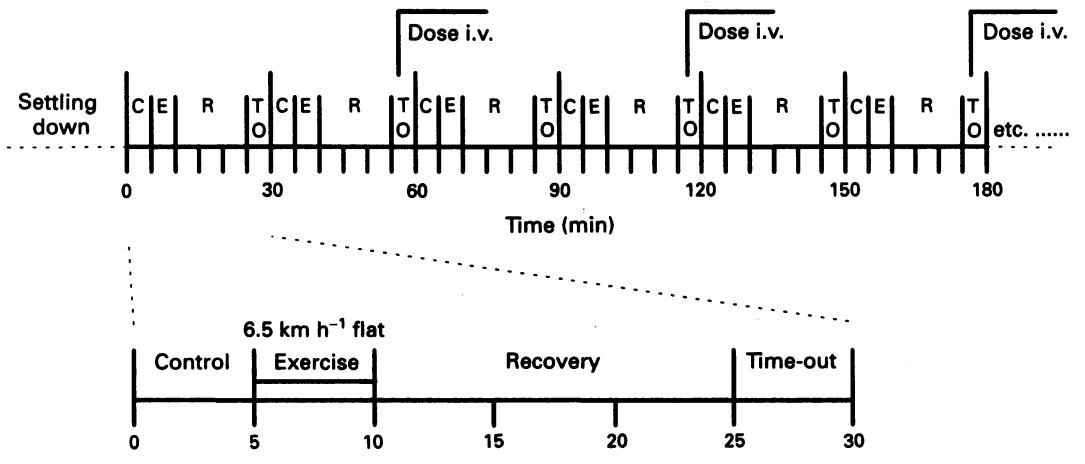


Figure 1 The upper part of the figure denotes the experimental protocol consisting of eight successive 30 min duration exercise runs following an acclimatization interval during which the dog was allowed to settle down. Each period comprised data collection during 5 min at rest, during 5 min of level running at 6.5 km h^{-1}, then during 15 min recovery. A 5 min interval was allowed between runs for catheter flushing, rearrangements of leads and drug administration. Drugs were given after pairs of exercise runs, the results from which were meaned.

stroke volume (ignoring coronary reverse flow). During each cardiac cycle, the integrator operated in two modes, sampling filtered diastolic flow as the initial set-point while developed left ventricular pressure was less than a pre-set level (approximately 50 mmHg), and integrating when left ventricular pressure was in excess of that level. Thus, a voltage indicative of stroke volume with compensation for any drift in input flow level was also derived on a beat-by-beat basis.

The analogue voltages were digitized by a Tandon PC equipped with an 8-channel analogue-to-digital converter board. Using purpose-written software, values sampled each minute (as clocked by the computer) were logged to hard disc as minute-meaned values together with cardiac output and systemic mean vascular resistance calculated from sampled values of stroke volume, heart rate and blood pressure. In addition, sampled data were displayed graphically on-screen to monitor progress of the experiment.

A paper chart recording of analogue aortic and left ventricular pressure, aortic flow velocity and stroke volume, together with beat-by-beat heart rate, was make on a 'Graftek' WR3502 heated stylus recorder equipped with alpha-numeric printers. Using the latter, minute-mean values of variables, including calculated cardiac output and systemic vascular resistance, were printed to the recording chart by the computer each minute.

Lotus 'Symphony' spreadsheet software was used subsequently for data manipulation and analysis.

Protocol

Drug effects were studied under the protocol illustrated by Figure 1. Each 30 min exercise period consisted of a 5 min control interval at rest followed by 5 min running at 6.5 km h^{-1} with a 20 min recovery interval. A between-exercise

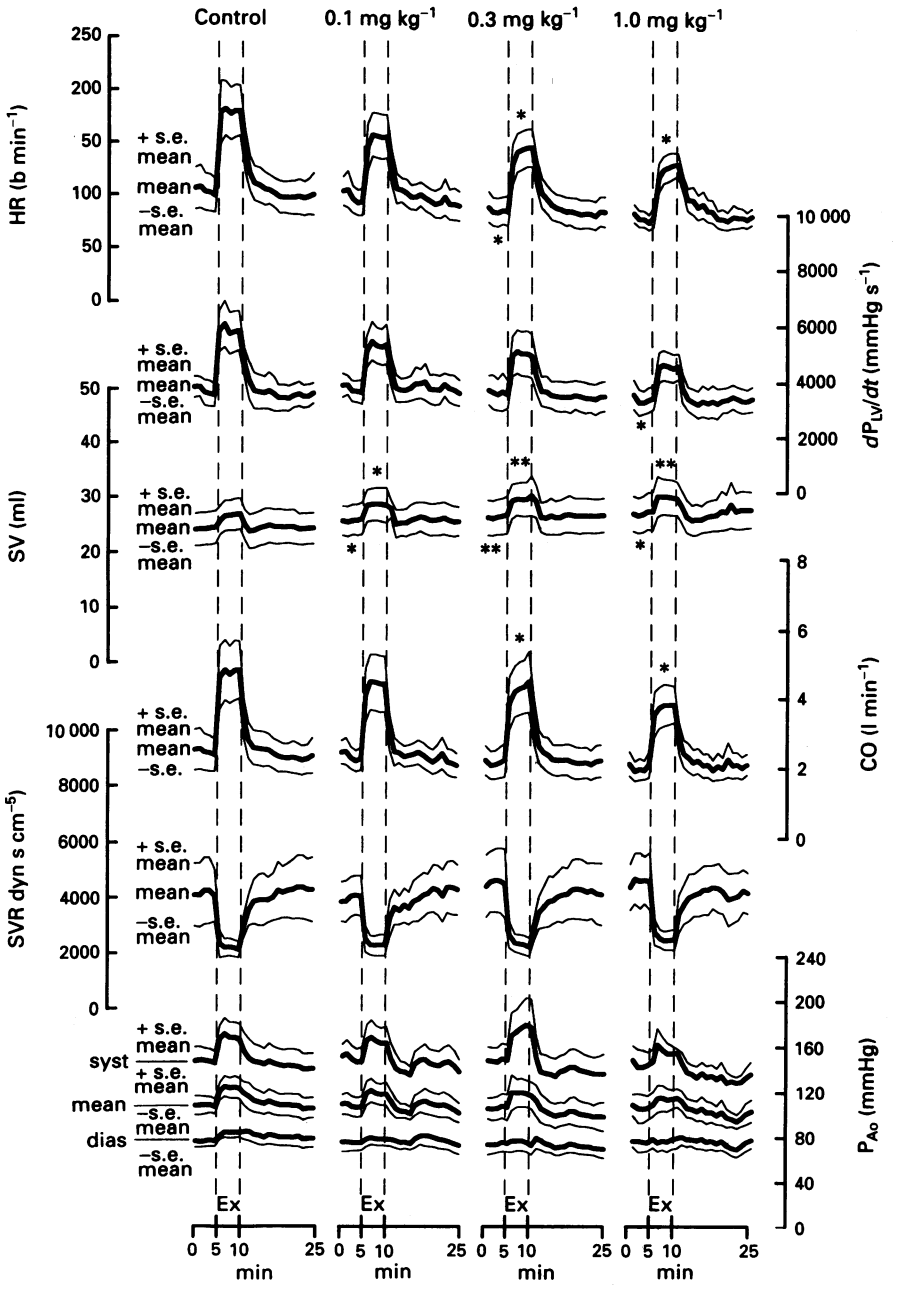


Figure 2 Effects of cumulative doses of ZD7288 on haemodynamic responses to treadmill exercise in dogs (n = 4). Mean changes in heart rate, contractile function (dP_{LV}/dt_{max}), stroke volume (SV), cardiac output (CO), calculated systemic vascular resistance (SVR) and aortic blood pressure (PAo) from four dogs, together with s.e.means are shown. Each response is the mean of paired successive periods of exercise on the level at 6.5 km h^{-1}. ZD7288 caused a decrease of exercise heart rate with concomitant decrease of cardiac output. Stroke volume increased both at rest and during exercise (Ex). (Differences from respective pre-dose control values: $^{*}P<0.05$, $^{**}P<0.01$ by Student's paired t test).

interval of 5 min, during which recording was suspended, was allowed for flushing of catheters, repositioning of recording leads if required, and for drug administration, when due.

An experiment consisted of 8 exercise runs over a period of 4 h. The drug under study was administered intravenously between each pair of exercise runs, so that three cumulative doses of drug were studied in each experiment. Results from pairs of exercise runs between drug doses were meaned.

Doses

Cumulative doses were dissolved in sterile physiological saline solution and given intravenously as follows: ZD7288 and zatebradine, 0.1, 0.3 and 1.0 mg kg^{-1}; and propranolol, 0.03, 0.1 and 0.3 mg kg^{-1}. In control experiments, sterile physiological saline was given as placebo at the appropriate intervals.

Ideally, all experiments would have been performed in the same four animal. However, this study involved six animals (mean weight 14.5 kg, range 13.3–16 kg), since the results described here were taken from a wider study involving other drugs, the results of which will not be described here.

Statistics

Statistical comparisons were made with Student's two-tailed paired t tests on absolute measurements in all instances.

Results

Control experiments demonstrated a degree of accommodation to repeated exercise over four hours, and heart rate, dP_{LV}/dt_{max} and cardiac output tended to decrease with time, although only changes in dP_{LV}/dt_{max} during exercise were statistically significant. Aortic pressure, cardiac output and calculated systemic vascular resistance, both at rest and during exercise, did not show any significant changes with time. It was considered that the response to repeated exercise was sufficiently reproducible to allow the study of the effects of drugs on the haemodynamic changes induced by exercise in this model.

Table 1 summarises the mean absolute values of results from all experiments, whilst Figure 2 illustrates the results obtained with ZD7288.

ZD7288 in the dose range 0.1 to 1.0 mg kg^{-1} caused a dose-related reduction of heart rate during exercise. The effects were statistically significant at the two higher doses. There was also a trend for heart rate at rest to be reduced, significant ($P<0.05$) only at 0.3 mg kg^{-1}, but similar in magnitude to that seen in the placebo experiments. The inotropic response during exercise was essentially unaffected by ZD7288 at any dose level, though resting dP_{LV}/dt_{max} before the top dose was significantly reduced ($P<0.05$). Effects were comparable to those seen in the placebo experiments. Stroke volume (SV), both at rest and during exercise, was

Table 1 Comparison of the haemodynamic effects of ZD7288, zatebradine and propranolol in beagles at rest and during level exercise at 6.5 km h^{-1}; responses during control experiments with the same time course are also shown

Dose (mg kg^{-1}, i.v.)		*HR* (min^{-1})	dP_{LV}/dt (mmHg s^{-1})	P_{Ao} *mean* (mmHg)	*SV* (ml)	*CO* (l min^{-1})	*SVR* (dyn s cm-5)
Controls (saline)							
hour 1	Rest	103.8 ± 7.7	3453 ± 433	99.2 ± 3.9	22.6 ± 4.8	2.39 ± 0.57	3802 ± 800
	Exercise	**204.7 ± 9.3**	**6743 ± 873**	**118.7 ± 3.3**	**24.0 ± 5.1**	**4.89 ± 1.18**	**2202 ± 482**
hour 2	Rest	89.9 ± 8.9	3147 ± 337	101.4 ± 7.6	23.1 ± 5.2	2.20 ± 0.67	4342 ± 776
	Exercise	**195.9 ± 12.2**	**6046 ± 902**	**119.4 ± 3.0**	**24.3 ± 5.0**	**4.88 ± 1.23**	**2196 ± 431**
hour 3	Rest	87.6 ± 10.5	3146 ± 371	92.8 ± 3.4	23.7 ± 5.4	2.24 ± 0.73	4172 ± 963
	Exercise	**191.3 ± 13.4**	**5831 ± 885[1]**	**113.7 ± 3.1**	**24.3 ± 5.1**	**4.82 ± 1.27**	**2145 ± 432**
hour 4	Rest	82.1 ± 5.8	3139 ± 330	93.4 ± 2.6	23.6 ± 5.2	2.06 ± 0.51	4201 ± 822
	Exercise	**187.4 ± 12.1**	**5605 ± 691[1]**	**112.4 ± 2.9**	**24.3 ± 5.2**	**4.74 ± 1.24**	**2127 ± 398**
ZD7288							
Control	Rest	103.6 ± 18.1	3702 ± 405	109.7 ± 7.6	24.0 ± 3.0	2.49 ± 0.54	4161 ± 1142
	Exercise	**179.7 ± 24.5**	**5888 ± 739**	**125.3 ± 9.2**	**26.5 ± 2.8**	**4.82 ± 0.85**	**2177 ± 303**
0.1	Rest	97.5 ± 13.5	3758 ± 399	109.3 ± 8.7	25.5 ± 2.8[1]	2.35 ± 0.33	3984 ± 727
	Exercise	**155.4 ± 21.1**	**5359 ± 666**	**120.4 ± 9.9**	**28.3 ± 3.0[1]**	**4.48 ± 0.81**	**2274 ± 357**
0.3	Rest	84.3 ± 13.3[1]	3623 ± 586	107.4 ± 10.3	26.1 ± 3.3[2]	2.17 ± 0.43	4554 ± 1155
	Exercise	**142.3 ± 18.4[1]**	**5034 ± 789**	**120.0 ± 12.3**	**29.4 ± 3.2[2]**	**4.63 ± 0.79**	**2301 ± 326[1]**
1	Rest	77.1 ± 8.1	3366 ± 458[1]	108.3 ± 11.0	26.7 ± 3.3[1]	2.02 ± 0.32	4589 ± 917
	Exercise	**125.4 ± 12.5[1]**	**4557 ± 504**	**115.4 ± 9.4**	**29.6 ± 3.2[2]**	**3.83 ± 0.58**	**2480 ± 338[1]**
Zatebradine							
Control	Rest	94.5 ± 12.2	3578 ± 484	98.0 ± 5.8	22.8 ± 3.9	2.25 ± 0.62	4228 ± 1108
	Exercise	**178.6 ± 18.9**	**5747 ± 862**	**117.5 ± 6.2**	**25.0 ± 3.7**	**4.51 ± 0.96**	**2200 ± 441**
0.1	Rest	91.3 ± 13.3	3690 ± 576	97.8 ± 5.9	23.5 ± 3.8	2.21 ± 0.59	4419 ± 1184
	Exercise	**164.6 ± 16.9[2]**	**5431 ± 1005**	**115.4 ± 4.4**	**26.0 ± 3.6**	**24.3 ± 0.89**	**2280 ± 468**
0.3	Rest	78.4 ± 12.1[1]	3533 ± 551	84.9 ± 1.4	24.6 ± 4.0	2.02 ± 0.65	5366 ± 2362
	Exercise	**141.8 ± 12.8[1]**	**4989 ± 761**	**102.5 ± 4.6**	**27.4 ± 3.8**	**4.04 ± 0.89**	**2302 ± 650**
1	Rest	67.2 ± 1.8	3616 ± 435	81.7 ± 3.2	25.9 ± 4.2[1]	1.66 ± 0.35	4913 ± 1594
	Exercise	**120.1 ± 6.4[1]**	**4701 ± 604**	**94.1 ± 5.6**	**28.2 ± 3.9[1]**	**3.44 ± 0.61**	**2367 ± 604**
Propanolol							
Control	Rest	92.6 ± 8.0	3830 ± 654	98.4 ± 5.6	25.4 ± 4.4	2.40 ± 0.48	3635 ± 769
	Exercise	**167.3 ± 13.8**	**5950 ± 843**	**113.6 ± 5.1**	**28.1 ± 3.9**	**4.88 ± 0.85**	**1886 ± 297**
0.03	Rest	68.8 ± 6.4	3334 ± 429	96.5 ± 6.3	26.3 ± 3.9	1.93 ± 0.46	4631 ± 981
	Exercise	**142.7 ± 13.6[1]**	**4185 ± 549[1]**	**117.3 ± 6.1**	**27.8 ± 3.8**	**4.18 ± 0.74[1]**	**2307 ± 330[2]**
0.1	Rest	64.0 ± 4.0[2]	3093 ± 409	98.4 ± 4.6	25.4 ± 3.9	1.69 ± 0.35[1]	5271 ± 1197
	Exercise	**134.5 ± 10.0[1]**	**3536 ± 438[1]**	**117.0 ± 3.6**	**26.6 ± 3.8**	**3.77 ± 0.66[1]**	**2567 ± 407[2]**
0.3	Rest	60.3 ± 1.9[1]	2958 ± 405	97.3 ± 4.0	25.4 ± 3.8	1.56 ± 0.28[1]	5377 ± 960[1]
	Exercise	**126.7 ± 11.2[1]**	**3273 ± 347[1]**	**111.7 ± 6.9**	**26.7 ± 3.7**	**3.59 ± 0.64[2]**	**2538 ± 361[2]**

Means and s.e.mean: $n = 4$ for all groups: [1]$P<0.05$, [2]$P<0.01$ by Student's paired t test versus respective initial control.

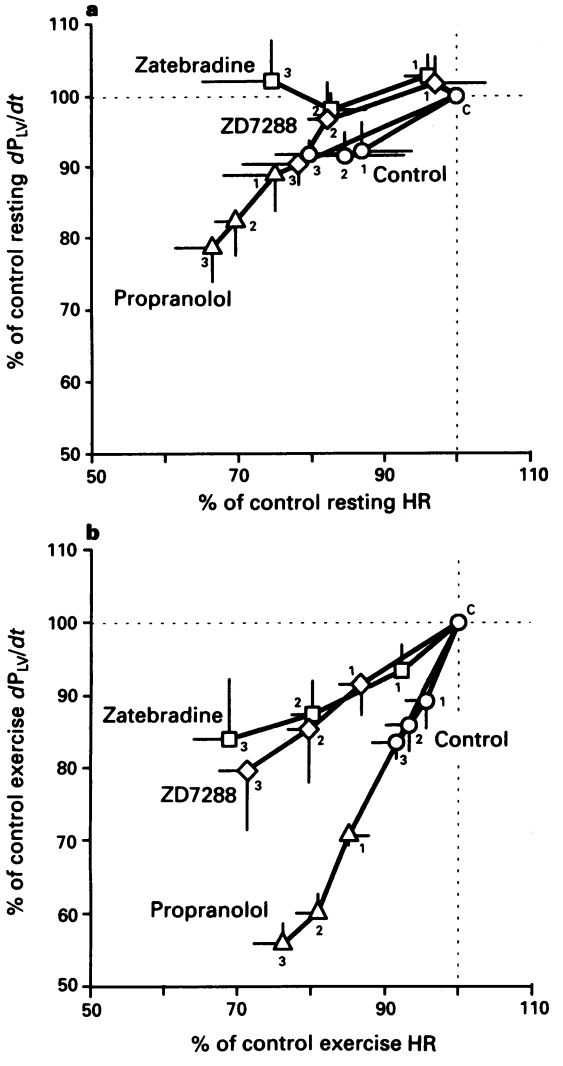


Figure 3 (a) The relationship between heart rate (HR) and contractile function (dP_{LV}/dt_{max}) at rest, each normalized with respect to initial control values, was similar whether animals were treated with saline in control experiments (○), or cumulative doses of ZD7288 (◇), zatebradine (□), each at 0.1, 0.3 and 1.0 mg kg^{-1} i.v., or propranolol (△) 0.03, 0.1 and 0.3 mg kg^{-1}i.v. (n = 4, means and s.e.mean at each dose). The effects of saline may be taken to represent changes with the progress of time common to all experiments both in this figure and in Figure 4. Points on trend lines are labelled in ascending dose order; C represents pre-drug controls. (b) During level treadmill exercise level at 6.5 km h^{-1}, the relationship between heart rate and contractile function normalized with respect to initial control exercise values clearly differentiate between the effects of propranolol, which prevents sympathetically mediated inotropic support of the myocardium, and sino-atrial node function modulators ZD7288 and zatebradine, which selectively reduce heart rate.

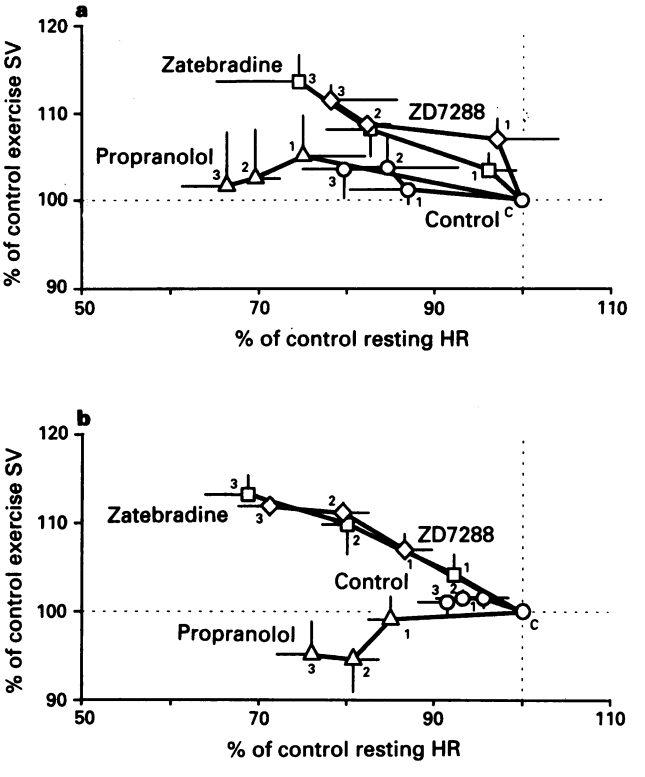


Figure 4 (a) The relationship between heart rate (HR) and stroke volume (SV) at rest (normalized with respect to initial resting levels) in control (○) and propranolol-dosed (△) animals shows little change of stroke volume as heart rate declines, but under the influence of ZD7288 (◇) or zatebradine (□), the relationship shows a more marked increase in stroke volume with less slowing of rate. (b) Propranolol decreased stroke volume response during exercise as heart rate decreased, whereas ZD7288 and zatebradine allowed stroke volume to increase as heart rate during exercise was lowered. (Cumulative drug doses as in Figure 3)

significantly increased (see Table 1) after all doses of ZD7288. As a consequence of this increase in stroke volume, even though there was a tendency for cardiac output to decrease, the latter was well maintained, despite the decrease in heart rate during exercise. Systemic vascular resistance at rest was unaffected by ZD7288, but the vasodilation during exercise was less at the two higher dose levels.

Zatebradine caused effects essentially similar to those seen after ZD7288: resting and exercise heart rates were reduced with no significant effects on contractile function: stroke volume increased dose-dependently both at rest and during exercise, though these changes only attained statistical significance after 1.0 mg kg^{-1} zatebradine. Cardiac output was well maintained and aortic blood pressure and systemic vascular resistance were not significantly affected.

In contrast, β-adrenoceptor antagonism by propranolol produced a different pattern of changes. Heart rate both at rest and during exercise were significantly reduced to a similar degree, so that the incremental responses to exercise remained relatively unchanged. Contractile function during exercise and the inotropic response to exercise, however, were grossly and significantly impaired at all doses studied (see Table 1). Stroke volume at rest did not change, but tended to decrease during exercise. Cardiac output was significantly reduced both at rest and during exercise. Aortic blood pressure was maintained, ostensibly as a consequence of increased systemic vascular resistance, but the dilator response to exercise increased (significantly after 0.3 mg kg^{-1}, $P<0.01$).

Because of the limited dose-response data obtained in these experiments, it is not possible to compare results directly on a dose for dose basis. However, the relative effects of the compounds studied may be illustrated as in Figures 3 and 4, which relate heart rates, normalized with respect to pre-drug control values, to corresponding contractile function and stroke volume, both at rest and during exercise. These figures clearly differentiate between the effects of blockade of sympathetic drive and the effects of ZD7288 or zatebradine.

Discussion

ZD7288 has been described as a sino-atrial node modulating agent which affects heart rate through a direct action on sino-atrial pacemaker cells (Briggs & Heapy, 1992; Marshall *et al.*, 1993; BoSmith *et al.*, 1993). A previous study in the

anaesthetized dog (Rouse & Johnson, 1992) has shown the drug to have a direct effect principally on intrinsic heart rate. Other observed haemodynamic changes (such as increases in stroke volume and systemic vascular resistance, fall in cardiac output and myocardial contractile function) were secondary and proportional to the reduction in heart rate, since they were reversed during atrial pacing. There was also dose-dependent prolongation of atrio-ventricular conduction during pacing at 180 beats per minute (an effect also seen after zatebradine and atenolol administration). The present studies have examined the effects of ZD7288 on the cardiovascular system in the conscious dog, and its effects on the haemodynamic response during exercise.

In the Alderley Park beagle, 5 min of mild exercise on a treadmill induced the expected increases of heart rate, cardiac output and left ventricular dP_{LV}/dt_{max}, whilst systemic vascular resistance was reduced overall (see Table 1). However, changes in stroke volume in response to exercise were marginal at this exercise level, increases in cardiac output being achieved predominantly as a consequence of increased heart rate. Responses to exercise were consistent over a period of 4 h, although there was a tendency for the resting haemodynamic variables to change in directions indicative of decreasing sympathetic-drive, as the animals presumably became more relaxed during the experimental procedure. This notion is consistent with Figures 3 and 4, in which control relationships tend to follow the trends occurring during removal of sympathetic drive by β-adrenoceptor antagonism. Although heart rate response to exercise, together with cardiac output and systemic vascular resistance during exercise remained constant, dP_{LV}/dt_{max} response to exercise declined.

The principal effect of ZD7288 on such exercise-induced responses was to reduce heart rate during exercise, which resulted in a further increase of stroke volume (see Figure 4). These effects mirrored those reported in the anaesthetized dog (Rouse & Johnson, 1994). As the tachycardic response to exercise was further reduced (by over 30%), so the increases of cardiac output and the vasodilator responses (falls in systemic vascular resistance) were blunted. Myocardial contractile function (dP_{LV}/dt_{max}) was only significantly reduced following the highest dose, and then only at rest. As the effect was similar to that seen in control (placebo) experiments, this result is also likely to be a consequence of the animals becoming more relaxed, rather than being due to any negative inotropic effects of ZD7288. It is probable that the blunted cardiac output response and the increase of systemic vascular resistance seen following ZD7288 administration were secondary to the large reduction of exercise tachycardia following the higher doses of ZD7288. These effects, again, were not seen in the anaesthetized dog when the heart rate was held constant during atrial pacing (Rouse & Johnson, 1994).

Our results are similar to those reported by Krumpl *et al.* (1988), in their study on zatebradine. This agent has also been shown to attenuate the heart rate response to exercise in the dog, a change which was accompanied by an increase in stroke volume. Both drugs were of a similar potency in the present studies, as has been described in studies of their electrophysiological actions on isolated sino-atrial node cells (Briggs & Heapy, 1993). ZD7288, therefore, could be described as a 'selective bradycardic agent', despite being chemically dissimilar from previously described drugs of this class (Hargreaves *et al.*, 1992).

In contrast to the haemodynamic effects of ZD7288 and zatebradine, when contractile function was well maintained during exercise, β-adrenoceptor antagonism following administration of propranolol prevented the positive inotropic effects mediated by the sympathetic nervous system in response to exercise, causing an apparent marked negative inotropic effect in the exercising dog (see Figure 3). It was noticeable, in our strain of beagles, that although resting heart rate and heart rate during exercise were each significantly reduced by propranolol, the tachycardic response to exercise was diminished by only 11%: this can be adequately accounted for by withdrawal during exercise of vagally-mediated slowing of resting heart rate (sinus arrhythmia). The reduction of heart rate produced by propranolol was not associated with an increase of stroke volume, as was the case after treatment with ZD7288 (see Figure 4: relationships shown in this figure echo results from conscious pig experiments described by van Woerkens *et al.*, 1992, where 'propranolol and (zatebradine) had opposite effects on stroke volume', as shown in Figure 3 of their paper). In addition, propranolol significantly impaired the vasodilator response to exercise.

β-Adrenoceptor antagonists were originally developed for the treatment of ischaemic heart disease, based upon their ability to attenuate the increase of myocardial oxygen demand resulting from sympathetic nerve activity (Shanks, 1966). Their efficacy as anti-ischaemic agents is well proven (Vedin & Wilhelmsson, 1985), but the concomitant antagonism of increases in inotropic activity limits their use in patients with left ventricular dysfunction. An alternative approach to the treatment of ischaemic heart disease is provided by the vasodilator actions of calcium channel blockers. These agents reduce cardiac afterload, thereby reducing cardiac work, as well as affording varying degrees of coronary vasodilatation (Warltier *et al.*, 1981). However, the use of such drugs can be offset by the incidence of side-effects which are consequent upon their peripheral vasodilator activity (Julian, 1985). Recently, a new class of potential anti-ischaemic drugs, the 'specific bradycardic agents', has been described (Kobinger & Lillie, 1987). These agents attenuate heart rate increases through a selective action on the sino-atrial node (Seidl *et al.*, 1991) and, particularly the most recent agent, zatebradine, are essentially devoid of negative inotropic and vasodilator activity (Riley *et al*, 1987). Zatebradine has shown anti-anginal efficacy in a small number of clinical trials (Baiker *et al.*, 1991) and may represent the prototype of a new class of anti-anginal agents suitable for clinical use.

In summary, ZD7288 has been shown to possess a direct effect only on heart rate in the exercising dog. Other haemodynamic effects associated with the drug were considered to be secondary to the reduced heart rate. Thus, the drug shares a cardiovascular profile of activity similar to the selective bradycardic agent, zatebradine. Both drugs show significant differences in their activity from β-adrenoceptor antagonists. Being devoid of direct negative inotropic effects, ZD7288 would be expected to be of use for the treatment of ischaemic heart diseas, especially in those patients in whom β-adrenoceptor antagonists might be contra-indicated.

References

BAIKER, E., VON CZAKO, E., KECK, M. & NEHMIZ, G. (1991) Efficacy and duration of action of three doses of Zatebradine (ULFS 49 CL) in patients with chronic angina pectoris compared to placebo. In *Sinus Node Inhibitors: a New Concept in Angina Pectoris*. ed Hjalmarson, A. & Remme, W., pp. 55–63, Darmstadt, Steinkopff, New York: Springer.

BOSMITH, R.E., BRIGGS, I. & STURGESS, N.C. (1993). Inhibitory actions of ZENECA ZD7288 on whole-cell hyperpolarization activated inward current (I_f) in guinea pig dissociated sinoatrial node cells. *Br. J. Pharmacol.*, **110**, 343–349.

BRIGGS, I. & HEAPY, C. (1992). Actions of ICI D7288 on sinoatrial node electrophysiology: action potentials. *Br. J. Pharmacol.*, **107**, 382P.

GROSS, G.J. & DÄMMGEN, J.W. (1987). Effects of bradycardic agents on ischaemic myocardium and perfusion in anaesthetized dogs. *Eur. Heart J.*, **8**, (Suppl. L), 69–74.

GUTH, B.D., HEUSCH, G., SEITELBERGER, R., MATSUZAKI, M. & ROSS, J. Jr. (1987). Role of heart rate reduction in the treatment of exercise-induced myocardia ischaemia. *Eur. Heart J.*, **8**, (Suppl. L), 61–68.

HARGREAVES, R.B., MILLS, S.D., MCLOUGHLIN, B.J. & MARSHALL, P.W. (1992). ICI D7288, a novel sino-atrial node modulator: synthesis and pharmacological activity. *23rd National Medicinal Chemistry Symposium, American Chemical Society*. Buffalo, June 1992: abstract 21.

JULIAN, D.G. (1985). Comparisons and combinations in antianginal therapy. *Eur. Heart J.*, **6**, (Suppl. A), 37–45.

KOBINGER, W. & LILLIE, C. (1987). Specific bradycardic agents – a novel pharmacological class? *Eur. Heart J.*, **8**, (Suppl. L), 7–15.

KRUMPL, G., WINKLER, M., SCHNEIDER, W., & RABERGER, G. (1988). Comparison of the haemodynamic effects of the selective bradycardic agent UL-FS 49, with those of propranolol during treadmill exercise in dogs. *Br. J. Pharmacol.*, **94**, 55–64.

LILLIE, C. (1991). ULFS 49 CL, a prototype of a novel pharmacological concept. In *Sinus Node Inhibitors: a New Concept in Angina Pectoris*, ed. HJALMARSON, Å. & REMME, W., pp 9–21, Darmstadt, Steinkopff, New York: Springer.

MARSHALL, P.W., ROUSE, W., BRIGGS, I., HARGREAVES, R.B., MILLS, S.D. & MCLOUGHLIN B.J. (1993). ICI D7288, a novel sinoatrial modulator. *J. Cardiovas. Pharmacol.*, **21**, 902–906.

RABERGER, G., KRUMPL, G. & SCHNEIDER, W. (1987). Effects of specific bradycardic agents on exercise-induced regional myocardial dysfunction in dogs. *Int. J. Cardiol.*, **14**, 343–354.

RILEY, D.C., GROSS, G.J. KAMPINE, J.P. & WARLTIER, D.C. (1987). Specific bradycardic agents, a new therapeutic modality for anaesthesiology: haemodynamic effects of UL-FS 49 and propranolol in conscious and isofluorane-anaesthetized dogs. *Anaesthesiology*, **67**, 707–716.

ROUSE, W. & JOHNSON, I.R. (1992). Haemodynamic actions of ICI D7288, a novel sino-atrial node modulator. *Br. J. Pharmacol.*, **107**, 383P.

ROUSE, W. & JOHNSON, I.R. (1994). Haemodynamic action of a novel sino-atrial node function modulator, ZENECA ZD7288 in the anaesthetized dog: a comparison with zatebradine, atenolol and nitrendipine. *Br. J. Pharmacol.*,

SEIDL, K. HAUER, B., LENGFELDER, W. & SENGES, J. (1991). Electrophysiological effects of ULFS 49 CL. In *Sinus Node Inhibitors: a New Concept in Angina Pectoris*. ed. HJALMARSON, Å. & REMME, W., pp. 37–44, Darmstadt, Steinkopff, New York: Springer.

SHANKS R.G. (1966). The pharmacology of beta sympathetic blockade. *Am. J. Cardiol.*, **3**, 308–316.

VAN WOERKENS, L.J., VAN DER GIESSEN, W.J. & VERDOUW. P.D. (1992). The selective bradycardic effects of zatebradine (UL-FS 49) do not adversely affect left ventricular function in conscious pigs with chronic coronary artery occlusion. *Cardiovasc. Drugs Therapy*, **6**, 59–65.

VEDIN, A. & WILHELMSSON, C. (1985). Medical treatment of ischaemic heart disease – beta blockers. *Eur. Heart J.*, **6**, (Suppl. A) 13–27.

WARLTIER, D.C., MEILS, C.C., GROSS, G.J. & BROOKS, H.L. (1981). Blood flow in normal and acutely ischaemic myocardium after verapamil, diltiazem and nisoldipine (Bay K 5552), a new dihydropyridine calcium antagonist. *J. Pharmacol. Exp. Ther.*, **218**, 296–302.

(Received January 31, 1994
Revised June 12, 1994
Accepted July 22, 1994)

British Journal of Pharmacology

VOLUME 113 (3) NOVEMBER 1994

SPECIAL REPORTS

A.J. Sellers & M.L.J. Ashford. Activation of BK_{Ca} channels in acutely dissociated neurones from the rat ventromedial hypothalamus by NS 1619 659

S. Kim, K. Ohta, A. Hamaguchi, T. Omura, K. Tominaga, T. Yukimura, K. Miura, M. Tanaka & H. Iwao. AT_1 receptor-mediated stimulation by angiotensin II of rat aortic fibronectin gene expression *in vivo* 662

PAPERS

K. Tschaikowsky, M. Meisner, F. Schönhuber & E. Rügheimer. Induction of nitric oxide synthase activity in phagocytic cells inhibited by tricyclodecan-9-yl-xanthogenate (D609) 664

A.U. Ziganshina, C.H.V. Hoyle, L.E. Ziganshin & G. Burnstock. Effects of cyclopiazonic acid on contractility and ecto-ATPase activity in guinea-pig urinary bladder and vas deferens 669

D.M. Grassi-Kassisse, E. Antunes, P.G. Withrington & G. de Nucci. Modulation by endogenous prostanoids of the vasoconstrictor activity of endothelin-1 in the canine isolated, perfused spleen 675

P. Soediono & G. Burnstock. Contribution of ATP and nitric oxide to NANC inhibitory transmission in rat pyloric sphincter 681

B.-L. Källström, J. Sjöberg & B. Waldeck. The interaction between salmeterol and β_2-adrenoceptor agonists with higher efficacy on guinea-pig trachea and human bronchus *in vitro* 687

A. Tomlinson, I. Appleton, A.R. Moore, D.W. Gilroy, D. Willis, J.A. Mitchell & D.A. Willoughby. Cyclo-oxygenase and nitric oxide synthase isoforms in rat carrageenin-induced pleurisy 693

M.A. Oriowo. Atypical β-adrenoceptors in the rat isolated common carotid artery 699

F.L. Christofi & J.D. Wood. Electrophysiological subtypes of inhibitory P_1 purinoceptors on myenteric neurones of guinea-pig small bowel 703

A. Sagrada, G.B. Schiavi, E. Cereda & H. Ladinsky. Antagonistic properties of McNeil-A-343 at 5-HT_4 and 5-HT_3 receptors 711

H. Bouaziz, Y. Joulin, M. Safar & A. Benetos. Effects of bradykinin B_2 receptor antagonism on the hypotensive effects of ACE inhibition 717

A. Hatano, H. Takahashi, M. Tamaki, T. Komeyama, T. Koizumi & M. Takeda. Pharmacological evidence of distinct α_1-adrenoceptor subtypes mediating the contraction of human prostatic urethra and peripheral artery 723

M.D. Tricklebank, L.J. Bristow, P.H. Hutson, P.D. Leeson, M. Rowley, K. Saywell, L. Singh, F.D. Tattersall, L. Thorn & B.J. Williams. The anticonvulsant and behavioural profile of L-697,414, a partial agonist acting at the glycine modulatory site on the N-methyl-D-aspartate (NMDA) receptor complex 729

S. Greber, C. Schwarzer & G. Sperk. Neuropeptide Y inhibits potassium-stimulated glutamate release through Y_2 receptors in rat hippocampal slices *in vitro* 737

M. Patel, M.J. Sheehan & P. Strong. Failure of CGS15943A to block the hypotensive action of agonists acting at the adenosine A_3 receptor 741

E. Coëffier, D. Joseph & B.B. Vargaftig. Role of interleukin-5 in enhanced migration of eosinophils from airways of immunized guinea-pigs 749

C. Szabó, G.J. Southan, C. Thiemermann & J.R. Vane. The mechanism of the inhibitory effect of polyamines on the induction of nitric oxide synthase: role of aldehyde metabolites 757

Y.-M. Leung, C.-Y. Kwan & T.-T. Loh. Dual effects of tetrandrine on cytosolic calcium in human leukaemic HL-60 cells: intracellular calcium release and calcium entry blockade 767

P. Onali, A.J. Aasen & M.C. Olianas. Antagonism by (R)- and (S)-trihexyphenidyl of muscarinic stimulation of adenylyl cyclase in rat olfactory bulb and inhibition in striatum and heart 775

P. Kotsonis & H. Majewski. Facilitation by procaterol, a β-adrenoceptor agonist, of noradrenaline release in the pithed rat independently of angiotensin II formation 781

M.J. Neal, S.J. Paterson & J.R. Cunningham. Enhancement of retinal acetylcholine release by DAMGO: possibly a direct opioid receptor-mediated excitatory effect 789

T. Katsuragi, S. Ogawa & T. Furukawa. Contribution of intra- and extracellular Ca^{2+} to noradrenaline exocytosis induced by ouabain and monensin from guinea-pig vas deferens 795

P.D. Taylor & L. Poston. The effect of hyperglycaemia on function of rat isolated mesenteric resistance artery 801

A.K. Bahl, M.M. Dale & J.C. Foreman. The effect of non-steroidal anti-inflammatory drugs on the accumulation and release of interleukin-1-like activity by peritoneal macrophages from the mouse 809

I. von Kügelgen, L. Späth & K. Starke. Evidence for P_2-purinoceptor-mediated inhibition of noradrenaline release in rat brain cortex 815

G. McCreath, I.P. Hall & S.J. Hill. Agonist-induced desensitization of histamine H_1 receptor-mediated inositol phospholipid hydrolysis in human umbilical vein endothelial cells 823

N.B. Mercuri, A. Bonci, P. Calabresi, F. Stratta, A. Stefani & G. Bernardi. Effects of dihydropyridine calcium antagonists on rat mid-brain dopaminergic neurones 831

S.A. Daly & J.L. Waddington. The effects of clozapine on behavioural responses to the selective 'D_1-like' dopamine receptor agonist, A 68930, and to the selective 'D_2-like' agonist, RU 24213 839

J.G. Filep, M. Clozel, A. Fournier & É. Földes-Filep. Characterization of receptors mediating vascular responses to endothelin-1 in the conscious rat 845

R.J. Evans & C. Kennedy. Characterization of P_2-purinoceptors in the smooth muscle of the rat tail artery: a comparison between contractile and electrophysiological responses 853

S.C. Chung, T.V. McDonald & P. Gardner. Inhibition by SK&F 96365 of Ca^{2+} current, IL-2 production and activation in T lymphocytes **861**

V. Richard, N. Kaeffer, M. Hogie, C. Tron, T. Blanc & C. Thuillez. Role of endogenous endothelin in myocardial and coronary endothelial injury after ischaemia and reperfusion in rats: studies with bosentan, a mixed ET_A-ET_B antagonist **869**

M.M. Iravani & M.A. Zar. Presence of neuropeptide Y in the rat seminal vesicle and its effects on noradrenaline- and nerve-induced contractions **877**

S.M.C. Cunningham, S. Mihara & G.M. Lees. Y_2-receptor-mediated selective inhibition of slow, inhibitory postsynaptic potential in submucous neurones of guinea-pig caecum **883**

K. Kamei, S. Yoshida, J. Imagawa, H. Nabata & H. Kuriyama. Regional and species differences in glyburide-sensitive K^+ channels in airway smooth muscles as estimated from actions of KC 128 and levcromakalim **889**

W.-X. Shen, P. Jobling & J.P. Horn. The sensitivity of nicotinic synapses in bullfrog sympathetic ganglia to α-bungarotoxin and neuronal-bungarotoxin **898**

M. Schwanstecher, C. Schwanstecher, C. Dickel, F. Chudziak, A. Moshiri & U. Panten. Location of the sulphonylurea receptor at the cytoplasmic face of the β-cell membrane **903**

F. Squadrito, D. Altavilla, P. Canale, M.P. Ioculano, G.M. Campo, L. Ammendolia, G. Squadrito, A. Saitta, G. Calapai & A.P. Caputi. Contribution of intercellular adhesion molecule 1 (ICAM-1) to the pathogenesis of splanchnic artery occlusion shock in the rat **912**

H. El-Bizri & P.B.S. Clarke. Regulation of nicotinic receptors in rat brain following quasi-irreversible nicotinic blockade by chlorisondamine and chronic treatment with nicotine **917**

J.S. Edwards & J.M. Ritter. Effect of cytoplasmic pH on Ca^{2+}-stimulated eicosanoid biosynthesis in human platelets **926**

R.A.D. Rutherford, Y. Matsuda, M.R. Wilkins, J.M. Polak & J. Wharton. Identification of renal natriuretic peptide receptor subpopulations by use of the non-peptide antagonist, HS-142-1 **931**

S.C. Cruwys, N.E. Garrett, M.N. Perkins, D.R. Blake & B.L. Kidd. The role of bradykinin B_1 receptors in the maintenance of intra-articular plasma extravasation in chronic antigen-induced arthritis **940**

J.P. Wang, S.L. Raung, M.F. Hsu & C.C. Chen. Inhibition by gomisin C (a lignan from *Schizandra chinensis*) of the respiratory burst of rat neutrophils **945**

D. Fulton, J.C. McGiff & J. Quilley. Role of K^+ channels in the vasodilator response to bradykinin in the rat heart **954**

A. Hall, J. Stow, R. Sorensen, J.O. Dolly & D. Owen. Blockade by dendrotoxin homologues of voltage-dependent K^+ currents in cultured sensory neurones from neonatal rats **959**

A. Zazpe, I. Artaiz & J. Del Río. Role of 5-HT_3 receptors in basal and K^+-evoked dopamine release from rat olfactory tubercle and striatal slices **968**

A. Delaunois, P. Gustin, C. Dessy-Doize & M. Ansay. Modulatory effect of neuropeptide Y on acetylcholine-induced oedema and vasoconstriction in isolated perfused lungs of rabbit **973**

F. Scamps & G. Vassort. Pharmacological profile oif the ATP-mediated increase in L-type calcium current amplitude and activation of a non-specific cationic current in rat ventricular cells **982**

D.J. Browse, R.T. Mathie, I.S. Benjamin & B. Alexander. The transhepatic action of ATP on the hepatic arterial and portal venous vascular beds of the rabbit: the role of nitric oxide **987**

A.L.A. Pires, P.M.R. e Silva, C. Pasquale, H.C. Castro-Faria-Neto, P.T. Bozza, R.S.B. Cordeiro, G.A. Rae, P. Braquet, V. Lagente & M.A. Martins. Long-lasting inhibitory activity of the hetrazepinic BN 50730 on exudation and cellular alterations evoked by PAF and LPS **994**

N.J. Yard, M. Chiesi & H.A. Ball. Effect of cyclopiazonic acid, an inhibitor of sarcoplasmic reticulum Ca^{2+}-ATPase, on the frequency-dependence of the contraction-relaxation cycle of the guinea-pig isolated atrium **1001**

J.A. Mitchell, M.G. Belvisi, P. Akarasereenont, R.A. Robbins, O.-J. Kwon, J. Croxtell, P.J. Barnes & J.R. Vane. Induction of cyclo-oxygenase-2 by cytokines in human pulmonary epithelial cells: regulation by dexamethasone **1008**

U. Windscheif, V. Ralevic, H.G. Bäumert, E. Mutschler, G. Lambrecht & G. Burnstock. Vasoconstrictor and vasodilator responses to various agonists in the rat perfused mesenteric arterial bed: selective inhibition by PPADS of contractions mediated via P_{2x}-purinoceptors **1015**

E.G. Silva, E. Frediani-Neto, A.T. Ferreira, A.C.M. Paiva & T.B. Paiva. Role of Ca^{2+}-dependent K-channels in the membrane potential and contractility of aorta from spontaneously hypertensive rats **1022**

C.-C. Huang & P -W. Gean. Paired-pulse depression of the N-methyl-D-aspartate receptor-mediated synaptic potentials in the amygdala **1029**

G. Pethö, M. Jocič & P. Holzer. Role of bradykinin in the hyperaemia following acid challenge of the rat gastric mucosa **1036**

R.W. Hauck, Ch. Schulz, H.P. Emslander & M. Böhm. Pharmacological actions of the selective and non-selective β-adrenoceptor antagonists celiprolol, bisoprolol and propranolol on human bronchi **1043**

D.T. Thwaites, B.H. Hirst & N.L. Simmons. Substrate specificity of the di/tripeptide transporter in human intestinal epithelia (Caco-2): identification of substrates that undergo H^+-coupled absorption **1050**

R.G. Humphries, W. Tomlinson, A.H. Ingall, P.A. Cage & P. Leff. FPL 66096: a novel, highly potent and selective antagonist at human platelet P_{2T}-purinoceptors **1057**

W. Rouse & I.R. Johnson. Haemodynamic actions of a novel sino-atrial node function modulator, ZENECA ZD7288, in the anaesthetized dog: a comparison with zatebradine, atenolol and nitrendipine **1064**

W. Rouse, P.J. Stafford & I.R. Johnson. The haemodynamic actions of ZENECA ZD7288, a novel sino-atrial node function modulator, in the exercising beagle: a comparison with zatebradine and propranolol **1071**

BRITISH JOURNAL OF PHARMACOLOGY

The *British Journal of Pharmacology* welcomes contributions in all fields of experimental pharmacology including neuroscience, biochemical, cellular and molecular pharmacology. The Board of Editors represents a wide range of expertise and ensures that well-presented work is published as promptly as possible, consistent with maintaining the overall quality of the journal.

Edited for the British Pharmacological Society by

A.T. Birmingham
(Chairman)

R.W. Horton **W.A. Large**
(Secretaries)

Editorial Board

J.A. Angus *Melbourne, Australia*
M.L.J. Ashford *Cambridge*
G.W. Bennett *Nottingham*
W.C. Bowman *Glasgow*
N.G. Bowery *London*
Alison F. Brading *Oxford*
S.D. Brain *London*
K.D. Butler *Horsham*
M. Caulfield *London*
R. Chess-Williams *Sheffield*
M.K. Church *Southampton*
T. Cocks *Melbourne, Australia*
S.J. Coker *Liverpool*
R.A. Coleman *Ware*
Helen M. Cox *London*
A.J. Cross *London*
V. Crunelli *Cardiff*
T.C. Cunnane *Oxford*
F. Cunningham *London*
A. Dray *London*
J.R. Docherty *Dublin*
J.M. Edwardson *Cambridge*
P.C. Emson *Cambridge*
W. Feniuk *Cambridge*
J.R. Fozard *Basle, Switzerland*
Allison D. Fryer *Baltimore, USA*
Sheila M. Gardiner *Nottingham*
C.J. Garland *Bristol*
L.G. Garland *Beckenham*
A. Gibson *London*
R. W. Gristwood *Cambridge*
D.W.P. Hay *Philadelphia, USA*
P.G. Hellewell *London*
P.E. Hicks *Edinburgh*
S.J. Hill *Nottingham*
S.M.O. Hourani *Guildford*
J.C. Hunter *Cambridge*
C.C. Jordan *Ware*
D.A. Kendall *Nottingham*
P. Leff *Loughborough*
R. McMillan *Macclesfield*
J. Maclagan *London*
C.A. Maggi *Florence, Italy*
Janice M. Marshall *Birmingham*
G. Martin *Beckenham*
W. Martin *Glasgow*
A. Mathie *London*
D.N. Middlemiss *Harlow*
P.K. Moore *London*
R.J. Naylor *Bradford*
C.D. Nicholson *Oss, The Netherlands*
C.P. Page *London*
A.N. Payne *Beckenham*
F.L. Pearce *London*
J.D. Pearson *London*
A.G. Renwick *Southampton*
M.H.T. Roberts *Cardiff*
C. Robinson *London*
G.J. Sanger *Harlow*
M.A. Simmonds *London*
J.M. Sneddon *Sunderland*
P. Sneddon *Glasgow*
K. Starke *Freiburg, Germany*
R.J. Summers *Melbourne, Australia*
P.V. Taberner *Bristol*
J. Tamargo *Madrid, Spain*
C. Thiemermann *London*
M.D. Tricklebank *Harlow*
M.B. Tyers *Ware*
S.P. Watson *Oxford*
K.J. Watling *Boston, USA*
A.H. Weston *Manchester*
B.J.R. Whittle *Beckenham*
Eileen Winslow *Riom, France*
B. Woodward *Bath*
E.H.F. Wong *California, USA*

Corresponding Editors

P.R. Adams *Stony Brook, U.S.A.*
C. Bell *Melbourne, Australia*
F.E. Bloom *La Jolla, U.S.A.*
A.L.A. Boura *Newcastle, Australia*
N.J. Dun *Toledo, U.S.A.*
R.F. Furchgott *New York, U.S.A.*
T. Godfraind *Brussels, Belgium*
S.Z. Langer *Paris, France*
R.J. Miller *Chicago, U.S.A.*
R.C. Murphy *Denver, U.S.A.*
E. Muscholl *Mainz, Germany*
R.A. North *Portland, U.S.A.*
M. Otsuka *Tokyo, Japan*
M.J. Rand *Melbourne, Australia*
S. Rosell *Södertalje, Sweden*
P. Seeman *Toronto, Canada*
L. Szekeres *Szeged, Hungary*
B. Uvnas *Stockholm, Sweden*
P.A. Van Zwieten *Amsterdam, Netherlands*
V.M. Varagič *Belgrade, Yugoslavia*
G. Velo *Verona, Italy*
Wang Zhen Gang *Beijing, China*
M.B.H. Youdim *Haifa, Israel*

Submission of manuscripts: Manuscripts (two copies) should be sent to The Editorial Office, British Journal of Pharmacology, St. George's Hospital Medical School, Cranmer Terrace, London SW17 0RE.

Authors should consult the Instructions to Authors and the Nomenclature Guidelines for Authors in Vol. **111,** 378–387. These Instructions and Guidelines also appear with the journal Index for Volumes **108–110,** 1993. A checklist of the essential requirements is summarised in each issue of the journal, or as the last page of the issue.

Whilst every effort is made by the publishers and editorial committee to see that no inaccurate or misleading data, opinion or statement appears in this Journal, they and the *British Pharmacological Society* wish to make it clear that the data and opinions appearing in the articles and advertisements herein are the responsibility of the contributor or advertiser concerned. Accordingly, the *British Pharmacological Society*, the publishers and the editorial committee and their respective employees, officers and agents accept no liability whatsoever for the consequences of any such inaccurate or misleading data, opinion or statement.

Featured Products

Aequorin
Photoprotein isolated from the jellyfish *Aequorea;* a Ca^{2+} indicator
Cat. No. A-205

α-Cobrotoxin
Selectively blocks nicotinic receptors; isolated from the venom of the snake *Naja Naja Kaouthia*
Cat. No. C-206

3-Morpholinosydnonimine HCl (SIN-1)
Nitric oxide source *Cat. No. M-184*

PD-123,319 ditrifluoroacetate
Potent and selective non-peptide angiotensin II AT_2 receptor antagonist (Sold with the permission of Warner-Lambert)
Cat. No. P-186

Cyclic ADP ribose
Potent intracellular Ca^{2+} releaser *Cat. No. C-201*

Rapamycin
A microlide immunosuppressant; binds to the FK506 binding protein (FKBP) through a FK506-calcineurin independent mechanism
Cat. No. R-117

Tamoxifen, (E)-4-hydroxy-
Metabolite of Tamoxifen (Cat. No. T-126); displays high affinity for the estrogen receptor
Cat. No. T-155

Tamoxifen, (Z)-4-hydroxy-
Less potent isomer *Cat. No. T-156*

RBI RESEARCH BIOCHEMICALS INTERNATIONAL

One Strathmore Road, Natick, MA 01760-2447 USA
508-651-8151 • 800-736-3690 • Fax 508-655-1359 • 800-736-2480

Local Distributors

Australia, Arncliffe • 2-567-5258
Denmark, Roedovre • 44-948822
France, Illkirch • 88-67-14-14
Germany, Köln • 221-497-2034
Israel, Jerusalem • 2-794951
Italy, Milano • 02-509-7720
Japan, Tokyo • 03-5684-1622
Korea, Seoul • 2-945-2431
Norway, Oslo • 22-220411
South Africa, Port Elizabeth • 41-4841
Switzerland, Zurich • 01-312-2124
Taiwan, Taipei • 2-918-1206
United Kingdom, St. Albans • 0727-841414

The *British Journal of Pharmacology* is published by Macmillan Press Ltd.

Scope The *British Journal of Pharmacology* is published monthly. It welcomes contribution in all field of experimental pharmacology including neuroscience, biochemical, cellular and molecular pharmacology. The Board of Editors represents a wide range of expertise and ensures that well-presented work is published as promptly as possible, consistent with maintaining the overall qulaity of the journal

This journal is covered by Current Contents, Excerpta Medica, BIOSIS and Index Medicus.

Editorial Manuscripts (plus two copies) and all editorial correspondence should be sent to: The Editorial Office, British Journal of Pharmacology, St George's Hospital Medical School, Cranmere Terrace, London SW17 0RE, UK. Tel: +44 81 767 6765; Fax: +44 81 767 5645.

Advertisements Enquires concerning advertisements should be addressed to: Michael Rowley, Hasler House, High Street, Great Dunmow, Essex CM6 1AP. Tel: +44 371 874613; Fax: +44 371 872273.

Publisher All business correspondence, supplement enquiries and reprint requests should be addressed to British Journal of Pharmacology, Scientific and Medical Division, Macmillan Press Ltd, Houndmills, Basingstoke, Hampshire RG21 2XS, UK. Tel: +44 256 29242; Fax: +44 256 810526. Publisher: Marija Vukovojac. Editorial Assistant: Alice Ellingham. Production Controller: Kath Parr.

Subscription Subscription price per annum (one volume, twelve issues) £540, rest of world £714 (Airmail), £595 (Surface mail) or equivalent in any other currency. Orders must be accompanied by remittance. Cheques should be made payable to Macmillan Magazines and sent to: The Subscription Department, Macmillan Press Ltd, Houndmills, Basingstoke, Hampshire RG21 2XS, UK. Where appropriate, subscribers may make payments into UK Post Office Giro Account No. 519 2455. Full details must accompany the payment. Subscribers from EC territories should add sales tax at the local rate.

British Journal of Pharmacology (ISSN 0007–1188) is published monthly by Macmillan Press Ltd, c/o Mercury Airfreight International Ltd, 2323 Randolph Avenue, Avenel, NJ 07001, USA. Subscription price for institutions is $950 per annum. 2nd class postage is paid at Rahway NJ. Postmaster: send address corrections to Macmillan Press Ltd, c/o Mercury Airfreight International Ltd, 2323 Randolph Avenue, Avenel NJ 07001.

Reprints of any article in this journal are available from Scientific and Medical Division, Macmillan Press Ltd, Houndmills, Basingstoke, Hampshire RG21 2XS, UK. Tel: +44 256 29242; Fax: +44 256 810526.

Copyright © 1994 The Macmillan Press Ltd

ISSN 0007–1188

All rights of reproduction are reserved in respect of all papers, articles, illustrations, etc., published in this journal in all countries of the world.

All material published in this journal is protected by copyright, which covers exclusive rights to reproduce and distribute the material. No material published in this journal may be reproduced or stored on microfilm or in electronic, optical or magnetic form without the written authorisation of the Publisher.

Authorisation to photocopy items for internal or personal use of specific clients, is granted by Macmillan Press Ltd, for libraries and other users registered with the Copyright Clearance Center (CCC) Transaction Reporting Service, provided that the base fee of $9.00 per copy is paid directly to CCC, 21 Congress St., Salem, MA 01970, USA. 0007-1188/94 $9.00 + $0.00.

Apart from any fair dealing for the purposes of research or private study, or criticism or review, as permitted under the Copyright, Designs and Patent Act 1988, this publication may be reproduced, stored or transmitted, in any form or by any means, only with the prior permission in writing of the publishers, or in the case of reprographic reproduction, in accordance with the terms of licences issued by the Copyright Licensing Agency.

Official publication of the British Pharmacological Society.

PREPARATION OF MANUSCRIPTS

Authors are strongly recommended to read the full *Instructions to Authors* and *Nomenclature Guidelines for Authors* (*Br. J. Pharmacol.* 1994, **111**, 378–387) before submitting a manuscript for publication in the *British Journal of Pharmacology*. The manuscript and cover letter should be checked against the following list before mailing.

The original and one copy of the manuscript must be supplied. Manuscripts must be typed in double-line spacing on one side of A4 paper, in type not smaller than 12 characters per inch or 10 point. Both copies to include Tables and a set of labelled Figures. One set of Figures without numbers or letters is also to be included. The text to be arranged in the following subsections:

1. **Title**—To have no more than 150 characters on a separate page, which should also include a Short Title (50 characters maximum) and the name and address of the author for correspondence.
2. **Summary**—To be arranged in numbered paragraphs (Full Papers) or a single paragraph (Special Reports).
   —to include aims, principal results and conclusions.
   —to include Key words (10 maximum) at end of summary.
3. **Introduction**—To contain concise statements of the problem and the aims of the investigation.
4. **Methods**—To have brief but adequate account of the procedures; *full names of drugs* (*including those referred to by manufacturer's code*), sources of drugs and statistical tests to be stated.
5. **Results**—To have no repetition of data in Figures, Tables and text.
6. **Discussion**—Findings and conclusions to be placed in context of other relevant work.
   NB Simple repetition of results and unwarranted speculation are not acceptable.
7. **Acknowledgements**—Sources of support. Sources of drugs not widely available commercially.
8. **References**—All references in the text to be included in the Reference List and *vice versa*. References in alphabetical order with complete citations; Journals publishing 'in press' papers identified.
   References to manuscripts submitted to other journals but not yet accepted are not allowed.
9. **Tables**—Each on a separate page and prepared in accordance with current requirements of the Journal.
10. **Figures**—Both labelled and non-labelled Figures to be prepared in accordance with current requirements of the Journal (see *Instructions to Authors*, 1993, **108**, 275–281) and provided with Figure Number and Authors' names on back (*in pencil*).
    —each legend to be typed on a separate page and carrying keys to symbols.
    —keys to symbols and histograms must not appear on the figures themselves, but in the respective legends.
    —'box style' figures are not in keeping with the Journal style; line drawings etc must have only left-hand and bottom axes.
11. **Manuscripts**—To be accompanied by a declaration signed by each author that
    (a) results are original
    (b) approval of all persons concerned has been given to submit manuscripts for consideration (see also 12b)
    (c) the same material is neither 'in press' (i.e. is in proof or has definitely been accepted for publication) nor under consideration elsewhere. Furthermore it will not be submitted or published elsewhere before a decision has been reached by the Editorial Board of the *British Journal of Pharmacology* and will not be submitted elsewhere if accepted by the *British Journal of Pharmacology*.
    (d) Copyright assignment is included.
12. **Cover letter**—To state clearly
    (a) Corresponding author's full postal address, telephone, telex or Fax number
    (b) where appropriate, that *either* ethical approval has been given for investigation *or* Company or Institutional permission to publish work has been received.
13. **Reminder**—Packaging to be sufficiently robust to protect Figures and to withstand mailing.

Failure to comply with *Instructions to Authors* may lead to substantial delays in processing, review and publication and may even jeopardize acceptance of the manuscript.

NOMENCLATURE

Authors are reminded that accepted receptor and associated terminology is laid out in *Nomenclature Guidelines for Authors*, as published in the *British Journal of Pharmacology*, *Br. J. Pharmacol.*, 1994, **111**, 385–387.

SPECIAL REPORTS

The purpose of *Special Reports* is to provide rapid publication for **new** and **important** results which the Editorial Board considers are likely to be of special pharmacological significance. *Special Reports* will have publication priority over all other material and so authors are asked to consider carefully the status of their work before submission.

In order to speed publication there is normally no revision allowed beyond very minor typographical or grammatical corrections. If significant revision is required, the Board may either invite rapid re-submission or, more probably, propose that it be re-written as a Full Paper and be re-submitted for consideration. In order to reduce delays, proofs of *Special Reports* will be sent to authors but **essential corrections must reach the Production Office within 48 hours of receipt.** Authors should ensure that their submitted material conforms exactly to the following requirements.

Special Reports should normally occupy no more than two printed pages of the Journal; two illustrations (Figures or Tables, with legends) are permitted. As a guideline, with type face of 12 pitch and double-line spacing, a page of A4 paper could contain about 400 words. The absolute maximum length of the *Special Report* is 1700 words. For each Figure or Table, please deduct 200 words. The manuscript should comprise a Title page with key words (maximum of 10), a Summary consisting of a single short paragraph, followed by Introduction, Methods, Results, Discussion and References (maximum of 10). In all other respects, the requirements are the same as for Full Papers (see current 'Instructions to Authors').

BRITISH JOURNAL OF PHARMACOLOGY VOLUME 113 (3) 1994

SPECIAL REPORTS

A.J. Sellers & M.L.J. Ashford. Activation of BK_{Ca} channels in acutely dissociated neurones from the rat ventromedial hypothalamus by NS 1619 659

S. Kim, K. Ohta, A. Hamaguchi, T. Omura, K. Tominaga, T. Yukimura, K. Miura, M. Tanaka & H. Iwao. AT_1 receptor-mediated stimulation by angiotensin II of rat aortic fibronectin gene expression *in vivo* 662

PAPERS

K. Tschaikowsky, M. Meisner, F. Schönhuber & E. Rügheimer. Induction of nitric oxide synthase activity in phagocytic cells inhibited by tricyclodecan-9-yl-xanthogenate (D609) 664

A.U. Ziganshin, C.H.V. Hoyle, L.E. Ziganshina & G. Burnstock. Effects of cyclopiazonic acid on contractility and ecto-ATPase activity in guinea-pig urinary bladder and vas deferens 669

D.M. Grassi-Kassisse, E. Antunes, P.G. Withrington & G. de Nucci. Modulation by endogenous prostanoids of the vasoconstrictor activity of endothelin-1 in the canine isolated, perfused spleen 675

P. Soediono & G. Burnstock. Contribution of ATP and nitric oxide to NANC inhibitory transmission in rat pyloric sphincter 681

B.-L. Källström, J. Sjöberg & B. Waldeck. The interaction between salmeterol and β_2-adrenoceptor agonists with higher efficacy on guinea-pig trachea and human bronchus *in vitro* 687

A. Tomlinson, I. Appleton, A.R. Moore, D.W. Gilroy, D. Willis, J.A. Mitchell & D.A. Willoughby. Cyclo-oxygenase and nitric oxide synthase isoforms in rat carrageenin-induced pleurisy 693

M.A. Oriowo. Atypical β-adrenoceptors in the rat isolated common carotid artery 699

F.L. Christofi & J.D. Wood. Electrophysiological subtypes of inhibitory P_1 purinoceptors on myenteric neurones of guinea-pig small bowel 703

A. Sagrada, G.B. Schiavi, E. Cereda & H. Ladinsky. Antagonistic properties of McNeil-A-343 at 5-HT_4 and 5-HT_3 receptors 711

H. Bouaziz, Y. Joulin, M. Safar & A. Benetos. Effects of bradykinin B_2 receptor antagonism on the hypotensive effects of ACE inhibition 717

A. Hatano, H. Takahashi, M. Tamaki, T. Komeyama, T. Koizumi & M. Takeda. Pharmacological evidence of distinct α_1-adrenoceptor subtypes mediating the contraction of human prostatic urethra and peripheral artery 723

M.D. Tricklebank, L.J. Bristow, P.H. Hutson, P.D. Leeson, M. Rowley, K. Saywell, L. Singh, F.D. Tattersall, L. Thorn & B.J. Williams. The anticonvulsant and behavioural profile of L-697,414, a partial agonist acting at the glycine modulatory site on the N-methyl-D-aspartate (NMDA) receptor complex 729

S. Greber, C. Schwarzer & G. Sperk. Neuropeptide Y inhibits potassium-stimulated glutamate release through Y_2 receptors in rat hippocampal slices *in vitro* 737

M. Patel, M.J. Sheehan & P. Strong. Failure of CGS15943A to block the hypotensive action of agonists acting at the adenosine A_3 receptor 741

E. Coëffier, D. Joseph & B.B. Vargaftig. Role of interleukin-5 in enhanced migration of eosinophils from airways of immunized guinea-pigs 749

C. Szabó, G.J. Southan, C. Thiemermann & J.R. Vane. The mechanism of the inhibitory effect of polyamines on the induction of nitric oxide synthase: role of aldehyde metabolites 757

Y.-M. Leung, C.-Y. Kwan & T.-T. Loh. Dual effects of tetrandrine on cytosolic calcium in human leukaemic HL-60 cells: intracellular calcium release and calcium entry blockade 767

P. Onali, A.J. Aasen & M.C. Olianas. Antagonism by (R)- and (S)-trihexyphenidyl of muscarinic stimulation of adenylyl cyclase in rat olfactory bulb and inhibition in striatum and heart 775

P. Kotsonis & H. Majewski. Facilitation by procaterol, a β-adrenoceptor agonist, of noradrenaline release in the pithed rat independently of angiotensin II formation 781

M.J. Neal, S.J. Paterson & J.R. Cunningham. Enhancement of retinal acetylcholine release by DAMGO: possibly a direct opioid receptor-mediated excitatory effect 789

T. Katsuragi, S. Ogawa & T. Furukawa. Contribution of intra- and extracellular Ca^{2+} to noradrenaline exocytosis induced by ouabain and monensin from guinea-pig vas deferens 795

P.D. Taylor & L. Poston. The effect of hyperglycaemia on function of rat isolated mesenteric resistance artery 801

A.K. Bahl, M.M. Dale & J.C. Foreman. The effect of non-steroidal anti-inflammatory drugs on the accumulation and release of interleukin-1-like activity by peritoneal macrophages from the mouse 809

I. von Kügelgen, L. Späth & K. Starke. Evidence for P_2-purinoceptor-mediated inhibition of noradrenaline release in rat brain cortex 815

G. McCreath, I.P. Hall & S.J. Hill. Agonist-induced desensitization of histamine H_1 receptor-mediated inositol phospholipid hydrolysis in human umbilical vein endothelial cells 823

N.B. Mercuri, A. Bonci, P. Calabresi, F. Stratta, A. Stefani & G. Bernardi. Effects of dihydropyridine calcium antagonists on rat mid-brain dopaminergic neurones 831

S.A. Daly & J.L. Waddington. The effects of clozapine on behavioural responses to the selective 'D_1-like' dopamine receptor agonist, A 68930, and to the selective 'D_2-like' agonist, RU 24213 839

J.G. Filep, M. Clozel, A. Fournier & É. Földes-Filep. Characterization of receptors mediating vascular responses to endothelin-1 in the conscious rat 845

R.J. Evans & C. Kennedy. Characterization of P_2-purinoceptors in the smooth muscle of the rat tail artery: a comparison between contractile and electrophysiological responses 853

S.C. Chung, T.V. McDonald & P. Gardner. Inhibition by SK&F 96365 of Ca^{2+} current, IL-2 production and activation in T lymphocytes 861

V. Richard, N. Kaeffer, M. Hogie, C. Tron, T. Blanc & C. Thuillez. Role of endogenous endothelin in myocardial and coronary endothelial injury after ischaemia and reperfusion in rats: studies with bosentan, a mixed ET_A-ET_B antagonist 869

M.M. Iravani & M.A. Zar. Presence of neuropeptide Y in the rat seminal vesicle and its effects on noradrenaline- and nerve-induced contractions 877

S.M.C. Cunningham, S. Mihara & G.M. Lees. Y_2-receptor-mediated selective inhibition of slow, inhibitory postsynaptic potential in submucous neurones of guinea-pig caecum 883

K. Kamei, S. Yoshida, J. Imagawa, H. Nabata & H. Kuriyama. Regional and species differences in glyburide-sensitive K^+ channels in airway smooth muscles as estimated from actions of KC 128 and levcromakalim 889

W.-X. Shen, P. Jobling & J.P. Horn. The sensitivity of nicotinic synapses in bullfrog sympathetic ganglia to α-bungarotoxin and neuronal-bungarotoxin 898

M. Schwanstecher, C. Schwanstecher, C. Dickel, F. Chudziak, A. Moshiri & U. Panten. Location of the sulphonylurea receptor at the cytoplasmic face of the β-cell membrane 903

F. Squadrito, D. Altavilla, P. Canale, M.P. Ioculano, G.M. Campo, L. Ammendolia, G. Squadrito, A. Saitta, G. Calapai & A.P. Caputi. Contribution of intercellular adhesion molecule 1 (ICAM-1) to the pathogenesis of splanchnic artery occlusion shock in the rat 912

H. El-Bizri & P.B.S. Clarke. Regulation of nicotinic receptors in rat brain following quasi-irreversible nicotinic blockade by chlorisondamine and chronic treatment with nicotine 917

J.S. Edwards & J.M. Ritter. Effect of cytoplasmic pH on Ca^{2+}-stimulated eicosanoid biosynthesis in human platelets 926

R.A.D. Rutherford, Y. Matsuda, M.R. Wilkins, J.M. Polak & J. Wharton. Identification of renal natriuretic peptide receptor subpopulations by use of the non-peptide antagonist, HS-142-1 931

Contents continue inside back cover

Typeset by Elite Typesetting Techniques, Eastleigh, Hants
and printed in Great Britain by Unwin Brothers Ltd., The Gresham Press, Old Woking, Surrey

S.C. Cruwys, N.E. Garrett, M.N. Perkins, D.R. Blake & B.L. Kidd. The role of bradykinin B_1 receptors in the maintenance of intra-articular plasma extravasation in chronic antigen-induced arthritis **940**

J.P. Wang, S.L. Raung, M.F. Hsu & C.C. Chen. Inhibition by gomisin C (a lignan from *Schizandra chinensis*) of the respiratory burst of rat neutrophils **945**

D. Fulton, J.C. McGiff & J. Quilley. Role of K^+ channels in the vasodilator response to bradykinin in the rat heart **954**

A. Hall, J. Stow, R. Sorensen, J.O. Dolly & D. Owen. Blockade by dendrotoxin homologues of voltage-dependent K^+ currents in cultured sensory neurones from neonatal rats **959**

A. Zazpe, I. Artaiz & J. Del Río. Role of 5-HT_3 receptors in basal and K^+-evoked dopamine release from rat olfactory tubercle and striatal slices **968**

A. Delaunois, P. Gustin, C. Dessy-Doize & M. Ansay. Modulatory effect of neuropeptide Y on acetylcholine-induced oedema and vasoconstriction in isolated perfused lungs of rabbit **973**

F. Scamps & G. Vassort. Pharmacological profile oif the ATP-mediated increase in L-type calcium current amplitude and activation of a non-specific cationic current in rat ventricular cells **982**

D.J. Browse, R.T. Mathie, I.S. Benjamin & B. Alexander. The transhepatic action of ATP on the hepatic arterial and portal venous vascular beds of the rabbit: the role of nitric oxide **987**

A.L.A. Pires, P.M.R. e Silva, C. Pasquale, H.C. Castro-Faria-Neto, P.T. Bozza, R.S.B. Cordeiro, G.A. Rae, P. Braquet, V. Lagente & M.A. Martins. Long-lasting inhibitory activity of the hetrazepinic BN 50730 on exudation and cellular alterations evoked by PAF and LPS **994**

N.J. Yard, M. Chiesi & H.A. Ball. Effect of cyclopiazonic acid, an inhibitor of sarcoplasmic reticulum Ca^{2+}-ATPase, on the frequency-dependence of the contraction-relaxation cycle of the guinea-pig isolated atrium **1001**

J.A. Mitchell, M.G. Belvisi, P. Akarasereenont, R.A. Robbins, O.-J. Kwon, J. Croxtell, P.J. Barnes & J.R. Vane. Induction of cyclo-oxygenase-2 by cytokines in human pulmonary epithelial cells: regulation by dexamethasone **1008**

U. Windscheif, V. Ralevic, H.G. Bäumert, E. Mutschler, G. Lambrecht & G. Burnstock. Vasoconstrictor and vasodilator responses to various agonists in the rat perfused mesenteric arterial bed: selective inhibition by PPADS of contractions mediated via P_{2x}-purinoceptors **1015**

E.G. Silva, E. Frediani-Neto, A.T. Ferreira, A.C.M. Paiva & T.B. Paiva. Role of Ca^{2+}-dependent K-channels in the membrane potential and contractility of aorta from spontaneously hypertensive rats **1022**

C.-C. Huang & P -W. Gean. Paired-pulse depression of the N-methyl-D-aspartate receptor-mediated synaptic potentials in the amygdala **1029**

G. Pethö, M. Jocič & P. Holzer. Role of bradykinin in the hyperaemia following acid challenge of the rat gastric mucosa **1036**

R.W. Hauck, Ch. Schulz, H.P. Emslander & M. Böhm. Pharmacological actions of the selective and non-selective β-adrenoceptor antagonists celiprolol, bisoprolol and propranolol on human bronchi **1043**

D.T. Thwaites, B.H. Hirst & N.L. Simmons. Substrate specificity of the di/tripeptide transporter in human intestinal epithelia (Caco-2): identification of substrates that undergo H^+-coupled absorption **1050**

R.G. Humphries, W. Tomlinson, A.H. Ingall, P.A. Cage & P. Leff. FPL 66096: a novel, highly potent and selective antagonist at human platelet P_{2T}-purinoceptors **1057**

W. Rouse & I.R. Johnson. Haemodynamic actions of a novel sino-atrial node function modulator, ZENECA ZD7288, in the anaesthetized dog: a comparison with zatebradine, atenolol and nitrendipine **1064**

W. Rouse, P.J. Stafford & I.R. Johnson. The haemodynamic actions of ZENECA ZD7288, a novel sino-atrial node function modulator, in the exercising beagle: a comparison with zatebradine and propranolol **1071**